

# Cover

---

## Excerpt

Why should one study a worm? This simple creature is one of several “model” organisms that together have provided tremendous insight into how all organisms are put together. It has become increasingly clear over the past two decades that knowledge from one organism, even one so simple as a worm, can provide tremendous power when connected with knowledge from other organisms. And because of the experimental accessibility of nematodes, knowledge about worms can come more quickly and cheaply than knowledge about higher organisms.

## Contents

- [Reviewers](#)
- [Preface](#)
- [Foreword](#)
- [Chapter 1. Introduction to \*C. elegans\*](#)
  - Donald L Riddle, Thomas Blumenthal, Barbara J Meyer, and James R Priess.
    - [I The Biological Model](#)
    - [II Origins of the Model](#)
    - [III Life History And Evolution](#)
    - [IV Anatomy](#)
    - [V Resources](#)
    - [VI Current Issues](#)
    - [Acknowledgments](#)
- [Chapter 2. The Genome](#)
  - Robert H Waterston, John E Sulston, and Alan R Coulson.
    - [I General Properties](#)
    - [II The Physical Map](#)
    - [III Genetics, Genes, and the Physical Map](#)
    - [IV Genome Sequencing](#)
    - [V EST Sequencing](#)
    - [VI Interpretation of the Sequence](#)
    - [VII Tentative Conclusions](#)
    - [VIII Prospects](#)
    - [Acknowledgments](#)
- [Chapter 3. Chromosome Organization, Mitosis, and Meiosis](#)
  - Donna G Albertson, Ann M Rose, and Anne M Villeneuve.
    - [I Introduction](#)
    - [II Mitosis](#)
    - [III Meiosis](#)
    - [IV Prospects](#)
- [Chapter 4. Mutation](#)
  - Robert C Johnsen and David L Baillie.
    - [I Introduction](#)
    - [II Induced Mutations](#)
    - [III Genetic Balancers](#)
    - [IV Genetically Detectable Genes](#)
    - [V What are Essential Genes?](#)
    - [VI Gene Distribution](#)

- [VII Summary](#)
- [Acknowledgment](#)
- [Chapter 5. Transposons](#)

Ronald H A Plasterk and Henri G A M van Luenen.

  - [I Introduction](#)
  - [II Tc1 and Tc3](#)
  - [III Other Elements](#)
  - [IV The Tc1/\*mariner\* Family](#)
  - [V Regulation of Tc1/\*mariner\* Transposition](#)
  - [VI Mechanism of Tc1 Transposition](#)
  - [VII Repair After Tc1 Excision](#)
  - [VIII Tc1 as a Tool in \*C. elegans\* Research](#)
  - [Acknowledgments](#)
- [Chapter 6. RNA Processing and Gene Structure](#)

Thomas Blumenthal and Keith Steward.

  - [I Introduction](#)
  - [II Cis -Splicing in Worms](#)
  - [III Trans -Splicing](#)
  - [IV SL2 Trans -Splicing and Operons](#)
  - [V Trans -Splicing in Vitro](#)
  - [VI Frequency of Operons and Trans -Splicing](#)
  - [VII Organization and Transcription of Spliced Leader RNA Genes](#)
  - [VIII 3'-End Formation](#)
  - [IX Translation Initiation and Termination Signals](#)
  - [X Conclusions](#)
  - [Acknowledgments](#)
- [Chapter 7. Transcription Factors and Transcriptional Regulation](#)

James D McGhee and Michael W. Krause.

  - [I Introduction](#)
  - [II The Basal Transcription Machinery](#)
  - [III Transcription Factors](#)
  - [IV Analysis of \*C. elegans\* Promoters](#)
  - [V Future Prospects](#)
- [Chapter 8. mRNA and Translation](#)

Philip Anderson and Judith Kimble.

  - [I Introduction](#)
  - [II The Translational Apparatus](#)
  - [III Informational Suppressors](#)
  - [IV Regulation of Translation During Development](#)
  - [Acknowledgments](#)
- [Chapter 9. Sex Determination and X Chromosome Dosage Compensation](#)

Barbara J Meyer.

  - [I Introduction](#)
  - [II Sexual Dimorphism](#)
  - [III The Primary Sex-Determination Signal and its Gene Target](#)
  - [IV Hermaphrodite-Specific Genes that Coordinately Control Sex Determination and Dosage Compensation](#)
  - [V X Chromosome Dosage Compensation](#)
  - [VI Somatic Sex Determination](#)
  - [VII Sex Determination in The Germ Line Versus the Soma](#)
  - [VIII Concluding Remarks](#)

- [Acknowledgments](#)
- [Chapter 10. Developmental Genetics of the Germ Line](#)  
Tim Schedl.
  - [I Introduction](#)
  - [II Summary of Anatomy and Development of the Germ Line](#)
  - [III Genetic Analysis of Germ-Line Development](#)
  - [IV Somatic Gonad](#)
  - [V Germ-Line Specification and Survival](#)
  - [VI Germ-Line Sex Determination](#)
  - [VII Control of Proliferation and Entry into the Meiotic Pathway](#)
  - [VIII Meiotic Prophase Progression and Gametogenesis](#)
  - [IX Oocyte Development, Maturation, and Ovulation](#)
  - [X Future Prospects](#)
  - [Acknowledgments](#)
- [Chapter 11. Spermatogenesis](#)  
Steven W L'Hernault.
  - [I Overview](#)
  - [II Organelle Morphogenesis During Spermatogenesis](#)
  - [III Spermiogenesis](#)
  - [IV Acquisition and Mechanism of Spermatozoan Motility](#)
  - [V Role of Motility During Oocyte Recognition](#)
  - [VI Future Prospects](#)
  - [Acknowledgments](#)
- [Chapter 12. Male Development and Mating Behavior](#)  
Scott W Emmons and Paul W Sternberg.
  - [I Introduction and Overview of Male Anatomy](#)
  - [II Behavior](#)
  - [III Development](#)
  - [IV Concluding Remarks](#)
  - [Acknowledgments](#)
- [Chapter 13. Fertilization and Establishment of Polarity in the Embryo](#)  
Kenneth J Kemphues and Susan Strome.
  - [I Introduction](#)
  - [II Fertilization](#)
  - [III Establishment of Polarity in the One-Cell Embryo](#)
  - [IV Cell Division Patterns in the Early Embryo](#)
  - [V Summary and Speculation](#)
- [Chapter 14. Specification of Cell Fates in the Early Embryo](#)  
Ralf Schnabel and James R Priess.
  - [I Introduction](#)
  - [II Specification of Cell Fates in the AB Lineage](#)
  - [III Specification of the P<sub>1</sub> Descendants](#)
  - [IV Future Prospects](#)
- [Chapter 15. Cell Death](#)  
Michael O Hengartner.
  - [I Introduction](#)
  - [II Programmed Cell Death in \*C. elegans\*](#)
  - [III Genetics of Programmed Cell Death](#)
  - [IV Programmed Cell Death in Specific Cell Types](#)
  - [V Cell Deaths not Mediated by the Common Death Program](#)

- [VI Evolution of Programmed Cell Death](#)
  - [Acknowledgments](#)
- [Chapter 16. Muscle: Structure, Function, and Development](#)  
 Donald G Moerman and Andrew Fire.
  - [I Introduction](#)
  - [II The Organization, Structure, and Function of Muscle](#)
  - [III Specification of Muscle Patterns: Programs for Muscle Determination and Differentiation](#)
  - [Acknowledgments](#)
- [Chapter 17. Extracellular Matrix](#)  
 James M Kramer.
  - [I Introduction](#)
  - [II Cuticle](#)
  - [III Basement Membranes](#)
  - [IV Conclusions](#)
  - [Acknowledgments](#)
- [Chapter 18. Heterochronic Genes](#)  
 Victor Ambros.
  - [I Introduction](#)
  - [II Heterochronic Phenotypes](#)
  - [III Control of Larval Development by \*lin-14\*](#)
  - [IV Developmental Programs and Regulatory Targets](#)
  - [V Postdauer Reprogramming of Heterochronic Phenotypes](#)
  - [VI Perspectives](#)
  - [Acknowledgments](#)
- [Chapter 19. Development of the Vulva](#)  
 Iva Greenwald.
  - [I Introduction and Overview](#)
  - [II The Anchor Cell](#)
  - [III VPC Generation and Identity](#)
  - [IV VPC Specification](#)
  - [V Execution](#)
  - [VI Morphogenesis](#)
  - [VII Evolution of Vulval Development](#)
  - [VIII Future Prospects](#)
  - [Acknowledgments](#)
- [Chapter 20. Patterning the Nervous System](#)  
 Gary Ruvkun.
  - [I Introduction](#)
  - [II Invariant Cell Lineages in \*C. elegans\* Neurogenesis](#)
  - [III Specification of Sensory Neuronal Development](#)
  - [IV Generation of Reiterated Neurons by Reiterated Cell Lineages](#)
  - [V Spatial Patterning by the \*C. elegans\* HOM-C Gene Cluster](#)
  - [VI Concluding Remarks](#)
- [Chapter 21. Cell and Growth Cone Migrations](#)  
 Adam Antebi, Carolyn R Norris, Edward M Hedgecock, and Gian Garriga.
  - [I Introduction](#)
  - [II Neuroglia and Pioneers](#)
  - [III Netrins Guide Circumferential Migrations](#)
  - [IV Hierarchies Of Guidance Cues](#)
  - [V Genetic Requirements for Axonal Growth](#)
  - [VI Cell Migration and other Aspects of Cellular Phenotype](#)

- [VII Muscle Positioning on the Body Wall and Muscle Arm Chemotropism](#)
  - [VIII Future Directions](#)
  - [Acknowledgments](#)
- [Chapter 22. Synaptic Transmission](#)  
 James B Rand and Michael L Nonet.  
  - [I Introduction](#)
  - [II Neurotransmitter Metabolism and Function](#)
  - [III Components Regulating Neurotransmitter Release in all Neurons](#)
  - [IV Conclusions and Future Perspectives](#)
  - [Acknowledgments](#)
- [Chapter 23. Mechanotransduction](#)  
 Monica Driscoll and Joshua Kaplan.  
  - [I Introduction: the Neural Circuit For Locomotion](#)
  - [II Mechanosensory Control of Locomotion](#)
  - [III Touch Receptor Development and Differentiation](#)
  - [IV Genes Required for Touch Receptor Function](#)
  - [V Conclusions](#)
  - [Acknowledgments](#)
- [Chapter 24. Feeding and Defecation](#)  
 Leon Avery and James H Thomas.  
  - [I Introduction: Nematode Hydrostatics](#)
  - [II Feeding](#)
  - [III Defecation Motor Program](#)
  - [IV Conclusions](#)
  - [Acknowledgments](#)
- [Chapter 25. Chemotaxis and Thermotaxis](#)  
 Cornelia I Bargmann and Ikue Mori.  
  - [I Introduction](#)
  - [II \*C. elegans\* Responds to a Variety of Chemicals](#)
  - [III The Behavioral Mechanism of Chemotaxis and Thermotaxis](#)
  - [IV Cellular Analysis of Chemosensory and Thermosensory Neurons](#)
  - [V Genetic and Molecular Analysis of Chemosensation and Thermosensation](#)
  - [VI Regulation of Chemotaxis and Thermotaxis by Experience](#)
  - [VII Conclusions and Prospects](#)
  - [Acknowledgments](#)
- [Chapter 26. Genetic and Environmental Regulation of Dauer Larva Development](#)  
 Donald L Riddle and Patrice S Albert.  
  - [I Introduction](#)
  - [II The Dauer State](#)
  - [III Developmental Transitions](#)
  - [IV A Network of Gene Functions](#)
  - [V Summary and Conclusions](#)
  - [Acknowledgments](#)
- [Chapter 27. Neural Plasticity](#)  
 Erik M Jorgensen and Catharine Rankin.  
  - [I Introduction: Connectivity and Plasticity](#)
  - [II Synaptic Plasticity During Development](#)
  - [III Behavioral Plasticity in the Adult](#)
  - [IV Conclusions](#)
  - [Acknowledgments](#)
- [Chapter 28. Environmental Factors and Gene Activities That Influence Life Span](#)

Cynthia Kenyon.

- [I The Study of Life Span](#)
- [II Theories of Aging](#)
- [III Aging in \*C. elegans\*](#)
- [IV The Search for Genes that Control the Rate of Aging](#)
- [V Prospects](#)
- [Acknowledgments](#)

- [Chapter 29. Evolution](#)

David H A Fitch and W. Kelley Thomas.

- [I Introduction](#)
- [II Phylogenetic Context for \*C. elegans\*](#)
- [III Character Evolution](#)
- [IV Other Directions](#)
- [V Conclusions](#)
- [Acknowledgments](#)

- [Chapter 30. Parasitic Nematodes](#)

Mark Blaxter and David Bird.

- [I The Nematode World](#)
- [II An Introduction to Some Nematode Parasites](#)
- [III Antinematode Compounds and Their Targets](#)
- [IV The Nematode Surface](#)
- [V Parasite Genes and Genomes](#)
- [VI Future Prospects](#)
- [Acknowledgments](#)

- [Appendix 1 Genetics](#)

Jonathan Hodgkin.

- [Part A Genetic Nomenclature](#)
- [Part B List of Laboratory Strain and Allele Designations](#)
- [Part C Skeleton Genetic Map](#)
- [Part D List of Characterized Genes](#)
- [Acknowledgments](#)
- [Gene List](#)

- [Appendix 2 Neurotransmitter Assignments for Specific Neurons](#)

James B Rand and Michael L Nonet.

- [Appendix 3 Codon Usage in \*C. elegans\*](#)

Paul M Sharp and Keith R Bradnam.

- [Appendix 4 On-line \*C. elegans\* Resources](#)

Mark L Edgley, Carolyn A Turner, and Donald L Riddle.

- [Part A ACeDB Resources](#)
- [Part B \*C. elegans\* Genome Project and Related Sources](#)
- [Part C Other Information Sources](#)

- [Bibliography](#)

## Reviewers

---

- Kathryn Anderson, *Sloan-Kettering Cancer Center*
- Phillip Anderson, *University of Wisconsin, Madison*
- Leon Avery, *University of Texas Southwestern Medical Center*
- Cori Bargmann, *University of California, San Francisco*
- Thomas Barnes, *McGill University, Montreal*
- Robert Barstead, *Oakland Medical Research Foundation, Oklahoma City*
- Martin Chalfie, *Columbia University*
- David J. Chitwood, *Nematology Laboratory, USDA, Beltsville, Maryland*
- John Connolly, *Cold Spring Harbor Laboratory*
- Victor Corces, *Johns Hopkins University*
- Joseph Culotti, *Samuel Lunenfeld Research Institute, Mount Sinai Hospital, Toronto*
- Scott Emmons, *Albert Einstein College of Medicine*
- Andrew Fire, *Carnegie Institution of Washington*
- Margaret Fuller, *Stanford University*
- Gian Garriga, *University of California, Berkeley*
- Timothy G. Geary, *The Upjohn Company, Kalamazoo, Michigan*
- Corey S. Goodman, *Howard Hughes Medical Institute, University of California, Berkeley*
- Jeff Hall, *Brandeis University*
- Scott Hawley, *University of California, Davis*
- Michael Hengartner, *Cold Spring Harbor Laboratory*
- Robert K. Herman, *University of Minnesota, St. Paul*
- Winship Herr, *Cold Spring Harbor Laboratory*
- Jonathan Hodgkin, *MRC Laboratory of Molecular Biology*
- Richard Hynes, *Massachusetts Institute of Technology*
- Thomas E. Johnson, *University of Colorado, Boulder*
- Joshua Kaplan, *Harvard University, Massachusetts General Hospital*
- Cynthia Kenyon, *University of California, San Francisco*
- Stuart Kim, *Stanford University*
- Judith Kimble, *University of Wisconsin, Madison*
- Mark Kirk, *University of Missouri, Columbia*
- Michael W. Krause, *NIDDK, National Institutes of Health, Bethesda*
- Mitzi Kuroda, *Baylor College of Medicine*
- Pamela Larsen, *University of Southern California*
- Ruth Lehmann, *Massachusetts Institute of Technology*
- Marco Marra, *Washington University*
- Elliot Meyerowitz, *California Institute of Technology*
- Steve Mount, *University of Maryland, College Park*
- Susan Parkhurst, *Fred Hutchinson Cancer Research Center, University of Washington, Seattle*
- Ronald H.A. Plasterk, *The Netherlands Cancer Institute, Amsterdam*
- Samuel M. Politz, *Worcester Polytechnic Institute, Massachusetts*
- Rudolph A. Raff, *Indiana University, Bloomington*
- Jasper Rine, *University of California, Berkeley*
- Donald Rio, *University of California, Berkeley*
- Joel Rothman, *University of California, Santa Barbara*
- Richard H. Scheller, *Howard Hughes Medical Institute, Stanford University Medical Center*
- Trudi Schupbach, *Princeton University*
- Hermann Steller, *Massachusetts Institute of Technology*
- Michael Stern, *Yale University School of Medicine*

- Paul Sternberg, *California Institute of Technology, Pasadena*
- Susan Strome, *Indiana University, Bloomington*
- Suzanne Tharin, *Cold Spring Harbor Laboratory*
- James H. Thomas, *University of Washington, Seattle*
- Laurie Tompkins, *Temple University*
- Timothy Tully, *Cold Spring Harbor Laboratory*
- Eugenia Wang, *Lady Davis Institute for Medical Research, Montreal*
- Sam Ward, *University of Arizona*
- John White, *University of Wisconsin, Madison*
- Marvin Wickins, *University of Wisconsin, Madison*
- William Wood, *University of Colorado, Boulder*
- S. Larry Zipursky, *Howard Hughes Medical Institute, University of California, Los Angeles*

## **Footnotes**

\*

Additional Reviewers who wish to remain anonymous also receive the thanks of the Editors.

Generated from local HTML

## Preface

---

It is a pleasure for me to have the opportunity to begin this volume with a tribute to the large community of scientists who have been devoting their life to studies of *Caenorhabditis elegans*. Should this preface be read by individuals outside the scientific community, they may well wonder what it is that motivates the thousands of individuals around the world who spend 80 hours a week thinking and dreaming about this tiny nematode worm, only about 1 mm long and formed from 959 body cells. To the uninitiated, let me begin by making it clear that this is not one of those inexplicable personality cults. The person who started it all in 1965, Sydney Brenner, often exudes both karma and charisma in his monthly essay in the journal, *Current Biology*. Nevertheless, it is an attempt to understand the worm that grips and inspires those thousands of scientists—not Sydney.

I was fortunate to begin my own career in molecular biology at a time when the traditions of the early bacteriophage workers, led by Max Delbrück, still predominated. Our research was performed in a relatively small community of scientists, where most heads of laboratories knew each other well. Much data were freely shared, with the confidence that personal integrity would ensure proper credit for the source of new discoveries, without the need for priority established by a publication record. The enormous growth of our enterprise has eroded this feeling of trust during the past 35 years. But a strong tradition of sharing and trust persists in the worm community. In part, this is due to the stepwise growth of this field, which allows most worm researchers today to view themselves as being united through a close-knit lineage of former laboratory mentors. Most of the credit clearly belongs to those mentors themselves, who—starting with Sydney, John Sulston, and others—have set a high standard for both science and cooperation that their descendants have faithfully followed.

The cooperation and sharing in the worm community have played a major part in the success of everyone's science. The many shared *C. elegans* techniques, meetings abstracts, upcoming events, mutants, and DNA sequences can be viewed by all on the Internet (at <http://eatworms.swmed.edu>). In fact, this community's early effort at electronic sharing was selected as a "model collaborative" in a publication from the Computer Science and Telecommunications Board of the National Research Council (National Collaboratories: Applying Information Technology for Scientific Research, 1993), the organization that I chair as president of the National Academy of Sciences.

The major assumption behind the Research Council report was that our marvelous new electronic communication tools will greatly speed up the science that is done in many different fields in the future. We can see why this is true when we review the driving force for the explosive development of biological knowledge in recent years. Science is fundamentally a knowledge-building process, in which each advance comes from combining units of previous knowledge in new ways. In short, the advance of scientific knowledge is all about making new connections. The more units of knowledge we have, and the more efficiently they are shared, the faster science proceeds. Biology is exploding both because with each passing year we have more knowledge to build on and because there is a great deal of sharing. Other factors being equal, those particular fields of biology in which the sharing is most efficient will move the fastest. In science, therefore, a tradition of good deeds is generally well rewarded.

Why should one study a worm? This simple creature is one of several "model" organisms that together have provided tremendous insight into how all organisms are put together. It has become increasingly clear over the past two decades that knowledge from one organism, even one so simple as a worm, can provide tremendous power when connected with knowledge from other organisms. And because of the experimental accessibility of nematodes, knowledge about worms can come more quickly and cheaply than knowledge about higher organisms.

Today, the most prominent of the model organisms are the bacterium *Escherichia coli*, the yeast *Saccharomyces cerevisiae*, the fruit fly *Drosophila melanogaster*, the plant *Arabidopsis thaliana*, the mouse, the human—and of course *C. elegans*. In each of these cases, the intensive study of the organism has led to the accumulation of enough knowledge about it that unexpected relationships between the genes and proteins of that organism are constantly being uncovered. These surprises are providing new insights into fundamental biological mechanisms

that are of profound significance. In other words, unanticipated synergies cause the impact of our knowledge from the many individual studies on an organism to be much greater than the simple sum of its parts. In addition, over time, a large armament of powerful organism-specific methods are developed that become powerful research tools for everyone who is interested in the organism. For *C. elegans*, for example, recent years have seen the development of reliable methods for knocking out the function of any desired gene by either antisense RNA or transposon-mediated techniques, an essentially complete library of ordered cosmid clones that provides the DNA corresponding to any mapped gene, a complete three-dimensional lineage map of what each cell does in the developing embryo as a function of time, the ability to separate and isolate blastomeres from the early embryos, and the DNA sequence of 58 million of the total of 100 million nucleotide pairs in the nematode genome (through a transcontinental project scheduled for completion in late 1998).

When I stand back and consider what I have learned from the studies of *C. elegans*, what do I remember most? I think first of all of that famous lineage diagram, which traces the ancestry of all 959 cells back to the fertilized egg and tells us exactly which cell divided—and at what time—to produce every cell in the embryo and adult. That such a diagram can be made at all is enormously significant. It tells us that each cell in a multicellular organism can act like a precisely timed robot that constantly senses its environment and acts accordingly, having the ability to remember what it detected (and therefore where it was) earlier in the embryo and to change its pattern of cell determination according to this memory, including setting a precise time for its next cell division. It is as if there were a time-counting “computer” inside each cell that inputs present events, stores them in memory along with the inputs from past events, and then performs the calculations that makes the cell behave appropriately with regard to its subsequent behavior. In other words, I learned from *C. elegans* that each cell in a multicellular organism must be incredibly sophisticated with regard to its input, storage, and output devices. Such a cell deserves tremendous respect from scientists.

I have also learned that a cell has amazing abilities to determine its movements and its precise spatial patterning. During the course of the worm's development, certain cells will move one way and then another, marching their way through a host of other cells in the embryo with great precision. And the mapping of all 302 nerve cells and their interconnections has revealed a remarkable consistency in the exact pattern of their more than 7000 branching synaptic interconnections. This result provides dramatic proof that incredible spatial control is possible in a multicellular aggregate, and it has given me a new feeling for the abilities that cells have for sculpting space.

We have come to realize in recent years that the basic molecules that make life possible are nearly the same in [all cells](#). So much so, that—to our surprise—we can learn an enormous amount about how a human develops from a fertilized egg by studying a model organism such as a worm. In fact, because worms are so much easier to study than humans, we can say with confidence that the fastest and most efficient way of acquiring an understanding of ourselves is to devote an enormous effort to trying to understand these, and other, relatively “simple” organisms.

In attempting to unscramble this wonderful puzzle of how life works, we have embarked on an intellectual adventure of the highest kind. By late 1998, when the genome sequence is completed, we will have the complete catalog of the 10,000 or so proteins from which a worm is made. Since we now know that most proteins function in groups of ten or more to form “protein machines,” this means that all the remarkable complexity of structure and behavior that we see in *C. elegans* is somehow possible with only about a thousand protein machines. Quite clearly, even a small living thing like a worm is by far more elaborate and fascinating than the most complicated human constructions that we can imagine on this planet.

Scientists who are investigating how cells work in an organism today know that they are on a true frontier, peering out across unknown and mysterious territory where many surprises are certain to be found. It is this realization that motivates so many biologists to live and dream about science, and it is this that explains the typical 80-hour weeks familiar to all of our families and colleagues.

**Bruce Alberts**

November 20, 1996

Generated from local HTML

## Foreword

---

Genetics today is a very different field from the one I entered more than 50 years ago when I began to study the chromosomes of *Elephantulus*, a South African insectivore. I taught myself cytogenetics by struggling for seven months with the 1937 edition of C.D. Darlington's book *Recent Advances in Cytology*, something, I am pleased to note, no student has to do today. The circumstances of my scientific education gave me broad knowledge of biology, and, more importantly, there were no boundaries between different subjects. Embryology, neurology, genetics, physiology, and even paleontology were seamlessly joined, something which cannot be said of biology today, where almost everybody is locked into a highly specialized compartment. As a student of medical science, I thought nothing of reconstructing embryos in the morning, doing experiments on the neuromuscular junction in the afternoon, and arguing about philosophy, politics, and life all night. Later, when I started research, I had enough of that particular form of self-confidence and courage that comes from sheer ignorance, to enable me to build ultracentrifuges, synthesize dyes, and even learn mathematics to pursue a life in science.

I can trace my path in genetics without any break from those early days through the work on bacteriophage begun in Oxford, my first illuminating meeting with Jim Watson and Francis Crick and the Double Helix in April 1953, continuing into the years at Cambridge, where the worm was born, and to my present preoccupation with the genome of another curious animal, the pufferfish. There has been only one quest, the quest to find out how organisms are encoded by their genes, to study that unique property of biological systems that distinguishes them from all other complex natural systems of containing an internal description of themselves. Genetics is the fundamental biological science, and it is also the unifying science, encompassing everything: How living systems work, how they are built and how they got that way—physiology, development, and evolution.

Everybody knows that while deep, global questions are the important ones to ask, they cannot be tackled directly and need to be decomposed in some way to allow something to be done about them. The nature of this decomposition has always been the critical question in my mind, and I manage to smuggle what was essentially a manifesto into my first paper on the genetics of *C. elegans*. One would not be allowed to do this today, because referees would ban it as speculative, irrelevant, and uninteresting. I wrote:

In principle, it should be possible to dissect the genetic specification of a [nervous system](#) in much the same way as was done for biosynthetic pathways in bacteria or for bacteriophage assembly. However, one surmises that genetical analysis alone would have provided only a very general picture of the organization of those processes. Only when genetics was coupled with methods of analyzing other properties of the mutants, by assays of enzymes or *in vitro* assembly, did the full power of this approach develop. In the same way, the isolation and genetical characterization of mutants with behavioral alterations must be supported by analysis at a level intermediate between the gene and behavior. Behavior is the result of a complex and ill-understood set of computations performed by nervous systems and it seems essential to decompose the problem into two: one concerned with the question of the genetic specification of nervous systems and the other with the way nervous systems work to produce behavior. Both require that we must have somehow of analyzing a [nervous system](#)... Some eight years ago, when I embarked on this problem, I decided that what was needed was an experimental organism which was suitable for genetical study and in which one could determine the complete structure of the [nervous system](#). *Drosophila*, with about  $10^5$  neurons, is much too large, and, looking for a simpler organism, my choice eventually settled on the small nematode, *Caenorhabditis elegans*....

Readers of "Worm I" will recall that these thoughts were there at the beginning of the work, but saying them aloud in 1974 caused great consternation, especially among the neurophysiologists. To say that the nervous systems included problems beyond the electrical properties of neurons was heresy and to talk about genes and development and combine these with old fashioned anatomy confirmed in their minds that this could only be a lunatic adventure. But all I proposed was an obvious extension to a higher level of organization of what previous research in molecular biology had already accomplished. Notice also the introduction of the word "computation"

not as applied to computers but to biological systems themselves, another of my passions which is becoming more prominent in biological research.

In these days where genetics is pursued by the alternative means of sequencing, we have the inverse question of how we can obtain function from sequence. The simple answer is by studying functions and finding out what sequences correspond to them much as we have done in the past in experimental genetics. We may hope one day to compute organisms from their DNA sequences; it will not be accomplished by some magic programme but only by doing genetics in the world of real organisms.

Here, 10 years later, is the second book of *The Worm*. It continues to flourish and to open new areas. All of biology is encompassed—physiology, development, behavior, and even ecology. And it still preserves that wonderful feature that I experienced first and which everybody has experienced since: that with a few toothpicks, some petri dishes and a microscope, you can open the door to all of biology.

**Sydney Brenner**

*November, 1996*

Generated from local HTML

# **Chapter 1. Introduction to *C. elegans***

---

## **Contents**

[I The Biological Model](#)

[II Origins of the Model](#)

[III Life History And Evolution](#)

[IV Anatomy](#)

[V Resources](#)

[VI Current Issues](#)

[Acknowledgments](#)

Generated from local HTML

# Chapter 1. Introduction to *C. elegans* — I The Biological Model

---

In 1965, Sydney Brenner settled on *Caenorhabditis elegans* as a model organism to study animal development and behavior for reasons that are now well known ([Brenner, 1973, 1988](#)). This soil nematode offered great potential for genetic analysis, partly because of its rapid (3-day) life cycle, small size (1.5-mm-long adult), and ease of laboratory cultivation. One might imagine how the ability to grow thousands of animals on a single petri dish seeded with a lawn of *Escherichia coli* as the food source had a certain appeal to a bacteriophage geneticist such as Brenner. Indeed, the 300—350 progeny produced by a single animal is even greater than the burst of progeny produced by a T4 phage upon lysis of its *E. coli* host. The natural *C. elegans* mode of inbreeding by the self-fertilizing hermaphrodite combined with the ability to cross hermaphrodites with males ([Fig. 1](#)) offered conveniences previously enjoyed only in plant genetic systems such as *Zea mays*, in which crossing or selfing can be manipulated at will. Other key features were the nematode's small genome (only 20 times that of *E. coli*) and anatomical simplicity (>1000 cells), including the 302-cell hermaphrodite [nervous system](#). With a [nervous system](#) that small, Brenner proposed that its complete circuitry could be determined by serial-section electron microscopy, a vision realized 20 years later ([White et al. 1986, 1988](#)). The ultimate goal was to determine the role of each gene involved in [neural](#) development and function.

An important reason *C. elegans* was chosen for study was that high-quality electron micrographs had been obtained from specimens of this species by Nichol Thomson, who was hired by Brenner in October, 1964. Initially, Brenner began reconstructing the [nervous system](#) by hand. He thought it might be possible to discern some principles of [neural](#) wiring by concentrating on one small part of the [nervous system](#), so he started with the [retrovesicular ganglion](#) (RVG) at the anterior end of the [ventral nerve cord](#). By the beginning of the 1970s, he began writing software for computer reconstruction of cell morphology from tracings of serial-section electron micrographs. Other investigators characterized responses to chemoattractants ([Dusenberry 1973; Ward 1973](#)) and the sensory ultra-structure of the wild type ([Ward et al. 1975; Ware et al. 1975](#)) and of mutants defective in chemotaxis ([Lewis and Hodgkin 1977](#)). Ultimately, the wild-type reconstructions showed all the connections of all the [neurons](#) in the hermaphrodite [nervous system](#); the 381-cell [male nervous system](#) has been partially reconstructed at the EM level ([White et al. 1988](#)). Analysis of the wild-type circuitry allowed detailed models of how [neurons](#) function together to generate behavior. Furthermore, comparison of [neural](#) ultrastructure at different developmental stages revealed some surprising examples of developmental plasticity ([Jorgensen and Rankin, this volume](#)). In recent years, the wild-type circuit diagram has provided the foundation for interpreting the phenotypes of behavioral and locomotory mutants and the spatial deployment and function of neurotransmitters ([Driscoll and Kaplan; Rand and Nonet, both this volume](#)).

A criticism raised by early skeptics was that the animal has few morphological and behavioral traits. The organism was viewed as an almost featureless tube that moves forward or backward in a simple sine wave. It was suggested that with so few visible characters, it would be difficult to distinguish the functions of genes by mutant phenotypes, thus diminishing the power of genetics as a tool to reveal genes of interest. This criticism was somewhat dampened by the publication of the first *C. elegans* genetic map ([Brenner 1974](#)) containing more than 100 genetic loci dispersed over the six chromosomes, all of which are behavioral or morphological markers.

It was soon made clear that most of the interesting features are inside the animal. The transparency of the body, the constancy of cell number (eutely), and the constancy of cell position from individual to individual have perhaps been the most unique advantages offered by this organism for the study of development. It is a nearly ideal specimen for observation with differential interference contrast microscopy, and virtually every cell in the body is accessible to laser microsurgery. Eutely is of fundamental importance to the detection and reliable scoring of mutant phenotypes that alter cell lineages. The complete wild-type cell lineage from fertilized egg to adult was determined by observation of cell divisions and cell migrations in living animals ([Sulston et al. 1988](#)). This landmark provided a foundation on which much of the research in this book is based.

Brenner's overall plan could not be accomplished with the technologies available at the time. Major technical advances, such as the cloning and physical mapping of virtually the entire *C. elegans* genome, the development of transposon-tagging, reverse genetics, germ-line DNA transformation, genetic mosaics, and laser microsurgery,

were essential to maintain and expand the usefulness of this model. Recently, Epstein and Shakes (1995) have compiled the most comprehensive collection of methods and information resources to date for analysis of *C. elegans*, including all of the methods mentioned above.

The early molecular genetic approach to *C. elegans* biology necessarily concentrated on genes encoding biochemically tractable products. This requirement effectively eliminated genes affecting [neural](#) development and function, but the genetics opened the door to address the problem of muscle assembly and function. The [unc-54](#) gene, encoding the major body-wall myosin heavy chain, was chosen for study because its 210-kD product is one of the most abundant proteins in the body, and the protein was readily analyzed by SDS-PAGE ([Epstein et al. 1974](#)). A large number of mutant alleles with an easily recognized slow-paralyzed phenotype had been collected in Cambridge, including recessive, temperature-sensitive, and dominant alleles. One semidominant allele, e675, is a small deletion that results in a stable messenger RNA and a stable protein lacking 100 amino acids near the carboxyl terminus. The difference in mRNA size was crucial for identifying [unc-54](#) complementary DNA clones, which were constructed from cDNA fragments synthesized from [unc-54](#) mRNA that had been partially purified on sucrose gradients ([MacLeod et al. 1981](#)). Although ribosomal RNA repeats were cloned and characterized in the same year ([Files and Hirsh 1981](#)), [unc-54](#) was the first genetically identified *C. elegans* gene to be cloned. It had a major impact on the muscle field because it provided the first myosin heavy-chain sequence. Up to that point, biochemists were proposing to sequence myosin using protein chemistry. [unc-54](#) also provided a probe to clone homologous genes in other organisms. Studies on [unc-54](#) quickly broadened to other muscle genes and muscle protein components, and the analysis of muscle assembly and function has been an important component in the exploitation of this experimental model ([Moerman and Fire](#), this volume).

The long-term problem of having to curate stocks of the wild type and many mutant derivatives was solved in 1969 when John Sulston developed convenient methods for permanent storage of nematode stocks. Methods for storing viable stocks of nematodes frozen in liquid nitrogen were similar to those used for mammalian cell lines ([Sulston and Hodgkin 1988](#)). Stocks stored in liquid nitrogen for 25 years have retained their viability, as have stocks frozen at -80°C for the past 12 years. Laboratory strains maintained in growing cultures for long periods have been found to diverge with respect to fecundity and life span. Also, spontaneous activation of Tc1 transposition has been observed. This problem, by no means unique to *C. elegans*, has been minimized by the ability to return to frozen reference stocks at any time. Furthermore, the cost of faithfully maintaining large collections of mutants and the potential loss or mislabeling of strains that can occur with repeated transfer of growing cultures have been substantially reduced.

Brenner's initial emphasis clearly centered on the development and function of the [nervous system](#), but a similar genetic approach to other aspects of developmental biology soon produced results, including the study of embryogenesis ([Vanderslice and Hirsh 1976](#); [von Ehrenstein et al. 1979](#)), sex determination ([Hodgkin and Brenner 1977](#)), and larval development ([Cassada and Russell 1975](#)). Developmental genetics gained momentum as the postembryonic cell lineage was completed ([Sulston and Horvitz 1977](#)) and progressed faster than the neurobiology for a number of years, but a distinct shift back to neurobiology, including developmental neurobiology, is evident in this volume. Knowledge gained from the molecular genetics of development has provided new tools for analysis of the [nervous system](#) ([Antebi et al.; Ruvkun](#); both this volume). This illustrates the value of "high-connectivity models," such as *C. elegans*, yeast, *Drosophila*, the mouse, and mammalian cells in culture, in which many different aspects of their biology are intensively investigated ([National Research Council Committee on Models for Biomedical Research 1985](#)). In such a system, knowledge gained in one area of research ultimately "connects" with research in other areas. This connectivity both expands and reinforces understanding and speeds research progress. The more research areas that are investigated in a given model system, the greater the chance for connectivity. A read of this volume shows that this ideal has been realized.

Whether by chance or by design, basic biomedical research in the past 30 years has concentrated on a relatively small number of model systems (primarily prokaryotic cells, yeast, protozoans, *C. elegans*, *Drosophila*, *Xenopus*, *Mus*, primates, and mammalian cells in culture). Although these are quite different from each other, an astounding degree of connectivity between them has been revealed in the past decade. The emerging parallels between the development of the body plan in nematodes, flies, and mice ([Ruvkun](#), this volume), and the fact that

similar proteins are used for programmed cell death in both nematodes and humans ([Hengartner](#), this volume), provide two examples.

*C. elegans II* attempts to provide a core of knowledge that builds upon the first book produced by the *C. elegans* community, *The Nematode Caenorhabditis elegans*, edited by W.B. Wood and the Community of *C. elegans* Researchers (1988). This 669-page book has been the “bible” of *C. elegans* biology for nearly a decade, and it will continue to be a fundamental resource for years to come. It synthesized the description of the organism, including its genetics, anatomy, cell lineage, development, reproduction, [neural](#) anatomy, and basic features of its genome. Here we profile knowledge that has accumulated within the past decade to apply this model system to solving current biological problems.

## Figures

Figure 1. Photomicrographs showing major anatomical features of the *C.*

### Figure 1

Photomicrographs showing major anatomical features of the *C. elegans* adult hermaphrodite (*top*) and male (*bottom*). Shown are lateral views under bright-field illumination. Bar, 20  $\mu\text{m}$ . (Reprinted, with permission, from [Sulston and Horvitz 1977](#).)

Generated from local HTML

## Chapter 1. Introduction to *C. elegans* — II Origins of the Model

---

The potential value of *Rhabditis* species for genetic research was pointed out by Dougherty and Calhoun (1948). *C. elegans* was initially described and named *Rhabditis elegans* by Maupas (1900); it was subsequently placed in the subgenus *Caenorhabditis* by Osche (1952) and then raised to generic status by Dougherty (1955). The name is a blend of Greek and Latin (*Caeno*, recent; *rhabditis*, rod; *elegans*, nice). Two strains have historical importance. One strain, Bergerac, was collected from the soil in France by Victor Nigon of the Université de Lyon ([Nigon 1949](#)), and the other strain, Bristol, was isolated by L.N. Staniland (National Agricultural Advisory Service, London) from mushroom compost near Bristol, England ([Nicholas et al. 1959](#)). At high inoculum, *C. elegans* and its associated bacteria are reported to cause losses in mushroom yield and quality ([Grewal 1991](#)).

Using the Bergerac isolate, Nigon (1949) observed a haploid chromosome number of six and documented the two modes of reproduction, by selfing and by crossing with males. Males of the Bristol strain were obtained in Nigon's laboratory for taxonomic classification, and the arrangement and morphology of the caudal papillae, or "rays," in the male copulatory bursa ([Emmons and Sternberg](#), this volume) were found to be the same as that already described for *C. elegans* var. Bergerac ([Nigon and Dougherty 1949](#)). Bristol males were then successfully crossed with hermaphrodites of the French strain.

Ellsworth Dougherty brought *C. elegans* to his laboratory at the Kaiser Foundation Research Institute in Richmond, California. He subsequently moved to the nearby Department of Nutritional Sciences at the University of California at Berkeley in 1961, and he continued to study the nutritional requirements and axenic cultivation of *Caenorhabditis* species, particularly *C. briggsae*, until his death in 1965. Although permanent cultures were maintained on nutrient agar slants inoculated with *E. coli*, an axenic medium (having no organism present) with chemically undefined supplements was developed in 1954 ([Dougherty et al. 1959](#)). Subsequently either monoxenic or axenic cultures of *C. elegans* and *C. briggsae* were provided to numerous investigators for research on nutrition, reproduction, genetics, and aging. Much of this early work on the biochemistry, physiology, culture, and nutrition of *Caenorhabditis* and other free-living nematodes can be found in Nicholas (1975) *The Biology of Free-living Nematodes* and in Zuckerman (1980) *Nematodes as Biological Models*, Volumes 1 and 2. Volume 1 includes chapters on *C. elegans* genetics, development, and behavior. More recently, anatomical and physiological information from *C. elegans* has been integrated with that from plant and animal parasitic species by Bird and Bird (1991) in the second edition of the classic monograph *The Structure of Nematodes*.

The Bergerac strain was found to exhibit a high spontaneous mutation frequency owing to transposition of the Tc1 transposon, which is present in high copy number (300—400 copies) in this strain ([Moerman and Waterston 1984](#)). It was crossed repeatedly with the low-copy-number (30 copies) Bristol strain to generate some of the "mutator" strains used for transposon tagging ([Mori et al. 1988a](#)). In part because the Bergerac males are essentially infertile and the hermaphrodites are temperature-sensitive sterile mutants ([Fatt and Dougherty 1963](#)), virtually all *C. elegans* genetics has been done with the Bristol strain, i.e., the N2 line that Sydney Brenner derived from the Bristol culture he obtained from Ellsworth Dougherty in the spring of 1964. However, some genetic work on the Bergerac strain was carried out in the laboratory of Jean-Louis Brun at Claude-Bernard University, Villeurbanne, France ([Dion and Brun 1971; Abdul-Kader and Brun 1978](#)). The Bergerac strain survives today as two diverged sublines, N62 (CB4851) and BO (RW7000). Several dumpy and lethal mutant lines derived from the Bergerac strain are also available.

Other wild-type strains of *C. elegans* have been isolated from numerous sites around the world ([Fitch and Thomas](#), this volume). These strains sometimes display different traits (see, e.g., [Barker 1994](#)), but they are all interfertile with the N2 laboratory strain, which was defined in 1965 as the wild-type reference. *C. briggsae* seems to be much less common in nature. One isolate (G16) from Gujarat, India, has been reported and compared with the Dougherty strain of *C. briggsae* and with *C. elegans* N2 ([Fodor et al. 1983](#)). This analysis revealed that the *C. briggsae* strain, which descended from a single worm isolated in 1944 from soil on the Stanford University campus by Margaret Briggs Gochnauer ([Gochnauer and McCoy 1954](#)), had accumulated numerous mutations in its 40 years of laboratory cultivation. Consequently, the G16 isolate replaced the Briggs isolate as the wild-type reference, and currently available DNA libraries are derived from G16. Prior to Brenner (1974), *C. briggsae* had

been the species of choice for most research, including a genetic study of a spontaneous "dwarf" mutant ([Nigon and Dougherty 1950](#)). It lost popularity in the 1970s because Brenner's work stimulated the adoption of *C. elegans* as a biological model ([Edgar and Wood 1977](#)), and because several *Caenorhabditis* laboratory lines thought to be *C. briggsae* were actually *C. elegans* ([Friedman et al. 1977](#)). *C. briggsae* had, in fact, been originally identified as *C. elegans* but was later reclassified and named as a new species (Dougherty and [Nigon 1949](#)).

Generated from local HTML

## Chapter 1. Introduction to *C. elegans* — III Life History And Evolution

---

The characteristics that make *C. elegans* an attractive experimental model reflect its survival strategy in the soil. Survival strategies have classically been considered in terms of “*r*-selection versus *K*-selection,” in which reproductive scheduling is selected on the basis of mortality rates and environmental stability. In unstable environments with high mortality rates, *r*-selection favors rapid development and early reproduction, whereas in stable environments with low mortality rates, *K*-selection favors genotypes resulting in slower development, larger size, longer reproductive period, and longer life span. The soil is presumably an unstable environment, with an uneven distribution of microbial food and considerable risk of death from environmental fluctuations in temperature or moisture, or from encounters with predators such as nematode-trapping fungi ([Gray 1988](#)).

*C. elegans* is itself a voracious predator that will eat anything that fits in its [mouth](#). In the laboratory, it converts *E. coli* into *C. elegans* with an efficiency of nearly 50% ([Lewis and Fleming 1995](#)). In the soil, it apparently seeks to consume all available resources as quickly as possible as a means to overgrow its competitors. Both the rapid life cycle (14-hour embryogenesis and 36-hour postembryonic development through four larval stages, L1—L4 to the adult at 25°C) and large brood size favor this strategy, but a compromise must be reached between these two traits. The hermaphrodite is protandrous, first producing sperm in the late L4 stage then turning to the production of oocytes as an adult ([L'Hernault; Schedl](#); both this volume). The adult is structurally a female, with its previously produced sperm stored in its [spermathecae](#). The typical hermaphrodite produces many more oocytes than sperm, so the size of the brood is limited by the number of sperm. Oocyte production is stimulated by mating with males; a single hermaphrodite has the potential to produce more than 1000 progeny when mated. Why does the hermaphrodite not maximize its reproduction by producing more sperm? With the protandrous reproductive system, producing more sperm delays the onset of egg laying, effectively slowing the generation time. In this case, more is not better ([Hodgkin and Barnes 1991](#)).

Given its “boom and bust” strategy of rapid habitat depletion (consumption of all microbial food resources), an effective mechanism for dispersal to more favorable soil locations is important for evolutionary success. This is a predicament shared with nematode parasites that must migrate from one host to another through a harsh environment that will not support growth ([Evans and Perry 1976](#)). The nondeveloping dauer (“enduring”) stage of *C. elegans* and analogous third-stage “infective” larvae of parasitic species are specialized to perform the needed dispersal function ([Blaxter and Bird](#), this volume). In many parasites, the dauer larva is an obligate stage of diapause, whereas in *C. elegans*, it is facultative. Dauer larvae are not formed as long as the food supply is sufficient to support continued growth of the population, but as the food supply is diminished, dauer larvae are formed at the second larval molt ([Riddle](#), this volume). Preparation for the nonfeeding dauer stage involves alteration of energy metabolism and accumulation of fat in intestinal and hypodermal cells; dauer-specific behaviors are specialized to favor dispersal. Dauer larvae can survive for many months, approximately ten times the normal life span, and when they encounter food, they resume development. Thus, *C. elegans* may successfully migrate through sparse soil resources from one region of microbial bloom to another.

Successful dauer dispersal is favored by hermaphrodite reproduction, since a single animal can establish a new population. Hence, the boom and bust lifestyle may be an important factor contributing to the persistence of hermaphrodite reproduction despite the normally deleterious effects of inbreeding. *C. elegans* males are rarely, if ever, isolated from soil, so if dauer dispersal is a prominent phase in the natural habitat, most populations may be clonal. This survival strategy selects against the accumulation of genetic load. In fact, neither inbreeding depression nor hybrid vigor (heterosis) has been observed in *C. elegans* ([Johnson and Wood 1982; Johnson and Hutchinson 1993](#)). The lack of heterosis eliminates a major complication for analysis of interstrain crosses and is particularly important for genetic analysis of life history traits such as life span, which is acutely dependent on the overall health of the organism. The short (2-week) life span of *C. elegans* and the availability of mutants with greatly increased longevity have stimulated its use as a model for research on aging ([Kenyon](#), this volume).

If the simple scenario of dauer dispersal followed by clonal reproduction is correct, one might predict that *C. elegans* should reproduce by parthenogenesis rather than sex. The origin and evolution of sex, in fact, remain a controversial issue in evolutionary biology, but sex is generally rationalized as a necessary means to obtain favorable recombinant genotypes. In *C. elegans*, XO males arise spontaneously in XX hermaphrodite populations by means of X chromosome nondisjunction at a frequency of about 0.1% (Hodgkin et al. 1979; [Meyer](#), this volume). The males mate with hermaphrodites ([Emmons and Sternberg](#), this volume) to produce a 1:1 ratio of male and hermaphrodite cross-progeny, but additional hermaphrodites are almost always produced by selfing. Hence, the sex ratio is skewed toward the hermaphrodite. Petri dish populations starve before males have had time to cross sufficiently with a hermaphrodite to maximize the male to hermaphrodite ratio. In these small laboratory populations, males normally disappear after a few generations if the sex ratio is not actively maintained.

Choice of reproductive mode may be a simple matter of economics. Limited resources in nature may favor hermaphrodite reproduction, but more uniform environments, such as a compost heap that supports a large population originating from numerous individuals (reproducing for many generations prior to dauer dispersal), may be more favorable for crossing. It pays to be a hermaphrodite if there are diminishing returns in producing gametes. In other words, producing twice as many gametes may not produce twice as many surviving progeny if those progeny simply compete with one another for limited food or space. In contrast, an abundance of food would favor crossing with males to maximize the number of offspring. The choice between hermaphroditic and gonochoric (dioecious) reproduction may allow *C. elegans* to proliferate in a spectrum of soil environments.

Generated from local HTML

## Chapter 1. Introduction to *C. elegans* — IV Anatomy

---

Nematodes live almost everywhere. Diverse genera have adapted to free-living habitats in virtually all terrestrial and marine environments, and they parasitize virtually all species of plant and animal ([Blaxter and Bird](#), this volume). Although they are of ancient evolutionary origin, their phylogeny is unclear because there is no fossil record ([Fitch and Thomas](#), this volume). Nevertheless, all nematodes are built on the same basic body plan, which is made up of two concentric tubes separated by a fluid-filled space, the [pseudocoelom](#). The animal's shape is maintained by internal hydrostatic pressure. *C. elegans* anatomy has been reviewed by White (1988). The outer tube is covered by the collagenous, extracellular cuticle, which is secreted by the underlying [hypodermis](#) ([Kramer](#), this volume). At each of the four larval molts, a new cuticle of stage-specific composition is secreted, and the old cuticle is shed. The body musculature is arranged in four longitudinal strips which are attached to the cuticle through a thin layer of [hypodermis](#) ([Moerman and Fire](#), this volume). Contraction of the two subventral muscle strips with relaxation of the subdorsal strips, and vice versa, generates sinusoidal movement in the dorsal-ventral plane ([Driscoll and Kaplan](#), this volume). On an agar dish, the animals move forward or backward on either lateral side and are confined to the surface by the surface tension of the water in the medium. The [nervous system](#), gonad, [coelomocytes](#), and [excretory](#)/secretory system are the other components of this outer tube ([Sulston and White 1988](#)).

The inner tube is composed of the muscular [pharynx](#) with its nearly autonomous [nervous system](#) and the intestine. [Figure 2](#) shows a schematic cross section through an adult hermaphrodite. The conserved nematode anatomy is generated by conserved developmental patterns. The early blastomeres, called founder cells, are generated by a series of asymmetric, asynchronous cleavages in which the germ-line precursor cell sequentially gives rise to the four founder cells for the somatic lineages and one germ-line cell (Schnabel and Priess; see [Fig. 1](#) in [Kemphues and Stone](#), this volume). The embryonic lineages generate 671 cells, but 113 of these undergo programmed cell death ([Hengartner](#), this volume). By the time a larva hatches from the egg, it possesses 558 cells. Approximately 10% of these are somatic blast cells that divide further to generate additional somatic tissues in the adult.

The cell bodies of most [neurons](#) are positioned around the [pharynx](#), along the ventral midline and in the tail. Most of their cell processes form a ring around the basement membrane that surrounds the [pharynx](#), or they join the dorsal or ventral nerve cords ([Rand and Nonet](#), this volume). Most chemosensory and [mechanosensory neurons](#) extend afferent processes from the region of the [nerve ring](#) to sensory organs near the tip of the head. Other [sensory neurons](#) extend their processes along the body or to the tail. The [nerve ring](#) receives and integrates sensory information and connects to [motor neurons](#) in the head or along the nerve cords.

The bilobed [pharynx](#) pumps food into the intestine, grinding it as it passes through the second bulb ([Fig. 3](#)). The intestinal cells surround a central lumen which connects to the [anus](#) near the [tail](#) (see [Fig. 1](#)). The [excretory](#)/secretory system is involved in osmoregulation and in secretion of glycoproteins thought to make up a replenishable surface coat over the epicuticle. The [excretory](#) cell is the largest cell in the animal, with [excretory](#) canals running the length of the body that are connected to an [excretory](#)/secretory pore on the ventral side of the head.

The hermaphrodite reproductive system consists of functionally independent anterior and posterior arms. Each arm is reflexed with an ovary that is distal to the [vulva](#), a more proximal oviduct, and a spermatheca connected to a common [uterus](#) centered around the [vulva](#) ([Schedl; Greenwald](#); both this volume). The adult [uterus](#) contains fertilized eggs and embryos in the early stages of development. Vulval contractions, mediated by the hermaphrodite-specific [neurons](#), are required for egg laying.

The [male gonad](#) is a single reflexed organ extending anteriorly from its distal tip, then posteriorly to connect via the [vas deferens](#) to the [cloaca](#) near the [anus](#) (see [Fig. 1](#)). As with the hermaphrodite ovary, the germ-line nuclei are mitotic near the distal end. Meiotic cells in progressively later stages of spermatogenesis are distributed along the gonad to the [seminal vesicle](#), in which [spermatids](#) are stored for release during copulation ([Schedl](#);

[L'Hernault](#), both this volume). Male-specific [neurons](#), muscles, and hypodermal structures are required for mating with hermaphrodites ([Emmons and Sternberg](#), this volume).

Although nematodes have evolved many specializations for their survival, all nematodes are built on a basic developmental and anatomical framework ([Bird and Bird 1991](#); [Blaxter and Bird](#); [Fitch and Thomas](#), both this volume). As the commonalities between *C. elegans* and parasitic species have become clearer, *C. elegans* biology and parasitology have interfaced with progressively more detail. Placing *C. elegans* in a properly detailed phylogenetic framework will help formulate this interface, but such placement remains a challenge because the characters traditionally used for nematode taxonomy have been so limited and the phylum is so old that evolutionary divergence is great, even within anatomically similar genera ([Fitch and Thomas](#), this volume).

It is not understood why all nematodes molt four times. Some species even molt once in the egg and hatch as second-stage larvae ([Bird and Bird 1991](#)). Molting is not required for growth as is the case for many insects. *C. elegans* increases in size by about one-third during each larval stage and again as an adult after the final molt ([Byerly et al. 1976](#)). The large intestinal parasite *Ascaris* is only slightly larger than *C. elegans* at its final molt, but it increases in size manyfold as an adult. The necessity to change surface composition to survive changing environments is an explanation for molting in parasites ([Blaxter and Bird](#), this volume), and for free-living nematodes that form dispersal stages, but not for many other free-living species. It seems likely that basic developmental cues controlling postembryonic cell lineages, and even developmental plasticity in cell morphology and function, are activated by the molting cycle, and such linkages may have stabilized the molting regimen in evolution. The molting process in *C. elegans* has been described ([Singh and Sulston 1978](#)), but little is known about hormonal control of molting in any nematode. *C. elegans* does not biosynthesize ecdysteroids, although cholesterol is required in the diet ([Chitwood and Feldlaufer 1990](#)).

## Figures

Figure 2. Diagram of a posterior cross section through the adult hermaphrodite.

### Figure 2

Diagram of a posterior cross section through the adult hermaphrodite. (g) Gonad; (h) [hypodermal ridge](#); (i) intestine; (m) muscle; (nc) nerve cord. (Reprinted, with permission, from [Edwards and Wood 1983](#).)

Figure 3. Electron micrograph of a feeding L4 larva showing a transverse section through the posterior bulb of the pharynx.

### Figure 3

Electron micrograph of a feeding L4 larva showing a transverse section through the posterior bulb of the [pharynx](#). The “grinder” disrupts the bacterial cells (*center*) with its tooth-like projections and forces the mixture posteriorly through the pharyngeal-intestinal valve into the intestine ([Avery and Thomas](#), this volume). Bar, 1  $\mu\text{m}$ . (Courtesy of P.S. Albert.)

Generated from local HTML

# Chapter 1. Introduction to *C. elegans* — V Resources

---

## A. Strains and Information Exchange

The success of long-term storage of *C. elegans* mutant strains made it feasible to maintain, at a single location, a comprehensive collection of genetic stocks representing all published genes and chromosomal rearrangements for distribution to the biomedical research community. The concept of the Caenorhabditis Genetics Center (CGC) was promoted by Donald G. Murphy, a research administrator at the National Institutes of Health, National Institute on Aging (NIA). Murphy closely watched the emergence of *C. elegans* research in the United States ([Edgar and Wood 1977](#)) and saw great potential for its growth as a biomedical model, particularly with respect to basic research on aging. With general agreement that the best way to promote use of this model was to establish a genetic stock center, and with scientific advice for creating a project description, Murphy assembled the resources for the NIA to release a Request for Proposals that led to the establishment of the Caenorhabditis Genetics Center at the University of Missouri in 1979. Not only was the CGC to be a comprehensive central repository for mutant strains, but it was also given responsibility to act as a clearing house for genetic nomenclature and act as an information resource ([Appendix 1](#)), with descriptive data on genes and strains, annual updating and publication of the genetic map, and maintenance of a complete bibliography of publications on *C. elegans*.

The CGC, now under contract with the NIH National Center for Research Resources, moved to its current location at the University of Minnesota in 1992. From its Minnesota location, the CGC continues to distribute *Caenorhabditis* strains upon request free of charge for research purposes. The genetic map has been integrated with the physical map of *C. elegans* and is maintained in conjunction with computing support from the Genome Sequencing Project. The complete *C. elegans* bibliography, the list of available genetic stocks, and the addresses of Worm Breeder's Gazette (WBG) subscribers are available on the Internet at the CGC gopher site ([Appendix 4](#)). The "traditional" genetic map of *C. elegans* ([Edgley and Riddle 1993](#)) is no longer published, but the map and its supporting data are made available by means of the *C. elegans* database, ACeDB. A modified genetic map with associated information is released in the WBG biannually.

The WBG met the need for an informal *C. elegans* research newsletter ([Goldberg 1991](#)). It was first assembled by Robert S. Edgar at the University of California, Santa Cruz, in December, 1975, and was circulated at no charge to 18 subscriber laboratories. As interest and demand grew, responsibility for the Gazette was transferred to the CGC in 1983, with 91 paying subscribers. The WBG now has more than 700 subscribers to the hard copy, and many more view the electronic edition of the WBG maintained on the *C. elegans* World Wide Web server at University of Texas Southwestern Medical Center (see [Appendix 4](#)). A *C. elegans* bionet electronic discussion group provides an additional avenue for information exchange. The WBG is an informal instrument for rapid communication in the research community, and WBG articles are not to be cited in published literature. Instead, WBG authors may be contacted to obtain personal communications.

In keeping with the concept of the high connectivity model, the biannual international *C. elegans* meetings (held in odd-numbered years) have been both markers and catalysts for research progress and development of the field. Despite the diverse biological problems addressed by attendees, an early consensus developed that this was the most immediately relevant professional meeting for most participants. The organism-based meeting remains a high point generally regarded in the not-to-be-missed category. Growth in the size of the field has profoundly changed the atmosphere of the International Meeting. Seventy-five people attended the 1977 meeting in Woods Hole, Massachusetts, and 750 attended the 1995 meeting in Madison, Wisconsin. It is no longer possible to meet all the people attending the meeting or to absorb all the material presented. Regional meetings in even-numbered years (West Coast, Midwest, East Coast, European) have filled the need for smaller meetings, and these meetings are assuming greater importance.

## B. Genomics

The physical map of the *C. elegans* genome is based on overlapping cosmid and yeast artificial chromosome (YAC) clones ([Waterston et al.](#), this volume). Overlaps were determined by a cosmid fingerprinting procedure ([Coulson et al. 1986](#)) and by YAC hybridization ([Coulson et al. 1988](#)). The clones that constitute the map are available from the Sanger Centre in Cambridge, U.K., as a central resource, essentially eliminating the need for other genomic libraries. This central resource facilitated a long-term collaboration in the *C. elegans* community. As investigators cloned mapped genes, the clones were fingerprinted to identify overlapping cosmids, thus providing anchor points for alignment of the physical and genetic maps in progressively greater detail. Initially, the clones of mapped genes assisted the process of ordering cosmid contigs. More recently, the genome map has provided the means for positional cloning. Mapped cDNA clones are available from the sequencing centers in Cambridge and at Washington University in St. Louis, Missouri ([Appendix 4](#)). YAC grids ("polytene grids") representing about 95% of the *C. elegans* coding sequences are also available to determine by hybridization the position of a cloned sequence in the genome, with an average resolution of about 100 kb.

The small size of the *C. elegans* genome (100 million base pairs, about the size of a single human chromosome) and the advanced state of the physical map made it an appropriate model for developing the strategies and technologies for analyzing the human genome. The genome sequence is made available in finished and "in-process" forms from Web sites at the two sequencing centers. The sequence is expected to be completed by the end of 1998 ([Waterston et al.](#), this volume). Transgenic lines carrying sequenced cosmids as extra minichromosomes are available from Simon Fraser University, Vancouver, Canada ([Appendix 4](#)).

ACeDB is a system of data management and display that integrates the various kinds of information about *C. elegans*, including genomic data ([Eckman and Durbin 1995](#)). It has been under development by Jean Thierry-Mieg and Richard Durbin since 1990, and genome projects related to other organisms have used it to develop databases of their own.

Research on *C. elegans* has benefited enormously from the network of resources that has been established during the past 20 years. No single individual can be credited with the construction of that network. Instead, a relatively small group of leaders by their actions supported open sharing of biological materials and information, both published and unpublished, for the common good. The accrued benefits have now become increasingly relevant to the wider scope of biomedical research, and the potential impact of *C. elegans* research over the next decade is enormous.

Generated from local HTML

# Chapter 1. Introduction to *C. elegans* — VI Current Issues

---

## A. The Genome

The *C. elegans* genomic sequence has revolutionized *C. elegans* biology. Together with genetic, developmental, and anatomical data, it also provides a powerful resource for research in other systems. Completion of the sequence will result in a tentative list of all the genes and a description of other sequence features that, in combination with information from other genomes, will surely advance our understanding of fundamental life processes in ways not yet foreseen. When all the gene products can be identified by their sequence, the challenge remains to relate this knowledge to the biology of the organism. At present, only about 10% of the genes in *C. elegans* have been identified by mutation ([Appendix 1; Johnsen and Baillie](#), this volume). Although methods for reverse genetics have been developed ([Plasterk and van Leunen](#), this volume), efficient methods analogous to the gene replacement technologies in yeast and mammalian cells will be required to utilize the enormous amount of information that is now available. Although coding sequences attract immediate interest, analysis of noncoding chromosomal sequences should contribute to the analysis of regulatory elements and to the identification of *cis*-acting elements of the meiotic and mitotic machinery, including sites necessary for proper segregation of chromosomes ([Albertson et al.](#), this volume).

## B. Gene Expression and Development

*Trans-splicing* of mRNA, first observed in *C. elegans* ([Krause and Hirsh 1987](#)) and later found in other nematodes, led to the discovery of operons ([Blumenthal and Steward](#), this volume). Unexpected aspects of mRNA processing have been described, but the significance of multigenic transcription units is yet to be understood. Now that operon sequences are available, the potential relationship of gene organization and structure to developmental expression can be addressed. Mechanisms for additional controls on translation and mRNA stability are being elucidated ([Anderson and Kimble](#), this volume). Although it is clear that maternally inherited mRNAs must be stored, then activated in specific patterns of expression observed within the early embryo, the full significance of translational regulation during development is not understood. At present, one can only guess at the complexity of this process.

The molecular analyses of genes affecting development have revealed much about the machinery of sex determination ([Meyer](#), this volume) and intercellular signal transduction ([Greenwald; Schedl; Schnabel and Priess; Antebi et al.; Riddle](#); all this volume) and revealed a multitude of transcription factors ([McGhee and Krause](#), this volume). The genes encoding transcription factors couple cell lineage cues and spatial patterning cues to the generation of cell type. A current challenge is to determine the relative importance of different signaling inputs and to understand how they are integrated. The task is to connect the individual examples of transcriptional control to the network of developmental events that impinge on each cell, and ultimately to the regulatory network that is the living animal. Similar signaling molecules and transcription factors have been found in *Drosophila* and in vertebrates. If they function in homologous processes, then it is possible that the downstream targets of these transcription factors may also be conserved. If so, analysis of the critical downstream developmental pathways will be much easier.

An important finding has been that many genes affecting the specification of cell fate function in lineages that are quite different from one another ([Emmons and Sternberg; Schnabel and Priess; Greenwald](#); all this volume). Comparison of these different effects offers the opportunity to study how the general mechanisms of cell fate determination interact with the lineage-specific, or tissue-specific, differentiation programs. Although cells of similar fate often come from similar lineages, there are notable exceptions ([Moerman and Fire](#), this volume).

Some differences between *C. elegans* and other models are notable. For example, the molecular mechanisms for sex determination and dosage compensation in *C. elegans* ([Meyer](#), this volume) seem to differ markedly from those in *Drosophila* or mammals, although the overall genetic strategies between *Caenorhabditis* and *Drosophila* are similar. A novel regulatory mechanism involved in temporal control of developmental processes has been

discovered by molecular analysis of the *lin-4* gene, which encodes a regulatory antisense RNA ([Ambros; Anderson and Kimble](#); both this volume). Although heterochronic mutants have been identified in other organisms, it is not yet known whether there are conserved pathways for control of biological timing. Finally, there are fundamental differences between *C. elegans* and *Drosophila* embryogenesis, yet some of the molecular components may be the same. Molecules that are similar in structure and function may be utilized in different ways.

Cell-cell interactions have been discovered that revise previous concepts about cell fate specification ([Schnabel and Priess](#), this volume) in the early embryo. Asymmetrically distributed factors that account for some differences between early blastomeres have also been identified ([Kemphues and Strome](#), this volume). The mode of action of these proteins should become clearer with identification of additional components of these systems and determination of the functional interactions between these components. The Genome Sequencing Project will speed these studies by eliminating the need for the initial cloning and sequencing steps that necessarily precede further molecular analysis.

The green fluorescent protein (GFP) reporter ([Chalfie et al. 1994](#)) is now widely used for analysis of the timing and tissue specificity of transcription in living transgenic animals. Whereas Nomarski DIC microscopy allows one to follow cell nuclei in development, the fluorescent protein should allow visualization of changes in cell size, shape, and position. For example, the paths of migrating cells or neuronal growth cones ([Antebi et al.](#), this volume) can now be documented in much more detail in wild-type and mutant strains. Furthermore, GFP expression provides a new tool for mutant screens.

Approaches to *C. elegans* cell biology have been limited by the inability to purify specific cell types. The lack of a *C. elegans* cell culture system is a notable absence in an otherwise impressive array of experimental tools. However, cell biology has had notable successes. For example, the ability to purify sperm from males has allowed a detailed description of sperm cell biology, including a novel mechanism for cell motility ([L'Hernault](#), this volume). The abundance and repetitive organization of muscle have allowed biochemical, ultrastructural, and immunochemical analyses that complement the genetic approaches ([Moerman and Fire](#), this volume). The genetic approach also has produced considerable information about the structure and function of the extracellular matrix, including the collagenous cuticle ([Kramer](#), this volume). Since the proteins that compose the extracellular matrix typically contain characteristic sequence motifs, the Genome Sequencing Project should identify most of the genes encoding matrix proteins. This will allow further characterization of the function of these components genetically.

## C. Neural Networks and Behavior

An organism so well suited for genetics and electron microscopy was originally thought unlikely to be advantageous for either cell biology or physiology, particularly with regard to the [nervous system](#). However, electrophysiological analysis of the homologous *Ascaris* [nervous system](#), together with genetic and ultrastructural data from *C. elegans*, is producing an integrated view of neurotransmission in nematodes ([Rand and Nonet](#), this volume). A neurophysiological approach to the neuromuscular control of pharyngeal pumping has characterized the circuitry and provided novel assays for mutant phenotypes ([Avery and Thomas](#), this volume).

An early approach to the analysis of synaptic transmission in *C. elegans* involved the selection of mutants resistant to neurotransmitter agonists or antagonists ([Brenner 1974](#)). Subsequent molecular analysis revealed that some of these genes encode synaptic proteins previously identified in vertebrates, whereas others were found to encode novel proteins, and the vertebrate homologs were discovered later ([Rand and Nonet](#), this volume). Hence, the process of synaptic transmission has been conserved, and metazoan models with tractable genetics provide unique information relevant to other animals. This is another case in which the Genome Sequencing Project will speed the identification of all the conserved components of the synaptic machinery.

A major step in the past decade has been the functional definition of [neural](#) circuits, using genetic, molecular, and cell ablation technologies. One lesson to emerge from the study of *C. elegans* behavior is the surprising

prevalence of redundancy or overlap between [neural](#) functions. Such redundancy is best revealed by cell ablation experiments ([Avery and Thomas; Bargmann and Mori](#); both this volume). In this sense, the *C. elegans* [nervous system](#) is no different from that of other animals. With only 302 [neurons](#), it was tempting to presume that each had an essential function, but this seems not to be true based on the existing behavioral assays. However, a closer look sometimes reveals more subtle adverse effects of cell loss, so that the apparent functional redundancy is not complete ([Avery and Thomas](#), this volume).

Because the [nervous system](#) is so well described, the roles of individual [neurons](#) in behavior can be defined despite functional overlaps. A current goal is to identify the molecules that function in sensory recognition and signaling (Bargmann and Mori; Driscoll and Kaplan; both this volume). Furthermore, the study of [neural](#) differentiation (the recognition of synaptic targets and the acquisition of chemical and behavioral specificity) has now become accessible at the organismal level by using molecular and cell ablation technologies. The problem of how sensory information is integrated can be addressed once individual behavioral circuits are characterized. Finally, the regulation of behavior over time has been demonstrated in *C. elegans*, but the mechanisms for this are not well understood ([Jorgensen and Rankin; Bargmann and Mori](#); both this volume). The possible complexity of learning and memory will only become known as *C. elegans* learning paradigms are better established. Once it is understood how behavioral changes result from morphological or physiological changes in a [neural](#) circuit, then those specific changes can be traced back to functions of gene products in individual cells. The nematode *Ascaris* possesses a diversity of neuropeptides with distinct patterns of cellular localization ([Cowden and Stretton 1995](#)). It seems likely that behavior will involve a complex interplay between peptide neurotransmitters and neuromodulators ([Rand and Nonet; Riddle](#); both this volume).

The developmental and behavioral strategies employed by *C. elegans* are now emerging to provide a portrait of the animal as an integrated network of molecular functions. The portrait remains incomplete, and many parts lack clear outline or detail, but the way seems open to complete the portrait with ultimate resolution.

Generated from local HTML

## **Chapter 1. Introduction to *C. elegans* — Acknowledgments**

---

We thank the National Center for Research Resources for its consistent, highly valued support of *C. elegans* resources, J. Hodgkin for helpful comments, L. Hatley for processing the manuscript, and the staff and scientists at Cold Spring Harbor Laboratory for their gracious hospitality during Don Riddle's stay.

Generated from local HTML

# **Chapter 2. The Genome**

---

## **Contents**

[I General Properties](#)

[II The Physical Map](#)

[III Genetics, Genes, and the Physical Map](#)

[IV Genome Sequencing](#)

[V EST Sequencing](#)

[VI Interpretation of the Sequence](#)

[VII Tentative Conclusions](#)

[VIII Prospects](#)

[Acknowledgments](#)

Generated from local HTML

## Chapter 2. The Genome — I General Properties

---

Our knowledge of the *Caenorhabditis elegans* genome has increased substantially since the publication of the 1988 *C. elegans* book ([Emmons 1988](#)); even the genome size has changed from an estimated  $80 \times 10^6$  base pairs to  $100 \times 10^6$  base pairs. Systematic study of the genome in the intervening years has seen the construction of a nearly complete physical map and the release of more than half the assembled sequence. Yet it is an awkward time to be writing about the genome, since our view of the genome is changing rapidly (~2 Mb of newly assembled sequence is being released per month), and as yet most of the sequence has been obtained from the gene-rich regions of the genome, with very little from the gene-poor autosomal arms. As a result, analysis of the overall sequence remains frustratingly anecdotal. Nevertheless, much has been learned, and this chapter will attempt to summarize our current understanding of the *C. elegans* genome.

The genome is the physical basis for genetics and includes both nuclear and cytoplasmic DNAs. For *C. elegans*, the mitochondrial genome (13,794 bp) has been fully sequenced ([Okimoto et al. 1992](#)). The nuclear genome contains approximately  $100 \times 10^6$  base pairs, organized into six chromosomes ranging in size from  $14 \times 10^6$  to  $22 \times 10^6$  base pairs ([Coulson et al. 1991](#)), which is approximately 20 times the size of *Escherichia coli* (the underestimate of the *E. coli* genome size, used as a standard, led to the underestimate of the *C. elegans* genome size by reassociation kinetics) and about 1/30 the size of the human genome. Most of the sequence is unique, with only 17% assigned to the repetitive class by reassociation kinetics (Sulston and [Brenner 1974](#)). The genome is on average 36% GC (Sulston and [Brenner 1974](#)). Although coding sequences are clearly higher in GC content and noncoding sequences are higher in AT content, surprisingly little variation in content exists over larger regions as determined first by isopycnic banding of genomic DNA and confirmed more recently by sequencing ([Brenner and Sulston 1974; Wilson et al. 1994](#) and unpubl.). The exception to this is the ribosomal gene cluster containing about 70–100 copies of the genes for 18S and 28S rRNAs: it is 51% GC ([Ellis et al. 1986](#)). No methylated bases have been detected, despite the use of methods capable of detecting 1 methylcytosine in 10,000 cytosine residues ([Simpson et al. 1986](#)).

Generated from local HTML

## Chapter 2. The Genome — II The Physical Map

---

The construction of the clonal physical map of the *C. elegans* genome began in response to the need for an efficient means to recover DNA segments corresponding to genes defined through mutation. Of the various methods available in the early 1980s, the most powerful and broadly applicable approach was one that has become known as positional cloning. Meiotic mapping is used in this method to position a gene between markers which are available as cloned DNA. Recovery of the DNA between these markers assures that a clone for the gene of interest is in hand. DNA transformation or other means can then be used to identify precisely on which segment the gene lies.

To assist in this process and to avoid unnecessary duplication, the community of *C. elegans* workers joined together at an early stage to generate a clone-based physical map of the entire genome, which would be progressively correlated with the genetic map. Two central laboratories took on the task of establishing the relationship of random clones with respect to one another, and the larger community associated specific genes and markers with the growing map. This has resulted in a map that spans more than 99% of the genes, with only seven gaps at present ([Fig. 1](#)).

The map consists of mostly overlapping bacterial cosmid clones and yeast artificial chromosome (YAC) clones ([Fig. 2](#)). The overlaps of the cosmid clones were established through a fingerprinting technique that relies on shared restriction fragments to determine the extent of overlap between randomly selected clones ([Coulson et al. 1986](#)). Analysis of the restriction fragment information and assembly was aided significantly by computer programs, but human validation of each proposed new overlap was critical, especially in the early phases, in preventing misassemblies. Biases in the representation of the genome in the bacterially based cosmid clones, however, severely compromised the level of continuity achieved; after the analysis of more than 17,000 clones, the genome remained in some 700 contigs (80 contigs would be expected from a truly random library).

The representation of the genome in YACs is more complete. This, combined with their larger size (average insert size in the initial sets was ~250 kb), allowed these clones to bridge many of the gaps between the cosmid contigs ([Coulson et al. 1988](#)). Hybridization of the YACs to grids of cosmid clones representing the mapped contigs and singlets, as well as hybridization of selected cosmids to grids of random YAC clones, was used to establish the overlaps between the clone sets, which brought down the contig number to just over 100.

Finally, a more laborious effort was undertaken to establish overlaps directly between YACs in those cases where gaps were not spanned by single YACs ([Coulson et al. 1991](#)). For this purpose, sequence was obtained from the insert end and used to develop a polymerase chain reaction (PCR) assay for the site, both to make a probe to hybridize against the YAC set and to verify any potential overlaps. A complementary approach involved the construction of additional YAC libraries, including the use of alternative enzymes in the partial digestion of the genomic DNA and the selection of larger inserts (average insert size >700 kb).

Telomeres in *C. elegans* consist of the repeated hexamer sequence TTAGGC ([Wicky et al. 1996](#)). These sequences are also present internally on the chromosomes, along the chromosome arms, complicating the identification of clones derived from the telomeres. Bal31 digestion experiments show that there are 4–9 kb of the repeat at the ends of chromosomes. Using a combination of Bal31 digestion and restriction digests yielding staggered ends on large DNA, [Wicky et al. \(1996\)](#) have obtained candidate clones for 11 of the 12 telomeres. These clones will be linked to clones on the current map to provide end markers.

Representative YAC clones have been selected across the entire map, arrayed in map order on nylon membranes and distributed to the community as the so-called polytene filters ([Coulson et al. 1991](#)). Using this grid, any cloned sequence can be localized on average to a 100-kb interval. Cosmids from the region can then be used to derive finer positioning.

Despite the small size of the *C. elegans* chromosomes, cytogenetics has played an invaluable part throughout the mapping project to position sequences onto chromosomes and to confirm the physical map order by *in situ* hybridization ([Albertson 1985](#)). The resolution of the method is limited, but the results clearly confirm the overall

physical map order (Fig. 3) (Coulson 1994). From comparisons of the clonal map and cytogenetic map distances between markers, it is also clear that the *C. elegans* chromosomes are not uniformly condensed. This is particularly true near the right (lower) end of chromosome I, where the *in situ* distance between markers is much greater than the physical map suggests. Unfortunately, this region includes one of the seven remaining gaps in the physical map, and thus a more definitive statement cannot be made. Nevertheless, fluorescent staining of the region does appear under the microscope to be attenuated, as if the region is stretched out (D. Albertson, pers. comm.).

Work from a large number of laboratories has led to an increasingly refined correlation between the genetic and physical maps. Cloned genes provided most of the early markers, and laboratories often shared the clones with the central laboratories at early stages in investigations. In addition, restriction fragment length polymorphisms (RFLPs) between the standard laboratory strain of *C. elegans* (var. Bristol) and other cross-fertile strains have played an increasingly important part. These RFLPs can often be identified at a frequency of one per cosmid or better, providing very tight mapping resolution where necessary. One of the most useful sources of such polymorphisms is the transposable element Tc1 of the Tc1-mariner class. The Bristol strain has about 30 copies of the element, whereas others have more than 500, distributed widely throughout the entire genome (Plasterk and van Leunen, this volume). Many of these elements have been cloned and positioned on both the meiotic and physical maps. An increasing number have been used to generate sequence tagged sites, which provide mapping tools for PCR-based mapping strategies (Williams et al. 1992; R. Plasterk and A. Coulson, pers. comm.).

The result has been a true genome map. With the substantial amounts of various data available, the need for a convenient database for entering and viewing all the relationships became critical. The need has been met by ACeDB (R. Durbin and J. Thierry-Mieg, pers. comm.), which offers interactive displays of the genetic and physical maps plus the underlying information, including genetic data, genomic and cDNA sequences, and much else besides (for examples, see Figs. 2 and 6).

## Figures



### Figure 1

The *C. elegans* genome. The contigs that make up the six chromosomes are represented by blocks, with the remaining seven gaps indicated. The progress in genome sequencing is indicated. The scale to the left of each chromosome is in millions of base pairs (Mb).



### Figure 2

A detail of the physical map. This representation taken from an ACeDB screen shows, from the top of the figure, the positions of (1) cDNAs, determined by hybridization against YACs representing the genome (the "polytene"YAC grid); (2) YACs, determined by hybridization to selected cosmids; and (3) cosmids, whose overlap was established by fingerprint analysis. The discontinuous bar beneath the cosmids indicates the extent of available genomic sequence. The bar across the window provides rapid access within ACeDB to the same position on the genetic map. Below this bar are shown the positions of defined genes, along with various remarks relating to the assembly of the map. At the bottom is an overview of the region of chromosome III in which the above map lies. The extent covered is represented by the solid rectangle. The YAC and cosmid clones shown with heavy lines are those clones selected for either the YAC "polytene"grid or the cosmid grid. Cosmids marked with an asterisk indicate the presence of additional analyzed clones not shown on this view.

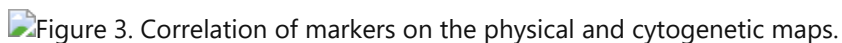


### Figure 3

Correlation of markers on the physical and cytogenetic maps. Small boxes show the physical map location of probes, and bars show the *in situ* signal localization on the right. The scales at the left represent the percentage of chromosome length (*in situ*) and megabases (physical map). (Reprinted, with permission, from [Coulson 1994](#).)

Generated from local HTML

## Chapter 2. The Genome — III Genetics, Genes, and the Physical Map

---

The availability of the genome map has allowed investigation of issues such as the rates of recombination per physical distance and gene density across chromosomes.

Brenner's early studies of the genetic map ([Brenner 1974](#)) showed that mutationally defined genes were tightly clustered near the centers of the autosomes, with about 80–90% of the genes lying in approximately 5 cM of each ~50-cM autosome ([Fig. 4](#)). Genes on the X appeared to be more uniformly distributed. Once the genome map was developed, it was clear that this recombinational clustering on the autosomes resulted both from higher recombination frequencies per physical distance on the arms (and lower rates in the clusters) and from differences in gene density per physical map distance ([Greenwald et al. 1987; Barnes 1991; Waterston et al. 1992](#)).

[Barnes et al. \(1995\)](#) have now systematically reviewed the data. Within the autosomal clusters, recombination frequencies are approximately 1 cM/1500 kb of DNA, with variations of less than a factor of two between different clusters. The physical sizes of the autosomal clusters are also similar (~7 Mb). Recombination frequencies on the arms are sharply higher than in the clusters, and they vary considerably between chromosomes and arms, ranging from 1 cM/50 kb on the right arm of chromosome IV, to 1 cM/100 kb on the left arm of chromosome I, to 1 cM/300 kb on the left arm of chromosome V. The physical size of the chromosomal arms varies as well, with longer arms having lower and shorter arms having higher recombination frequencies, thus maintaining similar genetic distances across arms.

Gene density, as measured by the number of cDNAs hybridizing to YACs within physical map intervals, varies by a factor of more than two between chromosome clusters and their arms, again with a relatively sharp boundary ([Fig. 5](#)). The largest chromosomes have lower gene densities by this measure. This led to the surprising conclusion that each of the autosomes has approximately the same number of genes, regardless of size (from 13 Mb for chromosome I to 21 Mb for chromosome V).

The X chromosome in contrast has more uniform distributions of both recombination and genes as judged from cDNA distribution. The cDNA density of the central X is only about 70% that of the autosomal clusters. Recombination frequencies in the central regions differ by no more than a factor of four from the peripheral portions, and gene density on the arms is about 65% that of the central region. Overall, the X chromosome appears to have as many genes as any of the autosomes.

Several repetitive elements have been characterized through molecular cloning ([Felsenstein and Emmons 1987; Naclerio et al. 1992; Cangiano and La Volpe 1993](#)), and the chromosomal distribution of seven such classes has been determined, using the YAC representation of the genome. Five of these classes were distributed in both clusters and arms, but two classes (CeRep3 and RcS5) were distributed preferentially outside the clusters. In particular, CeRep3 is found almost exclusively in the arms and not in the clusters of the autosomes ([Barnes et al. 1995](#)), but it is more uniformly distributed on the X.

### Figures

Figure 4. Correlation of markers on the physical and genetic maps for chromosome IV.

### Figure 4

Correlation of markers on the physical and genetic maps for chromosome IV. The positions of markers (*right*) are indicated on the physical (*center*) and genetic (*left*) maps. The scales on the left indicate the percentage of physical map length and centimorgans on the genetic map. (Reprinted, with permission, from [Coulson 1994](#).)

Figure 5. Variation of gene density along the chromosome.

### Figure 5

Variation of gene density along the chromosome. (Reprinted, with permission, from [Barnes et al. 1995](#).) The density of hybridizing cDNAs is plotted against chromosomal position for the second chromosome (*open boxes*).

Recombination frequencies across the chromosome of the left end are also indicated (*closed boxes*). The limits of the central gene clusters are shown by the vertical lines as determined by recombination. The positions of CeRep3 are also shown along the x-axis (*closed diamonds*). For other chromosomes and additional details, see [Barnes et al. \(1995\)](#).

Generated from local HTML

## Chapter 2. The Genome — IV Genome Sequencing

---

With a nearly complete clonal physical map available in 1989, systematic sequencing of the genome was an obvious next step. However, the resources required for such an effort were considerable and the available technology was inadequate. Fortunately, the *C. elegans* genome was included in the list of genomes whose analysis was considered important for the interpretation of the human sequence and for the development and testing of technology to accomplish this much larger task. In 1990, with funding from the Medical Research Council in England and the National Center for Human Genome Research in the United States, the two core laboratories that had been involved in the physical mapping began the sequencing effort. The laboratories have grown in efficiency with the development of improved technologies and increased scale during the past 5 years, so that presently more than 45 Mb of sequence has been completed and another 25 Mb is available in an assembled, but not yet completed, state ([Sulston et al. 1992](#); [Waterston et al. 1994](#); [Wilson et al. 1994](#)). Current throughput of the combined laboratories exceeds 2 Mb of completed sequence per month, and the project is on target for completion in 1998 (see [Fig. 1](#)).

The current program is based mainly on the mapped cosmids, because they provide a cost-effective way to proceed in an orderly fashion through the genome. Fingerprint information allows a reasonable choice of minimally overlapping clones through each of the approximately 520 cosmid contigs. Given the importance of genes, the decision was made to focus the initial effort on the gene-rich, central portions of the autosomes and the whole of the X (see [Fig. 1](#)). Fortunately, cosmid coverage was high over these regions.

The basic sequencing strategy involves two distinct phases. In the first phase, random subclones are generated from each selected cosmid and sequenced in a highly efficient, mechanized process (the "shotgun" phase). Currently, a successful sequencing tract (or read) from each subclone yields on average about 400 bases of high quality data, and a total of approximately 600 good tracts are collected for each cosmid, to produce an initial coverage of sixfold redundancy per cosmid. With the present methods, about 1 week of a junior technician's time is required to produce the data required for one cosmid. The random reads are assembled automatically with the program phrap (P. Green and L. Hillier, pers. comm.) or other assembly algorithms to produce not only the bulk of the final sequence, but also a map of all the sequenced subclones. Although generally accurate (>99% correct), the assembled sequence often still contains gaps (amounting to no more than 5% of the final sequence). In addition, there are regions where sequence is available on only one strand (and thus of lower average accuracy), and there are regions where compressions or other problems yield ambiguous sequence. Occasionally, assembly errors occur as well. Nevertheless, the community has found it useful to have access to the data at this early stage via an ftp site and the World Wide Web (WWW).

To achieve full continuity and high accuracy (estimated at 99.99% by comparison to preexisting *C. elegans* sequences in the databases), each cosmid project is subjected in the second stage of the process to human review. At this point, discrepancies between different sequence reads of the same region are resolved, and additional sequence reads are obtained in a directed manner to close gaps and to recover sequence from both strands in all regions. The mapped subclones produced by the assembly step are critical for this stage, as each subclone has an insert size about four to five times the initial sequence read length. Thus, in most cases, subclones are available that contain the missing sequence on the needed strand. Alternative chemistries are used to resolve compressions, as a substitute for the second-strand sequence and other problems. For regions where subcloned DNA is not available, custom oligonucleotides and PCR are usually sufficient to recover the desired DNA.

The sequence of the regions represented in cosmids (~60–65 Mb in the central autosomal clusters and X; 80 Mb total) is expected to be complete by early 1997. This should contain the large majority of coding and regulatory sequences (see below). The remaining 20% or so is presently represented only in YACs. Much of this sequence is probably represented in  $\lambda$  clones grown on severely recombination-deficient hosts, as determined by several regional studies. The small insert size of  $\lambda$  clones, however, combined with the difficulty of growing them on the debilitated hosts, makes them unattractive alternatives for sequencing. Another possibility is provided by newer vectors, maintained in single copy through the use of either [P1](#) or [F](#) origins. Preliminary evidence suggests that

some of the DNA missing from cosmid libraries might be recoverable in fosmid libraries, a vector system combining the *E* origin with the  $\lambda$  packaging sites (S. Chissoe et al., pers. comm.).

Completion of the genome sequence, however, will most likely depend on sequencing subclones prepared directly from YACs ([Vaudin et al. 1995](#)). The expectation is that most of the sequence will be recoverable in small clones and that map information can be used to orient the assembled contigs relative to one another, even if some segments cannot be cloned in *E. coli*. The principal technical difficulty is the unavoidable contamination of purified YACs with substantial amounts of yeast DNA, leading to wasted effort and additional complexities in finishing. However, with the completion of the yeast genomic sequence in early 1996, this latter problem can be dealt with effectively, since it is feasible to recognize sequence reads from yeast and discard them.

Generated from local HTML

## Chapter 2. The Genome — V EST Sequencing

---

Although the sequence of all the genes would be expected to come from the genome sequencing project, this project was obviously going to take several years to complete. To get an early look into the genes of *C. elegans*, several projects have been undertaken to obtain end sequences from cDNA clones. Such partial sequences, or expressed sequence tags (ESTs), can provide quick insight into a useful fraction of genes prior to genomic sequencing. The sequences are often invaluable aids in the interpretation of the genomic sequence, once obtained.

By far, the largest project undertaken is that of Yuji Kohara (pers. comm.). The project has used as starting material size-selected, poly(A)<sup>+</sup> RNA from total worms, and the resultant cDNA has been directionally cloned into a λ vector. More than 30,000 different clones were picked, and sequencing of clones begun. Repeated sequencing of abundantly represented clones has been minimized by periodically identifying and avoiding such clones in the full set by hybridization to the arrayed clones with pools of multiply represented clones. Both 5' and 3' ends have been sequenced from most clones. At present, there are 18,755 sequences from 11,852 clones, representing more than 3500 different genes. About half of these have significant database matches, providing clues as to their likely function in *C. elegans*. In the set, there are clear examples of alternative splicing (89 cases) and alternative poly(A)-addition sites (71 pairs). Of these ESTs, 1412 have been positioned on the genome map by hybridization of clones to the polytene YAC grid of the genome (>99% of these clones are represented in the currently mapped set of YACs). Placement of additional clones is now being done "in silico" by searching against the genomic sequence for matches. Clones are available to investigators by request.

Other earlier projects were much smaller in scale. In one such study, 5'-end sequences were obtained using a selected set of approximately 1500 cDNAs derived by an iterative procedure that used pools of previously picked clones as hybridization probes to avoid repicking clones with the same sequence ([Waterston et al. 1992](#)). Cluster analysis showed that these ESTs represented 1152 nonoverlapping sequences, but because only 5'-end sequences were obtained, there was no assurance that these represented that many different genes. Most of the corresponding 1152 clones were positioned on the YAC grids, and they remain available upon request. Another contemporaneous study generated 720 ESTs from 585 random clones from an unselected library, the inserts of which were not oriented ([McCombie et al. 1992](#)). Sequence from only one end was obtained from most clones. Although little map information was obtained initially, these sequences are also being positioned "in silico" and act as useful aids in sequence interpretation.

Generated from local HTML

## Chapter 2. The Genome — VI Interpretation of the Sequence

---

Discovering the meaning of the sequence is obviously the ultimate motivation behind the sequencing effort. This will undoubtedly require years of study involving many investigators in many disciplines. However, some aspects of function, particularly coding sequence, can be deciphered now, just from the sequence itself. For this purpose, each completed sequence is subjected to a variety of analyses, and the resulting data are collated within ACeDB and reviewed interactively before the annotated sequence is submitted to GenBank or EMBL databases ([Fig. 6](#)). These analyses include homology searches using BLAST and several other tools against various databases and direct analysis of the signals within the sequence using the program GENEFINDER. The latter takes advantage of biases in coding sequence versus noncoding sequence, in splice site signals, in initiator methionine signals, and in termination codons to identify likely exons (using a log-likelihood approach). It then uses a dynamic programming algorithm to combine the predicted exons into genes. Although generally reliable and more successful than similar programs used in more complex genomes, GENEFINDER is not infallible, nor can it predict alternatively spliced transcripts.

The GENEFINDER interpretations are often buttressed by the other information. Similarity segments not only provide insight into the function of the predicted gene, but also help in assembling the gene. As described above, systematic end sequencing of selected cDNAs has so far sampled more than 3500 different genes, or approximately one quarter of the total number of genes. These sequences now often confirm predicted splice patterns or suggest alternatives, and they are critical in interpreting unusual features such as alternative splicing and in establishing where genes begin and end, a task with which GENEFINDER has particular difficulties. Neither similarity nor cDNA information is used within GENEFINDER, but both are taken into account in the interactive review.

Other sequence features are also noted. Candidate tRNA genes are found using the program tRNAscan ([Fichant and Burks 1991](#)); the resultant set is filtered through the use of hidden Markov models (HMMs), which, although computationally intensive, help to distinguish genes from pseudogenes. Sequences that are repeated either locally or more globally are recognized through various algorithms. The locally repeated sequences are categorized as either tandem, direct, or inverted repeats. Repeat sequence families can also be identified. The first of the repeat families were identified through hybridization ([Felsenstein and Emmons 1987; Ciaramella et al. 1988](#)), but computer searches using HMMs and other tools have revealed a great variety of repeat families (see below). As computational tools improve, additional annotation is added.

## Figures

Figure 6. Sequence features in ACeDB.

### Figure 6

Sequence features in ACeDB. The columns from left to right represent (1) the cosmid, (2) the scale bar (yellow), (3) predicted genes indicated as open rectangles (exons) connected by lines (introns), (4) repeat families matches, (5–7) protein homologies from the public databases in each of three reading frames (blue), (8) matches with *C. elegans* ESTs (yellow), (9) nucleotide matches to a *Caenorhabditis briggsae* cosmid in which synteny is conserved (red), (10) local inverted repeats, (11) matches of the translated sequences to the *C. briggsae* cosmid (purple), and (12) gene names and comments. The matches to the several ESTs on the bottom gene confirm the gene prediction, and the conservation of the exon sequences between species in the upper gene confirms the gene predictions here. The conservation of additional sequences in the regions between the two genes and above the top gene suggests that these sequences are also functionally important.

## Chapter 2. The Genome — VII Tentative Conclusions

---

Sufficient data are now available from genomic sequencing and other sources to provide some insight into the arrangement of sequence in the genome as a whole, although unfortunately at this time little sequence is available from the autosome arms. This section deals with some of the major conclusions so far.

### A. Gene Number and Distribution

The reasonable reliability of the GENEFINDER predictions combined with the end sequencing of cDNAs has allowed an estimate to be made of the total protein-coding gene number. The ratio of predicted genes to cDNA sequences exactly matching them should be equal to the ratio of the total number of genes to total cDNAs; current data predict a total in the region of 14,000 genes. This number is much higher than expected, based on the estimations of 2000 to 4000 essential genes through genetic studies ([Brenner 1974](#); [Meneely and Herman 1979](#); [Sigurdson et al. 1984](#)). Presumably, this discrepancy means that a large number of *C. elegans* genes are dispensable, either because of redundancy or because under conditions tested, the loss of gene function does not result in a detectable mutant phenotype. A similar discrepancy between gene number revealed by sequence and essential gene number determined by genetics has been found for yeast, and it seems likely to be a general feature of eukaryotic genomes.

The accuracy of this gene number prediction is limited by several factors beyond random sampling errors. For example, the signals defining the ends of genes are at present poorly understood, leading at times to the probable fusion of genes in operons or in other sites where genes are closely spaced. In other areas where exons are more distantly spaced, a single gene may be split in two. These effects tend to balance each other, but if overprediction predominates, an exaggerated estimate of gene number will result. The calculation of total gene number also makes the assumption that gene expression levels are not biased by location, an assumption that seems likely to be true for regions of the genome with similar organization, i.e., the central gene-rich clusters. Whether this assumption holds true genome-wide seems increasingly unlikely.

These assumptions have come under increasing scrutiny as sequence has become available outside the autosomal gene clusters. At least two differences are apparent in preliminary analyses of available data. The density of predicted genes on the X chromosome in the regions sequenced to date is only 1 per 6.2 kb, with 20% of the total sequence coding, as compared to 1 per 4.6 kb, with 31% coding in the clusters of chromosomes II and III. The average predicted message length is about 13% smaller on the X than on the autosomes, whereas introns and intergenic regions are larger (40% and 60% greater, respectively). Another difference is that on the X chromosome, the fraction of genes that match a cDNA tag is lower than for the autosomal clusters (23% vs. 35%). Together, the difference in predicted gene density and the smaller fraction matching an EST approximately account for the difference in gene density observed with EST hybridization data for chromosome II and III clusters versus the X overall ([Barnes et al. 1995](#)).

Part of the difference between the autosomes and the X in the fraction of predicted genes matching a cDNA tag could result from overprediction of genes on the X. The lower coding density and larger introns could contribute to an artificial division of some genes with a correspondingly higher false-positive prediction rate on the X, as suggested by the shorter predicted message length on the X.

The remaining difference may reflect a lower average level of gene expression on the X. Dosage compensation, in which gene expression on the X is reduced in hermaphrodites ([Villeneuve and Meyer 1990b](#)), provides one plausible explanation as to why this might be so. Alternatively, the postulated difference in gene expression might reflect some other feature of chromosome structure or organization, such as those reflected in the distribution and density of certain repeated sequences and in the frequencies of recombination per unit of physical distance. Sequence from the autosome arms will provide additional comparisons between these parameters.

Whatever the explanation for the lower density of genes on the X and their lower match rate with ESTs, the practical effect at the moment is that predicted gene number has been rising as more sequence from the X is

incorporated into the total.

Coding density through the gene clusters is fairly uniform at the sequence level and does not show the local fluctuations in gene density observed in the analysis of the EST map data ([Barnes et al. 1995](#)). However, those fluctuations probably represent simply a combination of statistical and experimental artifacts, resulting from the relatively few cDNAs positioned and the uncertainties inherent in positioning YACs by hybridization data. A reduced coding density is evident in a small contig near the end of III (20% exonic in this 300-kb region as compared to 32% for III overall) and at the left end of the sequenced region on II, as would be expected from the cDNA hybridization data ([Waterston et al. 1992](#); [Barnes et al. 1995](#)). More data will be required for a more detailed comparison, but perhaps differences in gene expression levels will be a factor on the autosomal arms and on the X.

## B. tRNA Genes

More than 240 tRNA genes have been predicted in the first 27 Mb sequenced in the genome project, for an average of about ten genes per megabase (S. Eddy and T. Lowe, pers. comm.). No data comparable to the EST matches exist to predict how many tRNA genes there will be in the total genome. However, if tRNA genes have a distribution similar to that of the protein-coding genes, the genome would be expected to contain about 700–800 tRNA genes, far more than the 300 expected from filter hybridization experiments (Sulston and [Brenner 1974](#)). This could reflect an overprediction of tRNA genes or more likely an underprediction by the hybridization methods.

tRNA genes for all 20 amino acids are represented. The tRNA gene copy number approximately correlates with the known codon bias, but full analysis must await the complete sequence. The tRNA genes often occur singly, but small clusters have been seen, with one cosmid having nine candidate tRNA genes and three cosmids having six. A few tRNA genes have been observed in the introns of protein-coding genes, on either strand relative to the protein coding strand. About 5% of the genes are interrupted by introns.

## C. Repetitive DNA

Although little of the sequence is from the autosomal arms that are probably enriched in repetitive sequences, the central clusters of the autosomes and the X chromosome present the full spectrum of repetitive DNA typical of eukaryotes, including simple sequence, tandem, direct, inverted, and dispersed repeats. In the first 2.2 Mb of sequence, for example, more than 5% of the DNA was classified as repetitive.

Mononucleotide runs have been evaluated over the available portions of chromosomes II (3.12 Mb) and III (3.76 Mb) and the X (5.76 Mb) chromosomes (L. Hillier and R. Waterston, unpubl.; S. Jones and M. Berks, pers. comm.). The frequency of such runs by chance alone is determined by base composition. Overall, the GC content is quite constant (34–38% is the full range found in samples of up to 300 kb over regions of II, III, and X) and quite close to the fraction measured for the genome as a whole (36%). This contrasts with mammalian DNA, where large regional differences are found. Local variation does occur, however, with exons having a higher GC content than introns and intergenic regions.

The distribution of A and T run lengths does indeed follow a negative log linear plot, suggesting that their occurrence is largely explicable by chance alone. The slope of the line, however, would predict a higher effective AT content than is seen on average. This could reflect the local inhomogeneities in base composition discussed above, but we cannot rule out other contributing mechanisms.

In contrast, the distribution of G and C run lengths is distinctly different from that expected by chance. Although the number of runs of eight nucleotides is not far different from that predicted, on the basis of sequence composition, the number of longer runs does not decrease, but actually increases in runs with lengths between 11 and 16. (With an average composition of 36% GC, the probability by chance alone of a run of 11 bases or longer is less than one in the whole *C. elegans* genome.) Not until runs of 20 or greater are reached does the frequency fall off sharply.

The G and C runs are also more frequent on the X than on the autosomes (about threefold higher overall), although the distribution of run lengths is similar on all three chromosomes. The density of runs does vary along the length of the chromosomes, particularly on the autosomes, where the frequency increases on the edges of the gene-rich clusters. The strong deviation from random and the differential distribution between and along chromosomes strongly suggest that there may be a biological role for these runs. The prevalence on X might possibly reflect a role in dosage compensation. However, as pointed out previously, the X chromosome also differs from the autosomal gene clusters (and autosomal arms) in other significant ways, including recombination frequency and repeat distribution. It may be that the G and C runs are correlated with one of these, and the hint of increased frequency of G and C runs at the edges of the autosomal clusters is at present suggestive of this alternative correlation.

The nematode genome also appears to be rich in inverted repeats, in which a segment of genomic sequence lies within a few hundred bases of an inverted copy of itself. In the first 2.2 Mb of sequence, inverted repeats accounted for more than 2.5% of the sequence, with an inverted repeat found on average every 5.5 kb ([Wilson et al. 1994](#)). Most were quite small, with an average segment length of 70 bp and an average loop size of 164 bp. Occasionally, much larger segments (>1 kb) are found with complete or nearly complete identity. A high proportion of these inverted repeats fall in introns (43%), which represent only 20–25% of the sequence. Many of the inverted repeats fall into families and may be remnants of mobile elements (see below).

Tandem repeats, in which a segment of genomic sequence lies adjacent to one or more copies of itself, accounted for 1.5% of the sequence and occurred on average every 10 kb in the first 2.2 Mb ([Wilson et al. 1994](#)). Most of these were small, with an average segment length of 17 bp and an average copy number of 14. In contrast to inverted repeats, only 17% of these fell in introns, 20% fell in exons, and 63% fell between genes. Only triplet repeats, which formed the most common category of tandem repeat, were found in exons with any frequency. Large and complicated tandem repeats have been found, e.g., approximately 100 copies of a 200-base segment.

In addition to local repeats, many dispersed families of sequences appear to share a common consensus and are therefore probably duplicated and diverged from common ancestral sequences. In a few cases, these turn out to be examples of transposons. In addition to examples of known Tc transposons, the genome sequence has revealed examples of mariner-type transposons distantly related to Tc elements, two families of non-LTR (long terminal repeat) transposons and one example of a gypsy-class LTR retrotransposon. Most or all of these elements are probably inactive, or they would have revealed themselves as insertional mutagens.

Most dispersed repetitive elements are small (50–150 bp or so), and their function (if any) and the mechanism of their propagation are unclear. In addition to the families of elements previously identified through hybridization ([Felsenstein and Emmons 1988](#); [Naclerio et al. 1992](#)), new families are being systematically identified and classified by computer methods (R. Durbin; S. Lewis and S. Eddy; P. Agarwal and D. States; all unpubl.). *C. elegans* does not have any sequence as striking as the human *Alu* family, which makes up more than 10% of the human genome. The most numerous *C. elegans* interspersed repeat family, repA, has about a 98-bp core consensus, occurs in probably about 10,000 full-length and fragmentary copies, and accounts for 0.7% of the genome. Sixteen other dispersed repeat families have been identified and are routinely annotated in ACeDB. This number, however, is increasing, with 14 more likely to be added in the near future. In some cases, these dispersed families have short terminal inverted repeats similar or identical to the Tc2 or Tc3 terminal inverted repeats ([Plasterk and van Leunen](#), this volume); it seems plausible that these families are “hitchhikers,” mobilized in trans by Tc transposases.

In addition to these short dispersed repeats, larger segments are repeated at great distances, with up to 98% similarity ([Wilson et al. 1994](#)). These apparent duplications can have a complex structure wherein segments from regions are repeated in a second location, but with different spacings and orientations. Some involve coding regions and could represent exon shuffling; more likely, one copy probably represents a nontranscribed copy.

## D. Homologies

Overall, approximately 48% of the 6157 predicted genes in the region sequenced to date have significant similarities to genes previously characterized in other organisms. These similarities have often suggested a function for those predicted genes and have been used to find candidate genes associated with certain mutants. In turn, scientists working on genes in other organisms are turning to *C. elegans* to learn more about their genes. An illustration of the potential of the latter approach is the fact that more than half of all positionally cloned human disease genes have similarities to *C. elegans* genes, and in some cases, the *C. elegans* gene is the only similar gene in all of the public databases.

With so many genes now found in the finished sequence (an estimated 50% of all *C. elegans* genes), it is not surprising that many of the predicted genes fall into gene families ([Table 1](#)), with the largest family being the G-protein-coupled receptors and the protein kinases. Some quite large families which had been classified originally as "*C. elegans*-specific," based on lack of similarity to any known proteins, have recently been reclassified as probably G-protein-coupled receptors. Alignment and comparison of the sequences along with those from other organisms can help show which residues are important in protein function. The predominance of regulatory proteins ("G-protein-coupled receptors," kinases, GTPase, homeobox proteins) in the list provides a glimpse of the complexity of regulatory phenomena in a metazoan.

Why do half of *C. elegans* genes not find similar sequences in other organisms? The facile answer is, of course, that the similar gene from other organisms has not yet been sequenced. But this appears unlikely. [Green et al. \(1993\)](#) used statistical methods to examine the question in detail, when the first nematode genome and EST data were becoming available, along with similar systematically obtained data from yeast, *E. coli*, and humans. The clear prediction from that analysis was that even with their full sequences known, organisms in different phyla would show significant similarities for only about half their genes, using the programs and criteria delineated in the study. This result was reaffirmed when the analysis was repeated with additional data (P. Green, pers. comm.).

Although one could postulate that these genes have arisen *de novo*, the more probable explanation is that they have simply diverged too far to allow recognition of their ancestral relationships. One means of establishing these relationships is to find a homologous gene from more closely related species within the same phylum and use these to predict the ancestral gene, which in turn can be used to look more powerfully for related genes in other phyla. These ancestral genes can be found in *C. elegans* itself in the case of families of genes without known similarities, alluded to above. Indeed, in one instance, it has proven possible to identify a mammalian relative for what had been a nematode-specific gene family. Other examples will undoubtedly follow. To what extent the function of such divergent genes has been conserved is unclear, but even conservation of general function may be useful in understanding how genotype leads to phenotype.

## Tables

**Table 1**The current "top ten" protein families in the nematode

G-protein-coupled receptors	179
Protein kinases	169
Collagens	97
C4 zinc finger (nuclear hormone receptor) proteins	54
GTPase superfamily (Ras, G proteins, EF-Tu)	52
Homeobox proteins	45
RNA recognition motif (RNA-binding) proteins	43
Short-chain dehydrogenases (ADH-like)	34
Tyrosine protein phosphatases	33
ABC transporters	32

Based on computational analysis of 7299 predicted genes (Wormpep release 11). The numbers are preliminary and should be considered illustrative, not definitive.

Generated from local HTML

## Chapter 2. The Genome — VIII Prospects

---

The genome sequence should be completed by the end of 1998, given present rates of sequence production and support commitments. With that should come a tentative list of all the genes and many other sequence features. This, in combination with the complete lineage and the complete anatomy of the [nervous system](#), will provide unparalleled resources for the study of fundamental biological processes, including development and neurobiology. Understanding the function of this sequence will be the challenge for decades to come.

Central in gaining this understanding will be a ready means for associating variation in sequence with changes in phenotype. Methods exist to introduce DNA into the worm through germ-line transformation, and mutations can be recovered through transposon insertion and deletion ([Plasterk and van Leunen](#), this volume). However, to match the scale of the information now available, efficient methods will have to be developed to target introduced DNA to specific regions, in the manner available in yeast and mammalian cell culture. Localizing mRNA and protein products of the genes (preferably in real time) would provide critical information about these genes, and again the challenge will be to devise methods that will allow the thousands of predicted genes to be surveyed rapidly.

Comparative sequencing of other nematode genomes may also provide useful insights into which sequences are functionally important. More closely related worms will be useful in the investigation of regulatory and other noncoding sequences. More distantly related nematodes and organisms from other phyla are likely to be more useful in deciphering protein function.

Integrating information about related genes in other organisms with what is known about *C. elegans* will be an increasingly valuable activity as the complete genome sequences become available not only for bacteria, yeast, and *C. elegans*, but also for *Drosophila melanogaster* and humans. Databases such as ACeDB will be critical in making this vast amount of information available to the bench scientist.

Generated from local HTML

## **Chapter 2. The Genome — Acknowledgments**

---

We thank Steve Jones and Richard Durbin for comments on the manuscript and Sean Eddy for assistance in the discussion of repetitive DNA and tRNAs.

Generated from local HTML

# **Chapter 3. Chromosome Organization, Mitosis, and Meiosis**

---

## **Contents**

[I Introduction](#)

[II Mitosis](#)

[III Meiosis](#)

[IV Prospects](#)

Generated from local HTML

## Chapter 3. Chromosome Organization, Mitosis, and Meiosis — I

### Introduction

---

The mitotic chromosomes of *Caenorhabditis elegans*, and those of certain other organisms, including some plants, protozoa, insects, and other nematodes, are remarkable for having a well-differentiated kinetochore that extends along the entire poleward face of the metaphase chromosome. Microtubule attachment is distributed along the chromosome, and the chromosomes move broadside on toward the spindle poles. Chromosomes with this structure are referred to as holocentric or holokinetic, in contrast to monocentric chromosomes in which a single centromeric region may be distinguished at the primary constriction. Holocentric chromosomes typically behave differently in meiosis and mitosis. In meiosis, the nonlocalized kinetochore is absent, and in most organisms that have been examined, no structural differentiation of a kinetochore can be seen. Instead, microtubules appear to insert directly into the chromatin. The ends of the chromosomes are also said to adopt "kinetic activity" in meiosis, referring to the fact that in the meiotic divisions, the chromosomes move end on toward the spindle poles.

Studies on mitotic and meiotic segregation of *C. elegans* chromosomes have established that despite their holokinetic organization, these chromosomes share many features and behaviors with the more commonly studied higher eukaryotic monocentric chromosomes. They have similar telomere sequences and a trilaminar kinetochore structure which resembles that of monocentric chromosomes. *C. elegans* chromosomes undergo all of the classically described stages of meiotic prophase, culminating in a reductional division at meiosis I and equational division at meiosis II. Further homologous chromosomes in *C. elegans* rely on the formation of crossovers to ensure their proper disjunction at meiosis I. Thus, the study of mitotic and meiotic chromosome behavior in *C. elegans* can provide insight about conserved mechanisms governing chromosome behavior as well as about mechanisms specific to the segregation of holokinetic chromosomes.

In this chapter, we first review what is known about the structure and organization of mitotic chromosomes and discuss mitotic segregation of fusion chromosomes, chromosome fragments, and microinjected DNA in the context of holokinetic chromosome organization. We also briefly mention several mutations affecting mitotic segregation and cell division. In the second part of the chapter, we review the meiotic process, beginning with a cytological description of meiotic prophase and the meiotic divisions. This includes a discussion of the role of chiasma formation in determining the orientation of homologous chromosomes in late prophase and metaphase I, evidence that chromosome ends may adopt some centromeric functions during both meiosis I and meiosis II, and the genetic identification of *trans*-acting factors involved in assembly of the oocyte meiotic spindle. We then go on to discuss how the requirement for, and regulation of, crossover formation during meiosis is reflected in the organization of the genetic and physical maps. We review evidence for, and properties of, *cis*-acting chromosomal features that have key roles in promoting pairing and crossover formation between homologous chromosomes. Finally, we discuss how the analysis of mutants defective in meiotic segregation has led to the identification of numerous genes encoding *trans*-acting factors involved in pairing and crossover formation.

Generated from local HTML

## **Chapter 3. Chromosome Organization, Mitosis, and Meiosis — II**

### **Mitosis**

---

#### **A. The Wild-type Karyotype**

The wild-type metaphase karyotype of *C. elegans* consists of 12 chromosomes in hermaphrodites, five pairs of autosomes and two sex chromosomes, and 11 chromosomes in males, which have a single sex chromosome. Mitotic stages are most easily visualized in developing embryos, where the chromosomes display many of the characteristic features of holocentric chromosomes that distinguish them from monocentric chromosomes. At metaphase, each chromosome as a whole orients and lies within the spindle, parallel to the equator of the spindle, whereas anaphase figures suggest that the entire chromosome moves broadside on toward the spindle pole ([Albertson and Thomson 1982](#)).

Cytological preparations of metaphase chromosomes are made by squashing younger embryos, which contain a higher proportion of dividing cells. The chromosomes lack a primary constriction and are rods, a few microns in length. The length decreases with the developmental age of the embryo. Few distinguishing features are apparent on the chromosomes. Variably, regions of the chromosomes may show some differential fluorescence after staining with nucleic-acid-specific fluorochromes, but there is no consistent banding pattern as is seen with mammalian chromosomes. After staining with Hoechst 33258, a dark band has been observed on the right third of linkage group V, coincident with hybridization of a probe for the 5S gene cluster ([Albertson 1984a](#)) and may reflect a lower affinity of the dye for the DNA sequence composition at this locus.

#### **B. Holokinetic Organization**

In electron micrographs of sections taken longitudinally through embryonic metaphase chromosomes, the kinetochore appears as a trilaminar plaque covering the poleward face of the chromosomes. It resembles the monocentric kinetochore in structure, as it is composed of inner and outer layers, 0.02  $\mu\text{m}$  in width, separated by a more electron lucent layer, 0.03  $\mu\text{m}$  in width. Analysis of electron micrographs of serial sections taken through dividing embryonic cells revealed that from 0 to 8 microtubules were attached to the kinetochore. When several microtubules were present, they were distributed along the kinetochore, with the greater number of microtubules being recorded on the longer kinetochores ([Albertson and Thomson 1982](#)). However, the actual number of microtubules per kinetochore is likely to be larger, since microtubule stabilization buffers were not used in the preparation of the specimens. If the number were on the order of tens, then for *C. elegans* chromosomes, which vary in length from 12 to 20 Mb, there would be approximately one kinetochore microtubule for every  $10^6$  base pairs of DNA, similar to the microtubule density observed for monocentric chromosomes ([Bloom 1993](#)). A conservation of microtubule density for the two types of kinetochore structure may reflect similar requirements for movement and microtubule capture during mitosis in higher eukaryotes ([Pluta et al. 1995](#)). Furthermore, the presence of multiple microtubule attachment sites at both the holocentric and the monocentric kinetochore requires coordination of the structural and cell cycle control mechanisms ([Bloom 1993](#)). For example, in order to prevent nondisjunction, the microtubule-binding sites must be properly spaced so that they are oriented toward one spindle pole at metaphase, and cell cycle checkpoints must be able to sense orientation and number of bound microtubules prior to the onset of anaphase ([Pluta et al. 1995](#)).

The holocentric organization of *C. elegans* chromosomes has also been demonstrated by experimentally inducing chromosome breaks and observing the maintenance of the fragments through several mitotic cell divisions ([Albertson and Thomson 1982](#)). Such tests are considered diagnostic of holocentric chromosomes ([White 1973](#)), since when monocentric chromosomes are treated in the same way, acentric fragments are formed that are not mitotically stable. Breakage of holocentric chromosomes, on the other hand, should not produce acentric fragments. Similarly, irradiation of monocentric chromosomes can result in the formation of dicentric translocation chromosomes, which suffer breakage-fusion-bridge cycles. In organisms with holocentric chromosomes, dicentrics are not formed, even when two entire chromosomes are fused. In *C. elegans*,

segregation of both experimentally induced chromosome fragments and genetically characterized chromosome fragments, called free duplications (see below), appears cytologically to be nearly normal. Some abnormalities have been observed, however, suggesting that the fragments or small chromosomes behave somewhat differently compared to normal chromosomes. The fragments are often found at the edges of the metaphase plate in squash preparations, and they show evidence of abnormal segregation, including the presence of the fragments in the cytoplasm adjacent to the nucleus at interphase and lagging at anaphase ([Albertson and Thomson 1982](#)).

In addition to chromosomes and chromosomal fragments, extrachromosomal high-copy-number arrays of DNA injected into the germ line are transmitted through both meiosis and mitosis ([Mello et al. 1991](#)). The DNA arrays are propagated less efficiently than chromosomes and at different rates for different arrays formed from the same DNA. Rates of mitotic loss per cell division of  $1-2 \times 10^{-2}$  and  $3 \times 10^{-3}$  have been measured for two arrays ([Herman et al. 1995](#); L. Miller and S.K. Kim, pers. comm.). In comparison, the reported rate of mitotic loss per cell division for several free duplications varies from  $10^{-4}$  to  $5 \times 10^{-3}$  ([Herman 1995](#) and see below). The structure of the extrachromosomal DNA arrays has not been fully characterized, but it seems to differ from that of chromosomes and free duplications. The arrays appear to lack telomeres, since a probe for the *C. elegans* telomere failed to hybridize to several different arrays, although the presence of telomeres on several free duplications could be demonstrated using this same probe (D.G. Albertson, unpubl.). These observations are consistent with other independent evidence suggesting that at least some extrachromosomal arrays are circular in structure (S.K. Kim, pers. comm.), and therefore arrays and chromosomes might be expected to differ in their segregational behavior. Other aspects of array structure remain to be determined. For example, it is not known if a kinetochore is assembled on the arrays or what proteins interact with the arrays to package the DNA.

The observation that any DNA can be propagated as an extrachromosomal array in *C. elegans* suggests that there may be no specialized sequences required for segregation of holocentric chromosomes. On the other hand, the fact that neither free duplications nor DNA arrays segregate with the fidelity of normal chromosomes suggests that arrays and free duplications lack certain features that promote mitotic stability of wild-type chromosomes. Whether some of these features will turn out to be *cis*-acting sequences with properties and functions similar to those of monocentric centromeres remains to be determined. Monocentric centromeres carry out several functions in mitosis. They mediate attachment of the chromosome to the mitotic apparatus via the kinetochore. The centromere is also the site of the last attachment of sister chromatids and therefore may be expected to contain proteins directing sister chromatid segregation, as well as proteins involved in cell cycle control ([Pluta et al. 1995](#)). The role of specific DNA sequences in these various aspects of centromere function is best understood for the small, point centromeres of some yeasts, whereas for the larger, regional centromeres, such as those found in higher eukaryotes, it is not clear which of the various DNA sequence classes located at the centromeric constriction perform the different centromeric functions. In monocentric organisms, certain aspects of mitotic segregation can also be accomplished in the absence of a centromere, including the nucleation of microtubules, and their assembly into bipolar arrays on chromatin in egg or early embryo extracts ([Sawin and Mitchison 1991](#); A. Hyman, quoted in [Raff and Allan 1996](#)), and the transmission, albeit inefficient, of acentric fragments ([Steiner and Clarke 1994](#); [Brown and Tyler-Smith 1995](#); [Murphy and Karpen 1995](#)). Therefore, some mechanisms may exist that promote segregation in the absence of a normal centromere, and the fact that DNA arrays can be transmitted in *C. elegans* should not be interpreted as conclusive evidence that *cis*-acting factors are not required for holocentric chromosome segregation. Further study of both monocentric and holocentric chromosomes will be required to understand the role of *cis*-acting factors and different segregation mechanisms.

## C. Mutant Karyotypes

Reciprocal translocations between many pairs of chromosomes have been described. They have been useful for a variety of genetic analyses, including the characterization of *cis*-acting features involved in pairing and crossing over (see below) and as genetic balancers (for review, see Edgely et al. 1995). In some cases, the position of the breakpoints generates translocation chromosomes that are morphologically distinct in the light microscope, and these have been used for cytogenetics ([Albertson 1985](#)). Two additional types of chromosome rearrangements

can be stably propagated because of the holocentric organization of the chromosomes. They are small chromosome fragments, called free duplications, and translocations involving fusion of two entire chromosomes.

## 1. Chromosomal Rearrangements

The first fusion chromosome to be described in *C. elegans* was the *mnT12(IV;X)* chromosome, in which the right end of *X* is joined to the left end of *IV* ([Sigurdson et al. 1986](#)). Animals homozygous for *mnT12(IV;X)* are viable and fertile, indicating that all essential genes on *X* and *IV* have been retained on the translocation chromosome. However, telomeric sequences could not be observed at the breakpoint by fluorescent in situ hybridization with a telomere probe, and therefore have been eliminated or reduced below the sensitivity of the assay by the fusion event. The metaphase karyotype of *mnT12(IV;X)* homozygotes consists of ten chromosomes, with the *mnT12(IV;X)* chromosomes easily distinguished cytologically by their length ([Fig. 1a](#)).

Another fusion chromosome, *mnT13(I;X)*, has been characterized cytologically and consists of the left end of *X* joined to the right end of *I* ([Albertson and Thomson 1993](#)). Two observations suggest that some essential genes have been lost from linkage group *I* in the formation of the translocation. First, animals homozygous for *mnT13(I;X)* also carry an additional copy of linkage group *I*. Second, the ribosomal gene locus (which maps to the right end of linkage group *I*) appears to be partially deleted on the translocation chromosome, since hybridization of a probe for the ribosomal genes results in a fluorescent hybridization signal of reduced intensity on the *mnT13* chromosome ([Albertson and Thomson 1993](#); D.G. Albertson, unpubl.). The possible loss of other linkage group *I* gene sequences from *mnT13* has not been investigated.

Recently, [Hodgkin and Albertson \(1995\)](#) described the generation of attached *X* chromosomes (*X<sup>^</sup>X*) in *C. elegans*. These chromosomes resulted from rare recombination events involving attached inverted duplications of the *X* chromosome, and they should therefore be composed of two *X* chromosomes attached at their left ends (see Fig. 6 in [Hodgkin and Albertson 1995](#)). Although animals with *X<sup>^</sup>X* chromosomes were viable and the *X<sup>^</sup>X* could be propagated through both mitosis and meiosis, the chromosome broke down frequently. This behavior differs from the behavior of attached chromosomes studied in other organisms ([White 1973](#)) and may be due to breakage occurring as a result of the kinetic activity of the chromosome ends during meiotic segregation of these holocentric chromosomes (see below). Similar behavior has been reported for the *szT1(X)* translocation chromosome ([McKim et al. 1988](#)).

Free duplications appear cytologically as small chromosomes or chromosome fragments ([Fig. 1b](#)) ([Herman et al. 1976](#)). Approximately half of the genetic map is covered by different duplications ([Herman 1995](#)). The free duplications are usually present in one copy per cell, and they are transmitted through both somatic and germ-line divisions with lower fidelity than a normal chromosome. This segregational behavior has been exploited for the generation of genetic mosaics (for review, see [Herman 1995](#)). Three general observations about duplication behavior have been made from the genetic mosaic studies. First, larger duplications tend to be mitotically more stable than smaller duplications. This behavior can be seen by comparison of the mitotic stability of duplications and their derivatives that have been made either smaller by deletion or larger by fusion with other duplications. The deletion derivatives show decreased mitotic stability, whereas the fusion derivatives show increased mitotic stability relative to the progenitor duplication(s). There are exceptions to this rule, however ([McKim and Rose 1990](#); Hedgecock and [Herman 1995](#)). For example, the mitotic stability of *qDp3(III, f)* is about 20 times greater than that of *sDp3(III, f)*, although the physical size of the duplicated region of linkage group *III* included in *qDp3* appears to be equal to or less than that of *sDp3* ([Hedgecock and Herman 1995](#); [Herman 1995](#); D.G. Albertson, unpubl.). Second, it has been observed that the germ-line transmission frequency and mitotic stability of the duplications are correlated, although the germ-line transmission of the duplication, *ctDp2*, is lower than expected from its mitotic stability ([Hunter and Wood 1990](#)). Third, free duplications have been observed to undergo spontaneous rearrangement (deletion) in the germ line at a high frequency compared to normal chromosomes ([Herman 1984](#); [McKim and Rose 1990, 1994](#); [Villeneuve and Meyer 1990a](#)).

Two general explanations have been offered as to why free duplications should be less stable than the normal chromosomes. Cytological observations on chromosome fragments led to the suggestion that the probability of microtubule capture may depend on chromosome length ([Albertson and Thomson 1982](#)). Therefore, the somatic

loss of duplications, which has been observed to occur either by simple loss or by nondisjunction (Hedgecock and [Herman 1995](#); [Herman 1995](#)), might be explained by failure of the duplication to attach to the mitotic apparatus or by mal-orientation on the mitotic spindle. It has also been suggested that the different mitotic stabilities of free duplications might be due to the fact that they are ring chromosomes, rather than linear chromosomes ([McKim and Rose 1990](#), [1994](#); C.P. Hunter and W.B. Wood, pers. comm.). Whether free duplications are linear or ring chromosomes is at present not known, since the small size of the duplications makes it impossible to distinguish between these two structures by light microscopy. However, the demonstration of telomere sequences on two duplications of linkage group *III*, *qDp3* and *eDp6* (D.G. Albertson, unpubl.), suggests that at least some free duplications are linear. It is also possible that loss of free duplications may occur because of malfunctions occurring in interphase, including, for example, incorrect inclusion in the interphase nuclear organization or aberrant DNA replication.

The composition of most chromosome rearrangements has been determined by inspection of specific markers, usually by genetic mapping ([Edgley et al. 1995](#)), or in a few cases by mapping relative to the physical map by cytological or molecular methods (see, e.g., [Kramer et al. 1988](#); [Albertson 1993](#)). The rearrangements have therefore been mapped with respect to only a small portion of the genome, and the possibility remains that the free duplications, as well as other chromosome rearrangements, are highly complex rearrangements. They may contain other, as yet undetected regions of the genome important for proper segregation and stability. For example, addition of telomeres to *qDp3*, a duplication of the central portion of linkage group *III*, may have occurred *de novo* or may have been formed by translocation of other chromosome ends. Determination of the composition of chromosome rearrangements with respect to the entire genome by chromosome painting ([Chuang et al. 1994](#)) or comparative genomic hybridization ([Kallioniemi et al. 1992](#)) may reveal some surprises, as well as information on how rearrangements are formed and the requirements for their stable meiotic and mitotic segregation.

## 2. Aneuploidy

Both whole chromosome and segmental aneuploidies are observed in *C. elegans*. Nondisjunction of the *X* chromosome gives rise to viable hermaphrodites that are trisomic for the *X*, but otherwise diploid ([Hodgkin et al. 1979](#)). These animals may be distinguished from wild type by their dumpy morphology. Animals trisomic for linkage group *IV* are also viable ([Sigurdson et al. 1986](#)). They have small brood sizes but are indistinguishable morphologically from wild-type diploids. Tetrasomics in *C. elegans* appear to be lethal, since progeny tetrasomic for the *X*, for example, are not recovered from appropriate crosses ([Hodgkin et al. 1979](#)). In contrast, four copies of some chromosomal regions have been observed, for example, in animals homozygous for a translocated duplication ([Rogalski and Riddle 1988](#)) or a single copy of a free duplication that itself contains two copies of a chromosomal region (e.g.,  $+/-/eDp27$ ).

## D. Telomeres and Telomerase

The *C. elegans* chromosomes terminate in 4–9-kb blocks of the tandemly repeated sequence TTAGGC ([Wicky et al. 1996](#)), which is closely related to the telomeric repeats found in other, highly diverged eukaryotes and is most similar to the TTAGGG repeat characteristic of vertebrate and trypanosome telomeres ([Zakian 1989](#)). The TTAGGC sequence appears to be a general feature of nematode telomeres, since it is also found at the telomeres of the parasitic nematodes *Ascaris* and *Parascaris* ([Müller et al. 1991](#); [Zetka and Müller 1996](#)). In addition to the telomeric blocks of TTAGGC repeats, the *C. elegans* genome contains numerous dispersed internal blocks of perfect ([Cangiano and La Volpe 1993](#)) and degenerate (D.G. Albertson, unpubl.) TTAGGC repeats concentrated in the terminal 30% of the chromosomes.

In *C. elegans*, the terminal TTAGGC repeats alone appear to be sufficient for the general chromosome capping functions attributed to telomeres. Of the 12 telomeres, 11 have been cloned, and sequence analysis of the subtelomeric regions reveals that the 11 telomeres do not have any sequences in common apart from the TTAGGC repeats ([Wicky et al. 1996](#)). Moreover, TTAGGC repeats are joined immediately adjacent to a nearly complete ribosomal DNA repeat unit at the telomere corresponding to the right end of chromosome *I*. The fact

that each of the *C. elegans* subtelomeric regions is unique suggests that no specific DNA sequence apart from the TTAGGC repeats is required for basic telomere function. The absence of similarity among the *C. elegans* subtelomeric regions contrasts with the subtelomeric regions of other species, which often contain homologous and repeated sequences (Biessmann and Mason 1992; Kirk and Blackburn 1995). Although the *C. elegans* subtelomeric regions do not have sequences in common with each other, many do contain repetitive DNA. Three contain satellite-like tandem repeats, and five contain repeated sequences that cross-hybridize with internal genomic DNA fragments (Wicky et al. 1996).

The cloned telomeres represent an important resource for completion of the *C. elegans* physical map (Waterston et al., this volume), since most of the few remaining gaps in the map are located at the chromosome ends. Three of the cloned telomeres have been assigned to their chromosome ends of origin (Wicky et al. 1996; A. Rose et al., pers. comm.), and mapping of the remaining telomeric clones is in progress.

Recent experiments have provided molecular genetic evidence for telomerase activity in *C. elegans*. Wicky et al. (1996) demonstrated that a terminally deleted chromosome had acquired a new telomere and showed that this new telomere had arisen by *de novo* addition of telomeric repeats at a site that lacked preexisting TTAGGC repeats. The junction site contains three bases present in both the ancestral DNA sequence and the telomeric repeat; these three bases presumably acted as a primer for telomere addition by allowing limited pairing with the RNA template of the telomerase enzyme. This healing event is analogous to the new telomere formation that occurs during the developmentally regulated process of chromatin diminution in *Ascaris* (Tobler et al. 1992), where telomeric repeats are also added *de novo* at chromosomal sites that have one to four bases of overlap with the TTAGGC repeat (Müller et al. 1991; S. Jentsch and F. Müller, pers. comm.). Similar ambiguity at the junctions between subtelomeric satellite or ribosomal DNA repeat sequences and the TTAGGC telomeric repeats at several of the endogenous *C. elegans* telomeres further suggests that these telomeres may also have arisen by telomerase-mediated healing events and that *de novo* telomere formation by telomerase may play a part in genome evolution.

## 1. Mutations Affecting Chromosome Segregation

The mutation *him-10(e1511ts)* causes a temperature-sensitive defect in mitotic chromosome segregation (A.M. Villeneuve, unpubl.). In *him-10* hermaphrodites shifted to 25°C during larval growth, oocyte nuclei contain widely varying numbers of chromosomes, some having many more chromosomes than normal and some having many fewer. Since *C. elegans* oocyte nuclei are paused in meiotic prophase, prior to the meiosis I division (Schedl, this volume), an aberrant number of chromosomes at this stage is clear evidence of defective chromosome segregation during the mitotic proliferation of the germ line. Further investigation will be required to determine the underlying malfunction (e.g., in assembly or function of the mitotic spindle) responsible for these errors in chromosome segregation.

It is likely that *him-10(e1511)* affects mitotic chromosome segregation in *somatic cells* as well as in the germ line. Although this has not yet been demonstrated for whole chromosomes, the *him-10* mutation was found to cause a four- to sevenfold increase in the frequency of somatic mitotic loss of several free duplications, making it a useful tool for genetic mosaic analysis (Hedgecock and Herman 1995).

## 2. Mutations Affecting the Mitotic Cell Cycle

Mutations in several genes result in uncoupling of the chromosome and cell division cycles during postembryonic development. Newly hatched L1 larvae carrying these mutations are normal, perhaps because embryonic cell divisions are controlled by stored maternal products. Most postembryonic cell divisions are defective, resulting in a characteristic Sterile-Uncoordinated (Unc) phenotype since the development of the gonad and the later larval and adult *nervous system* requires cell division (Albertson et al. 1978; Sulston and Horvitz 1981). In one class of mutants, typified by *lin-5*, nuclear division and cytokinesis fail but DNA synthesis continues, resulting in polyploid blast cells. In *lin-5* mutants, many nuclei undergo abortive cycles of chromosome condensation and nuclear envelope breakdown, but metaphase and anaphase fail and the nuclear envelope reforms. In another class of mutants, typified by *unc-59* and *unc-85*, polyploid nuclei appear to arise

both by failed nuclear division and by nuclear fusion following failed cytokineses. In [\*lin-6\*](#) mutants, in contrast, cell divisions continue in the absence of DNA replication, producing smaller and smaller cells that eventually die.

Postembryonic cells of these Sterile-Unc mutants are unable to coordinate cell cycle events to ensure that they occur in the proper order; some aspects of the cell cycle continue unchecked despite the fact that events that normally precede them have failed. Cell division in *C. elegans* is governed by a classical checkpoint regulation program, however, as evidenced by the fact that pharmacological disruption of specific cell cycle events can elicit cell cycle arrest. For example, cell division in L1 larvae can be arrested prior to entry into mitosis (presumably in S phase) by treatment with the DNA synthesis inhibitor hydroxyurea (S. van den Heuvel, pers. comm.). Either the Sterile-Unc mutants cannot sense whether a prior event in the cycle has been completed or else their specific defects do not result in production of a signal capable of eliciting cell cycle arrest by a checkpoint mechanism.

In contrast to the Sterile-Unc genes, two genes have been identified that appear to be involved in regulating progression through the cell cycle: [\*emb-29\*](#), which is required for late embryonic mitoses ([Hecht et al. 1987](#)), and [\*glp-3\*](#), which is required for germ-line mitoses (L. Kaydyk et al., pers. comm.). Mutations in these genes cause an apparent arrest of the cell cycle prior to entry into mitosis, at the G<sub>2</sub>/M transition.

## Figures

Figure 1. Mitotic chromosome preparations with chromosome rearrangements.

### Figure 1

Mitotic chromosome preparations with chromosome rearrangements. The holocentric structure of *C. elegans* chromosomes allows the stable propagation of chromosome fragments and translocation chromosomes resulting from the fusion of two entire chromosomes. (a) Early prometaphase chromosomes from an embryo homozygous for *mnT12(IV;X)*. The karyotype consists of eight normal-size chromosomes and two double-length *mnT12* chromosomes (one *mnT12* chromosome is indicated by the arrow). (b) Embryonic late prometaphase/metaphase chromosomes including the free duplication, *eDp6* (arrow). In these embryos, the karyotype consists of 12 normal-size chromosomes and the small *eDp6* chromosome. The chromosomes in a are from an older embryo than those in b. As development progresses, the size of the chromosomes decreases. Bar, 10 μm.

Generated from local HTML

## Chapter 3. Chromosome Organization, Mitosis, and Meiosis — III

### Meiosis

---

#### A. Cytology of Meiotic Prophase

*C. elegans* chromosomes undergo all of the classically described stages of meiotic prophase in preparation for meiosis I, the reductional division. In both males and hermaphrodites, germ-cell nuclei representing all stages of meiotic prophase are arranged in temporal order along the distal-proximal axis of the adult gonads. As nuclei enter the extended prophase that precedes the first meiotic division, homologous chromosomes partially condense and pair, becoming aligned and physically associated, or synapsed, in a side-by-side configuration along their entire lengths. Alignment of homologs is complete at the pachytene stage, with the chromosomes localized to the periphery of the nucleus ([Fig. 2a](#)).

Electron micrographs of sectioned pachytene nuclei show normal-appearing synaptonemal complexes (SC), the highly ordered proteinaceous structures located at the interface of synapsed homologs ([Goldstein and Slaton 1982](#)). Hermaphrodite pachytene nuclei contain six tripartite SCs (corresponding to five autosomal bivalents and one X chromosome bivalent) composed of two lateral elements (each 35  $\mu\text{m}$  width) flanking a striated central element (20  $\mu\text{m}$  width). One end of each SC is attached to the nuclear envelope. Males, which have only a single X chromosome, contain five SCs, and the univalent X chromosome is present in a condensed heterochromatic state ([Goldstein 1982](#)).

Later in prophase, at the diplotene stage ([Fig. 2b](#)), the chromosomes desynapse but remain condensed and are held together by chiasmata. The chromosomes detach from the nuclear envelope and continue to condense as nuclei move into the diakinesis stage of meiotic prophase. In developing oocytes, nuclear volume increases as chromosome condensation proceeds, allowing individual bivalents to be visualized and counted ([Fig. 2c](#)). Wild-type oocytes reliably have six bivalents at diakinesis, consistent with all six homolog pairs having undergone a crossover ([Villeneuve 1994](#)). The chiasmata can no longer be readily distinguished at this stage due to the extremely condensed state of the bivalents, but their presence can be inferred from the fact that the homologs remain attached; when chiasmata are absent due to failure in crossing over, unattached univalent chromosomes are observed ([Fig. 2d](#)) ([Villeneuve 1994](#); see below). In developing [spermatocytes](#), the nuclear volume is much more compact, making it difficult to distinguish individual chromosomes or bivalents.

At diakinesis (and at metaphase I), the homologous chromosomes that constitute the bivalent are associated in an apparent end-to-end configuration ([Nigon and Brun 1955](#); [Herman et al. 1979](#); [Albertson and Thomson 1993](#)). *in situ* hybridization studies have shown that either end can be oriented toward the outside. For most chromosomes, which end is outside appears to be random, but chromosome I exhibits a bias such that the right ends (which contain the ribosomal DNA gene cluster) are more frequently located on the outside ([Albertson and Thomson 1993](#)). The apparent end-to-end association of homologs at this stage has been taken to reflect terminalization of the chiasmata, although there is debate in the literature over whether terminalization actually occurs in organisms for which meiosis I is the reductional division ([Jones 1987](#)). The end-to-end appearance of the bivalents at late diakinesis might instead be a consequence both of the original distribution of crossover events and of the progressive condensation of the chromosomes that occurs as prophase proceeds: Nearly 90% of autosomal crossovers occur in the terminal thirds of the chromosomes ([Barnes et al. 1995](#); see below), and condensation results in an estimated three- to tenfold shortening in chromosome length (concomitant with an increase in width) between the pachytene stage and late diakinesis. Thus, lateral projections observable at diplotene may be absorbed into the width of the bivalent by late diakinesis, resulting in bivalents that appear terminally associated. Whether or not terminalization occurs, the inside/outside orientation of the bivalents is most likely determined by the initial position of the crossover, with the end nearest the crossover becoming the inside end. If this hypothesis is correct, then the inside/outside orientation at diakinesis should be predictable for any bivalent in which the location of crossovers is constrained by regional crossover suppression. This prediction

has been borne out for a number of different rearrangements, an example of which is shown in Figure 3 ([Albertson et al. 1995](#); D.G. Albertson, unpubl.; see below).

In oocytes, meiosis pauses in diakinesis, and the oocyte nucleus does not go on to complete the meiotic divisions until after ovulation and fertilization have occurred (for a description of oocyte maturation and ovulation, see [Schedl](#), this volume); similar delay or arrest during meiotic prophase is a common feature of oocyte meiosis in animals. Spermatocytes, in contrast, proceed immediately into the first and second meiotic divisions.

## B. Cytology of Metaphase I and II

At metaphase I of meiosis in both spermatogenesis and oogenesis, the meiotic bivalents appear highly condensed, and ultrastructural studies have failed to differentiate a kinetochore structure on the chromosome. However, in certain species of the plant genus *Luzula*, in which nonlocalized kinetochores have been demonstrated in mitosis ([Braselton 1971](#); [Bokhari and Godward 1980](#)), a single, localized kinetochore-like structure has been distinguished on meiotic chromosomes ([Braselton 1981](#)). By using different fixation or staining procedures, it might also be possible to reveal kinetochore-like structures on the meiotic chromosomes of *C. elegans*. In electron micrographs of *C. elegans* meiotic chromosomes, microtubules appear to insert directly into the chromatin ([Albertson and Thomson 1993](#)), but it is currently not known where the microtubules attach or if there is a specific site of attachment.

At metaphase I and II, the chromosomes congress to the spindle equator with an outer ring of five chromosomes surrounding a central sixth chromosome. At metaphase I in males, the central chromosome was identified as the univalent *X* chromosome from reconstruction of electron micrographs of serial sections through metaphase I spindles. The autosomal bivalents formed the outer ring, with each half bivalent joined at the spindle equator by a chromatin thread, possibly corresponding to a chiasma. The central location of the *X* was also suggested by light microscopic observations of metaphase I. In hermaphrodites and at metaphase II in both sexes, the *X* chromosome cannot be distinguished morphologically from the autosomes ([Albertson and Thomson 1993](#)). We speculate that the observed differential placement of the *X* chromosome at metaphase I may be a consequence of unspecified mechanisms operating to ensure proper disjunction of the unpaired *X* in males ([Hodgkin et al. 1979](#)), which do not function in *XO* animals that have been transformed into hermaphrodites by a [her-1](#) mutation ([Hodgkin 1980](#)).

### 1. The Meiotic Spindle

Ultrastructural studies revealed that the meiotic spindle apparatus is organized differently in spermatogenesis and oogenesis ([Albertson and Thomson 1993](#)). In spermatogenesis, centrioles are present in the poles of the spindle, and the spindle appears similar to mitotic metaphase spindles. Segregation of the chromosomes to the spindle poles in the two maturation divisions results in four sperm, each with a centriole closely associated with the chromatin. The sperm contributes centrioles to the oocyte, and following fertilization, the sperm centrosome divides and organizes the first mitotic cleavage spindle ([Albertson 1984b](#)).

The meiotic maturation divisions of oogenesis take place in the oocyte after fertilization. At both meiotic divisions, the spindles are acentriolar and have a barrel-shaped morphology typically seen in oogenesis of many organisms (for review, see [McKim and Hawley 1995](#)). Formation of the meiotic spindles has been studied in fixed specimens by indirect immunofluorescent staining with antitubulin antibodies ([Albertson and Thomson 1993](#)). The early stages of meiotic spindle formation appear to proceed without well-defined organizing centers, since microtubules are first seen in an apparently disorganized array around the chromosomes. As the chromosomes congress, two well-defined poles at the ends of an elongated spindle can be distinguished. At this stage, a maximum pole-to-pole length of 13 μm was measured. Progression toward metaphase results in shortening of the spindle to less than one third of the initial length, reaching a minimum pole-to-pole length of 3–4 μm at anaphase. Prior to metaphase, the spindles are oriented parallel to the surface of the embryo, but by anaphase, they rotate to lie perpendicular to the surface with one end of the spindle closely apposed to the membrane. At

telophase, the blocks of chromatin separate to a maximum of 3–4 µm, leaving all antitubulin staining material lying between them.

## 2. Genes Involved in Formation of the Acentriolar Meiotic Spindle

The assembly of the acentriolar spindle takes place within a cytoplasm that will shortly undergo mitosis on a conventional centriolar spindle. This raises questions as to how assembly of these two different spindle structures is regulated. Genetic analysis is providing insights into both the process and the regulatory pathways associated with acentriolar spindle formation and coordination of mitosis and meiosis in a common cytoplasm. The [\*mei-1\*](#) gene is required for spindle formation in the female germ line, since loss-of-function mutations in this gene disrupt meiotic spindle formation ([Mains et al. 1990a, b](#)). However, *mei-1* gene activity must be eliminated prior to metaphase, since dominant gain-of-function alleles of *mei-1(ct46)* disrupt mitotic divisions ([Clandinin and Mains 1993](#)). Molecular cloning and sequencing of [\*mei-1\*](#) revealed that the protein product is a member of a family of ATPases that share a highly conserved nucleotide-binding site ([Clark-Maguire and Mains 1994a](#)). Immunolocalization of the protein in metaphase I meiotic spindles revealed staining distributed throughout the spindle, with the highest concentration at the spindle poles. In [\*mei-1\*](#) loss-of-function (lf) mutants, antitubulin staining at metaphase I remains diffuse, whereas no MEI-1 immunostaining is detected, suggesting that MEI-1 may play a part in promoting the organization of spindle poles ([Clark-Maguire and Mains 1994b](#)). Two genes have been identified that restrict [\*mei-1\*](#) activity to meiotic divisions: [\*mel-26\*](#) appears to be a postmeiotic inhibitor of [\*mei-1\*](#) activity, whereas [\*mei-2\*](#) is required to localize [\*mei-1\*](#) to meiotic spindles ([Clark-Maguire and Mains 1994b](#)).

## 3. Alignment and Segregation of Chromosomes in Meiosis

Observations on a variety of organisms with holocentric chromosomes indicate that in a given species, alignment of the meiotic bivalent on the metaphase I spindle takes one of two possible orientations ([White 1973](#)). The bivalent can lie parallel to the equator of the spindle (equatorial orientation) or it can be aligned with the long axis parallel to the spindle pole axis (axial orientation). When bivalents orient axially, sister chromatids segregate to the same pole at anaphase I, so that the first meiotic division is reductional, as occurs in meiosis in species with monocentric chromosomes.

In *C. elegans*, the meiotic chromosomes adopt the axial orientation at both metaphase I and II ([Albertson and Thomson 1993](#); D.G. Albertson, unpubl.). Because the bivalents are small and highly condensed, *in situ* hybridization was used to label one end of the chromatids of linkage groups I, II, or V. If the bivalent were to adopt the axial orientation, then the expectation would be that some metaphase figures should contain chromosomes in which the labeled ends are proximal to the spindle poles and not located on the spindle equator. If the chromosomes adopt the equatorial orientation, then the labeled ends should always lie on the equator. The axial orientation was demonstrated by the observation that in some metaphase I and II figures, the labeled ends of the chromatids were seen proximal to the spindle poles.

The monocentric centromere ensures the orderly disjunction of the chromatids by performing two functions in meiosis. First, it provides the site of attachment of the spindle microtubules. Second, it holds the sister chromatids together through meiosis I and then directs their splitting in meiosis II. In the absence of any cytologically visible centromeric structure in meiosis, the question arises as to the nature of the meiotic centromere on *C. elegans* chromosomes. It has so far not been possible to identify with certainty the site of attachment of microtubules to the meiotic bivalent because of the density of microtubules in the meiotic spindle ([Albertson and Thomson 1993](#)). However, it seems likely that attachment is made at the poleward end of the chromatids in metaphase I, and therefore this end of the chromatid performs one of the functions of the monocentric centromere at meiosis I. Does this end of the chromosome also hold the sister chromatids together and so perform both of the classical functions of the centromere? For the heterozygous translocation of chromosome I, *hT3(I;X)*, the answer is yes (D.G. Albertson, unpubl.). Since the bivalent of the heterozygous translocation adopts a fixed orientation in diakinesis, the poleward ends of the chromatids are also fixed at metaphase I. It was therefore possible to ask whether the chromatid ends that were poleward at metaphase I

also held the chromatids together in metaphase II. As shown in Figure 3, labeling one end of the chromatids by *in situ* hybridization revealed that the end of the chromatid that had been poleward at metaphase I was always at the equator at metaphase II. Therefore, one end of the sister chromatids performs both functions of the monocentric centromere. However, it is worth noting two differences in the behavior of these holocentric chromosomes compared to monocentric chromosomes. First, either end of the chromatid can perform the centromeric functions in metaphase I. Second, at metaphase II, the opposite end of the chromatid is proximal to the spindle pole compared to metaphase I, and so presumably spindle attachment takes place at different ends of the chromatids in the two divisions.

## C. Genetic Organization of Chromosomes

The genetic length of the *C. elegans* chromosomes is independent of their physical length and is a reflection of the functional regulation of the meiotic process. Although the chromosomes range in size from 12 to 20 Mb of DNA, the genetic map of each of the six chromosomes is approximately 50 map units in length, consistent with approximately one crossover event per bivalent per meiosis ([Brenner 1974](#); [Barnes et al. 1995](#)). Since crossing over between homologs is required to ensure their disjunction at the meiosis I division ([Hawley 1988](#); [Zetka and Rose 1992](#)), recombination must be carefully regulated to guarantee that a limited number of crossover events are distributed so that each bivalent undergoes a crossover. This regulation is exemplified by the observation that when crossing over is eliminated from one portion of a chromosome (e.g., due to heterozygosity for a regional crossover suppressor), there is often a compensatory elevation of crossing over in other regions of the chromosome ([McKim et al. 1988, 1993](#); [Zetka and Rose 1992](#)). In an extreme example, when crossing over was restricted to a small (normally 6-map-unit) interval on chromosome I in hermaphrodites heterozygous for two different rearranged chromosomes, the frequency of exchange in that interval was nearly the full amount expected for the entire length of the chromosome ([Zetka and Rose 1992](#)).

The *C. elegans* genetic map represents the synthesis of a large volume of data from 2-factor mapping experiments (measuring recombination frequency between genetic markers in hermaphrodites), 3-factor and multifactor mapping experiments (determining the relative order of genetic markers), and deficiency and duplication mapping experiments (testing for complementation of marker mutant phenotypes) ([Edgely and Riddle 1993](#)). The current genetic map, as well as the data used to construct it, can be accessed using ACeDB ([Eckman and Durbin 1995](#)). A striking feature of the meiotic maps of each of the autosomes, but not the *X* chromosome, is a central region where the number of meiotic exchanges per unit length of DNA is greatly reduced relative to the genomic average of 300 kb per map unit ([Greenwald et al. 1987](#); [Prasad and Baillie 1989](#); [Starr et al. 1989](#); [Barnes et al. 1995](#)). On chromosome I, for example, the number varies from as much as 1200 kb per map unit in the *dpy-5 unc-13* region to as little as 100 kb per map unit in the *unc-101 unc-54* region ([Barnes et al. 1995](#); [Zetka and Rose 1995b](#)). These regions of low recombination have been called “gene clusters” because of their appearance on the genetic map ([Brenner 1974](#)), but they are also regions where the genes are physically closer together (see [Sulston et al. 1992](#); [Barnes et al. 1995](#); [Waterston et al. this volume](#)). Flanking the gene clusters are regions (referred to as the chromosome “arms”) where exchange preferentially occurs. In some cases, these regions have been shown to contain recombinational hot regions, which have crossover frequencies as much as tenfold higher than the genomic average ([Hodgkin 1993](#); [Pilgrim 1993](#); [Clark-Maguire and Mains 1994a](#)). A comparison of the frequency of crossing over and gene density across the entire genome has shown that most recombination occurs in gene-poor regions, and it has been proposed that recombination-promoting sequences exist at high density in the chromosome arms ([Cangiano and LaVolpe 1993](#); [Barnes et al. 1995](#)).

The meiotic pattern of crossing over that gives rise to the genetic map is under genetic control and can be altered by a mutation in the *rec-1* gene. Animals carrying the *rec-1* mutation have the same total number of exchange events per chromosome each meiosis, but the placement of exchanges is altered, indicating that meiotic mechanisms determining the number of crossovers are separable from mechanisms determining their positions ([Zetka and Rose 1995b](#)). On chromosome I, for example, genetic distances expand across the medial gene cluster ([Rose and Baillie 1979b](#); [Rattray and Rose 1988](#)) and contract near the right end of the chromosome ([Zetka and Rose 1995b](#)), resulting in a map that is more consistent with the physical distances than is the meiotic

map. Despite causing a redistribution of autosomal crossover events during meiosis, the [rec-1](#) mutation does not appear to have any effect on the fidelity of chromosome segregation or on growth and viability. This result suggests that the wild-type distribution of crossover events is neither required for faithful meiosis nor is it an indirect consequence of a feature of chromosome organization that serves some other essential function, raising questions about how the wild-type crossover distribution originated and how or why it is maintained. Mutations in several other genes also disrupt the distribution of meiotic exchanges (see below). Unlike [rec-1](#), however, these mutations cause an overall reduction in the amount of crossing over, leading to nondisjunction.

## 1. Factors Influencing Crossover Frequency

Crossing over occurs in all three *C. elegans* germ lines (oocyte and spermatocyte in the hermaphrodite, spermatocyte in the male), and the frequency of recombination between genetic markers can be affected by a variety of environmental and physiological factors. These include temperature, age, and sex of the parent ([Rose and Baillie 1979a](#); [Kim and Rose 1987](#); [Zetka and Rose 1990](#)). For several pairs of markers within medial gene clusters, and one genetic interval spanning a cluster/arm boundary, crossover frequencies in both males and hermaphrodites were observed to increase with temperature and to decrease with parental age. Furthermore, for both genetic intervals tested, recombination frequencies were higher in hermaphrodite [spermatocytes](#) than in oocytes. Since [spermatocytes](#) are produced in the fourth larval stage, before the switch is made to oocyte production, these differences may also be attributable to differences in parental age. The effects of temperature and age have not been measured for other regions of the chromosomes, however. It is possible that the observed increases and decreases in crossover frequencies within the gene clusters may be offset by compensatory changes in crossover frequencies on the chromosome arms, as has been observed in certain cases of crossover suppression ([McKim et al. 1988](#)). Because many factors can influence the frequency of crossing over between markers, standardized conditions are recommended for genetic mapping experiments and for experiments comparing recombination frequencies in different strains ([Rose and Baillie 1979a](#)).

## 2. Crossing Over and Segregation in Spermatocytes

Recombination frequencies in males have been measured along the entire length of chromosome I, yielding a male genetic map that is approximately one-third shorter than the standard chromosome I map derived from measurements of genetic recombination frequencies in hermaphrodites ([Zetka and Rose 1990](#)). Although double crossovers have been detected in *C. elegans* males, their frequency is not high enough to account for the reduced size of the male map ([Hodgkin et al. 1979](#); [Zetka and Rose 1995b](#)). Unless there are undetected crossovers in regions at the tips of the chromosomes beyond known genetic markers, the length of the male map suggests that a significant fraction of chromosomes in male [spermatocytes](#) may be achiasmate. (Unfortunately, the frequency of achiasmate chromosomes in [spermatocytes](#) cannot be readily assessed cytologically as it can in oocytes due to the compact structure of the spermatocyte nucleus.) Nevertheless, males reliably segregate their homologous chromosomes, raising the possibility that in *C. elegans* males, a crossover per bivalent is not necessary for proper disjunction of homologs.

Mechanisms for ensuring the segregation of achiasmate chromosomes have been described for other organisms ([Hawley et al. 1992](#)), and several lines of evidence suggest that similar mechanisms may operate in *C. elegans* [spermatocytes](#) but not in oocytes. For example, in hermaphrodites mutant in either of two loci required specifically for normal X chromosome crossing over, the frequency of X chromosome nondisjunction is substantially higher in oocytes (which rely on chiasmata for X chromosome disjunction) than in [spermatocytes](#), despite the fact that recombination appears to be strongly reduced in both gamete lines ([Broverman and Meneely 1994](#); [Villeneuve 1994](#)). Unless there is a particularly high frequency of undetected crossovers near the X chromosome ends in these mutants, these data suggest that hermaphrodite [spermatocytes](#) may have the capacity to segregate achiasmate X chromosomes, at least when autosomal crossing over is normal. The existence of a recombination-independent segregation system is also supported by the observation that free duplications ([Herman et al. 1979](#); [McKim and Rose 1990](#)) and extrachromosomal arrays exhibit a modest

tendency to segregate from the lone X chromosome in male [spermatocytes](#). There is, however, no direct evidence for a system of this type that would be stringent enough to ensure faithful segregation.

## D. *Cis*- acting Chromosomal Features Involved in Pairing and Crossing Over

Genetic studies examining the meiotic behavior of chromosomal rearrangements have provided evidence that each of the six *C. elegans* chromosomes has a specialized chromosomal domain located near one end that has an important role in the pairing of homologous chromosomes. A key observation is that many reciprocal translocations behave as efficient crossover suppressors in *C. elegans* ([Rosenbluth and Baillie 1981](#); [Herman et al. 1982](#); [Ferguson and Horvitz 1985](#); [Fodor and Deak 1985](#); [McKim et al. 1988](#) [1993](#)). In individuals heterozygous for such reciprocal translocations, crossing over readily occurs in chromosomal segments extending from one end of the chromosome to the translocation breakpoint, but it is strongly suppressed or eliminated from the breakpoint to the other end of the chromosome ([Rosenbluth and Baillie 1981](#); [McKim et al. 1988](#) [1993](#)). Thus, each of the half-translocations consistently recombines with, and segregates from, only one of the two normal sequence chromosomes ([Rosenbluth and Baillie 1981](#); [McKim et al. 1988](#)). In the case of *eT1(III;V)*, for example, one half-translocation (consisting of the left portion of chromosome III and the left portion of chromosome V) always crosses over with and segregates from the normal chromosome III, whereas the reciprocal half-translocation consistently crosses over with and disjoins from the normal chromosome V. At the same time, crossing over is essentially eliminated for the right portion of chromosome III and the left portion of chromosome V. The fact that crossing over is strongly suppressed along the entire length of these translocated segments suggests that the absence of crossing over may result from a failure of these segments to pair with their homologs. Moreover, the ability of the reciprocal segments to recombine with their normal homologs suggests that features which facilitate homologous pairing are asymmetrically distributed on the chromosomes. Several translocations exhibit similar asymmetries in exchange and segregation behavior, and the accumulated data are all consistent with the proposal that each of the six chromosomes has a single localized domain, probably near one end, that facilitates crossing over, presumably through involvement in the process of homolog pairing ([Fig. 4](#)) ([McKim et al. 1988](#)).

What is the basis for crossover suppression in the reciprocal translocation heterozygotes? In many organisms, cytologically observable tetravalents form during meiotic prophase in reciprocal translocation heterozygotes, with each segment of the translocation chromosomes successfully pairing and forming crossovers with the corresponding segment of the normal sequence chromosomes ([Fig. 5a](#)). In *C. elegans*, the patterns of crossing over and segregation in balancer translocation heterozygotes are compatible with the absence of a tetravalent ([Fig. 5b](#)) and suggest instead that two separate bivalents may form, each of which includes a segment of homologous synapsis (where crossovers can occur) adjacent to a segment of nonhomologous synapsis (where crossovers cannot occur) ([Rosenbluth and Baillie 1981](#)). Reconstructions from electron microscope serial sections of pachytene nuclei from one translocation heterozygote suggest that this is in fact the case; six normal-appearing bivalents were observed, indicating that translocated chromosome segments had participated in nonhomologous synapsis ([Goldstein 1986](#)). Thus, crossing over is apparently suppressed because the translocated segments are sequestered away from their partners in a nonproductive synapsed configuration ([Villeneuve 1994](#)). The simplest interpretation of the genetic data is that only one of the two possible pairing configurations is adopted for a given translocation, despite the fact that in many cases, both configurations have comparable amounts of sequence identity. The dominant configuration is determined by the location of the specialized pairing domains involved in initiating an early event in the homolog pairing process.

Further evidence for these important pairing domains is the asymmetrical ability of chromosomal duplications derived from different ends of a chromosome to undergo meiotic exchange with a normal full-length chromosome. For example, of a pair of duplications that cover different ends of chromosome I (*sDp1* and *sDp2*), only the duplication of the right portion of chromosome I can undergo exchange with the normal homolog ([Rose et al. 1984](#)). Similar behaviors have been observed for duplications of the X chromosome ([Herman and Kari 1989](#)) and chromosome IV ([Rogalski and Riddle 1988](#)). In all of these cases, only duplications that are derived from the region of the chromosome predicted to contain the pairing domain (based on translocation studies) can recombine with the normal homolog, whereas duplications of other chromosomal regions do not.

These domains have been termed “homolog recognition regions” (HRRs) to denote their role in promoting the pairing of homologous chromosomes ([McKim et al. 1988, 1993](#)). They have also been referred to as “meiotic pairing centers” ([Villeneuve 1994](#)), employing terminology applied to potentially analogous chromosomal domains in maize ([Maguire 1986](#)). Although there is agreement that these chromosomal domains have an important role in homolog pairing, it is not known whether they function in the initial step of homolog recognition or in a later aspect of the pairing process.

Experiments examining the meiotic behavior of *X* chromosomes carrying deletions of the *X* chromosome HRR/pairing center region have provided additional information about the homolog pairing process ([Villeneuve 1994](#)). In hermaphrodites heterozygous for deficiencies of the left end of the *X* chromosome and a normal-sequence *X* chromosome, most *X* chromosomes were able to form crossovers with and disjoin from their homologs. This was true even for deficiencies that apparently removed the entire 4–5-map-unit region to which the HRR/pairing center had been localized by previous studies using translocations and duplications ([Herman et al. 1982; McKim et al. 1988; Herman and Kari 1989](#)). Only when the region was deleted from both homologs was a high frequency of noncrossover *X* chromosomes and a concomitant high frequency of *X* chromosome nondisjunction observed. Thus, the HRR/pairing center can apparently function even when it is present on only one of the two homologs. This meiotic behavior is inconsistent with the predictions of models proposing that the information content for homolog recognition is restricted to this region of the chromosome. According to this class of model, deletion of the region from only one of the two homologs would be just as detrimental as deleting it from both homologs, in either case rendering the homologs unable to find each other. The data instead suggest that the chromosomes utilize information outside the HRR/pairing center region to identify their pairing partners. It is not known whether autosomes deleted for their HRR/pairing center regions would exhibit meiotic behavior similar to that of the *X* chromosomes with HRR/pairing center deletions, since no comparable studies have been carried out.

How might an HRR/pairing center located near one end of a chromosome function to promote normal levels of crossing over along the entire length of the chromosome? Various related models have been proposed. One possibility is that the HRR/pairing center functions as an organizing center that nucleates the assembly of a bivalent which is competent to undergo crossing over, by acting as a binding site that loads *trans*-acting factors onto the chromosomes. These proposed *trans*-acting factors might function in the initial homolog recognition process, perhaps through involvement in a directional search for DNA homology that is initiated at the HRR/pairing center end of the chromosome. Alternatively, these *trans*-acting factors might function after homolog recognition, by promoting the initiation of homologous synapsis between prealigned chromosomes. In either case, the initial nucleation event would be followed by movement or distribution of factors along the length of the chromosomes, in a manner that would allow a chromosome with an intact HRR/pairing center to interact with a homolog from which the domain had been deleted. Initiation of synapsis in the vicinity of the HRR/pairing center would readily account for the observed and inferred synapsed configurations of various translocation heterozygotes. Furthermore, independent cytological evidence is consistent with a single site of synapsis initiation for the *X* chromosomes ([Goldstein 1984](#)). A variation on the above models is that the HRR/pairing center functions as a molecular address, targeting the end of the chromosome to a particular subnuclear location. This subnuclear localization would then serve to facilitate proper alignment and/or synapsis of homologous chromosomes.

Although the function of the HRR/pairing centers is required to promote normal levels of crossing over between homologs, it is unlikely that they are themselves the sites of initiation of recombination events (e.g., via the formation of double-strand breaks in the DNA), based on several considerations. First, crossovers frequently occur in regions of the chromosomes that are many megabases away from the HRR/pairing centers. Furthermore, in hermaphrodites heterozygous for some deletions ([Rosenbluth et al. 1990](#)), inversions ([Zetka and Rose 1992](#)), or insertions ([McKim et al. 1993](#)), crossovers have been observed to occur in intervals separated from the proposed HRR/pairing center by large stretches of nonhomologous DNA. It is difficult to envision how branch migration of hypothetical recombination intermediates could occur over such distances or through such obstacles. Moreover, initiation of a recombination event requires the presence of homologous DNA sequences

on both homologs, whereas the analysis of deletion heterozygotes has suggested that the *X* chromosome HRR/pairing center can function even when it is present on only one of the two homologs ([Villeneuve 1994](#)).

Growing evidence indicates that multiple additional meiotic sites may be involved in alignment of homologous chromosomes and/or the initiation of recombination. In particular, studies examining crossover distribution in deficiency heterozygotes have suggested that the autosomes may have secondary sites, near the ends of the chromosomes opposite to the HRR/pairing centers, that participate in homolog alignment ([Rosenbluth et al. 1990](#); [McKim et al. 1993](#)). Whereas these sites might be considered pairing sites, they are functionally distinct from, and subordinate to, the HRR/pairing centers.

Genetic and cytological experiments have provided evidence for chromosomal sites or domains in other organisms that may be analogous to the *C. elegans* HRR/pairing centers, although they differ in their chromosomal distribution. Whereas HRR/pairing center function appears to be concentrated to a single region on the small *C. elegans* chromosomes, the data suggest that there may be several pairing centers per chromosome in maize ([Maguire 1986](#)) and *Drosophila* ([Hawley 1980](#)).

## E. Genes Required for Wild-type Level and Distribution of Meiotic Crossovers

Because pairing and crossing over between homologs are required to ensure their disjunction at the meiosis I division, mutations in genes involved in these processes can be identified among mutations causing a high frequency of meiotic nondisjunction. The chromosomal sex determination mechanism and reproductive lifestyle of *C. elegans* can be exploited to isolate such mutations in a straightforward fashion ([Hodgkin et al. 1979](#); [Herman et al. 1982](#); [Villeneuve 1994](#)). Since males (XO) arise among hermaphrodite (XX) self-progeny at a frequency of 0.2% due to spontaneous nondisjunction of the *X* chromosome in the hermaphrodite germ line ([Hodgkin et al. 1979](#)), *C. elegans* mutants with increased nondisjunction are readily identifiable as hermaphrodites that produce increased frequencies of male self-progeny. Such mutants have been termed *him* mutants, for high incidence of males ([Hodgkin et al. 1979](#)).

### 1. Mutations Preferentially Affecting the X Chromosomes

Mutations in several genes, [\*him-1\*](#), [\*him-5\*](#), and [\*him-8\*](#), preferentially affect the segregation of the *X* chromosomes. These mutations cause not only a reduction in crossing over on the *X* chromosomes ([Hodgkin et al. 1979](#); [Herman and Kari 1989](#); [Broverman and Meneely 1994](#)), but also an altered distribution of the crossover events that do occur ([Broverman and Meneely 1994](#)). Although the mutants exhibit reduced recombination over most of the length of the *X* chromosomes, they have normal or elevated levels of recombination in genetic intervals at the left end of *X*, near the region proposed to contain the HRR/meiotic pairing center (see above). Such an altered distribution of crossovers suggests that these mutations do not cause defects in the recombination machinery itself, which might be expected to produce a more uniform reduction in crossover frequency. Rather, these mutations may instead affect a function involved in regulating the formation of crossovers, most likely some aspect of the pairing process responsible for identification and alignment of homologous chromosomes in a configuration that is productive for crossover formation, or some feature of chromosome architecture that mediates access of the recombination machinery to its chromosomal DNA substrates. Independent evidence that [\*him-8\*](#) may function in chromosome pairing comes from experiments showing that [\*him-8\*](#) mutants exhibit elevated levels of intrachromosomal and/or unequal crossing over between tandemly duplicated segments of the *X* chromosome; these events are normally inhibited by homolog pairing (A.M. Villeneuve, unpubl.; K. Tanner et al., pers. comm.).

Of these three genes, only [\*him-8\*](#) functions specifically in ensuring *X* chromosome segregation. Cytological analysis consistently reveals only a single pair of achiasmate chromosomes (the noncrossover *X* chromosomes) at diakinesis in [\*him-8\*](#) oocytes (D.G. Albertson; A.M. Villeneuve; both unpubl.). In contrast, [\*him-5\*](#) mutants exhibit some achiasmate autosomes (D.G. Albertson, unpubl.), as well as autosomal nondisjunction, and sterility at elevated temperatures (P. Meneely, pers. comm.). Furthermore, the isolation of several lethal [\*him-1\*](#) alleles

([Howell et al. 1987](#)) indicates that the *him-1* gene is required for some other essential function in addition to its role in meiosis.

## 2. Mutations Affecting All Chromosomes

Mutants defective for the segregation of the autosomes as well as the X chromosomes have been identified in either of two ways: (1) as *him* mutants that also produce a high frequency of inviable aneuploid zygotes ([Hodgkin et al. 1979](#); A.M. Villeneuve, unpubl.) or (2) as apparent maternal-effect embryonic lethal mutants that produce a low frequency of anatomically normal, fertile adult survivors, many of which are male, that by chance received a euploid (or near euploid) chromosome complement ([Kemphues et al. 1988a](#); J. Ahringer, pers. comm.). These include mutants defective in *him-2*, *him-3*, *him-6*, *emb-26*, and *him-14* ([Hodgkin et al. 1979](#); [Kemphues et al. 1988a](#); A.M. Villeneuve, unpubl.), as well as at least ten new complementation groups identified by directly screening for meiotic mutants (A.M. Villeneuve, unpubl.).

In the vast majority of these mutants, high nondisjunction apparently results from a failure to form crossovers between homologous chromosomes. Cytological analysis of oocyte chromosomes revealed a high frequency of achiasmate chromosomes at diakinesis in most of the mutants examined (K. Kemphues, pers. comm.; D.G. Albertson; A.M. Villeneuve; both unpubl.). Furthermore, in all cases tested, this high frequency of achiasmate chromosomes correlates with a substantial reduction in crossover frequencies measured in genetic mapping experiments ([McKim and Rose 1994](#); [Zetka and Rose 1995b](#); K. Kemphues, pers. comm.; A.M. Villeneuve, unpubl.). This indicates that the absence of chiasmata late in meiotic prophase is likely due to defects in chiasma formation rather than chiasma maintenance.

An altered distribution of a reduced number of crossovers was detected in strains carrying presumptive partial loss-of-function mutations in several of these genes, *him-3*, *him-6*, *him-14*, and *him(me9)* ([McKim 1990](#); [Zetka and Rose 1995b](#); L. Yip and A. M. Villeneuve, unpubl.). Thus, in every case examined in sufficient detail, *C. elegans* mutations that cause a reduction in the overall frequency of crossovers also cause an altered distribution of the residual crossover events. This observation suggests that screens for *C. elegans* mutants that produce viable gametes with abnormal chromosome complements may preferentially yield mutations in genes involved in regulating the formation of crossovers (e.g., through effects on pairing and alignment of homologous chromosomes, chromosome architecture, or crossover interference) rather than in genes encoding components of the recombination machinery itself. This apparent bias might reflect a requirement for recombination enzymes in essential functions such as DNA replication or repair. Alternatively, some recombination defects may prevent the formation of functional gametes, perhaps by triggering arrest of the cell cycle in response to unresolved or defective recombination intermediates. Another possible interpretation of the altered distribution of residual crossovers is that two (or more) separate pathways exist for meiotic recombination and that a given mutation affects only one of the pathways.

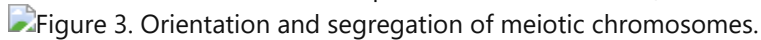
## Figures

Figure 2. Stages of meiotic prophase.

### Figure 2

Stages of meiotic prophase. (**a,b**) Chromosomes in unfixed dissected germ-cell nuclei stained with Hoechst 33342; (**c,d**) oocyte chromosomes fixed and stained with DAPI. (**a**) Nuclei at the pachytene stage of prophase I. Each of the brightly fluorescing elements is a pair of homologous chromosomes that are closely juxtaposed, or synapsed, in a side-by-side configuration along their entire lengths. The chromosomes are localized to the periphery of the nuclei. The arrow points to a homolog pair where it is possible to discern the two chromosomes. (**b**) Two nuclei at diplotene/diakinesis. Chromosomes have desynapsed and detached from the nuclear envelope. Arrows indicate chiasmata, the only remaining point of attachment between the homologs. (**c**) Late diakinesis in a wild-type oocyte. Chromosomes are maximally condensed and the six homolog pairs remain attached,

although the chiasmata can no longer be distinguished. (d) Late diakinesis in a mutant defective for crossing over on the X chromosomes. Arrows point to the achiasmate (noncrossover) X chromosomes. Bar, 5  $\mu$ m.

Figure 3. Orientation and segregation of meiotic chromosomes.

### Figure 3

Orientation and segregation of meiotic chromosomes. The axial orientation of the meiotic chromosomes at metaphase I and II was determined using fluorescent *in situ* hybridization with a probe for the ribosomal genes to label the ends of wild-type and translocation chromosomes. (a) Diagram of the *hT3(I)* and normal linkage group I chromosomes. In hermaphrodites heterozygous for the translocation *hT3(I;X)*, the *hT3(I)* chromosome, composed of material from the right end of *X* (*unshaded*) and the right end of *I* (*shaded*), pairs with and disjoins from the normal linkage group I chromosome ([McKim et al. 1993](#)). Both chromosomes carry wild-type copies of the ribosomal genes on the right end of the chromosome (*closed circles*). (b) Organization and orientation of the chromatids of the *+/hT3(I)* bivalent at diakinesis and metaphase I and the linkage group I chromatids at metaphase II. At diakinesis, the heterozygous bivalent is composed of the two half bivalents with the right ends in contact, so that at both diakinesis and metaphase I, the hybridization of the ribosomal probe is to the central portion of the bivalent. At metaphase II, hybridization of the ribosomal probe was to the ends of the chromatids proximal to the spindle poles on the axially oriented chromosomes. In the diagram, the normal linkage group I chromosome is shown at metaphase II, although either the *hT3(I)* or linkage group I chromosomes would adopt the same orientation and would not be distinguishable experimentally.

Figure 4. Physical map locations of the HRR/pairing centers.

### Figure 4

Physical map locations of the HRR/pairing centers. Each of the six *C. elegans* chromosomes is predicted to contain a specialized *cis*-acting chromosomal domain, termed the HRR or meiotic pairing center, that promotes pairing and crossing over between homologous chromosomes. For each chromosome, the shading indicates the region to which the proposed HRR/pairing center has been localized by experiments analyzing the recombination and segregation properties of translocations and duplications; the resolution of this mapping varies due to availability of informative chromosome rearrangements. The physical map was drawn using data from [Barnes et al. \(1995\)](#).

Figure 5. Possible pachytene pairing configurations in reciprocal translocation heterozygotes.

### Figure 5

Possible pachytene pairing configurations in reciprocal translocation heterozygotes. (a) Tetraploid structure predicted to form if DNA sequence identity alone were the sole determinant of the pachytene pairing configuration. The Xs indicate that crossovers can form in each chromosome segment. (b) Proposed pachytene pairing configuration for reciprocal translocations that act as crossover suppressors in *C. elegans*. Instead of a tetraploid, the data suggest that two bivalents form. The chromosome segments that are able to synapse with and form crossovers with their normal sequence homologs are those segments that contain the proposed HRR/pairing center, a specialized chromosomal domain located near one end of the chromosome that promotes homolog pairing. The remaining segments participate in nonhomologous synapsis and are thus unable to form crossovers.

## **Chapter 3. Chromosome Organization, Mitosis, and Meiosis — IV Prospects**

---

The combination of genetic, cytological, and molecular tools available for *C. elegans* has provided an initial picture of how the holocentric chromosomes are organized and how they segregate during mitosis and meiosis. In the future, our understanding of these processes will be extended by identification and characterization of *cis*-acting sites important for promoting segregation of normal and rearranged chromosomes in mitosis and meiosis and by the use of genetic screens to identify *trans*-acting factors required for the mitotic segregation of holocentric chromosomes. Continuing analysis of nematode telomeres and telomerases may also take advantage of *C. elegans* genetics to investigate the function, regulation, and maintenance of telomeres during development, to explore possible roles of telomeres and telomerase in aging, and to identify regulators of telomerase activity.

Genetic studies have led to the identification of both *cis*- and *trans*-acting components of the meiotic machinery responsible for pairing and crossing over between homologous chromosomes and for ensuring their disjunction at the meiosis I division. This analysis has entered the molecular phase. Gene products that direct the assembly of the oocyte meiotic spindle have already been identified. It will soon be possible to investigate how *trans*-acting factors involved in homolog pairing and crossover formation interact with each other and with the chromosomes themselves to achieve a normal level and distribution of meiotic crossovers. A major challenge will be to uncover the molecular nature of the *cis*-acting chromosomal domains involved in homolog pairing. Efforts in this area may be aided by completion of the physical map and the genome sequence.

Generated from local HTML

# **Chapter 4. Mutation**

---

## **Contents**

[I Introduction](#)

[II Induced Mutations](#)

[III Genetic Balancers](#)

[IV Genetically Detectable Genes](#)

[V What are Essential Genes?](#)

[VI Gene Distribution](#)

[VII Summary](#)

[Acknowledgment](#)

Generated from local HTML

## Chapter 4. Mutation — I Introduction

Mutations are tools that can be used to study the organization and function of the elements of a genome. Small random alterations in the DNA sequence can provide clues to the number of functional sequences in the genome, the mutability of the various sequences, and the functions of the various sequences. The study of DNA rearrangements such as translocations, duplications, deficiencies, and inversions can lead to an understanding of how homologs recognize each other and how they pair, recombine, and segregate (see [Albertson et al.](#), this volume). A sequenced genome may allow for the identification of all the proteins in the organism, but this does not provide sufficient information to identify the pathways and structures in which those proteins function. To take full advantage of the sequence information, it is necessary to integrate it with the cellular and developmental biology of the organism. This integration requires functional analysis of as many genes as possible, and this is most easily accomplished by mutation. Methods for generating mutations in *Caenorhabditis elegans* have been reviewed recently ([Anderson 1995](#)). In this chapter, we discuss the analysis of mutations.

The three types of mutagenesis are target-selected, spontaneous, and induced; the latter two are nonspecific. Target-selected mutagenesis is a powerful tool for generating mutations in any selected sequence ([Plasterk and van Leunen](#), this volume). A sequence is generally selected because it is known to have some function. The sequence may be a known gene, it may have matches in existing databases, or it may have been identified by sequence analyzing programs. Nonspecific mutagenic methods, on the other hand, have the advantage that they are inexpensive and, more importantly, are not limited to our current understanding of DNA sequences. Nonspecific mutagenesis can identify important sequences that may not have been identified by computer-assisted gene prediction methods. For example, genes such as *lin-4*, which encode small RNAs (see [Ambros](#), this volume), would not be detected as functional units by sequence analysis. Thus, mutagenesis can be viewed two ways: as a tool for specific sequence alteration and as a method to detect unknown aspects of genome function.

In general terms, recessive mutant phenotypes can be divided into three overlapping categories: visible, lethal, and conditional. Many genes have been altered to produce more than one category of mutants. The first two sets of spontaneous mutations studied in *C. elegans* were (1) in a locus controlling heat tolerance ([Fatt and Dougherty 1963](#)) and (2) two mutations giving dwarf phenotypes in the *Bergerac* strain ([Dion and Brun 1971](#)). The first mutants isolated in large mutagenic screens were viable with visibly altered morphology or movement ([Brenner 1974](#)). To date, 150 different categories of genes have been identified. Fourteen are categories of essential genes, mutations which result in lethal or conditional-lethal phenotypes. These include *emb* (abnormal embryogenesis), *let* (lethal), *mel* (maternal-effect-lethal), *mes* (maternal-effect sterile), *stu* (sterile uncoordinated), and *zyg* (zygote-defective). Twenty-six are categories of genes that have both visible and lethal alleles. In fact, more than one half of the known genetic loci in *C. elegans* have been mutated to produce a lethal phenotype ([Table 1](#)). Essential genes make up the largest class of genes in *C. elegans*; we estimate that 15–30% of the genes in *C. elegans* are essential. Similarly, in the yeast *Saccharomyces cerevisiae*, one quarter of the genes on chromosome I are essential ([Bussey et al. 1995](#)).

### Tables

**Table 1 Major gene classes**

Name	Phenotype	Number in class	Number with lethal alleles
<i>let</i>	lethality	464	464
<i>unc</i>	uncoordinated	114	13
<i>lin</i>	lineage-defective	48	14
<i>egl</i>	egg-laying-defective	46	3
<i>sup</i>	suppressor	37	6
<i>emb</i>	embryonic arrest	34	34

Name	Phenotype	Number in class	Number with lethal alleles
<i>daf</i>	dauer-defective or -constitutive	31	12
<i>mel</i>	maternal-effect lethal	29	29
<i>dpy</i>	umpy	26	2
<i>evl</i>	eversion of vulva	24	24
<i>che</i>	homeobox	21	2
<i>mab</i>	male abnormal	21	2
<i>spe</i>	sperm-defective	19	12
<i>eat</i>	eating abnormal	17	0
<i>mec</i>	mechanosensory abnormal	15	1
<i>him</i>	high-incidence male	14	0
<i>dyf</i>	dye-filling	13	0
<i>ced</i>	cell death	11	1
<i>zyg</i>	zygotic-arrest	11	11
<i>pat</i>	twofold arrest	9	9
Others		499	148
Total		1503	787

407 genes have been identified molecularly, but they have not yet been positioned genetically.

Generated from local HTML

## Chapter 4. Mutation — II Induced Mutations

---

### A. Classes of Mutagenesis

As stated above, mutagenesis, or the production of mutations, can be divided into three classes: spontaneous, induced, and target-selected. The first class, spontaneous mutagenesis, which is often unintentionally employed, is the production of mutations without the deliberate introduction of a mutagenic agent. The nature and frequency of the most common type of spontaneous mutations can vary between strains. In some strains, such as mutator strains, the majority of mutations appear to be the result of transposable element activity (see [Plasterk and van Leunen](#), this volume). In other strains, most mutational events are probably due to replication error, background irradiation damage, or environmental chemical mutagenesis, the latter type occurring fairly frequently in wild-type *C. elegans* (N2 strain). [Rosenbluth et al. \(1983\)](#) concluded that the frequency of spontaneous lethal mutations in the 15% of the genome that is balanced by the reciprocal translocation *eT1* is on the order of one mutation per 2000–3000 animals per generation. These authors pointed out that mutations accumulate in the balanced regions of strains that are propagated for extended periods of time.

The second class, induced mutagenesis, is the one most favored by geneticists. The range of usable mutagens is potentially quite large, although only a few have been well documented in *C. elegans* (for review, see [Anderson 1995](#)). These mutagens include (1) specific chemicals such as ethylmethanesulfonate (EMS), diethyl sulfate (DES), *N*-nitroso-*N*-ethylurea (ENU), or formaldehyde; (2) irradiation with X-rays,  $\gamma$ -rays, UV light, or ionizing particles; and (3) the introduction of a mutator locus such as [\*mut-2\*](#) into the genome, which in turn activates transposable element movement.

### B. Choice of Mutagen

Mutagenic methods provide either “point mutations” or larger-scale “chromosomal rearrangements.” Point mutations are defined by localized changes, i.e., transitions, transversions, or nucleotide additions or deletions (one or a few nucleotides). Chromosomal rearrangements include duplications (tandem, insertional, or free), deficiencies (deletions of DNA sequence), inversions, translocations, and more complex combinations of events. Rearrangements are frequently induced by irradiation, although they can be generated by some chemical mutagens. The distinction between point mutations and rearrangements can be a matter of degree. Deficiencies, for example, were traditionally defined by the genetic criterion that two or more adjacent loci were phenotypically “deficient,” and mutations in those loci failed to complement the deficiency. With the availability of the DNA sequence, however, the polymerase chain reaction (PCR) amplification of specific sequences can be used to determine if putative point mutations are actually small deficiencies. To achieve efficient induction of loss-of-function mutations in single genes, a mutagen that yields “point mutations” should be used. If the goal is to isolate larger mutations such as multigene deficiencies or chromosomal balancers, a “chromosome rearrangement” inducing mutagen should be used.

EMS is a potent and efficient mutagen for generating point mutations. The common effect is to cause G/C-A/T transitions, although it does produce some small deletions and other chromosomal rearrangements (see [Anderson 1995](#)). A potential alternative to EMS is ENU, which has about the same efficiency as EMS but produces both transitions and transversions, as well as some small deletions and other chromosomal rearrangements (B. De Stasio, pers. comm.).

Small deletions or rearrangements that disrupt one or a few genes can be generated by formaldehyde ([Moerman and Baillie 1981; Johnsen and Baillie 1988](#)), UV-irradiation ([Stewart et al. 1991](#)), or trimethylpsoralin (TMP) treatment followed by UV activation ([Lee et al. 1994; Yandell et al. 1994](#)). Both formaldehyde and UV mutagenesis yield similar types of mutations. Of 52 [\*unc-22\*](#) mutations, induced by either formaldehyde (17/27) or UV-irradiation (14/25), 31 were homozygous viable (J. Schein pers. comm.). Although a PCR-based method showed that only 2 of the 31 homozygous viable mutations were small deficiencies, the others could be very small deficiencies or point mutations. The 21 homozygous inviable mutations all proved to be deficiencies that

included adjacent essential genes. [Yandell et al. \(1994\)](#) reported the nature of 23 TMP-induced alleles of either [\*unc-22\*](#) or [\*pal-1\*](#). More than one-half (13) were deletions, and eight of these deletions ranged in size from 0.10 to 15 kb.

In addition to the induction of small deletions, formaldehyde, UV irradiation, TMP, and diepoxyoctane (DEO) ([Anderson and Brenner 1984](#)) are useful for generating intermediate-size deletions, duplications, and possibly inversions or translocations. Overlapping sets of intermediate-size chromosomal deficiencies and duplications allow mapping of genes to specific regions along a chromosome, whereas inversions and translocations are useful as balancers.

$\gamma$ -Irradiation ([Greenwald and Horvitz 1980](#); [Rosenbluth et al. 1985](#); [Finney et al. 1988](#); [Ruvkun et al. 1989](#); [Levin and Horvitz 1992](#); [Klein and Meyer 1993](#)), X-irradiation ([Sigurdson et al. 1984](#)), and UV-irradiation ([Stewart et al. 1991](#)) cause major rearrangements such as translocations, large duplications, inversions, and deficiencies, which are useful as balancers or for mapping genes to relatively large regions of the genome. A comparison of the number of genes deleted by formaldehyde-, UV-, or  $\gamma$ -irradiation-induced deficiencies in the *eT1*-balanced region of chromosome V shows that on average,  $\gamma$ -irradiation-induced deficiencies delete approximately twice as many genes as either formaldehyde- or UV-induced deficiencies ([Rosenbluth et al. 1985](#); [Johnsen and Baillie 1988, 1991](#); [Stewart et al. 1991](#)).

Mutators can mobilize transposable elements in the genome to generate a form of rearrangement. The [\*mut-2\*](#) locus can activate several families of transposons including Tc1, Tc3, Tc4, and Tc5 ([Collins et al. 1987, 1989](#); [Yuan et al. 1991](#); [Collins and Anderson 1994](#)). [\*mut-6\*](#) is effective at activating *Tc1* mobility ([Mori et al. 1988a](#)). The integrated transposons can be excised precisely to give revertants or imprecisely to yield a localized mutation. In some cases, even imprecise excision results in phenotypic reversion (see [Plasterk and van Leunen](#), this volume).

The mobilization of Tc1 can also generate large deficiencies extending to chromosome ends. [Clark et al. \(1990\)](#) generated Tc1 mutations in the *nT1(IV;V)* balanced region using the mutator [\*mut-4\*](#). Fifteen mutations that mapped to the left arm chromosome V were analyzed: Six were allelic with [\*lin-40\*](#), two identified other genes, and the remaining seven were deficiencies that were putative deletions of the end of the chromosome with breakpoints near [\*lin-40\*](#). The deficiencies of the chromosome end could be explained by the mobilization of resident Tc1 elements that were not followed by repair of the chromosome breaks. [Engels et al. \(1990\)](#) proposed that *P*-element loss in *Drosophila* is homolog-dependent and argued that *P* transposition created a double-strand break that was repaired by using the homolog as a template. [Johnsen and Baillie \(1991\)](#) proposed that a similar mechanism could explain the high incidence of chromosome end deficiencies generated by [\*mut-4\*](#) in the crossover-suppressed *nT1* translocated region. Translocations that act as crossover suppressors do not pair at meiosis ([Rosenbluth and Baillie 1981](#)). Therefore, the homolog of the crossover-suppressed region would not be available for use as a template to effect the type of repair proposed by [Engels et al. \(1990\)](#). If the homologous chromosome is used by *C. elegans* to repair Tc1 excision (see [Plasterk and van Leunen](#), this volume), then the mobilization of Tc1 in a translocation-balanced region would often be accompanied by a loss of the chromosome arm distal to the centromere.

## C. Application of Mutagens

Young adulthood is a good stage to mutagenize hermaphroditic worms because the number of germ-line nuclei is at its maximum. Young adults have all their sperm and also have oocytes in various stages of maturation. Treating younger worms increases the likelihood of "jackpots" or many mutants arising from one event. Young larvae contain a small number of rapidly dividing germ-line nuclei, and a mutation in one of these might be propagated to many gametes. "Jackpots" do not seem to pose a problem when young adults are mutagenized with EMS ([Johnsen and Baillie 1991](#)).

The interpretation of the results of a mutagenesis experiment requires caution. Most mutagens produce some level of all types of mutations, due to varied modes of action or because spontaneous mutations are often recovered along with the induced mutations. To avoid isolating strains that carry more than one mutation, the lowest possible level of mutagen required to achieve the desired results should be used. In addition, newly

isolated mutant strains should be backcrossed to an unmutagenized background and the desired mutations resegregated (see [Anderson 1995](#)). The number of backcrosses needed to adequately reduce the number of second-site alterations in the mutant stock depends on the dose of the mutagen used. For low doses of mutagen, where the probability of second-site mutations is low (described by [Rosenbluth et al. 1983, 1985](#)), backcrossing may not be necessary. Rosenbluth et al. (1983, 1985), [Johnsen and Baillie \(1988\)](#), and [Stewart et al. \(1991\)](#) have provided guidelines for appropriate doses of EMS,  $\gamma$ -irradiation, formaldehyde, and UV-irradiation (see [Anderson 1995](#)).

## D. Strategies for Mutagenesis

Two main strategies for obtaining mutations are forward genetics and reverse genetics. Forward genetics starts with a phenotype of interest and seeks mutants of that phenotype for analysis. Reverse genetics starts with a gene sequence and seeks to find animals with the gene of interest mutated. Both approaches have the goal of relating genotype to phenotype, but forward genetics starts with the phenotype, whereas reverse genetics starts with the genotype. Both approaches have strengths and weaknesses. Forward genetics ensures a phenotype of interest but may miss redundant genes or genes that do not play an important part under the set of conditions chosen for the mutant hunt. Reverse genetics ensures focus on a biochemically defined type of gene(s) but may lead to very diverse phenotypes (ranging from lethality to no obvious phenotype at all).

Forward genetic screening methods require no prior knowledge of the sequence function. The standard methodology is to apply a chosen mutagen to organisms with a phenotype that was selected to facilitate the screening for the desired type of mutation. For example, when screening for lethal mutations in a specific chromosomal region, an appropriate marker gene should be used. The absence of progeny with the marker phenotype indicates a linked lethal mutation. Forward genetic screens can be used to select for mutations in the entire genome or in localized regions. These types of screens can also be scaled to suit the researcher's requirements. For a review of the use of large-scale genetic screens for specific phenotypes, see [Rose et al. \(1994\)](#).

Reverse genetic methods require some knowledge of the sequence of the gene of interest. These target-selected methods include screens for Tc1 insertions ([Rushforth et al. 1993; Zwaal et al. 1993; Plasterk and van Leunen](#), this volume), promoter trapping ([Hope 1991](#)), and enhancer trapping ([Bellen et al. 1989; Bier et al. 1989; Wilson et al. 1989](#)). Induced mutagenesis can also be used to do reverse genetics. For example, [Yandell et al. \(1994\)](#) used chemical mutagenesis to isolate deletions that were recognized by a PCR assay. [Barstead and Waterston \(1991a\)](#) isolated mutants in the vinculin gene, [\*deb-1\*](#), by performing a screen for lethal mutations linked to a marker in the region of the genetic map corresponding to the physical location of the sequenced [\*deb-1\*](#) gene.

Generated from local HTML

## Chapter 4. Mutation — III Genetic Balancers

---

Although recessive lethal and sterile mutations cannot be maintained homozygously, methods using balancers have been developed that allow them to be maintained in heterozygous stocks fairly easily ([Rose and Baillie 1980](#); [Moerman and Baillie 1981](#); [Rogalski et al. 1982](#)). An early approach involved putting a lethal mutation in *trans* to a marker gene and then maintaining it by selecting wild-type animals. These wild types all contain the lethal mutation unless a crossover between the lethal mutation and the marker occurred to generate a wild-type chromosome. Progeny testing can be used to prevent loss of the lethal from the stock, but this is time consuming especially when a large number of lethal mutations are being maintained. A better method for isolating and maintaining large numbers of lethal mutations is the use of genetic balancers. [Edgley et al. \(1995\)](#) have produced a “field guide to balancers” listing the types of balancers, practical considerations for use, and the regions of the genome that have well-characterized balancers.

Balancers can be divided into two classes: (1) those that reduce or eliminate recombination between a mutation-bearing chromosome and a homolog that carries the wild-type allele, e.g., translocations, inversions, and possibly deficiencies, and (2) those that provide an extrachromosomal or integrated exogenous piece of DNA that complements a homozygous mutation, e.g., duplications and extrachromosomal transgenic arrays. In general, the first class of balancers are rearrangements that balance large genomic regions, allowing for the isolation and maintenance of lethal mutants in many genes. They also allow for choice in markers that are useful for following the lethal mutations since the only requirement is that the marker lie within the balanced region. Variants of the balancers can be generated or constructed that are useful for the analysis of the balanced region as well as the balancer itself.

### A. Translocations, Duplications, Inversions, and Deficiencies

The first reciprocal translocation identified in *C. elegans* was *eT1(III;V)* ([Rosenbluth and Baillie 1981](#)), which is a reciprocal exchange of the left half of chromosome V with the right half of chromosome III. The exchanged segments have never been shown to recombine with their normal homologs, whereas the nonexchanged ends undergo homologous recombination. In fact, the boundaries of *eT1*'s crossover suppression have been shown to correspond to the translocation breakpoints ([Rosenbluth and Baillie 1981](#)). The regions that recombine segregate from each other during meiosis ([Rosenbluth and Baillie 1981](#); [McKim et al. 1988, 1993](#); [Albertson et al., this volume](#)). [Rosenbluth and Baillie \(1981\)](#) proposed that regions do not recombine because they cannot pair with their normal homologs, in contrast to most other organisms studied in which translocated regions do recombine with their partners. This failure to recombine (balancing) provides a powerful tool for *C. elegans* genetics. Reciprocal translocations that balance regions of other chromosomes have been identified (see [Edgley et al. 1995](#)), and the results suggest that only one end of each chromosome can be involved in an exchange (see below). These regions are the left arms of chromosomes I and V and the right arms of chromosomes II, III, IV, and X. Therefore, reciprocal translocations cannot be used to balance the entire genome.

Duplications have also proven to be effective balancers. Some free duplications recombine with the normal homolog ([Rose et al. 1984](#)), but most do not ([Herman et al. 1979](#)). Those that recombine do so on the same end of each chromosome that recombines in translocation heterozygotes. It has been proposed that one end of the chromosome contains a homolog-pairing region that initiates subsequent meiotic events such as recombination and disjunction ([Rosenbluth and Baillie 1981](#); [McKim et al. 1988](#)). Duplications that do not recombine make good balancers for some regions that are not balanced by a translocation. A good example of this is *sDp3* (a duplication of chromosome III), which balances almost all of the chromosome not balanced by *eT1* (H. Stewart and D. Baillie, unpubl.). Another advantage of using large free duplications as balancers is that progressively smaller duplications can be derived and used as mapping tools. For example, *sDp2*, which balances almost the entire left half of chromosome I ([Howell et al. 1987](#)), was broken into shortened derivatives by means of  $\gamma$ -irradiation ([McKim and Rose 1990](#)). These derivatives were used for mapping essential genes to localized areas ([Howell and Rose 1990](#); [Peters et al. 1991](#); [McKim et al. 1992](#); [McDowall 1990, 1996](#)). However, some free duplications can shorten spontaneously ([McKim and Rose 1990](#)) and their use for mapping mutations should be

avoided. Free duplications have also been shown to be excellent tools for the analysis of gene function. They can be lost in [somatic cells](#) during development, allowing for mosaic analysis of chosen genes ([Herman 1984, 1987](#) ; [Bucher and Greenwald 1991](#)).

One proven inversion, *hln-1*, has been characterized ([Zetka and Rose 1992](#)). It inverts a region on the right half of chromosome I ([unc-75](#) to [unc-54](#)) and has proven to be an effective balancer for that region.

Deficiencies can also dominantly suppress recombination ([Rosenbluth et al. 1990](#); [McKim et al. 1992](#)). Several deficiencies on the left half of chromosome V were shown to suppress recombination toward the center of the chromosome but not toward the left end ([Rosenbluth et al. 1990](#)). This suppression can extend 15–20 map units and in some cases suppresses more than 90% of the expected recombination events. Thus, deficiencies could prove to be useful as balancers.

## B. Transgenic Rescue of (Lethal) Mutations

Balancers generally cover large regions of the genome and, although invaluable for maintaining lethal mutations, are of limited use as fine-scale mapping instruments. A number of balanced regions have been subdivided into zones by sets of overlapping duplications and/or deficiencies ([Edgley et al. 1995](#)). These are useful for mapping lethal mutations to relatively small regions by classical genetic techniques but are still not sufficient to correlate genetically identified genes with their physical map positions. A technique for mapping lethal mutations to the physical map using transgenic strains ([McKay 1993](#); J.S. McDowall and A.M. Rose, unpubl.) consists of constructing transgenic strains, which carry small free duplications created by microinjection of overlapping cosmids, and using them in complementation tests against lethal mutations. These transgenic arrays can also be used as balancers or even for masking phenotypes during strain construction. Twenty-two transgenic strains were used in large-scale experiments to rescue lethal mutations in the *dpy-5* to *dpy-14* region of chromosome I ([McKay 1993](#); [McDowall 1996](#)). The physical map of *C. elegans*, including the *dpy-14* region, is essentially complete ([Coulson et al. 1986, 1991](#) ; [Waterston et al.](#), this volume), and one half to three quarters of the essential genes in the *dpy-5 dpy-14* region have been identified genetically ([McDowall 1990](#)). Overlapping cosmids were microinjected to create transgenic strains and 25 mutant genes were rescued, providing links between the genetic and cosmid maps and ultimately the sequence map. This technology allows researchers to go directly from a gene of interest identified from the genomic sequence map to mutations in that gene.

A large-scale cosmid rescue project is in progress on chromosome III, where 50% of the sequenced portion of the chromosome is represented by more than 100 transgenic strains carrying groups of overlapping cosmids as extrachromosomal arrays. These arrays behave like free duplications in genetic crosses, and, so far, more than 50 lethal mutations have been rescued using those transgenic strains (D. Janke et al., unpubl.). Similar projects, using transgenic lines carrying cosmids or yeast artificial chromosomes (YACs) to rescue mutant phenotypes, have been carried out in the *unc-22* (IV) region ([Clark and Baillie 1992](#); J.E. Schein et al., unpubl.) and in the *rol-3* (V) region (B. Barbazuk, unpubl.).

Generated from local HTML

## Chapter 4. Mutation — IV Genetically Detectable Genes

---

For regions of the genome where the complete sequence is known, it is possible to estimate what fraction of the genes can be revealed by mutagenesis. To do this, one must be able to identify all of the genes in the sequence and to calculate how many genes are detectable through saturation mutagenesis of the region. There are several commonly used criteria for determining if a sequence is a gene. One is to match the putative coding sequence to the coding sequences of known genes. The presence of appropriately positioned strong splice sequences and open reading frames are also used to determine whether a sequence is likely to contain a gene regardless of whether the sequence exhibits database similarity. A more compelling criterion comes from showing the existence of RNA products or cDNAs derived from them. Gene-finding programs generally appear to do a good job of predicting the existence of genes, although they may not correctly identify all features of a gene.

The second requirement for determining the fraction of genes that have detectable phenotypes calls for a calculation of the number the genes that could be detected by saturation mutagenesis. Saturation mutagenesis itself is impossibly stringent for a number of reasons. First, the mutagens used may not be able to mutate every gene to a detectable phenotype. Second, the phenotype produced may not be easily recognized. For example, dauer-defective mutants are unable to produce dauer larvae (see [Riddle](#), this volume), a phenotype that would not be detected if the screened worms were not starved and overcrowded. An additional difficulty is that the dauer induction pathway is itself temperature-dependent ([Golden and Riddle 1984a](#)), and null alleles of several genes in the pathway are temperature-sensitive. Such mutants would not be detected unless the screens were performed at restrictive temperature. Multiple copy or functionally redundant genes are usually not detected unless mutations in them are dominant neomorphic alleles. An example of this is the [act-1](#), [act-2](#), [act-3](#) family ([Landel et al. 1984](#); [Waterston et al. 1984](#); see [Moerman and Fire](#), this volume). These types of problems are mitigated by combining the skills and genetic screens of the entire *C. elegans* community, but all phenotypes have not yet been detected. Third, some genes are very small targets for mutagenesis and will not be detected very often, whereas other genes are large targets. Fourth, the amount of effort needed to screen for and identify every mutable gene is prohibitively large. The identification of new genes by screening for mutants approximates a Poisson distribution, so that for each consecutive screening of the same number of chromosomes, fewer and fewer new genes are identified. The diminishing returns for the time and effort invested make complete saturation for genes untenable.

Without the complete genetic saturation of large sequenced regions, we must extrapolate the number of mutationally identifiable genes from the regions where some form of saturation mutagenesis has been attempted (about half the genome). From the regions where saturation mutagenesis for lethals has been attempted, we can estimate the percentage of genes that can be mutated to a lethal phenotype. The gene densities for each region were calculated by [Barnes et al. \(1995\)](#). The *sDp2* balanced region of chromosome I has a minimum of 225 essential genes ([Howell and Rose 1990](#); [McDowall 1996](#)), which is approximately 22% of all the genes in the region. The *unc-93* to *dpy-19* region of chromosome III has a minimum of 293 essential genes (H. Stewart, pers. comm.), which is approximately 24% of the genes identified in the genomic sequence. The *unc-22* region of chromosome IV has a minimum of 55 genes ([Clark et al. 1988](#)), which is approximately 10% of the total genes. The *eT1*-balanced region of chromosome V has a minimum of 120 essential genes ([Johnsen and Baillie 1991](#)), which again is about 10% of the total. It should be noted that the calculations for total gene numbers are inherently biased and yield only minimum estimates. We postulate that between 15% and 30% of *C. elegans* genes are essential.

To date, 10% (1503) of the 15,000 total genes estimated by the genome sequencing project ([Waterston et al. 1992](#); [Wilson et al. 1994](#); M. Marra; S. Jones; both pers. comm.) have been genetically identified. They consist of 716 visible and 787 essential genes that have been classified into 150 categories (see Appendix 1). If 15–30% of all genes are essential, then there is a total of 2250–4500 essential genes, and the 787 identified essential genes represent one third to one sixth of this total. R. Feichtinger, H. Schnabel, and R. Schnabel (pers. comm.) estimate an additional 450 (280–1000) maternal-effect lethal genes in *C. elegans*, but the essential genes and maternal-

effect gene classes are not exclusive sets. At least 7% of the characterized essential genes also have maternal-effect lethal alleles ([Johnsen and Baillie 1991](#)).

[Park and Horvitz \(1986a\)](#) estimated that mutants in up to 50% of *C. elegans* genes may be wild type when null. The analysis of deficiencies of the *let-56* - *unc-22* region of chromosome IV showed that the deletion of at least two of the four genes immediately to the left of *unc-22* yields no obvious phenotype in an *unc-22* background ([Schein et al. 1993](#)). This supports the idea that a large fraction of *C. elegans* genes have no obvious null phenotype. The genes that show no null phenotype are probably redundant genes, genes in redundant pathways, or genes that need specific environmental factors to reveal a phenotype. Functionally redundant genes have been detected genetically by dominant, neomorphic mutations ([Waterston et al. 1984; Park and Horvitz 1986a](#)).

Generated from local HTML

## Chapter 4. Mutation — V What are Essential Genes?

---

The most common class of identified genes is composed of essential genes. The categories of essential genes include a broad range of lethal mutant phenotypes that block survival or reproduction. Lethal mutations range in developmental blocking stages from egg to larval, sterile, and maternal-effect. Examination of the lethal phenotypes can provide information about the function of the gene product. Some, like [let-653](#), show gross morphological defects ([Jones and Baillie 1995](#)), and others can be correlated with physiological or developmental pathways by mosaic analysis ([Bucher and Greenwald 1991](#)) or gene interactions ([Barbazuk et al. 1994](#)). In one case, suppression of a lethal phenotype was used as a selection for genetic duplications ([Marra and Baillie 1994](#)).

Some categories of mutations cannot be readily defined as essential or nonessential. Examples of this are the *daf* mutations in which dauer-constitutive mutants cannot mature and are lethal, whereas dauer-defective mutants go through the normal life cycle and could only be considered lethal under conditions that require dauer formation. Another example is the *lin* mutations, which are defined by altered cell lineage development. Some of these defects are lethal, whereas others are not. Taking these caveats into account, approximately 20% of the genes originally represented by visible mutations, and more than one half (787/1503) of all identified genes, now have lethal alleles ([Table 1](#)). As more work is done, an even larger proportion of genes may prove to be mutable to lethality, and many of the genes identified only by lethal alleles may yield visible alleles.

In screens for visible mutations, lethals are generally not recovered, and in screens for lethals, visibles are usually missed. In some cases, the original phenotype has been shown to be atypical. Examples include *bli-4* for which only the original allele (e937) results in blistered cuticle ([Brenner 1974](#)), and all 12 other alleles result in late embryonic arrest ([Peters et al. 1991; Thacker et al. 1995](#)); *unc-70*, for which the original allele (e524) results in an uncoordinated phenotype ([Brenner 1974](#)), whereas at least seven other alleles are lethal ([Johnsen and Baillie 1991](#)); and *rol-3*, for which two alleles (e754 and e202) result in rolling ([Higgins and Hirsh 1977](#)), one allele is a temperature-sensitive lethal and there are 11 nonconditional lethal alleles ([Johnsen and Baillie 1991](#)). In contrast, *unc-60* is an example of a gene for which most of the alleles give a visible phenotype. However, one allele, which proved to be a small internal deletion, is lethal. *unc-60* encodes two alternatively spliced products, and it appears that both must be deleted in order for the essential function to be revealed ([McKim et al. 1994](#)). The *unc-52* gene also encodes alternatively spliced mRNAs, and the protein products function in the basement membranes underlying muscle cells. Nonlethal alleles are clustered in three adjacent, alternatively spliced exons that affect some, but not all, of these proteins, whereas lethal alleles eliminate gene function ([Rogulski et al 1995](#)).

Are essential genes mostly “housekeeping” genes, i.e., are they mainly required in general processes necessary for cell operation such as intermediary metabolism or are they mainly important in specific developmental processes such as determination, differentiation, or morphogenesis? Many essential genes function in both embryogenesis and later stages ([Hirsh and Vanderslice 1976; Vanderslice and Hirsh 1976](#); Schierenberg et al. 1980; [Miwa et al. 1980; Wood et al. 1980; Cassada et al. 1981](#)), and numerous genes are expressed throughout embryogenesis ([Schauer and Wood 1990](#)). These results led to the proposal that most zygotic essential genes have “housekeeping” functions. [Bucher and Greenwald \(1991\)](#) tested this by designing an elegant mosaic screen that circumvented the difficulties of analyzing the phenotypes of early blocking lethal mutations. These authors screened for zygotic lethal mutants in an *unc-36 glp-1 ncl-1* triple-mutant genetic background using the duplication *qDp3*, which covers the major gene cluster on chromosome III, including the markers. The duplication is occasionally lost in mitotic cells, resulting in genetic mosaicism. The genetic marker *ncl-1* results in enlarged nucleoli, enabling the cell division at which loss of the duplication occurred to be precisely defined. The foci of *unc-36* and *glp-1* are in different, nonoverlapping, parts of the lineage. The *unc-36* focus is in the early blastomere ABp, whereas the *glp-1* focus is P<sub>4</sub>, so loss of *qDp3* in AB or ABp results in an Unc phenotype; loss in P<sub>1</sub>, P<sub>2</sub>, P<sub>3</sub>, or P<sub>4</sub> results in a sterile worm. The genetic mosaic screen classified zygotic-lethal mutations based on their foci. Genes involved in general “housekeeping” functions should be required in all lineages, whereas genes involved in specific processes would have their foci in only defined parts of the lineages. The majority of genes examined (12/17) functioned in specific early pathways and therefore were not “housekeeping” genes. This is comparable to findings in *Drosophila*, where 60% of the lines containing reporter gene insertions associated with

recessive zygotic-lethal mutations have cell-type-specific expression ([Bier et al. 1989](#)). These results imply that the majority of essential genes in higher organisms are developmentally regulated.

Generated from local HTML

## Chapter 4. Mutation — VI Gene Distribution

---

The haploid *C. elegans* genome consists of 100 Mbp of DNA on five autosomes and an X chromosome. Each chromosome participates in about one recombination event per meiosis (see [Albertson et al.](#), this volume). As a result of this high level of interference, each chromosome is about 50 map units long. [Brenner \(1974\)](#) mapped visible mutations and found that each autosome has a central cluster of genes and smaller tip clusters separated by gene-sparse regions, whereas the X chromosome has a more even spacing of genes. The distributions noted by Brenner for the visible mutations continue to hold. The large regions in which essential genes have been intensively mapped follow the same pattern of distribution; i.e., chromosome I ([Howell et al. 1987](#)) and chromosome V ([Rosenbluth et al. 1988](#); [Johnsen and Baillie 1991](#)) both show the same distribution pattern. The distribution of recombination events along the chromosomes may be under the control of repetitive elements. At least two families of repeats show nonrandom distribution along the chromosomes (CeRep3 and RcS5). The approximately 120 copies of CeRep3 follow *C. elegans* recombinational distribution with no or few repeats in the central clusters and concentrations of repeats in the regions of high recombination. Cangiano and La Volpe (1993) have proposed that CeRep3, in conjunction with other elements, may promote recombination. The meiotic clustering of crossover events can be eliminated by a mutation in the gene [rec-1](#), demonstrating that the distribution of recombination events is under genetic control ([Zetka and Rose 1995b](#)).

Each chromosome has approximately the same number of genes, with two thirds of them in the central clusters, which is only about 5 map units long, and one third of them in the arms ([Barnes et al. 1995](#)). Not only are the genes clustered recombinationally, but they are also clustered physically (see [Waterston et al.](#), this volume). There is a higher density of genes in the central portions of the autosomes (about one per 5 kb on chromosome III) than in the arms (about one per 11 kb for chromosome III) ([Wilson et al. 1994](#)). The gene-dense regions have well-defined boundaries and are of similar physical lengths for each autosome (4.8– 7.7 map units) ([Barnes et al. 1995](#)). The boundaries of the recombinationally defined clustering and the physically defined clustering also appear to correspond. The differential gene spacing between the clusters and the arms is not sufficient to explain the degree of clustering shown on the genetic maps. Thus, the gene clustering on the genetic map is the combined effect of both gene density and regional differences in recombination frequency.

Generated from local HTML

## Chapter 4. Mutation — VII Summary

---

The sequencing of entire genomes is revolutionizing the study of higher organisms. When all of the proteins encoded in a genome can be identified, the challenge becomes to relate the knowledge gained from sequence analysis to the organism's biology. The study of mutant phenotypes is a key to achieving this goal. Currently, there are two bottlenecks blocking the integration of the two types of information. First, the biological information is lagging behind the sequence information in that only about 10% of the 15,000 genes of *C. elegans* are represented by mutations. The largest class of mutable genes (15–30% of all genes) are those with essential functions (lethals). The analysis of the lethals obviously will play an important part in the deciphering of the genome and developing a deeper understanding of *C. elegans* biology. Second, mapping sequences to mutants is a slow process. The Rose and Baillie laboratories have undertaken a large-scale effort to construct transgenic strains using cosmids that have been sequenced by the Genome Sequencing Centers in Hinxton, U.K., and St. Louis, U.S.A. These strains are being made available to the research community to facilitate high-resolution genetic mapping of the sequenced region of the genome. Information about the transgenic strains is available at <http://darwin.mbb.sfu.ca/imbb/dbaillie/cosmid.html>

This high-resolution approach to alignment of the genetic and physical maps is made possible by the high density of lethal mutations that have been identified in selected regions of the genome. Currently, more than 50 lethals have been localized to cosmids by means of transgenic rescue, and it is anticipated that this project will ultimately result in the alignment of at least one essential gene per cosmid in regions approaching genetic saturation. With the completion of the genome map, these resources will allow researchers to move rapidly from sequence to biological function.

Generated from local HTML

## **Chapter 4. Mutation — Acknowledgment**

---

We thank Ann Rose for discussion and comments on the manuscript.

Generated from local HTML

# **Chapter 5. Transposons**

---

## **Contents**

- [I Introduction](#)
- [II Tc1 and Tc3](#)
- [III Other Elements](#)
- [IV The Tc1/\*mariner\* Family](#)
- [V Regulation of Tc1/\*mariner\* Transposition](#)
- [VI Mechanism of Tc1 Transposition](#)
- [VII Repair After Tc1 Excision](#)
- [VIII Tc1 as a Tool in \*C. elegans\* Research](#)
- [Acknowledgments](#)

Generated from local HTML

## Chapter 5. Transposons — I Introduction

---

The *Caenorhabditis elegans* genome is approximately 30 times smaller than the human genome, but it is estimated to contain only 5 times fewer genes ([Wilson et al. 1994](#); [Waterston et al.](#), this volume). The compact worm genome results from shorter unique noncoding sequences (such as introns) and from fewer repeated sequences. It is not yet clear what role repeated sequences have in the *C. elegans* genome. An interesting hypothesis is that these elements are involved in meiotic recombination ([La Volpe et al. 1988](#); [Naclerio et al. 1992](#)). Part of the repetitive DNA probably has no function for the nematode at all; it may represent parasitic or selfish DNA. In their simplest form, these molecular parasites or transposons are single genes. They ensure their own spread by initiation of their own replication within genomes (see [Plasterk 1993](#)).

In this chapter, we review what is known about transposable elements in *C. elegans*, their mechanism of transposition, and their regulation. We discuss how transposons are used for the genetic analysis of *C. elegans*, and we focus on elements that have been shown to be mobile. The *C. elegans* genome also contains elements whose structure suggests that they are or were transposons, such as retroelement-like sequences ([Britten 1995](#); [Youngman et al. 1996](#)); these elements are not described in detail here. Emphasis is placed on the Tc1 element, which causes the majority of gene inactivations in certain natural strains of the worm. It is also the transposon that has been studied in most detail and is used most often for gene mapping and for gene inactivation. In parallel, we discuss the related element Tc3, which is the second most active transposon in the nematode.

Generated from local HTML

## Chapter 5. Transposons — II Tc1 and Tc3

---

Molecular and genetic approaches led to the discovery of the first transposable element in *C. elegans*: Tc1 (an amusing account of its discovery was published by [Anderson et al. \[1992\]](#)). Emmons and Hirsh noticed the frequent polymorphism between genomic clones of different strains ([Emmons et al. 1979](#)), one of which proved to be caused by a Tc1 insertion ([Emmons et al. 1983](#)). [Rozenzweig et al. \(1983a\)](#) and [Liao et al. \(1983\)](#) discovered a Tc1 element while cloning and sequencing actin genes. These molecular approaches identified Tc1 elements, but it took genetic approaches to establish the mobile nature of Tc1. [Eide and Anderson \(1985b\), 1988](#) used the [unc-54](#) myosin gene as a target to trap transposons, and [Moerman and Waterston \(1984\)](#) and [Moerman et al. \(1986\)](#) made use of the mobile nature of Tc1 to clone another muscle gene, [unc-22](#), by transposon tagging.

Tc1 is an element of 1610 bp with 54-bp terminal inverted repeats ([Fig. 1](#)) ([Rozenzweig et al. 1983a](#)). Tc1 elements always integrate into the sequence TA ([Rozenzweig et al. 1983a; Eide and Anderson 1988; Mori et al. 1988b; Zwaal et al. 1993; van Luenen and Plasterk 1994](#)). The copy number of Tc1 is strain-dependent: The Bristol N2 strain contains approximately 30 copies of Tc1, whereas the Bergerac BO strain contains more than 500 Tc1 copies per haploid genome ([Emmons et al. 1983; Liao et al. 1983; Egilmez et al. 1995](#)).

The Tc1 insertion pattern within the *C. elegans* species shows interesting features. The copies present in the standard laboratory strain Bristol N2 (the genome of which is being sequenced) are also present in high-copy-number strains ([Egilmez et al. 1995](#)). In addition, high-copy-number strains such as Bergerac contain at least 500 additional Tc1 insertions. Comparison of a limited number of Tc1 insertion sites among different high-copy-number strains shows that these strains often contain a subset of the Bergerac elements, such that regions of the genome either are completely devoid of the Bergerac Tc1 copies or contain the entire set ([Egilmez et al. 1995](#)). This patchy distribution suggests that these strains arose by crosses of a high-copy-number strain with a low-copy-number strain.

The Tc1 element contains one large open reading frame that was initially thought to encode a 273-amino-acid Tc1 transposase ([Rozenzweig et al. 1983a](#)). This protein was produced in *Escherichia coli* and was found to have a strong but nonspecific affinity for DNA ([Schukkink and Plasterk 1990](#)). However, transposition requires a specific interaction of the transposase with the transposon DNA. Sequence comparisons with other *Caenorhabditis* species ([Schukkink and Plasterk 1990; Prasad et al. 1991](#)) and cDNA analysis ([Vos et al. 1993](#)) indicated the presence of a small 5' exon and suggested that the complete coding region might be 343 triplets long. Expression of this larger protein (Tc1A) in the Bristol N2 strain results in enhanced somatic transposition of Tc1 ([Vos et al. 1993](#)). Furthermore, Tc1A purified to 95% homogeneity from a recombinant *E. coli* strain was recently shown to be sufficient for mediating Tc1 excision and transposition in vitro ([Vos et al. 1996](#)). The Tc1A-specific DNA-binding domain is largely contained within the extra 5' exon, explaining the lack of specific binding by the 273-amino-acid protein. The properties of 343-amino-acid Tc1 transposase (Tc1A) are discussed below.

The Tc3 element is present in approximately 15 copies per haploid genome in all strains analyzed thus far ([Collins et al. 1989](#)). Tc3 is 2335 bp long and has terminal inverted repeats of 462 bp ([Fig. 1](#)). The element contains a gene composed of two exons encoding Tc3A, the 327-amino-acid transposase of Tc3 ([van Luenen et al. 1993](#)). This conclusion is based on arguments similar to those for Tc1A. Forced expression of Tc3A induces Tc3 transposition in vivo, and recombinant Tc3A binds specifically to the Tc3 inverted repeats in vitro.

Tc1 and Tc3 have several common characteristics ([Collins et al. 1989](#)). The proteins encoded by the two elements are 34% identical. The terminal nine nucleotides of Tc1 and Tc3 are almost identical. Both elements integrate exclusively into the sequence TA, and transposition activity of both elements is affected by the same "host" mutation (the [mut-2](#) mutation discussed below).

## Figures

Figure 1. Structure of the DNA transposons of *C. elegans*.

### Figure 1

Structure of the DNA transposons of *C. elegans*. (Black boxes) Inverted repeats; (arrows) open reading frames.

Generated from local HTML

## Chapter 5. Transposons — III Other Elements

---

Tc2 elements are heterogeneous in length. The longest and most abundant Tc2 species (see [Fig. 1](#)) is 2074 bp in length and has 24-bp terminal inverted repeats ([Ruvolo et al. 1992](#)). The subterminal Tc2 sequence contains multiple direct repeats. Tc2 contains several large open reading frames, but transcripts have not been analyzed to confirm the intron/exon structure of the gene. The open reading frames have no homology with known proteins. Tc2 integrates into the sequence TA. Transposition of Tc2 has thus far only been detected in the offspring of inter-strain crosses between Bristol N2 and Bergerac BO ([Levitt and Emmons 1989](#)). Transposition of Tc1 and Tc2 might be coregulated, because *C. elegans* strains with a high Tc1 copy number also contain a high Tc2 copy number (20—25 elements), whereas strains with a low Tc1 copy number contain only 4—6 copies of Tc2 ([Levitt and Emmons 1989; Ruvolo et al. 1992](#)).

The Tc4 element is different from the previously described transposons because it is a fold-back element ([Yuan et al. 1991](#)). This type of transposable element consists mainly of two large inverted repeats. Examples of fold-back elements have been found in *Drosophila* ([Truett et al. 1981; Potter 1982](#)) and in sea urchin ([Liebermann et al. 1983](#)). Tc4 is approximately 1.6 kb in length and consists of almost perfect inverted repeats of 774 bp separated by a short unique sequence ([Fig. 1](#)). There is some heterogeneity among the elements. No open reading frame has been found in the Tc4 sequence. The element duplicates a 3-bp target sequence (TNA) upon integration. Approximately 20 copies of Tc4 per haploid genome occur in both Bristol N2 and Bergerac BO. A subpopulation of Tc4 elements (Tc4v, approximately five elements per haploid genome) contains a 2343-bp unique sequence which replaces a 477-bp internal fragment in one of the inverted repeats ([Li and Shaw 1993](#)). A transcript from the Tc4v element has been isolated that could encode a 537-amino-acid protein. This larger element could provide in trans the transposase needed for mobilization of all Tc4 elements. Tc4 elements have been found to transpose in the germ line of the Bergerac TR679 strain ([Collins et al. 1987](#)). This strain carries [mut-2](#), which also affects transposition of Tc1, Tc3, and Tc5.

The Tc5 element is present in four to six copies per haploid genome ([Collins and Anderson 1994](#)). Transposition of Tc5 is only detected in the [mut-2](#) genetic background. The element is 3171 bp long ([Fig. 1](#)) and has terminal inverted repeats of 491 bp (J. Collins, pers. comm.). Tc4 and Tc5 have a few common characteristics. The terminal nucleotides of Tc4 and Tc5 have an eight out of ten match; the Tc5 inverted repeat contains a 7-bp repeated sequence that is also present in the Tc4 inverted repeat, and the Tc5 transcript encodes a putative protein of 532 amino acids, which has an overall identity of 33% with the Tc4v protein. Furthermore, integration of Tc4 and Tc5 results in duplication of the same trinucleotide sequence.

Tc6 is a fold-back element ([Fig. 1](#)) consisting of 765-bp inverted repeats separated by a short unique sequence ([Dreyfus and Emmons 1991](#)). The Tc6 elements are heterogeneous in size because of internal deletions and insertions. All strains that have been analyzed contain 20—30 Tc6 copies per haploid genome. Transposition activity of Tc6 in the germ line or the soma has not yet been detected. The terminal six nucleotides of Tc6 are identical to the terminal nucleotides of Tc1 and Tc3, and Tc6 integrates into the sequence TA just like Tc1 and Tc3. No open reading frames have been found in the Tc6 sequence.

Generated from local HTML

## Chapter 5. Transposons — IV The Tc1/mariner Family

Members of the Tc1/mariner family of transposable elements have been identified in many species from different phyla ([Table 1](#)). The best-characterized elements from this large family of transposons are the Tc1 element from *C. elegans* and the mariner element from *Drosophila mauritiana*. Family members have terminal inverted repeats that end with a highly conserved sequence (5'-CAGTGC), they integrate into the sequence TA, and they contain a single gene encoding a related polypeptide. An alignment of the open reading frames found in the Tc1-like elements has been published by [Henikoff \(1992\)](#).

Other Tc1/mariner elements have been detected by hybridization, polymerase chain reaction (PCR) amplification, or database searches in different nematode species ([Abad et al. 1991](#); [Sedensky et al. 1994](#)), planarians ([Garcia-Fernández et al. 1993](#)), arthropods ([Brierly and Potter 1985](#); [Harris et al. 1988](#); [Lidholm et al. 1991](#); [Robertson et al. 1992](#); [Robertson 1993](#); [Bigot et al. 1994](#)), and vertebrates, including humans ([Henikoff 1992](#); [Goodier and Davidson 1994](#); [Auge-Gouillou et al. 1995](#); [Oosumi et al. 1995](#)), and have not yet been analyzed in detail. More distantly related members of the Tc1/mariner family have been found in bacteria (the IS630 element [[Tenzen et al. 1990](#); [Doak et al. 1994](#)]) and in ciliated protozoa (the Tec1, Tec2, and TBE1 elements [[Klobutcher and Jahn 1991](#); [Doak et al. 1994](#)]).

The wide distribution of Tc1/mariner elements could be explained by the presence of an early ancestor of the element before these species diverged, or by horizontal transfer, or by a combination of both ([Capy et al. 1994](#)). The data obtained for the mariner-like elements suggest horizontal transmission, because highly homologous elements were isolated from distantly related fly species; more closely related fly species contain less conserved elements ([Robertson 1995](#)). In addition, the mariner-like element (MLE) of *C. elegans* is more closely related to the fly mariner elements than to the *C. elegans* Tc1 element ([Sedensky et al. 1994](#)). Sequence comparison of the Tc1-like elements does not always imply horizontal transmission; the phylogeny of the elements studied by [Radice et al. \(1994\)](#) is consistent with the evolutionary phylogeny of the species.

### Tables

**Table 1** Characteristics of Tc1/mariner elements in different species

Phylum	Species	Name	Length (bp)	IR (aa)	ORF Tc1 (%)	Identity to	Target duplication	Terminal nucleotides	Reference
Fungi	<i>Fusarium</i>	Fot1	1928	44	542		TA	AGTCAA	<a href="#">Daboussi et al. (1992)</a>
	<i>oxysporum</i>	impala	1280	27			TA	CAGTGG	<a href="#">Langin et al. (1995)</a>
Nematode	<i>Caenorhabditis</i>	Tc1	1610	54	343	—	TA	CAGTGC	<a href="#">Rosenzweig et al. (1983a)</a>
	<i>elegans</i>	Tc3	2335	462	329	34	TA	CAGTGT	<a href="#">Collins et al. (1989)</a>
		Tc6	1603	765			TA	CAGTGC	<a href="#">Dreyfus and Emmons (1991)</a>
		MLE		28	339				<a href="#">Sedensky et al. (1994)</a>
	<i>Caenorhabditis briggsae</i>	Tcb1	1616	80	336	74	TA	CAGTAC	<a href="#">Harris et al. (1988)</a>

<b>Phylum</b>	<b>Species</b>	<b>Name</b>	<b>Length (bp)</b>	<b>IR (aa)</b>	<b>ORF Tc1 (%)</b>	<b>Identity to</b>	<b>Target duplication</b>	<b>Terminal nucleotides</b>	<b>Reference</b>
Arthropod	<i>Drosophila melanogaster</i>	Bari-1	1728	28	339	27	TA	ACAGTC	<a href="#">Caizzi et al. (1993)</a>
		pogo	2121	21	499		TA	CAGTAT	<a href="#">Tudor et al. (1992)</a>
		HB1	1655	30	320	27	TA	CAGCTG	<a href="#">Brierly and Potter (1985)</a>
	<i>Drosophila hydei</i>	Minos	1775	255	341	32	TA	CAGTGC	<a href="#">Franz and Savakis (1991)</a>
	<i>Drosophila heteroneura</i>	Uhu	1646–1655	46–50	273	40	TA	CAGTGT	<a href="#">Brezinsky et al. (1990)</a>
	<i>Drosophila mauritiana</i>	mariner	1286	28	345	36	TA	C/TCAGGT	<a href="#">Jacobson et al. (1986)</a>
Vertebrate	<i>Eptatretus stouti</i>	Tes1	1495	64	407	40	TA	CTCTAC	<a href="#">Heierhorst et al. (1992)</a>
		Brachydanio rerio	1205	52			TA	CAGT	<a href="#">Radice et al. (1994)</a>
		<i>Salmo gairdneri</i>	Tsg1	1689		335		CAGT	<a href="#">Radice et al. (1994)</a>
	<i>Salmo salar</i>	SALT1	1535	35	385		TA	CAGTGC	<a href="#">Goodier and Davidson (1994)</a>
			Tss1-2	1619	27	399		CAGT	<a href="#">Radice et al. (1994)</a>
		IpTc1	1135	85					<a href="#">Henikoff (1992)</a>

Generated from local HTML

# Chapter 5. Transposons — V Regulation of Tc1/mariner Transposition

---

Although all natural isolates of *C. elegans* contain Tc1, frequent germ-line transposition occurs only in some isolates, such as Bergerac BO ([Emmons et al. 1983](#), 1986; [Emmons and Yesner 1984](#); [Moerman and Waterston 1984](#); [Eide and Anderson 1985b](#)). It has not been detected in others, such as the Bristol N2 strain ([Emmons et al. 1983](#); [Emmons and Yesner 1984](#); [Moerman and Waterston 1984](#); [Eide and Anderson 1985a,b](#)). Transposition frequency is both strain-specific and tissue-specific ([Emmons and Yesner 1984](#); [Eide and Anderson 1985b](#), 1988; [Emmons et al. 1986](#); [Harris and Rose 1986](#); [Moerman et al. 1986](#); [Collins et al. 1987](#)). Tc1 elements in the soma of Bristol N2 excise frequently, whereas Tc1 elements in the germ line do not. The difference in transposition frequencies between strains is not simply explained by the copy number of Tc1 elements, since no correlation exists between Tc1 copy number and transpositional activity ([Eide and Anderson 1985b](#); [Mori et al. 1988a](#)). Transposition in the germ line most likely requires the expression of specific copies of the transposon (mutators).

## A. Mutators

Transposition proficiency can be attributed to genetic factors, so-called mutators or *mut* genes ([Mori et al. 1988a](#); [Mori 1989](#)). The transposition-proficient strain Bergerac BO contains several *mut* loci dispersed over the genome, and these *mut* genes appear to be mobile themselves ([Moerman and Waterston 1984](#); [Mori et al. 1988a](#)). It has therefore been suggested that these genes may represent copies of the Tc1 element. Mapping of the *mut-5* gene has identified three copies of Tc1 that cosegregate with *mut-5* and are therefore candidates for this mutator ([Mori et al. 1988a](#); [Mori 1989](#)).

One explanation of why these copies are germ-line mutators, whereas other Tc1 elements are not, could be that internal deletions or point mutations make these latter elements unable to produce transposase. Such nonautonomous elements have been observed for many types of transposons (e.g., the Ds element in maize [[McClintock 1951](#); for review, see [Fedoroff 1989](#)]). However, all Tc1 elements are of the same size ([Emmons et al. 1983](#); [Liao et al. 1983](#); [Egilmez et al. 1995](#)), and there are only a few sequence polymorphisms between the Tc1 elements ([Eide and Anderson 1985b](#); [Rose et al. 1985](#)). Only one of the sequenced Tc1 elements contains a premature stop codon and is therefore unable to produce a complete transposase protein ([Plasterk 1987](#)). A more likely explanation is that chromosomal position is important for establishment of an expression pattern that turns a Tc1 element into a mutator. The mutator of *mariner* in *D. mauritiana* referred to as the *Mos* factor ([Bryan et al. 1987](#); [Medhora et al. 1988](#)) has been cloned and found to be a copy of the *mariner* element ([Medhora et al. 1991](#); [Capy et al. 1992](#)). The *Mos* factor is most likely an activator of *mariner* elements because of its chromosomal location.

[van Luenen et al. \(1993\)](#) showed that forced expression of Tc3 transposase in a Bristol N2 strain activated jumping of endogenous Tc3 elements. A Tc3 element taken out of its chromosomal context and fused to an inducible promoter can activate transposition of other Tc3 elements when expression of Tc3A is induced; this element has become a somatic mutator. This result is consistent with the chromosomal location model suggested above, but it is also compatible with the alternative explanation. The Tc3 element introduced in N2 was isolated from a mutator strain, TR679 ([Collins et al. 1989](#)). This element could produce an active transposase, whereas all Tc3 elements in Bristol N2 are mutated and therefore inactive. The same is true for the observation that occasionally the N2 strain gives rise to a mutator strain (see [Moerman and Waterston 1989](#); [Babity et al. 1990](#)). It is conceivable that a mutation may occur within one of the nonautonomous transposons to make it a mutator, but perhaps a more likely explanation is that the absence of transposase expression in the germ line of N2 is not absolute, so that occasionally Tc1 elements in N2 may jump. If one of these elements lands in a region where it can be expressed in the germ line, it then becomes a mutator.

## B. *mut-2* and High-hopper Strains

The *mut* genes discussed above should not be confused with another factor affecting Tc1 and Tc3 transposition, the *mut-2* gene ([Collins et al. 1987](#)). The *mut-2* mutant was isolated after a mutagenic treatment of a Bergerac BO derivative (which is already transposition-proficient) and was initially recognized as a factor that enhanced reversion of a Tc1 insertion mutant of the *unc-54* gene. It was subsequently found to enhance transposition and excision of Tc1 and also of Tc3 and other transposons ([Collins et al. 1987](#), 1989; [Yuan et al. 1991](#); [Collins and Anderson 1994](#)). The *mut-2* mutation in this high-hopper strain (TR679) was mapped to chromosome I (Finney 1987). It is unlikely that *mut-2* is also a copy of Tc1, since it activates other transposons. Studies with Tc1 and Tc3 transposase in transgenic N2 strains have shown that the transposase of one element cannot activate jumping of the other ([Vos et al. 1993](#)). Mutagenic treatment of a nonmutator strain also resulted in a mutation (*mut-7*) that activates transposition of different transposons in the germ line (R. Ketting and R. Plasterk, unpubl.). It will be interesting to define the molecular nature of *mut-2* and *mut-7*.

Generated from local HTML

# Chapter 5. Transposons — VI Mechanism of Tc1 Transposition

---

## A. *Trans* Requirements

Transposition of DNA transposons is dependent on two factors: *cis*-acting factors (the transposon sequence and the target sequence) and *trans*-acting factors (the transposase and possibly additional host factors). The Tc1 and Tc3 transposases are, respectively, 343 and 329 amino acids in length (Fig. 2). The transposase protein contains two DNA-binding activities: a site-specific DNA-binding activity contained within the first 68 amino acids and a second nonspecific DNA-binding activity within the central part of the protein (Vos et al. 1993; Colloms et al. 1994; Vos and Plasterk 1994). The minimal sequence-specific DNA-binding domain of Tc1A (amino acids 1–68) recognizes the terminal sequence of the Tc1 inverted repeat (between positions 12 and 26). Additional sequence-specific contacts (between nucleotides 7 and 13) are made by an extended DNA-binding domain (amino acids 1–142). This second specific DNA-binding domain is not able to bind independently of the first domain.

A weak sequence homology has been noted between the paired domain and the DNA-binding domains of the Tc1 transposase and the transposase encoded by the Minos element from *Drosophila* (Franz et al. 1994). The paired domain is a conserved amino acid motif found in mammalian and *Drosophila* developmental genes (for review, see Gruss and Walther 1992). The significance of this homology is strengthened by the similar way in which these domains interact with their DNA-binding site (Vos and Plasterk 1994). The amino-terminal part of the bipartite domain (for Tc1A amino acids 1–68) interacts with the 3' part of the binding site (for Tc1 between positions 12 and 26), and the carboxy-terminal half of the domain (for Tc1A amino acids 68–142) binds to the 5' part of the binding site (for Tc1 between positions 7 and 13).

Differential splicing of P transposase results in either an active or an inactive transposase, and this leads to a tissue-specific regulation (Laski et al. 1986). A systematic analysis of the transposase transcripts in *C. elegans* has been complicated by the presence of multiple Tc1 copies in all *C. elegans* strains. Furthermore, it has not yet been possible to distinguish relevant transposase transcripts from irrelevant read-through transcripts. There are, however, indications that truncated Tc1 transposase proteins could be involved in regulation of transposition (Vos et al. 1993). Truncated versions of transposase proteins regulate P-element (Misra and Rio 1990), Tn5 (Isberg et al. 1982; Johnson et al. 1982), and IS7 (Escoubas et al. 1991) transposition.

The Tc1 and Tc3 transposases have no extensive homology with other transposases other than the Tc1/*mariner* family. However, the Tc1/*mariner* transposases contain a so-called DDE motif (Doak et al. 1994). This motif (two aspartic acid residues and a glutamic acid residue, the latter two separated by 35 residues) was first identified in retroviral integrases and bacterial IS transposases (Fayet et al. 1990; Khan et al. 1991). The DDE motif is part of the catalytic domain of the transposase (Fig. 2) and is thought to position a cation that plays an important part in the phosphoryl transfer reaction (Engelman and Craigie 1992; Kulkosky et al. 1992; van Gent et al. 1992; Skalka 1993). The retroviral integrases and bacteriophage Mu transposase are inactive when the DDE motif is mutated (Drelich et al. 1992; Engelman and Craigie 1992; Kulkosky et al. 1992; LaFemina et al. 1992; van Gent et al. 1992; Leavitt et al. 1993; Baker and Luo 1994). The DDE motif is not so well conserved in the Tc1/*mariner* family. The second aspartic acid residue and the glutamic acid residue are separated by only 34 residues, and an aspartic acid residue is found at the position of the glutamic acid residue in the *mariner*-like elements. However, Tc1A and Tc3A are inactive when any of these residues is mutated (van Luenen et al. 1994; Vos and Plasterk 1994). The DDE motif is indeed important for function. Thus, there may be a fundamental similarity in the catalysis of transposition of different types of elements: bacterial transposons, retroviruses, and DNA transposons in eukaryotes.

It has recently been demonstrated that Tc1A is the only nematode protein required for the Tc1 transposition reaction (Vos et al. 1996). Tc1A produced in insect cells or in *E. coli* can mediate precise Tc1 excision and transposition in vitro. The protein purified from *E. coli* is more than 95% pure, which strongly argues that Tc1A is the only protein required for transposition. However, a contribution of a contaminating protein to the transposition reaction cannot be fully excluded. Although transposase alone seems to be capable of mediating

transposition, there might be other *trans*-acting factors that stimulate transposition, similar perhaps to IHF and HU which are involved in bacterial recombination events ([Mizuuchi 1992a](#)) or HMG proteins which are involved in eukaryotic DNA transactions ([Grosschedl et al. 1994](#)).

## B. *Cis* Requirements

The inverted repeat of Tc1 (54 bp) contains a binding site for Tc1A located between positions 7 and 26 ([Vos et al. 1993; Vos and Plasterk 1994](#)). The Tc3 inverted repeat is longer (462 bp), and each inverted repeat contains two sequences that are recognized by the DNA-binding domain of Tc3A ([Colloms et al. 1994](#)). The terminal binding site for Tc3A is located between positions 9 and 28 and a second Tc3A-binding site is located around position 190. It is not without precedent that termini of transposons contain multiple binding sites for their transposase ([Mizuuchi 1992a](#)). Each Mu end contains three MuA-binding sites ([Craigie et al. 1984](#)), most of which are required for Mu transposition ([Groenen et al. 1985](#)), and many plant transposable elements have long arrays of transposase-binding sites near their termini ([Gierl et al. 1988; Kunze and Starlinger 1989](#)). The transposition frequency of these plant transposons is reduced when one or more of the binding sites are removed. However, when the internal Tc3 sequence was deleted, so that only the terminal 94 bp of each end were present, the deleted element was still able to transpose at a normal frequency (H.G.A.M. van Luenen and R.H.A. Plasterk, unpubl.).

The inverted repeats of Tc1, Tc3, and some other members of the Tc1/*mariner* family end with a well-conserved sequence, 5'-CAGTGC (see [Table 1](#)), suggesting that this sequence has an important functional role. In vitro, these bases are not protected by the transposase in a DNase I protection assay using partially purified transposase ([Vos et al. 1993; Colloms et al. 1994; Vos and Plasterk 1994](#)); they are probably transiently recognized during the catalytic step of the transposition reaction. When this conserved sequence is mutated in Tc1, the ends are no longer cleaved by Tc1A in vitro ([Vos and Plasterk 1994; Vos et al. 1996](#)). However, Tc3 elements with mutated ends do transpose in vivo with a reduced efficiency (H.G.A.M. van Luenen and R.H.A. Plasterk, unpubl.). A similar organization is found in bacterial transposons, where the most terminal base pairs are not important for binding of the transposase but are required during the catalysis of the transposition reaction ([Mizuuchi 1992a](#)).

## C. Target-site Selection

Tc1 and Tc3 exclusively integrate into the sequence TA ([Rosenzweig et al. 1983a,b; Eide and Anderson 1988; Mori et al. 1988b; Collins et al. 1989; Franz and Savakis 1991; Zwaal et al. 1993; van Luenen and Plasterk 1994](#)). The integration sites of Tc1 and Tc3 are not randomly distributed among the TA dinucleotides in the genome; there are hot spots and cold spots for integration, and this preference is Tc1- or Tc3-specific ([van Luenen and Plasterk 1994](#)). One Tc1 element inserted in a hot spot for integration in the *unc-54* gene was shown to revert with a higher frequency than elements inserted in cold spots ([Eide and Anderson 1988](#)). However, Anderson and co-workers recently found that the most common footprint left after loss of this element (four additional base pairs) fortuitously results in reversion. For most insertions, the most common footprint will not result in a phenotypic reversion ([Rushforth and Anderson 1995](#)). Thus, the frequency of Tc1 loss is generally greater than the reversion frequency.

Although hot spots and cold spots are not clustered, they can be close together, separated by only a few nucleotides ([van Luenen and Plasterk 1994](#)). There are also regional differences in insertion and excision frequency. A good example is the *unc-22* gene, which is hit approximately 100 times more frequently than the *unc-54* gene, whereas the coding region of *unc-22* is only three times larger than that of *unc-54* ([Moerman and Waterston 1984; Eide and Anderson 1985b](#)). Again, these estimates of gene inactivation frequencies reflect insertion frequencies corrected for the chance that an insertion fails to inactivate the gene.

What makes one TA dinucleotide a more preferred target over another? The most likely explanation for the target choice is the sequence flanking the TA dinucleotide. Alignment of the flanking sequences of all Tc1 and Tc3 insertion sites suggests a weak sequence preference ([Eide and Anderson 1988; Mori et al. 1988b; van Luenen and Plasterk 1994; H.C. Korswagen et al., in prep.](#)). Note that in some studies, germ-line insertions were

compared, whereas in other cases, somatic insertions were compared. Theoretically, this might result in different hot spots, although recent work on in vitro integrations with purified transposase strongly suggests that the target-site choice is made by the transposase only ([Vos et al. 1996](#)). For reviews on this subject for other transposons, see [Sandmeyer et al. \(1990\)](#), [Craigie \(1992\)](#), and [Bushman \(1993\)](#).

## D. Target Duplication

Integration of Tc1/*mariner* elements results in a duplication of the TA sequence into which they integrate, as does the bacterial IS630 element ([Tenzen et al. 1990](#); [van Luenen et al. 1994](#)). It was noted that the T on one side and the A on the other side of the transposon might actually be part of the inverted repeat of the transposon ([Rosenzweig et al. 1983b](#); [Ruan and Emmons 1987](#); [Eide and Anderson 1988](#)). This alternative explanation for the target duplication was investigated for Tc3 by replacing the flanking TA dinucleotides with another sequence ([van Luenen et al. 1994](#)). The elements with modified flanking sequences transposed normally (indicating that the immediate flanking sequence did not affect excision of the element), and the newly integrated elements were again flanked by TA nucleotides. This, in combination with the biochemical analysis of the transposon intermediate described below, shows that the T and the A are part of the flank and not the transposon and that integration results in a 2-bp target duplication.

## E. Transposition Intermediates

Transposition of DNA transposons is initiated by single- or double-strand cleavages at the ends of the element. The intermediate in the transposition reaction of Tn10, Tn7, Mu, and retroviruses always carries a 3'-hydroxyl group at the 3'end, and this 3'end coincides with the last nucleotide of the transposon sequence ([Mizuuchi 1992a](#)). Extrachromosomal Tc1 and Tc3 DNAs that could be part of the intermediate in the transposition reaction have been detected ([Rose and Snutch 1984](#); [Ruan and Emmons 1984](#); [van Luenen et al. 1993](#)). The majority of extrachromosomal Tc3 elements are present as linear DNA molecules ([van Luenen et al. 1993](#)). This DNA has been purified and the structure determined ([van Luenen et al. 1994](#)). Again, the 3'end of the excised transposon coincides with the last nucleotide of the element, and it contains a 3'-hydroxyl group. The 5'end is phosphorylated and is located two nucleotides within the element ([Fig. 3](#)). The excised Tc1 fragment observed in an in vitro system has a similar structure ([Vos et al. 1996](#)). The consequences of this structure for the integration reaction are discussed in the next section.

Excised circular Tc1 elements have also been observed ([Rose and Snutch 1984](#); [Ruan and Emmons 1984](#)). PCR amplification and sequence analysis of these elements reveal a heterogeneous population either with complete ends separated by one or more TA dinucleotides or with one or two deleted ends ([Radice and Emmons 1993](#)). The heterogeneity of the extrachromosomal circular Tc1 elements and the deletions of the ends strongly suggest that they are not intermediates but side products of the transposition reaction.

## F. Chemistry of the Transposition Reaction

The chemistry of Mu transposition (for review, see [Mizuuchi 1992b](#)) and retroviral integration (for reviews, see [Varmus and Brown 1989](#); [Goff 1992](#); [Mizuuchi 1992b](#); [Skalka 1993](#); [Vink and Plasterk 1993](#)) has largely been elucidated. Tc3 has three features in common with Mu and retroviruses: the structure of the transposition intermediate (a free 3'-hydroxyl group attached to the last nucleotide at the 3'ends of the element), the presence of a DDE motif in the transposase, and the target duplication upon integration. This suggests that the chemistry of Mu and retroviral transposition applies to Tc3 transposition ([van Luenen et al. 1994](#)). The element is excised, creating a 3'-hydroxyl group at the 3'end ([Fig. 3](#)). This end contains the complete Tc3 sequence, whereas the 5'end lacks two nucleotides. The 3'-hydroxyl groups of both ends are linked with a 2-bp stagger to the TA target sequence in a concerted reaction. After repair, this results in the integration of a complete Tc3 sequence plus the duplication of the TA.

## Figures

Figure 2. Structure of Tc1 and Tc3 transposases.

## Figure 2

Structure of Tc1 and Tc3 transposases. The DDE motifs, minimal sequence-specific DNA-binding domains (*solid line*), and nonspecific DNA-binding domains (*dotted line*) are indicated.

Figure 3. A schematic model for Tc1/Tc3 transposition explaining the excision and integration of the element, the target duplication, and the generation of the footprint.

## Figure 3

A schematic model for Tc1/Tc3 transposition explaining the excision and integration of the element, the target duplication, and the generation of the footprint. The model is described in the text. Black arrows indicate the cleavage sites at the ends of the transposon and also where strand transfer reactions take place during integration. Only the most common somatic footprint is indicated.

Generated from local HTML

## Chapter 5. Transposons — VII Repair After Tc1 Excision

---

It is important to distinguish transposon excision—the reaction by which the transposon is released from flanking DNA sequences by two double-strand DNA breaks—from transposon loss. The latter event consists of excision followed by repair of the double-strand break left behind in the donor DNA. Strictly speaking, the excision is probably always precise, and it is the subsequent repair that can result in precise or imprecise loss of the transposon. It is likely that the transposon does not “care” what happens to the break it leaves behind, in the sense that the repair is probably mechanistically identical to that of any double-strand DNA break in the worm genome and totally carried out by proteins that are not transposon-encoded. [Emmons et al. \(1983\)](#) showed that somatic excision of Tc1 could be monitored by Southern blot analysis, which reveals an empty donor restriction fragment, i.e., a fragment of which the size would suggest that the transposon is more or less precisely lost. Apparently, the cell puts the two flanks together again without much loss or addition of sequences. Analysis of the sequence at the junctions of the repaired somatic donor sites indicates that some microheterogeneity exists, resulting in “footprints” of only a few base pairs ([Ruan and Emmons 1987](#); [Eide and Anderson 1988](#); [van Luenen et al. 1994](#)). As shown in Figure 3, the excision leaves two nucleotides of each 5' transposon end behind at each end of the double-strand break, and indeed some of these are present in the footprint. The difference between excision and transposon loss has been visualized by synchronized induction of transposase expression. Expression leads to the appearance of a broken DNA donor fragment, which is subsequently chased into a repaired fragment (R.H.A. Plasterk and H.G.A.M. van Luenen, unpubl.).

Repair of the donor break in the germ line is discussed here in some detail because it is important for several applications of the transposon in genetic analysis. It has not yet been possible to detect the products of germ-line excision in a direct physical assay. Only repair products that result in reversion of a phenotype have been analyzed, and this implies a bias in product selection. Nevertheless, a common footprint is TAcaTA ([Eide and Anderson 1988](#); [Plasterk 1991](#)), which would indicate that the direct ligation of the broken ends occurs in [germ cells](#) as well. The resulting 4-bp footprint would of course lead to a frameshift in a coding region and therefore usually goes unnoticed in a reversion screen.

[Kiff et al. \(1988\)](#) noted that among revertants of an *unc-22* Tc1-insertion allele, there were rare alleles that contained a deletion. [Zwaal et al. \(1993\)](#) took a reverse genetic approach to show that such deletions occur among the progeny of most Tc1 insertion mutants. The endpoints of these deletions are often at short direct repeats, suggesting that the two broken DNA ends scan each other's flank until a match is found, after which the break is sealed at that point and the intervening sequence is lost. Anecdotal evidence suggests that the events occur at widely different frequencies for different insertion alleles, and thus the excision frequency may be different for each genomic position or the preferred repair products may be sequence-dependent.

A third class of repair products differs from direct ligation or deletion and results from a template-dependent repair process. [Plasterk \(1991\)](#) found that frequent precise loss of a Tc1 element depends on the presence of a wild-type sequence on the homologous chromosome. The wild-type sequence is used to repair the double-strand break, resulting in an apparent precise excision. Among rare revertants of a homozygous Tc1 allele are products that result from partial template-directed repair, and these contain short stretches of the transposon ends as a footprint. The same template-dependent repair process has been described by Engels for the *Drosophila* P element ([Engels et al. 1990](#)).

Mechanistically similar to this allelic template-directed repair is repair that uses an ectopic template. The main difference is the searching process that precedes the alignment of template and broken ends; the relative inefficiency of this process may explain the reduced frequency of ectopic template usage. [Plasterk and Groenen \(1992\)](#) showed that an extrachromosomal transgenic array could be used as template to repair the break after excision of Tc1 from a chromosomal *unc-22* gene. The transgene contained *unc-22* sequences marked with some polymorphisms, and these polymorphisms were found copied into the repaired *unc-22* gene. This method can in principle be used to shuttle any point mutation into the chromosome, provided a nearby transposon insertion is present.

Generated from local HTML

## Chapter 5. Transposons — VIII Tc1 as a Tool in *C. elegans* Research

---

Tc1 is the only member of the Tc1/*mariner* family that has been used extensively as a tool for genetic analysis. We discuss three present applications of Tc1, and three possible future applications.

### A. Identification and Isolation of Genes

The frequency of gene inactivation by Tc1 insertion varies among different strains and different genes, but in mutator strains such as RW7000 and “high-hopper” strains such as TR679, the frequency of transposon insertion mutants of some genes is approximately 1 per 1000 meioses ([Moerman and Waterston 1984](#); [Collins et al. 1987](#)). For a more detailed description of strain, gene, and transposon specificity of insertion frequencies, see [Anderson \(1995\)](#). Since not all transposon insertions result in functional mutations of the target gene ([Rushforth et al. 1993](#); [Rushforth and Anderson 1995](#)), the estimate based on forward mutant hunts may differ significantly from insertion frequencies based on reverse genetic screens. In many cases, it has been possible, after a gene has initially been defined by an ethylmethanesulfonate (EMS)-induced mutation, to isolate a Tc1-tagged allele of that gene. After several backcrosses with the low Tc1 copy number N2 strain, Southern blot analysis is done to identify a possible copy of Tc1 that cosegregates with the mutant allele. A size-selected plasmid library is generated and screened with a Tc1-specific probe. The flanks of the Tc1-containing plasmids are isolated and the insertion site is identified. Firm evidence that this transposon insertion is responsible for the mutant phenotype is usually obtained after the isolation of a revertant that will have lost the transposon, and its restriction pattern will be (virtually) identical to that of the wild type. This strategy of transposon tagging was followed for the cloning of [unc-22](#) ([Moerman et al. 1986](#)), [lin-12](#) ([Greenwald 1985](#)), and many genes since.

### B. Gene Mapping

In cases where no Tc1-tagged allele of a gene of interest was available or could easily be obtained, Tc1 has been used for mapping. The high Tc1 copy number strains contain up to 500 copies of Tc1, approximately 1 per 200 kbp (Egilmez and Shmookler Reis 1994). These can be used to align the genetic and physical map in areas of interest, and thus lead to map-based cloning of genes, for example, [lin-14](#) ([Ruvkun et al. 1989](#)).

A variant of this approach has become available. [Williams et al. \(1992\)](#) devised a multiplex PCR strategy that allows quick mapping of genes after a single cross with a high Tc1 copy number strain. They described a set of 40 Tc1 alleles for this purpose. Recently, H.C. Korswagen et al. (in prep.) characterized Tc1 alleles at more than 500 positions in a high Tc1 copy number strain and generated PCR primers that, in combination with Tc1-specific primers, can be used to visualize insertions. Each of these Tc1 alleles can be viewed as a “conditional visible” mutation and can be used to map any new gene quickly. This is particularly important since it is usually not possible to look at more than a few visible mutations independently within single animals. Genes are mapped as follows: A mutation generated in a low Tc1 copy number strain is crossed into a high-copy-number strain that contains the identified Tc1 alleles. Homozygous F<sub>2</sub> mutants are individually picked from the heterozygous parents and typed by PCR. Any Tc1 allele that is genetically linked to the gene of interest will be underrepresented in homozygous mutants. After an initial experiment identifies the chromosome that contains the mutation, a subsequent experiment is done to map the gene within that chromosome using Tc1 alleles that are specific for that chromosome.

### C. Target-selected Gene Inactivation

The method of target-selected gene inactivation was initially developed for the P element of *Drosophila* ([Ballinger and Benzer 1989](#); [Kaiser and Goodwin 1990](#)). Its usefulness is limited by the logistics of sibling selection on very large pools of flies, particularly since the target choice of the P element is far from random, so that many genes are not frequently hit. The method has been applied to Tc1 of *C. elegans* ([Rushforth et al. 1993](#)) and has been used to isolate transposon insertion alleles of many genes. Isolation of Tc1 alleles has been much facilitated by the generation of a frozen transposon insertion bank ([Zwaal et al. 1993](#); [Hodgkin et al. 1995](#)).

Many Tc1 insertions do not inactivate gene function, either because they are in introns, and therefore absent in mRNA, or because they are removed from exons by aberrant splicing ([Rushforth et al. 1993](#); [Rushforth and Anderson 1995](#)). Fortunately, the imprecise repair of double-strand breaks can be used to isolate null alleles.

Among the progeny of the animals containing a Tc1 allele are worms that have lost that Tc1 element, plus a few kilobase pairs of flanking DNA ([Zwaal et al. 1993](#)). These deleted derivatives usually have the gene of interest fully inactivated.

## D. Potential Future Applications of Tc1 for Genetic Analysis

### 1. Site-directed Mutagenesis

A Tc1 insertion can be used to introduce specific point mutations into the genome ([Plasterk and Groenen 1992](#)).

Although the method has not yet been used in a fully reverse genetic approach, where site-directed point mutants were identified by DNA analysis (e.g., PCR), such an approach in principle seems to be possible.

Application of the method may be demonstrated in cases where specific point mutants have been found to be interesting in gene homologs of other species (e.g., *trans*-dominant mutations and thermosensitive alleles), and where one wants to introduce these into the proper chromosomal context, rather than into an ectopic transgenic copy of the gene.

### 2. Enhancer Trapping

The method of enhancer trapping by screening large numbers of transposon insertion alleles, using a transgenic transposon marked with a reporter gene such as *lacZ*, has been used extensively in *Drosophila* genetics ([Bellen et al. 1989](#); [Wilson et al. 1989](#)). The method has not yet been applied to *C. elegans*, largely because attempts to integrate transgenic Tc1 elements into the nematode germ line have failed. As discussed above, we have succeeded in demonstrating jumping of Tc1 and Tc3 elements from transgenic arrays into the chromosome in *somatic cells* ([van Luenen and Plasterk 1994](#); [van Luenen et al. 1994](#)). This demonstrates that it is possible for a transposon to jump from an extrachromosomal transgenic array into a chromosome, and therefore the remaining obstacles to transposon-mediated germ-line transformation lie in the choice of proper selectable markers and the availability of a good (inducible) promoter for germ-line expression of transposase.

### 3. Transgenesis of Other Species

The wide spread of the Tc1/*mariner* transposon family suggests that if host factors are required for transposition, they will be ubiquitous. Therefore, these transposons are probably well suited for the introduction of foreign DNA into organisms that are not very well defined genetically. [Lidholm et al. \(1993\)](#) have shown that the *mariner* transposon from *D. mauritiana* can be used successfully to transform *Drosophila melanogaster*. In contrast, the P element of *Drosophila* transposes only in a limited number of fly species ([O'Brochta et al. 1991](#)). The years to come will probably witness many attempts to use Tc1/*mariner* transposons for the generation of transgenic species of economic and/or medical importance. For example, the discovery of Tc1 homologs in zebrafish ([Izsvák et al. 1995](#)) has raised interest in using Tc1 or its relatives for the generation of transgenic zebrafish.

## **Chapter 5. Transposons — Acknowledgments**

---

We to thank P. Anderson, T. Blumenthal, P. Borst, and J.C. Vos for their useful comments on the manuscript.

Generated from local HTML

# **Chapter 6. RNA Processing and Gene Structure**

---

## **Contents**

- [I Introduction](#)
- [II Cis -Splicing in Worms](#)
- [III Trans -Splicing](#)
- [IV SL2 Trans -Splicing and Operons](#)
- [V Trans -Splicing in Vitro](#)
- [VI Frequency of Operons and Trans -Splicing](#)
- [VII Organization and Transcription of Spliced Leader RNA Genes](#)
- [VIII 3'-End Formation](#)
- [IX Translation Initiation and Termination Signals](#)
- [X Conclusions](#)
- [Acknowledgments](#)

Generated from local HTML

# Chapter 6. RNA Processing and Gene Structure — I Introduction

---

The emphasis in this chapter is on various aspects of the basic molecular biology of information transfer in *Caenorhabditis elegans*. Overall, the genes of *C. elegans* have characteristics that are quite similar to those of other animals. In broad outline, the mechanisms involved in transcription, RNA processing, and translation of messenger RNA are shared with those of other animals. However, some aspects are not shared by the yeast, fly, plant, and vertebrate model organisms. Here, we briefly outline the major features of RNA processing that are shared by all of these systems (for recent reviews, see [Moore et al. 1993](#); [Madhani and Guthrie 1994](#)) and then concentrate on aspects that make the *C. elegans* system especially interesting (for recent reviews, see [Nilsen 1993](#); [Blumenthal 1995](#); [Davis 1996](#)).

## A. The Splicing Process

Genes are composed of alternating exons and introns. When these are transcribed to make pre-mRNAs, the intron sequences are removed, and adjacent exon sequences are spliced together. RNA splicing is catalyzed by a large complex of RNAs and proteins called the spliceosome, components of which recognize and cleave the 5'and 3'ends of each intron and catalyze the joining of the exons. At the 3'end of the gene, RNA polymerase proceeds past the end of the last exon, but the RNA is cleaved at this point, and the 3'end of the mRNA is matured by the addition of a poly(A) sequence, which is not represented in the gene. Collectively, these events are known as pre-mRNA processing. It is important to understand the mechanisms the cell uses in these crucial steps of gene expression. The introns are thought not to be important for gene function, although they may have roles in maximizing gene expression.

In all eukaryotes, introns are bordered by highly conserved sequences and also contain conserved sequences within them. These sequences constitute the splicing signals. They serve as binding sites for components of the spliceosome as well as the sites that are cleaved and spliced together. Splicing is a two-step process. In the first step, the upstream exon is cleaved from the downstream portion of the pre-mRNA and a lariat-like molecule is formed, in which the 5'end of the intron is linked to an adenosine moiety within the intron (called the branch site) by an unusual 2' 5'linkage. In the second step of splicing, the intron is cleaved from the downstream exon and the two exons are ligated together by a phosphodiester strand-transfer reaction. Key components in this complex process are the small nuclear ribonucleoprotein complexes (snRNPs) and various associated proteins. Five separate RNAs and as many as 100 proteins may have roles in this complex process. The snRNPs each contains single short RNAs with characteristic secondary structures, as well as several different proteins. There are proteins that bind to U-rich sites on U1, U2, U4, and U5 RNAs, called Sm proteins, as well as a variety of proteins bound uniquely to each snRNP.

Virtually all introns in eukaryotic nuclear pre-mRNAs begin with the dinucleotide GU (although GC is used infrequently) and end with the dinucleotide AG. This is known as the GU-AG rule. The 5'splice site, which in vertebrates has the consensus sequence G/GURAG (R = A or G), is recognized by the U1 snRNP through base pairing between the 5' splice site consensus sequence and a sequence near the 5'end of U1 snRNA. The branch site is also recognized by base pairing with an snRNP, this time U2. To bind productively with the branch-site consensus sequence, U2 requires another consensus sequence called the polypyrimidine tract. This U-rich sequence is found just downstream from the branch site and just upstream of the 3'splice site. It binds U2AF, an essential splicing protein required for the U2 branch-site interaction. Other snRNPs that have required roles in splicing are U4, U5, and U6. These three snRNPs enter the spliceosome later in the process as a group. U5 interacts with both exons by base pairing at the intron boundaries. U6 is the most highly conserved of the snRNPs and is thought to be responsible for catalyzing the splicing reaction. U4 appears to be a molecular chaperone for U6; it base pairs with U6 extensively, but it is released so that U6 can carry out its role. The spliceosome also contains numerous non-snRNP proteins that have crucial roles in carrying out the reaction. These include RNA helicases and SR proteins (named for their alternating Ser-Arg motifs), which bind to exon sequences and participate in splice site choice.

## B. A New Survey

By and large, the brief description of splicing outlined above applies to splicing in *C. elegans*. However, there are some interesting, perhaps even unique, aspects of splicing in *C. elegans* on which we will elaborate below. *C. elegans* splicing consensus sequences have been reported previously ([Blumenthal and Thomas 1988](#); [Emmons 1988](#); [Fields 1990](#)), but since so many more genes have been characterized from *C. elegans* since the last survey, we have recently performed a much more extensive computer-based survey, and the results are included in this chapter. More than 200 *C. elegans* genes, with over 650 introns (those reported to Genbank by 1/95 [release 88]), were included in this survey.

Generated from local HTML

# Chapter 6. RNA Processing and Gene Structure — II Cis -Splicing in Worms

---

## A. Intron and Exon Length

*C. elegans* introns have some unusual properties ([Blumenthal and Thomas 1988](#)). First of all, they tend to be much shorter than vertebrate, or even yeast, introns. [Figure 1](#) shows the size distribution of introns and exons in *C. elegans*. More than half of all *C. elegans* introns in the survey are shorter than 60 nucleotides, much too small to be spliced in vertebrates ([Weiringa et al. 1984](#); [Ogg et al. 1990](#)). The inset in [Figure 1](#) (top) shows the size distribution of the very short introns. It appears to represent a skewed distribution with a peak at 48 nucleotides but with greater than expected numbers of introns at 44 and 52 nucleotides. The reason for this uneven distribution is unknown, but it may reflect some constraint imposed by spliceosome formation. The shortest intron in the survey is 30 nucleotides long (in the  $\alpha 2$ [IV] collagen gene [[Sibley et al. 1993](#)]), but only 4 of 659 are shorter than 40 nucleotides. It is also worth noting that the *C. elegans* splicing machinery does retain the ability to splice very long introns. For example, the first intron of the *unc-7* gene is 18 kb ([Starich et al. 1993](#)).

*C. elegans* introns are not the shortest among free-living nematodes. *Caenorhabditis briggsae* introns tend to be somewhat shorter than those of *C. elegans*. For example, the introns of the *C. elegans* *ges-1* gene are much longer than those of the *C. briggsae* homolog ([Kennedy et al. 1993](#)). An informal survey of 39 homologous introns from the two species shows that 17 are substantially longer in *C. elegans*, whereas only 4 are longer in *C. briggsae* (T. Blumenthal, unpubl.), and the 4 known introns of another rhabditid nematode, CEW1, are between 38 and 41 nucleotides long ([Winter et al. 1996](#)). Other organisms have also been reported to have short introns: *Schizosaccharomyces pombe* introns have a median length of 63 bp ([Zhang and Marr 1994](#)); *Drosophila* introns show a sharp distribution around a modal length of 63 bp ([Mount et al. 1992](#)); introns in the flatworm, *Schistosoma mansoni*, are 31–42 bp long ([Craig et al. 1989](#)); and *Paramecium* introns all seem to be between 20 and 33 nucleotides in length ([Russell et al. 1994](#)). This is in sharp contrast to the much longer introns of vertebrates, plants, and even *Saccharomyces cerevisiae*.

*C. elegans* exons are most frequently about 80–250 bp in length ([Fig. 1](#), bottom), similar to vertebrate exons. However, they can be much longer. Several are larger than 4 kb, and the longest identified exon is 9 kb, in *unc-22* ([Benian et al. 1989](#)). The survey also shows that the typical *C. elegans* gene has a relatively small number of introns and exons ([Fig. 2](#); median = 3 introns/gene). The 100 fully characterized genes in the survey range in their exon content from 21% to 95% (median = 71%).

## B. Sequences That Signal Splicing

The vertebrate and *C. elegans* splice site consensus sequences are compared in [Figure 3](#). *C. elegans* introns obey the GU-AG rule (with very rare use of GC as a 5'splice site), and their 5'splice site consensus is essentially the same as that for vertebrates. However, several interesting differences exist between *C. elegans* and other species. *C. elegans* introns have an extended, very highly conserved 3'splice site consensus sequence, UUUUCAG, in which the U at the –5 position is almost perfectly conserved, whereas introns from most other organisms have only a combination of an upstream polypyrimidine tract and a YAG consensus at their 3'boundaries. This suggests that the 3'intron boundary may be a more important element in *C. elegans* intron recognition than in other organisms. This supposition has recently gained experimental support (see below). On the other hand, *C. elegans* introns have no obvious polypyrimidine tract (other than the 3'splice site consensus), nor have they any convincing branch site consensus similar to consensus sequences of yeast or mammalian introns. Since branch sites mapped in other species generally occur at A residues, it is reasonable to suppose that branching in *C. elegans* also tends to occur at A residues. It has been observed that although the entire intron is rich in U residues, A residues are more frequent at positions –16, –17, and –18 from the 3'splice site (T. Blumenthal and K. Steward, unpubl.), so it is reasonable to propose that branching may occur at these A residues.

Although *C. elegans* introns conform to the GU-AG rule, the *C. elegans* splicing machinery can recognize variants of this sequence at both ends of the intron ([Aroian et al. 1993](#)). Several mutations in the *let-23* and *dpy-10* genes were caused by mutation of the AG at the 3'splice site. Since these mutations resulted in only a partial loss-of-function phenotype, the RNA products of these mutant genes were examined, and at least a portion of the RNAs were found to be spliced at the normal site, now consisting of AA in place of AG. Furthermore, splicing occurred at other non-AG sites in the surrounding sequence, including UG, AU, and GG. In another study, it was discovered that mutations caused by insertion of the transposon Tc1 often produced weak phenotypes because the entire transposon was spliced out utilizing cryptic sites at the ends of the transposon or in surrounding DNA ([Rushforth et al. 1993; Rushforth and Anderson 1996](#)). In several instances, these sites did not conform to the GU-AG rule: UU and AU were used as 5'splice sites, and UG, AC, GC, and GG were used as 3'splice sites.

These results demonstrate that AG is not an obligatory component of the 3'splice site recognition process in *C. elegans*, although the fact that it is so highly conserved indicates that it certainly contributes information to the process. To determine where the additional information for 3'splice site choice is located, a mutational analysis of the site was performed ([Zhang and Blumenthal 1996](#)). When a 3'splice site, UUUCAAG/AAG, was mutated to UUUCAAAAAA, splicing occurred 100% of the time at the second A in the string of five A residues, which is the position where splicing occurs in the wild-type sequence. When additional single-base changes were introduced into the UUUC portion of the sequence, splicing failed to occur, or it occurred at a different site. Thus, the highly conserved UUUC that precedes the AG also provides important information to the spliceosomal machinery. It may be that this short stretch of pyrimidines replaces the polypyrimidine tract (which is typically 15–20 nucleotides long in vertebrates). If so, one would expect that it would serve as the recognition site for U2AF. It is worth noting that U to C changes in this short sequence clearly reduce its effectiveness, suggesting that if this is a polypyrimidine tract, it is not just a random sequence of pyrimidines (the strong UUUC consensus also supports this observation). However, U and C do not have equivalent functions in vertebrate polypyrimidine tracts either ([Roscigno et al. 1993](#)). Furthermore, the optimal binding sequence for mammalian U2AF, which acts at the polypyrimidine tract, has recently been shown to require several contiguous U residues ([Singh et al. 1995](#)).

*C. elegans* introns are very A + U-rich (~70%) compared with surrounding exons (~54%) ([Table 1](#)), a property they share with introns of other invertebrates and plants ([Goodall and Filipowicz 1989; Csank et al. 1990](#)). In plants, A + U richness has been demonstrated to represent an important aspect of intron recognition: Insertion of an A + U-rich sequence within an exon, even without splice sites, has been shown to result in splicing of the inserted sequence utilizing fortuitous matches to the splice site consensus sequences present in the surrounding exon ([Luehrs and Walbot 1994](#)). In worms, A + U richness has also been shown to be an important feature of 3'splice site recognition. In one case where two alternative 3'splice sites 20 nucleotides apart were available, the downstream site was always utilized; however, when the region between the two splice sites was made more G + C-rich, the upstream site was chosen, indicating that the border between A + U-rich and more G + C-rich RNA is one of the criteria *C. elegans* spliceosomes use in choosing splice sites ([Conrad et al. 1993a](#)). The data in [Table 1](#) also suggest that recognition of short and long introns may not be identical processes. The short introns appear to be richer in U nucleotides than are large introns. Furthermore, an analysis of information content of short and long introns of *C. elegans* showed that they were significantly different at both splice boundaries ([Fields 1990](#)). The data in [Table 1](#) also show that the regions of the exons specifying untranslated regions tend to be A + U-rich compared with protein-coding regions.

In summary, intron recognition in *C. elegans* appears to involve recognition of the general boundaries of the intron based on A + U richness, recognition of the 5'splice site (by U1 snRNP, as in all other organisms), and recognition of the 3'splice site by currently undefined components of the spliceosome that interact with the UUUUCAG sequence. Since there is neither a good match to the branch-site consensus, which would base pair with U2 snRNA, nor a polypyrimidine tract that would interact with U2AF, it seems most likely that the information provided in vertebrates by those consensus sequences, resulting in U2AF-assisted binding of U2-snRNP to the branch site, is provided in *C. elegans* by the highly conserved UUUUCAG instead. Tight binding of U2AF (or some other component) could result in recruitment of U2 to a very loosely defined branch-site sequence and simultaneous definition of the 3'splice site.

## C. The Splicing Machinery

Those portions of the splicing machinery that have been characterized so far are very highly conserved throughout the eukaryotes. This includes *C. elegans*, which has been found to have all the spliceosomal snRNAs ([Thomas et al. 1988](#)). The sequences and lengths of these RNAs are quite similar to those of other animals. In particular, the sequence in U1 that interacts with the 5'splice site and the sequence in U5 that interacts with both exon borders have both been perfectly conserved between vertebrates and *C. elegans* ([Thomas et al. 1990](#)). The sequence in U2 that base pairs with the branch site has been perfectly conserved in *C. elegans*, even though the branch-site sequence in *C. elegans* introns is so loosely defined that it is unrecognizable. When it was found that *C. elegans* introns were unusually short, it was thought that the snRNAs which catalyze their splicing might also be shorter than in other species. However, the *C. elegans* snRNAs are about the same lengths as their homologs in vertebrates. It may be that constraints imposed by snRNA size do not determine minimum or optimal intron length.

The genes that encode the snRNAs are also similar to those found in other species ([Thomas et al. 1990](#)). The spliceosomal snRNAs are each encoded by small multigene families of 6–12 members each. A few of the genes are clustered, but in general they are spread throughout the genome. These genes are transcribed in other animals, and probably *C. elegans* as well, by RNA polymerase II, except U6, which is transcribed by RNA polymerase III. The snRNA genes are each preceded at their 5'ends by a very highly conserved sequence called the proximal sequence element (PSE). In vertebrates, the PSE has been shown to be the site where a transcriptional activation complex called SNAPc forms. The *C. elegans* PSE sequence has diverged totally from the vertebrate PSE, but it is very highly conserved between the different *C. elegans* snRNA genes, and it occupies the same position as the vertebrate PSE, and thus it is likely to perform the same function.

Several genes that encode protein components of the *C. elegans* splicing machinery have been identified. These genes encode U2AF ([Zorio et al. 1997](#)); PRP21, a U2-associated protein ([Spikes et al. 1994](#)); PRP8, a U5 snRNP-associated protein involved in 3'splice site recognition ([Hodges et al. 1995](#); [Umen and Guthrie 1995](#)); and several SR proteins (M.L. Morrison et al., pers. comm.). Presumably, *C. elegans* homologs to the many other proteins involved in splicing also exist, and many have been identified in the partial *C. elegans* genomic sequence and in sequenced cDNA clones.

The pre-mRNA for the U2AF large subunit is alternatively spliced in a potentially interesting way (see [Zorio et al. 1997](#)). In addition to the RNA that encodes the full-length protein, an alternatively spliced RNA results from choice of a more proximal 3'splice site and removal of a short intron. This alternative splicing results in insertion of an approximately 300-bp exon, containing an in-frame stop codon, and a similar alternative splice occurs in the *C. briggsae* U2AF homolog. The *C. briggsae* gene is quite highly conserved in the exons surrounding the alternative splice, but it is essentially unrelated in the introns and in the exon inserted by the alternative splice. However, downstream from the alternatively used splice site, the *C. elegans* insert contains 10 good matches to the 3'splice site consensus, UUUUCAG/(A or G), and the *C. briggsae* insert contains 18 such matches. There is no evidence that these sequences serve as splice sites, so they may instead play a part in regulating U2AF levels. This autogenous regulation might occur by binding of excess U2AF to the 3'splice-site-like sequences in the pre-mRNA or in the alternative mRNA.

## D. Alternative Splicing

Alternative splicing is a frequently used mechanism for producing multiple mRNAs and protein products from a single gene. In *C. elegans*, there are numerous examples of alternative splicing, in which alternative splice sites are chosen (e.g., *xol-1* [[Rhind et al. 1995](#)], *fip-1* [[Rosoff et al. 1992](#)], *hlh-1* [[Krause et al. 1990](#)], IFa<sub>1</sub> [[Dodemont et al. 1994](#)]), entire exons are skipped (e.g., *lin-14* [[Wightman et al. 1991](#)], *tmy-1* [[Kagawa et al. 1995](#)]), or groups of exons are skipped (e.g. *unc-52* [[Rogalski et al. 1993, 1995](#)] and *bli-4* [[Thacker et al. 1995](#)]). One particularly interesting example is the case of *unc-17*, which encodes a synaptic vesicle-associated acetylcholine transporter, and *cha-1*, which encodes choline acetyltransferase (see [Rand and Nonet](#), this volume). These two independently identified genes are encoded by a single polycistronic cluster ([Alfonso et al. 1994b](#)). They share a

first noncoding exon, but the coding regions of the two genes are entirely separate (Fig. 4). The coding exons of *unc-17* are all contained within the unusually long first intron of *cha-1*. Hence, a given transcript can encode either the *unc-17* product or the *cha-1* product, but never both. This appears to be a unique use of alternative splicing to ensure that the products of the two genes are not produced simultaneously. This kind of arrangement also has been reported for the *unc-60* gene, which encodes two separate, but homologous, actin-depolymerizing proteins (McKim et al. 1994). The two share a first exon, which encodes only the methionine at which translation initiates.

The mechanisms by which these documented cases of alternative splicing are regulated remain mysterious. In one case, however, a *trans*-acting factor that regulates a variety of alternative splicing events has been identified genetically (Lundquist and Herman 1994). The *mec-8* gene was originally identified by mutations that cause defects in mechanosensation. Strong mutations at this locus resulted in a variety of seemingly unrelated defects including larval lethality. These mutations were shown to enhance the phenotype of mutations in the *unc-52* gene (which encodes perlecan), causing paralysis and embryonic arrest (see Fire and Moerman, this volume). The *unc-52* pre-mRNA undergoes a complex array of alternative splicing events involving exon skipping (Rogalski et al. 1993; 1995). Recent results have demonstrated that *mec-8* mutations alter the ratio of the *unc-52* alternatively spliced products (Lundquist et al. 1996). Specifically, *mec-8* mutations appear to reduce the level of exon skipping in the *unc-52* pre-mRNA. In addition, *mec-8* itself produces several RNA products, and *mec-8* mutations affect levels of these products as well, suggesting that its product is a splicing factor that autogenously regulates its own expression at the level of splicing. This idea is supported by characterization of the MEC-8 protein, which has two RNA recognition motifs (RRMs). These highly conserved sequences have been found previously in many proteins that bind RNA, especially proteins that are involved in catalysis of splicing or alternative splice site choice. Thus, it is reasonable to suppose that the MEC-8 protein is involved in splice site choice in *C. elegans* and that based on its pleiotropic mutant phenotype, its targets may include pre-mRNAs from a wide variety of genes.

Alternative *cis*-splicing is not the only means by which *C. elegans* creates diverse products from single genes. Several genes have been reported to have alternative first exons that may arise through promoters contained within introns or by alternative *trans*-splicing (see below) (e.g., *unc-87* [Goetinck and Waterston 1994b]; *unc-5* [Leung-Hagesteijn et al. 1992]; and *sdc-1* [Nonet and Meyer 1991]). The *unc-33* gene produces a shortened transcript due to either a second promoter or *trans*-splicing following a long fourth intron (Li et al. 1992). In the case of the *her-1* gene, the existence of a second promoter within the large second intron has been demonstrated (Perry et al. 1993). So far, no function has been ascribed to this shorter transcript. The *tmy-1* gene, which encodes several different tropomyosin isoforms, contains a promoter within the large third intron, and this promoter has a developmental specificity different from the upstream promoter (Kagawa et al. 1995). It is also possible for genes to be contained entirely within other genes: The *spe-26* gene, which is itself composed of six exons, is contained entirely within the first intron of a gene encoded on the other strand (Varkey et al. 1995).

## Figures

Figure 1. Intron and exon length distribution.

### Figure 1

Intron and exon length distribution. Each bar represents the number of introns or exons in each size class. The survey includes 669 introns and 862 exons. (Inset) Expanded plot of the small introns. Each bar represents introns of a specific length: 0–20, 21–40, 41–60, etc.

Figure 2. Intron/exon structure of *C. elegans*.

### Figure 2

Intron/exon structure of *C. elegans* genes. Each bar represents the number of genes having the number of introns shown. The survey includes 117 genes.

Figure 3. *C. elegans* genes.

### Figure 3

*C. elegans* intron consensus sequences. Splicing occurs at the vertical lines. Positions are numbered with respect to the splice sites, and the percentage of each nucleotide at each position is given. All 669 introns surveyed for Fig. 1 are included in the calculations. The derived *C. elegans* consensus sequence is given below. For comparison, the general consensus derived from a large data set including all organisms (Mount 1982) is included below the *C. elegans* consensus.

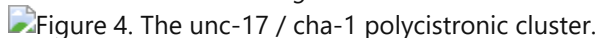


### Figure 4

The *unc-17* / *cha-1* polycistronic cluster. The two genes share a noncoding first exon, and the two products are generated by alternative splicing. The gene structures are redrawn to scale from the data of Alfonso et al. (1994b). Exons are shown as bars joined as shown.

## Tables

**Table 1** Base composition of *C. elegans* introns and exons

	Introns		Exons		
	small	large	protein coding	5'UTR	3'UTR
G	14	16	24	18	14
A	32	33	30	37	29
U	42	35	24	24	39
C	12	16	22	21	18
A+T	74	68	54	61	68

Base compositions for each intron, coding exon, or untranslated region (UTR) were calculated separately and then averaged to avoid weighting the results toward the base compositions of longer regions. Small introns are those of less than 100 nucleotides. The survey includes 407 small introns, 262 large introns, 548 protein coding exons, and 69 5'and 3'UTRs.

Generated from local HTML

# Chapter 6. RNA Processing and Gene Structure — III Trans -Splicing

---

## A. The Discovery of *Trans* -splicing

*Trans*-splicing, in which an identical short leader sequence, the spliced leader (SL), is spliced onto the 5'ends of multiple mRNAs (for reviews, see [Agabian 1990](#); [Donelson and Zeng 1990](#); [Bonen 1993](#)), was first discovered in the primitive eukaryotes, the trypanosomatids ([Murphy et al. 1986](#); [Sutton and Boothroyd 1986](#)), and later shown to occur also in *C. elegans* and other nematodes ([Krause and Hirsh 1987](#); for reviews, see [Nilsen 1993](#); [Davis 1996](#)), in Euglena ([Tessier et al. 1991](#)), and in flatworms ([Rajkovic et al. 1990](#); [Davis et al. 1994](#)). In trypanosomes, all splicing is *trans*-splicing; all mRNAs begin with the SL, and genes do not contain introns. Transcription is polycistronic, and *trans*-splicing is responsible for separating the long polycistronic transcripts into monocistronic units. In contrast, in nematodes, the genes do contain introns, and the pre-mRNA products of many genes are not subject to *trans*-splicing.

*Trans*-splicing in *C. elegans* was first found during molecular analysis of the actin genes ([Krause and Hirsh 1987](#)). It was discovered that mRNAs of three of the four actin genes begin with the identical 22-nucleotide sequence, a sequence that is not associated with the gene. Instead, the 22-nucleotide SL is donated by a 100-nucleotide small RNA, SL RNA, by a *trans*-splicing reaction. This *trans*-splicing process is closely related to *cis*-splicing (intron removal). A reasonable match to the 5'splice site consensus is present on the SL RNA, and a good match to the 3'splice site consensus is present at the site of SL addition (*trans*-splice site) on the pre-mRNA. Furthermore, the reaction proceeds by way of a branched intermediate similar to the lariat of *cis*-splicing ([Bektesh and Hirsh 1988](#); [Thomas et al. 1988](#); [Hannon et al. 1990a](#)). *Trans*-splicing also requires spliceosomal components including U2, U4, U5, and U6 snRNPs ([Hannon et al. 1991](#); [Maroney et al. 1996](#); see below).

## B. The Spliced Leader snRNP

The donor in the *trans*-splicing reaction, the SL RNA, exists in the form of an snRNP ([Bruzik et al. 1988](#); [Thomas et al. 1988](#); [Van Doren and Hirsh 1988](#)). It is bound to the Sm proteins found associated with U1, U2, U4, and U5 RNAs, and it has the unusual modified cap structure, trimethylguanosine (TMG), found on these snRNAs. The secondary structure predicted for the SL RNA resembles that of other snRNAs. It has the 5'splice site base-paired to the upstream part of the SL sequence in a manner resembling the U1-5'splice site base pairing. It was hypothesized that this intramolecular interaction might replace in *trans*-splicing the interaction between U1 and the 5'splice site required for initiation of *cis*-splicing ([Bruzik et al. 1988](#)). Subsequent work has demonstrated that the U1 snRNP is indeed dispensable for nematode *trans*-splicing in vitro (see below).

## C. *Trans* -splicing Signals

The *trans*-splice site consensus is the same as the intron 3'splice site consensus ([Table 2](#)), so it is not immediately obvious how the two reactions can be faithfully carried out. However, it is now clear that the signal for *trans*-splicing is simply the presence of an intron-like sequence at the 5'end of the mRNA with no functional 5'splice site upstream ([Conrad et al. 1991](#), 1993b, 1995). The region of the pre-mRNA from the 5'end to the *trans*-splice site is called the outron ([Conrad et al. 1991](#)). Genes whose pre-mRNAs are subject to *trans*-splicing are distinguished from those that are not only by the presence of an outron. Considerable experimental evidence has been adduced to support this view. A conventional gene can be converted into a *trans*-spliced gene by placing at the gene's 5'end either an intron from another gene or an A + T-rich synthetic sequence followed by a canonical 3'splice site. Furthermore, a *trans*-spliced gene can be converted into a conventional gene by inserting a 5'splice site into its outron. These experiments demonstrate that the only difference between *trans*-spliced and conventional genes is the presence of an outron, and they show that no sequence-specific recognition is involved in the decision to *trans*-splice. They also show that the intron and outron 3'splice sites are the same; the choice between *cis*- and *trans*-splicing is based solely on the presence or absence of an upstream 5'splice site.

Because *trans*-splicing is a relatively efficient reaction (like *cis*-splicing), it is generally impossible to isolate outron-containing pre-mRNAs, and so very few natural outrons have been defined. Nevertheless, in a few cases, the promoters of *trans*-spliced genes or start sites of outrons have been identified (e.g., [col-13](#) has a 64-bp outron [[Park and Kramer 1990](#)]). It might be possible to determine *trans*-spliced gene start sites by deleting the *trans*-splice site and analyzing the RNA product from a transgenic strain carrying the mutated gene. However, in the few cases in which this technique has been attempted, it has been unsuccessful because *trans*-splicing occurred at an alternative site. One proven successful technique is to introduce a 5'splice site consensus sequence into the outron. In this case, the introduced splice site splices to the *trans*-splice site, and the outron length can be calculated from the length of the 5'-untranslated region (5'UTR). This procedure was used to determine outron length (173 bp) for [rol-6](#) ([Conrad et al. 1993](#)). Although few natural outrons have been characterized, synthetic sequences have been introduced into the 5'UTR of a gene that is not normally *trans*-spliced in order to determine whether they can function as outrons. A + U-rich sequences of 51 nucleotides or longer resulted in efficient *trans*-splicing, whereas sequences that were 41 nucleotides or shorter (or not A + U-rich) were much less effective ([Conrad et al. 1995](#)). Thus, the same constraints that set the lower size limit on introns may be acting on outrons.

## D. Function of *Trans* -splicing

*Trans*-splicing occurs throughout the nematode phylum, and there is a remarkable degree of conservation of the SL sequence (although the portions of the SL RNAs downstream from the splice site have diverged widely) ([Bektesh and Hirsh 1988](#); [Tackacks et al. 1988](#); [Nilsen et al. 1989](#); [Zeng et al. 1990](#)). In the many free-living species, as well as animal and plant parasitic nematodes, that have been examined, only one single-base change has been found in the SL sequence ([Ray et al. 1994](#)). It is not known what selection pressure has kept this sequence so stable. In fact, it is not yet known precisely what function the SL has in the cell. In *C. elegans*, SL tends to be spliced very close to the initiating methionine codon (often immediately adjacent) ([Fig. 5](#)), so it seems likely to play a part in translation initiation. The unusual cap structure, trimethylguanosine (TMG), present at the 5'end of the SL becomes the 5'end of *trans*-spliced mRNAs, and this cap remains on the mRNA during translation ([Liou and Blumenthal 1990](#); [Van Doren and Hirsh 1990](#)). A TMG cap is known to inhibit translation in mammalian extracts ([Darzynkiewicz et al. 1988](#)), but it may actually stimulate translation in a nematode extract, at least when it is present at the 5'end of the SL sequence ([Maroney et al. 1995](#)).

In *Ascaris lumbricoides*, an animal parasite, the SL sequence in the DNA is needed for transcription of the SL RNA gene, which may be one reason why it has been so highly conserved ([Hannon et al. 1990b](#)). Although it is not known precisely what roles the SL sequence itself may perform, *trans*-splicing is in fact required for viability ([Ferguson et al. 1996](#)). An embryonic lethal mutation in the [rrs-1](#) gene is a deletion of all 100 tandem copies of the 1-kb sequence that encodes both 5S ribosomal RNA and SL RNA (see below). Remarkably, the embryonic lethality is rescued by a tandem array carrying the SL RNA gene alone (presumably the maternal supply of 5S RNA can carry the homozygous mutants through embryogenesis). Mutations in the SL RNA gene that eliminate the Sm-binding site prevent rescue, so it is fair to conclude that the SL snRNP is required for embryogenesis. Its required role could be a positive effect such as providing a sequence needed for translation initiation, mRNA stability, or localization, or it could be required for suppression of a negative effect such as inhibition of translation initiation by AUG codons in the outron. At least some of the mRNAs that normally are *trans*-spliced to SL1 have been found to be *trans*-spliced to the alternative spliced leader, SL2 (see below), in the [rrs-1](#) mutant strain ([Ferguson et al. 1996](#)).

## Figures

Figure 5. Distance from the trans-splice site to the translation initiation site.

### Figure 5

Distance from the *trans*-splice site to the translation initiation site. The survey includes 83 *trans*-spliced genes, both SL1- and SL2-acceptors. Each bar represents the number of genes in the indicated distance class (shown in

bp: 0–5, 6–10, 11–15, etc.).

## Tables

**Table 2Comparison of *cis*- and *trans*-3' splice sites**

	<b>-7</b>	<b>-6</b>	<b>-5</b>	<b>-4</b>	<b>-3</b>	<b>-2</b>	<b>-1</b>	<b>+1</b>
	<b>U</b>	<b>U</b>	<b>U</b>	<b>U</b>	<b>C</b>	<b>A</b>	<b>G</b>	<b>A/G</b>
<i>Cis</i>	53	89	98	70	83	100	100	74
SL1	57	92	97	64	82	100	100	79
SL2	66	66	84	66	78	100	100	75

The percentage of splice sites that match the consensus at each position is given. The survey includes 669 *cis*-splice sites, 58 SL1 *trans*-splice sites, and 32 SL2 *trans*-splice sites.

Generated from local HTML

# Chapter 6. RNA Processing and Gene Structure — IV SL2 Trans - Splicing and Operons

---

## A. The Discovery of a Second Spliced Leader

In 1989, a second SL was discovered in *C. elegans*. [Huang and Hirsh \(1989\)](#) reported that the SL at the 5'end of the *gpd-3* gene, although it is the same length as the SL found at the 5'ends of other mRNAs, has a different sequence, which they called SL2. Using this sequence, they identified a different SL RNA (SL2 RNA) with a potential secondary structure similar to that of the original SL (now called SL1). SL2 RNA is also present as an snRNP; it is bound to Sm antigen and has a TMG cap. Like SL1, SL2 is *trans*-spliced to a variety of mRNAs. Initial evidence suggested that *gpd-3* mRNA receives SL2, but no SL1, whereas other mRNAs receive only SL1. How is this specificity achieved? If SL1 is specific for *trans*-splicing at the 3'splice sites following outrons, and outrons are simply A + U-rich RNA of any sequence, where is the information to specify SL2?

## B. The Discovery of Operons

A look at the organization of the *gpd-3* genomic region ([Huang et al. 1989](#)) provides the answer ([Fig. 6](#)). The *gpd-3* gene and all other genes whose mRNAs receive SL2 at their 5'ends occur at downstream positions in closely spaced clusters of genes with the same 5'to 3'orientations ([Spieth et al. 1993; Zorio et al. 1994](#); for review, see [Blumenthal 1995](#)). The *gpd-3* gene is the third gene in a three-gene cluster, and both of the downstream genes receive SL2. The upstream gene in the cluster, *mai-1*, is not *trans*-spliced, although many first genes in such clusters are *trans*-spliced to SL1. Since the original discovery of this cluster, many more SL2-accepting mRNAs have been reported, and many more such clusters have also been found. In all cases (>30 are now known), mRNAs for genes that reside in downstream positions in clusters begin with SL2. Furthermore, every gene found to reside in such a position has turned out to encode mRNA that receives SL2. So it is now clear that the product of a gene in a downstream location in a closely spaced cluster is SL2 *trans*-spliced ([Zorio et al. 1994](#)).

How might chromosomal position translate into specificity of *trans*-splicing? [Spieth et al. \(1993\)](#) hypothesized that the gene clusters are in fact similar to bacterial operons in the sense that the entire cluster is transcribed from a single promoter and regulatory region at the 5'end of the cluster. However, whereas bacterial operon mRNA remains polycistronic and is translated by internal ribosome binding at the 5'end of each cistron, the *C. elegans* polycistronic pre-mRNA is converted into monocistronic mRNAs. This occurs by cleavage and polyadenylation at the 3'ends of the upstream genes, accompanied by SL2-specific *trans*-splicing at the 5'ends of the downstream genes. Several experimental observations support this hypothesis. First, polycistronic cDNA clones were isolated that contained the entire coding sequences of *mai-1* and *gpd-2*, the first two genes of the operon, joined by the 100-nucleotide sequence between them, which demonstrates that these two genes are cotranscribed. Second, in worms carrying a construct containing the *gpd-2* / *gpd-3* gene pair downstream from the heat shock promoter, expression of the downstream gene *gpd-3* is dependent on heat shock, and its product is *trans*-spliced to SL2. This shows that a controllable operon gives mature mRNA with correct splicing specificity. Third, SL2 specificity in this construct is dependent on the promoter being upstream of the first gene. Fourth, when the poly(A) site of the upstream gene is mutated, polycistronic precursor accumulates, indicating that expression of the mature downstream product is dependent on correct maturation of the upstream gene product. Finally, when a gene whose product normally receives SL1 is inserted between *gpd-2* and *gpd-3*, such that the intercistronic DNA between *gpd-2* and the inserted gene is composed of sequences from the outron of the inserted gene, its product receives primarily SL2, indicating that being a downstream gene in an operon is sufficient to result in SL2-specific *trans*-splicing.

## C. Properties of *C. elegans* Operons

In *C. elegans*, an operon is a cluster of closely spaced genes, transcribed from a regulatory region at the 5'end of the cluster, and whose monocistronic mRNAs are created from the polycistronic precursor RNA by conventional

3'-end formation (cleavage and polyadenylation) accompanied by *trans*-splicing to SL2 or a mixture of the two SLs. An analysis of more than 30 such operons has revealed some interesting properties. First, the genes are quite close together. [Figure 7](#) shows the distances between the poly(A) sites of the upstream genes and the *trans*-splice sites of the downstream genes. In most cases, the genes are about 100 bp apart, whereas a few are about 300–400 bp apart. It is not yet clear what aspect of the evolution or function of the operons requires that they be spaced so uniformly. It also is not clear whether the data in [Figure 7](#) represent a true bimodal distribution, which would suggest that there might be multiple constraints, resulting in two different favored lengths. The evolution of the operons and possible mechanistic constraints are discussed below.

Second, although some genes in downstream positions in operons receive SL2 exclusively, others receive a mixture of SL1 and SL2 ([Spieth et al. 1993](#); [Zorio et al. 1994](#)). In contrast, *trans*-splice sites near promoters accept only SL1 ([Zorio et al. 1994](#); [Conrad et al. 1995](#)). Why some downstream genes receive a mixture is not yet clear. One possibility is that these operons have internal promoters, so the SL1-containing message arises from pre-mRNA started at the internal promoter. A second possibility is that when 3'-end formation fails, the *trans*-splice site is no longer an SL2 substrate but can still be spliced to SL1. According to this idea, the entire upstream gene is read as an outron by the splicing machinery. So far, all of the genes following a 300–400-bp intercistronic region have been found to receive a mixture of the two SLs, whereas only a third of the genes following a 100-bp intercistronic region receive the mixture ([Zorio et al. 1994](#)). The reason for this difference is not known.

Although it was possible to isolate polycistronic cDNA clones for the *mai-1/gpd-2* operon, in most cases, no evidence of polycistronic pre-mRNA has been found. Even when the sensitive reverse transcriptase–polymerase chain reaction (RT-PCR) technique has been used to search for RNA crossing the boundary between two genes, it has not been detected for most operons (D. Zorio et al., in prep.), suggesting that 3'-end formation and SL2 *trans*-splicing occur cotranscriptionally. It even suggests the possibility that 3'-end formation occurs before RNA polymerase has passed into the downstream gene. Alternatively, the two RNA processing events may occur in a concerted fashion, such that RNA containing sequences from both genes never exists. Only when 3'-end formation is, for some reason, inefficient can such RNA be detected.

## D. Purpose of Operons in *C. elegans*

In bacteria, operons serve an important regulatory purpose: They allow coexpression from a single promoter/regulatory region of genes whose products function together. This both assures coordinate expression and results in efficient use of the cell's regulatory machinery. Do the *C. elegans* operons exist to assure coordinate regulation of genes whose products function together? Where it has been examined, the genes in *C. elegans* operons are indeed coexpressed (e.g., *kup-1* and *kin-13* [[Land et al. 1994](#)]). Because the functions of many operon genes are not known, no strong argument can be made for most of the operons (e.g., *dpy-30* and *rnp-1* [[Hsu et al. 1995](#)] and *mes-3* and *dom-3* [[Paulsen et al. 1995](#)]). However, there appear to be a few clear examples of purposeful coregulation. For instance, the two *lin-15* genes are contained in an operon; although it is not known how these two unrelated proteins function, it is known that they collaborate in an aspect of signal transduction in formation of the *vulva* ([Huang et al. 1994](#); [Clark et al. 1994](#); see [Greenwald](#), this volume). A second example is the *deg-3* gene, which encodes an acetylcholine receptor subunit (see [Treinin and Chalfie 1995](#)). When it was discovered that this gene's product received SL2, the upstream DNA was sequenced and found to contain another gene, appropriately spaced and in the same orientation, that is likely to be another subunit of the same receptor (M. Treinin and M. Chalfie, pers. comm.). Since they have shown that these two genes are expressed in the same cells, a good case can be made that their presence together in the operon serves the purpose of coexpression of proteins whose products function together. Many of the operons contain genes whose products would be expected to be expressed ubiquitously; for example, one operon contains the gene for fibrillarin, a protein needed for rRNA processing, and a gene for a ribosomal protein, *rps-16* ([Zorio et al. 1994](#)). Another contains genes for a chromosomal protein and for topoisomerase II. In these cases, they may be in the same operon simply to take advantage of a single ubiquitously expressed promoter.

It seems likely that the *C. elegans* operons are not ancient but are instead an innovation, perhaps having evolved as a response to selection for a small genome (although it is not clear what aspect of *C. elegans*' lifestyle or

development might require a small genome). Regions of DNA between genes might have been deleted such that the two genes are so close together that they can be cotranscribed from the upstream gene's promoter. If both of their products happen to be required together, or everywhere, an evolutionary advantage of reducing the genome size will accrue with no cost due to losing a regulatory region. Any new associations between genes will be tolerated as long as the benefits outweigh the costs. One of the benefits would be coregulation of genes whose products are needed in the same cells. Operons that fulfill this purpose should accumulate in the genome over time, whereas others might be lost.

It is not yet clear how widespread operons of the type found in *C. elegans* are in eukaryotes. So far, they have been observed only in free-living nematodes: *C. elegans* and its sibling species, *C. briggsae*, and a distantly related rhabditid nematode, CEW1 (D. Evans et al., unpubl.). In general, where *C. briggsae* homologs of *C. elegans* genes that occur in operons have been examined, the *C. briggsae* homologs have been shown to be present in the same genomic arrangement ([Lee et al. 1992](#); [Hengartner and Horvitz 1994b](#); [Kuwabara and Shah 1994](#); D. Zorio et al., in prep.). In CEW1, an operon containing two ribosomal proteins has been discovered, with 87 bp between the genes, and the downstream gene is *trans*-spliced to a sequence quite similar to SL2 (D. Evans et al., unpubl.). The fact that 80–90% of gene products of the parasitic species, *Ascaris lumbricoides*, are *trans*-spliced to SL1 ([Maroney et al. 1995](#)), whereas others are not *trans*-spliced, suggests that if operons exist in this species, either a specialized spliced leader is not used at internal *trans*-splice sites or operons are much less common than they are in *C. elegans*. It should be emphasized, however, that no systematic search for operons outside of *C. elegans* has yet been undertaken.

## B. E. Another Kind of Operon

Recently, a second type of operon has been discovered ([Hengartner and Horvitz 1994b](#); I. Korf and S. Strome, pers. comm.) that is different in two significant ways: (1) The mRNA of the downstream gene is *trans*-spliced to SL1, rather than SL2, and (2) there is no intercistronic sequence. The site of polyadenylation of the upstream gene and the *trans*-splice site are at adjacent nucleotides. The first such operon to be reported contains the [cyt-1](#) and [ced-9](#) genes, and the second contains the [mes-6](#) and [cks-1](#) genes. Operons containing the U170K and SRP54 genes are also apparently of this type (L. Xu and T. Blumenthal, unpubl.). It seems likely that this kind of operon may be functionally no different from the more common SL2 type but that the mechanism of processing of its polycistronic precursor may be quite different (see below).

## F. Mechanism of SL2-specific *Trans*-splicing and 3'-end Formation

How is SL2 *trans*-splicing specified? SL2-accepting *trans*-splice sites have the same consensus sequences as do intron 3'splice sites and SL1-accepting *trans*-splice sites (see [Table 2](#)). However, they appear to have more mismatches to the consensus than do the others, suggesting a mechanistic difference. One obvious idea is that 3'end formation, which occurs just upstream, is somehow directly or indirectly involved. The downstream product of the cleavage event in 3'-end formation is a free 5'phosphate (for review, see [Wahle and Keller 1992](#)). One might expect this product to be rapidly degraded because it is not protected by a cap. Why is the RNA coding for the downstream gene not subject to such degradation? Perhaps it binds to the SL2 snRNP, which subsequently splices at the *trans*-splice site 100–400 nucleotides downstream. In this view, SL2 is attracted to the appropriate sites by the 5'phosphate end. A somewhat more palatable idea is that the SL2 snRNP has affinity for the 3'-end formation machinery itself. According to this idea, a single complex involving the 3'-end formation machinery and the splicing machinery forms to accomplish both processes, perhaps simultaneously.

Both of these models suggest that the 3'-end formation machinery would be needed for SL2-specific splicing, and there is some experimental support for such a relationship. It has been shown in other systems that 3'-end formation is less efficient if the promoter is moved closer to the 3'end (see, e.g., [Iwasaki and Temin 1990](#)). [Spieth et al. \(1993\)](#) inserted the heat shock promoter at various positions within the [gpd-2](#) gene and found that the closer the promoter is to the 3'-end signals, the less SL2 splicing occurs. It was subsequently shown that SL1 *trans*-splicing occurs instead and that 3'-end formation is indeed less efficient when the promoter is positioned closer to the 3'end (S. Kuersten et al., unpubl.), supporting the idea that 3'-end formation and SL2 *trans*-splicing

are connected. The most direct experiment would be to inactivate the 3'-end formation signal. [Spieth et al. \(1993\)](#) mutated this signal, such that it was weakened but not eliminated, and found that polycistronic transcript accumulated. Thus, even though the *trans*-splice signal remained intact, it was only inefficiently used. This experiment suggests that the upstream 3'-end formation signal must remain intact for efficient SL2-specific *trans*-splicing. However, it does not answer whether 3'-end formation or the machinery that normally binds there is needed. The fact that in the [\*rrs-1\*](#) mutant strain, missing SL1, SL2 is *trans*-spliced onto normally SL1 accepting RNAs indicates that they are in competition, presumably for use of all *trans*-splice sites ([Ferguson et al. 1996](#)). The fact that an extrachromosomal array carrying the SL2 RNA gene can suppress the embryonic lethality of the [\*rrs-1\*](#) mutation lends further support to the idea that SL2 can be utilized in place of SL1 when SL1 is missing ([Ferguson et al. 1996](#)).

## Figures

Figure 6. The *mai-1* operon.

## Figure 6

The [\*mai-1\*](#) operon. Boxes indicate exons, lines introns, and wavy lines intercistronic regions. This figure is based on the data in [Huang et al. \(1989\)](#) and [Spieth et al. \(1993\)](#).

Figure 7. Distance between genes in operons.

## Figure 7

Distance between genes in operons. Each bar represents the number of genes with the indicated distance between the 3'end of the upstream gene and the 5'end of the downstream gene (shown in bp: 91–100, 101–110, 111–120, etc.). Thirty-nine intercistronic distances are included in the survey.

Generated from local HTML

## Chapter 6. RNA Processing and Gene Structure — V Trans -Splicing in Vitro

---

Important information about mechanisms of splicing has been obtained by recreation of the reaction in crude in vitro systems. Nilsen and co-workers have developed an extract from embryos of the nematode *Ascaris lumbricoides* capable of *trans*-splicing in vitro and have exploited this system to study mechanistic aspects of the reaction ([Hannon et al. 1990a](#); [Maroney et al. 1990a](#); [Yu et al. 1993](#)). They determined that branch-site formation occurs at either of two A residues contained in a sequence with no capability of base pairing with U2 snRNA. So far, no other branch sites have been mapped in nematode introns or outrons. These authors also discovered that the SL sequence itself is not required for the SL snRNP to function in *trans*-splicing in vitro ([Maroney et al. 1991](#)). Even when the first 20 nucleotides of the 22-nucleotide SL are deleted, *trans*-splicing of the remaining 2-nucleotide exon occurs accurately. In contrast, a region of the “intron” portion of the SL snRNP, including the Sm-binding site and adjacent nucleotides, is critically important for *trans*-splicing. Subsequent cross-linking experiments demonstrated that this region is involved in a base-pairing interaction with U6 snRNA ([Hannon et al. 1992](#)). It seems likely that this interaction is an important aspect of the mechanism of *trans*-splicing, bringing one of the substrates into contact with critical elements of the spliceosome.

The *A. lumbricoides* in vitro system has also been exploited to determine which snRNAs are required for *trans*-splicing ([Hannon et al. 1991](#); [Maroney et al. 1996](#)). It has been found that depletion of U2, U4, U5, or U6 by oligonucleotide/RNase H cleavage eliminates both *trans*- and *cis*-splicing. However, depletion of U1 inhibits only the latter. This result supports a prediction made by [Bruzik et al. \(1988\)](#) that the part played by U1 in *cis*-splicing, base pairing with the 5'splice site, is replaced in *trans*-splicing by the SL exon itself.

Generated from local HTML

## Chapter 6. RNA Processing and Gene Structure — VI Frequency of Operons and Trans -Splicing

---

Although it was originally estimated that the products of only 10–15% of *C. elegans* genes were subjected to *trans*-splicing ([Bektesh et al. 1988](#)), it is now clear that approximately 70% are *trans*-spliced ([Zorio et al. 1994](#)). The original estimate, based on a hybrid-arrest translation experiment with an SL1 antisense oligonucleotide, failed to take account of the fact that the TMG caps on the *trans*-spliced mRNAs inhibit translation in the rabbit reticulocyte system ([Darzynkiewicz et al. 1988](#)). This resulted in a large underestimation of the frequency of *trans*-splicing. [Zorio et al. \(1994\)](#) estimated the frequency of SL1 and SL2 *trans*-splicing by two different methods. First, the published literature was surveyed for genes for which the 5'ends had been determined. Of the 115 genes included in the survey, 57% were *trans*-spliced to SL1, 13% to SL2, and 30% were not *trans*-spliced. Second, 2 Mb of sequenced genomic DNA were surveyed for the presence of potential *trans*-splice sites upstream of predicted genes, and genes in clusters were tested for SL2 specificity to determine whether they were likely to be in operons. The results of this analysis are remarkably congruent with the survey of reported genes. The products of 57% of genes are estimated to be *trans*-spliced to SL1, 16% to SL2, and 27% are not *trans*-spliced. Taken together, these estimates indicate that the products of about 70% of *C. elegans* genes are *trans*-spliced and about 25% of *C. elegans* genes are transcribed in operons.

Generated from local HTML

## Chapter 6. RNA Processing and Gene Structure — VII Organization and Transcription of Spliced Leader RNA Genes

---

As mentioned above, the approximately 100 SL1 RNA genes are clustered with the 5S rRNA genes on a 1-kb repeat ([Krause and Hirsh 1987](#)). The 5S and SL1 RNA genes are arranged with their 5'ends apposed, with less than 200 bp between them. Although it is not clear whether this arrangement has any functional significance, it suggests that the 5S and SL RNA genes could share a regulatory region. However, the 5S rRNA gene is transcribed by RNA polymerase III, whereas the SL1 RNA gene is transcribed by RNA polymerase II ([Maroney et al. 1990b](#)). The presence of SL RNA and 5S genes in a short tandemly repeated unit is found in other nematodes (e.g., the parasites *Brugia malayi* and *Onchocerca volvulus* [[Tackacks et al. 1988; Zeng et al. 1990](#)]), and even in some trypanosomes (*Herpetomonas samuelpessoai* and *Trypanosoma vivax*) and *Euglena gracilis* ([Aksoy 1992; Keller et al. 1992; Roditi 1992](#)); however, in other nematodes and in the trypanosomes, both genes are on the same strand. Furthermore, there are nematode species in which the SL RNA genes are not clustered with the 5S genes (e.g., the free-living species *Panagrellus redivivus* and the parasite *Haemonchus contortus* [[Bektesh et al. 1988](#)]).

Transcription of the SL1 RNA gene requires the SL1 sequence itself, which serves as a binding site for a transcriptional activator ([Hannon et al. 1990b](#)). In addition, the SL1 RNA gene has a good match to the consensus *C. elegans* proximal sequence element (PSE), found upstream of all the *C. elegans* snRNA genes ([Thomas et al. 1990](#)). By analogy with the vertebrate PSEs, which have a different sequence, this sequence is presumed to be the site at which the SNAPc complex binds to activate transcription of both the SL RNA and the other snRNA genes ([Henry et al. 1995](#)).

SL2 RNA is encoded by a small gene family scattered throughout the *C. elegans* genome ([Huang and Hirsh 1989](#)), as are the other snRNA genes. Recently, a variety of SL2-related sequences have been identified ([Kuwabara et al. 1992; Ross et al. 1995](#)). These variant SL2s are *trans*-spliced onto the same set of mRNAs that receive SL2. They are also encoded by genes with sequences quite closely related to SL2 RNA. The existence of these variants suggests that the SL2 sequence may not serve as a binding site for a transcription factor, as the SL1 sequence does, since it has not been as highly conserved.

Generated from local HTML

## Chapter 6. RNA Processing and Gene Structure — VIII 3'-End Formation

---

In vertebrates, formation of 3'ends of mRNAs is dependent on a complex of proteins binding to signals just upstream of and just downstream from the future cleavage site, followed by cleavage of the pre-mRNA and polyadenylation of the resulting free 3'end (for review, see [Wahle and Keller 1992](#)). The upstream site is the almost perfectly conserved sequence, AAUAAA, which occurs between 10 and 35 nucleotides upstream of the cleavage site. This site binds a complex of three polypeptides called CPSF. The downstream site is a much less highly conserved U-rich or GU-rich sequence that binds another three-subunit protein called CStF. In addition, other proteins are required for the cleavage and polyadenylation reactions.

It appears that signals for 3'-end formation have diverged more rapidly than have signals for splicing. Although these signals have been very well defined in vertebrates, it has not proved possible to use this information to identify 3'-end formation signals in yeast or plants. In contrast, many *C. elegans* genes do have the AAUAAA sequence just upstream of the site of poly(A) addition. On the other hand, many do not. In an effort to determine what the 3'-end formation signal is in *C. elegans*, we have surveyed the 3'ends of published genes and cDNAs for matches to the AAUAAA consensus ([Table 3](#) and [Fig. 8](#)). In addition, an analysis of 3'-end sequences from a random set of 1500 *C. elegans* cDNA clones came to very similar conclusions (T. Blumenthal et al., unpubl.). These surveys clearly show that *C. elegans* uses the same signal as vertebrates, but the sequence requirements are less stringent. Just over half of *C. elegans* genes have a perfect match to the consensus AAUAAA. Most of the remaining genes have one of a limited group of tolerated mismatches to the consensus. AAUGAA (11%) and UAUAAA (8%) are the most commonly used variants. Furthermore, AAUAAA and variants occur in a very limited region, generally 11–17 nucleotides upstream of the cleavage site. Interestingly, 7% of *C. elegans* genes do not have any sequence related to AAUAAA in this region. This suggests that *C. elegans* may have an alternative, but much less commonly used, mechanism for 3'-end formation.

Because the *C. elegans* 3'-end formation machinery can accurately locate the correct cleavage site with several variants of the AAUAAA sequence, it is reasonable to suppose that the downstream signal might have a more highly conserved sequence than that in vertebrates. However, there is no obvious U-rich or GU-rich element in the downstream region. Furthermore, a search for an alternative consensus sequence in this region has not revealed any candidates. Additional sequences needed for 3'-end formation in *C. elegans* await identification.

One alternative mechanism for 3'-end formation that does appear to occur in *C. elegans* is polyadenylation at the free 3'end created by *trans*- splicing. [Spieth et al. \(1993\)](#) isolated cDNA clones in which the *mai-1* mRNA was polyadenylated at, or just a base or two upstream of, the *gpd-2* *trans*-splice site, instead of the normal site 100 nucleotides upstream. They hypothesized that these arose by polyadenylation of the free 3'end created by *trans*-splicing. This might require that the intronic region be debranched, and it would require that the *mai-1* AAUAAA sequence 100 nucleotides upstream serve as a binding site for CPSF to allow polyadenylation at a distance. This sequence has been shown to be able to function at a distance in vertebrates ([Manley et al. 1985](#)). The *mai-1* sequence, AGUAAA, is used very rarely, which may explain why a portion of the mRNA does not form 3'ends in the normal way. This alternative mechanism for 3'-end formation is probably used as well in the rare operons in which the site of polyadenylation of the upstream gene and the *trans*-splice site of the downstream gene are the same ([Hengartner and Horvitz 1994b](#); I. Korf and S. Strome, pers. comm.). Presumably, the mature mRNAs are formed by internal *trans*-splicing by the SL1 snRNP, followed by polyadenylation of the upstream mRNA at the free 3'end created by *trans*-splicing. Again, the upstream mRNA might have to be debranched, but in these cases, there is a proximal AAUAAA for binding CPSF to catalyze polyadenylation. It should be mentioned that, in general, 3'ends of genes within operons are signaled by AAUAAA and that the degree of conservation of this sequence at these locations is similar to that shown in [Table 3](#).

### Figures

 [Figure 8](#). Distance between the AAUAAA and the poly(A) site.

## Figure 8

Distance between the AAUAAA and the poly(A) site. Each bar represents the number of genes with the precise number of base pairs between the 3' end of the AAUAAA and the cleavage site indicated below. The survey includes 142 genes in which a match to the AAUAAA consensus was identified.

## Tables

**Table 3Polyadenylation and cleavage signal**

	No.	Percent
AAUAAA	86	56
AA <u>UG</u> AA	17	11
<u>UA</u> UAAA	13	8
None	10	7
<u>G</u> AUAAA	7	5
AAA <u>AAA</u>	6	4
<u>G</u> AUGAA	3	2
<u>C</u> AUAAA	2	1
AAUAA <u>U</u>	2	1
<u>A</u> GUAAA	2	1
<u>A</u> UUAAA	1	<1
AAU <u>CAA</u>	1	<1
<u>U</u> AUGAA	1	<1
AAUAC <u>A</u>	1	<1

The survey includes 153 genes in which the location of the 3'end has been experimentally verified. Matches to the AAUAAA consensus were identified visually. Mismatches to the consensus are underlined.

Generated from local HTML

## Chapter 6. RNA Processing and Gene Structure — IX Translation Initiation and Termination Signals

---

Initiation of translation in metazoans always occurs at an AUG codon. In addition to these three nucleotides, there appears to be information content in the preceding nucleotides, where the consensus is (A/G)CCAUG in vertebrates. In 211 genes included in the survey reported here, there is also a consensus in the nucleotides preceding the AUG, but it is quite different from the vertebrate consensus. *C. elegans* genes prefer A residues at each of the four positions preceding the AUG ([Fig. 9](#)). This is similar to the consensus proposed for ciliates and yeast, AAAAUG ([Cigan and Donahue 1987](#); [Brunk and Sadler 1990](#)).

There are also consensus sequences preceding and following the stop codon in *C. elegans*. The consensus is A/U, C/U—stop codon—A, U. Furthermore, not all termination codons are utilized with equal frequency: 61% are UAA, 17% UAG, and 22% UGA ([Fig. 9](#)).

### Figures

Figure 9. Translation initiation and termination sequences.

#### Figure 9

Translation initiation and termination sequences. The frequency (percent) of each nucleotide at each position with respect to the translation initiation codon, AUG (*above*) or translation termination codons (*below*), is given along with the derived consensus sequences. The frequency of use of each of the three termination codons is shown in the box. The survey includes 211 identified initiation codons and 142 identified termination codons.

Generated from local HTML

## Chapter 6. RNA Processing and Gene Structure — X Conclusions

---

*C. elegans* gene structure is similar to the gene structure of other animals. However, some special aspects of *C. elegans* genes are worthy of note. In general, the *C. elegans* genome appears to have been selected to be small. This has resulted in fewer introns per gene, in unusually small introns, and in less "junk" DNA between genes. The most dramatic difference reported to date between *Caenorhabditis* and other animals is the utilization of polycistronic transcription. This common bacterial trait has not been found so far in other animals. The existence of operons has allowed additional genome compaction. Although mechanisms of RNA splicing in *C. elegans* are quite closely related to the mechanisms utilized by other animals, the existence of *trans*-splicing coexisting with *cis*-splicing in the same cells to process the same pre-mRNAs makes study of splicing mechanisms in *C. elegans* especially interesting. Understanding the unique interplay of *trans*-splicing and 3'-end formation within the operons provides an interesting challenge for the future.

Generated from local HTML

## **Chapter 6. RNA Processing and Gene Structure — Acknowledgments**

---

We are grateful to members of the lab for critical reading of the manuscript and to John Spieth for extensive work on the figures. The survey was supported by a research grant from the National Institute of General Medical Sciences.

Generated from local HTML

# **Chapter 7. Transcription Factors and Transcriptional Regulation**

---

## **Contents**

- [I Introduction](#)
- [II The Basal Transcription Machinery](#)
- [III Transcription Factors](#)
- [IV Analysis of \*C. elegans\* Promoters](#)
- [V Future Prospects](#)

Generated from local HTML

## Chapter 7. Transcription Factors and Transcriptional Regulation — I Introduction

---

Particular aspects of *Caenorhabditis elegans* biology—embryonic development, sex determination, muscle and nerve biology, and so on—are considered in other chapters in this volume. This chapter focuses on a theme common to many of these chapters, namely, transcription factors and the regulation of genes transcribed by RNA polymerase II.

A recent compendium of human gene sequences ([Adams et al. 1995](#)) suggests that 7–8% of all genes code for transcription factors. If the same gene distribution applies to the approximately 13,000 genes in the *C. elegans* genome, then *C. elegans* must have 1000 such factors. *C. elegans* sequence databases contain many examples of classes of proteins that are known to control transcription in other organisms, and the genome sequencing project will soon provide a complete inventory. The task will then be to identify the genes that all of these factors regulate.

The first section of the present chapter summarizes information on the basal transcription machinery in *C. elegans*. The second section describes the most important properties of known transcription factors in *C. elegans*. The final section summarizes studies that have begun to unravel the transcriptional control of particular genes by analyzing their promoters.

Generated from local HTML

## Chapter 7. Transcription Factors and Transcriptional Regulation — II

### The Basal Transcription Machinery

---

Although several features of *C. elegans* transcription are unusual (e.g., *trans*-splicing and the arrangement of genes in operons), the basic transcriptional machinery is likely to be highly similar, both structurally and functionally, to that found in other eukaryotes. For example, RNA polymerase II from *C. elegans* behaves much like its counterpart in other eukaryotes, as judged from chromatographic behavior, immunological cross-reactivity, multisubunit composition, and  $\alpha$ -amanitin sensitivity ([Sanford et al. 1983, 1985](#)). The gene encoding the largest subunit of *C. elegans* polymerase II was cloned by heterologous screening with a *Drosophila* probe ([Bird and Riddle 1989](#)); sequence similarity is high throughout the encoded protein (80% or so, even when compared to animals as distant as mouse). The carboxy-terminal domain contains 42 heptad repeats, which is like the *Drosophila* enzyme but unlike the enzymes from yeast and mammals that have 26 and 52 repeats, respectively ([Bird and Riddle 1989](#)). Mutations in this gene can confer  $\alpha$ -amanitin resistance to worms, which has allowed extensive genetic analysis ([Rogalski et al. 1988, 1990](#)).

A second basal factor of crucial importance to transcription is TBP, the TATA-element-binding protein. The *C. elegans* TBP, like TBPs cloned from other organisms, has a rather highly diverged amino-terminal region. However, the carboxy-terminal region is highly conserved, with 75–85% sequence identity to the carboxy-terminal regions of TBP from yeast, *Drosophila*, and humans ([Lichtsteiner and Tjian 1993](#)). *C. elegans* TBP has been shown to interact directly with basal transcription factors from other organisms, for example, with TFIIA from yeast and with TFIIB from either humans or *Drosophila*. The *C. elegans* TBP can also replace human TBP in a depleted HeLa cell transcription system and can act on at least two different promoters ([Lichtsteiner and Tjian 1993](#)).

Experimental systems to investigate basal transcription are now becoming available in *C. elegans*. Active “nuclear run-on” systems have been described both in *C. elegans* ([Jones et al. 1989; Honda and Epstein 1990; Schauer and Wood 1990; Edgar et al. 1994](#)) and in *Ascaris* ([Cleavinger et al. 1989](#)). Furthermore, in vitro extracts of *Ascaris* embryos have been shown to be capable of transcribing the SL1 spliced leader RNA ([Maroney et al. 1990a](#)). An important experimental advance has been the preparation of transcriptionally active extracts from *C. elegans* embryos ([Lichtsteiner and Tjian 1995](#)). These extracts can accurately initiate transcription on *C. elegans* promoters (both promoters such as *hsp-16* that contain a TATAA element and promoters such as *her-1* that do not), as well as on heterologous promoters such as adenovirus. Basal transcription rates can be stimulated 10–40-fold by addition of either homologous or heterologous transcriptional activators, containing different types of activation domains. An important part of this initial study was to demonstrate that in-vitro-produced proteins (in this case, MEC-3 and UNC-86) could stimulate transcription from a particular *C. elegans* promoter (from the *mec-3* gene) in a manner consistent with extensive genetic evidence ([Lichtsteiner and Tjian 1995](#); see *Ruvkun*, this volume and below). Such biochemical experiments are likely to become increasingly important in the future, as genes that have originally been identified and studied by classical genetics become studied at the molecular level.

The phenomena of *trans*-splicing and of transcriptional operons ([Krause and Hirsh 1987; Zorio et al. 1994](#)) are two ways in which transcription in *C. elegans* can clearly differ from transcription in the best-studied experimental systems, such as yeast, *Drosophila*, or HeLa cells. The implications of these two phenomena for the overall biology of *C. elegans* are not yet clear (see Blumenthal and Steward, this volume), but they add one more level of complexity to the study of transcriptional regulation. For example, before the transcriptional control of a particular gene is investigated, it must be determined whether or not the gene is part of a transcriptional operon. *Trans*-splicing makes the determination of the transcription initiation site difficult but not impossible ([Conrad et al. 1993b](#)); it also raises the possibility that transcription initiation on a particular gene could occur at multiple sites, with *trans*-splicing subsequently converting heterogeneous primary transcripts into a unique mature messenger RNA. Partly because of the complications introduced by *trans*-splicing, relatively few genes in *C. elegans* have had their transcriptional initiation sites mapped unambiguously. Common promoter elements found in other systems, for example, the TATAA element, have often been assigned rather subjectively.

Relatively little is known about the general chromatin environment in which *C. elegans* transcription takes place, but there is no reason to think it will be much different from that in the majority of eukaryotes. *C. elegans* histone gene sequences have been well-conserved ([Vanfleteren 1983](#); [Roberts et al. 1987, 1989](#); [Vanfleteren et al. 1989](#); [Sanicola et al. 1990](#)) and show sequence variability only in regions where variability is found in other organisms. The repeating nucleosome architecture of *C. elegans* chromatin has been investigated by standard nuclease digestion experiments ([Dixon et al. 1990](#)). The basic repeat size appears to depend on the extent of digestion, perhaps pointing to different chromatin characteristics in the different cell types of the animal. Because of such unavoidable heterogeneity of starting material, it will be difficult to study detailed chromatin changes in subclasses of cells, the question of greatest biological interest.

The study of dosage compensation has provided the strongest connection between chromatin structure and transcriptional activity in *C. elegans* (see Meyer, this volume). Chuang *et al.* (1994) have shown that the product of the [\*dpy-27\*](#) gene belongs to a family of "chromosome condensation" proteins. Moreover, DPY-27 is localized to the two X chromosomes of hermaphrodites but not to the single X chromosome in males. The suggested model is that DPY-27 condenses the hermaphrodite X chromosomes, leading to approximately twofold repression of genes needed for correct dosage compensation.

Generated from local HTML

## Chapter 7. Transcription Factors and Transcriptional Regulation —

### III Transcription Factors

---

Dozens of transcription factors have now been identified and characterized in *C. elegans* by a combination of genetics, molecular screens, and the genome sequencing project. We describe below those factors for which sufficient information is available to suggest important roles in cell determination, differentiation, or function. Factors are grouped by family and subfamily (if appropriate), as summarized in [Table 1](#). Many of these genes and their products are discussed in greater detail elsewhere in this volume. The purpose of the present description is to provide a concise catalog of transcription factors characterized to date, their expression patterns, and their candidate target genes. It will be clear that only a small fraction (perhaps fewer than 5%) of *C. elegans* transcription factors have so far been identified and studied. It is equally clear that the combination of the genome sequencing information and the expanding understanding of *C. elegans* as a model biological system will result in an explosion of information about the control of transcription over the next few years.

#### A. Homeodomain Family

The homeodomain is a 60-amino-acid DNA-binding motif first recognized as a common feature in *Drosophila* homeotic proteins ([Laughon and Scott 1984](#); [McGinnis et al. 1984](#)). A number of different homeodomains have now been crystallized, and their overall structures all turn out to be highly similar (see, e.g., [Wolberger et al. 1991](#)). The homeodomain folds into a three-helix bundle that can bind to DNA through interactions between the "recognition" helix (helix no. 3) and groups in the DNA major groove. Additional interactions can occur between homeodomain flanking regions and the DNA minor groove.

*C. elegans* homeodomain genes identified on the basis of cross-hybridization were sequentially numbered under the *ceh* gene designation (*C.elegans* homeodomain). The evolution of homeodomain proteins, including several from *C. elegans*, has been reviewed recently by Bürglin (1995).

##### 1. HOX Class

As in *Drosophila* and vertebrates ([McGinnis and Krumlauf 1992](#)), *C. elegans* has a clustered set of homeodomain genes that appear to function in overlapping compartments arranged sequentially along the anterior-posterior axis of the animal. The HOX cluster in *C. elegans* maps to the central region of chromosome III and consists of five genes: [ceh-23](#), [egl-5](#), [mab-5](#), [lin-39](#), and [ceh-13](#) ([Bürglin et al. 1991](#); [Kenyon and Wang 1991](#); [Wang et al. 1993](#); [Bürglin 1995](#); [Hunter and Kenyon 1995](#)). As yet, insufficient information is available to elaborate on [ceh-23](#), but the other *C. elegans* HOX genes are discussed below (also see [Ruvkun](#), this volume).

##### **egl-5**

The [egl-5](#) gene was originally identified in genetic screens for egg-laying-defective animals ([Trent et al. 1983](#)) and subsequently identified in molecular screens for homeobox genes under the designation [ceh-11](#) ([Hawkins and McGhee 1990](#); [Schaller et al. 1990](#)). Consistent with its location at the "posterior" end of the HOX cluster, [egl-5](#) shows greatest similarity to the *Drosophila* gene *Abdominal B* ([Wang et al. 1993](#)). [egl-5](#) ::*lacZ* reporter genes are expressed in the [anal](#) and tail region of twofold embryos. In L1 animals, expression is detected in descendants of tail blast cells, in posterior body-wall muscle cells, and in the HSN cells that originate in the tail and migrate anteriorly during development ([Wang et al. 1993](#)); it is the HSN cell fate that is affected in [egl-5](#) mutants ([Chisholm 1991](#)). [egl-5](#) presumably functions in the regional specification of tail cell fates.

##### **mab-5**

The [mab-5](#) gene was identified in a genetic screen for [males](#) with [abnormal](#) morphology ([Hodgkin 1983](#); [Kenyon 1986](#)) and shows sequence similarity to the *Drosophila* gene *Antennapedia*. As assayed by *lacZ* fusions, [mab-5](#) is expressed in the posterior regions of the embryo, beginning at about the 200-cell stage ([Cowing and Kenyon 1992](#)); expression continues in posterior regions of larvae as demonstrated by *in situ* hybridization ([Costa et al.](#)

[1988](#); [Salser and Kenyon 1992](#)). Cells that express [\*mab-5\*](#) bear no obvious lineage relation to each other but rather are related by their ultimate position in the posterior of the animal. Consistent with the molecular expression data, [\*mab-5\*](#) appears to regulate cell fates in a region-specific manner; in particular, [\*mab-5\*](#) mutations alter a number of posterior [\*neuronal\*](#) cell fates, cell deaths, and cell migrations ([Kenyon 1986](#)).

### **lin-39**

The [\*lin-39\*](#) gene was originally identified through its effects on the [lineage](#) of a subset of vulval precursor cells (VPCs) and [\*neurons\*](#) involved in egg laying (see [Fixen et al. 1985](#)). More recently, [\*lin-39\*](#) was identified under the designation of [\*ceh-15\*](#) by molecular screens for homeodomain-containing genes ([Kamb et al. 1989](#); [Wang et al. 1993](#)). The LIN-39 homeodomain shows greatest sequence similarity to the *Drosophila* genes *sex combs reduced*, *deformed*, and *proboscipedia*, as might be predicted from its location in the cluster. During larval development, a [\*lin-39\* ::\*lacZ\*](#) reporter construct is expressed in the Q cells (and their descendants) and in some of the P cells. Expression can also be detected in the eight muscle cells of the adult [\*vulva\*](#). These patterns of expression are consistent with genetic data which demonstrate that [\*lin-39\*](#) plays a part in mid-body development.

### **ceh-13**

The [\*ceh-13\*](#) gene ([Schaller et al. 1990](#)), a putative ortholog of *Drosophila labial*, might be expected to determine the fates of cells anterior to cells influenced by [\*lin-39\*](#). CEH-13 is detected as early as the 28-cell stage in the [\*AB\*](#) and [\*E\*](#) lineages. Later in development, the gene product appears either transiently or continuously in cells from the [\*AB\*](#), [\*E\*](#), [\*MS\*](#), and [\*D\*](#) lineages and seems to be, at least partially, controlled by spatial cues. During larval and adult stages, [\*ceh-13\*](#) is expressed in hypodermal and [\*ventral nerve cord\*](#) cells (C. Whittman and F. Mueller, pers. comm.). The fact that CEH-13 is present in cells located anteriorly to [\*lin-39\*](#)-expressing cells suggests that the gene might indeed be involved in anterior morphogenesis. A genetic function for [\*ceh-13\*](#) is not yet clear.

## **2. POU Class**

The POU class of homeodomain proteins was named after the first identified class members: the mammalian transcription factors [\*Pit-1\*](#), [\*Oct-1\*](#), and [\*Oct-2\*](#) and the *C. elegans* gene product [\*UNC-86\*](#) ([Finney et al. 1988](#); [Herr et al. 1988](#)). In addition to sequence similarity in the homeodomain, POU members share further sequence similarity in an adjacent approximately 100-amino-acid region termed the POU domain.

### **unc-86**

The [\*unc-86\*](#) mutants were identified in the original *C. elegans* genetic screens as [uncoordinated](#) animals ([Brenner 1974](#); [Sulston and Horvitz 1981](#)). Lineage analysis of [\*unc-86\*](#) mutants demonstrated that in a number of neuroblast cell lineages, [\*unc-86\*](#) function is required for daughter cells to become different from their mothers. [\*unc-86\*](#) is also required for certain cells to adopt a specific [\*neuronal\*](#) cell fate ([Chalfie et al. 1981](#); [Finney et al. 1988](#)). Antibodies to UNC-86 locate the protein in nuclei of 47 [\*neurons\*](#) in L1 larvae and 57 [\*neurons\*](#) in adult hermaphrodites ([Finney and Ruvkun 1990](#)). The best studied function of [\*unc-86\*](#) in cell fate specification is the generation of the six touch receptor cells. UNC-86 functions in the [\*touch cells\*](#), at least in part, by activating the expression of the LIM class homeodomain gene [\*mec-3\*](#). *In vitro* studies have shown that UNC-86 binds the sequence AAATTCAT, that the binding is enhanced by interaction with the binding of MEC-3 to an adjacent site, and that this heterodimeric combination positively autoregulates [\*mec-3\*](#) ([Xue et al. 1992](#), 1993). These results have largely been confirmed by *in vitro* transcription assays ([Lichtsteiner and Tjian 1995](#)). Analysis of the [\*unc-86\*](#) promoter is summarized below. For a description of [\*unc-86\*](#) function, see Ruvkun (this volume).

### **ceh-6**

The [\*ceh-6\*](#) gene was identified in a molecular screen of a cDNA library using a degenerate homeodomain oligonucleotide as probe ([Bürglin et al. 1989](#)). CEH-6 has been detected in nuclei of four pairs of [\*head neurons\*](#), in the SABV cells, and in the [\*excretory\*](#) cell. *lacZ* reporter gene constructs show this same pattern of expression, as well as expression in several vulval and tail cells. Mutations in [\*ceh-6\*](#) have been isolated via Tc1 excisions and

display a severe tail defect that often results in tail rupture during late embryogenesis (T.R. Bürglin and G. Ruvkun, pers. comm.).

### **ceh-18**

Like [\*ceh-6\*](#), the [\*ceh-18\*](#) gene was isolated from a cDNA library using a degenerate homeodomain oligonucleotide probe ([Bürglin et al. 1989](#)). CEH-18 can be detected in nuclei of many cells at the threefold stage of embryogenesis. During larval development, CEH-18 is present in gonadal sheath cells, epidermal cells, and the [distal tip cells](#). A [\*ceh-18\*](#) null mutant shows defects that can be correlated with the gene's postembryonic expression pattern: meiotic cell cycle defects (presumably because of a defect in the sheath cells), gonad migration defects, and problems in epidermal cell differentiation ([Greenstein et al. 1994](#)).

## **3. LIM Class**

The LIM class of homeodomain proteins is named for the first three identified class members: *lin-11* from *C. elegans*, *Isl-1* from mammals, and *mec-3* from *C. elegans*; all share sequence similarities in regions distinct from the homeodomain ([Freyd et al. 1990](#)). Each LIM motif is composed of a double zinc finger structure reminiscent of DNA-binding fingers. Despite this similarity, LIM domains do not appear to function as DNA-binding elements, but they have been suggested to mediate protein-protein interactions. LIM domains may also negatively autoregulate the DNA-binding activity of the linked homeodomain (for review, see [Dawid et al. 1995](#)).

### **lin-11**

The [\*lin-11\*](#) gene was identified in genetic screens for lineage abnormalities resulting in a Vulvaless phenotype ([Ferguson and Horvitz 1985](#)). In [\*lin-11\*](#) mutants, the secondary vulval blast cells fail to produce daughter cells of different fates ([Ferguson et al. 1987](#)). The metal-binding properties of the [\*lin-11\*](#) LIM region raise the possibility that these proteins may function as redox-sensitive transcriptional regulators ([Li et al. 1991](#)).

### **mec-3**

The [\*mec-3\*](#) gene was identified as one of several genes involved in mechanosensation. Mutants in [\*mec-3\*](#) fail to generate the six touch cell receptor [neurons](#) ([Way and Chalfie 1988](#); see [Driscoll](#)) ([Kaplan](#)). *m3c-3::lacZ* reporter constructs are expressed in the six touch receptor cells from the time the cells are born, throughout the remainder of development ([Way and Chalfie 1989](#)). Expression is also seen in the pairs of FLP and [PWD neurons](#). Analysis of the [\*mec-3\*](#) promoter is discussed below. MEC-3 appears to act as a positive autoregulatory factor that can interact synergistically with UNC-86 to stimulate [\*mec-3\*](#) expression ([Xue et al. 1992](#), 1993). In vitro transcription studies demonstrate a similar enhancement of transcription by MEC-3 via interaction with UNC-86 ([Lichtsteiner and Tjian 1995](#)). Interactions with UNC-86 appear to be independent of the LIM domain. A carboxy-terminal acidic region of MEC-3 appears to function in transcriptional activation.

## **4. Paired and Paired-like Class**

The paired domain is a discrete 128-amino-acid motif found in proteins that may or may not also contain a homeodomain ([Burri et al. 1989](#); [Walther and Gruss 1991](#)). The paired domain alone can bind DNA ([Treisman et al. 1991](#)). The crystal structure reveals two globular domains with the amino-terminal domain making contacts with both the major and minor grooves of the DNA-binding site ([Xu et al. 1995](#)). If present, the homeodomain is highly conserved among paired domain proteins and is called a "paired-type" homeodomain.

### **vab-3**

The [\*vab-3\*](#) gene (variable abnormal morphology) is part of a complex locus that also includes the overlapping gene [\*mab-18\*](#). This locus has also been referred to as the *C. elegans* *Pax-6* gene because it encodes a homeodomain protein related to the *eyeless* and *Pax-6* gene products of *Drosophila* and vertebrates, respectively ([Chisholm and Horvitz 1995](#); [Zhang and Emmons 1995](#)). [\*vab-3\*](#) mutants have a variable phenotype affecting the head of the animal ([Lewis and Hodgkin 1977](#)). [\*vab-3::lacZ\*](#) reporter constructs first show embryonic expression at

about 300 minutes of development; expression is detected in 20–30 cells in the anterior-dorsal region corresponding in position to hypodermal and neuronal cells and their precursors ([Chisholm and Horvitz 1995](#)). Expression persists in anterior hypodermal cells and [neurons](#) into the L1 stage, and the mutant phenotype presumably results from a misspecification of anterior cell fates. In *Drosophila* and vertebrates, *eyeless/Pax-6* genes regulate eye development; [vab-3](#) function in *C. elegans* may reflect some primordial role for this evolutionarily conserved gene ([Chisholm and Horvitz 1995](#)).

### **mab-18**

The [mab-18](#) gene is also part of the [vab-3](#)-encoding locus described above. [mab-18](#) does not itself contain a paired domain because its transcriptional start site lies downstream from the [vab-3](#) paired-domain-encoding exon. However, a homeodomain of the type generally associated with paired-box factors is common to both [vab-3](#) and [mab-18](#) ([Chisholm and Horvitz 1995](#); [Zhang and Emmons 1995](#)). Expression of a [mab-18::lacZ](#) reporter construct is detected in the male ray 8 lineage beginning at the late L3 stage and in the ray 6 lineage beginning at the L4 stage ([Zhang and Emmons 1995](#)). The reporter gene is also expressed in several head hypodermal nuclei and [neurons](#) at the L4 stage. Consistent with the reporter gene expression patterns, [mab-18](#) mutations cause defects in the male rays, resulting in the male abnormal phenotype ([Baird et al. 1991](#); [Chow and Emmons 1994](#)).

### **unc-4**

The [unc-4](#) gene was genetically identified by mutations that cause uncoordinated movement ([Brenner 1974](#)) and was isolated in molecular screens for homeobox genes under the designation [ceh-4](#) ([Miller et al. 1992](#)). [unc-4](#) regulates the synaptic input of the VA motor [neurons](#), and [unc-4::lacZ](#) reporter genes are indeed expressed in these [neurons](#) in L1 larvae ([Miller and Niemeyer 1995](#); see [Ruvkun](#), this volume). The [unc-4::lacZ](#) reporter is also expressed in approximately a dozen other [neurons](#) beginning late in embryogenesis; however, defects in these latter cell types have not yet been observed in [unc-4](#) mutants.

### **ceh-10**

The [ceh-10](#) gene was identified in molecular screens for homeodomain-containing genes ([Hawkins and McGhee 1990](#)). [ceh-10](#) also shows strong similarity to two vertebrate genes, *Chx10* and *Vsx1*, both in the “paired-like” homeodomain and in a 60-amino-acid adjoining region termed the CVC domain ([Svendsen and McGhee 1995](#)). Both *Chx10* and *Vsx1* are highly (almost exclusively) expressed in cells of the vertebrate retina. A [ceh-10::lacZ](#) reporter construct is expressed in about a dozen anterior [neurons](#), including the [interneuron AIY](#). It was suggested that [AIY](#) may share properties with the vertebrate retinal cells expressing *Chx10/Vsx1*. Worm strains transformed with the [ceh-10::lacZ](#) reporter frequently display a Wit (withered tail) phenotype, possibly because expression of the transgene in the CAN cell interferes with normal cell function ([Svendsen and McGhee 1995](#)).

### **unc-30**

The [unc-30](#) gene was identified in the genetic screens of [Brenner \(1974\)](#) and is required for the development and function of all 19 GABAergic type-D motor [neurons](#) ([McIntire et al. 1993a](#)). Antibody staining shows that UNC-30 is present in nuclei of the D-class motor [neurons](#) in young larvae, with lower levels detected in adults. UNC-30 is also present in several non-GABAergic [neurons](#) but is absent from several non-D-type GABAergic [neurons](#). Ectopic expression of [unc-30](#) can induce GABA in some but not [all neurons](#) as well as in certain nonneuronal cells. It was suggested that [unc-30](#) controls terminal differentiation of the GABAergic type-D [neurons](#) ([Jin et al. 1994](#)).

## **5. NK Class**

### **ceh-22**

The [ceh-22](#) gene was cloned from an expression library using a [myo-2](#) (pharyngeal-specific myosin gene) promoter fragment as a probe ([Okkema and Fire 1994](#)). Antibody and *lacZ* reporter studies (see below) detect

similar patterns of pharyngeal-specific [ceh-22](#) expression beginning at the lima bean stage of embryogenesis. By the threefold stage, CEH-22 is present in nuclei of the pharyngeal muscles [m1](#), [m3](#), [m4](#), [m5](#), and [m7](#) ([Okkema and Fire 1994](#)). CEH-22 can bind to the sequence TAAAGTGGTTGTG, consistent with the NK-class core consensus binding site TNNAGTG. Ectopic expression of [ceh-22](#) can induce ectopic [myo-2](#) expression in body-wall muscles, demonstrating its positive role in activating [pharyngeal muscle](#)-specific genes (P. Okkema, pers. comm.).

## 6. Other Homeodomain Genes

### **pal-1**

The [pal-1](#) (posterior *alae* of males abnormal) gene was initially identified in genetic screens for abnormal males ([Waring and Kenyon 1990](#)), as well as in screens for embryonic lethals under the name [nob-2](#) (*no backend*; L. Edgar, pers. comm.). The [pal-1](#) gene was cloned using transformation rescue of the mutant ([Waring and Kenyon 1991](#)) and also in molecular screens for homeobox genes under the designation [ceh-3](#) ([Bürglin et al. 1989](#)). [pal-1](#) is very similar to the *caudal* gene of *Drosophila*. The genetically defined, postembryonic consequence of [pal-1](#) (e2097) is to disrupt the production of [mab-5](#) -dependent V6-derived rays ([Waring and Kenyon 1990](#)). Although the molecular nature of the alleles displaying a Pal phenotype is unknown, the embryonic Nob phenotype seems to result from loss-of-function mutations. Both genetic and molecular data suggest a critical role for [pal-1](#) function in posterior cell fate determination throughout development. Interestingly, high-copy-number transgenic [pal-1](#) ::*lacZ* strains produce some embryos with a Nob phenocopy (L. Edgar, pers. comm.), suggesting that positive regulators of [pal-1](#) may be titrated out.

### **vab-7**

Originally identified in genetic screens for morphological defects, [vab-7](#) has subsequently been shown to encode a homolog of the *Drosophila* gene *even-skipped* ([Ahringer 1996](#)). Expression of [vab-7](#) has been assayed both by *in situ* hybridization and by reporter gene expression in transgenic animals. Expression of [vab-7](#) begins in four muscle and epidermal precursor cells in the posterior of gastrulating embryos. Expression is later detected in posterior body-wall muscle cells and in posterior hypodermis. Analyses of [vab-7](#) mutants suggest that [vab-7](#) functions in posterior patterning, possibly reminiscent of *even-skipped* function in *Drosophila* ([Carroll and Scott 1986](#)).

## B. Zinc Finger Transcription Factors

The zinc finger motif, first described in the *Xenopus* transcription factor IIIA, is a small protein domain that uses zinc to stabilize its structure ([Miller et al. 1985](#)). Multiple zinc fingers are common features of a large number of proteins, and several subfamilies of zinc finger proteins have now been recognized (for review, see [Klug and Schwabe 1995](#)). Most, but not all, zinc fingers are found in transcription factors and function in DNA binding; they have also been ascribed a role in protein-protein interactions.

### **1. GATA Class**

The GATA class of zinc finger transcription factors are named after the founding member of the class, GATA-1, a factor crucial for vertebrate erythropoiesis ([Weiss and Orkin 1995](#)). GATA factors contain distinctive zinc finger domains (usually two) and bind to the DNA target sequence (A/T)GATA(A/G) ([Omichinski et al. 1993](#)).

### **elt-1**

The [elt-1](#) (erythrocyte-like or erythroid-like transcription factor) gene was identified in a molecular screen for GATA-factor homologs ([Spieth et al. 1991b](#)). The two zinc fingers of [elt-1](#) are highly similar (75% or so) to regions found in the GATA factors of vertebrates. Although the aim in cloning [elt-1](#) was to identify factors controlling transcription of the vitellogenin genes in the adult hermaphrodite intestine (see below), [elt-1](#) has recently been

found to be the same as [\*hyd-1\*](#), mutations in which cause embryonic hypodermal defects (B. Page et al., pers. comm.). Consistent with this latter role, [\*elt-1\*](#) mRNA is highly enriched in embryos ([Spieth et al. 1991b](#)).

### **elt-2**

The [\*elt-2\*](#) gene was cloned from an expression library using a GATA sequence from the intestinal-specific [\*ges-1\*](#) gene promoter as a probe ([Egan et al. 1995](#); [Hawkins and McGhee 1995](#); and see below). [\*elt-2\*](#) encodes a protein with only a single zinc finger, which nevertheless shows 72–84% identity to the carboxy-terminal DNA-binding finger of two-finger GATA proteins from vertebrates ([Hawkins and McGhee 1995](#)). Transformation experiments with [\*elt-2\* ::\*lacZ\*](#) reporter constructs suggest that [\*elt-2\*](#) expression is indeed intestinal-specific, beginning around the 2E cell stage of embryogenesis (M.G. Hawkins et al., unpubl.). [\*elt-2\*](#) mRNA is highly enriched in embryos and was not detected in oocytes. ELT-2 produced in vitro binds to an oligonucleotide containing the [\*ges-1\*](#) gene GATA sequences, and the resulting complex has electrophoretic properties similar to those of a complex produced with embryonic nuclear extracts ([Stroher et al. 1994](#); [Hawkins and McGhee 1995](#)). Forced expression of [\*elt-2\*](#) by means of a heat shock construct leads to ectopic expression of [\*ges-1\*](#) in the early embryo (T. Fukushige and J.D. McGhee, unpubl.). Thus, [\*elt-2\*](#) appears to be a good candidate to control [\*ges-1\*](#) transcription, but this has not yet been demonstrated genetically.

### **end-1**

The [\*end-1\*](#) gene was isolated in a genetic screen for mutant embryos that completely lack intestinal cells. END-1 has recently been shown to be a GATA factor, and [\*end-1\* ::\*lacZ\*](#) reporter constructs are expressed at the 2E cell stage of gut development (J. Rothman, pers. comm.). [\*end-1\*](#) must clearly have an important role in gut development, and it will be interesting to work out the relationship between [\*end-1\*](#) and [\*elt-2\*](#).

## **2. Other Genes Encoding Zinc Finger Proteins**

*tra-1*: The [\*tra-1\*](#) (sex transformer) gene was first identified genetically as the terminal gene in the sex determination pathway ([Hodgkin 1987a](#)). Alternative splicing can produce two different zinc finger proteins, one with two fingers and the other with an additional three fingers ([Zarkower and Hodgkin 1992](#)). The five-finger protein, TRA-1L, binds DNA with the sequence TGGG(T/A)GGTC; in contrast, the two-finger protein, TRA-1S, does not bind DNA ([Zarkower and Hodgkin 1993](#)). The zinc fingers of TRA-1L show greatest similarity to the *Drosophila* gene *cubitus interruptus Dominant* and the human genes *GLI* and *GLI3* ([Zarkower and Hodgkin 1993](#)). Both [\*tra-1\*](#) transcripts are present throughout development but are not sex-specific, suggesting that the regulation of [\*tra-1\*](#) activity is posttranscriptional ([Zarkower and Hodgkin 1992](#)). Indeed, the clustered distribution of sequence alterations in a series of gain-of-function alleles has led to the proposal that TRA-1 is regulated posttranslationally by interaction with one or more inhibitory proteins ([de Bono et al. 1995](#)).

### **sdc-1**

The *sdc* genes were identified in genetic screens for mutations involved in sex determination and dosage compensation ([Villeneuve and Meyer 1987](#)). The function of [\*sdc-1\*](#), as defined genetically, is to negatively regulate the [\*her-1\*](#) sex determination gene and to activate genes required in XX animals for the correct mode of dosage compensation ([Villeneuve and Meyer 1990a](#); [Nonet and Meyer 1991](#)). SDC-1 contains seven zinc finger domains, five of which show similarity to the TFIIIA type of DNA-binding finger ([Nonet and Meyer 1991](#)). Unlike the clustered distribution of most multiple zinc finger domains, the fingers of SDC-1 are dispersed throughout the protein. [\*sdc-1\*](#) RNA is most abundant in embryos, and analysis of temperature-sensitive mutations shows that [\*sdc-1\*](#) functions during the first half of embryogenesis ([Villeneuve and Meyer 1990a](#); [Nonet and Meyer 1991](#)).

### **sdc-3**

Like [\*sdc-1\*](#), the [\*sdc-3\*](#) gene regulates both sex determination and dosage compensation ([DeLong et al. 1993](#)) and is expressed in embryos and early larval stages of both sexes ([Klein and Meyer 1993](#)). SDC-3 has two zinc fingers (related to TFIIIA) and a region with limited similarity to the ATP-binding domain of myosin. Mutations affecting

only dosage compensation map to the zinc finger region, whereas mutations affecting sex determination map to the putative ATP-binding domain ([DeLong et al. 1993](#); [Klein and Meyer 1993](#)).

### **egl-43**

The [\*egl-43\*](#) gene was first identified because of the egg-laying-defective phenotype that results from the failed migration of hermaphrodite-specific [neurons](#) (HSNs) ([Desai et al. 1988](#); [Desai and Horvitz 1989](#)). *egl-43* is also required for the proper development of the tail [phasmid neurons](#) PHA and PHB. *egl-43* encodes two proteins, one with six zinc fingers and the other with three zinc fingers; these motifs are related to zinc fingers in the murine oncogene Evi-1 ([Garriga et al. 1993c](#)). Antibodies to EGL-43 reveal a complex expression pattern beginning in early embryogenesis and continuing into larval development. EGL-43 is present both in the cells affected by *egl-43* mutations (the migrating HSNs and the [phasmid neurons](#)) and in other apparently unaffected cell types (G. Garriga, pers. comm.).

### **lin-26**

The [\*lin-26\*](#) gene was identified in genetic screens for vulvaless animals ([Ferguson and Horvitz 1985](#)) caused by a defect in Pn.p cell development ([Ferguson et al. 1987](#)). LIN-26 contains two zinc fingers of the TFIIIA type and is required for all hypodermal cell development; a null mutation in *lin-26* results in degeneration of hypodermal cells leading to embryonic arrest at the comma stage ([Labouesse et al. 1994](#)). LIN-26 can be detected postembryonically in nuclei of all hypodermal cells, socket and sheath cells, P cells, tail blast cells, and precursors of the [somatic gonad](#). The phenotype of *lin-26* mutants coupled with the distribution of LIN-26 protein suggests that it may act in all nonneuronal ectodermal cells by repressing neuronal-specific genes ([Labouesse et al. 1996](#)).

### **lin-29**

The [\*lin-29\*](#) gene was identified in genetic screens for heterochronic genes ([Papp et al. 1991](#)). *lin-29* is expressed as two transcripts beginning during the L1 stage and peaking in abundance during the L4 stage ([Rougvie and Ambros 1995](#)). *lin-29* encodes a five zinc finger protein (TFIIIA type) that regulates the development of the lateral [hypodermal seam cells](#) during the larval to adult molt ([Ambros 1989](#); [Rougvie and Ambros 1995](#)). LIN-29 was shown to be capable of binding to the promoter regions of both the [\*col-19\*](#) gene (turned on in L4 animals) and the [\*col-17\*](#) gene (turned off at the L4 stage), suggesting that these genes may be direct targets for LIN-29 regulation in vivo and that LIN-29 can act as both a positive and a negative transcriptional regulator ([Rougvie and Ambros 1995](#); [Liu et al. 1995](#); and see below).

## **C. Helix-Loop-Helix Genes**

Helix-loop-helix (HLH) genes derive their name from a conserved domain that spans approximately 40 amino acids and mediates dimerization between family members. Most HLH factors also have an adjacent stretch of basic amino acids (~20 residues) that functions in DNA binding, recognizing the canonical DNA sequence CANNNTG (known as an E-box). The crystal structure of HLH homodimers reveals a parallel, left-handed, four helix bundle (two  $\alpha$  helices contributed by each monomer), from which the  $\alpha$ -helical basic domain protrudes into the major groove of the DNA-binding site ([Ma et al. 1994](#)).

### **hlh-1**

The [\*hlh-1\*](#) gene, encoding CeMyoD, was identified in molecular screens for homologs of vertebrate MyoD family members ([Krause et al. 1990, 1992](#)). CeMyoD is expressed in two phases during development, a transient early phase in [MS](#) daughters and granddaughters, followed by a second, stable pattern of expression beginning at the approximately 90-cell stage of embryogenesis in the two daughters of the [D](#) blastomere. CeMyoD protein subsequently accumulates in all body-wall muscle cells and their precursors, as well as in the six [GLR](#) cells in the head, remaining in these cells throughout development ([Krause et al. 1990, 1994](#)). Although no in vivo binding targets are known, CeMyoD efficiently homodimerizes and binds to the sequence CAGCTG in vitro (T.K. Blackwell and M. Krause, unpubl.). A null mutation in *hlh-1* shows that CeMyoD is required for proper myogenesis and

morphogenesis but is not required for cells to adopt the body-wall muscle cell fate ([Chen et al. 1992, 1994](#); see also [MoermanFire](#)).

## hlh-2

The [hlh-2](#) gene was identified by random cDNA sequencing ([McCombie et al. 1992](#)), and it encodes CeE12/Da, the *C. elegans* homolog of vertebrate E proteins and the *Drosophila Daughterless (Da)* protein. In vertebrates and *Drosophila*, E/Da protein-encoding genes are ubiquitously expressed and serve as the heterodimeric partner to cell-specific HLH factors such as the MyoD family in striated muscle (see [Weintraub 1993](#)) and the *achaete-scute* family in [neurons](#) ([Caudy et al. 1988; Cabrera and Alonso 1991](#)). In *C. elegans*, [hlh-2](#) expression can be detected in the nuclei of all blastomeres from the 2-cell stage through the approximately 200-cell stage of embryogenesis. The distribution of CeE12/Da becomes progressively restricted until, by hatching, protein is detected only in about 14 [head neurons](#) and [pharyngeal cells](#) and in seven cells of the tail. Surprisingly, CeE12/Da is not coexpressed in CeMyoD-expressing body-wall muscle precursors (M. Krause, unpubl.); such coexpression might have been anticipated from studies on vertebrate myogenesis. The function of CeE12/Da is presently unknown, but its early widespread expression raises the possibility of a role in sex determination, like the function of *Da* in *Drosophila* ([Caudy et al. 1988; Parkhurst et al. 1993](#)). The later restriction of CeE12/Da to [neurons](#) might suggest an interaction with members of the *C. elegans* *achaete-scute* family; similar interactions are known to occur in vertebrate and *Drosophila* neurogenesis (see, e.g., [Cabrera 1992](#)).

## lin-22

In [lin-22](#) mutant males, the anterior V cells adopt a neuronal, rather than epidermal, cell fate ([Horvitz et al. 1983](#)). Recent cloning of the [lin-22](#) gene (L. Wrischnik and C. Kenyon, in prep.) shows that it encodes a protein related to the *Drosophila hairy* gene product, an HLH protein that acts as a negative regulator of other HLH proteins involved in a number of developmental processes, including neurogenesis ([Ingham et al. 1985; Rushlow et al. 1989](#)). [lin-22](#) regulates the [lin-32](#) gene (see below), which encodes an HLH protein related to the *achaete-scute* family of *Drosophila*. The production of ectopic neuronal structures (rays and [postdeirids](#)) in a [lin-22](#) mutant in *C. elegans* appears to be similar to the situation in *Drosophila*, where the absence of *hairy* activity leads to ectopic neuronal cell types (i.e., bristles and hence the Hairy phenotype).

## lin-32

LIN-32 is related to the *achaete-scute* gene products required for *Drosophila* neurogenesis. Mutations in the [lin-32](#) gene cause a variety of phenotypes, all affecting neurogenesis ([Chalfie and Au 1989; Zhao and Emmons 1995](#)). One common phenotype of [lin-32](#) alleles is the lack of rays in males due to a transformation of ray [neuroblasts](#) into hypodermal cells ([Zhao and Emmons 1995](#)). Ectopic expression of [lin-32](#) can cause neurogenesis in other cells, demonstrating that LIN-32 has a key role in postembryonic neuronal cell fate determination ([Zhao and Emmons 1995](#); see [Ruvkun](#), this volume).

## D. Hormone Receptor Genes

The nuclear hormone receptors form a large family of transcription factors, originally characterized in vertebrates ([Evans 1988](#)). The three-dimensional structures of several hormone receptors have been determined (see, e.g., [Luisi et al. 1991; Schwabe et al. 1993](#)). Each of the two zinc-coordinating regions overlap with  $\alpha$ -helical domains that are folded into a large globular structure, rather than forming independent zinc finger domains. DNA binding is in the major groove through contacts with the amino-terminal  $\alpha$ -helix.

Hormone receptor genes of *C. elegans* have been cloned by molecular screens and have been variously referred to in the past as *crf* (*C. elegans receptor finger*), *cnr* (*C. elegans nuclear receptor*), and *chr* (*C. elegans hormone receptor*). More recently, the uniform nomenclature of *nhr* (*nuclear hormone receptor*) has been adopted. More than 20 distinct *nhr* genes have been cloned to date, and the most extensively characterized are described below ([Kostrouch et al. 1995; A.E. Sluder and G. Ruvkun, in prep.; B. Honda; D. Riddle; both pers. comm.](#)).

## **nhr-2**

The [\*nhr-2\*](#) (previously referred to as [\*crf-2\*](#)) gene was identified by molecular screens for hormone-receptor-related sequences. No natural ligand is known, but the core [\*nhr-2\*](#) DNA-binding domain shows sequence similarity to thyroid hormone receptors (A.E. Sluder and G. Ruvkun, in prep.). Antibodies detect NHR-2 protein in the nuclei of 2-cell stage embryos; NHR-2 persists in all nuclei until the 16–22-cell stage, at which point, it can no longer be detected in the blastomeres P<sub>4</sub> and D. Beyond the 28-cell stage, protein distribution becomes complex and disappears around the comma stage of embryogenesis (A.E. Sluder and G. Ruvkun, in prep.). The function of NHR-2 is as yet unknown.

## **daf-12**

The [\*daf-12\*](#) (*dauer formation abnormal*) gene was identified genetically as being required for dauer larva development ([Riddle et al. 1981](#)). Subsequent cloning of the [\*daf-12\*](#) gene shows that it is related to the nuclear hormone receptor family (D. Riddle, pers. comm.). More recently, a set of mutations perturbing gonadal cell migration have been shown to lie in the same gene (A. Antebi and E. Hedgecock, pers. comm.).

## **odr-7**

The [\*odr-7\*](#) (*odorant response*) gene was identified in genetic screens for mutants that failed to move to certain volatile attractants ([Bargmann et al. 1993](#); [Sengupta et al. 1994](#)). ODR-7 is related to the nuclear hormone receptors; however, it has unusual features in its putative DNA-binding domain and does not have a recognizable ligand-binding domain ([Sengupta et al. 1994](#)). In [\*odr-7\*](#) mutants, the function of the two AWA olfactory neurons is defective. [\*odr-7\*](#) ::GFP reporter genes are expressed at high levels in only the two AWA [\*neurons\*](#) in all larval stages. Since the AWA [\*neurons\*](#) are present in a putative null allele, [\*osdr-7\*](#) is proposed to regulate the expression of genes required in AWA to respond to certain olfactory signaling molecules.

## **E. fork head /HNF-3 Genes**

The *fork head*/HNF-3 family of transcription factors derives its name from the founding members: *fork head* in *Drosophila* and hepatocyte nuclear factor 3 (HNF-3) in rodents ([Weigel et al. 1989](#); [Lai et al. 1990](#)). Members of the family are also known as the “winged helix” proteins because of their three-dimensional structure. The proteins bind DNA as monomers, forming a globular three α-helix bundle with a β-sheet projecting from one side and a carboxy-terminal loop projecting from the other side. These latter two extensions constitute the “wings.” The third α-helix sits in the major groove of the DNA-binding site and the “wings” contact the phosphodiester backbone and the minor groove ([Clark et al. 1993](#); for review, see [Lai et al. 1993](#)).

## **lin-31**

The [\*lin-31\*](#) gene regulates [\*vulva\*](#) precursor cell fate and may be close to the terminal gene in the genetic cascade underlying [\*vulva\*](#) induction and formation ([Miller et al. 1993](#)). [\*lin-31\*](#) promoter-driven reporter gene expression is seen in all [\*VPC\*](#) cells, but it becomes down-regulated in [\*P5.p\*](#), [\*P6.p\*](#), and [\*P7.p\*](#) when they are induced to form a [\*vulva\*](#) (P. Tan and S. Kim, pers. comm.). It is suggested that [\*lin-31\*](#) might act as a cell-specific integrator of signaling events mediated by kinase cascades.

## **fkh-1**

The [\*fkh-1\*](#) gene was identified in a molecular screen for *C. elegans* homologs closely related to the original *fork head*/HNF-3 genes ([Azzaria et al. 1996](#)). The highest levels of [\*fkh-1\*](#) message are detected in embryos, with much lower levels present in oocytes and larval stages. At least three isoforms of the protein are produced by alternative *trans*-splicing. [\*fkh-1\*](#) ::*lacZ* reporter constructs are expressed in the intestinal cells of the early embryo beginning at the four to eight E-cell stage. Reporter gene expression can also be detected embryonically in the developing [\*pharynx\*](#) and postembryonically in the developing [\*somatic gonad\*](#). The original *fork head*/HNF-3 genes had a clear involvement with digestive tract formation. Because expression of the *Ce-fkh-1* reporter gene

first appears in the intestinal cells two to three cell divisions after the intestine is clonally established, it is unlikely that *Ce-fkh-1* by itself specifies the fate of *C. elegans* endoderm.

### **pes-1**

The *pes-1* (patterned expression site) gene was identified in a novel promoter trap screen ([Hope 1991](#)). PES-1 is rather distantly related to the *fork head/HNF-3* family in the DNA-binding domain and shows no particular similarity to any specific member of the family. The *pes-1* ::*lacZ* expression pattern appears to have three distinct components, occurring in 56 descendants of [AB](#), 16 descendants of D, and later in [Z1](#) and Z4. Two different protein forms can be produced by different *pes-1* transcripts ([Hope 1994](#)). As yet, the function of *pes-1* is unknown.

## **F. bZIP and Related Genes**

The bZIP family of transcription factors contains genes such as *GCN4*, *Fos*, and *Jun*, which contact DNA via a basic region protruding into the major groove. bZIP proteins dimerize by means of  $\alpha$ -helical "leucine zipper" regions adjacent to the basic DNA-binding regions, thereby stabilizing the overall interaction ([O'Shea et al. 1991](#); [Ellenberger et al. 1992](#)).

### **skn-1**

The *skn-1* (skin excess) gene was identified in genetic screens for maternal-effect lethal mutations that alter the fates of early blastomeres ([Bowerman et al. 1992a](#)). Although lacking a leucine zipper motif, SKN-1 is clearly related to the bZIP factors in primary sequence and in specificity of DNA binding. SKN-1 is required for the [EMS](#) blastomere of the four-cell embryo to develop correctly. In the absence of SKN-1, the [MS](#) and [E](#) daughters of [EMS](#) both produce hypodermal cells rather than pharyngeal and intestinal cells, respectively ([Bowerman et al. 1992a](#)). Although (maternally provided) *skn-1* mRNA appears to be uniformly distributed in the early embryo ([Seydoux and Fire 1994](#)), SKN-1 protein is present at a higher level in the posterior  $P_1$  blastomere than it is in the anterior [AB](#) blastomere. Following the next cell division, the daughters of  $P_1$  ( $P_2$  and [EMS](#)) both have higher levels of SKN-1 than do daughters of AB. Near the end of this cell cycle, SKN-1 levels drop and by the eight-cell stage of the embryo, SKN-1 protein is undetectable ([Bowerman et al. 1993](#)). SKN-1 binds as a monomer, preferably to one of two sequence motifs (GTCAT or ATCAT), associated with an adjacent AT-rich sequence ([Blackwell et al. 1994](#)). A proposed model for SKN-1 binding suggests that the  $\alpha$ -helical basic region interacts with the major groove of DNA, with binding stabilized by an amino-terminal arm that interacts with the DNA minor groove in a manner reminiscent of homeodomain binding ([Blackwell et al. 1994](#)).

### **pha-1**

The *pha-1* (pharynx development abnormal) gene is involved in formation of the [pharynx](#) ([Schnabel and Schnabel 1990](#)). The *pha-1* gene product shows general similarity to other bZIP proteins but differs in that the leucine zipper motif of PHA-1 is not adjacent to the basic region ([Granato et al. 1994](#)). *pha-1* RNA is detected throughout development but expression peaks at 3–5 hours, corresponding to the time of pharyngeal organogenesis ([Granato et al. 1994](#)). *pha-1* ::*lacZ* reporter constructs show expression transiently in the developing pharyngeal region and in body-wall muscle precursors; however, there is as yet no genetic evidence that *pha-1* has an essential role in body-wall muscle cells. *pha-1* does not appear to specify particular pharyngeal cell fates but may act throughout the pharyngeal organ to coordinate pharyngeal morphogenesis and terminal differentiation ([Granato et al. 1994](#)).

## **G. Other Transcription Factor Genes**

### **cey-1**

The [cey-1](#) (*C. elegans* Y-box) gene encodes a member of the Y-box family of transcription factors, which have been proposed to function in a variety of processes, including chromatin modification, transcriptional activation and repression, and mRNA masking (for review, see [Wolffe 1994](#)). [cey-1](#) was identified ([Jantsch-Plunger 1993](#)) in a molecular screen of an expression library using an enhancer fragment from the [unc-54](#) gene (body-wall muscle myosin heavy chain). Some proteins of this family bind DNA with only limited sequence specificity; the function of [cey-1](#) remains to be investigated. The [cey-1](#) transcript is widely expressed in cleaving embryos and subsequent expression occurs predominantly in mesodermal tissue ([Seydoux and Fire 1994](#)).

## **lin-1**

ETS domain proteins are transcription factors, some of which are regulated by kinase cascades (for review, see [Janknecht and Nordheim 1993](#)). The LIN-1 protein encodes an ETS domain protein most similar to the Elk-1/SAP-1/Net subfamily ([Beitel et al. 1995](#)). [lin-1](#) null mutants display ectopic induction of the [vulva](#) precursor cells, resulting in a Multivulva phenotype; wild-type [lin-1](#) activity therefore appears to function by negatively regulating primary and secondary vulval cell fates ([Beitel et al. 1995](#)). There may be parallels between the negative regulation of *C. elegans* [VPC](#) induction by the ETS protein LIN-1 and the negative regulation of *Drosophila* photoreceptor R7 induction by the ETS protein Yan ([Beitel et al. 1995; Rebay and Rubin 1995](#)).

## **mef-2**

The *C. elegans* [mef-2](#) gene was identified in a molecular screen for homologs of vertebrate and *Drosophila* [mef-2](#) genes (myocyte enhancer-binding factor; see [Gossett et al. 1989](#)). These belong to the MADS box family of transcription factors, named after its founding members: the yeast gene [MCM1](#), the plant genes [agamous](#) and [deficiens](#), and serum response factor or SRF ([Schwartz-Sommer et al. 1990](#)). CeMEF-2 is 94% identical in sequence to the vertebrate MEF-2A protein in the MADS domain and in an adjacent region characteristic of the subclass. CeMEF-2 binds the canonical MEF-2 DNA-binding site sequence CTAAAAATA in vitro, but no in vivo target site is known. A [mef-2](#) ::*lacZ* reporter construct is first expressed at the comma stage in a few presumptive [head neurons](#), but expression then spreads to essentially [all cells](#) (with the possible exception of the intestinal cells) by late embryogenesis (M. Park et al., unpubl.). Embryos homozygous for chromosomal deficiencies that remove the [mef-2](#) gene can still produce body-wall muscle. Thus, unlike the situation in *Drosophila*, zygotic [mef-2](#) activity does not appear to be necessary for terminal differentiation in [pharynx](#) or body-wall muscle types in *C. elegans* (J. Ahnn et al., unpubl.).

## **pop-1**

The [pop-1](#) (posterior pharynx-defective) gene was identified in genetic screens for maternal-effect lethal mutations that alter the fate of the [MS](#) blastomere. In [pop-1](#) mutants, the [MS](#) blastomere adopts the fate of its sister, the E blastomere; [MS](#) descendants that would normally make up the posterior part of the [pharynx](#) instead become intestinal cells. [pop-1](#) encodes a putative transcription factor with a single DNA-binding HMG box, most similar to the TCF/SOX subfamily of HMG-box-containing factors ([Lin et al. 1995](#)). HMG box factors of this subfamily can alter DNA structure and may thereby facilitate the interaction between other gene-specific transcription factors ([Giese et al. 1992](#)). Antibody staining reveals POP-1 protein in nuclei of maturing oocytes; after fertilization, the nuclear staining persists in most early blastomeres ([Lin et al. 1995](#)). POP-1 may be present at a higher level in the [MS](#) cell than in its [E](#) cell sister and may function permissively with SKN-1 (see above) in [MS](#) blastomere determination.

## **lag-1**

The [lag-1](#) gene was identified in a genetic screen for mutants displaying a phenotype characteristic of the double-mutant combination [lin-12](#) and [glp-1](#) ([Christensen et al. 1996](#)). [lag-1](#) encodes a nuclear-localized DNA-binding factor related to vertebrate CBF1/KBF2 and *Drosophila* Suppressor of Hairless SU(H) ([Israel et al. 1989; Furukawa et al. 1991; Schweiguth and Posakony 1992](#)). In vertebrates and flies, these transcription factors work downstream from the Notch signaling pathway to repress the function of helix-loop-helix proteins regulating

myogenesis and neurogenesis ([Kopan et al. 1994](#); [Nye et al. 1994](#); [Jarriault et al. 1995](#)). Similarly, LAG-1 functions downstream from the LIN-12/GLP-1 signaling pathway in *C. elegans*. In vitro studies show that LAG-1 can bind the SU(H)/CBF1/KBF2 consensus binding site (G/ATGGGAA) and can interact with the ankyrin repeats of GLP-1 (and presumably LIN-12 as well) ([Christensen et al. 1996](#)).

## pie-1

The [pie-1](#) (pharyngeal and intestinal excess) gene was identified in a genetic screen for maternal-effect mutations and results in the P<sub>2</sub> blastomere adopting an [EMS](#)-like cell fate. The consequences of this cell fate transformation is an excess of [MS](#) and [E](#) cell types and a loss of the germ-line precursors ([Mello et al. 1992](#)). [pie-1](#) encodes a protein with two zinc fingers of the C3-H1 type related to a variety of eukaryotic genes including at least ten other *C. elegans* genes, a mammalian growth hormone inducible factor TIS-11, and the splicing accessory factor U2AF35 ([Mello et al. 1996](#)). Although none of these factors have yet been shown to bind nucleic acids, PIE-1 is able to suppress [skn-1](#)-dependent transcription in a cultured cell assay (K. Blackwell and C. Mello, pers. comm.). Moreover, ectopic expression of [pie-1](#) in *C. elegans* embryos can cause embryonic death and can apparently suppress endogenous transcription as assayed by *in situ* hybridization ([Seydoux et al. 1996](#)). Antibodies to PIE-1 show that the protein is associated specifically with the future P<sub>1</sub> centrosome in a one-cell embryo (C. Schubert and J. Priess, pers. comm.). By the two-cell stage, PIE-1 is broadly distributed in the P<sub>1</sub> blastomere; by the four-cell stage, PIE-1 becomes strongly localized to the nucleus of P<sub>2</sub>. Staining continues to be restricted to the nucleus of germ-line precursors until about the 100-cell stage of embryogenesis. The distribution of PIE-1 and its known functions suggest that it may be involved in germ-line formation by preventing transcription in the embryonic germ-line precursors ([Mello et al. 1996](#); [Seydoux et al. 1996](#)).

## Tables

**Table 1** Transcription factors characterized in *C. elegans*

Homeodomain Superfamily	
HOX class:	<a href="#">egl-5</a> , <a href="#">mab-5</a> , <a href="#">lin-39</a> , <a href="#">ceh-13</a>
POU class:	<a href="#">unc-86</a> , <a href="#">ceh-6</a> , <a href="#">ceh-18</a>
LIM class:	<a href="#">lin-11</a> , <a href="#">mec-3</a>
Paired and paired-like class:	<a href="#">vab-3</a> , <a href="#">mab-18</a> , <a href="#">unc-4</a> , <a href="#">ceh-10</a> , <a href="#">unc-30</a>
NK Class:	<a href="#">ceh-22</a>
Others:	<a href="#">pal-1</a> , <a href="#">vab-7</a>
Zinc Finger Family	
GATA class:	<a href="#">elt-1</a> , <a href="#">elt-2</a> , <a href="#">end-1</a>
Others:	<a href="#">tra-1</a> , <a href="#">sdc-1</a> , <a href="#">sdc-3</a> , <a href="#">egl-43</a> , <a href="#">lin-26</a> , <a href="#">lin-29</a>
Helix-Loop-Helix Family	<a href="#">hhl-1</a> , <a href="#">hhl-2</a> , <a href="#">lin-22</a> , <a href="#">lin-32</a>
Hormone Receptor Family	<a href="#">nhr-2</a> , <a href="#">daf-12</a> , <a href="#">odr-7</a>
<i>fork head</i> /HNF-3 Family	<a href="#">lin-31</a> , <a href="#">fkh-1</a> , <a href="#">pes-1</a>
bZIP Family	<a href="#">skn-1</a> , <a href="#">pha-1</a>
Miscellaneous	<a href="#">cey-1</a> , <a href="#">lin-1</a> , <a href="#">mef-2</a> , <a href="#">pop-1</a> , <a href="#">lag-1</a> , <a href="#">pie-1</a>

## Chapter 7. Transcription Factors and Transcriptional Regulation —

### IV Analysis of *C. elegans* Promoters

---

Expression patterns of several dozen *C. elegans* genes have now been investigated by fusing the gene sequences to a *lacZ* reporter construct, introducing the gene fusion into worms, and then staining for β-galactosidase activity. This approach has been greatly facilitated by a convenient series of modular vectors provided by [Fire et al. \(1990\)](#). Possible limitations of DNA-mediated transformation as a method to study gene control are discussed below in Summary and Conclusions (see also [Mello and Fire 1995](#)), but, by and large, this approach has worked well. The advent of new reporter genes such as GFP or “green fluorescent protein” ([Chalfie et al. 1994](#)) promises to make this approach even more useful in the future. In the present section, we consider only those studies in which promoters have been analyzed in sufficient detail to identify *cis*-elements in the DNA that could control transcription patterns.

#### A. The Vitellogenin Genes

The *C. elegans* vitellogenins (or yolk proteins) are encoded by a family of six genes that provide an excellent experimental system in which to investigate multiple interlocking transcriptional controls. Vitellogenin genes are expressed in a manner that is sex-specific (only in hermaphrodites), stage-specific (only in late L4 and adults), and tissue-specific (only in the intestine) ([Kimble and Sharrock 1983; Sharrock et al. 1983; Blumenthal et al. 1984](#)). Such properties, combined with the genes' massive rates of RNA production, made control of the vitellogenin genes among the first to be investigated biochemically in *C. elegans*.

The initial study ([Spieth et al. 1988](#)) produced transgenic nematodes by the low-copy-number integration scheme developed by Fire (1986). A fusion between the *vit-2* and *vit-6* genes was designed as a reporter gene, whose expression could be detected immunologically and by nuclease protection. The initial construct included 3.9 kb of *vit-2* upstream sequence and 0.6 kb of *vit-6* downstream sequence and clearly showed the main elements of correct regulation: Upon transformation into wild-type worms, expression of the *vit-2* / *vit-6* reporter was detected only in the intestine of adult hermaphrodites. The number of integrated genes was low (in the range of 1–10 copies/genome), expression levels approximately depended on the copy number, and RNA from the transforming gene was of the expected size. Although there were examples of rearranged and mutated genes, presumably introduced by the genomic integration events, the overall conclusion was that regulation was correct. Indeed, correct sex/stage/tissue regulation could be achieved with only 247 base pairs of 5'-flanking region upstream of the transcriptional start site ([MacMorris et al. 1992](#)).

Two highly conserved sequence motifs (named vitellogenin promoter elements or VPEs) were identified by comparing the sequences of the different genes in the *C. elegans* vitellogenin family and by comparing the *C. elegans* genes with the homologous vitellogenins from *Caenorhabditis briggsae* ([Blumenthal et al. 1984; Spieth et al. 1985b, 1991a; Zucker-Aprison and Blumenthal 1989](#)). VPE1 has the sequence TGTCAAT, and VPE2 has the sequence CTGATAA, a subset of the WGATAR sequences that are involved in gene regulation during vertebrate erythropoiesis ([Weiss and Orkin 1995](#)). MacMorris et al. (1992) focused on the importance of certain of these elements in controlling the fused *vit-2/vit-6* reporter gene. The primary conclusion was that alteration of these elements could change the levels of reporter gene expression, but no alterations were identified that changed the sex/stage/tissue specificity of expression (see also [MacMorris and Blumenthal 1993](#)). Ablation of the VPE1 site closest to the TATAA box (~45 bp) inactivated the gene, but ablation of other VPE1 sites farther upstream had little effect. Ablation of one conserved VPE2 site (at ~150) or of an overlapping VPE1-VPE2 site also inactivated the promoter. Independently produced transgenic strains could show a substantial quantitative variability in expression level, suggesting that the precise site of chromosome integration could influence expression level of the transgene.

A further study from the same group ([MacMorris et al. 1994](#)) retained the *vit-2* / *vit-6* reporter (with both wild-type and mutated 247-bp promoters) but switched to a transformation procedure that produces multicopy extrachromosomal arrays ([Mello et al. 1991](#)). Copy numbers ranged up to several hundred copies per haploid

genome but expression levels showed only weak correlation with copy number. However, as assayed by the relative expression levels obtained with each promoter-mutated construct, the two transformation techniques (i.e., producing a small number of integrated copies or a large number of nonintegrated copies) did indeed lead to the same general conclusions: Mutation of some (but not all) of the conserved VPE1 and VPE2 sites greatly decreased the level of vitellogenin expression. In addition, single mutations that by themselves had little effect on expression could be combined to produce a drastic reduction in reporter gene activity.

Clearly, much remains to be done before vitellogenin control is understood. The VPE1 and VPE2 sequences are obvious candidate binding sites for transcription factors that confer specificity to vitellogenin expression. However, no such factors have yet been defined nor have the isolated elements (multimerized if necessary) been shown to be capable of directing correctly regulated expression of a "neutral" promoter. In principle, the elements could be general factor-binding sites, perhaps contributing to the massive levels of vitellogenin gene expression. The true sex/stage/tissue controlling sites may lie elsewhere, perhaps interspersed between the VPE1 and VPE2 sequences.

## B. The *unc-54* Gene

The [\*unc-54\*](#) gene encodes the major myosin heavy chain expressed in the body-wall muscle and has long been the focus of genetic and biochemical analyses ([MacLeod et al. 1981](#); [Moerman et al. 1982](#); [Miller et al. 1983](#); [Anderson and Brenner 1984](#)). [\*unc-54\*](#) is also expressed in muscles of the [\*vulva\*](#), intestine, and [\*somatic gonad\*](#) but is not expressed in muscles of the [\*pharynx\*](#) ([Ardizzi and Epstein 1987](#); see also [Moerman](#)[Fire](#)).

[Fire and Waterston \(1989\)](#) introduced cosmid DNA containing the [\*unc-54\*](#) locus into [\*unc-54\*](#) mutant worms, using the protocol ([Fire 1986](#)) that yields a low number of integrated gene copies. The general conclusion was that the exogenous genes could rescue wild-type movement and egg-laying ability. Monoclonal antibodies to the product of the [\*unc-54\*](#) gene were used to demonstrate that [\*unc-54\*](#) expression was correct, appearing in body-wall muscle cells but not in [\*pharyngeal muscle\*](#) cells. By comparing expression levels with those obtained in previous gene dosage experiments, the authors were able to conclude that the expression level of each copy of the transforming gene was within a factor of two of the expression level of the endogenous chromosomal gene ([Fire and Waterston 1989](#)).

The transcription initiation site of the [\*unc-54\*](#) gene has been mapped approximately 80 base pairs upstream of the ATG translation initiation codon ([Dibb et al. 1989](#); [Okkema et al. 1993](#)). There is no obvious TATAA element 25–30 base pairs farther upstream, but a polypyrimidine-polypurine sequence found nearby is also found in a comparable position in other myosin heavy-chain genes. Okkema *et al.* (1993) continued the transgenic analysis of the [\*unc-54\*](#) promoter, using transformation by multicopy extrachromosomal arrays. Gene expression was most frequently assayed in the first-generation progeny of the injected worms. In such an F<sub>1</sub> assay, expression of the transgene is mosaic, but expression patterns can still be deduced by investigating large numbers of individual animals. Two different reporter genes were used. The first reporter was the intact [\*unc-54\*](#) gene itself; correct expression could be assayed by rescue of the paralysis and egg-laying defects of [\*unc-54\*](#) mutants and by using [\*unc-54\*](#)-specific antibodies. The second reporter consisted of various *lacZ* vectors fused to [\*unc-54\*](#) or to pieces of [\*unc-54\*](#) placed upstream of a "neutral" promoter. A series of undirectional 5' deletions were constructed and introduced into worms. It was found that deletions to within six base pairs of the translation initiation codon (and which deleted the normal site of transcription initiation) were still able to confer phenotypic rescue; [\*unc-54\*](#) expression now derived from multiple start sites located in the newly juxtaposed vector. (Control experiments showed that muscle specificity did not derive from the sequences in the vector.) One of the models suggested by the authors was that an "initiator element" within the body of the gene directed transcription to begin a measured number of base pairs upstream. A second model proposed the existence of a mechanism to eliminate transcripts that cannot be properly processed ([Okkema et al. 1993](#)).

Using both deletions of the [\*unc-54\*](#) gene and deletions of a [\*unc-54\* ::\*lacZ\*](#) fusion construct, [Okkema et al. \(1993\)](#) were able to conclude that [\*unc-54\*](#) expression in the body-wall muscles could be directed by either of two tissue-specific control elements: The first such element is situated within 200 base pairs of the beginning of the [\*unc-54\*](#).

gene, and the second element behaves as an enhancer and is situated within the third intron. These two enhancers appear to be redundant since either by itself directs body-wall muscle expression. There was the possibility of upstream elements that controlled expression level but not tissue specificity.

The body-wall muscle enhancer in the third intron of the [unc-54](#) gene was investigated in more detail by [Jantsch-Plunger and Fire \(1994\)](#). As in the previous study, expression of various *lacZ* fusion constructs was assayed in the F<sub>1</sub> generation produced by injected worms. The basic strategy was to place mutated (or multimerized) third intron enhancers upstream of a minimal [myo-2](#) promoter (potentially pharyngeal-specific but inactive by itself) or upstream of the postulated non-tissue-specific promoter of the [glp-1](#) gene; appropriate enhancer-promoter pairs were then fused to *lacZ* reporters. The third intron enhancer was found to lie within a 90-base-pair region, which was then extensively mutated. The general result was that the [unc-54](#) intron enhancer consists of at least four distinct subelements; not only the sequence of these subelements, but also the spacing between subelements are important for expression. Gene expression destroyed by mutations in a particular element could sometimes be restored by duplication of the mutated site. Some individual elements could act by themselves if multimerized, but other elements could not. Moreover, there was clear interplay between the elements in the [unc-54](#) enhancer and the particular promoter that was being used. In general, the [myo-2](#) promoter gave higher levels of expression and more clear-cut results than did the [glp-1](#) promoter. None of the identified sites have yet been matched with the binding site of a transcription factor. Although it might have been expected that the *C. elegans* MyoD homolog interacts with [unc-54](#), the authors point out that the [unc-54](#) gene is still expressed in body-wall muscle in an [hlh-1](#) mutant.

## C. The *myo-3* and *myo-2* Genes

The second major myosin heavy chain expressed in the body-wall muscle cells is encoded by the [myo-3](#) gene. Less is known about the [myo-3](#) promoter than about the [unc-54](#) promoter, but several observations are pertinent. Low-copy-number integrants of the intact [myo-3](#) gene were able to rescue the lethality of a [myo-3](#) mutation and to recreate the wild-type staining pattern seen with an anti-MYO-3 monoclonal antibody ([Fire and Waterston 1989](#)). As with the [unc-54](#) gene, the reintroduced copies of the [myo-3](#) gene were estimated to be expressed at approximately the same level as the endogenous genes.

Subsequent studies assayed the ability of fragments of the [myo-3](#) gene to direct expression of [myo-2](#) promoter::*lacZ* fusion constructs into body-wall muscle cells ([Okkema et al. 1993](#)). Three separable elements with body-wall muscle enhancer activity were detected: Two elements lie within 2.5 kb upstream of the [myo-3](#) ATG ([myo-3](#) is *trans*-spliced), and the third element lies within the first [myo-3](#) intron.

The [myo-2](#) gene encodes a myosin heavy chain expressed exclusively in muscle cells of the [pharynx](#), not in muscle cells of the body wall. The 5'end of the primary transcript has been mapped ([Okkema et al. 1993](#)) and, like the [unc-54](#) and [myo-1](#) genes, no appropriately spaced TATAA element can be identified. Using transgenic *lacZ* fusion constructs, the major [pharyngeal muscle](#) enhancer of the [myo-2](#) gene was located several hundred base pairs upstream of the transcription initiation region. More detailed analysis ([Okkema and Fire 1994](#)) divided the [myo-2](#) enhancer into three overlapping fragments, each separately inactive but active when combined in pairs or when duplicated. Whereas the intact enhancer directed *lacZ* expression in all eight classes of [pharyngeal muscle](#) cells, enhancer subelements (when duplicated) showed selectivity for expression in only some of these cells. None of the enhancer elements showed strict lineage specificity. Furthermore, one such element appeared to lose strict muscle specificity when studied in isolation; however, the element appeared to retain specificity for cells of the [pharynx](#), as if it were organ-specific rather than cell-type-specific.

The overall picture of the [myo-2](#) enhancer is a collection of elements with overlapping specificity, the ultimate expression pattern arising from combinatorial interactions between the various elements. [Okkema and Fire \(1994\)](#) suggest that the complex interactions between different elements in such an enhancer might be necessary to coordinate the separate differentiation programs of muscle cells and other cells within the developing [pharynx](#). One particular enhancer subelement was used to screen an expression library, thereby

isolating the candidate controlling gene [ceh-22](#), an NK class homeobox transcription factor described above ([Okkema and Fire 1994](#)).

## D. The *col-19* Gene

The [col-19](#) gene encodes a collagen protein incorporated into the cuticle of the adult; expression of [col-19](#) is regulated by the heterochronic pathway ([Ambros and Horvitz 1984](#); [Cox and Hirsh 1985](#)). Liu et al. (1995) showed that 2.7 kb of [col-19](#) upstream sequence could direct expression of a *lacZ* reporter construct in the spatial and temporal pattern expected, namely, in hypodermal cells beginning at the L4 to adult molt. When introduced into heterochronic mutants in which the production of the adult cuticle is either "precocious" or "retarded," expression of the [col-19](#) ::*lacZ* fusion was also precocious or retarded, suggesting that the heterochronic pathway controls the downstream "effector" genes at the level of transcription. Adult-specific expression could be directed by an approximately 150-bp region located several hundred base pairs upstream of the [col-19](#) gene, with the possibility that separate elements control expression specificity and expression level. DNA fragments from within this region were shown to bind to recombinant LIN-29 protein ([Rougvie and Ambros 1995](#)). From genetic evidence, [lin-29](#) is an obvious candidate for controlling downstream genes in the heterochronic pathway (see Ambros, this volume), and these biochemical experiments suggest that the control might actually be direct. As described above, the [lin-29](#) gene encodes a zinc finger protein.

## E. The *hlh-1* Gene

As noted above, the [hlh-1](#) gene encodes the *C. elegans* homolog of MyoD, a member of the class of helix-loop-helix transcription factors that have a central role in muscle development in vertebrates (for review, see [Olson 1990](#); [Weintraub 1993](#)). The role of [hlh-1](#) in muscle biology is considered by Moerman and Fire (this volume).

To understand how the [hlh-1](#) gene is controlled, the promoter has been analyzed in considerable detail by [Krause et al. \(1994\)](#). A construct containing 3.1 kb of [hlh-1](#) upstream sequence and 2 kb of gene sequence (including a large first intron) fused to a *lacZ* reporter gene is expressed in transgenic worms in a pattern that accurately recapitulates the distribution of the endogenous *HLH-1* protein. Specifically, the reporter construct is expressed in mature body-wall muscles and their clonal precursors, in a set of six glial-like cells, and transiently in the granddaughters of the [MS](#) blastomere. A series of both unidirectional and internal deletions in the 5-kb region surrounding the [hlh-1](#) initiation codon identified a number of control elements that influence different aspects of the overall expression pattern. For example, elements that direct expression in embryonic muscle precursor cells could be distinguished from elements that function in mature body-wall muscles. The control elements associated with embryonic muscles did not seem to have exclusive control over expression in a particular lineage but rather only "favored" expression: Some elements favored expression in the [C](#) over the [MS](#) + [D](#) lineages, and others favored the reverse. A common "core" element, lying between base pairs -551 and -435 relative to the [hlh-1](#) ATG codon, appeared to be necessary for [hlh-1](#) ::*lacZ* expression in all aspects of the pattern, both adult and embryonic. Two different elements were identified that controlled the transient expression in the [MS](#) granddaughter cells; a further distinct element in the first intron influenced expression in the glial-like cells. The suspected enhancer sequences were introduced upstream of a neutral promoter, either that of the [myo-2](#) gene or that of the [glp-1](#) gene. By and large, this latter assay supported the conclusions arrived at by the unidirectional deletions.

To aid in the precise identification of control sequences, the [hlh-1](#) homolog from the related nematode *C. briggsae* was cloned and sequenced ([Krause et al. 1994](#)). Several conserved sequences could be identified within the enhancers previously defined by the functional assays, supporting the potential of these regions to be transcription factor targets. A number of "E-box" sequences (CAXTG, binding sites for helix-loop-helix proteins) were noted in these conserved regions but none has yet been demonstrated actually to interact with protein. The authors showed that the *C. briggsae* *hlh-1* gene could rescue *C. elegans* [hlh-1](#) mutants and that the *C. briggsae* expression pattern was highly similar to that seen in *C. elegans*, with the interesting exception that the transient phase of [hlh-1](#) expression in the [MS](#) granddaughters was not detected.

The above studies appear to have eliminated at least the simplest and most extreme model in which completely distinct enhancers control expression in distinct *hlh-1*-expressing cell lineages. Rather, the *hlh-1* promoter appears to be an array of overlapping influences. One short region just upstream of the ATG is required for all expression, but other regions influence the different spatial and temporal aspects of *hlh-1* expression, in short, a complex piecemeal type of control.

## F. The *mec-3* Gene

*mec-3* has been one of the most intensely studied genes in *C. elegans*. As noted above, *mec-3* encodes a LIM-type homeoprotein necessary for the correct production of differentiated [touch cells](#). The genetic studies of *mec-3* are described by Driscoll and Kaplan (this volume). In this section, we review studies analyzing the *mec-3* promoter.

In the original report of *mec-3* cloning, [Way and Chalfie \(1988\)](#) showed that touch-insensitive mutants could indeed be rescued by germ-line transformation with nonintegrated multicopy arrays of *mec-3*. Phenotypes usually diagnostic for [touch cells](#) (e.g., degeneration induced by a dominant allele of *mec-4*) could be identified in a few ectopic cells, presumably as a result of *mec-3* overexpression or misexpression from the transforming array. A *mec-3* ::*lacZ* fusion construct containing several kilobases of 5'-flanking DNA was expressed in a total of ten [neurons](#). This reporter expression apparently mirrors native MEC-3 distribution, although this has not yet been verified by immunocytochemical analysis of the endogenous protein: The reporter-expressing cells include the six [touch cells](#) plus four other cells for which there is evidence both for a role in mechanosensation and for *mec-3* involvement in cell function ([Way and Chalfie 1989](#)). Moreover, transgenes respond as expected to appropriate genetic backgrounds. Expression is abolished in [unc-86](#) mutants, in which the lineages that produce the [touch cells](#) are altered, and expression is reduced or transient in *mec-3* mutants, suggesting elements of autoregulation. The response of this full-length reporter construct to a variety of genetic backgrounds has been studied ([Way and Chalfie 1989; Way et al. 1992; Mitani et al. 1993](#)).

The *mec-3* promoter has been analyzed both by deletions and by site-directed mutations ([Way et al. 1991; Xue et al. 1992](#)). The *mec-3* control region appears to be compact, and several hundred base pairs upstream of the *mec-3* ATG (the site of transcription initiation is not known) are sufficient to generate the appropriate *lacZ* staining patterns. Comparison of 5'-flanking DNA sequences among the *mec-3* homologs from three species (*C. elegans*, *C. briggsae*, and *C. remanei* strain VT733 [previously called *C. vulgarensis*, see Fitch and Thomas, this volume]) reveals at least four highly conserved regions, and these are obvious candidates for *cis*-acting control sequences. Moreover, sites in the 5'-flanking region have been shown directly to bind recombinant versions of the UNC-86 and the MEC-3 proteins ([Xue et al. 1992, 1993](#)), and, by and large, the UNC-86- and MEC-3-binding sites do lie in the conserved regions.

Several key features of *mec-3* regulation and touch cell specification have been illuminated by the analysis of the *mec-3* promoter. Alteration of UNC-86-binding sites leads to reduced *mec-3* ::*lacZ* expression in both the establishment and the maintenance phase. Similarly, MEC-3-binding sites appear to be directly involved in the maintenance of *mec-3* expression. This *in vivo* analysis is made far more interesting because recombinant UNC-86 and MEC-3 proteins have been shown *in vitro* to form heterodimers on the DNA ([Xue et al. 1992, 1993](#)). Moreover, the possibility of synergistic UNC-86-MEC-3-binding interactions fits within the genetic framework ([Mitani et al. 1993](#)) and with evidence from *in vitro* transcription ([Lichtsteiner and Tjian 1995](#)). At least two issues remain to be resolved—whether there is a negative element that keeps *mec-3* repressed in sister cells and whether there are cell-type-specific (or lineage-specific) subelements within the *mec-3* promoter.

## G. The *unc-86* Gene

The *unc-86* gene product is one of the founding members of the POU class of homeodomain proteins (see above). The regulation of *unc-86* activity exemplifies central problems in *C. elegans* development: How do transcription factors become asymmetrically expressed within a lineage and how does such an asymmetric expression of a transcription factor bring about different fates of different cells (for a detailed review of *unc-86*

function in neurogenesis, see [Ruvkun](#), this volume). This section summarizes studies that analyze the [\*unc-86\*](#) promoter.

As detected by antibody staining, [\*unc-86\*](#) is expressed in 57 of the 302 [neurons](#) in adult *C. elegans* ([Finney and Ruvkun 1990](#)), and in general, these are the same cells that are altered in [\*unc-86\*](#) mutants. Besides the fact that the [\*unc-86\*](#)-expressing cells are [neurons](#), common features are not obvious. The cells are not spatially clustered, they do not show obvious clonal or lineage relations, and they do not have the same function. The central question is: How can a transcription factor become deployed in such a complex pattern in the developing animal? One model can probably be ruled out. In lineages that are transformed by [\*unc-86\*](#) mutations, immunologically detectable UNC-86 protein can appear in cell nuclei shortly after cell birth, i.e., UNC-86 does not appear to be produced in a mother cell and then segregated asymmetrically into only one of the daughters.

A recent transgenic analysis has provided important new insights into [\*unc-86\*](#) regulation ([Baumeister et al. 1996](#)). A 10-kb region of the [\*unc-86\*](#) locus (including ~5 kb of upstream DNA and 2-kb downstream from the gene), when introduced as multicopy arrays into an [\*unc-86\*](#) mutant, is able to rescue mutant phenotypes such as defective mechanosensation and chemotaxis. Moreover, antibody staining showed that the transgene product is expressed only in cells that normally express [\*unc-86\*](#). Reporter constructs in which the 5 kb of [\*unc-86\*](#) 5'-flanking region was fused to *lacZ* or to GFP (and excluding all sequences from [\*unc-86\*](#) mRNA) were also expressed in the correct pattern, allowing the important conclusion that the complex [\*unc-86\*](#) expression pattern is regulated at the level of [\*unc-86\*](#) transcription.

Like the [\*mec-3\*](#) gene described in the previous section, [\*unc-86\*](#) appears to have two phases of expression, one of establishment and one of (autoregulatory) maintenance; i.e., the reporter constructs in an [\*unc-86\*](#) mutant background show correct initial expression in the appropriate cells, but this expression is transitory. Moreover, promoter elements controlling establishment can be separated from elements controlling maintenance. A series of promoter deletions was used to explore the [\*unc-86\*](#) establishment phase. The principal result was that distinct promoter regions directed reporter expression in distinct sets of the [\*unc-86\*](#)-expressing cells. This important finding indicates that asymmetric [\*unc-86\*](#) expression does not result from some unitary animal-wide control mechanism applied to all cell lineages that express [\*unc-86\*](#). Rather, the promoter appears to be modular, although many further constructs must be investigated to determine how discrete such a promoter module can actually be.

[Baumeister et al. \(1996\)](#) also introduced the (intact) promoter::reporter fusion into a number of genetic backgrounds and found that certain genes ([\*lin-11\*](#), [\*ham-1\*](#), [\*lin-17\*](#)) affect [\*unc-86\*](#) expression in some cell lineages, whereas other genes ([\*lin-32\*](#), [\*vab-3\*](#), [\*egl-5\*](#)) affect expression in other lineages. This response is what would be expected for a modular promoter, in which different modules respond to different upstream genes. One task for the future will be to map the action of each potential [\*unc-86\*](#) regulatory gene onto discrete elements in the [\*unc-86\*](#) promoter. This will be a formidable amount of work, but the problem is both general and important.

## H. The *ges-1* Gene

The [\*ges-1\*](#) gene encodes a carboxylesterase enzyme expressed exclusively in the intestinal cell lineage. Esterase expression can be first detected when the developing gut has four to eight cells and expression continues throughout the life cycle ([Edgar and McGhee 1986, 1988](#)). Studies on [\*ges-1\*](#) control have focused on the establishment of the gut-specific expression patterns during the first half of embryogenesis (up to the comma or 1.5-fold stage); during these stages, the [\*ges-1\*](#) esterase is the only detectable esterase in the embryonic intestine. Mutations that abolish [\*ges-1\*](#) esterase activity have been produced ([McGhee et al. 1990](#)). The availability of these (viable) nonexpressing mutants and the cloned [\*ges-1\*](#) gene ([Kennedy et al. 1993](#)) has allowed the gene to be used as its own reporter in transformation studies aimed at understanding control of the [\*ges-1\*](#) promoter.

The basic approach has been to introduce [\*ges-1\*](#) constructs into the [\*ges-1\*](#) null mutant, to produce stable transgenic lines, in which the [\*ges-1\*](#) gene is present in multicopy nonintegrated arrays, and then to stain transformed embryos for esterase activity. The initial analyses of the [\*ges-1\*](#) promoter used unidirectional

deletions (Aamodt et al. 1991; Kennedy et al. 1993). A subsequent study (Egan et al. 1995) has used more closely spaced internal deletions and site-directed mutations and, by and large, has confirmed the main conclusions of the earlier work. The results of this latter study can be summarized as follows. Control of the *ges-1* gene centers on a region lying 800–1300 base pairs upstream of the *ges-1* ATG codon (*ges-1* is *trans*-spliced so the point of transcription initiation is not yet known). A deletion that removes 1300–1100 base pairs upstream of the ATG abolishes *ges-1* expression in the embryonic intestine, but this same construct now expresses *ges-1* in cells of the pharynx and the tail.

It has been a matter of concern that the “pharynx/tail” pattern of expression seen with modified *ges-1* promoters could have features in common with the “ectopic pharynx/posterior intestine” expression noted with a number of transgenic promoter-reporter constructs (see, e.g., Hope 1991; Krause et al. 1994). Furthermore, a significant fraction of promoter trap lines have been found to express in the pharynx. Nevertheless, all control experiments done to date suggest that the pharynx/tail expression patterns seen with modified *ges-1* constructs do indeed reflect endogenous regulatory mechanisms associated with the *ges-1* gene: Pharynx/tail expression has been observed in multiple stably transformed transgenic lines (using both integrated and nonintegrated arrays), in the absence of any vector sequences, with a variety of coinjected marker genes, and with several dozen different *ges-1* deletion constructs. However, probably the strongest validation of the *ges-1* transgenic analysis is that deletions in the endogenous chromosomal copies of the *ges-1* promoter (isolated by imprecise transposon excisions) give rise to weak but significant *ges-1* expression in the embryonic pharynx (Fukushige et al. 1996).

Sequences involved in this gut-to-pharynx/tail switch in *ges-1* expression have been explored in more detail. The switch centers on a 36-base-pair region that contains two WGATAR sites. Deletion of these two sites is sufficient to abolish gut expression and to activate expression in the pharynx/tail pattern. As noted above, WGATAR sequences are known to be involved in gene control during vertebrate erythropoiesis (for review, see Weiss and Orkin 1995). Furthermore, the downstream WGATAR element sits in a region that matches (13/13 base pairs) a sequence implicated in control of the (gut-specific) vitellogenin genes (see above). This tandem pair of WGATAR sites act as an embryonic gut enhancer. Reintroduction of the sequences several hundred base pairs downstream from the normal location in the WGATAR-deleted *ges-1* construct (and in either orientation) returns *ges-1* expression to the gut and silences expression in the pharynx/tail. Moreover, the sites (at least when multimerized) can direct expression of a naive promoter/reporter gene construct in the embryonic intestine. No evidence could be produced that the sites were capable of repressing expression from a heat shock promoter (Egan et al. 1995).

Laser microsurgery experiments combined with genetic analysis have shown that the embryonic cells expressing the WGATAR deleted *ges-1* construct belong to all three non-gut modules of the digestive tract: the ABa-derived anterior pharynx, the MS-derived posterior pharynx, and the ABp-derived rectum. Furthermore, this non-gut digestive tract expression of the WGATAR deleted gene is abolished by mutations in the zygotic gene *pha-4* and responds appropriately to mutations in a series of maternal-effect genes that alter early blastomere fate (*skn-1*, *mex-1*, *pie-1*, and *pop-1*) (Fukushige et al. 1996). Thus, *ges-1* appears to be regulated at the level of the entire digestive tract, not just at the level of separation of the E and MS blastomere fates as had originally been suggested (Aamodt et al. 1991; Egan et al. 1995). Furthermore, this digestive-tract-wide level of control is normally hidden, perhaps reflecting the evolutionary history of the *ges-1* gene.

The transgenic studies of *ges-1* expression also appear to have uncovered distinct control mechanisms within the gut lineage. Deletion of either the upstream or downstream WGATAR site directed *ges-1* expression only in the anterior gut, not the posterior gut. Deletion of a neighboring fragment (called δ4, spanning base pairs –811 to –1100) also causes *ges-1* expression only in the anterior gut. These deletions thus accentuate the normal tendency of *ges-1* staining to be stronger in the gut anterior (Edgar and McGhee 1986). Deletion of any two of the three elements (i.e., upstream WGATAR, downstream WGATAR, or the adjoining δ4 region) led to complete abolition of *ges-1* expression in the gut and to activation of *ges-1* in the pharynx/tail. Deletion of all three of these elements greatly reduced *ges-1* expression in all sets of cells. A rather detailed molecular model attempting to condense all the above results has been proposed (Egan et al. 1995). However, inconsistencies within the model were

already apparent; for example, deletion of all three promoter elements would not be predicted to cause extinction of *ges-1* expression in the pharynx/tail.

A biochemical system has been developed to study DNA-protein interactions in the early embryo ([Stroher et al. 1994](#)). Nuclear extracts of blocked embryos (but not of oocytes) were shown to contain a factor that binds specifically to the tandem WGATAR sites. As described earlier, the tandem WGATAR sequences from the *ges-1* promoter have been used to isolate the *elt-2* gene, which encodes a *C. elegans* zinc finger "GATA-factor" and which is a candidate for direct *ges-1* control ([Hawkins and McGhee 1995](#)).

## I. Promoter Trapping

The above discussion concerns specific cloned genes whose expression pattern was then investigated by transformation. [Hope \(1991\)](#) has established a "promoter trap" approach that takes the opposite direction. By fusing random genomic fragments to *lacZ* reporters, expression patterns in transformed worms can be investigated without prior knowledge of the gene. This approach has revealed a number of intriguing expression patterns worthy of further study and, in the particular case of *pes-1* ([Hope 1994](#)), has identified what could be an important regulatory factor in embryogenesis. A recent extension of this approach has investigated *lacZ* expression patterns directed by potential gene regulatory regions assigned by the genome sequencing project ([Lynch et al. 1995](#)).

## J. Summary and Conclusions

From the above examples, it seems clear that transformation "works" reasonably well as an experimental tool to investigate gene expression and gene regulation in *C. elegans*. Yet, there are limitations and potential biases in the method that should be kept in mind. It is of crucial importance to have some independent means of detecting where a gene is normally expressed, either by endogenous enzyme activity, antibody staining, or in situ hybridization. By introducing a foreign reporter sequence into a *C. elegans* gene, control signals could in principle be disrupted, deleted, or misspaced; posttranscriptional regulation of both mRNA (see, e.g., [Seydoux and Fire 1994](#); [Wilkinson and Greenwald 1995](#)) and protein could also be aberrant. Even when a gene acts as its own reporter, as in the case of *ges-1*, potential concerns arise about the influence of multiple gene copies, interspersed with marker genes and divorced from any long-range chromosomal context. Some of the concerns can be addressed by suitable controls and cautious interpretations, but many of the problems will not be solved until an efficient gene replacement technology is developed for *C. elegans*. With these cautions, there are important reasons for optimism: As one example, transformation of worms with fusions to the GFP reporter raises the possibility of watching gene activity in real time within particular cells inside the living animal.

We should also note several aspects of transformation in *C. elegans*, especially transformation using multicopy arrays, that are unexplained but potentially interesting. First, where it can be measured, multicopy arrays clearly lead to overexpression of the transforming genes ([Kennedy et al. 1993](#); [Egan et al. 1995](#)). This can possibly lead to low-level ectopic expression in particular cells, but misexpression might also be due to rearrangement of some small fraction of the transforming genes. The possibility of mosaic loss of the transforming array is a constant source of uncertainty, but it is curious that even integration of the array into the genome may still not raise the expression penetrance to 100% ([Krause et al. 1994](#); R. Baumeister and G. Ruvkun, in prep.). There have also been reports of the transforming gene somehow interfering with the function of the endogenous gene. As one example, a *ceh-10::lacZ* transgene apparently impaired the normal function of the CAN cell, a cell in which the transgene is expressed ([Swendsen and McGhee 1995](#)). It is not known whether this effect arises at the level of transcription (e.g., due to competition for limiting transcription factors, antisense inhibition because of unregulated transcription from the transforming array, or some ectopic pairing phenomenon between the endogenous gene and the extrachromosomal array) or at the level of protein function (e.g., the *ceh-10* fusion protein improperly dimerizing with its normal *ceh-10* homeodomain partner). Phenocopies have also been reported in *hlh-1* and *pal-1* transformants. Perhaps some of the above unexplained phenomena can be turned to advantage to produce novel insights into gene regulation.

Overall, what has transgenic analysis revealed about transcriptional control in *C. elegans*? It is not surprising that *C. elegans* genes, like those of other eukaryotes, are controlled by arrays of enhancers and repressors. Although none of these *C. elegans* elements or arrays of elements have yet been investigated in sufficient detail that we can say that we really understand a certain promoter, the array of controls seems to be compact. Most of the genes investigated by transformation have been "correctly" controlled by flanking regions no longer than several kilobases and, in certain cases, a few hundred base pairs seem adequate. On the one hand, this may reflect the imperfections of the current transformation assays in which long-range influences might not have been detected. On the other hand, these local controls certainly seem to be capable of producing a good first-order approximation of correct gene regulation. It also seems that compared to genes in other animals, a higher fraction of genes in *C. elegans* have transcriptional control elements in introns and at the 3'end. Perhaps this is a necessary consequence of gene compactness, but it is a feature that should be considered in gene expression studies because reporter construct strategies usually do away with such elements.

Generated from local HTML

## **Chapter 7. Transcription Factors and Transcriptional Regulation — V**

### **Future Prospects**

---

We end this chapter with two questions that face the field in the future. The first question is: How do these complex transcription patterns arise during development? We already have examples of gene expression patterns that are lineage-specific, cell-type-specific, organ-specific, sex-specific, region-specific, stage-specific, and even quasi-universal. Indeed, we also have examples of transcription factors that can be classified into many of the same categories. Do these gene expression patterns arise in a lineage autonomous fashion, by some directional and combinatorial sorting of transcription factors or do they arise by each piece of the expression pattern responding to cues in the local environment? The answer to the problem will undoubtedly lie somewhere between these two extreme options, and it is exciting that answers are beginning to emerge.

The second question is: How complex will it all be? It has taken us many pages to summarize our present imperfect knowledge of a small fraction of *C. elegans* transcription factors. How many pages will it take when we understand what is really going on? At what point must we stop collecting individual examples of gene control and begin looking for some underlying explanatory mechanisms, if indeed there are any? The challenge will be to connect these individual examples of gene control to the network of control mechanisms operating in each cell and then to the overall regulatory network that is the living animal, operated on by the forces of evolution.

Generated from local HTML

# **Chapter 8. mRNA and Translation**

---

## **Contents**

[I Introduction](#)

[II The Translational Apparatus](#)

[III Informational Suppressors](#)

[IV Regulation of Translation During Development](#)

[Acknowledgments](#)

Generated from local HTML

## Chapter 8. mRNA and Translation — I Introduction

---

The process of gene expression, during which the nucleotide sequence of a gene is converted to the amino acid sequence of a protein, is long and tortuous. An expressed gene must be transcribed, its pre-mRNA must be capped, polyadenylated, spliced, and transported to the cytoplasm, and the mature mRNA must be loaded onto polysomes and faithfully translated. In principle, gene expression can be regulated by modulating any of these molecularly complex steps. Indeed, examples of biological regulation occurring at each of these steps have been described in various organisms. We focus in this chapter on translation and translational regulation in *Caenorhabditis elegans*. Recent work with several *C. elegans* genes demonstrates that the level, timing, and pattern of gene expression can be regulated at the level of translation by elements contained within a messenger RNA's 3'-untranslated region (3'UTR). We also review the genetic and molecular effects of mutations that affect the translational apparatus itself. By altering the mechanics of translation, such mutations can influence the phenotypic consequences of mutations in many different genes.

Generated from local HTML

# Chapter 8. mRNA and Translation — II The Translational Apparatus

---

## A. Cytoplasmic Translation

Many components of the translational apparatus have been identified and studied, including ribosomal RNAs and the ribosomal DNA repeat ([Sulston and Brenner 1974](#); [Files and Hirsh 1981](#); [Albertson 1984a](#); [Ellis et al. 1986](#)); 5S rRNA and the 5S rDNA repeat ([Kumazaki et al. 1982](#); [Nelson and Honda 1985, 1986](#)); ribosomal proteins L29, L21, L35, L37, S9, and S16 ([Bektesh et al. 1988](#); [Wilson et al. 1994](#); [Zorio et al. 1994](#)); a 93-amino-acid ribosomal protein ([Jones and Candido 1993](#)); numerous tRNAs ([Tranquilla et al. 1982](#); [Khosla and Honda 1989](#); [Lee et al. 1990](#); [Schaller et al. 1991](#); [Wilson et al. 1994](#)); tRNA synthetases and modifying enzymes ([Gabius et al. 1983](#); [Amaar and Baillie 1993](#)); and translation elongation factor 2 ([Ofulue and Candido 1991, 1992](#)) and initiation factor 4A ([Roussel and Bennett 1992](#)). An in vitro system of *C. elegans* translation has unfortunately not yet been developed. *C. elegans* contains selenocysteine tRNA<sup>[Ser]Sec</sup> ([Lee et al. 1990](#)), a specialized tRNA that inserts selenocysteine (a rare amino acid) in response to specific UGA codons in many organisms. The presence of tRNA<sup>[Ser]Sec</sup> suggests that some *C. elegans* UGA codons are not translational terminators. Genes that are expressed highly tend to have greater bias in codon usage than those that are expressed at low abundance ([Stenico et al. 1994](#)), although the bias is not as strongly correlated with levels of expression as in yeast (see [Appendix 3](#)).

Cytoplasmic translation is noteworthy in that the 5' termini of many mRNAs are added posttranscriptionally by *trans*-splicing, using either of two different *trans*-spliced leader sequences ([Krause and Hirsh 1987](#); [Huang and Hirsh 1989](#)). *Trans*-spliced mRNAs retain trimethylguanosine caps of the *trans*-spliced leader ([Liou and Blumenthal 1990](#)). Messages *trans*-spliced with SL2 are derived from polycistronic precursors ([Spieth et al. 1993](#)). It appears that the role of SL2 *trans*-splicing is to generate monocistronic mRNAs from polycistronic precursors. The role of SL1 *trans*-splicing is less clear, but SL1 might contribute to efficient translation of SL1-containing mRNAs. For a more thorough review of *cis*- and *trans*-splicing in *C. elegans*, see [Blumenthal and Steward](#) (this volume).

## B. Mitochondrial Translation

The translational apparatus of *C. elegans* mitochondria is remarkable in that many of its components are the smallest ever described. The small- and large-subunit rRNAs are the smallest metazoan rRNAs described to date ([Okimoto et al. 1994](#)). Models of their secondary structure are remarkably similar to the universal core structures of *Escherichia coli* 16S and 23S rRNAs. *C. elegans* mitochondrial tRNAs are also among the smallest known and do not conform to the standard “folded cloverleaf” structure. Instead, 22 mitochondrial sequences are found that can be folded into structures that resemble tRNAs in which the TΨC arm and adjacent variable loop are missing and replaced with a single loop of 6–12 nucleotides ([Wolstenholme et al. 1987](#); [Okimoto and Wolstenholme 1990](#)). After 3'-CCA addition, these sequences constitute the complete set of mitochondrial tRNAs ([Okimoto et al. 1992](#)). Such tRNAs may represent the smallest adapters capable of functional translation. As in certain other vertebrate and invertebrate mitochondria, the codon AUA specifies methionine (rather than isoleucine in the standard code), UGA specifies tryptophan (rather than stop), and AGA and AGG specify serine (rather than arginine). None of the 12 encoded mitochondrial proteins initiates with the traditional AUG codon. Rather, three initiate with UUG, three with AUA, and six with AUU. Open reading frames terminate with either UAG or UAA. One or both of the “A” residues of UAA terminators are added posttranscriptionally following cleavage and polyadenylation ([Okimoto et al. 1990](#)).

## Chapter 8. mRNA and Translation — III Informational Suppressors

---

Isolating and analyzing genetic suppressors are a fundamental part of “forward” genetic analysis. Suppressors are defined classically as mutations that correct the phenotypic defects of another mutation without restoring its wild-type sequence. Suppressors may be intragenic (affecting the same gene) or they may be extragenic (affecting a different gene). Exogenous suppressors are particularly useful during genetic analyses, because they often identify additional components of a biological system or process. *Informational* suppressors are those that alter the genetic apparatus with which genes are expressed.

Two distinct types of informational suppressors have been identified in *C. elegans*. First, at least 13 different amber suppressors have been described, most of which affect defined tRNA genes. Both genetic and molecular criteria indicate that such suppressors are analogous to classical amber suppressors of microorganisms. Second, mutations affecting seven *smg* genes eliminate the *C. elegans* system of nonsense-mediated mRNA decay. Because of their effects on mRNA abundance, *smg* mutations can either suppress or enhance the phenotypic affects of other mutations.

### A. Amber Suppressors

Amber mutations introduce UAG nonsense codons within affected mRNAs. Amber suppressors decode such codons as “sense,” thereby restoring gene product and function. *C. elegans* is the only metazoan in which amber suppressors have been identified by traditional reversion analysis. Amber suppressors have been identified among the revertants of at least six different *C. elegans* genes. Literally hundreds of revertants of amber alleles affecting [unc-15](#), [unc-13](#), [tra-3](#), [unc-51](#), [dpy-20](#), and [lin-1](#) have been tested for the presence of amber (or other informational) suppressors ([Waterston and Brenner 1978](#); [Waterston 1981](#); [Hodgkin 1985](#); [Kondo et al. 1990](#)); 13 different suppressors have been identified from these studies.

#### 1. Genetic Properties of Amber Suppressors

[Table 1](#) summarizes genetic and molecular properties of *C. elegans* amber suppressors. Analysis of the suppressors listed in [Table 1](#), and of amber mutations themselves, leads to the following conclusions concerning amber suppression in *C. elegans*:

a.

Suppression is allele-specific, but not gene-specific. Amber alleles of many different genes are suppressed, but for any specific gene, only certain alleles (the amber alleles) are suppressed.

b.

Suppression is dose-dependent. The efficiency of phenotypic suppression depends on how many copies of an amber suppressor are present in a strain. Suppressor homozygotes suppress more strongly than suppressor heterozygotes. Amber suppressors are thus semidominant.

c.

Different suppressors have different strengths. The suppressors in [Table 1](#) differ greatly in the degree to which they suppress known amber mutations. When strengths of suppression are compared, [sup-7](#) is almost always the strongest suppressor, whereas [sup-29](#) is the weakest ([Kondo et al. 1990](#)). Amber alleles of [tra-3](#) provide the most sensitive test for amber suppression. [sup-29](#), for example, strongly suppresses amber alleles of [tra-3](#) but does not detectably suppress amber alleles of several other genes ([Kondo et al. 1988](#)). The proportion of UAG nonsense codons that are translated as sense can be remarkably high. For example, when [unc-15](#) (amber); [sup-7](#) mutants are grown at 15°C (see below for temperature effects), the quantity of full-length paramyosin is 39–45% of that found in wild type ([Waterston 1981](#)).

d.

The strength of suppression is often temperature-dependent. Phenotypic suppression by *sup-5*, *sup-7*, *sup-21*, *sup-28*, and *sup-34* is stronger at 15°C than at higher temperatures (Waterston and Brenner 1978; Waterston 1981; Kondo et al. 1990). The effect of temperature can be substantial. *unc-15* (amber); *sup-7* mutants grown at 15°C accumulate almost twice as much full-length paramyosin as those grown at 20°C (20–25% of wild type compared to ~10% of wild type, respectively) (Waterston and Brenner 1978; Waterston 1981).

e.

The strength of suppression is tissue-specific. Amber mutations have been identified in a wide variety of *C. elegans* genes, including those expressed in the nervous system, muscle, hypodermis, and germ line. The suppressors in Table 1 show consistent tissue-specific differences when tests of suppression are performed against a battery of amber alleles. For example, *sup-21*, *sup-28*, *sup-33*, and *sup-34* are strong suppressors when tested against genes expressed in the hypodermis, but they do not suppress (or do so only weakly) when tested against genes expressed in the nervous system (Kondo et al. 1988, 1990).

f.

Strong suppression is deleterious. Both *sup-5* and *sup-7* exhibit dose-dependent and temperature-dependent growth abnormalities that result from high levels of suppression. When grown at 15°C, *sup-5* (e1464) has a longer generation time than wild type (7.5 days vs. 5.5 days) and exhibits increased sterility. *sup-7* (st5), the strongest of the suppressors, cannot be grown as a homozygote for more than one generation at 15°C. Deleterious effects of strong amber suppression presumably result from inappropriate translation of natural UAG translation terminators.

Amber suppressors are valuable tools for interpreting genetic data. They are especially valuable because they provide molecular insights into gene function. Amber alleles of a gene (those phenotypically suppressed by amber suppressors) are usually null alleles, although there are occasional exceptions (Ferguson and Horvitz 1985; Hodgkin 1985, 1987a; Charest et al. 1990). Amber suppressors and amber alleles can be manipulated to confer conditional phenotypes to essential genes. Because amber suppressors are semidominant, varying the gene dose of a suppressor varies the amount of a suppressed gene product. Because the strength of amber suppression is tissue-specific, varying the suppressor varies the tissues in which suppression (and hence gene function) occurs. Amber suppressors can be effective markers to identify transgenic animals (Fire 1986). The toxicity of multiple copies of amber suppressors can be used to select for low-copy integrated transgenes.

## 2. Molecular Analysis of Amber Suppressors

Long before they were identified as tRNA genes, the genetic properties of *sup-5* and *sup-7* suggested strongly that they were analogous to classic tRNA-mediated suppressors of microorganisms (Waterston and Brenner 1978; Waterston 1981). Three lines of evidence demonstrate that this is true and that *sup-7* is, in fact, an amber suppressor. First, a purified tRNA fraction from *sup-7* mutants was shown to possess suppressor activity when microinjected into the gonad (Kimble et al. 1982) or when used to program an in vitro translation system (Wills et al. 1983). Second, *unc-54* (e1300), a *sup-7*-suppressible allele of a myosin heavy-chain gene, was shown to be an amber mutation (Wills et al. 1983). Third, *sup-7* was cloned, sequenced, and shown to encode a tRNA<sup>Trp</sup><sub>UGG</sub> (Bolten et al. 1984). Further analysis of amber suppressors and of the tRNA<sup>Trp</sup><sub>UGG</sub> gene family demonstrated that 8 of the 13 amber suppressors described in Table 1 are mutations of tRNA<sup>Trp</sup><sub>UGG</sub> genes (Bolten et al. 1984; Kondo et al. 1988, 1990). All eight suppressors encode identical tRNAs in which a single C→T substitution changes the anticodon of a tRNA<sup>Trp</sup> gene from 5'-CCA-3' to 5'-CUA-3'. The anticodon change thus allows mutant tRNAs to read the amber codon UAG. It is not certain, however, whether tryptophan is inserted at suppressed amber sites. Analogous tRNA<sup>Trp</sup><sub>UGG</sub> suppressors have been identified in *E. coli* (Hirsh 1971), but the anticodon change causes mischarging of tRNA<sup>Trp</sup> with glutamine rather than tryptophan (Yaniv et al. 1981). It is unknown whether this is also true of *C. elegans* tRNA<sup>Trp</sup> amber suppressors. Certain of the gene assignments of Table 1 are

derived from molecular analysis of tRNA<sup>Trp</sup><sub>UGG</sub> genes. For example, five alleles of "[sup-21](#)" were originally defined on the basis of their similar map positions ([Hodgkin 1985](#)). Subsequent molecular analyses of these alleles and of the tRNA<sup>Trp</sup><sub>UGG</sub> gene family ([Kondo et al. 1990](#)) demonstrated that these five alleles affect at least three distinct genes ([sup-21](#), [sup-28](#), and [sup-32](#)). Similarly, alleles originally defined as affecting "[sup-22](#)" proved to affect two distinct genes ([sup-22](#) and [sup-29](#)) ([Kondo et al. 1988](#)).

*C. elegans* contains 12 tRNA<sup>Trp</sup><sub>UGG</sub> genes, 8 of which have been mutated to suppressor alleles. When one tRNA<sup>Trp</sup><sub>UGG</sub> gene is converted to a suppressor allele, the remaining 11 genes provide sufficient tRNA<sup>Trp</sup> for translation of UGG codons during translation. Thus, at least some of the 12 wild-type genes are functionally redundant with regard to their ability to translate UGG codons. Consistent with this, animals that are homozygous for probable null alleles of [sup-7](#) are phenotypically wild type ([Waterston 1981](#)).

Of the 12 tRNA<sup>Trp</sup><sub>UGG</sub> genes, 4 have not been mutated to suppressor alleles. Such "silent" tRNA<sup>Trp</sup><sub>UGG</sub> genes may simply have been missed during reversion analyses performed to date or their pattern of expression may preclude isolating suppressor alleles. For example, [rtw-3](#) and [rtw-5](#) may be pseudogenes ([Kondo et al. 1990](#)). [rtw-6](#) and [rtw-7](#) may be expressed in insufficient or excessive quantities, such that suppressor alleles either have no detectable effect on phenotype or have such deleterious effects that suppressor alleles are dominant lethals.

Five amber suppressors in [Table 1](#) are not alleles of tRNA<sup>Trp</sup><sub>UGG</sub> genes ([sup-22](#), [sup-23](#), [sup-32](#), [sup\[st402\]](#), and [sup\[st414\]](#); [Hodgkin 1985](#); [Kondo et al. 1990](#)). Such suppressors are suspected, but not proved, to be mutations affecting other tRNA genes, such as tRNA<sup>Gln</sup><sub>CAG</sub> or tRNA<sup>Lys</sup><sub>AAG</sub>. An amber-suppressing tRNA<sup>Ser</sup> gene of *Drosophila* functions efficiently as an amber suppressor when transformed into *C. elegans* ([Pilgrim and Bell 1993](#)). Such manipulations of transgenic tRNA genes may eventually allow direct control of the inserted amino acid or of the resulting pattern of tRNA expression.

## B. *smg* Suppressors

Amber suppressors are "textbook" examples of how alterations of the genetic apparatus can influence the phenotypic consequences of mutations in many different genes. In principle, any of the many steps required for gene expression might be targets for informational suppression. For example, modification of the spliceosome can overcome defects resulting from mutant splice sites ([Parker et al. 1987](#)). Genetic and molecular analyses of informational suppressors are valuable both because they identify basic mechanisms of gene expression and because they provide technical tools for unrelated investigations. The seven *C. elegans smg* genes are informational suppressors whose wild-type mode of action involves selective mRNA degradation.

Independent work in three different laboratories identified *smg* mutations as extragenic suppressors of mutations affecting either sex determination, developmental timing, or muscle filament assembly ([Hodgkin et al. 1989](#)). Subsequent investigations established that *smg* mutations eliminate a specific system of mRNA turnover ([Pulak and Anderson 1993](#)). All eukaryotes examined to date have a system that selectively degrades mRNAs containing premature stop codons ([Peltz et al. 1994](#); [Maquat 1995](#)). This system, termed nonsense-mediated mRNA decay (NMD), has been proposed to protect cells against the deleterious effects of expressing nonsense-fragment polypeptides produced either by somatic mutation or by errors of "normal" gene expression ("mRNA surveillance"; [Pulak and Anderson 1993](#)). Genes required for nonsense-mediated decay have been identified in both yeasts (the *UPF/NMD* genes; [Leeds et al. 1991](#); [Peltz et al. 1994](#); [Cui et al. 1995](#); [He and Jacobson 1995](#); [Lee and Culbertson 1995](#)) and nematodes (the *smg* genes) ([Pulak and Anderson 1993](#)).

Six *smg* genes ([smg-1](#) through [smg-6](#)) were originally identified as allele-specific suppressors of mutations affecting either [tra-3](#), [lin-29](#), or [unc-54](#) ([Hodgkin et al. 1989](#)). A seventh gene, [smg-7](#), has been identified more recently as a suppressor of [unc-54](#) (B. Cali and P. Anderson, unpubl.). *smg*-suppressible alleles of numerous additional genes have been identified either by reversion analysis or by direct tests of suppression. These include alleles of [unc-17](#) (M. Nguyen et al., pers. comm.), [dpy-5](#) ([Hodgkin et al. 1989](#)), [glp-1](#) ([Mango et al. 1991](#)), [gon-2](#) (Y. Sun and E. Lambie, pers. comm.), [pha-1](#) ([Schnabel et al. 1991](#)), [tra-1](#) ([Hodgkin et al. 1989](#); [Zarkower et al. 1994](#)),

[\*tra-2\*](#) (Hodgkin et al. 1989), [\*unc-30\*](#) (R. Hoskins, pers. comm.), and [\*unc-76\*](#) (L. Bloom and R. Horvitz, pers. comm.). In each case, it is known (or believed) that phenotypic suppression occurs because (1) the mutant mRNAs are unstable in a *smg*(+) background, (2) the mutant mRNAs are stable in *smg*(-) backgrounds, (3) the mutant mRNAs are translated in a manner that yields partially or fully functional gene product, and (4) the elevated levels of gene product in *smg*(-) backgrounds are sufficient to confer a phenotypic effect. This molecular explanation has been rigorously demonstrated, however, only for certain *smg*-affected alleles of [\*unc-54\*](#) and [\*tra-1\*](#) (Pulak and Anderson 1993; Zarkower et al. 1994). The steady-state levels of [\*unc-54\*](#) nonsense-mutant mRNAs are about 5% of normal in a *smg*(+) background and about normal in *smg*(-) backgrounds. Nonsense mutations nearer the [\*unc-54\*](#) normal translational terminator have a less pronounced effect on mRNA stability.

Table 2 summarizes genetic properties of the *smg* genes. Analysis of the suppressors listed in Table 2 and of *smg*-suppressible mutations, leads to the following conclusions:

a.

*smg* genes act globally. *smg*-suppressible (see above) and *smg*-en-hanced (see below) alleles of many different genes have been identified, including genes expressed in the muscle, nervous system, hypodermis, pharynx, developing vulva, and germ line. The existence of *smg*-affected alleles indicates that the *smg* genes themselves function in all of those tissues. An allele that is suppressed (or enhanced) by any *smg* mutation is suppressed (or enhanced) by all *smg* mutations.

b.

Nonsense-mediated mRNA decay is not essential. As measured by the steady-state abundance of [\*unc-54\*](#) (*nonsense*) mRNA, nonsense-mediated mRNA decay is eliminated in all tested alleles of [\*smg-1\*](#), [\*smg-2\*](#), [\*smg-3\*](#), [\*smg-4\*](#), [\*smg-5\*](#), and [\*smg-7\*](#) (Pulak and Anderson 1993). Thus, the system of nonsense-mediated decay is not essential, consistent with its proposed role in mRNA surveillance. Nonsense-mediated decay is reduced, but not eliminated, in the only tested allele of [\*smg-6\*](#).

c.

*smg* mutants exhibit mild morphogenetic abnormalities. The designation "smg" (suppressor with morphogenetic effects on genitalia) describes the only conspicuous phenotype of *smg* mutants. Adult hermaphrodites exhibit protruding vulvae, and adult males have abnormal bursae. Despite these abnormalities, *smg*(-) hermaphrodites are egg-laying-proficient, and *smg*(-) males are cross-fertile, albeit with low efficiency. Young *smg*(-) males mate more efficiently than older males. The morphogenetic abnormalities of *smg* mutants suggest a subtle role for nonsense-mediated decay in the expression of normal genes. Both the suppression and morphological phenotypes of *smg* mutants are recessive, but certain synthetic dominant interactions between *smg* genes have been noted (Hodgkin et al. 1989).

d.

At least three *smg* genes ([\*smg-1\*](#), [\*smg-2\*](#), and [\*smg-5\*](#)) are nonessential. *smg*(-) single mutants, including alleles identified by either their suppression or morphological phenotypes, are viable, healthy, and exhibit only the mild abnormalities described above. *smg* alleles isolated in such screens, however, are of necessity viable and fertile, so this alone does not establish the null phenotype. Continuing molecular analyses of *smg* genes have identified known (or probable) null alleles of [\*smg-1\*](#), [\*smg-2\*](#), and [\*smg-5\*](#) (S. O'Connor and P. Anderson; B. Carr and P. Anderson; K. Anders and P. Anderson; all unpubl.). Thus, [\*smg-1\*](#), [\*smg-2\*](#), and [\*smg-5\*](#) are nonessential genes, and they appear by genetic criteria to function only in nonsense-mediated mRNA decay.

e.

Certain *smg* genes may be essential. Alleles of [\*smg-6\*](#) and [\*smg-7\*](#) isolated in a "noncomplementation" screen are often lethal when homozygous (B. Cali and P. Anderson, unpubl.). Thus, [\*smg-6\*](#) and [\*smg-7\*](#) may be essential genes, performing vital functions in addition to their role in nonsense-mediated decay.

f.

Certain *smg* genes exhibit a maternal effect. Suppression by *smg-3*, *smg-4*, and *smg-6* can be affected by maternal genotype. Specifically, animals of genotype *unc-54* (r293);*smg*(-), when derived as offspring of *smg*+/+ heterozygous mothers, are only partially suppressed. Suppression of *lin-29* (n546) exhibits a similar maternal effect for *smg-6* but not for *smg-3* or *smg-4*. Maternal effects have not been detected with alleles of *smg-1*, *smg-2*, and *smg-5*.

g.

*smg*-suppressible alleles are often, but not always, nonsense mutations. Although many *smg*-suppressible alleles are nonsense mutations ([Mango et al. 1991](#); J. Hodgkin, pers. comm.), others are deletions or rearrangements affecting the 3'end of a gene ([Pulak and Anderson 1988](#); [Hodgkin 1993](#); [Alfonso et al. 1994a](#); [Zarkower et al. 1994](#)). In cases of suppressed nonsense mutations, suppression likely occurs either because the nonsense-fragment polypeptide is partially active or because certain nonsense codons are occasionally mistranslated as "sense" in *smg*(-) backgrounds, similar to that observed in yeast ([Peltz et al. 1994](#)). In cases of *smg*-suppressible rearrangements, deletions or other mutations affecting the 3'UTR cause an upstream stop codon (which, in some cases, can be the normal translational terminator codon) to be recognized as "premature" by the NMD system, thereby resulting in degradation of the mutant message. Such mRNAs are unstable in *smg*(+) backgrounds but stable in *smg*(-) backgrounds.

## C. *smg* -dependent Dominance

Although *smg* mutations were first isolated as informational *suppressors* of recessive mutant phenotypes, one of their most striking (and useful) genetic properties is that they are informational *enhancers* of many dominant mutant phenotypes. Mutations that are recessive or only weakly dominant in *smg*(+) genetic backgrounds can be strongly dominant in *smg*(-) backgrounds. *smg* mutations can enhance the heterozygous phenotypes of either dominant-negative or dominant gain-of-function alleles. Conditional dominance of this type was first noted during genetic mapping of *smg* genes and during tests of suppression ([Hodgkin et al. 1989](#); [Mango et al. 1991](#)), but this phenomenon appears to be remarkably common. Of 14 tested *unc-54* nonsense mutations, 4 are recessive when *smg*(+) and dominant when *smg*(-) ([Pulak and Anderson 1993](#)). Of 10 feminizing *tra-1* alleles isolated in a *smg*(-) genetic background, 8 are *smg*-sensitive; i.e., expression of the mutant phenotype is greatly reduced in a wild-type background ([Zarkower et al. 1994](#)). Similarly, approximately 2/3 of dominant visible mutations isolated in a *smg*(-) background, affecting 12–14 different genes, become recessive (or only weakly dominant) when crossed into a *smg*(+) background (B. Cali and P. Anderson, in prep.). In *smg*(+) backgrounds, many of these mutations are recessive-lethals. Thus, *smg*(-) mutations can be valuable because they confer conditional viable phenotypes to recessive-lethal mutations.

*smg*-dependent dominance likely results from expression of nonsense-fragment polypeptides that have dominant-negative activities. Such polypeptide fragments are expected to be expressed at higher levels in *smg*(-) strains, because the nonsense-mutant mRNAs are present in greater abundance. The location of *smg*-dependent dominant mutations in the *unc-54* myosin heavy-chain gene is striking. Only myosins truncated near the myosin head/rod junction exhibit synthetic dominance ([Pulak and Anderson 1993](#)). Genetic tests demonstrate that the nonsense-fragment polypeptides themselves are the disruptive gene product (B. Cali and P. Anderson, in prep.). In principle, *smg*-dependent dominance may be especially pronounced in proteins like myosin that interact in macromolecular complexes. Nonsense-fragment polypeptides that are sufficiently stable to assemble into a complex with wild-type proteins may sufficiently disrupt the function of the complex to result in a dominant mutant phenotype. The location of *smg*-affected alleles can often define functional domains of a protein ([Mango et al. 1991](#); [Zarkower et al. 1994](#)).

## D. Mechanism(s) of Nonsense-mediated mRNA Decay

Nonsense-mutant mRNAs are unstable in most, if not all, eukaryotes ([Peltz et al. 1991](#); [Sachs 1993](#)). How are nonsense-mutant mRNAs targeted for selective degradation? The mechanisms are not understood in detail, but

insights from yeast and from cultured mammalian cells provide some clues. Selective turnover of nonsense-mutant mRNAs is coupled to translation ([Belgrader et al. 1993](#); [Peltz et al. 1993](#)) and is preceded by decapping of the mutant message ([Muhlrad and Parker 1994](#)). Nonsense-mutant mRNAs are not deadenylated prior to decapping, unlike many wild-type mRNAs ([Shyu et al. 1991](#); [Muhlrad and Parker 1994](#)). Cis-acting elements that either promote ([Peltz et al. 1993](#); [Cheng et al. 1994](#); [Zhang et al. 1995](#)) or inhibit ([Peltz et al. 1993](#)) nonsense-mediated mRNA decay have been defined. Such elements likely provide the means by which normal stop codons are distinguished from premature stop codons, although details of how they function are unclear.

As discussed above, the *C. elegans smg* genes and the yeast *UPF/NMD* genes encode *trans*-acting factors required for nonsense-mediated mRNA decay. How similar are the yeast and nematode proteins? *SMG-2* and *UPF1* are strong sequence homologs, being approximately 50% identical over most of their length ([Leeds et al. 1992](#); K. Anders et al., unpubl.). Despite these similarities, expression of *UPF1* in worms and expression of *smg-2* in yeast do not appear to rescue NMD function in appropriate mutants (K. Anders and P. Anderson, unpubl.). The sequences of *UPF2*, *UPF3*, *smg-1*, *smg-5*, and *smg-7* do not reveal any further strong homologies among *UPF* and *smg* genes ([Cui et al. 1995](#); [He and Jacobson 1995](#); [Lee and Culbertson 1995](#); S. O'Connor et al., unpubl.). This might indicate that additional yeast and nematode genes remain to be discovered or that components of the NMD system are not strongly conserved. Both *SMG-5* and *SMG-7* are novel proteins; *SMG-1* is a large protein that contains a "PI-3/protein" kinase domain at its carboxyl terminus (S. O'Connor and P. Anderson, unpubl.).

An unresolved issue concerning nonsense-mediated mRNA decay is where within the cell turnover occurs. A requirement for translation would suggest that turnover occurs in the cytoplasm, but observations involving several mammalian genes suggest that certain mRNAs are degraded while associated with nuclei (either within the nucleus or possibly during transport to the cytoplasm) ([Maquat 1995](#)). It is unclear at present whether there are distinct cytoplasmic and nuclear mechanisms of NMD. The *UPF1* protein of yeast is located predominantly, if not exclusively, in the cytoplasm and is associated with polysomes ([Atkin et al. 1995](#)). It will be important to determine where within the cell the *smg* gene products are located.

## Tables

**Table 1** Genetic and molecular properties of amber suppressors

Gene	Reference allele	Linkage group	Affected tRNA	Reference
<i>sup-5</i>	<i>e1424</i>	III	tRNA <sup>Trp</sup> <sub>UGG</sub>	<a href="#">Waterston and Brenner (1978)</a>
<i>sup-7</i>	<i>st5</i>	X	tRNA <sup>Trp</sup> <sub>UGG</sub>	<a href="#">Waterston (1981)</a>
<i>sup-21</i>	<i>e1957</i>	X	tRNA <sup>Trp</sup> <sub>UGG</sub>	<a href="#">Hodgkin (1985)</a>
<i>sup-22</i>	<i>e2057</i>	IV	unknown	<a href="#">Hodgkin (1985)</a>
<i>sup-23</i>	<i>e2059</i>	IV	unknown	<a href="#">Hodgkin (1985)</a>
<i>sup-24</i>	<i>st354</i>	IV	tRNA <sup>Trp</sup> <sub>UGG</sub>	<a href="#">Kondo et al. (1988)</a>
<i>sup-28</i>	<i>e1958</i>	X	tRNA <sup>Trp</sup> <sub>UGG</sub>	<a href="#">Kondo et al. (1988)</a>
<i>sup-29</i>	<i>e1986</i>	IV	tRNA <sup>Trp</sup> <sub>UGG</sub>	<a href="#">Kondo et al. (1988)</a>
<i>sup-32</i>	<i>e2058</i>	X	unknown	<a href="#">Hodgkin (1985)</a>
<i>sup-33</i>	<i>st389</i>	X	tRNA <sup>Trp</sup> <sub>UGG</sub>	<a href="#">Kondo et al. (1990)</a>
<i>sup-34</i>	<i>e2227</i>	I	tRNA <sup>Trp</sup> <sub>UGG</sub>	<a href="#">Kondo et al. (1990)</a>
<i>sup(st402)</i>	<i>st402</i>	unknown	unknown	<a href="#">Kondo et al. (1990)</a>
<i>sup(st414)</i>	<i>st414</i>	unknown	unknown	<a href="#">Kondo et al. (1990)</a>

**Table 2**Genetic properties of *smg* genes

Gene	Reference allele	Linkage group	Notes
<a href="#"><u>smg-1</u></a>	e1228	I	formerly <a href="#"><u>mab-1</u></a>
<a href="#"><u>smg-2</u></a>	e2008	I	formerly <a href="#"><u>mab-2</u></a>
<a href="#"><u>smg-3</u></a>	ma117	IV	maternal presence effect
<a href="#"><u>smg-4</u></a>	ma116	V	maternal presence effect
<a href="#"><u>smg-5</u></a>	r860	I	
<a href="#"><u>smg-6</u></a>	r896	III	maternal presence effect
<a href="#"><u>smg-7</u></a>	r1131	IV	suppression is temperature-sensitive

Generated from local HTML

# Chapter 8. mRNA and Translation — IV Regulation of Translation During Development

The regulation of translation is crucial to at least three aspects of *C. elegans* development: progression through the life cycle ([\*lin-14\*](#)), sex determination ([\*tra-2\*](#), [\*fem-3\*](#)), and early embryogenesis ([\*glp-1\*](#)). In the following sections, we discuss each control within its developmental context, but we focus on those experiments supporting a role for translational control. Although progress on *cis*-acting translational regulatory elements has been rapid, only one *trans*-acting regulator ([\*lin-4\*](#)) has been unambiguously identified.

## A. Translational Control and Progression through the Life Cycle

*C. elegans* passes through four distinct larval stages, termed L1, L2, L3, and L4, before reaching sexual maturity. This progression from L1 to adulthood depends on several “heterochronic” genes, including [\*lin-14\*](#) and [\*lin-4\*](#). During the past few years, a series of elegant genetic and molecular experiments demonstrated that [\*lin-14\*](#) is translationally regulated by [\*lin-4\*](#) to achieve normal progression through the life cycle (see [Ambros](#), this volume).

[\*lin-14\*](#) directs L1-specific events ([Ambros and Horvitz 1984](#)). Normally, L1 larvae possess abundant LIN-14 protein, whereas later stages possess little or none ([Ruvkun and Giusto 1989](#)). In contrast, [\*lin-14\*](#) mRNA is present at approximately the same level throughout larval development ([Wightman et al. 1993](#)). Two [\*lin-14\* \(gf\)](#) “gain-of-function” mutants reiterate L1 larval stages and possess LIN-14 protein throughout larval development ([Ambros and Horvitz 1984; Ruvkun and Giusto 1989](#)). The molecular defects associated with [\*lin-14\* \(gf\)](#) mutations reside in the [\*lin-14\* 3'UTR](#) ([Ruvkun et al. 1989; Wightman et al. 1991](#)). The [\*lin-14\* 3'UTR](#), furthermore, can confer upon a chimeric reporter gene a pattern of expression typical of LIN-14 protein ([Wightman et al. 1993](#)). Therefore, the [\*lin-14\* 3'UTR](#) is essential for the translational down-regulation of [\*lin-14\*](#) and hence for progression to the L2 stage.

The [\*lin-4\*](#) gene is required for translational repression of [\*lin-14\*](#) ([Ambros 1989; Arasu et al. 1991](#)). Mutants lacking [\*lin-4\*](#) activity reiterate L1-specific events ([Chalfie et al. 1981](#)), a phenotype that is strikingly similar to that of misregulated [\*lin-14\* \(gf\)](#) mutants. [\*lin-4\*](#) activity is essential for the translational repression of a chimeric reporter gene conferred by the [\*lin-14\* 3'UTR](#) ([Wightman et al. 1993](#)). Remarkably, [\*lin-4\*](#) encodes two short RNAs (22 and 61 nucleotides) with no apparent coding capacity for a protein. Instead, both RNAs are complementary to each of seven conserved sequence elements located in the [\*lin-14\* 3'UTR](#) (see [Fig. 1](#)) ([Lee et al. 1993; Wightman et al. 1993](#)). The small [\*lin-4\*](#) RNAs are themselves likely to be at least part of the *trans*-acting machinery that regulates [\*lin-14\*](#) translation. Proteins may also be critical, but none has yet been identified. The secondary structures of each potential hybrid, and the sequence of the “looped-out” regions (see [Fig. 1B](#)), are quite similar and could serve as protein-binding sites.

Figure 1A diagrams a simple binary switch, in which [\*lin-14\*](#) is translationally active during L1 and repressed in late L1 to effect the transition to L2. Various lines of evidence suggest that the control may be somewhat more complex than that of Figure 1A. Although data are not yet definitive, a temporal gradient for [\*lin-14\*](#) activity has been suggested, with high, intermediate, and low levels of [\*lin-14\*](#) activity directing the L1, L2, and L3 stages of the life cycle, respectively ([Austin and Kenyon 1994b](#) and references therein). The presence of seven *cis*-acting elements in the [\*lin-14\* 3'UTR](#) provides a plausible molecular mechanism for generating such a temporal gradient: Increasing occupancy of [\*lin-14\*](#) sites by [\*lin-4\*](#) RNA might result in graded repression of translation.

## B. Translational Control and Establishment of Embryonic Asymmetry

Asymmetry along the future anterior-posterior axis is established in the *C. elegans* embryo as the zygote divides into two daughter blastomeres. The anterior daughter, called AB, is larger than its posterior sister, P1, and AB and P1 have distinct developmental potentials ([Laufer et al. 1980; Cowan and McIntosh 1985; Schierenberg 1985; Edgar and McGhee 1986; Priess and Thomson 1987](#)). Strikingly, a cluster of cytoplasmic granules, called P

granules, are segregated into P1 at the two-cell stage ([Strome and Wood 1982, 1983](#); see [Kemphues and Strome](#), this volume). We focus here on the role that translational control has in regulating early embryonic asymmetry.

The newly fertilized egg contains a rich supply of maternal components that regulate early embryonic events. Of particular importance in this chapter is the maternal contribution of mRNA encoding the GLP-1 membrane receptor, which is required for several inductive cell interactions in the early embryo ([Priess et al. 1987; Hutter and Schnabel 1994; Mello et al. 1994; Moskowitz et al. 1994](#); see [Schedl](#), this volume). Maternal *glp-1* mRNA is distributed uniformly in maturing oocytes, in the newly fertilized zygote, and in early embryos until the eight-cell stage ([Evans et al. 1994; Seydoux and Fire 1994](#)). In contrast, GLP-1 protein first appears at the two- to four-cell stage and is detected in anterior, but not posterior, blastomeres ([Evans et al. 1994](#)). Therefore, the early embryonic distribution of maternally encoded GLP-1 does not depend on localization of maternal mRNA or on its differential stability.

To explore the regulation of maternal mRNAs, a reporter assay was developed (see [Fig. 2](#)) ([Evans et al. 1994](#)). The first step in this assay is the synthesis in vitro of a chimeric mRNA composed of a reporter-coding region (e.g., *lacZ*) fused to a proposed regulatory element (e.g., a 3'UTR). To enhance detection of reporter protein, a nuclear localization signal (NLS) is included. Reporter mRNA is injected into the syncytial germ line of adult hermaphrodites, and its translation is assayed by examining expressed reporter proteins. Using this assay, the *glp-1* 3'UTR was found to confer upon β-galactosidase virtually the same pattern of embryonic expression as observed for endogenous GLP-1 ([Evans et al. 1994](#)). The pattern of early embryonic GLP-1 expression is therefore directed by the *glp-1* 3'UTR. Since neither RNA localization nor stability seems to have a role in controlling GLP-1 expression in the early embryo, translational control has been inferred ([Evans et al. 1994](#)).

Generation of the pattern of *glp-1* mRNA appears to depend on two distinct aspects of translational control ([Evans et al. 1994](#)). One is temporal: *glp-1* mRNA is translationally silent in oocytes and one-celled embryos but becomes active by the two- to four-cell stage. The second is spatial: *glp-1* is translationally silent in posterior blastomeres but active in anterior blastomeres. The elements responsible for both controls reside in the 3'UTR. Sequences responsible for spatial regulation lie in a 39-nucleotide element in the central region of the 3'UTR, whereas those required for temporal control lie within an AU-rich region at the 3'end of the 3'UTR ([Evans et al. 1994; T. Evans and J. Kimble, unpubl.](#)). Within the 39-nucleotide region is a bipartite sequence with striking similarity to a *nanos* response element (NRE) of *Drosophila* ([Wharton and Struhl 1991](#)). Therefore, asymmetry in early *C. elegans* and *Drosophila* embryos may be established by analogous mechanisms in which translation of uniformly distributed maternal transcripts is restricted to anterior regions of the embryo through spatially controlled translational repression. The significance of the apparent similarity of *Drosophila* NREs with *C. elegans* NRE-like sequences has not been established.

A role for translational control of other maternal mRNAs in the early *C. elegans* embryo is not yet established, yet there are hints that this mechanism may be widespread. For example, *mex-3*, which is critical for the establishment of blastomere identity, contains a known RNA-binding motif, the KH domain, and has been implicated in the control of *pal-1* expression (B. Draper et al., in prep.; J. Priess, pers. comm.). Furthermore, other mRNAs expressed in the *C. elegans* germ line possess NRE-like sequences in their 3'UTRs ([Roussell and Bennett 1993; M. Grindl and K. Bennett, pers. comm.](#)). The extent to which translational control contributes to early blastomere fate specification and pattern formation will clearly be a major focus of research in the future.

## C. Translational Control and Sex Determination

Specification of *C. elegans* as a hermaphrodite or male is regulated by a group of sex determination genes (see [Meyer](#), this volume). One of these genes, *tra-2*, is clearly regulated at the level of translation ([Goodwin et al. 1993](#)), and a second, *fem-3*, appears to be translationally regulated ([Ahringer and Kimble 1991](#)). Mutations identifying *cis*-acting regulatory elements in both *tra-2* and *fem-3* were isolated by genetic selections (see [Fig. 3](#)) ([Barton et al. 1987; Schedl and Kimble 1988](#)). These controls have been most extensively explored in studies of the hermaphrodite germ line, although they function in somatic tissues as well.

## 1. Molecular Analysis of Amber Suppressors Regulation of *tra-2*

The *tra-2* gene normally directs female development ([Hodgkin and Brenner 1977](#)). Six *tra-2* (*gf*) regulatory mutations feminize the hermaphrodite germ line such that only oocytes are made ([Doniach 1986; Schedl and Kimble 1988](#)). Therefore, in hermaphrodites, *tra-2* is normally repressed to achieve the onset of spermatogenesis. In addition, XO *tra-2* mutants are slightly feminized, with the production of oocytes and yolk in animals homozygous for the strongest *tra-2* alleles.

*tra-2* mutants are altered in a 28-nucleotide tandem repeat located in the *tra-2* 3'UTR (see [Fig. 4A](#)) ([Goodwin et al. 1993](#)). Each 28-nucleotide repeat is called a direct repeat element, or DRE. The strongest *tra-2* allele deletes both DREs, whereas intermediate-strength and weaker alleles affect only one DRE. A role for the DREs in controlling the translational activity of *tra-2* mRNA is suggested by a comparison of *tra-2* mRNAs from wild-type and *tra-2* mutants. Whereas the steady-state quantity of *tra-2* mRNAs is normal, *tra-2* mRNAs are associated with larger polysomes than are wild-type *tra-2* mRNAs ([Goodwin et al. 1993](#)). Furthermore, chimeric reporter mRNA constructs, as described above (see [Fig. 2](#)), demonstrate that a wild-type *tra-2* 3'UTR represses expression of β-galactosidase in the germ line, whereas a *tra-2* 3'UTR lacking DREs does not ([Goodwin et al. 1993](#)). The extent of *tra-2* translation varies with the number of DREs ([Goodwin et al. 1993](#)). A *tra-2* mutant without DREs is more severely affected than a mutant with a single DRE. Thus, *tra-2* mRNAs containing no DRE are associated with larger polysomes than mRNAs having one DRE, which in turn are associated with larger polysomes than mRNAs containing two DREs. By several criteria, DREs therefore appear to function as *cis*-acting negative regulatory elements that mediate translational repression of *tra-2* mRNA.

Candidates for the translational repressor of *tra-2* have been identified. Each DRE specifically binds a factor, the DRE-binding factor (DRF), in crude extracts ([Goodwin et al. 1993](#)). A recently identified gene, *laf-1*, is predicted to either encode DRF or influence its activity (E. Goodwin and J. Kimble, unpubl.). A decrease in *laf-1* disrupts translational repression of a chimeric reporter gene mediated by the *tra-2* 3'UTR (E. Goodwin and J. Kimble, unpubl.).

## 2. Regulation of *fem-3*

*fem-3* normally directs male development ([Hodgkin 1986; Barton et al. 1987](#)). Nineteen *fem-3* (*gf*) mutations masculinize the hermaphrodite germ line such that it produces a vast excess of sperm and no oocytes ([Barton et al. 1987](#)). Therefore, *fem-3* is normally repressed to achieve the switch in the hermaphrodite germ line from spermatogenesis to oogenesis. Remarkably, all *fem-3* (*gf*) mutations either alter or remove nucleotides in a 5-bp region of the 3'UTR that is presumably part of a *cis*-acting negative regulatory element (see [Fig. 4B](#)) ([Ahringer 1991; Ahringer and Kimble 1991](#)). For simplicity, we refer to this 5-bp region as the point mutation element, or PME, although the regulatory element may comprise more than just these five nucleotides.

Disruption of the PME appears to disrupt translational control of *fem-3*. The *fem-3* (*gf*) mutations do not detectably affect transcription, splicing, or stability of *fem-3* mRNA, and the *fem-3* (*gf*) mutant RNAs possess a longer poly(A) tail than their wild-type counterparts ([Ahringer and Kimble 1991](#)). The evidence that *fem-3* is controlled at the translational level is not as strong as that for other genes discussed in this chapter, but all observations are consistent with translational regulation.

The *fem-3* 3'UTR is likely to be regulated by a *trans*-acting factor that can be titrated out in transgenic animals. Animals carrying a transgenic *fem-3* 3'UTR driven by the *fem-3* promoter exhibit germ-line masculinization, suggesting titration of a negative regulator from endogenous pools of mRNA ([Ahringer and Kimble 1991](#)). In gel-shift assays, the PME binds specifically to a factor in worm extracts, which we term here PMF (point mutation element-binding factor) ([Ahringer 1991](#)). Strong candidates for *trans*-acting regulators of *fem-3* via its 3'UTR are the six *mog* genes. *mog-1* loss-of-function mutants fail to switch from spermatogenesis to oogenesis, much like *fem-3* gain-of-function mutants ([Graham and Kimble 1993](#)). Mutants of *mog-2* through *mog-6* are similarly masculinized in the hermaphrodite germ line ([Graham et al. 1993](#)). Intriguingly, all six *mog* genes act maternally to influence embryogenesis in addition to controlling the sperm/oocyte switch. Therefore, if indeed the *mog* genes control *fem-3*, they are likely to encode factors that regulate numerous other mRNAs as well.

### 3. Spatial Differentiation in the Germ Line

Figure 5 diagrams a model of two controls that appear to be important for establishing the spatial pattern of differentiation in the germ line. The presence of sperm in proximal regions of the germ line and oocytes in distal regions depends on sequential regulation of both *tra-2* and *fem-3* via their 3'UTRs. In early stages, translational repression of *tra-2* permits the onset of spermatogenesis. In later stages, translational repression of *fem-3* appears to mediate the switch from spermatogenesis to oogenesis in more distal cells. Other controls (e.g., *fog-2*; [Schedl and Kimble 1988](#)) also contribute to the establishment of this pattern (see [Meyer](#), this volume).

### D. Comparison of 3'UTR Regulatory Elements

As discussed above, *cis*-acting regulatory elements have been identified in four *C. elegans* regulatory genes. The *cis*-acting regulatory elements of *lin-14*, *glp-1*, *tra-2*, and *fem-3* have several features in common. First, all elements reside in the 3'UTR. This similarity is particularly striking for *lin-14*, *tra-2*, and *fem-3*. The gain-of-function alleles of these genes were discovered by genetic screens that had no bias for the position of identified regulatory elements. In contrast, the *glp-1* elements were revealed by experiments that focused on the 3'UTR. Although other regions of the mRNAs (e.g., 5'UTRs) may also possess translational (or other) control elements, the 3'UTRs appear to be a common target for such regulation. Second, all five elements mediate negative control. Since disruption of positive control elements might be expected to have the same effect as a mutation that reduces gene function, such elements might be more difficult to detect genetically. Third, two of the 3'UTR control elements (*lin-14* and *tra-2*) may function as rheostats. In both genes, elements are repeated, and elimination of some but not all elements yields an intermediate level of translation ([Goodwin et al. 1993](#); [Wightman et al. 1993](#)). In wild-type mRNAs, partial occupancy of multiple sites might allow translation to be modulated incrementally. Alternatively, multiple elements might facilitate cooperative binding of regulatory factors and thereby facilitate concerted repression.

Although few 3'UTR regulatory elements are presently known, more will likely be discovered in the near future. A major effort is currently focused on the analysis of maternal mRNAs that control early embryonic decisions (e.g., *skn-1*, *apx-1*, *pie-1*; see [Schnabel and Priess](#), this volume). Such maternal mRNAs, many of which are expressed in specific patterns within the early embryo (e.g., see [Seydoux and Fire 1994](#)), are of necessity controlled posttranscriptionally. A likely site for *cis*-acting elements that confer such regulation is the 3'UTR. With a battery of regulatory elements in hand, we can begin to understand some of the 3'UTR ground rules. What level of regulatory complexity can a single 3'UTR possess? What elements are conserved between *C. elegans* and other species? What are the *trans*-acting factors? And how do these elements affect translation?

The full significance of translational regulation is not yet known. In some respects, work on 3'UTRs may be at a stage equivalent to the early days of analyzing promoters. Regulatory elements in 3'UTRs should prove useful in controlling translation, much as promoters are useful in controlling transcription. The manipulation of 3'UTR regulatory elements provides a powerful way of manipulating gene expression. For example, production of a protein in AB descendants of the early embryo can be achieved by judicious use of the *glp-1* 3'UTR.

## Figures



### Figure 1



### Figure 2

Reporter assay for 3'UTR regulation by injection of in-vitro-synthesized mRNA. Reporter RNA is synthesized in vitro (*top*) and injected into the syncytial germ line of an adult hermaphrodite (*middle*). After a period of a few hours, in which oocytes and early embryos incorporate injected reporter mRNA, expression is assayed by standard methods (e.g., antibody staining and X-gal).

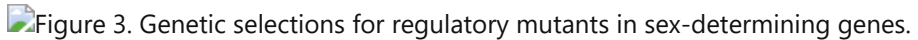


### Figure 3

Genetic selections for regulatory mutants in sex-determining genes. (A) General selection schemes. XX animals bearing only oocytes or only sperm are self-sterile. Mutations that permit either type of animal to make both sperm and oocytes generate self-fertile hermaphrodites. Such selections can be used to identify mutants that occur at frequencies of less than 1/200,000 animals. (B) Specific examples of selection schemes. *fem-1(ts)* animals are self-fertile at permissive temperature but are self-sterile at the restrictive temperature, making only oocytes. Therefore, *fem-1(ts)* animals can be grown as a homozygous strain at permissive temperature and then shifted to nonpermissive temperature to select for self-fertile animals. *fem-3(gf)* mutations were isolated as dominant suppressors of both *fem-1(ts)* and *fem-2(ts)* (Barton et al. 1987). Similarly, *fem-3(gf)* animals are self-fertile at permissive temperature but self-sterile at restrictive temperature, making only sperm. *tra-2* mutations were isolated as dominant suppressors of *fem-3(gf)* (Rosenquist and Kimble 1988).



### Figure 4

Regulatory elements in *tra-2* and *fem-3* mRNAs. (A) *tra-2* 3'UTR regulatory elements. (Top, shaded box) *tra-2* - coding region; (thin lines) the 5' and 3'UTRs; (bottom) expanded view of wild-type and mutant *tra-2* 3'UTRs. The wild-type 3'UTR possesses two DREs (arrows) separated by four nucleotides; each DRE has the same 28-nucleotide sequence,

UAGAUUAUGAGUAGAUAGAAAUAUAAAUA

The strongest *tra-2* allele lacks both DREs, an intermediate-strength allele harbors a transposable element (Tc1) in the more 5'DRE, and weakest alleles have a single remaining DRE, due to either a deletion or a Tc1 insertion into the more 3'DRE. Disruption of the 5'DRE is more severe than disruption of the 3'DRE; perhaps access to the DREs is limited by a process that moves from 5'to 3', such as transcription or translation. For details, see text and Goodwin et al. (1993). (B) *fem-3* 3'UTR regulatory element. (Top, shaded box) *fem-3* -coding region; (thin lines) 5'and 3'UTRs; (bottom) expanded view of wild-type and mutant *fem-3* 3'UTRs. The sequence UCUUG, which is altered in *fem-3(gf)* mutants, is located in approximately the middle of the wild-type *fem-3* 3'UTR. A deletion of the region has the most severe phenotype. Single nucleotide changes within the sequence alter the RNA as shown; the number of independently isolated mutants with each specific change is shown in parentheses above the altered nucleotide, or beside the deletion. For details, see text and Ahringer and Kimble (1991). (Reprinted, with permission, from Wickens et al. 1996.)

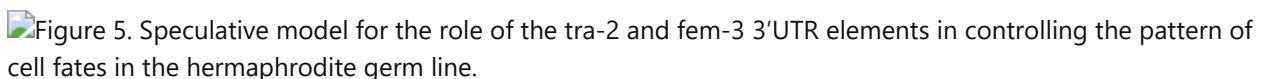


### Figure 5

Speculative model for the role of the *tra-2* and *fem-3* 3'UTR elements in controlling the pattern of cell fates in the hermaphrodite germ line. (Top) Translational activity of *tra-2* or *fem-3*; (bottom) pattern of cell fates. Pattern is generated as differentiation proceeds from proximal (left) to distal (right). First, repression of *tra-2* is required for the onset of spermatogenesis. DRF is proposed to bind DREs during larval development, thereby repressing *tra-2* translation and permitting spermatogenesis. *fem-3*, which is translationally active at this time, directs spermatogenesis for a period of hours in the proximal region of the gonad. At later times, repression of *fem-3* is required for the switch from spermatogenesis to oogenesis. PMF is proposed to bind the PME, thereby repressing *fem-3* translation and permitting oogenesis. The translational activity of *tra-2* during oogenesis is at present unknown. (Reprinted, with permission, from Wickens et al. 1996.)

Generated from local HTML

## **Chapter 8. mRNA and Translation — Acknowledgments**

---

We thank Marv Wickens for comments on the manuscript and the National Institutes of Health (P.A. and J.K.), the National Science Foundation (J.K.), the Council for Tobacco Research (J.K.), and the Howard Hughes Medical Institute (J.K.) for their research support during the course of this work.

Generated from local HTML

# **Chapter 9. Sex Determination and X Chromosome Dosage Compensation**

---

## **Contents**

- [I Introduction](#)
- [II Sexual Dimorphism](#)
- [III The Primary Sex-Determination Signal and its Gene Target](#)
- [IV Hermaphrodite-Specific Genes that Coordinately Control Sex Determination and Dosage Compensation](#)
- [V X Chromosome Dosage Compensation](#)
- [VI Somatic Sex Determination](#)
- [VII Sex Determination in The Germ Line Versus the Soma](#)
- [VIII Concluding Remarks](#)
- [Acknowledgments](#)

Generated from local HTML

# **Chapter 9. Sex Determination and X Chromosome Dosage Compensation — I Introduction**

---

The choice of sexual fate is an early developmental decision with far reaching consequences. In *Caenorhabditis elegans*, this decision not only specifies the overt sexual characteristics evident in adults, but also sets the level of X chromosome gene expression in [all somatic cells](#) throughout development, starting at the 30-cell stage. The sex determination decision itself must be made with considerable fidelity, despite the fact that only a twofold difference in X chromosome number triggers this major developmental event.

Studies during the last two decades have identified many of the genes in the complex regulatory hierarchy that determines sexual fate in *C. elegans*, stemming from those that comprise the sex-determining signal itself to those that control sexual dimorphism and X chromosome expression. Molecular mechanisms underlying many aspects of sex determination and differentiation have also been revealed. Indeed, studies of sex determination in *C. elegans* have proven it to be a rich source of information concerning the molecular nature of developmental decisions and how they are regulated. These studies have intersected work in many areas including transcriptional regulation, translational regulation, RNA processing, signal transduction, and chromosome structure.

This chapter summarizes our current understanding of the genetic and molecular basis for sex determination and the related process of dosage compensation. The extensive information obtained will facilitate future efforts to tap the enormous potential that this system holds for addressing fundamental biological and biochemical questions.

Generated from local HTML

## Chapter 9. Sex Determination and X Chromosome Dosage Compensation — II Sexual Dimorphism

---

*C. elegans* has two natural sexes, XO males and XX hermaphrodites. The hermaphrodites are simply self-fertile females whose only male character is the ability to make the limited number of sperm used solely for internal self-fertilization. This modified female is therefore able to reproduce in the absence of any other individual. However, given the opportunity, she will mate with a male, use his sperm preferentially, and produce more progeny as a consequence. Males can be produced from rare, spontaneous X chromosome nondisjunction events during hermaphrodite reproduction or as 50% of the outcross progeny in a mating between a male and a hermaphrodite.

Sex is determined by an X chromosome counting mechanism in which the dose of X chromosomes is measured relative to the ploidy, the number of sets of autosomes ([Nigon 1951](#); [Madl and Herman 1979](#)). Worms with an X:A ratio of 1.0 are hermaphrodites, and those with an X:A ratio of 0.5 are males. Animals can discriminate between even smaller differences in the signal: Those with an X:A ratio of 0.67 (2X:3A) are males, whereas those with an X:A ratio of 0.75 (3X:4A) are hermaphrodites. Although the organism uses an "X:A mechanism" of sex determination, wild-type animals are diploid and therefore normally only count X chromosomes.

The degree of overt sexual dimorphism in *C. elegans* is extensive, with 30% of the 959 somatic nuclei in the adult hermaphrodite and 40% of the 1031 somatic nuclei in the adult male being sexually specialized. In fact, sexual dimorphism occurs in all tissue types and arises in almost all major branches of the cell lineage ([Sulston and Horvitz 1977](#); [Kimble and Hirsh 1979](#); [Kimble and Sharrock 1983](#); [Sulston et al. 1983](#); [Hodgkin 1988](#)). Although some adult structures such as the [pharynx](#) and the main body musculature appear to be identical between the sexes, other aspects of the anatomy and many aspects of behavior are dramatically different ([Fig. 1](#)). For example, the hermaphrodite has a two-armed gonad in which spermatogenesis (160 sperm produced per arm) occurs during the last larval stage, followed by oogenesis during adulthood. In each arm, the sperm are stored internally in a specialized compartment, and the oocytes are fertilized as they pass through the compartment into the [uterus](#). The embryos are laid through the [vulva](#), an opening in the ventral hypodermis that also serves as the site of entry for male-produced sperm. The hermaphrodite tail is relatively unspecialized and tapers to a thin point. In contrast, the male is both shorter (~30%) and thinner than the hermaphrodite and is highly specialized for mating (see also [Emmons and Sternberg](#), this volume). For example, the [male tail](#) is equipped with various specialized sensory and copulatory structures that enable him to locate the [vulva](#) and successfully inseminate the hermaphrodite. The male also differs in that it has a single-armed gonad, which produces approximately 3000 sperm. The hypodermal cells that divide and give rise to the [vulva](#) in hermaphrodites fail to divide in the male and instead join the hypodermal syncytium. Extensive dimorphism also occurs in both the musculature and the [nervous system](#). Sex-specific muscles and [neurons](#) are involved in egg-laying behavior in hermaphrodites as well as mating behavior, copulation, and locomotory behavior in males. The intestine is functionally specialized for yolk production only in hermaphrodites ([Kimble and Sharrock 1983](#)).

Embryonic development is almost identical between the sexes. The first visible sign of sexual dimorphism appears two thirds of the way through embryogenesis with the programmed cell deaths of two hermaphrodite-specific motor [neurons](#) in the male and four male-specific [sensory neurons](#) in the hermaphrodite ([Sulston et al. 1983](#)). Other sexual dimorphisms arise during embryogenesis and the first three larval stages, but the differences in males and hermaphrodites become most prominent in the L4 larval stage and in the adult ([Sulston and Horvitz 1977](#)). Diverse strategies are used to generate sexual dimorphism, including sex-specific programmed cell death, generation of sex-specific blast cells, alternative lineages adopted by a common primordium, and differential gene expression in tissues with identical cell lineages.

The first aspect of sexual dimorphism to develop in worms is one shared by [all somatic cells](#): a difference in the average rate of X-linked gene expression, a consequence of dosage compensation. The process of dosage compensation equalizes the amount of X-linked gene products between the sexes despite a twofold difference in X chromosome dose ([Wood et al. 1985](#); [Meyer and Casson 1986](#); [DeLong et al. 1987](#); [Meneely and Wood 1987](#)).

The onset of dosage compensation occurs at approximately the 30-cell stage ([Chuang et al. 1994](#)). Dosage compensation is achieved by modulating the transcript levels of active X-linked genes, rather than by inactivating an X chromosome. In particular, hermaphrodites reduce transcript levels from both X chromosomes by half ([Meyer and Casson 1986](#); [Chuang et al. 1994](#)). This hermaphrodite-specific process is essential for the viability of XX animals ([Hodgkin 1983](#); [Meyer and Casson 1986](#); [Nusbaum and Meyer 1989](#); [Plenefisch et al. 1989](#)) and is lethal if implemented in males ([Miller et al. 1988](#)).

Achieving proper differentiation of the two sexes requires the coordination of a large number of developmental events that are spatially, mechanistically, and temporally distinct. All of the numerous aspects of sexual dimorphism, stemming from the earliest regulation of zygotic gene expression soon after fertilization to some of the latest events during gametogenesis in the mature adult, are controlled and coordinated by a regulatory gene hierarchy. This hierarchy includes genes that comprise the X:A signal itself, genes that respond directly to the signal to control coordinately both sex determination and dosage compensation, and more specialized genes that regulate either sex determination or dosage compensation.

## Figures

Figure 1. Sexual dimorphism in adult males and hermaphrodites.

### Figure 1

Sexual dimorphism in adult males and hermaphrodites.

Generated from local HTML

# **Chapter 9. Sex Determination and X Chromosome Dosage Compensation — III The Primary Sex-Determination Signal and its Gene Target**

---

## **A. X:A Signal Target Gene**

The primary effect of X chromosome dose is on a single gene target very early in development. This target of the X:A signal is the male-specific switch gene *xol-1* (XO lethal), which controls both sex determination and dosage compensation (Miller et al. 1988; Rhind et al. 1995; M. Nicoll et al., in prep.). *xol-1* is regulated by the X:A signal primarily at the level of transcription (M. Nicoll et al., in prep.). A male dose of X chromosomes results in a high level of *xol-1* transcripts and a hermaphrodite dose results in a low level (Rhind et al. 1995). A secondary level of *xol-1* regulation is posttranscriptional (M. Nicoll et al., in prep.).

The key to understanding the earliest events in the male/hermaphrodite decision was the appreciation that dosage compensation is a sex-specific process and that upsets in dosage compensation cause sex-specific lethality. Thus, mutations that perturb either the X:A signal or the gene targets of that signal would be expected to cause both sex-specific lethality and sexual transformation. *xol-1* was discovered after it had been shown that sex determination and dosage compensation are coordinately regulated in worms by a group of hermaphrodite-specific genes, the *sdc* genes (sex and dosage compensation) (Villeneuve and Meyer 1987; Nusbaum and Meyer 1989) and that dosage compensation is implemented by “dosage compensation *dumpy*” (*dpy*) genes (Hodgkin 1983; Meyer and Casson 1986; Plenefisch 1989), which function in hermaphrodites to down-regulate expression of both X chromosomes. Genetic epistasis studies placed *xol-1* upstream of the *sdc* and *dpy* genes, indicating that *xol-1* is the gene nearest to the X:A signal and might therefore be a direct target of that signal (Miller et al. 1988).

Null alleles of *xol-1* have no effect on otherwise wild-type XX animals, but they cause the feminization and death of XO animals. This XO-specific lethality results from inappropriately low X chromosome gene expression. Lethality but not feminization is suppressed by the dosage compensation *dpy* mutations, indicating that lethality is caused by inappropriate activation of the XX-specific dosage compensation machinery in XO mutants. Rescued XO *dpy*; *xol-1* animals are non-Dpy phenotypic hermaphrodites that express nearly wild-type levels of X-linked transcripts. Indeed, the first *xol-1* mutation arose spontaneously in a *dpy* mutant culture as just such an XO animal masquerading as a wild-type hermaphrodite. Mutations in the *sdc* genes fully suppress both the feminization and lethality of *xol-1* mutations, resulting in viable XO males. Together, these genetic interactions demonstrated that *xol-1* promotes male development by ensuring that downstream genes controlling hermaphrodite sexual development and dosage compensation are inactive in XO animals. The primary sequence of the 417-amino-acid XOL-1 protein provides no clue as to its mechanism of action.

The possibility that *xol-1* might be the only direct target of the X:A signal was suggested from the discovery that *xol-1* acts as an early switch in the sex determination decision (Rhind et al. 1995). Ectopic expression of *xol-1* transcripts in XX animals activates the male program of development and causes death by disrupting dosage compensation. The time in development during which expression of *xol-1* transcripts from a heat shock promoter kills XX animals is the same as that required to rescue *xol-1* null XO mutant animals—from the 28-cell stage through gastrulation, indicating that the effects of *xol-1* on XX animals mimics the action of *xol-1* in XO animals. This timing also agrees with the time of *xol-1* transcription in XO animals as assayed by a *xol-1::lacZ* reporter transgene. The very early time of *xol-1* action is consistent with its being the direct target of the primary sex determination signal. The fact that *xol-1* expression becomes dispensable toward the end of gastrulation suggests that an irreversible commitment to a particular sexual fate has occurred by then and that assessment of the X:A ratio is no longer necessary or consequential. Thus, the X:A signal target in worms does not appear to be involved in maintaining the sexual commitment.

Although [\*xol-1\*](#) produces three alternatively spliced transcripts that differ in their 3'ends, these three [\*xol-1\*](#) transcripts are present in both sexes, and only a single transcript mediates all [\*xol-1\*](#) functions in XO animals. Hence, alternative splicing does not play an essential part in the sex-specific control of the X:A target.

## B. X Chromosome Signal Elements

Genetic and molecular results indicate that the X:A signal is polygenic and that a small set of specific X-linked genes communicate X chromosome dose to the primary target, [\*xol-1\*](#) (Fig. 2) ([Akerib and Meyer 1994](#); [Hodgkin et al. 1994](#); [Hodgkin and Albertson 1995](#); M. Nicoll et al., in prep.; I. Carmi et al., unpubl.). Once the gene target of the X:A signal was identified and its roles in sex determination and dosage compensation were appreciated, criteria were established for recognizing the X:A signal genes whose relative dose communicates X chromosome number ([Cline 1988](#)). Increases in the zygotic dose of X:A numerator elements should specifically kill males, whereas decreases should specifically kill females. Changes in the dose of denominator elements should display the opposite sex specificity. These sex-specific lethal dose effects should be suppressed by the appropriate class of mutation in the X:A signal target. For example, increasing the dose of the X:A numerator elements should specifically kill males and be suppressed by hermaphrodite-lethal transgenes that constitutively transcribe [\*xol-1\*](#), whereas decreasing the zygotic dose of these same numerator genes should specifically kill hermaphrodites and be suppressed by male-lethal null alleles of [\*xol-1\*](#).

X-linked genes have been identified in worms that satisfy these and other criteria for X:A numerator elements. Moreover, the ability of mutations in [\*xol-1\*](#) to suppress completely the effects of changes in these X:A signal genes argues that there is only a single signal target. Thus, sex is determined by a polygenic zygotic signal acting on a single switch-gene target. These signal genes interact in a semi-additive fashion, with changes in the dose of any one gene enhancing the effects of similar changes in another and suppressing the effects of the opposite dose change. Synergism is indicated by the fact that simultaneous changes in the dose of two elements have more effect than twice the change in the dose of a single element. This behavior has been exploited in suppression screens for isolating X:A element mutations. Point mutations exist for only two worm numerator genes (see below). Dose effects of chromosome rearrangements have identified at least two other regions that harbor numerator elements ([Akerib and Meyer 1994](#)).

The polygenic nature of the X:A signal delayed the initial discovery of mutations in individual elements. Although duplications and deletions had been obtained that covered most of the worm X chromosome, none caused sex-specific lethality. Some of these duplications and deficiencies were subsequently found to include some X signal elements ([Akerib and Meyer 1994](#); I. Carmi et al., unpubl.). In retrospect, it is clear why there was little indication of specific X:A signal genes. Although these duplications and deficiencies harbored some X signal elements, the X:A ratio was not perturbed sufficiently by the gain or loss of a single copy of these individual elements to cause sex-specific lethality. On the other hand, any X chromosome rearrangement that was sufficiently large to affect the dose of several elements simultaneously and thereby cause sex-specific lethality ([Akerib and Meyer 1994](#); [Hodgkin et al. 1994](#); [Hodgkin and Albertson 1995](#)) would not have been recovered, since most of the schemes used to recover these rearrangements demanded that both XO and XX animals be viable.

With the knowledge that perturbations in the X:A signal could cause sex-specific lethality due to misregulation of specific regulatory genes, it was possible to devise strategies that would allow the recovery of duplications ([Akerib and Meyer 1994](#); [Hodgkin et al. 1994](#); [Hodgkin and Albertson 1995](#)) and deletions ([Akerib and Meyer 1994](#)) regardless of how many numerator elements they might contain. Duplications were recovered in XO animals carrying a mutation in an XX-specific dosage compensation gene (either an *sdc* or a *dpy* gene) that prevented males from activating the XX mode of dosage compensation, whereas deletions were recovered in XX animals carrying a [\*xol-1\*](#) mutation that prevented hermaphrodites from activating the XO mode of dosage compensation. Subsequently, deletions of signal elements were obtained as suppressors of the male-lethal effect of duplications.

Characterization of the rearrangements obtained in this way identified a region near the left end of X that contributes so strongly to the X:A signal that duplications of it cause nearly all males to die from misregulation of

*xol-1* (Akerib and Meyer 1994; Hodgkin et al. 1994). It is the increased dose of three smaller subregions within this duplication that is responsible for male lethality (Akerib and Meyer 1994). Most or all males survive if only one or two of these regions are duplicated. Once it was apparent that only a duplication containing all three subregions would kill nearly all the males, a screen was undertaken to isolate suppressors of the male lethality as a means of identifying point mutations in the numerator elements of this region (Akerib and Meyer 1994). An independent molecular approach had already identified a cosmid in the vicinity of this mutation that causes *sdc*-suppressible male lethality when present in multiple copies in transgenic animals, behavior suggesting that the cosmid harbored a numerator element (Hodgkin et al. 1994). The activity within this cosmid was referred to as *fox-1* (feminizing locus on X), although the gene or genes responsible for the male lethality had not been determined (Hodgkin et al. 1994). When DNA sequence analysis of the new loss-of-function numerator mutations (M. Nicoll et al., in prep.) revealed that they altered an RNA-binding protein encoded by a gene within this cosmid (Hodgkin et al. 1994), the gene identified by these mutations was given the name *fox-1*. XX mutants homozygous for a null allele of *fox-1* appear to be wild-type, indicating that this signal element is relatively weak (M. Nicoll et al., in prep.).

Mutations in a much stronger numerator gene *sex-1* (signal element on X), located in the center of X, were obtained in a genetic screen for mutations that activate an *xol-1::lacZ* transcriptional fusion reporter gene inappropriately in XX animals (J. Kopczynski et al., unpubl.). Not only does the loss of two copies of *sex-1* cause severe phenotypes in XX animals including masculinization and lethality, but the gain of two copies also causes extensive male-specific lethality (I. Carmi et al., unpubl.). Mutations in *xol-1* suppress all the XX-specific phenotypes.

The extent of masculinization and lethality caused by signal elements depends on the particular element or combination of elements whose dose is changed (Fig. 2). This observation provides additional evidence that worm numerator elements are not all equally effective in setting the expression state of their target. Synergism among the elements is shown by the fact that the *trans*-heterozygous combination of a *sex-1* mutation and a deficiency (*yDf20*) that eliminates two other X elements also causes extensive masculinization and lethality of XX animals, yet neither heterozygous mutation by itself has any obvious effect (I. Carmi et al., unpubl.). All XX animals homozygous for both a *sex-1* and a *fox-1* mutation are dead, even though *fox-1* mutations cause no lethality and *sex-1* mutations cause only partial lethality (I. Carmi et al., unpubl.). XX animals heterozygous for a deletion of the three elements included in *yDf17* are masculinized and display a Dpy phenotype indicative of a perturbation of dosage compensation, but their viability is not reduced (Akerib and Meyer 1994). The observation of incomplete masculinization and nonlethal dosage compensation upsets in XX animals with a reduced numerator element dose suggests that *xol-1* is capable of being expressed at intermediate activity states and that quantitative changes in *xol-1* expression are manifested by the intersexuality of XX animals.

The various worm numerator elements vary not just in their strength, but also in the molecular mechanism by which they influence *xol-1*. These differences are revealed by the different effects of signal element changes on the expression of an *xol-1::lacZ* transcriptional reporter transgene. The effects of *sex-1* or the *yDf19* region on *xol-1* are transcriptional, since deletion of these genes dramatically increases expression of this *xol-1* reporter in XX animals, whereas their duplication in XO animals decreases it (M. Nicoll et al., in prep.; I. Carmi et al., unpubl.). In contrast, *fox-1* and the *yDf20* region have no effect on the transcriptional reporter in either sex, indicating that these genes do not control the transcription of *xol-1*, despite robust genetic evidence that these elements are *xol-1* regulators (Akerib and Meyer 1994; M. Nicoll et al., in prep.). For example, elevating the expression of *xol-1* by increasing its copy number suppresses male lethality caused by duplications of these elements. However, multiple copies of transgenic *fox-1* sufficient to kill all XO animals do turn off the activity of a *xol-1::gfp* transgene in XO animals (M. Nicoll et al., in prep.). In this transgene, the sequences encoding the green fluorescence protein were inserted in frame into the coding region of a complete *xol-1* genomic clone. The *xol-1::gfp* fusion protein made from this transgene is active and complements an *xol-1* mutation in XO animals. Thus, *xol-1* is also regulated at a posttranscriptional level by signal elements. Since *fox-1* encodes a putative RNA-binding protein, a posttranscriptional effect of this gene on *xol-1* function would not be unexpected.

*xol-1* appears to be controlled sex-specifically via two different mechanisms, transcriptional and posttranscriptional. Both forms of control serve in the initial assessment of the X:A signal (M. Nicoll et al., in prep.). The primary form of *xol-1* regulation is transcriptional. A hermaphrodite dose of X signal elements represses transcription of *xol-1*. However, it appears that a second mechanism of repression involving an RNA-binding protein can function in hermaphrodites to inactivate *xol-1* activity, by affecting either *xol-1* mRNA stability, processing, transport, or translation. Such a mechanism might be important to fine-tune the level of *xol-1* activity or to compensate for a mistake in interpreting the X:A signal that causes *xol-1* transcripts to be produced inappropriately in XX animals. Thus, the worm appears to use the combination of two mechanisms to achieve the on/off regulation of *xol-1* through a nonlinear response to a small change in X chromosome dose.

What is the "A" part of the X:A signal? To date, no denominator genes have been identified for the worm. On the other hand, many potential candidates among a variety of uncharacterized dominant and recessive autosomal mutations have been isolated either as suppressors of the male lethality of X chromosome duplications or as mutations that elevate *xol-1* expression in XX animals. Although it is convenient to consider denominator elements as functionally analogous to numerator elements, arguments have been presented as to why this may be inappropriate (Cline 1993). Perhaps most important is the fact that changes in denominator element dose are not normally involved in the male/female decision for worms.

## Figures

Figure 2. Sex determination signal and its immediate target.

### Figure 2

Sex determination signal and its immediate target. The target of the primary sex-determining signal is the X-linked, male-specific switch gene *xol-1* that is repressed in response to a female dose of X chromosomes. *xol-1* is controlled by the zygotic dose of the X-linked genes (X:A numerator elements) indicated in the figure. Deficiencies (Df) and duplications (Dp) that perturb the dose of X signal elements are shown above the chromosome. T and P specify whether the regions or genes affect *xol-1* at the transcriptional or the posttranscriptional level. No autosomal genes (X:A denominator genes) have yet been identified. Nongenetical factors such as nuclear volume and total DNA accompany changes in ploidy and may contribute to the denominator.

Generated from local HTML

## Chapter 9. Sex Determination and X Chromosome Dosage Compensation — IV Hermaphrodite-Specific Genes that Coordinately Control Sex Determination and Dosage Compensation

---

The target of the worm X:A signal, [\*xol-1\*](#), coordinately controls sex determination and dosage compensation through its negative regulatory effects on another coordinate control switch gene ([Fig. 3](#)). This gene, [\*sdc-2\*](#), functions exclusively in hermaphrodites and requires the participation of at least two other coordinate control genes, [\*sdc-1\*](#) and [\*sdc-3\*](#), to activate the hermaphrodite mode of sex determination and dosage compensation ([Villeneuve and Meyer 1987](#), 1990b; [Nusbaum and Meyer 1989](#); [DeLong et al. 1993](#)).

The first [\*sdc-2\*](#) mutation was recovered in a screen for X-linked, hermaphrodite-specific lethal mutations, and subsequent alleles were recovered as suppressors of [\*xol-1\*](#) XO-specific lethality ([Nusbaum and Meyer 1989](#)). Although null [\*sdc-2\*](#) alleles have no effect on otherwise wild-type XO worms, in XX animals, they cause complete reversal of sexual fate, similar to mutations in the hermaphrodite sex-determination switch gene [\*tra-1\*](#), and cause extensive (>95%) XX-specific lethality, similar to mutations in the dosage compensation [\*dpy\*](#) genes. Direct measurement of X-linked transcript levels confirmed that [\*sdc-2\*](#) mutations disrupt dosage compensation and cause elevated X-linked transcript levels in XX animals but not in XO animals.

The effects of [\*sdc-2\*](#) mutations on sex determination and dosage compensation are implemented by independent pathways ([Nusbaum and Meyer 1989](#)). This point is illustrated by the fact that masculinization but not lethality is blocked by a mutation in [\*her-1\*](#), a male-specific switch gene that heads the sex determination branch of the regulatory hierarchy. The functioning of [\*sdc-2\*](#) as a negative regulator of [\*her-1\*](#) was shown more directly by the fact that in [\*sdc-2\*](#) XX mutants, [\*her-1\*](#) transcripts are present at the level normal for males but not for hermaphrodites ([Trent et al. 1991](#)). [\*sdc-2\*](#) could not be positioned in the dosage compensation hierarchy by such epistasis analysis since mutations in [\*sdc-2\*](#) and the dosage compensation [\*dpy\*](#) genes have the same effect on dosage compensation. A position for [\*sdc-2\*](#) upstream of the [\*dpy\*](#) genes could be inferred from the fact that [\*sdc-2\*](#) controls both sex determination and dosage compensation, whereas the [\*dpy\*](#) genes have a direct effect only on dosage compensation. Recent molecular experiments (see below) confirm this placement and demonstrate that SDC-2 is sex-specifically localized to the hermaphrodite X chromosomes (D. Lapidus et al., unpubl.) and activates dosage compensation by localizing the dosage compensation DPY proteins to the hermaphrodite X chromosomes ([Chuang et al. 1996](#); [Lieb et al. 1996](#)).

Recent experiments also demonstrate that [\*sdc-2\*](#) is a hermaphrodite switch gene (H. Dawes et al., unpubl.). Antibody staining revealed that SDC-2 is made exclusively in XX animals, confirming that the [\*sdc-2\*](#) gene is regulated by the X:A signal. Moreover, ectopic expression of [\*sdc-2\*](#) transcripts in XO animals causes extensive (~90%) XO-specific lethality that is suppressed by XX-specific dosage compensation mutations. Many rescued XO animals develop as hermaphrodites. These results indicate that the death of XO animals induced by ectopic SDC-2 is a consequence of dosage compensation upsets. From the switch nature of [\*sdc-2\*](#) and its exclusively zygotic expression, it seems likely that [\*sdc-2\*](#) is the target for negative regulation by [\*xol-1\*](#) in males to prevent activation of dosage compensation and hermaphrodite sexual development. In support of this hypothesis, an extrachromosomal array carrying numerous copies of a truncated [\*sdc-2\*](#) gene was found to have no adverse effect on males because it made no functional [\*sdc-2\*](#) gene product, yet it partially suppressed the XX-specific lethality caused by overproduction of [\*xol-1\*](#) transcripts ([Rhind et al. 1995](#)). The truncation left intact the 5' [\*sdc-2\*](#) regulatory region and three fourths of the structural gene; hence, that portion of the [\*sdc-2\*](#) gene may contain the [\*xol-1\*](#) target. SDC-2 is a very large protein (350 kD) with no similarity to sequences in current databases (D. Berlin et al., unpubl.). Although [\*sdc-2\*](#) initiates all aspects of hermaphrodite development, it is not yet known whether it is involved in maintaining that developmental mode.

The first gene to be discovered that demonstrated the link between sex determination and dosage compensation was [\*sdc-1\*](#) ([Villeneuve and Meyer 1987](#), 1990b). It acts at the same place in the hierarchy as [\*sdc-2\*](#), but it is maternally rescueable and its null phenotype is relatively weak: Not all XX animals are masculinized, and

the masculinization itself is incomplete. Moreover, null *sdc-1* alleles cause no significant XX-specific lethality, despite causing overexpression of X-linked genes. Nevertheless, there is synergism between alleles of *sdc-1* and *sdc-2* that demonstrates the importance of their joint participation in development. The combination of a weak *sdc-2* allele that causes little or no lethality by itself and a null *sdc-1* allele that is also nonlethal results in complete XX-specific lethality. Temperature-shift experiments demonstrated that *sdc-1* is required in the first half of embryogenesis for proper sex determination and for establishing the XX mode of dosage compensation. Consistent with a role for *sdc-1* as a negative regulator of *her-1* transcription, the gene encodes a 139-kD protein that contains seven zinc finger motifs of the TFIIIA variety and may therefore be a DNA-binding protein ([Nonet and Meyer 1991](#)).

Another partner for *sdc-2* is *sdc-3*. The intimate relationship between these two genes is dramatically illustrated by the fact that the localization of SDC-2 protein to the hermaphrodite X chromosomes requires *sdc-3* activity (H. Dawes et al., unpubl.), and conversely, localization of SDC-3 to X requires *sdc-2* (T.L. Davis and B.J. Meyer, in prep.). The stability and/or synthesis of SDC-3 is reduced by mutations in *sdc-2*.

Analysis of *sdc-3* was complicated by its unusual genetic properties, which nevertheless ultimately shed considerable light on its function ([DeLong et al. 1993](#)). This gene differs from the other coordinate control genes in that its sex determination and dosage compensation activities are separately mutable, indicating that they function independently. Three different classes of mutant *sdc-3* alleles were identified genetically. One class disrupts sex determination, causing masculinization of XX animals, but has no obvious effect on dosage compensation. The masculinized XX animals have levels of *her-1* transcripts appropriate for XO animals, indicating that *sdc-3*, like the other two *sdc* genes, represses *her-1* in hermaphrodites. A second class disrupts dosage compensation and causes greater than 95% XX-specific lethality but has little or no effect on sex determination. These two classes of mutations complement each other as if they represent two separate genes. However, a third class composed of true null alleles fails to complement alleles in either of the first two classes, indicating that all three classes are defective in the same gene. Ironically, the null phenotype itself is misleading, since it does not reflect the gene's involvement in sex determination: Escapers are not masculinized. Extensive genetic and molecular analyses revealed that the dosage compensation defect of *sdc-3* null alleles suppresses their own sex determination defect as a consequence of a feedback between sex determination and dosage compensation as discussed below.

Molecular analysis of *sdc-3* ([Klein and Meyer 1993](#)) confirmed the genetic conclusions and revealed that the sex determination mutations cluster to a region of the 250-kD SDC-3 protein that has limited homology with the ATP-binding domain of myosin, whereas dosage compensation mutations eliminate a pair of TFIIIA zinc finger motifs at the carboxyl terminus. Null mutations all abort translation of the SDC-3 protein prior to its sex determination and dosage compensation domains. The zinc finger motifs are essential for the localization of SDC-3 to X for dosage compensation (T.L. Davis and B.J. Meyer, in prep.). The mechanism by which SDC-3 represses *her-1* in sex determination is not yet known.

## Figures

Figure 3. Regulatory hierarchy that controls somatic sex determination and differentiation in hermaphrodites and males.

### Figure 3

Regulatory hierarchy that controls somatic sex determination and differentiation in hermaphrodites and males. Genes in the regulatory cascade that are functionally active are boxed and boldfaced. A dark bar indicates a negative regulatory interaction, and a dashed bar indicates the lack of negative regulation because the upstream regulator is inactive. The most likely direct target of *xol-1* is *sdc-2*, which together with *sdc-1* and *sdc-3* controls *her-1* at the level of transcription. The dosage-compensation-specific branch of the hierarchy diverges from the sex determination branch after the *sdc* genes and is not shown. A model of the molecular mechanisms used in the sex determination branch of the pathway is shown above each regulatory cascade.

Generated from local HTML

# **Chapter 9. Sex Determination and X Chromosome Dosage Compensation — V X Chromosome Dosage Compensation**

---

The results of extensive genetic, molecular, and biochemical experiments summarized below indicate that a set of sex-specific vital genes controls dosage compensation and has no direct effect on sex determination. These genes are XX-specific in their function and achieve dosage compensation by reducing hermaphrodite X chromosome gene expression through a direct association with the X chromosomes.

## **A. Genes That Control Somatic Dosage Compensation**

The correlation between sex-specific lethality and upsets in dosage compensation has been well established in *Drosophila melanogaster* ([Cline 1976, 1978](#); [Belote and Lucchesi 1980a,b](#)) and was influential in the interpretation of similar phenotypes in worms several years later. In the first report concluding that worms might dosage-compensate ([Hodgkin 1983](#)), *dpy-26* mutations were shown to cause a maternal-effect, XX-specific lethal phenotype. The gene was named for the fact that rare XX escapers have a distinctive Dumpy phenotype (short and fat). In contrast, *dpy-21* mutations were found to cause a recessive, XX-specific Dpy phenotype without lethality. *dpy-21* mutant hermaphrodites are killed, however, by one extra X, whereas it takes two extra X chromosomes to kill an otherwise wild-type diploid hermaphrodite. The XX-specific phenotypes of *dpy-21* and *dpy-26* mutants are similar to the Dpy and lethal phenotypes of diploid animals with 3X and 4X chromosomes, animals that might be expected to have an excess of X-linked products. It was therefore hypothesized that these mutant phenotypes are due to elevated X chromosome expression and that worms must undergo dosage compensation. Three additional maternal-effect, XX-specific lethals ([Plenefisch et al. 1989](#); [Hsu and Meyer 1994](#)) were subsequently identified in screens for sex-specific lethal mutations and for suppressors of *xol-1* XO-specific lethality: *dpy-27*, *dpy-28*, and *dpy-30*. Mutations in *dpy-27* and *dpy-28* cause a degree of lethality (~95%) similar to that of *dpy-26* mutations, but *dpy-30* mutations cause complete lethality.

The phenomenon of dosage compensation in worms, as well as the involvement of these *dpy* genes in that process, was shown using a phenotypic assay similar to the one that first demonstrated dosage compensation in flies ([Wood et al. 1995](#); [DeLong et al. 1987](#); [Meneely and Wood 1987](#)). By this assay, XX and XO animals exhibit equal expression of X-linked genes, and mutations in *dpy-26*, *dpy-27*, and *dpy-28* elevate this expression in XX animals but not in XO animals. *dpy-21* mutations also elevate X expression in XX animals, but they have a minor effect on X expression in XO animals as well. About the same time, dosage compensation and its perturbation by mutations in *dpy-21*, *dpy-27*, and *dpy-28* were demonstrated at the molecular level through quantitation of X-linked transcript levels ([Meyer and Casson 1986](#)). XX and XO animals have similar levels of X-linked transcripts, and mutations in the *dpy* genes disrupt dosage compensation, causing elevated X chromosome transcript levels in XX animals. Similar genetic and molecular assays subsequently demonstrated that mutations in *dpy-30* specifically elevate X chromosome expression in XX animals ([Hsu and Meyer 1994](#)). Together, these experiments indicate that the *dpy* genes equalize X chromosome gene expression between the sexes, most likely by reducing the levels of transcripts produced by both hermaphrodite X chromosomes.

The lack of interactions between mutant alleles of *dpy-26*, *dpy-27*, and *dpy-28* suggests that these genes act together to control X chromosome expression. However, *dpy-21* again behaves differently: Its mutant alleles alleviate some of the XX-specific lethality caused by the other *dpy* mutations, suggesting that the role of *dpy-21* in dosage compensation is different from that of the other genes.

The function of some dosage compensation *dpy* genes is not limited to dosage compensation. The pleiotropic nature of the mutations indicates that some *dpy* genes are clearly involved in other aspects of development. Mutations in *dpy-26* and *dpy-28* increase meiotic nondisjunction, suggesting a relationship between two very different aspects of chromosome dynamics: chromosome expression and segregation ([Hodgkin 1983](#); [Plenefisch et al. 1989](#)). Mutations in *dpy-30* cause a variety of deleterious effects on the morphology and behavior of even XO animals ([Hsu and Meyer 1994](#)). Perhaps the XX-specific lethal effect of *dpy-30* mutations is so unusually strong because it is a combined result of a standard XX-specific dosage compensation upset and a non-sex-

specific disruption of development that can be tolerated by individuals not also suffering a dosage compensation upset.

Abundant evidence exists for interactions between the dosage compensation and sex determination regulatory pathways. An inappropriate shift of dosage compensation toward the male mode can cause a shift of sexual differentiation toward the hermaphrodite mode. This feedback of dosage compensation onto sex determination appears to arise as an indirect consequence of perturbations in X chromosome expression, rather than as a direct action of *dpy* gene products on genes of the sex determination hierarchy. Perhaps it serves a homeostatic function in the wild-type worm to compensate for chance errors in X:A signal assessment. This feedback is vividly illustrated by *sdc-3* mutations (DeLong et al. 1993). XX worms homozygous for a sex-transforming allele of *sdc-3* develop as males, yet if they are also mutant in any of the dosage compensation *dpy* genes or in the dosage compensation domain of *sdc-3* itself, the surviving animals develop as fertile hermaphrodites. Since the level of *her-1* transcripts is appropriate for the phenotypic sex of the animal in all cases, suppression of *sdc-3* masculinization must occur via the sex determination pathway, by effects either on *her-1* itself or on some gene upstream of it. Other examples of interactions between dosage compensation and sex determination include the fact that mutations in any of the dosage compensation *dpy* genes suppress the masculinization of XX animals caused by *her-1* gain-of-function mutations (Trent et al. 1988; Plenefisch et al. 1989). Moreover, mutations in *dpy-21*, *dpy-27*, or *dpy-28* cause some 2X:3A animals to develop as fertile hermaphrodites instead of males (Hodgkin 1987b; Plenefisch et al. 1989).

## B. A Dosage Compensation Protein Complex

Proteins made by many of the dosage compensation genes associate with the X chromosome in a sex-specific fashion to modulate gene expression. (Fig. 4A,B,C). Molecular analysis of *dpy-27* first provided this insight (Chuang et al. 1994). DPY-27 is localized to both hermaphrodite X chromosomes throughout most of development. Although it is also produced and localized to the nucleus in males, it does not bind to the single male X chromosome. Thus, only the sex that actively implements dosage compensation has its X chromosomes decorated with dosage compensation proteins. The localization of DPY-27 to X at the 30-cell stage reflects the onset of dosage compensation in worms. There is no need for dosage compensation to begin earlier, since the onset of embryonic transcription is between the 8-cell and 16-cell stage (Edgar et al. 1994).

DPY-26 behaves like DPY-27: It is produced in both sexes but localizes to X only in XX animals around the 30-cell stage (Fig. 4A,B) (Lieb et al. 1996). The DPY-26 antibody staining pattern is more complex than the DPY-27 pattern, however, reflecting the role of DPY-26 in other processes. Consistent with the involvement of *dpy-26* in meiosis, DPY-26 protein associates with all meiotic chromosomes in the *germ cells* of both sexes (Fig. 4C–F). DPY-26 also associates with all chromosomes in mitotic *germ cells*. In contrast, DPY-27 is absent from the germ line. In young embryos that have not yet begun dosage compensation, DPY-26 is diffusely distributed throughout interphase nuclei, but unlike DPY-27, it associates with all condensed mitotic chromosomes. A few cell divisions later, it becomes specifically localized to X for the remainder of (somatic) development.

The dosage compensation proteins assemble on X as a complex (Chuang et al. 1996). DPY-27 antibodies immunoprecipitate DPY-26 from partially purified wild-type nuclear extracts but not from *dpy-26*, *dpy-27*, or *dpy-28* mutant extracts. Conversely, DPY-26 antibodies immunoprecipitate DPY-27 from wild-type but not from *dpy-27* mutant nuclear extracts. This complex contains at least two other proteins. On the basis of their size, they cannot be the products of previously cloned dosage compensation genes, but one may be DPY-28 by the following rationale: Both DPY-27 and DPY-26 proteins are undetectable in *dpy-28* mutants, despite the fact that the *dpy-27* and *dpy-26* transcript levels are nearly wild type. This result indicates that *dpy-28* affects either the production or stability of DPY-26 and DPY-27. If DPY-27 and DPY-26 function in a complex with DPY-28, both might become unstable in the absence of their DPY-28 partner. There is precedent for such destabilization in the case of DPY-27 in a *dpy-26* mutant background.

Although *dpy-27* mutations disrupt the stability of DPY-26 and its localization to X, they do not interfere with the role of DPY-26 in meiosis or its association with mitotic chromosomes. In contrast, *dpy-28* mutations do interfere

with the role of DPY-26 in these three processes ([Lieb et al. 1996](#)). The participation of DPY-26 in meiosis, dosage compensation, and perhaps mitosis may therefore be a consequence of its association with different protein partners in each of these different roles.

An important clue as to the mechanism of dosage compensation in worms came from the deduced amino acid sequence of DPY-27. DPY-27 is a member of the SMC (Structural Maintenance of Chromosomes) family of proteins known to be involved in several aspects of chromosome dynamics. Yeast SMC proteins are essential for mitotic chromosome condensation and segregation ([Strunnikov et al. 1993, 1995; Saka et al. 1994](#)). In frogs, they have been shown to participate in the induction and maintenance of chromosome condensation ([Hirano and Mitchison 1994](#)). The similarity of DPY-27 to the SMC proteins, together with its X localization, suggests that DPY-27 may reduce X chromosome transcript levels by inducing partial X chromosome condensation in interphase nuclei. Perhaps worms have adopted an evolutionarily conserved mechanism of chromosome condensation, used previously in mitosis, to achieve dosage compensation.

## C. Sex-specific Assembly of the Dosage Compensation Complex on X

An understanding of how the worm coordinate-control genes regulate dosage compensation came from analyzing the effects of *sdc* and *xol* mutations on the X chromosome localization of DPY-26 and DPY-27 ([Fig. 5](#)). From the genetics, it could be inferred that in XO animals, *xol-1* should prevent both DPY-26 and DPY-27 from localizing to the X chromosome by repressing the XX-specific *sdc* genes that activate the dosage compensation process. As predicted, both DPY-26 and DPY-27 decorate the single X of mutant *xol-1* males, consistent with the wild-type role of this male-specific switch gene to block the hermaphrodite program of dosage compensation ([Chuang et al. 1994; Lieb et al. 1996](#)).

Predictions for the effects of the *sdc* and *dpy* genes were less clear, since it had not been possible previously to order these genes with respect to their functions in dosage compensation. Mutations in *sdc-2*, *sdc-3*, and *dpy-30* cause XX animals to behave like XO males in that they produce DPY-26 and DPY-27 proteins but fail to localize them to X ([Chuang et al. 1996; Lieb et al. 1996](#)). Thus, *sdc-2*, *sdc-3*, and *dpy-30* are essential for the association of the dosage compensation complex with the X chromosome. Because the SDC-2 and SDC-3 proteins are themselves localized to X, they most likely regulate dosage compensation gene function by recruiting the DPY proteins to the X chromosome (T. Davis et al., in prep.). Consistent with this view, ectopic expression of *sdc-2* in XO animals is sufficient to assemble the dosage compensation complex on the single male X chromosome (H. Dawes et al., unpubl.). In contrast, DPY-30 has an indirect role in X localization. The novel, 123-amino-acid DPY-30 protein is diffusely distributed throughout the nuclei of both sexes, and its staining pattern is not affected by any dosage compensation mutations ([Hsu et al. 1995](#)). Hence, DPY-30 is not part of the dosage compensation complex. DPY-30 influences dosage compensation through its effects on *sdc-3*, since SDC-3 protein does not accumulate in the absence of DPY-30 (T.L. Davis et al., in prep.). Null alleles of *dpy-30* and *sdc-3* cause a similar cryptic sex determination defect, confirming the regulatory relationship between these two genes ([Hsu and Meyer 1994](#)). Thus, some dosage compensation genes act as regulators of others and do not participate in the dosage compensation process through an association with the X chromosome.

In contrast to mutations in *sdc-2*, *sdc-3*, and *dpy-30*, mutations in *sdc-1* and *dpy-21* have no effect on the DPY-26 and DPY-27 staining pattern ([Chuang et al. 1996; Lieb et al. 1996](#)). These two genes must affect some aspect of the dosage compensation process other than localizing or stabilizing DPY-26 and DPY-27.

All evidence supports the view that the dosage compensation *dpy* genes and the *sdc* genes work together in all aspects of dosage compensation and that males inactivate that process rather than activate a male-specific expression system. First, all dosage compensation genes with XX-specific lethal phenotypes are involved in the sex-specific assembly of the same large dosage compensation complex on the hermaphrodite X chromosomes. Second, a male will die if it inappropriately assembles that dosage compensation complex on its X. Such inappropriate assembly will occur if a male lacks *xol-1* or if he inappropriately expresses *sdc-2*, but in either case, the lethality can be suppressed by loss-of-function alleles of any *sdc* or *dpy* gene, indicating that this set of genes regulates and implements a single dosage compensation process. Such suppression could not occur if any

significant part of the male lethality were due to the failure to activate a male-specific X chromosome expression system, rather than the failure to inactivate the XX-specific dosage compensation system.

Figure 5 presents a model for the sex-specific assembly of the dosage compensation complex in worms based on all information currently available. In hermaphrodites, the XX-specific *sdc-2* switch gene is active and produces SDC-2 protein in the presence of the maternally supplied SDC-3 and DPY-30 proteins. Around the 30-cell stage of embryogenesis, SDC-2, in collaboration with SDC-3, localizes to the X chromosomes and recruits a protein complex consisting of at least DPY-26, DPY-27, and possibly DPY-28. These dosage compensation proteins then alter the structure of interphase X chromosomes and thereby cause a reduction in X-linked transcript levels. In males, the XO-specific *xol-1* switch gene is active and represses the *sdc-2* gene, thus preventing the recruitment of a dosage compensation protein complex to X.

## D. Dosage Compensation and the Germ Line

Mutations in worm dosage compensation genes can affect the fertility of XO animals in non-wild-type situations, suggesting effects on germ-line growth. For example, *her-1* and *tra-2* (eg) XO hermaphrodites make many more progeny if they are also mutant for a *dpy-26* mutation (Hodgkin 1983; Kuwabara 1996). However, it is not known whether it is *dpy* gene expression in the *germ cells* themselves that is relevant or even whether elevated X chromosome expression is involved. The fact that *dpy-27* has a similar effect on *her-1* XO hermaphrodites argues against this effect being related to germ-line dosage compensation, since DPY-27 appears to be absent from proliferating *germ cells* and therefore is unlikely to participate in germ-line dosage compensation. If the germ line is dosage-compensated, the genes *mes-2*, *mes-3*, *mes-4*, and *mes-6* (maternal-effect sterile) (Capowski et al. 1991) are potential candidates for this role, since mutations in them cause germ-cell-specific death that is greater for XX than XO cells (Paulsen et al. 1995; C. Garvin and S. Strome, pers. comm.).

## Figures

Figure 4. Localization of dosage compensation proteins.

### Figure 4

Localization of dosage compensation proteins. (A) Image of a wild-type XX embryo (>200-cell stage) that was triply stained with anti-DPY-27 antibody (red), anti-DPY-26 antibody (green), and the DNA-intercalating molecule diamidophenylindole (DAPI) (blue). In this merged image, DPY-26 and DPY-27 are colocalized to the X chromosomes of XX animals that have activated the dosage compensation process. (B) Enlargement of the boxed nucleus in A. In this optical section, both X chromosomes are distinctly visible, and the coincident positions of DPY-26 and DPY-27 on the X chromosomes are apparent. Embryos were analyzed through wide-field fluorescence microscopy followed by the use of deconvolution software. (C) DPY-26 is present in the germ line and is associated with meiotic chromosomes. Confocal image of the posterior half of a young wild-type XX adult worm stained with PI (red) and DPY-26 antibodies (green) to create the merged image. The left half of the image shows the gonad. DPY-26 colocalizes with all meiotic chromosomes in the germ cell nuclei (yellow arrow) but is localized only to the X chromosomes in *somatic cells* (white arrows). Confocal images of germ cell nuclei in pachytene stained with DPY-26 antibodies (D; green) and PI (E; red). The merged image in F shows that DPY-26 colocalizes with all meiotic chromosomes. Unlike DPY-26, DPY-27 is not present in the germ line. (Photos in this figure were provided by Jason Lieb.)

Figure 5. Model for the sex-specific assembly of an X chromosome dosage compensation complex.

### Figure 5

Model for the sex-specific assembly of an X chromosome dosage compensation complex. In males, *xol-1* inactivates *sdc-2*, thereby preventing a dosage compensation complex from assembling on X. In hermaphrodites, *sdc-2* is active and together with *dpy-30* activates *sdc-3*. Both the SDC-2 and SDC-3 proteins

localize to X and assemble a DPY protein complex that reduces expression of both hermaphrodite X chromosomes.

Generated from local HTML

# Chapter 9. Sex Determination and X Chromosome Dosage Compensation — VI Somatic Sex Determination

---

## A. A Regulatory Cascade of Sex Determination Genes

All aspects of sexual differentiation in worms are controlled by a complex regulatory cascade that includes several switch genes (see Fig. 3) (for review, see [Hodgkin 1988; Villeneuve and Meyer 1990a](#)). This cascade determines the functional state of *tra-1*, the terminal switch gene that imposes the hermaphrodite-specific pattern of differentiation. This cascade uses diverse forms of gene regulation. The terminal switch gene (*tra-1*) encodes a transcription factor that is sex-specific in its action, at least in the soma (Zarkower and [Hodgkin 1992](#)). A factor adding complexity to the worm cascade may be the involvement of its genes in germ-line as well as somatic sex determination, plus the complication that hermaphrodites are programmed to make both sperm and oocytes (see [Schedl](#), this volume).

Null mutations in the first three sex determination genes identified transform XX animals into males ([Hodgkin and Brenner 1977](#)). The most severe null phenotype of these transformer genes (*tra*) is that of *tra-1*: XX *tra-1* worms are transformed into fertile phenotypic males. Mutations in *tra-2* and *tra-3* cause incomplete transformation toward the male fate. Four additional genes were discovered subsequently: *her-1* ([hermaphroditization](#)) ([Hodgkin 1980](#)) and three *fem* ([feminization](#)) genes ([Doniach and Hodgkin 1984; Kimble et al. 1984; Hodgkin 1986](#)). All four are required for male development, and the *fem* genes are also required for spermatogenesis in hermaphrodites. Null *her-1* XO worms are fertile hermaphrodites, whereas null *fem-1*, *fem-2*, and *fem-3* XX and XO animals are fertile, spermless hermaphrodites that function as females.

*her-1*, *tra-1*, and *tra-2* all serve as switch genes, with constitutive activity of their products being sufficient to set sexual fate regardless of the X:A signal. For all three genes, dominant alleles exist that have phenotypic effects opposite to those of null alleles. Dominant *tra-1* mutations transform XO animals into either hermaphrodites or females ([Hodgkin 1980, 1987a](#)); dominant *tra-2* (eg) mutations transform XO animals into hermaphrodites ([Hodgkin and Albertson 1995](#)); and dominant *her-1* mutations partially masculinize XX animals ([Trent et al. 1988](#)).

A negative regulatory cascade was deduced from analysis of the epistatic interactions among these dominant and recessive mutations (see Fig. 3) ([Hodgkin 1980, 1986](#)). *tra-1* was identified as the terminal regulator because its activity is sufficient to trigger hermaphrodite development, whereas loss of its activity specifies male development, regardless of the activities of other genes in the pathway. Genetic analysis further indicated that *tra-1* activity is set in the following way: In XO animals, *her-1*, the first gene in the pathway, negatively regulates *tra-2* and thereby activates the *fem* genes. The *fem* genes inactivate *tra-1* to elicit male development. *her-1* must remain active throughout male development to prevent yolk production ([Schedin et al. 1994](#)). In XX animals, *her-1* is repressed and *tra-2* negatively regulates the *fem* genes and thereby activates *tra-1* to elicit hermaphrodite development. The proposed role of *tra-3* in the pathway is to potentiate *tra-2* activity. Recent experiments have identified mutations in the gene *laf-1* (lethal and feminized) that act as dominant suppressors of the masculinization caused by *tra-3* mutations but not by *tra-2* mutations (B. Goodwin and J. Kimble, pers. comm.). These results suggest that *tra-3* stimulates *tra-2* activity by repressing *laf-1*. Homozygous *laf-1* mutations cause embryonic lethality in both sexes, suggesting that it has multiple roles in development (B. Goodwin and J. Kimble, pers. comm.).

## B. Molecular Mechanisms

Molecular analysis confirmed this view of the regulatory cascade and revealed the great diversity of molecular mechanisms that operate in it (see Fig. 3). Transcriptional control is central for the first and last steps of the pathway, but cell-cell signaling and signal transduction are central for the middle steps to coordinate the sexual fates of the sexually dimorphic cells. *her-1* is regulated at the level of transcription by the *sdc* genes, which function as *her-1* repressors in XX animals ([Trent et al. 1991; DeLong et al. 1993](#)). This negative regulation can be overcome by mutations in any of the *sdc* genes ([Trent et al. 1991; DeLong et al. 1993](#)) or by dominant mutations

in the *her-1* promoter region (Trent et al. 1991; Perry et al. 1994). The functional *tra-1* gene product is a protein with five tandem zinc fingers resembling those in two human oncogenes associated with glioblastoma tumors, *GLI* and *GLI3*, and those in the *Drosophila cubitus interruptus* protein (Ci) required for the patterning of embryonic segments and imaginal discs (Zarkower and Hodgkin 1992). TRA-1 binds DNA and most likely acts as a transcription factor to control downstream sex differentiation genes (Zarkower and Hodgkin 1993). In support of this view, the Ci protein of *Drosophila* has been shown to function as a transcriptional activator (Alexandre et al. 1996).

No direct TRA-1 targets have yet been found. However, in response to *tra-1* action, genes required for male-specific development such as those involved in forming the complex tail structures or in mating behavior (Emmons and Sternberg, this volume) must be repressed, and genes required for hermaphrodite-specific development such as those essential for vulval development (Greenwald, this volume) and yolk production (Kimble and Sharrock 1983; Blumenthal et al. 1984) must be activated. Perhaps the best candidate for a TRA-1 target is *mab-3*, a gene required to prevent yolk protein production in males and to activate a male-specific cell lineage (Shen and Hodgkin 1988). In contrast, the yolk protein genes themselves are not likely to be the direct targets of TRA-1, since the critical promoter region required for sex-specific regulation of the yolk protein genes does not contain the TRA-1 recognition sequence (Spieth et al. 1985b; MacMorris et al. 1992; M. MacMorris and T. Blumenthal, pers. comm.).

The *tra-1* gene itself can be rendered insensitive to negative regulation by the sex determination pathway through dominant *tra-1* mutations that cluster to a small region at the amino terminus of the protein. These mutations suggest that the sex-specific regulation of *tra-1* is achieved posttranslationally via inhibitory protein-protein interactions, presumably with one or more of the FEM proteins (de Bono et al. 1995).

*her-1* participates in signal transduction (Hunter and Wood 1992; Perry et al. 1993). It encodes a small novel protein with a predicted signal sequence. Ectopic *her-1* expression directed by a promoter specific to the myosin body wall muscles is sufficient to masculinize the soma and germ line of XX animals, suggesting that HER-1 protein functions as a secreted signaling molecule. The masculinization requires the putative signal sequence. Crucial evidence for a signal transduction cascade is the cell-nonautonomous behavior of *her-1* described below (Hunter and Wood 1992).

The likely receptor of the putative HER-1 ligand is TRA-2A protein, which is present in both sexes. It has nine potential membrane-spanning domains and a putative signal sequence, and it has similarity to the *Drosophila patched* gene, a segment polarity gene in *Drosophila* involved in signal transduction (Okkema and Kimble 1991; Kuwabara et al. 1992). Overexpression of TRA-2A from a transgene driven by a heat shock promoter transforms XO animals into fertile hermaphrodites, indicating that TRA-2A is normally inactivated in males and that this negative regulation can be overridden by overexpression (Kuwabara and Kimble 1995). If HER-1 ligand inactivates the putative TRA-2A receptor protein by binding to its extracellular domain, one might expect to find *tra-2* mutations that interfere with the HER-1 binding but not with the TRA-2A feminizing activity. Such dominant *tra-2* mutations have been identified, and they have the properties expected for constitutively active TRA-2A. The mutations alter a predicted extracellular domain of TRA-2A and transform XO animals into hermaphrodites (Hodgkin and Albertson 1995; Kuwabara 1996).

It has been proposed that TRA-2A inactivates one or all of the intracellular FEM proteins in XX animals through a physical association with its carboxy-terminal cytoplasmic domain, thereby preventing TRA-1 inactivation (Kuwabara et al. 1992). By this model, HER-1 binding to TRA-2A releases the FEM proteins from TRA-2A, allowing them to inactivate TRA-1. Support of this proposal is of two types: First, expression of the TRA-2A carboxy-terminal cytoplasmic domain from a heat shock promoter feminizes phenotypic males, implying that extra copies of this domain titrate a male-specific protein (Kuwabara and Kimble 1995). Second, FEM-3, a novel protein (Ahringer et al. 1992), physically associates with the TRA-2A carboxy-terminal cytoplasmic domain, as assayed by the yeast two-hybrid system and by coimmunoprecipitation of the two proteins synthesized in vitro (A. Mehra et al., pers. comm.). Whether this physical association is sufficient to inactivate FEM-3 is not yet known.

How the FEM proteins inactivate TRA-1 has not been established, although all three FEM proteins are clearly required. For example, do the FEM proteins interact to form a regulatory complex, do they act sequentially to produce one inhibitory activity, or do they function independently? FEM-1 contains six copies of an ankyrin motif, which in other proteins mediates specific protein-protein interaction ([Spence et al. 1990](#)). FEM-2 interacts directly with FEM-3, as demonstrated by the yeast two-hybrid system and by coimmunoprecipitation ([Chin-Sang and Spence 1996](#)). Finally, FEM-2 is related to type-2C protein serine/threonine phosphatases, and FEM-2 possesses protein phosphatase activity in vitro ([Pilgrim et al. 1995; Chin-Sang and Spence 1996](#)). Mutational analysis showed that this activity is necessary for FEM-2 to promote male development in vivo ([Chin-Sang and Spence 1996](#)). Thus, protein phosphorylation appears to be involved in the signal transduction steps that coordinate worm sexual fate.

Although *tra-3* potentiates *tra-2*, it does not have a direct role in the signal transduction aspect of the function of TRA-2A. TRA-3 is a member of the calpain regulatory protease family ([Barnes and Hodgkin 1996](#)). Recent experiments indicate that TRA-3 may affect TRA-2A by inactivating a translational repressor of *tra-2*; this repressor may be the product of *laf-1* (B. Goodwin and J. Kimble, pers. comm.).

## C. Nonautonomy of Sex Determination

Cell-cell signaling is an important feature in somatic sex determination. Analysis of both *sdc-1* genetic mosaics ([Villeneuve and Meyer 1990b](#)) and triploid intersexes ([Schedin et al. 1991](#)) showed that worm cells do not choose their sexual fates independently. Since *tra-1* behaves in a strictly autonomous manner, only genes upstream of it can be responsible for this nonautonomy ([Hunter and Wood 1990](#)). *her-1* is one of the culprits. Its nonautonomous behavior in mosaic studies is striking ([Hunter and Wood 1992](#)). Not only can *her-1*(-) cells express a wild-type fate if surrounded by *her-1*(+) cells, the converse is also true: *her-1*(-) cells can force their *her-1*(+) neighbors to express a mutant fate! Not all *her-1*(-) cells are equivalent in their effects on *her-1*(+) cells. Generally, it is *her-1*(-) cells derived from the posterior blastomere ( $P_1$ ) of the two-celled embryo that influence *her-1*(+) cells derived from the anterior blastomere (**AB**). The converse is rarely, if ever, true. However, *her-1*(-) cells can affect *her-1*(+) cells even within the [AB lineage](#). These results indicate that *her-1* activity in sexually dimorphic cells is neither necessary nor sufficient for their male development. The cell-cell communication indicated by these results can be accounted for by the model in which HER-1 acts as a secreted ligand to inactivate the TRA-2A receptor ([Kuwabara et al. 1992](#)). The difference in potency of *her-1*(-) cells in affecting *her-1*(+) cells could be explained if the concentration of TRA-2A receptors differs from cell to cell.

It has been suggested that the nonautonomy in nematode sex determination serves as an error correction mechanism for an organism that does not have the luxury of a regulatory strategy of development ([Hodgkin 1992; Hunter and Wood 1992](#)). However, it is not obvious how practical such a mechanism would be if mistakes made by a minority of specific cells (derived from  $P_1$ ) prevent the majority of cells from making the correct choice. Moreover, if the original mistake were caused by misreading the X:A signal, a mechanism for correcting errors in sexual fate would only be useful if it were accompanied by an equivalent mechanism for correcting upsets in dosage compensation. In this connection, it is not yet known whether the regulation of dosage compensation, or indeed the assessment of the X:A signal, is cell-autonomous.

## D. Pathway Complexities

Current molecular models lend an appealing clarity to the regulatory complexities of worm sex determination. Nevertheless, several branches and feedback mechanisms exist throughout the pathway that can have profound effects on sexual phenotype but have no molecular explanation. One such subtlety is revealed by the fact that a null mutation in the terminal hermaphrodite switch gene *tra-1* has a greater masculinizing effect on XX animals than a null mutation in the upstream hermaphrodite switch gene, *tra-2*: Null *tra-1* XX animals are fertile males, whereas null *tra-2* XX animals are nonmating, incomplete males ([Hodgkin 1980](#)). Thus, control of *tra-1* by the X:A signal cannot all be exerted through *tra-2*. There must be an additional feminizing activity in hermaphrodites that contributes to *tra-1* activation. Ironically, this minor feminizing activity in XX animals is mediated by *xol-1*,

the coordinate-control switch gene that sets the male state in XO animals ([Miller et al. 1988](#)). The wild-type appearance of XX *xol-1* mutant animals gives no hint of such a role, but it is revealed in XX animals that have been incompletely masculinized by mutations in other genes such as *tra-2*. The *tra-2; xol-1* XX double mutants are fertile males. Similarly, *xol-1* mutations enhance partially masculinizing mutant alleles of *sdc-1*, *sdc-3*, and *tra-3*. This masculinizing effect of *xol-1* mutations is independent of the masculinizing switch gene *her-1*, which lies between *xol-1* and *tra-1* in the hierarchy. Thus, this feminizing effect of wild-type *xol-1* most likely occurs via a parallel pathway that intersects the main pathway between *tra-2* and *tra-1*. The feminizing activity of *xol-1* (+) in XX animals is separately mutable from the masculinizing activity in XO animals, and the two activities function at different times in development ([Rhind et al. 1995](#)). Hence, these two *xol-1* functions act independently and are likely to be mechanistically distinct.

Evidence also exists for positive feedback in the sex determination pathway. This idea derives from the fact that, unexpectedly, *tra-2* RNA is found at a “male” level in *tra-1* XX males ([Okkema and Kimble 1991](#)). If the sex-specific level of *tra-2* RNA were set by genes acting upstream, then the activity state of *tra-1* should be irrelevant. The opposite was found: The level of *tra-2* mRNA correlates with the sexual phenotype rather than the X:A signal. Although it is not yet known whether *tra-1* itself feeds back onto *tra-2*, the idea of regulation via positive feedback seems very likely to explain these results. The similarities between *tra-2* and *patched* as well as those between *tra-1* and *Ci* suggest the highly speculative possibility that TRA-1 may activate *tra-2* transcription in hermaphrodites just as *Ci* activates *patched* transcription in the embryo and imaginal discs of *Drosophila* ([Alexandre et al. 1996](#)).

Generated from local HTML

# **Chapter 9. Sex Determination and X Chromosome Dosage**

## **Compensation — VII Sex Determination in The Germ Line Versus the Soma**

---

The gene hierarchy that controls sex determination in the soma also controls sex determination in the germ line. In the germ line of males, the hierarchy directs spermatogenesis (see [Schedl; L'Hernault](#); both this volume), whereas in the germ line of hermaphrodites, the hierarchy must first specify spermatogenesis and then switch to oogenesis (see [Schedl; Anderson and Kimble](#); both this volume). Although there are major similarities between sex determination in the soma and in the germ line, these two processes differ in fundamental ways to allow each sex to specify the appropriate germ cell fate at the appropriate time: (1) The *her*, *tra*, and *fem* genes are essential for germ-line sex determination, but some of these genes (*tra-2* and *fem-3*) exhibit germ-line-specific regulation that differs in mechanism from their soma-specific regulation ([Schedl; Anderson and Kimble](#); both this volume). (2) Germ-line sex determination requires genes not needed for somatic sex determination, the *fog* genes (feminization of the germ line) for spermatogenesis ([Schedl and Kimble 1988; Barton and Kimble 1990; Ellis and Kimble 1995; Schedl](#), this volume) and the *mog* genes (masculinization of the germ line) for oogenesis ([Graham and Kimble 1993; Graham et al. 1993; Schedl](#), this volume). (3) In the soma, *tra-1* is a terminal switch gene whose product imposes the hermaphrodite pathway of differentiation, whereas in the germ line, this gene is not a switch gene ([Hodgkin 1987a; Schedl et al. 1989](#)). It participates in both female and male aspects of germ-line development. (4) The *fem* genes act at the terminal position in the gene hierarchy controlling germ-line sex determination (along with *tra-1*, *fog-1*, and *fog-3*). *fem-3* acts as a germ-line switch gene: Active *fem-3* triggers spermatogenesis and inactive *fem-3* triggers oogenesis ([Barton et al. 1987](#)). The details of germ-line sex determination in males and hermaphrodites are reviewed by [Schedl](#) (this volume). The analysis presented below simply compares the roles of *tra-1* and the *fem* genes in the soma versus the germ line.

In the soma, *tra-1* is an XX-specific terminal switch gene that promotes hermaphrodite development. Male development ensues in XO animals because *tra-1* is turned off by the *fem* genes and that is the only known role of the *fem* genes in the male soma. In the germ line, however, *tra-1* functions in males to promote abundant spermatogenesis and block oogenesis; in its absence, small amounts of both sperm and oocytes are produced ([Hodgkin 1987a; Schedl et al. 1989](#)). Moreover, rather than simply acting to turn off *tra-1*, the *fem* genes participate with *tra-1* in promoting male development in the germ line. In so doing, the *fem* genes occupy a terminal position in the regulatory hierarchy. In the absence of FEM proteins, males produce only oocytes and do so even in the absence of *tra-1* ([Doniach and Hodgkin 1984; Hodgkin 1986](#)). Hence, the block to oogenesis in wild-type males requires both the *fem* genes and *tra-1*. Recall that in the soma, feminization by the loss of the *fem* genes is blocked by loss of *tra-1*, one piece of evidence placing *tra-1* downstream from the *fem* genes in that tissue type.

*tra-1* also functions in the hermaphrodite germ line, but in the opposite capacity: to block spermatogenesis and promote abundant oogenesis, a role more in keeping with its somatic functions ([Hodgkin 1987a; Schedl et al. 1989](#)). Hence, with regard to its role in the germ line, it is more appropriate to think of *tra-1* as playing an active but different part in XX and XO animals, rather than being functionally "on" in XX and "off" in XO animals, as it is in the soma. The following model for *tra-1* germ-line functioning is consistent with known genetic and molecular data for this gene, but it departs from the conventional presentation of linear pathways and unifunctional elements. The basic idea is that in the germ line, *tra-1* has opposite effects on *germ cells* that depend on its interactions with the *fem* genes. *tra-1* promotes abundant spermatogenesis and blocks oogenesis when it interacts with (or is modified by) one or more of the *fem* genes, but in the absence of these interactions, it promotes abundant oogenesis and blocks spermatogenesis. *tra-1* gain-of-function mutants rarely make sperm regardless of the activity state of the *fem* genes. This result can be rationalized by the view that the TRA-1 protein is refractory to interactions with the *fem* genes and hence constitutively functions in its female mode, only promoting oogenesis. A parallel situation may exist for *fem-3* gain-of-function mutations. These alleles can fully masculinize the germ lines of either XX or XO animals independent of *tra-1*. In the course of eliminating the

normal controls on this gene, these dominant mutations appear to eliminate the need for the participation of *tra-1* in the masculinizing activities of this gene.

Generated from local HTML

## Chapter 9. Sex Determination and X Chromosome Dosage Compensation — VIII Concluding Remarks

---

Advances in elucidating the genetic and molecular control of *C. elegans* sex determination and X chromosome dosage compensation made during the last decade provide the means to address broader issues in the next decade. These include how sexual behavior is programmed, how sexual morphology arises, how molecular assessment of the X:A signal occurs, how individual elements of the polygenic X:A signal are recruited and eliminated, how changes in chromosome structure affect chromosome-wide regulation of gene expression, how a dosage compensation mechanism copes with rapid changes in sex chromosomes, and how quickly changes arise between the germ line and the soma.

These advances also make possible comparisons between sex determination and dosage compensation mechanisms in *C. elegans* and those in other organisms such as *Drosophila*, for which comparable information is available. Such a comparison reveals that the fly and the worm use strikingly similar genetic strategies to differentiate their sexes; nevertheless, there is a remarkable lack of overlap between the molecules and mechanisms used to achieve sexual differentiation and proper X chromosome expression (for review, see [Cline and Meyer 1996](#)). Moreover, virtually no genetic or molecular overlap has been found in the sex determination and dosage compensation strategies used by worms and mammals. These profound differences contrast strongly with the similarities in the genetic and molecular programming for the basic body plan. The suggestion that sex determination strategies evolve far more rapidly than those that govern the body plan is strengthened by the remarkable differences in how a house fly and a fruit fly specify sexual fate ([Dübendorfer et al. 1992](#)). The worm is no exception. Comparison of [tra-1](#) ([deBono and Hodgkin 1996](#)) and [tra-2](#) ([Kuwabara 1996](#)) between *C. elegans* and *C. briggsae*, species that diverged 20–50 Myr ago, revealed a far greater divergence between the two species' sex determination genes than between their cell death, vulval, or locomotion genes. Because the sex determination genes diverge so rapidly, analysis of how the *C. elegans* sex determination hierarchy has changed among more closely related species should provide unique insight into the molecular mechanics of evolution and elucidate such issues as the origins of hermaphroditism. One need not look far to determine how hermaphroditism arises, only to the genetic and molecular differences between sex determination in *C. elegans* and a relative, *C. remaneae*, which reproduces as a male/ female strain instead of a male/hermaphrodite strain.

Generated from local HTML

## **Chapter 9. Sex Determination and X Chromosome Dosage Compensation — Acknowledgments**

---

I gratefully acknowledge T. Blumenthal, T. Cline, and J. Kimble for comments on the manuscript, T. Schedl for many helpful conversations, and J. Lieb for the images in Figure 4. I also thank the *C. elegans* sex determination community for providing information and manuscripts prior to publication. Funding to B.J.M. is provided by grants from the National Institutes of Health and the American Cancer Society.

Generated from local HTML

# **Chapter 10. Developmental Genetics of the Germ Line**

---

## **Contents**

- [I Introduction](#)
- [II Summary of Anatomy and Development of the Germ Line](#)
- [III Genetic Analysis of Germ-Line Development](#)
- [IV Somatic Gonad](#)
- [V Germ-Line Specification and Survival](#)
- [VI Germ-Line Sex Determination](#)
- [VII Control of Proliferation and Entry into the Meiotic Pathway](#)
- [VIII Meiotic Prophase Progression and Gametogenesis](#)
- [IX Oocyte Development, Maturation, and Ovulation](#)
- [X Future Prospects](#)
- [Acknowledgments](#)

Generated from local HTML

# **Chapter 10. Developmental Genetics of the Germ Line — I**

## **Introduction**

---

The function of the germ line is to produce specialized cells, sperm, and oocytes, whose union results in the production of a new individual. Germ cells differ fundamentally from [somatic cells](#): They undergo a specialized cell cycle, meiosis, in which haploid gametes are formed following genetic recombination and chromosome reassortment; they are totipotent, as their descendants will form every tissue in the individual; and they are immortal in that they will give rise to progeny with a new germ line, thus ensuring continued propagation of genetic information.

The study of germ-line development addresses a number of issues, some of which are specific to [germ cells](#), whereas others relate to general aspects of biology. How is the germ-line lineage specified as distinct from somatic lineages? How is sexual identity determined? How is proliferation controlled? How is the decision to exit the mitotic cycle and enter the meiotic pathway made? What activities control the transitions between different stages of meiotic prophase? How are the specialized gametes formed? How are meiotic prophase progression and gametogenesis coordinated? How are the development and function of the germ line and [somatic gonad](#) coordinated?

Research by the *Caenorhabditis elegans* community addressing these questions is reviewed here. Additional features of germ-line development are described in other chapters in this volume: recombination and meiotic divisions (Albertson et al.), programmed cell death (Hengartner), spermatogenesis (L'Hernault), and fertilization (Kemphues and Strome).

Generated from local HTML

## Chapter 10. Developmental Genetics of the Germ Line — II

### Summary of Anatomy and Development of the Germ Line

The development of the reproductive systems in the hermaphrodite and male is diagrammed in Figure 1, and the anatomy of the adult germ line is shown in Figure 2 (cellular morphology) and Figure 3 (nuclear morphology). For detailed descriptions, consult original papers by Hirsh et al. (1976), Klass et al. (1976), Kimble and Hirsh (1979), Kimble and White (1981), Strome (1986b), and Crittenden et al. (1994).

The adult [hermaphrodite gonad](#) consists of two U-shaped tubular arms, each terminating proximally at a spermatheca. The two [spermathecae](#) join the centrally located [uterus](#). The adult [male gonad](#) consists of a single U-shaped tubular [testis](#) that terminates proximally at the [seminal vesicle](#) and [vas deferens](#). (The distal-proximal axis is relative to the proximal opening of the gonad to the exterior: the [vulva](#) in the hermaphrodite and the [cloaca](#) in the male.) A basement membrane completely encloses the gonad of both sexes. At the distal end of the gonad arms are the somatic [distal tip cells](#) (DTC, one per hermaphrodite arm and two in the [testis](#)). In the hermaphrodite, ten epithelial sheath cells are in direct contact with a large part of the germ line. In the male, [seminal vesicle](#) cells contact only the most proximal part of the germ line. Much of the germ line is syncytial, with each nucleus partially enclosed by plasma membrane. For simplicity, the term germ cell is used to describe a nucleus, its cytoplasm, and surrounding membranes.

The germ line displays distal-to-proximal polarity in its pattern of proliferation, meiotic prophase progression, and gametogenesis. The distal-most [germ cells](#) (from 1 to ~20 cell diameters from the tip) are proliferative and serve as a stem-cell population. Moving proximally, [germ cells](#) exit the mitotic cycle to enter and progress through stages of meiotic prophase. Spermatogenesis in the male and the hermaphrodite normally occurs only in the proximal gonad. Oogenesis occurs in the loop region and the proximal gonad. An anucleate cytoplasmic core (or rachis) is prominent in the pachytene region of the [hermaphrodite gonad](#) during oogenesis; a core is present, but less prominent, in the [testis](#). The core appears to supply cytoplasmic constituents to the proximal developing gametes (Gibert et al. 1984). Although the germ line is syncytial, the activities and/or distribution of molecules must be spatially controlled to achieve the observed distal-proximal polarity of development.

At hatching, the L1 larva of both sexes contains a gonad primordium of four cells: two [somatic gonad](#) precursors, [Z1](#) and [Z4](#), and two germ line precursors, [Z2](#) and [Z3](#). The [somatic gonad](#) precursors divide by an essentially invariant pattern during larval development to produce 143 cells in the hermaphrodite and 56 cells in the male. In hermaphrodites (late L2), ten [somatic gonad](#) blast cells (not including the DTCs) reorganize to form a centrally located [somatic gonad](#) primordium that separates the [germ cells](#) into anterior and posterior populations. The blast cells of the [somatic gonad](#) primordium divide during L3 and L4 to produce the sheath, spermatheca, and [uterus](#). Led by the DTC, each gonad arm grows and elongates/migrates to form a U shape. In males, the asymmetric structure is generated (in L1/L2) by a reorganization that places both DTCs at the future distal end and eight somatic blast cells at the future proximal end of the gonad. The proximal [somatic cells](#) (in L3 and L4) migrate/reflex to form the U-shaped [testis](#) and divide to produce the [seminal vesicle](#) and [vas deferens](#).

Germ cells divide in a variable pattern throughout the larval stages and the adult, generating about 1000 cells per gonad arm in the hermaphrodite and more than 1000 cells in the male. Distal-proximal germ-line polarity is first evident in the L3 stage when the most proximal [germ cells](#) enter meiotic prophase. Proximally located [germ cells](#) continue to enter meiosis so that, as development continues, a successively greater proportion of the germ line is in meiotic prophase. By adulthood, proliferation is limited to the distal mitotic stem-cell population. In hermaphrodites, the first approximately 40 [germ cells](#) that enter meiotic prophase in each gonad arm develop as male, producing about 160 sperm. Thereafter, a switch in sexual fate occurs so that all additional [germ cells](#) differentiate as oocytes. In males, [germ cells](#) differentiate continuously as sperm.

### Figures

Figure 1. Gonadogenesis in the hermaphrodite and male.

## Figure 1

Gonadogenesis in the hermaphrodite and male. (A) Newly hatched first-stage larva of both sexes with a mid-ventrally located gonad primordium. Shown are diagrams of the adult hermaphrodite (B) and male (C) gonad and selected stages of larval development. Somatic gonad cells are shaded, with the myoepithelial sheath cells (*stipples*) only shown in the adult. (DTC) Distal tip cell; (AC) anchor cell. Germ line: (*closed circles*) mitotic nuclei; (*open circles*) meiotic prophase nuclei; (*closed triangles*) primary spermatocytes; (*open triangles*) sperm. Anterior is left. (Adapted from Hirsh et al. 1976; Kimble and Hirsh 1979).

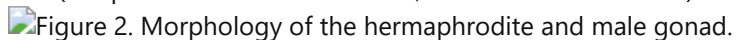


## Figure 2

Morphology of the hermaphrodite and male gonad. Nomarski photomicrographs of the anterior gonad arm of a young adult hermaphrodite (*top*) and a male testis (*bottom*). Internal view shows the anuclear core in the distal arm of the hermaphrodite. (*Open triangle*) Distal tip of the gonad; (*arrowhead*) primary spermatocyte. Anterior is left. Bar, 10 µm. (From R. Francis and T. Schedl, unpubl.)

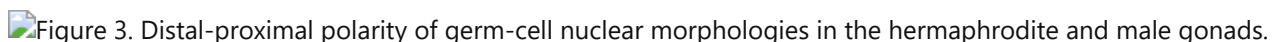


## Figure 3

Distal-proximal polarity of germ-cell nuclear morphologies in the hermaphrodite and male gonads. Fluorescence photomicrograph of a single young adult hermaphrodite gonad arm (*A*) or male gonad (*B*), released by microdissection and stained with DAPI (surface view). Somatic gonad nuclei are not indicated. The transition (Trans) zone is where nuclei undergo the transition from the mitotic cell cycle through early stages of meiotic prophase. Arrows indicate nuclei in mitotic telophase. Bar, 10 µm. (From R. Francis and T. Schedl, unpubl.)

Generated from local HTML

# Chapter 10. Developmental Genetics of the Germ Line — III Genetic Analysis of Germ-Line Development

---

Genes that participate in germ-line development can be genetically identified by isolating mutations with sterile phenotypes. Genetic and developmental studies can reveal the wild-type gene function, the point at which the mutation disrupts a morphological progression of germ-line developmental events, and the position of the gene in genetic regulatory pathways. Molecular analysis can provide information about biochemical processes underlying the regulatory pathways and morphological events.

## A. Identification of Genes That Function in Germ-line

Many of the well-characterized genes that function in germ-line development were identified in screens for recessive, loss-of-function (lf) mutations. Following ethylmethanesulfonate (EMS) mutagenesis, the progeny of individual F<sub>1</sub> hermaphrodites were screened for approximately 1/4 of animals displaying a sterile phenotype (see, e.g., Austin and Kimble 1987). Sterility is defined as the failure of XX animals to produce embryos. This narrow definition excludes maternal-effect embryonic lethal mutations (see [Kemphues and Stone; Preiss and Schnabel](#), both this volume) that, in many cases, display no obvious defect in germ-line development. Recessive sterile mutations were recovered at very high frequency, about  $1 \times 10^{-1}$  per haploid genome (J. McCarter et al., unpubl.; E. Lambie, pers. comm.) under standard mutagenesis conditions (Brenner 1974). Since the frequency for isolation of loss-of-function mutations in typical genes is  $1 \times 10^{-3}$  to  $1 \times 10^{-4}$  per mutagenized haploid genome (Brenner 1974; Greenwald and Horvitz 1980), the number of genes that can mutate to a sterile phenotype is large (>500). For some of the identified genes, null alleles have a sterile phenotype (a null sterile gene such as [glp-1](#) [Austin and Kimble 1987]), but for others, non-null alleles have a sterile phenotype and null mutations are embryonic or larval lethal (an essential gene like [lag-1](#) [Lambie and Kimble 1991]). Thus, an accurate estimate of the number of genes required for germ-line development and function is not possible because of the difficulty in determining the frequency at which non-null sterile alleles of essential genes can be recovered.

Because of both the large number of recessive sterile mutations obtained and the wide variety of phenotypes observed, only mutants with a select set of phenotypes have been studied in detail to date. One of the major sterile phenotypes chosen for further study was alteration in germ-line sexual fate: feminization of the germ line (e.g., [fog-2](#), [Schedl and Kimble 1988](#)) or masculinization of the germ line (e.g., [mog-1](#), Graham and Kimble 1993), where [germ cells](#) that would normally develop as one sex instead develop as the other sex. Other sterile phenotypes examined include germ-line proliferation-defective (e.g., [glp-1](#), Austin and Kimble 1987), germ-line tumorigenesis (e.g., [gld-1](#), Francis et al. 1995b), ectopic or proximal germ-line proliferation (e.g., [lin-12](#), Seydoux et al. 1990), failure to exit pachytene (e.g., [mek-2](#), [Church et al. 1995](#)), endomitotic oocytes (e.g. [emo-1](#), K. Iwasaki et al., unpubl.), and defective [somatic gonad](#) lineages. Additional sterile phenotypes that were frequently observed but have not been extensively studied include vacuolated germ lines; small germ lines consisting of undifferentiated cells (often with abnormal nuclear morphologies); small germ lines that produce sperm, then undifferentiated cells, and/or defective oocytes; uncoordinated animals with [somatic gonad](#)/vulval abnormalities and small germ lines with variable defects. The last group of sterile phenotypes may result from cell cycle defects analogous to those seen in [lin-5](#) and [lin-6](#) (Albertson et al. 1978; Sulston and Horvitz 1981; see [Albertson et al.](#), this volume) where postembryonic cell cycles variably fail, but embryonic cell cycles are unaffected, presumably because of maternal rescue. Screens for XO male sterile phenotypes have not been conducted, although mutants defective in spermatogenesis and fertilization have been readily isolated as hermaphrodites that are self-sterile but cross-fertile (see [L'Hernault](#), this volume).

Genes that can mutate to produce a sterile phenotype have also been identified in screens for recessive lethal/sterile mutations that were sought in selected regions of the genome (see, e.g., [Howell et al. 1987; Johnsen and Baillie 1991; Johnsen and Baillie](#), this volume). The phenotypes of most of these sterile mutations are uncharacterized, with the exception of those mapping to the [dpy-5 - unc-13](#) region (J. McDowell and A. Rose, pers. comm.).

Searches for maternal-effect sterile and for dominant sterile mutants have also been conducted. [Capowski et al. \(1991\)](#) identified five loci that frequently mutate to maternal-effect sterility (Mes) in screens of the F<sub>3</sub> generation following mutagenesis. Doniach (1986) identified gain-of-function (gf) alleles of *tra-2* in screens for dominant feminizing mutations. Dominant mutations in genes that control germ-line sex determination have also been isolated in selections for extragenic suppressor mutations that restore either self-fertility (see, e.g., [Barton et al. 1987](#)) or cross-fertility ([Hodgkin 1986](#)) to otherwise sterile strains.

Although non-null alleles of essential genes can be recovered in screens for sterile mutations, many essential genes that have critical roles in germ-line development may go undetected because non-null alleles affecting only fertility may be rare or nonexistent. Two strategies can be used to screen lethal mutations for sterile phenotypes. First, temperature-sensitive lethal mutations can be examined for sterile phenotypes by allowing mutant animals to develop at the permissive temperature through the lethal period and then shifting them to the restrictive temperature during later development. Large collections of temperature-sensitive embryonic lethal mutations exist (for review, see [Kemphues 1988](#)) and are currently being examined, with the promising result that some mutants (e.g., [zyg-13](#)) display intriguing temperature-sensitive zygotic sterile phenotypes (J. Hubbard and I. Greenwald, pers. comm.). Second, a genetic mosaic screen analogous to that described by Bucher and Greenwald (1991) can generate sterile animals that lack gene activity in the germ-line and/or somatic gonad lineages but are alive because wild-type gene activity is supplied to lineages that are necessary for viability. Currently, the genetic mosaic method is impractical for large-scale screening because of the low frequency of mosaic animals.

In summary, genetic methods have identified a number of genes that have important functions in development of the germ line, many of which are discussed below. These screens are likely to be far from saturation, particularly for the essential genes.

## B. Phenotypic Characterization

Sterile mutants are usually selected for further study on the basis of examination of adult gonad morphology by Nomarski microscopy and nuclear morphology by DAPI staining. The terminal adult phenotype, however, may provide misleading information about the cellular basis of the mutant phenotype. An early primary defect can lead to an array of secondary defects that are a combination of (1) dependent events that fail to be executed and (2) independent processes that proceed normally. Furthermore, a gene may function at more than one time or place in germline development, with the terminal phenotype representing the sum of the defects. To examine the different aspects of the phenotype (e.g., where and when do mitotic cycling, meiotic prophase progression, and gametogenesis occur), a time course analysis should be performed. In situ staining methods can be used to ask when, where, or if molecular markers for particular aspects of germ-line and somatic gonad development appear. Genetic mosaic analysis (see, e.g., Austin and Kimble 1987) can be used to determine if gene function is required in the germ line or soma. For mutants that affect the somatic gonad, the cell lineage (Kimble and Hirsh 1979) can be examined to determine if there are alterations in cell fate, cell position, or differentiation. For dynamic processes (e.g., ovulation), time-lapse video microscopy can provide information not readily available from static observations. Germ-line development is sensitive to environmental conditions (temperature, starvation, passage through the dauer stage) and genetic background (morphological and behavioral markers, etc.), which must be controlled to ensure accurate assessment of the mutant phenotype.

Genetic epistasis experiments can provide information on dependency relationships for some mutant phenotypes as well as place certain genes within known regulatory hierarchies. Analysis of XO male phenotypes for hermaphrodite sterile mutations can provide information about sex specificity. If the phenotype is hermaphrodite-specific, examination of double mutants with the sex determination genes can distinguish whether the phenotype is dependent on germ-line sex, somatic sex, or X/A ratio.

For sterile alleles of essential genes, it can be difficult to distinguish whether a gene has a specific or nonspecific function in germ-line development. As much of the metabolic activity of the late larva and adult worm is devoted to germ-line development, partial loss-of-function mutations in genes involved in metabolism and the

RNA/protein synthetic process are likely to affect the germ line more severely than other tissues. One such gene is [\*ama-1\*](#), which encodes an RNA polymerase II subunit ([Rogalski et al. 1988](#)). Because the sterile phenotypes of certain non-null [\*ama-1\*](#) mutations are likely to result from global defects in gene expression, its nonspecific nature is not particularly illuminating to our understanding of germ-line development. As more genes involved in germ-line development are characterized, the ability to distinguish between specific and nonspecific defects should improve.

Generated from local HTML

## Chapter 10. Developmental Genetics of the Germ Line — IV Somatic Gonad

---

Ablation of [somatic gonad](#) cells with a laser microbeam has been used to investigate the role of these cells in germ-line development. Ablation of the DTC(s) at any time during larval development and in the adult results in all [germ cells](#) entering the meiotic pathway ([Kimble and White 1981](#)). By ablating certain [somatic gonad](#) cells, the DTC can be mispositioned. When this occurs, [germ cells](#) adjacent to the DTC proliferate, whereas those at a distance enter meiosis. These experiments demonstrate that the DTC promotes proliferation (or inhibits entry into the meiotic pathway) locally, and its position at the end of the gonad arm helps to establish the distal-proximal germ-line polarity.

Ablation of the DTC (hermaphrodite) or the linker cell (male) indicates that these cells control the reflexed shape of the gonad arms ([Kimble and White 1981](#)). The U-shaped gonad is not crucial for normal germ-line development: Mutations that alter the migratory behavior of the DTC or linker cell, and thus change the shape of the gonad arm (Hedgecock et al. 1987; see [Antebi et al.](#), this volume), display essentially normal germ-line development.

Sterile mutations in a number of genes seem to affect primarily the [somatic gonad](#). These include [gon-2](#), where [Z1](#) and [Z4](#) fail to divide (E. Lambie, pers. comm.); [gon-4](#), which displays early lineage defects, and [gon-1](#), which displays later lineage defects (S. Santa Anna-Arriola et al., pers. comm.); [mig-5](#) (C. Guo and E. Hedgecock, pers. comm.); and [gon\(q7\)](#) (J. Bork and J. Kimble, pers. comm.), which may be defective in specification of the DTC fate; and [shv](#) mutants, where abnormal lineages give rise to ectopic DTCs (and gonad arms) (R. Francis et al., unpubl.). Genetic and molecular characterizations of these and other genes affecting the [somatic gonad](#) are in their early stages.

Generated from local HTML

## Chapter 10. Developmental Genetics of the Germ Line — V Germ-Line Specification and Survival

---

Germ-line granules, which have been observed in both invertebrates and vertebrates ([Eddy 1975](#)), have properties consistent with cytoplasmic determinants that function in specification of the germ-line fate (Illumsee and Mahowald 1974). Studies with *Drosophila* provide strong support for the hypothesis that germ (polar) granules are essential for the formation of [germ cells](#) in the embryo (for review, see Lehmann and Ephrussi 1994).

Germ-line granules have been detected in *C. elegans* by antibody staining ([Strome Wood 1982, 1983; Yamaguchi et al. 1983](#)) and electron microscopy (Wolf et al. 1983). During early embryogenesis, the granules are asymmetrically segregated in the P-cell lineage to the germ-line founder cell P<sub>4</sub> (thus termed P granules) and are present in all progeny [germ cells](#) except mature sperm. Consistent with the idea that P granules have a role in determination of the germ line is the grandchildless phenotype (absence of [Z2](#) and [Z3](#)) of certain alleles of each of the *par* genes and all [mes-1](#) alleles, where P granules of normal morphology are mispartitioned in the early embryo ([Kemphues 1988; Capowski et al. 1991; Kemphues and Stone, this volume](#)). However, P granules are not sufficient to specify the germ-cell fate. In [mes-1](#) mutants, P granules are found in both P<sub>4</sub> and D about 75% of the time, with the progeny of P<sub>4</sub> and D differentiating as muscle cells, rather than [germ cells](#) (Strome et al. 1995).

Two strategies are currently being used to identify P-granule components. First, an RNA helicase gene ([glh-1](#)) with significant sequence similarity to the *Drosophila* polar granule constituent *vasa* was identified by degenerate polymerase chain reaction (PCR) (Roussell and Bennett 1993). Immunohistochemical staining indicates that GLH-1 is a P-granule component (M. Gruidl and K. Bennett, pers. comm.), suggesting that some P/polar-granule components may be evolutionarily conserved. Second, [pgl-1](#) was identified in a screen for recessive mutants that fail to stain with a subset of anti-P-granule monoclonal antibodies (I. Kawasaki and S. Strome, pers. comm.). [pgl-1](#) encodes a novel protein with a putative RNA-binding motif and mutants display a maternal-effect temperature-sensitive sterile phenotype. The existing [pgl-1](#) mutants indicate that P-granule components are important for fertility but have not yet addressed whether they are important for germ-cell determination.

The genes [mes-2](#), [mes-3](#), [mes-4](#), and [mes-6](#) are necessary for germ-cell survival ([Capowski et al. 1991; Strome et al. 1994](#)). The maternal-effect sterile phenotype of [mes-3](#) mutations, which has been investigated in the most detail, results from germ-cell degeneration (distinct from programmed cell death; [Hengartner, this volume](#)), decreased proliferation, and a failure to differentiate even under conditions that would normally promote entry into meiotic prophase (Paulsen et al. 1995). The maternal-effect sterile phenotype displayed by the four *mes* genes is more severe in XX than XO animals, independent of somatic sexual phenotype (C. Garvin and S. Strome, pers. comm.). Possibly, the *mes* genes control X chromosome dosage compensation in the germ line, although it is not yet known whether the germ line even undergoes dosage compensation. The [mes-2](#) gene shows striking sequence similarity to the *Drosophila* *Enhancer of zeste* gene, especially in a putative chromatin-binding domain (R. Holdeman and S. Strome, pers. comm.). Molecular analysis of [mes-3](#) and [mes-6](#) has not thus far provided biochemical clues about their function in germ-cell viability as the gene sequences are novel (Paulsen et al. 1995; I. Korf and S. Strome, pers. comm.).

# Chapter 10. Developmental Genetics of the Germ Line — VI Germ-Line Sex Determination

---

The primary signal for sexual identity in *C. elegans* is the ratio of X chromosomes to autosomes (see [Meyer](#), this volume). XO animals develop as males and XX animals develop as hermaphrodites (somatic females whose [germ cells](#) adopt either sexual identity). Genetic methods have identified two types of genes downstream from the primary signal that controls germ-line sexual fate ([Table 1](#)): genes that function in both germ-line and somatic sex determination ([her-1](#), the [fem](#) genes, and the [tra](#) genes), and genes that function only in germ-line sex determination (e.g., [fog](#) and [mog](#) genes). Genetic epistasis experiments indicate that these genes are part of a negative regulatory pathway controlling germ-line sex determination ([Fig. 4](#)) (for discussion of somatic sex determination and dosage compensation, see [Meyer](#), this volume).

## A. The XO Male Germ Line

Genetic experiments argue that [her-1](#) promotes male development indirectly, by negatively regulating [tra-2](#) and [tra-3](#), genes that promote female development ([Hodgkin and Brenner 1977](#); [Hodgkin 1980](#)). [tra-2](#) and [tra-3](#), in turn, negatively regulate the [fem](#) genes ([fem-1](#), [fem-2](#), and [fem-3](#)) and [fog-1](#) and [fog-3](#), loci which direct spermatogenesis and/or inhibit oogenesis ([Doniach and Hodgkin 1984](#); [Hodgkin 1986](#); [Barton and Kimble 1990](#); [Ellis and Kimble 1995](#)).

Molecular analysis is beginning to provide a biochemical framework for the pathway. The [her-1](#) gene appears to encode a masculinizing hormone that is expressed specifically in the XO animal. Genetic mosaic analysis demonstrates that [her-1](#) behaves cell-nonautonomously ([Hunter and Wood 1992](#)). [her-1](#) encodes a novel 175-amino-acid product with a potential signal sequence ([Perry et al. 1993](#)). The signal sequence is necessary for ectopically expressed HER-1, driven by the body-wall myosin promoter, to masculinize XX germ-line and somatic tissues ([Perry et al. 1993](#)).

TRA-2A, a protein with a predicted signal sequence and nine potential membrane-spanning domains ([Kuwabara et al. 1992](#)), is the likely receptor for the HER-1 ligand. Kuwabara et al. (1992) proposed that in the absence of ligand, the predicted carboxy-terminal cytoplasmic domain of TRA-2A physically interacts with and negatively regulates one or more of the [fem](#) gene products. Binding of HER-1 to the extracellular domain of TRA-2A would lead to receptor inactivation, relieving negative regulation of the [fem](#) genes, [fog-1](#) and [fog-3](#), allowing male development to occur. Recent results are consistent with this model. Missense gain-of-function mutations in a predicted extracellular domain of TRA-2A produce a constitutively active receptor, possibly because the receptor does not bind or respond to binding of HER-1 ([Hodgkin and Albertson 1995](#); P. Kuwabara, pers. comm.). Ectopic expression of the TRA-2A intracellular carboxyl terminus alone can direct female development ([Kuwabara and Kimble 1995](#)). Physical association of FEM-3, a novel protein ([Ahringer et al. 1992](#)), with part of the TRA-2A carboxyl terminus has been demonstrated using the yeast two-hybrid system and coimmunoprecipitation of products synthesized in a reticulocyte lysate (A. Mehra et al., pers. comm.). FEM-3 may be activated or released from a complex with the cytoplasmic domain of TRA-2A following HER-1 binding. FEM-2, a protein with sequence similarity to serine/threonine phosphatases of the PP2C family ([Pilgrim et al. 1995](#)), physically associates with FEM-3 as assayed by the two-hybrid system and coimmunoprecipitation (I. Chin Sang and A. Spence, pers. comm.). FEM-3 may control the activity, specificity, or localization of FEM-2.

The [tra-3](#) gene encodes a protein related to the protease calpain, but with a divergent carboxyl terminus that lacks the calcium-binding motif (T. Barnes and J. Hodgkin, pers. comm.). Putative [tra-3](#) null alleles are temperature sensitive and suppressed by certain gain-of-function alleles of [tra-2](#) ([Hodgkin 1986](#)), suggesting that [tra-3](#) might be a cofactor for [tra-2](#). Alternatively, genes that are partially redundant with [tra-3](#) may exist.

The [fem-1](#) gene product contains six copies of the ankyrin motif ([Spence et al. 1990](#)) which is thought to mediate protein-protein interaction. Currently, neither the intracellular location nor the proteins with which FEM-1

associates are known. Sequence information is not known for *fog-1* or *fog-3*, either of which might act as a transcriptional regulator.

The similarity of FEM-2 to serine/threonine phosphatases and the similarity of TRA-3 to calpain indicate that protein phosphorylation-dephosphorylation and proteolytic cleavage are used as control mechanisms in the sex determination process. Once these biochemical activities are demonstrated, identification of their respective substrates (and for FEM-2, the requisite kinase) will be crucial for understanding the pathway.

In males, the sex determination pathway must be maintained in the male mode for spermatogenesis to occur throughout adulthood. Loss of *her-1* (Schedin et al. 1994), *fem-1* or *fem-2* (Kimble et al. 1984), or *fog-1* (Barton and Kimble 1990) activity in the adult (following a shift of temperature-sensitive mutants to the restrictive temperature) can result in the initiation of oogenesis in males. *tra-1* null mutant XO males (and XX males, see Meyer, this volume) produce first sperm and then oocytes, indicating that *tra-1* (+) is necessary for maintenance of spermatogenesis in the male (Hodgkin 1987a; Schedl et al. 1989). Additionally, the null phenotype suggests that although *tra-1* activity promotes maintenance of spermatogenesis, it is not essential for either spermatogenesis or oogenesis, at least in animals with a male soma. The *tra-1* gene encodes two products with zinc finger motifs (Zarkower and Hodgkin 1992), one of which binds DNA in vitro (Zarkower and Hodgkin 1993).

## B. The XX Hermaphrodite Germ Line

### 1. Spermatogenesis

In the hermaphrodite, activities of the sex determination genes are modulated: The *fem* genes, *fog-1*, and *fog-3*, must be active early to allow a brief period of spermatogenesis in the L4, but then must be inactive later to allow continuous oogenesis in the adult (Fig. 4). This regulation is independent of HER-1, as *her-1* null mutants do not affect hermaphrodite spermatogenesis, and the relevant mRNA is not expressed in XX animals (Trent et al. 1991).

Negative regulation of *tra-2* and *tra-3* is important to permit hermaphrodite spermatogenesis. Two classes of dominant gain-of-function mutations in *tra-2* exist that appear to be defective in down-regulation (Doniach 1986; Schedl and Kimble 1988). The first class, *tra-2(gf)*, displays strong feminization of the germ line in XX animals and weak feminization in XO animals. The *tra-2(gf)* mutations contain lesions in the 3'-untranslated region (3'UTR) and appear to disrupt translational repression (Okkema and Kimble 1991; Goodwin et al. 1993; Anderson and Kimble, this volume). Whether translational control is an important part of the normal mechanism for permitting hermaphrodite spermatogenesis awaits studies of TRA-2 levels. The second class, *tra-2(mx)*, displays dominant feminization of the germ line, as well as recessive partial masculinization of the soma in XX animals (*mx* is for mixed character, gain-of-function germ-line feminization and loss-of-function somatic masculinization). The *tra-2(mx)* mutations are missense lesions in a 22-amino-acid stretch (MX region) of the predicted cytoplasmic domain (P. Kuwabara et al., pers. comm.). The MX region is adjacent to, but separable from, the FEM-3-binding site (P. Kuwabara, pers. comm.). Thus, it is possible that a germ-line-negative regulator of TRA-2A might bind the MX region, precluding FEM-3 binding and thereby freeing FEM-3/FEM-2 to promote spermatogenesis.

Ectopic expression of HER-1 can, under certain conditions, result in a fully masculinized germ line within a somatically female XX animal (Perry et al. 1993; M. Perry, pers. comm.). The extracellular domain of TRA-2A is thus capable of influencing sex determination in the hermaphrodite germ line. The XX *somatic gonad* may normally promote male sex determination in the hermaphrodite germ line. Laser ablation of certain *somatic gonad* cells (sheath/spermathecal or dorsal *uterine* precursor cells) and the *shv-1(gf)* mutation that alters *somatic gonad* lineages all result in feminization of the germ line (J. McCarter et al., unpubl.). These data lead to the speculative hypothesis that the XX *somatic gonad* may produce a ligand that negatively regulates TRA-2A to allow hermaphrodite spermatogenesis. Down-regulation of the TRA-2A receptor to permit hermaphrodite spermatogenesis may thus occur at three levels: binding of an as yet hypothetical ligand produced by the *somatic gonad*, binding of a negative regulator to the MX region of the cytoplasmic domain, and translational repression.

A number of genes that specifically promote male germ-line sex determination in the hermaphrodite have been identified, but their modes of action are uncertain. In *fog-2* null mutants, all *germ cells* in animals with a female soma develop as oocytes, whereas male germ-line development is unaffected in animals with a male soma (Schedl and Kimble 1988). *fog-2* may promote hermaphrodite spermatogenesis by negatively regulating *tra-2*, *tra-3*, and the *mog* genes (Fig. 4). Alternatively, *fog-2* might positively regulate the *fem* genes and *fog-1* and *fog-3*. *laf-1* is an essential gene (mutations display recessive lethal and dominant hermaphrodite feminization phenotypes) that appears to have a role in promoting spermatogenesis (B. Goodwin and J. Kimble, pers. comm.). The *gld-1* gene has a nonessential function to promote hermaphrodite spermatogenesis and appears to act downstream from *tra-2* and *tra-3* (Francis et al. 1995a, 1995b).

## 2. Oogenesis

The switch to oogenesis requires negative regulation of the *fem* gene products, which are known to be present in the female germ line based on maternal-effect mutant phenotypes (see, e.g., Hodgkin 1986). Down-regulation of *fem-3* is crucial, as gain-of-function mutations exist that have a Mog phenotype and thus fail to switch to oogenesis (Barton et al. 1987). The *fem-3*(*gf*) mutations are in the 3'UTR and appear to disrupt translational negative regulation (Ahringer and Kimble 1991; see Anderson and Kimble, this volume). The *mog* genes (*mog-1* through *mog-6*) are candidate loci for negative regulators of the *fem* gene products, possibly as translational regulators of *fem-3* (Graham and Kimble 1993; Graham et al. 1993).

The *tra-1* and *tra-2* gene products may assist the switch to oogenesis. Constitutively active *tra-1*(*gf*) mutations exist that feminize the hermaphrodite germ line (Hodgkin 1987a; Schedl et al. 1989; de Bono et al. 1995), possibly by causing a premature switch to oogenesis. The *tra-2* locus expresses a female germ-line-specific messenger RNA that can encode TRA-2B, the carboxy-terminal cytoplasmic domain of TRA-2A (P. Kuwabara and J. Kimble, pers. comm.). TRA-2B may assist the switch by sequestering the negative regulatory factor that binds to the MX region and/or FEM-3 or the RNA may titrate negative regulatory factors that bind the 3'UTR.

Genes that specify the oocyte fate, analogous to the *fem* genes and *fog-1* and *fog-3* that specify the sperm fate, have not yet been identified. Such genes may be essential, with pleiotropic mutant phenotypes.

Comparison of the germ-line and somatic sex determination pathways reveals four major differences: (1) The germ-line pathway employs genes not found in the somatic pathway (e.g., *fog* and *mog*); (2) genes common to both sex determination pathways can display germ-line-specific regulation (e.g., TRA-2, as indicated by the MX region); (3) the *tra-1* gene performs regulatory functions that assist germ-line sex determination, but it has a more direct role in specifying the female fate in the somatic pathway; and (4) the *fem* genes have a direct role in specification of the male germ-line fate but only an indirect role in specification of the male somatic fate.

Much remains to be learned about germ-line sex determination. In addition to molecular characterization of previously defined genes, mutations in a number of new genes exist that have yet to be characterized.

Temperature-shift studies with conditional mutants indicate that sexual fate is not irreversibly determined in the male and hermaphrodite germ lines (Barton et al. 1987; Barton and Kimble 1990; Schedin et al. 1994), suggesting that a population of sexually uncommitted *germ cells* may exist in the adult. When and where germ-line sexual commitment and sex-specific gene expression occur remains to be determined. Most nematodes, including close relatives of *C. elegans* such as *Caenorhabditis remanei* (Baird et al. 1994), are female/male species. Comparative studies of sex determination gene homologs from *C. remanei* may provide molecular details of how germ-line sex determination has evolved.

## Figures

Figure 4. Genetic pathway for germ-line sex determination in the XO male and the XX hermaphrodite.

### Figure 4

Genetic pathway for germ-line sex determination in the XO male and the XX hermaphrodite. Arrow indicates positive regulation, and barred line indicates negative regulation. Genes involved in transducing the X/A ratio to

the diagrammed pathway are discussed in [Meyer](#) (this volume).

## Tables

**Table 1** Genes regulating germ-line sex determination in *C. elegans*

Gene	Loss-of-function germ-line phenotype	Proposed germ-line function	Predicted product
<b>(A) Genes that regulate germ-line and somatic sex determination</b>			
Wild type	XX: sperm, then oocytes	–	–
	XO: sperm only		
<i>her-1</i>	XX: wild type	initiates and maintains male fate in XO	novel secreted protein
	XO: sperm, then oocytes		
<i>fem-1</i> <sup>a</sup>	XX: oocytes only	specifies male fate	protein with six ankyrin motifs
	XO: oocytes only		
<i>fem-2</i> <sup>a</sup>	XX: oocytes only	specifies male fate	Ser/Thr phosphatase
	XO: oocytes only		
<i>fem-3</i> <sup>a</sup>	XX: oocytes only	specifies male fate	novel protein
	XO: oocytes only		
<i>tra-1</i>	XX: sperm and some oocytes	inhibits male fate in XX	two isoforms of a zinc finger
	XO: sperm and some oocytes	maintains male fate in XO	DNA-binding protein
<i>tra-2</i>	XX: sperm only	promotes female fate	integral membrane protein
	XO: wild type		
<i>tra-3</i> <sup>a</sup>	XX: sperm and some oocytes	promotes female fate	calpain-related protease
	XO: wild type		
<i>laf-1</i> <sup>b</sup>	XX: oocytes only	promotes male fate in hermaphrodites	unknown
	XO: wild type		
<b>(B) Genes that regulate germ-line, but not somatic, sex determination</b>			
<i>fog-1</i>	XX: oocytes only	specifies male fate	unknown
	XO: oocytes only		
<i>fog-2</i>	XX: oocytes only	promotes male germ-cell fate in somatically	unknown
	XO: wild type	female animals	
<i>fog-3</i>	XX: oocytes only	specifies male fate	unknown
	XO: oocytes only		
<i>mog-1</i> <sup>to</sup>	XX: sperm only	promotes switch from male to female fate	unknown

<b>Gene</b>	<b>Loss-of-function germ-line phenotype</b>	<b>Proposed germ-line function</b>	<b>Predicted product</b>
<i>moq-6<sup>c</sup></i>	XO: wild type	in hermaphrodites	
<i>gld-1</i>	XX: oocytes only	essential for oocyte differentiation	putative cytoplasmic RNA-
	XO: wild type	promotes male germ-cell fate in somatically	binding protein
		female animals	

For references, see text, and for somatic functions of *her-1* and the *fem* and *tra* genes, see [Meyer](#) (this volume).

a

The gene product is maternally provided; the phenotypes indicated are for mutant animals derived from homozygous mothers.

b

Phenotype of *laf-1* /+ heterozygotes; homozygotes are lethal.

c

*mog-2* to *mog-6* mutations are recessive and thus probably loss-of-function.

Generated from local HTML

# Chapter 10. Developmental Genetics of the Germ Line — VII

## Control of Proliferation and Entry into the Meiotic Pathway

---

### A. The *glp-1* Signaling Pathway

In both the hermaphrodite and male, a signal from the somatic DTC promotes germ-line proliferation and/or inhibits germ-cell entry into meiotic prophase (also see Section IV, Somatic Gonad). Three genes that directly mediate DTC signaling are *glp-1*, *lag-1*, and *lag-2*. Genetic and molecular characterization of these genes indicates that the *glp-1* signaling pathway is homologous to the *Notch* signaling pathway, which functions in cell fate specification in *Drosophila* (Artavanis-Tsakonas et al. 1995; for the related *lin-12* signaling pathway, see [Greenwald](#), this volume; for the role of *glp-1* in embryogenesis, see [Priess and Schnabel](#), this volume). Partial loss-of-function mutations in *lag-1* and *lag-2* and null mutations in *glp-1* have essentially the same phenotype as that resulting from DTC ablation: entry of all [germ cells](#) into the meiotic pathway. The *glp-1* gene, the function of which is required continuously in the germ line (Austin and Kimble 1987), encodes a transmembrane protein related to the receptors Notch and LIN-12 (Austin and Kimble 1989; Yochem and Greenwald 1989). The *lag-2* gene encodes a transmembrane protein homologous to *Drosophila Delta*, the ligand for *Notch*, and is expressed in the DTC but not the germ line ([Henderson et al. 1994](#); Tax et al. 1994). The *lag-1* gene encodes an intracellular protein homologous to *Drosophila suppressor of hairless* (Su[H]) and the CBF1 (also known as RBPJ $\kappa$ ) family of mammalian DNA-binding proteins (Christensen et al. 1996).

The GLP-1/Notch family receptors possess cytoplasmic ankyrin repeats that are critical for signaling. Mutations in the ankyrin repeats of GLP-1 disrupt receptor activity ([Kodoyianni et al. 1992](#); [Lissemore et al. 1993](#)).

Overexpression of the cycloplasmic domain, including the ankyrin repeats, from GLP-1, LIN-12, and Notch leads to constitutive signaling (for review, see [Greenwald 1994](#)). In *Drosophila* tissue culture cells, when Notch binds ligand, Su(H) is displaced from the ankyrin repeats and translocates to the nucleus (Fortini and Artavanis-Tsakonas 1994). *glp-1* signaling may be mechanistically similar in that LAG-1 binds to a portion of cytoplasmic domain that includes the ankyrin repeats of GLP-1 (M. Bosenberg and J. Kimble, pers. comm.). It is important to note that the GLP-1 cytoplasmic domain does not simply function to regulate LAG-1 negatively as *glp-1* and *lag-1* have the same germ-line loss-of-function phenotype. Thus, both act to promote germ-line proliferation (an analogous argument holds for Notch/ Su[H] signaling pathways).

Signaling activity of the *glp-1* pathway must be spatially restricted to establish and maintain normal germ-line polarity. LAG-2, expressed by the DTC, is a localized ligand ([Henderson et al. 1994](#)). Tethering of LAG-2 via its transmembrane domain is important for normal germ-line polarity as a secreted form of the ligand, driven from the *lag-2* promoter, produces ectopic germ-line proliferation (Fitzgerald and Greenwald 1995).

*glp-1* expression is also spatially restricted ([Crittenden et al. 1994](#)). In young adult hermaphrodites and males, immunohistochemical staining shows that membrane-associated GLP-1 is present in the proliferating germ-cell population (1 to ~20 cell diameters from the DTC). Membrane-associated GLP-1 decreases rapidly in the transition zone and is not detected in the pachytene region. *glp-1* RNA is found throughout the hermaphrodite germ line but limited to the more distal region in males. Thus, *glp-1* expression appears to be regulated at both translational and transcriptional levels.

Germ-line polarity is lost in a *glp-1(gf)* mutant which displays a tumorous phenotype (L. Wilson Berry and T. Schedl, unpubl.). The *glp-1(gf)* mutant receptor is constitutively active; germ-cell proliferation occurs after elimination of the ligand (double mutant with *lag-2(lf)*) or its source (DTC ablation). The receptor encoded by the *glp-1(gf)* allele contains an amino acid substitution at a conserved residue in a region of the extracellular domain adjacent to the transmembrane domain. In *glp-1(gf)* homozygous hermaphrodites and males, [germ cells](#) proliferate continuously. In *glp-1(gf)/glp-1(lf)* animals, normal germ-line polarity is initially established, but as adults age, the population of proliferating [germ cells](#) expands proximally to more than 60 germ-cell diameters from the distal tip. Spatial restriction of *glp-1* expression is also lost in *glp-1(gf)* animals: Ectopically proliferating [germ cells](#) contain membrane-associated GLP-1. The correlation between proliferation and expression, both in

wild type where *glp-1* signaling is limited by the localized ligand and in *glp-1(gf)* where signaling is independent of ligand, suggests that proliferation (or *glp-1* signaling) positively regulates *glp-1* expression.

How does DTC signaling influence proliferation up to approximately 20 germ cell diameters away from its cell body ([Crittenden et al. 1994](#))? The DTC sends out cytoplasmic processes (D. Hall, pers. comm.). Visualization of these processes by expression of green fluorescent protein (Chalfie et al. 1994) in the DTC reveals that they extend more than ten germ-cell diameters from the distal tip of adult gonads (Fitzgerald and Greenwald 1995). If such processes contained LAG-2, they might directly signal GLP-1 in [germ cells](#) that are some distance from the distal tip. An alternative hypothesis is based on the observation that LAG-2 produced by the DTC is internalized into the germ line and appears to colocalize with the internal punctate GLP-1 ([Henderson et al. 1994](#)). The internalized LAG-2–GLP-1 complexes may produce a signal that is propagated locally in the germ-line syncytium.

In principle, the absence of signaling activity by the *glp-1* pathway may be sufficient for [germ cells](#) to enter the meiotic pathway. Initial entry into meiosis in the L3 may occur solely because proximal [germ cells](#) have escaped the influence of the DTC ([Kimble and White 1981](#)). It is also possible that [somatic gonad](#) cells that neighbor proximal [germ cells](#) have an active role in promoting entry into meiotic prophase in L3.

## B. Suppressors and Enhancers of *glp-1*

To identify additional components of the *glp-1* signaling pathway and genes that modulate its activity, mutations that suppress (*sog* genes; [Maine and Kimble 1993](#)) or enhance (*ego* genes; Qiao et al. 1995) the phenotype of *glp-1* (ts) mutants have been sought. *sog* mutants do not bypass the requirement of *glp-1*, as they fail to suppress a *glp-1* null mutation. Since partial loss-of-function alleles of *lag-1* represent one class of *ego* mutants, this enhancer screen can identify components of the *glp-1* signaling pathway. The remaining *ego* mutants display a heterogeneous mix of sterile phenotypes. Future characterization will determine the null phenotype and the molecular nature of the *sog* and *ego* genes.

## C. Proximal Proliferation

Mutations in more than ten genes display a proximal proliferation (Pro) phenotype, for example, *lin-12(lf)* (Seydoux et al. 1990), *shv* mutants (R. Francis et al., unpubl.), *pro(q540)* (L. Kadyk and J. Kimble, pers. comm.), *let-42(gf)* (B. Westlund and T. Schedl, unpubl.), and *ego-3* (Qiao et al. 1995). In most cases, it is not yet known whether the mutations affect components of the *glp-1* signaling pathway or disrupt meiotic prophase functions (see *gld-1* below). In the case of *lin-12(lf)*, inappropriate signaling between the [somatic gonad](#) and the germ line is the likely cause of the proximal proliferation phenotype. During the L1 and L2 stages, the gonadal anchor cell (AC) and its precursors contact the germ line. In *lin-12(lf)* mutants and in the wild type when certain [somatic gonad](#) blast cells are ablated, proximal [germ cells](#) fail to enter the meiotic prophase, resulting in proximal proliferation (Seydoux et al. 1990). A likely scenario for the *lin-12(lf)* Pro phenotype is that LAG-2 expressed in the AC and its precursors (for the anchor cell/ventral [uterine](#) decision, see [Greenwald](#), this volume) inappropriately activates germ-line GLP-1, a process that is normally blocked or limited by surrounding [somatic gonad](#) cells and *lin-12* (+) activity.

# Chapter 10. Developmental Genetics of the Germ Line — VIII

## Meiotic Prophase Progression and Gametogenesis

---

Following entry into the meiotic pathway, germ nuclei in the distal arm and loop progress through the meiotic prophase and gamete formation begins. Meiotic prophase progression and gametogenesis appear to be coupled, as mutations in several genes disrupt both processes.

Two genes, *glp-3* and *glp-4*, appear to function in both mitotic and meiotic prophase cell cycle progression in the hermaphrodite and male germ lines. The original *glp-4* mutation, *bn2*, displays a temperature-sensitive proliferation defect, in which nuclei appear to be arrested in mitotic prophase ([Beanan and Strome 1992](#)). In *glp-4(bn2);glp-1(lf)* double mutants, [germ cells](#) fail to enter the meiotic pathway. Three nonconditional *glp-4* alleles (Qiao et al. 1995) show only minor defects in proliferation but major defects in meiotic prophase (the transition zone is expanded with an accompanying reduction in the mitotic and pachytene regions) and oogenesis (oocytes are small and irregularly shaped). Mutations in *glp-3* display a proliferation defect in which nuclei appear to be arrested in late G<sub>2</sub> or prophase of the mitotic cell cycle (L. Kadyk et al., pers. comm.). In *glp-3 glp-1(lf)* double mutants, [germ cells](#) enter the meiotic pathway but appear to arrest in pachytene. Existing *glp-3* and *glp-4* alleles have no obvious somatic cell cycle defects.

### A. The RAS/MAP Kinase Pathway

The transition from pachytene to diplotene/diakinesis of meiotic prophase I (termed pachytene exit) is mediated by the RAS/MAP kinase signaling pathway ([Church et al. 1995](#); E. Lambie, pers. comm.; R. Francis and T. Schedl, unpubl.). Mutations in *let-60* RAS, *lin-45* RAF, *mek-2* MAP kinase kinase (also known as *let-537*), and *mpk-1* MAP kinase (also known as *sur-1*) result in a pachytene arrest phenotype as well as major defects in gametogenesis. Both hermaphrodites and males are affected. On the basis of genetic mosaic analysis with *mpk-1*, the RAS/MAP kinase pathway functions in the germ line to promote pachytene exit. The RAS/MAP kinase pathway genes also function in vulval induction ([Greenwald](#), this volume) and are necessary for viability. However, genes upstream of RAS and downstream from MAP kinase in the vulval induction pathway appear not to be required for pachytene exit. Two downstream vulval genes (*lin-1* and *lin-12*) do not appear to function in pachytene exit ([Church et al. 1995](#)), and the upstream receptor tyrosine kinase (*let-23*) that initiates vulval development also does not appear to function in pachytene exit.

The source of the signal that activates the RAS/MAP kinase pathway in the germ line is unknown ([Church et al. 1995](#)). The somatic gonadal sheath cells of the hermaphrodite are positioned appropriately to signal [germ cells](#) to exit pachytene. Ablation of all the sheath cells (and spermathecal cells) results in an impairment of pachytene progression and gametogenesis (J. McCarter and T. Schedl, unpubl.), consistent with the sheath cells playing a part in meiotic prophase progression. However, the region of the [male gonad](#) where [germ cells](#) exit pachytene lacks [somatic cells](#) and is surrounded only by a basement membrane. One possibility, for both sexes, is that proximal and/or distal [germ cells](#) signal intervening [germ cells](#) to control pachytene exit. Another possibility is that the pathways in the male and [hermaphrodite gonad](#) differ in one or more steps.

### B. Meiotic Prophase Progression in Oogenesis

The *gld-1* gene has an essential function for meiotic prophase progression in oogenesis but not in spermatogenesis ([Francis et al. 1995a, 1995b](#)). In *gld-1* null hermaphrodites, a germ-line tumor forms where oogenesis would normally occur. Germ cells enter the meiotic pathway normally but then exit pachytene and return to mitotic proliferation. Genetic epistasis experiments with sex determination gene mutations demonstrate that the tumorous phenotype is female germ-line-specific. Furthermore, although there is no morphological evidence of oogenesis, the *gld-1* null mutant germ line initiates oogenesis as multiple female germ-line-specific markers are expressed (R. Francis and T. Schedl, unpubl.). The *gld-1* gene thus has an essential function in oocyte differentiation and pachytene progression, and this function is regulated by the sex determination pathway. *gld-1* encodes a protein that contains a KH RNA-binding motif (hnRNP K homology motif; Siomi et al. 1993) within a

larger, approximately 200-amino-acid evolutionarily conserved region (Jones and Schedl 1995). GLD-1 is found only in the germ-line cytoplasm (A. Jones and T. Schedl, unpubl.), suggesting that it may control meiotic prophase progression by affecting RNA translation or stability.

The sex-specific *gld-1* tumorous germ-line phenotype can be explained as follows. The female germ line is likely to synthesize mRNAs that encode cell cycle factors which will be used subsequently for the meiotic divisions and/or embryonic cleavages. If GLD-1 functions as a translational repressor to mask such mRNAs, then cell cycle factors in a *gld-1* null mutant will be inappropriately translated in pachytene, resulting in activities that lead to meiotic prophase exit and proliferation. Biochemical experiments will be necessary to determine the molecular function of GLD-1.

Generated from local HTML

# Chapter 10. Developmental Genetics of the Germ Line — IX Oocyte Development, Maturation, and Ovulation

---

## A. Oocyte Development

Late stages of oogenesis occur during diakinesis of meiotic prophase I. As distal germ-line nuclei progress around the loop and through the proximal gonad, they become more fully enclosed by membrane, cell and nuclear volumes increase, and chromosomes become increasingly condensed. Oocyte surface/membrane-associated antigens appear at this time ([Strome 1986a](#); [Guo and Kemphues 1995](#)). Approximately five of the most mature oocytes accumulate large amounts of yolk proteins (S. Strome, pers. comm.), which are synthesized in the [intestine](#) (Kimble and Sharrock 1983).

Time-lapse Nomarski microscopy ([Ward and Carrel 1979](#)) has been used to define a pathway of landmark events in late oocyte development, meiotic maturation, and ovulation ([Fig. 5](#)) (J. McCarter and T. Schedl, unpubl.). In hermaphrodites, the oocyte nucleolus disappears about 70 minutes before ovulation. Subsequently, the nucleus migrates to the distal surface of the cell. The distal surface can also invaginate toward the nucleus, suggesting a physical connection that is under tension. With the exception of the acentrally placed nucleus (the importance of which is not currently known), the oocyte does not show an obvious polarization; no symmetry is observed in the cytoskeleton or the distribution of P granules ([Strome 1986a](#)) or PAR-1 ([Guo and Kemphues 1995](#)). Thus, unlike the *Drosophila* oocyte, which exhibits asymmetries that reflect a “prepattern” of the embryonic body axes (see, e.g., Roth et al. 1995), asymmetries in the *C. elegans* embryo appear to be established *de novo* at fertilization or during early zygotic development (see [Kemphues and Stone](#), this volume).

## B. Oocyte Maturation

Meiotic maturation describes the transition from diakinesis to metaphase of meiosis I. The first indication of maturation is nuclear envelope breakdown (NEBD) which begins at 5.7 minutes before ovulation. At 3.0 minutes before ovulation, the oocyte begins to change shape from a cube to a sphere (oocyte cortical rearrangement). Vigorous sheath contractions occur at the same time. Analysis of sheath-ablated animals and mutants defective in sheath activity indicates that NEBD and oocyte cortical rearrangement do not depend on myoepithelial sheath contractile activity (Myers et al. 1996; J. McCarter and T. Schedl, unpubl.).

## C. Ovulation

Ovulation, the exit of the most proximal oocyte from the gonad arm into the spermatheca, requires contraction of the eight proximal sheath cells (which are myoepithelial) and dilation of the distal spermatheca (oviduct valve). The rate of sheath contractions increases prior to NEBD and peaks at ovulation when the sheath appears to contract tonically as it pulls the dilating distal spermatheca over the oocyte. As the distal spermatheca closes, cytoplasmic streaming is visible in the oocyte, possibly indicating fertilization. The divisions of meiosis I and II occur in the [uterus](#).

## D. Meiotic Prophase Arrest

In unmated females, oocytes arrest in diakinesis, failing to undergo meiotic maturation and ovulation. Numerous oocytes accumulate, each with an enlarged, distally placed nucleus without a nucleolus. Sheath contractile activity in females is lower than the background level observed between ovulations in hermaphrodites. (At a low rate, oocytes in females stochastically exit from arrest and are ovulated.) It is unclear whether arrest is an active inhibition of progression or a failure to provide a positive signal that is necessary for progression.

In hermaphrodites with abundant sperm, oocyte development, maturation, and ovulation occur in an assembly-line-like fashion, with the time between successive ovulations averaging about 25 minutes. In this situation, the

time an oocyte spends in diakinesis may reflect a developmental requirement for the execution of certain events and thus might not be a true “arrest” of the meiotic cell cycle.

## E. Mutants with Endomitotic Oocytes

Mutants with polyploid oocytes in the gonad arm due to endomitosis (Emo) arise frequently in recessive sterile screens and are beginning to be characterized. Mutants with an Emo phenotype include *ceh-18(mg57)* (Greenstein et al. 1994) and certain non-null alleles of *emo-1* ([Iwasaki et al. 1996](#)), *lin-3*, *let-23* (Aroian and Sternberg 1991), and *mup-2* (Myers et al. 1996). Most Emo mutants examined to date by time-lapse microscopy show ovulation defects (J. McCarter and T. Schedl, unpubl.). Both *lin-3(n1058)* and *let-23(sy10)*, for instance, show an additional 20-minute delay between NEBD and ovulation. The distal spermatheca fails to dilate during this time and the oocyte is damaged upon ovulation, with contents relapsing into the gonad arm.

The Emo phenotype can arise from germ-line or somatic defects. Mosaic analysis of *emo-1* indicates a germ-line focus of action ([Iwasaki et al. 1996](#)). CEH-18 is found in sheath cell nuclei (Greenstein et al. 1994) and laser ablation of sheath, distal spermatheca, or their precursors can also result in an Emo phenotype (J. McCarter and T. Schedl, unpubl.). A current hypothesis is that the maturing oocyte signals the surrounding sheath and distal spermatheca cells to trigger ovulation, and failure of this process traps the mature oocyte in the gonad where it begins mitotic cycling. Karyokinesis and cytokinesis do not occur because unfertilized oocytes lack mitotic centrioles (Albertson 1984b).

## Figures

Figure 5. Landmark morphological events in late oocyte development, meiotic maturation, and ovulation.

### Figure 5

Landmark morphological events in late oocyte development, meiotic maturation, and ovulation. Events are shown for a single oocyte, as deduced by time-lapse Nomarski microscopy. Time is relative to the end of ovulation (0.0) at 20–22°C. The time at which nuclear migration occurs is variable; the bar indicates the time range during which most migrations are completed. Somatic myoepithelial sheath events repeat each ovulation. The dependency relationships for most of these events are not known. (From J. McCarter and T. Schedl, unpubl.)

Generated from local HTML

## Chapter 10. Developmental Genetics of the Germ Line — X Future Prospects

---

Developmental genetic studies have begun to provide a solid outline of germ-line development in *C. elegans*. A number of genes important for germ-line development have been identified and are in the process of being characterized. An even larger set of essential genes remains to be identified.

Two major technical obstacles must be overcome for studies of germ-line development to progress at a rapid pace. First, a lack of molecular markers for various aspects of germ-line development has limited the analysis of mutant phenotypes and dependency relationships. New *in situ* RNA and protein markers will be generated as more genes are characterized. Second, expression of transgenes is unusually inefficient and often variable in the germ line as compared to somatic tissues. "Promoter trap" screens have identified a number of transgenic lines that display specific *lacZ* expression patterns in somatic lineages, but not lines that display *lacZ* expression in the larval or adult germ line ([Hope 1991](#)). Transformation rescue of some genes can be very efficient and reproducible (e.g., [mes-3](#), Paulsen et al. 1995), but for other genes, rescue of the sterile phenotype occurs only at a very low frequency (or not at all) among worms containing the transgene. Furthermore, in some cases, a wild-type transgene in a wild-type host can produce variable dominant phenotypes similar to those observed for loss-of-function mutations in the gene (e.g., [gld-1](#), Jones and Schedl 1995). The development of improved methods for expressing gene products in the germ line will greatly speed molecular characterization of sterile loci (e.g., cloning, structure/function studies, and manipulating the temporal/spatial pattern of gene expression) and would permit the development of "enhancer/ promoter trap" methods to generate new germ-line markers and identify additional genes involved in germ-line development.

Molecules and signaling pathways utilized in germ-line development as well as in other aspects of *C. elegans* biology are evolutionarily conserved. Studies of these conserved pathways in the *C. elegans* germ line can provide new insights into their mode of action. An important question is whether molecular pathways that mediate the execution of a given step in *C. elegans* germ-line development mediate the same step in germ-line development of other organisms. The answer to this question is currently unknown because of our incomplete knowledge of germ-line development in *C. elegans* and other organisms. Emerging data from genome-sequencing projects should help answer whether molecules important for germ-line development in one organism perform similar functions in other organisms.

Generated from local HTML

## **Chapter 10. Developmental Genetics of the Germ Line — Acknowledgments**

---

I thank the many *C. elegans* researchers for providing unpublished results; Ross Francis for providing Figures 1, 2, and 3; Bob Clifford for Figure 4; and Jim McCarter for Figure 5. I also thank members of my laboratory, particularly Bob Clifford, for comments on the manuscript and stimulating discussions. I would also like to thank Susan Strome, Judith Kimble, Jane Hubbard, Eric Lambie, and Andrew Spence for comments on the manuscript. Research in my laboratory is supported by the National Institutes of Health and the National Science foundation.

Generated from local HTML

# **Chapter 11. Spermatogenesis**

---

## **Contents**

[I Overview](#)

[II Organelle Morphogenesis During Spermatogenesis](#)

[III Spermiogenesis](#)

[IV Acquisition and Mechanism of Spermatozoan Motility](#)

[V Role of Motility During Oocyte Recognition](#)

[VI Future Prospects](#)

[Acknowledgments](#)

Generated from local HTML

## Chapter 11. Spermatogenesis — I Overview

---

Spermatogenesis in *Caenorhabditis elegans*, as in most animals, is a differentiation pathway in which [spermatogonial](#) stem cells differentiate into spermatozoa. This process involves mitotic proliferation of [spermatogonial](#) cells to form primary [spermatocytes](#) and two subsequent meiotic divisions of the nucleus during spermatid formation. Spermiogenesis then follows, which is the maturation of [spermatids](#) into spermatozoa. As in other nematodes, *C. elegans* spermatozoa lack an acrosome and flagellum (for review, see [Foor 1983](#)) and move by crawling across the substrate (for review, see [Theriot 1996](#)). Although *C. elegans* sperm differ from flagellated sperm in a number of significant ways, both types of sperm engage in meiosis and in unusual cell divisions characterized by extremely asymmetric cytoplasmic partitioning.

*C. elegans* offers several advantages over other organisms in which spermatogenesis has been studied. Primary [spermatocytes](#) differentiate into [spermatids](#) in only 90 minutes and wild-type cells can be easily studied under simple culture conditions *in vitro* ([Ward et al. 1981](#); [L'Hernault and Roberts 1995](#)). Differentiation of [spermatocytes](#) into [spermatids](#) *in vivo* is much slower in organisms that produce flagellated sperm, taking about 32 days in humans, 24 days in rats (for review, see [Fawcett 1994](#)), and 5 days in *Drosophila* ([Lindsley and Tokuyasu 1980](#)). Although *in vitro* development of mouse sperm is possible, it has only been attained when [germ cells](#) are cocultured with transformed Sertoli-like cells under complex culture conditions ([Rassoulzadegan et al. 1993](#); [Hofmann et al. 1994, 1995](#)). Most animals produce sperm that can only be studied by microscopic techniques following dissection of the testes. In contrast, *C. elegans* is small and transparent, permitting microscopic observations of sperm development and motility in a living, undissected animal ([Ward and Carrel 1979](#)). Finally, *C. elegans* sperm develop without any of the accessory cells that complicate analysis of flagellated sperm development (for review, see [Skinner et al. 1991](#)). The steps of *C. elegans* spermatogenesis have been determined by light and electron microscopy ([Klass et al. 1976](#); [Wolf et al. 1978](#); [Ward et al. 1981](#)), and they have also been studied in a large collection of mutants ([Fig. 1](#)).

In hermaphrodites, spermatogenesis begins during the L4 larval stage and is completed in the young adult shortly after molting, requiring about 6–7 hours at 25°C ([Hirsh et al. 1976](#)). In males, spermatogenesis starts in the L4 and continues through adult life. Although the gonad anatomies of hermaphrodites and males differ (see [Schedl](#); [Emmons and Sternberg](#); both this volume), the process of spermatogenesis is similar at the cellular level. Spermatozoa derived from males closely resemble those of the hermaphrodite, with a few exceptions noted below.

Spermatocytes initially form in a syncytium with a central cytoplasmic core named the rachis ([Fig. 1A](#)) ([Hirsh et al. 1976](#)). The stages of cellular differentiation within the germ line proceed from the distal tip toward the [seminal vesicle](#) (in males; see [Emmons and Sternberg](#), this volume) or the spermatheca (in hermaphrodites; see [Schedl](#), this volume). Mitotic proliferation of the [spermatogonial](#) nuclei occurs near the distal tip. As the syncytial nuclei approach the loop region, where the gonad turns posteriorly, meiosis is initiated and a zone of nuclei in pachytene of the first meiotic division can be identified (see [Schedl](#), this volume). At this point, [spermatocytes](#) bud off the rachis ([Fig. 1B](#)), and individual cells complete meiosis. There is no apparent analog of the Sertoli cell, which is the somatic cell component of the mammalian seminiferous epithelium that provides nourishment and structural support to developing sperm cells (for review, see [Skinner et al. 1991](#)). *C. elegans* [spermatocytes](#) completely separate as each one buds from the rachis, while adjacent mammalian [spermatocytes](#) form a syncytium (for review, see [Fawcett 1994](#)). Metaphase I follows shortly with either of two results ([Fig. 1](#)) ([Ward et al. 1981](#)): The primary spermatocyte can divide completely into two secondary [spermatocytes](#) ([Fig. 1D](#)) or it can incompletely divide, with the two halves remaining in syncytium ([Fig. 1D'](#)). In both cases, the second meiotic division occurs with concomitant formation of a cytoplasm, called the residual body, between the developing [spermatids](#) (speckled structures at D and D' in [Fig. 1](#)). In many mammalian species, a residual body does not form until after release of elongate [spermatids](#), well after completion of meiosis (for review, see [Fawcett 1994](#)). Mammalian spermatogenesis is characterized by a lengthy period of differentiation between completion of meiosis and conversion of the spermatid into the spermatozoon. After a *C. elegans* spermatid has budded from

the residual body, it is not known whether there are required differentiation steps that must occur prior to competence to initiate spermatogenesis.

Spermatogenesis occurs in hermaphrodites when [spermatids](#) are moved into the spermatheca. In males, [spermatids](#) are stored in the [seminal vesicle](#) until ejaculation into the hermaphrodite. Shortly after ejaculation, [spermatids](#) (Figs. 1E and 2a) differentiate into spermatozoa (Figs. 1H and 2b,c). This differentiation occurs within the [uterus](#) just inside the [vulva](#), and some [spermatids](#) that remain in the male after copulation also undergo spermatogenesis ([Ward and Carrel 1979](#)). *C. elegans* spermatozoa, like all examined nematode spermatozoa ([Foor 1983](#)), lack both a flagellum and an acrosome ([Wolf et al. 1978; Ward et al. 1981](#)). Instead, the *C. elegans* spermatozoan cell body has a single pseudopod ([Fig. 2](#)), and directed membrane flow allows it to crawl over the substratum (Figs. 1H and 2b) ([Nelson et al. 1982; Roberts and Ward 1982a,b](#)). All mitochondria, the nucleus, and other organelles reside only in the cell body, which is separated from the pseudopod by laminar membranes ([Fig. 2c](#)). Much of the *in vivo* development discussed above can also be studied *in vitro* because [spermatocytes](#) that have detached from the rachis can complete differentiation into spermatozoa in simple media (for review, see L'Hernault and Roberts 1995; K. Machaca and S. L'Hernault, unpubl.).

The unusual reproductive biology of *C. elegans* offers advantages for mutational analyses of spermatogenesis. Hermaphrodite self-fertilization is extraordinarily efficient, and nearly every spermatozoon successfully fertilizes an oocyte in the young hermaphrodite ([Ward and Carrel 1979](#)). Whereas young wild-type hermaphrodites usually lay eggs containing developing embryos, mutant self-sterile hermaphrodites that contain defective sperm lay oocytes. When such mutants are mated to wild-type males, cross-progeny form, demonstrating that normal spermatozoa can rescue the sterile phenotype of the mutant hermaphrodite. A genetic screen using this strategy has identified more than 60 genes that affect spermatogenesis ([Hirsh and Vanderslice 1976; Ward and Miwa 1978; Argon and Ward 1980; Ward et al. 1981, 1982, 1983; Edgar 1982; Nelson et al. 1982; L'Hernault et al. 1987, 1988, 1993; Shakes 1988; Shakes and Ward 1989a,b; L'Hernault and Arduengo 1992; Varkey et al. 1993, 1995; Minniti et al. 1996](#)). Figure 1 summarizes how some of these mutants alter or arrest spermatogenesis. Many of these mutants appear to be spermatogenesis-specific in their mutant defects (see, e.g., [L'Hernault et al. 1988](#)), and, in those cases that have been analyzed, transcription of the encoded gene product is limited to the male germ line ([L'Hernault and Arduengo 1992; L'Hernault et al. 1993; Varkey et al. 1995; Minniti et al. 1996](#)). The phenotypes of many of these mutants are discussed below in the context of normal sperm function. Table 1 summarizes all of the mutants discussed in this chapter.

## Figures

Figure 1. Wild-type spermatogenesis is shown as a pathway of morphogenesis labeled (vertically) A–H.

### Figure 1

Wild-type spermatogenesis is shown as a pathway of morphogenesis labeled (vertically) A–H. Genes discussed here are placed on the pathway at the cytological stage that is altered when mutants are viewed by light microscopy. In most cases, mutants arrest spermatogenesis at a stage that resembles a wild type (all mutants placed near vertical arrows pointing down, and [spe-9](#), [spe-13](#), [spe-16](#), and [fer-14](#)). Mutants positioned to the right of the vertical pathway ([spe-4](#), [spe-5](#), [spe-26](#), [fer-2](#), [fer-3](#), [fer-4](#), and [fer-6](#)) produce cells with cytology unlike wild type. Placement of these mutants before an arrow indicates that they produce cells similar to those depicted to the right of the arrowhead. Placement of a mutant before a bifurcating arrow indicates that they produce cells similar to those depicted to the right of either arrowhead. [spe-5](#) null mutants have a variable phenotype; they usually arrest cellular morphogenesis as an abnormal spermatocyte, but a few [spermatids](#) capable of forming fertilization-competent spermatozoa are also produced. The placement of genes in this figure does not imply knowledge of how these spermatogenesis (*spe*)/fertility (*fer*)-defective genes should be ordered relative to one another and does not take into account ultrastructural defects.

# Chapter 11. Spermatogenesis — II Organelle Morphogenesis During Spermatogenesis

---

## A. Nuclei and Perinuclear Material

Nuclei of primary [spermatocytes](#) undergo two meiotic divisions to give rise to spermatid nuclei, which are haploid. The spermatid and spermatozoan nuclei are highly condensed ([Fig. 2a,c](#)) and stay in this state until they are within the oocyte during fertilization. (A condensed nucleus is also observed in most flagellated spermatozoa.) The nuclear division of secondary [spermatocytes](#) is rapid (~2–5 minutes; [Ward et al. 1981](#)), and chromatin condensation apparently occurs as meiosis II is completed. However, unlike flagellated sperm, *C. elegans* spermatid and spermatozoan nuclei are not surrounded by an envelope or any type of membrane. The highly condensed spermatid chromatin is not associated with protamines (B. Nathans and S. Ward, unpubl.), unlike the chromatin of mammalian spermatozoa. However, a novel sperm-specific histone H1 in *C. elegans* is expressed during spermatogenesis ([Sanicola et al. 1990](#)), as is the case for a number of species that have flagellated sperm (see, e.g., [Cole et al. 1986](#)). It is possible that this histone H1 plays a part in formation of the highly condensed chromatin that characterizes sperm. The spherical nucleus has a closely applied layer of perinuclear material (forming a halo that surrounds the nucleus) in which the centriole pair is embedded ([Fig. 2a,c](#)). Ultrastructural analyses after cytochemical staining suggest that this material is enriched in RNA ([Ward et al. 1981](#)).

## B. Plasma and Internal Membranes

Formation of [spermatids](#) involves dramatic rearrangements of the cytoplasm. At two points, sperm undergo an unequal division ([Fig. 1A,D,D'](#)). Several types of membrane-bounded organelles are confined to and segregate with [spermatocytes](#) as these cells separate from the rachis, despite a coenocytic association prior to division ([Fig. 1A](#)). The second unequal division is observed when [spermatids](#) bud from a common residual body ([Fig. 1D,D'](#)). This second division involves formation of a membrane boundary by accretion of vesicles at the site of division ([Ward et al. 1981](#); [Roberts et al. 1986](#)); no microfilament-containing contractile ring can be detected and division is insensitive to cytochalasins (G. Nelson and S. Ward, unpubl.). These features of spermatid budding ([Ward et al. 1981](#)) resemble platelet formation from a megakaryocyte ([Yamada 1957](#)) or plant cell division ([O'Brien and McCully 1969](#)).

Some type of mechanism must ensure that cellular divisions are associated with the proper partitioning of cytoplasm and plasma membrane into the developing spermatid. For instance, recent data indicate that voltage-dependent ion channels in the plasma membrane are sorted so that most of these channels in [spermatocytes](#) are segregated into the residual body ([Machaca et al. 1996](#)). Intracellularly, the major mechanism employed to ensure proper cytoplasmic partitioning involves an unusual organelle called the fibrous body–membranous organelle complex (FB-MO; also referred to as the special vesicle) ([Wolf et al. 1978](#); [Ward et al. 1981](#)), and this organelle appears to be peculiar to nematode sperm. The membranous organelle (MO) portion of the FB-MO is first observed after [spermatogonial](#) cells have initiated meiosis, but before they bud from the rachis (Figs. 1A and 3A). They first appear as vesicular swellings at the edges of the abundant Golgi complexes that are evident at this stage, and each cell forms a number of individual MOs. These vesicles are constricted at their base by a collar structure that forms an electron-dense necklace. As the MOs form, the fibrous body (FB) is first detected at their bases. The major constituent of the FB is the major sperm protein, or MSP ([Fig. 3a](#)). [Roberts et al. \(1986\)](#) examined developing MO membranes by monoclonal anti-MSP antibody labeling ([Ward et al. 1986](#)) and serial-section electron microscopy and showed that they are associated with MSP from their earliest identifiable stage.

As mentioned above, the FB-MO complexes are a major mechanism to prepackage proteins for delivery to [spermatids](#) during their budding division from the residual body. Their cargo includes proteins that will ultimately reside on the cell surface, as well as those that remain within the cytoplasm. As the FB-MO develops, it increases in size and soon has three distinct compartments ([Fig. 3B](#)). The head is a membrane vesicle that has an

electron-dense interior that lacks internal membrane structure. An electron-dense collar separates the main body of the MO from the head, forming a noose-like structure that appears to constrict the membrane. The body of the MO has an internal membrane compartment continuous with the head. The body membrane folds around the FB but does not seal it off from the rest of the cytoplasm. The interior membrane of the FB is the only site in [spermatocytes](#) and developing [spermatids](#) where the MSP forms fibers that constitute the bulk of the FB.

Another protein, sperm-specific protein SSP-10, also becomes associated with the MSP fibers (Sosnowski 1987). The FB-MO reaches its maximum size in budding [spermatids](#) where these structures (which fill ~35% of the spermatid volume; [Ward et al. 1981](#)) are segregated along with mitochondria and the nucleus into the budding spermatid ([Fig. 2a](#)). In contrast, all ribosomes, actin, myosin, nearly all tubulin (except that in the centrosome), and many internal membranes are segregated into the residual body ([Nelson et al. 1982](#); Ward 1986).

How FB-MOs segregate into developing *C. elegans* [spermatids](#) is unknown, but in *Ascaris*, FB-MOs localize near the centrosomes, and [spermatids](#) form around the haploid nucleus that is very close to the centrosome after completion of the second meiotic division (T. Roberts, pers. comm.). Reorganization of the FB occurs once [spermatids](#) bud from the residual body. The double membrane surrounding the MSP fibers is retracted and folds in on itself to form a compact, bilobed MO ([Fig. 3C](#)). The MSP fibers from the FB depolymerize and the MSP is scattered throughout the cytoplasm, as detected by antibody labeling (Roberts et al 1986). This basic protein (pI 8.6; Klass and Hirsh 1981; Burke and Ward 1983) renders the spermatid more electron-dense following depolymerization of the FB, but it has no known role during this developmental stage. The MO localizes below the plasma membrane ([Fig. 3D](#)).

MOs have a secretory function during spermiogenesis. Well before fertilization, the MO head fuses with the plasma membrane and releases its contents onto the cell surface (Figs. 2c and 3E). Much of this material stains with fluorescent wheat-germ agglutinin and is removed by proteases, suggesting that it is glycoprotein ([Ward et al. 1983](#)). The collar structure of the MO forms a permanent fusion pore with the plasma membrane, and the interior of the MO body is open to the cell's exterior. The MSP, which had scattered throughout the spermatid cytoplasm, concentrates in the single pseudopod and forms 2-nm filaments that appear to play a part in spermatozoan motility (see below).

## C. Mutants with Organelle Defects

### 1. Chromosome Segregation Defects

The [spe-6](#) and [spe-26](#) genes have been shown to be involved in proper chromosome segregation ([Varkey et al. 1993](#), 1995). Mutants defective in [spe-6](#) contain [spermatocytes](#) that arrest meiotic nuclear divisions at diakinesis. DAPI staining of [spe-6](#) mutant testes reveals terminal [spermatocytes](#) that contain condensed meiotic chromosomes, usually located near the center of the cell. Mutants lacking [spe-26](#) form normal-appearing primary [spermatocytes](#) that are incapable of forming [spermatids](#). The mutant cells arrest as terminal [spermatocytes](#) that frequently contain four DAPI-positive regions, suggesting that the nuclear divisions of meiosis have occurred. However, about half of the examined [spe-26](#) terminal [spermatocytes](#) contain 5–12 regions of chromatin, indicating that aberrant meiotic nuclear divisions are also common. The [spe-26](#) gene encodes a protein that has homology with a family of actin-binding proteins, suggesting that mutant defects in meiosis might be due to improper function of microfilaments ([Varkey et al. 1995](#)).

### 2. Defects in Perinuclear Material

The [fer-2](#), [fer-3](#), [fer-4](#) ([Ward et al. 1981](#)), and [spe-11](#) mutations ([Hill et al. 1989](#); [Browning and Strome 1996](#)) cause defects in the structure and organization of the perinuclear halo. A perinuclear halo is absent in [fer-2](#), [fer-3](#), and [fer-4](#) mutants, but it is replaced by an accumulation of large tubules. The aberrant ultrastructure of the perinuclear halo is evident from its first appearance during development of [fer-4](#) sperm, whereas the [fer-2](#) perinuclear material initially is almost wild type in appearance, becoming progressively more tubular in appearance. In addition to perinuclear defects, [fer-2](#), [fer-3](#), and [fer-4](#) sperm also have defects in the pseudopod, which are presumably responsible for their defects in both motility and fertilization (see below). It is unclear how

the perinuclear defects might be related to these pseudopod defects ([Ward et al. 1981](#)). In contrast, the only evident cytological defects in *spe-11* sperm are in the perinuclear region ([Hill et al. 1989](#)). The most penetrant *spe-11* mutant lacks most of the perinuclear halo, except for a small amount surrounding the centriolar region. Mutant *spe-11* spermatozoa are competent to enter the oocyte but result in a paternal-effect lethal phenotype ([Kemphues and Stone](#), this volume), suggesting that the perinuclear region is essential for embryonic viability.

### 3. FB-MO Defects

Mutant *spe-4*, *spe-5*, *spe-6*, *spe-10*, *spe-17*, *fer-1*, and *fer-6* sperm all exhibit defects in FB-MO morphogenesis and/or function. The most striking defects are found in sperm lacking *spe-4* or *spe-6*, which never make *spermatids* and always arrest as cells that, by Nomarski optics, are similar to *spermatocytes*, except that they contain four haploid nuclei. Such cells are called “terminal *spermatocytes*” ([L'Hernault and Arduengo 1992](#); [Varkey et al. 1993](#)). The earliest defects are observed in *spe-6* mutant sperm, which never make an identifiable FB containing MSP filaments ([Varkey et al. 1993](#)). Instead, antibody staining reveals that MSP is present throughout the terminal spermatocyte cytoplasm. This result suggests that *spe-6* lacks the normal site(s) required for the nucleated assembly of MSP filaments normally found in the FB. Developing MOs become distended and vacuolated in *spe-6* mutants and are scattered throughout the cytoplasm.

Ultrastructural analyses reveal that *spe-4* mutants have defects in FB-MO morphogenesis. Although examination of wild-type *spermatocytes* has revealed that the FB normally develops in intimate association with the MO, in *spe-4* mutants, the FB and MO seem to develop as discrete structures. It is not known if there is a transient association between the FB and MO during their development or if there is an alternative pathway for formation of the FB in *spe-4* mutants. Nevertheless, the end result is a terminal spermatocyte that contains distended MOs and separate FBs. The *spe-4* gene encodes an integral membrane protein that appears to be localized to the FB-MO during sperm development ([Arduengo et al. 1994](#)). The precise biochemical function of SPE-4 is unknown, although this protein shows homology with the presenilins (Levy-Lahad et al. 1995; Rogaev et al. 1995; Sherrington et al. 1995) and the *C. elegans* SEL-12 protein (Levitian and Greenwald 1995). The presenilins are integral membrane proteins implicated in the development of Alzheimer's disease, and *sel-12* mutations were identified as suppressors of *lin-12*. The SEL-12 protein facilitates reception of intercellular signals by LIN-12 (see [Greenwald](#), this volume).

Mutations in *spe-5*, *spe-10*, *spe-17*, *fer-1*, and *fer-6* all affect FB-MO morphogenesis, but allow formation of at least a few *spermatids*. These *spermatids* usually have ultrastructural defects in their FB-MOs, although they occasionally develop into spermatozoa that successfully fertilize oocytes. The *spe-5*, *spe-10*, and *spe-17* mutants show defects in FB-MO morphogenesis in *spermatocytes*. In *spe-5*, defects are first evident in primary *spermatocytes*. The MO portion of the FB-MO appears to be distended and vacuolated, and in most cases, *spermatids* do not form and cells arrest in a manner reminiscent of *spe-4* mutants described above. Occasionally, *spermatids* with vacuolated MOs form, and some of these differentiate into functional spermatozoa. Putative null mutants are slightly self-fertile ([L'Hernault et al. 1988](#); K. Machaca and S. L'Hernault, unpubl.).

The *spe-17* FB-MOs assemble in a manner that appears superficially normal except that the membranes appear to be studded with ribosomes ([Shakes and Ward 1989b](#)); wild-type FB-MO membranes are never associated with ribosomes (Wolf et al. 1978; [Ward et al. 1981](#)). Normally, ribosomes are segregated to the residual body during the second meiotic division, but, in *spe-17*, ribosomes associated with the FB-MO are carried into the spermatid. The FB appears to disassemble normally, but many MOs do not fuse with the cell surface during spermiogenesis. Nevertheless, many *spe-17* spermatozoa are able to crawl in vitro ([Shakes and Ward 1989b](#)) and a few can fertilize oocytes in vivo (L'Hernault et al. 1993). The *spe-17*-encoded protein is not homologous to any known protein, and it does not appear to be an integral membrane protein ([L'Hernault et al. 1993](#)).

Morphogenesis of FB-MOs appears to be superficially normal in *spe-10* mutants until *spermatids* start to form ([Shakes and Ward 1989b](#)). In this mutant, the membrane around the FB appears to retract prematurely and the membrane-free fibrous body ends up in the residual body. The MO is segregated into the spermatid without an attached FB, and it becomes distended and vacuolated. The *spe-10* mutants do not have any MOs that fuse with the cell surface during spermiogenesis, and *spe-10* spermatozoa do not crawl.

In contrast to the above-mentioned mutants, many *fer-6* spermatids contain FBs that fail to disassemble. The membrane that normally surrounds the FB is apparently retracted into the MO during spermatid budding, but the naked MSP fiber bundles fail to disassemble and can be observed in the cytoplasm of cells that have extended pseudopods. Additionally, *fer-6* spermatozoa contain many MOs that fail to fuse with the plasma membrane ([Ward et al. 1981](#)).

The latest FB-MO defects are shown by *fer-1* mutants, which appear indistinguishable from wild type until spermiogenesis ([Ward et al. 1981](#)). During spermiogenesis, the MOs in *fer-1* mutants do not fuse with the cell surface. The resulting spermatozoa have abnormally short pseudopods (see [Fig. 1G](#)) and do not crawl. These observations, together with those from *spe-10* mutants, suggest that MO fusion with the cell surface is an essential prerequisite for proper spermatozoan motility. MO fusions introduce permanent fusion pores into the plasma membrane, probably insert MO-derived membrane components into the plasma membrane (Roberts et al. 1986), and release extracellular matrix constituents onto the cellular surface ([Fig. 2c](#)) ([Ward et al. 1981](#)). However, no MO-derived component has been shown to have a direct function in motility.

## Figures

Figure 2. (a) Transmission electron micrograph of a budded spermatid containing one fused membranous organelle (MO) in the upper left corner and one labeled, unfused MO.

## Figure 2

(a) Transmission electron micrograph of a budded spermatid containing one fused membranous organelle (MO) in the upper left corner and one labeled, unfused MO. The centrioles (C) are embedded in the pericentriolar material that surrounds the dense nucleus to its right. Laminar membranes (LM) are evident on the right side of the cell. (b) Scanning electron micrograph of spermatozoa. Prior to fixation, the cell at the lower left was using its pseudopod to crawl across the substrate (arrow). Bar, 2 μm. (c) Transmission electron micrograph of a spermatozoon. The nucleus (Nuc), centrioles (c), fused MOs, and mitochondria are localized within the cell body, which is separated from the pseudopod by the laminar membrane (LM). Bar, 0.5 μm. (a, reprinted, with permission and slight modification, from [Nelson et al. 1982](#); c, reprinted, with permission, from [Nelson et al. 1982](#) [by copyright permission of the Rockefeller University Press].)

Figure 3. Summary of morphogenesis of the FB-MO complex.

## Figure 3

Summary of morphogenesis of the FB-MO complex. (A) The fibrous body (fb) develops in close association with, and is almost surrounded by, the MO within the primary spermatocyte. The MO is separated by a collar (c) region into a head (bracketed speckled region, labeled h) and body (bracketed region to the right of the collar, labeled b). (B) The FB-MO complex reaches its largest size within mature *spermatocytes*. The double-layered MO-derived membrane surrounds the striped fibers within the FB, and the fibers of the FB contain the MSP. (C) The membranes surrounding the FB retract and fold up as the FB begins to disappear and disperse its contents during budding of *spermatids* from the residual body. (D) The head (arrow labeled h) of each MO moves to a position just below the plasma membrane (pm) of the spermatid, and the fibrous bodies have disappeared. (E) The head of the MO fuses at the collar (c) to the plasma membrane and exocytoses its contents (fibers at the arrow) onto the cell surface. A permanent fusion pore remains at the point of each MO fusion. (Reprinted, with permission and slight modification, from [L'Hernault and Arduengo 1992](#) [by copyright permission of the Rockefeller University Press].)

## Tables

### Table 1 *spe* genes discussed in this chapter

<b>Gene/Phenotype</b>
<u><a href="#">fer-1</a></u>
MOs do not fuse with plasma membrane during spermiogenesis. Spermatozoon has a short pseudopod and defective motility. ( <a href="#">Ward and Miwa 1978</a> ; <a href="#">Argon 1980</a> ; <a href="#">Argon and Ward 1980</a> ; <a href="#">Ward et al. 1981</a> ; <a href="#">Roberts and Ward 1982a,b</a> ; <a href="#">L'Hernault et al. 1988</a> )
<u><a href="#">fer-2</a></u>
Spermatids either lack or have an abnormal pseudopod. Defective perinuclear halo. ( <a href="#">Argon 1980</a> ; <a href="#">Argon and Ward 1980</a> ; <a href="#">Ward et al. 1981</a> )
<u><a href="#">fer-3</a></u>
Occasional abnormal pseudopod. Defective perinuclear halo. ( <a href="#">Argon 1980</a> ; <a href="#">Argon and Ward 1980</a> ; <a href="#">Ward et al. 1981</a> )
<u><a href="#">fer-4</a></u>
Abnormal pseudopods with very few projections. Defective perinuclear halo. ( <a href="#">Argon 1980</a> ; <a href="#">Argon and Ward 1980</a> ; <a href="#">Ward et al. 1981</a> )
<u><a href="#">fer-6</a></u>
Defective FB-MO morphogenesis. Spermatids occasionally form. ( <a href="#">Argon 1980</a> ; <a href="#">Argon and Ward 1980</a> ; <a href="#">Ward et al. 1981</a> ; <a href="#">L'Hernault et al. 1988</a> )
<u><a href="#">fer-14</a></u>
Sperm are defective in oocyte entry after gamete contact. ( <a href="#">Roberts and Ward 1982b</a> ; <a href="#">Nelson et al. 1982</a> )
<u><a href="#">fer-15</a></u>
Both males and hermaphrodites produce <u><a href="#">spermatids</a></u> that do not activate. ( <a href="#">Roberts and Ward 1982a</a> )
<u><a href="#">spe-4</a></u>
Defective FB-MO morphogenesis. No normal <u><a href="#">spermatids</a></u> form. ( <a href="#">L'Hernault et al. 1988</a> ; <a href="#">L'Hernault and Arduengo 1992</a> )
<u><a href="#">spe-5</a></u>
Defective FB-MO morphogenesis. Spermatids occasionally form. ( <a href="#">L'Hernault et al. 1988</a> ; K.A. Machaca and S.W. L'Hernault, unpubl.)
<u><a href="#">spe-6</a></u>
Defective FB-MO morphogenesis. Defective chromosome segregation. ( <a href="#">Varkey et al. 1993</a> )
<u><a href="#">spe-8</a></u>
Activation-defective. Males are cross-fertile and hermaphrodites are self-sterile. ( <a href="#">L'Hernault et al. 1988</a> ; <a href="#">Shakes and Ward 1989b</a> ; <a href="#">Machaca et al. 1996</a> )
<u><a href="#">spe-9</a></u>
Sperm are defective in oocyte entry after gamete contact. ( <a href="#">L'Hernault et al. 1988</a> ; K. Mercer et al., unpubl.)
<u><a href="#">spe-10</a></u>
Defective FB-MOs. Spermatids with short pseudopods occasionally form. ( <a href="#">Shakes and Ward 1989a</a> )
<u><a href="#">spe-11</a></u>
Defective perinuclear halo. Paternal-effect lethal. ( <a href="#">L'Hernault et al. 1988</a> ; <a href="#">Hill et al. 1989</a> ; <a href="#">Browning and Strome 1996</a> )
<u><a href="#">spe-12</a></u>
Activation-defective. Males are cross-fertile and hermaphrodites are self-sterile. ( <a href="#">L'Hernault et al. 1988</a> ; <a href="#">Shakes and Ward 1989b</a> ; <a href="#">Machaca et al. 1996</a> ; A. Minniti et al., unpubl.)
<u><a href="#">spe-13</a></u>
Sperm are defective in oocyte entry after gamete contact. ( <a href="#">L'Hernault et al. 1988</a> ; K.B. Mercer et al., unpubl.)

<b>Gene/Phenotype</b>
<u><a href="#">spe-16</a></u>
Sperm are defective in oocyte entry after gamete contact. ( <a href="#">Shakes 1988</a> ; K.B. Mercer et al., unpubl.)
<u><a href="#">spe-17</a></u>
Defective MOs with bound ribosomes. Spermatids are small and have a short pseudopod and a mispositioned nucleus. ( <a href="#">Shakes and Ward 1989a</a> ; <a href="#">L'Hernault et al. 1993</a> ; S. Cordovado and S.W. L'Hernault, unpubl.)
<u><a href="#">spe-26</a></u>
Defective chromosome segregation. Spermatids do not form. ( <a href="#">Varkey et al. 1995</a> )
<u><a href="#">spe-27</a></u>
Activation-defective. Males are cross-fertile and hermaphrodites are self-sterile. ( <a href="#">Machaca et al. 1996</a> ; <a href="#">Minniti et al. 1996</a> )
<u><a href="#">spe-29</a></u>
Activation-defective. Males are cross-fertile and hermaphrodites are self-sterile. ( <a href="#">Machaca et al. 1996</a> ; P. Muhlrad and S. Ward; J. Nance et al.; both unpubl.)

Generated from local HTML

# Chapter 11. Spermatogenesis — III Spermiogenesis

---

## A. Spermatid Activation

Activation initiates spermatogenesis in both hermaphrodites and males. Nonmotile, symmetrical [spermatids](#) become motile, asymmetrical spermatozoa when a single pseudopod extends from one side of the cell during activation (see [Fig. 2](#)). Most studies of activation have been performed on male-derived [spermatids](#) because they are easily dissected and can be processed in bulk for larger-scale experiments (for review, see [L'Hernault and Roberts 1995](#)). Unlike *Ascaris* (Burghardt and Foor 1978; Sepsenwol and Taft 1990), the natural *in vivo* activating substance from *C. elegans* is unknown. However, a number of drugs and proteases have been discovered that can activate *C. elegans* [spermatids](#) *in vitro*.

The first successful report of *in vitro* activation ([Nelson and Ward 1980](#)) employed the cationic ionophore monensin, which exchanges intracellular H<sup>+</sup> for extracellular monovalent cations, particularly K<sup>+</sup> (Pressman 1976). Subsequently, cell surface proteolysis and a number of agents, including monensin and triethanolamine (TEA), that were capable of elevating intracellular pH 0.4–1.0 unit were shown to initiate activation ([Ward et al. 1983](#)). Although the effect of TEA on intracellular pH is almost instantaneous, sperm need to be exposed to it continuously for more than 6 minutes in order to complete spermatogenesis, since spermatid activation is a two-step process ([Shakes and Ward 1989a](#)). Video recordings during spermatid activation revealed a transient intermediate stage characterized by extension of several spike-like projections at or adjacent to the site where the single pseudopod subsequently appeared ([Fig. 1F](#)). Brief treatment with TEA followed by a wash in TEA-free medium resulted in [spermatids](#) that were arrested at this spike-containing stage. Subsequent exposure to TEA-containing medium allowed formation of a pseudopod. It was also possible to obtain [spermatids](#) arrested at the spike-bearing stage by treatment with any of several putative calmodulin antagonists; inactive analogs were not able to elicit spike formation. In this case, continuous exposure to the calmodulin antagonist inhibited subsequent formation of a pseudopod, but, if the cells were washed into drug-free medium, normal pseudopod-bearing spermatozoa formed. It is not clear how calmodulin antagonists affect spermatid activation because no detectable calmodulin is present in sperm by immunofluorescence. Furthermore, activation also does not require extracellular Ca<sup>++</sup> and is not influenced by the calcium ionophore A23187 ([Nelson and Ward 1980; Ward et al. 1983](#)).

Several components of sperm medium have been investigated in attempts to understand how various *in vitro* activators function. Monensin and TEA were more effective at a pH of 7.8 than at 7.0, consistent with a role in facilitating a rise in intracellular pH ([Ward et al. 1983](#)). Monensin required extracellular Na<sup>+</sup> or K<sup>+</sup> ([Nelson and Ward 1980](#)), but TEA-induced spermatogenesis was reduced only by 30% in Na<sup>+</sup>/K<sup>+</sup>-free medium. In contrast, Pronase-induced spermatogenesis was insensitive to extracellular pH but was reduced approximately 40% in K<sup>+</sup>-free medium; Na<sup>+</sup>-free medium had no effect on activation efficiency. These data suggest two activation pathways, one associated with a rise in intracellular pH (TEA and monensin) and one independent of a change in pH (Pronase). Analysis of mutants (see below) has confirmed that there are two distinct pathways of activation ([Shakes and Ward 1989a](#)), but how these two *in vivo* pathways relate to the *in vitro* activation results is not clear.

The above experiments indicate that ion traffic across the plasma membrane has a role in spermatid activation. Molecular mechanisms that might mediate aspects of this process have recently been assessed by patch-clamp electrophysiological techniques. Surprisingly, these experiments revealed that the only detectable voltage-dependent ion channel in [spermatids](#) is a Cl<sup>-</sup> channel that is inward rectifying (Clir). This channel can be inhibited by several Cl<sup>-</sup> channel-blocking drugs, the most effective being the stilbene 4, 4'diisothiocyanostilbene-2, 2'-disulfonic acid (DIDS). Furthermore, treatment of [spermatids](#) with DIDS results in activation and formation of apparently normal spermatozoa ([Machaca et al. 1996](#)). These patch-clamp experiments suggest that Clir is involved in activation and also indicate that much ion traffic (especially cations) across the plasma membrane probably occurs through ion carriers, transporters, and/or pumps. However, it is unclear why inhibition of Clir should lead to spermatid activation.

A number of substances are capable of eliciting spermatid activation, but the relation of how in vitro activation with any of these substances is related to in vivo activation is unclear. Recently, techniques have been developed to assess in-vitro-activated [spermatids](#) for fertility by artificial insemination ([LaMunyon and Ward 1994](#)). These experiments show that TEA in-vitro-activated [spermatids](#) are capable of fertilization, whereas Pronase-activated [spermatids](#) are not. These data do not rule out the possibility that a protease could be an in vivo activator, especially since proteases are the only agents that will activate both *C. elegans* ([Ward et al. 1983](#)) and *Ascaris* ([Sepsenwol and Taft 1990](#)) [spermatids](#) in vitro. Pronase is a mixture of proteases with a broad substrate specificity ([Narahashi 1970](#)). Perhaps only one or a few surface molecules need to be subjected to proteolysis to initiate spermatid activation. The Cl<sup>-</sup> channel might be involved in parallel with a cation channel that transports protons and alters pH. Proteases might act by altering these channels.

## B. Mutants Defective in Spermatid Activation

[fer-15](#) mutants accumulate [spermatids](#) that do not activate (<1%) in vivo in either hermaphrodites or males ([Roberts and Ward 1982a](#); S. L'Hernault and S. Ward, unpubl.). Furthermore, [fer-15 spermatids](#) from males do not make normal pseudopods in the presence of either Pronase, monensin, TEA, calmodulin antagonists such as trifluoperazine (TFP), or chloride channel inhibitors such as DIDS (S. L'Hernault and S. Ward; D. Shakes and S. Ward; K. Machaca and S. L'Hernault; all unpubl.). Consequently, [fer-15 spermatids](#) do not respond to any of the known mechanisms of activation.

Mutations in four genes, [spe-8](#), [spe-12](#) ([Shakes and Ward 1989a](#)), [spe-27](#) ([Minniti et al. 1996](#)), and [spe-29](#) (A. Minniti et al., unpubl.), result in hermaphrodites that are self-sterile because they accumulate [spermatids](#) that do not activate. Males are fertile because they make [spermatids](#) that activate normally during mating. Consequently, each mutant can be propagated as a gonochoristic male/"female" homozygous strain. One surprising result is that [spe-8](#), [spe-12](#), [spe-27](#), or [spe-29](#) mutant hermaphrodites are capable of producing a number of self-progeny after males have transferred "competent" seminal fluid ([Shakes and Ward 1989a](#)). "Competent" seminal fluid can be provided by wild-type males or a variety of tested spe mutant males. For instance, [fer-1](#) males ejaculate spermatozoa that do not crawl in vivo ([Ward and Carrel 1979](#)), yet [fer-1](#) seminal fluid is competent to activate [spe-8](#) hermaphrodite-derived [spermatids](#) in vivo ([Shakes and Ward 1989a](#)). These results suggest that a component of male seminal fluid acts in *trans* to activate [spe-8](#) hermaphrodite [spermatids](#). Consistent with this interpretation, artificial insemination with seminal-fluid-free [spe-27](#) male-derived [spermatids](#) into [spe-27](#) recipient hermaphrodites did not result in any cross-progeny, whereas a control experiment using wild-type seminal-fluid-free male-derived [spermatids](#) did result in cross-progeny ([Minniti et al. 1996](#)). This experiment suggests that males and hermaphrodites produce different activators and that the hermaphrodite-produced activator can act on male-derived [spermatids](#) within the [uterus](#) and at some distance from its presumed normal site of action within the spermatheca. The nature of this signal transduction pathway is not yet clear, because the [spe-12](#) and [spe-27](#) genes both encode novel proteins ([Minniti et al. 1996](#); J. Nance and A. Minniti, unpubl.).

The [spe-8](#), [spe-12](#), and [spe-27](#) mutants have helped to classify in vitro spermatid activators and determine the sequence of ultrastructural changes that accompany activation. Monensin and TEA activate [spe-8](#), [spe-12](#), and [spe-27 spermatids](#) (from either males or hermaphrodites) normally ([Shakes and Ward 1989a](#); [Minniti et al. 1996](#)). In contrast, Pronase ([Shakes and Ward 1989a](#); [Minniti et al. 1996](#)) causes these [spermatids](#) to arrest as a spiky intermediate ([Fig. 1F](#)). DIDS efficiently stimulates formation of spikes on [spe-8 spermatids](#) and not on other members of this group ([Machaca et al. 1996](#)). This spiky intermediate is a transient unstable stage in wild-type sperm (discussed above) that is not preserved with fixatives commonly employed to prepare cells for ultrastructural analyses. In contrast, the spike stage produced by [spe-8](#) or [spe-12 spermatids](#) after Pronase treatment is stable and can be fixed for ultrastructural analyses. These studies revealed that spike extension can precede fusion of the MOs during spermatid activation. Subsequent exposure of Pronase-treated [spe-8](#) or [spe-12 spermatids](#) to TEA, monensin, or TFP allows them to complete differentiation and become apparently normal spermatozoa.

The above data indicate that the [spe-8](#), [spe-12](#), and [spe-27](#) mutants produce [spermatids](#) that do not activate in response to the normal hermaphrodite signal. If provided with the male-derived activator, either in a male or by

insemination of competent seminal fluid, [\*spe-8\*](#), [\*spe-12\*](#), and [\*spe-27\* spermatids](#) activate normally. These data are consistent with two modes of activation, one hermaphrodite-specific and one male-specific. Artificial insemination ([LaMunyon and Ward 1994](#)) of [\*spe-8\*](#) hermaphrodites might provide a means to identify the male activator, since self-sterile hermaphrodites should only produce progeny when injected with a fraction containing the male activator. Direct analysis of an activator candidate could be confirmed by in vitro spermatid activation experiments.

Spermatids in the *C. elegans* hermaphrodite are activated to become spermatozoa as they enter the spermatheca ([Ward and Carrel 1979](#)). This occurs concomitantly with the first ovulation, where the spermatheca is pulled forward over [\*spermatids\*](#) that are between it and the first oocyte (see [Schedl](#), this volume). In mammals, capacitation must occur prior to egg contact for fertilization to occur. This was revealed by in vitro studies showing that freshly ejaculated spermatozoa were incapable of fertilization (Austin 1951; Chang 1951). Capacitation is associated with a number of biochemical changes within the female reproductive tract and takes several hours to complete (for review, see Cohen-Dayag and Eisenbach 1994). There is no evidence that *C. elegans* sperm activation, where the sessile spermatid is converted into a crawling spermatozoon, is in any way analogous to this process. In fact, the [\*spermatids\*](#) produced by a hermaphrodite appear to be activated and capable of fertilization within 1–2 minutes after their entry into the spermatheca (J. McCarter and T. Schedl, pers. comm.). Male-derived *C. elegans* spermatozoa must crawl the length of the hermaphrodite [\*uterus\*](#) and into the spermatheca prior to fertilization, and it is unknown if this journey is associated with capacitation-like changes to the cell. The existence of a capacitation-like phenomenon could be tested by in vitro fertilization, but this procedure has not been developed for *C. elegans*.

Generated from local HTML

# Chapter 11. Spermatogenesis — IV Acquisition and Mechanism of Spermatozoan Motility

---

Nematode spermatozoa differ substantially from vertebrate and many other invertebrate spermatozoa by lacking both a flagellum and acrosome ([Fig. 2](#)) (for review, see Foor 1970, 1983; Heath 1992; Roberts and Stewart 1995). Spermatozoan motility in *C. elegans* and *Ascaris* has been reviewed previously (see, e.g., Ward et al. 1982; [Roberts et al. 1989](#); Roberts and Stewart 1995). The amoeboid motility exhibited by *C. elegans* and other nematode spermatozoa is unusual in that a single pseudopod with a position that is fixed relative to the cell body is employed ([Fig. 2](#)). The availability of both in vitro activators and a suitable medium has permitted detailed in vitro analyses of spermatozoan motility (for review, see Ward et al. 1982). Translocating cells are attached to the substrate by knobs on their pseudopodial surface, whereas the cell body is unattached ([Nelson et al. 1982](#); Roberts and Streitmatter 1984). The pseudopod promotes forward movement by directed bulk membrane flow, which includes glycoproteins and lipids. These movements have been studied by nonspecific probes, such as latex beads and fluorescent lipid probes ([Roberts and Ward 1982a,b](#)), as well as by monoclonal antibodies to membrane proteins (Pavalko and Roberts 1987, 1989). The results all indicate that membrane components are inserted at the tip of pseudopodial projections and move back toward the junction of the cell body and pseudopod. The rate of bulk membrane flow closely approximates the rate of forward movement (~20–30 μm per minute). It is not known if surface components are internalized and recycled.

## A. Major Sperm Protein and the Cytoskeleton

Nematode spermatozoa are unusual among crawling cells in that they lack appreciable amounts of most conventional cytoskeletal proteins (for review, see [Roberts et al. 1989](#)). In *C. elegans*, less than 0.02% of sperm protein is actin, no microfilaments can be detected, and there is no detectable myosin in bulk preparations of [spermatids](#) or spermatozoa. The trace amount of actin probably resides mostly within the few [spermatocytes](#) that always contaminate spermatid preparations, although small dots of staining are also detected in pseudopods ([Nelson et al. 1982](#)). Spermatozoan motility is unaffected by cytochalasin B, D, or E under conditions where [spermatocytes](#) (which do contain actin) do not properly divide. *C. elegans* [spermatids](#) and spermatozoa also do not have microtubules except those that form the pair of centrioles (Wolf et al. 1978; [Ward et al. 1981](#); Ward 1986). Not surprisingly, the tubulin-depolymerizing drugs colchicine and oncobendazole are without effect on spermatozoan motility. Yet, as mentioned above, the vigorous surface movements and remodeling of the *C. elegans* pseudopod that occur as the cell moves forward suggest cytoskeleton-mediated membrane flow.

Electron microscopic examination of the pseudopod reveals a dense, granular cytoplasm devoid of organelles, which are confined to the cell body ([Fig. 2](#)). Under certain conditions of preparation for ultrastructural analyses, it is possible to observe approximately 2-nm filaments that form a loose meshwork within the granular cytoplasm (Roberts 1983). One of the major components of the pseudopod is MSP (Ward and Klass 1982; Roberts et al. 1986), a protein that comprises about 10–15% of total sperm protein (Klass and Hirsh 1981). The multigene family that encodes the *C. elegans* MSPs has been extensively analyzed and is highly conserved (Burke and Ward 1983; Klass et al. 1984, 1988; Ward et al. 1988). Unfortunately, the small size and dense distribution of fine filaments within the pseudopod have made it difficult to use immunogold localization to determine the identity of the 2-nm filaments *in vivo*. However, polyclonal (Klass and Hirsh 1981) and monoclonal (Roberts et al. 1986) antibodies to *C. elegans* MSP cross-react with similar proteins in *Ascaris* (for review, see [Roberts et al. 1989](#)). In *Ascaris*, anti-MSP antibodies decorate filament bundles in the pseudopod that extend into substrate contact areas and play a dynamic part in cell motility (Sepsenwol et al. 1989).

Purified *Ascaris* MSP will assemble into 11-nm filaments in vitro ([King et al. 1992, 1994a; Stewart et al. 1994](#)). Filament assembly is pH-sensitive (Roberts and King 1991), and a pH gradient in the *Ascaris* pseudopod might modulate MSP assembly and filament/membrane interactions *in vivo* (King et al. 1994b). The sequence of MSPs from *Ascaris* (Bennett and Ward 1986; King et al. 1992) is 82% identical to the deduced consensus derived from *C. elegans* MSP gene sequences (Bennett and Ward 1986; Ward et al. 1988). Preliminary data suggest that *C.*

*elegans* MSP proteins also assemble into filaments in vitro (M. Smith et al., pers. comm.). *Ascaris* MSP filament bundles move retrograde (from the pseudopodial tip toward the cell body) with a velocity that is similar to the retrograde movement of pseudopodial surface components ([Roberts and Ward 1982a,b](#); Royal et al. 1995). Membrane components isolated from the leading edge of the pseudopod appear to facilitate MSP assembly into filament bundles in vitro (Italiano et al. 1996). These bundles are then capable of moving vesicles and, as is true in vivo for both *C. elegans* ([Ward et al. 1983](#)) and *Ascaris* (Roberts and King 1991), motility is dependent on ATP production. These observations suggest that an ATPase(s) and/or kinase(s) plays an important part, but no candidate proteins have yet been identified from either species.

MSP association with membranes appears to be analogous to actin association with membranes in other amoeboid cells (for review, see [Condeelis 1993](#)), with some important differences. Unlike actin, the ATP requirement for MSP filament function is indirect, since the protein does not contain a nucleotide-binding consensus motif (King et al. 1992) and does not seem to bind ATP in solution (J.E. Italiano and P. Fajer, unpubl.). The sperm MSP cytoskeleton also has no known analog of myosin, which can cross-link actin filaments and provide contractile activity in many types of cells (for review, see Ruppel and Spudich 1995). However, myosin might have a secondary role in membrane expansion during amoeboid movement (for review, see Zigmond 1993), and actual protrusive activity could be based on specific actin filament–membrane interactions, as is the case for MSP-membrane interactions (Italiano et al. 1996). How membrane interactions lead to actin-based protrusion in amoeboid cells is unclear. For instance, ponticulin is the membrane protein that accounts for nearly all actin-plasma membrane interactions in *Dictyostelium*, but mutants lacking this protein can still crawl (Shariff and Luna 1990; Chia et al. 1993; Hitt et al. 1994).

## B. Mutants Defective in Motility

In most *spe* mutants, sperm are defective in motility because they fail to make pseudopods. However, a few mutants make sperm that exhibit defective motility despite extending pseudopods. Such motility-defective sperm have cytological defects in either MOs (caused by [fer-1](#) or [spe-10](#) mutation) or perinuclear material (caused by [fer-2](#), [fer-3](#), or [fer-4](#) mutation). However, the connection between these defects and motility, if any, is unclear ([Ward et al. 1981](#); [Shakes and Ward 1989b](#)). Abnormally short pseudopods are present on [fer-1](#) and [spe-10](#) spermatozoa. These pseudopods do not move properly in either mutant, and neither [fer-1](#) nor [spe-10](#) spermatozoa crawl across the substrate in vitro. [fer-1](#) spermatozoa appear to be defective in the directed membrane flow characteristic of wild-type spermatozoan motility ([Roberts and Ward 1982a,b](#)). Latex beads bound to the pseudopodial surface of [fer-1](#) sperm frequently move randomly and can move across the pseudopod/cell body junction; beads on pseudopods of wild-type cells always move from tip to pseudopod/cell body junction and never cross this junction. Short pseudopods per se do not preclude active motility. [spe-17](#) spermatozoa are only about 66% wild type in size and have abnormally short pseudopods, yet they are able to crawl in vitro and in vivo ([Shakes and Ward 1989b](#); [L'Hernault et al. 1993](#)). [fer-2](#) spermatozoa either lack pseudopods or have pseudopods of variable morphology, for example, short or helically twisted ([Ward et al. 1981](#)). [fer-3](#) and [fer-4](#) mutant sperm make pseudopods that frequently appear normal ([fer-3](#)) or have abnormally few pseudopodial projections ([fer-4](#)) ([Ward et al. 1981](#)). Lectin-binding experiments with [fer-2](#), [fer-3](#), and [fer-4](#) sperm reveal that membrane glycoproteins move much more slowly across the pseudopodial surface of any of the three mutants when compared to wild-type cells ([Argon 1980](#); [Nelson et al. 1982](#); [Roberts and Ward 1982b](#)).

# Chapter 11. Spermatogenesis — V Role of Motility During Oocyte Recognition

---

## A. Fertilization

The motility described above is essential for spermatozoa to function properly before and during penetration of the oocyte. Both hermaphrodite and male-derived spermatozoa wait in the spermatheca for an oocyte to be ovulated through this structure, which is the site of spermatozoon-oocyte recognition and fusion ([Ward and Carrel 1979](#); [Kemphues and Stone](#), this volume). Hermaphrodite-derived spermatozoa are placed into the spermatheca when the gonad begins to produce oocytes. Male-derived spermatozoa crawl toward the spermatheca after insemination during mating. The spermatheca has complex infolds of its surface, and spermatozoa seem to attach to its walls and extend pseudopodial processes into these infolds ([Ward and Carrel 1979](#); [Shakes and Ward 1989a](#)). Fertilization occurs rapidly after gamete contact, and the resulting fertilized egg exits the spermatheca. Since the spermatheca is not much larger in volume than an oocyte, a number of spermatozoa can be carried into the [uterus](#) on the surface of the egg during its exit. These spermatozoa are observed to crawl back rapidly into the spermatheca and re-attach to its walls to await the next ovulated oocyte. Thus, motility is required to maintain proper position because spermatozoa that become displaced from the spermatheca crawl back into this structure.

## B. Mutants Defective in Oocyte Recognition

Any mutant that produces sperm incapable of proper movement will be fertilization-defective. Most such mutants, as described above, have some type of cytologically visible defect. However, sperm-defective mutants in either [spe-9](#), [spe-13](#) ([L'Hernault et al. 1988](#)), [spe-16](#) ([Shakes 1988](#); K. Hill and S. L'Hernault, unpubl.), or [fer-14](#) ([Nelson et al. 1982](#); [Roberts and Ward 1982b](#)) have superficially normal cytology and motility, yet they are incapable of fertilizing an oocyte when they contact it. Spermatozoa defective in [spe-9](#) and [spe-13](#) are rapidly displaced from the hermaphrodite spermatheca into the [uterus](#) by passing oocytes. These displaced mutant spermatozoa do not efficiently crawl back into the spermatheca ([L'Hernault et al. 1988](#); K. Mercer et al., unpubl.). In contrast, male-derived [spe-9](#), [spe-13](#), and [spe-16](#) spermatozoa target toward and crawl into the spermatheca, suggesting that they, like wild-type spermatozoa, are attracted to this structure. Whether these male-derived spermatozoa are similar to hermaphrodite-derived spermatozoa in being displaced by passing oocytes is not known (K. Mercer et al., unpubl.). Establishment of the molecular identity of these *C. elegans* *spe* gene products will reveal if they are similar to mammalian spermatozoan proteins involved in fertilization (Wasserman 1995).

Generated from local HTML

## Chapter 11. Spermatogenesis — VI Future Prospects

---

Although many aspects of *C. elegans* sperm development and motility have been described, much remains to be answered. Many genes affect sperm cell division, yet how these genes interact to specify proper cell division is not clear. Segregation of cellular components during spermatogenesis has been studied by genetic, cytological, and electrophysiological methods. These diverse approaches could be integrated, for example, to identify mutants defective in ion channel segregation during spermatogenesis. Many substances cause in vitro spermatid activation, but their relevance is unclear because the in vivo activators need to be identified. The spermatozoon has a novel motility mechanism, and further analysis should reveal how it is utilized to locate and fertilize oocytes. Perhaps the most important future challenge is to order the many known *spe* mutants into pathways by analyzing double mutants, suppressors, and other gene interactions.

Generated from local HTML

## **Chapter 11. Spermatogenesis — Acknowledgments**

---

The author thanks Drs. Samuel Ward and Thomas Roberts and their laboratories for communicating unpublished data and many helpful suggestions for this manuscript. The author also thanks members of his laboratory and two anonymous reviewers for helpful editorial suggestions. Work in the author's laboratory is supported by National Institutes of Health and National Science Foundation grants.

Generated from local HTML

# **Chapter 12. Male Development and Mating Behavior**

---

## **Contents**

[I Introduction and Overview of Male Anatomy](#)

[II Behavior](#)

[III Development](#)

[IV Concluding Remarks](#)

[Acknowledgments](#)

Generated from local HTML

# Chapter 12. Male Development and Mating Behavior — I

## Introduction and Overview of Male Anatomy

The complexity of the anatomy and mating behavior of *Caenorhabditis elegans* males poses a variety of interesting questions in neurobiology and developmental biology. The mating structures of the [male tail](#) differ in form between nematode species and hence provide an opportunity to study the determinants of morphology and their evolution. The fact that the male is dispensable for laboratory culture makes genetic analysis of the male attractive because strains can be easily maintained as hermaphrodites, and their defective males can be studied. In particular, mutant males are often examined as the progeny of Him ([high incidence of males](#)) hermaphrodites (Hodgkin et al. 1979), which segregate XO male progeny by X chromosome nondisjunction during meiosis. We discuss here the major features of male development and behavior and those aspects that have been analyzed most intensively. We begin with an overview of male anatomy, discuss mating behavior, and then discuss the development of each structure. [Table 1](#) summarizes the male-specific [neurons](#), [Table 2](#) summarizes the other cells discussed in this chapter, and [Table 3](#) summarizes the genes discussed in this chapter.

The male anatomy differs from that of the hermaphrodite in that the male has a single-armed [somatic gonad](#) of only 55 cells as well as 41 specialized muscles, 79 additional [neurons](#) (87 sex-specific; [White et al. 1976](#); [Sulston et al. 1980](#)), 36 extra neuronal support cells (socket and sheath cells), 23 [proctodeal cells](#), and 16 hypodermal cells associated with mating structures. Most of these cells are located in the [tail](#), which is composed of an elongated bursa, cuticularized fan (caudal alae), and [proctodeum](#) (Fig. 1). Nine pairs of sensory rays (caudal papillae) are embedded in the fan. The two spicules, each with two [sensory neurons](#), and the [gubernaculum](#) are in the [proctodeum](#). Specialized muscle cells attach to the spicules and the [gubernaculum](#) (sclerotized cuticle secreted by the [proctodeum](#)) that guides the spicules as they are protracted. In addition, there are longitudinal, diagonal, and caudal muscles in the posterior body region and [tail](#). The hook and associated sensillae are located just anterior to the [cloaca](#), whereas the two postcloacal sensillae are located posterior to the [cloaca](#). The J-shaped gonad consists of a [testis](#), [seminal vesicle](#) and valve region, and [vas deferens](#)/ejaculatory duct that connects to the [cloaca](#). There is also one male-specific sensory [neuron](#) in each of the four cephalic [sensilla](#) in the head (Ward et al. 1975). The [male nervous system](#) has not been fully reconstructed (see [Sulston et al. 1980](#)).

## Figures



## Figure 1

Male anatomy. (A) Ventral view of an adult [male tail](#) (anterior is to the left). (1–9) The nine pairs of sensory rays. (B) Lateral view of a [male tail](#) (ventral is down). The left spicule, fan, hook, and postcloacal sensillae (p.c.s.) are indicated. (C) Plumbing of the [male reproductive system](#) and [proctodeum](#). Sperm are stored in the [seminal vesicle](#) anterior to the “valve” region. The [vas deferens](#) connects the [seminal vesicle](#) to the [proctodeum](#). The lumen of the [intestine](#) connects to the [proctodeum](#). The [anal](#) sphincter surrounds the recto-intestinal valve and shuts off the opening during mating.

## Tables

**Table 1** Male-specific [neurons](#) and their roles in mating behavior

Neuron	Structure	Class	Role
CAn	ventral cord	motor	?
CPn	ventral cord	motor	turning
CEMn	head	sensory	?

<b>Neuron</b>	<b>Structure</b>	<b>Class</b>	<b>Role</b>
DXn		motor	?
DVE		inter	?sperm activation or transfer
DVF		inter	?sperm activation or transfer
EFn			turning
<u>HOA</u>	hook	sensory	vulval location
<u>HOB</u>	hook	sensory	vulval location
PCA	p.c.s.	sensory	vulval location
PCB	p.c.s.	sensory	vulval location
PCC	p.c.s.	sensory	vulval location
<u>PDC</u>	p.a.g.	inter	?
<u>PGA</u>	p.a.g.	inter	?
<u>PVV</u>	p.a.g.	inter	?
<u>PVY</u>	p.a.g.	inter	backing
R1A	ray	sensory	dorsal response?
R1B	ray	sensory	dorsal response?
R2A	ray	sensory	ventral response?
R2B	ray	sensory	ventral response?
R3A	ray	sensory	?
R3B	ray	sensory	?
R4A	ray	sensory	ventral response?
R4B	ray	sensory	ventral response?
R5A	ray	sensory	dorsal response?; turning?
R5B	ray	sensory	dorsal response?
R6A	ray	sensory	?
R6B	ray	sensory	?
R7A	ray	sensory	dorsal response?; turning?
R7B	ray	sensory	dorsal response?; turning?
R8A	ray	sensory	ventral response?; turning?
R8B	ray	sensory	ventral response?; turning?
<u>R9A</u>	ray	sensory	turning?
R9B	ray	sensory	turning?
SPC	spicule	motor/proprio	necessary for spicule insertion
SPD	spicule	sensory	necessary for spicule insertion
SPV	spicule	sensory	inhibits ejaculation

A question mark indicates not known or tentative assignment. Due to partial redundancy, many of the [ray neurons](#) cannot be assigned specific roles by the behavioral assays so far employed.

**Table 2Prominent male blast cells**

L1 blast cell	Late blast cell	Notable progeny
Z1, Z4	VD, SV	gonad somatic structures, linker cell
M	SM	sex muscles, coelomocyte
P	Pn.p (n = 9–11),	hook, <a href="#">interneurons</a> , CA, CP Pn.aap (n = 3–11)
V5, V6, T	Rn (n = 1–9)	rays
B	α, β, γ, δ, ε, ζ, <a href="#">B.pa</a> , <a href="#">B.pp</a>	spicules
Y	<a href="#">Y.p</a>	postcloacal sensilla
U, F	U.x, F.x	killer of linker cell, <a href="#">neurons</a>

**Table 3 Some genes controlling male development and behavior**

Gene	Product/homologs	Lineage	Role
<a href="#">cat-1</a>		behavior	turning
<a href="#">cat-2</a>		behavior	turning
<a href="#">cat-4</a>		behavior	turning
<a href="#">che-2</a>		behavior	response to contact
<a href="#">che-3</a>		behavior	response to contact
<a href="#">che-10</a>		behavior	response to contact
<a href="#">cod-1</a>	n.d.	behavior	spicule insertion
<a href="#">cod-2</a>	n.d.	behavior	spicule insertion
<a href="#">cod-4</a>	n.d.	behavior	spicule insertion
<a href="#">cod-5</a>	n.d.	behavior	turning
<a href="#">cod-6</a>	n.d.	behavior	spicule insertion
<a href="#">cod-7</a>	n.d.	behavior	spicule insertion
<a href="#">cod-8</a> ,	n.d.	behavior	spicule insertion (synthetic)
<a href="#">cod-9</a>			
<a href="#">cod-10</a>	n.d.	behavior	response to contact
<a href="#">cod-11</a>	n.d.	behavior	turning, SM migrations
<a href="#">cod-12</a>	n.d.	behavior	<a href="#">vulva</a> location
<a href="#">cod-13</a>	n.d.	behavior	<a href="#">vulva</a> location
<a href="#">cod-14</a>	n.d.	behavior	<a href="#">vulva</a> location
<a href="#">cod-15</a>	n.d.	behavior	<a href="#">vulva</a> location
<i>cod-16</i>	n.d.	behavior	response to contact
<a href="#">daf-4</a> receptor	TGF-β type II	rays 5, 6, 7	specification of ray identity
<a href="#">daf-10</a>	n.d.		response to contact
<a href="#">daf-19</a>	n.d.		response to contact
<a href="#">egl-5</a>	Hox class txn factor	multiple	anterior-posterior patterning in ventral and lateral epidermis
<a href="#">egl-44</a>	n.d.		backing

<b>Gene</b>	<b>Product/homologs</b>	<b>Lineage</b>	<b>Role</b>
<a href="#"><i>egl-45</i></a>	n.d.		backing
<a href="#"><i>goa-1</i></a>	α-subunit of G-protein G <sub>o</sub>	behavior	turning, spicule insertion
<a href="#"><i>let-23</i></a>	tyrosine kinase		induction of anterior fates in <a href="#">B lineage</a>
<a href="#"><i>let-60</i></a>	Ras, small G-protein	B	induction of anterior fates in <a href="#">B lineage</a>
<a href="#"><i>lin-1</i></a>	ets domain txn factor	B	promotes posterior fates in <a href="#">B lineage</a>
<a href="#"><i>lin-3</i></a>	EGF-like growth factor	B	induces anterior B.axxx
<a href="#"><i>lin-12</i></a>	receptor	<a href="#">B.p</a>	promotes <a href="#">B.pa</a> fate
		hook	promotes 2 <sup>o</sup> p.a.g. lineage
		Bγ/δ	promotes Bδ fate
<a href="#"><i>lin-14</i></a>	txn factors	multiple	stage-specific timing of events
<a href="#"><i>lin-15</i></a>	two novel proteins	B	negative regulation of <a href="#"><i>let-23</i></a> in <a href="#">B lineage</a>
		hook	promotes 3 <sup>o</sup> fate
<a href="#"><i>lin-17</i></a>	frizzled	Z,P,M,T,B	asymmetric cell division
<a href="#"><i>lin-22</i></a>	hairy bHLH transcription factor	seam	inhibits ray production
<a href="#"><i>lin-32</i></a>	achaete/scute bHLH txn factor	seam	specifies neuroblast cell fate
<a href="#"><i>lin-44</i></a>	signaling protein/Wnt	B,T, etc.	orients cell division, expressed by <a href="#">hyp8-11</a>
<a href="#"><i>lin-45</i></a>	Raf serine/threonine kinase	B	induction of anterior fates in <a href="#">B lineage</a>
<a href="#"><i>lin-48</i></a>	n.d.	F and U	
<a href="#"><i>lin-49</i></a>	n.d.	F and U	
<a href="#"><i>mab-3</i></a>	n.d.		male specification in <a href="#">tail</a> and gut
<a href="#"><i>mab-5</i></a>	Hox class txn factor	V5,V6,P	anterior-posterior patterning in ventral and lateral epidermis
<a href="#"><i>mab-9</i></a>	n.d.	B,F	cell fate determination
<a href="#"><i>mab-18</i></a>	Pax-6 txn factor	ray 6	necessary for ray 6 identity
<a href="#"><i>mab-19</i></a>	n.d.	T	specification of cell fates, division polarity
<a href="#"><i>mab-20</i></a>	n.d.	V5, V6	ray identity specification
<a href="#"><i>mab-21</i></a>	novel	ray 6,	ray 6 identity,
	T.apapa		hypodermal fate of T.apapa
<i>mab-26</i>	n.d.	V5, V6	ray identity specification
<a href="#"><i>mig-5</i></a>	n.d.		<a href="#">P12</a> fate
<a href="#"><i>plg-1</i></a>			allows mating plug
<a href="#"><i>ram-1</i></a>	n.d.		ray morphology
<a href="#"><i>ram-2</i></a>	n.d.		ray morphology
<a href="#"><i>ram-3</i></a>	n.d.		ray morphology
<a href="#"><i>ram-4</i></a>	n.d.		ray morphology
<a href="#"><i>ram-5</i></a>	n.d.		ray morphology

<b>Gene</b>	<b>Product/homologs</b>	<b>Lineage</b>	<b>Role</b>
<u><a href="#">sem-5</a></u>	SH3-SH2-SH3 adaptor	B	induction of anterior fates in
protein			<u><a href="#">B lineage</a></u>
<u><a href="#">sma-2</a></u>	novel, called DWARFIN	rays 5, 6, 7	specification of ray identity
<u><a href="#">sma-3</a></u>	novel, called DWARFIN	rays 5, 6, 7	specification of ray identity
<u><a href="#">sma-4</a></u>	novel, called DWARFIN	rays 5, 6, 7	specification of ray identity
<u><a href="#">unc-4</a></u>	Hox class txn factor	nerve chords	fail to back during mating
<u><a href="#">unc-6</a></u>	netrin	nerve chords	fail to back during mating
<u><a href="#">vab-3</a></u>	Pax-6 txn factor	B,V,T	ray specification; <u><a href="#">B.a</a></u> specification

txn indicates transcription; see text for references.

n.d. indicates not determined.

Generated from local HTML

## Chapter 12. Male Development and Mating Behavior — II Behavior

Male copulatory behavior is composed of a series of sub-behaviors, which are under separate neuronal and genetic control. For a description of mating behavior, see [Liu and Sternberg \(1995\)](#), Dusenbery (1980a), Ward and Carrel (1979), Baird et al. (1992), and Loer and Kenyon (1993). Although the hermaphrodites are behaviorally passive during the mating process (males will successfully mate with paralyzed hermaphrodites), there are cues from the hermaphrodite for at least several of the steps of mating behavior. The mating process is depicted in [Figure 2](#). A male responds to contact with a hermaphrodite by apposing his tail against her body; he moves backward until he approaches the end of the hermaphrodite, at which time he turns and continues backing until he locates the [vulva](#). At the [vulva](#), he inserts his [copulatory spicules](#) and forms a seal with his [cloaca](#) apposed to the [vulva](#); he then transfers sperm and seminal fluid, retracts his spicules, and moves away. A simple scheme relating the cues that elicit male behavior to the male sensory structures through which they likely act is shown in [Figure 3](#).

Although mating behavior follows a stereotypical series of steps, some of the early steps in the behavior are not obligatory. If a male locates the [vulva](#) prior to reaching the head or tail of the hermaphrodite, turning behavior is obviated. If a male is forced to back into a hermaphrodite such that the ventral surface of his tail contacts her, he will initiate backing and search for the [vulva](#), even if unable to respond to contact with the hermaphrodite without help.

### A. Sensory Contact

The question of whether males actively seek hermaphrodites (taxis) or just accumulate once they are in the vicinity (kinesis) is open. However, it is clear that there is a chemical signal of some sort: Males will accumulate at hermaphrodites (E. Jorgensen; J. Sulston; both pers. comm.) or at agar conditioned with *C. elegans* hermaphrodites or females of another *Caenorhabditis* species (K. Liu et al., unpubl.), which appear to be a stronger source of attraction to *C. elegans* males than are *C. elegans* hermaphrodites. In many other nematode species, a mutual attraction exists between males and females (for review, see Anya 1976; see, e.g., Duggal 1978).

Males sense contact with the hermaphrodite via their sensory rays. In the absence of the dorsally opening rays (ray 1, ray 5, and ray 7; [Sulston et al. 1980](#)), males fail to respond to dorsal contact ([Liu and Sternberg 1995](#)). In the absence of the ventrally opening rays (ray 2, ray 4, and ray 8), the males still respond to ventral contact, using other ventrally located sensillae (hook or [postcloacal sensilla](#) or spicules).

The rays have apparent chemosensory openings, but their elongated structure raises the possibility that they are mechanosensory ([Sulston et al. 1980](#)). One argument for a chemosensory role is that mutations which disrupt other mechanosensory behaviors do not eliminate response to contact, whereas some but not all mutations that disrupt chemosensory responses (chemosensory-defective, Che; osmotic-avoidance-defective, Osm; or dye-filling defective, Dfy; see, e.g., Starich et al. 1995) eliminate response ([Hodgkin 1983](#); K. Liu et al., in prep.). Moreover, most of the copulation-defective (Cod) mutants with defects in response to contact are defective in uptake of dye by amphid and [phasmid neurons](#), indicative of a general chemosensory defect (K. Liu et al., in prep.).

### B. Backing

Males place their ventral side against the hermaphrodite and move backward. The [PVY interneuron](#) ([Sulston et al. 1980](#)) is required for continued backing (K. Liu and P. Sternberg, in prep.). Mutants defective in backing due to motor system defects ([unc-4](#), [unc-6](#) mutants) result in failure to back, suggesting that at least the [ventral cord motor neurons](#) are required. Although males will initially respond to themselves and chunks of agar, they do not persist in backing beyond a few seconds. Thus, it is likely that males respond to a nonspecific cue, but they then require a hermaphrodite-specific cue to maintain the backing behavior.

### C. Turning

Males turn at approximately 10% or 90% hermaphrodite body length if they have not yet located the [vulva](#). Turning occurs at the appropriate body position on long mutant hermaphrodites and thus is not controlled by a preset time or distance (K. Liu, pers. comm.). Turning involves recognition of the approaching end of the hermaphrodite (either by tapering or by end-specific chemosensory cues) and a coordinated and well-timed ventral flexure, followed by relaxation of the turn.

A subset of the sensory rays are necessary for the turn, although it has not been determined precisely which ones are necessary. Ablation of the posterior three rays on each side prevents turning: The males move backward off the end of the hermaphrodite. Ablation of the presumed dopaminergic [ray neurons](#) R5A, R7A, and [R9A](#) results in abnormal “loose” turns; a similar defect is seen in [cat-2](#) males, which have reduced dopamine ([Sulston et al. 1975](#); K. Liu et al., in prep.; cf. [Loer and Kenyon 1993](#)). Ablation of the EF [interneurons](#) results in males backing to the end of the hermaphrodite and stopping without initiating a turn (K. Liu and P. Sternberg, in prep.), suggesting that the ray [sensory neurons](#) involved in turning might act via the EF [interneurons](#).

CP motor [neurons](#) express serotonin and are necessary for normal turning behavior ([Loer and Kenyon 1993](#)). Exogenously supplied serotonin stimulates [tail](#) curling (ventral flexure) and rescues the lack of ventral flexure in [cat-4](#) mutants, which do not synthesize serotonin ([Sulston et al. 1975](#)). The diagonal muscles contribute to the ventral flexure of the [male tail](#) ([Loer and Kenyon 1993](#); K. Liu et al., in prep.). The simplest hypothesis is that [CP neurons](#) stimulate the diagonal muscles. Loer and Kenyon (1993) argue that the [CP neurons](#) might also indirectly inhibit dorsal [body wall muscle](#). Males without diagonal muscles still respond somewhat to serotonin, indicating another role for [CP neurons](#) (or other serotonergic [neurons](#)). CP-ablated males are less defective in turning than are sex-muscle-defective males, suggesting that there is another input to the sex muscles ([Loer and Kenyon 1993](#)).

## D. Vulval Location and Spicule Insertion

Vulval location is mediated through three sensillae ([Liu and Sternberg 1995](#)). The male locates the approximate position of the [vulva](#) using the hook [sensilla](#) and then uses the spicules and the postcloacal sensillae (p.c.s.) to locate the [vulva](#) precisely. A simple model is that the p.c.s. potentiates spicule function. In the absence of the hook [sensilla](#), the male circles the hermaphrodite for several minutes and then backs slowly and protracts his spicules until the [vulva](#) is located. This apparently alternative search mode may well be an expansion of a normal aspect of vulval location. The postcloacal sensillae are required for the initiation of this slow search, suggesting that the postcloacal sensillae trigger the search mediated by the spicules. Both [HOA](#) and [HOB sensory neurons](#) are required for locating the [vulva](#), suggesting that there might be two or more cues. The three p.c.s. [sensory neurons](#) are partially redundant: Ablation of one [neuron](#) results in a less severe defect than ablation of two or all three [neurons](#) ([Liu and Sternberg 1995](#)). The relative role of chemosensation and mechanosensation in locating the [vulva](#) is an open question; both may be involved.

Spicule insertion requires the SPD sensory [neuron](#) and the SPC motor neuron ([Liu and Sternberg 1995](#)) and the spicule protractor muscles ([Sulston et al. 1980](#); K. Liu et al., in prep.). Since the spicules are used in vulval location, the separation of these “steps” in behavior is somewhat arbitrary.

## E. Sperm Transfer and Spicule Withdrawal

A signal from the hermaphrodite [uterus](#) appears to be necessary for sperm release. Males lacking the SPV [neuron](#) ejaculate prematurely if near the [vulva](#) ([Liu and Sternberg 1995](#)). This suggests that the SPV inhibits sperm release, and a signal inhibits the activity of SPV. Males will insert their spicules but will not release sperm into hermaphrodites lacking a gonad (K. Liu, pers. comm.). Since SPD and SPC are necessary for premature ejaculation, there must also be a positive input (see [Fig. 3](#)).

The mechanism of sperm transfer is relatively unknown. There is no known [neural](#) connection to the gonad, and thus there might be humoral factors (e.g., neuropeptides) that trigger sperm release from the [seminal vesicle](#); another possibility is that sperm release acts via body wall muscles. The sperm are stored in the [seminal vesicle](#) ([Hirsh et al. 1976](#); [Ward and Carrel 1979](#)).

Defecation ceases during mating (K. Liu, pers. comm.). The periodicity of defecation in males when not mating is less regular than in hermaphrodites (J. Thomas; K. Liu; both pers. comm.). The [anal](#) sphincter, which surrounds the intestinal-rectal valve, not only closes off the [intestine](#) during ejaculation, but also pulls it dorsally out of the way of the [vas deferens](#) ([Sulston et al. 1980](#)). The sphincter is helpful but not essential for sperm release ([Sulston et al. 1980](#)).

The spicules remain inserted for approximately 25–30 seconds after ejaculation, for males paired with paralyzed hermaphrodites. In [plg-1](#) strains (variants of *C. elegans* that have the capacity to deposit a copulatory plug) and other *Caenorhabditis* species, the male deposits a copulatory plug during this time ([Barker 1994](#); [Liu and Sternberg 1995](#); J. Hodgkin, pers. comm.). Withdrawal of the spicules takes approximately 20 seconds and presumably requires the spicule retractor muscles.

## F. Genetic Analysis

Genetic analysis of mating behavior began with [Hodgkin \(1983\)](#), who screened for mating-defective male strains and characterized those with abnormal morphology (*mab*; [male abnormal](#)). In addition, he described the efficiency of mating (the number of progeny sired by a male in a given time period) of most extant mutant strains. Using a Hodgkin-style screen, new genes have been defined by mutations that disrupt mating behavior but in general do not affect morphology (K. Liu et al., in prep.). Additional genes were identified in a screen in which the ability of males to deposit a copulatory plug was used to assay successful mating. About three quarters of the Cod ([copulation defective](#)) strains failed to backcross as single gene traits, indicating that many genes with partial mating defects exist. This result is not surprising given the results of [Hodgkin \(1983\)](#), who demonstrated that most mutants have at least a partial defect in the efficiency of male copulation, and of [Liu and Sternberg \(1995\)](#), who demonstrated that there is considerable redundancy in the sensory control of male mating behavior. On the basis of the fact that most loci are identified by single alleles, it is likely that many genes involved in male mating remain to be discovered.

[che-2](#), [che-3](#), [che-10](#), [cod-10](#), [cod-16](#), [daf-10](#), and [daf-19](#) mutants are defective in response to contact. [egl-44](#), [egl-45](#), and [unc-4](#) mutants are defective in backing. [cod-5](#), [cod-11](#), [cat-1](#), [cat-2](#), and [cat-4](#) mutant males are defective in turning. [cod-12](#), [cod-13](#), [cod-14](#), and [cod-15](#) mutant males are defective in vulval location. [cod-1](#), [cod-2](#), [cod-4](#), [cod-6](#), and [cod-7](#) are defective in spicule insertion. Some *cod* mutants have defects in more than one gene. One strain defective in spicule insertion has been shown to harbor mutations in two unlinked loci, [cod-8](#) and [cod-9](#).

Many of the *cod* mutations analyzed so far affect single steps in mating behavior. For example, the [cod-1](#) mutation disrupts spicule insertion but not response, turning, and vulval location; steps subsequent to spicule insertion have not been examined. This genetic separability supports the dissection of mating behavior into component steps based on the cell ablation experiments discussed above. These results suggest that there might be genes specific to individual steps in mating behavior. However, it is not known whether these *cod* mutations represent complete loss-of-function alleles, a necessary prerequisite to addressing whether the *cod* genes are specific to male mating behavior.

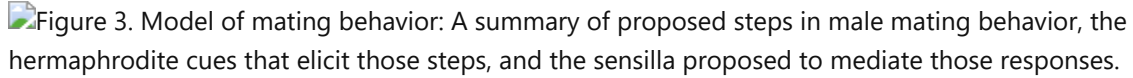
Only one *cod* mutant has been molecularly analyzed: [goa-1](#) was cloned as a *C. elegans* homolog of the  $\alpha$ -subunit of the heterotrimeric G- protein  $G_o$  ([Lochrie et al. 1991](#)). [goa-1](#) mutants were identified by their Cod phenotype, by altered movement, and by polymerase chain reaction (PCR)-based detection of a transposon insertion ([Mendel et al. 1995](#); [Ségalat et al. 1995](#)). This broadly expressed G-protein is required for both turning and spicule insertion ([Mendel et al. 1995](#)).

## Figures

Figure 2. Sequence of steps in male mating behavior.

## Figure 2

Sequence of steps in male mating behavior. (A) Response to contact with the hermaphrodite. Male arches the posterior third of his body and apposes the ventral side of his [tail](#) to her body. (B) Male is shown turning from the dorsal side to the ventral side of the hermaphrodite. The turn is initiated before the male reaches the end of the hermaphrodite and comprises a deep ventral flexion of the [tail](#). (C) Male has located the hermaphrodite [vulva](#). (D) Male has inserted his spicules into the [vulva](#). Bar, 0.1 mm. (Reprinted, with permission, from [Liu and Sternberg 1995](#); copyright by Cell Press.)

Figure 3. Model of mating behavior: A summary of proposed steps in male mating behavior, the hermaphrodite cues that elicit those steps, and the sensilla proposed to mediate those responses.

### Figure 3

Model of mating behavior: A summary of proposed steps in male mating behavior, the hermaphrodite cues that elicit those steps, and the [sensilla](#) proposed to mediate those responses. (A) Males respond by shape or chemosensation to certain structures by apposing [tail](#) to body and initiating backing. This response to contact is mediated by the sensory rays and ventral sensillae. (B) Continued backing requires specific cues from the hermaphrodite, mediated by the sensory rays. (C) Prior to reaching the end of the hermaphrodite, the male turns. This is mediated by sensory rays, probably a distinct subset of the rays that mediate response to contact. (D) Approximate location of the [vulva](#) is sensed by the hook and causes the male to cease backward motion. (E) The male remains in the vicinity of the [vulva](#) via a cue sensed by the postcloacal sensillae (p.c.s.) and protrudes his spicules. This cue might be from the [vulva](#) or the [uterus](#). (F) Spicule protrusion requires SPD. (G) The spicules sense insertion into the [uterus](#), via at least SPV, which inhibits sperm transfer until inhibited by a [uterine](#) signal. Another signal is required to promote sperm release, and this is possibly mediated through SPD. (H) After sperm release, the spicules are retracted. Model based on [Liu and Sternberg \(1995\)](#) and K. Liu and P. Sternberg (in prep.).

Generated from local HTML

## Chapter 12. Male Development and Mating Behavior — III

### Development

---

Although the sex of the embryo is set early (see [Meyer](#), this volume), male and hermaphrodite embryos are nearly identical. The only sex-specific anatomical differences at hatching are the positions of the [coelomocytes](#), the presence of the HSN or CEMs, and the size of the B cell. Most of the differences between male and hermaphrodite adults result from differences in postembryonic development. Certain cells that are terminally differentiated in the hermaphrodite larva are postembryonic blast cells in the male and divide to generate male-specific tissues ([Fig. 4](#)). The major example is the B cell, which is a rectal epidermal cell in the hermaphrodite, but which divides in the male, giving rise to 43 surviving progeny. Other cells divide postembryonically in both sexes but follow different lineages and generate different progeny cells. Examples of this are [Z1](#) and [Z4](#), which give rise to the somatic tissues of the gonad. Finally, some cells undergo different terminal differentiation in the two sexes. For example, the HSN [neurons](#) of the hermaphrodite undergo programmed cell death in the male. Pn.aap ventral chord cells die or differentiate into VC motor [neurons](#) in the hermaphrodite, but they survive, divide once, and differentiate into CA and CP motor [neurons](#) in the male.

Male development appears to utilize many of the same genes as does hermaphrodite development. The differences between the sexes ultimately arise from the action of [tra-1](#), the master control transcription factor at the end of the sex determination pathway. Evidence so far suggests that this gene exerts its influence continuously and at many points in the developmental pathway, rather than by regulating a small number of male-specific or hermaphrodite-specific genes.

How does the postembryonic developmental program generate the male-specific structures necessary to achieve mating? The reconstruction by [Sulston et al. \(1980\)](#) reveals impressively complex sensory, structural, and mechanical components. This complicated cellular machine appears to arise in two stages. In the first stage, cell lineages generate the many epidermal, neuronal, support, and muscle cell types necessary, in nearly their correct relative positions. In the second stage, which occurs primarily during L4, cells terminally differentiate and carry out their fixed roles in morphogenesis. If one asks where in the genetic complement of the organism the information for the overall structure lies, the answer is that much of it must be in the cell fate specification program that generates cells with distinct properties. The remainder is accounted for by the probably largely autonomous morphogenetic activities of individual cells.

#### A. Specification of Cell Fates

Complex postembryonic cell lineages producing the cells of the adult male arise from reproducible cell-cell interactions as well as asymmetric cell divisions. In this section, we discuss mechanisms of cell fate specification for each tissue or lineage separately.

##### 1. Spicules and Proctodeum

The [B](#), [Y](#), [U](#), and [F](#) cells ([Fig. 4](#)) divide postembryonically to generate the spicules, postcloacal sensillae, and [proctodeum](#). Thus, the simple tube that connects the [intestine](#) to the [anus](#) is extensively remodeled to accommodate the connection to the [vas deferens](#) and the addition of the spicules and [gubernaculum](#) (see [Fig. 1C](#)). At hatching, these cells form the anterior ([U](#), [Y](#)) and posterior ([F](#), [B](#)) walls of the [rectum](#) and thus topologically maintain a connection from the [intestine](#) to the [anus](#) throughout development. Remodeling of this region occurs during the L4 lethargus ([Sulston et al. 1980](#)). A series of asymmetric cell divisions and cell-cell interactions specify the fates of these cells and their descendants. In particular, the asymmetric division of the B cell is one of the best understood asymmetric cell divisions. The specification of the intermediate precursor cells at the ten-cell stage of the [B lineage](#) provides a superb example of a network of cell-cell interactions.

The identity of the B cell requires [mab-9](#); in [mab-9](#) mutants, [B](#) acts as does [Y](#), its anterior-ventral neighbor. The B cell is also affected in hermaphrodites ([Chisholm and Hodgkin 1989](#)). [egl-5](#) provides regional specification for the

B cell and is necessary for a complete [B lineage](#) (Chisholm 1991). Whether [egl-5](#) acts early or continuously is an open question.

The B cell divides asymmetrically with a large anterior-dorsal daughter ([B.a](#)) and a smaller posterior-ventral daughter ([B.p](#)) ([Fig. 5A](#)). [B.a](#) generates [all cells](#) of the spicules, and [B.p](#) generates two neurons and four [proctodeal cells](#) ([Sulston et al. 1980](#)). The asymmetry of the B division is controlled by the [lin-44](#), [lin-17](#), and [vab-3](#) genes. [lin-44](#) is necessary for the orientation of the division: In [lin-44](#) mutants, the asymmetric cytokinesis and subsequent lineage are reversed ([Fig. 5B](#)) (Herman and Horvitz 1994). LIN-44 is a member of the Wnt protein family expressed in the posterior epidermis (see [Fig. 7](#)), suggesting that a signal from the posterior acts on [B](#) (Herman et al. 1995). The change in size of the B daughter that correlates with changes in fate implies that specification occurs partially in the B cell itself, rather than solely in the daughters or their progeny. [lin-17](#) is necessary for polarity and asymmetry ([Fig. 5C](#)) ([Sternberg and Horvitz 1988](#)). LIN-17 is a homolog of the *Drosophila* frizzled protein (H. Sawa and R. Horvitz, unpubl.), a transmembrane protein involved in tissue polarity (Park et al. 1994). Thus, it is possible that LIN-17 is the receptor for LIN-44 or that it is required to maintain the polarity and asymmetry of the B cell. [vab-3](#) is necessary for two aspects of the B division ([Fig. 5D](#)) ([Chamberlin and Sternberg 1995](#)): the asymmetry of the B division and the [B.a](#) fate. VAB-3 is a Pax-6 class transcription factor similar to *Drosophila eyeless*, mouse *Small eye*, and human aniridia ([Chisholm and Horvitz 1995](#)). Double-mutant experiments ([Fig. 5E-F](#)) (Herman and Horvitz 1994; [Chamberlin and Sternberg 1995](#)) suggest that LIN-44 acts via LIN-17 to control the polarity of the B-cell division, and LIN-17 controls the [B.a](#) versus [B.p](#) fate via VAB-3. Of course, this represents only the skeleton of a pathway, and many aspects of B asymmetry remain to be elucidated.

LIN-12 controls the fates of [B.pa](#) (which generates two [proctodeal cells](#)) versus [B.pp](#) (which generates [neurons](#), [proctodeum](#), and an apoptotic cell) ([Greenwald et al. 1983](#)). LIN-12 activity is required for the [B.pa](#) fate. [lin-17](#) also acts during the [B.p](#) lineage: In [lin-17](#) animals with normal B divisions, [B.pp](#) often generated fewer progeny, suggesting that LIN-17 acts at the [B.p](#) division and might be required for the [B.pp](#) fate ([Chamberlin and Sternberg 1995](#)). The phenotypes of [lin-12](#) and [lin-17](#) mutations provide an example of how genes are used repeatedly during development for analogous processes.

[B.a](#) divides to form a ring of eight cells, which intercalate to form two rings of four cells each around the [rectum](#). These cells are conveniently called **aa**, **ap**, **pa**, and **pp** on the basis of their ancestry (e.g., [B.alaa](#) and [B.araa](#) are the **aa** cells; [Fig. 6A](#)). A network of cell-cell interactions occurs during this stage, as revealed by cell ablation experiments (Chamberlin and Sternberg 1993). These interactions lead to what is viewed, to a first approximation, as six distinct precursor cell types ( $\alpha$ ,  $\beta$ ,  $\gamma$ ,  $\delta$ ,  $\epsilon$ ,  $\zeta$ ) ([Fig. 6B](#)). Each cell then divides one to three rounds, followed by differentiation or death ([Sulston et al. 1980](#)). Many aspects of these sublineages appear to be autonomous, but this proposal needs to be tested rigorously. In each pair, there is an anterior fate ( $\alpha$ ,  $\gamma$ ,  $\epsilon$ ) and a posterior fate ( $\beta$ ,  $\delta$ ,  $\zeta$ ) ([Fig. 6A](#)).

The anterior fate in each pair is promoted by a signal that requires the [E](#) and [U](#) cells ([Fig. 6C](#)). This signal requires LIN-3, LET-23, SEM-5, LET-60, and LIN-45; the [B lineages](#) of mutants defective in any of these genes resemble those of males that lack [E](#) and [U](#) (Chamberlin and Sternberg 1994). Decreased activity of the LET-23–LET-60 pathway results in anterior to posterior transformation in precursor cell fate, whereas increased activity of the pathway results in posterior to anterior transformation in cell fates. The epidermal growth factor (EGF) domain of LIN-3 expressed under control of a heat shock promoter (Katz et al. 1995) overcomes the lack of [E](#) and [U](#) (Chamberlin and Sternberg 1994). Specification of the [B.a](#) grandprogeny thus has a strong parallel to specification of the vulval precursor cells (see [Greenwald](#), this volume): In both cases, cells are induced by a LIN-3–LET-23–LET-60–LIN-45 pathway. However, there are genes that are specific to vulval induction. Specifically, [lin-2](#), [lin-7](#), and [lin-10](#) are necessary for vulval induction but apparently not spicule formation by the LET-23-mediated pathway (Ferguson and Horvitz 1985). Genes specific to spicule induction might be defined by mutations that affect spicule formation but not vulval induction (see, e.g., Chamberlin 1994).

The posterior fates are promoted by a signal from the [Y.p](#) cell, or more likely its progeny, and by a distinct signal from the other great-grandprogeny of the [B.a](#) cell. Yet another cell-cell interaction appears to be merely an

insulating function, passively preventing one cell from responding to a signal from a third cell: The presence of the **pa** cells prevents the **Y.p** signal from affecting the anterior pp cells (the presumptive  $\gamma$  cell). *lin-15* promotes posterior fates, presumably by negative regulation of LET-23-mediated signal transduction (Chamberlin and Sternberg 1994). The *lin-15* phenotype is suppressed by decreased *let-23* function, as is the case during vulval development (Ferguson et al. 1987; Ferguson and Horvitz 1989; Huang et al. 1994). The **Y.p** signal is likely to impinge on signal transduction downstream from LIN-45 Raf (and possibly far downstream), since *lin-45* mutants do not block the abnormal  $\delta$  fate after **Y.p** ablation (Fig. 6C) (Chamberlin and Sternberg 1994). Thus, *lin-15* is not the mediator of the **Y.p** signal. However, whether the **B.a** signal is equivalent to the *lin-15*-mediated signal is unresolved.

The existence of another signal is inferred from genetic analysis: *lin-12(lf)* and *lin-12(gf)* mutations have opposite effects on the **pp** cells (the  $\gamma/\delta$  pair), with *lin-12(lf)* mutations having two  $\gamma$  fates and *lin-12(gf)* mutations having two  $\delta$  fates (if other cells are ablated); thus, *lin-12* promotes the  $\delta$  fate (Greenwald et al. 1983; Chamberlin and Sternberg 1994). LIN-12-mediated signaling is important, but it can be overridden by LET-23-mediated signaling (the **E** and **U** signal overrides the *lin-12(gf)* effect on the **pp** cells, whereas the anchor cell overrides a *lin-12(gf)* effect on **P6.p** during vulval development [Sternberg and Horvitz 1989; Chamberlin and Sternberg 1994]).

Multiple intercellular signals specify precursor cell types in both hermaphrodite **vulva** and male spicule development. In contrast to the **vulva**, in the case of the **B lineage**, the existence of negative signals acting antagonistically to a LIN-3 inductive signal can be demonstrated by cell ablation, rather than inferred from genetic analysis. *lin-17* also acts late during the **B lineage** affecting the  $\gamma$ ,  $\epsilon$ , and  $\zeta$  lineages (Chamberlin and Sternberg 1995). These sublineages include unequal cell divisions (Fig. 6B) and might require LIN-17. Little is known about the late neurogenesis of the male, but the *cod* mutants with spicule insertion defects might define genes necessary for neuronal cell-type specification.

Comparison of the  $\alpha$  with the  $\beta$ , the  $\gamma$  with the  $\delta$ , and the  $\epsilon$  with the  $\zeta$  lineages (Fig. 6B) leads to the conclusion that a signal through a Ras-mediated signal transduction pathway is not merely stimulating proliferation, but rather controlling alternative cell fates. Specifically, the LET-60 Ras pathway can control the choice of cell fate, but the details of those fates are set by other factors. For these cells, **neurons** are produced only by cells that adopt posterior fates ( $\beta$  and  $\epsilon$ ). Thus, the LET-23–LET-60 pathway acts to inhibit neuronal differentiation.

However, in other aspects of development, notably the specification of the **P11** and **P12** neuroblast (see below), the LET-23–LET-60 pathway controls the types of **neurons** produced, rather than whether **neurons** are produced. Differences exist in the extent of proliferation:  $\alpha$  generates four progeny,  $\beta$  generates six progeny;  $\gamma$  generates six progeny, and  $\delta$  only generates two progeny (Fig. 6B).

The **Y** cell generates the postcloacal sensillae. LIN-12 is necessary to specify the **Y** versus **DA9** fate. In *lin-12(gf)* mutants, there are two **Y** cells, as evidenced by their generation of **Y** lineages. EGL-5 is necessary for normal **Y** development (Chisholm 1991).

**E** and **U** are sister cells (Sulston et al. 1983), and they generate similar lineages (Sulston et al. 1980). Both are able to induce the anterior fates in the **B.a** great-grandprogeny (Chamberlin and Sternberg 1993). In a *mab-9* mutant, **E** is abnormal and acts more like **U**, although there is not much difference between the lineages (Chisholm and Hodgkin 1989). The presence of the **B** cell is necessary for normal **E** and **U** polarity (Chisholm and Hodgkin 1989). *lin-44* mutants have a similar polarity defect, and the reversed **B**-cell polarity is proposed to have an indirect effect on the polarity of **E** and **U** lineages (Herman and Horvitz 1994). Other mutants that affect **E** and **U** lineages include those that define *lin-48* and *lin-49* (Chamberlin 1994 and pers. comm.).

## 2. Specification of Cell Fates in the Seam

The rays and probably also the fan are generated by lateral epidermal cells. Cells of the lateral epidermis, or **seam cells**, divide regularly during development of both male and hermaphrodite to provide hypodermal nuclei and a postdeirid neuroblast. In the male, extra divisions in the posterior lineages and specification of ray **neuroblasts** result in generation of the nine rays (Fig. 7B,C). Each ray has a distinct identity characterized by its size, shape, and position in the fan, neurotransmitter use, independent developmental assembly, and behavioral

role (Sulston and Horvitz 1977; [Sulston et al. 1980](#); [Baird et al. 1991](#); [Loer and Kenyon 1993](#); [Liu and Sternberg 1995](#)).

The reproducible patterns of cell divisions, the postdeirid and ray [neuroblasts](#), and the multiple ray identities arise by a pattern formation mechanism that progressively specifies alternate cell fates as the [seam cells](#) divide. This mechanism involves interactions between neighboring [seam cells](#), but, unlike the [vulva](#) or the B-cell lineages described above, a role for the [lin-3 - let-23](#) or the [lin-12](#) signaling pathways has not been demonstrated. Instead, [seam cell](#) lineages utilize the anterior-posterior axial patterning functions of the HOM-C/Hox cluster genes ([Wang et al. 1993](#); see [Ruvkun](#), this volume). The two posterior HOM-C/Hox genes [mab-5](#) and [egl-5](#) have primary roles in patterning the posterior [seam](#) and, in particular, are necessary for generation and correct morphology of the rays. One important consequence of signaling between [seam cells](#) appears to be regulation of these two genes.

### 3. Signaling between Seam Cells

Four different signaling functions are known to act in the [seam](#) ([Fig. 7A](#)), and two additional signals are known to be involved in specification of ray identities. The presence of these signals has been revealed by cell ablation studies or been inferred from genetic results. The first extensive cell ablation analysis by laser microsurgery was carried out by [Sulston and White \(1980\)](#); their observations have been extended by others (Waring and Kenyon 1990; Waring et al. 1992; Austin and Kenyon 1994a; [Chow and Emmons 1994](#); Chow et al. 1995; [Zhang and Emmons 1995](#)).

In the male, the three most posterior [seam cells](#), V5, V6, and T, generate rays, whereas anterior [seam cells](#) generate cuticular alae. This pattern is set up by the combined action of a [seam](#) cell prepattern and a series of cell signals. A signal ([Fig. 7A](#), signal 1) is sent by each [seam](#) cell to inhibit its anterior neighbor from generating rays ([Sulston and White 1980](#)). Thus, if V6 is ablated, V5 generates five rays instead of only one; if V5 is ablated, V4 generates one ray, and so forth. Rays are generated by certain cells despite these ubiquitous inhibitory signals because of differences in their responsiveness. V6 escapes the inhibitory influence of its posterior neighbor, T, by expression of the homeobox transcription factor gene [pal-1](#), a *Drosophila caudal* homolog (Waring and Kenyon 1990, 1991). In mutants for [pal-1](#), V6 generates no rays unless the T cell is ablated. V1 through V4, on the other hand, are made sensitive to the inhibitory signal by the presumably cell-autonomous action of the basic helix-loop-helix transcription factor gene [lin-22](#), a *Drosophila hairy* homolog (L. Wrisschnick and C. Kenyon, pers. comm.). In mutants for [lin-22](#), V1–V5 all express identical lineages and generate two rays (Horvitz et al. 1983). Thus, the [seam cells](#) are inherently different in their response to posterior neighbor signaling: V1–V4 are sensitized to inhibition, whereas V6 is immune. How the [seam](#) cell prepattern is established is not known.

The cell division pattern of [seam cells](#) is also influenced by neighbor signaling in both sexes. At most divisions, [seam cells](#) divide following a stem cell pattern to give an anterior daughter that fuses with the hypodermal syncytium, *hyp* 7, and a posterior daughter that remains in the [seam](#), capable of further division. This pattern is altered after ablation of cell neighbors. [Sulston and White \(1980\)](#) found that if a sufficiently large number of [seam cells](#) were ablated, thus producing a large gap, the stem cell division pattern of the remaining [seam cells](#) was sometimes transformed to a symmetric proliferative division, thus effectively repopulating the [seam](#) with cells capable of continued division. Under these conditions of extensive ablation, the polarity of asymmetric divisions was sometimes reversed, indicating a further role of cell signaling in determining the orientation of asymmetric cell division ([Fig. 7A](#), signal 2).

Most [seam cells](#) undergo a proliferative as well as a stem cell division at the end of the L1 stage. V5.p instead produces an anterior neuroblast that generates the postdeirid. This asymmetric division requires signals ([Fig. 7A](#), signal 3) from both V5.p neighbors (Waring et al. 1992; Austin and Kenyon 1994a). If either neighbor of V5.p is ablated, the postdeirid neuroblast, V5.pa, is transformed into a proliferative [seam](#) cell identical to its sister, V5.pp. In a [lin-22](#) mutant background, [seam cells](#) V1–V4 behave like V5 in wild type and respond to neighbor signaling by generating a postdeirid. In these experiments, a requirement for direct cell-cell contact was demonstrated for generation of the signal. This observation suggests that the signaling mechanism involves cell adhesion molecules, either directly as part of the signaling pathway or indirectly to juxtapose the signaling cells closely.

A fourth signal (Fig. 7A, signal 4) affecting [seam cells](#) has been identified by genetic analysis. Mutations in the [lin-44](#) gene cause severe disruption of [male tail](#) development as a result of abnormalities in both the [B](#) and [T](#) lineages. Many of these abnormalities can be characterized as reversals in polarity of asymmetric cell divisions (see Fig. 5) (Herman and Horvitz 1994). The product of [lin-44](#) is homologous to mammalian Wnt and *Drosophila wingless*, well-known extracellular signaling proteins (Herman et al. 1995). The gene is expressed by the four embryonic hypodermal cells that make up the very tip of the [tail](#) (Fig. 7A). It is not known whether these cells are in direct contact with responding cells or whether LIN-44 can diffuse to a target cell and influence the polarity of its division.

#### 4. Determination of Cell Fates in the Seam by *mab-5* and *egl-5*

The effect of the cell signals described above appears to be to regulate the expression of transcription-factor-encoding genes. These genes, in turn, determine cell fate. Thus, there is a progressive specification of alternate cell states through the lineage. Each cell state is characterized by a particular pattern of transcription factor gene expression and by a specific division pattern and subset of progeny. No doubt, this is a general paradigm for cell fate specification in many cell lineages.

The most extensive expression data are for the gene [mab-5](#) (Fig. 7B,C) (Costa et al. 1988; [Salser and Kenyon 1996](#)). [mab-5](#) is not expressed in the anterior [seam](#) lineages of V1–V4. In the V5 lineage, expression cycles on and off, dictating the fates of the various branches. Expression must be off in V5.p to allow generation of the postdeirid, on in V5.pp and V5.ppp to allow a proliferative cell division in late L2, off in V5.pppa to allow production of alae, on in V5.pppp to allow generation of a ray, and finally off in progeny of V5.pppp to allow specification of the ray 1 identity. Expression is modulated in a different way in V6: The gene is initially on, and this is necessary for the wild-type pattern of division of V6, for the proliferative divisions at the end of L1 and beginning of L3, and for generation of the rays. Later, the gene is gradually turned off in the posterior branches, but continued expression in rays 2 and 4 is necessary for expression of ray 2 and ray 4 identity. These conclusions are based on levels of MAB-5 as determined by antibody studies, on the phenotypes of [mab-5](#) loss-of-function and gain-of-function mutants, and on the effects of ectopic expression from a heat-shock-driven transgene.

Although not yet as extensively characterized, [egl-5](#) appears to be regulated in the V6 lineage in a manner similar to that of [mab-5](#) in the V5 lineage; i.e., it is preferentially expressed in the posterior branches and is necessary for posterior fates (Fig. 7B,C) (Y. Zhang and S.W. Emmons, unpubl.; S. Salser and C. Kenyon, pers. comm.). It appears to be on in V6.ppp and off in V6.pap, and this expression pattern is necessary for the differences between these two branches. Later, it is expressed more strongly in the posterior V6.pppp branch than in the anterior V6.pppa branch, and this influences specification of ray identity.

These results run counter to the generally held view of the action of HOM-C/Hox genes. Models initially proposed to account for the properties of HOM-C mutations in *Drosophila* viewed HOM-C gene expression as an indelible marker of positional cell identity. As such, the HOM-C expression pattern in each cell was thought to be set at an early stage in development and to be maintained throughout life in order to confine cell fate to that appropriate to a particular body region (Lawrence 1992). Here we see that [mab-5](#) and [egl-5](#) expression cycles on and off. It is confined to some branches of a lineage and not others, and this is necessary to specify a variety of cell properties, including cell division, assumption of the neuroblast cell fate, and morphogenetic identity. Thus, regulation of HOM-C/Hox genes may be a more dynamic and pervasive aspect of the developmental program than previously thought.

Two additional genes have been described with effects confined to subsets of rays. In loss-of-function mutants at the [mab-3](#) locus, rays 1–6 are absent, as in [mab-5](#) mutants ([Shen and Hodgkin 1988](#)). [mab-3](#) mutations also affect sex-specific differentiation of endoderm (see below), leading to speculation that the function of [mab-3](#) is to implement the program of sexual differentiation at the tissue level. A gene whose action is confined to the [I lineage](#) is [mab-19](#) (Sutherlin and Emmons 1994). In mutants defective in this gene, ray expression from the [I lineage](#) is reduced and variable because of transformations of polarity and loss of specific cell divisions and ray [neuroblasts](#).

## 5. *lin-32* May Be a Target of *mab-5* and *egl-5* Gene Action

HOM-C/Hox genes such as *mab-5* and *egl-5* appear to function abstractly to impart differences to cells belonging to different body regions. They act in all cell types and tissue layers. They must therefore be able to influence the transcription of many genes. The binding specificities of the HOM-C/Hox genes themselves differ from one another only subtly. It remains somewhat of a mystery how these subtle differences are translated into regionally specific patterns of expression of a broad range of target genes. Detailed studies of the interaction between HOM-C/Hox genes and their transcriptional targets are necessary to resolve this issue. In the male *seam*, the *lin-32* gene is a good candidate for a direct target of *mab-5* and *egl-5* regulation.

*lin-32* is required for generation of the postdeirid neuroblast in both sexes and the ray *neuroblasts* in the *male tail*. It encodes a transcription factor of the basic helix-loop-helix family and is most closely related to the *achaete/scute* subfamily (Zhao and Emmons 1995). Basic helix-loop-helix transcription factors are thought to function to designate tissues. Genes of the *achaete/scute* subfamily regulate expression of the neuronal cell fate. *lin-32* is also required for generation of *touch cells* (Chalfie and Au 1989) and is likely to be required for the fates of many additional neuroblast cells, as the gene appears to be widely expressed in the developing *nervous system*, and the null phenotype is probably lethality (Zhao and Emmons 1995).

Ectopic expression of *lin-32* from a heat-shock-driven transgene resulted in expression of the ray sublineage by anterior *seam cells* V1–V4 (Zhao and Emmons 1995), indicating that it is only lack of LIN-32 that prevents these cells from generating rays. It further suggests that regional regulation of *lin-32* is transcriptional, because regulation can be circumvented by replacement of the *lin-32* promoter region with the heat shock promoter.

The best candidates for *lin-32* regional transcriptional regulators are *mab-5*, *egl-5*, and *lin-22*. Genetically, *mab-5* activates the ray sublineage in the posterior body region, and *lin-22* inhibits it in the anterior body region. A similar inhibitory relationship is found in *Drosophila*, where *hairy* binds the promoter of *achaete* to regulate its transcription negatively (Ohsako et al. 1994; Van Doren et al. 1994).

MAB-5 is present in the anterior ray lineages leading to rays 1, 2, and 3 (Salser and Kenyon 1996) and could directly activate *lin-32* in those lineages. It is present only at low levels or not at all in the posterior V6 lineages leading to rays 4, 5, and 6, but genetic evidence suggests an even stronger activation of *lin-32* in these lineages (C. Zhao and S.W. Emmons, in prep.). The lack of correlation between MAB-5 level and apparent potency of *lin-32* activation suggests an additional gene activates *lin-32* in the posterior V6 lineages. The strong expression of *egl-5* in these same lineages makes *egl-5* a candidate. Thus, *mab-5* may activate *lin-32* in rays 1, 2, and 3, whereas *egl-5*, alone or together with *mab-5*, may activate *lin-32* in rays 4, 5, and 6. If such a model is correct, it is necessary to invoke hypothetical interactions between *mab-5* and *egl-5* to explain the mutant phenotypes of these genes: All rays are lost in a *mab-5(0)* mutant (Kenyon 1986), whereas only ray 6 is lost in an *egl-5(0)* mutant (Chisholm 1991). These phenotypes may be explained if, first, *mab-5* activates transcription of *egl-5*. This hypothesis is consistent with the observation of Salser and Kenyon (1996) that activation during the L1 stage of a *mab-5* heat shock transgene in a *mab-5(0)* background results in generation of rays in the V6 lineage much later, during L3. Second, *egl-5* may inhibit *mab-5* in rays 4 and 5. In an *egl-5(0)* mutant, *mab-5* would be released from this inhibition and could turn on *lin-32*.

## 6. Specification of Ray Identities

Once *lin-32* is activated, the ray sublineage is expressed and generates the three cells of each ray during L4 (Fig. 7C). Each of these rays has a unique identity. The necessity for separate ray identities can be understood in the context of ray differentiation. After they are born, the ray cells immediately commence to differentiate into the two ultrastructurally distinct *ray neurons* and the ray support cell, termed the structural cell. Processes of these three cells assemble into a ray at a predetermined site in the epidermis (Fig. 8A), whereas the connected cell body migrates into the *preanal ganglion*. The ray assembly process must involve the function of ray-specific cell recognition and adhesion molecules that allow each ray cell to recognize its correct assembly partners and to reject association with cells belonging to the other rays. Perhaps the best evidence for the presence of these specific recognition functions is the existence of a set of assembly mutants in which the specificity of the process

breaks down and pairs or groups of adjacent rays fuse together (Fig. 8B) (Baird et al. 1991; Chow et al. 1995). Formation of specific homotypic and heterotypic cell associations of this sort must be a widespread process in metazoan development, but its molecular basis is little understood.

The specificity of ray assembly lies at least in part with the structural cell. This cell alone, in the absence of the [neurons](#), is sufficient to generate a ray at the correct position and with appropriate morphology ([Zhang and Emmons 1995](#)). These properties of the structural cell are transformed in a ray identity transformation mutant.

A pattern formation mechanism must underlie generation of the multiple ray identities. The problem presents a fine example of differentiation among members of a set of serially repeated structures. Two general types of pattern formation mechanisms have been ruled out: mechanisms involving positional signaling and mechanisms involving nearest-neighbor signaling. Neither the position along the anterior-posterior axis of the body at which a ray forms nor the identities of its neighbors determine the identity of the ray generated by a particular ray precursor cell ([Chow and Emmons 1994](#)). Rather, each ray precursor cell appears to be born with the identity of the ray it will generate predetermined. Thus, ray identities are generated by a lineage mechanism similar to that discussed above which determines the pattern of cell divisions and cell fate specifications.

Not surprisingly, two key players are once again [mab-5](#) and [egl-5](#). Gene dosage studies ([Chow and Emmons 1994](#)) revealed that the level of [mab-5](#) activity helps to discriminate between ray 1 identity (low activity) and ray 2 identity (high activity), and between ray 3 (low activity) and ray 4 (high activity). [egl-5](#) activity helps to discriminate between ray 4 identity (low activity) and ray 6 identity (high activity). Ectopic expression of [mab-5](#) from a heat shock transgene resulted in transformations affecting rays 1, 2, and 3, including the transformation of ray 1 into ray 2 ([Salser and Kenyon 1996](#)). These results are consistent with the observed expression domains and expression levels of [mab-5](#) and [egl-5](#) (Fig. 7B,C). Furthermore, the ratio as well as the absolute numbers of [mab-5\(+\)](#) and [egl-5\(+\)](#) gene copies had an effect ([Chow and Emmons 1994](#)), suggesting cross-regulatory interactions between the two genes, as proposed above under regulation of [lin-32](#).

In addition to [mab-5](#) and [egl-5](#), eight genes have so far been identified that are involved in specification of ray identities: [mab-18](#), [mab-20](#), [mab-21](#), [mab-26](#), [daf-4](#), [sma-2](#), [sma-3](#), and [sma-4](#) ([Baird et al. 1991](#); [Chow and Emmons 1994](#); [Savage et al. 1996](#)). Mutations in [mab-20](#) and [mab-26](#) result in massive fusions involving many rays. They also cause epidermal deformities elsewhere on the body. Interactions between mutations in [mab-20](#) and [mab-26](#), on the one hand, and mutations in [mab-5](#) and [egl-5](#), on the other, suggest that these genes all act at a similar step in the ray determination pathway ([Chow and Emmons 1994](#)).

Mutations in the remaining genes have effects on rays that are mainly limited to a pathway leading to the identity of just a single ray, ray 6. Ray 6 is unique among the rays in having a fat, tapering morphology, little or no opening to the exterior, and certain ultrastructural features (see Fig. 1A) (Sulston et al 1980; Chow et al. 1995). Furthermore, it is one of only two rays, along with ray 8, that is born from an anterior lineage branch (Fig. 7B). Thus, it is not surprising to find genetic functions responsible for or related to these unique properties.

A key gene in the ray 6 differentiation pathway appears to be [mab-18](#). [mab-18](#) encodes the homeodomain portion of a *C. elegans* Pax-6 homolog, in which paired domain mutations define the separate genetic locus [vab-3](#) ([Chisholm and Horvitz 1995](#); [Zhang and Emmons 1995](#)). [mab-18](#) transcription is turned on permanently in the ray 6 sublineage and transiently in the ray 8 sublineage. In the absence of [mab-18](#) function, ray 6 assumes a ray 4 identity ([Baird et al. 1991](#); [Zhang and Emmons 1995](#)). Mutations in [mab-21](#), which encodes a novel protein of unknown function, have a similar ray 6 to ray 4 transformation phenotype (Chow et al. 1995). In addition, in [mab-21](#) mutants, the [seam](#) cell T.apapa, the anterior sister of R7, sometimes generates a ray. MAB-21 appears to act redundantly in both R6 and T.apapa to block the effect of an inductive signal from R6 that causes T.apapa to take the neuroblast cell fate.

The genes [daf-4](#), a type II transforming growth factor- $\beta$  (TGF- $\beta$ ) family receptor (Estevez et al. 1993), and [sma-2](#), [sma-3](#), and [sma-4](#), which define a family of novel proteins also found in vertebrates and fruit flies, are components of a TGF- $\beta$ -like signaling pathway ([Savage et al. 1996](#)). They thus define a further cell signal specifying ray identities. Mutations in these genes cause a [male tail](#) phenotype primarily involving rays 5, 6, and 7, which appears to be best interpreted as a transformation of ray 5 and ray 7 identities to ray 6 identity. In

support of this interpretation, in these mutants, a *mab-18* reporter gene is expressed in rays 5 and 7, and *mab-18* mutations are epistatic for the ray phenotype. The source of the ligand that normally binds the putative DAF-4 receptor and blocks rays 5 and 7 from activating *mab-18* and the ray 6 identity pathway is not known.

## 7. Hook and Preanal Ganglion

Like the hermaphrodite *vulva*, the hook develops postembryonically from a subset of ventral epidermal precursor cells (Pn.p cells). There are at least two stages of specification. During the L1 stage, the *P11* and *P12* neuroectoblasts become different from each other; during the L3 stage, the posterior progeny *P9.p*, *P10.p* and *P11.p* form an equivalence group for hook formation ([Sulston and White 1980](#)). Although specification of the *P11* and *P12* fates proceeds similarly in both sexes, the importance of their progeny in hook and *preanal ganglion* formation highlights their role in male development.

The specification of Pn cell fate during the L1 stage proceeds essentially as in the hermaphrodite (see [Ferguson et al. 1987](#); [Greenwald](#), this volume). Mutations in a number of developmental control genes affect the fates of *P11* and *P12*, in particular, LIN-44, the LET-23 signaling pathway, and the HOM-C genes. The interrelationship among these has not been established. (Note that in many cases, the fate of only *P11.p* and *P12.p* has been assayed, and thus there may be an added level of complexity.) *let-23*, *let-60*, *lin-44*, *egl-5*, and *mig-5* are all at least partially required for the *P12* fate (Fixsen et al. 1985; Aroian and Sternberg 1991; Chisholm 1991; Herman and Horvitz 1994; C. Guo and E. Hedgecock, pers. comm.). *lin-44* might be necessary for the development of the cell(s) that signals to *P12* since it is expressed in cells that do not contact *P11* and *P12* (see Figs. 4 and 7A) (Herman and Horvitz 1994). Overexpression of the EGF domain of LIN-3 or loss of *lin-15* function, both of which activate the LET-23 pathway, results in a *P11* to *P12* transformation (Fixsen et al., 1985; L. Jiang et al., unpubl.) Thus, there is a complex signaling pathway involving at least two intercellular signals. *P11* and *P12* fates in *mab-5* mutants are variably misspecified, with transformations in both directions observed (Kenyon 1986). The effects of the HOM-C/Hox genes might be complex as they could be affecting both signaling and responding cells involved in *P12* specification.

A fascinating aspect of cell fate specification is how precursor cells choose among three potential fates ([Fig. 9](#)). The *preanal ganglion* precursor cells provide a second example to that of the vulval precursor cells.

In intact wild-type males, *P10.p* generates the hook and its associated sensillum ([Sulston et al. 1980](#)). *P11.p* generates *interneurons* and epidermis; *P9.p* fuses with *hyp7* syncytial epidermis or divides and its progeny fuse. These three cells form an equivalence group. After ablation of *P11.p*, *P10.p* acts as does *P11.p* in the intact animal and *P9.p* generates the hook. After ablation of *P10.p* and *P11.p*, *P9.p* has the fate of *P11.p*. Thus, the *P11.p* fate is the primary fate, the *P10.p* fate is the secondary fate, and the *P9.p* fate is the tertiary fate. In mutants with additional cells because *P12* is transformed to *P11* fate, *P12.p* adopts the primary fate (generation of *interneurons* and epidermis) and *P11.p* generates the hook (Chisholm 1991; P. Sternberg and R. Horvitz, unpubl.). Thus, it is likely that *P9.p*, *P10.p*, and *P11.p* are each tripotent.

Genes necessary for hook and *preanal ganglion* development (during the L3 stage) have been identified by screens for other phenotypes. These genes include the HOM-C/Hox genes and the LET-23- and LIN-12-mediated signaling pathways. *mab-5* is necessary for hook development (Kenyon 1986). In *mab-5* males, *P9.p* and *P10.p* fuse with *hyp7*, rather than retaining the potential to participate in hook development. In addition, *P11.p* often acts like *P12.p* and thus fails to generate the *preanal ganglion neurons* that it usually generates. In hermaphrodites, MAB-5 protein decreases in *P11.p* by the L2 stage, whereas in males, it remains expressed; *P10* has higher levels of protein than *P9* and *P11* (Salser et al. 1993).

The LET-23 and LIN-12 signaling pathways may have roles in *preanal ganglion* fate specification similar to their roles in vulval precursor fate specification, consistent with the hypothesis that these lineally equivalent Pn.p cells respond to similar intercellular signaling pathways to specify distinct fates that are sex-specific ([Greenwald et al. 1983](#); M. Herman et al., unpubl.). One apparent difference between the *vulva* and hook equivalence groups is that no source of inductive signal has been found in the *male tail*. Moreover, an isolated distal *VPC* can become 2° (Katz et al. 1995), whereas an isolated *P9.p* apparently cannot (Herman 1991) ([Fig. 9](#)). In *lin-15* mutants, *P9.p*

generates a 2° lineage and an ectopic hook. In males with normal [P11](#), isolated [P9.p](#) generates a 1° lineage. In strong *lin-12(gf)* mutants, all three P(9-11).p cells generate 2° lineages ([Greenwald et al. 1983](#)). In *lin-12(lf)* males, [P10.p](#) generates either a 3° or a 1° lineage. In *lin-12(lf);lin-15(lf)* double-mutant males, all three cells generate a 1° lineage (P. Sternberg and R. Horvitz, unpubl.).

What is the source of patterning information? One class of model assumes specification similar to that of the vulval precursor cells in *C. elegans*; another class is based on specification of the vulval precursor cells in *Mesorhabditis* ([Sommer and Sternberg 1994](#)). First, there might be a redundant source of LIN-3 in the [tail](#) (by analogy with [B.a](#) sublineage specification; Chamberlin and Sternberg 1993) that cannot be removed by ablation as numerous attempts to do so have failed (M. Herman; L. Jiang; R. Hill; all pers. comms.). The difficulty in finding an “organizer” for the [male tail](#) has been partially overcome by ablation of sets of cells (Chamberlin and Sternberg 1993). A second possibility is that the anterior-posterior positional differences in HOM-C expression contribute to the pattern of [preanal ganglion](#) fates, with the LIN-12 pathway used to specify the 2° fate. In particular, [P11](#) is different from [P9](#) and [P10](#) in that only [P11](#) can replace [P12](#) during the L1 stage ([Sulston and White 1980](#)). Pn.p cells might become different from each other by virtue of their anterior-posterior position and the action of the Hox genes. The Hox genes might provide a prepattern that is reinforced by intercellular signals, notably a LIN-12-mediated lateral signal. The role of LET-23 during the L3 stage might be nil, or it might be the target of the HOM-C/Hox prepattern.

## 8. Mesoderm and Endoderm

The male-specific muscles are generated postembryonically from a single precursor cell, [M](#) (see [Fig. 4](#)). During the L1 stage, [M](#) generates [body muscle](#) and three sex myoblasts (SM1, SM2, SM3) on each side. During the L3 stage, the SMs divide to generate distinct sets of muscles and one coelomocyte ([Sulston et al. 1980](#)). The sex myoblast lineages are asymmetric between the left and right sides. For example, SM2L.pp is a coelomocyte and [SM2R.pp](#) is the male-specific gubernacular erector muscle. This asymmetry suggests the effect of positional information, but the cell ablation experiments of [Sulston and White \(1980\)](#) did not reveal cell interactions. As with, for example, spicule development ([B lineage](#)), there may be redundant sources of signals, and a combination of mutations and cell ablations might be necessary to identify the source of the patterning information.

LIN-12 specifies the number of sex myoblasts in the male. In the absence of [lin-12](#), there are four SMs on either side, rather than the three per side present in wild-type males ([Greenwald et al. 1983](#)). A [cod-11](#) mutation disrupts SM migrations and leads most notably to disorganized diagonal muscles and a turning defect (K. Liu et al., in prep.). LIN-17 also affects the [M lineage](#), although the precise defect(s) has not been elucidated ([Sternberg and Horvitz 1988](#)). [egl-5](#) mutants have abnormally positioned sex muscles and often have a second dorsal coelomocyte (Chisholm 1991).

There are also sex-specific differences in the [intestine](#). Hermaphrodites but not males produce yolk. In [mab-3](#) mutants, the male [intestine](#) produces yolk, and this phenotype is interpreted as a specific defect in sexual identity ([Shen and Hodgkin 1988](#)). The two diverse roles of [mab-3](#) in ray development and regulation of yolk production might be explained if the function of [mab-3](#) is to mediate the control of sex-specific differentiation in response to the major sex determining loci (see [Meyer](#), this volume).

Finally, [Z1](#) and [Z4](#) divide asymmetrically to generate two [distal tip cells](#), four [vas deferens](#) precursor cells, three [seminal vesicle](#) precursor cells, and one linker cell. The asymmetry of the [Z1](#) and [Z4](#) divisions requires [lin-17](#) ([Sternberg and Horvitz 1988](#)). The linker cell is specified by [lin-12](#) in a process analogous to that of the anchor cell (Kimble and Hirsh 1979; Kimble 1981; [Greenwald et al. 1983](#)). Linker cells can autonomously migrate to the [tail](#) in mutants in which they detach from the gonad ([Sternberg and Horvitz 1988](#); Chisholm 1991). [egl-5](#) is necessary for late somatic lineages (VD and SV sublineages) in the [male gonad](#) (Chisholm 1991).

## B. Morphogenesis

How multicellular structure is generated through the morphogenetic activities of individual cells is a biological problem that remains largely unsolved. The process must involve many diverse cellular activities. These may include the formation of junctions with correct neighbors, changes in cell shape, changes in cell volume, and the synthesis of both intracellular and extracellular macromolecular structures. Only a preliminary survey of the cellular activities that underlie formation of the male-specific [tail](#) structures has been made so far. Although a number of *mab* mutations have been isolated that appear to define genes which act during morphogenesis, these have not been studied at the molecular level.

## 1. Retraction and Fan Formation

Up until the L4 larval stage, the external morphologies of males and hermaphrodites are nearly identical. The adult [male tail](#) is formed inside the L4 cuticle following cell differentiation during the L4 stage, so that a mature male emerges at the final molt. [Male tail](#) morphogenesis involves a retraction process that remodels the [tail](#) region, during which the fan forms and the rays extend ([Fig. 10](#)) ([Sulston et al. 1980](#)). The mechanism of retraction undoubtedly involves the participation of several tissues and processes. Contractions of the posterior oblique muscle and other muscles, including the diagonal muscles, can be observed to draw the ventral region upward. This results in the [tail](#) region having a reduced volume. Reduction in volume must be accompanied by the extrusion of fluid into the growing cavity that separates the retreating future adult body surface from the overlying L4 cuticle. Fluid pressure built up in this cavity may be another driving force for retraction, since integrity of the L4 cuticle appears to be necessary for the process to proceed (S.W. Emmons, unpubl.).

As retraction proceeds, the fan gradually forms. The fan consists of a fold of the outer (cortical) layer of the two-layered adult cuticle ([Sulston et al. 1980](#); Cox et al. 1981b). During retraction, this outer layer comes away from the body, whereas the inner (basal) layer bunches up at the retreating body surface ([Sulston et al. 1980](#)). Why this occurs only in the posterior region, and not more anteriorly, where retraction still occurs but where the two layers of the adult cuticle remain attached by struts (Cox et al. 1981b), is not known. One possibility is that [Rn.p cells](#), which underlie the presumptive dorsal fan region ([Baird et al. 1991](#)), synthesize a special type of fan-specific cuticle incapable of strut formation. Specific binding of a monoclonal antibody and wheat-germ agglutinin to the fan indicates either the presence of fan-specific molecular components or fan-specific exposure of ubiquitous components (Link et al. 1988).

A modest collection of *mab* mutations may have their effects during retraction and fan morphogenesis (see, e.g., [Hodgkin 1983](#); S.W. Emmons, unpubl.). By and large, these have been passed over in favor of genes thought to act at the earlier regulatory steps of development. They remain a source for future analysis of the molecular basis of morphology itself.

## 2. Rays

Ray cells are born within the lateral epithelium during the L4 stage and immediately commence to differentiate. The structural cell (Rnst) retains junctions with the epidermis, whereas the two [neurons](#) delaminate. Cell bodies of all three cells migrate into the lumbar [ganglia](#), leaving behind dendritic processes extending to the surface (see [Fig. 8A](#)); the [neurons](#) extend axonal processes through commissures into the [preanal ganglion](#) ([Sulston et al. 1980](#)). Correct assembly of the dendritic processes together with structural cell processes into mature rays requires the specification of separate ray identities, as described above.

How the rays come to be located at reproducible positions within the fan presents a well-defined problem in morphogenesis. Ray positions are determined by the sites at which the ray structural cells make attachments to the surface during L4 ([Fig. 10](#)). In part, these sites are determined by the cell lineage: The anterior-posterior order of the rays is the same as the order of the Rn cells in the [seam](#), with the exception of ray 6, which is born between ray 4 and ray 5 (see [Fig. 7B](#)). Studies of cell positions during ray differentiation of mutants and of ray patterns in other nematode species suggest, however, that additional active processes are required. After the ray sublineages are complete, the cells of each ray come to take up specific positions within a complex pattern of Rn.p epidermal cells ([Fig. 11](#)) ([Baird et al. 1991](#)). The arrangement suggests that the position of each ray might be determined by specific ray cell–epidermal cell interactions. Just as rays have distinct identities, [Rn.p cells](#) are

nonequivalent: R1.p–R5.p fuse together forming a syncytium called the tail [seam](#) (SET), whereas R6.p–R9.p fuse with [hyp7](#) ([Sulston et al. 1980](#)). In mutants that alter ray identities, both the positions of individual rays and the fates of [Rn.p cells](#) are transformed ([Baird et al. 1991](#); [Chow et al. 1995](#); [Zhang and Emmons 1995](#)). Thus, ray placement, like ray assembly, is an example of a possibly very general and not well understood aspect of differentiation, involving the expression by cells of specific cell recognition and adhesion functions that allow them to make a correct set of homotypic and heterotypic cell contacts. Analysis of ray evolution (see [Fitch and Thomas](#), this volume) suggests that ray identities, expression of cell recognition and adhesion functions, or both may be important foci of evolutionary change in [male tail](#) morphology ([Fitch and Emmons 1995](#)).

Finally, simultaneously with retraction and fan formation, the rays extend. The bulk of each ray consists of [hyp7](#) (see [Fig. 8A](#)) ([Chow et al. 1995](#)). Why and how this syncytial cell, undoubtedly under the local influence of the ray processes, generates these thin, snake-like protrusions of the cell surface and cytoplasm is unknown. A class of five genes (*ram*, [ray morphology](#)) has been described in which mutations cause the rays to have a lumpy, amorphous morphology ([Baird and Emmons 1990](#)). These mutations might disrupt the interaction between the ray surface and the overlying fan.

### 3. Spicules

Spicules are intricate structures whose final form depends on a variety of cell types. Analysis of spicule morphogenesis might well provide an opportunity to study how cell differentiation can lead to structures of particular size and shape. Morphogenesis of the spicules is described by [Sulston et al. \(1980\)](#). A variety of cell lineage mutants have abnormal spicules. Ablation of muscle results in a failure of spicule elongation ([Sulston and White 1980](#)). The spicule defect of [mab-5](#) mutations is due to muscle as shown by mosaic analysis ([Kenyon 1986](#)). Similarly, [egl-5](#) mosaics with mutant sex muscle, but wild-type spicules, have crumpled spicules ([Chisholm 1991](#)).

### 4. Vas Deferens/Cloaca

The linker cell leads the migration of the gonad and is induced to undergo apoptosis by [U.ip](#) or [U.rp](#) ([Sulston and White 1980](#)). This relatively understudied aspect of male development affords the chance to study the connection of tubes and the induction of programmed cell death in response to intercellular signals.

## Figures

Figure 4. Postembryonic blast cells in the L1 male.

### Figure 4

Postembryonic blast cells in the L1 male. Shown are the positions of the major male blast cells listed in [Table 2](#) (underlined cells), as well as other cells mentioned in the text. The [somatic gonad](#) precursor cells, [Z1](#) and [Z4](#), lie within the gonad primordium, flanking the germ line precursor cells ([Z2](#) and [Z3](#)). (*Top*) Lateral view; (*bottom*) mid-sagittal view. The following are sources for this figure: Sulston and Horvitz (1977), White (1988), Austin and Kenyon (1994a), Podbilewicz and White (1994), S.W. Emmons (unpubl.), and D.H. Hall and D.H.A. Fitch (in prep.).

Figure 5. Roles of LIN-44, LIN-17, and VAB-3 in B lineage asymmetry.

### Figure 5

Roles of LIN-44, LIN-17, and VAB-3 in [B lineage](#) asymmetry. (A) In the wild type, [B](#) divides unequally with a larger anterior daughter ([B.a](#)) indicated by the “greater than” sign). [B.a](#) generates two identical daughters, which undergo a characteristic lineage (boxed A, for anterior). [B.p](#) generates a distinct lineage (circled P, for posterior). (B) In a [lin-44](#) mutant, the asymmetry is often reversed ([Herman and Horvitz 1994](#)). (C) In a [lin-17](#) mutant, [B](#) divides equally (indicated by the “equal” sign) and both daughters generate two A cells ([Sternberg and Horvitz 1988](#)). (D) In some [vab-3](#) mutant animals, the [B lineage](#) is unequal as in wild type, but only progeny with the P fate are produced; in other animals, the B-cell division is equal, indicating a role of VAB-3 in the asymmetric cell division as well ([Chamberlin and Sternberg 1995](#)). (E) In a [lin-17 lin-44](#) double mutant, the [B lineage](#) is equal and

thus similar to [lin-17](#) (Herman and Horvitz 1994). (F) In a *lin-17; vab-3* double mutant, the B division is often symmetric, but all progeny have the P fate ([Chamberlin and Sternberg 1995](#)). Some *vab-3* mutations also cause an equal B division, but the mutation used for the double-mutant analysis does not.

Figure 6. Sublineage choice in the B lineage.

## Figure 6

Sublineage choice in the [B lineage](#). (A) Position of the eight [B.a](#) great-grandprogeny at the  $B = 10$  cell stage, along with [E](#), [U](#), and [Y.p](#) progeny. aa, ap, pa, and pp refer to [B.a](#) great-grandprogeny. These cells become specified to generate the lineages  $\alpha$ ,  $\beta$ ,  $\gamma$ ,  $\delta$ ,  $\alpha$ ,  $\epsilon$ , and  $\zeta$  shown in part B. (B) Sublineages generated by the eight [B.a](#) great-grandprogeny. (so) Spicule socket cell; (sh) sheath cell; (n) [neuron](#); (p) proctodeal cell; (p/X) becomes a proctodeal cell or dies, depending on its homolog. (l) Left; (r) right; (d) dorsal; (v) ventral; (a) anterior; (p) posterior. (C) Model for signal transduction and integration. LIN-3 is an excellent candidate for the signal from [E](#) and [U](#) (or their progeny) that promotes anterior fates. This signal is mediated by LET-23, SEM-5, LET-60, and LIN-45. LIN-15 acts antagonistically to LET-23. [Y.p](#) also acts antagonistically to the [E](#) and [U](#) signal, but intersects downstream from LIN-45. The signal from the [B.a](#) progeny has not been analyzed and conceivably is equivalent to the LIN-15 signal. Based on model of Chamberlin and Sternberg (1994).

Figure 7. Specification of cell fates in the seam.

## Figure 7

Specification of cell fates in the [seam](#). (A) Four effects of signals on lateral epidermal [seam cells](#): (1) Seam cells inhibit their anterior neighbors from generating rays; (2) [seam cells](#) induce stem cell division and polarize the asymmetric divisions of their neighbors; (3) [seam cells](#) induce their neighbors to make a postdeirid; (4) LIN-44 (Wnt), expressed by shaded cells, orients division polarity in the [T lineage](#). (B,C) HOM-C/Hox gene expression patterns in the [seam](#) lineages. (Circles) [mab-5](#) expression; (diamonds) [egl-5](#) expression. Shading indicates approximate relative level of expression. The vertical axis indicates the period of postembryonic development. (B) Postembryonic [seam](#) lineages beginning with the posthatching L1 larva (shown in A), up to mid L3. Arrangement of the ray precursor cells (Rn) in the mid L3 larva is shown. (C) Lineages from late L3 to early L4. The arrangement of the ray precursor cells is shown just before they divide in late L3. B and C are adapted from Salser and Kenyon (1996); [egl-5](#) expression data are from Y. Zhang and S.W. Emmons (unpubl.).

Figure 8. Structure of a ray.

## Figure 8

Structure of a ray. (A) Diagrammatic section in the plane of the fan of a ray (*left*) and a ray tip (*right*). The structural cell (Rnst) holds the dendritic endings of the A (RnA) and B (RnB) [neurons](#) and generates an opening through [hyp7](#) to the exterior. The cell processes connect to cell bodies lying in the lumbar [ganglia](#), anterior of the [anus](#). d indicates a density characteristic of the B-type [neuron](#) of all the rays except ray 6. The body of the ray consists primarily of [hyp7](#). (B) A ray 4/ray 6 fusion in a [mab-21](#) mutant male, in which ray 6 assumes a ray 4 identity. A single structural cell, which is likely to arise by fusion of R4st and R6st, holds a B-type [neuron](#) in each of two openings (note the density in *both* B-type [neurons](#)). Two A-type [neurons](#) are also present, but one fails to extend to the ray tip. Figure adapted from Chow et al. (1995). N indicates a [hyp7](#) nucleus present in the base of the ray.

Figure 9. Specification of the P(9-11).

## Figure 9

Specification of the P(9-11).p lineages. (A) Schematic drawing of the positions of the relevant cells during the early L3 stage. (B) The lineages of [P9.p](#), [P10.p](#), and [P11.p](#). ([hyp7](#)) Joins the large epidermal syncytium [hyp7](#); (H) forms the hook; (so) hook socket cell; (B) [HOB neuron](#); (A) [HOA neuron](#); (Z) [PVZ](#) neuron; (sh) hook sheath cell; (V) [PVV neuron](#); (Y) [PVY neuron](#); (C) [PDC neuron](#); (G) [PGA neuron](#); (awhs) epidermal cells associated with the [hook](#)

sensillum. Dotted lines indicate that [P9.p](#) only sometimes divides (data from [Sulston et al. 1980](#)). (C) Fates of P(9-11).p after certain cell ablations (–) or in fate specification mutants. (gf) Gain-of-function mutation; (lf) loss-of-function mutation (data from [Sulston and White 1980](#); [Greenwald et al. 1983](#); P. Sternberg et al., unpubl.). Slash indicates that [P10.p](#) can be either 3° or 1° in *lin-12(lf)* mutants.

Figure 10. Morphogenesis of the male tail.

## Figure 10

Morphogenesis of the [male tail](#). Morphogenesis of the fan and rays during the L4 larval stage. (A) Nuclei of epidermal cells and ray cells are clustered in the posterior region (36 hr after hatching). (B) Beginning of retraction. Ray papillae are visible; the papilla of ray 2 is below the plane of focus. The final positions of the rays in the fan are set at this stage by the positions at which the respective ray papillae form on the surface (40 hr after hatching). (C) Mid-retraction; fan and rays are forming (43 hr after hatching). The tips of rays 1, 5, and 7 can be seen to lie in the dorsal surface of the fan. (D) Retraction complete. A fully formed [male tail](#) is present inside the L4 cuticle (45 hr after hatching). Bar, 10  $\mu$ m. (Reprinted, with permission, from [Baird et al. 1991](#).)

Figure 11. Cell arrangement in the lateral epidermis during ray differentiation.

## Figure 11

Cell arrangement in the lateral epidermis during ray differentiation. The positions where the rays will form is determined by a complex set of cell interactions in the lateral [tail](#) epidermis. Here, cell boundaries during the L4 larval stage have been traced from preparations stained with an antibody (MH27) to a cell junctional antigen (indirect immunofluorescence photomicrograph shown in E). In A and B, cells are shown during and immediately after execution of the ray sublineages. At progressively later times, the ray cells differentiate, leaving the structural cells attached at precise locations that will determine the positions where the rays will form (F). These positions remain fixed during retraction (G). (se) Seam; (Ph) phasmid; (tsy) tip syncytium; (set) [tail seam](#). (Reprinted, with permission, from Fitch and Emmons 1995.)

Generated from local HTML

## Chapter 12. Male Development and Mating Behavior — IV

### Concluding Remarks

---

The studies described here have shown that male-specific structures arise from rather complex lineages in which cells of many different types and characteristics are specified. Studies of cell fate specification in these lineages are proving to be a rich source of insight into general problems of development. One striking finding is that many genes (or pathways) affect cell fate specification in different cells. For example, [\*lin-17\*](#) is necessary for a variety of asymmetric cell divisions, whereas [\*lin-12\*](#) specifies alternative cell fates for many pairs of cells. Since the cell types produced are often quite different, comparison of different aspects of development might allow an understanding of how general mechanisms of cell fate specification interact with tissue-specific differentiation programs. How these cell types, once specified, differentiate into functional organs and structures should help us understand the principles of morphogenesis. The [\*male nervous system\*](#) affords a chance to relate [\*nervous system\*](#) structure to behavior. It will be invaluable to have a reconstruction of the [\*male nervous system\*](#), but light microscopic methods might substitute in part. Comparisons of male and hermaphrodite development and behavior provide opportunities to analyze the sex specificity of gene action. Although a comprehensive understanding of the *C. elegans* genome will require insight into the role each gene has in both sexes, the beauty of their anatomy and subtlety of their behavior, coupled with their dispensability, make *C. elegans* males a worthy subject of study in their own right.

Generated from local HTML

## **Chapter 12. Male Development and Mating Behavior — Acknowledgments**

---

Work in S.W.E.'s laboratory is funded by the National Institutes of Health and the National Science Foundation. P.W.S. is an investigator with the Howard Hughes Medical Institute, which has funded the research in his laboratory discussed here. Katharine Liu, Helen Chamberlin, Michael Herman, and the reviewers provided invaluable criticism.

Generated from local HTML

# **Chapter 13. Fertilization and Establishment of Polarity in the Embryo**

---

## **Contents**

[I Introduction](#)

[II Fertilization](#)

[III Establishment of Polarity in the One-Cell Embryo](#)

[IV Cell Division Patterns in the Early Embryo](#)

[V Summary and Speculation](#)

Generated from local HTML

# Chapter 13. Fertilization and Establishment of Polarity in the Embryo — I Introduction

---

The body plan of the *Caenorhabditis elegans* embryo is established during the first few cleavages. The reproducible orientations of these cleavages coupled with asymmetric localization of cytoplasmic components initiate processes that establish the three principal axes of the body and set the fates of the six founder cells. In this chapter, we review the current understanding of mechanisms controlling the early cleavages, and we address the following issues: (1) when and how embryonic polarity is established, (2) how cytoplasmic factors are differentially partitioned along an axis, and (3) how spindle positioning is controlled to generate cells of the correct sizes, in the correct positions, and with the correct contents.

## A. Overview of Embryogenesis

For detailed descriptions of *C. elegans* embryogenesis, see [Sulston et al. \(1983\)](#), which describes the entire embryonic lineage, and [Wood \(1988\)](#) and [Strome \(1989\)](#). It takes 14 hours at 20°C for a newly fertilized embryo to complete embryogenesis and hatch from its eggshell into a juvenile worm. During the first few hours, the embryo undergoes a series of four unequal divisions, to produce five somatic founder cells ([AB](#), [E](#), [MS](#), [C](#), and [D](#)) and the primordial germ cell ( $P_4$ ) by the 28-cell stage (Figs. 1 and 2a–i). Gastrulation begins at the 28-cell stage when the two daughters of [E](#) move to the interior of the embryo (Fig. 2i), followed later by  $P_4$  and some of the descendants of [MS](#), [C](#), [D](#), and [AB](#). These cell movements, coupled with continued proliferation, result in a generally triploblastic embryo of 300 cells, with an internal cylinder of [pharynx](#) and gut primordia, an outer layer of hypodermal and [neuronal precursors](#), and four quadrants of body wall myoblasts between the two layers. Cell divisions cease when the embryo contains 550 cells (Fig. 3). During the second half of embryogenesis, tissues differentiate and become more highly organized and separated from each other, and the spherical embryo is squeezed by circumferential microfilaments and microtubules into a vermiform worm (Figs. 2j–l and 3).

## B. Overview of Early Embryonic Polarity

Figure 4 summarizes known anterior-posterior (A-P) asymmetries of the early embryo (also see [Goldstein et al. 1993](#)). The unfertilized oocyte shows no asymmetry other than the eccentric placement of the egg nucleus and the presence of a cytoplasmic bridge linking each oocyte to the common cytoplasm of the germ line ([Strome 1986a; White 1988](#)). During the first cell cycle, however, the [zygote](#) becomes discernibly polarized along its long axis. The first cleavage bisects this axis, producing two daughter cells of different sizes with different developmental potentials ([Laufer et al. 1980; Cowan and Macintosh 1985; Priess and Thomson 1987](#)). The blastomeres also differ in cell division timing, centrosome behavior, and cytoplasmic composition.

P granules are perhaps the best known marker of early embryonic polarity ([Strome and Wood 1982, 1983](#)). These granules are present in the cytoplasm of oocytes and early embryos, become localized to the posterior of the [zygote](#), and are partitioned to the posterior blastomere,  $P_1$ . They continue to be partitioned asymmetrically at each of the unequal cleavages in the [germ-line cells](#) ( $P_1$ ,  $P_2$ , and  $P_3$ ) and remain associated with the germ lineage throughout the life of the worm. Because of their polar distribution and their association with the germ line, it is possible that they play a part in establishing embryonic polarity or germ-cell fate or both. P granules appear to be ribonucleoprotein particles. *In situ* hybridization studies have shown that P granules are associated with SL1-containing, poly(A)<sup>+</sup> RNAs ([Seydoux and Fire 1994](#)). In addition to unidentified proteins that are recognized by monoclonal antibodies ([Strome and Wood 1983; Yamaguchi et al. 1983](#)), two known proteins, GLH-1, a putative RNA helicase, and MEX-3, a protein with putative RNA-binding domains, have been detected in P granules by immunolocalization studies ([Roussell and Bennett 1993](#); M. Gruidl and K. Bennett; B. Draper and J. Priess, both pers. comm.). PGL-1, a novel protein with a putative RNA-binding domain, may be another component of P granules. [pgl-1](#) mutant worms lack some P-granule epitopes and show a maternal-effect sterile phenotype (I).

Kawasaki, and S. Strome, unpubl.). This is consistent with the notion that P granules are indeed involved in some aspect of germ-line development.

Important developmental regulators also exhibit asymmetric distributions in early embryos: SKN-1 ([Bowerman et al. 1993](#)), GLP-1 ([Evans et al. 1994](#)), PIE-1 (C. Mello et al., pers. comm.), and PAL-1 (C. Hunter and C. Kenyon, pers. comm.). SKN-1, PIE-1, and PAL-1 are localized to posterior cells via unknown mechanisms. GLP-1 is detected in only the anterior cell, [AB](#), and its immediate descendants and is restricted to these cells by translational control ([Evans et al. 1994](#)).

Some maternal messenger RNAs are also asymmetrically distributed in early embryos. In most cases, the differences are due to differential mRNA stability in germ-line versus [somatic cells](#) ([Seydoux and Fire 1994](#)), but two cases of mRNAs with graded distributions in one-cell embryos have been reported ([pos-1](#), H. Tabara et al., pers. comm.; [mex-3](#), B. Draper and J. Priess, pers. comm.).

The roles of some of these localized molecules are discussed in [Schnabel and Priess](#) (this volume). In the remainder of this chapter, we provide a more detailed description of the events of early embryogenesis and review progress toward understanding the mechanisms responsible for establishing polarity.

## Figures

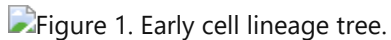


### Figure 1

Early cell lineage tree. Cell divisions are indicated by horizontal lines; the anterior daughter of each division is placed on the left. A series of unequal divisions of the germ-line or P cells results in formation of five somatic founder cells ([AB](#), [MS](#), [E](#), [C](#), and [D](#)) and the primordial germ cell ( $P_4$ ). The tissues generated by each founder cell are indicated. (Adapted from [Sulston et al. \[1983\]](#) and [Schierenberg \[1987\]](#).)



### Figure 2

Nomarski differential interference-contrast images of living embryos. Anterior is left, and ventral is down. (a) Appearance of the oocyte (o) and sperm (s) pronuclei; (b) pronuclear migration and pseudocleavage; (c) pronuclear meeting; (d) Rotation of the mitotic spindle onto the A-P axis; (e) first mitosis; (f) two-cell embryo; (g) four-cell embryo; (h) eight-cell embryo; (i) embryo beginning gastrulation; (j) "comma"-stage embryo; (k) "tadpole"-stage embryo; (l) "pretzel"-stage embryo. Bar, 10  $\mu\text{m}$ . (Reprinted, with permission, from Schierenberg 1986.)

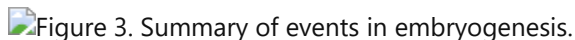


### Figure 3

Summary of events in embryogenesis. The timing of key events and stages of elongation (at 20°C) are shown on the left. The number of living nuclei in different stage embryos is plotted on the right. Fertilization is normally at ~50 minutes. (Reprinted, with permission, from [Strome \[1989\]](#), as adapted from [Sulston et al. \[1983\]](#).)

## Chapter 13. Fertilization and Establishment of Polarity in the Embryo — II Fertilization

---

The process of fertilization in *C. elegans* occurs within the spermatheca of the adult hermaphrodite: Contractions of the oviduct force an oocyte into the spermatheca, where the leading end of the oocyte appears to engulf a single sperm ([Ward and Carrel 1979](#)). The newly fertilized egg exits its prophase arrest state and completes meioses I and II, extruding two polar bodies at the future anterior end of the embryo. Concurrently, a hard and impermeable eggshell forms around the embryo.

As in many other invertebrate embryos, in *C. elegans*, the vast majority of factors needed to nourish and guide the development of the early embryo appear to be maternally supplied (see this chapter and [Schnabel and Priess](#), this volume). Nevertheless, the sperm makes several essential contributions to the embryo.

First, sperm entry appears to activate the oocyte to begin embryogenesis. Unfertilized oocytes do not complete meiosis or become surrounded by an eggshell; they undergo rounds of DNA replication, but in the absence of functional microtubule-organizing centers (MTOCs), they do not undergo mitosis or cytokinesis ([Ward and Carrel 1979](#)). A sperm-supplied product, encoded by the *spe-11* gene, has been implicated in the activation process. Mutations in *spe-11* lead to a paternal-effect embryonic-lethal phenotype: Fertilization of wild-type oocytes by sperm from homozygous mutant animals leads to abnormal embryonic development ([Hill et al. 1989](#)). The abnormal embryos fail to complete meiosis, form a weak eggshell, show defects in spindle orientation, and fail to undergo cytokinesis. The similarities between Spe-11 embryos and unfertilized oocytes suggest that SPE-11 participates in at least some aspects of egg activation. SPE-11 is normally supplied via the sperm but can by genetic engineering be supplied via the oocyte instead ([Browning and Strome 1996](#)). This finding that SPE-11 can be supplied through either gamete suggests that it serves a direct function in the early embryo, as opposed to an indirect role during spermatogenesis.

Second, centrosomes are paternally inherited in *C. elegans*. The poles of the oocyte meiotic spindle lack centrioles ([Albertson and Thomson 1993](#)) and are apparently incapable of functioning as MTOCs for mitosis. The centriole-containing centrosome present in the sperm duplicates after fertilization, and the resulting MTOCs nucleate the microtubules that mediate pronuclear migration and compose the mitotic spindle ([Albertson 1984b](#)).

Third, the site of sperm entry specifies the future posterior end of the embryo. The sperm normally enters the end of the oocyte that first penetrates the spermatheca, and this end becomes posterior. The oocyte nucleus normally resides at the opposite end, and its polar body products usually mark the future anterior of the embryo (see [Fig. 2a](#)). Recently, [Goldstein and Hird \(1996\)](#) demonstrated that when the rate of passage of oocytes into the spermatheca is speeded up, the position of sperm entry into the oocyte is frequently altered, and in all cases, the pole of sperm entry becomes posterior. Thus, the unfertilized *C. elegans* oocyte has no predetermined axis. The sperm is thought to specify the initial asymmetries in the embryo by directing cytoplasmic rearrangements that cause determinants to become asymmetrically localized (see below).

Generated from local HTML

## Chapter 13. Fertilization and Establishment of Polarity in the Embryo — III Establishment of Polarity in the One-Cell Embryo

Following sperm entry and completion of meiosis by the oocyte nucleus, the sperm and oocyte pronuclei form at the posterior and anterior ends, respectively, of the embryo (see [Fig. 2a](#)). The next phase of the first cell cycle is marked by dramatic cytoplasmic reorganization: Internal cytoplasm streams posteriorly, whereas cortical cytoplasm streams anteriorly ([Hird and White 1993](#)). The anterior cortex undergoes a series of contractions, which eventually result in the formation of a pseudocleavage furrow at 50% egg length ([Fig. 2b](#)); the oocyte pronucleus migrates posteriorly toward the sperm pronucleus, and the two meet in the posterior hemisphere and move to the center of the embryo ([Fig. 2c,d](#)). P granules become localized in the posterior half of the embryo, concentrated around the cortex (see [Fig. 4](#)). After cytoplasmic streaming ceases and the pseudocleavage furrow relaxes, the growing mitotic spindle rotates onto the A-P axis, the nuclear membranes break down, and the chromosomes align along the metaphase plate. The initially symmetrical spindle becomes asymmetric during anaphase ([Fig. 2e](#)); the anterior aster remains fixed in position, whereas the posterior aster swings from side to side and becomes smaller as it moves closer to the posterior cortex ([Albertson 1984b; Kemphues et al. 1988b](#)). The anterior and posterior centrosomes also take on different appearances as mitosis progresses, the anterior centrosome being spherical and the posterior being disc-shaped. Finally, the cleavage furrow bisects the asymmetric spindle to generate a large anterior cell, the somatic founder cell [AB](#), and a smaller posterior cell, the germ-line cell [P<sub>1</sub>](#) ([Fig. 2f](#)).

### A. Cytoplasmic Streaming

The period of cytoplasmic reorganization, which comprises only about 15 minutes of the first 100-minute cell cycle (at 16°C), converts the initially symmetrical egg into a highly polarized embryo. The cytoplasmic streaming observed during this period appears to have a crucial role in generating asymmetry. The streaming was first reported by [Nigon et al. \(1960\)](#) and later carefully documented by [Hird and White \(1993\)](#) using time-lapse video microscopy to follow individual cytoplasmic granules observed with Nomarski microscopy. Internal granules flow posteriorly toward the sperm pronucleus, whereas cortical granules flow anteriorly away from the sperm pronucleus. This “fountainhead” pattern of cytoplasmic streaming may be directed by the sperm pronucleus, the associated centrosomes and nascent microtubules, or a localized cortical change induced by sperm entry, since embryos in which the sperm entered laterally display cytoplasmic streaming that is laterally directed toward the sperm pronucleus ([Goldstein and Hird 1996](#)). The direction of streaming becomes shifted toward the nearest (future posterior) pole as the sperm pronucleus, associated centrosomes, and perhaps overlying membrane shift toward that pole.

Cytoplasmic streaming appears to have a major role in localizing germ-line-specific P granules to the posterior cortex of the one-cell embryo. This insight has come from monitoring the behavior of fluorescently tagged P granules in living embryos ([Hird et al. 1996](#)). The granules are distributed throughout the cytoplasm of newly fertilized embryos. The majority of granules flow toward the posterior pole at the same time and with the same speed as general cytoplasmic streaming occurs. In addition, as observed with general cytoplasmic streaming, P granules at the posterior cortex show some anterior movement away from the sperm pronucleus. Differential stability of P granules in different regions of the cytoplasm also appears to contribute to P-granule partitioning in the one-cell embryo; P granules in the anterior-most region of the embryo do not move posteriorly and instead disappear from view ([Hird et al. 1996](#)). This is thought to reflect disassembly or degradation of P granules in cytoplasm that is destined for the somatic daughter cell. This would suggest that, in addition to asymmetric localization of P granules, there is asymmetric localization of the ability to maintain P granules. The consequence of partitioning P granules to the posterior cortex is that the granules are inherited exclusively by [P<sub>1</sub>](#). During subsequent divisions, they are passed to [P<sub>2</sub>](#), [P<sub>3</sub>](#), and then [P<sub>4</sub>](#), the primordial germ cell.

### B. The Crucial Role of Microfilaments

The actin cytoskeleton is required to generate asymmetry in the one-cell embryo. Treatment of embryos with the microfilament inhibitor cytochalasin D disrupts the microfilament cytoskeleton ([Strome 1986b](#)) and prevents cytoplasmic streaming ([Hird and White 1993](#)), P-granule segregation to the posterior, and the development of spindle asymmetry ([Strome and Wood 1983](#)). In cytochalasin-treated embryos, the pronuclei meet centrally and P granules coalesce in the center of the embryo, both asters of the spindle behave similarly, and the spindle remains symmetrically located ([Fig. 5b](#)). Cytokinesis does not occur ([Strome and Wood 1983](#)). On the basis of analysis of embryos treated with cytochalasin D for only brief intervals in the first cell cycle ([Fig. 5c–e](#)), the crucial time interval for microfilament function is the interval of cytoplasmic reorganization described above. Drug treatment of embryos during this interval, but not before or after, prevents P-granule partitioning and spindle asymmetry, leading to symmetrical division and distribution of P granules to both daughters ([Hill and Strome 1988](#)). Analysis of the resulting two-cell embryos further reveals that microfilament disruption during the one-cell stage also leads to missegregation of the potential for future unequal divisions and unequal partitioning of P granules ([Hill and Strome 1990](#); see below). Thus, microfilaments appear to be involved in many or all aspects of asymmetry in the one-cell embryo.

Where are microfilaments located when they perform their crucial role(s) in the one-cell embryo? Staining of embryos with rhodamine phalloidin revealed that microfilaments exist as a meshwork of fine fibers just below the cell surface and as cortical dots or foci ([Strome 1986b](#)). The fine fibers remain around the entire periphery throughout the first cell cycle. However, the foci become concentrated in the anterior cortex during the period of cytoplasmic reorganization. Although this striking asymmetry in microfilament foci correlates roughly with the time of cytochalasin sensitivity, it is not essential for establishing polarity. Embryos from *nop-1* (for no pseudocleavage) mutant mothers lack the asymmetrically distributed microfilament foci, yet are viable and undergo cytoplasmic streaming and P-granule localization ([Rose et al. 1995](#)). Thus, the anteriorly concentrated microfilament foci observed in wild-type embryos apparently are not responsible for generating asymmetry, but instead are another manifestation of asymmetry in the one-cell embryo. The component of the actin cytoskeleton that appears to be critical for the establishment of asymmetry is the uniform cortical meshwork. This meshwork may serve as a scaffold upon which other factors become asymmetrically localized.

## C. The Role of the *par* Genes

Maternal-effect lethal mutations have identified several genes with roles in establishing early embryonic polarity: *mex-1* ([Mello et al. 1992](#)) and the six *par* genes ([Kemphues et al. 1988b; Kemphues 1989; Kirby et al. 1990; Morton et al. 1992; Cheng et al. 1995](#); J. Watts et al., in prep.). *mex-1* has a role in localization of SKN-1 and P granules (see [Schnabel and Priess](#), this volume). Mutations in the six *par* genes (for partitioning-defective) lead to disruption of several aspects of A-P polarity in the [zygote](#), including P-granule localization, pseudocleavage and cytoplasmic streaming, and asymmetric placement of the first cleavage spindle ([Kemphues et al. 1988b; Kirby et al. 1990](#)). The daughter cells that result do not exhibit typical polar behaviors. They divide synchronously and in many cases have altered spindle orientations. In addition, molecules that are normally restricted to either anterior or posterior blastomeres have abnormal distributions in *par* mutant embryos. SKN-1 or GLP-1 or both fail to localize in *par-1*, *par-2*, and *par-3* mutant embryos ([Bowerman et al. 1993](#); B. Bowerman; S. Crittenden and J. Kimble, both pers. comm.), and PAL-1 and PIE-1 are undetectable in *par-1* embryos (C. Hunter and C. Kenyon; C. Schubert et al., both pers. comm.). Subsequent development is aberrant, with alterations in timing and spindle orientation in later cleavages and alterations in cell fates. Embryos arrest as amorphous masses of differentiated cells.

Although mutations in all of the *par* genes affect the same processes, the mutant phenotypes are gene-specific (see [Table 1](#)) ([Kemphues et al. 1988b; Morton et al. 1992; Cheng et al. 1995](#)). For example, *par-1* and *par-4* strongly affect P-granule localization but only weakly affect spindle positioning and orientation, whereas the remaining four *par* genes have a strong effect on spindle behavior and a weaker effect on P-granule localization. The differences are not simply quantitative: *par-2* and *par-5* affect spindle orientation in the P<sub>1</sub> cell, and *par-3* and *par-6* affect spindle orientation in the AB cell. Similarly, *par-1*, *par-3*, and *par-6* mislocalize SKN-1 and *par-2* does not.

The *par* genes appear to be exerting their primary effects during the first cell cycle. First, as described above, the earliest deviation from normal occurs in the *zygote* (Kirby et al. 1990). Second, temperature-sensitive mutations in *par-2* and *par-4* are insensitive to nonpermissive temperature after the one-cell stage (Morton et al. 1992; Cheng et al. 1995). Consistent with this view, the *PAR* proteins are present in the one-cell embryo (Fig. 6 and see below). However, the *PAR* proteins may also play a part in germ-line development. At least one allele at each locus is incompletely expressed; i.e., some embryos escape the maternal-effect lethality and grow to be adult worms. Most such worms are agametic (Kemphues et al. 1988b; Morton et al. 1992; Cheng et al. 1995; K.J. Kemphues, unpubl.). This could be a secondary consequence of a weak defect at the one-cell stage or could reflect a requirement for the *par* genes in later germ-line development. The protein distributions described below are consistent with the latter possibility.

## D. Mode of Action of the *par* Genes

Although it is not yet known how the *par* genes work, information obtained by cloning of three of the *par* genes gives some important clues. PAR-1 is a 126-kD protein that includes near its amino terminus a serine/threonine protein kinase domain with strong similarity to a small subclass of widely conserved kinases. PAR-1 shares with these kinases an additional domain of unknown activity at the carboxyl terminus (Guo and Kemphues 1995). The kinase activity appears to be important for *par-1* function, since two mutations affecting conserved amino acids of the kinase domain produce phenotypes indistinguishable from the putative null allele. PAR-2 is a novel protein with a predicted size of 72 kD and contains a zinc-binding domain of the "ring finger" class and a myosin-type ATP-binding site (Levitian et al. 1994). PAR-3 is a novel protein of 138 kD (Etemad-Moghadam et al. 1995).

All three proteins become localized to the cell periphery of the *zygote* in an asymmetric fashion (Fig. 6). PAR-1 and PAR-2 are restricted to the posterior 40–50% of the *zygote* (Guo and Kemphues 1995; L. Boyd and K. Kemphues, unpubl.), whereas PAR-3 is restricted to the anterior 50–60% of the *zygote* (Etemad-Moghadam et al. 1995). None of the protein sequences have features consistent with membrane localization, so it seems likely that the proteins are associated with the cortical cytoskeleton. It is possible that the effects of cytochalasin on polarity (Hill and Strome 1988, 1990) could be due in part to the mislocalization of the PAR proteins.

Analysis of PAR protein distributions in *par* mutant embryos has revealed relationships among the *par* genes with respect to control of their localization (for summary, see Fig. 7a) (Etemad-Moghadam et al. 1995; Watts et al. 1996; L. Boyd and K.J. Kemphues, unpubl.). The major conclusions are (1) PAR-2 and PAR-3 are mutually dependent for their localization, (2) PAR-3 restricts PAR-1 to the posterior, (3) *par-6* acts to stabilize PAR-3 at the cortex, and (4) *par-4* is not involved in localizing PAR-1, PAR-2, or PAR-3. The role of *par-5* is unclear. The results suggest the following model (Fig. 7b): A graded distribution of PAR-3 along the future A-P axis is generated in response to the polarity cue provided by the sperm. This graded distribution is reinforced by the activity of PAR-2, which excludes PAR-3 from the posterior cortex. PAR-1 is excluded from the anterior cortex by PAR-3.

This model for localization can explain an unexpected genetic interaction. Reducing wild-type *par-6* activity suppresses *par-2* loss-of-function mutations (J. Watts et al., in prep.). Two observations of PAR-3 distribution suggest a likely explanation. First, in *par-6* mutant embryos, PAR-3 is not maintained at the cortex. Second, in *par-2* mutant embryos, PAR-3 is not restricted to the anterior but rather is present at the cell periphery in a gradient along the A-P axis. Suppression of the *par-2* mutations by reducing *par-6* could be the result of a uniform decrease in the amount of PAR-3 at the cortex. Because of the graded distribution of PAR-3 in *par-2* mutants, an overall reduction of PAR-3 in the cortex would reduce the amount of PAR-3 at the posterior periphery to negligible levels, but would leave significant amounts of PAR-3 at the anterior, resulting in a more nearly normal distribution of PAR-3. This would, in turn, lead to a nearly normal distribution of PAR-1. Preliminary results from examining the distribution of PAR-3 in the suppressed embryos support this view (J. Watts and B. Etemad-Moghadam, pers. comm.). If this interpretation is correct, then the primary function of PAR-2 is to restrict PAR-3 protein to the anterior periphery.

The modes of action of PAR-3 and PAR-1 are less clear. PAR-3 has at least two functions. One, as described below, is control of spindle orientation, and the other is the localization of PAR-1. It is possible that localizing

PAR-1 is the major way that PAR-3 influences intracellular polarity. Alternatively, PAR-3 could be mediating the localization of multiple cellular components including PAR-1. PAR-1 presumably acts via phosphorylation, but its substrates and site of action are unknown. Although its localization to the posterior periphery suggests that it has a role there, a detectable amount of PAR-1 protein is found in the cytoplasm ([Guo and Kemphues 1995](#)). Furthermore, the PAR-1 protein exhibits partial function when it is not localized, as occurs in *par-2* mutant embryos (see [Fig. 7a](#)). In *par-2* mutants, P granules become localized to the posterior of the zygote ([Cheng 1991](#)) despite the fact that PAR-1 is not localized to the cortex. Because *par-1* activity is required for P-granule localization ([Kemphues et al. 1988b](#); [Guo and Kemphues 1995](#)), these observations indicate that asymmetric peripheral localization of PAR-1 is not necessary for it to mediate the posterior localization of P granules. Why is PAR-1 localized? Perhaps events in the zygote other than localization of P granules require high concentrations of PAR-1 at the posterior periphery. Alternatively, asymmetric cortical localization may be required to assure proper amounts of PAR-1 in P<sub>1</sub>, P<sub>2</sub>, and P<sub>3</sub> (see next section).

## Figures



### Figure 4

Asymmetries of the early embryo. (Left) Cellular components that are predominantly anterior; (right) components that are predominantly posterior. Components in parentheses are not shown in the diagram. Late one-cell embryo (P<sub>0</sub>): P granules are localized in the posterior; pronuclei meet in the posterior; microfilament foci are concentrated in the anterior cortex; *mex-1* mRNA is present in an anterior-to-posterior gradient; and *pos-1* mRNA is present in a posterior-to-anterior gradient. Two-cell embryo: AB is larger than P<sub>1</sub>; GLP-1 protein is variably detected in the AB cell; P granules become localized to the posterior of P<sub>1</sub>; SKN-1 protein is present in higher concentration in the P<sub>1</sub> nucleus; PIE-1 is present only in P<sub>1</sub>; and class II mRNAs disappear from AB. Four-cell embryo: GLP-1 is found exclusively in the AB daughters, both in the cytoplasm and at the cell periphery; SKN-1 and PAL-1 are found almost exclusively in EMS and P<sub>2</sub>; PIE-1 is present only in P<sub>2</sub>; class II mRNAs are found only in P<sub>2</sub>; and P granules localize to the ventral half of P<sub>2</sub>. For references, see text.

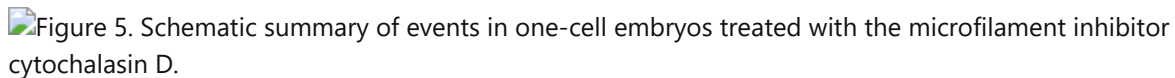


### Figure 5

Schematic summary of events in one-cell embryos treated with the microfilament inhibitor cytochalasin D. Anterior is left. (a) Untreated embryo; (b) embryo exposed to cytochalasin D at or after meiosis and left continuously in inhibitor; (c–e) embryos treated briefly with cytochalasin D from meiosis until the commencement of pronuclear migration (c), during pronuclear migration (d), and after pronuclear migration and pseudocleavage (e). (Reprinted, with permission, from [Strome \[1989\]](#), as adapted from [Hill and Strome \[1988\]](#).)



### Figure 6

Distribution of PAR-1, PAR-2, and PAR-3 in one-cell embryos. Embryos were stained by indirect immunofluorescence using antibodies specific for each protein. Anterior is left. (a) PAR-1; (b) PAR-2; (c) PAR-3. Bright spots in the center of the embryos are the metaphase chromosomes, which have been stained with DAPI and are visible in these double exposures.



### Figure 7

Overview and model. (a) Distribution of PAR-1, PAR-2, and PAR-3 proteins in various *par* mutant backgrounds. PAR-1 is shown in blue, PAR-2 in red, and PAR-3 in green. The genotypes are indicated on the left; interpretations of the distributions are shown at the right. (b) Current model describing the localization of the PAR proteins. This model shows functional relationships and is not meant to indicate temporal order. (1) The sperm provides a polarity cue, arbitrarily shown as a gradient. (2) PAR-3 responds to that cue by establishing a graded distribution, high in the anterior and low in the posterior. (3) PAR-3 and PAR-2 interact, leading to a mutually exclusive distribution, with PAR-3 restricted to the anterior. (4) PAR-3 restricts the distribution of PAR-1 to the posterior. (5) By unknown mechanisms, these proteins mediate the asymmetric distribution of a large number of other cellular components.

## Tables

**Table 1** Par mutant phenotypes

Genotype	First cleavage	Timing of second cleavage	P granual distribution	<b>AB</b> spindle orientation	<b>P1</b> spindle orientation	SKN-1 localization at two-cell stage <sup>a</sup>	Intestine differentiation
Wild-type	unequal	asynchronous	localized	transverse	longitudinal	asymmetric	all embryos
<i>par-1</i>	equal (sl. var.)	synchronous	unlocalized	transverse (~20% of embryos)	transverse	symmetric	no embryos
<i>par-2</i>	equal	nearly synchronous	localized at first division, unlocalized thereafter	transverse	transverse	asymmetric	~10% of embryos
<i>par-3</i>	equal	nearly synchronous	localized in some embryos	longitudinal	longitudinal	symmetric in many embryos	~30% of embryos
<i>par-4</i>	unequal	synchronous	unlocalized	transverse	transverse (~20% of embryos)	n.d.	no embryos
<i>par-5</i>	equal	synchronous	unlocalized	transverse	transverse	n.d.	~20% of embryos
<i>par-6</i>	equal	nearly synchronous	partly localized	longitudinal	longitudinal	symmetric in many embryos	~60% of embryos

a

n.d. indicates not determined.

Generated from local HTML

# Chapter 13. Fertilization and Establishment of Polarity in the Embryo — IV Cell Division Patterns in the Early Embryo

---

## A. The Unequal Divisions of the P Cells

The [germ-line cells](#)  $P_0$ ,  $P_1$ ,  $P_2$ , and  $P_3$  divide unequally and along the A-P axis. (The orientation of division refers to the orientation of the mitotic spindle and hence the daughter cells.) In contrast, most of the [somatic cells](#) in the early embryo divide equally and orthogonally to the previous division. This somatic pattern is essentially the default pattern. This section deals with the mechanisms employed by the P cells to undergo a nondefault pattern of division.

The potential for unequal division appears to be localized in the posterior of the one-cell embryo. This is based on the results of embryo extrusion experiments ([Schierenberg 1988](#)). When the posterior 25% of the cytoplasm and membrane is extruded through a laser-induced hole in the eggshell, the partial embryo left inside the eggshell seals its membrane and subsequently divides equally. When the pronuclei or [zygote](#) nucleus is extruded along with the posterior cytoplasm and membrane, the extruded embryonic fragment divides unequally. Similar operations at the anterior of the embryo do not extrude the potential for unequal division. Thus, this potential is localized posteriorly and apparently is passed on to the  $P_1$  daughter.

The posterior localization of the potential for unequal division appears to be labile and depends on intact microfilaments. As mentioned above, brief disruption of the microfilament cytoskeleton during the crucial period in the one-cell stage results in an equal first division and distribution of P granules to both daughter cells ([Hill and Strome 1988](#)). These unusual two-cell embryos show four different patterns of subsequent division, which indicate that the potential for unequal division was inherited by only the posterior daughter cell (the normal situation), only the anterior daughter cell (a reverse polarity situation), both daughter cells (a mirror-image situation with two  $P_1$ -like cells), or neither daughter cell (a mirror-image situation with two [AB](#)-like cells) ([Hill and Strome 1990](#)). Furthermore, the unequal divisions are accompanied by P-granule partitioning to the small daughter cell, and equal divisions are accompanied by P granules being distributed to both daughters. These results demonstrate that unequal division and unequal partitioning are coupled, perhaps mechanistically.

The biochemical nature of the “potential for unequal division and P-granule partitioning” has not been elucidated. The P granules are not responsible because, based on the extrusion experiments described above ([Schierenberg 1988](#)), the potential for unequal division is localized to the posterior end of the one-cell embryo before P granules become localized posteriorly. The *par* gene products are good candidates, since *par* mutant embryos have apparently lost the potential for unequal division and partitioning. Furthermore, the asymmetric peripheral distribution of the PAR proteins is consistent with this view. During each of the unequal P-cell divisions ( $P_0$ ,  $P_1$ ,  $P_2$ , and  $P_3$ ), PAR-1, PAR-2, and PAR-3 establish asymmetric peripheral distributions. PAR-3 becomes distributed along the half of the cell opposite the P granules, and PAR-1 and PAR-2 take up a reciprocal distribution on the P-granule side of the cell. PAR-1 and PAR-2 are present at high concentrations only at the periphery of the P cells; PAR-3, although present in all early blastomeres, only becomes asymmetrically localized in unequally dividing P cells. Thus, the PAR proteins are in the right place at the right time to participate in localizing P granules posteriorly and then generating spindle asymmetry.

## B. The Anterior-Posterior Orientation of P-cell Divisions

The default pattern of division,  $90^\circ$  to the previous division axis, can be explained by the movements of the centrosomes. Prior to mitosis, the centrosome in a cell duplicates, and the two daughter centrosomes migrate away from each other to opposite sides of the nucleus (see [AB](#) cell in [Fig. 8a](#)), where they serve as the MTOCs of the mitotic spindle (for review, see [Strome 1993](#)). Deviations from this  $90^\circ$  pattern require alternative or additional movements of the centrosomes. In the P cells, there is an additional rotation of the centrosome-nucleus complex, which results in the spindle being oriented along the A-P axis during each P-cell division. The

rotation ([Fig. 8a](#)) has been best studied in two-cell embryos ([Hyman and White 1987; Hyman 1989](#)). The duplicated centrosomes in P<sub>1</sub> are initially oriented perpendicular to the A-P axis, with astral microtubules from each centrosome extending toward a site on the anterior cortex. Preferential interaction of the cortical site with the microtubules from one aster pulls that aster toward the anterior cortex, thereby rotating the entire centrosome-nucleus complex 90° and pulling the complex toward the anterior end of the cell. The evidence that either aster's microtubules can win the competition for the anterior cortical site comes from laser surgery experiments. When one centrosome or the microtubules from one centrosome are damaged with a laser microbeam, then the other centrosome is always pulled toward the anterior cortex ([Hyman 1989](#)). A similar rotation of the centrosome-nucleus complex is observed in P<sub>2</sub> and P<sub>3</sub>, as well as in P<sub>1</sub>.

What components mediate centrosome-nucleus rotation in the P cells? As expected, intact microtubules are required, as is an intact microfilament cytoskeleton ([Hyman and White 1987](#)). The anterior cortical site in P<sub>1</sub> is located at the junction of [AB](#) and P<sub>1</sub>, perhaps at the remnant of the division of P<sub>0</sub>. This site has been shown to contain actin and actin capping protein ([Waddle et al. 1994](#)). The model is that a protein complex, minimally consisting of actin, actin capping protein, and perhaps a tethered microtubule motor protein, captures some of the microtubules of one aster and reels the microtubules into the complex. If the microtubule motor is indeed located in the cortical site ([Fig. 8b](#)), then it is predicted to be a minus-end directed motor, such as cytoplasmic dynein, or a minus-end directed kinesin. Alternatively, microtubule movement could involve a plus-end directed motor, such as a kinesin, located in the centrosomes. In a third variation, the driving force for the rotation would be provided by microtubule depolymerization.

The *par* gene products also participate in controlling rotation of the centrosome-nucleus complex. In [par-2](#) mutant embryos, P<sub>1</sub> fails to undergo this rotation and therefore divides transversely (both P<sub>1</sub> and [AB](#) divide like a normal [AB](#)), and in [par-3](#) and [par-6](#) mutant embryos, a centrosome-nucleus rotation occurs in [AB](#), resulting in an A-P division (see [Fig. 8c](#)), i.e., both P<sub>1</sub> and [AB](#) divide like a normal P<sub>1</sub> ([Cheng et al. 1995](#); J. Watts et al., in prep.). The finding that [par-3](#) is epistatic to [par-2](#) (in double mutants, both P<sub>1</sub> and [AB](#) divide like P<sub>1</sub>) indicates that neither gene is required specifically for rotation of the centrosome-nucleus complex.

The current model is that PAR-3 acts to prevent rotation of the centrosome-nucleus complex, and PAR-2 is required to restrict PAR-3 activity to the [AB](#) cell ([Cheng et al. 1995](#)). The distribution of PAR-3 supports this model ([Etemad-Moghadam et al. 1995](#)). PAR-3 is found in all early cells (up to about the 50-cell stage) but is uniformly distributed at the periphery of [somatic cells](#) and asymmetrically distributed in the unequally dividing P cells. In two-cell [par-2](#) embryos, PAR-3 is distributed uniformly at the periphery of both blastomeres. In fact, at the two-cell stage, in all blastomeres with a transverse spindle orientation (wild-type [AB](#) and both cells of [par-2](#), [par-5](#), and some [par-1](#) and [par-4](#) two-cell embryos), PAR-3 is distributed uniformly, but in blastomeres with longitudinal spindles (wild-type P<sub>1</sub> and both cells of [par-3](#) and [par-6](#) two-cells), PAR-3 is either absent or distributed asymmetrically ([Fig. 8c](#)). A uniform distribution of PAR-3 around the periphery of transversely dividing cells could prevent spindle rotation in one of two ways. PAR-3 may either prevent formation of the cortical site or override the activity of the cortical site by promoting strong interactions between the asters and the cortex at multiple sites. Two observations favor the latter. First, PAR-3 appears to be present at the division remnant in both [AB](#) and P<sub>1</sub> throughout the cell cycle. Second, spindle position is more easily perturbed in P<sub>1</sub> cells in [par-3](#) mutant embryos than in wild type ([Cheng et al. 1995](#)). This implies that PAR-3 normally stabilizes the spindle in P<sub>1</sub> and would be consistent with it promoting an association between the cortex and the microtubules of the aster.

## C. Polarity Reversal in P<sub>2</sub>

The orientations of cell divisions are most easily observed in partial embryos that have been freed from the constraints of the eggshell, either by extruding portions of the embryo through a laser-induced hole in the eggshell or by removing the eggshell using chitinase. Analysis of partial embryos clearly reveals that there is a reversal in the polarity of division and cytoplasmic partitioning in P<sub>2</sub> relative to the earlier P cells ([Schierenberg](#)

[1987](#)): P<sub>0</sub> and P<sub>1</sub> segregate P granules posteriorly and generate a posterior P-cell daughter, whereas P<sub>2</sub> and P<sub>3</sub> segregate P granules anteriorly and generate an anterior P-cell daughter. (In intact embryos, the steric constraints of the eggshell and neighboring cells cause the P<sub>2</sub> and P<sub>3</sub> segregation and division axis to assume a dorsal-ventral orientation, with P granules and the P cell on the ventral side.) The mechanism by which polarity is reversed in P<sub>2</sub> is not understood, although it may involve the [mes-1](#) gene. Mutations in this maternal-effect gene cause defects in P-granule partitioning and division orientation and asymmetry in P<sub>2</sub> and P<sub>3</sub> ([Strome et al. 1995](#)). One explanation for observing [mes-1](#)-induced defects only in P<sub>2</sub> and P<sub>3</sub> is that [mes-1](#)<sup>+</sup> functions specifically in polarity reversal. However, an alternative and somewhat favored hypothesis is that the role of [mes-1](#)<sup>+</sup> is to stabilize whatever controls the polarized divisions and partitioning events of the P cells (perhaps the PAR proteins) and that the later-stage P cells (P<sub>2</sub> and P<sub>3</sub>) suffer the consequences of the progressive loss of polarity.

Why does polarity reversal occur in *C. elegans*? One possibility is that it enables the germ line and the intestinal lineage to stay in contact. Electron microscopy has revealed a close association between the primordial [germ cells Z2](#) and [Z3](#) and nearby intestinal cells during embryogenesis and in the newly hatched larva ([Sulston et al. 1983](#)). Based on this, it has been speculated that the intestine nourishes the germ line. In the absence of polarity reversal, the germ lineage would become separated from the intestinal lineage by other embryonic cells. This is indeed what is observed in embryos of the soil *Rhabditid cephalobus*, in which polarity reversal does not occur. Interestingly, later in *R. cephalobus* embryogenesis, cellular rearrangements restore contact between the primordial germ cell and the intestinal precursor, and by the onset of gastrulation, the spatial order of cells is similar to that in *C. elegans* ([Skiba and Schierenberg 1992](#)).

## D. Control of the Division Axis in the EMS Cell

Like the P cells, [EMS](#) divides along the A-P axis and generates daughter cells ([E](#) and [MS](#)) with different developmental fates. These properties of [EMS](#) require interaction with P<sub>2</sub> at the four-cell stage. This was demonstrated by studying the division axis and developmental potential of isolated [EMS](#) cells versus [EMS](#) cells recombined with P<sub>2</sub> or another blastomere ([Goldstein 1992, 1993, 1995a, b](#)). Contact between P<sub>2</sub> and [EMS](#) induces an A-P orientation of the mitotic spindle, and hence the division axis of [EMS](#), apparently by establishing a cortical site in [EMS](#) similar to that described above in the P cells. One centrosome in [EMS](#) rotates toward the site of cell-cell contact and this requires intact microtubules ([Goldstein 1995a](#)). In the absence of P<sub>2</sub>, centrosome rotation does not occur in [EMS](#), and in addition both daughters of [EMS](#) follow an [MS](#)-like fate ([Goldstein 1992, 1995b, 1995b](#)). The current model is that P<sub>2</sub> contact with [EMS](#) serves two distinct roles: to orient the mitotic spindle correctly and to induce the segregation of factors to one daughter of EMS. The proposed segregation event concentrates either gut-specifying factors in the [E](#) daughter or gut-inhibiting factors in the [MS](#) daughter ([Goldstein, 1995a, 1995b](#); also see [Schnabel and Priess, this volume](#)).

Although the oriented division of [EMS](#) is similar to those in the [P lineage](#) in many aspects, there are two distinguishing features. First, as discussed above, the orientation signal is cell-autonomous in the P cells, but nonautonomous in EMS. Second, all three PAR proteins are present and asymmetrically distributed at the cortex in the P cells, whereas only PAR-3 is present in [EMS](#), and it is uniformly distributed at the cortex ([Etemad-Moghadam et al. 1995](#)).

## E. Establishment of the Dorsal-Ventral and Left-Right Axes

Most of the discussion thus far has been of polarity along the A-P axis. Unlike the A-P axis, specification of the dorsal-ventral (D-V) and left-right (L-R) axes does not appear to involve differentially partitioned factors. Instead, these axes are determined by the chance positioning of blastomeres at the four-cell stage, followed by cell-cell interactions. The D-V axis becomes apparent as the two-cell embryo divides. Due to the constraints of the eggshell, the growing mitotic spindle in [AB](#) shifts from a strictly transverse orientation to an oblique orientation, and this in turn shifts the orientation of the P<sub>1</sub> spindle from longitudinal to oblique. In the resulting four-cell embryo, the position of the posterior daughter of [AB](#) ([ABp](#)) defines dorsal, and [EMS](#) is ventral (see [Fig. 2g](#)). [Priess](#)

[and Thomson \(1987\)](#) investigated whether the two daughters of [AB](#), which give rise to distinct dorsal- and ventral-specific lineages, become committed to their different fates during the division of AB. These investigators used a blunt-ended microneedle to reorient the [AB](#) spindle and thereby switch the positions of the [AB](#) daughters. This operation reversed the D-V axis but gave an otherwise normal worm. This result demonstrated that the two daughters of [AB](#) are developmentally equivalent at the four-cell stage. Further studies of manipulated embryos and maternal-effect lethal mutant embryos (for discussion, see [Schnabel and Priess](#), this volume) support the view that the differences in the fates of the two daughters of [AB](#) are due to differences in position, leading to differential cell-cell signaling.

The L-R axis is operationally defined by the establishment of the A-P and D-V axes. L-R asymmetries are first apparent as the four-cell embryo divides; the skewed spindle orientations in the two [AB](#) daughters ([ABA](#) and [ABp](#)) cause the two leftward [AB](#) granddaughters ([ABal](#) and [ABpl](#)) to be positioned slightly anterior of the two rightward [AB](#) granddaughters ([ABar](#) and [ABpr](#)). This slight A-P difference in position of the leftward and rightward [AB](#) cell pairs is evidently responsible for subsequent L-R differences in their development. [Wood \(1991\)](#) demonstrated this by micromanipulating four-cell embryos to reverse the relative A-P positioning of the leftward and rightward [AB](#) cell pairs. This caused the leftward [AB cells](#) to execute lineages typical of the right-hand side of the animal, and the rightward [AB cells](#) to execute left-hand lineages. Thus, in the six-cell embryo, the pair of [AB cells](#) on the right is developmentally equivalent to the pair on the left. As with D-V differences in development, L-R differences in development are dictated by cell-cell interactions, most of which probably occur early in embryogenesis (see [Schnabel and Priess](#), this volume).

## Figures

Figure 8. Centrosome movements and spindle orientations in two-cell embryos.

### Figure 8

Centrosome movements and spindle orientations in two-cell embryos. Black dots represent centrosomes, open circles are nuclei, and lines are microtubules. Anterior is left. (a) In wild-type embryos, centrosomes duplicate and migrate in both [AB](#) and [P<sub>1</sub>](#); in [P<sub>1</sub>](#) only, the centrosome-nucleus complex undergoes an additional rotation to align the spindle along the A-P axis. (Astral microtubules are not shown.) (Adapted from [Cheng et al. 1995](#).) (b) One model proposed to explain centrosome rotation in [P<sub>1</sub>](#). Minus-end directed microtubule motor proteins (e.g., cytoplasmic dynein or a minus-end directed kinesin, shown here as a lowercase y) are tethered to an anterior cortical site containing actin and actin capping protein. The motors capture astral microtubules from one centrosome, translocate toward the minus end of the microtubule, and pull that centrosome toward the cortical site. (Adapted from [Waddle et al. 1994](#).) (c) Centrosome positions and cortical distribution of PAR-3 protein at the two-cell stage in wild type and in various *par* mutant genetic backgrounds. PAR-3 distribution is indicated by shading.

Generated from local HTML

## Chapter 13. Fertilization and Establishment of Polarity in the Embryo — V Summary and Speculation

---

A-P polarity arises after fertilization. The sperm, in addition to providing components important for early development, determines the posterior of the embryo by providing a positional cue for a polarized reorganization of cytoplasmic components. The reorganization appears to be mediated, at least in part, by directed cytoplasmic flow. Known consequences of the reorganization are the localization of P granules to the posterior and the transient accumulation of microfilaments in the anterior. It is likely that other cytoplasmic components are affected as well. The first cleavage spindle aligns along the newly defined A-P axis and is positioned asymmetrically, resulting in an unequal cleavage. The [germ-line cells](#), P<sub>1</sub>, P<sub>2</sub>, and P<sub>3</sub>, also develop intracellular polarity, orient their spindles along the axis of polarity, and divide unequally. This series of unequal cleavages generates qualitative differences in the cytoplasm of the blastomeres. Such differences probably have important roles in distinguishing the fates of the founder cells and contribute to the cell-cell interactions that determine fates of cells on the D-V and L-R axes.

Our current understanding of the mechanistic basis for the reorganization in P<sub>0</sub> and reproducible spindle alignments in the P-cell lineage remains sketchy, but the results thus far provide a strong foundation for subsequent analyses. Cytoplasmic reorganization and spindle alignment appear to be mechanistically linked. Both depend on microfilaments, probably those at the cell cortex, and both depend on the activities of the *par* gene products. Attention is focused on the cortical cytoskeleton because both microfilaments and the PAR proteins are concentrated at the cell periphery. The PAR proteins become asymmetrically distributed prior to the localization of the P granules and are essential for proper localization of the granules.

Future progress in understanding the establishment of polarity depends on answering the following questions: What is the nature of the polarity cue provided by the sperm? How do the PAR proteins respond to that cue? What role does the actin cytoskeleton serve? How do the PAR proteins interact to establish their distributions along the A-P axis? How do the PAR proteins facilitate cytoplasmic reorganization? What roles do P granules and PAR proteins have in the control of protein asymmetries in subsequent stages?

Current results allow for some speculation. One very attractive unifying hypothesis has been proposed, based on a comparison of certain features of A-P polarity in *C. elegans* and *Drosophila* embryos ([Evans et al. 1994](#)). It is possible that the most essential aspect of A-P polarity in *C. elegans* is localization of the P granules. The granules may contain mRNAs and proteins that act as regulators of protein distribution. P-granule factors may determine whether specific proteins accumulate in the germ-line daughter or the somatic daughter of each unequal division. This control of protein accumulation could be at the level of mRNA stability, mRNA translation, protein stability, or a combination of these. Observations of translational control of [glp-1](#) mRNA and of differential stability of several mRNAs in germ-line versus somatic blastomeres are consistent with this view. In this model, all the genes required for A-P polarity function to localize or stabilize P granules and to orient the spindle in such a way that the P granules will be partitioned to one daughter cell. Although this model is consistent with results from a variety of analyses, there is no direct evidence for a causative link between P granules and polarity. It is possible that the role of P granules is limited to germ-line development and that rather than being an essential component of the polarity system, the granules are one of the cellular components that respond to the polarity system.

A key to future progress lies in determining the mode of action of the essential proteins that have been identified thus far and in identifying additional components of the polarity system. Molecular, biochemical, and genetic approaches are being used to identify proteins that interact with actin or with the PAR proteins. Elucidating the activities and cellular locations of these proteins should add structure and depth to the picture that has already emerged.



# **Chapter 14. Specification of Cell Fates in the Early Embryo**

---

## **Contents**

[I Introduction](#)

[II Specification of Cell Fates in the AB Lineage](#)

[III Specification of the P<sub>1</sub> Descendants](#)

[IV Future Prospects](#)

Generated from local HTML

# Chapter 14. Specification of Cell Fates in the Early Embryo — I

## Introduction

Classical studies in embryology showed that in certain animals, the descent, or lineage, of cells was correlated strictly with cell fate; these animals were described as having a determinate, autonomous, or mosaic mode of development. Nematodes like *Caenorhabditis elegans* have an invariant lineage and have been a paradigm of the determinate mode. Results from experiments on *C. elegans* in the 1980s were, and remain, consistent with the classical notion that some specification of cell fates in nematodes occurs autonomously ([Laufer et al. 1980](#); [Cowan and McIntosh 1985](#); [Edgar and McGhee 1986](#); [Schierenberg 1988](#)). For example, it was shown that certain cleavage-arrested blastomeres are nevertheless able to undergo tissue-specific differentiation. However, as described in this chapter, a large number of cell-cell interactions have now been identified in the *C. elegans* embryo. The invariant lineage of the embryo may result largely from the fact that invariant cleavage patterns set up reproducible patterns of cell-cell interactions.

All of *C. elegans* embryogenesis occurs within a transparent egg shell; the egg measures about 50 µm in length and 30 µm in diameter. The small size of the egg and the small number of cells at hatching (55) have made it possible to observe with the light microscope the pattern of cell cleavage and differentiation of [all cells](#) in the living embryo. A major conclusion from these studies is that this pattern, or lineage, is largely invariant between different embryos. Thus, it has been possible to construct a single diagram representing the entire cell lineage of the *C. elegans* embryo ([Deppe et al. 1978](#); [Sulston et al. 1983](#)).

During the first four cleavages of the embryo, five cells, or blastomeres, are produced that generate distinct sets of somatic tissues. These blastomeres, called [AB](#), [MS](#), [E](#), [C](#), and [D](#), often are referred to as somatic founder cells. The sister of D is the P<sub>4</sub> blastomere and is the precursor of the germ line ([Fig. 1](#)). We will discuss embryogenesis by focusing on how the fates of the individual founder cells are specified and by describing how P<sub>4</sub> becomes the germ-line precursor.

## Tables

**Table 1** Localization of gene products described in this chapter

Gene	Product	Localization	Mutant phenotype	References
<a href="#">apx-1</a>	transmembrane protein similar to LAG-2 in <i>C. elegans</i> and Delta in <i>Drosophila</i>	protein is in P <sub>1</sub> at the 2-cell stage and P <sub>2</sub> at the 4-cell stage RNA is maternal class II <sup>a</sup>	maternal-effect lethal mutations cause <a href="#">ABp</a> into <a href="#">ABA</a> transformation in fate	<a href="#">Mango et al. (1994a)</a> ; <a href="#">Mello et al. (1994)</a> ; <a href="#">Mickey et al. (1996)</a>
<a href="#">elt-2</a>	GATA-like transcription factor	preliminary data suggest <a href="#">elt-2</a> is expressed in Ea and Ep	embryonically expressed gene; mutant phenotype not known	<a href="#">Egan et al. (1995)</a> ; <a href="#">Hawkins and McGhee (1995)</a>
<a href="#">end-1</a>	GATA-like transcription factor	preliminary data suggest <a href="#">end-1</a> is expressed in Ea and Ep	embryonically expressed gene; null mutations cause E to adopt a C-like fate	J. Zhu and J. Rothman (pers. comm.)
<a href="#">glp-1</a>	transmembrane receptor protein related to LIN-12 in <i>C. elegans</i> and Notch in <i>Drosophila</i>	expression begins in <a href="#">AB</a> at the 2-cell stage; present at the surfaces of all <a href="#">AB</a> descendants until about the 28-cell stage RNA is maternal class II	maternal-effect lethal alleles exist that are defective primarily in the 12-cell stage interaction between the <a href="#">MS</a> blastomere and <a href="#">AB</a> descendants; other alleles also are defective in the 4-cell stage interaction between P <sub>2</sub> and <a href="#">ABp</a> ; see <a href="#">Fig. 2</a> for summary of	<a href="#">Austin and Kimble (1987)</a> ; <a href="#">Priess et al. (1987)</a> ; <a href="#">Yochem and Greenwald (1989)</a> ; <a href="#">Evans et al. (1994)</a> ; <a href="#">Hutter and Schnabel (1994)</a> , <a href="#">1995a</a> ; <a href="#">Mello et al. (1994)</a> ; <a href="#">Moskowitz (1994)</a>

<b>Gene</b>	<b>Product</b>	<b>Localization</b>	<b>Mutant phenotype</b>	<b>References</b>
			transformations in cell fate; the <a href="#">MS</a> blastomere does not produce muscle in <a href="#">glp-1</a> mutants RNA is maternal class II	<a href="#">et al. (1994); Schnabel (1994)</a>
<a href="#">mex-3</a>	probable RNA-binding protein with two KH domains	cytoplasmic protein present in oocytes and all early blastomeres; most abundant in <a href="#">AB</a> and <a href="#">AB</a> daughters; MEX-3 is a component of P granules; mRNA most abundant in <a href="#">AB</a> and <a href="#">AB</a> daughters, disappears from embryo in class II pattern	maternal-effect lethal mutations cause <a href="#">AB</a> descendants to adopt C fates; mutants have PAL-1 misexpressed in <a href="#">AB</a> descendants; mutants also have extra cells that resemble <a href="#">Z2</a> or <a href="#">Z3</a> ; correlated with variable defect in P <sub>3</sub> development	E. Draper et al. (in prep.); C. Hunter and C. Kenyon (in prep.)
<a href="#">pal-1</a>	product is a homeodomain protein that is most similar to the Caudal protein of <i>Drosophila</i>	nuclear protein appears in <a href="#">EMS</a> and P <sub>2</sub> late in the 4-cell stage RNA is maternal class II	removing maternal expression prevents P <sub>2</sub> from producing muscle	<a href="#">Waring and Kenyon (1991); C. Hunter and C. Kenyon (in prep.)</a>
<a href="#">pie-1</a>	novel nuclear protein	nuclear protein present exclusively in germ-line blastomeres during the early cleavages RNA is maternal class II	maternal-effect lethal mutations cause P <sub>2</sub> blastomeres to produce <a href="#">EMS</a> -like cell types including intestinal cells and <a href="#">pharyngeal cells</a> ; mutations result in inappropriate transcription in the germ-line blastomeres	<a href="#">Mello et al. (1992); C. Mello et al. (in prep.); G. Seydoux et al. (1996)</a>
<a href="#">pop-1</a>	HMG-box transcription factor	nuclear protein present in oocytes and in all early blastomeres RNA pattern not determined	a maternal-effect lethal mutation causes <a href="#">MS</a> to adopt an E fate	<a href="#">Lin et al. (1995)</a>
<a href="#">skn-1</a>	probable transcription factor with DNA-binding domain	nuclear protein; higher level in P <sub>1</sub> than in <a href="#">AB</a> at 2-cell stage, highest levels in <a href="#">EMS</a> and P <sub>2</sub> at 4-cell stage; present in <a href="#">MS</a> , E, P <sub>3</sub> , and C at 8-cell stage; not detectable after the 8-cell stage in early embryo RNA is maternal class II	in maternal-effect lethal mutants, the <a href="#">EMS</a> blastomere does not produce <a href="#">pharyngeal cells</a> and frequently does not produce intestinal cells; <a href="#">EMS</a> instead produces hypodermal cells and muscles similar to a wild-type C blastomere	<a href="#">Bowerman et al. (1992a, 1993), 1993; Blackwell et al. (1994)</a>

a

Maternal class II RNAs are described in [Seydoux and Fire \(1994\)](#). These RNAs are present uniformly in 2-cell and 4-cell stage embryos. In 8-cell stage embryos these RNAs persist in the P<sub>3</sub> and C blastomeres, but disappear from all other blastomeres. After the next round of cleavage, these RNAs persist only in P<sub>4</sub> and D.

## Chapter 14. Specification of Cell Fates in the Early Embryo — II

### Specification of Cell Fates in the AB Lineage

Most cells of the hatching larva, 389 of 558, are derived from the [AB lineage](#). [AB](#) descendants contribute to three major tissues, the [nervous system](#) (200 neurons and 40 supporting cells), the hypodermis (72 cells), and about half of the [pharynx](#) (49 cells). The [nervous system](#) and the hypodermis classically have been considered to be the ectoderm. The pattern of [AB](#) development appears to be very complex; for the most part, cell types do not arise from single progenitors. Instead, multiple [AB](#) descendants that are not closely related can produce the same type of cell.

The first, unequal cleavage of the fertilized [zygote](#),  $P_0$ , produces an anterior blastomere called [AB](#) and a slightly smaller posterior blastomere called  $P_1$  ([Fig. 1](#)). The cleavage of the [AB](#) blastomere is initiated parallel to the future dorsal-ventral axis of the embryo. However, as [AB](#) completes division, the daughter blastomeres shift positions such that one daughter is more anterior than the other; these daughters therefore are named [ABA](#) and [ABp](#), respectively ([Sulston et al. 1983](#)). The cleavage of the [AB](#) daughters initially is parallel to the future left-right axis of the embryo. These blastomeres also become shifted in position such that the left daughter of each blastomere pair is slightly anterior to the right daughter of each pair. This, together with the unequal divisions of the  $P_1$  descendants, results in an embryo with anterior-posterior, dorsal-ventral, and left-right asymmetries; thus, in three divisions, the fertilized egg becomes an asymmetric, or chiral, embryo.

The development of the left and right daughters of the [ABA](#) blastomere is asymmetrical. These daughters produce neurons and hypodermal and [pharyngeal cells](#) from distinct and complicated lineages ([Figs. 1](#) and [2](#)). In contrast, the left and right daughters of the [ABp](#) blastomere have almost symmetrical patterns of development. For example, [ABpla](#) and [ABpra](#) both produce mostly hypodermis, and [ABplp](#) and [ABprp](#) both contribute predominantly to the [nervous system](#).

Experiments in which blastomere positions were altered or specific blastomeres were killed with a laser microbeam indicated that cell-cell interactions had to play a major part in the specification of [AB](#) descendants ([Priess and Thomson 1987](#); [Schnabel 1991](#); [Wood 1991](#)). If the positions of [ABA](#) and [ABp](#) are interchanged as these blastomeres form, the embryo develops normally and hatches into a fertile worm ([Priess and Thomson 1987](#)). These experiments demonstrated that neither the dorsal-ventral nor the left-right axis of the embryo is fixed before the four-cell stage. If the relative left-right positions of the daughters of [ABA](#), and three of the daughters of [ABp](#), are switched simultaneously, the embryo hatches into a larva that grows to a fertile adult with an inverted left-right axis ([Wood 1991](#)). In other words, a blastomere on the left of the embryo, like [ABA](#), must initially have the potential to adopt the fate of a blastomere on the right of the embryo, like [ABp](#), just as [ABA](#) initially has the potential to adopt the normal fate of [ABp](#). The observation that the positions of sister blastomeres are critical for their developmental patterns suggested that these blastomeres are initially equivalent and that cell-cell interactions which depend on the general topology of the embryo must be taking place in the early embryo to break this equivalence.

To simplify the discussion of the specification of the [AB lineage](#), we focus on how the fates (identities) of the eight [AB](#) great-granddaughters are established in the early embryo ([Fig. 2](#)). It appears that the eight basic fates are established by three major and two minor binary switches, each switch serving to discriminate between otherwise equivalent fates. There is no evidence of major interactions after the onset of gastrulation; however, at least three lateral interactions in late embryogenesis specify the fates of three pairs of bilaterally homologous cells ([Sulston et al. 1983](#); [Bowerman et al. 1992b](#)).

#### A. A Cellular Interaction That Makes the Daughters of AB Different

Experiments by [Bowerman et al. \(1992a\)](#) showed that the formation of one type of cell normally made by [ABp](#), but not [ABA](#), required the  $P_2$  blastomere. This result suggested that interactions were occurring between the [ABp](#) and  $P_2$  blastomeres, but it did not explain the major differences observed between the [ABp](#) and [ABA](#).

blastomeres. Work by several laboratories then showed that the P<sub>2</sub> blastomere is responsible for breaking the initial equivalence of ABa and ABp by specifying the entire ABp identity (Hutter and Schnabel 1994; Mango et al. 1994b; Mello et al. 1994; Moskowitz et al. 1994). In a normal four-cell embryo, P<sub>2</sub> contacts the ABp blastomere but not the ABa blastomere. If ABp is prevented from contacting P<sub>2</sub> (Mello et al. 1994) or P<sub>2</sub> is removed from the embryo (Mango et al. 1994b; Moskowitz et al. 1994), then ABp does not produce the cell types it makes in normal development, and instead undergoes an ABa-specific pattern of differentiation. When ABa contacts descendants of the P lineage, it acquires an ABp-like fate (Hutter and Schnabel 1994; Mello et al. 1994). The interaction between ABp and P<sub>2</sub> has been shown by staining manipulated embryos with antibodies that recognize tissues normally produced by ABp (Mango et al. 1994b; Mello et al. 1994), and by directly following large parts of the AB lineage by four-dimensional microscopy (Hutter and Schnabel 1994; Moskowitz et al. 1994). The interaction does not induce a simple type of tissue differentiation, but rather results in a complex pattern of development involving the formation of several distinct tissues.

## B. Cellular Interactions That Generate Left-Right Asymmetry

Although interactions with P<sub>2</sub> appear to make ABp different from ABa, the left and right daughters of ABp are initially equivalent, as are the left and right daughters of ABa (Wood 1991). Evidence that EMS, or an EMS descendant, influences ABa development came initially from the finding that when the EMS blastomere was removed or killed, embryos did not produce the pharyngeal cells that normally are made by ABa (Priess and Thomson 1987). Further analysis of this interaction showed that the signaling cell was the daughter of EMS, the MS blastomere (Hutter and Schnabel 1994; Mango et al. 1994a). Remarkably, when signaling from MS was prevented, the entire AB lineage became left-right symmetrical (Fig. 2) (Hutter and Schnabel 1994). In these experiments, the blastomere ABara adopted the fate of its bilateral homolog, ABala, and ABalp adopted the fate of its bilateral homolog, ABarp. Thus, in wild-type embryogenesis, most of the left-right asymmetries in the fates of AB descendants are a consequence of signaling by the MS lineage (Fig. 3).

Two minor left-right asymmetries are specified by at least two additional later interactions (Hutter and Schnabel 1994, 1995a). The first is between descendants of ABala and ABpla. The second interaction is between an MS descendant, called MSap, and ABplp descendants. Unlike the induction specifying the primary left-right asymmetry in ABa, the specificity of these inductions is not conferred by discriminative cell-cell contacts on the left and right side of the embryo but by a restriction of the inductive competence to one of two bilateral homologs (Hutter and Schnabel 1995a). The establishment of left-right asymmetry is therefore a multistep process involving three inductions that depend on cell-cell contacts and that specify blastomere identities. The pattern of cell-cell contacts is a consequence of the invariant cleavage pattern of the embryo (see Kemphues and Stone, this volume). The left-right asymmetry in blastomere positions begins with the anterior-posterior skewing of the ABa and ABp cleavage planes; the basis for this skewing is not known. The oval egg shell surrounding the embryo may facilitate the skewing of the AB cleavage plane, but it is not essential because the majority of embryos still develop normally after removal of the egg shell (Hyman and White 1987; Wood and Kershaw 1991; Schierenberg and Junkersdorf 1992).

The interactions described above make the AB daughters different and the left-right pairs of AB granddaughters different. The diversification of the pairs of AB great-granddaughters, such as ABala and ABalp, can be described as the general problem of what makes ABxxa different from ABxp. The establishment of ABxxa/ABxp differences have been analyzed in two studies. Work by Gendreau et al. (1994) suggested that the ABxxa and ABxp fates may differ because of an anterior-posterior asymmetry in the embryo that already is present in AB by the first cleavage of the embryo. These authors removed the P<sub>1</sub> blastomere and found that the AB blastomere nevertheless produced pairs of great-granddaughters that had distinct ABxxa and ABxp fates as judged from the differentiation of hypodermal fates in posterior ABxp lineages. In contrast, Hutter and Schnabel (1995b) found that ablation of the P<sub>1</sub> blastomere with a laser microbeam at the two-cell stage could affect the ABxxa and ABxp differences. ABxp blastomeres executed complete ABxxa identities, suggesting that P<sub>1</sub> may contribute to the anterior-posterior polarization of AB (Fig. 3). Although the basis for these different results is not understood

at present, the [AB](#) and P<sub>1</sub> blastomeres remained in contact for a few minutes before removal of P<sub>1</sub> in the experiments of [Gendreau et al. \(1994\)](#). Thus, it is possible that P<sub>1</sub> needs only a brief period of time to interact with [AB](#) and had already polarized [AB](#) before it could be removed.

## C. Molecular Specification of AB Fates

Some of the genes involved in the P<sub>2</sub> and [MS](#) interactions have been identified. The [glp-1](#) gene ([Austin and Kimble 1987; Priess et al. 1987](#)) is a homolog of the *Notch* gene of *Drosophila* and the [lin-12](#) gene of *C. elegans* ([Yochem and Greenwald 1989](#)). [glp-1](#) is expressed maternally, and GLP-1 protein accumulates on the surfaces of [AB](#), but not P<sub>1</sub>, descendants ([Evans et al. 1994](#)). GLP-1 appears to function as a receptor in both the P<sub>2</sub> and [MS](#) interactions ([Hutter and Schnabel 1994; Mello et al. 1994; Moskowitz et al. 1994](#)); GLP-1 is a receptor for other cell-cell interactions as well (see [Schedl; Greenwald](#); both this volume). It appears to function with LIN-12 in the interactions that establish the minor left-right asymmetries described above (I. Moskowitz and J. Rothman, unpubl.).

Maternal-effect lethal mutations in the gene [gpx-1](#) were found to prevent the P<sub>2</sub> interaction with [ABp](#) ([Mango et al. 1994b; Mello et al. 1994](#)), resulting in defects in the development of [ABp](#) that were very similar to those observed in [glp-1](#) mutants ([Hutter and Schnabel 1994; Mello et al. 1994](#)). Cloning of [gpx-1](#) showed that it encoded a homolog of the *Drosophila* protein *Delta*, a ligand for *Drosophila Notch* ([Mello et al. 1994](#)). Immunolocalization studies have shown that the APX-1 protein is expressed in the P<sub>2</sub> blastomere and localized to the junction between [ABp](#) and P<sub>2</sub> ([Mickey et al. 1996](#)). Thus, it appears that APX-1 is the ligand for GLP-1 in the P<sub>2</sub> interaction.

APX-1 does not appear to be the ligand for the [MS](#) interaction since the left-right induction still occurs in [apx-1](#) mutants, and APX-1 protein has not been detected in [MS](#) in wild-type embryos ([Mickey et al. 1996](#)). Injection of antisense [apx-1](#) RNA into wild-type mothers should remove maternally expressed [apx-1](#) mRNA from embryos, and embryonically transcribed [apx-1](#) mRNA should not be present in embryos homozygous for a deficiency of the [apx-1](#) gene. However, the [MS](#) interaction still occurs in both types of embryos. Similar studies suggest that the [lag-2](#) and [arg-1](#) genes, which are homologs of [apx-1](#), also are not likely to encode the [MS](#) ligand (C. Mello, unpubl.). However, it remains possible that these genes have redundant functions in [MS](#) signaling.

The different responses of [AB](#) descendants to the P<sub>2</sub> and [MS](#) interactions have been proposed to result from a change of competence in the [AB](#) descendants between the times that the interactions occur ([Hutter and Schnabel 1994; Mango et al. 1994b; Mello et al. 1994](#)). The question of whether the P<sub>2</sub> and [MS](#) signals are different has been tested directly by replacing the [MS](#) blastomere in one embryo with a P<sub>2</sub> blastomere from a second embryo (C.A. Shelton and B. Bowerman, in prep.). The resulting chimeric embryos produced [pharyngeal cells](#) that normally result from the [MS](#), but not the P<sub>2</sub>, interaction, suggesting that the P<sub>2</sub> signal is functionally equivalent, although not identical, to the [MS](#) signal.

## D. Summary of Events Controlling AB Development

The early embryo up to the four-cell stage shows no visible left-right asymmetry. The embryo becomes asymmetric (chiral) only after the next cleavage. Later in embryogenesis, the body once again becomes bilaterally symmetrical as a consequence of cell migrations. Thus, the embryo makes successive transitions between topological symmetry, then topological and fate asymmetry, before returning to a general bilateral symmetry.

Theoretically, the different fates of the eight [AB](#) great-granddaughters could be established by three binary switches, each switch breaking the equivalence of a pair of blastomeres. *C. elegans* apparently uses only a few more, namely, five, binary switches to establish the identities of the eight great-granddaughters of [AB](#) ([Fig. 3](#)). The inductions described here have the following properties in common: (1) they all depend on cell-cell contacts, (2) they all act as binary switches to differentiate otherwise equivalent cells, (3) they all establish blastomere identities, i.e., complex lineage patterns and not tissues, and (4) they all act in combination. The first three

switches specify six different fates. Two more identities are established later by the two left-right switches specifying the minor asymmetries in [ABp](#). Four of the switches are specified by inductions. The switch specifying the anterior-posterior differences of the eight great-granddaughters of [AB](#) may represent either the autonomous expression of the potential to form hypodermis or an additional inductive interaction that specifies discrete blastomere identities ([Gendreau et al. 1994](#); [Hutter and Schnabel 1995b](#)).

Two major questions concerning the early specification of the [AB lineage](#) still remain open: (1) How is the initial identity of the [AB](#) blastomere specified? (2) How is its general polarity specified? When all the inductions are prevented by ablating the  $P_1$  blastomere in a [glp-1](#) mutant, all eight [AB](#) great-granddaughters develop like the wild-type ABala blastomere, and thus the [ABala](#) fate may be considered a ground state of the [AB lineage](#) (H. Hutter and R. Schnabel, unpubl.). The observed ABala lineages show a proper anterior-posterior polarity, indicating that the [AB](#) descendants still have anterior-posterior information. It is not known whether this polarity is determined autonomously or nonautonomously in the [AB](#) blastomere.

## Figures



### Figure 1

Early development of *C. elegans*. The lineage diagram shows the timing of the early cell divisions from the first cleavage. (Adapted, with permission, from [Sulston et al. 1983](#).) The vertical axis indicates time of development at 25°C. The stem-cell-like P blastomeres produce in unequal divisions the somatic founder cells [AB](#), [MS](#), [E](#), [C](#), [D](#), and the germ-line precursor  $P_4$ . The main tissues produced by the founder cells are shown under the lineage diagram.



### Figure 2

Specification of left-right asymmetry in the *C. elegans* embryo. The [AB lineage](#) is drawn to emphasize symmetry relationships. (Adapted, with permission, from [Sulston et al. 1983](#).) The dashed lines indicate the cells whose fates were compared in wild-type (outer columns) and in [glp-1\(e2072\)](#) mutant embryos (middle columns) or in wild-type embryos after ablation of the [MS](#) blastomere (inner columns). The key at the bottom of the figure lists the symbols for cell deaths, hypodermal cells, mitotic cells, nondividing cells, and unidentified cells. Symmetrical parts of the lineage are shaded. For example, [ABpla](#) on the left of the embryo normally has a pattern of development that is almost identical to [ABpra](#) on the right of the embryo. In contrast, [ABalp](#) in wild-type embryos is very different from [ABarp](#). However, the chart shows that these blastomeres have very similar patterns of development in [glp-1\(e2072\)](#) mutants and in wild-type embryos after ablation of the [MS](#) blastomere. The bold arrowheads indicate that this pattern of development represents a right to left transformation in cell fate relative to the normal fate of [ABarp](#). These results are summarized schematically on the right of the figure, with separate icons representing the patterns of development of the eight [AB](#) granddaughters in normal embryos and in symmetrical embryos (such as [glp-1\(e2072\)](#) or wild-type embryos after the [MS](#) blastomere is ablated). (Adapted, with permission, from [Hutter and Schnabel 1994](#).)



### Figure 3

Specification of the [AB lineage](#). (A) Schematic representations of the early stages of the *C. elegans* embryo showing the inductions of blastomere identities. At the 4-cell stage, the  $P_2$  blastomere induces the [ABp](#) fate. At the 6-cell stage, the embryo has visible left-right asymmetry in the positions of blastomeres (dorsal view shown). At the 12-cell stage, [MS](#) induces the first left-right asymmetry in cell fates in the ABa lineage by inducing the [ABara](#) and [ABalp](#) identities. At the 24- and 26-cell stages, the minor left-right asymmetries in the ABp lineage are

induced. (B) The logic of the specification of the identities of the eight great-granddaughters of AB. The induction of anterior-posterior identities can be achieved by two binary switches establishing the four different fates present before the left-right inductions occur. In one, the difference between ABa and ABp is induced. The second switch corresponds to the specification of the anterior-posterior differences of the eight great-granddaughters of AB indicated by the gray shading. This AB polarization may be intrinsic to the AB blastomere, or it may be determined by a polarizing interaction with P<sub>1</sub>. The icons for the final fates of the AB granddaughters are the same as those in [Fig. 2](#). (Adapted, with permission, from [Hutter and Schnabel 1995c](#).)

Generated from local HTML

## Chapter 14. Specification of Cell Fates in the Early Embryo — III Specification of the P1 Descendants

---

### A. P<sub>4</sub>, the Germ Cell Precursor

At hatching, the *C. elegans* larva contains two cells, Z2 and Z3, that are the precursors for all of the germ-line tissue. Z2 and Z3 are generated during early embryogenesis from the division sequence P<sub>0</sub>, P<sub>1</sub>, P<sub>2</sub>, P<sub>3</sub>, through P<sub>4</sub> (see Fig. 1). The P<sub>4</sub> blastomere divides only once more during early embryogenesis, producing Z2 and Z3. Each of the blastomeres P<sub>0</sub>–P<sub>4</sub> can be described as germ-line blastomeres, in contrast to all other embryonic blastomeres that produce only somatic cell types. The unique ability of the *germ cells* to reproduce the entire organism at the next generation often is described as totipotency, and the question of how certain embryonic cells remain totipotent has been a long-standing problem in developmental biology. In *Drosophila*, the germ-cell lineage is separated from *all somatic* cell lineages before the general cellularization of the embryo (Foe and Alberts 1983; Warn et al. 1985). In contrast, the germ-cell precursors in *C. elegans* and most animals share a common lineage with somatic cell precursors for the first several embryonic cleavages. In the nematode *Ascaris*, studies almost 100 years ago demonstrated that as somatic precursors were generated during the early cleavages, they lost chromosomal material, a phenomenon described as chromosomal diminution (Boveri 1910). This loss did not occur in any of the germ-line blastomeres, presumably allowing only these precursors to remain totipotent.

Although there is no evidence for chromosomal diminution in *C. elegans*, several characteristics of the germ-line blastomeres distinguish them from somatic blastomeres. Each germ-line blastomere is born from an unequal cleavage in which it is the smaller of two daughters. Before each unequal cleavage, cytoplasmic particles called P granules move toward the side of the parental blastomere from which the germ-line blastomere is born (Strome and Wood 1983). Thus, at all stages of embryogenesis, the P granules are localized exclusively in germ-line blastomeres (see also Kempfues and Stone, this volume).

Very little is known about the function and molecular composition of P granules or how P granules are localized to the germ-line blastomeres. Although it is possible that P granules are necessary for germ-cell differentiation, several experiments indicate that the presence of P granules does not preclude somatic cell differentiation. If germ-line blastomeres are prevented from dividing by treatment with microfilament and microtubule inhibitors, gene products are expressed in the undivided cell that normally are expressed only in that blastomere's somatic descendants (Laufer et al. 1980; Cowan and McIntosh 1985; Edgar and McGhee 1986). Maternally expressed genes, such as the *par* genes, *cib-1*, *pie-1*, *mes-1*, and *mex-1*, have been identified that are required for germ-cell development (Kempfues et al. 1988b; Schnabel and Schnabel 1990; Capowski et al. 1991; Mello et al. 1992; Schnabel et al. 1996), and mutations in some of these genes result in mislocalization of P granules. For example, mutations in the *mes-1* gene result in P-granule mislocalization into both P<sub>4</sub> and D; in these embryos, both P<sub>4</sub> and D produce muscle cells (Capowski et al. 1991; Strome et al. 1995; see also Kempfues and Stone, this volume). Similarly, in *pie-1* mutants, P<sub>4</sub> and D both contain P granules and both blastomeres can produce intestinal cells (Mello et al. 1992). Several antibodies recognize P granules in fixed embryos (Strome and Wood 1982; Yamaguchi et al. 1983); however, it has not yet been possible to identify these antigens molecularly. The MEX-3 protein, described below, appears to associate transiently with P granules during the early cleavage stages of embryogenesis, but it is not found in P granules in adult gonads or late-stage embryos (Draper et al. 1996).

Transcription appears to be inhibited in each of the germ-line blastomeres at periods when somatic blastomeres become transcriptionally active. Incorporation of [<sup>3</sup>H]UTP can be detected by autoradiography in 8–12-cell embryos (Edgar et al. 1994), and several genes have been identified that are transcribed during the early cleavage stages (Schauer and Wood 1990). Transcription of the *pes-10* gene can be detected by *in situ* hybridization in 4-cell-stage embryos in all three somatic blastomeres (AB<sub>a</sub>, AB<sub>p</sub>, and EMS) but not in the germ-

cell precursor, P<sub>2</sub> (Fig. 4) (Seydoux and Fire 1994). Other genes have been identified that are expressed at the 8-cell stage or later in all blastomeres except the germ-line blastomeres P<sub>3</sub> or P<sub>4</sub> (Seydoux et al. 1996). Thus, there appears to be a significant, if not complete, repression of transcription in the germ-line blastomeres. This finding provides an explanation for why transcription factors, such as SKN-1 and PAL-1, which are present in germ-line blastomeres as well as in somatic blastomeres, appear to function only in the somatic blastomeres (Bowerman et al. 1992a, 1993; C. Hunter and C. Kenyon, in prep.). RNA synthesis also appears to be inhibited in the early germ-cell precursors of *Drosophila* (Zalokar 1976), suggesting that transcriptional repression may be a general characteristic of the germ-cell lineage in animal embryos.

The maternal gene *pie-1* is required for germ-cell development and appears to play a part in the repression of transcription in the germ-line blastomeres. The *pie-1* gene was identified by mutations that caused the germ-line blastomere P<sub>2</sub> to produce somatic cell types much like its sister EMS (Mello et al. 1992). In *pie-1* mutants, the SKN-1 transcription factor functions in the P<sub>2</sub> blastomere, promoting somatic differentiation. Genes, such as *pes-10*, that normally are expressed only in somatic blastomeres also are expressed in germ-line blastomeres in *pie-1* mutants (Fig. 4) (Seydoux et al. 1996). The biochemical role of PIE-1 in transcriptional repression is not known. PIE-1 appears to be tightly associated with chromatin in interphase nuclei and has two potential zinc finger domains that are similar to the zinc fingers of TIS-11, a vertebrate protein with unknown function (C.C. Mello et al., in prep.).

The PIE-1 protein is expressed in the nuclei of each of the germ-line blastomeres P<sub>1</sub>, P<sub>2</sub>, P<sub>3</sub>, and P<sub>4</sub> in the early embryo, and only in these blastomeres (Fig. 5) (C.C. Mello et al., in prep.). Thus, the PIE-1 protein, like P granules, is localized asymmetrically to the germ-line blastomeres after cell division. The PIE-1 protein apparently leaves the nucleus during prophase of the cell cycle and associates with the two centrosomes in the nascent mitotic spindle (C.C. Mello et al., in prep.). As the parental cell undergoes mitosis, PIE-1 can no longer be detected in the centrosome of its somatic daughter, but it persists in the centrosome of the daughter that is the germ-line blastomere. Finally, PIE-1 becomes localized again to the nucleus of that germ-line blastomere.

## B. E and MS Blastomeres

E and MS are sister blastomeres in an eight-cell embryo. In normal development, E produces only intestinal cells and MS produces primarily mesodermal cell types such as body-wall muscles and pharyngeal cells. The *skn-1* gene is expressed maternally and encodes a putative transcription factor that is required for proper MS and E development (Bowerman et al. 1992a, 1993). The SKN-1 protein has a basic domain very similar to the DNA-binding domain found in a class of transcription factors called basic leucine zipper (bZIP) proteins (see McGhee and Krause, this volume). The leucine zipper is a sequence of regularly spaced leucines required for dimerization of all known bZIP proteins. SKN-1 is unique in lacking this dimerization domain and indeed can bind DNA as a monomer (Blackwell et al. 1994). *skn-1* mRNA appears to be distributed uniformly in two-cell and four-cell embryos, but SKN-1 protein accumulates at much higher levels in the P<sub>1</sub> nucleus than in the AB nucleus (Fig. 5) (Bowerman et al. 1993a; Seydoux and Fire 1994). Several mutations have been identified that result in high levels of SKN-1 expression in the AB blastomere. In each of these mutants, AB produces pharyngeal cells characteristic of a normal MS blastomere (Mello et al. 1992; J. Watts et al., in prep.). For example, the AB blastomere in a *mex-1* mutant embryo produces these pharyngeal cells, but an AB blastomere from a *mex-1;skn-1* double mutant does not. The effect of expressing high levels of SKN-1 in a wild-type AB blastomere has not been determined, but it is likely that the asymmetric localization of the SKN-1 protein in P<sub>1</sub> is at least part of the reason a wild-type P<sub>1</sub> produces a descendant with the properties of MS and the AB blastomere does not. The distribution of SKN-1 provides a dramatic example of AB/P<sub>1</sub> asymmetry in the early embryo, but it is not yet known how this asymmetry is established.

The P<sub>1</sub> daughters, and the P<sub>1</sub> granddaughters, each appears to have equal levels of SKN-1 (Fig. 5). Thus, other embryonic asymmetries must determine whether or not SKN-1 influences the development of individual P<sub>1</sub> descendants. At the four-cell stage, SKN-1 function appears to be prevented in P<sub>2</sub> by the PIE-1 protein, as

described above. The development of both of the [EMS](#) daughters, [MS](#) and E, are affected by mutations in [skn-1](#). The *skn-1(zu67)* mutation is predicted to result in a severely truncated SKN-1 protein lacking the presumptive DNA-binding domain (C. Schubert, unpubl.). In *skn-1(zu67)* mutant embryos, the [MS](#) blastomere produces hypodermal cells and muscles, and in about 80% of such embryos, E also produces hypodermal cells and muscles. However, in the remaining 20% of the *skn-1(zu67)* mutant embryos, the E blastomere produces cells with some intestinal characteristics, such as the birefringent gut granules ([Bowerman et al. 1992a](#)). Thus, other factors in the embryo appear to be sufficient to specify at least some E-specific differentiation. Screens for maternal-effect lethal mutants lacking intestinal cells have identified ten genes, collectively called the *gut* genes (T. Stiernagle et al., in prep.). Mutations in *gut* genes, like mutations in [skn-1](#), affect development of both E and MS. However, in *gut* mutants, cells derived from the E blastomere produce gut granules in less than 10% of embryos.

Several experimental studies have focused on how the fate of E is specified during early embryogenesis and have shown that the P<sub>1</sub> blastomere has an intrinsic ability to produce intestinal cells that is not present in the [AB](#) blastomere ([Laufer et al. 1980](#); [Cowan and McIntosh 1985](#); [Edgar and McGhee 1986](#); [Priess and Thomson 1987](#)). Although these experiments suggested that [EMS](#) also had an intrinsic ability to produce intestinal cells, more recent work has shown that a cell-cell interaction between [EMS](#) and its sister P<sub>2</sub> at the beginning of the four-cell stage is essential for E-specific differentiation ([Schierenberg 1987](#); [Goldstein 1992, 1993, 1995b](#)). If P<sub>2</sub> is removed from the embryo during this early period, [EMS](#) divides into daughter blastomeres that both have characteristics of [MS](#) blastomeres, but have no apparent characteristics of E blastomeres. In normal development, P<sub>2</sub> contacts the posterior side of [EMS](#), and it is the posterior daughter of [EMS](#) that normally becomes the intestinal precursor, E. If P<sub>2</sub> is repositioned in an embryo such that it instead contacts the anterior side of [EMS](#), the anterior daughter of [EMS](#) becomes an intestinal precursor ([Goldstein 1995b](#)). Thus, in normal development, interactions between P<sub>2</sub> and [EMS](#) could result in asymmetries within [EMS](#) in the activity, or localization, of factors that specify the [MS](#) or E fates.

The molecular basis for P<sub>2</sub>-[EMS](#) interaction has not been determined. Mutations in gene products directly involved in P<sub>2</sub> signaling, or in signal reception, might be expected to result in [EMS](#) producing only [MS](#)-like daughters; such mutants have not yet been described. However, maternal-effect lethal mutations in the [pop-1](#) gene have been identified that result in [EMS](#) producing only E-like daughters, suggesting that *pop-1*(+) activity is essential for specification of the [MS](#) fate and that [pop-1](#) may function downstream from the P<sub>2</sub>-[EMS](#) interaction in normal development ([Lin et al. 1995](#)). Thus, the P<sub>2</sub>-[EMS](#) interaction may be necessary for the activation of [pop-1](#) in the [EMS](#) daughter that becomes MS.

The [pop-1](#) gene encodes a nuclear protein that is present in each of the four-cell-stage blastomeres, [ABa](#), [ABp](#), [EMS](#), and P<sub>2</sub> ([Lin et al. 1995](#)). After [EMS](#) divides, the E blastomere in many embryos stains less intensely with the POP-1 antisera than does the [MS](#) blastomere. At present, it is not clear whether this difference in staining results from differences in the level of POP-1 protein, protein modifications, or different associations between POP-1 and other proteins that influence staining. The predicted POP-1 protein has a domain called an HMG box that is very similar to the HMG boxes of the vertebrate lymphoid-specific transcriptional regulators TCF-1 and LEF-1 ([Travis et al. 1991](#); [van de Wetering et al. 1991](#); [Waterman et al. 1991](#); [Lin et al. 1995](#)). The function of proteins such as TCF-1 and LEF-1 in transcriptional regulation is not fully understood. However, the HMG boxes from these proteins are capable of binding to and bending DNA, and they may alter chromatin structure to permit interactions between other transcription factors ([Giese et al. 1992](#)). Such studies suggest the possibility that in *C. elegans*, POP-1 may interact with factors such as SKN-1 to specify [MS](#) development.

Understanding how the action of maternally expressed genes such as [skn-1](#) and [pop-1](#) results in [MS](#) or E patterns of development will require the identification and analysis of the genes they regulate. Biochemical and genetic approaches have been used to try to find embryonically expressed genes that are required for E development. The [ges-1](#) gene encodes an intestine-specific esterase that is expressed early in the [E lineage](#), and an analysis of the [ges-1](#) 5'promoter identified a small region required for expression in the [E lineage](#) ([Edgar and McGhee 1986](#);

[McGhee 1987](#); [Aamodt and McGhee, 1991](#); [Kennedy et al. 1993](#); [Stroher et al. 1994](#)). This region contained two copies of a consensus GATA-factor binding sequence, suggesting that a GATA-like transcription factor might be involved in [ges-1](#) expression in the [E lineage](#).

The [elt-2](#) gene was cloned from an expression library using the [ges-1](#) GATA sequence as a probe ([Hawkins and McGhee 1995](#); [Egan et al. 1995](#); see [McGhee and Krause](#), this volume). [elt-2](#) encodes a protein with a putative zinc finger that is 72–84% identical to the carboxy-terminal DNA-binding finger of two-finger GATA proteins from vertebrates ([Hawkins and McGhee 1995](#)). Transformation experiments with [elt-2::lacZ](#) reporter constructs suggest that [elt-2](#) expression is indeed intestinal-specific, beginning in the two daughters of the E blastomere, Ea and Ep (M.G. Hawkins et al., unpubl.). Forced expression of [elt-2](#) by means of a heat shock construct has been shown to cause ectopic, nonintestinal expression of [ges-1](#) in the early embryo (T. Fukushige and J. McGhee, unpubl.). Thus, [elt-2](#) is an embryonically expressed gene that appears to be a good candidate for controlling [ges-1](#) transcription in normal gut development, although this has not yet been demonstrated genetically.

Several groups have begun to look for embryonically expressed genes that control cell fate by characterizing the terminal phenotypes of embryos that are homozygous for chromosomal deficiencies ([Ahnn and Fire 1994](#); [Storfer-Glazer and Wood 1994](#); R.M. Terns et al., in prep.). A phenotypic analysis of embryos that were homozygous for various chromosomal deficiencies identified a region on chromosome V that was required for the E blastomere to produce intestinal cells (R.M. Terns et al., in prep.). Subsequent genetic screens identified an embryonically expressed gene in this region called [end-1](#) in which mutations prevent intestinal development (J. Zhu et al., in prep.). Molecular cloning of [end-1](#) has shown that it encodes a GATA-like transcription factor that is expressed in both daughters of the E blastomere, and thus [end-1](#) also is a candidate for a regulator of the [ges-1](#) esterase and early E-lineage differentiation (J. Zhu and J. Rothman, pers. comm.; see [McGhee and Krause](#), this volume). The E-lineage defect in [end-1](#) mutants is very similar to the E-lineage defect in most [skn-1](#) mutant embryos, suggesting that maternal SKN-1 could play a part in the zygotic expression of [end-1](#). DNA sequences 5' of the [end-1](#) gene contain consensus SKN-1-binding sites, but the functional significance of these sequences has not yet been determined ([Blackwell et al. 1994](#); J. Zhu and J. Rothman, pers. comm.).

## C, C and D Blastomeres

In normal embryogenesis, all but one of the body-wall muscles are descendants of the P<sub>1</sub> blastomere. The C, [MS](#), and D blastomeres each produces body-wall muscles, but do so through distinct patterns of division and differentiation. Most C descendants become either body-wall muscles or hypodermal cells, most [MS](#) descendants become either body-wall muscles or [pharyngeal cells](#), and all D descendants become body-wall muscles. If either C, [MS](#), or D is allowed to develop after all other blastomeres are killed with a laser microbeam, the resulting partial embryo contains muscle cells ([Mello et al. 1992](#); [Schnabel 1994, 1995](#)). These experiments suggest that the C, [MS](#), and D blastomeres are able to produce muscles in the absence of interactions with other blastomeres. However, analysis of mutant or wild-type embryos in which sets of embryonic blastomeres are allowed to develop simultaneously suggests that cell-cell interactions play an important permissive part in muscle production from [MS](#) and D ([Schnabel 1994, 1995](#)). For example, the D blastomere, derived from the P<sub>2</sub> lineage, appears to exert an inhibitory effect on muscle development from [MS](#) that, in normal embryogenesis, is blocked by [AB](#) descendants. Thus, only when both P<sub>2</sub> and [AB](#) are killed does [MS](#) produce muscles. In contrast, no cell-cell interactions have been identified that are required for the C blastomere to produce muscles.

The [pal-1](#) gene appears to be involved in specifying the correct developmental patterns of the C and D blastomeres (C. Hunter, unpubl.). The [pal-1](#) gene encodes a protein with a homeodomain that is most similar to the homeodomain of the *Drosophila* protein Caudal ([Waring and Kenyon 1991](#); see [McGhee and Krause](#), this volume). [pal-1](#) was identified initially through mutations that affected larval development ([Waring and Kenyon 1990](#)); however, further analysis has shown that [pal-1](#) also is expressed maternally (C. Hunter and C. Kenyon, in prep.) and embryonically (L.G. Edgar and W.B. Wood, in prep.). The PAL-1 protein is present in four-cell embryos in the nuclei of the [EMS](#) and P<sub>2</sub> blastomeres, and in eight-cell embryos, PAL-1 is present in [MS](#), E, P<sub>3</sub>, and C (Fig. 5). Thus, the distribution of the PAL-1 protein is similar to that of the SKN-1 protein in four-cell and eight-cell

embryos. Adults with germ lines that are homozygous for a *pal-1* mutation produce abnormal embryos in which neither the C nor the D blastomeres produce body-wall muscles (C. Hunter and C. Kenyon, in prep.).

In normal development, the expression of PAL-1 appears to be regulated by the *mex-3* gene product. In *mex-3* mutants, the PAL-1 protein is expressed inappropriately in the AB granddaughters (B. Draper et al.; C. Hunter and C. Kenyon; both in prep.); each of these granddaughters produces body-wall muscles and hypodermal cells, as does a C blastomere in wild-type embryos (B. Draper et al., in prep.). *mex-3* encodes a cytoplasmic protein with two repeats called KH domains that are thought to mediate interactions with RNA, and missense mutations in one of the KH domains of the *mex-3* gene result in a mutant phenotype indistinguishable from that of null mutations (B. Draper et al., in prep.). An interesting possibility is that in wild-type embryos, MEX-3 binds to the *pal-1* mRNA and prevents its translation in AB descendants. This model would require MEX-3 to function in AB descendants, but not in P<sub>1</sub> descendants where PAL-1 normally is expressed. In wild-type embryos, MEX-3 is present at slightly higher levels in AB descendants than in P<sub>1</sub> descendants (B. Draper et al., in prep.); however, other embryonic asymmetries could also result in different levels of MEX-3 function. In particular, there is genetic evidence that the PAR-1 kinase, which is localized to the posterior cortex of P<sub>1</sub> (Guo and Kemphues 1995), is required for the proper regulation of *mex-3* activity (B. Draper et al., in prep.; see Kemphues and Stone, this volume).

## Figures



### Figure 4

Transcription in the early *C. elegans* embryo. Embryonically expressed *pes-10* can be detected by in situ hybridization (Seydoux and Fire 1994) in the EMS nucleus in a wild-type (WT) embryo. In a *pie-1* mutant embryo, *pes-10* message is expressed in both EMS and P<sub>2</sub>. Embryos are 40 µm in length. (Reprinted, with permission, from Seydoux et al. 1996.)

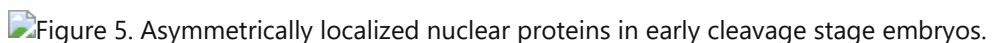


### Figure 5

Asymmetrically localized nuclear proteins in early cleavage stage embryos. The expression patterns of the SKN-1, PIE-1, and PAL-1 proteins are shown schematically in 2-cell, 4-cell, and 8-cell embryos. The relative amounts of each protein at the different stages are indicated by shading, with the darker color representing the most protein.

Generated from local HTML

## Chapter 14. Specification of Cell Fates in the Early Embryo — IV Future Prospects

---

There have been several important advances in our understanding of nematode embryogenesis in the last few years. New cell-cell interactions have been discovered that have clarified the logic of fate specification of both the AB- and the P<sub>1</sub>-derived lineages. We have learned the identity of a few factors that are asymmetrically distributed between the early blastomeres and that appear to account for some of the different properties of these blastomeres. However, it is clear that very much remains to be discovered. We have no molecular information about how the anterior-posterior polarity of the embryo is established initially, leading to the unequal distributions of the *par* gene products. We do not understand how the *par* genes affect the expression patterns of many of the maternal products described in this chapter that are required for proper fate specification, nor have we established direct links between any of these maternal products and the expression of embryonically transcribed genes. Although GLP-1 has been shown to have a critical role in multiple embryonic cell-cell interactions, we do not understand why these interactions have different outcomes.

At present, the differences between the general outlines of early embryogenesis in *C. elegans* and *Drosophila* are more apparent than the similarities. However, there are hints that at least some of the molecular machinery may be the same, although utilized for different purposes. Analysis of GLP-1 localization suggests that similar factors may regulate mRNA translation ([Evans et al. 1994](#)), and PAL-1 has been shown to be related to the *Drosophila* protein Caudal (C. Hunter and C. Kenyon, in prep.). From the genome sequencing projects now under way in nematodes, flies, and humans, we may soon learn how well the genes that control embryogenesis have been conserved in animal evolution. We anticipate that these databases, coupled with techniques for eliminating gene function, will provide important resources for molecular dissection of the *C. elegans* embryo.

Generated from local HTML

# **Chapter 15. Cell Death**

---

## **Contents**

- [I Introduction](#)
- [II Programmed Cell Death in \*C. elegans\*](#)
- [III Genetics of Programmed Cell Death](#)
- [IV Programmed Cell Death in Specific Cell Types](#)
- [V Cell Deaths not Mediated by the Common Death Program](#)
- [VI Evolution of Programmed Cell Death](#)
- [Acknowledgments](#)

Generated from local HTML

## Chapter 15. Cell Death — I Introduction

---

Programmed cell death is a common cell fate in most if not all multicellular animals. Cell death is used extensively during development, as well as later in life, to eliminate cells that are either useless or potentially detrimental to the organism. Programmed cell death is basically cell suicide, in the sense that the cell which is to die actively participates in—and often itself induces—its own demise and removal from the organism. Proper control of programmed cell death is crucial, and breakdown in the regulation of this process can result in a number of pathologies: Inactivation of the death program has been associated with the development of cancer and autoimmune diseases, whereas aberrant activation of the apoptotic machinery is thought to contribute to the extensive cell deaths observed in neurodegenerative diseases and stroke ([Vaux 1993; Thompson 1995](#)).

Programmed cell death is often also called apoptosis, particularly in vertebrates. The term apoptosis was introduced by [Kerr et al. \(1972\)](#) to emphasize that programmed cell deaths are morphologically very different from necrotic deaths. Because the original definition of apoptosis was based on strict morphological criteria, there has been considerable debate as to whether all programmed cell deaths in mammals were of the apoptotic type. It is now generally agreed that most, if not all, programmed cell deaths in mammals occur by apoptosis.

As its name implies, programmed cell death is thought to be mediated by a specific molecular program activated by the cell if and when it needs to die. In a sense, programmed cell death is not much different from any other terminal differentiation program, except that the end state is somewhat less tangible in the former case. The term “programmed” cell death has sometimes been applied specifically to deaths that occur reproducibly during organismal development, excluding apoptotic deaths that are dependent on interactions with other cells or with the extracellular milieu. In this chapter, the term programmed cell death will be applied to all deaths that share the genetic and morphological characteristics that are described below, regardless of how the deaths are induced.

Generated from local HTML

# Chapter 15. Cell Death — II Programmed Cell Death in *C. elegans*

---

## A. Identity and Origin of Dying Cells

Of the 1090 cells generated during *C. elegans* hermaphrodite somatic development, 131 undergo programmed cell death ([Sulston and Horvitz 1977](#); [Kimble and Hirsh 1979](#); [Sulston et al. 1983](#)). As with most of *C. elegans* development, these deaths are highly reproducible: The identity of the dying cells and the time in development at which these cells die are essentially invariant among individuals. This feature allows for the study of programmed cell death at single-cell resolution in this organism, a powerful advantage, as it allows the study of mutations that might have only a very weak effect on cell death or affect only specific cell types.

Most (113/131) developmental deaths occur during embryogenesis, mainly between 250 and 450 minutes after fertilization ([Sulston et al. 1983](#)). A second, smaller wave of death is observed in the second larval stage, following the divisions of several [neuroblasts](#). In hermaphrodites, no more deaths are observed in the soma after the L2 stage; a few more deaths occur in male-specific lineages well into the fourth larval stage. In addition to the developmental deaths, a large number of cells undergo programmed cell death in the adult hermaphrodite germ line.

Many different cell types undergo programmed cell deaths. Ectodermal cells, mainly [neurons](#) and neuron-associated cells but also hypodermal cells, make up the bulk of dying cells. A small number of mesodermal cells, such as muscle cells and the sisters of the [pharyngeal gland cells](#), also die. No intestinal cells die in *C. elegans*, but they have been observed to die in other nematodes species ([Sternberg and Horvitz 1982](#)). Deaths are not confined to any specific part of the cell lineage, although most of them are descendants of [AB](#), presumably a reflection of the high number of dying [neurons](#). Only a single [C](#) descendant dies, and no deaths are found in the D and E lineages. Germ cells ( $P_4$  descendants) die in large numbers but only in adult hermaphrodites.

## B. Morphological Characteristics of Dying Cells

Cells dying by programmed cell death in *C. elegans* undergo a series of morphological changes that have been extensively characterized by both light and electron microscopy ([Sulston and Horvitz 1977](#); [Robertson and Thomson 1982](#)). The first morphological changes that can be observed under Nomarski (DIC) optics are a decrease in the refractivity of the cytoplasm, followed by a loss of texture and an increase in refractivity of the nucleus. Soon thereafter, both cytoplasm and nucleus become highly refractive. At this stage, the dead cell can readily be identified as a flat, round disk ([Sulston and Horvitz 1977](#)). In the wild type, this refractive disk gradually disappears as the cell is digested by a neighboring cell. Although engulfment usually accompanies (or sometimes can even precede) the changes observed under DIC optics, it is not required for the latter to occur, as the characteristic morphological and ultrastructural changes are still observed in mutants that are defective in engulfment ([Hedgecock et al. 1983](#); [Ellis et al. 1991a](#)).

At the ultrastructural level, programmed cell deaths are characterized by an early nuclear chromatin condensation and reduction in cell volume. Cytosolic organelles (e.g., mitochondria) appear to be normal until very late in the process. At later stages, the dying cell breaks up into membrane-bound fragments, and autophagic vacuoles and membranous whorls appear in the cytoplasm. The engulfed cell fragments finally fuse with vacuoles, thus completing the elimination of the dead cell ([Robertson and Thomson 1982](#); [Ellis et al. 1991a](#)).

## C. Morphological Similarities with Apoptotic Cell Deaths in Vertebrates

Apoptotic deaths in mammals share several of the morphological features observed in programmed cell deaths in *C. elegans* ([Wyllie et al. 1980](#)). The first ultrastructural changes that can be detected in apoptotic deaths are condensation of the cytoplasm and compaction of the nuclear chromatin into sharply circumscribed, uniformly dense masses that abut the nuclear membrane. Further condensation is then often accompanied by convolution of the nuclear and cellular outlines. Finally, the dying cell breaks up into membrane-bound fragments containing normal-looking organelles and sometimes nuclear fragments ([Kerr and Harmon 1991](#)). The extent of nuclear

fragmentation and cellular budding varies by cell type, with small cells showing less extensive fragmentation. In tissues, apoptotic fragments are rapidly engulfed by adjacent cells and degraded within lysosomes, as is the case in nematodes. In single-layer epithelia, the dying cells are sometimes extruded from the epithelial surface. A similar phenomenon can be observed during *C. elegans* embryonic development, where corpses on the surface of early embryos sometimes detach ([Hedgecock et al. 1983](#)). Whether nucleosomal DNA ladders, another hallmark of apoptotic death ([Wyllie 1980](#); [Walker and Skorska 1994](#)), also occur in *C. elegans* remains to be determined.

Generated from local HTML

# Chapter 15. Cell Death — III Genetics of Programmed Cell Death

---

## A. The Genetic Pathway for Programmed Cell Death

Genetic screens have led to the isolation of well over 100 mutations that affect programmed cell death in *C. elegans* ([Sulston 1976](#); [Hedgecock et al. 1983](#); H.M. [Ellis and Horvitz 1986](#); R.E. [Ellis and Horvitz 1991](#); [Desai et al. 1988](#); [Ellis et al. 1991a](#); [Hengartner et al. 1992](#)). These mutations identify more than a dozen genes that affect all programmed cell deaths, as well as a handful of genes that alter the pattern of deaths ([Table 1](#)). Analysis of the phenotypes conferred by the various double-mutant combinations has allowed these genes to be placed into a genetic pathway for programmed cell death that contains four distinct, genetically separable steps: the decision of individual cells whether to live or die, the execution of the death sentence in a cell that has decided to die, the engulfment of the dying cell by one of its neighbors, and finally the degradation of the dead cell within the engulfing cell ([Fig. 1](#)). Genes in the first step affect only a limited number of cells, often a single cell type. In contrast, the 11 genes that function in the last three steps affect all cell deaths and are therefore thought to act in a central pathway common to all deaths. These genes are described below.

## B. *ced-3* and *ced-4*

### 1. *ced-3* and *ced-4* Are Essential for Programmed Cell Death

The [\*ced-3\*](#) and [\*ced-4\*](#) ([cell death abnormal](#)) genes are essential for programmed cell death in *C. elegans*. Mutations that completely inactivate either gene prevent all programmed cell deaths, with the exception of a handful of deaths in the [male tail](#) ([Ellis and Horvitz 1986](#)). Weaker mutations, e.g., *ced-3(n2438)* and *ced-4(n2273)*, result in a partial suppression of death, where only a fraction of cells survive. Which cells survive and which cells die is to a large extent stochastic, although a bias is evident in some cases. For example, the sisters of the pharyngeal I2 [neuron](#) and [m1](#) muscle cell are more easily rescued from death than other [pharyngeal cells](#), whereas the sister of the [M4](#) motor [neuron](#) is rescued at a lower than average frequency. That mutations in [\*ced-3\*](#) and [\*ced-4\*](#) completely eliminate cell deaths suggests that all programmed cells deaths in *C. elegans* (except as noted above) share a common molecular mechanism.

Since all of the surviving cells differentiate (see below), [\*ced-3\*](#) and [\*ced-4\*](#) mutants end up with 12% more [somatic cells](#) than their wild-type counterparts, and a [nervous system](#) that is larger by about one third (407 vs. 302 cells in hermaphrodites). Despite these dramatic increases in cell numbers, [\*ced-3\*](#) and [\*ced-4\*](#) mutants do not show any obvious morphological or behavioral abnormalities. They are viable and fertile and are indistinguishable from the wild type for life span, locomotion, feeding, and several other behaviors ([Ellis and Horvitz 1986](#); M. Hengartner et al., unpubl.). A more detailed analysis, however, reveals a number of subtle defects: [\*ced-3\*](#) and [\*ced-4\*](#) mutants grow more slowly than the wild type, show a slightly reduced fertility, and are somewhat defective in complex tasks such as chemotaxis ([Ellis et al. 1991b](#); C. Bargmann, pers. comm.).

### 2. Fate of Undead Cells

The surviving, or “undead,” cells in [\*ced-3\*](#) and [\*ced-4\*](#) mutants never divide again, but rather differentiate. In many cases, they appear to adopt a cell fate very similar to the one adopted by their sister cell, although some also adopt the fate of their aunt or of cells at equivalent positions in other lineages ([Ellis and Horvitz 1986](#); [Avery and Horvitz 1987](#); [White et al. 1991](#)). However, undead cells exhibit considerably greater variability than normal cells, both in their position and in the expression of particular traits. For example, V5.paapp, an undead cell of the postembryonic group, frequently synthesizes dopamine, suggesting that this cell can adopt a fate similar to that of its aunt, the dopaminergic cell V5.paaa ([Ellis and Horvitz 1986](#)). However, unlike V5.paaa, which always stains for dopamine, only about 60% of V5.paapp cells stain. The other 40% might synthesize very low levels of dopamine, have only partially differentiated, or might have adopted a different cell fate altogether.

At the ultrastructural level, most undead [neurons](#) have connectivity patterns that are not characteristic of any normally surviving cell ([White et al. 1991](#)), suggesting again that the undead cells adopt fates that are distinct from those adopted by normal cells. As the synaptic patterns were determined only once for each undead cell, it is not clear how variable these patterns are. Whether the novel synaptic patterns are those of cryptic cell types that once were used but now are superfluous and therefore eliminated or rather abortive attempts by slightly confused cells to adopt a known pattern has not been resolved.

Despite this greater variability in position and fate, undead cells are clearly healthy. Several observations also suggest that they are capable of normal function at least part of the time. For example, the pharyngeal motor [neuron M4](#), which is essential for feeding and thus for viability, has a sister that dies in the wild type. This sister can substitute for the normal [M4 neuron](#) following ablation of the latter by laser microsurgery: Whereas ablation of the [M4 neuron](#) in a wild-type animal invariably results in death by starvation, the elimination of [M4](#) in a [ced-3](#) mutant rarely results in the death of the animal. However, if both [M4](#) and its undead sister are ablated in [ced-3](#) mutants, the animal again invariably dies ([Avery and Horvitz 1987](#)). An even more interesting case can be found in the ventral cord: In [ced-3](#) mutants, the undead sister of the rectal epithelial cell usurps its sister's position and performs its function, while the "rightful" rectal epithelial cell (P12.pa), pushed aside, adopts a slightly altered epithelial fate and fails to play any significant part ([White et al. 1991](#)).

### **3. *ced-3* and *ced-4* Act Cell-autonomously**

Mosaic analysis of [ced-3](#) and [ced-4](#) indicates that both genes are likely to act cell-autonomously to promote the death of cells that are fated to die: For both genes, a perfect correlation is observed between the loss of wild-type gene function and survival of cells fated to die ([Yuan and Horvitz 1990](#)). Although mosaic analysis cannot exclude the possibility that [ced-3](#) and [ced-4](#) function within cells that are closely related to the dying cell by lineage (such as its mother or surviving sister), ectopic expression experiments support the cell-autonomous hypothesis. For example, overexpression of either [ced-3](#) or [ced-4](#) under the control of the [mec-7](#) promoter, which directs expression in the six [touch cells](#) ([Savage et al. 1989](#)), results in the programmed death of these cells in a significant fraction of transgenic animals ([Shaham and Horvitz 1996a](#)). Thus, high levels of [ced-3](#) or [ced-4](#) can bypass the protective effect of [ced-9](#) (see below). Interestingly, unlike normal programmed cell deaths, which require both [ced-3](#) and [ced-4](#) activities, killing by the [mec-7-ced-3](#) constructs was still observed (albeit at reduced levels) in the absence of endogenous [ced-4](#), suggesting that high levels of [ced-3](#) can at least partially bypass the requirement for [ced-4](#). The converse experiment showed that [ced-4](#) is completely dependent on [ced-3](#) for its killing activity, suggesting that, in the genetic sense, [ced-4](#) acts either upstream or independently of [ced-3](#) ([Shaham and Horvitz 1996a](#)).

### **4. *ced-4* Encodes a Novel Protein and Can Both Promote and Prevent Cell Death**

The [ced-4](#) gene encodes a novel 549-amino-acid protein that shows no significant overall sequence similarity with any other known protein ([Yuan and Horvitz 1992](#)). Two regions within the CED-4 protein show some similarity to the EF-hand family of Ca<sup>++</sup>-binding domains. However, these regions are not conserved in the CED-4 protein sequence from the related species *C. briggsae* and *C. vulgaris*, and site-directed mutagenesis of residues in these regions indicates that they are not essential for the ability of [ced-4](#) to kill ([Horvitz et al. 1994](#)).

The [ced-4](#) transcript is most abundant in embryos, the period during which most developmental deaths occur. However, the [ced-4](#) message can be detected at all developmental stages, including stages where no cell deaths occur, suggesting that [ced-4](#) expression is not restricted to dying cells. A similar conclusion was reached using genetic arguments ([Hengartner et al. 1992](#); S. Shaham and H.R. Horvitz, pers. comm.).

Recent work suggests that [ced-4](#) produces multiple, alternatively spliced transcripts ([Shaham and Horvitz 1996b](#)). In addition to the message originally identified by Yuan and Horvitz (1992), [ced-4](#) produces a second, much less abundant transcript that encodes a slightly larger protein (CED-4<sub>L</sub>). Interestingly, overexpression of CED-4<sub>L</sub> prevents cell death, suggesting that the large isoform has an effect on cell death opposite from that of the major shorter protein (CED-4<sub>S</sub>). Genetic evidence for the presence of CED-4<sub>L</sub> is provided by the weak allele [ced-](#)

*4(n2273)*, which affects the *ced-4* S-specific splice acceptor site ([Yuan and Horvitz 1992](#); [Shaham and Horvitz 1996b](#)). This mutation only partially blocks usage of this splice site but results in a dramatic increase in the use of the alternative, *ced-4* L-specific site, which might contribute to the death-suppressing activity of this mutation. The expression patterns of the short and long forms and the part played by CED-4<sub>L</sub> during normal nematode development remain to be determined.

## 5. CED-3 Is a Member of the ICE Family of Cysteine Proteases

CED-3 shows significant sequence similarity to a new family of cysteine proteases ([Yuan et al. 1993](#)), of which interleukin-1β-converting enzyme (ICE) is the prototype member. At least ten additional family members exist in mammals ([Schwartz and Osborne 1994](#); [Kumar 1995](#)); little to nothing is known about the biological function of most of them (but see below).

ICE substrate specificity studies using synthetic peptides indicate that ICE cleaves after aspartate residues, with a preference for the following residue to be a small hydrophobic amino acid ([Howard et al. 1991](#)). This cleavage specificity is characteristic of all proteases in this family. The three residues preceding aspartate strongly affect the affinity of the enzyme for substrate peptides, and the ICE family members show distinct, but slightly overlapping, sequence preferences at these positions ([Thornberry et al. 1992](#); [Nicholson et al. 1995](#)), suggesting that each enzyme acts on a different set of substrates.

Like many proteases, ICE is synthesized as a larger inactive precursor (proICE). Proteolytic cleavage of the 45-kD proenzyme (p45) at three sites generates the active form, which consists of a (p20/p10)<sub>2</sub> tetramer ([Thornberry et al. 1992](#); [Walker et al. 1994](#); [Wilson et al. 1994](#)). All other ICE family members, including CED-3, appear to be synthesized and processed in a similar manner ([Rotonda et al. 1996](#); [Xue et al. 1996](#)). Interestingly, the proenzyme processing sites are also after aspartates, suggesting that activation of ICE family members might occur autocatalytically. In support of this hypothesis, proICE translated in rabbit reticulocyte lysates remains in the inactive, uncleaved form but is rapidly cleaved to the mature form upon addition of small amounts of active ICE enzyme ([Thornberry et al. 1992](#)).

As expected from the strong sequence similarity observed between CED-3 and mammalian ICE family members, the CED-3 protein shows a protease activity similar to that observed for ICE ([Xue and Horvitz 1995](#)). Most missense mutations that strongly impair *ced-3* activity alter residues that are conserved between CED-3 and ICE ([Yuan et al. 1993](#)). Analysis of the residual enzymatic activity of several mutant CED-3 proteins shows a direct correlation between the reduction in protease activity and the strength of the mutation *in vivo*, indicating that the ability of CED-3 to promote programmed cell death is dependent on its ability to function as a protease ([Xue and Horvitz 1995](#)).

Overexpression of CED-3 or any of the other ICE family members induces apoptotic cell death in mammalian cells ([Miura et al. 1993](#); [Kumar et al. 1994](#); [Wang et al. 1994](#)). Under most conditions, these deaths can be prevented by simultaneous overexpression of either *bcl-2* or, in the case of ICE and CED-3, *crmA*, a cowpox-virus-encoded ICE protease inhibitor ([Ray et al. 1992](#)). That *crmA* can block ICE- and CED-3-induced apoptosis suggests that, as is the case in *C. elegans*, it is the protease activity of these proteins, rather than another, previously unrecognized activity, that induces programmed death.

Similar conclusions have been reached from the study of the baculovirus gene *p35*. This gene is required to block baculovirus-infected insect cells from undergoing programmed cell death ([Clem et al. 1991](#)). Interestingly, *p35* also efficiently prevents programmed cell death when overexpressed in *C. elegans* ([Sugimoto et al. 1994](#)), *Drosophila* ([Hay et al. 1994](#)), and mammalian cells ([Rabizadeh et al. 1993](#); [Martinou et al. 1995](#)). That *p35* can prevent death in these phylogenetically diverse species suggests that its cellular target is evolutionarily conserved. This target is most likely a member of the CED-3/ICE protease family, as *p35* can act as a specific inhibitor of, and is specifically cleaved by, these proteases ([Bump et al. 1995](#); [Xue and Horvitz 1995](#)). If correct, this would imply that *Drosophila* also harbors ICE-like proteases (none have been described so far) and that these proteases will act as positive regulators of apoptosis, just as they do in worms and mammals.

## C. *ced-9*

### 1. *ced-9* Is Required to Protect Cells from Programmed Cell Death

The *ced-9* gene is a negative regulator of programmed cell death in *C. elegans* ([Hengartner et al. 1992](#)).

Overexpression of *ced-9* results in the survival of cells that should die and causes a phenotype similar to the one observed in animals that lack either *ced-3* or *ced-4* ([Hengartner and Horvitz 1994a](#)). Survival of cells fated to die is also observed in mutants heterozygous or homozygous for the dominant gain-of-function mutation *ced-9* (*n1950*). Interestingly, *n1950* does not result in overexpression of the wild-type protein but rather affects a conserved residue in the *ced-9* open reading frame (see [Hengartner and Horvitz 1994a](#) and below).

In contrast, mutations that reduce or eliminate *ced-9* function cause many cells that normally live to inappropriately activate the cell death pathway and undergo programmed cell death ([Hengartner et al. 1992](#)). The extent of ectopic death is dependent on the maternal *ced-9* genotype: Homozygous *ced-9* (*lf*) mutants derived from *ced-9* (*lf*)/+ mothers (*F*<sub>1</sub> mutants) have a few extra cell deaths, but they are viable and grow up to adulthood, whereas their own progeny (*F*<sub>2</sub> mutants) tend to have many extra deaths and invariably die during embryogenesis. The pattern of extra deaths is not fixed; different cells die in different animals, although general trends are evident. For example, cells in neuronal lineages are particularly prone to die. In *F*<sub>1</sub> mutants, ectopic deaths tend to be restricted mostly to *germ cells* and *neurons*. For example, in the ventral cord, many of the Pn.a descendants die, whereas the Pn.p descendants tend to survive ([Hengartner et al. 1992](#)). These ectopic deaths result in a number of defects in *F*<sub>1</sub> mutants that are visible in the dissecting microscope, including a backward Unc phenotype similar to the one observed in *unc-59* and *unc-85* mutants and, in the strong mutants, an incompletely penetrant sterility. Most embryonically generated cells are not affected in *F*<sub>1</sub> mutants, presumably because the maternal contribution of the *ced-9* product is still sufficient to protect these cells from death. One notable exception is the pair of HSN neurons, which appear to be extremely sensitive to the loss of *ced-9* function, as they die even in mutants homozygous for the weak hypomorphic allele *ced-9* (*n1653*) ([Hengartner et al. 1992](#)).

Mutations in *ced-3* and *ced-4* block the ectopic cell deaths as well as the lethality caused by the absence of *ced-9* function ([Hengartner et al. 1992](#)), suggesting that *ced-9* acts genetically upstream of *ced-3* and *ced-4* and normally prevents cell death by antagonizing the activities of *ced-3* and *ced-4* (Fig. 1). Furthermore, *ced-9* (*lf*); *ced-3* and *ced-4* *ced-9* (*lf*) mutants are indistinguishable from the *ced-3* or *ced-4* single mutants (with the exception of weak *ced-3* or *ced-4* mutations, see below), indicating that the sole function of *ced-9* in *C. elegans* is to modulate the activities of *ced-3* and *ced-4*.

### 2. *ced-9* and Human *bcl-2* Are Members of a Family of Death Regulators

*ced-9* is the downstream gene of a polycistronic locus that also contains the gene *cyt-1*, which encodes a protein similar to cytochrome *b*<sub>560</sub> of complex II of the mitochondrial respiratory chain ([Hengartner and Horvitz 1994b](#)). Unlike most polycistronic loci in *C. elegans* ([Spieth et al. 1993](#)), the *ced-9* message starts immediately after the end of the *cyt-1* transcript (the *ced-9* SL-acceptor site overlaps with the *cyt-1* poly(A)-addition site), and *ced-9* is mostly *trans*-spliced to SL1 rather than to SL2.

*ced-9* encodes a 280-amino-acid protein with sequence and structural similarity to the mammalian proto-oncogene *bcl-2* ([Hengartner and Horvitz 1994b](#)). *C. elegans* CED-9 and mouse Bcl-2 show 24% overall identity (49% similarity), including several stretches with much higher conservation (see below). Interestingly, these two proteins show not only sequence similarity, but also a striking functional similarity: Overexpression of *bcl-2* protects from cell death (see, e.g., [Vaux et al. 1988](#); [Garcia et al. 1992](#); [Allsopp et al. 1993](#)), whereas a reduction or loss of *bcl-2* function, e.g., by expression of antisense mRNA ([Reed et al. 1990](#)) or by gene disruption ([Nakayama et al. 1993](#); [Veis et al. 1993](#)), renders cells hypersensitive to death-inducing signals. These observations have led to the suggestion that like *ced-9* in *C. elegans*, *bcl-2* is required to protect mammalian cells that should live from apoptosis (for review, see [Korsmeyer et al. 1993](#); [Vaux 1993](#); [Reed 1994](#)). Further evidence that these two genes perform similar functions comes from the observation that human *bcl-2* can prevent programmed cell death in *C.*

*elegans* (Vaux et al. 1992; Hengartner and Horvitz 1994b) and can even substitute for *ced-9* in animals deficient in *ced-9* function (Hengartner and Horvitz 1994b).

The finding that *ced-9* is cotranscribed with a protein predicted to be involved in the mitochondrial respiratory chain is particularly intriguing given that (1) Bcl-2 is an integral membrane protein that in mammalian cells copurifies with enzymes located in the inner mitochondrial membrane (Hockenberry et al. 1990) and (2) Bcl-2 has been suggested to prevent death by acting in an antioxidant pathway (Hockenberry et al. 1993). However, immunofluorescence and ultrastructural studies suggest that Bcl-2 is localized not only to mitochondria, but also to the endoplasmic reticulum and outer nuclear membranes (Alnemri et al. 1992; Monaghan et al. 1992; Jacobson et al. 1993; Krajewski et al. 1993), and the proposed role of Bcl-2 in regulating an antioxidant pathway is still the subject of considerable debate (Jacobson and Raff 1995; Shimizu et al. 1995). There is currently no evidence that *cyt-1* has any role in *C. elegans* programmed cell death; however, some reports implicated cytochromes in mammalian apoptosis (Liu et al. 1996).

Dominant gain-of-function mutations have been described in both *ced-9* and *bcl-2* (Yunis et al. 1982; Tsujimoto et al. 1984; Hengartner et al. 1992). The *bcl-2* mutations, which are commonly found in follicular lymphoma, are translocations that result in overexpression of a normal Bcl-2 protein in B cells (Yunis et al. 1982; Tsujimoto et al. 1984; Cleary et al. 1986; Tsujimoto and Croce 1986; Seto et al. 1988). In contrast, the *ced-9* (*n1950*) gain-of-function mutation affects the open reading frame of *ced-9* and results in a glycine to glutamate substitution in a region highly conserved among all *ced-9* / *bcl-2* family members (Hengartner and Horvitz 1994a). This region has been shown to be required for heterodimerization of Bcl-2 with Bax (Yin et al. 1994), suggesting that the *n1950* mutation might affect the ability of CED-9 to interact with other proteins.

*ced-9* and *bcl-2* are two members of a rapidly growing gene family which contains members from vertebrates (*bcl-2*, *bax*, *bcl-x*, *bak*, *bad*, *bfl-1*, *MCL1*, and *A1*), invertebrates (*C. elegans* and *C. briggsae ced-9*), and viruses (Epstein-Barr virus BHRF1, African swine fever virus LMW5-HL, adenovirus E1B 19K, and possibly herpesvirus Saimiri ORF16) (for review, see Hengartner and Horvitz 1994d; Haecker and Vaux 1995). Although the overall conservation among the various members of this family is rather low, a few regions are more highly conserved and might identify domains important for structure and/or function (for review, see Williams and Smith 1993; Hengartner and Horvitz 1994d). Most family members, including CED-9 and Bcl-2, have a carboxy-terminal hydrophobic tail, which in the case of Bcl-2 has been shown to be important for membrane localization (Hockenberry et al. 1993; Tanaka et al. 1993).

Many, but not all, of the members of the *ced-9* / *bcl-2* gene family have been shown to affect programmed cell death. Rather surprisingly, these genes can influence the process in quite different ways: Whereas *bcl-2* and the viral genes prevent programmed cell death (see Williams and Smith 1993), Bax and Bak render cells more susceptible to death-inducing signals, and Bcl-x can either prevent or stimulate apoptotic cell death by acting via two distinct *bcl-x* gene products, Bcl-x<sub>L</sub> and Bcl-x<sub>S</sub>, that are generated by alternative RNA splicing. Furthermore, many members of this family can interact to form heterodimers, and it has been suggested that this heterodimerization is the mechanism by which the antagonistic effects of these various proteins on cell death are effected (for review, see Haecker and Vaux 1995). This observation suggests that *C. elegans* contains one or more *ced-9* homologs that act like Bax and Bak. Alternatively, *ced-9* might, like *bcl-x*, be capable of providing both Bcl-2-like (protecting) and Bax-like (death-promoting) functions.

### 3. CED-9 Promotes the Death of Cells That Should Die

Two lines of evidence suggest that although CED-9 prevents cell death in cells that should live, it stimulates cell death in cells that should die (Hengartner and Horvitz 1994a): (1) CED-9(+) antagonizes the death suppressing activity of CED-9(G169E) [the protein encoded by the gain-of-function allele *ced-9* (*n1950*)]: Fewer cells survive in *ced-9* (*n1950*)/+ heterozygotes than in *ced-9* (*n1950*)/*Df* hemizygotes. (2) Double mutants between *ced-9* (*lf*) and weak *ced-3* alleles have more surviving cells than do the corresponding *ced-3* single mutants (Hengartner and Horvitz 1994a), an observation opposite of what would be predicted if the sole function of *ced-9* is to prevent cell death. How *ced-9* functions to promote death is not known.

## D. Conservation of the Death Pathway between Nematodes and Mammals

The central roles members of the *ced-9 / bcl-2* and *ced-3/ICE* gene families have in mediating programmed cell death in both *C. elegans* and humans—and the observation that these structurally similar genes are functionally interchangeable—strongly suggest that nematodes and mammals share a common molecular pathway for programmed cell death. If so, then it seems likely that not only CED-9 and CED-3, but also the rest of the cell death pathway that has been characterized in *C. elegans* will be conserved through evolution and that homologs of these genes will function in apoptotic death in mammals. That this common genetic program for cell death predates the evolutionary separation of nematodes and vertebrates also shows that it is of ancient origin, possibly arising with the advent of metazoa or soon thereafter.

## E. *dad-1*

A second *C. elegans* cell death suppressor gene, *dad-1* (defender against apoptotic death), has been described recently ([Sugimoto et al. 1995](#)). *C. elegans dad-1* is a homolog of a gene originally found mutated in a temperature-sensitive mutant hamster cell line that undergoes apoptosis at the restrictive temperature ([Nakashima et al. 1993](#)). Transfection with a wild-type copy of *dad-1* rescues the death of the hamster cells at the restrictive temperature, confirming that the apoptotic phenotype resulted from the loss of *dad-1* function. Although these observations suggest that *dad-1* might encode a negative regulator of cell death, they do not eliminate the more trivial possibility that the absence of *dad-1* function only indirectly results in cell death, possibly by affecting the overall health of the cell.

[Sugimoto et al. \(1995\)](#) went some way toward addressing this question by isolating and characterizing the *C. elegans* homolog, which shows a high degree of sequence conservation with its mammalian counterpart. Interestingly, overexpression of either worm or human *dad-1* weakly prevents programmed cell death in *C. elegans* ([Sugimoto et al. 1995](#)). Many different cell types appear to be rescued from death, suggesting that *dad-1* might indeed be a proximal inhibitor of the cell death machinery. Where *dad-1* acts with respect to the other *C. elegans* cell death genes (*ced-3*, *ced-4*, *ced-9*) remains to be determined.

*dad-1* homologs have also been identified in plants and in the yeast *Saccharomyces cerevisiae* ([Silberstein et al. 1995](#)). The yeast protein, which shows about 35% sequence identity with the nematode and human DAD-1 proteins, is a subunit of oligosaccharyltransferase, an enzyme required for N-linked protein glycosylation in the endoplasmic reticulum. Whether the metazoan DAD-1 proteins perform a similar function has yet to be determined. If it is the case, this result would suggest that glycosylation is important in controlling apoptotic death.

## F. Genes Required for the Engulfment of Dying Cells

Engulfment of cells undergoing programmed cell death is a highly efficient process in *C. elegans*; dying cells are phagocytosed and mostly digested within less than 1 hour. Ultrastructural studies suggest that engulfing cells can recognize a dying cell before it shows any overt morphological changes and even before the cell division generating the dying cell has been completed ([Robertson and Thomson 1982; Ellis et al. 1991a](#)). Thus, generation of the engulfment-promoting signal must be an early event in the death process. No professional phagocytes exist in *C. elegans*, and most cells appear to be able to recognize and engulf programmed cell deaths. During embryogenesis, the sister of the dying cell will often be the engulfing cell; during postembryonic development, epithelial cells tend to take over this role.

Mutations in six genes (*ced-1*, 2, 5, 6, 7, 10) result in a persistent corpse phenotype ([Hedgecock et al. 1983; Ellis et al. 1991a](#)). In animals mutant for any one of these genes, cells die as usual, but many of the dying cells fail to be engulfed and remain in the worm for many hours, or even days, readily visible under Nomarski optics as flat refractile disks. Ultrastructural studies confirmed that these cells show all the morphological changes that are found in normal cell death, but for phagocytosis and degradation within the engulfed cell. Corpses in engulfment-defective mutants do eventually disappear. Some undergo secondary necrosis and break up, and others might be recognized after a delay and engulfed after all.

Indeed, none of these six genes are absolutely essential for engulfment. Engulfment of most cells is delayed in all mutants, but eventually most cell corpses disappear. Even in the strongest mutants, less than 30% of the embryonic programmed cell deaths are still visible as corpses at hatching. Nevertheless, all six genes contribute to the efficient engulfment of any given cell, although to different degrees. For example, the corpses of the pharyngeal I2 sister cells can persist in mutants in all six genes, but they are more likely to be present in *ced-2* or *ced-5* mutants than in *ced-1* or *ced-6* mutants. Other cell corpses (e.g., those of the NSM sister cells) show a different spectrum of persistence, but again they can be observed in most mutants at some detectable frequency (Ellis et al. 1991a). Thus, the low expressivity observed in these mutants cannot solely be ascribed to the six genes acting on distinct and mutually exclusive groups of dying cells, but rather suggests that there is at least some functional redundancy in the engulfment process.

## 1. Two Partially Redundant Pathways for Engulfment

Analysis of all possible double-mutant combinations among the six engulfment genes suggests that these six genes can be divided into two distinct, partially redundant groups—*ced-1*,6,7 and *ced-2*,5,10—that appear to act in parallel to promote the engulfment of dying cells (Ellis et al. 1991a). Combining two mutations within a single group usually leads to a phenotype no stronger than the stronger single mutant, suggesting that these genes act in the same genetic pathway (this is particularly true for *ced-2*,5,10; the rule breaks down in several cases in the other group). In contrast, double mutants carrying mutations in one gene in each class show a vastly increased engulfment defect.

Interestingly, the six engulfment genes can be divided into the same groups for two other apparently unrelated phenotypes. Mutations in *ced-2*,5,10, but not *ced-1*,6,7, partially suppress the Vulvaless phenotype conferred by gain-of-function mutations in *lin-24* and *lin-33* (Kim 1994; see below). Furthermore, mutations in *ced-2*,5,10 cause an incompletely penetrant distal tip cell (DTC) migration defect. In about 30% of such mutants, at least one of the two half gonads follows a meandering path that can include abnormal dorsal or ventral detours, additional turns, and in some cases failure to turn at the appropriate position (T. Gumienny and M.O. Hengartner, unpubl.; Y. Wu and H.R. Horvitz, pers. comm.).

It should be stressed that the six identified genes do not represent the full complement of genes involved in engulfment. One additional gene in the *ced-2*,5,10 class has been identified recently (F. Ross, pers. comm.). Furthermore, a large number of deficiencies result, in the homozygous state, in arrested embryos that contain unengulfed cell corpses (Ahnn and Fire 1994), suggesting that many genes function in engulfment. Mutations in these additional genes might not have been recovered in previous screens because the genes might also be required for other, possibly essential functions. Supporting this view, J. Rothman (pers. comm.) has identified a number of point mutations that result in embryonic lethality and a strong engulfment defect.

## 2. Molecular Basis of Recognition/Engulfment

How do the engulfment genes function to promote the engulfment of dying cells? The individual genes could be involved either in the generation of a signal by the dying cell, in the reception and interpretation of this signal by the engulfing cell, or in the actual phagocytosis. Neither the molecular nature nor the site of action (within the dying cell or the engulfing cell) of any of the cell death genes has been described. All of the engulfment genes but *ced-1* show maternal rescue for the engulfment of early (embryonic deaths). That either maternal (but not paternal) or zygotic expression is sufficient to rescue embryos suggests that these genes are expressed both in the germ line and in embryos and that either contribution is sufficient for wild-type levels of engulfment. Late deaths, as well as the DTC migration defect, do not show any maternal rescue.

The two groups of engulfment genes presumably identify two distinct pathways that independently promote the engulfment of dying cells. *ced-1*,6,7 might function in a process specific to programmed cell deaths, as mutations in these genes do not appear to have any other phenotypes. That *ced-2*,5,10 also promote the engulfment of the abnormal corpses caused by mutations in *lin-24* and *lin-33* suggests that these genes might be involved in a more general process; they could, for example, be involved in recognizing and eliminating all dead or very sick cells whose membrane integrity is threatened, irrespective of the cause of their demise.

[Hedgecock et al. \(1983\)](#) reported that mutations in *ced-1* or *ced-2* did not affect engulfment kinetics of abnormal (pathological) deaths, but more recent studies have suggested that at least some of the engulfment genes are required for the efficient removal of cellular debris resulting from *mec-4* -mediated neurodegenerative deaths (see below).

### 3. Conservation of the Engulfment Process?

The use of multiple mechanisms to promote the engulfment of dying cells is not confined to *C. elegans*. Mammalian macrophages are thought to be able to use at least three distinct recognition mechanisms to identify apoptotic cells (for review, see [Savill et al. 1993](#)). Depending on the nature and physiological state of the engulfing cell, and to some extent the nature of the dying cell, macrophages will rely to varying degrees on these three recognition mechanisms. The first system involves an as yet uncharacterized macrophage cell surface lectin that binds to sugar residues, such as glucosamine, that are postulated to become exposed on the surface of apoptotic cells. The second mechanism involves thrombospondin, which is thought to act as a bridge between the dying cell and the macrophage. Thrombospondin can bind to the surface of the macrophage via the vitronectin receptor; how it recognizes the apoptotic cell has yet to be elucidated. Finally, macrophages appear to be able to recognize the presence of phosphatidylserine on the outer surface of apoptotic cells. This phospholipid, usually confined to the inner leaflet of the plasma membrane, shows up on the outer leaflet in apoptotic cells. How phosphatidylserine flips to the outer surface and how it gets recognized by the macrophage have not been determined.

There is currently no evidence to support or refute the proposition that *C. elegans* and mammals use the same mechanism to identify cells undergoing programmed cell death, but since the cell death program (or at least its killing step) has remained conserved between nematodes and mammals, and since generation of the signal for engulfment is likely to be an integral part of the death program, one could expect that this part of the program would also be conserved through evolution.

### G. *ced-8*

*ced-8* had previously been classified as an engulfment-defective gene on the basis of the observation that, in *ced-8* mutants, threefold embryos show a significant higher number of cell corpses than the wild type ([Ellis et al. 1991a](#)). However, in *ced-8* mutants, both the appearance and engulfment of dying cells are slowed down, suggesting that *ced-8* is required for efficient and rapid execution of the death sentence rather than for engulfment per se (G. Stanfield et al., unpubl.).

### H. *nuc-1*

The *nuc-1* (nuclease-deficient) gene is required to digest the DNA of dead, engulfed cells ([Sulston 1976](#); [Hedgecock et al. 1983](#)). In *nuc-1* mutants, the DNA of engulfed cells is degraded much more slowly than in the wild type, and persistent nuclear remnants can readily be visualized, through the use of DNA stains such as DAPI, as small bright dots inside the engulfing cell. Biochemical studies indicated that *nuc-1* mutants lack the major DNase activity found in wild-type *C. elegans* ([Hevelone and Hartman 1988](#)). This nuclease, which is probably encoded by the *nuc-1* gene, has properties characteristic of the acid nucleases found in many animal cells and is also required to digest the DNA of the bacteria on which *C. elegans* feeds, since large amounts of DNA can be observed in the gut lumen of *nuc-1* mutants ([Hevelone and Hartman 1988](#)). These observations suggest that the nuclease missing in *nuc-1* mutants is probably a lysosomal enzyme normally involved in digesting the DNA present in ingested foods and scavenging endogenous DNA, and thus only has a peripheral role in programmed cell death.

## Figures



## Figure 1

Cell death pathways in *C. elegans*. (a) The pathway for programmed cell death that functions in most *C. elegans* cells. (b) Murder pathway, which functions in the death of the linker cell and of *B.a*/<sub>1</sub>,apaav. (c) Pathological deaths. Inferred regulatory interactions between genes are also shown. (→) Positive regulatory interaction; (—) negative regulatory interaction. (Adapted from [Ellis et al. 1991b](#); [Driscoll 1992](#); [Hengartner and Horvitz 1994c](#); [Kim 1994](#).)

## Tables

**Table 1C. *C. elegans* genes that affect cell death**

Gene	Gene product	Normal gene function	Mutant phenotype (If unless noted otherwise)
<i>ced-3</i>	cysteine protease	promotes PCD	no PCD
<i>ced-4</i>	novel	CED-4 <sub>S</sub> : promotes PCD CED-4 <sub>L</sub> : antagonizes PCD	no PCD
<i>ced-8</i>	unknown	promotes PCD	slowed down PCD kinetics; very weak suppression of PCD
<i>ced-9</i>	Bcl-2 homolog	protects cells that should live from PCD; promotes PCD in cells that should die	gf: no somatic PCD; germ cell death normal lf: many cells that normally live undergo PCD; maternal-effect lethal
<i>dad-1</i>	oligosaccharyltransferase	unknown	gf: protects cells that should die from PCD lf: unknown
<i>ced-1</i>	unknown	promotes engulfment of PCDs	persistent PCD corpses
<i>ced-6</i>	unknown	promotes engulfment of PCDs	persistent PCD corpses
<i>ced-7</i>	unknown	promotes engulfment of PCDs	persistent PCD corpses
<i>ced-2</i>	unknown	promotes engulfment of PCDs and pathological deaths	persistent PCD corpses; suppression of <i>lin-24</i> (gf) and <i>lin-33</i> (gf); DTC migration defect
<i>ced-5</i>	unknown	promotes engulfment of PCDs and pathological deaths	persistent PCD corpses; suppression of <i>lin-24</i> (gf) and <i>lin-24</i> (gf); DTC migration defect
<i>ced-10</i>	unknown	promotes engulfment of PCDs and pathological deaths	persistent PCD corpses; suppression of <i>lin-24</i> (gf) and <i>lin-24</i> (gf); DTC migration defect
<i>nuc-1</i>	DNase ?	digestion of DNA in lysosomes and gut	slow degradation of genomic DNA of engulfed cells; accumulation of DNA in gut
<i>ces-1</i>	unknown	unknown	gf: NSM and I2 sisters survive (4 cells) lf: no phenotype
<i>ces-2</i>	bZIP	promotes death of NSM sisters?	NSM sisters survive (2 cells)

<b>Gene</b>	<b>Gene product</b>	<b>Normal gene function</b>	<b>Mutant phenotype (If unless noted otherwise)</b>
<a href="#"><i>egl-1</i></a>	unknown	unknown	gf: HSNs undergo PCD in hermaphrodites lf: unknown
<a href="#"><i>lin-24</i></a>	novel	unknown	gf: Pn.p cells die or show abnormal lineages lf: no phenotype
<a href="#"><i>lin-33</i></a>	unknown	unknown	gf: Pn.p cells die or show abnormal lineages lf: no phenotype
<a href="#"><i>mec-4</i></a> , <a href="#"><i>mec-6</i></a> , <a href="#"><i>mec-10</i></a> , <a href="#"><i>deg-1</i></a> , <a href="#"><i>unc-105</i></a>	degenerins	see <a href="#">Driscoll and Kaplan</a> (this volume)	see <a href="#">Driscoll and Kaplan</a> (this volume)
<a href="#"><i>deg-3</i></a>	acetylcholine receptor subunit	see <a href="#">Driscoll and Kaplan</a> (this volume)	see <a href="#">Driscoll and Kaplan</a> (this volume)

(PCD) Programmed cell death; (gf) gain-of-function mutation; (lf) loss-of-function mutation; (DTC) distal tip cell. See text for references.

Generated from local HTML

# Chapter 15. Cell Death — IV Programmed Cell Death in Specific Cell Types

---

In addition to the genes that function in all programmed cell deaths, a number of genes have been identified that, when mutated, affect the survival of specific subsets of *C. elegans* cell deaths, often of a single cell type. Some of these genes are required for cells to acquire their proper fate (to know that they should die), whereas others might be required for the cells to activate (or repress) the death pathway in response to this fate.

## A. Mutations That Affect Cell Identity

Mutations in many cell fate determination genes alter the normal pattern of cell death. In most of these cases, such changes are brought about indirectly, as a secondary consequence of changes in cell lineages. The mutated gene is thus unlikely to participate directly in controlling the decision between life and death of individual cells. For example, the homeobox gene *lin-32* is required for neuroblast fate specification, and many neuronal lineages are either abnormal or missing altogether in *lin-32* mutants ([Chalfie and Au 1989](#); [Zhao and Emmons 1995](#)). Programmed cell deaths that would have been generated in the altered lineages therefore do not occur, as the cells that should die are not generated.

In other cases, determination genes might be directly involved in specifying life versus death even though they also affect other cell fate decisions. For example, the HOM-C homeobox gene *lin-39* is expressed in the midbody region and is involved, in combination with the genes *egl-5* and *mab-5*, in specifying the fates of many cells in this domain, including the P cells and their descendants ([Ellis 1985](#); [Clark et al. 1993](#); [Wang et al. 1993](#); see [Ruvkun](#), this volume). Depending on the exact genes that they express, lineally equivalent cells in the [P1–P12](#) lineages will adopt distinct fates: In [P1](#), [P2](#), and [P9–P12](#), the Pn.aap cells undergo programmed cell death, whereas P3.aap–[P8.aap](#) cells become [VC neurons](#) and innervate the vulval muscles. In *lin-39* mutants, the P3.aap– [P8.aap](#) cells appear to adopt the fate of their anterior or posterior equivalents and also undergo programmed cell death ([Ellis 1985](#); [Clark et al. 1993](#); [Wang et al. 1993](#)). Thus, *lin-39* activity is required to repress the death fate in the Pn.aap cells. How *lin-39* acts—directly by regulating the expression of one or several cell death genes or indirectly—remains to be determined.

## B. HSN Neurons

Mutations in the *egl-1* (egg-laying-defective) gene specifically affect the survival of the two serotonergic HSN neurons, which innervate the vulval muscles and drive egg laying in hermaphrodites ([Sulston and Horvitz 1977](#); [Trent et al. 1983](#); [Desai et al. 1988](#); [Desai and Horvitz 1989](#)). These [neurons](#) are sexually dimorphic: In males, the HSNs are not needed and undergo programmed cell death ([Sulston and Horvitz 1977](#)). Dominant mutations in the *egl-1* gene cause the HSNs to undergo programmed cell death in hermaphrodites, leading to a defect in egg laying. No other cells appear to be affected. These dominant mutations presumably result in a gain of *egl-1* function, since deficiencies that delete the *egl-1* locus do not cause the death of the HSN neurons. However, extensive suppression screens have so far failed to isolate intragenic revertants, but for the large deficiency *nDf42* (M.O. Hengartner and H.R. Horvitz, unpubl.). *ced-3*, *ced-4*, and *ced-9* (*n1950gf*) are epistatic to *egl-1*: In such double mutants, the HSNs survive and function normally, and the animals are non-Egl ([Ellis and Horvitz 1986](#); [Hengartner et al. 1992](#)), suggesting that the *egl-1* mutations specifically induce the cell death pathway in the HSN neurons, rather than causing some unrelated sickness that would induce cell death as a secondary consequence. One appealing hypothesis is that these mutations cause the HSNs to be sexually transformed and adopt a male fate rather than a hermaphrodite fate, which would lead them to activate the cell death program inappropriately.

## C. NSM Sister Cells

In wild-type animals, the sister cells of the pharyngeal serotonergic NSM neurons undergo programmed cell death. Mutations in two genes, *ces-1* and *ces-2* (cell death specification), specifically affect this decision ([Ellis and](#)

[Horvitz 1991](#)). Activation of *ces-1* or inactivation of *ces-2* leads to the survival of the NSM sisters, with the undead cells adopting a fate similar to that of their sisters. The single known mutation in *ces-2* is hypomorphic and temperature-sensitive. The identity of the null phenotype is not known. The three dominant *ces-1* gain-of-function mutations also lead to the survival of the sisters of the two pharyngeal I2 [neurons](#) (these cells die normally in *ces-2* mutants). Loss of *ces-1* function causes no obvious phenotype. In particular, the sisters of the NSM and I2 [neurons](#) die as they do in the wild type. However, *ces-1* (*lf*) mutations suppress the survival of the NSM sisters in *ces-1* (*lf*); *ces-2* double mutants, suggesting that *ces-2* acts as a negative upstream regulator of *ces-1*. In contrast, the NSM sisters survive in *ces-1* (*lf*); *ced-3* or *ces-1* (*lf*); *ced-4* double mutants (and in *ces-1* (*lf*) *ces-2*; *ced-3* triple mutants), indicating that *ces-1* itself acts upstream of the general cell death genes, consistent with the proposed role of *ces-1* in controlling cell death specifically in the NSM and I2 sisters. These genetic interactions suggest that *ces-1* has a cryptic capacity to rescue the NSM sisters from programmed cell death and that *ces-2* function is required to repress this activity. Whether *ces-1* is normally expressed in the NSM sisters and what the normal function of *ces-1* might be (since loss of its function apparently results in a wild-type phenotype) remain to be determined. The *ces-2* gene encodes a putative bZIP transcription factor ([Metzstein et al. 1996](#)), suggesting that, as in mammals, some nematode cell deaths might be regulated at the level of gene expression.

## D. Germ Line

Programmed cell deaths are very common in the adult hermaphrodite germ line ([White 1988](#); T. Gumienny and M.O. Hengartner, unpubl.). Germ cell deaths are very similar in appearance, both under Nomarski optics and in the electron microscope, to the developmental cell deaths, except for the generally larger size of the germ cell corpses. The kinetics of death are also very similar: Germ cell corpses are rapidly recognized and phagocytosed by the sheath cells, disappearing usually in less than 1 hour.

Programmed cell deaths in the germ line appear to be associated—either directly or indirectly—with oogenesis, because no [germ cells](#) normally die in larvae, nor in adult males. There is also a strong if not perfect correlation between the presence of oogenesis and programmed cell deaths in the various sex-determination mutants (T. Gumienny and M.O. Hengartner, unpubl.). Furthermore, deaths are only found in the region of the syncytium occupied by nuclei arrested in pachytene and are not observed in the mitotic region. More mature oocytes appear to be capable of undergoing programmed cell death, but they do so only infrequently in the wild type. Once oogenesis starts, germ cell deaths occur continuously and persist for at least as long as oogenesis persists. The rate of death appears to be constant (or to increase slightly) during this period. About five [germ cells](#) die every hour, suggesting that as many cells die as oocytes are produced. Thus, during the reproductive life of the animal, at least 300 [germ cells](#) are estimated to undergo programmed cell death, more than twice the total number of cell deaths that occur during development.

Most of the mutations that affect developmental deaths in the soma also affect programmed cell death in the germ line. *ced-3* and *ced-4* are required for [germ cells](#) to die, whereas *ced-9* is required to protect [germ cells](#) from death: In *ced-9* (*lf*) mutants, many more germ cell corpses can be observed. In the strongest alleles, almost all presumptive oocytes die, and only a handful of progeny are produced (which invariably appear sick and die early in embryogenesis). In engulfment-defective mutants, germ cell corpses accumulate between the syncytial germ line and the sheath cell. The older the animal, the more corpses can be found; up to 100 corpses have been observed in a single half-gonad. In older animals, the corpses are swept along the gonadal arm and can be observed among the mature oocytes in the proximal arm and in the [uterus](#). In *nuc-1* animals, large DAPI-positive vacuoles accumulate in the sheath cells. Both vacuoles and DAPI-positive material are absent in wild-type animals, as well as in mutants defective for engulfment of dying cells. No extra DAPI-positive material can be found in the germ line of *nuc-1* mutants, suggesting that dying [germ cells](#) are all engulfed by the sheath cell, rather than being resorbed and phagocytosed by the germ-line syncytium.

A unique aspect of germ cell deaths is that they occur in a syncytium. Time course studies in the light microscope and analysis of electron microscopic sections of dying [germ cells](#) indicate that the deaths are not nuclear deaths but rather that dying cells cellularize and pinch off the syncytium very early in the death process. This

sequestration might be important for avoiding the diffusion of death-promoting factors (such as active CED-3) from a dying cell to its neighbors. Cellularization does not occur in *ced-3* or *ced-4* mutants, indicating that this process is a subroutine activated by the death program in the *germ cells*.

A somewhat similar but even more curious phenomenon has been described in *lin-5* mutants. *lin-5* is required for most postembryonic nuclear and cell divisions but not for DNA replication (Albertson et al. 1978; Sulston and Horvitz 1981). Postembryonic blast cells in *lin-5* mutants thus become polyploid and often show some features of the various differentiated cells that they would have generated. In *lin-5* mutants, the P cells that normally generate programmed cell deaths occasionally appear themselves to adopt this fate and die. On other occasions, they will extrude from the large polyploid nucleus smaller, nuclear-like bodies that appear to undergo programmed cell death independently of the larger nucleus, which survives (Albertson et al. 1978). The exact nature of these smaller bodies, e.g., whether they cellularize, and their fate in the various *ced* mutant backgrounds have not been determined.

Why *germ cells* undergo programmed cell death has not been unambiguously determined. One possibility is that *germ cells* are subjected to a “quality control,” with the bad, e.g., mutated or damaged, genomes being eliminated through programmed cell death, in a mechanism similar to p53-induced apoptosis in mammals (Bates and Vousden 1996). Why such a control mechanism would operate only during oogenesis and not during spermatogenesis is unclear. Furthermore, in *ced-3* and *ced-4* mutants, all *germ cells* make functional oocytes. Although *ced-3* and *ced-4* mutants have slightly reduced brood sizes compared to the wild type (Ellis and Horvitz 1986), no increase in lethality or rate of spontaneous mutagenesis has been detected.

An alternative hypothesis can be proposed on the basis of the observation that the *germ cells* in hermaphrodites perform a double duty: In addition to their status as oocyte precursors, they also function as nurse cells, synthesizing cytoplasmic components that the oocytes incorporate when they cellularize (Gilbert et al. 1984; Kimble and Ward 1988; White 1988). It is possible that more such nurse cells are required than oocytes can be made and that the excess *germ cells* which will not become oocytes are then discarded by letting them die. Dying *germ cells* contain very little cytoplasm, which would be consistent with the idea that these deaths are mostly meant to eliminate excess nuclei. The observation that germ cell deaths are particularly abundant in starving and old animals (Sulston 1988) suggests that germ cell death might also have evolved to control the rate of oogenesis in response to environmental conditions or sperm availability.

## E. Other Programmed Cell Deaths

The cases discussed above represent only a small fraction of all cell types that undergo programmed cell death. It seems reasonable to assume that many more cell-type-specific cell death genes remain to be identified. As the survival of individual cells rarely leads to any obvious phenotype, isolation of mutations in such genes will unfortunately require direct screening for the presence of the undead cell.

Generated from local HTML

# Chapter 15. Cell Death — V Cell Deaths not Mediated by the Common Death Program

---

Not all developmental cell deaths occur by programmed cell death and not all programmed cell deaths need to be mediated by the same molecular pathway. Examples have been found of both programmed (naturally occurring) and unscheduled (pathological) cell deaths that are not mediated through the classical [ced-3](#) / [ced-4](#) -dependent pathway.

## A. Murders

A small number of deaths that occur during normal *C. elegans* male development appear to occur through a pathway distinct from the "classical" [ced-3](#) / [ced-4](#) -dependent pathway.

The linker cell is required to guide the developing [male gonad](#) to the [tail](#), where the reproductive and digestive system fuse ([Kimble and Hirsh 1979](#)). Once the destination is reached, the linker cell dies and is engulfed by either U.1p or [Urp](#), two cells of the [proctodeum](#) in an event that has been described as necessary for opening the channel between the [vas deferens](#) and the [cloaca](#). If the [U](#) progenitor cell is eliminated by laser microsurgery, or if the linker cell is prevented from reaching the [proctodeum](#) (by mutation or otherwise), the linker cell fails to die ([Sulston et al. 1980](#)). These observations suggest either that U descendants are required to signal the linker cell to commit suicide or that engulfment of the linker cell is required for it to die; in which case, this death would be described more aptly as a murder than as a suicide. In support of the latter interpretation, death of the linker cell still occurs about half the time in [ced-3](#) mutants, suggesting that although the cell death machinery does promote the death of the linker cell, it might not be essential for its demise ([Ellis and Horvitz 1986](#)).

The B descendants [B.a<sup>1</sup>/r](#)apaav form an equivalence group, with one cell forming part of the [vas deferens](#) and the other one being engulfed by P12.pa ([Sulston et al. 1980](#)). If the precursor to one of the two cells is ablated, the other invariably survives, suggesting that survival is the primary fate in this group. In P12.pa-ablated animals, and in [ced-1](#) or [ced-2](#) mutants, both [B.alapaav](#) and [B.arapaav](#) survive, suggesting that engulfment by P12.pa is the cause of death in this case ([Sulston et al. 1980; Hedgecock et al. 1983](#)). The effect of mutations in [ced-3](#), [ced-4](#), and the other engulfment genes on [B.a<sup>1</sup>/r](#)apaav death has not been investigated.

## B. *lin-24* and *lin-33*

Gain-of-function mutations in the genes [lin-24](#) and [lin-33](#) can cause the death of the Pn.p cells, resulting, in hermaphrodites, in a Vulvaless phenotype ([Ferguson and Horvitz 1985; Ferguson et al. 1987; Kim 1994](#)). The deaths induced by these mutations are morphologically and genetically distinct from programmed cell deaths and appear to be degenerative in nature.

Under Nomarski optics, the Pn.p nuclei in [lin-24](#) and [lin-33](#) mutants increase in refractivity during the late first or early second larval stage of development and form oval bodies that persist from a few minutes to up to 3 hours. These refractile bodies are distinguishable from the refractile corpses formed by programmed cell death because they are larger and less regular, affect the nucleus rather than the whole cell, and often contain an internal "depression." Once the refractivity decreases, the nucleus becomes granular and then resolves. At this point, one of three outcomes can be observed: (1) The cell dies, (2) the cell survives but the nucleus remains abnormally small, or (3) the cell survives and the nucleus appears to recover completely. Only a minority of the cells actually die; most recover completely. However, even the cells that recover show abnormal division patterns (most Pn.p cells fail to divide altogether). Thus, the Vulvaless phenotype is mostly the result of abnormal cell division patterns rather than of cell death. The refractile Pn.p cells also show ultrastructural features, including swelling of nuclear and mitochondrial membranes followed by karyolysis, that are distinct from the changes observed in programmed cell death and that are more reminiscent of cells undergoing necrosis than apoptosis ([Kim 1994](#)).

The mutations that cause the Pn.p deaths result in a gain of *lin-24* or *lin-33* function, and but for one recessive *lin-24* (*gf*) allele, all are semidominant. Dosage studies for several of these mutations point to the existence of complex interactions between mutant and wild-type alleles, and between different mutant alleles, but in general suggest that the mutant allele does not result in an overexpression of gene product but rather might direct the synthesis of an abnormal, cytotoxic gene product. Loss-of-function mutations have no obvious phenotype on their own, but they act as *cis*- and *trans*-dominant suppressors of gain-of-function mutations in the same gene. Furthermore, loss-of-function alleles of one gene can suppress gain-of-function mutations in the other gene, indicating that normal *lin-24* function is required for *lin-33* to kill cells, and *vice versa*. This mutual suppression suggests that these two genes function in the same step of a yet to be defined pathway (Kim 1994).

*ced-3*, *ced-4*, and *ced-9* (*gf*) do not prevent the Pn.p deaths in *lin-24* and *lin-33* mutants. However, rather intriguingly, mutations in *ced-2*, *ced-5*, and *ced-10*, which constitute one of the partially redundant group of genes required for the engulfment of programmed cell deaths, efficiently prevent the Pn.p deaths and partially suppress the Vulvaless phenotype (Kim 1994). One hypothesis consistent with this observation would be that *lin-24* (*gf*) and *lin-33* (*gf*) do not actually kill the Pn.p cells but make them very sick. The sick cells are then presumably recognized by neighboring cells in a *ced-2/ced-5/ced-10*-dependent manner and phagocytosed. If phagocytosis is prevented, the cells survive and eventually recover.

## C. Necrotic Deaths

Mutations in a number of genes, including but not limited to *mec-4*, *deg-1*, and *deg-3*, lead to the death of particular cells by causing them to swell and lyse. Analysis of these mutations has shown that in most cases, the degeneration-inducing mutation results in a gain of gene function, that the mutated gene encodes an ion channel subunit, and that the affected cells are neuronal. The molecular nature of these mutations and the cells that they affect are discussed in this volume by Driscoll and Kaplan and elsewhere (Ellis et al. 1991b; Driscoll 1992; Driscoll and Chalfie 1992). Reviewed in this chapter are the morphological and genetic features of these deaths that distinguish them from programmed cell deaths.

Swelling deaths induced by gain-of-function mutations in genes of the degenerin family, such as *mec-4*, *deg-1*, and *mec-10*, exhibit morphological features of necrotic cell death. Such deaths are distinct from programmed cell death in several ways: (1) Cells undergoing programmed cell death appear to be compacted and "button-like," whereas cells undergoing degenerative cell death appear to be swollen and enlarged, (2) distinct ultrastructural changes accompany the two types of death (Robertson and Thomson 1982; M. Driscoll, pers. comm.), (3) programmed cell deaths transpire within the hour, whereas degenerative deaths occur over several hours (Chalfie and Sulston 1981; Robertson and Thompson 1982), and (4) *ced-3* and *ced-4*, needed for execution of all programmed cell deaths, are not required for degenerin-induced deaths (Hedgecock et al. 1983; Ellis and Horvitz 1986; Chalfie and Wolinsky 1990).

The time of onset of degenerative death correlates with initiation of degenerin gene expression, and the rapidity with which death occurs correlates with dose of the toxic allele (Chalfie and Wolinsky 1990; Hall et al. 1997). These observations are consistent with the hypothesis that a threshold ion influx is needed to initiate the degenerative process. Ultrastructural analysis has established that degeneration initiates with striking infoldings of the plasma membrane (M. Driscoll, pers. comm.). Small tightly wrapped membranous whorls are the first indications of pathology. Subsequently, internalized whorls grow in size and large vacuoles appear. Cell body volume can increase 100-fold during this process. The nucleus becomes distorted and chromatin aggregates. Internal degradation of cell contents then follows shortly. Finally, corpse debris is removed in a process that requires the activities of the engulfment *ced* genes (Hedgecock et al. 1983; Ellis et al. 1991a), with *ced-2*, *ced-5*, and *ced-10* appearing to be most important (S. Chung and M. Driscoll, pers. comm.). Thus, although mechanisms of killing are distinct in programmed and degenerin-induced cell death, corpse recognition and removal mechanisms share common steps.

Degenerin-poisoned cells share features of subcellular pathology exhibited in disorders caused by mutations in mammalian ion channels (e.g., in the muscle Na<sup>+</sup> channel affected in hyperkalemic periodic paralysis; Engel et al.

[1970](#)) and under degenerative conditions such as neuronal ceroid lipofuscinosis ([March et al. 1995](#)). The dramatic endocytosis observed during neurodegeneration in *C. elegans* and the implication of altered intracellular membrane trafficking in Alzheimer's disease and Huntington's disease suggest that endocytotic responses provoked by diverse types of damage could be a common element of diverse degenerative conditions.

Additional genes can mutate to induce vacuolar degeneration of various *C. elegans* cells (M. Chalfie; A. Chisholm and H. R. Horvitz; both pers. comm.). Molecular analysis of one of these, [\*deg-3\*](#), established that degenerin family members are not the only channel genes capable of mutation to toxic forms. [\*deg-3\*](#) (*u662*) is a gain-of-function allele that leads to the degeneration of several [neurons](#), including the [touch receptor neurons](#) and the PVC [interneurons](#) ([Treinin and Chalfie 1995](#)). Loss-of-function [\*deg-3\*](#) alleles have no apparent phenotype. DEG-3 exhibits significant similarity to  $\alpha$  subunits of the neuronal nicotinic acetylcholine receptor and, in the pore-lining domain TMDII, is most like  $\alpha 7$  subunits. [\*deg-3\*](#) (*u662*) encodes an I293N substitution in TMDII at a site equivalent to the chicken  $\alpha 7$ -4 V251T mutant. Since the mutant chicken subunit exhibits defective desensitization when expressed as a homomeric channel in *Xenopus* oocytes, the *C. elegans* channel, which harbors a substitution of a polar for a hydrophobic residue at the equivalent site, is likely to permit excessive ion influx. Consistent with this hypothesis, some nicotinic antagonists partially suppress the [\*deg-3\*](#) (*u662*) Mec phenotype.

Generated from local HTML

# Chapter 15. Cell Death — VI Evolution of Programmed Cell Death

---

## A. Purpose of Programmed Cell Death in *C. elegans*

A significant fraction of the cells that are generated in *C. elegans* are subsequently eliminated by programmed cell death: about 12% during somatic development, even more in the germ line. Many a student of *C. elegans*, impressed by the efficiency and finesse of its development, has marveled at this apparent waste of energy. Why does this organism bother to generate cells if it will discard them afterward? In vertebrates, programmed cell death is used to eliminate cells that have been produced in excess, have already served their purpose, or are potentially detrimental to the organism. In *C. elegans*, most deaths appear to belong to either of the first two categories. However, because mutants with no cell death are less fit than their wild-type counterparts, at least some of the deaths (or combinations of deaths) can also be placed into the third group (if the definition of "detrimental" is taken loosely enough).

A small number of cells in *C. elegans* die after having fulfilled a function that is needed only transiently. These include the linker cell in the male and the "nurse cells" in the hermaphrodite germ line, both discussed in previous sections, as well as the spike cells ([AB.p](#)<sup>1</sup>/pppppp), which are required to form the [tail spike](#) during embryogenesis ([Sulston et al. 1983](#)). It is interesting to note that as with the linker cell, the [tail spike](#) cells appear to die by a mechanism that is slightly distinct from the normal cell death pathway (M.O. Hengartner, unpubl.).

Most cells that die in *C. elegans* are unlikely to have time to perform any function, since they are eliminated very shortly after their birth, often within the hour ([Sulston and Horvitz 1977](#); [Sulston et al. 1983](#)). Nevertheless, in most cases, a rationale for the original generation of the cells can be found.

Often, deaths are used to refine stereotypical lineages that are used repeatedly. In the ventral cord, for example, the 12 Pn.a [neuroblasts](#) follow a stereotypical pattern of division to generate five cells each (see [Ruvkun](#), this volume). However, not all five cells survive in all 12 lineages: [neurons](#) that are not needed in particular positions differentiate into other cell types or are eliminated by programmed cell death ([Sulston and Horvitz 1977](#); [White et al. 1986](#)). Thus, only P cells close to the presumptive [vulva](#) (P3–P8) generate [VC neurons](#), which will innervate the vulval muscles ([White et al. 1986](#)). The equivalent cells (Pn.aap) in [P1](#), [P2](#), and [P9–P12](#), which would presumably be too far from the [vulva](#), die. Similar arguments can explain the deaths of the [VB neurons](#), which extend axons posteriorly to synapse onto body-wall muscle ([White et al. 1986](#)), in the [P11](#) and [P12](#) lineages, as there would be no room for them to go anywhere. In these cases, it appears that it was simpler (or more expedient) to use programmed cell death to modify an existing lineage "subprogram" than to generate a new program that would not generate the superfluous cell. The corollary of this argument is that, although unlikely, the development of cell lineages in which the generation of useless cells is eliminated is possible and therefore should occur at a low but finite frequency. Lineage analysis in other nematode species suggests that this is indeed the case, as cells that die in *C. elegans* fail to be generated altogether in other species.

Cell death is also used to produce sexually dimorphic structures. Adult hermaphrodites and males differ significantly in the number and type of cells that they contain. Most postembryonically generated differences involve the use of sex-specific cell divisions. However, hermaphrodite and male embryos use identical patterns of cell divisions, and the few embryonically derived sexually dimorphic cells are generated through the sex-specific use of programmed cell death. Thus, the HSN neurons, discussed previously, undergo programmed cell death in males, whereas the four male-specific CEM cells die in the hermaphrodite ([Sulston et al. 1983](#)).

Finally, on the evolutionary scale, selective use of programmed cell death can also lead to the creation of novel structures. For example, the gonadal lineages in *C. elegans* hermaphrodites and *Panagrellus redivivus* females are very similar, even though the gonads of these animals are quite different. Whereas *C. elegans* have two symmetrically arranged ovaries, the ovary of *Panagrellus* is asymmetric, with the posterior arm failing to extend or contain [germ cells](#). Interestingly, [Sternberg and Horvitz \(1981\)](#) have found that the posterior distal tip cell in *Panagrellus* undergoes programmed cell death. Given the importance of this cell in *C. elegans* for gonad elongation and germ cell proliferation, it seems likely that the death of the posterior distal tip cell would be

sufficient (along with a few additional deaths observed in *Panagrellus* but not in *C. elegans*) to restrict gonadal development to the anterior arm and thus explain the striking differences in gonad morphology between these two species.

## B. Origin and Evolution of Programmed Cell Death as a Cellular Program

The conservation in sequence and function between *ced-9* and the *bcl-2* family and between *ced-3* and the *ICE* family strongly suggests that the apoptotic death program is of ancient origin and was probably in place before the separation of nematodes and vertebrates. Thus, we would expect that all species from this part of the evolutionary tree (i.e., all bilateria, which also includes arthropods and other smaller groups) possess a *ced-9* / *bcl-2* cell death pathway. As a phenomenon, programmed cell death is, however, much more widespread. It is used extensively not only by metazoans, but also by higher plants and basidiomycetes. The molecular basis of the death program in these phyla is, however, not known.

How far "down" the evolutionary ladder one can expect programmed cell death to exist depends on how one defines the phenomenon. Except for *dad-1*, no homologs of cell death genes have been found outside the bilateria. Morphological similarities to apoptotic deaths have been noted in dying differentiated cells in the slime mold *Dictyostelium discoidium* ([Cornillon et al. 1994](#)) and in dying trypanosomes ([Ameisen et al. 1995](#)). More limited similarities have been reported between the degeneration of macronuclei in conjugating *Tetrahymena* and the degradation of nuclei during apoptosis ([Davis et al. 1992](#)). It might well be that the apoptotic program found in nematodes and mammals evolved from such more restricted "subprograms" that had specific uses before the advent of metazoans.

It has been argued that for unicellular organisms, there would *a priori* appear to be no need for such a program, as cell death basically translates into organismal death and therefore would confer no evolutionary advantage (dead organisms do not procreate). However, if the unicellular organisms have the ability to recognize their kin, or simply tend to live in close proximity of each other, then this argument is no longer valid: One can easily envision that a unicellular organism could kill itself for the better good of its neighboring relatives, thus furthering the survival and multiplication of its own genes. Given the extreme biological diversity found in Nature, it would be surprising if programmed cell death did *not* occur in at least some unicellular organisms.

Generated from local HTML

## **Chapter 15. Cell Death — Acknowledgments**

---

The section on degenerin-mediated deaths was contributed by M. Driscoll. M.O.H. is a Rita Allen Foundation Scholar.

Generated from local HTML

# **Chapter 16. Muscle: Structure, Function, and Development**

---

*Owl Explained about the Necessary Dorsal Muscles. He had explained this to Pooh and Christopher Robin once before, and had been waiting ever since for a chance to do it again, because it is a thing which you can easily explain twice before anybody knows what you are talking about.* with apologies to A.A. Milne *The House at Pooh Corner* © 1928  
(E.P. Dutton)

## **Contents**

[I Introduction](#)

[II The Organization, Structure, and Function of Muscle](#)

[III Specification of Muscle Patterns: Programs for Muscle Determination and Differentiation](#)

[Acknowledgments](#)

Generated from local HTML

# Chapter 16. Muscle: Structure, Function, and Development — I

## Introduction

---

Muscle cells are characterized by a filament-lattice structure that generates contractile force in a regulated manner. *Caenorhabditis elegans* contains several groups of muscles with diverse functions. The most numerous (95 in adults) are striated (multiple sarcomere) muscles used for locomotion of the animal. Eighty one of these body-wall muscles are present at birth, with the remainder added early during postembryonic development ([Sulston and Horvitz 1977](#); [Sulston et al. 1983](#)). A variety of nonstriated (single-sarcomere) muscles are formed during embryogenesis. These muscles are used for diverse functions: pharyngeal pumping (20 [pharyngeal muscle](#) cells), intestinal contraction (2 intestinal muscles), and defecation control (1 [anal](#) sphincter and 1 [anal](#) depressor). During postembryonic development, the hermaphrodite adds a set of muscles for fertilization and egg laying (8 vulval and 8 [uterine](#) muscles and the contractile gonadal sheath), whereas the male adds a specialized set of 41 muscles to be used in mating. Anatomical simplicity has been a significant factor in the development of *C. elegans* as a model organism for studies of muscle. Due to the predominance of the body-wall muscle class, this class has been the most extensively analyzed; thus, much of the information in this chapter focuses on body-wall muscle.

Muscle has been a fertile ground for molecular genetic studies with *C. elegans*. Although muscle is essential for viability (see, e.g., [Waterston 1989](#)), partial muscle function is sufficient for growth under laboratory conditions. This allowed the isolation of many mutations affecting muscle (see, e.g., [Brenner 1974](#); Epstein and Thomson 1974; [Epstein et al. 1974](#); [Waterston et al. 1980](#); [Zengel and Epstein 1980](#); [Avery 1993a](#)). As the corresponding genes have been characterized, *C. elegans* has provided the larger community of muscle researchers with the first cloned genes and/or functional data on many fundamental components of muscle. The first example of this was the genetic analysis and complete sequence of a myosin heavy-chain gene ([Epstein et al. 1974](#); [Karn et al. 1983](#)). Many subsequent examples will be evident from this chapter. At the same time, muscle has been an excellent paradigm within *C. elegans* research for developing molecular genetic strategies and methods. These include the characterization of chemical and transposon mutagenesis ([Brenner 1974](#); Eide and Anderson 1985b; Moerman et al. 1986), the first cloning of genetically defined loci (MacCleod et al. 1981), DNA transformation-rescue assays (Fire and [Waterston 1989](#)), and development of technology for reverse genetics ([Waterston 1989](#); Plasterk and Groenen 1992; [Rushforth et al. 1993](#)).

[Waterston \(1988\)](#) provided an encyclopedic introduction to the biology of *C. elegans* muscle in *The Nematode Caenorhabditis elegans*. We have not attempted to duplicate that material, but rather have tried to build on Waterston's introduction by presenting some of what has been learned in the intervening eight years.

Generated from local HTML

## Chapter 16. Muscle: Structure, Function, and Development — II The Organization, Structure, and Function of Muscle

---

The fundamental repeat unit within muscle that is responsible for contraction is the sarcomere. The sarcomere consists of a bundle of myosin-containing thick filaments flanked and interdigitated with bundles of actin-containing thin filaments ([Fig. 1](#)). The striated appearance of muscle results from the alternation of thick-filament-containing (A-Band) and thin-filament-containing (I-band) regions. The center of each A-band consists of a specialized region (M-line). Unlike vertebrate muscle, nematode striated muscle cells do not fuse to form a multinucleate myotube. Instead, these mononucleate cells adhere tightly to adjacent muscle cells within a quadrant, as well as to the underlying extracellular matrix and [hypodermis](#) ([Francis and Waterston 1985](#), 1991; [Waterston 1988](#); [White 1988](#)). Within the body-wall muscle cell, the myofilament lattice lies just beneath the cell surface and is anchored to the membrane through a series of lateral attachments ([Fig. 2](#)) ([Waterston et al. 1980](#); [Francis and Waterston 1985](#), 1991; [Waterston 1988](#)). At the earliest stage that intact muscle is discernible, individual muscle cells are two "A-bands" wide. By the adult stage, an individual muscle may be as wide as ten A-bands.

For muscle function to have a global effect of moving any part of an animal, there must be anchoring between the filament arrays and skeletal structures. In *C. elegans*, this is accomplished by an intricate series of connections leading from the filament lattices to the exoskeleton (i.e., from muscle to cuticle). The aligned centers of muscle thick filaments (M-line) can be thought of as one end of this series of connections. Thick filaments emanating from the M-line are not directly attached to peripheral cellular structures but are instead "anchored" by their interactions with thin filaments. Thin filaments are in turn anchored at the opposite end by characteristic structures named dense bodies ([Waterston et al. 1980](#)). The dense bodies are finger-shaped structures that project from the sarcolemma (plasma membrane) into the cytoplasm. The dense bodies are functionally analogous to vertebrate Z-lines, one primary role being to maintain the alignment of the thin filaments. A transmembrane complex links the dense bodies to the basement membrane, which is interposed between the muscle cells and the overlying [hypodermis](#) ([Francis and Waterston 1985](#)). Contractile force must still be transmitted through the [hypodermis](#) to the overlying cuticle. Ultrastructural features of the [hypodermis](#) would be expected to reflect this process. The hypodermal face overlying muscle contains hemidesmosomal structures with associated tonofilament arrays that resemble intermediate filaments ([Bartrik et al. 1986](#); [Francis and Waterston 1991](#)). This arrangement of structures in muscle and [hypodermis](#) allows for coordinated contraction and relaxation within a muscle quadrant and for the direct transmission of muscle shortening to the cuticle of the animal.

Sarcomeric units within *C. elegans* body-wall muscle are organized differently from those in vertebrate striated muscle. Rather than being cross-striated as in vertebrate muscle, nematode muscle is obliquely striated ([Rosenbluth 1965](#); [Francis and Waterston 1985](#); [Waterston 1988](#)). The filaments lie parallel to the longitudinal axis of the animal, but adjacent units are offset by approximately 6°. In vertebrate muscle, adjacent units are held in lateral register. Thick and thin filaments in the nematode also differ in length and composition from vertebrate filaments. Whereas both nematode and vertebrate thick filaments contain myosin, nematode thick filaments contain an additional protein, paramyosin. Nematode thick filaments are nearly 10 μm in length and taper in diameter, from 33.4 nm centrally to 14 nm distally ([Mackenzie and Epstein 1980](#); [Epstein et al. 1985](#)). In contrast, vertebrate thick filaments are 1.6 μm in length and 12–14 nm in diameter (for review, see [Harrington 1979](#)). Thin filaments are also longer in nematodes than in vertebrates, being 6 μm in length as compared to 1 μm. Thin filaments are, however, similar in diameter in nematodes and vertebrates and appear to have a similar subunit composition of actin, tropomyosin, and troponins. A final major difference between nematode and vertebrate muscle pertains to the mode of attachment and transmission of tension. The ends of muscle cells contain attachment plaques in both nematodes and vertebrates; in the nematode, however, tension is not primarily transferred by these end attachments, but by a series of lateral attachments directly to the cuticle. As described above, this tension is mediated by the dense bodies and the M-line constituents.

Even with the availability of a large catalog of sarcomere constituents, important aspects of sarcomere assembly and the contractile process are still not understood. For example, the ability of myosin and actin to self-assemble into simple ensembles in vitro has been well-documented (for review, see [Davis 1988](#)), but many open questions remain concerning the more complex process of sarcomere assembly in vivo: How is dimerization regulated? What events lead to higher-order assembly? How is the final length of a filament determined? What cues determine the final positions of muscle filaments within a cell?

## A. Proteins Involved in Thick-filament Assembly and Regulation

The principal components of a nematode thick filament are myosin and paramyosin ([Fig. 1](#)). Twitchin is a less-abundant thick-filament-associated protein. Paramyosin is primarily an  $\alpha$ -helical coiled-coil rod and is composed of two identical subunits. Paramyosin forms the central region of the filament, with myosin molecules assembling around this “core.” Each myosin molecule has two identical heavy chains, each associated with a set of two light chains. Approximately one half of the myosin heavy chain is composed of an  $\alpha$ -helical coiled-coil rod similar to paramyosin; this rod region is responsible for heavy-chain dimer formation and assembly into the filament. The other half of the myosin heavy chain consists of a globular head domain that associates with the two light chains. The head region possesses ATPase activities, actin-binding domains and undergoes conformational changes during muscle contraction and relaxation.

### 1. Myosin Heavy Chains

*C. elegans* expresses four distinct muscle myosin heavy-chain (MHC) isoforms, each encoded by a separate gene (Schachat et al. 1977; Waterston et al. 1982; [Dibb et al. 1989](#)). Pharyngeal muscles contain MHC C and D, whereas MHC A and B are present in all other muscles including both striated and single-sarcomere body muscles ([Epstein et al. 1974](#); Garcea et al. 1978; MacKenzie et al. 1978a; Ardizzi and Epstein 1987). The gene encoding MHC B is designated [unc-54](#), as it was first identified mutationally in Brenner's screen for uncoordinated mutants. Miller et al. (1986) determined the correspondence between the remaining MHC isoforms and three other *C. elegans* MHC genes: [myo-3](#), [myo-2](#), and [myo-1](#) encode MHC A, C, and D, respectively.

Although individual thick filaments in body-wall muscle contain both MHC A and MHC B, these myosins primarily form homodimers rather than heterodimers ([Schachat et al. 1978](#)). The two isoforms are differentially localized within the filament (Miller et al. 1983). In an adult thick filament 10  $\mu\text{m}$  in length, MHC A forms the central 1.8  $\mu\text{m}$ , and the remaining 4  $\mu\text{m}$  at either end is composed predominantly of MHC B.

### The Rod Portion of MHC A and MHC B

The first available MHC sequence for any organism was that of MHC B ([MacLeod et al. 1981](#); [Karn et al. 1983](#)). The rod portion exhibits many features common to known  $\alpha$ -helical coiled-coil domains in which two  $\alpha$ -helices interact along a hydrophobic core ([McLachlan and Karn 1982](#), 1983). The rod has a seven-amino-acid periodicity (abcdefg) with hydrophobic residues at positions a and d. Charge distribution reveals an additional 28-residue periodicity with a biphasic charge structure. This 28-residue motif is repeated approximately 38.5 times, resulting in alternating bands of charge along the length of the rod. This stabilizes dimer-dimer interactions at stagger distances that are odd multiples of 14. Cumulative experimental and modeling data suggest a 98-residue stagger ( $14 \times 7$ ) between MHC rods, which would correspond to a 14.6-nm spacing ([McLachlan and Karn 1982](#)). This is very close to the 14.3-nm period of myosin heads in vertebrates determined using X-ray analysis.

McLachlan and Karn noted that four “skip” residues would be needed in the MHC B rod to maintain the heptad and 28-residue repeats. These additional residues affect the hydrophobic [seam](#) between two  $\alpha$ -helices. Skip residues are conserved in sarcomeric myosins from diverse organisms, although available sequences of nonmuscle myosins do not show regularly spaced skip residues (see [Dibb et al. 1989](#)). A likely possibility is that skip residues could be responsible for constraining rod-rod interactions during formation of highly ordered thick filaments.

Sequence comparisons between the four *C. elegans* myosins show only modest conservation of the rod portions (compared to strong conservation in the head portions) ([Dibb et al. 1989](#)). The rod portions of MHC A and MHC B are more similar to each other than to other isoforms; it has been suggested that this may reflect a functional constraint on rod divergence ([Dibb et al. 1989](#)). One possibility is that similarity between MHC A and B rods might reflect structural features needed to coassemble in regions of the thick filament where these two isoforms overlap.

The bipolar structure of thick filaments requires an antiparallel packing in the middle of the filament, with parallel packing in the two filament arms. The central antiparallel region is named the “bare zone” because this region lacks myosin heads. Antiparallel packing of myosin rods with complete overlap would predict a bare zone of approximately 160 nm, the measured size in several studies (see, e.g., [Craig 1977](#)). This region of the filament is occupied by MHC A (Miller et al. 1983). A direct implication of this observation is that MHC A dimers must be able to pack in an antiparallel manner and thus carry out the nucleating step in filament assembly ([Fig. 3b](#)).

Genetic studies support the idea that MHC A has a special role in filament assembly ([Brenner 1974](#); [Epstein et al. 1974](#); [MacLeod et al. 1977](#); [Waterston 1989](#)). Animals lacking MHC A die as embryos with completely nonfunctional muscles and severely impaired thick-filament assembly ([Waterston 1989](#)). In contrast, mutants lacking MHC B are viable with weakly contractile muscles that progress to near paralysis during later larval stages ([Epstein et al. 1974](#)). Mutants lacking MHC B have thick filaments, some of wild-type length, which consist entirely of MHC A (MacKenzie and Epstein 1980; Epstein et al. 1986). This indicates that MHC A dimers are capable of standard parallel packing, not just the antiparallel packing seen at the center of each filament. Indeed, MHC A appears to be capable of replacing MHC B if expressed at sufficient levels: An increase in *myo-3* (MHC A) gene copy number can rescue movement and thick-filament defects of animals lacking MHC B (Riddle and Brenner 1978; Maruyama et al. 1989). The converse is not true: Overexpression of MHC B cannot rescue mutants lacking MHC A ([Waterston 1989](#); P. Hoppe, pers. comm.).

These genetic observations suggest that unique feature(s) in the structure of MHC A must permit assembly at the M-line. The unique features could involve the capacity for antiparallel packing or interactions with specific M-line constituents. By making a set of DNA constructs encoding MHC A/MHC B chimeras, it has been possible to map two critical regions within the MHC A rod, either of which is sufficient to confer on MHC B the ability to rescue an MHC A null (P. Hoppe and R.H. Waterston, pers. comm.). The regions affecting myosin mutant rescue are a 263-residue segment toward the middle of the rod and a segment of 169 residues near the carboxyl end (the rod has a total length of ~1088 residues). In each of the critical segments, MHC A is more hydrophobic on the outer surface of the myosin dimer. This surface is thought to mediate dimer-dimer interactions for filament assembly; an exciting possibility is that hydrophobicity in this region may allow antiparallel packing of MHC A. Previous modeling has emphasized surface charge distribution along the rod surface in guiding filament assembly ([McLachlan and Karn 1982](#); [Kagawa et al. 1989](#)); these results may indicate additional guidance based on hydrophobicity profile.

## Functional Analysis of the Myosin Head

The sliding filament model ([Huxley and Hanson 1954](#)) provided an eloquent explanation of how sarcomeres and thus muscle could be shortened by sliding thick and thin filaments past one another. The process is ATP-dependent, requires direct interaction of the myosin head and actin, and requires a change in the conformation of the myosin head to transform chemical energy from ATP hydrolysis into mechanical energy of myosin head movement along an actin filament. The recently available crystal structure for the myosin head fragment of chicken skeletal muscle has been a major breakthrough in developing models of actomyosin function (Rayment et al. 1993a,b). The presence of an ATP-binding pocket was expected, as was the proximity of two conserved thiol residues (designated SH1 and SH2) to this pocket. The positions of the catalytic site and actin-binding region on opposite faces of the molecule were unexpected, as was the long narrow cleft that extends from underneath the catalytic site to the actin-binding face. These structural details have suggested that interactions between nucleotide and the active site not only affect the power-stroke determining myosin movement, but can also disrupt myosin-actin binding by opening the long cleft (Rayment et al. 1993b; Rayment and Holden 1994).

In light of recent structural information, it is of interest to consider functional data from mutations in the myosin head. Two broad classes of [\*unc-54\*](#) missense mutations within the head region have been identified.

The first class apparently affects the contraction-relaxation cycle in a manner that increases the duration of tight binding between myosin and actin. This class of mutations was isolated in a screen for intergenic suppressors of specific [\*unc-22\*](#) (twitchin) mutants (Moerman et al. 1982; Dibb et al. 1985). Although some of these suppressor mutations have global effects on motility and muscle structure, they are rare and often subtle; hence, their isolation was facilitated by the power of the reversion screen. Depending on the allele, homozygous mutant animals may exhibit little or no effect on motility, or they may have a slow rigid movement, comparable to a rigor state. Eight alleles of this class have been sequenced ([Table 1](#)) (Dibb et al. 1985; D.G. Moerman et al., unpubl.): Three affect amino acids flanking the myosin ATP-binding site (Walker et al. 1982), two alter amino acids near the conserved SH1 thiol residue (Wells and Yount 1979), two are in the actin-binding region (Mornet et al. 1981; Sutoh 1983), and one allele is a double mutation that may also affect the actin-binding region. Most of these mutations have near-normal muscle structure, but two mutations in the actin-binding region have some disorganization within the A-band (Moerman et al. 1982; D.G. Moerman, unpubl.). All substitutions are at residues conserved between nematode and vertebrate myosin.

This first class of [\*unc-54\*](#) missense mutations should be useful in defining different functional interactions of myosin. For example, the mutations located at the putative myosin-actin interface may permit tighter binding between actin and myosin to occur, whereas mutations near the ATP-binding site may affect ATP interactions with the pocket or consequent effects on the cleft. These mutant myosin forms should be particularly useful for biochemical analysis in combination with in vitro motility systems (for review, see [Cooke 1995](#); [Ruppel et al. 1995](#)), including systems to analyze single myosin molecules (Finer 1994; Ishijima et al. 1994).

The second class of [\*unc-54\*](#) myosin head mutants, identified as dominant-negative mutations, suggests a role for the myosin globular head in filament assembly ([Bejsovec and Anderson 1988, 1990](#)). Heterozygous *unc-54(d)* animals are slow, or paralyzed, and have disrupted thick-filament assembly and organization. Homozygous animals are very sick or inviable, depending on the allele, and accumulate only low levels of MHC B (Bejsovec and Anderson 1988). Since homozygous *unc-54(0)* mutants are paralyzed, not lethal, the *unc-54(d)*-induced lethality cannot be due to low levels of MHC B alone. Bejsovec and Anderson (1990) proposed that the remaining altered MHC B in these mutants acts as a poison for filament assembly. Considering this hypothesis, the location of these mutations came as a surprise: All of these dominant-negative mutations mapped to the head region of myosin (31 mutations spread over 15 different sites; Bejsovec and Anderson 1990), none mapped to the rod portion of the molecule. The mutations are located in two major clusters, one near the ATP-binding site and the other near a weak actin-binding site. There is precedence for the view that the MHC head portion is involved in assembly. ATP and actin have been shown to promote myosin aggregation in vitro (Mahajan et al. 1989), and phosphorylation of regulatory light chains has been shown to regulate assembly of smooth muscle and nonmuscle myosin filaments (Citi and Kendrick-Jones 1987). Although the results of Bejsovec and Anderson suggest a role for the head region in filament assembly, it remains possible that these mutations exert their effect in some other manner, for example, by facilitating turnover of myosin. How the head region of myosin might contribute to filament assembly or stability is not understood, and this constitutes a challenge for the future.

At least one dominant allele of [\*unc-54\*](#) affecting the rod region (*e1152*) has also been identified (Dibb et al. 1985). Unlike the class identified by Bejsovec and Anderson (1988), *e1152* animals accumulate normal amounts of MHC B ([MacLeod et al. 1977](#)). The MHC B in this mutant can form dimers but does not aggregate to properly organized thick filaments. Heterozygous animals are slow, whereas homozygous animals are severely paralyzed. Several other dominant alleles of [\*unc-54\*](#) result in similar heterozygote phenotypes and myosin accumulation patterns, but they have not been sequenced. A number of these alleles are lethal when homozygous.

## 2. Myosin Light Chains

The globular head region of a single MHC has two associated smaller polypeptides important for regulation of MHC activity. These two associated proteins are called the regulatory and essential (or alkali) myosin light chains

(MLCs). Calcium regulation of myosin ATPase occurs through the regulatory MLCs. Two electrophoretically separable bands of 16,000 daltons and 18,000 daltons have been identified that correspond to MLCs (Harris et al. 1977). The larger band represents the regulatory MLCs of which there are two almost identical isoforms (Cummins and Anderson 1988). The two regulatory MLC genes of the nematode, designated [\*mlc-1\*](#) and [\*mlc-2\*](#), are closely linked on the X chromosome, being separated by only 2.6 kb (Cummins and Anderson 1988). To date, one "essential MLC" gene ([\*mlc-3\*](#)) has been identified (S. Sprunger and P. Anderson; C. White and P. Anderson; both pers. comm.).

[\*mlc-1\*](#) and [\*mlc-2\*](#) perform redundant functions within body-wall muscle ([Rushforth et al. 1993](#); A. Rushforth and P. Anderson; C. White and P. Anderson; both pers. comm.); animals that are deleted for either the [\*mlc-1\*](#) or [\*mlc-2\*](#) gene appear to have wild-type body-wall muscle structure and normal movement. However, the double-mutant *mlc-1(0) mlc-2(0)* is paralyzed, muscle is defective, and animals die as L1/L2 larvae. Within the [\*pharynx\*](#), the redundancy appears to be incomplete: *mlc-1(0)* animals exhibit normal pharyngeal function, and *mlc-2(0)* animals often exhibit pumping defects and larval arrest.

### 3. Paramyosin

This protein is a major component of thick filaments in many invertebrates ([Cohen et al. 1970, 1971; Levine et al. 1976](#)). Paramyosin is encoded by a single gene in *C. elegans*, [\*unc-15\*](#) ([Kagawa et al. 1989](#)). Loss-of-function [\*unc-15\*](#) mutants are severely paralyzed and have disorganized body-wall muscle (Waterston et al. 1977). Paramyosin is also present in pharyngeal muscles, but it is apparently not essential in these cells (Waterston et al. 1974). Paramyosin is a major component of the core of thick filaments and as such interacts directly with both MHC A and MHC B (MacKenzie and Epstein 1980). Protein content estimates of late larval thick filaments show a ratio of 4.5 paramyosin:3.1 MHC B:1.0 MHC A (Honda and Epstein 1990). Thick filaments isolated from [\*unc-15\*](#) mutants are fragile and easily shear during isolation (MacKenzie and Epstein 1980), perhaps a clue regarding the *in vivo* role of paramyosin.

*C. elegans* paramyosin consists of 872 amino acid residues, with a structure characteristic of a myosin rod, including features of an  $\alpha$ -helical coiled-coil throughout most of its length ([Kagawa et al. 1989](#); H. Kagawa, pers. comm.). Like the myosin rod, paramyosin has a heptad periodicity (abcdefg)<sub>n</sub> with hydrophobic residues concentrated in the a and d positions and charged residues concentrated in the remaining positions. Paramyosin also has a 28-residue meta-repeat of alternating charge. Paramyosin and myosin also share skip residues in the same positions, although paramyosin has an additional skip residue between the positions of skip residues 3 and 4 of myosin.

While the myosin rod and paramyosin have an overall 40% sequence similarity, paramyosin has more hydrophobic residues and fewer glycine residues than do myosin rods. The increased hydrophobicity is consistent with the localization of paramyosin within the filament. Fewer glycine residues, as well as intradimer salt bridges, may lead to a paramyosin rod that is more rigid than the corresponding region of myosin ([Cohen et al. 1987; Kagawa et al. 1989](#)). This is perhaps required for a core structure within the thick filament. The carboxyl terminus of paramyosin is similar to the carboxyl termini of MHC A and B, but paramyosin has a unique 29-residue hydrophobic amino portion. This region contains seven serine residues; two of which are known to be phosphorylation targets in the nematode ([Schriefer and Waterston 1989](#)). In several systems, the phosphorylation of myosin can regulate filament assembly or enzymatic activity. Although there is no direct evidence as to the function of paramyosin phosphorylation, it is intriguing that only free (nonfilament-associated) paramyosin is phosphorylated (Dey et al. 1992). This suggests that phosphorylation of paramyosin could regulate its assembly *in vivo*.

### Assembly of Paramyosin

The presence of alternating zones of negative and positive charges along the outer surface of a paramyosin coiled-coil helix suggests that, like myosin, paramyosin assembly may be largely mediated by intermolecular ionic interactions ([McLachlan and Karn 1982; Kagawa et al. 1989](#)). An intriguing picture of thick-filament structure has come from "best fit" estimates of molecular packing based on these interactions. As more data become

available, it will be interesting to see this picture confirmed and/or modified. In particular, nonionic interactions could also affect molecular packing within the thick filament (e.g., paramyosin shares the hydrophobicity profile for the coat position residues implicated in antiparallel MHC A packing; P. Hoppe and R.H. Waterston, pers. comm.).

Unlike myosin rods, which have maximal interactions at a parallel stagger of 98 residues, paramyosin rods appear to interact optimally at parallel staggers of 493 residues (an overlap region of 330 residues) ([Kagawa et al. 1989](#)). This is an axial displacement of approximately 720 Å (nematode paramyosin is ~1211 Å in length) and is in good agreement with observations on paramyosin paracrystals ([Fig. 3a](#)) (Cohen et al. 1971; Waterston et al. 1974). To form and extend thick filaments *in vivo*, parallel paramyosin must interact with myosin rods. Models for this interaction based on charge distributions suggest an alignment with the myosin head almost contacting the amino terminus of paramyosin ([Fig. 3d](#)) ([Kagawa et al. 1989](#)).

Paramyosin might also be expected to pack in an antiparallel manner in the central zone of each filament. The existence of such "antiparallel" paramyosin is still under debate. [Ardizzi and Epstein \(1987\)](#) and Epstein et al. (1993) did not see labeling in the central zone with antibodies to paramyosin; this could reflect absence of paramyosin from the region or inaccessibility of epitopes. Charge distribution analysis suggests that antiparallel-packed paramyosin would be most stable with a stagger of 358 residues ([Fig. 3c](#)) ([Kagawa et al. 1989](#)).

A large-scale criterion can be used to assess the filament packing models above. It is believed that paramyosin acts as a template upon which the myosin is assembled ([Kagawa et al. 1989](#) and references therein). For this to occur, interactions between these molecules should allow adjacent packing with minimal requirement for gaps or bending. This higher-order constraint is well satisfied by the filament packing models described above ([Fig. 3d](#)).

Much of the above modeling is supported by analysis of mutations in [unc-15](#) ([Gengyo-Ando and Kagawa 1991](#)). Mutants lacking paramyosin have aggregated deposits of myosin but do not form structures resembling native thick filaments (Waterston et al. 1977). Missense alleles of paramyosin have disorganized muscle; under polarized light, large birefringent needle-shaped paramyosin aggregates can be observed within the muscle cells. These animals can be either weakly (e.g., *e1215*) or severely (e.g., *e73*) uncoordinated. *e73* is semidominant and has been used to isolate both intergenic and intragenic suppressor mutants (Riddle and Brenner 1978; Brown and Riddle 1985). *e73* results in a charge reversal in the middle portion of the molecule (D-342 to K). Three other missense alterations, *su228* (R-837 to C), *e1215* (Q-809 to R), and *e1402* (L-799 to F), are restricted to a small, unusually hydrophilic region near the carboxyl terminus.

The charge-based model for parallel paramyosin assembly described above would place the *e73* site opposite the region where the other three mutations are located (see [Fig. 4](#)). Further support of this model comes from the analysis of the intragenic revertants of *e73* (Brown and Riddle 1985; [Gengyo-Ando and Kagawa 1991](#)). Three revertant changes were sequenced: *m193* (E-586 to K) results in limited restoration of movement, whereas *m208* (R-826 to K) and *m209* (E-835 to K) allow more effective restoration of movement. When superimposed on the parallel assembly model described above, the latter two revertants contact the *e73* region. The *e73* and *m209* sites are directly opposite each other ([Fig. 4](#)). Gengyo-Ando and Kagawa (1991) propose that *e73* may promote abnormal paramyosin aggregate (paracrystal) formation by increasing the self-affinity of the molecule. *m209* could decrease this affinity by restoring the charge repulsion at this position.

The model of parallel paramyosin assembly was based on one-dimensional considerations of the ionic interactions between structures ([McLachlan and Karn 1982](#); [Kagawa et al. 1989](#)). As noted by Gengyo-Ando and Kagawa (1991), the situation is clearly more complex *in vivo*. The single charge reversals caused by paramyosin missense mutations do not significantly alter the calculated interaction scores, yet they dramatically affect assembly. Perhaps the mutations pinpoint regions of the molecule crucial for the initial steps of parallel paramyosin assembly. Just how complex the dynamic interactions between paramyosin self-association and paramyosin-myosin association are *in vivo* is illustrated by interactions between *e73* and its intergenic suppressor [myo-3](#) /*sup-3*. (Riddle and Brenner 1978; Brown and Riddle 1985; Maruyama et al. 1989). Motility can be partially restored to *e73* animals by increasing MHC A levels (Maruyama et al. 1989). How increasing myosin counters paramyosin self-assembly is not understood, but this *in vivo* result should give pause to those who rely

solely on in vitro reconstruction experiments to determine essential components in complex molecular assemblages.

### Paramyosin and the Thick-filament Core Structure

In experiments initially designed to map the relative positions of MHC A and B within a thick filament, [Epstein et al. \(1985\)](#) found a new substructure within the filament which they have called the "core." Successively higher salt concentrations (0.1 M to 0.75 M) applied to purified thick filaments will gradually solubilize the filaments, progressing from the ends toward the center. Using antibodies to mark the myosins, it was shown that, first MHC B was solubilized, and then MHC A, finally leaving an insoluble region with MHC A, a result that confirmed the differential distribution of these two myosin isoforms within the filament. When this minifilament was examined using electron microscopy, a "core structure" 15 nm in diameter was observed extending beyond the MHC A region of the filament.

New methods have allowed analysis of the filament core in more detail ([Fig. 5a](#)) (Epstein et al. 1988; [Deitiker and Epstein 1993](#)). Although some paramyosin is solubilized along with myosin in the above treatments, 30% of paramyosin remains with the core. Thus, paramyosin is a major component of core fractions ([Deitiker and Epstein 1993](#)). Paramyosin-rich core structures have also been identified in other invertebrates (e.g., *Limulus*; Levine et al. 1982). In *C. elegans*, minor protein constituents associated with the core have been identified ([Deitiker and Epstein 1993](#)), and a model for the nematode core structure has been proposed ([Fig. 5b,c,d,e](#)) (Epstein et al. 1995).

## 4. The Twitchin Protein Superfamily

The identification of the thick-filament protein twitchin in the nematode marked the first occurrence of a new muscle component being discovered through genetic analysis. Mutants in the *unc-22* gene ([Brenner 1974](#)) exhibit disorganized muscle sarcomeres and constant "twitch" of body muscles (Moerman and Baillie 1979; [Waterston et al. 1980](#)). The twitching phenotype suggests a role in regulating the actomyosin contraction-relaxation cycle. Early support for this hypothesis came from genetic reversion studies and immunofluorescence: (1) Rare missense alleles located in the head region of MHC B can suppress *unc-22*-induced twitching (Moerman et al. 1982) and (2) twitchin colocalizes with MHC B in muscle A-bands ([Moerman et al. 1988](#)).

Sequencing of *unc-22* revealed a large protein (6839 amino acids) with a single protein kinase domain near the carboxyl terminus, multiple copies of a fibronectin type-III-like domain (motif I, 31 copies), and an immunoglobulin superfamily C2-like domain (motif II, 30 copies) ([Benian et al. 1989, 1993](#)). Each motif is approximately 90–100 amino acids in length, and these motifs are arranged in a I-I-II pattern (and rarely as I-I-I-II) throughout most of the protein. Several additional motif II repeats are present at the amino and carboxyl termini ([Fig. 6](#)).

The discovery of an intracellular protein with fibronectin and immunoglobulin motifs was initially surprising, since previously described motifs of these types were all in extracellular proteins or domains. There are now several members of this protein family, including a set of vertebrate muscle components (titin/connectin [[Labeit et al. 1990; Labeit and Kolmerer 1995](#)], myosin light-chain kinase [[Olson et al. 1990; Shoemaker et al. 1990](#)], C protein [[Einheber and Fischman 1990](#)], 86-kD protein [[Fischman et al. 1991](#)], telokin [[Gallagher and Herring 1991; Collinge et al. 1992](#)], skelemin [[Price and Gomer 1993](#)], and M protein [[Noguchi et al. 1992](#)]) and several invertebrate variants of twitchin (the *Drosophila* twitchin homolog, projectin [Ayme-Southgate et al. 1991; Fyrberg et al. 1992] and a set of arthropod, annelid, and mollusc muscle components called "mini-titins" [Nave and Weber 1990; Lakey et al. 1990; Vibert et al. 1993; Probst et al. 1994; for review, see Ziegler 1994]). Titin, C protein, and twitchin have all been shown to associate with myosin (Labeit et al. 1992; Okagaki et al. 1993; cited in [Deitiker and Epstein 1993](#)). A possible unifying theme for members of this family might thus be association with myosin.

Although there are likely to be structural and other similarities, there is no reason *a priori* to assume that protein family members have identical functions. Despite similar structural motifs in titin and twitchin (immunoglobulin

and fibronectin domain repeats, and a serine/threonine protein kinase near the carboxyl end), their distribution and proposed functions are different. Titin, at 3000 kD, is the largest member of this muscle protein family; at approximately 1 μm in length, it can extend over half a vertebrate sarcomere, from M-line to Z-line (Wang et al. 1984; Furst et al. 1988). Two distinct functions for titin have been proposed on the basis of distribution within the sarcomere. Association of titin with thick filaments has led to the suggestion that it acts as a template or "protein ruler" for thick-filament assembly (Whiting et al. 1989; Trinick 1994; [Labeit and Kolmerer 1995](#)). The extension of titin across the I-band from the ends of thick filaments to the Z-line and its elastic nature suggested that it might be responsible for the passive elasticity of muscle (Maruyama et al. 1976 1977; Horowitz et al. 1986, 1989; for review, see Trinick 1994; Ziegler 1994; also see [Labeit and Kolmerer 1995](#)).

The phenotype of [unc-22](#) mutants, the localization of the protein product to the A-band region of the sarcomere, and the presence of a kinase domain within the protein have led to the suggestion that twitchin is involved in the regulation of muscle contraction ([Brenner 1974](#); [Moerman et al. 1988](#); [Benian et al. 1989](#)). Genetic studies on [unc-22](#) mutants demonstrate that twitchin does not function as a protein ruler to regulate thick-filament length. Lack of twitchin does not directly inhibit filament assembly, rather the constant twitching of the muscle cell destroys previously assembled filament integrity. Young animals have near-normal muscle structure, but this structure gets progressively more disorganized with increasing age (D.G. Moerman, unpubl.). Whereas lack of twitchin in a wild-type background leads to a phenotype of twitching and disorganized muscle, lack of twitchin in an [unc-54\(s75\)](#) background leads to relatively normal movement and muscle (Moerman et al. 1982; also see section on myosin head mutants). By altering the crossbridge cycle of myosin-actin interactions, one releases the animal from any requirement for twitchin. This would not be the expected result if twitchin were acting as a protein ruler determining thick-filament length and stability; this result is instead compatible with twitchin having a role in regulating contraction.

*Drosophila* projectin offers an instructive example of isoform diversity. Projectin in asynchronous indirect flight muscle is limited to the I-band region, whereas projectin in synchronous muscles is associated with the A-band region ([Vigoreaux et al. 1991](#)). Projectin isoforms vary in size but are the products of a single gene (Ayme-Southgate et al. 1991). The localization of different isoforms of projectin to different subcompartments of a sarcomere in different muscle types suggests that this protein may have multiple functions. *Drosophila* indirect flight muscles are stretch-activated; thus, the role of projectin in these muscles may be analogous to the elasticity function proposed for titin in vertebrate muscle. Conversely, the location of projectin to muscle A-bands in synchronous muscles has led to the suggestion that, similar to twitchin, it may be involved in the regulation of contraction (Ayme-Southgate et al. 1995).

Studies on the kinase domain of nematode twitchin have shed light on protein kinase structure and autoregulation in general. The kinase domain of twitchin has activity in vitro, with myosin light-chain peptides the preferred substrates ([Lei et al. 1994](#)). Similar to other myosin light-chain kinases, twitchin undergoes autophosphorylation: Thr-5910, a site just upstream of the catalytic core (residues 5940–6197) is the primary target ([Lei et al. 1994](#)). In addition, twitchin contains an autoinhibitory site just carboxy-terminal to the catalytic core which can bind to the catalytic site and inhibit its function (Hu et al. 1994; [Lei et al. 1994](#)). X-ray crystallographic studies of twitchin's kinase demonstrate the steric mechanism of this autoinhibition. The inhibitory fragment does not simply act as a "pseudosubstrate" but actually "mirrors" the active site making contacts with residues (Hu et al. 1994).

Whether myosin light chains are the normal phosphorylation target in vivo for twitchin is unknown (J. Heierhorst et al., in prep.). Since nematode muscle has both myosin-based and thin-filament-based calcium regulatory systems (Lehman and Szent-Gyorgyi 1975; Harris et al. 1977), a role for twitchin as part of a myosin-based regulatory system would be plausible. Recent results obtained in studies on *Aplysia californica* add strong circumstantial support to this suggestion. Experiments designed to identify proteins mediating muscle relaxation induced by neuropeptide cotransmitters (cardioactive peptides and myomodulins) identified a 750-kD phosphoprotein as a major substrate in this pathway (Probst et al. 1994). This protein is the *Aplysia* twitchin homolog; its level of phosphorylation was directly related to the change in muscle relaxation rate (Heierhorst et al. 1994; Probst et al. 1994). These physiological studies in *Aplysia*, when combined with genetic and molecular

studies from *C. elegans*, make a strong case for a dynamic role for twitchin in control of the actomyosin contraction-relaxation cycle.

Recent studies of the [\*unc-89\*](#) gene provide a genetic handle on other functions for the twitchin/titin superfamily. [\*unc-89\*](#) mutations affect the M-line at the center of the bare zone, the region of bipolar thick filaments free of myosin heads. The function of the M-line may be to maintain thick filaments in proper register. Examination of [\*unc-89\*](#) mutant body-wall muscle reveals a normal thick-filament number, but improper alignment of thick filaments; in addition, there is no M-line matrix ([Waterston et al. 1980](#)). [\*unc-89\*](#) mutants move well but are thinner and more transparent than wild-type animals. UNC-89 is a 732-kD member of the twitchin/titin intracellular immunoglobulin superfamily (Benian et al. 1996). The protein consists from amino to carboxyl end of a complex series of domains, including SH3, CDC24, and PH; seven immunoglobulin domains; a KSP-containing multiphosphorylation domain; and finally 46 immunoglobulin domains in tandem. The region of similarity to CDC24 suggests that UNC-89 may be coupled to a G-protein-mediated signal transduction pathway. UNC-89 has been localized to the middle of muscle A-bands and may be specifically associated with the M-line (Benian et al. 1996). In vertebrates, five nonmyosin proteins have been localized to the M-line: creatine kinase (Strehler et al. 1983), myomesin ([Vinkemeier et al. 1993](#)), skelemin ([Price and Gomer 1993](#)), M protein ([Noguchi et al. 1992](#)), and the carboxyl terminus of titin ([Gautel et al. 1993](#)). As with UNC-89, the latter four proteins are members of the twitchin family.

## B. Components of Thin Filaments

*C. elegans* thin filaments share many of the components of vertebrate thin filaments, including actins, tropomyosin, and troponins ([Files et al. 1983](#); [Krause et al. 1989](#); [Myers et al. 1996](#); H. Kagawa et al., in prep.). Mutations affecting several of these thin-filament components have been identified and characterized.

### 1. Actins

One of the most conserved proteins phylogenetically, actin forms the core component of thin filaments and binds and activates myosin. *C. elegans* has four known muscle actin genes ([Files et al. 1983](#); [Albertson 1985](#); [Waterston et al. 1984](#); [Landel et al. 1984](#); [Avery 1993a](#); [Stone and Shaw 1993](#)), encoding nearly identical proteins ([Krause et al. 1989](#)). These are typical invertebrate actins in that they resemble the sequence of vertebrate cytoplasmic actins, not vertebrate muscle actins (Vandekerckhove and Weber 1978). A candidate for cytoplasmic actin, [\*act-5\*](#), has been recently identified in *C. elegans* (L. Schriefer and R.H. Waterston; J. Waddle and R.H. Waterston; both pers. comm.). This actin is somewhat divergent from the previously identified actins, and, unlike these other actins, it is expressed in the intestine.

The study of *C. elegans* actin genes offers an instructive example of in vivo genetic analysis of a multigene family. Actin mutants were first identified as semidominant slow to paralyzed animals designated [\*unc-92\*](#). Genetic mapping and reversion analysis suggested that these might be actin mutations ([Landel et al. 1984](#); [Waterston et al. 1984](#)). These mutants have disorganized body-wall muscle and aggregates of thin filaments at the ends of muscle cells (Waterston, et al. 1984). Pharyngeal muscle is also disrupted. These early results suggested the possibility that the dominant mutations might be missense alleles of individual actin genes and that the frequent reversion could result from second-site loss-of-function mutations inactivating the aberrant gene. Molecular studies have confirmed these hypotheses ([Landel et al. 1984](#); L.A. Schriefer and R.H. Waterston, pers. comm.). The crystal structure of actin is known (Holmes et al. 1990; Kabsch et al. 1990), and the sequencing of dominant alleles reveals that several are amino acid substitutions located on an interactive actin face or near the ATP-binding pocket (L.A. Schriefer and R.H. Waterston, pers. comm.) The implication is that these alterations disrupt actin-actin interactions during filament assembly. Some of the revertants analyzed have insertions or deletions in [\*act-1\*](#) or [\*act-3\*](#), indicating that elimination of a particular actin isoform, not the repair of the lesion, is the mode of phenotypic reversion ([Landel et al. 1984](#)). This type of revertant is possible presumably because multiple actin genes are expressed in these muscle tissues and the level of actin required in these muscles is less than that produced when either [\*act-1\*](#) or [\*act-3\*](#) are deleted (no data yet for [\*act-4\*](#)).

## 2. The Troponin-Tropomyosin Complex

This complex regulates the calcium-sensitive interaction of actin with myosin. Genes for nematode tropomyosin, troponin C (TnC), and troponin T (TnT), have all been cloned and sequenced, and mutations have been identified ([Myers et al. 1996](#); H. Kagawa and B. Williams, pers. comm.; H. Kagawa et al., in prep.). Tropomyosin and TnC are encoded by the [lev-11](#) and [pat-10](#) genes, respectively ([Williams and Waterston 1994](#); H. Kagawa and B. Williams, pers. comm.); TnT is encoded by [mup-2](#) ([Myers et al. 1996](#)). There is evidence that multiple tropomyosin isoforms are encoded by a single-copy gene with alternative splicing (H. Kagawa et al., in prep.), but the situation is not yet clear for TnC and TnT, which may have other family members.

Loss-of-function mutations in [lev-11](#), [pat-10](#), or [mup-2](#) lead to late embryonic lethality. Interestingly, none of these genes affect early assembly of the sarcomere; all act after muscle contraction has begun ([Williams and Waterston 1994](#); [Myers et al. 1996](#)). Mutations in [lev-11](#) or [pat-10](#) result in an identical phenotype of severe paralysis from the earliest stages of development, whereas [mup-2](#) mutants are capable of muscle contraction and continue morphogenesis until the threefold stage. The primary defect noted in [mup-2](#) animals is a displacement of the dorsal muscle quadrants, particularly at the bends in the embryo. This displacement appears to be due to a loss of muscle attachment to the underlying matrix, since most [mup-2](#) animals at the twofold stage have properly organized and attached muscle quadrants.

The isolation of a temperature-sensitive (ts) allele for [mup-2](#) has permitted analysis of TnT function in later stages of muscle activity ([Myers et al. 1996](#)). This [mup-2](#) mutation allows growth but causes a contraction phenotype: The animals tremble in liquid medium with poor coordination between muscle cells along the animal's length ([Myers et al. 1996](#)). This phenotype is reminiscent of [unc-22](#) mutants and some non-null alleles of [lev-11](#) and [unc-54](#) ([Brenner 1974](#); Lewis et al. 1980a; Dibb et al. 1985). It is intriguing that similar phenotypes can arise from defective components of thick filaments ([unc-22](#) twitchin, [unc-54](#) myosin) or thin filaments ([lev-11](#) tropomyosin, [mup-2](#) troponin). The trembling/twitching phenotypes suggest regulatory defects in the muscle contractile cycle. Nematode muscles use both thick- and thin-filament-based calcium regulatory systems in controlling contraction (Harris et al. 1977). Analysis of mutations that perturb regulation in just one of the two filament types may illuminate the nature and purpose of this dual regulation.

A second phenotype of [mup-2](#) (ts) mutants grown at a restrictive temperature is that they are sterile ([Myers et al. 1996](#)). Sterility appears to result from lack of fertilization of the oocytes; the oviduct of these animals is enlarged and full of oocytes, but these oocytes fail to pass through the spermatheca. Oocyte movement along the oviduct and through the spermatheca is dependent on the myoepithelial sheath, a contractile structure (Hirsh et al. 1976) containing actin (Strome 1986b), myosin (Ardizzi and Epstein 1987), and attachment structures (e.g., perlecan; G. Mullen and D.G. Moerman, unpubl.). Comparative video recordings show that [mup-2](#) mutants are severely deficient in oviduct contractile function ([Myers et al. 1996](#)).

## 3. Other Thin-filament-associated Proteins

Two genes recently cloned and sequenced which have roles in thin-filament stability and function, [unc-60](#) and [unc-87](#), take us beyond the more familiar constituents of sarcomere thin filaments. Depending on the allele, [unc-60](#) mutant animals exhibit a limp paralysis, slow movement, or lethality ([Waterston et al. 1980](#); [McKim et al. 1994](#)). Large aggregates of thin filaments are observed at the ends of cells in all viable alleles examined ([Waterston et al. 1980](#)). [unc-60](#) is a complex locus encoding two transcripts that share an initiator methionine but have separate subsequent exons ([McKim et al. 1994](#)). The two encoded proteins are 165 and 153 amino acids in length, with 38% identity and show similarity to the cofilin/destrin family of actin-binding proteins, a group known to depolymerize actin (Yonezawa et al. 1985; Nishida et al. 1987; Abe et al. 1989, 1990; Moriyama et al. 1990). Whether UNC-60 has a function similar to these proteins is unknown, but the [unc-60](#) mutant phenotype of actin aggregates is consistent with this protein having a regulatory role in filament assembly. McKim et al. (1994) proposed that UNC-60 may have a function similar to actophorin in *Acanthamoeba castellani*, where actophorin acts in conjunction with  $\alpha$ -actinin to promote bundling of actin filaments in vitro (Maciver et al. 1991). In the absence of actophorin, *Acanthamoeba* actin filaments continue to grow and cannot be bundled by  $\alpha$ -actinin.

The single lethal allele, *unc-60(s1586)*, is a small deletion interrupting both open reading frames (ORFs) ([McKim et al. 1994](#)). Therefore, it may be that mutations affecting only one transcript give rise to the Unc class of alleles. It will be interesting to learn if these mutations are limited to one ORF or whether both are targets. The *s1586*-bearing animals arrest development at mid-larval stages, which is surprising given that thin-filament regulatory proteins (e.g., tropomyosin) lead to late embryonic lethality, as does the absence of other key sarcomere constituents (see below). Perhaps [\*unc-60\*](#) is a member of a functionally redundant gene family.

Mutations in [\*unc-87\*](#) result in a severe larval paralysis, whereas adults are somewhat less affected (they exhibit a limp paralysis). [\*unc-87\*](#) animals have disorganized body-wall muscle with collections of both thick and thin filaments. As with [\*unc-60\*](#) mutants, small clumps of thin filaments are visible at the ends of cells ([Waterston et al. 1980](#); Goetinck and Waterston 1994a). The [\*unc-87\*](#) gene has recently been sequenced and was found to encode a 357-amino-acid 40-kD protein with a portion showing sequence similarity to the actin-binding domain of vertebrate calponins (Goetinck and Waterston 1994b). Calponins were first identified in vertebrate smooth muscle as binding to F-actin, Ca<sup>++</sup>/calmodulin, and tropomyosin (Takahashi et al. 1986; Vancompernolle et al. 1990). Although their role in smooth muscle is not fully understood, one suggestion is that calponins form part of the thin-filament regulatory system (Abe et al. 1990; Winder and Walsh 1990). It is not clear whether UNC-87 has a regulatory role in muscle. In particular, it lacks homology with the calponin regions identified as tropomyosin- or calmodulin-binding sites (Vancompernolle et al. 1990; Mezqueldi et al. 1992; Goetinck and Waterston 1994b). However, it is clear that UNC-87 is closely associated with the thin filaments. In wild-type and tropomyosin mutant ([\*lev-11\*](#)) animals, UNC-87 is found in muscle I-bands, and in [\*act-3\*](#) mutants, UNC-87 colocalizes with the misplaced thin filaments (Goetinck and Waterston 1994b).

Since muscle contraction appears to exacerbate the [\*unc-87\*](#) phenotype, [Goetinck and Waterston \(1994a\)](#) speculated that retarding muscle contraction might alleviate the muscle disorder in these mutants. Indeed, [\*unc-54\*](#) missense alleles that retard the contraction/relaxation cycle can partially suppress [\*unc-87\*](#) disorders. Although the role of UNC-87 in muscle is unknown, it appears that this protein is not involved in the early stages of sarcomere assembly, since threefold-stage embryos have wild-type muscle which then becomes progressively more disorganized as the animals grow. On the basis of its structure, localization, and interaction with other muscle-affecting genes, [Goetinck and Waterston \(1994a\)](#) suggested that UNC-87 serves as a structural component to maintain lattice integrity during contraction.

## C. Building a Sarcomere

A description of some of the important steps in sarcomere assembly has accumulated from analysis of wild-type embryos using antibodies to the various sarcomere constituents ([Epstein et al. 1993](#); [Hresko et al. 1994](#); [Moerman et al. 1996](#)) and from careful analysis of mutants affecting each of these structural components ([Waterston 1989](#); [Venolia and Waterston 1990](#); [Barstead and Waterston 1991a](#); [Rogalski et al. 1993](#); [Williams and Waterston 1994](#); [Gettner et al. 1995](#)). The emerging view is similar in many respects to that held for vertebrate myofibril assembly (for review, see Epstein and Fischman 1991; Epstein and Bernstein 1992). Two similarities are particularly striking: the compartmental nature of the assembly process, and the importance of the membrane or membrane-associated components in initiating assembly.

In *C. elegans*, the compartmental nature of myofilament assembly can be deduced from examining muscle mutants. Most mutants exhibit either an A-band- or I-band-specific disruption; the reciprocal part of the sarcomere is reasonably intact, properly attached, and oriented appropriately ([Waterston et al. 1980](#); [Zengel and Epstein 1980](#); [Waterston 1989](#); [Barstead and Waterston 1991a](#)). Similar results have been observed in *Drosophila* in the analysis of actin and myosin mutants ([Beall et al. 1989](#)), and in cultured cardiac myocytes: I-Z-I-like (actin/α-actinin/titin/ troponin) complexes and MHC (myosin heavy chain) fibrils can assemble independently of one another ([Lu et al. 1992](#)). These observations from several disparate systems support the notion that during sarcomere assembly, A-bands and I-bands assemble independently, perhaps as M+A and db+I units (where M = M-line components and db = dense body components).

In *C. elegans*, the earliest stage that muscle structural proteins can be detected in embryos is 290 minutes after the first cleavage ([Fig. 7](#)) ([Epstein et al. 1993](#); [Hresko et al. 1994](#); [Moerman et al. 1996](#)). Muscle cells are just commencing migration from their initial lateral positions, and muscle components are diffusely distributed within the cells. Muscle cells that will eventually form dorsal and ventral quadrants are arranged as a single sheet of cells at this stage. Some of these muscle cells will divide again before assuming their final position within a muscle quadrant. By 350 minutes, myofilament components localize to membranes where muscle cells contact each other and the underlying [hypodermis](#) (referred to as muscle cell polarization in Hresko et al. [1994]). At this stage, muscle cells are arranged into quadrants adjacent to ventral or [dorsal hypodermis](#). By 420 minutes, the muscle cells have flattened and broadened ([Hresko et al. 1994](#)), and by 450 minutes, fully formed sarcomeres and attachment complexes can be observed. At 450 minutes, a muscle quadrant consists of a double row of spindle-shaped cells with four A-bands across each quadrant (two per cell; [Fig. 8](#)). It is at this time that the first muscle-generated movements of the embryo are detected ([Fig. 9](#)).

## 1. Genes Necessary for Early Sarcomere Organization

Two broad phenotypic classes of lethal mutations affecting early muscle have been described in *C. elegans*, the Mup class ([muscle positioning](#); [Hedgecock et al. 1987](#); [Goh and Bogaert 1991](#)), and the Pat class ([paralyzed and arrested elongation at twofold](#); [Williams and Waterston 1994](#)). These mutants are primarily embryonic or early larval lethals. The gene and product for some of these mutants are known; these are either components of the attachment complex (i.e., dense body and M-line: [deb-1](#) -vinculin, [Barstead and Waterston 1991a](#); [pat-3](#) - $\beta$ -integrin, [Gettner et al. 1995](#); [pat-2](#) - $\alpha$ -integrin, [Williams and Waterston 1994](#) and pers. comm.; [unc-52](#) -perlecan, [Rogalski et al. 1993](#)) or essential components within the sarcomere ([myo-3](#) -MHC A, [Waterston 1989](#); [lev-11](#) -tropomyosin, [Williams and Waterston 1994](#) and pers. comm., [Kagawa 1995](#) and pers. comm.; [mup-2](#) -troponin T, [Myers et al. 1996](#); [pat-10](#) -troponin C, B. Williams and H. Kagawa, pers. comm.). Several other Pat mutants have yet to be characterized on a molecular level ([Williams and Waterston 1994](#); K. Norman and D.G. Moerman, unpubl.).

The Pat phenotype offers a ready and efficient screen for mutants with disruptions in sarcomere assembly and organization, since animals arrested at the twofold stage of elongation are quite easy to identify. Elongation is the process whereby the embryo changes from a ball of cells to a worm. A hypodermal role in elongation had been described ([Sulston et al. 1983](#); [Priess and Hirsh 1986](#)). The demonstration that [myo-3](#) mutants arrested at the twofold stage of embryogenesis was the first indication that intact functional muscle is necessary to facilitate elongation of the embryo ([Waterston 1989](#)). Mutations in [myo-3](#) do not affect the early stages of elongation. [myo-3](#) mutants appear to develop normally until the 1.5-fold stage, when contraction would normally begin. These animals fail to initiate muscle contractions; the paralyzed animals cease elongation shortly thereafter (twofold stage; see [Fig. 9](#)). Pharyngeal morphogenesis continues in these animals and they hatch as inviable larvae.

That the Pat phenotype might be a common feature of mutations affecting early events in myofilament assembly was suggested by the results of [Barstead and Waterston \(1991a\)](#), who demonstrated that mutants lacking vinculin ([deb-1](#)) also have a Pat terminal phenotype. Lethal alleles of [unc-45](#), a gene involved in thick-filament assembly ([Epstein and Thomson 1974](#); [Waterston 1988](#)), also die as twofold-arrested and paralyzed animals ([Venolia and Waterston 1990](#)). Williams and Waterston (1994) carried out a screen designed to sample the whole genome for recessive-lethal mutations leading to the Pat phenotype. They identified ten novel genes and also obtained lethal "Pat" alleles of three genes previously identified only by non-null viable alleles ([unc-52](#), [unc-112](#), and [lev-11](#)). Although the screen has not yet been carried out to saturation, this new array of mutants has proven invaluable for deducing several of the essential events in myofilament formation.

## 2. Sarcomere Assembly and the Membrane

A physical linkage between the myofibril array and the membrane is critical in allowing myofilament contraction to move the animal. This linkage is provided by the dense body structure (see [Fig. 1](#)). Major intracellular constituents of this structure in *C. elegans* include  $\alpha$ -actinin, found throughout the dense body ([Francis and](#)

[Waterston 1985](#); Barstead et al. 1991b), and vinculin and talin, which are found nearer the sarcolemma (Barstead and [Waterston 1989](#); Moulder et al. 1996). A transmembrane complex containing  $\beta$ -1 and  $\alpha$ -integrin components anchors the myofilament lattice (Gettner et al. 1995; B. Williams, pers. comm.). Perlecan is a basement membrane component associated with the extracellular surface of these anchoring regions (Francis and Waterston. 1991; Rogalski et al. 1993).

The nematode dense body structure is similar in many respects to the vertebrate focal adhesion site ([Burridge et al. 1988](#)). Vertebrate models of myofibrillar assembly emphasize the importance of submembranous adhesion plaques as assembly points for myofibrillar components (for review, see Epstein and Fischman 1991). In cultured cardiac myocytes, myofibrillar components are found adjacent to the sarcolemma, and myofibril formation occurs at the plasma membrane (Dlugosz et al. 1984; Schultheiss et al. 1990). There is now direct evidence from studies in *C. elegans* and *Drosophila* demonstrating the essential role of membrane-associated proteins as nucleation sites for myofibril assembly.  $\beta$ -integrin is the transmembrane anchor at the base of dense bodies and M-lines in the nematode ([Francis and Waterston 1985](#); Gettner et al. 1995). Mutations in the structural gene for  $\beta$ -integrin, *pat-3*, lead to a twofold arrest, and myosin and actin are not organized into sarcomeres in muscle cells ([Williams and Waterston 1994](#)). These observations on *pat-3* mutants suggest that although this  $\beta$ -integrin is not necessary for muscle cell migration or the formation of muscle quadrants, it is essential for assembling the myofilament lattice within individual muscle cells in the nematode. Similar results have been obtained in *Drosophila* with the *lethal(1) myospheroid* locus which encodes a  $\beta$ -integrin subunit (Wright 1960; Newman and Wright 1981; MacKrell et al. 1988; Volk et al. 1990).

Components of muscle-associated basement membranes are also important contributors to myofibril assembly and organization and may act as anchors for the transmembrane integrin complex. For example, mutations in type IV collagen ([let-2](#) and [emb-9](#)), or perlecan ([unc-52](#)), or overexpression of SPARC/osteonectin all lead to alterations in muscle during embryogenesis and thus result in a lethal phenotype (Guo et al. 1991; Sibley et al. 1993; Rogalski et al. 1993, 1995; Schwarzbauer and Spencer 1993; [Williams and Waterston 1994](#); for review, see Kramer 1994b and this [volume](#)). Particularly striking is the similarity in the null phenotypes for [unc-52](#) and [pat-3](#) (Rogalski et al. 1993; [Williams and Waterston 1994](#)). Similar to *pat-3* mutants, [unc-52](#) Pat mutants fail to assemble a myofilament lattice, although all of the appropriate muscle constituents are present ([Fig. 10](#)); this appears to be the null phenotype of [unc-52](#) (Rogalski et al. 1995).

The [unc-52](#) gene encodes the nematode homolog of perlecan, the core protein of the mammalian basement membrane heparan sulfate proteoglycan ([Fig. 11](#)) (Noonan et al. 1991; Kallunki and Tryggvason 1992; Murdock et al. 1992; Rogalski et al. 1993; see [Kramer](#), this [volume](#)). Nematode perlecan is found in the extracellular matrix (ECM) linking muscle to [hypodermis](#) and is concentrated under the dense bodies and M-lines where integrin anchoring occurs ([Fig. 12](#)) ([Francis and Waterston 1991](#)). Mammalian perlecan co-aligns with focal adhesion sites in fibroblasts (Singer et al. 1987). Recent evidence suggests that mammalian perlecan and integrin may directly interact with each other (Chacravarti et al. 1995).

An attractive interpretation of these results is that perlecan and integrin form a nucleating complex for sarcomere assembly and that several sets of components assemble independently onto such centers. This model incorporates the current data and emphasizes the compartmental structure of the sarcomere. The limited effects of [myo-3](#) and [deb-1](#) mutations exemplify the compartmental nature of myofilament assembly ([Waterston 1989](#); [Barstead and Waterston 1991a](#); [Hresko et al. 1994](#); [Williams and Waterston 1994](#)). In [deb-1](#) mutants lacking vinculin, actin is not well organized, but integrin and talin are present and properly organized within the sarcolemma ([Hresko et al. 1994](#); Moulder et al. 1996). This observation implies that the base of the transmembrane complex is assembled at the membrane independent of other components of the dense body and thin filaments. This model of initiation of myofilament assembly does not address several key questions. For example, how are perlecan-integrin complexes recognized separately by talin/vinculin/ $\alpha$ -actinin assemblages and M-line constituent assemblages, and how is the spacing and alternating order between integrin transmembrane sites determined? These are clearly important parameters for initiating myofilament assembly and for determining the length and orientation of a myofilament unit.

One clear implication of studies to date is that spacing of transmembrane complexes is not dependent on intact ordered myofilaments, since sarcomere spacing is not perturbed in mutants with primary defects in either thick or thin filaments ([Waterston et al. 1980](#); [Zengel and Epstein 1980](#); [Waterston et al. 1984](#); also see [Waterston and Francis 1985](#); [Hresko et al. 1994](#)). The distance between dense bodies and the M-line does increase during growth (for review, see [Waterston and Francis 1985](#)). A body-wall muscle cell in a newly hatched L1 is two sarcomeres wide and has A-bands with approximately 100 filaments. As the animal increases its mass, muscle cells grow, so that as an adult each muscle cell is about 10 sarcomeres wide and each A-band has 600 or more filaments (MacKenzie et al. 1978b). To accommodate this growth, the number of A-bands and the size of individual A-bands both increase (L1: width = 0.5  $\mu\text{m}$ , depth = 0.4  $\mu\text{m}$ ; Adult: width = 1.1  $\mu\text{m}$ , depth = 1.4  $\mu\text{m}$ ). To maintain the stagger of the filaments when the width of the filaments is increased, individual filaments must grow longer, from 5  $\mu\text{m}$  in an L1 to approximately 10  $\mu\text{m}$  in an adult (see [Waterston and Francis 1985](#)). A direct implication of increased filament length is that spacing between integrin complexes must also increase during development; yet evidence to date suggests that the former does not determine the latter. This flexibility in the positioning of the integrin complex during growth stands as a major challenge that must be accommodated in any model of myofilament assembly.

Whether the “ruler” or “organizer” for determining the final position of integrin in the muscle membrane is internal or external to the cell is unknown. The identification of perlecan as important for sarcomere assembly and attachment in the nematode is the first evidence that forces outside a muscle cell can influence internal structure. At this time, only a few major proteins of the ECM are identified; we know little about their roles either in organizing the ECM or in cell attachment. One feature evident from this rudimentary dataset is that the ECM undergoes structural changes during development. In particular, [unc-52](#) expresses tissue- and temporal-specific perlecan isoforms (G. Mullen and D.G. Moerman, unpubl.). Viable mutations affecting a specific [unc-52](#) isoform lead to late larval defects, including muscle attachment defects and fracturing of dense bodies (MacKenzie et al. 1978b; [Waterston et al. 1980](#); Rogalski et al. 1995). Precise analysis of internal muscle structure as these mutants develop may illuminate the connection(s) between basement membrane structure and internal muscle organization (i.e., dense body positioning).

### 3. Muscle-Hypodermal Interactions

For muscle contraction to be useful to the animal, the series of links anchoring the myofilament lattice must eventually lead to the [hypodermis](#) and overlying cuticle. Studies on *Ascaris* as well as *C. elegans* reveal that the [hypodermis](#) in regions adjacent to muscle contains tonofilaments ([Bartnik et al. 1986](#); [Francis and Waterston 1991](#)). The tonofilament arrays are similar to intermediate filaments in size and morphology and react to antibodies specific for intermediate filaments ([Fig. 12](#)) ([Bartnik et al. 1986](#); [Francis and Waterston 1991](#)). A monoclonal antibody specific to nematode intermediate filaments, MH4, stains bands of tonofilaments running circumferentially from one side of a muscle quadrant to the other ([Francis and Waterston 1991](#)). Individual bands are about 1  $\mu\text{m}$  wide and can be resolved as a doublet with a narrow gap. Two other monoclonal antibodies, MH5 and MH46, identify other components of this attachment network. These antibodies show a pattern similar to that of MH4, although MH5 staining is punctate and MH46 staining is more uniform ([Francis and Waterston 1991](#)). MH5 staining is also more intense in regions overlying muscle-muscle contacts. MH5 may be reacting with a component of the hemidesmosome, the membrane attachment structure for the tonofilaments. The MH46 antigen is a large basement membrane component of hypodermal origin with several fibronectin type III repeats as well as novel sequences (M. Hresko and L. Shrieffer, pers. comm.).

The location of the tonofilament arrays and associated organelles in regions apposed to muscle suggests that this network may be the link between muscle and the cuticle. However, there is no direct or fixed relationship between the tonofilaments and hemidesmosomes of the [hypodermis](#) with the major attachment structures within muscle. In examining transverse and longitudinal sections of nematode cuticle and muscle, [Francis and Waterston \(1991\)](#) found tonofilaments and their associated organelles adjacent to all major components of muscle, including A-bands, I-bands, dense bodies, and M-lines. The periodicity of the tonofilaments and hemidesmosomes is not mediated by an interaction with muscle, but rather by their association with the annuli

(a pleated ridge) of the cuticle. Hemidesmosomes are located directly beneath the annuli. An implication of these observations is that tension developed by muscle may be distributed to the [hypodermis](#) by the basement membrane, perhaps through perlecan and the MH46 antigen. Interestingly, perlecan, a product of muscle, is distributed over the whole of the basement membrane underlying muscle but is concentrated at dense bodies and M-lines, whereas the MH46 antigen, a product of the [hypodermis](#), is distributed within the basement membrane underlying muscle in a pattern similar to the distribution of hemidesmosomes within the [hypodermis](#). How these two proteins may be linked is presently unknown.

From their birth, muscle cells are intimately associated with the [hypodermis](#). The migration of muscle cells from a lateral position adjacent to the [seam cells](#) to either a dorsal or ventral quadrant adjacent to [hypodermis](#) implies interaction between muscle and [hypodermis](#) ([Sulston et al. 1983](#); [Hedgecock et al. 1987](#); [Goh and Bogaert 1991](#)). Throughout the time when muscle cells are migrating from the midline to form the four muscle quadrants, a series of temporally related changes are occurring in the [hypodermis](#). These will eventually culminate in the formation of tonofilaments and hemidesmosomes in the region of the [hypodermis](#) adjacent to muscle (see [Fig. 7](#)). Gradually (from ~290 minutes after the first cleavage onward), antigens to MH4, MH5, and MH46 can be detected in dorsal and ventral, but not [seam](#), hypodermal cells. At 310 minutes, presumptive hypodermal attachment structures have started to concentrate under muscle cells. At 350 minutes, the MH46 antigen is found colocalized with perlecan at the boundaries of adjacent muscle cells and the [hypodermis](#), and by 390 minutes, the antigens to MH4 and MH5 are concentrated under the muscle contractile complex ([Goh and Bogaert 1991](#); [Hresko et al. 1994](#)). At 420 minutes, these hypodermal antigens, perlecan, and the myofilament lattice of muscle are co-extensive. By 430–450 minutes, the MH4 and MH5 antigens appear organized into tonofilaments and associated hemidesmosomes similar to those of an adult ([Francis and Waterston 1991](#); [Goh and Bogaert 1991](#); [Hresko et al. 1994](#)).

The close association of muscle and [hypodermis](#) throughout much of development, and the identification of hypodermal attachment structures only adjacent to muscle cells, suggests that these tissues may communicate to coordinate their development. The recruitment of a hemidesmosomal complex within the [hypodermis](#) does appear to be the result of a signal received from the underlying muscle. It has been shown that hypodermal cells organize hemidesmosomes only in regions adjacent to muscle cells and not in regions adjacent to areas where muscle cells have been experimentally removed (P. Shrimankar and R. H. Waterston, cited in [Hresko et al. 1994](#)).

A few genes have been identified which may have a role in muscle-hypodermal interactions. Mutations in some of the *mup* genes disturb muscle positioning as well as attachment ([Hedgecock et al. 1987](#); [Goh and Bogaert 1991](#); E. Gatewood and E. Bucher, pers. comm.). Another interesting group are the [muscle attachment](#) (*mua*) mutants described by J. Plenefisch and E. Hedgecock (pers. comm.). Body-wall muscle is initially properly placed and well organized in Mua animals, but during larval growth, muscle progressively detaches. Several complementation groups distinct from known *pat*, *mup*, or *unc* genes have been identified (J. Plenefisch and E. Hedgecock, pers. comm.). Alleles of [unc-23](#) and viable (Unc) alleles of [unc-52](#) convey phenotypes similar to this group of dystrophic mutants.

The fibronectin-like gene identified using the monoclonal antibody MH46 ([Francis and Waterston 1991](#); M. Hresko, pers. comm.) is an intriguing candidate for a hypodermal factor involved in muscle interactions; mutants with defects in this gene arrest at the twofold stage of elongation but are not paralyzed (M. Hresko, pers. comm.). Muscle twitching occurs, and the muscle detaches from the [hypodermis](#) when contraction begins. In these twofold-arrested animals, the hemidesmosomes are not restricted to the region adjacent to muscle, but are found throughout the dorsal and ventral [hypodermis](#). Mutants with specific defects in the [hypodermis](#) may help dissect the structure and function of the hemidesmosomal complex in a manner similar to what has been achieved for the muscle dense body. For example, it will be interesting to see if this structure has components common to mammalian hemidesmosomes, in particular an  $\alpha 6-\beta 4$  integrin complex (for review, see Garrod 1993). Beyond merely dissecting the attachment complexes of muscle and [hypodermis](#), we will need to resolve how these two tissues coordinate and facilitate their behavior during morphogenesis if we are to understand how a fully functional muscle quadrant is established.

## Figures

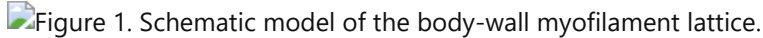


### Figure 1

Schematic model of the body-wall myofilament lattice. (*Bottom*) Contractile unit (sarcomere) of *C. elegans* body-wall muscle. This structure is similar to sarcomeres in vertebrate striated muscle. Thin filaments (*blue*) are anchored at one end to dense bodies (*mauve*, analogs of the vertebrate Z line) and overlap at the other end with bipolar thick filaments (*light orange*). Thick-filament alignment is maintained by M-line components (*purple*). Contractile force is generated by myosin heads (*yellow*), which interact with and pull on adjacent thin filaments. As a result, dense bodies are pulled more closely together. Contractile force is transferred to the outside of the animal through a series of attachments, including transmembrane integrin complexes underlying the dense body, an adjacent extracellular basement membrane (*light green*), *hypodermis* (clear with black hemidesmosomes) and eventually the cuticle (*dark green*). Above are shown detailed models of each filament type. Thick filaments (*top right*) have myosin heads (*yellow*) protruding from a surface composed of myosin rods, paramyosin, and other less abundant components (e.g., twitchin and UNC-89, not shown). Myosin has six subunits (two identical heavy chains and two pairs of light chains [*red*])); paramyosin has two identical subunits. Almost half of myosin heavy chain and all of paramyosin consist of  $\alpha$ -helical coiled-coil rod. Figs. 3 and 5 illustrate the detailed packing of paramyosin and myosin. The four-strand symmetry depicted here is based on filament structures determined for other invertebrate thick filaments of similar diameter (see [Waterston 1988](#)). The thin filament (*top left*) is built on a two-stranded actin helix (*blue*). Tropomyosin (*light purple*) and associated troponin (*green/pink/gold*) lie along the groove between the two actin strands and regulate contraction in response to calcium. Tropomyosin has two subunits arranged in a rodlike  $\alpha$ -helical coiled coil. The subunit composition of *C. elegans* troponin has not yet been defined; in mammalian muscle, troponin has three subunits: troponin-T (*green*) which binds tropomyosin, troponin-C (*gold*) which binds to calcium, and troponin-I (*pink*) which binds actin. The actin structure shown (large and small domains) is of the monomeric ("G") form. (Adapted, with permission, from [Waterston 1988](#); [Francis and Waterston 1991](#); [Hresko et al. 1994](#).)

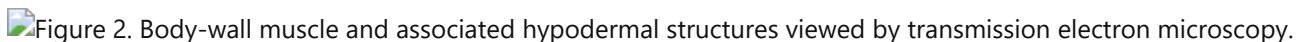


### Figure 2

Body-wall muscle and associated hypodermal structures viewed by transmission electron microscopy. (*a*) Transverse-section micrograph showing many features illustrated in Fig. 1. (*Black arrow*) Thick filament surrounded by thin filaments; (*white arrow*) thin filaments near the dense body (I-band region); (db) dense body; (M) M-line; (mcb) muscle cell body; (hyp) *hypodermis*. Mitochondria cluster at the boundary of the muscle lattice and the muscle cell body. (*b,c*) At high magnification, darkly staining patches in cuticle can be seen to overlie filament bundles in the *hypodermis*. These bundles extend between densely staining plaques on the inner and outer hypodermal cell membranes; the filament-plaque structures are called fibrous organelles (FO). A prominent basement membrane between the *hypodermis* and muscle is also apparent (*large open arrow*). Bar, 0.5 mm. (Adapted, with permission, from [Francis and Waterston 1991](#); copyright by the Rockefeller University Press.)



### Figure 3

Possible myosin and paramyosin interactions during assembly. (*Arrowheads*) Amino termini; (*open bars*) paramyosin molecules; (*closed bars*) myosin molecules. Short vertical bars in paramyosin indicate spacing of 28-residue repeats; long vertical bars in both molecules indicate the position of skip residues. Horizontal lengths are drawn to scale (note that  $725 \text{ \AA} \approx 493$  residues; vertical widths are not to scale). (*a*) Parallel form of paramyosin (shift = 493); 330-residue "overlaps" alternate with 163-residue "gaps." (*b*) Antiparallel myosin packing across the bare zone (shift = 0); complete overlap with 1120 residues between heads. (*c*) Antiparallel overlap of paramyosin molecules (shift = 593; overlapping region of 465 residues). (*d*) Myosin and paramyosin aligned antiparallel with

minimal distance between amino termini (shift = -296); two such pairs, placed antiparallel, would combine the interactions shown in *b* and *c*. (Adapted, with permission, from [Kagawa et al. 1989](#).)

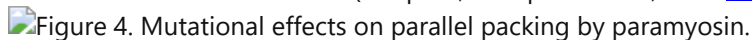


### Figure 4

Mutational effects on parallel packing by paramyosin. (A) Mutation sites are indicated by allele number. Paramyosin molecules are drawn as associated in the parallel model of Kagawa et al. (1989) (see [Fig. 3a](#)). *e73* is a missense mutation causing formation of paracrystals of paramyosin; *m193*, *m208*, and *m209* are intragenic revertants that improve assembly of paramyosin with the *e73* mutation. (B) Amino acid sequence of regions affected by mutations. The upper and lower lines of amino acid sequence correspond to the upper and lower paramyosin molecules diagrammed in A. Wild-type residues changed in the suppressor mutations are circled; arrows indicate the substituted amino acids. *a,b,c,d,e,f,g* indicate the positions within the heptad repeat; hydrophobic residues are concentrated in the *a* and *d* positions. Note that the substituted amino acid in *m209* lies directly opposite the *e73* mutation in the parallel model of paramyosin association. (Reprinted, with permission, from [Gengyo-Ando and Kagawa 1991](#).)



### Figure 5

Models of thick-filament substructures in *C. elegans*. (Reprinted, with permission, from [Deitiker and Epstein 1993](#).) (a) Layers of the thick filament (in each case, one half of a filament is shown): (*Top*) The outer layer of the filament, showing the positions of myosin isoforms MHC A and MHC B; (*middle*) outer myosin layer peeled away to reveal a middle (still dissociable) paramyosin compartment; (*bottom*) dissociable paramyosin removed to reveal a core structure containing a firmly associated paramyosin component and core proteins. (b,c,d,e) A model of the core structure. (Based, with permission, on Epstein et al. 1995.) The essential components of the model are (1) an outer sheath of seven subfilaments, each subfilament consisting of two strands of paramyosin staggered by 72 nm with respect to one another (also see [Kagawa et al. 1989](#)); and (2) an inner set of 54-nm-long tubules repeating every 72 nm. These are illustrated in *b* (longitudinal section) and *c* (transverse view). The composition of the inner tubules is unknown. The model requires consecutive paramyosin dimers to have a 22-nm gap, and it is proposed that this gap region and the unpaired ends of paramyosin contain sites for interaction with the inner tubule constituents (*c*). (*d*) Unrolled representation of the model. The unit cell is 144 nm long and 44 nm in circumference. The seven paramyosin subfilaments are shown in black, with the 22-nm gap indicated as a narrower region. The unrolled tubule is shown as a hatched rectangle interacting in an offset way with the gap region. Epstein et al. (1995) suggest that the gap region and the sites at which the ends of paramyosin (shown in *e*) interact with the inner tubule proteins may be important sites for assembly. Analysis of mutations supports the latter structure as important; no data are yet available to implicate the gap region (residues 372–522) directly in assembly.



### Figure 6

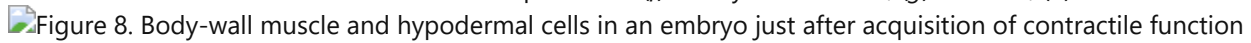
Schematic of domains in the deduced amino acid sequence of twitchin. (*Gray boxes*) Motif I (fibronectin type-III-like domain); (*white boxes*) motif II (immunoglobulin superfamily C2-like domain); (*hatched box*) the kinase domain. (Reprinted, with permission, from Benian et al. 1993.)



### Figure 7

Embryonic muscle differentiation. (A–D) Schematic diagram of muscle assembly in *C. elegans* depicting cross sections of embryos at various developmental stages. The diagram represents a view of body-wall muscle assembly based on the data presented in Hresko et al. (1994). (A) Embryo 290 min after the first cleavage.

Hypodermal cells (dorsal, [seam](#), ventral) are thin layers covering most of the embryo; only the ventral surface is exposed. Hypodermal components destined for hemidesmosomes are present in dorsal and ventral hypodermal cells (indicated by hatched regions). Muscle cells (*circles*) have begun to accumulate muscle components (*dots*). Muscles are adjacent to [seam cells](#) at this stage but will subsequently move to contact dorsal or ventral [hypodermis](#). Some muscle cells are postmitotic at this stage, others will divide once before assuming a final position. (B) 350-min embryo. Muscle cells (*circles*) are still rounded but have become asymmetric. Myofibrillar components (*dots*) localize to membranes adjacent to other muscle cells and to [hypodermis](#). Basement membrane components (*black*) are also localized to these contacts. Hypodermal hemidesmosome components (*hatched region*) have become restricted to regions of the [hypodermis](#) adjacent to muscle cells. (C,D) A dorsal quadrant is used to illustrate events that occur in each of the four quadrants. (C) 420-min embryo. Muscle cells (*ovals*) are flattened; myofilament components (*dots*), basement membrane (*black*), and the hemidesmosome components (*hatched regions*) are coextensive. (D) 450-min embryo. Organization of myofibril lattice and the hypodermal hemidesmosomes is evident. (Reprinted, with permission, from [Hresko et al. 1994](#).) (e–h) Left-lateral view of developing embryos stained with a muscle cell marker. (Reprinted, with permission, from [Moerman et al. 1996](#).) (e) Embryo at approximately 310 min. Note that muscles are a continuous sheet of cells when present on the lateral side of the embryo. Between 300 and 350 min, starting at the anterior end, this sheet separates as cells move to form the dorsal and ventral muscle quadrants. (f) Embryo at 330 min; (g) 350 min; (h) 420 min.

Figure 8. Body-wall muscle and hypodermal cells in an embryo just after acquisition of contractile function (longitudinal view).

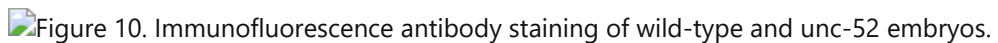
## Figure 8

Body-wall muscle and hypodermal cells in an embryo just after acquisition of contractile function (longitudinal view). An embryo at the 1-3/4 stage (~430 min) is diagrammed. (a) Left-dorsal surface of whole embryo. The dorsal muscle quadrant is a double row of spindle-shaped cells (*shaded*) that are attached to the thin hypodermal cells covering the embryo. (b) Detail of boxed region including the arrangement of myosin containing A-bands within the muscle cells. Note that there are four A-bands across the quadrant. Positions of hypodermal cell adherens junctions are indicated, including the circular junction formed at the deirid sensillum. Hypodermal adherens junctions are visualized with antibody MH27 ([Francis and Waterston 1985](#)). (Reprinted, with permission, from [Williams and Waterston 1994](#); copyright by the Rockefeller University Press.)

Figure 9. Embryogenesis in wild-type and Pat mutants.

## Figure 9

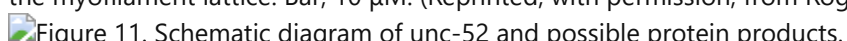
Embryogenesis in wild-type and Pat mutants. (a) Wild type. The first contractions of body-wall muscles occur as the embryos reach the 1.5-fold length. By twofold, embryos roll vigorously within the egg. (b) Pat mutants. 1.5-fold embryos fail to start moving and remain severely paralyzed. Elongation continues until the embryos are twofold, but then stops. Pharyngeal morphogenesis occurs. Embryos often hatch near the normal time as misshapen, inviable larvae. (Reprinted, with permission, from [Williams and Waterston 1994](#); copyright by the Rockefeller University Press.)

Figure 10. Immunofluorescence antibody staining of wild-type and *unc-52* embryos.

## Figure 10

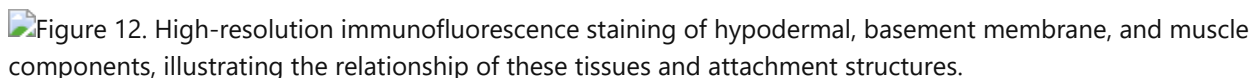
Immunofluorescence antibody staining of wild-type and *unc-52* embryos. Embryos are stained at approximately 420 min after the first cleavage. For reference, all samples are also stained with monoclonal antibody MH27, which decorates hypodermal adherens junctions of both wild-type and mutant embryos. (a) Wild-type embryos stained with MH27 + anti-perlecan monoclonal antibody MH3. MH27 staining gives a set of thin lines tracing hypodermal adherens junctions; these are easily distinguished from the broader band of MH3 (perlecan) staining, which is seen in each muscle quadrant. Two muscle quadrants are visible in this plane of focus; the arrowhead notes MH3 staining in a dorsal quadrant. (b) *unc-52* (st549) stained as in a. Staining of hypodermal adherens junctions is observed, but no staining is seen with the anti-perlecan antibody MH3. (c) Wild-type

embryos stained with a monoclonal antibody to myosin isoform A (mAb5.6; Miller et al. 1983) and MH27. Myosin isoform A is organized into nascent A-bands in body-wall muscle cells (*arrowhead*). (d) *unc-52* (*st549*) stained as in a. Muscle cells of the mutant embryo (*arrowhead*) are stained strongly but show extreme disorganization of the myofilament lattice. Bar, 10  $\mu$ M. (Reprinted, with permission, from Rogalski et al. 1993.)

Figure 11. Schematic diagram of *unc-52* and possible protein products.

### Figure 11

Schematic diagram of *unc-52* and possible protein products. *unc-52* consists of 26 exons and has three alternative poly(A)-addition sites (exons 10, 22, and 26). Protein motifs are illustrated by shading: (white) LDL receptor; (light gray shading) a laminin-like motif; (dark gray shading) an Ig motif. Note that in several (but not all) cases, a single structural motif is encoded precisely by a single exon. The amino terminus (dark shading) is unique to this protein. Two different isoforms of the protein based on differential splicing and poly(A) addition are illustrated at the bottom of the figure. Many exons are alternatively spliced, including exons 6, 16, 17, and 18. One consequence of alternative splicing is to alter the Ig repeat copy number within domain IV of the molecule. Sequenced mutations are shown above the gene. The mutations *ut111*, *st549*, and *st560* all lead to a Pat terminal phenotype, whereas the mutations clustered in the region of alternative splicing all lead to an Unc (non-null) phenotype. (Adapted, with permission, from Rogalski et al. 1993, 1995.)

Figure 12. High-resolution immunofluorescence staining of hypodermal, basement membrane, and muscle components, illustrating the relationship of these tissues and attachment structures.

### Figure 12

High-resolution immunofluorescence staining of hypodermal, basement membrane, and muscle components, illustrating the relationship of these tissues and attachment structures. Staining of adult muscle cells is shown. (a) Immunolocalization of an intermediate filament polypeptide (monoclonal antibody MH4; [Francis and Waterston 1985](#)). Signal is seen in the *hypodermis* underlying two ventral muscle quadrants. This antigen is present in a repeat pattern consisting of regularly spaced bands running circumferentially from one edge of each muscle quadrant to the other. (b,c) Staining with two monoclonal antibodies (MH5 and MH46, respectively) that recognize components of the attachment network within the *hypodermis*. Regions of the body-wall adjacent to muscle cells are labeled in a pattern of doublet bands resembling that obtained with MH4, but differing in detail. Bands revealed by MH5 are irregular and appear to be composed of a series of small dots; signal is more intense (white arrows) in regions of the *hypodermis* where the underlying muscle cells contact one another. MH46 bands are more uniform in appearance; these lack the increased signal over muscle-muscle cell junctions seen with MH5. (d) Immunolocalization of the basement membrane proteoglycan perlecan (monoclonal antibody MH2). Signal is detected over the entire basement membrane underlying muscle but is enhanced at muscle-muscle cell boundaries (black arrows) and at periodicities corresponding to the sites of the dense bodies and M-line structures. (e) Immunolocalization of  $\beta$ -integrin within the muscle cell membrane (monoclonal antibody MH25). Staining is present at the base of the dense bodies, at attachment plaques, and also at the base of the M-line. The model shown in [Fig. 1](#) incorporates many of these findings. Bar, 10  $\mu$ M. Occasional gaps (e.g., the longitudinal gap in c) may represent an artifact of preparation. (Adapted, with permission, from [Francis and Waterston 1991](#); copyright by the Rockefeller University Press.)

## Tables

**Table 1 Contractile activity mutations affecting the head region of the *unc-54* myosin heavy chain**

Allele	Sequence change	Myosin domain containing mutation	Phenotype
<i>st134</i>	C-T	2338 S1 25K peptide	slow, stiff
	Ser-Phe	117 near ATP-binding site	normal structure

<b>Allele</b>	<b>Sequence change</b>		<b>Myosin domain containing mutation</b>	<b>Phenotype</b>
<i>s95</i>	G-A	2340	S1 25K peptide	slow, stiff
	Gly-Arg	118	near ATP-binding site	normal structure
<i>s74</i>	C-T	2884	S1 50K peptide	slow, stiff
	Arg-Cys	273	near ATP-binding site	normal structure
<i>s75</i>	G-A	4074	S1 20K peptide	moves well;
	Gly-Arg	652	near conserved SH1 thiol	normal structure
<i>s77</i>	G-A	4272	S1 20K peptide	slow, stiff
	Gly-Arg	718	near conserved SH1 thiol	normal structure
<i>st130</i>	G-A	3739	S1 50K peptide	slow; disorganized
	Cys-Tyr	540	actin-binding region	A-bands
<i>st132</i>	G-A	3646	S1 50K peptide	slow; disorganized
	Glu-Lys	527	actin-binding region	A-bands
<i>st135</i>	G-A	3460	S1 50K peptide	slow, stiff
	Ala-Thr	465	near actin-binding region	normal structure
	C-T	3855	S1 50K peptide	
	His-Tyr	579	near actin-binding region	

This table describes a set of missense alleles of *unc-54* myosin that affect the contractile activity of the myofilament lattice. Mutations and amino acid changes associated with each sequenced allele of this class are given. "Myosin domain" refers to the portion of the myosin peptide affected by each mutation. Proximity to expected functional and/or structural features of the molecule are also noted. "Phenotype" describes the ability of animals to move, and the organization of the myofilament lattice (as viewed by polarized light microscopy). For reference, wild-type animals have vigorous movement and highly organized myofilament structure, whereas *unc-54* null mutants are severely paralyzed as late larvae and adults and have highly disorganized myofilament structure. Note that this class of mutations was isolated based on their ability to suppress twitching in an *unc-22* background (see text). Data for *s95* and *s74* are from Dibb et al. (1985); remainder are from D. Moerman et al. (unpubl.).

Generated from local HTML

# **Chapter 16. Muscle: Structure, Function, and Development — III**

## **Specification of Muscle Patterns: Programs for Muscle Determination and Differentiation**

---

### **A. Cellular Roles in Early Myogenesis**

To a first level of resolution, the questions of how muscles are formed in *C. elegans* can be addressed by examination of the cell lineage ([Sulston and Horvitz 1977](#); [Deppe et al. 1978](#); [Kimble and Hirsh 1979](#); [Sulston and White 1980](#); [Sulston et al. 1983](#)). The idea that all muscles might derive from clonal myogenic commitment of a few early blastomeres was appealing to earlier investigators, who had determined that muscle is predominantly derived from only two of the four-cell-stage blastomeres (Boveri 1888). However, a more detailed examination of the lineages makes a simple early-clonal-commitment model untenable. This is most dramatically seen by the presence of a single body-wall muscle derived from the [AB lineage](#) (Figs. 13 and 14) ([Sulston et al. 1983](#)). Although it is the only body-wall muscle to derive from this lineage, the differentiated cell exhibits no evident distinctions from its distant cousins that form body-wall muscles from the P<sub>1</sub> lineages. Body-wall muscles likewise arise in a piecemeal way from the [MS lineage](#), with clonal groups of one to four body-wall muscles interspersed in the lineage tree with branches yielding a variety of nonmuscle cells. Derivation of body-wall muscles from the C and D lineages exhibits a much less complex pattern: Two granddaughters of the [C](#) cell give rise to simple clones of muscle, while [D](#) gives rise precisely to 20 muscle cell descendants. The different muscle lineage patterns suggest that several different pathways might be responsible for the initiation of myogenesis in body-wall muscle (Fig. 14).

Pharyngeal muscles, derived from [AB](#) and [MS](#), are produced by a piecemeal pattern in a manner similar to that of the body-wall muscle lineages derived from these two founder cells ([Sulston et al. 1983](#)). The pharyngeal muscles are, however, not closely related to body-wall muscle lineages but are instead interspersed with lineages producing nonmuscle [pharyngeal cells](#). The remaining embryonic muscles (the four intestine-associated [nonstriated] body muscles) are also produced from [AB](#) and [MS](#); these are closely related in lineage to striated body-wall muscles.

### **B. Autonomy and Nonautonomy in Muscle Cell Commitment**

The invariance of the cell lineage does not necessarily imply a noninteractive commitment of early embryonic cells to specific patterns of descendants. A variety of cell ablation and isolation experiments have suggested that interactions of potential myogenic precursors with neighboring cells have a key role in determining the pattern of cells that eventually differentiate into muscle ([Priess and Thomson 1987](#); [Wood 1991](#); [Hutter and Schnabel 1994](#); [Schnabel 1994, 1995](#)). These studies are still in progress (see [Schnabel and Priess](#), this volume). From the viewpoint of muscle patterning, the most striking feature of the characterized cell interactions is that they occur very early in the affected cell lineages, several cell divisions before any overt differentiation of muscle cells is observed in the embryo ([Priess and Thomson 1987](#); [Schnabel 1995](#)). Thus, whatever information is imparted through the cell interactions must be stably maintained through several cell divisions before eventually becoming manifest in expression of muscle-specific differentiation products.

Given the large number of early cell interactions that influence later commitment to muscle cell fates, it is valid to ask if there is any point at which myogenic commitment has become an intrinsic feature of specific cells. In the case of the [D](#) blastomere, it has been possible to address this question with a conceptually simple isolation experiment. Starting from the first embryonic division, the cells *not* in the lineage leading to [D](#) can be ablated just as they are born ([Schnabel 1995](#)). This leaves an isolated [D](#) cell, surrounded by debris resulting from ablation of other embryonic cells. The resulting partial embryo yields approximately 20 cells that express components indicative of body-wall muscle differentiation. This experiment strongly suggests that some type of intrinsic commitment is indeed occurring in the early embryo.

The invariant cell lineage could be taken as suggesting that the myogenic differentiation program might be switched on by a mechanism that counts cell cycles. Mutations blocking cell division ([Gossett et al. 1982](#)) and pharmacological agents (Cowan and McIntosh 1985) have been used to examine embryos in which cell cleavage arrests while other developmental events (including DNA synthesis) proceed. Both sets of manipulations resulted in cleavage-arrested embryos (2–90 cells total) containing specific subsets of cells that had initiated the myogenic program, as assayed by production of muscle filament components. It thus appears that a myogenic commitment program can proceed in the absence of a fully operational cell cycle. These experiments do not rule out the possibility that some aspect of the cell cycle might continue in cleavage-blocked embryos and have a role in myogenic commitment.

Experiments by [Edgar and McGhee \(1988\)](#) have addressed the ability of muscle differentiation to occur in cases in which DNA replication (instead of cell cleavage) has been blocked. These experiments demonstrated that muscle differentiation can occur without the last several rounds of DNA synthesis. This argues against a model in which replication cycles are counted to precisely time the onset of muscle differentiation. Edgar and McGhee observed that earlier blockage of DNA replication (two to three divisions before final differentiation) could inhibit muscle differentiation. This was in contrast to their observations with gut differentiation markers and suggested that some feature(s) dependent on S phase of the cell cycle might have a role in executing the process of myogenic commitment.

## C. Genes Responsible for Muscle Patterning

Genetic and biochemical analyses have given us some understanding of the on events at the two temporal extremes of the muscle-patterning process: the early events preceding myogenic commitment and terminal events that give rise to differentiated muscle. The middle stages in this process are still a mystery and are the focus of research using a variety of experimental approaches.

### 1. The Early Body Plan

The establishment of the early blastomere identities is in large part controlled by maternally encoded factors, which have initial roles in determining patterns for both muscle and nonmuscle tissues. For a more extensive discussion of these genes, see [Schnabel and Priess](#) and [Kemphues and Strome](#) (both this volume). The influences of these genes on muscle can be summarized as follows:

a.

The earliest determinative events in the embryo may be the formation of the asymmetric anterior-posterior axis (see [Kemphues and Strome](#), this volume). As muscle is predominantly derived from the posterior daughter at the first cleavage ( $P_1$ ), it is not surprising that genes responsible for early anterior-posterior axis formation (*par* genes) also affect the pattern of muscle cells produced.

b.

Many of the cell-cell interactions in the early embryo (which both restrict and enable subsequent muscle-containing lineages) require the GLP-1 signaling pathway (see [Schnabel and Priess](#), this volume). Thus, mutations in [\*glp-1\*](#) lead to both missing muscles and ectopic muscle. Some of the other components required for this signaling pathway have also been identified, including one of several proposed GLP-1 ligands, APX-1, which functions in interactions between  $P_2$  and ABp (Mango et al. 1994b; Mello et al. 1994), and [\*lag-1\*](#), which may act downstream from [\*glp-1\*](#) (Lambie and Kimble 1991). There is as yet no working hypothesis of how [\*glp-1\*](#) function might result several divisions later in modifications to the pattern of differentiated muscle and nonmuscle cells.

c.

The myogenic potential of the [\*MS\*](#) and  $P_2$  lineages depends on separate programs that appear to set the initial identities of these blastomeres ([Mello et al. 1992](#)). Genetic analysis has implicated the gene [\*skn-1\*](#) in

setting the identity of [MS](#) (Bowerman et al. 1992a, 1993; [Mello et al. 1992](#)), with [pal-1](#) setting the identity of P<sub>2</sub>-derived muscle precursors (C.P. Hunter and C. Kenyon, pers. comm.). Both genes produce maternally encoded transcription factors.

## 2. The Terminal Differentiation Program

The structural proteins described in this chapter are the end products of the muscle differentiation pathway. As nucleic acid and antibody probes for these components are generated, it becomes possible to follow the onset of transcription and translation of the corresponding genes. The four muscle myosin heavy-chain genes were the first components for which such probes were available ([MacLeod et al. 1981](#); [Karn et al. 1983](#); [Dibb et al. 1989](#)), and thus they have been the most extensively analyzed. Myosin protein accumulation in body-wall muscle cells begins just before the terminal division of myogenic precursors ([Epstein et al. 1993](#); [Hresko et al. 1994](#)). If this is indeed the earliest expression of muscle-specific differentiation markers, it would contrast with the clonal gut lineage, for which expression of differentiated products can begin up to three divisions before cessation of cell division. In situ hybridization experiments demonstrated that expression of myosin genes is controlled at the level of mRNA accumulation (Evans et al. 1994; Seydoux and Fire 1994). Quantitative assays for mRNA and protein levels were consistent with this conclusion and with primary control at the level of transcription; the latter assays also suggested a modest posttranscriptional regulation modulating relative levels of the MHC isoforms (Honda and Epstein 1990).

An intensive genetic analysis of the major MHC isoform (encoded by [unc-54](#)) was facilitated by the fact that null mutations are viable and have an easily identified paralyzed phenotype ([Brenner 1974](#); Anderson and Brenner 1984). It was hoped initially that the large number of mutant alleles would provide both structural and regulatory mutations and that the regulatory mutations might point to specific modes of gene control. Surprisingly, none of the [unc-54](#) mutations that have been characterized appear to affect the regulation of the gene. Of more than 75 sequenced mutations, all but three affect the coding region by either changing critical amino acids, introducing stop codons, or affecting splice junctions (Dibb et al. 1985; Eide and Anderson 1985a,b; Bejsovec and Anderson 1990; D. Moerman, J. Kiff, and R.H. Waterston, unpubl.). Two alleles appear to be 5' duplications which are intriguing but do not immediately shed light on [unc-54](#) regulation (Eide and Anderson 1985c). The remaining allele is a deletion in the 3'UTR which leads to RNA degradation by the SMG system (Eide and Anderson 1985a; Pulak and Anderson 1993; see [Anderson and Kimble](#), this volume). The deleted sequences do not appear to have an essential role in determining the pattern of [unc-54](#) regulation, since the 3'deletion allele is fully functional and properly regulated in a Smg<sup>-</sup> genetic background (Okkema et al. 1993).

The analysis of *cis*-acting sequences was greatly bolstered by the development of a DNA transformation system which allowed reporter constructs (*lacZ* fusions) to be rapidly assayed for expression pattern (Fire et al. 1990). Using such assays, Okkema et al. (1993) found that each of the MHC genes contains several separated elements, each sufficient to direct muscle-type-specific expression. All of the elements identified were positively acting enhancer or promoter elements: There was no evidence for negative regulation mediated through specific promoter or enhancer elements. Given the multiplicity of positively acting regulatory sites for each gene, the failure in the original genetic screens to recover individual point mutations with large effects on expression is not surprising.

Several of the *cis*-acting elements responsible for MHC gene activation have been dissected in more detail, with the results suggesting combinatorial modes of action. Evidence for a combinatorial "AND" function comes from a strong enhancer within the [unc-54](#) third intron ([Jantsch-Plunger and Fire 1994](#)). This enhancer contains a set of four separable subelements, at least one of which has a broader specificity (body-wall muscle plus [body hypodermis](#)) than the complete enhancer (body-wall muscle only). Dissection of the [myo-2](#) upstream enhancer revealed both combinatorial "AND" and "OR" functions. This enhancer carries at least one element active throughout the [pharynx](#) (in muscle and nonmuscle tissue), as well as an element acting in only a subset of pharyngeal muscles ([Okkema and Fire 1994](#)).

It seems likely that the mechanisms regulating MHC gene promoter/ enhancer activities will be used for coordinated activation of a larger set of muscle filament components. Analysis of the tropomyosin gene [tmy-1](#) ([Kagawa et al. 1995](#)) provides a similar example of type-specific regulation (body-wall vs. [pharynx](#)) by promoter activation while indicating that additional complexity in regulation can be generated by differential splicing. Studies of basement membrane collagen and perlecan expression have similarly revealed a variety of differentially spliced mRNAs with distinct regulation, including both muscle-specific and more generally expressed forms (see [Kramer](#), this volume).

## D. Diversity within and between Muscle Cell Classes

Although all body-wall muscles have the same overall shape and organization, these cells are distinguishable by several features. First, as noted above, the cells derive from several different branches of the lineage tree. Second, cells have distinctive and fixed anterior-posterior (as well as dorsal-ventral) positions. In particular, the cells at the front and rear margins of the muscle quadrants might need special attachment properties in order to maintain overall integrity of the animal. Third, body-wall muscle cells in different parts of the animal have different connectivity patterns with the [nervous system](#) (White et al. 1986). These similarities and differences highlight the question of the extent of diversity in the body-wall muscle gene expression program.

At one extreme, body-wall muscle cells from different lineages (or in different parts of the body) might use completely different sets of regulatory factors in carrying out differentiation. Alternatively, it was conceivable that all body-wall striated muscles express a completely uniform differentiation program and that each is equivalent in gene expression (with any differences due to cellular context and/or posttranscriptional events). These extreme models both appear unlikely. The analysis of *cis*-acting sequences regulating body-wall MHC expression suggested at least some common elements to gene expression in the different cells, since each of the MHC promoter and enhancer elements (both wild-type and mutant) acts uniformly in all body-wall muscles (Okkema et al. 1993; [Jantsch-Plunger and Fire 1994](#)). Although MHC regulation may be uniform, indications of nonhomogeneity in body-wall muscle gene expression come from a variety of analyses. In a pilot screen for enhancers that act nonhomogeneously in body-wall muscles, two such elements were found: one with preferential expression in anterior body-wall muscles and a second with preferential expression posterior (A. Fire and S. Xu, unpubl.). In addition, expression of the homeotic selector gene [mab-5](#) has been observed in a subset of posterior muscles (D. Cowing and C. Kenyon, pers. comm.; also see Wang et al. 1993). Although the differential activity of the selector genes and the two characterized position-dependent body-wall muscle enhancers demonstrate a mechanism for expressing genes nonhomogeneously in this tissue, there is not yet any functional indication of how such a mechanism might be used by the animal.

The nonstriated single sarcomere muscles (pharyngeal, vulval, [uterine](#), and intestine-associated) have wide variation in their cellular morphology. The nonpharyngeal single-sarcomere muscles ("minor muscles") express many of the same differentiated components as body-wall muscles, including the same set of MHC isoforms (Ardizzi and Epstein 1987). Nevertheless, differences between striated and nonstriated muscle cells are readily observed in the timing and eventual levels of structural protein accumulation. This is exemplified by preferential expression of different [unc-52](#) splice variants in the different muscle classes (G. Mullen and D.G. Moerman, unpubl.) and by differential activity of promoter and enhancer elements from the [unc-54](#) gene (Okkema et al. 1993). Pharyngeal muscles are likewise a diverse group (see [Avery and Thomas](#), this volume), having in common perhaps only their pharyngeal location and expression of the MHC isoforms encoded by [myo-1](#) and [myo-2](#). One functional subgrouping within [pharyngeal muscle](#) is suggested by two independent experiments: embryonic staining with monoclonal antibody 3NB12, and activity assays for the "B" subelement of the [myo-2](#) enhancer. Both experiments define a subset of pharyngeal muscles that include cells [m3](#), [m4](#), [m5](#), [m7](#) but strikingly excludes the large muscle cell [m6](#) (see [Fig. 15](#)) (Okamoto and Thomson 1985; [Priess and Thomson 1987](#); [Okkema and Fire 1994](#)).

Several ongoing lines of research are suggesting that gene expression in nematode nonstriated muscles might have an even richer complexity than previously imagined. [Lynch et al. \(1995\)](#) have recently produced *lacZ* fusions to many genes defined solely from the genome sequencing project and have reported promoter regions active

in a variety of subsets of muscle cells, including subsets of the vulval and pharyngeal muscles. M. Krause and L. Avery (pers. comm.) have examined a striking restriction in the distribution of the HLH-2 protein, which is observed in muscle nuclei of the [m5](#) class, but only in a subset of these nuclei. Two distinct and very specific enhancer elements have been found upstream of the *C. elegans* gene [ceh-24](#). One is active only in the lone [m8 pharyngeal muscle](#), and the other is active only in vulval muscles (B. Harfe and A. Fire, unpubl.).

## E. A Mystery: Acquisition of Muscle Cell Fates in the Mid-stage Embryo

In principle, it should be possible to find the mechanistic links between the early events establishing blastomere identity and much later elucidation of the differentiated muscle pattern. A half dozen cell cleavages occur in the intervening period of embryogenesis, with the onset of extensive overt differentiation coinciding with the last cleavage. A detailed understanding of this "mystery" phase of embryogenesis will require the identification of genes and gene products that are differentially distributed or differentially active during late proliferation. This will potentially be informative (1) as markers for intermediate stages in cell-type-specific commitment and (2) as candidates for molecules with functional roles in the process.

Several types of screens are being undertaken to identify myogenic genes active in the mid-stage embryo. Working from control sequences known to be responsible for structural protein gene expression, it should be possible to isolate regulatory factors that provide successive steps backward through the regulatory pathway. This has been done successfully in the case of the pharyngeal-muscle-specific "B" element of the [myo-2](#) enhancer. A homeodomain protein, CEH-22, was identified by its ability to bind to that element and was subsequently shown to be expressed in precisely the cells in which the "B" element is active ([Okkema and Fire 1994](#)). CEH-22 is a member of the "NK2" family of homeodomain factors (see [McGhee and Krause](#), this volume). In several organisms so far examined, multiple members of this family have been found (*Drosophila*, Kim and Nierenberg 1990; *Planarians*, Garcia-Fernandez et al. 1991; vertebrates, Price et al. 1992; *C. elegans*, B. Harfe and A. Fire, unpubl.). These components have been implicated in mesodermal and ectodermal specification and differentiation, including most intriguingly the murine NKx2.5 factor, which has been implicated in cardiac differentiation (Lyons et al. 1995). The role of CEH-22 in pharyngeal development has been addressed by genetic analysis and misexpression studies. Loss-of-function mutations in the [ceh-22](#) gene result in loss of "B" element activity, whereas ectopic expression of CEH-22 in body-wall muscles can result in ectopic activity of the endogenous [myo-2](#) gene (P. Okkema and A. Fire, unpubl.). [ceh-22](#) expression is activated somewhat earlier than myosin gene expression, but it is limited to [pharyngeal muscle](#) precursors ([Okkema and Fire 1994](#)). Hence, although a step has been taken back through the series of regulatory events, more such steps will be essential before the process is completely charted.

At the same time, a more classical genetic approach has been taken to look for genes that are required for muscle differentiation and commitment. Mutations that fully disrupt these processes with no detectable differentiation of the affected muscle class would be expected to have lethal phenotypes ([Waterston 1989](#)). If muscle development is controlled by a consecutive series of differentiation factors, each dependent on previous factors for its expression, then one might expect to find a large number of such mutations. Lethal screens have been carried out for mutations affecting body-wall muscle differentiation (see, e.g., [Williams and Waterston 1994](#)), but no point mutations that specifically eliminate expression of muscle-specific differentiation markers have been isolated. Because the precise arrest phenotype to be expected from such a mutation is not clear, these screens focused on mutations that arrest as paralyzed twofold-elongated embryos (characteristic of complete loss of function for the contractile apparatus; [Waterston 1989](#)). A more general screen was carried out using deficiency mutations, assaying only for the production of terminally differentiated muscle components (Ahnn and Fire 1994). The surprise of the deficiency screens has been that very few loci in the zygotic genome are required uniquely for muscle differentiation. One candidate locus (yet to be identified on a molecular level) was identified in screening approximately 80% of the genome. These studies suggest extensive maternal contribution to later embryonic development, widespread redundancy in the commitment/differentiation program, or both.

Muscles associated with the reproductive system develop post-embryonically. The specific role of vulval muscles in egg laying allows them to be the object of a straightforward type of genetic screen. Animals without [vulval](#)

[muscle](#) function fail to lay eggs, leading to a "bag of worms" phenotype in which the young worms hatch inside of the parent. Many mutants that affect the functioning of body-wall muscles (e.g., [unc-54](#) null mutations) have similar effects on the vulval muscles, and thus exhibit egg-laying defects (Trent et. al. 1983). Mutations affecting [vulval muscle](#) function can be enriched for by prescreening for animals that fail to lay eggs and thus retain their eggs internally. A secondary screen can then be carried out to identify specific defects in [vulval muscle](#) (M. Stern and H.R. Horvitz, pers. comm.). The resulting genes are designated "[sem](#)" for [sex](#) muscle abnormality (some are called "[egl](#)" for egg-laying-defective). From these screens (Stern and Horvitz 1991; Garriga and Stern 1994; M. Stern, pers. comm.), mutations have been isolated that affect the generation and cell fate of sex muscle precursors (sex myoblasts) during larval development ([egl-31](#), [sem-1](#), [sem-4](#)), the divisions of sex myoblasts ([sem-1](#)), sex myoblast migrations ([egl-15](#), [egl-17](#); Stern and Horvitz 1991), and the attachment orientation of the vulval muscles ([unc-53](#); T. Bogaert, pers. comm.). The [sem-2](#) and [sem-4](#) genes have been proposed to cause presumptive sex myoblasts to adopt characteristics of body-wall muscle fate (M. Stern, pers. comm.). [sem-4](#) encodes a zinc-finger-containing factor that has roles in a variety of [neural](#) tissues in addition to muscle (Basson and Horvitz 1996). The [sem-2](#) locus may likewise be more general than just sex myoblast differentiation, since lethal mutations have been isolated that exhibit defective anterior body-wall muscles (C. Colledge and R.H. Waterston, pers. comm.).

Genetic screens for components affecting [pharyngeal muscle](#) development have likewise begun (Schnabel and Schnabel 1990; Avery 1993a; Mango et al. 1994a). So far, two mutations from these screens are of particular interest from the perspective of commitment. Both of these define zygotically acting genes required for all tissues within the [pharynx](#). [pha-1](#) encodes a putative DNA-binding protein required for complete differentiation of both muscle and nonmuscle tissue (Granato et al. 1994). The mutant animals produce only a rudimentary [pharynx](#). [pha-1](#) is evidently not required for [pharyngeal muscle](#) cell commitment, since the mutant embryos can still express [ceh-22](#) and low levels of pharyngeal myosin (P. Okkema, pers. comm.). [pha-4](#) mutants have a much more dramatic effect on pharyngeal development. Mutants lack an evident [pharynx](#) and all known pharyngeal markers, both muscle and nonmuscle (Mango et al. 1994a). It will be of interest to determine the connection among PHA-1, PHA-4, and the [pharynx](#)-specific (muscle+nonmuscle) enhancer subelements such as that upstream of [myo-2](#) (Okkema and Fire 1994).

A second type of functional screen seeks factors that can promote muscle differentiation when expressed ectopically. Transformation technology in *C. elegans* is inadequate to implement such a screen solely in *C. elegans*: As an alternative, Krause and colleagues have been isolating homologs of two classes of vertebrate myogenic factors that had been shown to promote muscle differentiation in tissue culture cells. The most extensively characterized family of vertebrate myogenic factors are the MyoD subfamily of helix-loop-helix (HLH) transcription factors. *C. elegans* apparently contains only a single member of this HLH subfamily (Krause et al. 1990; Chen et al. 1992). This factor (designated HLH-1) has a striking expression pattern, with expression activated in mid-stage embryonic cells whose clonal descendants will give rise only to striated muscles. This suggests that a myogenic program has indeed been activated in these cells and nominates *HLH-1* as a candidate execution factor for such a program. Mutational analysis indicates that *HLH-1* is not the only execution factor in this program. Striated muscle differentiation proceeds in mutant animals lacking *HLH-1*, with the number and overall grouping of the resulting muscle cells apparently normal (Chen et al. 1992, 1994). The resulting muscles contract only poorly, so that the animals are inviable.

The analysis of [hlh-1](#) function in *C. elegans* contrasts somewhat with similar studies in mice, where a double knockout of two myoD family members results in loss of muscle tissue (Rudnicki et al. 1993). The apparent paradox between the two systems is magnified in that the *C. elegans* factor can function in vertebrate tissue culture cells to promote muscle differentiation (Krause et al. 1992), and at least one of the vertebrate family members (myogenin) can substitute for *C. elegans* [hlh-1](#) (Chen et al. 1994). This paradox might reflect a fundamental difference in the primary function in the two species or alternatively could reflect distinct cellular consequences (cells absent vs. abnormal) resulting from a similar primary defect in the muscle differentiation program.

A second family of vertebrate myogenic factors, the "MEF2" family of MADS box factors ([Yu et al. 1992](#)), appears also to have a single *C. elegans* homolog (M. Park and M. Krause, pers. comm.; see [McGhee and Krause](#), this volume). In *Drosophila*, zygotic expression of the single [\*mef-2\*](#) homolog has been shown to be necessary for all muscle differentiation (Bour et al. 1995; Lilly et al. 1995). Embryos homozygous for deficiencies removing the known *C. elegans* [\*mef-2\*](#) homolog can still initiate muscle differentiation (J. Ahnn and A. Fire, unpubl.; M. Krause, pers. comm.). These deficiencies also delete considerable numbers of flanking genes, complicating further interpretation of the arrest phenotype. As point mutations in the locus become available, it should become clear what role this locus might have in myogenesis.

Searches based solely on expression pattern offer the possibility of directly obtaining genes that act at early stages in the myogenic pathway. A "gene-trap" screen ([Hope 1991](#)), as well as more directed schemes for expression pattern screening (Lynch et al. 1995), should be useful in this regard. Monoclonal antibody screens provide a variant of this approach. Two components with intriguing expression patterns have been identified in these screens. The glyoxylate cycle enzyme complex isocitrate lyase/ maleate synthetase (Liu et al. 1995) appears in myogenic lineages (although not exclusively), coincident with the onset of differentiation, and an unidentified protein recognized by the 3NB12 antibody appears in postcleavage pharyngeal precursors (Okamoto and Thomson 1985). Although the functional significance of these molecules is unclear, they provide useful markers for assessment of early muscle commitment events. In the case of [\*hlh-1\*](#), it has been instructive to view the gene as a marker for body-wall muscle cell commitment, leading to an investigation of regulatory sequences generating the myogenic precursor expression pattern. These studies have suggested that distinct lineage-specific signals in the [\*hlh-1\*](#) promoter are responsible for the complete expression pattern (Krause et al. 1994). The corresponding regulatory components are likely to be the more general mesoderm-specifying or blastomere-specifying factors that act in combination to generate the myogenic pattern.

## Figures

Figure 13. Striated body-wall muscle cells shown by position in the four muscle quadrants.

### Figure 13

Striated body-wall muscle cells shown by position in the four muscle quadrants. The diagram is designed to show an animal as it would look cut along the dorsal midline and splayed out laterally. Colors represent lineal origin: (Red) Embryonic [C lineage](#); (blue) embryonic [MS lineage](#); (purple) embryonic [AB lineage](#); (green) embryonic [D lineage](#). Yellow cells are derivatives of the [M](#) mesoblast that are born postembryonically. (Redrawn, with permission, from [Sulston and Horvitz 1977; Sulston et al. 1983](#).)

Figure 14. Early cell lineage of *C.*

### Figure 14

Early cell lineage of *C. elegans* showing the early founder cells that give rise to embryonic muscles and the number and types of these muscles. (Adapted, with permission, from [Sulston et al. 1983](#).)

Figure 15. Organization of the pharyngeal musculature into eight cell groups, [m1–m8](#), also called pm1–pm8 (see Avery and Thomas, this volume).

### Figure 15

Organization of the pharyngeal musculature into eight cell groups, [m1–m8](#), also called pm1–pm8 (see [Avery and Thomas](#), this volume). Anterior is at top; posterior is at bottom. The approximate shape of individual muscle cells is indicated; shaded circles indicate positions of [pharyngeal muscle](#) nuclei. [m1](#) is a single cell encircling the entire [pharynx](#) that contains three pairs of nuclei located in posterior bulges. Muscle groups [m2–m7](#) each consists of three cells in threefold radial symmetry. [m8](#) is a single, toroidal mononucleate cell at the posterior end of the [pharynx](#). Each cell of the [m2](#), [m3](#), [m4](#), and [m5](#) classes is binucleate, whereas the [m7](#) and [m8](#) cells are

mononucleate. (Redrawn, with permission, from Albertson and Thomson 1976 with corrections in the shape of [m2](#) as described by L. Avery [pers. comm.].)

Generated from local HTML

## **Chapter 16. Muscle: Structure, Function, and Development — Acknowledgments**

---

We thank the many members of the *C. elegans* muscle community for sharing their ideas and information. Valuable contributions to this manuscript have come from J. Ahnn, P. Anderson, L. Avery, R. Barstead, M. Basson, G. Benian, T. Bogaert, B. Bucher, J. Bush, C. College, D. Cowing, H. Epstein, R. Francis, B. Harfe, M. Gilbert, E. Hedgecock, P. Hoppe, B. Horvitz, C. Hresko, C. Hunter, V. Jantsch-Plunger, H. Kagawa, C. Kenyon, J. Kiff, M. Krause, M. Montgomery, G. Mullen, K. Norman, P. Okkema, R. Plasterk, J. Plenefisch, J. Priess, T. Rogalski, A. Rushforth, L. Schriefer, G. Seydoux, S. Sprunger, M. Stern, J. Sulston, R. Waterston, B. Williams, and S. Xu. We also thank G. Mullen and J. Bush for help with the figures. D.G.M. also wishes to thank Ralf and Heinke Schnabel for their hospitality during the early stages of this review.

Generated from local HTML

# **Chapter 17. Extracellular Matrix**

---

## **Contents**

[I Introduction](#)

[II Cuticle](#)

[III Basement Membranes](#)

[IV Conclusions](#)

[Acknowledgments](#)

Generated from local HTML

## Chapter 17. Extracellular Matrix — I Introduction

---

All metazoans produce extracellular matrices (ECMs) composed of complex mixtures of glycoproteins and carbohydrates. The structures and compositions of these matrices differ in different tissues, in regions of the same tissue, and at different times in development. ECMs can have many functions such as strengthening tissues under physical stress, acting as barriers that inhibit cell migration or substrates upon which cells migrate, serving as molecular filters, and providing signals that alter cell differentiation. Two types of ECMs have been identified in *Caenorhabditis elegans*: the cuticle and basement membranes. The cuticle covers the outside of the animal and lines the stomodeum and [rectum](#). Basement membranes cover most internal organs, separating them from the pseudocoelomic cavity. Although most metazoans contain interstitial matrix that lies between the cells within tissues, no interstitial matrix is seen in *C. elegans* or apparently in other nematodes.

*C. elegans* is an excellent system for genetic analysis of ECM structure and function. Many of the same molecules found in mammalian ECM (collagens, proteoglycans, laminins) have been identified in *C. elegans*, and for the most part, their sequences have been highly conserved. The simple, well-defined anatomy and powerful genetics of *C. elegans* allow for detailed analyses of ECM function that complement the intensive biochemical analyses performed in mammals. This chapter reviews the composition and genetic and molecular studies of the cuticle and basement membranes of *C. elegans*. Other reviews also describe molecular and genetic analyses of *C. elegans* (Edgar et al. 1982; Cox 1992; Johnstone 1994; Kramer 1994a,b) and mammalian (Yurchenco and Schittny 1990; Paulson 1992; Adams and Watt 1993; Hudson et al. 1993; Tilstra and Byers 1994; [Prockop and Kivirikko 1995](#)) extracellular matrix.

Generated from local HTML

## Chapter 17. Extracellular Matrix — II Cuticle

---

The cuticle is the animal's exoskeleton and is important for maintenance of morphology, protection from and/or interaction with the external environment, and motility. The cuticle is connected to the [hypodermis](#) via hemidesmosomes. Filaments extend from body wall muscles through the basement membrane and connect to the [hypodermis](#) ([Francis and Waterston 1985](#); [Francis and Waterston 1991](#)). It is through these connections that the force of muscle contraction is transmitted to the cuticle. Nematodes do not have opposing muscles. The elasticity of the cuticle and the animal's high internal hydrostatic pressure provide the restorative force that allows the animal to straighten after contracting muscles on one side of the body (like a water-filled balloon). The cuticle is a highly complex extracellular structure, presumably due to the many functions it must perform.

### A. Cuticle Structure

The cuticle has both surface specializations and internal layers that can differ at different developmental stages. Protruding ridges, termed alae, form over the left and right lateral rows of [hypodermal seam cells](#). The L1-, dauer-, and adult-stage alae have distinct structures; however, alae are not present on L2, L3, or L4 cuticles ([Cox et al. 1981b](#)). Ablation of [seam cells](#) with a laser microbeam causes gaps in the overlying alae, indicating that [seam cells](#) are responsible for formation of the alae ([Singh and Sulston 1978](#)). The surfaces of all cuticles have narrow circumferential indentations, uniformly spaced about 1  $\mu\text{m}$  apart, that define rings called annuli (Figs. [1](#) and [2](#)). Annuli run continuously around the animal but are absent over the lateral hypodermal cords. Annuli may function like pleats, allowing the cuticle to fold on the inner radius of a bend and extend over the outer radius.

The ultrastructure of the adult cuticle has been most carefully characterized. Six layers (epicuticle, external cortical, internal cortical, medial, fiber, and basal) have been identified in the adult cuticle, although not all layers are well defined using any one fixation/staining technique (Figs. [1](#) and [2](#)) ([Cox et al. 1981a,b](#); Peixoto and de Souza 1992). In addition, a loosely associated, carbohydrate-rich surface coat external to the epicuticle can be detected using specific fixation and staining methods (Zuckerman et al. 1979; Blaxter et al. 1992; Blaxter 1993a). The structure of the epicuticle is not well understood. It is trilaminar in appearance (two electron-dense layers separated by an electron-lucent layer), and evidence from studies on other nematodes indicates that it contains lipid. The epicuticle of *C. elegans* can be fractured into two faces, suggesting a bilayer structure, but its properties are distinct from those of plasma membranes (Blaxter 1993a; [Maizels et al. 1993](#); Peixoto and de Souza 1994).

The medial layer is composed of filamentous columns of material, termed struts, that connect the cortical and fiber layers. Struts spaced about 0.4  $\mu\text{m}$  apart form two rows located on either side of the annular indentations ([Fig. 1](#)). A smaller number of struts are found scattered between the annular indentations. The space between the struts is presumably filled with fluid. The fiber layer contains two highly organized layers of fibers that spiral around the animal in opposite directions. Each layer is oriented at about 65° from the long axis, with the outer layer running counterclockwise and the inner layer running clockwise relative to the animal's tail-to-head axis.

L1-, dauer-, and adult-stage cuticles are structurally distinct and differ from the L2, L3, and L4 cuticles, which are very similar in structure ([Cox et al. 1981b](#)). The cuticles from all stages have epicuticle, external, and internal cortical layers, although the structure of the layers can differ between stages. A distinct medial layer with struts is only apparent in the adult cuticle. The L2–L4 and adult cuticles have similar-appearing fiber layers. In place of a fiber layer, the L1 and dauer larva cuticles have a striated layer characterized by darkly staining bands of about 18 nm periodicity. The striations in the dauer larva cuticle are broader and more distinct than those in the L1. Glancing sections through the dauer larva cuticle show that the striated layer is composed of interwoven orthogonal fibers or laminae ([Popham and Webster 1978](#); [Cox et al. 1981b](#)). The dauer larva cuticle is especially thick, accounting for 10.2% of the animals' cross-sectional area versus 4.4% for the cuticle of other stages.

### B. Molting

At the end of each larval developmental stage, nematodes undergo a molt in which a new cuticle is formed and the old cuticle is shed ([Singh and Sulston 1978](#)). At molts, animals enter a period of lethargus lasting

approximately 2 hours, during which pharyngeal pumping and movement are suppressed. Two to four hours preceding lethargus, the cytoplasm of the lateral [seam cells](#) accumulates densely packed Golgi bodies. At the beginning of lethargus, connections between the [hypodermis](#) and cuticle are broken and a new cuticle begins forming. During the second half of lethargus, animals frequently spin or flip around their long axis. About 30 minutes before ecdysis (shedding of the old cuticle), the posterior bulb of the [pharynx](#) begins twitching and granules accumulate in the g1 pharyngeal gland cell bodies (Hall and Hedgecock 1991). Just preceding ecdysis, the granules are secreted and the [pharynx](#) begins spasmodic contractions. The cuticle lining the [pharynx](#) breaks, the old cuticle distends around the head, and the animal pulls back repeatedly to dislodge the cuticle remaining in the [pharynx](#). The animal pushes with its head until the old cuticle breaks and then crawls out of the remainder of the old cuticle.

Circumferential microfilament bundles form in the [hypodermis](#) at larval molts and disperse between molts (B. Draper and J. Priess, pers. comm.; J. Kramer, unpubl.). These filament bundles appear to assume structural functions of the cuticle during molting and may have an important role in defining cuticle structure. During the second half of embryogenesis, similar bundles of circumferential microfilaments and microtubules form immediately under the apical plasma membrane of the [hypodermis](#) (Priess and Hirsh 1986). These filament bundles are involved in elongation of the embryo, and they define the location of the circumferential indentations of the cuticle that delimit annuli. Just prior to hatching, the filaments disperse, and maintenance of morphology shifts to the newly formed cuticle.

## C. Cuticle Composition

In accord with its role in protection from the external environment, the cuticle is highly resistant to solubilization. The standard method for preparation of cuticles is to boil sonicated animals in 1% SDS. This treatment solubilizes essentially all other structures, leaving cuticles as the insoluble residue. Cuticles prepared in this manner retain their original ultrastructure remarkably well ([Cox et al. 1981a](#)). Treatment of the SDS-insoluble material with reducing agent solubilizes 70–75% of adult and L4-, 44% of L1-, and 26% of dauer-stage cuticle proteins ([Cox et al. 1981b](#)). Cuticle proteins are extensively cross-linked with disulfide bonds and also with nonreducible tyrosine-derived cross-links (see below). Solubilized cuticle proteins can be separated into about eight major and numerous minor molecular weight species on SDS-PAGE. The estimated molecular weights of the soluble cuticle proteins range from 53,000 to more than 200,000, with the majority being 90,000 and greater. Overlapping, but distinct, molecular weight forms are found in extracts from cuticles of different stages.

Most of the soluble cuticle proteins are digested by treatment with bacterial collagenase, indicating that they are collagenous in nature. The high glycine and imino acid content of adult soluble cuticle proteins (26% glycine, 11% proline, 12% hydroxyproline) is also consistent with a largely collagenous nature ([Cox et al. 1981a,b](#); Ouazana and Herbage 1981; Ouazana et al. 1984). The insoluble cuticle proteins have lower, although still substantial, glycine and hydroxyproline content (22% glycine, 13% proline, 7.5% hydroxyproline), indicating the presence of less collagenous material. A small amount of hydroxylsine, which is a common constituent of vertebrate collagens, is found in dauer larva cuticles but not at other stages. The soluble cuticle proteins exhibit two unusual properties that have also been noted for vertebrate collagens; they run at different apparent molecular weights on gels of different polyacrylamide concentration, and they stain pink with Coomassie brilliant blue R-250. Both the soluble and insoluble cuticle fractions contain a small amount of carbohydrate, about 1% by weight ([Cox et al. 1981c](#)).

## D. Cuticle Collagen Structure and Regulation

### 1. Gene Family

The collagens that constitute the major elements of the cuticle are encoded by an unusually large gene family estimated to contain between 50 and 150 genes ([Cox et al. 1984](#)). This estimate is based on the ratio of the number of collagen to actin-hybridizing clones in *C. elegans* genomic phage libraries, given that there are four actin genes in the genome. The genes are distributed throughout the genome, with multiple members mapping

to each chromosome (Cox et al. 1985). In general, the genes are dispersed, but there are examples of two or more collagen genes in close proximity ([Park and Kramer 1990](#); [Bird 1992](#); [Levy et al. 1993](#)). Collagen genes in close proximity usually show strong sequence similarity, as would be expected if they arose by gene duplication. However, not all gene pairs that have high sequence similarity are in close proximity.

## 2. Protein Structure

Complete genomic DNA sequences for more than 30 cuticle collagen genes have been determined ([Kramer et al. 1982, 1988, 1990](#); [von Mende et al. 1988](#); [Cox et al. 1989](#); [Park and Kramer 1990](#); [Bird 1992](#); [Johnstone et al. 1992](#); [Levy and Kramer 1993](#); [Levy et al. 1993](#)), and the genome sequencing project is adding to this number rapidly (Waterston and Sulston 1995). In general, the genes are small (<2 kb) and have just one to three short introns. The collagen chains they are predicted to encode range from 26 kD to 35 kD, with one exceptional gene that is predicted to encode a 107-kD product. All of the cuticle collagen chains have similar domain structures and several conserved motifs ([Fig. 3](#)). There is a long amino non-Gly-X-Y domain that is of variable length, a central Gly-X-Y repeat domain, and a variable length carboxyl non-Gly-X-Y domain.

Starting near the amino terminus are four short sequence motifs that are conserved in most or all cuticle collagens, named homology blocks D-A (HBD-A) in the amino to carboxyl direction ([Fig. 4](#)). HBD is very hydrophobic and is located within the predicted signal peptide. HBD is highly conserved in the [col-1](#) and [col-6](#) cysteine subfamilies (see below), but only weakly conserved in others. HBC is located six amino acids to the carboxyl side of HBD, and in most cases, it spans the predicted site for signal peptidase cleavage. HBB follows six amino acids after HBC, and it contains a conserved tryptophan, the only tryptophan in many of the cuticle collagens. About one half of the 38 cuticle collagen genes considered here ([Fig. 3](#)) have an intron between positions 6 and 7 of HBB. This is the only obviously conserved intron in the entire cuticle collagen gene family. HBA is located 19–44 amino acids after HBB, and it contains highly conserved arginine residues that constitute an endoproteolytic processing site (see below). The sequences between homology blocks do not have strongly conserved residues. However, since the spacing between HBD, HBC, and HBB is conserved, these blocks may constitute a single functional unit in the cuticle collagens. Mutations in HBC and HBA have been shown to affect collagen function ([Kramer and Johnson 1993](#); [Levy et al. 1993](#); [Yang and Kramer 1994](#)).

The region from HBA to the start of the Gly-X-Y repeat domain is highly variable in length (15–318 amino acids) and sequence. Closely preceding the Gly-X-Y domain, there are three cysteines in all but one collagen which has two cysteines. The Gly-X-Y repeat domain is broken into two major sections. The first section generally contains 10 repeats and is followed by an interruption of 10–21 amino acids that contains two or three cysteines. The second Gly-X-Y section contains about 40 repeats and can have one to three interruptions of from two to eight amino acids each. Closely following the end of the Gly-X-Y repeat domain are two cysteine residues in all cuticle collagens. The remainder of the carboxyl non-Gly-X-Y domain is short (9–19 amino acids) and conserved in the [col-1](#) and [col-6](#) subfamilies, but quite variable in length (13–393 amino acids) and sequence in other collagens.

The cuticle collagens can be divided into subfamilies based on the spacing of the cysteine residues that flank the Gly-X-Y domain ([Fig. 5](#)). Currently, there are nine cysteine subfamilies, but the number is likely to increase as more sequences are generated. Collagens in the same subfamilies generally have more sequence similarity to each other than to collagens in other subfamilies. The cysteine spacings are likely to be important for directing the formation of disulfide bonds between appropriate molecules in the cuticle. Whether cuticle collagen molecules form from three identical chains (homotrimeric) or a mix of nonidentical chains (heterotrimeric) has not been determined. Both homotrimeric and heterotrimeric collagens have been described in vertebrates, and it is possible that the cuticle contains both homotrimeric and heterotrimeric collagens.

Cuticle collagen gene sequences have been examined in several other nematode species. These collagens have all of the same conserved domain structures and sequence motifs that are found in *C. elegans*. One complete and two partial cuticle collagen sequences from the sheep parasite *Haemonchus contortus* have all of the conserved aspects of the [col-1](#) subfamily ([Shamansky et al. 1989](#); [Cox 1990](#); [Cox et al. 1990](#)). Partial sequences of two cuticle collagen genes from the pig parasite *Ascaris suum* (Kingston et al. 1989; Kingston and Pettitt 1990) and the complete sequence of one gene from the human parasite *Brugia malayi* (Scott et al. 1995) fit in the [col-6](#)

subfamily. The complete sequence of a cuticle collagen from the root knot nematode, *Meloidogyne incognita*, places it in the [\*col-8\*](#) subfamily (Vandereycken et al. 1994). On the basis of the numbers of Gly-X-Y hybridizing bands on genomic Southern blots, the size of the cuticle collagen gene families may be smaller in these parasitic nematodes than in *C. elegans*. However, the strong conservation of cuticle collagen structure among these diverse nematodes suggests that the roles of collagens in cuticle function have been conserved throughout the phylum.

### 3. Gene Expression

Synthesis of cuticle proteins occurs at high rates during molts and at lower rates between molts ([Cox et al. 1981c](#)). The levels of some cuticle collagen transcripts follow this same pattern ([Park and Kramer 1994](#)). Different members of the cuticle collagen gene family are expressed at different developmental stages. Two-dimensional gel analyses of  $^3\text{H}$ -proline-labeled in vitro translation products of RNA from the L4-adult- and L2d-dauer-stage molts identified at least 60 distinct collagenase-sensitive products in the 37,000 to 52,000 range (Politz and Edgar 1984). These apparent molecular weights are probably higher than expected (26,000–35,000) due to the fact that collagens migrate abnormally on SDS-PAGE (Furthmayr and Timpl 1971; Freytag et al. 1979). The number of spots on the gels is clearly an underestimate of the number of collagens expressed at these two molts, since different gene products may comigrate and a large class of collagens with more basic pIs would not have been detected (J. Kramer, unpubl.). Of the 32 collagenous products from L4 and 29 from L2d-dauer-stage molt RNA, only 3 were found in both molts. RNAs isolated early versus late in the L4 molt generate different sets of collagenase-sensitive products (Politz and Edgar 1984). Thus, there are qualitative and quantitative differences in collagen expression both between molts and at different times during a molt.

Expression of 20 cuticle collagen genes has been examined using several different techniques: hybridization of genomic collagen clones with labeled cDNA generated from poly(A) RNAs isolated from molting animals (Cox and Hirsh 1985), Northern hybridization with gene-specific probes (Kramer et al. 1985; [Park and Kramer 1990, 1994](#)), analysis of *lacZ* reporter constructs in transgenic animals (Liu and Ambros 1991; Liu et al. 1995), and reverse transcriptase–polymerase chain reaction (RT-PCR) ([Levy and Kramer 1993](#)). The results of these studies are summarized in a nonquantitative manner in [Table 1](#). Nine different expression patterns are indicated in the table, but this is certainly an underestimate since most studies have not looked at RNA from all stages or from different times within a molt or between molts. Additionally, there are large quantitative differences in expression between different collagen genes and for the same gene at different stages. Further complexity arises from studies of collagen promoter-*lacZ* reporters that show expression in different subsets of hypodermal nuclei (Liu and Ambros 1991; Liu et al. 1995; I. Johnstone, pers. comm.; J. Kramer, unpubl.). The combination of temporal, quantitative, and spatial expression controls with the large number of cuticle collagen genes makes for a potentially bewildering level of complexity.

### 4. Nonreducible Cross-links

The primary translation products of the cuticle collagens have, with one exception, predicted molecular masses of 26–35 kD, but the collagens extracted from cuticles have apparent molecular weights of 53,000 and larger. Some of this discrepancy is due to the abnormal migration of collagens on SDS-PAGE. However, the major cause is the presence of nonreducible covalent cross-links between collagen chains. Vertebrate collagens contain nonreducible cross-links that form between modified lysine residues. In contrast, the cross-links that have been identified in *Ascaris* ([Fujimoto 1975; Fujimoto et al. 1981](#)) and *C. elegans* (D. Eyre and J. Kramer, unpubl.) cuticles are di-, tri-, and/or isotryptophane residues. In *Ascaris* cuticles, isotryptophane is primarily found in cuticle collagens, and di- and triptophane in cuticlin. Cuticlin is defined as the insoluble cuticle residue that remains after extraction with reducing agents. After incubation of *Ascaris* in  $^3\text{H}$ -labeled tyrosine-containing medium, 20% of tyrosine incorporated into the cuticle was in the form of dityrosine and 6% was isotryptophane (Fetterer et al. 1993). The rate of formation of dityrosine was greater in the  $\beta$ -mercaptoethanol-insoluble (cuticlin) fraction of the cuticle and that of isotryptophane was greater in the soluble fraction, consistent with the distribution of the cross-links noted above. Formation of the cross-links was inhibited by several peroxidase inhibitors, suggesting the

involvement of a peroxidase in their formation. Indeed, formation of dityrosine cross-links in the sea urchin fertilization envelope has been shown to be dependent on oxidation of tyrosine residues by ovoperoxidase (Deits et al. 1984).

During molting in *C. elegans*, low-molecular-weight (38,000–52,000) collagenase-sensitive proteins can be detected on Western blots using antisera produced against high-molecular-weight (53,000 to greater than 200 kD) adult cuticle proteins (Politz et al. 1986), suggesting conversion of low- to high-molecular-mass products. Western blots of cuticle extracts probed with antiserum specific for the SQT-1 cuticle collagen show that low-molecular-weight forms of SQT-1 are most abundant at molts and are replaced by higher-molecular-weight forms following the molt (J. Yang and J. Kramer, unpubl.). A cross-link containing tryptic peptide was isolated from *C. elegans* cuticles, and its sequence was found to be identical to the carboxyl end of COL-2 (*col-1* cysteine subfamily in [Fig. 5](#)), with the tyrosine located between the conserved cysteines involved in the cross-link (D. Eyre and J. Kramer, unpubl.). Generally, a single conserved tyrosine residue is found in the carboxyl non-Gly-X-Y domain of most cuticle collagens, and these are likely to be involved in cross-linking. Tyrosine residues in the amino non-Gly-X-Y domain must also be involved in cross-linking to account for the very high-molecular-weight multimers that form in the cuticle.

Rotary shadowing of collagens extracted from *Ascaris* cuticle under reducing conditions primarily shows individual 47-nm-long molecules ([Betschart and Wyss 1990](#)). The dimensions of these molecules match those expected for triple-helical molecules formed from products of the known cuticle collagen genes. Extraction of *Ascaris* cuticle under nonreducing, nondenaturing conditions results in long fibers that appear to be chains of triple-helical molecules. These results suggest that isotryptophane cross-links primarily form between the three chains within a collagen molecule and that multiple molecules are linked end-to-end via disulfide bonds. The formation of higher-molecular-weight nonreducible material would result from further tyrosine cross-link formation occurring after the intramolecular cross-links had formed.

## E. Cuticle Genetics

A large number of mutations have been identified that cause gross changes in the animal's overall morphology and may result from defects in cuticle function ([Brenner 1974](#); [Higgins and Hirsh 1977](#); [Cox et al. 1980](#); [Hosono 1980](#); [Hosono et al. 1982](#); [Kusch and Edgar 1986](#)). These mutations can cause a variety of phenotypes, including blister (Bli), blisters on cuticle; dumpy (Dpy), short and fat; long (Lon), long and thin; left roller (LRol), twisted in a left-handed helix; and right roller (RRol), twisted in a right-handed helix (Figs. [6](#) and [7](#)). Additionally, mutations that cause dominant Rol and recessive Dpy phenotypes have been termed squat (Sqt). Combinations of these phenotypes can occur, e.g., dumpy and left roller (DLR), and the severities of the phenotypes can vary widely. There are currently 6 *bli* genes, 27 *dpy* genes, 3 *lon* genes, 6 *rol* genes, and 3 *sqt* genes. Five of the *dpy* genes are involved in X chromosome dosage compensation (see [Meyer](#), this volume) and only affect cuticle function indirectly. The *dpy* gene designation can also be misleading since many *dpy* genes have alleles that result in Rol and/or DpyRol, or Dpy, phenotypes. There is no evidence for lineage changes in these mutants, and their phenotypes appear to result from altered cell shape and position. In roller animals ([Fig. 7](#)), the cuticle and all of the internal organs are helically twisted ([Higgins and Hirsh 1977](#)). Roller animals rotate around their long axes and tend to move in circles. The fact that these severely abnormal animals can reproduce is testimony to the value of using a self-fertilizing hermaphroditic species for genetic studies, since most of these phenotypes render males incapable of mating.

Mutations in many of these genes only show phenotypes at particular developmental stages, and in some cases, the phenotype of a single allele can differ at different stages. For example, *sqt-1(e1350)* heterozygotes are RRol at all stages from L2 to adult, whereas homozygotes are wild type at L2, weak RRol at L3, weak Dpy at L4, and Dpy as adults ([Cox et al. 1980](#); [Park and Kramer 1994](#)). Passage through the dauer larva stage can also affect the phenotype of some *sqt-1* and *sqt-2* alleles; *e1350* homozygotes are variable RRol at L2d and dauer stages, as are adults that develop from dauer larvae. The phenotype is considered variable because individual animals range from strong Rol to apparently wild type. This stage specificity of phenotypes is likely to result from stage-specific expression of the particular gene as well as the influence of other gene products expressed at the same stages.

## F. Mutations in Cuticle Collagens

Several of the genes that are involved in determination of overall morphology have been shown to encode cuticle collagens ([Table 2](#)): [\*sqt-1\*](#) (Kramer et al. 1988; [Kramer and Johnson 1993](#)), [\*dpy-13\*](#) ([von Mende et al. 1988](#)), [\*rol-6\*](#) (Kramer et al. 1990; [Kramer and Johnson 1993](#)), [\*dpy-7\*](#) ([Johnstone et al. 1992](#)), [\*dpy-2\*](#) ([Levy et al. 1993](#)), [\*dpy-10\*](#) ([Levy et al. 1993](#)), and [\*sqt-3\*](#) ([Vanderkeyl et al. 1994](#)). Mutations in these cuticle collagens can generate all of the morphological phenotypes noted above and can additionally cause abnormal hermaphrodite tail morphology (Tal). The range of phenotypes indicates that these collagens can have different functions in the cuticle and that different mutations in a single collagen can alter its function in different ways.

Collagen chains with amino acid substitutions can aberrantly participate in the assembly pathway and interfere with normal collagen processing and assembly. For this reason, null mutations are critical for determining the function of a collagen. Null mutations in [\*sqt-1\*](#) and [\*rol-6\*](#) cause very weak phenotypes, Tal or very weak Dpy. Thus, the absence of these collagens has only a minor effect on morphology, even though the presence of abnormal SQT-1 or ROL-6 can produce severe morphological abnormalities. In contrast, null mutants of [\*dpy-10\*](#) or [\*dpy-13\*](#) have strong phenotypes, DLR or Dpy, demonstrating that these collagens are required for normal morphology.

In all organisms and collagens examined, the vast majority of collagen missense mutations are substitutions of glycine residues in the Gly-X-Y repeat domains. Commonly, glycine substitutions inhibit triple-helix formation, resulting in abnormal modification and degradation of much of the mutant collagen chain, as well as other chains associated with it ([Prockop and Kivirikko 1995](#)). As a result, a reduced amount of abnormal collagen is secreted into the matrix. Glycine substitutions cause weak phenotypes in [\*sqt-1\*](#) but strong phenotypes in other genes. In the three genes that have both null and glycine substitution mutations, the phenotypes of both types of mutations are generally similar, possibly reflecting severe reduction in collagen level in both cases. However, the glycine substitution phenotypes are slightly more severe than the null phenotypes (weak Lon and weak LRol phenotypes for [\*sqt-1\*](#), and a more severe DLR in [\*dpy-10\*](#)). Since glycine substitutions result in more severe phenotypes than null mutations, the abnormal collagens must interfere with the function of other molecules involved in cuticle synthesis, assembly, or structure.

### 1. Mutations Affecting Homology Blocks A through C

Substitutions for the highly conserved arginine residues at homology block A positions 2 and 5 (see [Fig. 4](#)) have been identified in [\*sqt-1\*](#), [\*rol-6\*](#), and [\*dpy-10\*](#) ([Kramer and Johnson 1993](#); [Levy et al. 1993](#)). Replacement of arginine with cysteine in [\*sqt-1\*](#) causes a dominant RRol, recessive Dpy phenotype, whereas the equivalent [\*dpy-10\*](#) mutant is dominant LRol, recessive DLR. The arginine to cysteine substitution in [\*rol-6\*](#) is semidominant RRol, whereas the arginine to histidine substitution is recessive RRol. The fact that the same mutation that causes RRol in [\*sqt-1\*](#) and [\*rol-6\*](#) causes the opposite, LRol, phenotype in [\*dpy-10\*](#) suggests that these collagens function in a mirror image manner. The two fiber layers in the cuticle are mirror image structures that spiral around the animal in opposite directions. Possibly, SQT-1 and ROL-6 are localized in one of the fiber layers and DPY-10 in the other.

Transgenic analyses of in-vitro-generated [\*sqt-1\*](#) and [\*rol-6\*](#) mutations indicate that arginine or lysine is required at positions 2 and 5 of HBA for normal collagen function ([Yang and Kramer 1994](#)). The spacing of the conserved arginine residues in HBA suggests that they could form the cleavage site for a subtilisin-like endoproteinase (see [\*bli-4\*](#) below). Western blot analyses using SQT-1-specific antisera show that HBA mutant forms of SQT-1 are larger than wild type by the amount expected if cleavage normally occurs at HBA and that sequences amino-terminal to HBA are retained in mutant but not wild-type SQT-1 (J. Yang and J. Kramer, unpubl.). These results indicate that cuticle collagens are synthesized as procollagens that are endoproteolytically processed at HBA to remove the amino-terminal pro-domain during their maturation. HBA mutant collagens retain the pro-domain, and this could interfere with their further processing and assembly into higher-order structures. Many, although not all, vertebrate collagens are also proteolytically processed during their maturation; however, the use of a subtilisin-like protease for this purpose is unique to nematodes. The inability to remove the amino pro-domain of vertebrate type I collagen causes dermatosparaxis, a fragile skin disease in which incorporation of the abnormal chains inhibits formation of collagen fibers (Smith et al. 1992).

Three ethylmethanesulfonate (EMS)-induced recessive LRol mutations of *sqt-1* are substitutions of the first of the two conserved carboxyl domain cysteines (Figs. 3 and 5) with tyrosine or serine. Analyses of in-vitro-generated mutations show that replacement of either of these two cysteine residues with serine in *sqt-1* or *rol-6* causes an LRol phenotype, although the phenotype is less severe for *rol-6* (Yang and Kramer 1994). Assembly of some vertebrate collagens requires disulfide bonding between the carboxyl domains of the three chains. Replacement of both carboxyl domain cysteine residues with serine in *sqt-1* also results in an LRol phenotype. Since this is a non-null phenotype, carboxyl domain disulfide bonding is not essential for assembly of SQT-1, although it is necessary for normal SQT-1 function. Western blot analyses of cuticle extracts from *sqt-1* LRol mutants show that nonreducible cross-link formation is severely inhibited (J. Yang and J. Kramer, unpubl.). A tyrosine immediately precedes the first carboxyl cysteine in both SQT-1 and ROL-6 (Fig. 5). Apparently, loss of the ability to form the adjacent disulfide bond inhibits cross-link formation at this tyrosine residue.

An unusual mutation has been identified in homology block C (Fig. 4) of *dpy-10* (Levy et al. 1993). The *dpy-10(m481m482)* mutation was generated by a Tc1 excision (see Plasterk and van Leunen, this volume) that resulted in the deletion of an isoleucine codon at position 5 of HBC (Levy et al. 1993). This allele causes no apparent abnormal phenotype, but it fails to complement other *dpy-10* alleles. Loss of the isoleucine residue may interfere with signal peptide cleavage, which is predicted to occur on the amino side of the deleted isoleucine residue. This mutant must provide enough *dpy-10* function such that homozygotes are normal, but not enough function to complement more severe *dpy-10* alleles.

## 2. Discordance of Expression and Phenotype in *sqt-1* and *rol-6*

As noted above, *sqt-1* and *rol-6* mutants can exhibit abnormal phenotypes at L2-adult and at L2d and dauer stages. Both *sqt-1* and *rol-6* transcripts are detected at each of the molts preceding these stages, except for the dauer stage (Park and Kramer 1994). Dauer larvae show strong Rol phenotypes, but no expression of the genes is detected after completion of the L1-L2d molt. Why then do dauer larvae exhibit the mutant phenotype? A likely explanation is that the hypodermal filament bundles that form at each molt (see above) “lock” the *hypodermis* into whatever shape it has at the beginning of the molt. Since L2d animals are Rol, the *hypodermis* would be locked into a helical configuration at the L2d-dauer molt. The twisted *hypodermis* would synthesize a wild-type dauer cuticle that has the form of the underlying twisted *hypodermis*. Thus, the phenotype of the dauer larva is derived from the pattern created in the preceding stage. Support for this notion comes from rhodamine-phalloidin staining of *sqt-1* and *rol-6* mutants, showing that the *hypodermis* remains twisted throughout the entire L2d-dauer molt period.

## G. Interactions between Cuticle Collagen Genes

Collagens generally do not function independently, but form complexes of increasing size and complexity during their maturation. The presence of an abnormal collagen chain can disturb the structure of the complex in subtle and unpredictable ways. As a result of their biochemical properties, collagens have somewhat unusual genetic properties (Cox et al. 1980; Kusch and Edgar 1986; Kramer and Johnson 1993). Collagen mutations are frequently dominant due to disruption of the complex in which they are a component. Genetic interactions between collagen genes, such as intergenic suppression or enhancement of phenotypes, occur frequently because multiple collagens are components of the same complex structure.

LRol or glycine substitution mutations of *sqt-1* are dominant suppressors of *rol-6* RRol alleles (Kramer and Johnson 1993), and *rol-6* LRol mutations can suppress *sqt-1* RRol phenotypes (Yang and Kramer 1994). Double mutants for RRol alleles of both genes are RRol, and thus no suppression occurs between these alleles. ROL-6 requires SQT-1 to function, since *rol-6* phenotypes are suppressed in the *sqt-1* null background. However, SQT-1 does not require ROL-6, since *sqt-1* phenotypes are apparent in the *rol-6* null background. These interactions suggest that SQT-1 and ROL-6 interact, possibly forming a single heterotrimeric collagen molecule. Recalling that the null phenotypes for both genes is nearly wild type, it is possible that suppression occurs by removal of the abnormal collagen chain(s). When certain mutations in the two collagen chains are combined, the end result may be complete loss of both collagens (mutual suicide), resulting in the null phenotype.

Mutant *dpy-10(e128)* animals have a Dpy phenotype that can be converted to DpyLRol (the more severe Dpy-10 phenotype) by the addition of a single copy of any non-null *sqt-1* mutation ([Kusch and Edgar 1986](#); [Kramer and Johnson 1993](#)). This enhancement of the Dpy-10 phenotype occurs with recessive LRol, dominant RRol, and recessive Lon alleles of *sqt-1*. Enhancement does not occur with a *sqt-1* null allele, showing that the effect is due to the presence of abnormal SQT-1 and not to the absence of normal SQT-1. Alleles of the *dpy-2* and *dpy-7* collagens also show enhancement by *sqt-1*, but *dpy-13* does not.

## H. Surface Molecules

The cuticle surface of nematodes is a major focus of studies on the interactions of parasites with their hosts ([Maizels et al. 1993](#)). The *C. elegans* cuticle surface is being studied as a model for parasites, as well as for its roles in cuticle function (Politz and Philipp 1992). Cuticle surface molecules are discussed in detail by Blaxter and Bird (this volume).

## I. Other Cuticle-related Genes

### 1. *bli-4*

The *bli-4* gene was originally identified by a single allele, *e937*, that results in blistering (Bli) of the adult cuticle ([Brenner 1974](#)). Eleven more alleles were subsequently identified that cause early larval lethality (Peters et al. 1991). Two of the lethal (Let) alleles fail to complement the other Let alleles, but they do complement the Bli allele. The noncomplementing alleles arrest in late embryogenesis, and the complementing alleles arrest as L1 larvae. The complementing alleles may retain some *bli-4* function, resulting in later arrest and the ability to complement the Bli allele. The *bli-4* gene encodes a protein with strong similarity to the Kex2/subtilisin family of serine endoproteases that are involved in processing prohormones and other precursor proteins (Thacker et al. 1995). Alternative splicing generates three BLI-4 variants that share common amino-terminal sequences, but differ in their carboxyl termini. Two of the noncomplementing lethal alleles affect common exons present in all transcripts, whereas the Bli allele, *e937*, deletes an exon found in only one BLI-4 variant. This BLI-4 variant may only be required for proper function of the adult cuticle. As noted above, cuticle collagen homology block A appears to be a cleavage site for a subtilisin-like proteinase. It is possible that one or more of the *bli-4* gene products are involved in cleavage of procollagens at HBA.

### 2. *rol-3*

The *rol-3* gene was originally identified by a single allele, *e754*, that caused an adult LRol phenotype. Subsequently, 12 further *rol-3* alleles were shown to be recessive larval lethals ([Barbazuk et al. 1994](#)). One temperature-sensitive mutant is lethal at high temperature but is a viable, weak LRol at low temperature. The temperature-sensitive period for *rol-3* was shown to be from mid-L1 to mid-L3, well before formation of the adult cuticle. The LRol phenotype appears only in adult-stage animals, not in L4 heterochronic mutants that have adult cuticles, making it unlikely that *rol-3* encodes an adult-specific cuticle component. Suppressors of the *rol-3* temperature-sensitive lethality were localized to two genes, *srl-1* and *srl-2* (suppressor of roller lethal). Some *rol-3;srl* double mutants show abnormal development in the posterior region of the animal. The *srl* hermaphrodites show no obvious abnormalities, but males have abnormal tail morphology. It is possible that these genes are involved in morphogenesis of the posterior region of the animal ([Barbazuk et al. 1994](#)).

### 3. *dpy-5*

Mutations in *dpy-5* result in a Dpy phenotype in animals from L2 to adult stages, and mutant animals have altered cuticle structure ([Quazana et al. 1985](#)). The *dpy-5* gene encodes a novel protein of approximately 25 kD. DPY-5 has a good predicted signal peptide and the carboxyl half of the protein is cysteine-rich. Whether DPY-5 is a cuticle component or affects cuticle structure indirectly is unknown.

### 4. *dpy-20*

Alleles of [\*dpy-20\*](#) result in Dpy phenotypes of differing severities and can also cause a rounded-head phenotype ([Hosono et al. 1982](#); [Clark et al. 1995](#)). The [\*dpy-20\*](#) gene encodes a novel protein with no signal peptide, making it unlikely that it is a component of the cuticle. [\*dpy-20\*](#) mRNA is most abundant in L2–L4 animals, corresponding to its temperature-sensitive period around the L2 stage ([Clark et al. 1995](#)). Whether [\*dpy-20\*](#) has any role in cuticle function is not clear.

## 5. Cuticlin Genes

The material that remains insoluble after extraction of *Ascaris* cuticles with 0.5 M NaCl, followed by 1%  $\beta$ -mercaptoethanol at 37°C, was originally termed cuticlin ([Fujimoto and Kanaya 1973](#)). The *C. elegans* cuticle material that remains insoluble after boiling in 1–2% SDS, 5%  $\beta$ -mercaptoethanol has also been called cuticlin, although there may be differences between this material and *Ascaris* cuticlin. Two *C. elegans* genes, [\*cut-1\*](#) and [\*cut-2\*](#), that encode proteins in the cuticlin fraction have been identified ([Sebastian et al. 1991](#); [Lassandro et al. 1994](#)). The [\*cut-1\*](#) gene encodes a novel protein of about 40 kD that is cysteine- and tyrosine-rich. Transcripts are detected in animals undergoing dauer larva formation. Antiserum directed against CUT-1 detects a 40-kD protein on Western blots of animals that are forming dauer larvae, but CUT-1 becomes insoluble in the mature dauer cuticle. Immunofluorescence localized CUT-1 to a 2- $\mu$ m-wide band underlying the dauer alae.

The [\*cut-2\*](#) gene encodes a novel 231-amino-acid protein that is also tyrosine-rich. CUT-2 contains 13 variable-length repeats that begin with AAP(A/V/I) and have a tyrosine present in most of the repeats. Similar repeats have been seen in vitelline membrane, chorion, and larval cuticle proteins of insects. Transcripts are detectable in RNA from animals of all stages, but they may only be produced around the time of molts. Anti-CUT-2 antibodies react with the insoluble cuticle residue of all stages. Immunogold localization shows that CUT-1 and CUT-2 are in the cortical layer of cuticles in all stages and are also localized under the dauer alae ([Ristoratore et al. 1994](#); [Favre et al. 1995](#)). Upon incubation with horseradish peroxidase and H<sub>2</sub>O<sub>2</sub>, recombinant CUT-2, but not CUT-1, is efficiently cross-linked via dityrosine residues. The structure of CUT-2 may promote the formation of tyrosine cross-links, resulting in its insolubility.

## Figures



### Figure 1

Scanning electron micrograph of adult *C. elegans* cuticle. On the left of the figure is the epicuticle/cortical layer, and an annulus is indicated. On the right, the cortical layer has been cracked off, revealing struts attached to the fiber layer. Note the rows of struts that are adjacent to the annular indentations. Magnification, 9750 $\times$ .



### Figure 2

Freeze-etch electron micrograph of adult cuticle. The cortical layer (C), strut (S), fiber layer (F), basal layer (B), and [\*hypodermis\*](#) (H) are indicated. An annular indentation can be seen in the upper right. Note the fibrous nature of the cuticle, which is not apparent by other visualization methods. Magnification, 50,000 $\times$ . (Micrograph kindly provided by Christina Peixoto.)



### Figure 3

General structure of *C. elegans* cuticle collagens. The domain structure is derived from the sequences of 38 collagen genes. (Hatched boxes) Gly-X-Y domain; (black boxes) interruptions; (horizontal lines) amino and carboxyl non-(Gly-X-Y) sequences; (vertical lines) conserved cysteines; (dashed lines) regions in the amino and carboxyl domains that show the greatest length and sequence divergence. Homology blocks are short stretches

of conserved sequence found in most or all cuticle collagens (see [Fig. 4](#)). The number of amino acids in different domains are indicated above the figure.



#### Figure 4

Cuticle collagen homology block (HB) consensus sequences. Consensus sequences were derived from 30 collagen gene sequences. The percentage of collagens that have a particular amino acid or type of amino acid at each position is indicated in superscript. When two amino acids or classes are frequent at one position, they are shown one above the other. HBD is located 1–24 amino acids in from the initiator methionine residue. Since HBD is not conserved in [dpy-7](#), [C09G5.6](#), or the [col-8](#) subfamily, these sequences were not included in the analysis of HBD. The standard single-letter code is used for amino acids. (+) D or E; (–) K or R; (O) hydrophobic; (Z) polar; (x) no conservation.



#### Figure 5

Cuticle collagen cysteine subfamilies. The amino acid sequences immediately amino and carboxyl to the Gly-X-Y repeat domain (written vertically in the figure) are shown. Also shown are the sequence of a single collagen that is representative for each subfamily and the number of genes in the subfamily. All members of a subfamily have identical cysteine spacings.



#### Figure 6

Nomarski micrographs of adult wild-type and mutant animals illustrating morphological phenotypes. (a) Wild-type N2 strain animal; (b) *dpy-10(e128)* animal, Dpy phenotype; (c) *lon-2(e678)* animal, Lon phenotype. Magnification, 75×.



#### Figure 7

Rhodamine phalloidin-stained RRol mutant animal, *rol-6(e187)*. Helical twisting of the four muscle quadrants in this L2 animal is evident. Magnification, 315×.

### Tables

**Table 1 Patterns of *C. elegans* cuticle collagen gene expression**

Canonical genes	No. genes in class	Developmental stage <sup>a</sup>						References
		embryo	L1	L2	L3	L4	L2d	
<a href="#">sgt-1</a> , <a href="#">rol-6</a>	2	–	+	+	+	+	–	<a href="#">Park and Kramer (1994)</a>
<a href="#">col-12</a> , <a href="#">col-13</a> b	2	–	n.d.	n.d.	+	+	–	<a href="#">Cox and Hirsh (1985)</a> ; Park and Kramer (1990)
<a href="#">col-1</a>	5	+	n.d.	n.d.	+	+	+	<a href="#">Cox and Hirsh (1985)</a> ; Kramer et al. (1985)
<a href="#">col-17</a>	1	+	+	+	+	–	n.d.	<a href="#">Liu et al. (1995)</a>
<a href="#">col-15</a>	2	–	n.d.	n.d.	+	+	+	<a href="#">Cox and Hirsh (1985)</a>
<a href="#">col-2</a> <sup>c</sup> , <a href="#">col-6</a>	2	–	n.d.	n.d.	–	+	++	<a href="#">Cox and Hirsh (1985)</a> ; Kramer et al. (1985)

		Developmental stage <sup>a</sup>						
Canonical genes	No. genes in class	embryo	L1	L2	L3	L4	L2d	References
<a href="#"><i>col-8</i></a>	4	–	n.d.	n.d.	–	+	+	<a href="#">Cox and Hirsh (1985)</a> ; Liu and Ambros (1991); <a href="#">Liu et al. (1995)</a> .
<a href="#"><i>col-36</i></a>	1	–	+	–	–	–	+	<a href="#">Levy and Kramer (1993)</a> .
<a href="#"><i>col-40</i></a>	1	–	(+) <sup>d</sup>	–	–	–	+	<a href="#">Levy and Kramer (1993)</a> .

Presented on an essentially nonquantitative basis, but note that large quantitative differences between genes within a class can occur. (+) mRNA detected; (–) mRNA not detected; (n.d.) not determined; (++) mRNA detected at a very high level.

a

RNAs isolated from animals in molt at end of stage indicated, except embryos.

b

By cDNA hybridization, also weakly in embryo and L2d.

c

[\*col-2\*](#) is weakly detected in L3–L4 by cDNA hybridization.

d

[\*col-40\*](#) is detected in L1 larvae before the molt but not at the L1–L2 molt.

**Table 2** Adult phenotypes of molecularly characterized cuticle collagen mutations

Gene (alias)	Type of mutation									
	putative null	allele	substitutions for Gly-X-Y glycine	allele	HBA Arg substitutions	allele	transposon insertions	allele	other mutations	allele
<a href="#"><i>sqt-1</i></a>	Tal	<i>sc103</i>	Tal wLon wLRol Tal wLon Tal Lon/wTal	<i>sc107</i> <i>sc99</i> <i>sc101</i>	Dpy/dRRol (3)	<i>e1350</i>	Tal	<i>cg1</i>	LRol Tal/wTal <sup>a</sup> (3)	<i>sc13</i>
<a href="#"><i>rol-6</i></a>	wDpy (3)	<i>n1178</i>			RRol sdRRol	<i>e187</i> <i>su1006</i>				
<a href="#"><i>dpy-2</i></a>			tsDLR (3) Dpy	<i>sc38</i> <i>q292</i>						
<a href="#"><i>dpy-10</i></a>	DLR	<i>cg36</i>	DLR (2) Dpy	<i>cg37</i> <i>q291</i>	DLR/dLRol	<i>cn64</i>	Dpy (2) DLR	<i>m481</i> <i>q323</i>	Dpy <sup>b</sup> WT <sup>c</sup>	<i>e128</i> <i>m481m482</i>
<a href="#"><i>dpy-13</i></a>	Dpy	<i>e458</i>	Dpy (2)	<i>e225</i>			Dpy (3)	<i>m399</i>	sdDpy <sup>d</sup> Dpy <sup>b</sup>	<i>e184</i> <i>e488</i>
<a href="#"><i>dpy-7</i></a>			Dpy (4)	<i>e88</i>						
<a href="#"><i>sqt-3</i></a>			tsDpy lethal	<i>e2117</i>						
( <a href="#"><i>col-1</i></a> )			ts sdDpy tsDpy/ts dLRol	<i>e24</i> <i>sc63</i>						

Phenotypes and references are described in the text. Where multiple alleles show the same phenotype(s), the number of such alleles is indicated in parentheses. One representative allele is shown to the right of the phenotype. Phenotypes included on a single line are all associated with the same allele(s). Phenotypes are recessive unless otherwise indicated. When recessive and dominant phenotypes of the same mutation differ, they are listed: recessive/dominant. Phenotypic modifiers are (d) dominant; (sd) semidominant; (ts) temperature-sensitive; (w) weak.

a

Replacement of conserved carboxyl domain Cys with Tyr or Ser.

b

Splicing mutations.

c

Deletion of Ile at position 5 of HBC. Fails to complement other [\*dpy-10\*](#) alleles.

d

Deletion of 36 bp in first Gly-X-Y domain.

Generated from local HTML

## Chapter 17. Extracellular Matrix — III Basement Membranes

---

Basement membranes can be recognized as thin sheets of extracellular matrix material closely associated with cell membranes. Studies in vertebrates indicate that basement membranes have roles in cell adhesion, migration, and differentiation, as well as acting as molecular filters, barriers to cell migration, and mechanical supports. In *C. elegans*, basement membranes cover the pseudocoelomic faces of the [hypodermis](#), [pharynx](#), [intestine](#), gonad, and some body wall muscles ([White et al. 1976](#)). The basement membrane covering the [pharynx](#) is thicker, 45 nm, than that found on other tissues, 20 nm (Albertson and Thomson 1976). There are generally few distinguishing features of basement membranes, but 30-nm striations have been noted in glancing sections ([White et al. 1976](#)), and thickening of the hypodermal basement membrane can be seen at sites of muscle cell attachment ([Francis and Waterston 1985](#); [Francis and Waterston 1991](#)). The major constituents of vertebrate basement membranes are type IV collagen, laminin, nidogen, and proteoglycans (Yurchenco and Schittny 1990; Paulsson 1992). With the exception of nidogen, genes encoding all of these molecules have been identified in *C. elegans*.

### A. Type IV Collagen

Type IV collagen is generally the most abundant constituent of basement membranes and is found only in basement membranes. The structure of type IV collagen has been conserved from sponges to humans. It has a short, non-triple-helical amino-terminal domain that contains several cysteines, a long Gly-X-Y repeat domain with numerous small interruptions, and a carboxy-terminal globular domain (NC1) with 12 highly conserved cysteines. Type IV collagen forms a polygonal network that is stabilized by disulfide-bonded NC1 domain dimers and amino-terminal domain tetramers, and poorly understood lateral interactions. There are at least six type IV collagen genes in mammals (Hudson et al. 1993). The ubiquitous form of type IV collagen, found in essentially all basement membranes, is a heterotrimer of two  $\alpha 1$  and one  $\alpha 2$ (IV) chains. The  $\alpha 3$ ,  $\alpha 4$ , and  $\alpha 5$ (IV) collagen chains are primarily localized to the kidney glomerular basement membrane, and mutations in these chains can cause the degenerative kidney disease Alport syndrome.

Two genes that encode type IV collagen chains, [emb-9](#) and [let-2](#) (previously called [clb-2](#) and [clb-1](#), respectively) have been characterized in *C. elegans* (Guo and Kramer 1989; [Guo et al. 1991](#); [Sibley et al. 1993](#), 1994). They have strong similarity to the human type IV chains, being most conserved in the NC1 domain, where [emb-9](#) and [let-2](#) are 63% and 72% identical to the human  $\alpha 1$  and  $\alpha 2$  chains, respectively. Sequences of  $\alpha 2$ (IV) collagen genes have also been determined from the parasitic nematodes *Ascaris* (Pettitt and Kingston 1991) and *Brugia* (Caulagi and Rajan 1995), and they have 74% amino acid sequence identity with *C. elegans* over the entire protein, 87% in the NC1 domain. In mammals, the  $\alpha 1/\alpha 2$ ,  $\alpha 3/\alpha 4$ , and  $\alpha 5/\alpha 6$  type IV gene pairs are in head-to-head orientation, separated by short promoter regions, allowing transcriptional control of gene pairs encoding chains that form a single type IV molecule. The *C. elegans* genes, [emb-9](#) and [let-2](#), are located on different chromosomes, III and X, respectively, ruling out such a control mechanism.

#### 1. Type IV Collagen Genetics

Alleles of [emb-9](#) and [let-2](#) were originally identified at high frequency in genetic screens for embryonic lethal mutations ([Meneely and Herman Herman, 1981](#); [Miwa et al. 1980](#); [Wood et al. 1980](#); [Cassada et al. 1981](#); [Isnenghi et al. 1983](#)). Multiple alleles of both genes cause embryonic lethality, demonstrating that normal type IV collagen is required for embryogenesis. Most alleles are temperature-sensitive, such that animals raised at 15°C develop normally, but at 25°C (20°C in some cases), they die during embryogenesis. At intermediate temperatures, animals often arrest during larval development or become sterile adults. The strongest alleles convey nonconditional lethal phenotypes. Arrest occurs at about the twofold stage of embryogenesis and is accompanied by extensive herniation of the [hypodermis](#) and disorganization of [body wall muscle](#). When mutant animals are shifted to 25°C as larvae, they arrest development or become subfertile adults, indicating that type IV collagen function is required throughout the life cycle.

Five alleles of [emb-9](#) (Guo et al. 1991; M. Gupta and J. Kramer, unpubl.) and 15 of [let-2](#) (Sibley et al. 1994) are substitutions of other amino acids for glycines in the Gly-X-Y repeat domain. Each type IV collagen chain normally contains about 20 interruptions in its Gly-X-Y repeat domain, but these "novel interruptions" are not compatible with normal function. Substitutions for different glycine residues can result in phenotypes of varying severity, ranging from embryonic lethality at 25°C, but not at 20°C, to unconditional lethality. The *let-2(mn114)* mutation is a glycine to glutamic acid substitution in the third Gly-X-Y repeat of the  $\alpha 2$ (IV) chain. It has a strong affect on adult fertility but only a mild affect on embryonic and larval development, suggesting that it affects gonad function preferentially. The *let-2(mn126)* mutation is an alanine to threonine substitution in the X position of a Gly-X-Y repeat immediately following a four-amino-acid interruption, and it causes a relatively severe phenotype. Substitutions for X- or Y-position amino acids are extremely rare in collagens. Such an alteration is not likely to have a major effect on triple-helix folding or stability, but it may define a region involved in interaction between type IV molecules or between type IV collagen and other basement membrane components.

Alleles of [emb-9](#) and [let-2](#) display temperature-sensitive dominant effects (P. Graham et al., unpubl.) that generally result in reduced viability and/or fertility in heterozygous animals. Some alleles, such as *emb-9(g23)* and *let-2(mn103)*, are in fact temperature-sensitive dominant lethals. Two putative null alleles of [emb-9](#), a 500-bp deletion and a nonsense mutation, have been generated by reversion of the *emb-9(g23)* temperature-sensitive dominant lethal phenotype (M. Gupta and J. Kramer, unpubl.). The putative null alleles result in recessive nonconditional embryonic lethality, but they allow animals to develop further in embryogenesis, to about the threefold stage. Since missense mutations cause more severe phenotypes than the null mutations, the presence of abnormal type IV collagen must interfere with the function of other basement membrane components.

The distribution of mutations in the type IV collagen genes is nonrandom. There are 940 potential target Gly-X-Y glycines in the two genes. Yet, among the 20 independently isolated type IV mutations, there are four cases in which two mutations affect the same glycine. This clustering could result if substitutions for most glycines do not cause obvious phenotypes, and would therefore not have been identified in genetic screens, or if they cause dominant lethality or sterility, making them impossible to maintain. Since the existing alleles show strong dominant effects, the latter explanation seems most likely.

An unusual feature of the [let-2](#)  $\alpha 2$ (IV) collagen gene is its complex pattern of interallelic complementation (Meneely and Herman 1981). Every [let-2](#) allele complements at least one other allele to some extent, such that *trans* heterozygote animals have milder phenotypes than either homozygote. If each *C. elegans* type IV molecule contains one  $\alpha 2$ (IV) chain, as in vertebrate type IV, then complementation between different  $\alpha 2$  chain alleles can only result from some type of intermolecular interaction. This interaction may be between type IV collagen molecules or between type IV collagen and other basement membrane components. A correlation exists between the degree of interallelic complementation for two alleles and the physical distance between the mutations (Sibley et al. 1994). Alleles must be at least 47 amino acids apart to show any complementation and at least 134 amino acids apart to show full complementation. The relationship between interallelic complementation and distance may reflect lateral interactions between *C. elegans* type IV collagen molecules.

## 2. Alternative Splicing of *let-2*

Transcripts of [let-2](#) are alternatively spliced into two forms that contain either exon 9 or exon 10, but not both (Sibley et al. 1993). Exons 9 and 10 are separated by just 30 bp and have unusual 5'-splice donor sequences. Exons 9 and 10 appear to be duplicates, having the general structure (Gly-X-Y)<sub>5</sub>\_9- or 10-amino-acid interruption \_ (Gly-X-Y)<sub>4</sub>. The interruption is nine amino acids long in exon 9, and ten amino acids long in exon 10. The ratio of exon-9-containing to exon-10-containing transcripts changes dramatically during development. Exon-9-containing transcripts are 90% of the total in embryos, decline to about 30% within 1 hour after hatching, and slowly decline during larval development to a level of about 10% in adults. Transcripts of the *Ascaris suum*  $\alpha 2$ (IV) collagen gene are also alternatively spliced at exactly the same sites (Pettitt and Kingston 1994). Exon 9 is more highly conserved between the two nematodes (81% amino acid identity) than is exon 10 (65% identity). The interruption of exon 9 is 100% conserved, whereas the interruption of exon 10 is only 70% conserved. A

similar temporal difference in expression of exon-9- versus exon-10-containing transcripts is seen in *Ascaris* and *C. elegans*.

The fact that alternative splicing of  $\alpha 2(IV)$  collagen has been maintained between these distantly related nematodes suggests that it may have an important role in basement membrane function. The shift from primarily the exon-9- to primarily the exon-10-containing variant of  $\alpha 2(IV)$  coincides with a dramatic shift in *C. elegans* development, from a phase of rapid and extensive morphological change (embryogenesis) to a phase that primarily entails symmetrical growth (early larval through adult stages). The morphological changes of embryogenesis may require basement membranes with properties different from those present in larvae or adults.

## B. Proteoglycan

Proteoglycans consist of a protein core to which at least one glycosaminoglycan chain is attached. In vertebrates, there is a large family of proteoglycans that can have different core proteins and/or different attached glycosaminoglycan chains. The *C. elegans* [\*unc-52\*](#) gene was shown to encode a homolog of the mammalian basement membrane heparan sulfate proteoglycan, perlecan ([Rogalski et al. 1993](#)). Perlecan is a common component of basement membranes and has been shown to interact with other basement membrane molecules as well as cell surface receptors. Three 65-kD heparan sulfate side chains are attached to domain I of mammalian perlecan. The *C. elegans* protein has no similarity to the mammalian protein in this region, but it does have two potential carbohydrate attachment sites. The *C. elegans* and mammalian proteins are very similar in domains II–IV. Domain II has three LDL receptor-like repeats, domain III has similarity to laminin, and domain IV contains 14 immunoglobulin C2-like repeats. Several variant forms of *UNC-52* result from alternatively spliced transcripts that are missing one or more exons from domains II–IV. Antibody staining shows that *UNC-52* is localized to basement membranes underlying body wall and [anal](#) muscles and surrounding the [pharynx](#) and gonad (G. Mullen and D. Moerman, pers. comm.).

Three classes of [\*unc-52\*](#) alleles have been identified: class-1 mutants are viable and develop progressive paralysis, the class-2 mutant arrests at the twofold stage of embryogenesis and is paralyzed (Pat phenotype) (Williams and Waterston 1994), and the class-3 mutant arrests at the twofold stage but is not paralyzed. Paralysis of class-1 alleles is due to fracture of muscle-dense bodies and separation of the myofilament lattice from the plasma membrane (Waterston et al. 1980). Class-1 mutations also cause structural defects of the [somatic gonad](#), possibly affecting the myoepithelial sheath cells ([Gilchrist and Moerman 1992](#)). The somatic gonadal defect of class-1 alleles is complemented by the class-3 allele, but it is more severe in animals heterozygous for class-1 and class-2 alleles.

The [\*unc-52\*](#) class-1 alleles are all localized to alternatively spliced exons in domain IV, including four nonsense mutations, one splice donor mutation, and one Tc1 insertion ([Rogalski et al. 1995](#)). Some of the alternatively spliced [\*unc-52\*](#) transcripts would be unaffected by these mutations. Thirteen intragenic revertants of class-1 mutations ([Gilchrist and Moerman 1992](#)) were found to alter the splice acceptor sites of these same alternatively spliced exons. Thus, removal of the mutated exon by altered splicing can result in intragenic suppression. The class-3 allele has a transposon insertion in domain II. The class-2 allele is a nonsense mutation in a domain III exon present in all [\*unc-52\*](#) transcripts. Thus, the Pat phenotype of the class-2 allele represents the complete loss of function for [\*unc-52\*](#).

Dominant intergenic suppressors of the Unc phenotype of [\*unc-52\*](#) class-1 alleles have been identified ([Gilchrist and Moerman 1992](#)). Five of the suppressor mutations were mapped to a single gene, *sup-38* IV. They are strong suppressors of the muscle defects but not of the gonadal defects. By themselves, the suppressor mutations cause mild muscle defects and variable gonadal defects. Putative [\*sup-38\*](#) null mutations were generated by reverting the dominant suppressor activity and were found to cause maternal-effect lethality. The progeny of [\*sup-38\*](#) null mutant hermaphrodites generally die during late larval development but have normal muscle structure. The function of [\*sup-38\*](#) is therefore not required for normal muscle formation.

## C. SPARC

SPARC (also known as BM-40 or osteonectin) is an anti-adhesive extracellular matrix-associated glycoprotein that can modulate the interaction of cells with the matrix (Lane and Sage 1994). A SPARC homolog has been identified in *C. elegans* that has 38% amino acid sequence identity to mammalian SPARC (Schwarzauer and Spencer 1993). Bacterial fusion proteins containing the amino- and carboxy-terminal domains of *C. elegans* SPARC bind calcium, as do the equivalent domains of mammalian SPARC. The *C. elegans* SPARC also contains intrachain disulfide bonds with properties similar to those in mammalian SPARC (Schwarzauer et al. 1994). Staining of transgenic strains carrying a SPARC-*lacZ* fusion indicates that SPARC is expressed from late embryogenesis to adulthood and is restricted to body wall and sex muscles. Transgenic overexpression of wild-type *C. elegans* SPARC causes several abnormal phenotypes (Schwarzauer and Spencer 1993). Animals develop an Unc phenotype as adults and in some cases become completely paralyzed in the posterior. The morphology of the [vulva](#) is abnormal, and sometimes the [intestine](#) or [gonad](#) protrudes through the [vulva](#). Coinjection of the SPARC gene with the *rol-6(su1006)* RRol gene produced Unc, but not RRol, transgenic animals, suggesting that overexpression of SPARC can suppress the Rol phenotype. Injections with high concentrations of SPARC DNA resulted in no transgenic offspring, suggesting that strong overexpression of the gene may be lethal. Overexpression of SPARC may interfere with the normal interactions of muscle cells with their associated basement membranes.

## D. Laminin

In mammals, the laminins are a family of basement membrane molecules composed of three disulfide-bonded subunits,  $\alpha\beta\gamma$  ([Tryggvason 1993](#); [Timpl and Brown 1994](#)). Association of different variant subunits generates at least seven distinct laminin molecules. Laminins can polymerize noncovalently and can bind to cell surface receptors. *C. elegans* homologs of the mammalian  $\alpha$  and  $\beta$  laminin chains have been identified (K. Joh et al., pers. comm.). The  $\alpha$  chain is encoded by the genetic locus [epi-1](#) and the  $\beta$  chain is encoded by [lam-1](#). Mutations in these genes can cause rupturing of basement membranes, migration defects, and [body wall muscle](#) disorganization.

The [unc-6](#) gene encodes a small laminin-related protein that is required for proper dorsal and ventral migrations of axons and mesodermal cells ([Ishii et al. 1992](#)). Closely related molecules named netrins have been identified in vertebrates where they have also been shown to promote axonal outgrowth (Serafini et al. 1994). For a complete description of the [unc-6](#) gene, see Hedgecock et al. (this volume).

Generated from local HTML

## Chapter 17. Extracellular Matrix — IV Conclusions

---

The structures and functions of some ECM molecules have begun to be established in *C. elegans*, but there is a vast amount that is yet to be understood. Since most ECM molecules contain characteristic protein motifs or modules ([Bork and Bairoch 1995](#)), completion of the genome sequence should make it possible to identify most, if not all, of the genes encoding ECM proteins in *C. elegans*. Using methods already available, it should then be possible to characterize genetically the functions of the complete repertoire of ECM molecules. The next level of analysis will be to characterize interactions between ECM molecules. In vertebrates, these interactions have largely been studied biochemically, but in *C. elegans* it should be possible to employ genetics for this as well.

There are several other areas relevant to ECMs that have not been examined in detail in *C. elegans* and that are promising areas for future investigations. Several potential matrix metalloproteinase (MMP) genes have been identified by the genome sequencing project. In vertebrates, the MMPs are the major proteases involved in turnover and remodeling of the ECM. The activities of the MMPs are closely regulated by a family of inhibitors, the tissue inhibitors of matrix metalloproteinases (TIMPs). It will be of interest to determine what roles MMPs and their inhibitors have in *C. elegans* development and ECM remodeling. Another unexplored area is the function of polysaccharides in the ECM, especially the large glycosaminoglycan (GAG) chains. In vertebrates, GAGs can be found separately or attached to the protein core of proteoglycans. GAG chains are likely to have important roles in ECM function in *C. elegans*. Finally, understanding the interactions of cell surface receptors, primarily integrins, with ECM ligands is an area that deserves further study. Cell-ECM interactions can function bidirectionally such that the ECM influences cellular behavior and the cells can modify the composition and organization of the ECM. Such interactions may have important roles in *C. elegans* development (see [Schnabel and Priess](#), this volume).

Generated from local HTML

## **Chapter 17. Extracellular Matrix — Acknowledgments**

---

I thank Don Moerman and Jean Schwarzbauer for helpful comments on the manuscript. Work from this laboratory was supported by the National Institutes of Health.

Generated from local HTML

# Chapter 18. Heterochronic Genes

---

## Contents

[I Introduction](#)

[II Heterochronic Phenotypes](#)

[III Control of Larval Development by \*lin-14\*](#)

[IV Developmental Programs and Regulatory Targets](#)

[V Postdauer Reprogramming of Heterochronic Phenotypes](#)

[VI Perspectives](#)

[Acknowledgments](#)

Generated from local HTML

## Chapter 18. Heterochronic Genes — I Introduction

---

*Caenorhabditis elegans* is a convenient animal for the genetic and molecular analysis of developmental timing, since the worm's developmental pattern is simple and well-characterized ([Sulston and Horvitz 1977](#); [Sulston et al. 1983](#)). Changes in the relative timing of developmental events are termed "heterochrony." Genes have been identified in *C. elegans* that appear to act almost exclusively in the control of the relative timing of stage-specific events (Chalfie et al. 1981; [Ambros and Horvitz 1984](#)). Mutations in these so-called "heterochronic genes," which include [\*lin-4\*](#), [\*lin-14\*](#), [\*lin-28\*](#), and [\*lin-29\*](#), cause precocious or retarded development of certain cell lineages, leading to, for example, larvae with adult tissues or adults with larval tissues. The genetic and molecular analysis of heterochronic genes affords an opportunity to examine in detail the regulatory principles underlying an organized developmental schedule. Because heterochrony may be a common mechanism for evolutionary variation (Gould 1977), the heterochronic genes of *C. elegans* are of potential evolutionary and developmental interest.

Genetic analysis of the heterochronic genes has revealed that they act in regulatory pathways that specify the proper sequence of developmental events through the larval stages to the adult ([Ambros and Horvitz 1984](#); [Ambros 1989](#); Liu and [Ambros 1989](#); [Euling and Ambros 1996a](#)). The heterochronic genes so far identified affect only postembryonic development, indicating that separate mechanisms control the steps of embryonic development. These genes also do not appreciably affect development of the gonad, suggesting that separate genetic circuitries control the timing of gonadal and nongonadal development in the larva. This chapter focuses on our current understanding of the *C. elegans* heterochronic gene pathway as determined by genetic characterization of the regulatory interactions among the genes ([Ambros and Horvitz 1987](#); [Ambros 1989](#); Liu and [Ambros 1989](#)) and recent progress on the cloning, sequencing, and molecular analysis of genes involved in this pathway ([Ruvkun et al. 1989](#); Arasu et al. 1991; [Papp et al. 1991](#); Wightman et al. 1991; [Lee et al. 1993](#); Rougvie and Ambros 1995; E. Moss et al., in prep). Primary emphasis is placed on the developmental decisions controlled by the heterochronic genes, the regulatory interactions among genes of the pathway, and the effects of [\*lin-14\*](#) on the expression of cell fates throughout larval development.

Generated from local HTML

## Chapter 18. Heterochronic Genes — II Heterochronic Phenotypes

A newly hatched *C. elegans* larva contains about 550 nuclei, and about 260 additional [somatic cells](#) are added in the hermaphrodite (somewhat more in the male) by stage-specific cell divisions during the subsequent four larval stages, L1–L4 ([Sulston and Horvitz 1977](#); [Wood et al. 1988](#)). Mutations in the heterochronic genes cause temporal transformations in cell fates so that cells express developmental programs normally specific for cells at a different larval stage ([Ambros and Horvitz 1984](#)). For example, [\*lin-14\*](#) loss-of-function (lf) mutations cause deletion of the L1-specific, or “S1,” patterns from hypodermal lineages, and precocious expression of L2-specific, or “S2,” patterns (see Figs. 1 and 2A). Semidominant gain-of-function (gf) mutations in [\*lin-14\*](#) result in retarded expression of events within the same lineage, so that S1 patterns are reiterated at L2 and later stages ([Fig. 1](#)). These deletions or reiterations of S1 cell lineage patterns occur in many different cell lineages of [\*lin-14\*](#) mutant larvae ([Ambros and Horvitz 1984](#)), indicating that [\*lin-14\*](#) controls a generic choice of “S1” versus “S2” cell lineage programs for cells at the L1 and L2 stages.

Other examples of temporal transformations in cell lineage fate in heterochronic mutants involve substitutions of larval fates for adult fates, or vice versa, in the lateral hypodermal cell lineage ([Fig. 3](#)). For example, mutations in [\*lin-28\*](#) cause cells that would normally divide at the L3 molt to express precociously a terminal differentiation event, termed the “L/A switch,” that is normally specific to the L4 molt ([Fig. 3](#)). Mutations in [\*lin-29\*](#) cause cells to fail to execute the L/A switch, and they divide instead of differentiating at the L4 molt. The temporal transformations in cell fates exhibited by heterochronic mutants always occur between lineal descendants of the same postembryonic blast cells, suggesting that in these particular cases, cells of equivalent developmental potential are generated at successive stages and that the fates they express are determined by heterochronic gene activity.

Heterochrony is not always manifested in alterations in cell lineage. For example, dauer larva arrest, which normally occurs at the L2 molt (see [Riddle](#), this volume), can occur at either the L1 molt or the L3 molt ([Fig. 4](#)) in heterochronic mutants ([Liu and Ambros 1989](#)). In this case, the heterochronic genes control the stage specificity of a developmental program involving cell cycle arrest and dauer-specific differentiation that ultimately affects all of the cells in the animal. In certain other cases, cell cycle progress is controlled by heterochronic genes ([Ambros and Horvitz 1984](#); [Euling and Ambros 1996a](#)). Cells that normally divide at a specific larval stage can divide earlier than normal in certain mutants. In other mutants, these cells are delayed or blocked in their divisions (see [Fig. 5](#)).

It is striking that the heterochronic genes generally affect the fates of cells at specific larval stages, but they do not affect the general rate of larval growth or the rate of progression through the cycle of molts. Therefore, it appears that the heterochronic genes provide information about developmental stage within an independently specified framework of molting and cell division.

### Figures

Figure 1. Temporal transformations in cell fates in the lateral hypodermal cell lineages of heterochronic mutants.

### Figure 1

Temporal transformations in cell fates in the lateral hypodermal cell lineages of heterochronic mutants. Anterior is to the left, and posterior to the right. The vertical axis indicates time during larval development, beginning at hatching. Only the first three larval stages (L1–L3) are shown. (A) In this example, the hermaphrodite [T lineage](#), an L1-specific cell fate (S1), and an L2-specific cell fate (S2) are distinguishable by the pattern of cell divisions and the differentiated fates of the cells produced. The posterior daughter of T is a neuroblast (NB) that produces five [neurons](#) and an extra cell that undergoes programmed cell death ([Sulston and Horvitz 1977](#)). Heterochronic mutations transform the fates of [T lineage](#) cells; [\*lin-14\(0\)\*](#) mutations cause precocious expression of the S2 pattern by the T cell, and deletion of the S1 pattern ([Ambros and Horvitz 1984](#)). In contrast, [\*lin-14\(gf\)\*](#) mutations cause reiteration of the S1 pattern by T.ap and its granddaughter. Additional reiterations can occur at later molts

in *lin-14(gf)* animals ([Ambros and Horvitz 1984](#)). (B) Analogous temporal transformations in cell fates occur in the lateral hypodermal V cell lineages (V6 is shown here). The S1 pattern is deleted in *lin-14(0)* animals, and S2 patterns and subsequent S3 patterns are precocious. Fates after the S3 are also precocious in these lineages (see [Fig. 3](#)). In *lin-14(gf)* animals, S1 patterns are reiterated in the V lineages, but in some weaker *lin-14(gf)* mutants, S2 lineage patterns can occur, and then be reiterated ([Ambros and Horvitz 1987](#)).

Figure 5. Control of the timing of cell division and developmental competence of vulval precursor cells (VPCs).

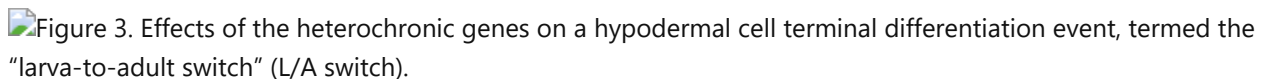
## Figure 5

Control of the timing of cell division and developmental competence of vulval precursor cells (VPCs). (A) The VPCs (P3.p-P8.p) are equivalent tripotent cells, three of which produce the [vulva](#) ([Greenwald](#), this volume). The VPCs are born in the L1 as daughters of P cells (one of which, [P6](#), is shown here), and in the wild type, they divide again in the middle of the L3 stage to produce differentiated vulval cells. In *lin-14(0)* or *lin-28(0)* mutants, the VPCs divide in the L2, and the rest of vulval morphogenesis follows during the late L2 and early L3, resulting in precocious completion of vulval morphogenesis by the L3 molt. *lin-4(0)* or *lin-14(gf)* mutations cause a delay in [VPC](#) division and also prevent VPCs from acquiring the ability to adopt vulval fates ([Ferguson et al. 1987; Euling and Ambros 1996a](#)). (B) Epistasis pathway controlling [VPC](#) cycle progress and [VPC](#) identity. A potential target for the heterochronic gene pathway for VPCs could include “[VPC](#) identity” genes ([Ferguson et al. 1987](#)).

Figure 2. Mutant phenotypes and genetic interactions controlling stage-specific lateral hypodermal cell fates.

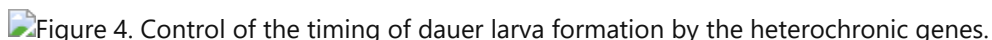
## Figure 2

Mutant phenotypes and genetic interactions controlling stage-specific lateral hypodermal cell fates. (S1–S4) Cell lineage patterns normally specific to the L1–L4 stages, respectively; (Ad) adult-specific terminal differentiation of the lateral [hypodermal seam cells](#) (see also [Fig. 3](#)). (A) Sequences of developmental events in the lateral hypodermal cell lineages in wild-type and heterochronic mutants. *lin-14a* and *lin-14b* represent mutant alleles that selectively affect L1- and L2-specific fates, respectively ([Ambros and Horvitz 1987](#)). (B) A progressive decrease in [lin-14](#) activity controls developmental programs specific to the L1–L3 stages. During the L1, high [lin-14](#) activity (corresponding to *lin-14a* level) specifies or permits L1 fates and prevents precocious expression of S2 and S3 fates. Either [lin-14](#) or [lin-28](#) is sufficient to repress the expression of S3 fates during the L1, whereas loss of both regulators leads to the S3 program. For the L2, [lin-4](#) down-regulates [lin-14](#) to low levels, corresponding to *lin-14(b)* level. In this case, [lin-14](#) and [lin-28](#) are both required to inhibit S3 fates in the L2. During the L3, [lin-14](#) is off, but the state of [lin-28](#) has not been determined. In this model, the *lin-14(a)* and *lin-14(b)* levels of [lin-14](#) activity correspond to the stage-specific *lin-14* alleles (see panel A) ([Ambros and Horvitz 1987](#)) but could also correspond to somewhat different *lin-14* gene products (Wightman et al. 1991).

Figure 3. Effects of the heterochronic genes on a hypodermal cell terminal differentiation event, termed the “larva-to-adult switch” (L/A switch).

## Figure 3

Effects of the heterochronic genes on a hypodermal cell terminal differentiation event, termed the “larva-to-adult switch” (L/A switch). Only the last three stages of lateral hypodermal cell lineages are shown. (A) In the wild type, hypodermal cells switch from expressing “larval molts” at earlier stages (corresponding to S3 and S4 programs) to expressing the “adult molt” (Ad) at the L4 stage. Three horizontal lines signify the stage of expression of the L/A switch. *lin-29(0)* mutants reiterate larval cell divisions (indicated by the dashed line) at extra molts. (B) The L/A switch involves several coordinate changes in the behavior of hypodermal cells at the fourth molt: cessation of cell division, formation of adult (instead of larval) cuticle, cell fusion, and cessation of the molting cycle (Liu et al. 1995; Rougvie and Ambros 1995). [lin-29](#) activates the L/A switch at the L4 molt, and the time of [lin-29](#) action is controlled by upstream genes of the heterochronic gene pathway, including [lin-4](#), [lin-14](#), and [lin-28](#).

Figure 4. Control of the timing of dauer larva formation by the heterochronic genes.

## Figure 4

Control of the timing of dauer larva formation by the heterochronic genes. (A) Dauer larva formation can only occur at the L2 molt in the wild type. Mutations in *lin-14* alter the stage of dauer larva formation, allowing dauer larva formation at the L1 or L2 molts in *lin-14(0)* animals or at the L2 or L3 molts in animals carrying *lin-14(gf)* mutations. (B) Among the identified heterochronic genes, only *lin-4* and *lin-14* affect the stage of dauer larva formation. Some *lin-14* regulatory target (X) may mediate the temporal control of dauer larva development. This proposed target might be one or more members of the pathway of genes required for normal dauer larva formation (Riddle, this volume).

Generated from local HTML

## Chapter 18. Heterochronic Genes — III Control of Larval Development by *lin-14*

---

### A. A Temporal Decrease of LIN-14 Protein Controls L1–L3 Events

Genetic analysis of *lin-14* has shown that the level of *lin-14* activity specifies the expression of stage-specific cell fates for diverse cell types and that a temporal decrease in *lin-14* activity is critical for specifying the timing of events during the larval stages (Ambros and Horvitz 1987). Semidominant *lin-14(gf)* mutations appear to cause an elevated level of *lin-14* activity in the L2 when it would normally be reduced and hence result in a reiteration of S1 cell lineage patterns (Ambros and Horvitz 1987). This suggests that *lin-14* activity must decrease for the proper expression of L2-specific and later cell fates. Temperature-shift experiments with *lin-14* (ts) alleles indicate that *lin-14* acts early in the L1 stage to specify the fates of L1 cells and at the end of the L1 stage to control the fates expressed by cells in the early L2. Finally, *lin-14* must be absent in the late L2 stage to permit the proper execution of L3-specific fates (Ambros and Horvitz 1987). Thus, *lin-14* seems to determine three different sets of stage-specific fates by acting at three successively reduced levels. Hence, the level of *lin-14* activity may be the determining factor for temporal cell fate specification in the L1 through L3 stages (Ambros and Horvitz 1987).

The *lin-14* gene was cloned by chromosomal walking (Ruvkun et al. 1989). The *LIN-14* protein is localized to the nuclei of most of the cells that are affected by *lin-14* mutations (Ruvkun and Giusto 1989), consistent with a direct role for *lin-14* in the regulation of gene expression. The predicted *LIN-14* protein sequence does not indicate homology with previously known proteins, suggesting that *lin-14* may represent a new class of regulatory molecule (Wightman et al. 1991). Molecular analysis of *lin-14* gene expression confirms that the level of *LIN-14* protein is temporally regulated. Western blots and *in situ* immunofluorescent staining indicated that *LIN-14* protein decreases in level between the early L1, when it is abundant, and the end of the L2, when it is undetectable (Ruvkun and Giusto 1989; Wightman et al. 1991). The level of *lin-14* mRNA seems to be relatively constant during this time, implying that posttranscriptional regulation is a significant component of the temporal decrease in *LIN-14* protein (Wightman et al. 1991, 1993).

Most *lin-14* mutations, including putative null alleles, transform the fates of certain L1 and L2 cells to those of L2 and L3 cells, respectively. Certain alleles have shown that the L1 and L2 effects of *lin-14* are independently mutable: *lin-14(a)* alleles selectively affect the fates of L1 cells and *lin-14(b)* alleles affect only cells after the L1. It was proposed that these independently mutable *lin-14* functions might selectively affect the level of a single gene product at particular stages (Ambros and Horvitz 1987). According to this view, three levels of *lin-14* gene activity would confer three different lineage-specific fates on cells through the L1–L3 stages. Alternatively, *lin-14(a)* and *lin-14(b)* mutations might selectively affect the function of distinct gene products that are each separately down-regulated (Ambros and Horvitz 1987). Several different *lin-14* transcripts have been identified from cDNA clones, and these could encode proteins that differ at their amino termini (Wightman et al. 1991). It is not yet known whether these transcripts are subject to tissue-specific or stage-specific regulation. It will be interesting to see if *lin-14* does indeed produce multiple protein products with distinct expression patterns or if different levels of a single *lin-14* gene product can direct normal development.

### B. *lin-4* Down-regulates LIN-14 Protein

Genetic and molecular experiments indicate that *lin-4* is a negative regulator of *lin-14* which has a critical role in *lin-14* down-regulation (Ambros 1989). A *lin-4(0)* mutation causes a retarded phenotype essentially identical to that of *lin-14(gf)* mutations (Chalfie et al. 1981; Ambros and Horvitz 1987), and epistasis experiments indicate that these *lin-4* defects depend on *lin-14* function (Ambros 1989). Furthermore, *lin-4* activity is required for the temporal decrease in *LIN-14* protein level; in *lin-4* mutant animals, *LIN-14* protein remains abnormally high later in development (Arasu et al. 1991). Since *lin-14* messenger RNA is not noticeably affected by *lin-4* mutations (Wightman et al. 1993), these findings suggest a posttranscriptional role for *lin-4* in *lin-14* down-regulation. *lin-14(gf)* alleles contain deletions of sequences from the 3'-untranslated region (3'UTR) of the *lin-14* transcripts.

This suggests that the 3'UTR of *lin-14* RNA contains a negative regulatory element that affects *lin-14* activity posttranscriptionally, and through which the *lin-4* gene product might act in *trans* (Ruvkun et al. 1989; Wightman et al. 1991).

*lin-4* has been cloned, and, surprisingly, it does not encode a protein (Lee et al. 1993). It encodes two small untranslated RNAs, and the more abundant of the two transcripts, *lin-4* S, is expressed beginning in the late L1 stage (R. Feinbaum and V. Ambros, in prep.). Since this is the time that LIN-14 protein begins to decrease, *lin-4* S may be directly responsible for reducing the level of LIN-14 protein. *lin-4* S RNA is 22 nucleotides long and contains two blocks of sequences that are complementary to an element repeated seven times in the 3'UTR of *lin-14* mRNA, suggesting that *lin-4* might inhibit *LIN-14* protein synthesis by a complementary base pairing with *lin-14* mRNA (Lee et al. 1993; Wightman et al. 1993; see also Anderson and Kimble, this volume). Although there has not yet been a direct demonstration of a *lin-4* – *lin-14* RNA interaction, the strong evolutionary conservation of the complementarity between *lin-4* S and *lin-14* 3'UTR sequences in other nematode species strongly suggests that base pairing is important. The precise mechanism by which *lin-4* S RNA down-regulates LIN-14 protein is not yet clear.

The temporal down-regulation of *LIN-14* protein synthesis by *lin-4* begins in response to signals that initiate larval development. In the absence of food, newly hatched L1 larvae do not develop; postembryonic cell divisions do not occur (Wood et al. 1988), and LIN-14 levels remain high (Arasu et al. 1991). After feeding, starvation-arrested larvae initiate postembryonic development, and *LIN-14* protein decreases. The mechanism of action of this “food signal” that initiates postembryonic development is unknown, but it must ultimately lead to activation of *lin-4* transcription because *lin-4* RNA is not detected until after feeding of L1 animals (R. Feinbaum and V. Ambros, in prep.). It will be of great interest to identify the temporal signals that coordinate the activation of *lin-4* transcription with L1 development.

## C. Stage-specific *lin-14* – *lin-28* Interactions

Mutations in *lin-28* result in defects generally similar to those of *lin-14(b)* alleles (Ambros and Horvitz 1984, 1987), where the L1 stage is unaffected, but the L2 stage events are deleted (Fig. 2A). Interestingly, *lin-28* mutants seem to have an abnormally low level of LIN-14 protein during the late L1, consistent with a role for *lin-28* in maintaining an appropriate level of LIN-14 expression (Arasu et al. 1991). These molecular observations, together with the similarity of *lin-14(b)* and *lin-28* phenotypes, suggest that the *lin-28* gene product might interact with the *lin-14* gene or gene product during the late L1 stage to control L2-specific fates. The *lin-28* gene product is not likely to function simply as an activator of *lin-14* gene expression, because the *lin-14* and *lin-28* null alleles do not result in equivalent phenotypes. In *lin-28(0)* animals, some hypodermal cells can express an adult-specific event at the L2 molt, whereas in *lin-14(0)* mutants, that event is never expressed before the L3 molt (Ambros and Horvitz 1984; Ambros 1989). Furthermore, in the absence of *lin-14*, the stage of expression of certain events still depends on *lin-28* activity (Ambros 1989). For example, *lin-28* is sufficient to prevent expression of L3-specific programs (S3) in the L1 even when *lin-14* is absent (Fig. 2). Thus, *lin-28* must have *lin-14*-independent functions.

The functional relationship between *lin-28* and *lin-14* changes between the L1 and L2. Specifically, either *lin-14* or *lin-28* is sufficient to inhibit expression of S3 fates in the L1; neither single mutant alone expresses precocious S3 fates in the L1, but the double mutant does. In contrast, both *lin-14* and *lin-28* are required to inhibit S3 programs in the L2; the single mutants express precocious S3 programs at that stage. These observations suggest that perhaps the level of *lin-28* activity also changes between the L1 and L2 stages. The recently cloned *lin-28* gene was found to be a member of a family of nucleic-acid-binding proteins that contain “cold-shock” domains (E. Moss et al. in prep). The molecular characterization of *lin-28* will allow tests of whether the *lin-28* gene product interacts physically with LIN-14 and also should allow the identification of potential regulatory targets of LIN-28. The fact that members of the cold-shock domain family of proteins can have both RNA- and DNA-binding activities (Wolffe 1994) leaves open the question of whether *lin-28* regulates gene expression at the transcriptional and/or posttranscriptional level.

Generated from local HTML

# Chapter 18. Heterochronic Genes — IV Developmental Programs and Regulatory Targets

---

The fact that the timing of events in different cell lineages and at essentially all larval stages originates with the down-regulation of one gene, *lin-14*, provides a basis for the organized execution of diverse stage-specific programs in different cell lineages. For some cells, particularly in the L1 stage, *lin-14* could directly regulate gene expression. In other cells, it may act in combination with other heterochronic genes. For cells at later stages, it likely acts indirectly, via downstream heterochronic genes, by allowing their regulation to occur. The diversity of developmental events whose expression is controlled by genes of the heterochronic pathway suggests that the ultimate regulatory targets of the pathway are cell-type-specific genes required to implement the stage-specific programs of particular cells. Below is a summary of our current understanding of three developmental events that have been the focus of study thus far.

## A. Dauer Larva Arrest

One stage-specific developmental event that involves every cell in the animal is the entry into the optional, developmentally arrested dauer larva stage. Dauer larva formation involves a global developmental decision, made in response to environmental stimuli (food levels and crowding), that results in developmental arrest and specialized differentiation at the L2 molt (Cassada and Russell 1975; Singh and Sulston 1978; [Riddle](#), this volume). Dauer larvae resume development when returned to favorable environmental conditions. The fact that dauer larvae can only form at the L2 molt in the wild type indicates that there is strict temporal control over execution of the dauer larva program. Mutations in *lin-14* or *lin-4* alter the stage of dauer larva formation (Liu and [Ambros 1989](#)), allowing dauer larvae to form at either the L1 molt or the L3 molt ([Fig. 4](#)). The results of epistasis experiments suggest a genetic regulatory pathway wherein *lin-14* normally represses dauer larva formation at the L1 molt, and *lin-4* represses *lin-14* in the L2, permitting dauer larva formation at the L2 molt. According to this model, were it not for *lin-14*, wild-type animals would be competent to enter dauer larva arrest at the L1 molt. Thus, in the case of dauer larva formation, *lin-14* may act to override or short circuit a signaling pathway whose output triggers a specific developmental program. Thus, the regulatory targets of *lin-14* for the temporal control of dauer larva development might include previously identified genes required to activate the process in the presence of appropriate environmental stimuli ([Riddle et al. 1981](#)).

One of these potential targets of *lin-14* is *daf-12*, a gene required for dauer larva developmental arrest ([Riddle et al. 1981](#)), and hence a potential activator of the dauer program that could be regulated by *lin-14*. Intriguingly, *daf-12* also has a role in the heterochronic gene pathway in the control of stage-specific cell fates. In addition to blocking dauer formation, *daf-12* mutations also cause lateral hypodermal cells to reiterate L2-specific cell lineage patterns (S2) in the L3 (A. Antebi and E.M. Hedgecock, in prep.). Thus, *daf-12* may be required for switching from L2 to L3 programs and may therefore interact with *lin-14* and *lin-28*. For example, *daf-12* could mediate the effects of *lin-14* on the expression of L3 fates and could also be a target for *lin-14* in its repression of dauer formation at the L1 molt. A simplifying model could be that *daf-12* is primarily a temporal regulator that is required for various L3-specific events, including S3 cell lineage patterns, and dauer larva formation.

Mutations in *daf-12* also affect morphogenesis of the gonad, indicating that *daf-12* functions in diverse developmental programs, and could potentially interact with multiple regulators in addition to *lin-14* and *lin-28*. *daf-12* encodes a member of the nuclear hormone receptor superfamily (W.-H. Yeh et al., in prep.), and although a ligand has not been identified, this suggests that DAF-12 might act by regulating gene expression in response to intercellular signals.

## B. Vulval Precursor Cells: Cell Cycle Length and Competence

Generally, the heterochronic genes do not affect the lengths of cell division cycles. However, for certain specific cells, including the male ectoblasts B, Y, and F, and the vulval precursor cells (VPCs), the heterochronic genes control cell cycle length ([Ambros and Horvitz 1984](#); [Euling and Ambros 1996a](#)). The effects of heterochronic

mutations on the [VPC](#) cycle have been studied in most detail. In [\*lin-4\*](#), [\*lin-14\*](#), and [\*lin-28\*](#) mutants, VPCs divide either earlier than normal (in precocious mutants) or later than normal (in retarded mutants) ([Fig. 5](#)) ([Ambros and Horvitz 1984](#); [Euling and Ambros 1996a](#)). In wild-type animals, the VPCs are born in the L1 and then divide in the middle of the L3 stage. In [\*lin-14\*](#) and [\*lin-28\*](#) mutants, the VPCs are born at the normal time but divide as much as one full stage early, in the L2. Vulval morphogenesis follows during the late L2 and early L3, resulting in precocious completion of vulval morphogenesis by the L3 molt. This shortening of the [VPC](#) cycle in [\*lin-14\*](#) or [\*lin-28\*](#) mutants can be accounted for by a shortened G<sub>1</sub> ([Euling and Ambros 1996a](#)). These results suggest that [\*lin-14\*](#) and [\*lin-28\*](#) normally act to restrict [vulva](#) development to the L3 by delaying progress through G<sub>1</sub> in VPCs or by holding the VPCs in G<sub>0</sub>. Down-regulation of [\*lin-14\*](#) after the L1 permits G<sub>1</sub> progression, leading to the eventual synchronous mitosis of the VPCs in the L3. Although G<sub>1</sub> is shortened in these mutants, it is not absent altogether. Even in the *lin-14;lin-28* double mutant, a G<sub>1</sub> still occurs, indicating that [\*lin-14\*](#) and [\*lin-28\*](#) are not the only factors controlling cell cycle progress in the VPCs (V. Ambros, unpubl.).

The manner in which the retarded phenotype of [\*lin-14\*](#) and [\*lin-4\*](#) mutants is expressed in the VPCs suggests that the heterochronic pathway controls a step in [VPC](#) development in addition to [VPC](#) cycle progress. Specifically, VPCs can divide in *lin-4(0)* or *lin-14(gf)* mutants, but they never produce differentiated vulval progeny, indicating the existence of a potent block in vulval differentiation by [\*lin-14\*](#) expression. This result suggests that the normal role of heterochronic genes is to control two aspects of [VPC](#) development: cell division and the acquisition of competence to respond to intercellular signals and select a 1<sup>o</sup>, 2<sup>o</sup>, or 3<sup>o</sup> cell fate (see [Greenwald](#), this volume). By regulating the timing of both cell division and competence in VPCs, the heterochronic genes may coordinate these processes and in so doing contribute to the fidelity of the spatial patterning of differentiated vulval cells.

Candidate regulatory targets for heterochronic gene control of the VPCs could be identified genetically by mutations that cause [vulva](#)-specific effects on the timing of cell division and differentiation. One such mutation is *n300*, which is associated with the *nT1* translocation ([Ferguson et al. 1987](#)). *n300* causes a retarded [vulva](#) defect like that caused by *lin-4(0)* or *lin-14(gf)* mutations and is epistatic to [\*lin-28\*](#) (S. Euling and V. Ambros, unpubl.). This suggests that *n300* may define a genetic target of [\*lin-28\*](#) for the VPCs. Since *n300* has not been characterized in sufficient detail to determine whether it represents a loss of gene function, or mutation of more than one gene, its role in normal development is difficult to assess.

## C. *lin-29* and Hypodermal Terminal Differentiation

The effects of [\*lin-14\*](#) mutations extend beyond the L3 stage to include the timing of lateral hypodermal cell terminal differentiation (the "L/A switch") at the L4-to-adult molt ([Fig. 3](#)) ([Ambros and Horvitz 1984](#); [Ambros 1989](#)). This event involves several coordinate changes in the behavior of hypodermal cells: cessation of [seam](#) cell division, formation of adult (instead of larval) cuticle, [seam](#) cell fusion, and cessation of the molting cycle. The execution of the L/A switch requires the heterochronic gene [\*lin-29\*](#), and the timing of the event is affected by mutations in the upstream heterochronic genes, including [\*lin-14\*](#) and [\*lin-28\*](#). In [\*lin-29\*](#) mutants, lateral hypodermal cells reiterate L4-specific cell divisions and larval cuticle synthesis, and in *lin-14(0)* or *lin-28(0)* mutants, the L/A switch occurs precociously ([Ambros and Horvitz 1984](#); Liu et al. 1995). Since the progressive down-regulation of [\*lin-14\*](#) can account for the sequential expression of L1–L3 events (see above), there must be an additional mechanism for coupling of L3 regulatory events to the expression of the L/A switch at the L4 molt. This mechanism could depend on the expression of L3- and L4-specific developmental events, or it could result from temporal changes in downstream regulatory genes. Among the known heterochronic genes, the one that appears to most directly regulate [\*lin-29\*](#) based on epistasis is [\*lin-28\*](#), since [\*lin-28\*](#) can affect the timing of the L/A switch in the absence of [\*lin-14\*](#) ([Ambros 1989](#)). However, the timing of [\*lin-28\*](#) expression has not been analyzed, and all of the genes acting between [\*lin-14\*](#) and the L/A switch may not have been identified. Three additional heterochronic genes, [\*lin-41\*](#), [\*lin-42\*](#), and [\*lin-46\*](#), have been identified by mutations that affect the timing of the L/A switch (E. Moss et al., unpubl.).

[\*lin-29\*](#) was cloned by physical genetic mapping ([Papp et al. 1991](#)) and was found to encode a zinc finger protein of the C2H2 class of transcription factors (Rougvie and Ambros 1995). In lateral hypodermal cell nuclei of wild-

type animals, *LIN-29* protein is first detected in the L4 stage (J. Bettinger and A.R. Rougvie, in prep.). Furthermore, the temporal accumulation of LIN-29 in these nuclei is altered in precocious or retarded *lin-4*, *lin-14*, and *lin-28* mutants (J. Bettinger and A.R. Rougvie, in prep.), consistent with its proposed status as a regulatory target of these upstream heterochronic genes. Since *lin-29* encodes an apparent transcription factor, it could activate the L/A switch by directly regulating the transcription of genes involved in the differentiation of lateral hypodermal cells. Hence, putative *lin-29* targets might include genes that control cell division, cell fusion, cuticle synthesis, and molting. Indeed, *LIN-29* protein synthesized in vitro binds to essential 5' regulatory sequences of the stage-specifically expressed collagen genes *col-17* and *col-19* (Liu et al. 1995; Rougvie and Ambros 1995). This finding strongly suggests that *lin-29* represents the end of the heterochronic pathway in the *hypodermis* for the timing of the L/A switch and provides a model for how the pathway may control other events.

## D. Other Heterochronic Genes

Although mutations in *lin-4* and *lin-14* are pleiotropic, they do not affect all stage-specific events of larval development, and thus these other events must be under other temporal controls. With the exception of *daf-12*, the heterochronic genes identified so far do not have major effects on the timing of gonadal development, suggesting the existence of an independent pathway that governs developmental timing for the gonad. Mutants in *lin-4*, *lin-14*, and *lin-28* do have minor effects on the timing of steps in gonadal distal tip migrations (V. Ambros, unpubl.). However, this might result indirectly from the heterochronic hypodermal defects of these mutants, since the *hypodermis* probably participates in guiding gonad morphogenesis (Hedgecock et al. 1990).

At least one new heterochronic gene, *srf(yj43)*, was identified by screening for mutations that cause the persistence of an L1-specific cuticle surface antigen (Hemmer et al. 1991). This mutant phenotype could result from the mutation of a temporal regulatory gene or of a gene that specifically affects the synthesis or accessibility of this particular antigen. Since the expression of this L1-specific antigen is not affected by mutations of *lin-4* or *lin-14* (S. Politz, pers. comm.), its temporal regulation is apparently separate from the previously identified heterochronic genes.

Generated from local HTML

## Chapter 18. Heterochronic Genes — V Postdauer Reprogramming of Heterochronic Phenotypes

Animals that undergo the optional dauer larva stage and then resume larval development reveal a surprising plasticity in the temporal programming of the larval stages. During “postdauer” development, certain heterochronic developmental defects of mutations in [\*lin-4\*](#), [\*lin-14\*](#), and [\*lin-28\*](#) are phenotypically suppressed ([Liu and Ambros 1991](#)). For example, [\*lin-14\*](#) and [\*lin-28\*](#) null mutations do not affect the timing of the L/A switch during postdauer development even though they drastically affect this switch during continuous development ([Fig. 6](#)). [\*lin-29\*](#), however, is critical for the L/A switch in both developmental pathways. These results indicate that development through the dauer larva stage must involve an override of the action of [\*lin-4\*](#), [\*lin-14\*](#), and [\*lin-28\*](#), followed by the engagement of an alternative mechanism for programming the stage-specific activation of [\*lin-29\*](#).

The [\*vulva\*](#) defects of [\*lin-14\*](#) and [\*lin-28\*](#) precocious mutants are also corrected by postdauer development, since these mutants have restored egg-laying ability after postdauer development. This is despite the fact that the precocious vulval development of these mutants begins before dauer larva arrest, resulting in dauer larvae with partially developed vulvae. Cell lineage analysis revealed that the postdauer vulval cell lineages of [\*lin-14\*](#) and [\*lin-28\*](#) animals are normal, regardless of the predauer lineage history of the vulval cells. Specifically, vulval cells that are formed by up to two rounds of vulval cell divisions prior to dauer larva arrest reverse their state of determination to that of multipotential VPCs ([Euling and Ambros 1996b](#)) and express complete 1<sup>o</sup>, 2<sup>o</sup>, or 3<sup>o</sup> vulval cell fates during postdauer development ([Fig. 6](#)). This surprising observation suggests that vulval cells which otherwise behave as if they were irreversibly determined nevertheless possess cryptic multipotency that is unmasked under novel temporal conditions of dauer larva arrest and postdauer development. The capacity of dauer larvae to reprogram [\*vulva\*](#) cells to the state of VPCs suggests that exit from dauer larva development respecifies the early L3 state of cells in general and reinforces the multipotential state of VPCs in particular.

### Figures

Figure 6. Postdauer reprogramming of hypodermal development.

### Figure 6

Postdauer reprogramming of hypodermal development. (A) Mutant [\*lin-28\*](#) patterns are used for illustration. During continuous development, [\*lin-28\*](#) animals delete L2-specific events from hypodermal lineages and precociously express S3 programs (including vulval development; see [Fig. 5](#)), S4 programs, and the L/A switch (see [Fig. 3](#)). The L3 molt is the final molt in these mutants. Dauer larvae arrest development at the L2 molt, and the lateral hypodermal and vulval cell lineages cease (indicated by the closed circles). The vulval cell lineages cease at variable points, three of which are shown. (B) The [\*lin-28\*](#) dauer larvae that resume larval development express a normal postdauer lateral hypodermal cell lineage, the number of postdauer stages is normal, and the L/A switch occurs at the normal time ([Liu and Ambros 1989](#)). Vulval cells formed prior to dauer larva arrest become reprogrammed to VPCs and express postdauer cell lineage patterns characteristic of VPCs, in this case, a “1<sup>o</sup>” cell lineage pattern ([Euling and Ambros 1996b](#)).

## Chapter 18. Heterochronic Genes — VI Perspectives

---

As a fundamental phenomenon, the problem of temporal control of developmental processes merits a detailed genetic and molecular study. The genetic regulatory mechanisms whereby heterochronic genes specify the developmental stage are likely to include the same kinds of transcriptional, posttranscriptional, and intercellular signaling mechanisms identified in other developmental contexts. However, surprises may be in store, since at least one novel regulatory mechanism has been identified through molecular analysis of the *lin-4* regulatory RNA gene product ([Lee et al. 1993](#); P. Olsen and V. Ambros, in prep.).

With the cloning and molecular analysis of more genes of the heterochronic gene pathway, it should be possible in the near future to arrive at a complete description of when and where the various genes are expressed and to work out the molecular basis of their regulatory interactions. The mechanisms that regulate *lin-29* during continuous and postdauer development will be of particular interest. Mosaic analysis should make it possible to establish the anatomical sites of action of the heterochronic genes and to establish the importance of cell-cell interactions in the organization of the larval developmental schedule. Other areas of interest will be the identification of genes that affect the timing of gonadal cell lineages and the molting cycle, since these processes seem to be programmed separately from the heterochronic gene pathway, yet must somehow be linked to the events controlled by the heterochronic genes. Finally, it should be possible to explore the control of cell cycle progression during larval development by analyzing the role of the heterochronic genes in controlling the divisions of the VPCs and other cell types.

Do the heterochronic genes further promise a unique perspective on developmental regulatory mechanisms and strategies? Uncovering the details of temporal control by the heterochronic genes will likely contribute to a general understanding of the molecular basis for biological timing mechanisms. Perhaps the requirement for accurate control of the relative order and synchrony of diverse developmental events imposes special regulatory constraints unique to the problem of developmental timing. Temporal control systems must be rigid enough to produce reproducible developmental patterns but must also be flexible enough to allow for developmental contingencies, such as optional developmental arrest in the dauer larva or diapause in insects. The study of *C. elegans* heterochronic genes should uncover the fundamental genetic designs and regulatory strategies that permit accurate, yet flexible, control of developmental timing.

Heterochronic mutants with developmental defects analogous to those in *C. elegans* have been identified in other organisms, including plants ([Poethig 1988a,b](#); [Lawson and Poethig 1995](#)), slime mold (Simon et al. 1992), and fungi (Adams et al. 1988). For example, the maize *Teopod* (*Tp*) mutations appear to be gain-of-function alleles of genes controlling a juvenile signal. Mutations in *Tp* cause persistence of juvenile developmental patterns abnormally late in development ([Poethig 1988a,b](#)) and so seem to be analogous, genetically and phenotypically, to *lin-14(gf)* mutations. *Tp1* has been shown to act cell-extrinsically, suggesting that *Tp1* controls the activity of a diffusible factor (Poethig 1988b). In *Drosophila*, mutations of the *anachronism* locus cause precocious cell cycle progression in certain neuroblast lineages (Ebens et al. 1993) analogous to the precocious vulval cell divisions caused by *lin-14* or *lin-28* mutations ([Euling and Ambros 1996a](#)).

In some animals, the mechanisms of spatial patterning of cell fates may involve temporally dynamic regulatory processes analogous to the specification of the developmental stage by the heterochronic genes of *C. elegans*. In the leech, the spatially diversified segmental identity is produced by the temporally sequential production of cells with different expression patterns of Hox genes ([Shankland 1994](#)). Since this process of spatial diversification is so closely associated with sequences of cell divisions, it may involve timing mechanisms that link changes in gene expression to cell lineage not unlike the situation during *C. elegans* larval development. It remains to be seen what regulatory features are in common between the control of developmental sequences in *C. elegans* and the control of developmental programs in other systems.

## **Chapter 18. Heterochronic Genes — Acknowledgments**

---

Thanks to Eric Lambie, Ann Rougvie, Adam Antebi, and members of my laboratory for critical reading of the manuscript and to Ann Rougvie, Adam Antebi, and Sam Politz for communicating results prior to publication.

Generated from local HTML

# **Chapter 19. Development of the Vulva**

---

## **Contents**

- [I Introduction and Overview](#)
- [II The Anchor Cell](#)
- [III VPC Generation and Identity](#)
- [IV VPC Specification](#)
- [V Execution](#)
- [VI Morphogenesis](#)
- [VII Evolution of Vulval Development](#)
- [VIII Future Prospects](#)
- [Acknowledgments](#)

Generated from local HTML

# Chapter 19. Development of the Vulva — I Introduction and Overview

Formation of the hermaphrodite [vulva](#) has been particularly amenable to genetic and developmental studies. These studies have revealed that [vulva](#) formation is a microcosm of events important in the development of all animals and that these events utilize molecules that appear to be conserved in all animals. Indeed, some of these molecules or their involvement in development were first identified through studies of vulval development in *Caenorhabditis elegans*.

The [vulva](#) consists of 22 cells and serves as the passageway through which sperm enter and fertilized eggs leave the gonad ([Fig. 1](#)). Vulval development may be roughly divided into four stages. First, in the L1 stage, the vulval precursor cells (VPCs) are born. The VPCs are six hypodermal cells, consecutively numbered [P3.p](#) through [P8.p](#), each of which has the potential to contribute cells to the [vulva](#). Second, in the early L3 stage, cell-cell interactions specify the fates of the VPCs. In wild-type hermaphrodites, three discrete signaling events specify [P5.p](#), [P6.p](#), and [P7.p](#) to adopt vulval fates (i.e., to undergo lineages that result in the production of vulval cells) and [P3.p](#), [P4.p](#), and [P8.p](#) to adopt a nonvulval fate (i.e., to produce additional hypodermal cells). Third, the VPCs execute the fates that have been specified, generating the appropriate number and types of vulval cells. Fourth, the vulval cells undergo cell movements, cell fusion, and eversion to form the mature [vulva](#).

The [somatic gonad](#) influences vulval development. The most pervasive influence is provided by the anchor cell (AC), which has many important roles in vulval development, from [VPC](#) fate specification and patterning to morphogenesis. In addition, other somatic gonadal cells also influence vulval morphogenesis and eversion.

Genetic screens have exploited the fact that a functional [vulva](#) is not necessary for viability. In the absence of a [vulva](#), eggs are produced by self-fertilization and mature internally, so that larvae hatch internally and ultimately devour their parent. This activity leads to the formation of a “bag of worms” ([Fig. 2](#)), which is essentially the parent’s cuticle surrounding its progeny. The bag of worms phenotype of Vulvaless mutants is distinctive and easily viewed in the dissecting microscope ([Fig. 2B](#)), enabling rapid and powerful screens for mutations affecting vulval development. Moreover, the absence of eggs on a plate of Vulvaless mutants is also readily apparent in the dissecting microscope, enabling the identification of suppressor mutations, which may define additional genes with related functions. Genetic screens have also exploited another possible anomaly of vulval development: A Multivulva phenotype, in which [P3.p](#), [P4.p](#), and [P8.p](#), which normally adopt a nonvulval fate, instead generate vulval cells. The Multivulva phenotype is readily visualized in the dissecting microscope by multiple pseudovulval protrusions ([Fig. 2C](#)) and is also easy to revert. Through genetic screens of these kinds, a large collection of genes involved in vulval development have been identified ([Table 1](#)).

In this chapter, I first consider aspects of the development and function of the AC. I then consider the four stages of vulval development, with a focus on key genes that have been identified through mutations. Because more is known about [VPC](#) specification than any other stage, there will be considerable detail about the cell-cell interactions that specify [VPC](#) fates and the cell signaling and signal transduction pathways that mediate these interactions.

## Figures

Figure 1. Overview of vulval development.

### Figure 1

Overview of vulval development. Left lateral view of nuclei, indicated by circles. (*Open circles*) Nuclei of [P6.p](#) and its descendants, produced by execution of the 1<sup>o</sup> fate; (*closed circles*) nuclei of [P5.p](#) and [P7.p](#) and their descendants, produced by execution of the 2<sup>o</sup> fate; (*gray circles*) nuclei of [P3.p](#), [P4.p](#), and [P8.p](#) and their progeny, produced by execution of the 3<sup>o</sup> fate. Times given are hours from hatching at 20°C. (Based on [Sulston and](#)

[Horvitz 1977](#).) (A) VPCs during the L3 stage, at the time that their fates are specified; (B) [VPC](#) daughters (L3 stage); (C) [VPC](#) granddaughters (L3 stage); (D) vulval cells (L4 stage); (E) mature [vulva](#) (adult).

Figure 2. Vulval mutants, viewed in the dissecting microscope.

## Figure 2

Vulval mutants, viewed in the dissecting microscope. (A) N2 (wild-type); (B) *let-23(sy97)*, Vulvaless; (C) *lin-15(e1763)*, Multivulva. Large arrow-head indicates the [vulva](#). Smaller arrowheads indicate pseudovulvae. (Photograph courtesy of Paul Sternberg.)

## Tables

**Table 1** Genes featured in this chapter

Gene	Protein product
A. Genes involved in the AC/VU decision	
<a href="#">lag-2</a>	ligand of the DSL family
<a href="#">lin-12</a>	receptor of the LIN-12/Notch family
B. Genes involved in <a href="#">VPC</a> generation or identity	
<a href="#">lin-26</a>	zinc finger protein
<a href="#">lin-39</a>	homeodomain protein
<i>lin(n300)</i>	no information
<a href="#">unc-83</a>	no information
<a href="#">unc-84</a>	no information
C. Genes of the inductive signaling pathway	
<a href="#">let-23</a>	receptor tyrosine kinase of the EGF receptor subfamily
<a href="#">let-60</a>	Ras
<a href="#">lin-3</a>	EGF-like ligand
<a href="#">lin-45</a>	Raf
<a href="#">mek-2</a>	MAP kinase kinase
<a href="#">mpk-1 / sur-1</a>	MAP kinase
<a href="#">sem-5</a>	SEM-5/GRB2 adaptor protein
D. Potential targets of the inductive signaling pathway	
<a href="#">lin-1</a>	putative transcription factor of the Ets family
<a href="#">lin-25</a>	novel protein
<a href="#">lin-31</a>	putative transcription factor of the HNF3/fork head family
<a href="#">sur-2</a>	novel protein
E. Genes that influence the activity of the inductive signaling pathway	
<a href="#">ksr-1</a>	protein kinase
<a href="#">let-341</a>	no information
<a href="#">lin-2</a>	putative cell junction protein
<a href="#">lin-7</a>	putative cell junction protein

<b>Gene</b>	<b>Protein product</b>
<a href="#"><i>lin-10</i></a>	novel protein
<a href="#"><i>sli-1</i></a>	<i>cbl</i> oncogene homolog
<a href="#"><i>unc-101</i></a>	clathrin adaptor protein
F. Genes involved in lateral signaling	
<a href="#"><i>lin-12</i></a>	receptor of LIN-12/Notch family
G. Genes that influence <a href="#"><i>lin-12</i></a> -mediated signaling	
<a href="#"><i>sel-1</i></a>	novel secreted protein
<a href="#"><i>sel-12</i></a>	presenilin homolog
H. Genes involved in inhibitory signaling	
<a href="#"><i>lin-9</i></a>	novel protein
<a href="#"><i>lin-13</i></a>	zinc finger protein
<a href="#"><i>lin-15</i></a>	two novel proteins
<a href="#"><i>lin-36</i></a>	novel protein
<a href="#"><i>lin-37</i></a>	no information
I. Genes involved in execution of vulval fates	
<a href="#"><i>lin-11</i></a>	LIM homeodomain protein
<a href="#"><i>lin-17</i></a>	multipass transmembrane protein
<a href="#"><i>lin-18</i></a>	no information
<a href="#"><i>vex-1</i></a>	no information
J. Genes involved in vulval morphogenesis	
<a href="#"><i>sel-12</i></a>	presenilin homolog
<a href="#"><i>spe-2</i></a>	novel protein
<a href="#"><i>sqv-3</i></a>	galactosyltransferase

See text for references.

Generated from local HTML

## Chapter 19. Development of the Vulva — II The Anchor Cell

---

The AC is the key organizer of vulval patterning and morphogenesis, and as a consequence, some mutations that affect the development of the AC also affect vulval development. Wild-type hermaphrodites have a single AC, generated after interactions between two equivalent cells ([Hirsh et al. 1976](#); [Kimble and Hirsh 1979](#); [Kimble 1981](#); [Seydoux and Greenwald 1989](#)). Studies of this process, the “AC/VU decision,” have illuminated the function of [\*lin-12\*](#), which also mediates lateral signaling involved in specifying the fates of the VPCs.

### A. The AC/VU Decision

During development of the [hermaphrodite gonad](#), each of two cells, named [\*Z1.ppp\*](#) and [\*Z4.aaa\*](#), has an equal chance of becoming the AC or a ventral [uterine](#) precursor cell (VU). However, in a given hermaphrodite, only one cell becomes the AC ([Kimble and Hirsh 1979](#)). Laser microsurgery experiments have shown that this outcome reflects interactions between [\*Z1.ppp\*](#) and [\*Z4.aaa\*](#) ([Kimble 1981](#); [Seydoux and Greenwald 1989](#)). If [all cells](#) in the developing [somatic gonad](#) are ablated except for [\*Z1.ppp\*](#) and [\*Z4.aaa\*](#), one of the two cells becomes the AC and the other becomes a VU. However, if [all cells](#) are ablated except for [\*Z1.ppp\*](#) or [\*Z4.aaa\*](#), the remaining cell always becomes an AC. Taken together, these results suggest that [\*Z1.ppp\*](#) and [\*Z4.aaa\*](#) each makes a decision between the AC and VU fates and that signaling between them ensures that only one becomes the AC (see [Fig. 3](#)).

### B. Genes Involved in the AC/VU Decision

The AC/VU decision is mediated by the activity of [\*lin-12\*](#) and [\*lag-2\*](#). *LIN-12* is thought to function as the receptor for LAG-2. [\*lin-12\*](#) was implicated in the control of the AC/VU decision by the observation that null alleles cause both [\*Z1.ppp\*](#) and [\*Z4.aaa\*](#) to become ACs, whereas hypermorphic or activated alleles cause both [\*Z1.ppp\*](#) and [\*Z4.aaa\*](#) to become VUs ([Greenwald et al. 1983](#)). The predicted *LIN-12* protein (Greenwald 1985; Yochem et al. 1988) is the archetype of the *LIN-12/Notch* protein family found in all animals (for review, see Greenwald 1994; Artavanis-Tsakonas et al. 1995). All members of this family are predicted transmembrane proteins with multiple epidermal growth factor (EGF)-like motifs and three LNR (*LIN-12/Notch repeat*) motifs in their extracellular domains and six cdc10/SWI6 motifs (also called ankyrin repeats) in their cytoplasmic domains. Genetic mosaic analysis suggested that [\*lin-12\*](#) functions as the receptor for the signal between [\*Z1.ppp\*](#) and [\*Z4.aaa\*](#) ([Seydoux and Greenwald 1989](#)). Many other aspects of [\*lin-12\*](#) expression, structure, and function have also been studied ([Greenwald and Seydoux 1990](#); Seydoux et al. 1990; [Lambie and Kimble 1991](#); Fitzgerald et al. 1993; [Struhl et al. 1993](#); Sundaram and Greenwald 1993a; Chamberlin and Sternberg 1994; Wilkinson et al. 1994; Newman et al. 1995; Wilkinson and Greenwald 1995).

[\*lag-2\*](#) was implicated in the AC/VU decision by loss-of-function alleles that lead to the production of two ACs ([Lambie and Kimble 1991](#)). Furthermore, rare gain-of-function alleles suppress the AC/VU decision defect caused by hypermorphic alleles of [\*lin-12\*](#) ([Tax et al. 1994](#); F. Tax et al., in prep.). [\*lag-2\*](#) is predicted to encode a transmembrane protein with EGF-like motifs and another cysteine-based motif, the DSL domain (Henderson et al. 1994; [Tax et al. 1994](#)). These structural features are apparent in all members of a family of “DSL” proteins (for Delta, Serrate, LAG-2) thought to function as ligands for *LIN-12/Notch* proteins in all animals. Other aspects of [\*lag-2\*](#) expression, structure, and function have also been studied ([Lambie and Kimble 1991](#); Henderson et al. 1994; [Tax et al. 1994](#); Wilkinson et al. 1994; Fitzgerald and Greenwald 1995).

### C. A Feedback Mechanism during the AC/VU Decision

Genetic mosaics in which [\*Z1.ppp\*](#) and [\*Z4.aaa\*](#) differed in [\*lin-12\*](#) activity illuminated an important aspect of the AC/VU decision ([Seydoux and Greenwald 1989](#)). Normally, the relative level of [\*lin-12\*](#) activity in [\*Z1.ppp\*](#) and [\*Z4.aaa\*](#) is somehow assessed by the two cells before either commits to the AC or VU fates, and a feedback mechanism reinforces a stochastic initial difference between the two cells so that only one becomes an AC ([Fig. 3](#)). Analysis of [\*lin-12\*](#) and [\*lag-2\*](#) expression suggested that transcriptional control is a component of the inferred feedback mechanism in the AC/VU decision (Wilkinson et al. 1994). Although both [\*lin-12\*](#) and [\*lag-2\*](#) are initially

expressed in both [Z1.hpp](#) and [Z4.aaa](#), [lin-12](#) expression becomes restricted to the presumptive VU and [lag-2](#) expression becomes restricted to the presumptive AC at some point prior to commitment. This change in the expression pattern depends on [lin-12](#) activity and appears to be functionally important for a normal AC/VU decision.

## Figures

Figure 3. The AC/VU decision.

### Figure 3

The AC/VU decision. The specification of the AC and VU fates may be viewed as having three steps prior to cell fate commitment ([Seydoux and Greenwald 1989](#)). (1) Uncommitted [Z1.hpp](#) and [Z4.aaa](#) initially have equal capacity to signal and/or receive. The ligand and receptor may interact, but signaling activity is below a critical threshold. Both [lin-12](#) and [lag-2](#) are expressed at low levels. (2) A stochastic event causes one cell to become a net signaler and the other cell to become a net receiver, above the critical threshold. (3) The tendency to be a signaler or a receiver is then reinforced by a feedback mechanism. [lin-12](#) activity positively autoregulates [lin-12](#) transcription and negatively regulates [lag-2](#) expression, possibly at the level of transcription ([Wilkinson et al. 1994](#)).

Generated from local HTML

# Chapter 19. Development of the Vulva — III VPC Generation and Identity

---

Twelve P cells are present at hatching. The VPCs are the posterior daughters of [P3–P8](#) (see [Fig. 4](#)). The nuclei of all of the P cells are initially present in a lateral position and migrate ventrally within the cells during the L1 stage ([Sulston and Horvitz 1977](#)). The migration appears to be an active process and requires the activity of the [unc-83](#) and [unc-84](#) genes ([Sulston and Horvitz 1981](#); Fixsen 1985; W. Fixsen and H.R. Horvitz, pers. comm.). After nuclear migration is completed, the P cells divide in an anterior-posterior manner ([Sulston and Horvitz 1977](#)). The anterior daughters are [neuroblasts](#) that contribute descendants to the [ventral nerve cord](#). The posterior daughters of [P3–P8](#) are the VPCs, whereas the posterior daughters of the other P cells fuse with [hyp7](#), the major hypodermal syncytium encompassing the animal. [P3.p–P8.p](#) are not specified to adopt vulval fates until the L3 stage.

## A. Genes Required for the Identity of P3.p–P8.p as VPCs

Genes required for the identity of [P3.p–P8.p](#) as VPCs have been identified by mutations that cause a Vulvaless phenotype. In [lin-39](#) mutants, [P3.p–P8.p](#) fuse with the hypodermis in the L1 stage and therefore behave like the posterior daughters of the other P cells ([Clark et al. 1993](#); [Wang et al. 1993](#)). [lin-39](#) is a member of the *C. elegans* Hox gene cluster and is generally involved in patterning cells of the mid-body region ([Clark et al. 1993](#); [Wang et al. 1993](#)). Thus, [VPC](#) identity appears to depend on the position of posterior daughters of P cells within the animal.

In [lin-26](#) partial loss-of-function mutants, [P3.p–P8.p](#) become [neurons](#) or [neuroblasts](#) instead of VPCs; null mutants are inviable, with much hypodermal cell death ([Ferguson et al. 1987](#); [Labouesse et al. 1994](#)). [lin-26](#) encodes a predicted protein with a zinc finger, suggesting that it functions as a transcription factor to repress expression of [neural](#) target genes or activate expression of hypodermal target genes ([Labouesse et al. 1994](#)).

## B. Heterochronic Genes and VPC Identity

Heterochronic genes are involved in cell identity by controlling the timing of stage-specific events. In retarded mutants, cells behave as if they belong to an earlier larval stage, and in precocious mutants, cells behave as if they belong to a later larval stage ([Chalfie et al. 1981](#); [Ambros and Horvitz 1984, 1987](#); see [Ambros](#), this volume). The global heterochronic genes [lin-4](#), [lin-14](#), and [lin-28](#) affect vulval development. They appear to affect the maturation of VPCs by controlling the length of their cell cycles ([Euling and Ambros 1996a](#)). [lin\(n300\)](#) also appears to have a [vulva](#)-specific heterochronic defect, and genetic epistasis tests suggest that it may be a target of the global heterochronic genes ([Euling and Ambros 1996a](#)).

## C. Other Genes Involved in VPC Generation or Identity

Two genes, [lin-25](#) and [lin-31](#), have been primarily studied for their roles in [VPC](#) specification, but they may also have roles in [VPC](#) generation or identity. Null alleles of [lin-25](#) and [lin-31](#) sometimes cause [P3.p–P8.p](#) to divide precociously to generate two cells, each of which can be a [VPC](#) (i.e., has the potential to adopt vulval fates) or, in the case of [lin-31](#), a neuroblast ([Ferguson et al. 1987](#); Miller et al. 1993; Tuck and Greenwald 1995). These genes are potential targets of the Ras-Raf-MEK-MAPK cascade of the inductive signaling pathway (see below), raising the possibility that this cascade is utilized in cell signaling events involved in [VPC](#) generation or identity.

# Chapter 19. Development of the Vulva — IV VPC Specification

[P3.p–P8.p](#) each has the potential to adopt one of three fates, which can be recognized by the lineages that they undergo ([Fig. 4](#)). The 1° fate and 2° fates are termed “vulval” fates, because they lead to the production of vulval cells. The 3° fate is termed the “nonvulval” or “hypodermal” fate, because it leads to the production of cells that join the [hyp7](#) hypodermal syncytium. In wild-type hermaphrodites, [P3.p–P8.p](#) always adopt the same pattern of fates: 3°-3°-2°-1°-2°-3°. It is now thought that this pattern reflects the outcome of three different signaling events: inductive signaling from the AC, lateral signaling among VPCs, and inhibitory signaling from the hypodermal syncytium. I first summarize what is known about each of these signaling pathways and then discuss how the different signals may be integrated by the VPCs.

## A. Inductive Signaling

Laser microsurgery experiments demonstrated that the AC of the [somatic gonad](#) induces underlying VPCs to adopt vulval fates ([Sulston and White 1980; Kimble 1981](#)). The AC is necessary to induce vulval development, since if the AC alone is ablated, [P5.p](#), [P6.p](#), and [P7.p](#) do not adopt vulval fates. Moreover, the AC is sufficient to induce vulval development, since if [all somatic](#) gonadal cells except for the AC are ablated, the [vulva](#) develops normally ([Kimble 1981](#)).

There is also evidence suggesting that inductive signaling from the AC influences the patterning of vulval fates. An isolated [VPC](#) may adopt either the 1° or 2° fate, depending on its distance from the AC or the dosage of the inductive signal, LIN-3 ([Sternberg and Horvitz 1986; Thomas et al. 1990; Katz et al. 1995](#)). These experiments suggested that the inductive signal may be spatially graded and that the amount of inductive signal received by a [VPC](#) may influence whether it adopts the 1° or 2° fate. The extreme form of the graded signal model would be that in wild-type hermaphrodites, [P6.p](#) (the [VPC](#) closest to the AC) receives a high level of inductive signal that specifies the 1° fate, and [P5.p](#) and [P7.p](#), which are further away, receive a lower level of inductive signal that specifies the 2° fate; [P3.p](#), [P4.p](#), and [P8.p](#) would receive less (or no) inductive signal and therefore not be induced to adopt vulval fates. However, as described below, another signaling event (lateral signaling) is critical for patterning the fates of the VPCs.

A large collection of genes involved in [VPC](#) fate specification have been identified in screens for Vulvaless and Multivulva mutants. Many of the mutants are defective in the inductive signaling process, and genetic epistasis experiments have led to the construction of a genetic pathway for vulval induction ([Fig. 5](#)). Remarkably, molecular analysis of the genes involved in vulval induction revealed that this genetic pathway corresponds to a well-conserved Ras-mediated signal transduction pathway ([Fig. 5](#)).

### 1. Genes of the Inductive Signaling Pathway

The genes that mediate the interaction between the AC and the VPCs have been identified in genetic screens for mutations affecting vulval development and for suppressors of extant vulval mutants. It is notable that many of the genes involved in inductive signaling and signal transduction are essential genes, i.e., complete absence of gene activity results in larval arrest. Genetic screens based on the Vulvaless and Multivulva phenotypes are so powerful that relatively rare events can be detected easily, enabling the identification of non-null alleles of these essential genes.

[lin-3](#) was defined by partial loss-of-function mutations that confer a Vulvaless phenotype ([Horvitz and Sulston 1980; Ferguson and Horvitz 1985; Ferguson et al. 1987](#)). It is predicted to encode a transmembrane protein containing a single EGF-like motif and is expressed in the AC at the time of vulval induction (Hill and Sternberg 1992). Overexpression of wild-type LIN-3 protein or just the LIN-3 EGF-like motif causes a Multivulva phenotype (Hill and Sternberg 1992; [Katz et al. 1995](#)).

[let-23](#) was implicated in vulval development by partial loss-of-function alleles that confer a Vulvaless phenotype ([Ferguson and Horvitz 1985; Ferguson et al. 1987; Aroian and Sternberg 1991](#)). The predicted LET-23 protein is a

receptor tyrosine kinase of the EGF receptor subfamily (Aroian et al. 1990). Genetic mosaic analysis has confirmed the inference that *let-23* acts in the VPCs (Koga and Ohshima 1995; Simske and Kim 1995). Other aspects of *let-23* expression and function have also been studied (Katz et al. 1996; Sakai et al. 1996).

*sem-5* was defined by partial loss-of-function alleles that confer a Vulvaless phenotype and defects in sex myoblast migration (Clark et al. 1992; Stern and Horvitz 1991). SEM-5 is composed of two SH3 domains and one SH2 domain and is structurally and functionally homologous to the human GRB2 protein (Clark et al. 1992; Stern et al. 1993). SEM-5/GRB2 appears to function as an adaptor between receptor tyrosine kinases and Ras.

*let-60* Ras was first implicated in vulval development by hypermorphic alleles that confer a Multivulva phenotype (Ferguson and Horvitz 1985; Ferguson et al. 1987; Beitel et al. 1990; Han et al. 1990). Antimorphic (dominant-negative) alleles and recessive partial loss-of-function alleles also exist and confer a Vulvaless phenotype (Beitel et al. 1990; Han and Sternberg 1990, 1991). The finding that *let-60* encoded a Ras protein (Han and Sternberg 1990) was the first indication in any organism that Ras proteins have roles in specification and differentiation as opposed to cell growth and proliferation.

*lin-45* Raf, *mek-2* MEK, and *mpk-1* / *sur-1* MAP kinase are the components of a protein kinase cascade that act after *let-60* Ras. They were all found as partial loss-of-function mutations in screens for suppressors of the Multivulva phenotype of activated *let-60* Ras, as well as in other screens (Han et al. 1993; Lackner et al. 1994; Wu and Han 1994; Church et al. 1995; Kornfeld et al. 1995a; Wu et al. 1995).

## 2. Probable Targets of the Inductive Signaling Pathway

The inductive signaling pathway leads to changes in gene expression so that different cell fates are executed. It is therefore no surprise that some genes which act downstream from the Ras-Raf-MEK-MAP kinase cascade, based on genetic criteria, encode proteins resembling known transcription factors. Others are novel proteins of unknown function (but which may prove to be transcription factors). Thus far, based on genetic epistasis, likely targets of the inductive signaling pathway are *lin-1*, which encodes a putative transcription factor of the ets family that acts as a negative regulator of vulval induction (Beitel et al. 1995); *lin-25* (Tuck and Greenwald 1995) and *sur-2* (Singh and Han 1995), which encode novel proteins and act as positive factors required for full induction; and *lin-31*, which encodes a putative transcription factor of the HNF3/fork head family and appears to be involved in specifying both vulval and nonvulval fates (Miller et al. 1993).

It is interesting that in contrast to the components of the inductive signaling pathway, the potential targets of the pathway thus far identified display little or no lethality even when gene activity is completely eliminated. Whether the viability of null mutants of potential target genes reflects a more restricted role in development or functional redundancy with other genes is not yet known.

## 3. Other Influences on Inductive Signaling

Many other genes have been defined by mutations that suppress activated Ras. The *ksr-1* gene identified by reverting an activated allele of *let-60* Ras encodes a protein kinase (Kornfeld et al. 1995b; Sundaram and Han 1995). KSR-1 could be an important, and hitherto missing, component of the system for Raf activation, or it could act on a component of the Ras signaling pathway downstream from Raf. Another gene, *let-341*, is a candidate for a guanine nucleotide exchange factor based on genetic epistasis (S. Clark et al., pers. comm.).

Three genes, *lin-2*, *lin-7*, and *lin-10*, were defined by null alleles that result in an incompletely penetrant Vulvaless phenotype (Horvitz and Sulston 1980; Ferguson and Horvitz 1985; Ferguson et al. 1987). *lin-10* encodes a novel protein (Kim and Horvitz 1990), and *lin-2* and *lin-7* encode potential cell junction proteins (Hoskins et al. 1996; Simske et al. 1996). Further characterization of these genes has suggested that they are involved in localizing LET-23 and that receptor mislocalization in *lin-2* and *lin-7* mutants reduces the efficacy of inductive signaling (Simske et al. 1996).

## B. Lateral Signaling

The existence of a lateral signal among VPCs was suggested by the observation that in Multivulva mutants, in which all VPCs adopt vulval fates independent of inductive signaling, adjacent VPCs do not adopt the 1<sup>o</sup> fate. The possibility of lateral signaling was tested by laser microsurgery (Sternberg 1988). In *lin-15* Multivulva mutants (see below), the pattern of VPC fates most closely approximates an alternating 1<sup>o</sup>-2<sup>o</sup> pattern. VPC-to-VPC communication was demonstrated by showing that if the AC and five VPCs are killed, the remaining VPC adopts the 1<sup>o</sup> fate, but if the AC and only four VPCs are killed, one VPC adopts the 1<sup>o</sup> fate and the other adopts the 2<sup>o</sup> fate.

*lin-12* appears to be the receptor for the lateral signal, since VPCs never adopt the 2<sup>o</sup> fate in mutants that lack *lin-12* activity and always adopt the 2<sup>o</sup> fate in mutants that have a high level of *lin-12* activation (Greenwald et al. 1983; Sternberg and Horvitz 1989; Struhl et al. 1993). However, LAG-2 does not appear to be the ligand for *LIN-12* in lateral signaling (Tax et al. 1994; K. Fitzgerald and I. Greenwald, unpubl.; S. Kaech and S. Kim, pers. comm.), and the identity of the lateral signal is as yet unknown.

Lateral signaling is an important input into VPC specification. Certain *lin-12* alleles result in apparent ligand-independent activation of LIN-12 and cause all six VPCs to adopt the 2<sup>o</sup> fate even in the absence of inductive signaling (Greenwald et al. 1983; Sternberg and Horvitz 1989; Greenwald and Seydoux 1990; Han et al. 1990; Levitan and Greenwald 1995). Thus, inductive signaling per se is not necessary, and lateral signaling alone is sufficient, to specify the 2<sup>o</sup> fate. Furthermore, vulval development can be normal even if P5.p and P7.p are incapable of responding to the inductive signal. Genetic mosaics in which P5.p lacked activity of *let-23*, and hence could not respond to the LIN-3 inductive signal, but in which P6.p had *let-23* activity, had normal vulval development (Koga and Ohshima 1995; Simske and Kim 1995). In these genetic mosaics, P5.p adopted the 2<sup>o</sup> fate, presumably because of lateral signaling from P6.p.

It is not yet known whether *lin-12* activity in the VPCs is subject to feedback modulation analogous to that occurring in the AC/VU decision. However, if there is a feedback mechanism involved in lateral signaling, it may not involve transcriptional regulation of *lin-12*, which appears to be expressed continuously and uniformly in the VPCs from the L2 stage through the time of their division in the L3 stage (Wilkinson and Greenwald 1995).

## C. Inhibitory Signaling

Genetic mosaic analysis of *lin-15* suggested that an inhibitory signal from hyp7, the syncytial hypodermal cell that encompasses much of the animal, prevents VPCs from adopting vulval fates. Mosaic hermaphrodites could have a Multivulva phenotype if cells in the hypodermis lacked *lin-15* activity even when the VPCs were genotypically wild type (Herman and Hedgecock 1990). The inference that hyp7 is involved in inhibitory signaling is particularly appealing since making a distinction between vulval hypodermis and syncytial hypodermis appears to be a recurring theme in vulval development. An early manifestation of the identity of a hypodermal cell as a VPC is that it is not part of a syncytium (Kenyon 1986), and nonvulval descendants of VPCs join the hyp7 syncytium (Sulston and Horvitz 1977).

The *lin-15* locus includes two genes that are members of a group of genes called "SynMuv" genes (a "Synthetic Multivulva" phenotype), because in some cases, a Multivulva phenotype is only visible if mutations in two different genes are combined (Horvitz and Sulston 1980; Ferguson and Horvitz 1989; J. Thomas and H.R. Horvitz, pers. comm.). The SynMuv genes are likely to be involved in the hyp7-VPC communication, but molecular analysis has not thus far provided any clues about the signaling mechanism. *lin-15* encodes two novel proteins (Clark et al. 1994; Huang et al. 1994) that are nuclear and broadly expressed (L. Huang and P. Sternberg, pers. comm.). *lin-9* and *lin-36* each encodes novel proteins (G. Beitel et al., pers. comm.). Genetic mosaic analyses have suggested that *lin-36* functions in VPCs (J. Thomas and H.R. Horvitz, pers. comm.) and that *lin-37*, like *lin-15*, has a focus in hyp7 (Hedgecock and Herman 1995). *lin-15*, *lin-36*, and *lin-37* may therefore be involved in reception or transduction of the inhibitory signal. *lin-3* encodes a protein with multiple zinc fingers (A. Meléndez and I. Greenwald, unpubl.), and it will be interesting to determine its cellular focus.

## D. Integration of Different Signaling Inputs

In wild-type hermaphrodites, the pattern of vulval fates is invariant: [P5.p](#), [P6.p](#), and [P7.p](#) adopt the 2<sup>o</sup>, 1<sup>o</sup>, and 2<sup>o</sup> fates, respectively ([Sulston and Horvitz 1977](#)). As described above, three different signaling systems are involved in the generation of this pattern: the inductive signal, the lateral signal, and the inhibitory signal. Somehow, these different signaling inputs are integrated so that the correct pattern of [VPC](#) fates is always specified.

This problem is a subject of great current interest and some controversy, particularly for the integration of the inductive and lateral signaling pathways. The key issue is determining which inputs [P5.p](#), [P6.p](#), and [P7.p](#) (the VPCs that adopt vulval fates) receive during normal development. Is the graded inductive signal the primary patterning agent? As described above, the fate of a [VPC](#) may be influenced by its position or the level of [lin-3](#) activity, indicating that a graded inductive signal may play a part in patterning ([Sternberg and Horvitz 1986](#); [Thomas et al. 1990](#); [Katz et al. 1995](#)). Is sequential induction the primary patterning agent, so that only [P6.p](#) is directly induced to produce the lateral signal that specifies the fates of [P5.p](#) and [P7.p](#)? Several lines of evidence suggest that lateral signaling by [P6.p](#) is important for patterning. Genetic mosaic studies indicate that vulval development can be normal even if only [P6.p](#) is induced by the AC (Koga and Ohshima 1995; Simske and Kim 1995). Furthermore, mutations in [lin-25](#) and [sur-2](#), apparent targets of the inductive signaling pathway, lead to a reduced lateral signaling, suggesting that the activity of the lateral signal is regulated by the inductive signaling pathway (Singh and Han 1995; Tuck and Greenwald 1995).

Currently, the prevalent view is that although either a graded inductive signal or a sequential induction mechanism may be sufficient to pattern the [vulva](#), both mechanisms may be utilized during normal development ([Fig. 6](#)) ([Beitel et al. 1995](#); [Katz et al. 1995](#); Koga and Ohshima 1995; Simske and Kim 1995). Indeed, there is some evidence that VPCs are able to assess the relative activity of the inductive and lateral signaling pathways. The vulval phenotypes of an allelic series of [lin-12](#) hypermorphs suggested that [lin-12](#) activity must be relatively high to bypass the need for inductive signaling ([Greenwald et al. 1983](#)). In addition, the presence of an anchor cell or activation of the inductive signaling pathway can override the effects of activating LIN-12 ([Sternberg and Horvitz 1989](#)). Furthermore, when the activity of the inductive signaling pathway is set at a high level by removing the activity of [lin-1](#), one copy of activated [lin-12](#) is insufficient to specify the 2<sup>o</sup> fate, but two copies of activated [lin-12](#) can specify the 2<sup>o</sup> fate ([Beitel et al. 1995](#)).

## E. Other Genes Involved in VPC Specification

In describing genes involved in intercellular signaling that specify [VPC](#) fates, I have focused primarily on genes that are known to be key players based directly on the analysis of mutant phenotypes. However, extragenic suppressors of vulval mutants are easily obtained by reverting egg-laying defects of Vulvaless mutants or morphology defects of Multivulva mutants. The primary roles of some of these "suppressor genes" may be in [VPC](#) fate specification. Indeed, as described above, many of the genes of the inductive signaling pathway were identified as suppressors of vulval defects. Other suppressor genes may influence [VPC](#) fate specification as a secondary consequence of more general roles in protein trafficking or stability. For example, [unc-101](#), identified by reverting the Vulvaless phenotype of [let-23](#) mutants, encodes a clathrin adaptor protein ([Lee et al. 1994](#)).

The genetic and molecular characterization of suppressors of vulval defects will no doubt be a future source of great insight into [VPC](#) specification and the conserved molecular mechanisms utilized in other developmental events and in other organisms. Thus far, many other new genes have been defined by reverting vulval defects. [suv-1](#) (suppressor of vulvaless) was identified by reverting the Vulvaless phenotype of [lin-10](#) mutants (Kim and Horvitz 1990). [sli-1](#), which was identified by reverting the Vulvaless phenotype of [let-23](#) mutants (Jongeward et al. 1995), was found to be similar to the mammalian proto-oncogene *c-cbl* (Yoon et al. 1995).

Fourteen genes have been identified by reverting phenotypes associated with reduced or elevated [lin-12](#) activity ([Ferguson and Horvitz 1985](#); [Sundaram and Greenwald 1993b](#); [Tax et al. 1994](#); [Levitin and Greenwald 1995](#); F. Tax et al., in prep.; I. Greenwald, unpubl.). As described above, one way that [lag-2](#), a ligand for [lin-12](#), was identified was by reverting [lin-12](#) mutant defects ([Tax et al. 1994](#)). Another gene, [sel-1](#) (suppressor/enhancer of [lin-12](#)), acts

as a negative regulator of *lin-12* activity and encodes a novel secreted protein (Sundaram and Greenwald 1993b; Grant and Greenwald 1996). A third gene, *sel-12*, appears to function in receiving cells to facilitate *lin-12*-mediated signaling and encodes a protein that is homologous to the human presenilins, which have been implicated in the development of Alzheimer's disease (Levitian and Greenwald 1995).

## Figures



### Figure 4

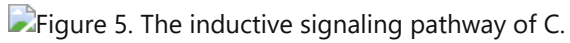


### Figure 5

The inductive signaling pathway of *C. elegans* and homologous pathways in the yeast *Schizosaccharomyces pombe* (for review, see Kurjan 1993) and in mammals (for review, see Khosravi and Der 1994).



### Figure 6

Cell signaling events during wild-type vulval development. Inductive signaling: The AC produces LIN-3 (arrows), which activates LET-23 (inverted arrow) in *P6.p*, and possibly in *P5.p* and *P7.p* (arrows with question marks). Lateral signaling: Induction causes expression or activation of a ligand (circle) for LIN-12 (C-shaped) in *P6.p* and possibly in *P5.p* and *P7.p*. Inhibitory signaling: The *hyp7* hypodermal syncytium may be the source of a signal that inhibits vulval induction or promotes the 3<sup>o</sup> fate.

Generated from local HTML

# Chapter 19. Development of the Vulva — V Execution

---

Laser microsurgery and temperature-shift experiments suggest that the VPCs become specified prior to their division ([Greenwald et al. 1983](#); [Sternberg and Horvitz 1986](#); [Ferguson et al. 1987](#); [Euling and Ambros 1996a](#)). After the VPCs are specified, the different fates must be correctly executed to generate the correct numbers and types of descendants. For the purposes of this chapter, I consider “execution” to be the phase of vulval development from the division of the VPCs until the termination of the vulval lineages at the end of the L3 stage.

## A. Intrinsic Programming or Extrinsic Influences?

Once the [VPC](#) fates have been specified, interactions among [VPC descendants](#) may not be important for the execution of vulval fates: For example, if [P5.pa](#) is ablated, [P5.pp](#) expresses its normal lineage (TN), and if [P5.pp](#) is ablated, [P5.pa](#) expresses its normal lineage (LL) ([Sternberg and Horvitz 1986](#)). However, there may be other extrinsic influences on the execution of vulval fates. Indeed, signaling from the [somatic gonad](#) appears to influence polarity of the 2<sup>o</sup> lineages (W. Katz and P. Sternberg, pers. comm.). Furthermore, many of the mutants in [VPC](#) specification display abnormal execution of vulval lineages (see, e.g., [Ferguson et al. 1987](#); [Sternberg and Horvitz 1989](#)). Although these abnormal lineages may reflect abnormal specification, it is also possible that the same signaling systems are involved in cell-cell interactions during execution. Finally, [lin-12](#) is expressed in cells during the 2<sup>o</sup> lineages, raising the possibility that [lin-12](#)-mediated signaling is also involved in execution of the 2<sup>o</sup> fate ([Wilkinson and Greenwald 1995](#)).

## B. Genes Involved in Execution

Genes involved in execution may be operationally defined by mutations that specifically alter either the 1<sup>o</sup> or the 2<sup>o</sup> lineages. Two criteria have been most useful: the plane of the final division and adherence properties of the penultimate and ultimate cells ([Sternberg and Horvitz 1986](#); [Ferguson et al. 1987](#)). Thus far, one gene that may be specifically required for the execution of the 1<sup>o</sup> lineage has been identified. In [vex-1](#) mutants, [P6.p](#) expresses an abnormal 1<sup>o</sup> lineage, but [P5.p](#) and [P7.p](#) express normal 2<sup>o</sup> lineages (P. Kayne and P. Sternberg, pers. comm.).

Three genes that appear to be involved in the execution of the 2<sup>o</sup> lineage have been identified. In [lin-11](#) mutants, the 2<sup>o</sup> lineages expressed by both [P5.p](#) and [P7.p](#) are affected and may be represented as **LLLL** instead of **LLTN** ([P5.p](#)) or **NTLL** ([P7.p](#)) as in wild type ([Ferguson et al. 1987](#)). [lin-11](#) encodes a transcription factor containing a homeodomain and a LIM metal-binding domain (Freyd et al. 1990). [lin-11](#) is expressed in the T and N cells and not in the other VPCs (and often not in the [VPC](#) daughters), suggesting that [lin-11](#) functions in the cells that are abnormal in [lin-11](#) mutants (Freyd 1991; G. Freyd and H.R. Horvitz, pers. comm.). The *lin-11::lacZ* transgene that was used in [lin-11](#) expression studies is an excellent marker for expression of the 2<sup>o</sup> fate by a [VPC](#).

Mutations in [lin-17](#) and [lin-18](#) have virtually no effect on the 2<sup>o</sup> lineage of [P5.p](#), but they alter the 2<sup>o</sup> lineage expressed by [P7.p](#), resulting in **LLLL** (symmetric) or **LLTN** (reversed polarity) lineages ([Ferguson et al. 1987](#); [Sternberg and Horvitz 1988](#)). [lin-17](#) is predicted to encode a multiple transmembrane domain protein that is similar to the *Drosophila* frizzled gene (Vinson et al. 1989), which is also involved in cell polarity (H. Sawa and H.R. Horvitz, pers. comm.). Expression of [lin-11](#) is altered in [lin-17](#) and [lin-18](#) mutants (Freyd 1991), suggesting that it may be a target of intercellular signaling mediated by [lin-17](#) and [lin-18](#).

# Chapter 19. Development of the Vulva — VI Morphogenesis

---

For the purposes of this chapter, I consider morphogenesis to be the events of the L4 stage. During the L4 stage, the vulval cells form an invagination, with vulval cells at the apex of the invagination attached to [uterine](#) cells; the anchor cell fuses with a specific multinucleate [uterine](#) cell, and defined vulval cells fuse with each other to generate a series of seven toroidal rings (see [Fig. 7](#)) (J. White et al., pers. comm.). At the L4 molt, the vulval invagination everts to form the mature [vulva](#).

## A. Role of Somatic Gonadal Cells

Laser microsurgery experiments have demonstrated that the AC and other gonadal cells (particularly of the [uterus](#)) are important for normal vulval morphogenesis. If the AC is ablated in the early L3 stage, before the VPCs divide, the correct number of vulval cells are generated in some cases, but the morphology of the vulval invagination is abnormal ([Kimble 1981](#)). Furthermore, if the AC is ablated somewhat later, in the mid-L3 stage, vulval invagination is normal but the attachment to the [uterus](#) is not made ([Kimble 1981](#)), and vulval eversion is abnormal ([Seydoux et al. 1993](#)). However, if the AC is ablated in the late L3 stage, the [vulva](#) everts normally, implying that the role of the AC is completed before the main events of morphogenesis occur ([Seydoux et al. 1993](#)).

## B. Morphogenetic Capacity of Vulval Cells

Vulval cells appear to have at least some intrinsic capacity to undergo morphogenesis. Genetic and laser microsurgery experiments have suggested that the eight vulval cells produced as a result of the expression of the 1<sup>o</sup> fate can sometimes form a functional [vulva](#) in the absence of the vulval cells descended from 2<sup>o</sup> lineages ([Sulston and White 1980](#); [Sulston and Horvitz 1981](#)). Furthermore, when [lin-12](#) is activated, causing all six VPCs to adopt the 2<sup>o</sup> fate, the resulting pseudovulvae consist of concentric rings, suggesting that the vulval cells produced as a result of the expression of the 2<sup>o</sup> fate also have the intrinsic capacity to organize, even when located far away from the anchor cell and [uterus](#) (J. White et al., pers. comm.).

## C. Genes Involved in Vulval Morphogenesis

One screen for genes involved in vulval morphogenesis was conducted by looking for mutants with a reduced vulval invagination at the mid-L4 stage but with normal cell lineages (T. Herman and H.R. Horvitz, pers. comm.). In this screen, mutations in eight different genes were found to cause reduced vulval invagination (with apparently normal cell lineages) and reduced fertility or viability. Two of these genes have been cloned (T. Herman and H.R. Horvitz, pers. comm.): [sqv-3](#) ([squashed vulva](#)) encodes a protein similar to a mammalian β-1,4 galactosyl transferase, suggesting that sugar groups may be important for cell-cell recognition events during morphogenesis, and [spe-2](#) encodes a novel protein.

Another screen for genes involved in vulval morphogenesis was conducted by looking for mutants with abnormal vulval eversion, leading to the production of a large vulval protrusion ([Seydoux et al. 1993](#)). Mutations in many different genes can cause this *Evl* ([abnormal eversion of the vulva](#)) phenotype, and germ-line and [somatic gonad](#) abnormalities were associated with virtually all of these mutants. Some of the *Evl* mutants appear to affect the integrity of the gonad without affecting the vulval lineages, and therefore their effects on vulval eversion may be a consequence of their effects on gonadal development.

The [sel-12](#) gene was identified in a screen for mutations that suppress the Multivulva phenotype associated with *LIN-12* activation ([Levitin and Greenwald 1995](#)). Genetic studies suggest that vulval morphogenesis may be particularly sensitive to reduced [sel-12](#) activity, although it is not yet clear if the effects of [sel-12](#) on vulval morphogenesis are independent of [lin-12](#) activity (D. Levitan and I. Greenwald, unpubl.).

## Figures

Figure 7. Schematic view of the morphology of the L4 vulva (based on J.

## Figure 7

Schematic view of the morphology of the L4 [vulva](#) (based on J.G. White et al., pers. comm.). In the early L4, the vulval primordium is a stack of seven multinucleate toroidal cells, with the anchor cell at the apex. The anchor cell appears to insinuate itself through the middle of the four F ring precursor cells, thereby opening up a passage at the apex of the [vulva](#) primordium. Later on, the anchor cell fuses with a multinucleate [uterine](#) cell, and the B1 and B2 cells of the stack fuse. After fusion, the apex opens out and the structure is no longer conical. The lineage relationships of cells that give rise to each toroid are indicated. (*Closed circles*) Nuclei produced by execution of the 2<sup>o</sup> fate; (*open circles*) nuclei produced by execution of the 1<sup>o</sup> fate.

Generated from local HTML

## Chapter 19. Development of the Vulva — VII Evolution of Vulval Development

---

Comparative studies of vulval development have provided insight into the evolution of vulval patterning ([Sternberg and Horvitz 1982](#); [Sommer and Sternberg 1994](#); [Fitch and Thomas, this volume](#)). In *Caenorhabditis*, the [vulva](#) forms at 50% body length. In other genera, however, the [vulva](#) forms more posteriorly. In *Panagrellus*, the [vulva](#) forms at 60% body length, and [P4.p–P9.p](#) are the VPCs, i.e., they have the potential to generate vulval cells ([Sternberg and Horvitz 1982](#)). However, a posterior shift in the Pn.p cells that become VPCs does not appear to be the mechanism for forming a [vulva](#) even more posteriorly: In several species characterized by [vulva](#) formation at 80–90% body length, [P3.p–P8.p](#) or [P4.p–P8.p](#) are VPCs ([Sommer and Sternberg 1994](#)). In these species, VPCs migrate posteriorly and adopt a species-specific position, and vulval induction is delayed until the gonad has extended posteriorly so that the AC lies over [P6.p](#) ([Sommer and Sternberg 1994](#)). Mutations affecting vulval development have been recently identified in other species (Sommer and Sternberg 1996a).

Generated from local HTML

## Chapter 19. Development of the Vulva — VIII Future Prospects

---

In the 8 years since the publication of the Genetics of Cell Lineage chapter in the original "worm book" ([Horvitz 1988](#)), the identification and molecular characterization of genes involved in vulval development have led to a great deal of progress toward understanding [VPC](#) specification. What will the next 8 years bring?

There are still many unresolved problems in [VPC](#) specification. A key issue is how different signaling inputs are integrated and the relative importance of the different signaling inputs in specifying [VPC](#) fates in wild-type hermaphrodites. Another area of current and future research is to describe the lateral and inhibitory signaling pathways as completely as the inductive signaling pathway. This description will involve the genetic identification of new components (perhaps largely through the isolation of suppressor mutations) and their molecular characterization.

In general, effects on vulval development will also be used more as an assay to work out details of the mechanism and function of conserved components of signaling pathways. Furthermore, the study of mutations that affect vulval development as a secondary consequence of more profound effects on fundamental processes such as protein trafficking will open new areas of *C. elegans* research. Finally, little is known about [VPC](#) generation and identity, the execution of [VPC](#) fates, and vulval morphogenesis. Genetic and molecular analyses of these aspects of vulval development will be forays into relatively uncharted territory and will no doubt yield insights that will be of general relevance to developmental biology.

Generated from local HTML

## **Chapter 19. Development of the Vulva — Acknowledgments**

---

I am grateful to Paul Sternberg, who was an invaluable consultant during the writing of this review. I also thank Simon Tuck for helpful comments, and Victor Ambros, Bob Horvitz, Stuart Kim, Paul Sternberg, and John White for permission to cite unpublished information.

Generated from local HTML

# **Chapter 20. Patterning the Nervous System**

---

## **Contents**

- [I Introduction](#)
- [II Invariant Cell Lineages in \*C. elegans\* Neurogenesis](#)
- [III Specification of Sensory Neuronal Development](#)
- [IV Generation of Reiterated Neurons by Reiterated Cell Lineages](#)
- [V Spatial Patterning by the \*C. elegans\* HOM-C Gene Cluster](#)
- [VI Concluding Remarks](#)

Generated from local HTML

# Chapter 20. Patterning the Nervous System — I Introduction

The *Caenorhabditis elegans* nervous system consists of 302 neurons of 118 types that interconnect in a reproducible manner to form a variety of neural circuits and pathways (White et al. 1986). This complex array of neurons is generated by invariant patterns of cell division and migration (Sulston et al. 1983). Many of the neural types are generated in groups by neuroblast sublineages that are reiterated along the symmetry axes of the animal. Some of these iterated cell lineages are modified to generate sets of neural descendants that are variations on a theme. The correlation of neural type with pattern of cell lineage suggests that there are genetic pathways which couple neural specification to lineage. The variations on the canonical cell lineages suggest that there are also pathways that modify the activity of such modular cell-lineage-generating mechanisms.

Genes that act to couple cell lineage to neural identity as well as genes that mediate the variations in these cell lineages have been detected in genetic screens for mutants with defects in neural development or function (Finney and Ruvkun 1990; Miller et al. 1993; Wang et al. 1993; Jin et al. 1994). Many of these genes encode transcription factors that regulate the patterned generation of neurons in stereotyped cell lineages (Way and Chalfie 1988; Finney and Ruvkun 1990; Miller et al. 1992; Jin et al. 1994) or in spatial domains (Salser et al. 1993). Some of these genes also control the detailed features of neural type, such as their migration paths (Kenyon 1986; Chisholm 1991), patterns of synaptic connectivity (White et al. 1992), and neurotransmitter production (Desai et al. 1988; Chisholm 1991; Jin et al. 1994). The expression of these genes is activated in complex patterns that presage the key neurogenic events. These neuronal transcription factors are thought to regulate the expression of entire repertoires of downstream genes (Xue et al. 1992) that actually mediate the complex recognition and signaling events necessary for neurogenesis and neural function.

In this chapter, I discuss the molecular genetic evidence that committed cell lineages generate a variety of neural types during *C. elegans* neurogenesis. The genes *lin-32*, *unc-86*, and *mec-3* encode components of such a cell-lineage-coupling mechanism in sensory neurogenesis. *unc-4* and *unc-30* act similarly in reiterated motor neuron lineages. Next, I discuss how the patterns of neural types specified by these reiterated cell lineages are modified along the anterior-posterior (A-P) axis by the action of the *C. elegans* homeobox cluster (HOM-C) genes. Finally, I speculate on how these genes conspire to specify the complexity of nervous system development and function.

## Tables

**Table 1** Summary of genes and neural types affected

Gene	Mutant phenotypes	Gene product	Expression pattern
<i>mec-3</i>	Mec	LIM homeodomain	mechanoreceptor neurons
<i>mec-7</i>	Mec	β-tubulin	mechanoreceptor neurons
<i>mec-4</i>	Mec	probable channel	mechanoreceptor neurons
<i>unc-86</i>	Mec, Odr, Ttx, Lin	POU homeodomain	a variety of neuroblasts and neurons
<i>lin-11</i>	Unc, Lin	LIM homeodomain	particular neurons and vulval cells
<i>ham-1</i>	symmetrization of HSN/PHB cell lineage	novel	asymmetrically localized on affected neuroblasts
<i>lin-32</i>	Mec, neuroblasts to ectoblast transformation	basic HLH	neuroblasts
<i>vab-3</i>	missing head structures and neurons	Pax homeodomain	anterior and posterior neuroblasts and neurons
<i>unc-4</i>	Unc: presynaptic VA neuron	Prd homeodomain	VA motor neurons, VA-like motor neurons defects

<b>Gene</b>	<b>Mutant phenotypes</b>	<b>Gene product</b>	<b>Expression pattern</b>
<a href="#"><i>unc-37</i></a>	Unc-like <a href="#"><i>unc-4</i></a> ; sterile	Groucho homolog	unknown
<a href="#"><i>unc-30</i></a>	Shrinker Unc	homeodomain	GABAergic <a href="#"><i>neurons</i></a>
<a href="#"><i>lin-26</i></a>	P neuroectoblast, ectodermal defects	zinc finger protein	all ectoblasts
<a href="#"><i>lin-39</i></a>	midbody region cell fates	HOX cluster homeodomain	midbody region cells
<a href="#"><i>mab-5</i></a>	post/midbody region cell fates	HOX cluster homeodomain	post/midbody region cells
<a href="#"><i>egl-5</i></a>	posterior body region cell fates	HOX cluster homeodomain	posterior body region cells
<a href="#"><i>ceh-20</i></a>	<a href="#"><i>lin-39</i></a> and <i>mab-5</i> -like defects	PBX homeodomain	<a href="#"><i>ventral nerve cord</i></a> , ectoblasts
<a href="#"><i>sem-4</i></a>	sex myoblast, HSN maturation defects	zinc finger protein	unknown
<a href="#"><i>vab-7</i></a>	maternal-effect lethal, zygotic	Eve homeodomain	posterior blastomeres

The genes discussed in this chapter are listed with the mutant phenotypes, type of protein encoded, and pattern of expression summarized. References for these results are listed in the text of the chapter. (Mec) Mechanosensory defective; (Odr) defective in taxis toward attractive odors; (Che) defective in taxis toward attractive water soluble chemicals; (Lin) cell lineage defects; (Ttx) defective thermotaxis; (Unc) uncoordinated, associated with defective motorneurons.

Generated from local HTML

## Chapter 20. Patterning the Nervous System — II Invariant Cell Lineages in *C. elegans* Neurogenesis

Stereotyped cell lineages generate reproducible patterns of [neurons](#) and support cells during the development of phylogenetically diverse organisms such as insects ([Bate and Grunewald 1981](#)), leeches (Weisblat and Blair 1984), and *C. elegans* ([Sulston and Horvitz 1977](#); [Sulston et al. 1983](#)). In many cases, these sublineages are reiterated along the symmetry axes of the animal to generate multiple sets of [neurons](#). For example, in *C. elegans*, the pattern of postembryonically generated motor [neurons](#) is reiterated 13 times along the A-P axis, albeit with some variation ([Fig. 1](#)) ([Sulston et al. 1983](#)). Most of the 13 neuroblast P cells generate one each of the motor [neuron](#) classes VA, VB, VC, VD, and AS; these classes differ in patterns of neurite outgrowth, connectivity, and neurotransmitter ([Fig. 1](#)) ([White et al. 1986](#)). For example, [VA neurons](#) are excitatory cholinergic neurons that connect to ventral targets, whereas [VD neurons](#) are inhibitory [GABAergic neurons](#) that connect to dorsal targets ([White et al. 1986](#)). In these cell lineages, most [VA neurons](#) are sisters of [VB neurons](#), are cousins to [VC neurons](#), and are more distantly related to the AS and [VD neurons](#) ([Fig. 1](#)). With some variation, each of 13 [neuroblasts](#) spaced along the A-P axis generates this set of five [neurons](#) by a similar pattern of cell division so that muscles along the entire body length of the animal are innervated by reiterated sets of motor [neurons](#).

In addition to the reiterations along the A-P axis, there are cell lineage symmetries relative to other axes ([Sulston et al. 1983](#)). For example, the six sets of IL1 and IL2 [sensory neurons](#) are generated by homologous patterns of cell lineage at six radial positions anterior to the [nerve ring](#). Analogous fourfold symmetric (URA, URB, URY, OLQ, etc.) and twofold symmetric [neurons](#) are generated along the bilateral axis of symmetry of the animal ([Sulston et al. 1983](#)).

The correlation of characteristic neuroblast divisions with patterns of [neural](#) differentiation suggests that a modular “program” for the generation of sets of [neurons](#) is activated at each point where the lineage is observed. Once triggered, this regulatory cascade may mediate the observed sequence of neuroblast cell divisions and [neural](#) specializations. Because the sublineages occur in a variety of locations with distinct neighboring cells, these sublineages either generate internal cues to control the characteristic patterns of [neural](#) types or respond to multiple or global extracellular cues. Cell killing studies using laser microsurgery showed no evidence of extracellular cues in, for example, the IL1/IL2 sublineages ([Sulston et al. 1983](#)), and molecular genetic analysis of the mechanism by which particular [neurons](#) such as the VDs ([Jin et al. 1994](#)) or [mechanosensory neurons](#) are generated (Chalfie and Au 1989) has not yet revealed evidence that extracellular signals are involved. However, the reproducible asymmetric cell lineages of the early *C. elegans* blastomeres (see [Schnabel and Priess](#), this volume) as well as those of postembryonic neuroectoderm blast cells (Herman and Horvitz 1994; Herman et al. 1995) have been shown to be mediated by intercellular signaling. Thus, the reproducibility of [neural](#) cell lineages does not rule out extracellular signals in the specification of neuroblast cell lineages. Similar analysis of *Drosophila* [neural](#) lineages has revealed segregated factors that appear to function in autonomous cell lineage control ([Rhyu et al. 1994](#)) as well as a Notch-based cell-cell signaling system (Hartenstein and Posakony 1990).

In *C. elegans*, the mechanism by which cell lineage asymmetry cues activate [neuron](#) specification genes has been analyzed most completely in the case of the control of sensory neurogenesis by [mec-3](#), [unc-86](#), and [lin-32](#).

### Figures

Figure 1. Cell lineages and fates of the postembryonically derived motor neurons.

### Figure 1

Cell lineages and fates of the postembryonically derived motor [neurons](#). The late developing motor [neurons](#) are derived from a set of 13 [neuroblasts](#) (P0 to P12) that each produce five cells via an identical lineage. In general, the [neuron](#) classes are produced in stereotyped positions on these lineages, but there are exceptions such as the substitution of an AVF [interneuron](#) in the normal location of a VA in two cases and the substitution of a cell death

(X) in the normal locations of VB (two cases) and VC (seven cases). (Reprinted, with permission, from Chalfie and White 1988; White et al. 1988.)

Generated from local HTML

# Chapter 20. Patterning the Nervous System — III Specification of Sensory Neuronal Development

---

Mutations in *mec-3*, *unc-86*, and *lin-32* affect *sensory neurons* almost exclusively. *mec-3* is a neuron-type specification gene that is necessary for the development of *mechanosensory neurons*. *lin-32* and *unc-86* couple cell lineage asymmetry cues to the asymmetric expression of *mec-3*, as well as to other genes.

## A. *mec-3* Specifies Neuron Type

Six *mechanosensory neurons* mediate response of *C. elegans* to gentle touch: *ALM* (left and right), *PLM* (left and right), *AVM*, and *PVM*.

These *mechanosensory neurons* are specialized for the detection of mechanical deformation: They show ultrastructural specializations and express the touch neuron-specific genes *mec-4* and *mec-7* (Hamelin et al. 1992; Mitani et al. 1993). *mec-4* and *mec-7* encode a probable sodium channel subunit and a specialized tubulin, respectively, that are specialized features of *mechanosensory neurons* (see Driscoll and Kaplan, this volume).

*mec-3* gene activity is necessary for the differentiation of these *mechanosensory neurons* (Fig. 2). In the absence of *mec-3* gene activity, these *neurons* do not express *mec-7* and *mec-4* (Mitani et al. 1993). *mec-3* encodes a homeobox gene that also bears an upstream LIM domain (Way and Chalfie 1988; Freyd et al. 1990). The LIM domain has been implicated in protein/protein interactions (Schmeichel and Beckerle 1994) and is associated with a class of homeodomain transcription factors, as well as in proteins that are not implicated in control of transcription (Freyd et al. 1990). *mec-3* is expressed in the six *touch receptor neurons* as well as two other *neurons*, *FLP* and *PVD* (Way and Chalfie 1989). MEC-3 protein binds to the *mec-4* and *mec-7* promoters (A. Duggan and M. Chalfie, pers. comm.). *mec-3* also autoregulates its own expression (Way and Chalfie 1989; Xue et al. 1992; Lichtsteiner and Tjian 1995). Thus, the expression of the MEC-3 transcription factor in the *mechanosensory neurons* activates and maintains the expression of mechanosensory-specific genes such as *mec-7* and *mec-4* that mediate the specialized features of *mechanosensory neurons* (see Driscoll and Kaplan, this volume).

All of the *neurons* that express *mec-3* are the most anterior daughters of a neuroblast that expresses the *unc-86* gene earlier (see below; Fig. 3). These data suggest that expression of *mec-3* is coupled to cell lineage cues. *mec-3* expression is dependent on *unc-86* and *lin-32* gene activities. In *unc-86* and *lin-32* mutants, neuroblast cell lineages are altered so that *mechanosensory neurons* are not generated (Fig. 4). However, in wild-type animals, after its earlier neuroblast specification function, UNC-86 protein continues to be expressed in *mechanosensory neurons* (Finney and Ruvkun 1990) and binds directly to the *mec-3*, *mec-4*, and *mec-7* promoter regions (Xue et al. 1992; A. Duggan and M. Chalfie, pers. comm.). Thus, *unc-86* could both act early in neurogenesis and continue to function later to regulate *mec-3* expression.

The *mec-3* transcriptional regulatory region bears evolutionarily conserved binding sites for UNC-86 and MEC-3 proteins that are important for regulation of the gene (Xue et al. 1992; see McGhee and Krause, this volume). For example, four segments of 71, 29, 28, and 24 bp are conserved between *C. elegans* and *C. remanei* strain VT733, formerly called *C. vulgarensis* (Way and Chalfie 1989; Xue et al. 1992). UNC-86-binding sites map to three of the conserved segments, but it appears that only UNC-86-binding sites in the second and third conserved segments are essential for establishment of *mec-3* expression (Xue et al. 1992). MEC-3 binds adjacent to UNC-86, and these two proteins synergistically activate transcription in vitro on the *mec-3* promoter (Xue et al. 1992; Lichtsteiner and Tjian 1995). The addition of the 71-bp *mec-3* regulatory element to a minimal promoter element is sufficient to recapitulate the *mec-3* expression pattern (Way and Chalfie 1989). However, deletion of this element from a wild-type promoter shows that it is not necessary for expression, suggesting redundancy in this regulatory region.

So far, none of the *mec-3* promoter deletion mutants have shown any evidence of cell-type-specific expression; i.e., each mutant expresses *mec-3* in either all or none of the mechanosensory cells. Thus, the *mec-3* promoter

may respond to the same activation cues in each of the cell types that expresses the gene. All *mec-3*-expressing *neurons* are the anterior-most daughters of an *unc-86*-expressing neuroblast (Fig. 2). Thus, the *mec-3* promoter may respond to a factor that is segregated or differentially activated in these anterior daughters. Although UNC-86 binds to the *mec-3* promoter and is necessary for *mec-3* expression, it is not sufficient to explain its expression: *mec-3* is only activated in a subset of the *neurons* that express *unc-86* (see below). Other factors must modify the activity of *unc-86* either in the cells that express *mec-3* or in those that do not. Candidates for these combinatorial factors are *sem-4*, *egl-44*, *egl-46*, and *lin-14*, which modulate the number of *neurons* that express mechanosensory *neural* markers (Mitani et al. 1993). Three of these genes, *sem-4*, *egl-44*, and *lin-14*, are known to encode nuclear proteins that are candidates to regulate UNC-86 activity directly (Ruvkun and Giusto 1989; M. Basson and H.R. Horvitz, pers. comm.).

The *neurons* that express *mec-3*, however, are not equivalent. First, the *PVD* and FLP *neurons* do not express abundant *mec-4* and *mec-7* (Hamelin et al. 1992; Mitani et al. 1993). Second, the anterior and posterior *mechanosensory neurons* differ in their postsynaptic partners: *AVM* and *ALM* mediate response to touch in the anterior body and couple to the backward command *neuron* AVD, whereas *PVM* and *PLM* mediate response to touch in the posterior body and couple to the forward command *neuron* PVC (see Driscoll and Kaplan, this volume). It is possible that a common cell-lineage-coupling mechanism activates *mec-3* expression in all of these *neurons* to specify their differentiation into *mechanosensory neurons* but that the differences between the connectivities of these *neurons* are specified by external cues or by spatial patterning genes such as *mab-5* (see below) (Chalfie et al. 1983).

The pattern of *mec-3* expression controls where and when *mechanosensory neurons* are generated. But expression of *mec-3* depends on *unc-86* and *lin-32*. These genes constitute parts of the cell lineage asymmetry generation and detection system for asymmetric activation of *mec-3* and other *neural* specification genes.

## B. *unc-86* Controls Neuroblast Cell Lineage Asymmetry

*unc-86* is a key component in the mechanism that detects cell lineage asymmetry to control *neural* fate in a variety of neuroblast cell lineages, including the mechanosensory *neural* lineages. *unc-86* mutants are mechanosensory-defective because of cell lineage defects that disrupt the generation of *mechanosensory neurons* (Chalfie et al. 1981). Analogous cell lineage defects in *unc-86* mutants affect the generation of other *sensory neurons*, motor neurons, and *interneurons*. In all of these cases, *unc-86* mutants disrupt the generation of mother/daughter asymmetry in neuroblast cell lineages: In *unc-86* mutants, one neuroblast daughter of the asymmetric division inappropriately repeats the pattern of cell lineage normally associated with its mother cell (Chalfie et al. 1981). The other daughter cell is not affected by *unc-86* mutations. Therefore, *unc-86* is necessary for one daughter, but not the other, to become distinct from its mother cell. *unc-86* null mutations cause defects in other *neurons* that are not associated with neuroblast cell lineage aberrations. For example, in *unc-86* mutants, the hermaphrodite-specific neuron (HSN) is generated and migrates to its normal position, but it fails to grow a normal axon or connect to its partners and does not accumulate the neurotransmitter serotonin (Desai et al. 1988). Thus, *unc-86* is necessary for the coupling of cell lineage asymmetry to neuroblast as well as *neuronal* cell fates.

*unc-86* encodes a POU-domain protein, a homeodomain transcription factor with two independent helix-turn-helix DNA-binding domains that have been found in many metazoans (Finney et al. 1988; see McGhee and Krause, this volume). UNC-86 protein is expressed in 57 of the 302 *neurons* during the development of the *C. elegans* *nervous system* (Fig. 3) (Finney and Ruvkun 1990). These include particular *sensory neurons*, motor neurons, and *interneurons*, some of which are known to be defective in *unc-86* mutants.

The lineages affected by *unc-86* mutants may constitute a “modular subprogram” of development that has been duplicated and modified repeatedly during evolution (Chalfie et al. 1981). Similarities among the six lineages known to be affected are summarized in Figure 2. All six lineages produce a sensory *neuron* in equivalent positions, as the anterior-most descendant of the first cell to express *unc-86*. In five of the six lineages, these *sensory neurons* express *mec-3* and are mechanosensory; they are the only five pairs of cells in the entire animal

to express *mec-3* (Way and Chalfie 1989). The expression of *unc-86* does not cause these lineages to be similar, because parts of the lineages that never express UNC-86 protein also produce similar *neuron* types (Fig. 2). Thus, the expression of *unc-86* in these lineages is an indication of an underlying similarity that must be set up by other genes.

The cell lineages that express *unc-86* have another common feature: *unc-86* expression is asymmetrically activated in the daughter cell affected by *unc-86* mutations (Fig. 4) (Finney and Ruvkun 1990). Therefore, asymmetric expression of UNC-86 must be sensitive to some factor segregated or activated asymmetrically at division, and *unc-86* must act in the daughter neuroblast or *neuron*. This asymmetric activation of *unc-86* expression may be an initial step in a cascade of regulatory changes that distinguish lineally related *neurons* and *neuroblasts*.

It is the *unc-86* transcriptional regulatory region that detects cell lineage asymmetry (Baumeister et al. 1996). This was established by monitoring the expression of fusion genes that bear *unc-86* regulatory regions in an *unc-86* null mutant, so that *unc-86* autoregulation (see below) did not confound the analysis. A fusion gene bearing 5.1 kb upstream of the *unc-86* gene recapitulates the entire *unc-86* expression pattern in an *unc-86* null mutant, suggesting that all of the regulatory elements necessary to activate *unc-86* expression are present in this 5-kb region. Distinct regions of the *unc-86* 5' region are responsive to cell lineage asymmetry cues in different sets of neuroblast cell lineages. For example, a fusion gene bearing 2.8 kb upstream of the start of transcription activates *unc-86* expression in *neurons RIH* and *RIR*, but not in *I1*, *NSM*, or *HSN* or in the *neuroblasts Q.p*, *V5.paap*, and *T.ppp*. In contrast, a fusion gene that bears -5.1 to -2.7 kb is expressed in neurons *I1*, *NSM*, and *HSN*, and in the *neuroblasts Q.p*, *V5.paaa*, and *T.ppppa*, but is not expressed in *RIH* or *RIR* (Baumeister et al. 1996). Similar analysis showed that enhancers for *unc-86* expression map 3' to the promoter as well (Baumeister et al. 1996).

Expression of these *unc-86* promoter-reporter genes is transient in an *unc-86* null mutant and fades soon after the expression is initiated. In contrast, the expression of the same genes is maintained in animals that express a functional UNC-86 protein. In addition, reporter genes that are activated in a subset of *unc-86*-regulated cell lineages in *unc-86* null mutants are expressed in all of these cell lineages in wild-type animals (Baumeister et al. 1996). These results indicate that *unc-86* autoregulates its own expression. Since *unc-86* encodes a transcription factor, it is a likely candidate to autoregulate its own expression directly (Finney et al. 1988; Xue et al. 1992). Analogous autoregulation of the mammalian POU gene *Pit-1* has been observed (Chen et al. 1990).

This analysis suggests that the complex *unc-86* regulatory region builds up the pattern of *unc-86* expression piece by piece using regulatory pathways that are unique to particular sets of cell lineages. These data suggest that distinct transcriptional regulatory proteins are differentially activated in particular cell lineages to asymmetrically regulate *unc-86* transcription from distinct enhancer elements on the gene. Once expression of *unc-86* is initiated, *unc-86* autoregulation can confer continued UNC-86 expression. In this way, the initial activators of asymmetric *unc-86* expression may be active only transiently to trigger *unc-86* autoregulation.

This model is supported by the observation that mutations in other genes such as *lin-11* affect only parts of the *unc-86* expression pattern. *lin-11* mutants express *unc-86* ectopically in the *interneuron AVG*, which is the sister of the *unc-86*-expressing *neuron RIR* (Baumeister et al. 1996). The pattern of *unc-86* expression in other cell lineages is normal in a *lin-11* mutant. These results suggest that LIN-11 activity in *AVG* may inhibit *unc-86* expression in this *interneuron*.

*ham-1* acts upstream of *unc-86*: Extra *unc-86*-expressing "HSN" *neurons* are evident in *ham-1(n1810)* animals (Baumeister et al. 1996). *ham-1* mutants generate extra HSN neurons due to symmetrization in the neuroblast cell lineage that generates these *neurons* (Desai et al. 1988; C. Guenther and G. Garriga, pers. comm.). *ham-1* encodes a novel protein that is localized asymmetrically to the periphery of the *neuroblasts* that generate PHB and HSN, as well as other *neuroblasts* (C. Guenther and G. Garriga, pers. comm.). Thus, HAM-1 is an asymmetrically segregated protein that functions in the asymmetric activation of UNC-86 and other proteins. Asymmetrically segregated cell lineage control proteins, for example, Numb and Prospero, have also been detected in *Drosophila* (see below) (Posakony 1994).

*vab-3* acts upstream of *unc-86* in other cell lineages that are spatially grouped in the anterior regions of the animal (Baumeister et al. 1996). *vab-3* mutants are defective in neuroectodermal patterning in the anterior and posterior regions, and the *vab-3* gene is expressed in those regions (Chisholm and Horvitz 1995; Zhang and Emmons 1995; see Emmons and Sternberg, this volume). *vab-3* encodes the *C. elegans* homolog of the *Drosophila* and mammalian *Pax-6* genes (Chisholm and Horvitz 1995; Zhang and Emmons 1995) that regulate eye development (Quiring et al. 1994; Halder et al. 1995). Similarly in mammals, *Pax-6* is likely to act upstream of the *unc-86* homolog Brn-3 (Xiang et al. 1993; Stoykova and Gruss 1994). It is possible that the morphogenetic pathways activated by *vab-3* in *C. elegans* are homologous to the *Pax-6*-regulated development of the *Drosophila* and vertebrate eye and that genes homologous to *unc-86* act downstream from *Pax-6* in these species as well.

POU protein transcription factors homologous to *unc-86* may mediate neuroblast cell lineage determination across metazoan phylogeny. For example, two *Drosophila* POU proteins, dPOU28 and dPOU19, mediate analogous neuroblast cell fate determinations in the developing CNS (Bhat et al. 1995; Yeo et al. 1995). Three vertebrate *unc-86* homologs, Brn-3a, Brn-3b, and Brn-3c, are expressed in subsets of retinal ganglion cells (Xiang et al. 1995). Although it has been shown that cell lineage mechanisms do not generate clones of particular neural types in the vertebrate retina (Turner et al. 1990), it has not been excluded that modular cell lineages analogous to those that utilize asymmetric activation of *unc-86* in *C. elegans* also couple expression of the *Brn-3* genes to cell lineage cues.

## C. *lin-32* Controls an Ectodermal to Neural Switch in Sensory Cell Lineages

*lin-32* mutants cause neuronal precursor cells such as Q or R.n or V5.paa to generate hypodermal seam cells rather than neuroblast and neuronal descendant cells. Lineage aberrations indicate that *lin-32* acts in these lineages prior to *unc-86* (Way and Chalfie 1989). *lin-32* mutants are mechanosensory-defective and perturb the expression of *unc-86* and *mec-3* in many neuroblast cell lineages (Way and Chalfie 1989; Mitani et al. 1993; Baumeister et al. 1996). For example, in *lin-32(u282)* mutant, the Q and V5.paa lineages do not generate *unc-86*-expressing neurons, the IL2 neurons are either missing or do not express *unc-86*, and fewer tail and deirid neurons express *unc-86*. The defects are not localized to a particular body region underlining the general role of *lin-32* in specification of neuroblast fate. Furthermore, the existing *lin-32* mutations may not be null, so it is possible that additional neuroblasts also require *lin-32* function.

*lin-32* encodes a basic helix-loop-helix (bHLH) transcription factor that is homologous to the *Drosophila* gene *atonal*, which functions only in peripheral nervous system development (Jarman et al. 1995; Zhao and Emmons 1995). A *lin-32* reporter gene is expressed widely in the embryo and in the ventral nerve cord of L1 and L2 larvae, as well as tail neuroectodermal cell lineages (C. Zhao and S.W. Emmons, pers. comm.). All of the lineages affected by *lin-32* normally produce sensory neurons (Q, V5.paa, AB.p(l/r)apaaa, AB.p(l/r)apapapp, IL2, T.ppp), consistent with the function of its *Drosophila* homolog *atonal* in the specification of sensory chordotonal and photoreceptor organs (Jarman et al. 1995). Because *lin-32* acts before *unc-86* and because *lin-32* encodes a probable transcription factor, it is a candidate for an activator of *unc-86* asymmetric expression.

Not only is *lin-32* necessary for neuroblast specification, but in some cells, it is also sufficient to specify neuroblasts. For example, expression of *lin-32* from a heat shock promoter can transform seam cells from their hypodermal fate toward a neuroblast fate; ectopic ray papillae are formed from cells which ectopically express *lin-32* (Zhao and Emmons 1995). Because widespread expression of *lin-32* can only transform particular epidermal cells, and because the consequences of normal *lin-32* expression in Q, V5.paa, and R.n cause distinct neuroblast fates, LIN-32 protein activity must be modified by other cellular factors to specify particular neuroblast cell fates.

In some cell lineages, the activity of *lin-32* may be regulated by *lin-22*. *lin-32* reporter gene expression expands in a *lin-22* mutant (C. Zhao and S.W. Emmons, pers. comm.), consistent with ectodermal to neuronal cell lineage transformations in this mutant (Waring and Kenyon 1990). *lin-22* has been shown to encode a *C. elegans* homolog of Hairy (L. Wrischnik and C. Kenyon, pers. comm.) which acts as a transcriptional corepressor to

Achaete/Scute in *Drosophila* ([Paroush et al. 1994](#)). *lin-22* may normally antagonize the activity of *lin-32* in these ectodermal cell lineages. It is not known how *lin-32* expression is regulated or how its activity is coupled to the asymmetric expression of *unc-86* in particular neuroblast cell lineages. However, precedents come from studies of how *Drosophila* neurogenesis is controlled by close relatives of *lin-32*, the members of the *achaete/scute* (*ac/sc*) complex (Guillemot et al. 1993; Ferreiro et al. 1994; Posakony 1994). These genes are activated early in neurogenesis in a subset of ectodermal cells which constitute a proneural cluster of cells. The pattern of *achaete/scute* activation is under the control of antagonist *emc* and *E-spl* genes and a lateral signaling pathway mediated by members of the *Notch* pathway (Posakony 1994). Earlier-acting genes that pattern the A-P and dorsal-ventral (D-V) axes may regulate *achaete/scute*, *E-spl*, and *emc* expression (Skeath et al. 1992).

Once *achaete* is expressed in *Drosophila* proneural clusters, this activates a Notch/Delta/Hairless/Suppressor of Hairless lateral inhibition mechanism so that finally only one isolated neuroblast precursor cell is specified ([Hartenstein and Posakony 1990](#)). *lin-12* and *glp-1* encode partially redundant *C. elegans* members of the Notch signaling family (Lambie and Kimble 1991), but neurogenesis is not obviously affected in these mutants. For example, *mec-3* expression is normal in a *lin-12 glp-1* double mutant (Way et al. 1992), suggesting that *lin-32*-mediated neurogenesis in the mechanosensory *neural* lineages is not dependent on these Notch signaling molecules. *mec-4*, a gene that acts downstream from *lin-12 / glp-1*, encodes a *Suppressor of Hairless* homolog (Christensen et al. 1996). *lag-2* encodes a *Delta* homolog (Henderson et al. 1994; Tax et al. 1994). *lag-1*, *lag-2*, *lin-12*, and *glp-1* mutants have not yet been checked for neurogenesis or normal patterns of *unc-86* or *mec-3* activation. Homologs of other *Drosophila* genes implicated in Notch signaling have been found in the *C. elegans* genome sequence.

In *Drosophila*, after a neuroblast precursor cell has been selected by the *Notch* pathway, segregated molecules have been shown to act downstream in the neuroblast cell lineages. For example, both Numb and Prospero proteins are differentially segregated in neuroblast cell lineages ([Rhyu et al. 1994](#); [Hirata et al. 1995](#); [Knoblich et al. 1995](#)). The Numb protein sequence does not suggest how this protein controls asymmetric cell lineage. Prospero encodes a homeodomain protein, suggesting that after it is asymmetrically segregated, it regulates gene expression in one daughter cell (Doe et al. 1991). A *C. briggsae* Numb homolog, pk02c05, and a *C. elegans* Prospero homolog (Bürglin 1994) have been identified by the genome sequencing project. *ham-1*, which also encodes a segregated protein (C. Guenther and G. Garriga, pers. comm.), may couple to asymmetry generating systems similar to those used by Numb and Prospero.

In *Drosophila*, the *achaete/scute* neurogenesis pathway couples to *groucho*. *groucho* mutants show broader activation of neurogenesis than wild type and this neurogenic phenotype depends on *achaete/scute* function ([Paroush et al. 1994](#)). These and other studies suggest that *Groucho*, a protein containing a WD40 repeat, acts as a transcriptional corepressor. It is possible that a *C. elegans* *Groucho* homolog, *unc-37* (see below; A. Pflugrad et al., pers. comm.), acts to regulate *lin-32* activity in this manner. *unc-37* has not been shown to interact genetically with *lin-32*. However, the null phenotype of *unc-37* is probably lethal, and only reduction of function *unc-37* alleles that genetically interact with the homeobox gene *unc-4* (see below) have been studied in detail. It will be interesting to observe the pattern of *lin-32* and *unc-86* expression and neurogenesis in general in an *unc-37* mutant.

## Figures

Figure 2. *unc-86* couples cell lineage to cell identity.

### Figure 2

*unc-86* couples cell lineage to cell identity. Each lineage is traced back as far as possible without including cells that are other than *neurons* or cell deaths. (*Thick lines*) Cells expressing *unc-86*. Parallels among these lineages are apparent from the characteristics of resulting *neurons* (neuron characteristics from [White et al. 1986](#) and [Way and Chalfie 1989](#)). For instance, all six of the anterior-most descendants of the first cell to express *unc-86* protein

are [sensory neurons](#), and five of the six are the only five cell types to express [\*mec-3\*](#). (Modified, with permission, from [Finney and Ruvkun 1990](#).)

Figure 3. Position and lineage origin of cells expressing UNC-86 protein.

### Figure 3

Position and lineage origin of cells expressing UNC-86 protein. (*Top*) Positions of [neurons](#) that express [\*unc-86\*](#) are shown (dark ellipses). Only one of bilaterally symmetrical cells is shown. (\*) Cells at asymmetric positions. Parentheses at SDQL/R indicate that the staining fades in late L1 as it is no longer visible afterward. (*Bottom*) Lineage origin of [\*unc-86\*](#)-expressing cells. (*Thick lines*) Cells staining with [\*unc-86\*](#) antibodies. Lineage branches not leading to [\*unc-86\*](#)-expressing cells have been trimmed. (X) Programmed cell death. (Modified, with permission, from Finney and Runkun 1990.)

Figure 4. *unc-86* regulates mother/daughter neuroblast asymmetry.

### Figure 4

[\*unc-86\*](#) regulates mother/daughter neuroblast asymmetry. The cell lineage of the neuroblast Q is shown on the left. In wild type, the [neurons AQR](#) and [PQR](#) are generated from the Q.a neuroblast, whereas the [neurons AVM](#), [PVM](#), and SDQ are generated from Q.p which expresses UNC-86, shown in thick line (X = programmed cell death). In an [\*unc-86\*](#) mutant, Q.p fails to express [\*unc-86\*](#), and the cell reiterates the fate of the mother cell Q, reiterating the Q.a sublineage to generate supernumerary [AQR](#) and [PQR neurons](#). Note that no mechanosensory [AVM](#) or [PVM neurons](#) are generated in the [\*unc-86\*](#) mutant.

Generated from local HTML

## Chapter 20. Patterning the Nervous System — IV Generation of Reiterated Neurons by Reiterated Cell Lineages

---

Although the body plan of *C. elegans* is not segmented in the obvious way that segmented insects or vertebrates are, there are reiterated structures in the final body plan, such as the reiterated P0 to P12 neuroectoblasts along the A-P axis (Figs. 1 and 5) (Chalfie et al. 1983). These reiterated [neuroblasts](#) generate multiple sets of VA, VB, VC, VD, and AS motor [neurons](#) (see [Fig. 1](#)). These P ectoblast cell lineages constitute a basic feature of the *C. elegans* "segment." Variations on the theme of these reiterated sublineages are mediated by the HOM-C genes to generate regional diversity in the [nervous system](#).

But how are the reiterated P neuroectoblast developmental units themselves generated? At present, this problem is only partly solved. Two genes that act in these sublineages to generate [neurons](#) reiterated over the A-P axis of the animal are [unc-4](#) and [unc-30](#). [unc-4](#) mutations disrupt the differentiation of particular attributes of particular [VA neurons](#) (White et al. 1992). [unc-30](#) mutations affect the differentiation of D-type neurons, including the [VD neurons](#) (Jin et al. 1994). Both of these genes encode homeodomain proteins and are expressed in patterns that presage the differentiation of those [neural](#) types. Thus, where and when [unc-4](#) and [unc-30](#) are expressed determine where and when these particular [neural](#) types are generated, and these genes constitute part of the system for generation of reiterated sublineages along the the A-P axis of the animal.

### A. [unc-4](#)

[unc-4](#) is necessary for the specification of particular attributes of the VA class of motor [neurons](#). Loss-of-function mutations in [unc-4](#) result in backward movement defects but affect forward movement much less dramatically. Laser microsurgery experiments have shown that the [VA neurons](#) control backward movement but not forward movement (Chalfie and Au 1989). The 12 VA motor neurons are generated via homologous cell lineages that are variations on a common theme: Generally, the [VA neurons](#) are generated as the most anterior daughters of homologous P-cell lineages (see [Fig. 1](#)). Of the 12 [VA neurons](#), 9 are generated from P-cell lineages where the sisters of the [VA neurons](#) are the [VB neurons](#). The remaining 3 [VA neurons](#) are generated from modified P-cell lineages where the sisters of VA are a cell death or a VD neuron ([Fig. 1](#)) (Sulston and Horvitz 1977).

The ventral cord of a probable [unc-4](#) null mutant has been reconstructed by serial electron microscopy section (White et al. 1992). In the reconstruction, three of the [VA neurons](#) generated from P-cell lineages where the sister of VA is VB (VA2, VA3, and VA10) are transformed to the presynaptic specificity of the VB, whereas the three [VA neurons](#) that are derived from lineages that do not produce VB sisters (VA1, VA11, and VA12) have normal connectivity. In the [unc-4](#) mutant, the presynaptic partners of the affected "VA2," "VA3," and "VA10" [neurons](#) are the PVC and AVB interneurons that are normally presynaptic to VB, rather than the AVA, AVD, and AVE interneurons that are normally presynaptic to VA motor neurons ([Fig. 6](#)). The anterior axonal pathfinding and postsynaptic muscles and [neurons](#) of these "VA" [neurons](#) are unaffected in an [unc-4](#) mutant. Thus, [unc-4](#) specifically controls only a subset of the VA fate: its presynaptic connections to the [interneurons](#) AVA, AVD, and AVE.

[unc-4](#) encodes a homeodomain protein that is most closely related to the Prd/Pax class but probably defines a new class (Miller et al. 1992). As a transcription factor, it must regulate presynaptic specificity indirectly, perhaps by controlling the expression of molecules that mediate specific connection between the affected [VA neurons](#) and their presynaptic partners. *lacZ* fusions to [unc-4](#) have shown that [unc-4](#) is expressed in the VA neuron itself, rather than in the connected [interneurons](#) or in the VB sister [neuron](#) (Miller and Niemeyer 1995). Thus, [unc-4](#) is likely to regulate the activity of genes in the VA neuron that mediate connectivity between VA and the interneurons AVA, AVD, and AVE.

Two general models can explain the transformation of VA to VB presynaptic fates (Miller and Niemeyer 1995): (1) In the [VA neurons](#) that are sisters to [VB neurons](#), UNC-4 may normally repress or antagonize either a VB specification gene or the genes regulated by a VB specification gene. The genes regulated by such a VB

specification gene might be normally expressed in and decorate the dendrites of the maturing VB neuron to mediate synapsis to the PVC [interneuron](#) and formation of gap junctions to the AVB [interneuron](#). In an [unc-4](#) mutant, such VB connectivity genes would be expressed in the VA sisters as well as [VB neurons](#) to mediate their inappropriate connectivity. (2) [unc-4](#) may normally up-regulate the expression or localization of surface recognition proteins in VA that mediate its connectivity to the presynaptic interneurons AVA, AVD, and AVE. In the absence of [unc-4](#), the VA [neuron](#) would express a default VB presynaptic specificity. The [unc-4](#)-regulated genes may normally supersede any VB specification genes. Such a model would not explain why [unc-4](#) is not necessary for presynaptic connectivity of [VA neurons](#) that are not sisters of [VB neurons](#).

[unc-4](#) also is expressed in a number of [neurons](#) that are similar to the [VA neurons](#) or which are generated by cell lineages homologous to those that generate the [VA neurons](#). For example, [unc-4](#) is expressed in the [DA neurons](#) as well as the [VA neurons](#) ([Miller and Niemeyer 1995](#)). The [DA neurons](#) are generated earlier than the [VA neurons](#), but they are connected to the same presynaptic [neurons](#) and postsynaptic targets as the [VA neurons](#) and subserve a similar function in motor control ([White et al. 1986](#)). However, the presynaptic connectivity of these [neurons](#) is normal in an [unc-4](#) mutant, suggesting that [unc-4](#) has no essential function (or it may be redundant in these cell lineages) in the development of the [DA neurons](#) ([White et al. 1992](#)). It is possible that, like the [VA neurons](#) generated by neuroectoblasts P0, P11, and P12, the [DA neurons](#) do not depend on [unc-4](#) because there is no competing VB specification cascade from the sisters of these A-type neurons. On the other hand, it is also possible that [unc-4](#) serves some other function (such as regulation of synaptic signaling) in these neurons that was not detected in the electron microscopic reconstruction of the [unc-4](#) mutant. However, the body posture of [unc-4](#) mutants shows a characteristic lack of VA function only in the central body region where VA and [VB neurons](#) are sisters, suggesting that the other VA and [DA neurons](#) are functional ([White et al. 1992](#)).

In addition to expression in the A-type [neurons](#), [unc-4](#) is expressed in the AVF [neurons](#) that are generated by nearly homologous cell lineages ([Fig. 6](#)). Although [unc-4](#) has no known function in these [neurons](#), the pattern of expression suggests that similar cell lineage cues are used to animate expression in AVF in addition to the [VA neurons](#). Thus, [unc-4](#) is likely to couple neuroblast cell lineage control genes to the expression of particular [neural](#) attributes in these distinct [neural](#) types.

It must be stressed, however, that the correlation of cell lineage and cell fate in *C. elegans* is not absolute—in many cases, similar cell types are generated by cell lineages that have no similarity. For example, the embryonic DA and DB motor [neurons](#) are generated by lineages that bear no relationship to the simple patterns of cell lineage that generate their functional homolog VA and VB motor [neurons](#); six of the nine [DA neurons](#) are generated as symmetric sisters, in distinction to the [VA neurons](#) which are always sisters of distinct neuron types. Cell lineage or other cues distinct from those used in the Pn.a neuroblast cell lineages are likely to activate expression of [unc-4](#) in the [DA neurons](#). Because no [unc-4](#) function has been detected in the DA and AVF neurons, the relevance of this regulation to neurogenesis has not yet been established.

[unc-37](#) has been shown to act in the same developmental pathway as [unc-4](#). Although the [unc-37](#) mutants have not been characterized in the same electron microscopic detail as [unc-4](#) mutants, some [unc-37](#) alleles cause uncoordinated behaviors quite similar to those of [unc-4](#) null mutants ([Miller et al. 1993](#)). These recessive [unc-37](#) mutant alleles do not affect expression of [unc-4](#) or the pattern of axon outgrowth of the [VA neurons](#), suggesting that [unc-37](#) does not regulate the generation of [VA neurons](#) per se or the expression of [unc-4](#) ([Miller and Niemeyer 1995](#)). In addition to the same characteristic Unc phenotype, severe loss-of-function [unc-37](#) alleles are sterile and show distorted gonad and vulval morphology ([McKim et al. 1992](#)), suggesting that [unc-37](#) may serve a larger role in development than that mediated by [unc-4](#) (A. Pflugrad et al., pers. comm.).

Rare gain-of-function mutations in [unc-37](#) can suppress a temperature-labile [unc-4](#) mutation that maps to the homeodomain ([Miller et al. 1992; Miller and Niemeyer 1995](#)). This [unc-4](#) mutation is predicted from the crystal structure of the homeodomain to perturb the structure of the hydrophobic core. These [unc-37](#) mutants cannot suppress null [unc-4](#) mutants ([Miller et al. 1993](#)). The combination of the similarity of recessive [unc-37](#) mutants to [unc-4](#) mutants and the genetic suppression by [unc-37](#) gain-of-function mutants of a labile [unc-4](#) mutant supports the hypothesis that the UNC-4 and UNC-37 proteins either interact or regulate common targets.

[unc-37](#) encodes a protein homologous to the *Drosophila* Groucho protein (A. Pflugrad et al., pers. comm.). In *Drosophila*, Groucho is expressed ubiquitously and acts as a corepressor of Achaete/Scute and other bHLH proteins, such as Hairy ([Paroush et al. 1994](#)). Hairy in turn negatively regulates the homeobox gene *ftz* in a *groucho*-dependent manner ([Paroush et al. 1994](#)). Given the *Drosophila* precedent, it is possible that UNC-37 acts as a corepressor with UNC-4 in the [VA neurons](#) to regulate negatively a VB specification gene or VB-specific presynaptic surface receptor genes. To explain the similarity of the [unc-37](#) and [unc-4](#) mutant phenotype, the main function of UNC-4 may be to repress VB fates in the [VA neurons](#), and UNC-37 may be an essential cofactor in that repression. If this repression depends on an interaction of UNC-4 and UNC-37, mutations in [unc-37](#) or [unc-4](#) that interfere with this interaction may allow the expression of a VB specification gene or VB-specific downstream genes in the [VA neurons](#). UNC-37 protein bearing the gain-of-function mutation may interact more potently to stabilize a labile UNC-4 protein to allow normal repression of downstream genes. The model that UNC-37 is an UNC-4 corepressor of the expression of a VB-presynaptic specification gene would suggest that such a gene would be misexpressed in the [VA neurons](#) that are sisters of VB in an [unc-4](#) or [unc-37](#) mutant.

The null phenotype of [unc-37](#) is probably larval-lethal ([McKim et al. 1992; Miller et al. 1992](#)), suggesting that the UNC-37 protein interacts with more than just UNC-4. For example, on the basis of precedents from *Drosophila* neurogenesis, UNC-37 may regulate the activity of the bHLH protein LIN-32.

## B. unc-30

[unc-30](#) is necessary for the development and function of the inhibitory D-type [GABAergic neurons](#), including the [VD neurons](#) generated by the P neuroectoblasts ([Jin et al. 1994](#)). In an [unc-30](#) mutant, these neurons do not synthesize the neurotransmitter GABA and show abnormalities in their pattern of synaptic targets even though gross pathfinding is normal ([Jin et al. 1994](#)). [unc-30](#) is not essential for the production of GABA in non-D-type GABAergic motor neurons, for example, the RME and [AVL](#) and [DVB](#) neurons.

[unc-30](#) encodes a homeodomain protein that defines a new class ([Jin et al. 1994](#)). [unc-30](#) is expressed in the VD and DD D-type [GABAergic neurons](#) that depend on [unc-30](#) function for production of GABA. It is not expressed in the other [GABAergic neurons](#) that are not dependent on [unc-30](#) for GABA production. [unc-30](#) is also expressed in the non-GABAergic PVP [neuron](#) and in the ASG, [RIH](#), and [RID neurons](#). These [neurons](#) bear no obvious relationship with the D-type neurons.

[unc-30](#) regulates the expression of [unc-25](#), the glutamate acid decarboxylase (GAD) gene in the D-type neurons ([Jin et al. 1994](#)). Not only is [unc-30](#) necessary for the expression of [unc-25](#) in the D-type neurons, but it is also sufficient for the expression of [unc-25](#) in other tissues. Expression of [unc-30](#) from a heat shock promoter can activate the accumulation of GABA in a large number of neurons as well as in hypodermal cells ([Jin et al. 1994](#)). In the non-[GABAergic neurons](#) that express [unc-30](#), other factors may inhibit UNC-30 activation of [unc-25](#). [unc-25](#) is probably also regulated by other factors in the [GABAergic neurons](#) which do not depend on [unc-30](#) but depend on [unc-25](#) for GABAergic function.

Like [unc-4](#), [unc-30](#) is thus expressed in neurons mainly of one type: the D type. And like [unc-4](#), expression of [unc-30](#) is activated in the reiterated P-cell lineages as well as in other cell lineages that produce D-type neurons. For example, the [VD neurons](#) are generated from the P.na [neuroblasts](#) (see [Fig. 1](#)), whereas the [DD neurons](#) are generated from other unrelated [neuroblasts](#).

## C. A Prepattern or Piece-by-Piece Generation of Reiterated Sublineages

The reiterated expression of [unc-4](#) and [unc-30](#) in all the Pn.a-derived neurons of a particular class suggests that these genes are a component of the pathway for generating the reiterated pattern of P-derived cells. A set of cues must be "read" to assemble the reiterated expression pattern of the P-cell lineage specification genes, either at the level of genes such as [unc-4](#) and [unc-30](#) that act in the daughter [neurons](#) of the P neuroectoblasts or upstream at the level of genes that generate the reiterated pattern of the P cells. Given that the P ectoblast patterns of cell lineage are spatially reiterated along the A-P axis of the animal before [unc-4](#) and [unc-30](#) are

activated in particular [neural](#) types, it is likely that the unknown genes that specify P-cell fate respond to such cues.

No known mutations affect only P-cell specification. [lin-26](#) is the best candidate to act at this step before [unc-4](#) and [unc-30](#) are activated. [lin-26](#) null mutants cause a variety of hypodermal defects, including P-cell defects ([Labouesse et al. 1994](#)). Weak [lin-26](#) alleles symmetrize the normally asymmetric P-cell division to yield daughters that both express the Pn.a neuroblast fate. [lin-26](#) encodes a zinc finger transcription factor that is expressed in the P cells as well as in all other hypodermal cells. The LIN-26 protein is not asymmetrically segregated to the Pn.p cell at the P-cell division, but rather it fades away in both daughters synchronously ([Labouesse et al. 1994](#)). [lin-26](#) is probably necessary for the differentiation of hypodermal cells, including the P cells and Pn.p cells. LIN-26 may constitute one combinatorial partner that is required for the activation of P-cell fates.

The [unc-4](#) and [unc-30](#) promoters may be activated by the same cell lineage cue, for example, [lin-26](#), in each of the Pn.a sublineages. It is also possible that the [unc-4](#) and [unc-30](#) genes are regulated by distinct sets of upstream genes in different regions of the animal to become active in a spatially reiterated set of cells. A dissection of the [unc-4](#) or [unc-30](#) promoters may shed light on whether these genes use the same cues in each reiterated P cell or utilize distinct cues at distinct positions. For example, if distinct spatial cues are used to activate these genes in particular P blast cells, promoter deletions may disrupt their activation in particular P-cell lineages but not others. On the other hand, if universal P-cell lineage cues or if the same extracellular signal activates their expression, then such mutations should disrupt gene activation in all P cells. Similar analysis of the [unc-86](#) promoter ([Baumeister et al. 1996](#)) and the *even skipped* and *hairy* promoters in *Drosophila* (Riddihough and Ish-Horowicz 1991; Small et al. 1991; Stanojevic et al. 1991) has revealed that the complex and patterned expression of these genes is built up piece by piece to generate reiterated domains of expression.

## Figures

Figure 5. Role of HOM-C genes in patterning the P cells (ventral ectoderm) in the male nematode.

### Figure 5

Role of HOM-C genes in patterning the P cells (ventral ectoderm) in the male nematode. (A,B) Location and division pattern of P cells; (C) overall domains of HOM-C gene activity. Distribution of Mab-5 protein and staining for [lin-39](#)-lacZ expression coincide with the indicated (filled) domains. (D) Fates of the individual descendants of each P cell. (A,B,S,D) Motor [neuron](#) types called VA, VB, AS, and DD, respectively. (E) Division to produce one cell death and one rectal epithelial cell; (F) fusion; (U) lack of fusion with the epidermal syncytium; (M) division to produce a pair of motor [neurons](#) (one serotonergic); (I) division to produce one [interneuron](#) and one neuron-like cell; (X) programmed cell death; (N,P,V,Z) other types of [neurons](#). Colors indicate the dependence of these fates on [lin-39](#) (red), [mab-5](#) (yellow), [egl-5](#) (blue), or [lin-39](#) plus [mab-5](#) (orange). Yellow cross-hatching indicates variable [mab-5](#) activity in promoting the I fate in a [lin-39](#) (-) background. Red cross-hatching indicates [lin-39](#) activity in promoting the N fate, which extends beyond the domain of other [lin-39](#) activities and beyond detectable [lin-39](#)-lacZ expression. (Reprinted, with permission, from Salser and Kenyon 1994.)

Figure 6. The [unc-4](#) gene defines the pattern of synaptic input to VA motor neurons.

### Figure 6

The [unc-4](#) gene defines the pattern of synaptic input to VA motor neurons. (A) Axons from interneurons in the head (AVA, AVD, AVE, AVB) and in the tail (PVC) project into the [ventral nerve cord](#) during embryonic development. Twelve VA motor [neurons](#) and 11 VB motor neurons are innervated by separate sets of interneurons (indicated by color shading). (B) Most of the VA and VB motor neurons are derived from a common precursor in the postembryonic motor neuron lineage. VA and VB axons adopt opposite trajectories with VAs projecting anteriorly and VBs posteriorly. In the wild type, VA motor [neurons](#) accept input from [interneurons](#) AVA

(gap junction and chemical synapse), AVD, and AVE (chemical synapse), whereas the VBs are connected to AVB (gap junction) and PVC (chemical synapse). In null mutant *unc-4(e120)*, VA motor neurons retain their normal morphology but assume the pattern of synaptic input normally reserved for their VB sisters (gap junction from AVB). These connections (*arrows*) are made *en passant* between parallel-oriented processes and do not require axonal branching ([White et al. 1992](#)). (C) Cell lineage of *unc-4-lacZ*-expressing [neurons](#). (*Thick lines*) *lacZ*-positive [neurons](#). Thirteen precursor cells or P cells (PO-P12) give rise to 12 VA motor [neurons](#) and to 2 AVF [neurons](#) in the L1 stage. (Reprinted, with permission, from [Miller and Niemeyer 1995](#).)

Generated from local HTML

# Chapter 20. Patterning the Nervous System — V Spatial Patterning by the *C. elegans* HOM-C Gene Cluster

---

## A. *C. elegans* HOM-C Gene Cluster

The basic pattern of Pn.a neuroblast cell lineage varies over the length of the animal. For example, the [VC neurons](#) that innervate the vulval muscles are only generated by 6 of the 12 Pn.a neuroblast cell lineages that are located in the middle of the animal, [P3.a](#) to [P8.a](#) (Fig. 5). In the other Pn.a cell lineages, the cells at the position in the cell lineage homologous to the VC [neuron](#) undergo programmed cell death. Such modifications to the reiterated neuroblast cell lineages are spatially clustered and are under the control of homeotic genes.

As in *Drosophila* and vertebrates, a cluster of homeobox genes regulates spatial patterning of *C. elegans*. Six members of the ancient metazoan homeobox cluster (HOM-C) genes (Kenyon and Wang 1991; Bürglin and Ruvkun 1993; [Wang et al. 1993](#)) have been detected in *C. elegans*, and mutations have been identified in four of them. The *C. elegans* homologs of the *Drosophila* *Dfd*, *Antp*, and *Abd-B* genes, called [lin-39](#), [mab-5](#), and [egl-5](#), respectively, control spatial patterning of mesodermal and ectodermal cells in adjacent spatial domains. These genes mediate the spatial variations on the canonical Pn.a neuroblast cell lineages and thus are likely to modulate the activity of, or response to, the [neural](#) patterning genes described above. The *C. elegans* homolog of *labial*, [ceh-13](#), has not yet been analyzed genetically, although it is expressed in a spatial pattern consistent with the function of *labial* in *Drosophila* (C. Wittmann and F. Muller, pers. comm.). [vab-7](#), the *C. elegans* homolog of *eve*, which in vertebrates is part of the HOM-C gene complex, is expressed in the posterior region of early embryos and is necessary for normal patterning in the most posterior regions of the animal (Ahringer 1996).

### **mab-5**

Mutations in [mab-5](#) affect cell identities in a region just anterior to that affected by [egl-5](#) and just posterior to the region affected by [lin-39](#) (Fig. 5) (Kenyon 1986; [Wang et al. 1993](#)). A variety of cell types are regulated by [mab-5](#). For example, the fates of the VB descendants of neuroectoblasts [P11](#) and [P12](#), the production of rays or alae by V-cell descendants in the male, the fate of ventral Pn.p hypodermal cells, and the migration of the descendants of the Q and [M](#) cells are all controlled by [mab-5](#). [mab-5](#) encodes a homeodomain protein most closely related to the *Antp* class (Costa et al. 1988). The finding that the spatial patterning function of [mab-5](#) is mediated by a homolog of a *Drosophila* spatial patterning gene was the first indication that *C. elegans* might also bear a homeotic gene cluster.

MAB-5 protein is expressed in a simple spatial pattern that includes the cells affected by [mab-5](#) mutations ([Salser et al. 1993](#); [Wang et al. 1993](#)). Genetic mosaic analysis revealed autonomous [mab-5](#) function in these patterning activities (Kenyon 1986). However, the [mab-5](#) activities in patterning are much more complex than its simple expression pattern would indicate—the boundaries of its activity vary depending on cell type ([Salser et al. 1993](#)). For example, [mab-5](#) is required for the death of the [VB neurons](#) in the [P11](#) and [P12](#) cell lineages only; in the absence of *mab-5*, these neurons survive, as is normally observed in P-cell lineages more anterior to [P11](#) and [P12](#). Thus, the boundary for [mab-5](#) activity in the [VB neurons](#) is between [P10](#) and [P11](#). The boundary for [mab-5](#) function in Pn.p specification is between [P6](#) and [P7](#). However, the expression pattern of MAB-5 spans the region from [P7](#) to [P12](#). The discordance between the simple [mab-5](#) expression pattern and complex pattern of genetic activities suggests that other developmental factors modify [mab-5](#) activity in each of these P-cell sublineages. Ectopic expression of MAB-5 from a heat shock promoter is not sufficient to confer apoptosis to [VB neurons](#) in other P-cell lineages, suggesting that some combinatorial partner to MAB-5 is essential to confer apoptosis in [P11](#) and [P12](#) ([Salser et al. 1993](#)). This partner has not been identified. However, it is known that [egl-5](#) is not the partner for VB cell death. [egl-5](#), however, is a possible regulator of [mab-5](#) expression, for all [P11](#) and [P12](#) descendants continue to express MAB-5 in an [egl-5](#) mutant, unlike wild type. Thus, [mab-5](#) modifies the canonical P-cell lineage in the Pn.p descendants of [P7](#) and [P8](#) and in the Pn.a descendants of [P11](#) and [P12](#).

## **lin-39**

*lin-39* controls fates in the region anterior to and partially overlapping that controlled by *mab-5*. The most obvious phenotype of *lin-39* null mutant hermaphrodites is that the Pn.p cells that normally generate the *vulva* fuse with the *hyp7* syncytium, rather than remaining unfused and competent to respond to signals from the anchor cell as they do in wild type (Fig. 6) (Clark et al. 1993; Wang et al. 1993). Thus, in *lin-39* mutants, the vulval equivalence group is not specified, and *P3.p* to *P8.p* fuse with an adjacent syncytium, as their spatial homologs *P1*, *P2*, *P9*–12 do normally. From the pattern of cell fate changes, it appears that *lin-39* acts in the P cells, because both anterior *neural* and posterior ectodermal derivatives of these P cells are affected. For example, in the hermaphrodite, *P3.a* to *P8.a* normally generate VC motor neurons, but in a *lin-39* mutant, these cells die, like their homologs in the Pn.a cell lineages normally generated by *P1*, *P2*, *P9*–12. Other neurons generated by *P3.a* to *P8.a* in a *lin-39* mutant migrate anteriorly, like the *P1*, *P2a* derived neurons in wild type, suggesting that *P3* to *P8* are transformed to a more anterior fate in a *lin-39* mutant. In *lin-39* mutant males, the Pn.aapp serotonergic neuron normally generated by *P3* to *P8* is not generated; instead, this cell in the *P3* to *P6* sublineages undergoes programmed cell death, more like *P1* and *P2*, whereas *P7* and *P8* generate neuronal cell lineages more like *P9* to *P11*. Hypodermal cells *P7.p* and *P8.p* are transformed in a *lin-39* mutant to the fate more similar to those of posterior cells. Thus, in *lin-39* mutants, cells located in the mid-body region are transformed to either more anterior or more posterior cell fates. Genetic mosaic analysis of *lin-39* revealed cell-autonomous function in P-cell specification as well as in Q-cell migration (see below).

*lin-39* encodes a homeodomain protein of the Dfd class, consistent with the spatial patterning functions of this gene class in other animals (Clark et al. 1993; Wang et al. 1993). A *lin-39/lacZ* fusion gene is expressed in *P5* to *P8* and to a lesser extent in *P3* and *P4*, as well as weakly in the V cells and in the Q cells also located in this spatial domain (Fig. 7). Muscle cells in the region also express the *lacZ* fusion gene.

The transformations of cell identity in a *lin-39* mutant involve both anterior transformations and posterior transformations of cell fate. The simplest interpretation of this observation is that *lin-39* modifies the activity of *mab-5* in the posterior region of the *lin-39* expression pattern but that in the anterior region of its expression pattern, *lin-39* modifies the activity of an unknown other gene, perhaps the HOM-C *labial* homolog *ceh-13*. There are not yet mutations in *ceh-13* to test this notion.

## **egl-5**

*egl-5* corresponds to the posterior-most homeobox gene in the cluster and may be the homolog of *Drosophila* Abd-B. Mutations in *egl-5* cause homeotic changes in cell fate in ectoblast cells and neurons that are clustered in the tail of the animal (Chisholm 1991). These cells become transformed toward the fates of more anterior homologs. An *egl-5/lacZ* fusion gene is expressed in the cells of the posterior region affected by *egl-5* mutations (Fig. 7) (Wang et al. 1993).

## **B. The Molecular Basis of Homeosis**

The cell fate transformations that result from mutations in HOM-C genes are homeotic because of their antagonistic regulation of other HOM-C genes. In *Drosophila*, Abd-A represses expression of Ubx in the posterior regions, so that in an Abd-A mutant, the Ubx expression domain is expanded posteriorly (Struhl and White 1985). This posterior expansion of the Ubx expression transforms posterior segment identity to that of anterior fates. In this case, homeosis results from cross-regulation of HOM-C cluster gene expression. In other cases, homeosis results not from cross-regulation of expression but from cross-regulation of activity. For example, in *Drosophila*, the expression of HOM-C genes from the posterior regions of the complex renders impotent the expression of other members of the complex (Mann and Hogness 1990). Examples of both these phenomena have been observed in the *C. elegans* HOM-C cluster genes.

The *C. elegans* HOM-C genes *lin-39* and *mab-5* do not regulate each other's expression. Rather, in this case, the homeosis results from combinatorial control of cell fates by *mab-5* and *lin-39*. For example, the fates of *P7* and *P8* descendants are controlled by the combination of *lin-39* and *mab-5* gene activities (see Fig. 5). In the absence

of *lin-39* gene product, the fates of *P7* and *P8* descendants are governed solely by MAB-5 and vice versa. Since the expression of *lin-39* is generally more anterior to *mab-5* and only overlaps in the region of *P7* and *P8*, in the absence of *lin-39* gene activity, *P7* and *P8* descendants take on the fates normally associated with cells in the *mab-5* expression domain that do not express *lin-39*, normally located more posteriorly. Similarly, in the absence of *mab-5* gene activity, *P7* and *P8* descendants take on the fates normally associated with cells in the *lin-39* expression domain that do not express *mab-5*, normally located more anteriorly. This *lin-39* / *mab-5* interaction in the *P7/P8* spatial domain is not due to cross-regulation of *mab-5* or *lin-39* gene expression; MAB-5 protein is expressed in the same low level in *P7* and *P8* even in a *lin-39* mutant, and *lin-39* / lacZ fusion gene expression is not altered in a *mab-5* mutant (Wang et al. 1993). Even more compelling is the observation that expression of *mab-5* in the *lin-39* expression domain caused all P cells in the *lin-39* domain to become transformed to the *P7* and *P8* fates, which, for example, include cell fusion of *P7.p* and *P8.p* in males (Salser et al. 1993). This fate depends on both *lin-39* and *mab-5* gene activities. Thus, expression of MAB-5 does not repress or neutralize LIN-39 expression; rather, it acts combinatorially with LIN-39 to respecify cells.

In the anterior regions, *lin-39* may conspire with *ceh-13* to specify *P1* to *P6* fates. The transformations in cell fate that accompany mutations in these genes are not automatically posterior or anterior; they rather reflect which HOM-C gene products combinatorially interact in particular regions. In the case of the *P11* and *P12* cell lineages, *egl-5* appears to repress the expression of *mab-5*. *mab-5* expression in *P11* and *P12* descendants continues in an *egl-5* mutant, unlike wild type.

## C. *ceh-20* Encodes a Combinatorial Partner to HOM-C Proteins

Mutations in *ceh-20* cause defects in spatial patterning in the *lin-39* and *mab-5* spatial domains, including defects in Pn.p specification and defects in M-cell migrations (E. Chen and M. Stern, pers. comm.). *ceh-20* encodes a homeodomain protein of the PBC type, which bears a divergent homeodomain as well as an upstream conserved domain that has been found in mammalian and *Drosophila* homologs (Bürglin and Ruvkun 1992). CEH-20 is expressed in a variety of mesodermal and ectodermal cells, including the Pn.a and Pn.p cells (T. Bürglin and G. Ruvkun, pers. comm.). The *Drosophila* homolog of CEH-20 is Exd, which has been shown to act as a combinatorial partner to Ubx and Antp (Rauskolb et al. 1993; Rauskolb and Wieschaus 1994). The probable bipartite DNA-binding domain of PBC proteins and their synergistic binding with HOM-C cluster homeodomain proteins probably increase the specificity of HOM-C gene action. For example, in isolation, HOM-C homeodomain proteins are rather promiscuous in their DNA-binding specificity, to the point that it has proven difficult to detect downstream genes biochemically using isolated HOM-C homeodomain proteins. But in combination with Exd, the Ubx and Antp proteins bind synergistically to downstream gene sequences (Chan et al. 1994; Lu et al. 1995; Popperl et al. 1995). The P-cell fate defects in the *ceh-20* mutant suggest that like Exd in *Drosophila*, *ceh-20* functions as a combinatorial partner for *C. elegans* HOM-C genes. The HOM-C proteins in combination with CEH-20 are likely to modify the activity of genes analogous to *unc-4* and *unc-30* (see below).

## D. Control of Cell Migration

*mab-5* and *lin-39* are also necessary for the normal migration of Q-cell descendants. In the wild type, *QL* and its descendants migrate posteriorly, whereas *QR* and its descendants migrate anteriorly (Fig. 8). In a *mab-5* mutant, *QL* descendants migrate anteriorly rather than posteriorly, but *QR* migrates normally. *lin-39* mutants disrupt anterior migrations of *QR* descendants but do not affect posterior migrations of *QL* descendants. In a *lin-39* mutant, *QR* and its descendants begin their anterior migration normally but do not continue migrating into the head region. In genetic mosaics, a Q-cell migration defect is always associated with a *mab-5* or *lin-39* mutant genotype in the Q cell (Kenyon 1986; Clark et al. 1993). The cell autonomy of *mab-5* and *lin-39* suggests that both activate the expression of signaling pathways that sense migration cues, rather than regulating the production of migration cues themselves.

*mab-5* is expressed in *QL* descendants but is not expressed in *QR* descendants (Salser and Kenyon 1992). Thus, the changes in *QL* migration that are observed in the *mab-5* mutant can be understood as a homeotic transformation from *QL* to *QR* fates. *mab-5* begins to be expressed as soon as the migrating Q cell moves into

the posterior region of the animal, where [\*mab-5\*](#) is expressed by other cells. Thus, a system that detects spatial cues in the migrating Q cell may activate *mab-5*. The [\*mab-5\*](#) gene activity in this migrating cell may modify this detection system or the mechanism by which detection of these cues is translated to directed migration to allow new cues or new migratory behaviors to be induced.

A [\*mab-5\*](#) gain-of-function mutation results in the opposite transformation: Both [\*QR\*](#) and [\*QL\*](#) descendants migrate posteriorly. [\*mab-5\*](#) may be expressed in both [\*QR\*](#) and [\*QL\*](#) in this mutant. Interestingly, expression of MAB-5 from a heat shock promoter at any point in the anterior migration of Q.a is sufficient to cause its neuroblast daughter Q.ap to migrate posteriorly ([Fig. 8](#)) ([Salser and Kenyon 1992](#)). Thus, if migratory cues are detected by a MAB-5-regulated gene, they must be distributed globally. The lag between heat shock and migration direction change is 4 hours, suggesting that a cascade of gene regulation could be necessary for the change in migration imposed by MAB-5 expression ([Salser and Kenyon 1992](#)). Within a few hours of MAB-5-induced posterior migration, the [\*neuroblasts\*](#) and [\*neurons\*](#) begin to migrate again anteriorly, but further heat shock induction of MAB-5 again causes these cells to reverse direction ([Salser and Kenyon 1992](#)). These observations show that [\*mab-5\*](#) does not cause an irreversible switch in migratory behavior.

The factors that asymmetrically activate [\*mab-5\*](#) expression in [\*QL\*](#) are not known. The *mab-5(gf)* mutation is a partial duplication of the entire gene that truncates the promoter of one of the duplicate [\*mab-5\*](#) genes at -4 kb ([Salser and Kenyon 1992](#)). The *Mab-5* gain-of-function phenotype is not suppressed in *trans* to a deficiency, suggesting that it is not a twofold increase in [\*mab-5\*](#) that creates the phenotype. Rather, it is more likely that the truncated [\*mab-5\*](#) promoter either removes a negative regulatory element or generates a novel positive regulatory element for [\*QR\*](#) to symmetrize [\*mab-5\*](#) expression. This suggests that repression of [\*mab-5\*](#) in [\*QR\*](#) is the basis of asymmetric expression.

The distinct activities of the closely related [\*lin-39\*](#) and [\*mab-5\*](#) genes in, for example, [\*QL\*](#) where both are expressed suggest that these genes regulate distinct sets of genes. [\*lin-39\*](#) may regulate the expression of genes that respond to anterior migration cues, whereas [\*mab-5\*](#) may regulate the expression of genes that respond to posterior migration cues. Precedent for how such related genes can have such distinct activities comes again from *Drosophila*. For example, ectopic expression of Ubx or Antp proteins cause distinct segmental transformations, and this specificity maps to particular residues in the homeodomain that are distinct between Antp and Ubx ([Mann and Hogness 1990](#)). These differences mediate the distinct biological activities of related homeobox genes presumably by controlling which combinatorial partners interact with each subtype.

[\*mab-5\*](#) and [\*lin-39\*](#) also regulate the migration of the P-cell descendants. Normally, just the [\*P1\*](#) and [\*P2\*](#) descendants migrate anteriorly, whereas in a [\*lin-39\*](#) mutant, [\*P1\*](#) to [\*P6\*](#) descendants all migrate anteriorly, and in a [\*lin-39\*](#); [\*mab-5\*](#) double mutant, [\*P1\*](#) to [\*P11\*](#) descendants migrate anteriorly ([Clark et al. 1993](#)). Thus, in these cases, expression of [\*lin-39\*](#) or [\*mab-5\*](#) inhibits anterior migration, whereas in the case of the Q cell, expression of [\*lin-39\*](#) activates anterior migration and expression of [\*mab-5\*](#) activates posterior migration. Other factors may modify the activity of [\*lin-39\*](#) and [\*mab-5\*](#) in P descendants versus Q descendants. On the other hand, differential splicing of [\*mab-5\*](#) or [\*lin-39\*](#) in the P cells and Q cells, analogous to the differential splicing observed in *Drosophila* HOM-C genes ([Weinzierl et al. 1987](#)), could modify the sets of downstream genes regulated, and thus the migration cues detected by P- and Q-cell descendants. For example, alternative microexons in Ubx confer differential ability of the protein to specify PNS [\*neural\*](#) fates, suggesting that these Ubx microvariants may cooperate with distinct sets of other transcription factors to activate PNS-specific genes ([Mann and Hogness 1990](#)).

[\*egl-5\*](#) also regulates cell migration ([Desai et al. 1988; Chisholm 1991](#)). The HSN neuron is born in the posterior [\*egl-5\*](#) spatial domain, and its migration and development depend on [\*egl-5\*](#) function. The HSN expresses an *egl-5 lacZ* fusion gene, even after this cell migrates away from the posterior regions. If this represents continued [\*egl-5\*](#) expression rather than β-galactosidase perdurance, it suggests that extracellular regional-specific cues are not necessary for maintenance of [\*egl-5\*](#) expression once it has been initiated. A similar perdurance of *mab-5/lacZ* expression has been noted in the migrating M cell ([Wang et al. 1993](#)).

Mammalian HOM-C genes are expressed in migrating [\*neural\*](#) crest cells and in migrating cells during gastrulation ([Lufkin et al. 1991; Dush and Martin 1992](#)). Together with the regulation of neuroblast migration by *C. elegans*

HOM-C genes, this suggests that the regulation of migration by HOM-C genes may be general. Interestingly, mammalian evx genes have been implicated in control of gastrulation, and *vab-7*, the *C. elegans* evx homolog, appears to act in an analogous region of the *C. elegans* embryo (Ahringer 1996). During such migrations, cell movements into the domains of signaling molecules may induce expression of particular HOM-C genes, as has been observed in the case of *mab-5*, and the expression of these genes may in turn cause changes in adhesive properties and the migratory properties of these cells.

The regulation of migration by such HOM-C genes may be mediated by membrane receptors whose expression is regulated by these transcription factors. In *Drosophila*, the gene for the surface adhesion protein Connectin was isolated based on binding to Ubx protein and regulation by Ubx (Gould and White 1992). This adhesion molecule may mediate recognition of particular muscle cells by motor *neurons*; expression of Connectin in both muscle and motor *neurons* may be regulated by HOM-C genes (Gould and White 1992; Nose et al. 1994). This precedent suggests that there is not a deep regulatory hierarchy downstream from HOM-C genes but that these transcription factors directly regulate, in some cases, molecules that mediate morphogenetic movements and adhesions.

Across phylogeny, HOM-C cluster genes continue to be expressed in *neurons* (Krumlauf et al. 1993). Because of the function of HOM-C genes in migration of *neuroblasts*, they may also function in *neural* pathfinding as well. It is possible that similar cues guide migrating cells and outgrowing *neurons* so that the same regulatory pathways from HOM-C genes to receptors for guidance cues control cell migration and *neural* pathfinding (see Antebi et al., this volume).

## E. Modification of Reiterated Pattern Elements

The HOM-C genes generate spatial diversity along the A-P axis of animals across phylogeny. Mutations in genes that specify particular spatial domains reveal underlying reiterated spatial domains in the A-P dimension that express similar patterns of cell identity. Thus, the HOM-C genes can be understood as evolutionary adaptations to diversify reiterated basic units of development, the segment in *Drosophila*, or the P-cell-based segmental unit in *C. elegans*. The HOM-C genes may modify the activity of other pattern formation genes that specify these more ancient pattern elements.

The modifications of the basic P-cell sublineages by the HOM-C genes suggest that these genes may modulate either the expression or the activity of genes that specify *neural* fates in these sublineages. The HOM-C genes probably do not modulate the expression or activity of *unc-4* and *unc-30*, which are expressed in all P-cell lineages. But, for example, the *VC neurons* that innervate the vulval muscles are only generated by 6 of the 12 Pn.a neuroblast cell lineages that are located in the middle of the animal, P3 to P8 (see Fig. 5). In the other Pn.a cell lineages, the cells at the position in the cell lineage homologous to the VC neuron undergo programmed cell death. The production of *VC neurons* is dependent on *lin-39*. In the absence of *lin-39*, these neurons undergo programmed cell death, like the homologous cells in the other P-cell lineages. On the other hand, in a *ced-3* mutant, where programmed cell death is inactivated, six additional *VC neurons* are generated from the cell lineages where a programmed cell death normally occurs (Schinkmann and Li 1992). Thus, the expression of *lin-39* in P3 to P8 may inactivate a cell death pathway directly or may act to control another transcription factor analogous to *unc-4* that controls the generation of *VC neurons* in these cell lineages.

In this sense, one can view HOM-C proteins as another tier of gene regulation that modulates an earlier-acting (and phylogenetically more ancient) system of gene regulation for patterning reiterated elements. It is at the promoters for genes analogous to *unc-4* and *unc-30* or at the promoters of the genes which they regulate that we should look for mechanistic answers to how HOM-C genes pattern spatial domains. And it is at these promoters that the slight sequence differences between HOM-C proteins such as LIN-39 and MAB-5 will induce distinct cellular responses.

## F. Regulation of Cellular Communication

One of the initial responses to *mab-5* expression in Q is the detection of migration cues, whereas the initial response to *mab-5* expression in P7 and P8 is the fusion of these cells with their neighbors. Both of these responses involve cell-cell communication. Interestingly, expression of *lin-39* defines the fates of the P3.p to P8.p hypodermal cells that constitute the vulval equivalence group. These cells respond to anchor cell signaling via a *let-23* signaling system (Arojan et al. 1990; see Greenwald, this volume). In the absence of *lin-39* gene activity, P3.p to P8.p fuse with adjacent *hypodermis* rather than become competent to respond to the anchor cell signal. Expression in these Pn.p cells of the LET-23 receptor for the anchor cell signal, LIN-3, may thus be under the control of *lin-39*. It will be interesting to see if *let-23* and other genes in the signaling pathway downstream from *let-23* are regulated directly by *lin-39*.

It is provocative that downstream from *Drosophila* segmentation genes, many of which encode homeobox proteins or other transcription factors, are the cell-cell signaling genes such as *dpp* and *hedgehog* that may define segmental boundaries (Basler and Struhl 1994). These boundaries may correspond to the *Drosophila* polyclonal compartments that may constitute cell migration barriers (Blair et al. 1994). Such migratory barriers could be due to surface adhesion molecule expression, which could seal off a region from other migrating cells and signals from other compartments. It is tantalizing that the vulval equivalence group, P3 to P8, is also defined by HOM-C genes and may define a similar signaling domain.

## G. What Regulates the HOM-C Genes?

Upstream of the HOM-C genes in *Drosophila* are the gap and pair rule genes that subdivide the embryo into domains. The pathway upstream of these genes in *C. elegans* is much less well characterized. However, candidate earlier-acting genes that may directly regulate the HOM-C genes have been identified.

The *pal-1* / *nob-2* gene is a candidate for a patterning gene that regulates HOM-C genes. Null mutations in *pal-1* cause the posterior regions of the embryo to be malformed (L. Edgar et al., pers. comm.). The *pal-1* mRNA is found in all blastomeres of the early embryo, but production of PAL-1 protein is repressed in particular nonposterior blastomeres by the maternal-effect patterning gene *mex-3* (C. Hunter et al., pers. comm.). PAL-1 encodes a homeodomain protein related to *Drosophila* Caudal and mouse Cdx-1 (Waring and Kenyon 1990; Gamer and Wright 1993). These genes have been shown to regulate expression of HOM-C genes in the posterior region of the embryo. Thus, *pal-1* may regulate HOM-C gene expression, as in distantly related organisms, but may be activated by cell lineage cues that are more parochial to *C. elegans*. This early blastomere regulation of *C. elegans* development is distinct from the syncytial mechanism of early *Drosophila* development. But flies, worms, and vertebrates clearly use the same HOM-C developmental mechanism after these distinct beginnings.

## Figures

Figure 7. Embryonic expression pattern of the *lin-39-lacZ*, *mab-5-lacZ*, and *egl-5-lacZ* fusion genes.

### Figure 7

Embryonic expression pattern of the *lin-39-lacZ*, *mab-5-lacZ*, and *egl-5-lacZ* fusion genes. The schematic drawing shows a mid-stage embryo (460 min after first cleavage) with the anterior (A) and posterior (P) ends indicated. Below are shown embryos that carry *lin-39*-lacZ, *mab-5*-lacZ, and *egl-5*-lacZ constructs. (Reprinted, with permission, from Wang et al. 1993.)

Figure 8. Dorsal view of the migration patterns of the Q neuroblast descendants.

### Figure 8

Dorsal view of the migration patterns of the Q neuroblast descendants. *QL* and *QR* (open circles) are initially located directly opposite each other, but early migrations (not shown) shift *QR* anteriorly and *QL* posteriorly (A). The subsequent migratory behaviors of Q descendants are under the control of HOM-C genes. (B–F) Migrations dependent on *mab-5* (yellow) and *lin-39* (red), and migrations independent of these gene activities (gray) are

indicated by colored arrows; (*D*) effects of *mab-5* expression induced using heat shock during the anterior migration of the [QR](#) descendants. (Reprinted, with permission, from Salser and Kenyon 1994.)

Generated from local HTML

## Chapter 20. Patterning the Nervous System — VI Concluding Remarks

---

The molecular genetic analyses of *C. elegans* neurogenesis described in this chapter have revealed transcription factor genes that couple cell lineage cues and spatial patterning cues to the generation of particular [neural](#) types. Homologs of many of these genes, for example, [unc-86](#), [lin-32](#), [vab-3](#), and the HOM-C genes have been found in vertebrates. These homologs are likely to function in homologous processes, for example, in the case of [unc-86](#), coupling cell lineage asymmetry cues to the regulation of [neural](#) specification genes. Similarly, it is possible that entire genetic pathways including the network of genes regulated by these transcription factors are conserved.

The complexity of gene expression in the [nervous system](#) appears to exceed that of other tissues. This probably reflects the larger number of genes that are necessary to mediate the complex connections and functions of the many cell types in the [nervous system](#). Given the distinct gene expression repertoires that may be associated with each [neural](#) type, it is not surprising to find that the pattern and type of [neurons](#) generated are controlled by transcription factors. The frontier for the future will be to connect the complex regulation of these transcription factors to the expression of distinct batteries of genes that subserve the specialized features of each [neural](#) type. These transcription factors are likely to bind to a large number of downstream genes that mediate the specialized features of neurons. The overlapping expression patterns of many of these transcription factors, for example, SEM-4 (M. Basson and B. Horvitz, pers. comm.), UNC-86, and EGL-5 in the HSN neuron, suggest that transcription factors are likely to conspire in the regulation of at least some downstream genes. For example, they may bind combinatorially and synergistically, as has been shown for UNC-86 and MEC-3, to regulate only certain genes in certain [neurons](#) (Xue et al. 1993).

The activities of these transcription factor genes in neurogenesis is mediated by the downstream genes that they regulate. The identification of the network of genes downstream from each of these transcription factor genes is a major goal for the future. Molecular approaches to the isolation of downstream genes may be fruitful in the future, but such analyses will demand genetic proof that genes so identified are bona fide and important in neurogenesis. Gene knockout techniques will allow such genetic studies of downstream genes identified by molecular criteria ([Zwaal et al. 1993](#); see [Plasterk and van Leunen](#), this volume). Genetic approaches to the identification of downstream genes have also been used. Mutations in the genes regulated by these transcription factors may lead to the same phenotype as mutations in the transcription factor genes in cases where few genes act downstream. For example, mutations in the mechanosensory [neuron](#) specification gene [mec-3](#) have behavioral phenotypes similar to mutations in the downstream [mec-7](#) tubulin or [mec-4](#) sodium channel genes (Chalfie and Au 1989). However, if many genes are regulated by these transcription factor genes, mutations in any one of these downstream genes may confer only a subset of the phenotypes. Thus, saturating screens for a phenotype may not reveal such downstream genes. They might show up in more subtle enhancer or suppressor screens. In addition, any genes negatively regulated by these transcription factor genes may mutate to opposite phenotypes; such genes would be revealed by suppressor screens. Another approach to the identification of downstream genes has utilized a hyperactivated transcription factor to activate increased or ectopic expression of downstream genes (J. Sze et al., pers. comm.). Suppression of the phenotypes conferred by such an activated transcription factor, or suppression of non-null mutations in downstream genes by an activated transcription factor, promises to identify downstream genes genetically.

Also key for future analyses of the pathways that include these transcription factors is the study of how their activities are regulated during neurogenesis. For example, the UNC-6/Netrin and UNC-5 receptor dorsal-ventral pathfinding system (see [Antebi et al.](#), this volume) has a transcriptional component: Expression of the UNC-5 dorsal pathfinding receptor appears to be transcriptionally controlled as [neurons](#) turn dorsalward (Hamelin et al. 1993; Y. Zhou and J. Culotti, pers. comm.). Thus, there may be a coupling of signals from growth cones to the nucleus to activate [unc-5](#) expression at the position where [neurons](#) turn dorsalward. Such transcriptional control of [neural](#) pathfinding molecules may be mediated by the modulation of transcription factor activities that are

specific to that system or by modulation of transcription factor activities that also mediate other neurogenic events. More theoretically, the labeled pathways model for neurogenesis posits that a variety of surface adhesion molecules decorate particular sets of axons and even particular regions of axons to attract or repel particular other neurites (Kolodkin et al. 1992; Schmucker et al. 1992; Meier et al. 1993). To express such a spectrum of surface molecules, the pattern of gene expression in the developing [neuron](#) might be dynamic so that a series of surface receptors are expressed over time to decorate a series of segments of a developing neurite. Modulation of transcription factor activities would be expected to mediate such changes in transcription during [neural](#) pathfinding.

Genes such as *unc-86*, *mab-5*, and [\*unc-30\*](#) continue to be expressed in the mature [nervous system](#) (Finney and Ruvkun 1990; Jin et al. 1994). Similarly, [\*unc-4\*](#) gene activity is necessary after its initial function in motor neurogenesis perhaps to maintain synaptic connections (Miller et al. 1992). It is likely that these transcription factors not only regulate the expression of downstream genes that mediate initial neurogenesis, but also continue to regulate the expression of these and other genes to maintain [neural](#) function. Maintenance of [neural](#) structure and function probably involves regulation of a repertoire of genes that may be similar to those that mediate initial neurogenesis. The emerging view that developmental changes requiring changes in gene expression underlie learning and memory points to the genetic pathways that control initial [neural](#) development as likely mediators of these functions. Modulation of CREB transcription factor activity in *Drosophila* and vertebrates by cAMP kinase may underlie the changes in synaptic strength that accompany learning (Bourtchuladze et al. 1994; Yin et al. 1995). It is tantalizing to imagine that activity regulation of transcription factors such as UNC-86, UNC-4, and UNC-30 by kinases whose activity is a measure of [neural](#) activity could modulate the expression of downstream genes that modify synaptic strength after [neural](#) activity.

Generated from local HTML

# **Chapter 21. Cell and Growth Cone Migrations**

---

## **Contents**

- [I Introduction](#)
- [II Neuroglia and Pioneers](#)
- [III Netrins Guide Circumferential Migrations](#)
- [IV Hierarchies Of Guidance Cues](#)
- [V Genetic Requirements for Axonal Growth](#)
- [VI Cell Migration and other Aspects of Cellular Phenotype](#)
- [VII Muscle Positioning on the Body Wall and Muscle Arm Chemotropism](#)
- [VIII Future Directions](#)
- [Acknowledgments](#)

Generated from local HTML

# Chapter 21. Cell and Growth Cone Migrations — I Introduction

---

During morphogenesis, some cells migrate from their origins to distant locations. The complex, stereotyped migrations of axonal growth cones, for example, determine the connectivity of the [nervous system](#). Motile cells and processes can undergo directed movements in response to spatially patterned molecules ([Keynes and Cook 1995](#); [Garrity and Zipursky 1995](#)), and recent studies suggest that specific directional cues are conserved from nematodes to chordates ([Hedgecock et al. 1990](#); [Ishii et al. 1992](#); [Kennedy et al. 1994](#); [Serafini et al. 1994](#); [Colamarino and Tessier-Lavigne 1995](#)).

Migrating cells may follow several different directional cues, often in strict sequence, during development. Moreover, they may halt migration at stereotyped positions or times either to divide or to differentiate. These changes in cell movements must reflect changes in the extracellular environment or changes within the motile cell itself. For example, cells might be constitutively responsive to multiple directional cues, changing course whenever they encounter a further cue within their repertoire. Instead, it appears that cells become responsive to new cues, or unresponsive to current ones, during the course of migration. Some transitions could be entirely autonomous, reflecting, for example, an intracellular clock, but many are contingent upon extracellular signals encountered during the course of migration. These transitions often involve new gene expression. Analysis of these transitions has identified signaling pathways and transcriptional cascades within migrating cells that help select substrate and direction of migration, or regulate transitions between motile and stationary states. One such pathway in nematodes responds to hormonal signals that advance developmental age throughout the larva, whereas others respond to growth factors that mark particular origins or migration paths. Together with cytoskeletal machinery for directed movement, these regulatory mechanisms form the intrinsic navigational programs of migrating cells.

This chapter reviews the developmental genetics of cell migration in *Caenorhabditis elegans* including growth cones and other motile cell processes. The origins and fates, including migrations and morphogenetic movements, of the [somatic cells](#) in both males and hermaphrodites have been traced in living embryos and larvae ([Sulston and Horvitz 1977](#); [Kimble and Hirsh 1979](#); [Sulston et al. 1980, 1983](#)). The cellular anatomy of the adult [nervous system](#), including axon trajectories and synaptic connectivity, has been completely reconstructed from serial electron micrographs ([Ward et al. 1975](#); [Ware et al. 1975](#); [Albertson and Thomson 1976](#); [White et al. 1976, 1986](#); [Hall and Russell 1991](#)). Several earlier reviews of cell and growth cone migrations in *C. elegans* ([Hedgecock et al. 1987](#); [Wadsworth and Hedgecock 1992](#); [Culotti 1994](#); [Garriga and Stern 1994](#)) and some recent general reviews of cell motility and pathfinding are highly recommended ([Burns and Augustine 1995](#); [Garrity and Zipursky 1995](#); [Keynes and Cook 1995](#); [Tanaka and Sabry 1995](#)).

Generated from local HTML

# Chapter 21. Cell and Growth Cone Migrations — II Neuroglia and Pioneers

---

In nematodes, as in other animals, the first growth cones, or pioneers, establish a simple scaffold of axon tracts on the basal surface of the ectoderm ([Wadsworth and Hedgecock 1992](#); [Wadsworth et al. 1996](#)). These tracts generally follow the natural longitudinal (anterior-posterior) and circumferential (dorsal-ventral) axes of the neurula. Pioneer growth cones are guided by molecules on neuroglia and [neuroblasts](#) (guideposts) along the migration paths and factors diffusing from more distant cells. Growth cones arriving later can follow these same directional cues or newer ones provided by the pioneer axons themselves. In *C. elegans*, it is possible to test the relative contributions of neuroglia, [neuroblasts](#), and pioneer axons, and their molecular cues, by ablating individual cells prior to axonogenesis or mutating individual genes.

The ectoderm, including the [nervous system](#), is remarkably simple in nematodes ([Albertson and Thomson 1976](#); [White et al. 1976](#), 1986; [Hall and Russell 1991](#)). By the middle of embryogenesis, an epithelium of hypodermal cells has spread across and enclosed the body to form the neurula, or comma stage. The hypodermal cells form the cuticle (exoskeleton) on their apical surface, but they have additional, specialized functions as neuroglia. Their basolateral surface serves as pathways for migrations of [neuroblasts](#) and pioneer growth cones ([Fig. 1](#)) ([White et al. 1986](#); [Durbin 1987](#); [Hedgecock et al. 1987](#); [Wadsworth and Hedgecock 1992](#)). As structural elements of the body wall, they support movement and attachment of various mesoblasts on their basal lamina. The largest cells, hypodermoblasts and hypodermal syncytium, are arranged in longitudinal rows along the body. Smaller cells, with characteristic arrangement and shapes, form the extreme head and tail, passageways to internal epithelia, and openings (sockets) for various [sensilla](#) ([Ward et al. 1975](#); [Perkins et al. 1986](#); [White et al. 1986](#)). Finally, a combination of hypodermal cells, known as marginal cells, and myoepithelial cells form the [pharynx](#), an internal epithelium involved in feeding ([Albertson and Thomson 1976](#); see [Avery and Thomas](#), this volume).

## A. Ventral Nerve Cord

Longitudinal axon tracts on the nematode body wall and [pharynx](#) tend to follow the centers or margins of the rows of hypodermal cells and associated muscles ([Hedgecock et al. 1987](#)). The largest such connective, the [ventral nerve cord](#), comprises paired axon tracts flanking a row of motor neurons along the ventral midline of the body wall ([Fig. 2](#)) ([White et al. 1976](#)). Most axon sorting occurs within small [ganglia](#) at its anterior (retrovesicular) and posterior (preanal) ends, where interneurons, and some sensory axons, enter or leave the nerve cord ([White et al. 1976](#), 1986; [Durbin 1987](#); [Hall and Russell 1991](#)). The small, highly asymmetrical ventral longitudinal tracts of modern nematodes apparently arose from a larger, more symmetrical nerve cord by a process of reduction and partial fusion ([Durbin 1987](#)). Excepting the head, nematodes flex strictly in the dorsal-ventral plane, and fusion of the longitudinal tracts in the nerve cords ensures that left and right body muscles receive identical synaptic inputs.

The behavior of paired axons as they enter the [ventral nerve cord](#) at either end is most revealing (Figs. 3 and 4) ([White et al. 1986](#); [Durbin 1987](#)). Some axons (e.g., RIF in the retrovesicular ganglion and PVP in the [preanal ganglion](#)) first cross the ventral midline and then travel in the contralateral tracts. Such reciprocal crossing of nerve tracts, or decussation, is common to all phyla, but its mechanism and purpose are obscure. Other axons (e.g., AVK, HSN, and PVQ) fasciculate and travel in the ipsilateral tracts without decussation. Finally, most axons entering from the left (e.g., [AVAR](#) and PVCL) first cross the ventral midline and then travel in the major (right) tract together with their homolog. Such unilateral decussation is probably a recent adaptation in nematodes, whereas the other two patterns are vestiges of an earlier, more symmetrical, [ventral nerve cord](#).

The early development of the [ventral nerve cord](#) has been studied by serial electron microscopic reconstruction of staged embryos ([Durbin 1987](#)). From the [retrovesicular ganglion](#), the midline neuron [AVG](#) extends the first axon posteriorly along the [ventral nerve cord](#) (Figs. 3 and 4a). This axon pioneers the right tract of the nerve cord. Next, the motor neurons DD extend axons anteriorly, fasciculating with AVG. These axons then turn dorsally and, along with axons from motor neurons DA and DB, establish the [dorsal nerve cord](#). During the same period,

the paired neurons PVP in the [preanal ganglion](#) extend axons anteriorly along the nerve cord. These axons first decussate at the ventral midline and then pioneer the contralateral tract. The paired neurons PVQ in the lumbar [ganglia](#) pioneer the lumbar commissures to the [preanal ganglion](#) where they fasciculate with the PVP axons and travel anteriorly in the ipsilateral tract. Finally, the paired neurons RIF in the [retrovesicular ganglion](#) extend axons anteriorly toward the developing [nerve ring](#). Like PVP in the [preanal ganglion](#), these axons first decussate at the ventral midline and then pioneer the contralateral tracts.

After the pioneering events, axons of various sensory and interneurons enter the [ventral nerve cord](#) via the [nerve ring](#) or lumbar commissures. Excepting [AVKR](#), axons that enter on the left (e.g., [AVAR](#), [AVBR](#), and [PVCL](#)) decussate unilaterally and travel with their homologs in the right tract of the [ventral nerve cord](#) ([Fig. 4d](#)). Further axons are added to the right tract during larval development. Finally, the paired motor neurons HSN enter the [ventral nerve cord](#) in the midbody during the L4 stage and grow anteriorly along the ipsilateral tracts without decussation ([White et al. 1986](#)). The vestigial left tract of the [ventral nerve cord](#) comprises just three interneurons ([AVKR](#), [PVPR](#), [PVQL](#)) and one motor neuron ([HSNL](#)) in the adult hermaphrodite ([Fig. 4e](#)).

## B. Nerve Ring

The [nerve ring](#), a bundle of approximately 100 axons encircling the outside of the [pharynx](#), is the principal circumferential tract in the [nervous system](#) ([White et al. 1986](#)). Axons from [sensory neurons](#) in the [anterior ganglia](#) form six labial nerves that enter the [nerve ring](#) at its anterior margin. Most axons from neurons in the [lateral ganglia](#) enter the [nerve ring](#) at its posterior margin either laterally (e.g., AVA) or ventrally (e.g., AVB) via the amphid commissures and ventral ganglion. In general, axons that enter from the lateral or ventral [ganglia](#) grow dorsally in the ring neuropil. Some terminate at the dorsal midline of the [nerve ring](#) (e.g., PVP, PVQ, and RIF), whereas others decussate and continue ventrally in the contralateral ring neuropil (e.g., AVA, AVB, and AVK). Unlike the [ventral nerve cord](#), the [nerve ring](#) is more or less symmetrical.

In comparison to the [ventral nerve cord](#), less is known about the developing [nerve ring](#). Sheath cells, resembling the radial glia of chordates, may provide a scaffold and directional cues for the developing [nerve ring](#) and labial nerves. In the mature [nervous system](#), sheaths envelop various sensory endings, coupling them to the hypodermal openings formed by socket cells ([Ward et al. 1975](#); [Ware et al. 1975](#); [Perkins et al. 1986](#)). In the neurula, the six inner labial sheaths leave processes trailing back to the [nerve ring](#) as they move toward the sensillar rudiments. These processes could guide labial axons to the [nerve ring](#) while their endfeet form a transient, ring-shaped substratum for axons within the ring itself ([Fig. 3](#)) ([Wadsworth et al. 1996](#)). The four cephalic sheaths extend sheet-like processes that anticipate the outer surface of the ring neuropil and persist through the adult ([White et al. 1986](#)). In particular, ventral and dorsal cephalic sheaths could provide the paths for pioneer axons entering the ring neuropil from the ventral and lateral [ganglia](#), respectively. Finally, the six mesoglia [GLR](#) extend sheet-like processes covering the inner surface of the [nerve ring](#). These processes could support and guide the muscle arms that form neuromuscular junctions with motor axons in the [nerve ring](#).

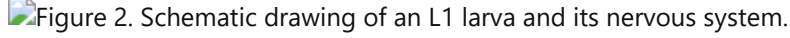
The pioneers of the [nerve ring](#) are still unknown. However, the four RME motor neurons are promising candidates on the basis of their unique morphology and connectivity in the adult ([White et al. 1986](#)). Like the ring neuropil itself, the cell bodies of these neurons are included within the basal endfeet of the cephalic sheaths ([Fig. 3](#)). From each cell body, two axons travel around the [nerve ring](#) in opposite directions to complete a circle at the anterior margin of the neuropil. These axons are synaptic targets of [inner labial neurons](#) IL1 and IL2 (discussed below). Conceivably, the inner labial sheath processes could guide the inner labial axons to the developing [nerve ring](#) where the labial and RME axons fasciculate. Finally, RMEs form gap junctions with [GLR](#) and neuromuscular junctions onto muscle arms.

## Figures

Figure 1. Topology of body wall.

### Figure 1

Topology of body wall. (*Left*) A neuron positioned between the hypodermal (epidermal) cell membrane and basal lamina (basement membrane). (*Middle*) A distal-tip cell, ensheathing the distalmost [germ cells](#) in the [hermaphrodite gonad](#), migrates along the basal laminae of either body wall muscles (not shown) or hypodermal cells. The arrow indicates the direction of migration. (*Right*) A body-wall muscle cell attached to the hypodermis. A muscle arm extends to a nearby nerve cord where it forms a neuromuscular junction (NMJ) traversing the basal laminae. (Reprinted, with permission, from [Hedgecock et al. 1987](#).)

Figure 2. Schematic drawing of an L1 larva and its nervous system.

## Figure 2

Schematic drawing of an L1 larva and its [nervous system](#). Shown are all neuronal cell bodies and process tracts behind the retrovesicular ganglion on the left, dorsal, and ventral sides. Adapted from [Sulston et al. \(1983\)](#) and [Durbin \(1987\)](#).

Figure 3. NC-6 expression in the embryonic ectoderm and proposed guidance functions.

## Figure 3

NC-6 expression in the embryonic ectoderm and proposed guidance functions. (*Top*) The [AVG](#) (red) axon runs posteriorly along the ventral midline. The body wall is shown opened along the dorsal midline in cylindrical projection, and the [nerve ring](#) is flattened in anterior projection (cf. [White et al. 1986](#)). Excepting neuron [J5](#) in the [pharynx](#), [all cells](#) that express UNC-6 in the embryo are shown. Stars mark additional cells, included for reference, that do not express UNC-6. Neurons are located within various [ganglia](#), i.e., lateral (AVA, AVB), retrovesicular ([AVG](#), RIF), preanal (PVP, [PVT](#)), or lumbar (PVQ). The [excretory pore](#) (*middle*) and [anus](#) (*right*) provide landmarks along the ventral midline. Cephalic sheaths (CEPsh) support RME and other axons within the ring neuropil. Inner labial sheaths (ILsh) may guide axons entering the neuropil from the anterior via the six labial nerves. Cephalic sheaths may guide axons entering the neuropil from the posterior via lateral (e.g., AVA) and ventral routes (e.g., AVB). AVA and AVB axons undergo reciprocal decussations at the dorsal midline of the ring. Ventral hypodermoblasts (epidermoblasts [P1/2-P11/12](#)) are represented by the six subdivisions shown on the body wall. These hypodermoblasts support axons within the [ventral nerve cord](#). Guidepost neurons [AVG](#) and [PVT](#) may mark the anterior and posterior boundaries of the nerve cord proper. (*Lower left*) The body wall and [nerve ring](#) are shown in cross section through the head. The ventral cephalic sheaths, which express UNC-6, are filled. Axons of neurons AVA and AVB in the lateral [ganglia](#) enter the [nerve ring](#) by lateral and ventral routes, respectively. (*Lower right*) The body wall is shown in cross section through the midbody. The ventral hypodermoblasts, which express UNC-6, are filled. Typical sensory and motor neurons are shown projecting to the ventral and dorsal nerve cords, respectively. (Reprinted, with permission, from [Wadsworth et al. 1996](#), copyright by Cell Press.)

Figure 4. Pioneers and their followers in the developing ventral nerve cord (after Durbin 1987; Garriga et al. 1993a).

## Figure 4

Pioneers and their followers in the developing [ventral nerve cord](#) (after [Durbin 1987](#); [Garriga et al. 1993a](#)). (*a*) [AVG](#) has pioneered the right tract, and PVP and PVQ growth cones extend anteriorly. Motor neurons in the right tract are omitted for clarity. (*b*) Removing [PVPR](#) causes [PVQL](#) to decussate; (*c*) removing [PVQL](#) has no effect on [PVPR](#); (*d*) AVK growth cones extend posteriorly; (*e*) HSN growth cones extend anteriorly; (*f*) removing [PVPR](#) and [PVQL](#) causes the [HSNL](#) to decussate.

## Chapter 21. Cell and Growth Cone Migrations — III Netrins Guide Circumferential Migrations

---

Three known genes, [\*unc-5\*](#), [\*unc-6\*](#), and [\*unc-40\*](#), are required to guide the circumferential migrations of neuronal growth cones and mesoblasts on the body wall ([Hedgecock et al. 1990](#)). [\*unc-6\*](#) is required for guiding both dorsal and ventral migrations, whereas [\*unc-5\*](#) is required only for dorsal migrations. [\*unc-40\*](#) is required for most or all [\*unc-6\*](#) functions; existing alleles of [\*unc-40\*](#) severely disrupt ventral migrations but also weakly affect dorsal migrations. Unlike [\*unc-5\*](#) and [\*unc-6\*](#), mutations in [\*unc-40\*](#) also affect hypodermal cell intercalations and Q neuroblast migrations.

UNC-6 is a laminin-related protein with a unique carboxyl terminus ([Fig. 5](#)) ([Ishii et al. 1992](#)). Recently, vertebrate orthologs, called netrins, have been isolated as growth cone chemoattractants expressed in the floorplate of the developing spinal cord ([Kennedy et al. 1994](#); [Serafini et al. 1994](#)). UNC-6 is expressed by 12 types of hypodermoblasts, sheaths, and neurons of ectodermal origin during embryonic or larval development in the hermaphrodite ([Wadsworth et al. 1996](#)). Like the vertebrate netrins ([Kennedy et al. 1994](#)), UNC-6 expression is restricted to the ventralmost cells within each region of the [nervous system](#) (see [Fig. 3](#)). A simple model is that netrin gradients on neuroepithelia, peaking along the ventral midline, act as attractive or repulsive cues, respectively, for ventral and dorsal migrations ([Colamarino and Tessier-Lavigne 1995](#); [Wadsworth et al. 1996](#)). Whether netrin is attractive or repulsive evidently depends on the motile cell itself and, particularly, on the current state of its navigational program.

The domain structure of netrins, which is conserved from nematodes to chordates, has several implications for their biological activities. The amino terminus is homologous to domains VI and V of laminin subunits  $\alpha$ ,  $\beta$ , and  $\gamma$  ([Fig. 5](#)). Laminin molecules, which are heterotrimers of all three subunits, self-assemble via their domain VI, forming a stable, polymeric scaffold for the basal lamina ([Yurchenco and Cheng 1993](#)). Thus, netrin domain VI could allow its incorporation into basal laminae by copolymerization with laminin. Several epidermal growth factor (EGF)-like modules in domains V and III of laminin subunits are proposed to form binding sites for integrins and other cellular receptors ([Beck et al. 1990](#); [Hynes and Lander 1992](#)). By inference, netrin modules V-1, V-2, or V-3 might be the ligands for receptors on growth cones and migrating cells that respond to netrin cues. Finally, the basic domain at the carboxyl terminus could tether netrin to other molecules for display on cell surfaces or unique matrix sites.

Molecular analysis of selective loss-of-function and null alleles of [\*unc-6\*](#) indicates that the biological activities of netrins are mediated through distinct protein domains ([Wadsworth et al. 1996](#)). Inframe deletions of the EGF-like module V-2 disrupt netrin-mediated repulsion but not attraction ([Fig. 5](#)). This module could provide a binding site for the repulsion receptor UNC-5 (discussed below). Missense and other subtle mutations in domain VI can produce other selective loss-of-function phenotypes. A mutation near the end of domain VI selectively disrupts mesoblast but not axonal migrations. Conceivably, this mutation could affect the display of UNC-6 on the outward face of basal laminae that contacts mesoblasts but not its display on the inward face or cell surfaces that contact neuronal growth cones. A mutation nearer the middle of domain VI selectively disrupts ventral migrations of both axons and mesoblasts. One possibility is that the receptor mediating attraction binds to this module. Alternatively, some distinct mechanism of tethering, affected by this mutation, may be used to maintain a high concentration of netrin along the ventral midline. Finally, deletions of the 3'exons coding for module V-3 and domain C result in a null phenotype.

UNC-5 is a novel cell surface receptor with an extracellular amino terminus comprising two immunoglobulin and two thrombospondin type I modules (T1 in [Fig. 5](#)) and a large intracellular carboxyl terminus including a potential SH3 module (SH in [Fig. 5](#)) ([Leung-Hagemeijer et al. 1992](#)). UNC-5 expression on the surface of motile cells appears both necessary and sufficient to orient them away from UNC-6 sources ([Hamelin et al. 1993](#); M. Su et al., in prep.). UNC-40 is a cell surface protein with an extracellular amino terminus comprising four immunoglobulin and six fibronectin III modules and a large intracellular carboxyl terminus ([Fig. 5](#)) (S. Chan et al., in prep.).

UNC-40 is closely related to DCC ([Chan et al. 1996](#)), a protein frequently inactivated in human colorectal cancer ([Hedrick et al. 1994](#)). DCC and its orthologs in other vertebrates are expressed in developing epithelia and in neurons undergoing axonogenesis ([Lawlor and Narayanan 1992](#); [Chuong et al. 1994](#); [Pierceall et al. 1994a,b](#); [Vielmetter et al. 1994](#)). UNC-40 is apparently expressed in all of the neurons and mesoblasts that are known to undergo netrin-guided movements (S. Chan et al., in prep.). Interestingly, certain neurons that grow strictly along the ventral midline also express this receptor; netrin attraction may help prevent these growth cones from straying from the midline as they migrate longitudinally along the ventral hypodermis ([Hedgecock et al. 1990](#); [Wadsworth et al. 1996](#)). In contrast to UNC-5, it is not yet known whether UNC-40 has an instructive role in netrin-guided movements. It evidently acts with UNC-5 to orient motile cells away from netrin sources; it may act either alone or with some unknown instructive partner to orient motile cells toward netrin sources. Vertebrate netrins may interact directly with DCC ([Keino-Masu et al. 1996](#)). The various netrin-independent phenotypes of *unc-40* mutants suggest that UNC-40/DCC have a widespread role in cell adhesion and motility.

## Figures

Figure 5. One-dimensional representations of *C. elegans*.

### Figure 5

One-dimensional representations of *C. elegans* gene products involved in cell and growth cone migrations. The modular organization of domains I–VI of mouse laminin  $\gamma$  is shown for comparison to UNC-6/netrin ([Yamada and Sasaki 1987](#); [Ishii et al. 1992](#); [Serafini et al. 1994](#)). References for other *C. elegans*-predicted gene products include UNC-5 ([Leung-Hagesteijn et al. 1992](#)), UNC-40/DCC ([Hedrick et al. 1994](#); S. Chan et al., in prep.), EGL-15/FGF ([DeVore et al. 1995](#)), PAT-3/B-integrin ([Gettner et al. 1995](#)), UNC-44/ankyrin ([Otsuka et al. 1995](#)), SEM-5/GRB2 ([Clark et al. 1992](#); [Lowenstein et al. 1992](#)), UNC-33/CRMP-62/TOAD-64 ([Li et al. 1992](#); [Goshima et al. 1995](#); [Minturn et al. 1995](#)), MIG-5/DSH ([Klingensmith et al. 1994](#); [Theisen et al. 1994](#); [Guo 1995](#)), UNC-104/KIF1A ([Otsuka et al. 1991](#); [Okada et al. 1995](#)), UNC-51 ([Ogura et al. 1994](#)), KSR-1 ([Sundaram and Han 1995](#)), LIN-39/Sex combs reduced ([Clark et al. 1993](#); [Wang et al. 1993](#)), MAB-5/Antennapedia ([Costa et al. 1988](#)), EGL-5/Abdominal B ([Wang et al. 1993](#)), UNC-30 ([Jin et al. 1994](#)), CEH-18 ([Greenstein et al. 1994](#)), VAB-3/PAX-6 ([Chisholm and Horvitz 1995](#); [Zhang and Emmons 1995](#)), EGL-43/Evi-1 ([Perkins et al. 1991](#); [Garriga et al. 1993b](#)), and DAF-12/DHR96 ([Yeh 1991](#); [Fisk and Thummel 1995](#)). Cartoons of various modules are adapted from [Bork and Bairoch \(1995\)](#).

Generated from local HTML

## Chapter 21. Cell and Growth Cone Migrations — IV Hierarchies Of Guidance Cues

---

The pattern of UNC-6 expression suggests how multiple netrin cues, each with a characteristic role, guide cells and axons in the developing [nervous system](#) (see [Fig. 3](#)) ([Wadsworth and Hedgecock 1996](#)). UNC-6 is first secreted by hypodermoblasts [P1/2-P11/12](#) as they slide over the neuroectoderm and meet together along the ventral midline. A proposed netrin gradient on the body wall may act as an attractive cue for [AVG](#) and PVP growth cones as they pioneer the ventral longitudinal tracts and as a repulsive cue for DA, DB, and DD growth cones as they grow away from the ventral midline. Next, midline [neuroblasts AVG](#) and [PVT](#) at either end of the [ventral nerve cord](#) express UNC-6. One possible function is to guide the decussations of the pioneer axons RIF and PVP, respectively. Remarkably, [RIFL](#) itself but not its homolog [RIFR](#) expresses UNC-6. Together, the [AVG](#) and [RIFL](#) axons may provide a continuous netrin-labeled pathway restricted to the right tract of the nerve cord during early stages of [nervous system](#) development. This asymmetric cue could guide the unilateral decussation of various paired axons from the [nerve ring](#) and lumbar commissures as they enter the [ventral nerve cord](#). Finally, the netrin cue from [PVT](#) could help attract the PVQ growth cones and facilitate their contact with the PVP axons. At the threefold stage, the neurons PVQ themselves express UNC-6. Hence, these pioneer axons could provide a netrin-labeled pathway in the lumbar commissures for guiding later axons.

The importance of netrin cues in the developing [nerve ring](#) is still uncertain ([Wadsworth et al. 1996](#)). Neurons IL1 in the [anterior ganglia](#) express the receptor UNC-5 (M. Su et al., in prep.), suggesting that these axons may pioneer the labial nerves into the [nerve ring](#) by moving down the UNC-6 gradient seen on the process of the inner labial sheath. The ventral cephalic sheaths express UNC-6 transiently in the neurula, but their dorsal homologs never express this netrin cue. Neurons AVA and AVB also express the receptor UNC-5 (M. Su et al., in prep.), suggesting that these axons may pioneer the lateral and ventral routes, respectively, from the lateral [ganglia](#) into the [nerve ring](#). A simple model for their complex trajectories is that AVA is first attracted and then repulsed by UNC-6 from the ventral cephalic sheaths, whereas AVB is first repulsed and then attracted by this same netrin cue (see [Fig. 3](#)). This model predicts specific temporal control of UNC-5 in AVA and AVB; a detailed analysis of UNC-5 temporal expression should shed light on this issue. After axonogenesis begins, AVA and AVB themselves express UNC-6. Like PVQ in the lumbar [ganglia](#), these axons could provide netrin-labeled pathways for guiding later axons to the [nerve ring](#) and ventral ganglion.

The roles of individual pioneer axons in guiding later growth cones in the developing [ventral nerve cord](#) have been examined by ablation of [neuronal precursors](#) ([Durbin 1987](#); [Garriga et al. 1993a](#)). Removing [AVG](#) results in a loss in cohesion of the right tract, which splits into multiple fascicles, and occasional shifting of axons to the left tract. When the [PVPR](#) precursor is removed, the [PVQL](#) and [AVKR](#) growth cones shift to the right tract ([Fig. 4b](#)). Removing the [PVQL](#) precursor has no effect on [PVPR](#) but prevents other growth cones of the left lumbar ganglion from reaching the [ventral nerve cord](#). Finally, removing both [PVPR](#) and [PVQL](#) during the first larval stage, after their axons have grown out, invariably causes the [HSNL](#) growth cone to shift to the right tract ([Fig. 4f](#)). However, removing [PVQL](#) alone at this stage only causes a shift in about 30% of the operated larvae, whereas removing [PVPR](#) alone has no effect on HSNL. Mosaic studies using [unc-6](#) null alleles might confirm whether the effects of removing [AVG](#) or PVQ reflect the loss of specific UNC-6 cues provided by these neurons ([Hedgecock et al. 1990](#); [Wadsworth et al. 1996](#)).

Several known genes are required for decussation and outgrowth of the PVP axons. In [unc-73](#), either one of the two axons may fail to decussate and travels instead in the ipsilateral tract in about 80% of all animals (H. Bhatt and E. Hedgecock, pers. comm.). [unc-73](#) mutants are pleiotropic, affecting the migrations of many cells and growth cones ([Hedgecock et al. 1985, 1987](#); [Desai et al. 1988](#); [Siddiqui 1990](#); [Siddiqui and Culotti 1991](#); [McIntire et al. 1992](#)). In [unc-6](#) and [unc-40](#), one axon fails to decussate in about 30% of all animals, whereas more rarely, a PVP axon leaves the [ventral nerve cord](#) entirely and travels anteriorly along the [lateral hypodermis](#) ([Wadsworth et al. 1996](#)). Finally, in [unc-30](#), the left tract of the [ventral nerve cord](#) is often missing, and PVP neurons fail to stain with the monoclonal antibody MAb M44 (H.B. Bhatt and E.M. Hedgecock, pers. comm.; B. Wightman et al., in

prep.). UNC-73 is related to the GTP/GDP exchange factor for Rho-type G proteins, and it is expressed in neurons (J. Culotti, pers. comm.). Rho-type G proteins are implicated in diverse actin-dependent processes including budding in yeast, assembly of focal adhesions and stress fibers, and filopodia and lamellapodia extension ([Ridley and Hall 1992](#); [Ridley et al. 1992](#); [Chant and Pringle 1995](#); [Nobes and Hall 1995](#)). Finally, UNC-30 is a homeobox transcription factor that is expressed in PVP and several other types of neurons ([Fig. 5](#)) ([Jin et al. 1994](#); see [McGhee and Krause](#), this volume).

Several genes, including [\*enu-1\*](#), [\*fax-1\*](#), [\*unc-42\*](#), and [\*unc-115\*](#), are required for HSN path selection in the [ventral nerve cord](#) (G. Wightman and G. Garriga, in prep.). Mutations in these genes cause the [HSNL](#) axon to cross the ventral midline and to travel anteriorly in the right tract together with the [HSNR](#) axon. These mutations apparently do not disrupt the outgrowth of the [PVPR](#) axon along the left tract and may identify genes specifically required for interactions between the [HSNL](#) growth cone and the [PVPR](#) and [PVQL](#) axons. UNC-115 is a novel cytoskeletal adaptor with three LIM domains and a sequence related to the actin-binding headpiece of villin (E. Lundquist et al., in prep.).

Generated from local HTML

# Chapter 21. Cell and Growth Cone Migrations — V Genetic Requirements for Axonal Growth

---

## A. Genes Required for Longitudinal Migrations

Several genes, including [\*vab-8\*](#) and [\*unc-53\*](#), are required for longitudinal migrations of diverse cells and growth cones. [\*vab-8\*](#), which affects posteriorly directed migrations, is the first shown to be essential for longitudinal migration in a specific direction ([Manser and Wood 1990](#); [Wightman et al. 1996](#)). Mutations in this gene disrupt 14 of 17 posterior migrations examined, yet only 2 of 17 anterior or circumferential migrations. In bipolar neurons, moreover, these mutations selectively disrupt the extension of the posterior growth cone. Interestingly, there are two classes of [\*vab-8\*](#) mutants, one with defects in both migration of the CAN and exons and a second defective only in axonal outgrowth (G. Garriga, pers. comm.). Finally, [\*unc-53\*](#) is required for many longitudinal growth cone migrations ([Hedgecock et al. 1987](#); [Siddiqui 1990](#); [Hekimi and Kershaw 1993](#)), as well as elongation of body wall and vulval muscles along the longitudinal axis (T. Bogaert, pers. comm.).

## B. Genes Involved in Growth Cone Extension and Collapsin Nerve Fascicles

The small size of the nematode [\*nervous system\*](#) allows axons to reach all their synaptic targets with a minimum of branching or terminal arborization. Most synapses occur en passant between axons running in parallel within the [\*nerve ring\*](#) and ventral cord ([White et al. 1986](#)). The relative arrangement of axons within these tracts is highly stereotyped and therefore constrains synaptic connectivity. For example, the axons of the embryonic neurons BDU provide a fasciculative cue that both induces collateral branching of the [\*AVM\*](#) axon and guides these growth cones to their synaptic targets in the ring neuropil during the L1 stage ([Walhall and Chalfie 1988](#)). Several genes are specifically required for axon assortment and fasciculation. In [\*unc-3\*](#), the arrangement of ventral cord interneurons appears to be normal, but motor axons of all classes are defasciculated ([Durbin 1987](#); [Chalfie and White 1988](#); J. White, pers. comm.). Mosaic analysis indicates that [\*unc-3\*](#) is required in the motor neurons for correct fasciculation ([Herman 1987](#)).

In [\*unc-34\*](#), [\*unc-71\*](#), and [\*unc-76\*](#) mutants, widespread defects in axon assortment and fasciculation are associated with failures of axonal elongation within the nerve tracts. In [\*unc-76\*](#) mutants, for example, amphidial axons defasciculate and halt prematurely upon entering the [\*nerve ring\*](#). Other axons terminate abruptly upon entering the [\*ventral nerve cord\*](#) (PHA, PHB) or terminate prematurely after extending a short distance along the ventral (e.g., HSN) or dorsal (e.g., DD and VD) nerve cords ([Hedgecock et al. 1985](#); [Desai et al. 1988](#); [McIntire et al. 1992](#)). Moreover, the nerve cords are frequently split into multiple bundles. Similar phenotypes are observed in [\*unc-34\*](#) and [\*unc-71\*](#) mutants, although the penetrance and spectrum of affected cell types vary ([McIntire et al. 1992](#)). A simple model is that these mutations disrupt, either directly or through altered axonal bundling, fasciculative signals that normally stimulate growth cone migration along the nerve tracts. [\*unc-76\*](#) mutants may also reveal cryptic signals that cause cessation of growth cone extension, which likely is mechanistically related to growth cone collapse. For example, PHA and PHB axons that fail to enter the [\*ventral nerve cord\*](#) in [\*unc-6\*](#); [\*unc-76\*](#) double mutants migrate for long distances along the [\*lateral hypodermis\*](#), suggesting that premature growth cone collapse requires contact with the preanal neuropil ([Hedgecock et al. 1985](#)). In these individuals, the contralateral PHA and PHB axons elongate for normal or supernormal distances in the [\*ventral nerve cord\*](#). Thus, contact with contralateral lumbar axons, possibly PHA and PHB themselves, may provide a collapsing cue for these growth cones. Indeed, in wild type, many axon classes terminate at points of contact with neurons of the same class ([White et al. 1986](#)).

## C. Genes Required for Axonogenesis

Many types of cells can extend short, irregular processes, but only neurons elaborate axons of constant caliber, and indefinite length, in response to mechanical tension applied at the process tip by growth cones or along the entire process by tissue growth ([Bray 1992](#)). The assembly and maintenance of axons require unique adaptations

of the cell membrane and cytoskeleton. Four known genes, [\*unc-14\*](#), [\*unc-33\*](#), [\*unc-44\*](#), and [\*unc-51\*](#), are believed to encode structural or regulatory proteins required for axonogenesis ([Hedgecock et al. 1985](#); [Desai et al. 1988](#); [Siddiqui 1990](#); [Siddiqui and Culotti 1991](#); [McIntire et al. 1992](#)). Mutations in these genes affect axon guidance of most or [\*all neurons\*](#) but do not alter cell migrations. The spectrum of axonal defects varies considerably with neuron type but commonly includes extra axons or axonal branches, poorly directed outgrowth, defective fasciculation, and premature termination ([Hedgecock et al. 1985](#); [Desai et al. 1988](#); [Siddiqui 1990](#); [Siddiqui and Culotti 1991](#); [McIntire et al. 1992](#)). Moreover, in [\*unc-14\*](#) and [\*unc-51\*](#) mutants, axons often have irregular caliber, including varicosities containing abnormal membranous vesicles and cisternae ([McIntire et al. 1992](#)). These ultrastructural defects are reminiscent of the *Drosophila shibire* mutant; *shibire* encodes a dynamin involved in membrane fusion and retrieval ([Poodry and Edgar 1979](#); [van der Bliek and Meyerowitz 1991](#)). UNC-51 is a serine/threonine protein kinase with a novel carboxy-terminal domain that is expressed throughout the [\*nervous system\*](#) ([Fig. 5](#)) ([Ogura et al. 1994](#)).

[\*unc-44\*](#) encodes multiple ankyrin isoforms, including a large isoform implicated in axonogenesis ([Otsuka et al. 1995](#)). Ankyrins are cytoskeletal adaptors that couple diverse membrane proteins to spectrin and actin filaments forming the membrane cytoskeleton. Distinct isoforms help establish and maintain stable membrane domains in epithelia (apical, basolateral), neurons (soma, axon, synapse), and other cell types ([Chan et al. 1993](#); [Lambert and Bennett 1993](#)). In particular, the L1/neuroglian family of cell surface receptors is implicated in coupling ankyrins to the extracellular environment along the axolemma ([Davis et al. 1993](#); [Burden-Gulley et al. 1995](#)).

In [\*unc-33\*](#) mutants, sensory endings have elevated numbers of microtubules, often with abnormal protofilament arrangements, suggesting a defect in the assembly of axonal microtubules ([Hedgecock et al. 1985](#)). [\*unc-33\*](#) encodes three cytoplasmic proteins localized in axons. Interestingly, in [\*unc-44\*](#) mutants, these proteins accumulate abnormally in the neuronal soma instead of axons ([Li et al. 1992](#); W. Li et al., pers. comm.). UNC-33 isoforms are homologous to the collapsin-response mediator protein CRMP-62 recently discovered in chicken ([Goshima et al. 1995](#)) and its ortholog in the rat, TOAD-64 ([Miturn et al. 1995](#)). CRMP-62 is proposed to couple the collapsin receptor to heterotrimeric GTPases that regulate growth cone collapse. A simple model is that UNC-33, perhaps tethered to the axolemma through ankyrin, stabilizes axonal microtubules and suppresses actin-based motility. These activities could prevent secondary axons forming at the soma, suppress collateral branching along the primary axon, convert kinetoplasm just behind the growth cone to axoplasm, and collapse the entire growth cone when signals for extension are absent.

Generated from local HTML

# Chapter 21. Cell and Growth Cone Migrations — VI Cell Migration and other Aspects of Cellular Phenotype

---

A handful of cells undergo long-range migrations during embryogenesis ([Sulston et al. 1983](#); [Hedgecock et al. 1987](#)). The somatic mesoblast M and its contralateral homolog, the right intestinal muscle cell, the gonadal mesoblasts [Z1/Z4](#), and the coelomocyte mother cells all migrate posteriorly along the ventral body wall from their origins in the head to stereotyped positions along the midbody. The head-mesodermal cells migrate dorsally alongside the developing [pharynx](#) using UNC-6, possibly that which is secreted from pharyngeal neuron [IS](#), as a repulsive cue ([Hedgecock et al. 1990](#); [Wadsworth et al. 1996](#)). Somewhat later, the [ALM](#) and CAN neurons migrate posteriorly along the [lateral hypodermis](#) from their origins in the head, whereas HSN migrates anteriorly from the tail. More than 20 known genes are required for these embryonic cell migrations ([Trent et al. 1983](#); [Hedgecock et al. 1987](#); [Desai et al. 1988](#); [Manser and Wood 1990](#); [Garriga et al. 1993b](#)). Some genes are highly specific, but most mutations affect the migrations of multiple cell types, often including both mesoblasts and [neuroblasts](#).

The navigational programs that regulate cell migration and process outgrowth are parts of larger programs that control all aspects of cellular phenotype including division, differentiation, and death. Genetic studies have identified the regulatory mechanisms that control migration and other cellular phenotypes. For example, whereas [egl-5](#) controls diverse aspects of HSN development including cell migration and neuronal differentiation (e.g., growth cone navigation and neurotransmitter synthesis), [egl-43](#) and [unc-86](#) are required specifically for HSN migration and differentiation, respectively ([Desai et al. 1988](#); [Finney et al. 1988](#)). All three genes encode transcription factors expressed in the HSN motor neurons; EGL-5, EGL-43, and UNC-86 are a Hox protein, a zinc-finger protein, and a POU-homeodomain protein, respectively ([Fig. 5](#)) ([Clark et al. 1993](#); [Garriga et al. 1993b](#); [Wang et al. 1993](#); [Finney et al. 1988](#); [Finney and Ruvkun 1990](#); C. Guenther and G. Garriga, unpubl.; see [McGhee and Krause](#), this volume).

## A. *wingless/wnt1* Signaling Pathway in Q Neuroblast Migrations

The postembryonic development of the paired [neuroblasts QR](#) and [QL](#) illustrates how migrations are interwoven with cell division, determination, and death in a simple cell lineage ([Sulston and Horvitz 1977](#); [Sulston et al. 1980](#); [Hedgecock et al. 1987](#)). Neuroblasts [QR](#) and [QL](#) each generates a small number of [sensory neurons](#) during the L1 stage ([Sulston and Horvitz 1977](#)). Starting in midbody, [QR](#) descendants migrate anteriorly for stereotyped distances along the right [lateral hypodermis](#), where they divide again or differentiate, whereas homologous [QL](#) descendants on the left-hand side remain stationary or migrate posteriorly. Nearly 20 genes have been identified that affect the navigational responses of the Q [neuroblasts](#) ([Chalfie et al. 1983](#); [Trent et al. 1983](#); [Kenyon 1986](#); [Hedgecock et al. 1987, 1990](#); [Clark et al. 1993](#); [Wang et al. 1993](#); [Harris et al. 1996](#); [Hishida et al. 1996](#); E.M. Hedgecock, unpubl.). The program of anteriorly oriented movement apparently represents a default program for Q [neuroblasts](#), whereas posteriorly oriented movement is contingent upon a developmental signal normally active only on the left side of the body. Expression of the Hox gene [mab-5](#) in Q cells is both necessary and sufficient for the latter program. In [mab-5](#) loss-of-function (lf) mutants, both [neuroblasts](#) follow the default program, but in [mab-5](#) gain-of-function (gf) mutants, both cells undergo posteriorly oriented movements ([Kenyon 1986](#); [Salser and Kenyon 1992](#)). The Q migrations share several features in common with sex-myoblast migrations (see below); both cell types evidently employ an integrin-dependent mechanism of cell motility ([Fig. 5](#)) ([Gettner et al. 1995](#); E.M. Hedgecock et al.; P.D. Baum and G. Garriga; both in prep.).

The distinct responses of the Q [neuroblasts](#) are controlled by the wingless signal-transduction pathway. In [mig-5](#) (lf) mutants, both [neuroblasts](#) follow similar default programs, migrating anteriorly like wild-type QR. In [mig-5](#)(lf) [mab-5](#)(gf) double mutants, both cells follow nondefault programs, placing [mig-5](#) upstream of [mab-5](#) in this signaling pathway ([Guo 1995](#)). Similarly in [lin-17](#) mutants, both Q [neuroblasts](#) often follow the default program. Moreover, [QR](#), which normally expresses MAB-5, often fails to express MAB-5 in [lin-17](#) mutants, placing [lin-17](#) upstream of [mab-5](#) ([Harris et al. 1996](#)). MIG-5 is an ortholog of the *Drosophila* protein Dishevelled ([Guo 1995](#))

(Fig. 5), the first known downstream component in the Wingless signaling pathway (Klingen-smith et al. 1994; Sussman et al. 1994; Theisen et al. 1994; Sokol et al. 1995), and LIN-17 is an ortholog of *Drosophila* Frizzled (Sawa et al. 1996). A new member of the *frizzled* gene family *Drosophila Dfz2* has recently been shown to encode a wingless receptor (Bhanot et al. 1996). *wingless/wnt1* and related genes encode a family of secreted proteins that control cell fates and planar polarity during epithelial development (Klingensmith and Nusse 1994). These proteins can organize cell patterning over large distances through both direct signaling and the relaying of Wingless-induced or related asymmetric polarity cues from cell to cell possibly via the *frizzled* pathway (Vinson and Adler 1987; Wong and Adler 1993; Theisen et al. 1994). A simple model is that *seam cells* on the left-hand side secrete a Wingless protein that signals *QL* and its descendants to remain stationary or navigate posteriorly by expressing MAB-5 and its target genes. *wingless* homologs have been identified in *C. elegans*, but it remains to be determined whether they play a part in Q neuroblast migrations (Kamb et al. 1989; Shackleford et al. 1993; Herman et al. 1995; Sawa et al. 1996).

## B. FGF Signaling Pathway in Sex-Myoblast Migration

The hermaphrodite sex myoblasts illustrate how a hierarchy of path and target cues position sex muscles precisely over the developing *uterus* and *vulva* (Thomas et al. 1990; Stern and Horvitz 1991; Clark et al. 1992; DeVore et al. 1995). In the late L1 stage, the mesoblast M generates paired sex myoblasts (Sulston and Horvitz 1977). During the L2 stage, these cells migrate anteriorly along the body wall to flank the gonad. During the L3, they divide to generate *uterine* and *vulval muscle* cells. During the L4, these muscles differentiate, forming stereotyped attachments to body wall, *uterus*, and *vulva*. In the adult, these muscles mediate egg laying.

Ablation of the gonad rudiment reveals that initial anterior movement of the sex myoblasts along the body wall is independent of the gonad (Thomas et al. 1990). However, these cells often undershoot or overshoot their destination in operated larvae, suggesting that a gonad-dependent cue is important for precise positioning. Indeed, sex myoblasts can accurately find the gonad in *dig-1* mutant larvae, in which the gonad rudiment is displaced to nearby sites on the body wall (Thomas et al. 1990). From these and related experiments, it was proposed that the anchor and *uterine* blast cells of the gonad provide a diffusible chemoattractant for refining the final positions of the sex myoblasts (Stern and Horvitz 1991).

In *egl-15* and *egl-17* mutants, gonadal cues actually repulse the sex myoblasts (Trent et al. 1983; Stern and Horvitz 1991; DeVore et al. 1995). In intact mutants, sex myoblasts halt their migration prematurely and occasionally even reverse direction. If the gonad is ablated, these cells can migrate farther anteriorly, although their final positions are more variable than similarly operated wild-type animals. Two models have been proposed to explain why the gonad repels the sex myoblasts in *egl-15* and *egl-17* mutants. In the first, the *egl-15* and *egl-17* mutations remove an attractive signal to reveal an underlying repulsive signal. In a second model, *egl-15* and *egl-17* mutations transform an attractive signal into a repulsive one. Several other genes cause similar sex myoblast migration defects when mutated alone (e.g., *ksr-1*) or in combination with mild *egl-15* alleles (e.g., *sem-5*) (Clark et al. 1992; DeVore et al. 1995; Sundaram and Han 1995).

EGL-15 is an ortholog of the fibroblast growth factor (FGF) receptor, SEM-5 is an ortholog of human Grb2 and *Drosophila* Drk, which couple receptor tyrosine kinases to Ras activators, and KSR-1 is a novel Raf-like protein (Fig. 5) (Clark et al. 1992; Lowenstein et al. 1992; Simon et al. 1993; Stern et al. 1993; DeVore et al. 1995; Sundaram and Han 1995). FGF signaling pathways have been widely implicated in cell migration and neurite outgrowth. Mutations in the *Drosophila* FGF receptor gene *breathless*, for example, disrupt migrations of both neuroglial and tracheal cells (Klambt et al. 1992; Reichman-Fried et al. 1994). Similarly, activation of FGF receptors on cultured *neurons* promotes neurite outgrowth, acting synergistically with several known cell adhesion molecules (Chao 1992; Williams et al. 1994). Knowledge of the sources and distribution of both ligands and receptors will no doubt be important for understanding the role of FGF signaling in these cell migration programs.

## C. A Hormonal Signaling Pathway in Gonadal Migrations

The multistage migrations of the gonadal leader cells illustrate how changes in cell substrate and direction, and transitions between motile and stationary states, can be programmed in postmitotic cells (Kimble and Hirsh 1979; Hedgecock et al. 1987). The gonadal leaders comprise two distinct cell types generated from mesoblasts Z1 and Z4 in the late L1 stage which organize gonadogenesis and polarize germ-line maturation along their distal-proximal axis (Kimble and Hirsh 1979). Depending on nematode species and sex, one or both types of leaders undergo complex, stereotyped migrations along the larval body wall which determine the shape and position of the mature gonad (Chitwood and Chitwood 1974). In *C. elegans* males, only the proximal leader (linker cell) migrates, whereas in hermaphrodites of this species, only the distal leaders (distal-tip cells) migrate (Kimble and Hirsh 1979; see Schedl, this volume). Each leader cell describes a unique trajectory on the body wall that can be analyzed as a succession of unidirectional migrations on uniform substrates (Fig. 6). Most segments follow the natural axes of the body wall, but the oblique movement of the linker cell near the start of L4 stage is best described as a ventral movement superimposed on a continuous posterior migration.

In principle, elaborate labeled pathways on the larval body wall might guide the migrations of each gonadal leader. Instead, it appears that these cells navigate by following several global directional cues, e.g., UNC-6, in strict sequence. Changes in cell direction do not correspond to obvious guidepost cells that could provide signals to advance the navigational program. Moreover, when leader cells are generated at ectopic sites on the body wall by reiterated division (e.g., unc-39) or displacement of the gonad rudiment (e.g., dig-1), they migrate for more or less normal times and distances, not to fixed landmarks (Thomas et al. 1990; E.M. Hedgecock, unpubl.). By inference, the navigational programs of these cells advance either autonomously or in response to hormonal signals available throughout the larva. For example, UNC-5 is expressed in the hermaphrodite distal-tip cells just hours before the L3 molt immediately presaging their dorsal movements (M. Su et al., in prep.). This and other differences in distal-tip and linker cell behavior reflect distinct navigational programs, not sex-specific extracellular signals. In particular, intersexes produced by mosaicism for tra-1, or mutations in tra-1 that selectively disrupt its activity in soma (e.g., e1488) or gonad (e.g., rh132), reveal that gonadal leaders are indifferent to the sexual phenotype of hypodermis and skeletal muscle which form the migration paths (Hodgkin 1987a; Herman and Hedgecock 1990; Hunter and Wood 1990).

Development of the gonad and soma is closely coordinated over a range of growth conditions in wild-type larvae. In particular, changes in gonadal leader direction or motility during the L2, L3, and L4 larval stages all occur soon after commitment to another molt cycle, as judged from new cuticle synthesis and DNA replication in the hypodermis. Moreover, migration ceases at the dauer molt, indicating that gonadal leaders respond to a general signal for developmental arrest. Mutations at several loci, known as heterochronic genes, can advance or delay stage-specific events in the hypodermis and other somatic tissues, but they have little or no effect on gonad and germ line (Ambros and Horvitz 1984; Ambros, this volume). Two new genes, mig-7 / daf-12 and mig-8, are required to advance aspects of gonadal development, including the navigational programs of the leader cells (A. Antebi et al., in prep.). In these mutants, leader cells may continue without turning or completely cease migration at various stage transitions. Like previously described heterochronic mutants, mig-7 / daf-12 also delays development of somatic tissues, causing repetitions of earlier events.

mig-7 mutants have proven to be novel alleles of the dauer pathway gene daf-12, which encodes a nuclear hormone receptor most similar to *Drosophila* DHR96 (Fig. 5) (Riddle et al. 1981; Yeh 1991; Fisk and Thummel 1995; Riddle, this volume). Conceivably, a hormone, acting through DAF-12 and related receptors, synchronizes development of soma and gonad at the commitment to each postembryonic stage. At these transitions, heterochronic gene activities within each tissue select stage-specific transcriptional cascades. The targets of DAF-12 activation or repression are unknown, but they may include tissue-specific transcription factors (e.g., Hox genes) as well as other heterochronic genes. Indeed, several transcription factors have been implicated in the gonadal leader migrations (Fig. 5) (EGL-5/Abdominal-B, Chisholm 1991; Wang et al. 1993; LIN-39/Sex combs reduced, Clark et al. 1993; CEH-18, Greenstein et al. 1994; and VAB-3/PAX-6, Chisholm and Horvitz 1995; Zhang and Emmons 1995; A.D. Chisholm and H.R. Horvitz, in prep.). In some cases, a gonadal focus has been demonstrated for the migration phenotype (Chisholm 1991; Greenstein et al. 1994). Finally, DAF-12 controls,

perhaps indirectly, the expression of UNC-5 and other cell surface receptors used in leader cell migration (M. Su et al., in prep.).

## Figures

Figure 6. Migrations of the hermaphrodite distal-tip cells (top) and male linker cell (bottom) on the larval body wall in C.

### Figure 6

Migrations of the hermaphrodite distal-tip cells (*top*) and male linker cell (*bottom*) on the larval body wall in *C. elegans* (Kimble and Hirsh 1979; Hedgecock et al. 1987; E. Hedgecock and D. Hall, unpubl.). Hypodermis (*white*) and body wall muscles (*shaded*) are shown as a cylindrical projection opened along the dorsal midline. The hypodermal basal lamina is exposed to the body cavity along each of four ridges. Individual cells (not shown) in the four body-wall muscles are named sequentially from head to tail, e.g., VR1 through VR24 in the ventral right muscle (White et al. 1976). The labeled circles along the migration paths mark transitions in the navigational programs corresponding to proposed commitments to the L2, L3, L4, and adult stages (2, 3, 4, A, respectively) (A. Antebi et al., pers. comm.; see Ambros, this volume). The hermaphrodite distal-tip cells are born around the L1 molt (16 hr) over *body muscle* cells VR15 and VL16, respectively, but remain stationary until mid L2 stage (21 hr). They then move in opposite directions along the ventral body muscles (~6  $\mu\text{m}/\text{hr}$ ), halting in mid L3 (30 hr) over *body muscle* cells VR12 and VL20, respectively. These cells slowly reorient over the next hour and then move dorsally across the *lateral hypodermis* (31–32.5 hr). As they near the dorsal body wall muscles, they quickly reorient (33 hr) and then migrate centripetally along these muscles (~10  $\mu\text{m}/\text{hr}$ ). They complete about 80% of this final segment by mid L4 (39 hr). Active migration then slows and ceases entirely by the L4 molt (45 hr), with cells positioned over muscle cells DR16 and DL17, respectively. From a starting position over VR15, the male linker cell begins moving anteriorly along the ventral right *body muscle* soon after its birth around the L1 molt (16 hr). It halts in mid L2 (21 hr) over VR13, reorients, and then moves dorsally across the *lateral hypodermis* (22–23.5 hr). It reorients on the dorsal right muscle and then migrates posteriorly along this muscle until mid L3 (30 hr) over DR16 where it reorients obliquely and migrates across the *lateral hypodermis* (31–32.5 hr). Crossing ventral *body muscle* VR17 (33 hr), the linker cell continues posteriorly along the ventral midline. It reaches the developing *cloaca* by mid L4 where it is engulfed (Sulston et al. 1980).

Generated from local HTML

## Chapter 21. Cell and Growth Cone Migrations — VII Muscle Positioning on the Body Wall and Muscle Arm Chemotropism

During embryonic elongation, body-wall (i.e., skeletal) myoblasts shift circumferentially to their final positions underlying dorsal or ventral hypodermis (Fig. 6). Resembling an unzipping, this partition of myoblasts into future dorsal and ventral body-wall muscles proceeds from head to tail along the neurula (Moerman et al. 1996). These movements require selective adhesion of the myoblasts to dorsal and ventral hypodermis, and perhaps repulsion from [lateral hypodermis \(seam\)](#). It is unknown whether myoblast positioning shares common mechanisms with the longer-range cell migrations described above. Myoblast positioning is severely disrupted in various *mup* mutants; *unc-5* and *unc-6* mutants also display mild *Mup* phenotypes (Hedgecock et al. 1990; Goh and Bogaert 1991; E.M. Hedgecock, unpubl.).

Body-wall muscles receive synaptic input by extending long processes, or arms, to the motor terminals. This unique muscle adaptation further reduces the need for axonal branching in nematodes. Muscle cells in the head form a precise topographic projection onto motor axons in the [nerve ring](#) (White et al. 1986). However, muscle cells in the body simply project to the nearest nerve cord, i.e., dorsal muscle cells project to motor axons in the dorsal cord and ventral cells project to axons in the ventral cord. In *unc-5* and *unc-6* mutants, motor axons that fail to reach the [dorsal nerve cord](#) can still recruit arms from dorsal muscle cells, which are their normal targets, as well as ectopic arms from nearby ventral muscle cells (Hedgecock et al. 1990). A simple model is that motor terminals provide a diffusible factor that induces or guides muscle arm outgrowth (Fig. 7). Alternatively, motor terminals might stabilize nascent muscle arms by a contact-dependent mechanism. Direct observation of muscle arm extension should distinguish between these possibilities.

Mutants defective in axonal transport suggest that the muscle arm recruitment factor is packaged and transported to the motor terminals in synaptic vesicle precursors. UNC-104 and its vertebrate ortholog KIF1A are kinesin-related proteins responsible for fast anterograde axonal transport of synaptic vesicle precursors (Hall and Hedgecock 1991; Otsuka et al. 1991; Okada et al. 1995). In *unc-104*, synaptic vesicle precursors are not transported to the axon terminals but instead accumulate in the [neuron](#) cell bodies. As a result, dorsal muscle cells ignore motor axons in the dorsal cord and project instead toward motor [neuron](#) cell bodies in the ventral cord.

Finally, sex muscles involved in egg laying receive synaptic input by conventional branching and arborization of the motor terminals. Interestingly, the cues for axonal branching come from path cells, not the muscle targets themselves (Li and Chalfie 1990; Garriga et al. 1993a). The specialized hypodermal cells forming the [vulva](#) guide HSN axons as they enter the [ventral nerve cord](#) and induce the primary branching of both HSN and VC axons where they innervate the sex muscles.

### Figures

Figure 7. A chemoattraction model of muscle arm targeting.

### Figure 7

A chemoattraction model of muscle arm targeting. More than 50 motor [neurons](#) are arranged in file along the [ventral nerve cord](#), but only two cells are shown (in black). Motor axons run along the ventral and dorsal nerve cords. Wild-type axon terminals transport and secrete a hypothetical substance (*small dots*) via synaptic vesicle precursors, which attracts arms (*dark gray*) from nearby muscles (*light gray*). In *unc-5* mutants, mispositioned motor axons run along the [lateral hypodermis](#) but still recruit arms from dorsal muscles and sometimes from ventral muscles as well. In *unc-104* mutants, the chemoattractant is not transported to the axon terminals but is released, instead, closer to the cell bodies. As a consequence, dorsal body muscles extend fewer arms than normal, and some arms home incorrectly toward cell bodies in the [ventral nerve cord](#) while ignoring nearby axon terminals. (Reprinted, with permission, from Hall and Hedgecock 1991.)

Generated from local HTML

## Chapter 21. Cell and Growth Cone Migrations — VIII Future Directions

---

Several themes have emerged from the study of cell migration and axon guidance in *C. elegans*. First, a few global directional cues orient cells and pioneer growth cones along the natural axes of the hypodermal and pharyngeal epithelia, and local path or target cues provide further specificity and fidelity. Second, substrate and direction of movement, and motility itself, are determined by the surface receptors and cytoskeletal adaptors expressed within each cell. Third, hormones and growth factors acting through conserved signal transduction pathways can regulate the navigational program, including gene expression and cytoskeletal responses.

From the perspective of both cell and developmental biology, many basic questions remain unanswered. What are the directional cues for anterior and posterior migrations? How are the circumferential positions of longitudinal axon tracts specified? What is the arrangement of neuroglia and pioneers, and their molecular cues, in the developing [nerve ring](#)? How do various fasciculative cues act together to establish reproducible neighborhoods within axon tracts? What is the relationship, if any, between fasciculation and synapse formation? What is the basic mechanism of cell motility? How does activation of UNC-5 or other receptors cause cytoskeletal orientation? Most developmental problems can likely be solved by current methods, but understanding their cellular mechanisms may require new insights and techniques.

Finally, two outstanding technical developments deserve mention. First, transgenes expressing the reporter GFP allow the visualization of migrating cells and growth cones in living animals ([Chalfie et al. 1994](#)). Moreover, the dynamics of key proteins, including subcellular distribution and colocalization, during cell migrations can be studied by introduction of GFP modules into otherwise functional proteins. Second, the genome sequencing project has identified a cornucopia of adhesion molecules, cytoskeletal adaptors, and transcription factors ([Sulston and al. 1992; Wilson et al. 1994](#); see [Waterston et al.](#), this volume) whose functions in development, and migrations in particular, can be explored by reverse genetics ([Zwaal et al. 1993](#); Plasterk and Van Luenen, this volume).

Generated from local HTML

## **Chapter 21. Cell and Growth Cone Migrations — Acknowledgments**

---

We thank our numerous colleagues for sharing their unpublished results and particularly Victor Ambros, Joseph Culotti, Chaobo Guo, Dave Hall, Donald Riddle, William Wadsworth, and Bruce Wightman for helpful discussions. A.A. and C.R.N. were supported by postdoctoral fellowships from the Damon Runyon–Walter Winchell Cancer Research Fund and National Institutes of Health. E.M.H. was supported by grants from the Muscular Dystrophy Association, the American Cancer Society, and the National Institutes of Health. G.G. was supported by the NIH and a McKnight Scholars award.

Generated from local HTML

# **Chapter 22. Synaptic Transmission**

---

## **Contents**

[I Introduction](#)

[II Neurotransmitter Metabolism and Function](#)

[III Components Regulating Neurotransmitter Release in all Neurons](#)

[IV Conclusions and Future Perspectives](#)

[Acknowledgments](#)

Generated from local HTML

## Chapter 22. Synaptic Transmission — I Introduction

---

Intercellular communication between [neurons](#) and their target cells is primarily accomplished by the regulated release of neurotransmitters at synapses. Extensive study of this vesicular-mediated process has revealed that many of the molecular components of the release apparatus are highly conserved in metazoans ([Bennett and Scheller 1994; Südhof 1995](#)). In vertebrates, biochemical approaches have led to the identification of components that participate in the release process, whereas the study of synaptic transmission in *Caenorhabditis* and *Drosophila* has proceeded in large part using genetic approaches. Each of these approaches has yielded insights. An extensive array of biochemically defined protein-protein interactions has provided the framework for building mechanistic models of neurotransmitter release. The genetic approach has identified novel components that eluded biochemical characterization and has provided functional data to refine the models. Clearly, a complete analysis at the functional level will require the use of electrophysiological techniques, and although such methods are becoming available for *C. elegans* ([Avery et al. 1995b; Avery and Thomas](#), this volume), they are more advanced in other organisms. In concert, the study of synaptic transmission in *C. elegans*, *Drosophila*, and vertebrates has begun to provide an outline of the molecular details of synaptic vesicle function and neurotransmitter release.

The entire [nervous system](#) of the adult *C. elegans* hermaphrodite, which contains 302 [neurons](#), has been reconstructed from serial section electron micrographs ([White et al. 1986](#)). The reconstruction yielded not only a connectivity pattern, but also an excellent understanding of the structure of synapses in *C. elegans*. The [nervous system](#) contains approximately 2000 neuromuscular junctions, 5000 chemical synapses between [neurons](#), and 700 gap junctions. Most [neurons](#) in *C. elegans* are extremely simple in structure and contain one or at most a few processes. The vast majority of synapses are formed *en passant* in the major process bundles of the nematode: the [nerve ring](#) and the ventral and dorsal nerve cords ([Fig. 1A](#)). [White et al. \(1986\)](#) and [Hall and Russell \(1991\)](#) showed that the specificity of synaptic contacts made by individual [neurons](#) was relatively invariant from animal to animal.

The presynaptic terminals are associated with varicosities of the axon and often contain a thick electron-dense specialization ([Fig. 2](#)). Vesicles are clustered around this specialization. Most vesicles in *C. elegans* synapses are approximately 35 nm in diameter; dense core vesicles of 35–50 nm in diameter are found in a minority of [neurons](#) at varying frequency. [Hall and Hedgecock \(1991\)](#) estimated that  $3.5 \times 10^5$  synaptic vesicles are present in the [nerve ring](#), yielding an average of approximately 100 vesicles per synapse. However, individual synapses vary widely in size and vesicle density ([Hall and Hedgecock 1991; Hall and Russell 1991](#)). Postsynaptic specializations are difficult to visualize at both neuron-neuron synapses and neuromuscular junctions ([White et al. 1986](#); but see [Fig. 2](#)), and the postsynaptic junctional folds observed in mammalian neuromuscular junctions are absent. The morphological differences between neuromuscular junctions and neuron-neuron synapses in *C. elegans* are minor compared with the differences between these two types of synapses observed in vertebrates.

In this chapter, we examine nematode synaptic transmission, and we consider the synaptic components in two groups. First, we discuss the molecular and genetic studies that have identified proteins required for the metabolism, transport, and function of specific neurotransmitters in *C. elegans*. Although we provide a brief overview of the role of cells using each particular neurotransmitter, we omit discussions of circuitry and behavior, as these are examined in depth in other chapters. In the second portion of the chapter, we explore the mechanisms underlying the calcium-regulated release of all neurotransmitters. We discuss molecular and genetic data that support the involvement of components in the transport, docking, fusion, and endocytosis of synaptic vesicles. In both sections, we compare the *C. elegans* data with results obtained using other invertebrates and mammals, emphasizing similarities and dramatic differences rather than subtle ones. Finally, we focus on the challenges that lie ahead to analyze *C. elegans* synaptic transmission, and we discuss how future work will lay foundations for understanding synaptic function in higher organisms.

## Figures



## Figure 1

Visualization of synapses in *C. elegans*. (A) Immunolocalization of synaptotagmin in an L2 hermaphrodite. The staining (using an affinity-purified rabbit antiserum) is restricted to synaptic regions of the animal ([Nonet et al. 1993](#)). The [nerve ring](#) stains intensely, and the punctate nature of the staining is apparent in the ventral and dorsal nerve cords. The synapses of the pharyngeal [nervous system](#) are also visible. (Photo courtesy of Janet Duerr, Oklahoma Medical Research Foundation.) (B) SNB-1:GFP fusion expressed in GABAergic VD motor [neurons](#) of an adult hermaphrodite animal. Two VD motor [neurons](#) are clearly visible, each with 9 to 11 fluorescent patches that demarcate synaptic vesicle-rich varicosities. The motor [neuron](#) cell bodies (out of focus) and the cell body of a third GABAergic motor [neuron](#) are also visible. (Photo courtesy of M.L. Nonet.)



## Figure 2

A chemical synapse from *C. elegans*. (Top) Electron micrograph; (bottom) schematic drawing of the same synapse. The presynaptic axon is locally enlarged and filled with synaptic vesicles. The “active zone” is usually defined morphologically by the juxtaposition of a presynaptic density and a cluster of vesicles. Vesicles closest to the active zone are smaller and somewhat less electron-dense than transport vesicles, which move along microtubules (MT) from the soma to the synapse. At vesicle release sites, an electron-dense tuft lines the cytoplasmic side of the presynaptic membrane. A less dramatic thickening of the postsynaptic membrane is sometimes seen, forming a postsynaptic density (PSD). The PSD is best seen in longitudinal sections of the synapse, as on the left, but is rarely evident in transverse views. (Figure courtesy of David H. Hall, Albert Einstein College of Medicine.)

Generated from local HTML

## Chapter 22. Synaptic Transmission — II Neurotransmitter Metabolism and Function

---

The synthesis, packaging, release, and re-uptake of neurotransmitter molecules by [neurons](#) are highly regulated ([Fig. 3](#)). Most neurotransmitters are synthesized from common cellular metabolites by enzymes expressed specifically in [neurons](#) using the transmitter. In addition to classical transmitters such as acetylcholine, serotonin, and GABA, a few amino acids are neurotransmitters. Neurotransmitters are loaded into synaptic vesicles by vesicular transporters using a proton gradient as the source of energy. Distinct transporters are responsible for loading different transmitters. After the neurotransmitter is released by vesicular fusion, it diffuses across the synaptic cleft separating the pre- and postsynaptic cells and binds to receptors on the postsynaptic cell. Such receptors are highly specific for transmitters, and their expression in specific cells determines the response of the cell to the chemical signal. Receptors influence electrical activity in the postsynaptic cell either directly by permitting selective entry of ions or indirectly by activating second-messenger pathways. The signaling event is usually terminated by re-uptake of the transmitter from the synaptic cleft by plasma membrane transporters.

Despite its simple anatomy, the *C. elegans* [nervous system](#) uses an array of classical neurotransmitters which approaches the complexity of vertebrate nervous systems. In this section, we review the molecules regulating the synthesis, packaging, and re-uptake of the major neurotransmitters in *C. elegans*, as well as the genetic and molecular analyses of transmitter receptors. We also briefly discuss neuropeptides in *C. elegans*, although we do not discuss the distinct mechanisms used in the biosynthesis, packaging, and release of these molecules. In many sections, we discuss results obtained using the large parasitic nematode *Ascaris*, which has the same number and organization of motor [neurons](#) in the [ventral nerve cord](#) as *C. elegans* ([Stretton et al. 1978](#)). These *Ascaris* studies provide electrophysiological data not yet available in *C. elegans*.

### A. Acetylcholine

Acetylcholine appears to be the primary excitatory neurotransmitter controlling motor functions in *C. elegans*. Although physiological data are lacking, evidence for acetylcholine function in *C. elegans* is quite compelling and comes from pharmacological studies using acetylcholine agonists and antagonists ([Lewis et al. 1980b](#)), direct measurement of the presence of the transmitter in extracts ([Hosono et al. 1987](#); [Hosono and Kamiya 1991](#); [Nguyen et al. 1995](#)), measurement and characterization of the enzymes of acetylcholine synthesis and degradation ([Johnson and Russell 1983](#); [Kolson and Russell 1985a](#); [Rand and Russell 1985a](#)), and genetic analysis of mutants defective in acetylcholine synthesis ([Rand and Russell 1984](#); [Hosono et al. 1985](#)).

There are several noteworthy aspects of acetylcholine metabolism in *C. elegans*. First, acetylcholine is the only neurotransmitter so far identified in *C. elegans* that is essential for viability. Animals totally deficient for acetylcholine synthesis ([cha-1](#) mutants, see below) are inviable, whereas animals deficient in GABA, serotonin, or dopamine are viable. In addition, the synthesis of the transmitter and its loading into synaptic vesicles are controlled by a novel type of eukaryotic operon with a novel nested structure (discussed below). This type of gene structure appears to be a general feature of cholinergic regulation in mammals as well ([Bejanin et al. 1994](#); [Erickson et al. 1994](#)).

#### 1. Synthesis and Vesicular Transport

Acetylcholine is synthesized by choline acetyltransferase (ChAT), which is encoded by the [cha-1](#) gene. The *C. elegans* protein is 36% identical to pig ChAT and 34% identical to *Drosophila* ChAT ([Alfonso et al. 1994a](#)). In mammals, the enzymes that synthesize neurotransmitters are often associated with synaptic vesicles ([Kuhn et al. 1990](#); [Bon et al. 1991](#); [Carroll 1994](#)), and biochemical and immunochemical studies in *C. elegans* suggest that at least part of the ChAT activity is membrane-associated ([Rand and Russell 1985a](#); J. Duerr, pers. comm.). Viable [cha-1](#) mutants are small, slow growing, and uncoordinated (coily and jerky going backward; [Rand and Russell 1984](#); [Hosono et al. 1985](#)). They also have slow pharyngeal pumping and a slow irregular defecation cycle ([Thomas 1990](#); [Avery 1993a](#)) and are resistant to inhibitors of acetylcholinesterase ([Rand and Russell 1984](#)). Rare

lethal alleles of *cha-1* (e.g., m324) represent the null phenotype; animals homozygous for such alleles are able to hatch, but they can barely move or feed and die as small, shrunken L1 larvae (Rand 1989; Avery and Horvitz 1990; Alfonso et al. 1994a). The temperature effects of some *cha-1* alleles make them particularly useful: *cn101* homozygotes are temperature-sensitive ts-Unc and *p1182* is ts-lethal (Hosono et al. 1985; Rand 1989).

Neurotransmitters are transported into synaptic vesicles by specific transporter molecules. The *C. elegans unc-17* gene was shown to encode a synaptic vesicle acetylcholine transporter (Alfonso et al. 1993). *unc-17* encodes a predicted 58-kD hydrophobic protein with 12 transmembrane domains and homology with two rat synaptic vesicle dopamine transporters (Erickson et al. 1992). Using the *unc-17* cDNA, Varoqui et al. (1994) were able to identify a homolog from *Torpedo*, and a *Torpedo* clone was then used to identify rat and human homologs (Erickson et al. 1994). Transfected mammalian cells expressing either the *C. elegans unc-17* gene or the *Torpedo*, rat, or human VACHT genes make a protein that binds a specific inhibitor of VACHT (vesamicol). The transfected rat gene was able to mediate specific vesamicol-inhibitable accumulation of acetylcholine. These results confirm that these homologs all encode acetylcholine transporters.

Both viable and lethal alleles of *unc-17* have been identified, and they lead to phenotypes similar to those of the *cha-1* mutants described above (Brenner 1974; Rand and Russell 1984; Alfonso et al. 1993). Thus, a total deficiency for the acetylcholine transporter seems to have the same effect as a total deficiency for acetylcholine synthesis, demonstrating that the transporter is essential for *neural* function and for survival. In addition, antibody staining of the developmentally arrested *cha-1* and *unc-17* hatchees revealed a superficially normal *nervous system* (J. Duerr, pers. comm.). It therefore appears that most (or perhaps all) of the processes required for proper *neural* development can occur in the complete absence of acetylcholine or cholinergic function.

## 2. A Cholinergic Operon with Conserved Structure

Molecular analysis indicated that the *cha-1* and *unc-17* mRNAs were derived by alternative splicing of a common precursor (Fig. 4). The two genes use a common 5'-untranslated exon; the remainder of the *unc-17* gene is nested within the long first intron of the *cha-1* gene (Alfonso et al. 1994b). Thus, the sequential steps of acetylcholine synthesis and vesicle loading are encoded by different genes within a single, complex transcription unit. This same genomic organization has also been shown in mammals: The human (and rat) VACHT gene is nested within the long first exon of the ChAT structural gene (Fig. 4) (Bejanin et al. 1994; Erickson et al. 1994). Although there are some clear differences between the nematode and mammalian genes (e.g., the number of introns in ChAT and in VACHT differ from nematodes to mammals, and the mammalian gene may have additional promoters not present or not yet identified in *C. elegans*), the overall similarity is striking and suggests that the gene structure is critical for function and/or regulation.

## 3. Cholinergic Neurons

The primary tools for identifying cholinergic *neurons* in *C. elegans* have been antibodies to ChAT and UNC-17. The cellular expression pattern of these two proteins is virtually identical (J. Duerr, pers. comm.). Immunoreactivity to both proteins is observed primarily in a punctate staining pattern in synaptic regions (Alfonso et al. 1993; J. Duerr, pers. comm.), as expected for synaptic or synaptic-vesicle-associated proteins. In addition, the anti-ChAT stain also appears weakly in nonsynaptic regions of cells (J. Duerr, pers. comm.). Transgenic animals that overexpress *cha-1* and *unc-17* have increased synaptic staining and also have enough staining in cell bodies to confirm the identification of cholinergic *neurons*.

Almost all of the ChAT-positive cells appear to be motor *neurons*. Strongly staining cells include six of the eight classes of *ventral cord motor neurons* (VA, VB, VC, DA, DB, AS), three types of *pharyngeal motor neurons* (M1, M2, M5), and putative sublateral motor neurons (SAA, SAB, SIA, SIB, SMB, SMD) (J. Duerr, pers. comm.). A few other neurons also appear to be cholinergic; these include ALN, PLN, and SDQ, as well as some cells yet to be identified (see Appendix 2) (J. Duerr, pers. comm.). These results are in agreement with published *Ascaris* enzyme and physiology data for *ventral nerve cord* motor *neurons*. The *Ascaris* counterparts of the DA, DB, and AS cells contain ChAT, and their excitatory output is blocked by cholinergic blockers, whereas the DD and VD

counterparts do not contain ChAT and their output is blocked by GABAergic, but not cholinergic, blockers ([Johnson and Stretton 1985](#); [Segerberg and Stretton 1993](#)).

#### 4. Acetylcholinesterase

Unlike other neurotransmitters, whose synaptic action is terminated by rapid re-uptake mechanisms, acetylcholine is hydrolyzed in the synaptic cleft by the enzyme acetylcholinesterase (AChE). Three classes of AChE activity (designated A, B, and C) have been identified, partially purified, and characterized from *C. elegans*. The classes have distinct kinetic properties, substrate specificities, and inhibitor sensitivities ([Johnson and Russell 1983](#); [Kolson and Russell 1985b](#)) and are controlled by three unlinked genes, *ace-1 X*, *ace-2 I*, and *ace-3 II* ([Culotti et al. 1981](#); [Johnson et al. 1981](#), 1988; [Kolson and Russell 1985a](#)). *ace-1* encodes the class-A enzyme which is 42% identical to AChE from *Torpedo* and humans, 41% identical to human butyryl-cholinesterase, and 35% identical to *Drosophila* AChE ([Johnson et al. 1981](#); [Arpagaus et al. 1994](#)). *ace-2* mutants lack class-B activity and *ace-3* mutants lack class-C activity; these genes are presumed to encode the respective AChE classes ([Culotti et al. 1981](#); [Johnson et al. 1988](#)). The existence of three *C. elegans* AChE genes is in contrast to *Drosophila*, which has only one AChE gene, *Ace* ([Hall and Kankel 1976](#)), and vertebrates, which have one AChE gene as well as a second gene encoding a closely related butyrylcholinesterase activity ([Taylor and Radic 1994](#)). Catalytically, classes A and B are both somewhat similar to vertebrate AChE ([Johnson and Russell 1983](#)), but the class-C enzyme is quite unusual: It has an extremely low  $K_m$  for acetylcholine and has so far been found only in nematodes ([Kolson and Russell 1985b](#)). Vertebrate AChE molecules are often covalently attached to collagen-like tails to help anchor them in the basement membrane ([Johnson et al. 1977](#)). In contrast, none of the *C. elegans* AChE forms appears to be covalently attached to a collagen-like tail. However, within each enzyme class are multiple size forms, some of which appear to be membrane-bound ([Johnson and Russell 1983](#)), so that much of the AChE activity is likely to be on the external surface of cell membranes.

The genetic analysis of *C. elegans* AChE was one of the early triumphs of *C. elegans* biochemical genetics. All of the mutants were identified by “brute-force” screening, using class-specific single-worm enzyme assays. Animals homozygous for any one of the *ace* genes have no discernible behavioral or developmental phenotype (although *ace-2* animals are hypersensitive to AChE inhibitors). Two of the double-mutant combinations (*ace-1 ; ace-3* and *ace-2 ; ace-3*) are also behaviorally and developmentally essentially normal ([Johnson et al. 1988](#)). However, the *ace-1 ; ace-2* double mutant is uncoordinated ([Culotti et al. 1981](#)), and the *ace-1 ; ace-2 ; ace-3* triple mutant is paralyzed and developmentally arrested. Embryonic development is relatively unimpaired, but the animals are unable to grow beyond the hatching stage ([Johnson et al. 1988](#)). Thus, most of the functions of the AChE isoforms are individually dispensable but collectively essential. Histochemical assays indicate that classes A and B are present in the [nerve ring](#) and the ventral ganglion, with somewhat less staining in the nerve cords and the [preanal ganglion](#) ([Culotti et al. 1981](#)). Mosaic analysis suggests that *ace-1* expression is required in muscle cells ([Herman and Kari 1985](#); [Johnson et al. 1988](#)). However, this analysis does not exclude the possibility that *ace-1* is also expressed in some [neurons](#).

#### 5. Acetylcholine Receptors and Other Postsynaptic Components

Pharmacological studies suggest that cholinergic transmission at *C. elegans* neuromuscular junctions is mediated postsynaptically by ligand-gated receptors of the nicotinic acetylcholine receptor (nAChR) family ([Lewis et al. 1980b](#); [Avery and Horvitz 1990](#)). Application of nicotine leads to hypercontraction of [body wall muscle](#) and modulates [pharyngeal muscle](#) action. Although the neuromuscular nAChRs from *C. elegans* and vertebrates have pharmacological similarities, there are some important differences ([Lewis et al. 1980b](#); [Fleming et al. 1993](#)). In particular, toxins such as  $\alpha$ -bungarotoxin, which bind very tightly to vertebrate nAChRs, are not effective against the *C. elegans* receptor, whereas the anti-helminthic levamisole is a potent agonist of *C. elegans* neuromuscular nAChR receptors. The sensitivity of nematodes to levamisole has provided an effective method of identifying mutants affecting nAChR subunits and associated proteins ([Lewis et al. 1980a](#)).

At least 16 nAChR subunit genes are thought to be expressed in *C. elegans* ([Fleming et al. 1993](#); T. Barnes, pers. comm.), and the role of five of these subunits in *C. elegans* neurotransmission has been studied in some detail.

The [unc-29](#), [unc-38](#), and [lev-1](#) genes encode three nAChR subunits that are components of the levamisole-sensitive receptor found in [body wall muscle](#). [unc-38](#) encodes an  $\alpha$ -subunit, whereas [lev-1](#) and [unc-29](#) encode non- $\alpha$  subunits (J.T. Fleming et al., in prep.). Coexpression of UNC-38, UNC-29, and LEV-1 in *Xenopus* oocytes results in levamisole-induced currents (J.T. Fleming et al., in prep.). Genetic and biochemical studies of [unc-38](#) and [unc-29](#) indicate that both of the subunits are essential for levamisole-sensitive nAChR function, but [lev-1](#) is not essential ([Lewis et al. 1987b](#); J.T. Fleming et al., in prep.). Direct evidence that [unc-29](#), [unc-38](#), and [lev-1](#) are present in muscle is lacking, although [unc-29](#) is required in the [MS](#), C, and D lineages, which give rise to most of the musculature, suggesting a requirement in muscle (L. Miller and S. Kim, pers. comm.). Because null mutants of all three genes retain some coordinated locomotion, it is likely that additional non-levamisole-sensitive nAChRs are expressed in muscle. Furthermore, cholinergic transmission in the [pharynx](#) is probably mediated by a distinct nicotinic receptor complex because [unc-29](#) mutants have normal pharyngeal pumping ([Avery 1990](#)). A candidate to encode such a receptor is [eat-18](#), a gene necessary for [pharyngeal muscle](#) to respond to nicotine ([Raizen et al. 1995](#)).

Two nAChR subunits expressed in [neurons](#) have also been characterized in detail. [deg-3](#) encodes an  $\alpha$ -7-like nAChR subunit expressed in [touch receptor neurons](#) and some other neurons ([Treinin and Chalfie 1995](#)). Dominant [deg-3](#) mutations result in neuronal degeneration of cells expressing this gene (presumably due to increased channel activity), whereas loss of [deg-3](#) activity confers no mutant phenotype. Another nAChR receptor subunit gene, now called [acr-2](#), is expressed in multiple classes of motor neurons ([Squire et al. 1995](#); Y. Jin and H.R. Horvitz, pers. comm.). An apparent dominant mutation in this gene, *n2420*, exhibits a shrinking uncoordinated phenotype (Y. Jin and H.R. Horvitz, pers. comm.). Coexpression of [acr-2](#) and [unc-38](#) in *Xenopus* oocytes is associated with levamisole-inducible currents ([Squire et al. 1995](#)). Mutations in [unc-38](#) are capable of suppressing the *n2420* phenotype (Y. Jin and H.R. Horvitz, pers. comm.); thus, UNC-38 may be expressed in [neurons](#) as well as muscle and may form a functional receptor complex with ACR-2 in vivo.

In addition to the 5 nAChR subunits already characterized, 11 apparent nicotinic receptor subunits are present in the genomic sequence data already released (T. Barnes, pers. comm.), suggesting that as many as 50 nAChR subunits may be expressed in *C. elegans*. Evidence also exists for muscarinic acetylcholine receptors in *C. elegans*: [Culotti and Klein \(1983\)](#) described a membrane-bound, high-affinity, saturable binding activity for *N*-methylscopolamine and quinuclidinyl benzilate, two potent muscarinic receptor blockers. In addition, [Avery and Horvitz \(1990\)](#) reported that muscarinic agonists and antagonists can modulate pharyngeal pumping. However, there are no known mutants defective in the putative muscarinic receptor(s).

Genetic and biochemical approaches have also identified several postsynaptic nonreceptor components required for cholinergic transmission. The levamisole resistance locus [unc-50](#) encodes a nonreceptor molecule of novel structure; homologs of [unc-50](#) exist in eukaryotes from yeast to vertebrates (M. Hengartner, pers. comm.). Because levamisole-binding activity appears to be decreased in [unc-50](#) mutants ([Lewis et al. 1987b](#)), the protein seems most likely to play a part in receptor gene transcription or receptor assembly. The levamisole resistance genes [unc-63](#) and [unc-74](#) are also candidates to encode nonreceptor components, since AChR homologs have not been found in the genomic intervals where these genes reside (T. Barnes, pers. comm.).

## B. GABA

The vast majority of GABAergic cells in *C. elegans* are inhibitory motor [neurons](#). However, there are also a few excitatory GABAergic motor [neurons](#). The evidence for GABA function in *C. elegans* includes pharmacological studies using GABA-related compounds, immunohistochemical demonstration of the presence of GABA in specific cells, and analysis of mutants defective in GABA synthesis and function ([McIntire et al. 1993a,b](#)). Mutants with GABAergic transmission defects are viable, although they have several motor defects. The most obvious phenotype is a tendency to contract dorsal and ventral [body wall muscle](#) simultaneously in response to touch ("shrinker" phenotype), which appears to result from lack of function of the GABA-containing DD and VD inhibitory motor [neurons](#) ([McIntire et al. 1993a,b](#)).

Three genes have been identified in *C. elegans* that are required in the presynaptic [neuron](#) for GABAergic transmission. [\*unc-25\*](#) encodes a protein that is approximately 45% identical to mammalian glutamic acid decarboxylase (GAD) (Y. Jin and H.R. Horvitz, pers. comm.), the enzyme that synthesizes GABA from glutamic acid. [\*unc-25\*](#) mutants have no apparent GABA ([McIntire 1993a](#)), and extracts prepared from these animals lack GAD activity (C. Johnson and A. Stretton, pers. comm.). After synthesis, GABA is transported into vesicles by a vesicular transporter, a molecule that has not been molecularly identified in vertebrates. [\*unc-47\*](#) mutants accumulate elevated levels of GABA immunoreactivity, a phenotype consistent with a defect in GABA transport. [\*unc-47\*](#) probably encodes the GABA vesicular transporter as UNC-47 contains a series of membrane-spanning domains similar to those of many other transporters (K. Schuske and E. Jorgensen, pers. comm.). Finally, there is evidence that the [\*unc-46\*](#) gene product is required presynaptically in [neurons](#) for GABAergic transmission ([McIntire et al. 1993a](#)); however, evidence also exists for postsynaptic [\*unc-46\*](#) function ([Reiner and Thomas 1995](#)).

Using anti-GABA antibodies, [McIntire et al. \(1993b\)](#) identified 26 [neurons](#) that contain GABA immunoreactivity, most of which are motor [neurons](#) (including DD, VD, RME, [AVL](#), and [DVB](#); see [Appendix 2](#)). In all of these cells, the GABA immunoreactivity was uniformly distributed throughout the cytoplasm and was clearly not restricted to synaptic regions. Expression of the [\*unc-25\*](#) GAD gene is restricted to the same 26 [neurons](#) (Y. Jin and H.R. Horvitz, pers. comm.), suggesting that all of the [GABAergic neurons](#) in *C. elegans* have been identified.

GABA uptake by a plasma membrane transporter (or transporters) was analyzed by exposing GABA-deficient [\*unc-25\*](#) animals to GABA and then staining for GABA immunoreactivity ([McIntire et al. 1993a](#)). Surprisingly, only 7 of the 26 GABA-immunoreactive cells take up GABA under these conditions, and there are also additional cells capable of GABA uptake. Thus, not all of the GABA-synthesizing cells express the GABA uptake activity and not all of the transporter-expressing cells can synthesize detectable levels of GABA ([McIntire et al. 1993a](#)).

Studies on GABA function, localization, and uptake in *Ascaris* are in good agreement with the *C. elegans* results. In *Ascaris*, GABA acts as an inhibitory transmitter at neuromuscular junctions ([del Castillo et al. 1964](#)). The 26 cells with strong and consistent GABA immunoreactivity appear to be the homologs of the 26 *C. elegans* GABA-positive cells ([Guastella et al. 1991](#)). An additional 10 *Ascaris* cells stain weakly or inconsistently with antisera specific for GABA, and many of these cells also contain GABA transport activity ([Guastella and Stretton 1991](#)). It is therefore likely that many (or all) of these cells correspond to the *C. elegans* cells described above which take up GABA but cannot synthesize it endogenously.

[\*unc-49\*](#) mutants share many phenotypic characteristics with [\*unc-25\*](#), [\*unc-46\*](#), and [\*unc-47\*](#) mutants. However, [\*unc-49\*](#) mutant animals are resistant to the GABA receptor agonist muscimol ([McIntire et al. 1993a](#)). Molecular analysis has revealed that the [\*unc-49\*](#) gene has the potential to encode several proteins with similarity to GABA<sub>A</sub> receptors of the ligand-gated ion channel superfamily (B. Bamber and E. Jorgensen, pers. comm.). Additionally, the [\*exp-1\*](#) gene may encode a postsynaptic component regulating excitatory GABAergic transmission in the enteric muscles ([Avery and Thomas, this volume](#); see also [McIntire et al. 1993a](#)).

## C. Dopamine

Dopamine (3,4-dihydroxyphenylethylamine) was originally identified in *C. elegans* using the technique of formaldehyde-induced fluorescence (FIF; [Sulston et al. 1975](#)). In most organisms, dopamine is produced by the hydroxylation of tyrosine by tyrosine hydroxylase to form 3,4-dihydroxy-phenylalanine (DOPA), and the subsequent decarboxylation of DOPA to dopamine by aromatic amino acid decarboxylase (AAAD). Evidence from several organisms suggests that AAAD also decarboxylates 5-hydroxy-tryptophan to produce serotonin. Exogenous dopamine inhibits locomotion and egg laying, and these behavioral responses habituate ([Schafer and Kenyon 1995](#); [Ségalat et al. 1995](#)), but it has not yet been proven that these responses are due to dopamine (as opposed to some related transmitter) in vivo.

Five *cat* (catecholamine-deficient) genes were identified that affected dopamine ([Sulston et al. 1975](#)). [\*cat-2\*](#), [\*cat-3\*](#), and [\*cat-5\*](#) seem to affect primarily the morphology of the [neurons](#) or the subcellular localization of the FIF, but in [\*cat-2\*](#) and [\*cat-4\*](#) mutants, the level of dopamine is greatly reduced or absent. Dopamine is normally present in eight sensory cells (two [ADE](#), two [PDE](#), and four CEP [neurons](#); [Sulston et al. 1975](#)). Unpublished data suggest that

dopamine is required for the function of these [neurons](#): Sensory behaviors (including foraging behavior and sensation of bacterial lawns) mediated by these cells are absent in dopamine-deficient [cat-2](#), [cat-4](#), or [bas-1](#) (see below) mutants (J. Kaplan, pers. comm.; B. Sawin and H.R. Horvitz, pers. comm.). Dopamine is also present in three pairs of [ray neurons](#) (R5A, R7A, [R9A](#)) in the [male tail](#) ([Sulston and Horvitz 1977](#)).

## D. Serotonin

Serotonin (5-hydroxytryptamine, or 5-HT) is a common neurotransmitter in vertebrates and invertebrates, and there is persuasive evidence for its function in *C. elegans*. It has been identified in *C. elegans* [neurons](#) by formaldehyde-induced fluorescence ([Horvitz et al. 1982](#)) and by anti-serotonin immunostaining ([Desai et al. 1988; McIntire et al. 1992](#)). In vertebrates, serotonin is usually synthesized from tryptophan in two steps: hydroxylation by the enzyme tryptophan hydroxylase, and decarboxylation by AAAD. In *C. elegans*, exogenous serotonin stimulates egg laying and pharyngeal pumping and inhibits locomotion and defecation ([Horvitz et al. 1982; Ségalat et al. 1995](#)). Serotonin is also required for male mating behavior ([Loer and Kenyon 1993](#)).

A number of genes have been identified that affect serotonin metabolism or function. Mutants in [bas-1](#) (biogenic amine synthesis-defective) are deficient in serotonin and dopamine ([Loer and Kenyon 1993](#)). However, these mutants can accumulate exogenous serotonin in the "normal" serotonin cells as well as the "dopamine" cells described above ([Loer and Kenyon 1993](#)). Wild-type animals are also able to accumulate exogenous 5-hydroxytryptophan (5-HTP, the precursor of serotonin) in the "serotonin" and "dopamine" cells and convert it to serotonin. Treatment of [bas-1](#) mutants with exogenous 5-HTP does not lead to any serotonin immunofluorescence ([Loer and Kenyon 1993](#)), which is consistent with [bas-1](#) mutants having a defect in AAAD. [bas-1](#) maps near (and could be the same as) a putative AAAD gene identified by the Genome Sequencing Project (C. Loer, pers. comm.). Other putative AAAD homologs have been identified (see, e.g., [Marra et al. 1993](#)), but it is not known what part, if any, these other genes may play in neurotransmitter metabolism.

The [cat-4](#) gene, originally identified because of its effect on dopamine cells ([Sulston et al. 1975](#)), is also deficient in serotonin ([Desai et al. 1988](#)), but it does not appear to have a defect in serotonin uptake or in the decarboxylation of 5-HTP to make serotonin ([Loer and Kenyon 1993](#)).

Several genes have also been identified that affect the response to exogenous serotonin ([Ségalat et al. 1995](#)). The best characterized such gene is [goa-1](#), which encodes a G<sub>o</sub> subunit apparently required for transduction of a signal from a metabotropic serotonin receptor ([Mendel et al. 1995; Ségalat et al. 1995; Jorgensen and Rankin, this volume](#)).

There are at least ten cells in *C. elegans* hermaphrodites (and a greater number in males) with significant anti-serotonin immunoreactivity (see [Appendix 2](#)) ([Desai et al. 1988; Loer and Kenyon 1993](#); G. Garriga; B. Sawin and H.R. Horvitz; both pers. comm.). The NSM cells have the strongest and most consistent staining. These [pharyngeal cells](#) have varicosities, fine branches, and endings on the surface of the [pharynx](#) ([Albertson and Thomson 1976](#)), suggesting that serotonin might be released into the [pseudocoelom](#) and have a humoral function. The male-specific [CP neurons](#) also have strong serotonin immunoreactivity; they are involved in male mating behavior, and animals lacking serotonin ([bas-1](#), [cat-4](#)) are defective in this behavior ([Loer and Kenyon 1993](#)). In addition, the HSN cells, which are required for egg laying ([Trent et al. 1983](#)), contain serotonin ([Desai et al. 1988](#)), but serotonin does not appear to be essential for HSN function ([Weinshenker et al. 1995](#)).

## E. Glutamate and Other Transmitters

Glutamate acts as both an excitatory and inhibitory neurotransmitter in *C. elegans*. In the [pharynx](#), the [M3 motor neurons](#) appear to be inhibitory and glutamatergic and act by opening a chloride channel (J. Dent et al., pers. comm.). [avr-15](#), a gene involved in resistance to avermectin (C. Johnson, pers. comm.), is a good candidate to encode a glutamate receptor (or a receptor subunit), because [pharyngeal muscle](#) of [avr-15](#) mutants does not respond to pulses of glutamate (J. Dent et al., pers. comm.; [Avery and Thomas, this volume](#)). Additionally, two genes encoding subunits of a glutamate-gated chloride channel have been isolated by functional expression cloning in *Xenopus* oocytes ([Cully et al. 1994](#)).

Analysis of *glr-1* mutants, lacking a protein with 40% identity to the vertebrate AMPA glutamate receptor subunit, suggests that several classes of [sensory neurons](#) use glutamate as an excitatory transmitter ([Hart et al. 1995](#); [Maricq et al. 1995](#)). The most compelling case exists for the sensory [neuron](#) ASH, but [Hart et al. \(1995\)](#) also proposed that certain [mechanosensory neurons](#) are glutamatergic (see [Driscoll and Kaplan](#), this volume). However, additional [neurons](#) are also likely to be glutamatergic since the *glr-1* receptor is expressed in 17 classes of [neurons](#) ([Hart et al. 1995](#); [Maricq et al. 1995](#)). Several other genes encoding homologs of mammalian excitatory glutamate receptors have been identified by polymerase chain reaction (PCR) methods and by the Genome Sequencing Project (A. Maricq and C. Bargmann, pers. comm.).

Octopamine (*p*-hydroxyphenyl~ethanolamine) has been detected in *C. elegans* extracts, and exogenous octopamine stimulates movement and inhibits egg laying ([Horvitz et al. 1982](#)). Thus, its biological actions appear to antagonize those of serotonin, but it is not yet known which cells contain octopamine.

Several additional small molecules known to be neurotransmitters in other organisms (including adenosine, epinephrine, glycine, aspartate, histamine, and norepinephrine) have not yet been identified as transmitters in *C. elegans*. In most cases, the technology (e.g., immunohistochemistry and enzyme assays) available for analysis of these transmitters is not as good as that available for the transmitters described above. Therefore, as new and more sensitive methods are developed, it is possible that the existence and function of some of these transmitters will be identified in *C. elegans*.

## F. Peptides

In general, peptide neurotransmitters/neuromodulators appear to be regulated, transported, and released by mechanisms different from those used by the classical small molecule neurotransmitters. In both invertebrates and vertebrates, families of related peptides are often processed from precursor proteins by specific peptidases, and this appears to be true in *C. elegans* as well. To date, only one class of peptide has been studied in *C. elegans*: the FMRFamide group, which includes FLRFamide peptides (the terminology is derived from the carboxy-terminal amino acid sequence of the peptides). The only gene to be analyzed thus far is *fip-1* (FMRFamide like peptide; [Rosoff et al. 1992](#)), which encodes an alternatively spliced transcript. *fip-1* encodes proteins that may be processed to give eight related FLRFamide peptides. Other possible peptide-precursor genes have been identified by the Genome Sequencing Project, but these genes and their putative products have not yet been studied.

*fip-1* mutants have not yet been characterized and the precise function(s) of the encoded peptides is not known. However, the peptide FLRFamide was shown to potentiate the effects of serotonin on vulval muscles ([Schinkmann and Li 1992](#)). Peptide immunolocalization was performed using an antibody recognizing carboxy-terminal Arg-Phe-NH<sub>2</sub> epitopes ([Schinkmann and Li 1992](#)). This antibody is expected to react with most or all FMRFamide and FLRFamide peptides and perhaps many others; it should thus identify all of the *fip-1* -containing peptides and perhaps many more. These peptides have been immunolocalized to the VC motor [neurons](#) of the [ventral nerve cord](#) and approximately 25 additional cells throughout the body, including both [interneurons](#) and motor [neurons](#) (see [Appendix 2](#)) ([Schinkmann and Li 1992](#)). It is quite possible that the different *fip-1* peptides are expressed in different sets of cells.

In *Ascaris*, where the identification and separation of neuropeptides have been more carefully analyzed, it is estimated that there may be as many as a dozen families of distinct bioactive peptides, many of which have highly specific cellular localizations and physiological effects ([Sithigorngul et al. 1990](#); [Stretton et al. 1991](#); [Cowden et al. 1993](#); [Cowden and Stretton 1995](#); see [Jorgensen and Rankin](#), this volume). It is therefore likely that a more intensive biochemical and cellular analysis of *C. elegans* will reveal comparable complexity.

## Figures

Figure 3. (A) Steps of the synaptic release cycle.

## Figure 3

**(A)** Steps of the synaptic release cycle. Synaptic vesicles (or vesicle precursors) are synthesized in the soma and transported to synaptic terminals by axonal transport. Vesicles are loaded with neurotransmitter which is synthesized from cellular metabolites. Loaded vesicles are translocated to and docked at release sites. The docked vesicles subsequently become poised for fusion through a process often referred to as priming. Calcium influx (not shown) initiates the rapid fusion of the vesicle with the plasma membrane to release neurotransmitter. The transmitter diffuses across the synaptic cleft and interacts with transmitter receptors on the postsynaptic cell. To terminate the neurotransmitter signal in the synaptic cleft, the transmitter is either destroyed or transported back into a cell via a transmitter uptake transporter. Vesicle membrane that is incorporated into the plasma membrane during fusion is recycled by endocytosis. Vesicular components are sequestered into clathrin-coated pits (in gray) and these membrane patches bud off from the plasma membrane as coated vesicles. After the vesicles are uncoated, they fuse with synaptic endosomes. Finally, mature vesicles bud from the synaptic endosomes. **(B)** Schematic diagram of the molecular interactions that accompany vesicle fusion. Although this model is likely to be incorrect in some details, we present it as a conceptual aid to the reader. Prior to vesicle docking, UNC-18 protein is thought to associate tightly with syntaxin, a component found at docking sites. The vesicle-associated rab3 GTP-binding protein is proposed to regulate docking by interacting with unidentified effectors. rab3 is known to dissociate from vesicles during the fusion process ([Fischer von Mollard et al. 1994](#)). Upon or subsequent to docking, a complex forms between the three SNAP receptors (in white; syntaxin, SNAP-25 and VAMP, also called synaptobrevin). UNC-18, which dissociates from syntaxin at this step, is proposed to mediate this complex formation. Subsequently, SNAP and NSF bind to the SNAP receptor complex. The complex is structurally altered following ATP hydrolysis by NSF. This priming reaction leads to dissociation of the NSF and SNAP and poises the vesicle for fusion. Synaptotagmin has been proposed to be the sensor that detects calcium influx. Genes encoding specific synaptic components in *C. elegans* are in parentheses.

Figure 4. The structure of the cholinergic gene locus is conserved from *C. elegans*.

## Figure 4

The structure of the cholinergic gene locus is conserved from *C. elegans* to mammals. In *C. elegans*, the [\*unc-17\*](#) gene, which encodes the vesicular acetylcholine transporter (VACHT), is nested within the long first intron of the [\*cha-1\*](#) gene, which encodes choline acetyltransferase (ChAT). Both genes use a common, 66-base untranslated 5' exon, with the [\*cha-1\*](#) and [\*unc-17\*](#) transcripts produced by alternative splicing ([Alfonso et al. 1994b](#)). A very similar gene organization has been observed in rats and humans ([Bejanin et al. 1994](#); [Erickson et al. 1994](#)). For each organism, the genomic region is shown schematically (not necessarily to scale) above the structures of the transcripts so far identified. In mammals, three independent promoter regions (designated R, M, and N) have been identified, as well as exon-specific alternative splicing. This leads to several types of VACHT and ChAT transcripts which have not yet been identified in *C. elegans*. The start codon (ATG) is indicated for each gene. Most of the ChAT-coding exons are not shown.

Generated from local HTML

## Chapter 22. Synaptic Transmission — III Components Regulating Neurotransmitter Release in all Neurons

---

The identification and molecular characterization of several proteins associated with vertebrate synaptic vesicles initiated an extensive biochemical characterization of proteins acting at synapses. *C. elegans* mutations have now been isolated in most of the genes encoding biochemically identified components of neurotransmitter release. Mutants have been isolated by two strategies: screening for mutants with behavioral defects and selecting for mutants resistant to neuroactive compounds. Surprisingly, most mutants (including null mutants) with general synaptic defects are viable. In contrast, mutations in analogous genes in *Drosophila* (and mouse) usually lead to lethality ([Südhof 1995](#)). Although this apparent difference may reflect differences in the function of the homologous proteins in the synapses of their respective organisms, the most likely interpretation is that many of these components are equally important, but not absolutely essential, for synaptic transmission in these organisms. *C. elegans* is able to survive even with its [neuronal](#) function severely (but not totally) compromised, whereas *Drosophila* and mice, with a far greater need for [neuronal](#) function for feeding and reproduction, are far less tolerant to impaired function. At present, the severity of *C. elegans* synaptic defects is determined indirectly by quantifying alterations in behavior, responses to pharmacological agents, synaptic vesicle densities at synaptic terminals, and accumulation of neurotransmitter. However, electrophysiological techniques in *C. elegans* are being developed and are beginning to provide a more direct measure of synaptic efficacy in mutant animals ([Avery et al. 1995b](#); [Raizen et al. 1995](#)).

### A. Models of the Release Mechanism

Quantal release of neurotransmitter occurs by fusion of transmitter-filled vesicles in response to calcium influx into the [neuron](#). After exocytosis, vesicles are recycled by endocytosis and subsequently reloaded with neurotransmitter. At a molecular level, the process of fusion requires more than a dozen molecules (and probably many more) that interact to form many different protein complexes ([Bennett and Scheller 1994](#); [Südhof 1995](#)). Many of these molecules were first discovered as proteins associated with synaptic vesicles, and additional components were isolated as molecules that interacted with vesicle-associated proteins. Finally, others were identified through the molecular characterization of mutants with synaptic transmission defects in *C. elegans* and *Drosophila*.

Current models describing the molecular mechanism of calcium-regulated synaptic vesicle exocytosis and endocytosis divide the process into multiple steps (see [Fig. 3](#)) ([Bennett and Scheller 1994](#); [Südhof 1995](#)). Exocytosis is initiated by the docking of vesicles near release sites. Subsequently, these vesicles are “primed” for the fusion reaction. This is thought to involve the formation of a complex between molecules on the synaptic vesicle and molecules attached to the plasma membrane. The complex (often called the [SNAP receptor](#), or SNARE complex) is proposed to act as the receptor for soluble fusion factors. Soluble NSF attachment proteins (SNAPs) bind to the SNARE complex and recruit NSF (*n*-ethylmaleimide-sensitive fusion protein) to the complex. Subsequently, ATP hydrolysis by NSF is thought to complete vesicle priming. Influx of calcium then leads to the rapid completion of membrane fusion and the release of the neurotransmitter cargo. After fusion, endocytosis recycles the vesicular components to replenish the synaptic vesicle pool.

In the following section, we describe the molecules identified in *C. elegans* that participate in vesicle release and endocytosis and the phenotypes of animals harboring mutations in these genes. Many of the proteins participating in docking and fusion of synaptic vesicles have cellular homologs that participate in regulating the fusion of other types of vesicles utilized in the general secretory pathways found in [all cells](#). However, except in instances where specific molecules operate in both pathways, we restrict our discussion to molecules acting at the synapse.

### B. Identification of Synaptic Mutants

In 1974, Brenner reported that the AChE inhibitor lannate was toxic to *C. elegans* and that it was possible to obtain mutants with increased resistance to the toxin. In particular, he noted that [\*unc-17\*](#) mutants were quite resistant to lannate. Over the years, many more genes have been identified that, when mutant, confer resistance to AChE inhibitors (the AChE inhibitors aldicarb and trichlorfon are now commonly used instead of lannate). These studies have included both direct testing of known uncoordinated mutants and selection schemes for toxin-resistant mutants ([Rand and Russell 1985b](#); [Hosono et al. 1989](#); [Nguyen et al. 1995](#); [Miller et al. 1996](#)).

Presumably, inhibition of AChE leads to a toxic overaccumulation of the excitatory neurotransmitter acetylcholine, causing paralysis and death. If the real toxin is not the AChE inhibitor but rather the neurotransmitter itself, then any mutation that reduces the buildup of acetylcholine in the synaptic cleft would provide some protection from the drug. In fact, mutational defects in many aspects of presynaptic acetylcholine metabolism, including synthesis, packaging, and release, have been shown to confer drug resistance ([Rand and Russell 1984](#); [Alfonso et al. 1993](#); [Nonet et al. 1993](#); [Nguyen et al. 1995](#); [Miller et al. 1996](#); M.L. Nonet et al., in prep.). Defects in acetylcholine receptors should also in principle confer resistance to AChE inhibitors. However, although levamisole-resistant AChR mutants are able to move better than wild type in the presence of aldicarb ([Lewis et al. 1980a](#)), they are unable to grow and reproduce. Hence, these genes were not identified in many of the selection schemes for aldicarb-resistant mutants ([Nguyen et al. 1995](#); [Miller et al. 1996](#)).

Aldicarb-resistant mutants may be classified as presynaptic or postsynaptic by two principal criteria. First, acetylcholine levels are usually elevated in mutants with presynaptic defects (because of the accumulation of unreleased transmitter) and normal in mutants with postsynaptic defects ([Hosono et al. 1989](#); [Nguyen et al. 1995](#)). Second, mutants with postsynaptic defects are resistant to the AChR agonist levamisole, but mutants with presynaptic defects have normal (or even hypersensitive) response to levamisole ([Nonet et al. 1993](#); [Miller et al. 1996](#)).

More than 20 genes are now known that, when mutated, can confer recessive resistance to AChE inhibitors ([Rand and Russell 1985b](#); [Hosono et al. 1989](#); [Nguyen et al. 1995](#); [Miller et al. 1996](#)), and most of them appear to encode presynaptic functions. Many of these genes had previously been identified on the basis of an uncoordinated phenotype. Several new genes have been named after the encoded protein, when known (e.g., [snb-1](#) and [snt-1](#)), or else given a *ric* (resistance to inhibitors of cholinesterase) designation if the gene product was not known ([Nguyen et al. 1995](#); [Miller et al. 1996](#)).

## C. Axonal Transport and Docking of Vesicles

Vesicles (or vesicle precursors) are synthesized in the soma and transported along axonal microtubules to synaptic terminals, where they are tightly clustered around the electron-dense release zone. It is possible that some maturation process is required in the terminal. The mature vesicles appear to be tethered to a cytoskeleton framework radiating from the release site ([Kelly 1988](#)). Upon stimulation, it is believed that synaptic vesicles are translocated along the cytoskeleton to docking sites and the depleted vesicle pool is replenished. The docking process probably includes mechanisms that distinguish between different types of membrane organelles present in the cell to ensure that only synaptic vesicles are docked. Unfortunately, few of the components participating in the docking process have been identified in any organism.

### 1. Axonal Transport

Motor molecules of the kinesin family are thought to mediate the transport of vesicles along microtubule tracks. The [\*unc-104\*](#) gene of *C. elegans* encodes a 180-kD kinesin-related protein ([Otsuka et al. 1991](#)). The primary cellular defect in [\*unc-104\*](#) mutants appears to be a failure to transport synaptic vesicles from the cell body along the axon to synapses ([Hall and Hedgecock 1991](#)). Electron microscopic reconstruction reveals a large decrease in the number of synapses and synaptic vesicles in axons. Vesicles are formed, but they aggregate in large clusters in neuronal cell bodies ([Hall and Hedgecock 1991](#)). The most severe [\*unc-104\*](#) mutants arrest growth as severely uncoordinated young larvae similar in phenotype to [\*cha-1\*](#) and [\*unc-17\*](#) mutants. However, unlike [\*cha-1\*](#) and [\*unc-17\*](#) mutants, [\*unc-104\*](#) mutants can survive to adulthood under certain culture conditions ([Hall and Hedgecock](#)

[1991](#)). The behavioral and developmental phenotypes were therefore interpreted as due to a severe deficiency in synaptic transmission ([Hall and Hedgecock 1991](#)). A mouse homolog of [unc-104](#), KIF1A, has recently been demonstrated to mediate anterograde axonal transport of most synaptic vesicle proteins but not of plasma membrane components of the synaptic machinery ([Okada et al. 1995](#)).

The altered subcellular distribution of synaptic vesicles in [unc-104](#) mutants provides a useful tool for determining whether or not any given protein is associated with synaptic vesicles. Thus, for example, immunoreactivity for the vesicle proteins synaptotagmin ([Nonet et al. 1993](#)), UNC-17 ([Alfonso et al. 1993](#)), synaptobrevin (M.L. Nonet et al., in prep.), and RAB-3 (M.L. Nonet et al., in prep.) are all mislocalized from synapses to the cell body in [unc-104](#) mutants. In contrast, the localization of nonvesicle-associated proteins, such as syntaxin (M.L. Nonet et al., in prep.) and SNAP-25 (J. Lee and B. Meyer, pers. comm.) is unchanged in [unc-104](#) animals. However, the assignment of a protein as a synaptic vesicle protein based on its mislocalization in [unc-104](#) animals may have some exceptions. For example, it is possible that some nonvesicular molecules may use the UNC-104 transporter or that some proteins associated with mature vesicles may use a different axonal transporter and not be incorporated into the vesicle until it reaches the terminal. In vertebrates, the synaptic vesicle protein SV2 appears to fall into the latter category ([Okada et al. 1995](#)).

## 2. Attachment of Vesicles to the Cytoskeleton

In vertebrates, the synapsins are thought to participate in anchoring synaptic vesicles to the actin cytoskeleton at synapses ([De Camilli et al. 1990](#); [Pieribone et al. 1995](#)). Molecules similar to synapsins have not yet been identified in *C. elegans*. In synapsin-deficient mice, synaptic vesicles still cluster normally at synapses, although vesicle populations are somewhat reduced ([Rosahl et al. 1995](#)). Thus, attachment is probably not regulated solely by the synapsins.

[unc-31](#) encodes another molecule that may regulate vesicle attachment to the cytoskeleton. [unc-31](#) mutations confer several distinct phenotypes which suggest that synaptic transmission is altered but not eliminated in the mutants ([Avery et al. 1993](#)). UNC-31 protein is expressed in all *C. elegans* [neurons](#) and is similar to CAPS, a calcium- and actin-binding protein ([Livingstone 1991](#)). CAPS (calcium-dependent activator protein for secretion) was originally purified as a factor required for calcium-dependent secretion in permeabilized neuroendocrine cells ([Walent et al. 1992](#)). However, the calcium-binding properties of CAPS suggest that the molecule could be suited either for regulating recruitment of vesicles to docking sites or for regulating fusion directly ([Martin 1994](#); K. Ann et al., in prep.). Many phenotypes of [unc-31](#) mutants are consistent with the disruption of regulatory pathway(s) that modulate the availability of the synaptic vesicle pool for release.

## 3. rab-3

Small GTP-binding proteins of the rab family have long been implicated in regulating membrane trafficking ([Simons and Zerial 1993](#)), and proteins of the rab3 family associate specifically with synaptic vesicles ([Fischer von Mollard et al. 1994](#)). In *C. elegans*, one rab3-like gene (*rab-3 II*) has been isolated; the RAB-3 protein (75% identical to rat rab3C) is found localized to synaptic regions of the [nervous system](#) (M.L. Nonet et al., in prep.). Surprisingly, [rab-3](#) null mutants exhibit only mild behavioral defects, suggesting that synaptic transmission remains relatively intact. Similarly, rab3A knockout mice show only subtle behavioral abnormalities ([Geppert et al. 1994a](#)), and synaptic transmission in cultured [neurons](#) from mice lacking rab3A is diminished only upon repetitive stimulation. *C. elegans* [rab-3](#) mutants are resistant to aldicarb and have a 50–70% decrease in vesicle populations at neuromuscular synapses (M.L. Nonet et al., in prep.). The abnormalities in both *C. elegans* and mice are consistent with a role for rab3 in regulation of vesicular pool size. The mild defects observed in rab3 mutants are strikingly different from yeast rab mutants that have severe secretory defects ([Novick and Brennwald 1993](#)). This may reflect fundamental differences in vesicular trafficking in these two secretory processes or redundancy in rab function at the synapse. In mouse, redundancy is a possibility because of the presence of rab3B and rab3C proteins at presynaptic sites ([Geppert et al. 1994a](#)). However, in *C. elegans*, no other gene encoding a rab3-like protein has been identified in extensive PCR-based searches which isolated many other members of the rab family (M.L. Nonet et al., in prep.).

rab3 activity is regulated by cycling from a rab3-GTP-bound to a rab3-GDP-bound state in a fashion similar to that of ras ([Fischer von Mollard et al. 1994](#)). A guanine nucleotide dissociation inhibitor (GDI) binds rab3 and many other rab proteins in their GDP-bound form ([Ullrich et al. 1993](#)). Rabphilin-3A, a protein that specifically binds rab3 in its GTP-bound form, is particularly intriguing because it contains protein kinase C2-like domains that bind calcium ([Shirataki et al. 1993](#)). In *C. elegans*, homologs of both GDI ([gdi-1](#)) and rabphilin-3A have been identified by the Genome Sequencing Project, suggesting that many aspects of the rab3 regulatory pathway may be conserved.

#### 4. *unc-18* A Link between Docking and Priming?

UNC-18 may participate in regulating the formation of a stable interaction between vesicles and the plasma membrane. [unc-18](#) null mutants are viable but severely paralyzed; they are strongly resistant to aldicarb and have elevated acetylcholine levels ([Hosono et al. 1987](#); [Nguyen et al. 1995](#)). Ultrastructural analysis indicates that an excess of synaptic vesicles accumulates at synaptic terminals (E. Hartwieg et al., pers. comm.). These phenotypes all suggest that synaptic function is severely impaired in the mutant. [unc-18](#) encodes a neuronally expressed protein with similarity to Sec1p, Slp1p, and Sly1p, three yeast proteins required for distinct steps of the secretory pathway ([Hosono et al. 1992](#); [Gengyo-Ando et al. 1993](#)). Mutants in the *Drosophila* *rop* gene, which encode a molecule with 60% identity to [unc-18](#), also exhibit severe synaptic defects ([Harrison et al. 1994](#); [Schulze et al. 1994](#)). Using several different approaches, a number of groups identified similar proteins that are expressed in the vertebrate [nervous system](#) (called Munc18, n-Sec1, or rb-Sec1) and demonstrated that these proteins interact tightly with syntaxin, a protein found at the plasma membrane ([Hata et al. 1993](#); [Garcia et al. 1994](#); [Pevsner et al. 1994](#); [Katagiri et al. 1995](#)).

Biochemical studies suggest that [unc-18](#) acts early in the vesicle release process: UNC-18 family members bind tightly to syntaxin, but they are not found in the biochemical complexes that are proposed to form during vesicle priming and fusion. Thus, UNC-18 probably dissociates from syntaxin when syntaxin interacts with vesicle-associated proteins. Since [unc-18](#) mutants appear to block synaptic transmission and accumulate vesicles, UNC-18 may be required for efficient complex formation. A role for UNC-18 in linking the rab3 GTP regulatory protein to complex formation is also suggested by genetic interactions in yeast between rab and Sec1p/Slp1p/Sly1p family members ([Ferro-Novick and Novick 1993](#)). For example, overexpression of the rab protein Sec4p will compensate for Sec1p deficiency, and overexpression of Sly1p will compensate for lack of the rab protein Ypt1p ([Salminen and Novick 1987](#); [Dascher et al. 1991](#)).

### D. Priming of Vesicles for Release

Release of neurotransmitter occurs very quickly after the depolarization of the nerve terminal. It therefore appears that many of the steps required for vesicle fusion must occur before depolarization. The distinction between the initiation of this priming process and end of the docking process is somewhat arbitrary. We define SNAP receptor complex formation as the beginning of priming because it appears that formation of this complex is unrelated to the specificity of the docking.

#### 1. SNAP Receptors

The vesicle protein synaptobrevin or VAMP (vesicle-associated membrane protein) and the plasma membrane proteins SNAP-25 and syntaxin are thought to form a complex to position vesicles adjacent to the plasma membrane in preparation for fusion (see [Fig. 3](#)) ([Bennett and Scheller 1994](#); [Südhof 1995](#)). In *C. elegans*, [ric-4](#) encodes a protein with 72% amino acid sequence identity to rat SNAP-25 and [unc-64](#) encodes a protein with 67% identity to rat syntaxin (J. Lee and B. Meyer, pers. comm.; M.L. Nonet et al., in prep). Mutants in these two genes have similar phenotypes (lethargic uncoordinated movement, resistance to aldicarb, and elevated levels of acetylcholine), suggesting that synaptic transmission is severely impaired ([Nguyen et al. 1995](#)). Surprisingly, both the syntaxin and SNAP-25 homologs are ubiquitously distributed on neuronal membranes in *C. elegans* (M.L. Nonet et al., in prep; J. Lee and B. Meyer, pers. comm.), supporting the idea that SNAP receptors do not participate in determining docking specificity and suggesting that these proteins may also have roles in other

vesicular fusion events (e.g., those required for axonal outgrowth). However, although it is not yet known if any of the [unc-64](#) and [ric-4](#) alleles are null, there seem to be no outgrowth defects associated with any of the known mutations in either gene.

[snb-1](#) encodes a neuronally expressed protein exclusively localized to vesicles that is 72% identical to rat synaptobrevin I. [snb-1](#) mutants are lethargic, uncoordinated, and resistant to aldicarb (M.L. Nonet et al., in prep.). Fusions of GFP to the penultimate amino acid of SNB-1 retain the capability of localizing specifically to synaptic-vesicle-rich regions of the [nervous system](#) (see Fig. 1B) (M. Nonet and B. Meyer, unpubl.). UNC-11 appears to be required for the proper localization of SNB-1 to synaptic regions (M. Nonet and Y. Jin, unpubl.). In [unc-11](#) mutants, SNB-1 protein is uniformly distributed on neuronal membranes in a pattern similar to that of UNC-64. However, RAB-3 and synaptotagmin remain synaptically localized in [unc-11](#) mutants (M. Nonet, unpubl.), and synaptic terminals remain intact at the ultrastructural level (E. Jorgensen et al., pers. comm.). [unc-11](#) encodes a soluble protein (A. Alfonso, pers. comm.) that appears to be involved in the sorting or localization of synaptobrevin to synaptic vesicles. Since [unc-11](#) mutants have more severe behavioral defects than [snb-1](#) mutants, UNC-11 may also have other roles in synaptic release.

## 2. NSF and SNAP

NSF (N-ethylmaleimide-sensitive factor) and SNAPS (soluble NSF attachment proteins) are strongly implicated in participating in neurotransmitter release ([Bennett and Scheller 1994](#); [Südhof 1995](#)). In *C. elegans*, mutants affecting these proteins have not yet been identified, although homologs have been identified by the Genome Sequencing Project. Because NSF and SNAPS presumably participate in all vesicular membrane fusion events, it is likely that complete elimination of such proteins would confer an embryonic-lethal phenotype. In *Drosophila*, there appear to be two NSF genes ([Ordway et al. 1994](#); [Boulianne and Trimble 1995](#)), and one of them corresponds to the temperature-sensitive paralytic mutant *comatose* ([Pallanck et al. 1995](#)). This suggests that certain hypomorphic lesions in an NSF gene might preferentially affect neuronal secretion. Thus, the *C. elegans* NSF and SNAPS may yet be identified genetically through the characterization of aldicarb-resistant mutants.

## E. Calcium Regulation and Fusion

Studies of secretion in chromaffin cells suggest that multiple steps in vesicle release are calcium-dependent ([Neher and Zucker 1993](#)). Biochemical studies suggest that interactions between synapsin and vesicles are regulated by calcium/calmodulin-dependent protein kinase II, supporting roles for calcium in earlier steps in the synaptic vesicle cycle ([De Camilli et al. 1990](#)). Vesicle fusion is calcium-dependent and can occur within 0.2 msec after influx of calcium into the presynaptic nerve terminal through calcium channels. The speed of this final step in transmitter release suggests that calcium acts to relieve a block of a trapped intermediate, rather than initiate a vesicle docking and fusion process. Furthermore, endocytosis of membrane can be regulated by calcium ([Neher and Zucker 1993](#); [von Gersdorff and Matthews 1994](#)). Although it is not surprising that multiple calcium-binding proteins are associated with synaptic terminals, it is noteworthy that three of these molecules, rabphilin-3A, UNC-13, and synaptotagmin, all interact with calcium via a domain similar to the C2 domain of protein kinase C.

Calcium influx through N-type calcium channels localized at release sites is thought to initiate vesicle fusion. In *C. elegans*, several genes encoding proteins with similarity to voltage-gated calcium channels have been identified, although none of these channels appear to be analogous to specific vertebrate channel subtypes (L, N, or P). [unc-2](#) and [unc-36](#) both encode voltage-gated calcium channel subunits. [unc-2](#) encodes an  $\alpha$ -1 type subunit ([Schafer and Kenyon 1995](#)), and [unc-36](#) encodes an  $\alpha$ -2 subunit (L. Lobel and H.R. Horvitz, pers. comm.). Both mutants are aldicarb-resistant and have similar lethargic uncoordinated phenotypes, suggesting that they have synaptic transmission defects ([Nguyen et al. 1995](#); [Miller et al. 1996](#); K. Yook and E. Jorgensen, pers. comm.). Localization of [unc-2](#) message by *in situ* hybridization and mosaic analysis of [unc-2](#) and [unc-36](#) suggest that both genes function in muscle and in [neurons](#) ([Schafer and Kenyon 1995](#); W. Schafer and C. Kenyon, pers. comm.). At the present time, it is unclear whether [unc-2](#) and [unc-36](#) are subunits of the voltage-gated channel at the active zone or whether they are subunits of other voltage-gated regulatory channel(s).

Synaptotagmin is an integral membrane protein associated with synaptic vesicles with the capacity to bind calcium and phospholipids in vitro (Brose et al. 1992). Because of its biochemical properties, synaptotagmin was originally thought to mediate the calcium dependence of vesicular fusion. The behavioral defects, aldicarb resistance, acetylcholine accumulation, and electrophysiological abnormalities observed in *snt-1* null mutants provide strong evidence that loss of synaptotagmin impairs synaptic transmission (Nonet et al. 1993; Raizen et al. 1995). However, *snt-1* animals remain relatively active and they respond to touch, suggesting that some regulated transmission remains in *snt-1* mutants. Electrophysiological studies of synaptic transmission in synaptotagmin mutants in *Drosophila* and mice have led to essentially the same conclusions: Synaptic transmission is drastically reduced in the absence of synaptotagmin, but some regulated transmission remains (DiAntonio and Schwarz 1994; Geppert et al. 1994b; Littleton et al. 1994). However, it is still not known if synaptotagmin acts by preventing fusion until calcium enters or promotes fusion of vesicles upon calcium influx. In addition, the study of synaptotagmins in vertebrates and *snt-1* mutants in *C. elegans* has uncovered evidence that synaptotagmin's role is not limited to regulating the calcium-sensitive step of release (Jorgensen et al. 1995), i.e., it appears that synaptotagmin may regulate both exocytosis and endocytosis (see below).

A role for *unc-13* in synaptic transmission was inferred from its mutant phenotype: resistance to AChE inhibitors and elevated acetylcholine levels (Rand and Russell 1985b; Hosono et al. 1989; Nguyen et al. 1995). In addition, *unc-13* null mutants are almost paralyzed and have some aberrant synaptic connections (Brenner 1974; Maruyama and Brenner 1991; Ahmed et al. 1992). It thus appears that *unc-13* encodes a protein important but not absolutely required for neuronal function. The UNC-13 protein has a mass of 200 kD and is essentially novel, except for a 300-amino-acid region that has homology with the C1 and C2 regulatory domains of protein kinase C (Maruyama and Brenner 1991). When expressed in bacteria, this domain bound phorbol ester in a calcium-dependent manner; the binding was inhibited competitively by diacylglycerol (Maruyama and Brenner 1991; Ahmed et al. 1992). These results suggest some role for UNC-13 in signal transduction, but its specific function(s) has not yet been established. Several mammalian *unc-13* homologs, called Munc13s, have been described recently (Brose et al. 1995).

## F. Endocytosis

Vesicle recycling appears to proceed in several steps (Morris and Schmid 1995). Vesicle membrane is first internalized by a clathrin-mediated process. Subsequently, these recycling vesicles fuse with synaptic endosomes. Finally, synaptic vesicles are formed by budding from the endosomal compartment. Although direct evidence for synaptic endosomes is missing in *C. elegans*, vesicular structures of 50–80 nM in diameter are often seen in electron micrographs at the periphery of synapses (E. Hartwieg et al., pers. comm.).

Many of the phenotypes of the *snt-1* synaptotagmin mutants can be explained by an exocytic block of synaptic transmission (Nonet et al. 1993). However, analysis of synaptic terminals of *snt-1* null mutants revealed that these terminals are greatly depleted of synaptic vesicles, even though synaptic vesicle components such as RAB-3 and SNB-1 remain diffusely localized in the synaptic-rich regions of the nervous system (Jorgensen et al. 1995; M. Nonet, unpubl.). This suggests that the synaptic components are present in the plasma membrane and argues that synaptotagmin is required for a step in vesicular membrane retrieval. This observation is supported by the study of the eight synaptotagmins identified in vertebrates. A subset of these proteins do not bind calcium and therefore appear not to be involved in calcium-mediated fusion (Li et al. 1995). In addition, all synaptotagmins tested bind to the AP-2 clathrin adapter complex which links integral membrane proteins to clathrin, when coated pits are formed during endocytosis (Zhang et al. 1994; Li et al. 1995). Thus, in *C. elegans*, an endocytic defect appears to account for the morphological defects observed at synaptic terminals; however, this does not preclude a role for synaptotagmin in exocytosis.

Dynamin is a large GTPase that plays a central part in endocytosis (Liu and Robinson 1995). The GTP-associated form of the protein is located at the neck of invaginating coated pits, suggesting that the molecule may be involved in pinching off vesicles during endocytosis (Hinshaw and Schmid 1995; Takel et al. 1995). In *Drosophila*, dynamin is encoded by the *shibire* gene (Chen et al. 1991; van der Bliek and Meyerowitz 1991). Analysis of *shibire* mutants has demonstrated that dynamin is required for endocytosis of vesicular membrane in neurons (Kosaka

[and Ikeda 1983](#); [Koenig and Ikeda 1989](#)). A *C. elegans* dynamin gene ([dyn-1](#)) encoding a protein with 62% identity to the *Drosophila* protein was cloned based on its sequence similarity (A. van der Bliek, pers. comm.).

Immunohistochemical staining indicates that *C. elegans* dynamin in the [nervous system](#) is localized in a pattern similar to that seen with synaptotagmin (A. van der Bliek, pers. comm.), suggesting that most dynamin in [neurons](#) is restricted to synaptic terminals, as has been demonstrated for dynamin I in rat ([Powell and Robinson 1995](#)). By analogy with the phenotype of *shibire* mutants, a [dyn-1](#) mutant was identified by screening for temperature-sensitive uncoordinated behavior (S. Clark and C. Bargmann, pers. comm.). Further genetic studies using [dyn-1](#) may lead to the identification of regulators of dynamin activity.

## G. Other Components Participating in Synaptic Transmission

Several other putative synaptic genes have been identified by analysis of aldicarb-resistant mutants, including [aex-3](#), [egl-10](#), [egl-30](#), [ric-1](#), [ric-3](#), [ric-6](#), [ric-7](#), [ric-8](#), [unc-10](#), [unc-26](#), [unc-41](#), and [unc-75](#) ([Nguyen et al. 1995](#); [Miller et al. 1996](#); E. Jorgensen, pers. comm.). Although many of these mutants have not yet been thoroughly analyzed, most of the genes appear to encode presynaptic functions ([Nguyen et al. 1995](#); [Miller et al. 1996](#)). In addition, preliminary genetic analysis suggests that there are at least six (and perhaps more than 12) additional aldicarb resistance loci (J. Rand, unpubl.). It is therefore likely that many (or most) of the known synaptic proteins are represented, as well as several novel genes.

Generated from local HTML

## Chapter 22. Synaptic Transmission — IV Conclusions and Future Perspectives

---

The process of synaptic transmission has been conserved throughout metazoan evolution. Consequently, the study of synaptic transmission in *C. elegans* has provided insights into the workings of the vertebrate synaptic machinery, and vice versa. In particular, the unique ability to isolate *C. elegans* mutants with synaptic defects using aldicarb and levamisole has identified more than 30 genes that participate in various aspects of synaptic transmission. Molecular characterization of a subset of these genes, identified through functional assay, has revealed that some encoded synaptic proteins previously characterized in vertebrates (e.g., synaptotagmin and syntaxin) and others encoded novel proteins. Vertebrate homologs of some of these genes have now been identified; these include [unc-13](#), [unc-17](#), [unc-18](#), and [unc-104](#).

Further analysis of *C. elegans* mutants with synaptic defects promises to lead to the discovery of other intriguing molecules. Physiological techniques with the sensitivity to dissect the roles of these molecules at a mechanistic level are now under development ([Avery et al. 1995b](#)). With the Genome Sequencing Project providing a complete description of the conserved components of the synaptic machinery, it appears that a mutational analysis of most genes encoding synaptic components in *C. elegans* (with the exception of postsynaptic receptors which are quite numerous) should be feasible in the near future. Combined with extensive biochemistry, physiology, cell biology, and genetics in other systems, such studies are likely to clarify the structure of the synaptic machinery in the coming years.

Although synaptic transmission underlies behavior, understanding the release mechanism at a molecular level is only one step toward a molecular description of behavior. Modeling and understanding the functions of [neural](#) circuits require a knowledge of the transmitters used by each cell and the types of signal (excitatory or inhibitory) used at each synapse. So far, only about half of the [neurons](#) in *C. elegans* have a transmitter assigned to them. It is likely that many of the remaining cells use transmitters such as glutamate, which is present in [all cells](#) and whose assignment as a transmitter is difficult to prove. It is also likely that additional transmitters, such as histamine or adenosine, may be utilized in *C. elegans*. The characterization of the expression pattern of genes encoding molecules responsible for the synthesis or vesicular transport of these additional transmitters should provide the most direct method of identifying cells that utilize these transmitters. Receptors for these transmitters must also be identified. With the exception of nAChRs, very little is yet known about the diversity and function of neurotransmitter receptors in *C. elegans*. The Genome Sequencing Project should aid in this endeavor, but it is the isolation of mutants that disrupt individual transmitter systems either pre- or postsynaptically that will provide the most information about the molecular mechanisms that underlie behavior.

Studies already published on *Ascaris* indicate a great diversity of neuropeptides with distinct cellular localization patterns ([Sithigorngul et al. 1990](#); [Stretton et al. 1991](#); [Cowden et al. 1993](#); [Cowden and Stretton 1995](#)). It is likely that *C. elegans* will have comparable diversity of peptides with diverse roles as transmitters, cotransmitters, and/or neuromodulators. Analysis of the roles of such peptides in neuronal function will be quite difficult not only because of the molecular and cellular complexity, but also because of the problems associated with identifying subtle yet specific behavioral paradigms. Nevertheless, understanding the functions of these molecules will be necessary for any eventual comprehensive description of the [neural](#) control of behavior.

Although an outline of the mechanism of synaptic transmission is evolving, several additional aspects of synaptic biology in metazoans are virtually undefined in molecular terms. In particular, distinctions between the mechanisms underlying peptidergic and classical neurotransmission have yet to be identified. Peptide and classical transmitters differ in many respects, including the mechanism and location of vesicle loading and the locations and kinetics of release. In addition, the mechanisms underlying the formation of synaptic specializations also remain poorly characterized at the molecular level. Components of a synapse must be transported and assembled into a complex structure at specific sites in both the presynaptic cell and the postsynaptic cell. Another critical area of research will involve determining the molecular basis of synaptic modulation and plasticity (see [Jorgensen and Rankin](#), this volume). Such modifications include altering the

number and size of synapses, as well as modulating the efficacy of transmission. Thus, plasticity probably consists, at least in part, of linkages between the synaptic function and synaptic assembly/disassembly processes. The prospect for a relatively complete description of synaptic transmission at a molecular level hinges upon the coordinated molecular, biochemical, physiological, and genetic characterization of many distinct properties of synapses. Even in an organism with a simple [nervous system](#) like *C. elegans*, this remains a difficult task.

Generated from local HTML

## **Chapter 22. Synaptic Transmission — Acknowledgments**

---

We are grateful to Erik Jorgensen, Carl Johnson, Joe Culotti, Bill Trimble, and the members of our laboratories for useful discussions and comments on the manuscript. We also wish to express our appreciation to David Hall and Janet Duerr for providing micrographs and to many members of the *C. elegans* community for permission to present unpublished data.

Generated from local HTML

# **Chapter 23. Mechanotransduction**

---

## **Contents**

- [I Introduction: the Neural Circuit For Locomotion](#)
- [II Mechanosensory Control of Locomotion](#)
- [III Touch Receptor Development and Differentiation](#)
- [IV Genes Required for Touch Receptor Function](#)
- [V Conclusions](#)
- [Acknowledgments](#)

Generated from local HTML

# Chapter 23. Mechanotransduction — I Introduction: the Neural Circuit For Locomotion

---

Diverse mechanical stimuli are likely to be encountered constantly in *Caenorhabditis elegans*' normal habitat, the soil. Therefore, it is not surprising that *C. elegans* utilizes [mechanosensory neurons](#) to regulate many of its behaviors. Touch regulates locomotion, foraging, egg laying, pharyngeal pumping, and defecation.

Mechanosensory inputs not only give rise to simple reflexive avoidance behaviors, but also appear to control the overall activity of the animal. In this chapter, we describe the [neural](#) circuits for locomotion, foraging, and touch avoidance, their genetic analysis, and a molecular model for mechanosensory transduction. Since understanding regulation of locomotion by mechanical stimuli requires knowledge of the [neural](#) circuit for locomotion, we first describe this circuit with a focus on three key questions: How is the sinusoidal pattern of body bends generated? How are the antagonistic behaviors of forward and backward locomotion coordinated? How is the sinusoidal wave propagated along the body axis?

## A. Musculature and Motor Neuron Innervation

The anatomy of the body wall muscles and of their synaptic inputs restricts locomotion to dorsal and ventral turns of the body. Locomotion consists of a sinusoidal pattern of alternating ventral and dorsal turns of the body musculature. The body wall muscles are organized into two dorsal rows and two ventral rows. Each row consists of 23 or 24 diploid mononucleate muscle cells arranged in an interleaved pattern ([Sulston and Horvitz 1977](#)). Dorsal and ventral body muscles are controlled by distinct classes of motor [neurons](#). Five types of [ventral cord motor neurons](#) (A, B, D, AS, and VC) are defined by similarities in axonal morphologies and patterns of synaptic connectivities ([White et al. 1986](#)). Motor neuron processes have presynaptic regions, which form neuromuscular junctions and provide input to other [neurons](#), and postsynaptic regions, which receive input from other [neurons](#). Some classes of [neurons](#) (VA, VB, VC, and VD) form neuromuscular junctions with the ventral body muscles, whereas others (AS, DA, DB, and DD) innervate the dorsal muscles. Each motor [neuron](#) class is composed of multiple members, which are arrayed along the length of the ventral cord in repeating units (e.g., VA1–VA6). Equivalent motor [neuron](#) classes are found in the [nervous system](#) of *Ascaris suum* (Stretton et al. 1978; Johnson and Stretton 1980). Unlike *C. elegans* [neurons](#), *Ascaris* [neurons](#) are large and amenable to electrophysiological study. Since the nervous systems of these two nematodes are largely homologous, neurophysiological properties of *C. elegans* [neurons](#) can be inferred from analyses in *Ascaris*.

To generate the sinusoidal pattern of movement, the contraction of the dorsal and ventral body muscles must be out of phase. For example, to turn the body dorsally, the dorsal muscles contract while the opposing ventral muscles relax. A pattern of alternating dorsal and ventral contractions is produced by interactions between excitatory and inhibitory motor [neurons](#). The A, B, and AS motor [neurons](#) utilize the neurotransmitter acetylcholine (J. Duerr and J. Rand, unpubl.) and are likely to be excitatory. Consistent with this are physiological measurements showing that the analogous *Ascaris* motor [neurons](#) are both cholinergic and excitatory (Johnson and Stretton 1985; Walrond et al. 1985a). The D-type [neurons](#) are inhibitory and utilize GABA as their transmitter ([McIntire et al. 1993b](#)).

The A- and B-type neuromuscular junctions are organized into characteristic dyadic complexes in which an A or B synaptic terminus is apposed to two distinct postsynaptic elements, a [body wall muscle](#) and a D neuron dendrite ([White et al. 1986](#)). The pattern of these dyadic synapses is highly asymmetric. The [VD neurons](#) receive input at the dorsal A- and B-type neuromuscular junctions (and hence are likely to be active during dorsal muscle contractions), and they form neuromuscular junctions ventrally that appear to relax the ventral muscles. The converse set of connections obtain for the [DD neurons](#). This pattern of connectivities led to the proposal that the D neurons act as cross-inhibitors that prevent the simultaneous contraction of the dorsal and ventral muscles ([White et al. 1986](#)).

This model for cross-inhibition is supported by genetic analysis and cell ablations in *C. elegans* and by physiological studies in *Ascaris*. In *C. elegans*, mutations in the [unc-25](#) gene, which encodes the GABA

biosynthetic enzyme glutamic acid decarboxylase (Y. Jin and R. Horvitz, unpubl.), or killing the D neurons with a laser microbeam causes the simultaneous contraction of the dorsal and ventral muscles so that animals shrink along their body axis (Brenner 1974; McIntire et al. 1993a,b). In *Ascaris*, the excitatory cholinergic motor [neurons](#) activate the inhibitory GABAergic motor [neurons](#), which in turn relax the opposing muscles (Walrond and Stretton 1985b). Together, these results strongly support the model that synaptic interactions between excitatory (A and B) and inhibitory (D) motor [neurons](#) prevent simultaneous contraction of dorsal and ventral muscles.

The [unc-25](#) phenotype suggested a second function for the D-type neurons. When at rest, [unc-25](#) mutants have a straight rather than sinusoidal posture, and when moving, they generate a wave with greatly reduced amplitude ([McIntire et al. 1993b](#)), implicating the D neurons in the regulation of wave amplitude. In *Ascaris*, the FMRFamide peptide AF1 modulates the activity of the cross-inhibitors, greatly reducing the domain of muscle relaxation (Cowden et al., 1989). The D-type neurons of *C. elegans* may also be modulated in this manner, since they are postsynaptic to the [VC neurons](#) that express FMRF-like immunoreactivity ([White et al. 1986](#); Li and Chalfie 1990; Schinkmann and Li 1992).

How does this circuit create the rhythmic pattern of locomotory movement? In several cases in other organisms, networks of [neurons](#) have been shown to control rhythmic behaviors, and specific cells in these networks have intrinsic oscillating activity that engenders the observed rhythm. These oscillating cells have been termed pattern generators (for review, see [Getting 1988](#)). In the case of *C. elegans* locomotion, relatively little is known about how the rhythmicity is engendered. In *Ascaris*, the GABA-containing [ventral cord motor neurons](#) (equivalent to the D-type motor neurons of *C. elegans*) have an oscillating pattern of electrical activity, leading to the speculation that the GABA motor neurons act as the pattern generator for locomotion (Angstadt and Stretton 1989; Davis and Stretton 1989). A similar pattern-generating mechanism seems unlikely in the case of *C. elegans* because [unc-25](#) and [unc-30](#) mutants that lack functional D neurons still generate rhythmic sinusoidal movement, albeit with a reduced amplitude. Given the recent success in obtaining electrophysiological recordings from *C. elegans* neurons (L. Avery et al., pers. comm.), the pattern-generating activity of the locomotory circuit should be elucidated in the near future.

## B. Circuits for Forward and Backward Locomotion

Forward locomotion and backward locomotion are antagonistic behaviors, controlled by distinct [neural](#) circuits ([Fig. 1](#)). Four bilaterally symmetric interneuron pairs (AVA, AVB, AVD, and PVC) have large-diameter axons that run the entire length of the [ventral nerve cord](#) and provide input to the [ventral cord motor neurons](#) ([White et al. 1976](#)). These interneurons have distinct patterns of connectivities. AVA and AVD provide input to the A-type motor neurons, whereas AVB and PVC provide input to the B-type motor [neurons](#). Cell-killing experiments have shown that the ventral cord interneurons and motor neurons can be subdivided according to their function in forward or backward movement ([Chalfie et al. 1985](#)). The circuit comprising AVB, PVC, and the B motor [neurons](#) drives forward locomotion, whereas the circuit comprising AVA, AVD, and the A motor [neurons](#) drives backward movement. The phenotype of [unc-4](#) mutants also supports the specific function of AVA, AVD, and the A-type [neurons](#) in backward movement. The UNC-4 homeodomain protein is expressed in the A-type [neurons](#) ([Miller et al. 1992](#); [Miller and Niemeyer 1995](#); see [Ruvkun](#), this volume). In [unc-4](#) mutants, type-A [neurons](#) have synaptic inputs characteristic of the B motor [neurons](#), and defective backward movement results ([White et al. 1992](#)).

Although to a first approximation forward and backward locomotion reflects the activities of competing circuits, there are several indications that these circuits functionally interact. First, disabling either circuit with a laser microbeam also causes mild defects in the opposing behavior (J. Kaplan; B. Sawin; both unpubl.). Second, mosaic analysis of GLR-1 glutamate receptors, which are expressed in the locomotory [interneurons](#), suggests that both the forward and backward interneurons play a part in backward movement ([Hart et al. 1995](#)). Third, simultaneous activation of the forward and backward circuits with a diffuse mechanical stimulus (tap, described below) reveals that these circuits functionally inhibit each other ([Wicks and Rankin 1995](#); see [Jorgensen and Rankin](#), this volume). Interaction between these opposing circuits may be mediated by the unusual connectivities of the ventral cord interneurons. The forward and backward interneurons have multiple reciprocal connections, which could mediate coordination of opposing circuits ([White et al. 1986](#)).

## C. Propagation of the Sinusoidal Wave

Relatively little is known about how the sinusoidal wave is propagated along the body axis. Adjacent muscle cells are electrically coupled via gap junctions, which could couple excitation of adjacent body muscles. Alternatively, [ventral cord motor neurons](#) could promote wave propagation since adjacent motor neurons of a given class are connected by gap junctions ([White et al. 1986](#)). A third possibility is that motor neurons could themselves act as stretch receptors so that contraction of body muscles could regulate adjacent motor neuron activities, thereby propagating the wave. This model (originally proposed by R.L. Russell and L. Byerly and described in [White et al. 1986](#)) was inspired by subtle morphological features of the [ventral cord motor neurons](#). Both A and B motor [neurons](#) have long undifferentiated processes distal to the regions containing their neuromuscular junctions ([White et al. 1976](#)). These terminal, undifferentiated processes have been proposed to be stretch-sensitive. Interestingly, the anterior-posterior polarity of motor [neuron](#) processes correlates with function in either forward or backward movement. A-type [neurons](#), required for backward movement (i.e., anteriorly propagated waves), have anteriorly directed processes, whereas B [neurons](#) drive forward movement (i.e., posteriorly propagated waves) and have posteriorly directed processes ([White et al. 1986](#)). It is not known whether motor [neurons](#) are actually stretch-sensitive, nor is the relationship between motor [neuron](#) function and axonal polarity understood.

## Figures

Figure 1. Locomotory circuitry.

### Figure 1

Locomotory circuitry. (*Inverted triangles*) Representatives of the six major motor [neuron](#) classes; (*rectangles*) [interneurons](#). Only one of each motor [neuron](#) class is shown, although each class has multiple members that are situated along the length of the ventral cord. The DA, DB, and DD motor [neurons](#) innervate dorsal muscles, and the VA, VB, and [VD neurons](#) innervate ventral muscles ([White et al. 1986](#)). The circuit comprising interneurons AVB and PVC and the B-type motor [neurons](#) directs forward locomotion; the circuit including [interneurons](#) AVA, AVD, and AVE and the A-type motor [neurons](#) directs backward locomotion ([Chalfie et al. 1985](#)). The A- and B-type motor [neurons](#) are excitatory and use the neurotransmitter acetylcholine (*open triangles*) (J. Duerr and J. Rand, pers. comm.); the D-class motor [neurons](#) are inhibitory and use the transmitter GABA (*closed triangles*) ([McIntire et al. 1993b](#)). The D-class motor [neurons](#) receive synaptic input from other motor [neuron](#) classes rather than from [interneurons](#)—the D-class motor neurons synapse onto muscles situated opposite to those innervated by their presynaptic partners and function as reciprocal inhibitors that coordinate forward and backward movements. Morphologies of motor [neuron](#) classes are diagrammed schematically. (Adapted, with permission, from Chalfie and White 1988.)

Generated from local HTML

# Chapter 23. Mechanotransduction — II Mechanosensory Control of Locomotion

---

Four behavioral paradigms have been developed to study mechanosensory control of locomotion: nose touch, gentle body touch, tap, and harsh body touch ([Chalfie et al. 1985](#); [Way and Chalfie 1989](#); [Chiba and Rankin 1990](#); [Rankin 1991](#); [Kaplan and Horvitz 1993](#)). The neuronal circuitry for each behavioral paradigm has been deduced and, to varying degrees, has been experimentally tested. We first describe here neuronal circuitry and genetic characterization of two behavioral responses to nose touch: nose touch avoidance and head withdrawal. We then discuss circuitry for responses to three distinct types of body touch: localized gentle touch, a diffuse tap delivered over the entire body, and localized harsh touch. Finally, we discuss in detail the molecular genetics of development and function of the six touch receptor cells, which have critical roles in sensory transduction of several of the aforementioned behaviors. In addition to modulation by mechanical stimuli, locomotion can be controlled by chemosensory and thermosensory cues (see [Bargmann and Mori](#), this volume).

## A. Nose Touch Avoidance

When animals collide nose-on with an object such as an eyelash they respond by initiating backward movement ([Croll 1976](#); [Kaplan and Horvitz 1993](#)). Three classes of [mechanosensory neurons](#) (ASH, FLP, and OLQ) act in parallel to mediate this avoidance response (see [Fig. 2A](#) for ASH circuitry diagram). These nose touch [neurons](#) have cell bodies in the [nerve ring ganglia](#) and send long dendritic processes to the tip of the worm's nose. The response to nose touch is quantitative (normal animals respond in 90% of trials), and each sensory [neuron](#) class accounts for a fraction of the normal response, as follows: ASH, 45%; FLP, 29%; and OLQ, 5% ([Kaplan and Horvitz 1993](#)). The remaining responses (~10%) are mediated by the [ALM](#) and [AVM neurons](#), which sense anterior body touch (J. Kaplan, unpubl.). It is unclear what distinguishes the function of the three nose touch [neurons](#). One attractive possibility is that these cells differ in their sensitivities and that the intensities of nose touch stimuli vary according to the violence of the collision. If this were the case, it would be expected that the most sensitive neuron (ASH) would account for the majority of responses and the less sensitive neurons (FLP and OLQ) would account for the remainder.

The mechanosensory function of the ASH neurons is surprising because these cells were thought to act solely as chemosensory [neurons](#). The ASH neurons are part of the amphid chemosensory organs, their sensory endings are exposed to the external environment, and they have two chemosensory functions mediating avoidance of osmotic and volatile repellents ([Bargmann et al. 1990](#); [Troemel et al. 1995](#); see [Bargmann and Mori](#), this volume). Thus, the ASH neurons are polymodal [sensory neurons](#). Several classes of chemosensory neurons respond to multiple chemical stimuli in *C. elegans*; however, ASH is unique among them in responding to such divergent stimuli. In this respect, ASH neurons are similar to vertebrate [neurons](#) that sense painful stimuli, which are called nociceptors (Besson and Chaouch 1987).

ASH and FLP provide direct synaptic input and OLQ provides indirect synaptic input (via RIC) to the AVA, AVB, and AVD interneurons ([Fig. 2A](#)) ([White et al. 1986](#)). Genetic evidence supports the function of these synaptic connections. The [glr-1](#) gene encodes an AMPA-type glutamate receptor that is expressed in both the forward (AVB and PVC) and backing (AVA and AVD) [interneurons](#) ([Hart et al. 1995](#); [Maricq et al. 1995](#)). [glr-1](#) mutants are defective for nose touch avoidance, which suggests that the sensory transmitter is glutamate and that [glr-1](#) encodes a subunit of the postsynaptic glutamate receptors at the nose touch neuron-to-interneuron synapses. Analysis of genetic mosaics revealed that GLR-1 receptors function in both [AB.a](#) and [AB.p](#) lineages, suggesting that GLR-1 receptors are required in both the forward and backing interneurons (which are derived from [AB.p](#) and [AB.a](#), respectively) and that the forward interneurons also have a role in backward movement ([Hart et al. 1995](#)).

GLR-1 glutamate receptors appear to play a part in distinguishing between the two ASH sensory modalities. [glr-1](#) mutants are defective for ASH-mediated touch sensitivity but are normal for ASH-mediated osmotic and volatile-repellent sensitivity ([Hart et al. 1995](#); [Maricq et al. 1995](#)). Although they are specifically required for ASH-

mediated touch sensitivity, GLR-1 receptors are expressed in synaptic targets of ASH. These results suggest that the ASH [neurons](#) produce different synaptic signals in response to the two stimuli. Consistent with this idea, ASH synaptic termini contain two distinct kinds of synaptic vesicles, clear and dense core vesicles, implying that ASH [neurons](#) utilize two distinct neurotransmitters ([White et al. 1986](#)). Separate signaling pathways for the two ASH sensory modalities are also supported by the phenotype of [osm-10](#) mutants, which are defective for ASH-mediated osmotic avoidance but are normal for ASH-mediated nose touch sensitivity (A. Hart and J. Kaplan, unpubl.). Thus, differential signaling at the ASH-to-[interneuron](#) synapses may allow animals to distinguish between the ASH sensory modalities.

## B. Foraging and Head Withdrawal

Touch also regulates movement of the animal's head, which is called foraging behavior. Foraging behavior consists of continuous, apparently exploratory, head movements. The patterns of head movements that occur during foraging are complex compared to the relatively simple sinusoidal movements that underlie locomotion. This difference is explained by the motor anatomy of the head. Head muscles are divided into eight radial symmetric sectors, and these are independently innervated by ten classes of motor [neurons](#) ([Ware et al. 1975](#); [White et al. 1986](#)). As a consequence of this motor circuitry, worms can move their head through 360°.

When worms are touched on either the dorsal or ventral sides of their nose with an eyelash, they interrupt the normal pattern of foraging and undergo an aversive head-withdrawal reflex. This simple reflex is mediated by two classes of [mechanosensory neurons](#) (OLQ and IL1) and their synaptic targets, the RMD motor neurons ([Fig. 2B](#)) ([Hart et al. 1995](#)). Killing any of these cells, alone or in combination, diminishes the head withdrawal reflex. Here again, the [sensory neurons](#) have nonredundant functions, OLQ accounting for the majority of the normal responses. Interestingly, IL1, OLQ, and RMD also regulate spontaneous foraging movements ([Hart et al. 1995](#)). Laser operated animals lacking IL1 and OLQ forage abnormally slowly and make exaggerated dorsal and ventral nose turns. These results suggest that mechanosensory stimuli (touch or stretch) regulate both the rate and pattern of spontaneous foraging movements. The function of the sensory neuron-to-RMD synapses is supported by the phenotype of [glr-1](#) mutants ([Hart et al. 1995](#)). The [RMD neurons](#) express GLR-1 glutamate receptors and [glr-1](#) mutants are defective for the head withdrawal reflex.

## C. Genetic Analysis of Nose Touch Avoidance and Foraging

The [mechanosensory neurons](#) that mediate nose touch avoidance and control foraging behavior have sensory endings that contain a single cilium ([Ward et al. 1975](#); [Albert et al. 1981](#); [Perkins et al. 1986](#)). Mutations in several genes (e.g., [che-3](#) and [osm-1](#)) disrupt the ultrastructure of ciliated sensory endings (Lewis and Hodgkin 1977; [Albert et al. 1981](#); [Perkins et al. 1986](#)). These cilium-structure mutants are all defective for nose touch avoidance and head withdrawal and have abnormally slow foraging behavior ([Kaplan and Horvitz 1993](#) and unpubl.). These results suggest that the nose touch [neurons](#) act as [sensory neurons](#) (rather than interneurons) in these behaviors.

Mutations in two genes ([daf-11](#) and [eat-4](#)) disrupt the function of nose touch [neurons](#) and other ciliated [sensory neurons](#). [daf-11](#) mutants are defective for the nose touch avoidance response (J. Kaplan, unpubl.). The [daf-11](#) gene encodes a membrane-bound guanylate cyclase (D. Birnby and J. Thomas, pers. comm.) that is also required for chemotaxis and for the regulation of dauer formation by ciliated chemosensory neurons. [eat-4](#) mutants are defective for nose touch avoidance and head withdrawal and have an abnormal pattern of foraging movements (A. Hart and J. Kaplan, unpubl.). As discussed below (see also [Avery and Thomas](#), this volume), several lines of evidence suggest that [eat-4](#) mutants are generally defective for glutamatergic neurotransmission, again implicating glutamate as the sensory transmitter.

## D. Response to Gentle Body Touch

### 1. The Neuronal Circuit

Animals respond to gentle touch (typically delivered with an eyelash) all along the length of their body ([Chalfie and Sulston 1981](#); [Chalfie et al. 1985](#)). Anterior touch elicits backward movement, whereas posterior touch elicits forward movement. Gentle body touch is sensed by the [mechanosensory neurons ALML/R, AVM, and PLML/R](#) ([Fig. 3A](#)). These [mechanosensory neurons](#) were previously called the microtubule cells because their long axonal processes are filled with bundles of distinctive large-diameter microtubules ([Fig. 3B](#)) ([Chalfie and Thomson 1979](#)). Several observations support the conclusion that these touch cell processes, which run longitudinally along the body wall, function in mechanoreception ([Chalfie and Sulston 1981](#); [Chalfie et al. 1985](#)). First, the touch cell processes lack synaptic specializations and hence are likely to be dendritic. Second, the touch cell processes are embedded in the hypodermis adjacent to the cuticle, a position expected to facilitate detection of mechanical stimuli. Third, the position of the processes along the body axis correlates with the sensory field of the touch cell. [ALM](#) and [AVM](#) have sensory receptor processes in the anterior half of the body, and ablation of these cells eliminates anterior touch sensitivity. Likewise, [PLM](#) has a posterior dendritic process, and ablation eliminates posterior touch sensitivity. The [PVM](#) neuron does not appear to have a critical role in touch sensitivity as it cannot mediate a touch response by itself. However, [PVM](#) is also considered a touch cell because it is ultrastructurally similar to the other [touch cells](#), and its differentiation is controlled by the same genetic pathway (see below).

The touch cell processes enter the neuropile and form connections with many other [neurons](#) ([Chalfie et al. 1985](#); [White et al. 1986](#)). [ALM](#) and [AVM](#) axons enter the [nerve ring](#), whereas [PLM](#) and [PVM](#) axons enter the [ventral nerve cord](#) ([Fig. 3A](#)). The [touch cells](#) provide direct input to the interneurons that control locomotion; however, the pattern of these connections is highly asymmetric. The anterior [touch cells ALM](#) and [AVM](#) form gap junctions with the backward movement interneuron [AVD](#), but they provide synaptic input to the forward interneurons ([AVB](#) and [PVC](#)). Conversely, [PLMR](#) provides input to the forward interneuron [PVC](#) via gap junctions, but it provides synaptic input to the backward interneurons [AVA](#) and [AVD](#) ([Fig. 2C](#)). Thus, the [touch cells](#) form gap junctions with agonist interneurons and chemical synapses with the antagonist interneurons. This reciprocal pattern of connectivities led to the proposal that the gap junctions are excitatory and the synaptic connections are inhibitory ([Chalfie et al. 1985](#)). The excitatory function of these gap junctions is supported by cell-killing experiments. Killing [AVD](#) in embryos eliminates anterior touch sensitivity in young larvae, whereas killing [PVC](#) eliminates posterior touch sensitivity. Analysis of the tap response (described below) provides some support for the inhibitory function of the touch cell-to-interneuron synapses ([Wicks and Rankin 1995](#)).

## 2. Roles for Touch Receptors in the Regulation of Multiple Behaviors

In addition to mediating touch avoidance, the [touch cells](#) also control the spontaneous rate of locomotion. Animals that lack functional [touch cells](#), either due to laser microsurgery or due to mutations that disrupt the sensory function of the [touch cells](#), are lethargic. Thus, in the same manner that [IL1](#) and [OLQ](#) regulate spontaneous foraging behavior, the [touch cells](#) play a part in spontaneous movement. In both cases, mechanical stimuli (sensed by these [mechanosensory neurons](#)) regulate spontaneous movements. The mechanical stimuli that drive spontaneous locomotion could be interaction with external objects or stretch produced by the locomotory movements themselves.

The [touch cells](#) synapse onto many cells that do not appear to be involved with locomotion ([White et al. 1986](#)). These include several putative [sensory neurons](#) ([CEP](#), [ADE](#), and [PDE](#)), the [RIP](#) interneurons, which connect the somatic [nervous system](#) with the pharyngeal [nervous system](#) (see [Avery and Thomas](#), this volume), and the [HSN](#) motor neurons, which control egg laying ([Chalfie et al. 1985](#)). Some of these connections are likely to be functional because body touch has been shown to regulate pharyngeal pumping ([Chalfie et al. 1985](#)), egg laying (B. Sawin, unpubl.), and defecation (Thomas 1990). However, the circuitry underlying these effects has not been experimentally verified. Although it apparently has no role in touch-mediated control of locomotion, [PVM](#) might mediate mechanosensory control of some of these other behaviors ([Chalfie et al. 1985](#)).

## 3. Changes in Touch Circuitry during Development

The circuit for gentle body touch sensitivity is modified during the course of development. Four [touch cells](#) ([ALML/R](#) and [PLML/R](#)) are born during embryogenesis and two ([AVM](#) and [PVM](#)) are born during larval development. At maturity, [AVM](#) forms gap junctions with the [ALM](#) cells in the [nerve ring](#), creating an anterior touch cell network. [AVM](#) can, however, mediate a partial touch response independently of the [ALM](#) neurons. When both [ALM](#) cells are killed in the embryo, the resulting larvae initially lack anterior touch sensitivity, but 35–40 hours after hatching, partial touch sensitivity returns ([Chalfie and Sulston 1981](#)). Similarly, killing the [AVD](#) interneurons in the embryo eliminates anterior touch sensitivity early in L1, yet touch sensitivity is restored later in larval development ([Chalfie et al. 1985](#)). In both cases, restoration of touch sensitivity requires a functional [AVM neuron](#). These results demonstrate that [AVM](#), which arises in the first larval stage, does not function until the fourth larval stage and that [AVM](#) makes at least two kinds of connections that can mediate touch sensitivity. The connections dependent on the [AVD](#) neurons are likely to be the identified gap junctions between [AVM](#) and [AVD](#). The second functional connections appear to be chemical synapses (since [AVM](#) forms gap junctions only with [ALM](#) and [AVD](#)). The other [AVM](#) target has been proposed to be [AVB](#), which receives synaptic input from [AVM](#). These [AVM](#)-to-[AVB](#) synapses are presumed to be inhibitory because [AVM](#) mediates touch stimulation of backward movement, whereas [AVB](#) promotes forward movement ([Chalfie et al. 1985](#)). However, because [AVM](#) also provides input to other [neurons](#), the identity of the functional [AVM](#) synaptic target is uncertain.

Although the [AVM](#) synaptic targets have not been unambiguously identified, the function of the [AVM](#) chemical synapses has been genetically characterized. The [avr-15](#) and [eat-4](#) genes are required for [AVM](#) function when the [AVD](#) neurons have been killed, implying that these genes are required for functional [AVM](#) chemical synapses (B. Sawin, pers. comm.). Several experiments suggest that [avr-15](#) and [eat-4](#) are components of glutamatergic synapses. First, both [avr-15](#) and [eat-4](#) are required for [pharyngeal muscle](#) relaxation, mediated by the inhibitory motor [neuron M3](#) (Raizen and Avery 1994; see [Avery and Thomas](#), this volume). [eat-4](#) is required for [M3](#) function and [avr-15](#) is required for the postsynaptic response to the [M3](#) neurotransmitter, which has been tentatively identified as glutamate (J. Dent and L. Avery, pers. comm.). Second, [eat-4](#) mutants are defective for other behaviors mediated by glutamatergic synapses, including nose touch, which has led to the proposal that the [EAT-4](#) protein is required globally for glutamatergic neurotransmission (A. Hart and J. Kaplan, unpubl.; R. Lee and L. Avery, pers. comm.). Third, mutations in the [avr-15](#) gene also confer resistance to the antihelminthic drug avermectin (C. Johnson, pers. comm.) which appears to affect a glutamate-gated chloride channel (Cully et al. 1994). On the basis of this evidence, Avery and colleagues have proposed that [AVM](#) is glutamatergic and that the [AVM](#)-to-[AVB](#) synapses are functional and inhibitory as originally suggested by Chalfie et al. (1985).

## E. Circuitry for the Tap Response

As mentioned above, the anterior and posterior touch circuits are interconnected in two ways: (1) Touch cells make reciprocal connections to the opposing classes of [interneurons](#) (described above) and (2) the forward and backward interneurons form reciprocal connections (see [Fig. 2C](#)). These interconnections suggest that the anterior and posterior touch circuits functionally interact, perhaps allowing integration of opposing mechanosensory inputs. The capacity of these circuits for integration is beginning to be understood through the analysis of the tap response. Worms respond to a diffuse mechanical stimulus (a tap to the side of the dish on which they are resting) either by accelerating forward movement or by initiating backward movement ([Chiba and Rankin 1990; Rankin 1991](#)). Given that the stimulus is not spatially coherent and that the animal's response is variable, it was proposed that the tap response reflects the simultaneous activation of the anterior and posterior [touch cells](#). The cellular basis of the tap response has been analyzed extensively (Wicks and Rankin 1995; see [Jorgensen and Rankin](#), this volume). Since the tap response can be quantitated (as prevalence or magnitude of accelerations vs. reversals), relatively subtle effects of cell killing can be detected. As predicted, both the anterior ([ALM](#) and [AVM](#)) and posterior ([PLM](#)) [touch cells](#), and their interneuron targets ([AVD](#) and [PVC](#)), contribute to the tap response, the anterior cells promoting reversals and the posterior cells promoting accelerations ([Fig. 2E](#)). Disabling either the anterior or posterior touch circuits results in exaggeration of the opposing response. For example, animals lacking [PLM neurons](#) respond to tap solely with reversals, and these reversals are of greater magnitude than those of unoperated controls. Similarly, animals lacking the [PVC](#) interneurons (which mediate accelerations) always respond to tap by reversing, although the magnitude of their reversals is indistinguishable

from that of unoperated controls. These results show that the anterior and posterior touch circuits functionally inhibit each other. Furthermore, since killing [PLM](#) and PVC produced distinct phenotypes, these results also suggest that [PLM neurons](#) make functional connections other than the gap junctions with PVC. One attractive possibility is that [PLM](#) inhibits the magnitude of reversals via chemical synapses with the backing interneurons AVA and AVD.

Although the tap response can be thought of as a competition between the anterior and posterior touch circuits, there also are [neurons](#) that promote the activities of both circuits. The [PVD](#) and [DVA neurons](#) are presynaptic to both the forward and backing [interneurons](#), and animals lacking these [neurons](#) respond to tap with diminished accelerations and reversals. Therefore, [PVD](#) and [DVA](#) appear to maintain the overall activity of the touch circuit. Since [PVD neurons](#) are mechanosensory ([Way and Chalfie 1989](#)), it is possible that the excitability of the touch circuit is modulated by mechanical stimuli. Thus, the tap response comprises the simultaneous activation of anterior and posterior [touch cells](#), with the behavioral outcome being determined by the integration of these two antagonistic circuits (see [Jorgensen and Rankin](#), this volume).

The tendency of animals to respond to tap with accelerations versus reversals varies over the course of development. Accelerations predominate in larvae and reversals predominate in adults ([Chiba and Rankin 1990](#)). Because this developmental switch occurs in young adults (i.e., 46–50 hours after hatching), it has been proposed that this change reflects the formation of functional connections by the [AVM neuron](#). However, adults lacking [AVM](#) do not behave like larvae, as they respond to tap by reversing much more often than accelerating ([Wicks and Rankin 1995](#)). Therefore, this developmental switch must reflect more than the addition of [AVM neurons](#) to the circuit—perhaps the addition of the [PVD neurons](#) contributes to the developmental switch.

## F. Circuitry for the Response to Harsh Touch

Although animals lacking functional [touch cells](#) are insensitive to touch with an eyelash, they remain sensitive to prodding with a platinum wire (typically responding by undergoing backward movement) ([Chalfie and Sulston 1981](#)). This result suggested that a separate mechanosensory circuit mediates sensitivity to harsh touch stimuli ([Fig. 2D](#)). The [PVD neurons](#) are thought to be harsh touch [sensory neurons](#) for several reasons. First, the [PVD neurons](#) have long undifferentiated processes that run along the lateral body wall, which could be mechanosensory ([White et al. 1986](#); E. Hedgecock, pers. comm.). Second, the [PVD neurons](#) express genes involved in touch cell differentiation (e.g., [mec-3](#), see below), implying that they may also be mechanosensory ([Way and Chalfie 1989](#)). Third, killing the [PVD neurons](#) in animals that lack touch cell function eliminates harsh touch sensitivity ([Way and Chalfie 1989](#)). The locomotion [interneurons](#) AVA and PVC are direct synaptic targets of PVD. Mutants lacking GLR-1 glutamate receptors (which are expressed by the locomotory [interneurons](#)) are insensitive to harsh touch, which suggests that these synapses are functional and that glutamate is the [PVD](#) transmitter ([Hart et al. 1995](#)).

## Figures

Figure 2. Mechanosensory circuits.

### Figure 2

Mechanosensory circuits. (Ovals) Sensory [neurons](#); (rectangles) [interneurons](#); (inverted triangles) motor [neurons](#). Cells that express [glr-1](#) glutamate receptors are black. Synaptic connections are indicated by lines with triangles; gap junctions by lines with bars. Connectivities are as described by White et al. (1986). To simplify the illustration, gap junctions between ASH and AVD and between PVC and AVA are not shown. (A) ASH neurons respond to three stimuli, all of which stimulate backward locomotion ([Bargmann et al. 1990](#); [Kaplan and Horvitz 1993](#); [Troemel et al. 1995](#)). ASH provides synaptic input to [interneurons](#) that control backward (AVA and AVD) and forward (AVB) movement. Animals lacking [glr-1](#) glutamate receptors are defective for ASH-mediated touch sensitivity but are normal for ASH-mediated osmotic and volatile-repellent sensitivity ([Hart and Kaplan 1995](#); [Maricq et al. 1995](#)). (B) Mechanosensory neurons IL1 and OLQ, and the RMD motor neurons regulate the rate of

spontaneous foraging and mediate an aversive response to touch to the ventral or dorsal tip of the nose (J. Kaplan and H.R. Horvitz, unpubl.). *glr-1* mutants forage abnormally slowly and are defective for the head withdrawal reflex (Hart and Kaplan 1995). (C) The mechanosensory neurons ALM, AVM, and PLM sense touch to the body and provide input to the command neurons via both synaptic connections and gap junctions (Chalfie et al. 1985). Anterior and posterior body touch stimulates backward and forward locomotion, respectively. The anterior touch cells ALM and AVM are connected by a gap junction, which creates an anterior touch cell network. AVM neurons also function independently of the ALM neurons, presumably via the gap junctions with AVD and the synaptic connections with AVB. (D) Harsh touch sensitivity is mediated by the PVD sensory neurons, which provide synaptic input to AVA and PVC (White et al. 1986; Way and Chalfie 1989). These synapses appear to require GLR-1 glutamate receptors, since *glr-1* mutants are insensitive to harsh touch (Hart and Kaplan 1995). (E) A diffuse mechanical stimulus (tap) simultaneously activates both the anterior and posterior touch circuits. Two behavioral responses to tap are observed, accelerations of forward movement and reversals. Which of these responses occurs appears to be determined by integration of the antagonistic activities of the anterior and posterior touch circuits (Wicks and Rankin 1995). Not shown are PVD (but see panel D) and DVA which provide input to both the anterior and posterior circuits and appear to enhance both reversals and accelerations.

Figure 3. The touch receptor neurons.

### Figure 3

The touch receptor neurons. (A) Positions and general structure (White et al. 1986). Cell bodies of the embryonically derived ALM cells are situated laterally; long processes extend anteriorly and branch near the nerve ring. Of the bilaterally symmetric pair, only ALML is shown. Most ALM synaptic connections, including the gap junctions with AVM, occur on the synaptic branch (magnified in inset). The postembryonically derived AVM cell joins the touch circuit late in development via connections made on its synaptic branch. The bilaterally symmetric PLMs are situated laterally and branch at their anterior termini to approach the ventral nerve cord—PLMR (not shown) enters the cord to connect to several interneurons; PLML is blocked by the hypodermal ridge and does not enter the ventral cord. PVM is generated postembryonically. The PVM process initially extends dorsally along a commissure and turns to extend anteriorly at the ventral edge of the ventral nerve cord, adjacent to the cuticle. PVM, which does not mediate a locomotory response to gentle touch (Chalfie and Sulston 1981), is unbranched. (B) Electron micrograph of a cross section of the touch receptor ALML. The ALM neuron is embedded in the hypodermis (H) and extends its process adjacent to the cuticle (C). Indicated also are darkened regions at the cuticle edge that are hypothesized to anchor the touch cell to the cuticle (D). Two distinguishing features of the touch receptors are the 15-protofilament microtubules (MT) and the osmophilic specialized extracellular matrix that surrounds the receptor process, the mantle (M). (Adapted, with permission, from Chalfie and Sulston 1981.)

Generated from local HTML

# Chapter 23. Mechanotransduction — III Touch Receptor Development and Differentiation

---

The best-studied [mechanosensory neurons](#) are the six touch receptor cells. More than 400 mutants that lack the ability to respond to gentle touch but exhibit otherwise normal locomotion and responsiveness to harsh touch have been identified ([Chalfie and Sulston 1981](#); [Chalfie and Au 1989](#)). These mutations define 18 genes that have various roles in touch cell development and differentiation. We briefly summarize current understanding of combinatorial gene action that culminates in establishment of the differentiated touch receptor fate. We then review molecular genetic studies of the genes needed for mechanoreceptor function and discuss a molecular model for mechanotransduction based on this work. Genes have been identified that function in the execution of the cell lineage that generates the [touch receptors](#), the specification of touch cell fate, the restricted expression of touch cell structural genes, cell migrations, and process outgrowth. Interestingly, none of these genes are devoted exclusively to development and differentiation of the [touch receptor neurons](#).

## A. Gene Action in Development

The [ALM](#), [PLM](#), and [AVM/PVM](#) cells are derived from three distinct lineages via different patterns of cell divisions, yet the six [touch receptor neurons](#) express nearly identical terminally differentiated features. How is touch receptor fate specified? The activities of at least three regulatory proteins are required in the final steps of the cell lineages that generate some or all of the [touch receptor neurons](#). LIN-14 is a nuclear protein that acts as a genetic switch controlling the choice to execute the sublineage which generates the postembryonic [touch cells](#) [AVM/PVM](#) ([Ambros and Horvitz 1984](#); [Ruvkun and Guisto 1989](#); [Mitani et al. 1993](#)). LIN-32, which encodes a member of the basic helix-loop-helix family of transcription factors related to the *Drosophila atonal* gene ([Zhao and Emmons 1995](#)), influences the generation of precursors for the [PLM](#) and the [AVM/PVM](#) cells. The UNC-86 POU homeodomain protein directs appropriate differentiation of [neuroblasts](#) that generate all six [touch receptor neurons](#) ([Chalfie et al. 1981](#); [Finney et al. 1988](#)). A key function of UNC-86 in touch receptor development is to initiate expression of [mec-3](#). MEC-3 is an LIM homeodomain protein ([Freyd et al. 1990](#)) that is expressed in the six [touch receptors](#) (as well as in FLP and [PVD](#)) and is needed for specification of the touch cell fate ([Way and Chalfie 1988](#); [Way and Chalfie 1989](#); [Way et al. 1991](#); [Xue et al. 1992](#)). [mec-3](#) is expressed only in the anterior daughters of a terminal cell division of [unc-86](#)-expressing cells, an asymmetric expression pattern that depends in part on the activities of the [lin-17](#), [unc-73](#), [unc-40](#), and [pag-3](#) genes ([Way et al. 1992](#); [Jia et al. 1996](#)).

In the absence of [mec-3](#), the lineages that generate the [touch cells](#) are normal, but the cells produced differentiate as [neurons](#) that fail to express touch-cell-specific features; in the case of the ALMs, the [neurons](#) express traits of the BDU cells, their lineage sisters ([Chalfie and Sulston 1981](#); [Way and Chalfie 1988](#)). The MEC-3 homeodomain protein has proven to direct expression of touch-cell-specific structural genes, including the [mec-7](#)  $\beta$ -tubulin and the [mec-4](#) channel subunit ([Way et al. 1991](#); [Hamelin et al. 1992](#); [Xue et al. 1992](#); [Mitani et al. 1993](#)). Critical to MEC-3 function is its association with UNC-86 to form heterodimers that bind to well-defined sites in the [mec-3](#) promoter and other touch cell promoters ([Xue et al. 1993](#); [Lichtsteiner and Tjian 1995](#); see [Ruvkun](#), this volume). Once MEC-3 is expressed in the [touch cells](#), it activates its own synthesis ([Way and Chalfie 1989](#)), probably as a heterodimer with UNC-86 ([Xue et al. 1993](#)). Later in development, [mec-17](#) also contributes to maintenance of [mec-3](#) expression. [unc-86](#) continues to be expressed in differentiated [touch receptors](#) ([Finney and Ruvkun 1990](#)) and is continuously needed for their function. [lin-32](#) appears to be needed for maintenance of touch-cell-specific gene expression in at least the [ALM](#) cells ([Hamelin et al. 1992](#)).

Several genes that act to inhibit expression of touch-cell-specific genes in inappropriate cells have been identified ([Mitani et al. 1993](#)). [egl-44](#) and [egl-46](#) turn off expression of the [mec-7](#)  $\beta$ -tubulin in the FLP neurons, [pag-3](#) turns off expression of [mec-7](#) in the lineage sisters of the [ALM](#) cells, the BDUs ([Jia et al. 1996](#)), and [sem-4](#) prevents [mec-3](#) expression in the tail [PHC neurons](#) ([Mitani et al. 1993](#)).

## B. Genes and Environmental Cues Influencing Cell Migration and Process Outgrowth

The [ALM neurons](#) arise in the anterior body and migrate posteriorly to the midbody during embryogenesis; the [AVM](#) and [PVM](#) positions are determined by the migrations of their precursor cells [QR](#) and [QL](#), respectively. The activities of the [egl-27](#), [hch-1](#), [mab-5](#), [unc-11](#), [unc-40](#), and [unc-73](#) influence the Q cell migrations ([Hedgecock et al. 1987](#); [Salser and Kenyon 1992](#); see [Antebi et al.](#), this volume). Mutations in many additional genes affect outgrowth of touch cell processes, resulting in premature termination; abnormal growth in dorsal, ventral, and lateral directions; abnormal varicosities; and abnormal branching of processes ([Siddiqui 1990](#); [Siddiqui and Culotti 1991](#); [McIntire et al. 1992](#)). Genes that act specifically in touch receptor outgrowth have not been identified.

Cell ablation studies established that there is a prolonged delay before [AVM](#) becomes functional. The [AVM neuron](#) arises in the L1 approximately 10 hours after hatching ([Sulston and Horvitz 1977](#)), yet its function cannot be detected until the L4, 35–40 hours after hatching ([Chalfie and Sulston 1981](#)). This discrepancy suggests that some aspect of [AVM](#) development (e.g., differentiation, axon outgrowth, or synapse formation) could be delayed. Factors that determine the timing of [AVM](#) development have not been characterized, but there are several other examples of delayed differentiation of postembryonic [neurons](#) (e.g., the HSNs and VCs). Perhaps the heterochronic genes (e.g., [lin-4](#) and [lin-14](#)), which control the timing of larval lineages ([Ambros and Horvitz 1984](#); [Ambros 1989](#); [Ruvkun and Giusto 1989](#); see [Ambros](#), this volume) and are involved in the lineage decision that generates the postembryonic [touch cells](#), also control the timing of development of [AVM](#) and other [neurons](#).

Outgrowth of the [AVM](#) process appears to depend on the BDU cell for guidance cues ([Walthall and Chalfie 1988](#)). As noted above, [AVM](#) forms functional connections about 25 hours after it is born. If BDU is killed early during process outgrowth, [AVM](#) can no longer mediate a touch response. If BDU is killed late in development, [AVM](#) function is not affected. Since BDU does not synapse onto [interneurons](#) needed for backward movement, and since many synapses are formed between [AVM](#) and BDU, it seems that BDU serves to guide [AVM](#) process outgrowth.

Environmental cues independent of those supplied by BDU influence branching of postembryonic [touch cells](#) near the [nerve ring](#) ([Chalfie et al. 1983](#); [Walthall and Chalfie 1988](#)). The [AVM](#) process normally branches near the [nerve ring](#), whereas the [PVM](#) process, which terminates in the midbody, does not branch. If the [AVM](#) precursor is prevented from migrating anteriorly by a barrier of debris created with a laser microbeam, the [neuron](#) differentiates and extends a process that does not reach the [nerve ring](#) and does not branch. Conversely, if the [PVM](#) precursor migrates anteriorly, as occurs in the [mab-5](#) background, its process branches and the cell can make functional connections. These data support the conclusion that local environmental signals dictate branch formation, although it cannot be ruled out that [PVM](#) adopts the [AVM](#) fate in the absence of [mab-5](#).

Generated from local HTML

# Chapter 23. Mechanotransduction — IV Genes Required for Touch Receptor Function

---

## A. *mec-7* and *mec-12* Tubulins

The touch receptor cell processes (Fig. 3B) are filled with a distinctive bundle of wide-diameter microtubules that contain 15 protofilaments (Chalfie and Thomson 1979, 1982). (Microtubules present in most *C. elegans* cells contain 11 protofilaments; those in most organisms contain 13 protofilaments.) Individual microtubules 10–20  $\mu\text{m}$  long do not span the full length of the touch cell processes, which is about 400–500  $\mu\text{m}$ . Rather, overlapping microtubules are positioned along the touch cell process. The microtubule ends appear to be structurally distinct—The end proximal to the cell body appears darkened and is preferentially found on the inside of a microtubule bundle, whereas the distal end is diffusely stained and is always situated outside of the microtubule bundle. Interestingly, the distal end is often juxtaposed to the plasma membrane and thus could potentially form a mechanical link between the microtubule network and mechanosensory receptors in the plasma membrane.

The 15-protofilament microtubules are required for mechanosensory function. In *mec-7* null mutants and some *mec-12* loss-of-function mutants, the 15-protofilament microtubules are absent from the [touch receptor neurons](#), and, consequently, the animals are touch-insensitive (Chalfie and Sulston 1981). *mec-7* encodes a 440-amino-acid  $\beta$ -tubulin and *mec-12* encodes a 450-amino-acid  $\alpha$ -tubulin (Savage et al. 1989; Hamelin et al. 1992). Both genes are highly expressed in the touch [neurons](#) (Mitani et al. 1993; Savage et al. 1994; M. Hamelin et al., pers. comm.). *mec-12* is also expressed at high levels in several other cells, including ventral cord DB, VA, and [VD neurons](#) and the CAN neuron. Unlike the touch [neurons](#), these cells do not have 15-protofilament microtubules; therefore, *mec-12* expression alone is not sufficient for formation of wide-diameter microtubules. Apart from the carboxy-terminal domain, which is highly variable among  $\beta$ -tubulins, only seven amino acid residues distinguish MEC-7 from other isoforms (Savage et al. 1989). These unique amino acids may have an instructive role in determination of protofilament number. Taken together, studies of *mec-7* and *mec-12* suggest that the 15-protofilament microtubules are composed of MEC-7 and MEC-12  $\beta$  and  $\alpha$  tubulins and are essential for mechanosensory transduction.

What role do the 15-protofilament microtubules have in touch cell function? These microtubules are not essential for axon outgrowth, since touch receptor processes are formed normally in *mec-7* mutants (Chalfie and Sulston 1981). Touch cell processes in *mec-7* (null) animals are not devoid of microtubules altogether—11-protofilament microtubules, normally all but absent in the [touch cells](#), partially replenish the microtubule content of the axons (Chalfie and Thomson 1982). This suggests that the 11-protofilament microtubules may partially compensate for the lack of MEC-7 tubulin, thereby allowing normal axon outgrowth. The 15-protofilament microtubules do, however, have some capacity to influence process outgrowth. Touch cell processes are extended or produced at ectopic sites as a consequence of two particular *mec-7* missense alleles (Savage et al. 1994). Whatever their contribution to touch cell development, microtubule integrity appears to be essential for mechanosensory function of the [touch receptor neurons](#). If touch cell microtubules are disrupted in low concentrations of colchicine, touch sensitivity is lost (Chalfie and Thomson 1982).

## B. Genes Affecting the Extracellular Mantle

A second distinguishing feature of the [touch receptor neurons](#) is that their processes are surrounded by a specialized extracellular matrix referred to as the mantle (see Fig. 3B) (Chalfie and Sulston 1981). Darkly staining cuticular specializations are positioned periodically along the length of the touch receptor process, in close contact with the mantle. The cuticular specializations look similar to muscle attachment sites and thus they may be sites at which the touch receptor process is fixed to the cuticle.

It appears that the touch cell processes must be closely apposed to the hypodermis for mantle production. In *mec-1* mutants, [touch cells](#) lack the mantle and associated periodic specializations of the overlying cuticle; the [ALM](#) processes run along body wall musculature, rather than within the hypodermis (Chalfie and Sulston 1981).

However, where portions of the touch processes are embedded within the hypodermis in *mec-1* mutants, the mantle is observed. Two equally plausible models could account for these results: The mantle may be essential for positioning the touch cell processes, or, conversely, failure to correctly position the processes results in the lack of the mantle. Molecular analysis of the *mec-1* gene should distinguish between these possibilities. *mec-1* action does not appear to be specific to the *touch cells* since amphidial defects have been noted in some *mec-1* mutants (Lewis and Hodgkin 1977; Chalfie and Sulston 1981; Perkins et al. 1986).

The *mec-5* and *mec-9* genes may encode structural components of the mantle. *mec-5* encodes a collagen expressed by the hypodermis (Du et al. 1996). No obvious ultrastructural defects are observed in *mec-5* mutants, although a subtle mantle abnormality—inability to bind peanut lectin—has been noted (Chalfie and Sulston 1981; E. Hedgecock and M. Chalfie, unpubl.). Mutations in the *mec-9* gene do not detectably alter the mantle, although *mec-9* encodes a secreted protein (Chalfie and Sulston 1981; Du et al. 1996). The *mec-9* gene encodes two transcripts, the larger of which encodes a 834-amino-acid protein that is expressed only in the *touch receptors*. The predicted MEC-9 protein contains a glutamic-acid-rich domain and several domains related to the Kunitz-type serine protease inhibitor domain, Ca<sup>+</sup>-binding EGF repeats and non-Ca<sup>+</sup>-binding EGF repeats (Du et al. 1996). *mec-9* mutations are dominant enhancers of a *mec-5* (*ts*) allele, suggesting that these proteins might interact in the extracellular matrix outside the touch receptor *neuron* (Du et al. 1996; Gu et al. 1996). Potential roles for MEC-5 and MEC-9 in mechanotransduction are discussed below.

## C. Genes That May Encode Subunits of a Mechanosensory Ion Channel

Loss-of-function mutations in *mec-4* and *mec-10* disrupt touch sensitivity but do not alter touch receptor ultrastructure (Chalfie and Sulston 1981). A few observations suggest that *mec-4* and *mec-10* could encode subunits of a mechanically gated ion channel. First, these genes encode proteins related to subunits of the vertebrate amiloride-sensitive Na<sup>+</sup> channels, which are required for ion transport across epithelia (Driscoll and Chalfie 1991; Huang and Chalfie 1993; Chalfie et al. 1994; Canessa et al. 1993, 1994b; Lai et al. 1996). Although channel activity has not yet been directly demonstrated for either MEC-4 or MEC-10, certain nematode/rat chimeric proteins function in *C. elegans* and *Xenopus* oocytes, implying that the nematode and rat proteins are functionally similar (Hong and Driscoll 1994; Waldmann et al. 1995). Second, *mec-4* and *mec-10* are coexpressed nearly exclusively in the *touch receptor neurons* (Mitani et al. 1993; Huang and Chalfie 1994). Third, *mec-4* and *mec-10* are crucial for the mechanosensitivity of the touch *neurons*. For these reasons, it has been proposed that MEC-4 and MEC-10 could function in a mechanically gated ion channel, i.e., one that opens in response to membrane stretch or to mechanical displacement of a channel domain. Alternatively, the MEC-4/MEC-10-containing channels could be required to maintain the ionic milieu of the *touch cells*.

Additional members of this Na<sup>+</sup> channel superfamily have been identified. *C. elegans* family members were called degenerins because dominant alleles of *mec-4* and *deg-1* induce neurodegeneration. These genes encode proteins similar in size (724–778 amino acids for currently characterized degenerins) which, like all family members, have two putative transmembrane domains. The more amino-terminal of these is hydrophobic, whereas the more carboxy-terminal of these (MSDII) is amphipathic. Genetic evidence (Hong and Driscoll 1994) and electrophysiological characterization of rat and rat/nematode chimeras (Waldmann et al. 1995) support the hypothesis that MSDII constitutes a pore-lining domain and that highly conserved hydrophilic residues in MSDII face into the channel lumen to influence ion flow. Interestingly, both hydrophobic domains are slightly longer than required for a single transmembrane domain. For this reason, it has been proposed that MSDI and MSDII include residues that loop back into the membrane forming a pore, similar to H5 domains of several characterized channel types (Jan and Jan 1994; Renard et al. 1994; García-Añoveros et al. 1995). Analysis of both the vertebrate and *C. elegans* proteins suggests that the amino and carboxyl termini are cytoplasmic and the central region is extracellular (Canessa et al. 1994a; Renard et al. 1994; Snyder et al. 1994; García-Añoveros et al. 1995; Lai et al. 1996).

Dominant gain-of-function *mec-4* alleles induce swelling and death of the *touch receptor neurons* (Chalfie and Sulston 1981; Chalfie and Au 1989; for discussion of degenerate cell death, see Hengartner, this volume). Toxic

*mec-4* (*d*) alleles encode substitutions of large side-chain amino acids for a conserved alanine residue (A713) situated adjacent to MSDII (Driscoll and Chalfie 1991; Lai et al. 1996). Since nontoxic *mec-4* alleles encode small side-chain amino acids at this position, steric hindrance is postulated to play a critical part in degeneration. A working model for the initiation of cell death is that the presence of a bulky side chain at position 713 prevents the channel from closing effectively, producing an increased influx of ions that proves toxic. Consistent with such a model, amino acid substitutions in the predicted pore domain (which are likely to disrupt ion influx) block or delay degeneration (Hong and Driscoll 1994). Substitutions at the site corresponding to MEC-4 (A713) in degenerin family members *deg-1* and *mec-10* (*mec-10* [A673V]) also cause neuronal swelling and death which can be blocked by the presence of a second-site substitution in the predicted pore-lining domain (Huang and Chalfie 1994; García-Añoveros et al. 1995; Shreffler et al. 1995). Thus, the conserved alanine residue and the potential for toxic misregulation of channel activity by large amino acid substitutions at this site thus far appear to be general features of the degenerin gene family.

What is the subunit composition of the degenerin-containing channels? Coexpression of three distinct but homologous subunits of the rat amiloride-sensitive Na<sup>+</sup> channel is required to reconstitute in vivo pharmacological properties of the channel in *Xenopus* oocytes (Canessa et al. 1994b). Furthermore, biochemical characterization of the mammalian epithelial Na<sup>+</sup> channels suggests as many as six different subunits (Benos et al. 1987; Ausiello et al. 1992). The *mec-6* gene may encode an additional subunit of the *C. elegans* degenerin ion channels. *mec-6* mutations disrupt touch cell function and block *mec-4* (*d*)-and *mec-10* (A673V)-induced degeneration (Chalfie and Wolinsky 1990; Huang and Chalfie 1994), consistent with the hypothesis that *mec-6* encodes a third protein required for channel assembly or function.

Genetic interactions between *mec-4* and *mec-10* alleles also suggest that the touch receptor channel is multimeric. Specific *mec-4* alleles suppress the toxicity of a *mec-4* (*d*) allele in *trans*-heterozygotes (Hong and Driscoll 1994). Likewise, one *mec-10* allele can act in *trans* to suppress degeneration induced by the engineered toxic variant of *mec-10*, *mec-10* (A673V) (Huang and Chalfie 1994). Thus, MEC-4 and MEC-10 homomultimeric interactions are likely to occur in vivo. The fact that *mec-4* (*lf*) mutations suppress cell death induced by *mec-10* (A673V) supports the idea that MEC-4 and MEC-10 also interact with each other (Huang and Chalfie 1994). One interpretation of the observed genetic interactions is that the minimal channel complex may include at least two subunits of MEC-4, two of MEC-10, and one of MEC-6. An alternative explanation for the heteroallelic interactions is that individual subunits compete for assembly into a multimeric complex.

## D. The Degenerin Gene Family

A relatively large family of degenerins is encoded in the *C. elegans* genome (at least 13 closely related members reported to date by the Genome Sequencing Project). Multiple subunit genes, differential splicing, and differential expression patterns seem to contribute to the diversity of channel functions mediated by *C. elegans* family members; this diversity appears to include signal transduction in specialized mechanosensory cells, muscle contraction, and possibly volume control in diverse cell types. Since characterization of other family members provides some insight into the function of the channel in the *touch receptors*, we briefly digress to review current data on the degenerin family here.

Although the *C. elegans* degenerins share approximately 25–30% sequence identity with their vertebrate counterparts, clear differences distinguish vertebrate and *C. elegans* family members. A cysteine-rich domain and a 22-amino-acid region in the ectodomain (García-Añoveros et al. 1995; see below) are unique to the *C. elegans* proteins. In addition, the carboxyl termini of *C. elegans* degenerins lack the proline-rich regions important to the function of the vertebrate proteins. In the rat, a proline-rich SH3-binding domain in the rat  $\alpha$ -subunit interacts with spectrin to direct the channel to the apical side of the epithelial cell (Rotin et al. 1994). In humans, the proline-rich carboxy-terminal domains of the  $\beta$  and  $\gamma$  subunits of the human epithelial Na<sup>+</sup> channel have important roles in regulating channel function since Liddle's syndrome, a hypertensive disorder caused by elevated channel activity, is caused by deletions of these domains (Shimkets et al. 1994; Hansson et al. 1995).

## 1. deg-1

The first molecularly characterized family member, [\*deg-1\*](#) (named for degeneration), was identified by a dominant gain-of-function allele (*u38*) that induces swelling and death of multiple [\*neurons\*](#) that are unrelated by cell lineage, position, or function (Chalfie and Wolinsky 1990). The PVC [\*interneuron\*](#) that mediates the posterior touch response dies late in larval development in the [\*deg-1\*](#) (*u38*) background, and thus the mutants have a Tab (touch abnormal) phenotype: They respond neither to gentle touch nor to strong prods on the posterior. The ASH neurons also die in [\*deg-1\*](#) (*u38*), rendering mutants insensitive to nose touch (A. Hart and J. Kaplan, unpubl.; C. Bargmann, pers. comm.). Interestingly, loss-of-function [\*deg-1\*](#) mutations isolated as intragenic suppressors of [\*deg-1\*](#) (*u38*) mediated death have no apparent phenotype, suggesting either that [\*deg-1\*](#) activity is not required for PVC and ASH function or that [\*deg-1\*](#) is functionally redundant (Chalfie and Wolinsky 1990; García-Añoveros 1995; A. Hart and J. Kaplan, unpubl.). [\*mec-6\*](#) mutations suppress [\*deg-1\*](#) (*u38*)-induced cell death, implying that the [\*deg-1\*](#) channel complex could include this candidate subunit.

[\*deg-1\*](#) encodes a predicted protein of 778 amino acids, although alternative processing of [\*deg-1\*](#) transcripts can remove up to 42 amino acids from the protein (Chalfie and Wolinsky 1990; García-Añoveros et al. 1995; Shreffler et al. 1995). As noted above, dominant death-inducing [\*deg-1\*](#) mutations affect the conserved alanine residue corresponding to the site affected by dominant degeneration-inducing mutations in the [\*mec-4\*](#) (*d*) mutant (García-Añoveros et al. 1995; Shreffler et al. 1995). A recessive degeneration-inducing [\*deg-1\*](#) allele, *u506*, encodes an A393T substitution in a 22-amino-acid sequence in the predicted extracellular domain that is conserved among the *C. elegans* family members but is missing from the mammalian proteins (García-Añoveros et al. 1995). Introduction of the same amino acid change into MEC-4 also creates a toxic allele. Ionic influx is implicated in toxicity by this extracellular substitution since mutations that disrupt the predicted channel pore block killing by the [\*deg-1\*](#) (A393T) mutation. These results suggest that the 22-amino-acid extracellular domain could regulate ionic flux through these channels. An extracellular gating domain unique to *C. elegans* family members could confer rapid channel gating properties, distinguishing it from the vertebrate epithelial channel, which has long open times.

## 2. unc-105

At least one member of the degenerin family can dramatically affect muscle function. Unusual semidominant alleles of the [\*unc-105\*](#) gene induce hypercontraction of body wall muscles (Park and Horvitz 1986a). Null alleles of [\*unc-105\*](#) do not have an apparent phenotype, suggesting functional redundancy. Molecular analysis established that [\*unc-105\*](#) encodes a degenerin and that semidominant [\*unc-105\*](#) mutations affect residues near, but not at, the site of the alanine residue affected in [\*mec-4\*](#) (*d*) and [\*deg-1\*](#) (*d*) (B. Shrank et al., pers. comm.). The [\*unc-105\*](#) (*sd*) mutation causes muscle hypercontraction presumably because muscle cells are depolarized by inappropriate ion influx. Specific alleles of [\*let-2\*](#) (also known as [\*sup-20\*](#)) restore locomotion to [\*unc-105\*](#) (*sd*) animals (Park and Horvitz 1986b; J. Liu and R. Waterston, pers. comm.). [\*let-2\*](#) encodes an essential basement membrane collagen (Sibley et al. 1993; see Kramer, this volume), suggesting that UNC-105 may function in a stretch-responsive channel in [\*body wall muscle\*](#) that is gated via attachment to collagen in the extracellular matrix. Alternatively, by analogy to the mammalian epithelial sodium channels, UNC-105 channels may primarily mediate vectorial ion transport. In this case, the functional interaction with the LET-2 collagen could reflect the need to localize channels to a particular domain of the plasma membrane. In either case, these results underscore the likely importance of extracellular matrix in the function of degenerin channels.

## 3. unc-8

Dominant [\*unc-8\*](#) alleles cause periodic swelling of subsets of embryonically derived motor [\*neurons\*](#) (DB3-DA7) and other [\*neurons\*](#) in the head and tail [\*ganglia\*](#) (Shreffler et al. 1995). Affected cells do not die—swelling of midbody motor [\*neurons\*](#) begins after hatching, peaks in severity late in L1 and L2, and then regresses. [\*unc-8\*](#) mutants coil and are unable to back up, they lay eggs constitutively, and at least some are resistant to NDG (*N*-dihydroguaiaretic acid), a lipoxygenase inhibitor. NDG blocks a signal transduction pathway that opens FMRF-sensitive S-K<sup>+</sup> channels in *Aplysia* (Belardetti et al. 1989). Analysis of mutations that suppress [\*unc-8\*](#) (*d*)-induced

defects established that (1) *unc-8* null alleles have no apparent phenotype; (2) specific *unc-8* alleles can suppress or enhance *unc-8* mutations in *trans*, suggesting that UNC-8:UNC-8 interactions occur; and (3) *mec-6* mutations can suppress *unc-8* (*d*)-induced phenotypes (Shreffler et al. 1995). Similar genetic properties are exhibited by *deg-1* and some other degenerins, and thus it has been hypothesized that *unc-8* could encode another family member. Indeed, molecular analysis has established that *unc-8* encodes a degenerin family member (N. Tavernarakis et al., unpubl.).

Further support for UNC-8 association with degenerin-like channels comes from analysis of the dominant extragenic suppressor *sup-41* (*lb125*). In addition to suppressing *unc-8* (*d*) phenotypes, this allele partially suppresses the posterior touch insensitivity (the Tab phenotype) of a *deg-1* (*d*) allele (Shreffler et al. 1995). In contrast, *sup-40* (*lb130*) suppresses all phenotypes associated with *unc-8* (*d*) but does not alter *deg-1* (*d*) induced cell death (Shreffler et al. 1995). Unselected phenotypes of *sup-40* (*lb130*) include slow growth, production of fragile enlarged oocytes, swelling and occasional detachment of adult hypodermal nuclei, and strong NDG resistance. These phenotypes are expressed independently of the *unc-8* locus and are not affected by *mec-6* mutations.

## E. MEC-2, a Potential Protein Link between the Mechanosensory Channel and the Cytoskeletal Network

Mutant *mec-2* alleles appear to disrupt touch receptor function specifically. Among the 54 *mec-2* alleles are some that are semidominant or fully dominant and exhibit a complex pattern of interallelic complementation (Chalfie and Sulston 1981); these genetic data imply that MEC-2 proteins functionally interact in vivo. Features of the predicted 481-amino-acid MEC-2 protein also imply involvement in protein-protein interactions (Huang et al. 1995). The carboxy-terminal domain of MEC-2 has a proline-rich region that is similar to that of the SH3-binding domains. The central MEC-2 domain (amino acids 114–363) includes a hydrophobic domain (amino acids 114–141) and a cytoplasmic hydrophilic domain that together exhibit 65% identity to the human red blood cell (RBC) protein stomatin. Stomatin is an integral membrane protein that associates with the cytoskeleton and affects ion balance via an unknown mechanism. Interestingly, RBCs that lack stomatin (i.e., hereditary stomatocytosis) swell and exhibit elevated Na<sup>+</sup> permeability (Stewart et al. 1993).

Genetic evidence suggests that the MEC-2 protein functionally interacts with both the degenerin channels and the microtubule network. Certain *mec-2* alleles partially suppress *mec-10* (*d*)-induced death (Huang and Chalfie 1994). In addition, some recessive *mec-2* alleles act as dominant enhancers of a weak *mec-4* (*ts*) allele (Huang et al. 1995; Gu et al. 1996). In a wild-type background, a MEC-2LacZ fusion protein is distributed along the touch receptor axon as well as in the cell body; this distribution depends on the integrity of the 118-amino-acid amino-terminal MEC-2 domain, which is situated in the cytoplasm (Huang et al. 1995). The axonal distribution of a MEC-2LacZ fusion protein is mildly disrupted in a *mec-7* (*null*) or *mec-12* strong loss-of-function background. More dramatically, two specific *mec-12* missense alleles interfere with localization of MEC-2 fusion proteins, restricting the fusion proteins to the cell body (Huang et al. 1995). If the implied interactions are direct, a simple hypothesis is that MEC-2 may tether the 15-protofilament microtubules to the degenerin channel, an association that might enable mechanical deflection of microtubules to open the channel (Huang et al. 1995). These models must be considered highly speculative until the predicted biochemical interactions have been documented.

## F. Molecular Biology of Other *mec* Genes

Mutations in *mec-14* disrupt touch receptor function without altering ultrastructure (Chalfie and Au 1989). *mec-14* encodes a member of the superfamily that includes the β subunits that associate with, and modify the activity of, Shaker-type K<sup>+</sup> channels (N. Hom and M. Chalfie, pers. comm.). Since *mec-14* alleles can partially suppress *mec-10* (A673V)-induced death (Huang and Chalfie 1994), it appears that MEC-14 influences mechanosensory channel function. However, whether MEC-14 interacts with the touch receptor channel directly to modify activity via mechanisms similar to that of K<sup>+</sup> channel β subunits (see, e.g., Rettig et al. 1994) is not known.

*mec-8* most likely affects touch cell function indirectly by influencing expression of other *mec* genes. *mec-8* alleles disrupt touch sensitivity (Chalfie and Sulston 1981), but they also affect amphid and phasmid development, attachment of [body wall muscle](#) to the hypodermis and cuticle, and embryonic and larval development (Perkins et al. 1986; Lundquist and Herman 1994). The MEC-8 protein, which includes two RNA-binding motifs, is required for proper splicing of several messages including its own, that of the UNC-52 protein and that of the MEC-2 protein (M. Huang 1995; Lundquist et al. 1996).

The molecular identities of *mec-1*, *mec-6*, *mec-15*, *mec-17*, and *mec-18* remain to be elucidated. A *mec-15* allele partially suppresses *mec-10* (A673V), and *mec-18* alleles enhance *mec-10* (A673V)-induced deaths (Huang and Chalfie 1994), suggesting that the products of these genes could directly influence channel function.

## G. A Model for Mechanotransduction in Touch Receptor Neurons

The molecular identities of genes required for touch cell function suggest a model for how a mechanical stimulus such as gentle touch is transduced into a locomotory response (for a discussion of this model, see [Huang et al. 1995](#); [Du et al. 1996](#); G. Gu et al., pers. comm.). This model shares features of the proposed gating mechanism of mechanosensory channels that respond to auditory stimuli in the vertebrate inner ear ([Fig. 4](#)) (for review, see [Hudspeth 1989](#); [Pickles and Corey 1992](#)). In the inner ear, hair cells that have bundles of a few hundred stereocilia on their apical surface mediate sensory transduction. The stereocilia are connected at their distal ends to neighboring stereocilia by filaments called tip links. Directional deflection of the stereocilia relative to each other creates tension on the tip links; this tension is proposed to open the channels directly. Consistent with this model, the integrity of the tip links is essential for channel opening, and the mechanosensitive channels appear to be situated at the ends of the stereocilia, near the connecting tip links (Hudspeth 1982; Assad et al. 1991; Lumpkin and Hudspeth 1995; Denk et al. 1996).

Central to the model of mechanotransduction in the [touch cells](#) ([Fig. 5](#)) is the heteromeric degenerin channel, composed of MEC-4, MEC-10, and MEC-6 subunits. These subunits assemble to form a pore in the membrane that is lined by hydrophilic residues in MSDII. Subunits are oriented such that their amino and carboxyl termini project into the cytoplasm and their cysteine-rich regions extend outside the cell. Localized tension, which is expected to be required for regulated opening and closing, is likely to be administered by tethering the extracellular channel domains to the specialized extracellular matrix and anchoring intracellular domains to the microtubule cytoskeleton. On the extracellular side, channel subunits may interact with MEC-1, MEC-5, and/or MEC-9 in the touch receptor mantle. Inside the cell, channel subunits are likely to interact with the 15-protofilament microtubules, which may contact the channel at their distal ends. Microtubules might be connected to the channel via MEC-2, a linker protein that may interact both with the MEC-12  $\alpha$ -tubulin and with intracellular channel domains.

How is the touch signal transduced? A touch stimulus could deform the microtubule network, which could tug the channel open from the intracellular side. Alternatively, a touch stimulus could perturb the mantle connections and pull the channel open from the extracellular side. In either case,  $\text{Na}^+$  influx would activate the touch receptor to signal via gap junction connections to [interneurons](#) in the touch relay circuit, eliciting locomotion in the appropriate direction. This model provides a number of specific predictions that can be easily tested with available tools, although experiments such as reconstituting channel triggering in heterologous expression systems will likely be challenging.

Is mechanotransduction in *C. elegans* similar to that in other organisms? One mechanosensitive ion channel gene, *mscL*, has been cloned from *Escherichia coli* ([Sukharev et al. 1994](#)). The MscL channel forms a large conductance nonselective ion channel. MscL encodes a 136-amino-acid protein that appears to have two transmembrane domains with intracellular amino and carboxyl termini (P. Blount and C. Kung, pers. comm.) but does not share striking primary sequence similarity to MEC-4 or MEC-10. Purified MscL reconstituted in liposomes is mechanosensitive, so it appears that membrane stretch is sufficient to generate the gating force for this channel. Overall, the primary sequence of the MscL channel and the means of delivering gating tension

appear to be different from that proposed to mediate mechanotransduction in the *C. elegans* [touch receptor neurons](#).

As discussed above, the mechanically gated ion channel that mediates auditory transduction in the vertebrate inner ear has been studied using elegant biophysical approaches (for review, see [Hudspeth 1989](#); [Pickles and Corey 1992](#)), but the genes encoding the auditory channel subunits have not been cloned. Might the hair cell channel be a degenerin family member? Such a possibility remains a plausible hypothesis, but it should be noted that the hair cell channel is a relatively nonselective cation channel that is clearly permeable to  $K^+$ , whereas indirect evidence (Waldmann et al., 1995) suggests that the touch cell channel, like the rENaC channel, may be  $Na^+$ -selective. In addition, if a degenerin family member is a component of the hair cell channel, it appears that the gene encoding that channel may not be highly conserved with MEC-4 and MEC-10, since PCR and low-stringency screening approaches have not quickly yielded a degenerin homolog expressed in the hair cells.

## Figures

Figure 4. A model for mechanotransduction in the ear.

### Figure 4

A model for mechanotransduction in the ear. Adjacent stereocilia in a hair bundle are connected at their apical surface by tip links (shown as springs). The short end of each tip link is thought to be connected directly to the transduction channel. Deflection of the hair bundle to the right increases tension in the tip links, causing the transduction channel to open. After prolonged deflections, the hair cells adapt to their new positions and the upper point of attachment of the tip links appears to slide downward. (Reprinted, with permission, from [Pickles and Corey 1992](#).)

Figure 5. Speculative model for mechanotransduction in the touch receptor neurons.

### Figure 5

Speculative model for mechanotransduction in the [touch receptor neurons](#). (A,B) The mechanosensitive channel in the [touch receptors](#) is hypothesized to include MEC-4 and MEC-10 (Driscoll and Chalfie 1991; Huang and Chalfie 1994), which are related to subunits of the vertebrate amiloride-sensitive  $Na^+$  channel (Chalfie et al. 1994). MEC-6 is hypothesized to be a third channel subunit because of its genetic properties ([Chalfie and Wolinsky 1990](#)); its molecular identity has not been established. MEC-5 collagen and the secreted MEC-9 protein are likely to be mantle components ([Du et al. 1996](#)). The MEC-5 collagen could directly attach to the channel to help maintain gating tension, an association that has not been biochemically demonstrated. MEC-1 is needed for mantle production ([Chalfie and Sulston 1981](#)), but its molecular identity is unknown. MEC-2 is thought to be membrane-associated ([Huang et al. 1995](#)) and might tether the specialized 15-protofilament microtubules, which is made up of MEC-12  $\alpha$ -tubulin and MEC-7  $\beta$ -tubulin subunits (Savage et al. 1989; M. Hamelin et al., pers. comm.), to the channel via a gating-spring-like attachment. Note that no biochemical data substantiate the hypothetical arrangement of any of the molecules depicted. (B) Response to a deflection of the cuticle administered by a stroke of an eyelash hair. Upon gentle touch, a domain of the channel is physically moved, inducing a conformational change that opens the channel to  $Na^+$  influx. Note that the gating tug could come from deflection of the microtubules as shown here or could come from the extracellular side, perhaps delivered by a collagen "spring" attachment.

## Chapter 23. Mechanotransduction — V Conclusions

---

The conversion of mechanical stimuli into cellular responses underlies diverse biological phenomena including cell volume regulation, fertilization, gravitaxis, involuntary muscle movement, and the senses of hearing, touch, and balance (for reviews, see [French 1992](#); [Sackin 1995](#)). The capacity to sense and respond to mechanical stimuli appears to be ubiquitous among living cells; indeed, from *E. coli* to a myriad of differentiated cell types from higher organisms, cells utilize mechanotransduction for essential functions. Electrophysiological investigations have established that specialized ion channels mediate cellular responses to mechanical stimuli. These channels, however, have proved difficult to purify; channels are not expressed at high levels within individual cells and specialized mechanosensory cells are not highly concentrated within tissues. Moreover, agonists/antagonists that specifically bind with high affinity to mechanically gated channels have not been identified. Consequently, genes encoding mechanically gated channels have remained largely elusive.

Knowledge of neuronal connectivity, cell ablation technology, and molecular genetic approaches have been employed to provide insight into the mechanisms by which mechanical stimuli are transduced into behavioral responses in *C. elegans*. Remarkably, none of the genes required for touch cell function (e.g., [mec-2](#), [mec-4](#), [mec-6](#), and [mec-10](#)) have proven to be required for nose touch sensitivity (J. Kaplan, unpubl.), suggesting that the [touch cells](#) and the ciliated [mechanosensory neurons](#) use distinct means to perform their sensory tasks. Future cellular, genetic, and molecular dissection of mechanosensory modalities should clarify mechanisms of sensory transduction and finally bring us to understand how the worm feels touch.

Generated from local HTML

## **Chapter 23. Mechanotransduction — Acknowledgments**

---

We thank our colleagues cited herein for communicating results prior to publication, and we thank the reviewers of this chapter for useful suggestions.

Generated from local HTML

# **Chapter 24. Feeding and Defecation**

---

## **Contents**

[I Introduction: Nematode Hydrostatics](#)

[II Feeding](#)

[III Defecation Motor Program](#)

[IV Conclusions](#)

[Acknowledgments](#)

Generated from local HTML

## Chapter 24. Feeding and Defecation — I Introduction: Nematode Hydrostatics

The observation that the interior of a nematode is under pressure was first documented for *Ascaris* by [Harris and Crofton \(1957\)](#). The common observation that a healthy worm bursts when the cuticle is punctured shows that it is true for *C. elegans* as well. This pressure is the “hydrostatic skeleton” ([Crofton 1966](#)) that allows the worm to maintain its shape against forces (such as surface tension) which would tend to squash it flat and provides the tension against which body muscles act in locomotion. The internal pressure is crucial to understanding the design of the digestive system.

The central part of the digestive system is the [intestine](#) ([Fig. 1](#), top), a flexible one-cell-thick epithelial tube that runs most of the length of the worm. It is composed of a series of toroids, the anteriormost consisting of four cells, and each of the rest of two cells ([Fig. 1](#), bottom) ([White 1988](#)), with microvilli on the luminal surface ([Sulston et al. 1983](#); [Albert and Riddle 1988](#)). Little is known about the physiology of the intestinal cells. In addition to absorbing nutrients, they may secrete digestive enzymes into the lumen, are thought to store nutrients ([White 1988](#)), and are known to synthesize yolk proteins ([Kimble and Sharrock 1983](#)). The basal surface of the [intestine](#) forms most of the inner boundary of the pseudocoelomic space, which extends beyond the ends of the [intestine](#) to contact all tissues. This space is filled with fluid that can be seen to flow constantly when the worm moves. Although there is no direct evidence, it is presumed that the pseudocoelomic fluid distributes throughout the body nutrients released from the basal surface of the [intestine](#). The pseudocoelomic fluid, the intestinal cells, and the contents of the intestinal lumen are all under pressure.

A crushed bacterial suspension is forced into the intestinal lumen by pharyngeal pumping. Nutrients must be absorbed with astonishing speed: Tracers such as mineral oil or iron particles remain in the [intestine](#) for only a few minutes (L. Avery and J.H. Thomas, unpubl.). This rapid flow is not propelled by the [intestine](#) itself, which is devoid of muscle cells along most of its length and is mechanically passive. Instead, the flow is controlled by two elaborate muscle complexes that seal off the ends of the [intestine](#). A powerful muscular pump at the anterior end, the [pharynx](#), is needed to force food against pressure into the [intestine](#). Smaller muscles at the posterior end of the [intestine](#) control the opening of the [anus](#), which facilitates the expulsion of intestinal contents by the high internal pressure. In addition, the body muscles, used primarily for locomotion, are exploited part of the time to move the intestinal contents. The residence time of intestinal contents must be a significant factor in achieving optimal nutrition, and this time is determined by the volume and frequency of defecation.

### Figures



### Figure 1

The *C. elegans* digestive tract. In all figures, anterior is to the left and dorsal is up. (Top) Schematic overview. The [pharynx](#) is at the anterior end and is shown in more detail in Figs. 2 through 4. The [intestine](#) connects to the posterior end of the [pharynx](#) and is a tube made up of a single layer of cells. The lumen runs down the center of the [intestine](#) and flares at the anterior end. The [anus](#) connects to the posterior end of the [intestine](#) and is shown closed. (Bottom) Intestinal cells in the mid embryo (430 minutes). The [intestine](#) is similar in the L1 through adult except that the germ-line lobes into int5 are absent. The bulk of the [intestine](#) is formed by the cell layers called int1 through int9. The four most anterior layers include the most posterior muscle of the [pharynx](#) ([m8](#)) and the pharyngeal-intestinal valve ([vpi](#)), although this probably does not function as a valve. At the posterior end of the [intestine](#) is a single layer that forms the intestinal-rectal valve ([vir](#)), followed by five layers of [rectal epithelium](#) ([rep](#) through [hyp7](#)). (Bottom figure is reprinted, with permission, from [Sulston et al. 1983](#).)

## Chapter 24. Feeding and Defecation — II Feeding

Topologically, the [pharynx](#) is part of the ectoderm. For an anatomical description of the [pharynx](#), see [Albertson and Thomson \(1976\)](#), unless otherwise specified. The muscle cells and marginal cells constitute a single-cell-thick epithelial tube, continuous at its anterior end with the tube of [hypodermis](#) that encloses the worm. Muscle and marginal cells are joined by tight junctions, which divide the membrane into apical and basal surfaces ([Fig. 2a](#)). The apical surfaces face the lumen and secrete cuticle, continuous with the cuticle made by the [hypodermis](#). Their basal surfaces face the [pseudocoelom](#) and secrete a basal lamina, continuous with the basal lamina that separates the [hypodermis](#) and [intestine](#) from the [pseudocoelom](#) and mesoderm. Pharyngeal neurons lie in folds of the [pharyngeal muscle](#) basal membrane, between the muscle and the basal lamina, just as the extrapharyngeal [nervous system](#) is between the basal membrane of the [hypodermis](#) and the basal lamina. No basal lamina separates pharyngeal motor neuron presynaptic terminals from the postsynaptic muscle membrane. In contrast, extrapharyngeal motor neurons are separated from the muscle cells on which they synapse by the basal lamina that separates the mesodermal muscle cells from the ectodermal neurons.

There are eight muscle types, arranged end to end along the anterior-posterior axis of the [pharynx](#) ([Fig. 2b](#)). These muscles can be divided into three functional groups. The corpus, containing muscles pm1 through pm4, constitutes the anterior half of the [pharynx](#). Its purpose is to take in and trap bacteria. The isthmus, muscle pm5, is the middle part of the [pharynx](#). It regulates flow of food from the corpus to the terminal bulb. The posterior part of the [pharynx](#), muscles pm6 through pm8, is the terminal bulb. It grinds up the bacteria.

### A. Normal Feeding

Normal feeding consists of two motions, pumping and isthmus peristalsis ([Fig. 3](#)) ([Albertson and Thomson 1976; Avery and Horvitz 1989](#)). A pump is a near-simultaneous contraction of the muscles of the corpus, anterior isthmus, and terminal bulb, followed by a near-simultaneous relaxation. The contractile fibers of the pharyngeal muscles are radially oriented, so contraction pulls the lumen open from its resting Y-shape ([Fig. 2a](#)) to a triangular shape. Because the posterior isthmus remains closed, the open lumen of the corpus is filled by liquid flowing in through the [mouth](#), along with suspended bacteria. The contraction of the terminal bulb muscles breaks up bacteria and passes the debris back to the [intestine](#) ([Doncaster 1962](#)). This near-simultaneous contraction is followed by a near-simultaneous relaxation, which returns the grinder to its resting position and allows the lumen of the corpus to close, expelling liquid while retaining bacteria.

The second motion, isthmus peristalsis, occurs after the main relaxation is complete. It is a peristaltic wave of contraction in the posterior isthmus that carries bacteria trapped in the anterior isthmus back to the grinder ([Doncaster 1962](#)). Typically, only every fourth pump is followed by an isthmus peristalsis ([Avery and Horvitz 1987](#)).

#### 1. Trapping and Transport of Bacteria in the Pharyngeal Lumen

*Caenorhabditis elegans* is a filter-feeder: The worms take in liquid with suspended particles (bacteria) and then spit out the liquid while retaining the particles. This separation, accomplished by the corpus and anterior isthmus, is poorly understood. In a microscopic system such as the [pharynx](#), fluid motions are reversible and linearly related to force ([Purcell 1977](#)). If the motions of the pharyngeal muscles during relaxation are the reverse of those during contraction, fluid and particle motions should also be reversed. Thus, if corpus and isthmus muscles contracted and relaxed in synchrony ([Fig. 3a](#)), bacteria that came in through the [mouth](#) should exit through the [mouth](#). In fact, they are trapped. This implies a complexity in the muscle motions not obvious to real-time visual inspection.

Relaxation is the key step in filtering. During contraction, bacteria move posteriorly with the fluid as one would expect. Relaxation expels the fluid, but somehow the bacteria remain trapped ([Avery 1993b](#)). The mechanism of trapping is not known, because the relaxation is so fast (<17 msec; [Avery 1993a](#)) that the motions cannot be seen

in videotapes. The speed of relaxation is likely to be important, since the pharyngeal motor neuron [M3](#), which regulates relaxation, is important for effective trapping of bacteria ([Avery 1993b](#)).

[Seymour et al. \(1983\)](#), analyzing [pharyngeal muscle](#) motions in ciné films, reported that the motions of the anterior isthmus are delayed compared to the corpus. Subsequent analysis of videotapes with better time resolution confirmed that isthmus contraction begins when corpus contraction is well advanced and that isthmus relaxation takes place well after corpus relaxation has ended (L. Avery, unpubl.). [Seymour et al. \(1983\)](#) also reported that procorpus motions precede those of [metacorpus](#), but this observation could not be confirmed on videotapes (L. Avery, unpubl.; L. Philipson, pers. comm.). This delay of the isthmus with respect to the corpus is interesting because it means that the motions of the pharyngeal muscles during relaxation are not the reverse of those during contraction, a theoretical requirement for trapping. [Seymour et al. \(1983\)](#) also described perplexing motions of the metastomal flaps. These flaps, operated by the pharyngeal pm1 and pm2 muscles, *prevent* bacteria from entering the [pharynx](#) during most of the corpus contraction. What function this serves is unknown.

There is clearly a great deal left to be learned about how these worms catch food. Laser ablation of the pm1 and pm2 muscles might reveal the role of the metastomal flaps in this process. High-speed video recordings of the motions of individual particles in the lumen would be useful for understanding trapping. Computer or physical models of fluid flow within the pharyngeal lumen could test the importance of the metastomal flaps and the timing of muscle motions.

## 2. Terminal Bulb Function

The terminal bulb grinds up food and passes the debris to the [intestine](#). The pm6 and pm7 muscle cells secrete a thick, ridged cuticle called the grinder on their luminal surfaces. The three segments of the grinder (made by the three pairs of muscle cells) engage one another. Contraction of the muscles rotates the segments (usually all three together, although occasionally individual segments turn); food caught between them is ground up and passed back to the [intestine](#) through the pharyngeal-intestinal valve, which is opened at this time ([Doncaster 1962](#)), probably by contraction of pm8. Relaxation of the terminal bulb has no active purpose—it merely returns the grinder to its resting position.

## 3. Isthmus Function

We believe that the isthmus acts as a double valve which separates high- and low-pressure regions of the [pharynx](#), allowing food to be forced into the [intestine](#) against the pressure gradient. Our model is shown in Figure 4. At rest, the pharyngeal lumen is closed except for a small region around the grinder, which is at high pressure ([Fig. 4a](#)). During a pump ([Fig. 4b](#)), the lumen of the corpus and anterior isthmus are at ambient pressure, open to the outside fluid. The lumen around the grinder is at high pressure, connected to the intestinal lumen by the open pharyngeal-intestinal valve. These two regions are separated by the closed posterior isthmus. Near the end of the peristalsis ([Fig. 4d](#)), the isthmus lumen is connected to the terminal bulb lumen and is at high pressure.

The movement of the bacteria occurs within isobaric regions. The region from the [mouth](#) to the middle of the isthmus is at low pressure during the pump, the region from the isthmus and terminal bulb is at high pressure during isthmus peristalsis, and the region from the terminal bulb to [intestine](#) is at high pressure during the pump. Food is transferred from low to high pressure between the end of the pump and the beginning of the isthmus peristalsis (i.e., between b and c in [Fig. 4](#)), as the anterior isthmus closes. This transfer occurs without motion of the food and therefore requires little energy. Most of the work done to move the bacteria against the pressure gradient is done when the corpus lumen opens against the internal/external pressure difference. This is analogous to the way a diver leaves a submarine through a lock. The diver moves from the submarine into the lock at low pressure, closes the hatch to the submarine, stands still while the hatch to the ocean is opened and the pressure rises, and then moves from the lock to the ocean at high pressure. The work necessary to move the diver from low to high pressure is done when the water is pumped out of the lock.

This model is supported by observations of air bubbles sucked into the [pharynx](#). They remain unchanged in size in the corpus and anterior isthmus, showing that these regions are at ambient pressure, then shrink in the isthmus and vanish into solution in the terminal bulb, showing that the pressure is high there ([Doncaster 1962](#); L. Avery, unpubl.). It is not known what determines when an isthmus peristalsis occurs, although it is likely to be controlled by the [M4](#) neuron (see below).

## B. Each Pump Corresponds to a Single Muscle Action Potential

### 1. The Pharyngeal Muscle Action Potential

Pharyngeal muscle was the first *C. elegans* cell type from which intracellular electrical recordings were achieved (S. Lockery, pers. comm.). Figure 5a shows a recording of the membrane potential of an active [pharyngeal muscle](#) cell ([Davis et al. 1995](#)). The action potentials are very similar to those recorded from *Ascaris* [pharyngeal muscle](#) ([del Castillo and Morales 1967](#); [Byerly and Masuda 1979](#)) and resemble action potentials of vertebrate heart muscle cells (particularly cells from the ventricles) in that they are long-lasting and have three phases, which [Raizen and Avery \(1994\)](#) called E, P, and R for excitation, plateau, and repolarization. The action potential begins with excitation: a rapid rise in the membrane potential from the resting value of -40 to -50 mV to a depolarized value of 30 to 40 mV. This is followed by a plateau phase during which the membrane remains depolarized. The length of the plateau phase can vary from 50 to 500 msec, but during normal wild-type pumping, it is typically about 150 msec. The plateau phase ends with an abrupt drop in membrane potential (repolarization) during which membrane potential becomes more negative than resting values. After repolarization, the membrane potential slowly rebounds. During slow pumping, as in Figure 5a, it relaxes back toward the resting potential, but during rapid pumping, the rebound continues right past the resting potential to trigger another action potential, typically 100 msec after repolarization. Each contraction-relaxation cycle corresponds to a single muscle action potential ([Raizen and Avery 1994](#); [Davis et al. 1995](#)). Contraction is first visible about 30 msec after excitation and proceeds during the plateau of the action potential. Relaxation immediately follows repolarization.

Intracellular recording methods have only recently been developed for *C. elegans*. Most of our knowledge of electrical events in the [pharynx](#) comes from a simpler recording method in which the electrical currents that flow in and out of the worm's [mouth](#) are measured ([Raizen and Avery 1994](#)). One of these recordings, called electropharyngeograms or EPGs, is shown in Figure 5b. The EPG is the time derivative of the membrane potential summed over all pharyngeal muscles. Thus, each rapid positive change in membrane potential is seen as a positive spike in the EPG, and each rapid negative potential change is seen as a negative spike. The largest features in the EPG, which correspond to the excitation and repolarization of the corpus muscles ([Raizen and Avery 1994](#); T.A. Starich et al., in prep.; M.W. Davis, pers. comm.), are labeled E and R in Figure 5b.

The [nervous system](#) is not necessary for generation of these potential changes—The capacity is probably intrinsic to the muscle cells. [Avery and Horvitz \(1989\)](#) showed that pumping continues even after the entire pharyngeal [nervous system](#) is killed. [Raizen and Avery \(1994\)](#) showed that E and R spikes are not greatly altered even after all [pharyngeal neurons](#) except [M4](#) are killed. (The essential neuron [M4](#) was spared in order to allow the worms to reach adulthood. [M4](#) is believed not to affect pumping [[Raizen et al. 1995](#)].)

### 2. Ionic Basis of the Action Potential

Although little is known for certain about the ionic basis of the [pharyngeal muscle](#) action potential, it is likely to be mediated by voltage-activated calcium channels. Except in chordates, muscle action potentials have been reported to be mostly or entirely calcium-mediated ([Hagiwara and Byerly 1981](#)), and there is no reason to suppose that nematode [pharyngeal muscle](#) is an exception. Thus, the sustained high potential during the plateau phase and some part of the rise in membrane potential during excitation are probably caused by influx of  $\text{Ca}^{++}$  through plasma membrane calcium channels. Recent genetic studies have identified a gene that probably encodes a subunit of the [pharyngeal muscle](#)  $\text{Ca}^{++}$  channel (R.Y.N. Lee et al., in prep.).

Muscle contraction results from a rise in the cytoplasmic  $\text{Ca}^{++}$  concentration. There are two potential sources for this  $\text{Ca}^{++}$ : the  $\text{Ca}^{++}$  that enters through the plasma membrane channel, and  $\text{Ca}^{++}$  release from intracellular stores. On excitation, most muscle cells release  $\text{Ca}^{++}$  from the endoplasmic reticulum (or sarcoplasmic reticulum, a specialized endoplasmic reticulum) into the cytoplasm through a calcium channel called the ryanodine receptor, which opens in response to the opening of the plasma membrane channel.

*C. elegans* possesses a ryanodine receptor ([Kim et al. 1992](#); Y. Sakube and H. Kagawa, pers. comm.) encoded by *unc-68* (E. Maryon and P. Anderson, pers. comm.). Ryanodine, which opens the ryanodine receptor channel, causes [body muscle](#) contraction in wild-type ([Kim et al. 1992](#)) but not *unc-68* worms (E. Maryon and P. Anderson, pers. comm.). Surprisingly, *unc-68* is not necessary for body or [pharyngeal muscle](#) contraction (E. Maryon and P. Anderson, pers. comm.). This result suggests that enough  $\text{Ca}^{++}$  may enter through the plasma membrane to cause contraction. (Although  $\text{Ca}^{++}$  release through a different intracellular channel such as the IP3 receptor [H. Baylis et al., pers. comm.] cannot be excluded, such a channel would not be expected to respond rapidly enough to plasma membrane potential changes to account for [pharyngeal muscle](#) motions.) *unc-68* mutants are uncoordinated ([Brenner 1974](#)) and have abnormal [pharyngeal muscle](#) motions (R.Y.N. Lee, pers. comm.). Furthermore, they do not respond as strongly as wild type to excitation of body muscles by the acetylcholine agonist levamisole ([Lewis et al. 1980a](#)). Thus, the ryanodine receptor does have a role in [body wall muscle](#) contraction. Perhaps it allows  $\text{Ca}^{++}$  concentration to rise more rapidly in response to membrane excitation than the plasma membrane channel alone could accomplish. This hypothesis could be tested by measuring the onset of contraction and the rise of  $\text{Ca}^{++}$  concentration in response to voltage pulses in *unc-68* and wild type.

If the action potential is sustained by a voltage-activated calcium channel, some other event at the beginning of the action potential must produce the initial rise in membrane potential that opens the calcium channel. The control of this event is a key behavioral function, since the frequency of such excitations determines the frequency of pumping, which is the major behavioral response of the [pharynx](#). During rapid pumping, the action potential is likely to be triggered by an excitatory postsynaptic potential from the motor neuron MC (see below). However, the muscle can also be excited in the absence of the [nervous system](#). Nothing is known about the muscle-intrinsic excitation.

The best-understood part of the action potential is the repolarization, thanks to voltage-clamp studies on *Ascaris* [pharyngeal muscle](#) by [Byerly and Masuda \(1979\)](#). They identified a voltage-gated potassium channel called the negative spike channel that closes when the membrane is depolarized but is opened by rapid negative potential changes. Its opening allows  $\text{K}^+$  to leave the cell, causing the potential to become more negative, which causes more negative spike channels to open, resulting in a fast regenerative negative-going spike. The effects of membrane potential on the rate of repolarization are consistent with the existence of such a channel in *C. elegans* [pharyngeal muscle](#) ([Davis et al. 1995](#)).

### 3. Synchronization of Pharyngeal Muscles

During a pump, corpus and terminal bulb muscles contract together. EPG recordings show that this synchronization of contraction is accomplished by synchronization of the action potentials. In the wild type, the excitation of the isthmus and corpus happens within a few milliseconds of each other, resulting in one large E spike ([Fig. 5b](#)). Repolarization is less tightly synchronized, but corpus and terminal bulb are still coupled: The terminal bulb R spike usually occurs less than 50 msec after the corpus R spike ([Raizen and Avery 1994](#)). Within the corpus or within the terminal bulb, synchronization is nearly perfect. In mutants homozygous for the *eat-5* mutation (only one allele is known), corpus and terminal bulb contractions often occur separately ([Avery 1993a](#)), and when this happens, separate excitation spikes are seen: Small spikes correlate with terminal bulb contraction and large spikes correlate with corpus contraction ([Starich et al. 1995](#)).

[Avery and Horvitz \(1989\)](#) proposed that pharyngeal contractions are synchronized by electrical coupling of pharyngeal muscles through gap junctions. Synchronization does not require the pharyngeal [nervous system](#).

([Avery and Horvitz 1989](#)), and it is difficult to imagine any nervous-system-independent mechanism other than electrical coupling that could synchronize muscle action potentials with millisecond precision.

The *eat-5* gene, which is necessary to synchronize the corpus and terminal bulb, encodes a member of the OPUS family of membrane proteins (T.A. Starich et al., in prep.), including *C. elegans* UNC-7 and *Drosophila* Ogre and Passover. On the basis of predicted protein structure and the *unc-7* and *Passover* mutant phenotypes, [Barnes \(1994\)](#) proposed that OPUS is a family of invertebrate gap junction proteins. If this proposal could be verified by functional expression of OPUS proteins, it would greatly strengthen the case for electrical coupling of pharyngeal muscles.

The purpose of corpus and terminal bulb synchronization is unknown. *eat-5* worms grow more slowly than wild type, but this may be because the terminal bulb pumps more slowly, perhaps because the pacemaker is in the corpus (see below). Nematodes of the genus *Panagrellus* feed efficiently with unsynchronized corpus and terminal bulb contractions ([Mapes 1965](#)). *Panagrellus silusiae* and *Panagrellus redivivus* are bacteria-eating soil nematodes with a [pharynx](#) similar in overall form to that of *C. elegans*. The terminal bulb pumps more rapidly than the corpus in both species ([Mapes 1965](#); L. Avery, unpubl.). Perhaps *Panagrellus* and *C. elegans* use different mechanisms to generate terminal bulb rhythm.

The isthmus does not contract in tight synchrony with the corpus and terminal bulb. In fact, the anterior and posterior isthmus do not contract at the same time, even though each muscle cell runs the entire length of the isthmus. Within the anterior or posterior isthmus, contraction occurs as a wave that propagates from anterior to posterior, instead of simultaneously along the length as in the corpus or terminal bulb. Furthermore, no EPG signal has ever been detected from the isthmus. This suggests that depolarization of the isthmus, like its contraction, is spread out in time, so that no single discrete excitation spike results. We believe that the capacity of the isthmus for unsynchronized contraction is functionally important. Asynchrony of the anterior and posterior halves allows the terminal bulb and corpus lumen to be at different pressures (see above), and the anterior to posterior waves of contraction appear to be important for transporting bacteria posteriorly.

The lack of synchrony in isthmus contraction can be explained by proposing that isthmus muscle, unlike terminal bulb or corpus muscle, is incapable of regenerative action potentials. In this case, local excitation of the muscle would produce a local depolarization and local contraction, both of which would tend to spread slowly from the site of excitation and decrease with distance. Thus, the delayed contraction of the anterior isthmus during a pump would be explained by excitation at the anterior end through electrical coupling to corpus muscle cells. Posterior isthmus peristalsis could be a result of excitation by the motor neuron [M4](#) (see below), which synapses on the posterior end of the isthmus muscle cells ([Albertson and Thomson 1976](#)). This idea could be tested by intracellular recording from the isthmus at various points along its length.

## C. Pharyngeal Nervous System Function

*C. elegans* has two nervous systems capable of independent function: the extrapharyngeal or somatic [nervous system](#), consisting in the adult hermaphrodite of 282 neurons of 104 anatomical types ([White et al. 1986](#)), and the pharyngeal [nervous system](#), containing 20 neurons, 8 unpaired and 6 bilaterally symmetric pairs, for a total of 14 anatomical types ([Albertson and Thomson 1976](#)). The pharyngeal and extrapharyngeal nervous systems are connected by a bilateral pair of gap junctions between the extrapharyngeal RIP neurons and the pharyngeal I1 neurons ([Albertson and Thomson 1976](#)). This connection can be severed with very little effect on pharyngeal function by killing the RIPs. (The only effect that has been seen is that pumping becomes unresponsive to light touch sensed by the extrapharyngeal [touch cells](#) [M. Chalfie and J.E. Sulston; J.H. Thomas et al.; both pers. comm.], which in intact worms briefly inhibits pumping [[Chalfie et al. 1985](#)].)

Although there may be humoral communication between the pharyngeal and extrapharyngeal nervous systems (see discussion of NSM function below), each of the nervous systems can function without such interaction.

When the [pharynx](#) is exposed by dissection, presumably eliminating any humoral influences the extrapharyngeal [nervous system](#) might have, pharyngeal behavior and electrophysiology are essentially normal ([Avery et al.](#)

1995a). Similarly, when the 19 nonessential [pharyngeal neurons](#) are killed with a laser, extrapharyngeal behaviors are not grossly abnormal ([Avery and Horvitz 1989](#); L. Avery, unpubl.).

The nervous control of feeding is thus almost exclusively the province of the pharyngeal [nervous system](#). The ability to identify all of the relevant neurons is a technical advantage unique to feeding. Although it is usually straightforward to identify the neurons that directly control other *C. elegans* behaviors, upstream circuitry is delimited only with difficulty. Because we can identify all of the neurons that control feeding, we can kill all of them. As described above, pumping continues in the absence of the [nervous system](#). Feeding behavior is not normal, however. The following are three principal abnormalities, each of which can be attributed to a single motor neuron type: (1) Relaxation is delayed in the absence of [M3](#); (2) pumping is slow in the absence of MC; and (3) there is no isthmus peristalsis in the absence of M4.

Not only are these three motor neuron types necessary for normal feeding, they are also sufficient for nearly normal feeding; i.e., when all [pharyngeal neurons](#) except [M4](#), MC, and [M3](#) are killed, feeding is nearly normal ([Avery 1993b; Raizen et al. 1995](#)). We therefore believe that [M4](#), MC, and [M3](#) execute the principal functions of the pharyngeal [nervous system](#). A fourth pharyngeal neuron type, NSM (neurosecretory motor neuron), may serve to communicate the presence of food to the rest of the worm. The other [pharyngeal neurons](#) may regulate these four, or they may have functions that are not exercised in the laboratory.

## 1. M3: A Single Neuron Proprioceptive Loop?

The M3s are inhibitory motor neurons that control the timing of pharyngeal relaxation. They are a bilaterally symmetric pair of motor neurons with output to the [metacorpus](#) and perhaps the isthmus ([Albertson and Thomson 1976](#)). When they fire, they produce fast negative changes in muscle membrane potential (inhibitory postsynaptic potentials) that can trigger repolarization and therefore relaxation ([Avery 1993b; Raizen and Avery 1994](#)). This regulation of the timing of relaxation seems to be important for effective transport of bacteria within the pharyngeal lumen ([Avery 1993b](#)).

Each [M3](#) may constitute a single-neuron proprioceptive loop, firing in response to corpus muscle contraction and causing relaxation. [Albertson and Thomson \(1976\)](#) first proposed that [M3](#) might be a sensorimotor neuron because it has free endings in the [metacorpus](#). Consistent with this idea, [Raizen and Avery \(1994\)](#) saw [M3](#) inhibitory postsynaptic potentials even when other [pharyngeal neurons](#) had been killed (showing that it is a motor neuron) and only when corpus muscle was contracted (suggesting it is sensory). The evidence still falls short of proof (for discussion, see [Raizen and Avery 1994](#)).

J.A. Dent et al. (in prep.) have tentatively identified the [M3](#) neurotransmitter as glutamate. The following are the key results: (1) Pulses of glutamate applied to the [pharyngeal muscle](#) mimic the effect of [M3](#); (2) *avr-15* (avermectin-resistant) mutants, whose [pharyngeal muscle](#) does not respond to glutamate pulses, also lack [M3](#) transmission (see below). Immunocytochemical detection of glutamate in the [M3](#) neurons has not yet been successful. Glutamate probably acts by opening an avermectin-sensitive glutamate-gated chloride channel in the [pharyngeal muscle](#) (see [Rand and Nonet](#), this volume). The avermectins are broad-spectrum nematocidal drugs that paralyze *Ascaris* [body muscle](#) by irreversibly opening  $\text{Cl}^-$  channels ([Martin 1993](#)). To identify avermectin targets, [Arena et al. \(1991\)](#) injected *C. elegans* mRNA into *Xenopus* oocytes and found a  $\text{Cl}^-$  channel that was irreversibly opened by avermectin. They subsequently cloned two cDNAs that encode such a channel ([Cully et al. 1994](#)). On the basis of the finding that expression of these cDNAs resulted in a glutamate-gated  $\text{Cl}^-$  conductance, they proposed that this channel might mediate fast inhibitory glutamatergic transmission ([Arena et al. 1992; Cully et al. 1994](#)).

*C. elegans* [pharyngeal muscle](#) is paralyzed by low concentrations of avermectin ([Avery and Horvitz 1990](#); M. Chalfie, pers. comm.), and this paralysis can be reversed by lowering the extracellular  $\text{Cl}^-$  concentration (J.A. Dent, pers. comm.), suggesting that in *C. elegans* [pharyngeal muscle](#) as in *Ascaris* [body muscle](#) ([Martin 1993](#)), avermectins open  $\text{Cl}^-$  channels. To test the hypothesis that [M3](#) transmission is mediated by an avermectin-sensitive glutamate-gated  $\text{Cl}^-$  channel, J.A. Dent et al. (in prep.) recorded EPGs from avermectin-resistant

mutants isolated by C.D. Johnson ([Rand and Johnson 1995](#); C.D. Johnson, unpubl., cited by [Anderson 1995](#)). One gene that can confer avermectin sensitivity, *avr-15*, was necessary for [M3](#) transmission. Furthermore, pulses of glutamate applied to wild-type but not *avr-15* mutant [pharyngeal muscle](#) mimic the effects of [M3](#) (J.A. Dent et al., in prep.; H. Li et al., unpubl.). Cloning of *avr-15* showed that it encodes a new member of the family of avermectin-sensitive glutamate-gated chloride channel subunits (J.A. Dent et al., in prep.).

## 2. MC Controls the Rate of Pumping

The MCs are excitatory motor neurons that control the initiation of [pharyngeal muscle](#) action potentials and therefore the frequency of pumping ([Avery and Horvitz 1989](#); [Raizen et al. 1995](#)). When they fire, they produce a fast positive change in muscle membrane potential (an excitatory postsynaptic potential), which usually triggers a muscle action potential. [Raizen et al. \(1995\)](#) proposed that MC is the pacemaker for rapid pharyngeal pumping; it is the sole neuron type necessary for this behavior. The rate of pharyngeal pumping is regulated by the presence of food, the nutritional state of the worm, and neurotransmitters such as serotonin ([Horvitz et al. 1982](#); [Avery and Horvitz 1990](#); [Raizen et al. 1995](#)). Most of this regulation requires MC ([Avery and Horvitz 1989](#); [Raizen et al. 1995](#)), so it is likely that MC is the major target of regulation of the rate of pumping. However, there is also a nervous-system-independent muscle response to serotonin (D.M. Raizen, pers. comm.).

MC appears to function as a motor neuron, because its ability to produce postsynaptic potentials in [pharyngeal muscle](#) does not depend on other neurons ([Raizen et al. 1995](#)). [Albertson and Thomson \(1976\)](#) found that the MCs synapse not on muscle, but on the marginal cells, which are structural cells located between the muscle cells (see [Fig. 2a](#)). Since nematodes lack obvious postsynaptic specializations, it cannot be excluded on the basis of electron microscopy that [pharyngeal muscle](#) is a postsynaptic partner. However, a more interesting possibility is that MC in fact excites the marginal cells, which then serve as a conduction pathway to excite electrically coupled muscle cells, somewhat like the Purkinje fibers of the vertebrate heart. In fact, gap junctions between marginal cells and muscle cells have been observed in electron micrographs (D. Hall, pers. comm.).

Like [M3](#), MC may be a sensorimotor neuron. It has a putative mechanosensory ending at the boundary between the procorpus and [metacorpus](#) ([Albertson and Thomson 1976](#)). Laser microsurgery and electrophysiological recordings suggest that MC is stimulated by bacteria in the [pharynx](#) and that the precise timing of its firing is adjusted in response to muscle motions ([Raizen et al. 1995](#)).

The identity of the MC neurotransmitter is not clear. Pharmacological and genetic data point to acetylcholine, but these are contradicted by immunocytochemical experiments. Acetylcholine agonists are excitatory to [pharyngeal muscle](#) ([Avery and Horvitz 1990](#); [Raizen et al. 1995](#)). This effect is probably mediated in part by a nicotinic receptor distinct from the levamisole receptor ([Avery and Horvitz 1990](#)), the major [body muscle](#) nicotinic receptor. The nicotinic blocker curare blocks MC neuromuscular transmission ([Raizen et al. 1995](#)). Furthermore, the *eat-18* gene is necessary both for [pharyngeal muscle](#) to respond to nicotine and for MC neuromuscular transmission. The phenotype of *eat-18* mutants is indistinguishable from that of worms in which MC has been killed. Worms that carry partial loss-of-function mutations in the *cha-1* and *unc-17* genes, which are necessary for cholinergic transmission (see [Rand and Nonet](#), this volume), pump slowly ([Avery 1993a](#)), and *cha-1* null mutants do not pump ([Avery and Horvitz 1990](#)). However, MC does not stain with antibodies against CHA-1 or UNC-17 protein (J. Duerr and J. Rand, pers. comm.). These antibodies stain extrapharyngeal motor neurons previously known to be cholinergic, and they stain certain pharyngeal neuron types other than MC (J. Duerr and J. Rand, pers. comm.). Molecular characterization of *eat-18* and mosaic analysis to determine the focus of the *cha-1/unc-17* slow-pumping defect might resolve this question.

Figure 6 summarizes the proposed actions of [M3](#) and MC on the [pharyngeal muscle](#) action potential. Parts of the model shown in this figure are speculative. In particular, since there is presently no way of recording directly from [pharyngeal neurons](#), the patterns of [M3](#) and MC firing are uncertain.

## 3. M4 Controls Isthmus Peristalsis

The [M4](#) motor neuron synapses on the posterior half of the isthmus muscles ([Albertson and Thomson 1976](#)) and is necessary for posterior isthmus peristalsis ([Avery and Horvitz 1987](#)). Worms lacking [M4](#) swallow little or no food and therefore fail to grow. (Like intact worms deprived of food, [M4<sup>-</sup>](#) worms may survive up to 2 weeks.) They continue to pump, and the pumping appears to be functional in that bacteria are concentrated in the anterior isthmus and corpus, which become stuffed ([Avery and Horvitz 1987](#)). Although [M4<sup>-</sup>](#) worms pump slowly, this is probably a consequence of the stuffing, since if the corpus is cleared by placing the [M4<sup>-</sup>](#) worms on drugs that excite isthmus muscle, they will pump rapidly until the lumen is again full (see [Raizen et al. 1995](#)).

Little is known about [M4](#) activity or communication between [M4](#) and isthmus muscle. Isthmus peristalsis occurs after some pumps but not others ([Avery and Horvitz 1989](#)) and appears to be an all-or-none event. All pumping cycles in an [M4<sup>-</sup>](#) worm are similar to those cycles in intact worms in which isthmus peristalsis does not occur. This suggests that isthmus peristalses may be signaled by single [M4](#) action potentials. However, no [M4](#) postsynaptic potentials are detected in the EPG, suggesting that its direct effect is not fast electrical excitation. It might, for instance, activate intracellular signals that allow the muscle to contract in response to depolarization from the terminal bulb. However, there are several alternative explanations: Perhaps [M4](#) is merely permissive for posterior isthmus contraction, and the muscle has an intrinsic mechanism for making an all-or-none decision to contract, or perhaps postsynaptic potentials in the isthmus cannot be detected in the EPG.

[M4](#) stains with antibodies against UNC-17, suggesting that it may use acetylcholine as its transmitter (J. Duerr and J. Rand, pers. comm.). However, [Albertson and Thomson \(1976\)](#) saw large dense-core vesicles at [M4](#) neuromuscular junctions, so if acetylcholine is an [M4](#) neurotransmitter, it is probably not the only one. Furthermore, mutations that weaken cholinergic transmission have no striking effect on isthmus peristalsis (L. Avery, unpubl.).

#### 4. NSM: A Signal of the Presence of Food?

Although they are not as important as MC, [M3](#), and [M4](#) in the control of feeding, the NSMs have received as much attention. This pair of neurons has synapses in the isthmus not only on the muscle, but also on the basal lamina that bounds the [pharynx](#) ([Albertson and Thomson 1976](#)). Because the extrapharyngeal [nerve ring](#) (the closest thing a nematode has to a brain) lies on the other side of this basal lamina and because the NSMs have putative sensory endings at the boundary between the corpus and isthmus (where bacteria accumulate), [Albertson and Thomson \(1976\)](#) proposed that they might secrete something into the [pseudocoelom](#) when their endings detected food in the pharyngeal lumen. This proposal was supported by the discovery that the NSMs contain serotonin ([Albertson and Thomson 1976](#)). Serotonin has three obvious effects on hermaphrodites: It depresses locomotion, stimulates egg laying, and stimulates pumping ([Croll 1975a; Horvitz et al. 1982](#)). These are all sensible responses to the presence of food and are in fact all seen in the presence of bacteria ([Croll 1975b; Croll and Smith 1978](#)).

Unfortunately, proof of a neurohumoral function of the NSMs has been hard to come by. Killing them has almost no effect on behavior, although subtle effects in the expected direction have been seen ([Avery et al. 1993](#); E. Sawin; D.M. Raizen; both pers. comm.). The meagerness of these effects can be reconciled with the evidence that NSM signals the presence of food by proposing that NSM is redundant with other neurons that detect bacteria, depress locomotion, and stimulate pumping and egg laying. Proof will require identifying the redundant neurons. Unfortunately, the best candidate for the redundant neuron that stimulates feeding is MC, which is probably also the major target through which the NSMs stimulate feeding; i.e., serotonin probably stimulates pumping largely by increasing the firing frequency of MC, but MC also accelerates its firing in response to bacteria in the absence of serotonin (D.M. Raizen, pers. comm.). Thus, the usual sign of redundancy—a synergistic effect when both redundant neurons are killed—cannot be tested in this case because killing MC effectively eliminates both pathways. If this model is correct, demonstration of a substantial effect of NSM on feeding will require specific elimination of the NSM-independent sensory function.

#### 5. Other Neurons

We have discussed 4 of the 14 pharyngeal neuron types in detail. For most of the remaining 10, there is even less functional information than for NSM. What are these remaining 10 neuron types doing? Some of them unquestionably regulate MC, [M3](#), and M4. The I1s, for instance, receive the gap junctions from the R1Ps, which connect the pharyngeal [nervous system](#) to the extrapharyngeal [nervous system](#). They synapse on MC ([Albertson and Thomson 1976](#)) and affect the rate of pumping in the absence of bacteria (D.M. Raizen, pers. comm.). Similarly, [I5](#) is a sensory neuron that synapses on [M3](#) ([Albertson and Thomson 1976](#)). Killing [I5](#) hastens relaxation, but killing both [I5](#) and [M3](#) results in a delay in relaxation indistinguishable from that caused by killing [M3](#) alone. Thus, it is likely that [I5](#) inhibits M3. ([I5](#) also has [M3](#)-independent effects on the isthmus.) Other neurons might have small or redundant effects. Another possibility is that some of these neurons are evolutionary detritus. Nematodes have extraordinarily varied pharyngeal morphology and feeding patterns. Perhaps some [pharyngeal neurons](#) serve a purpose in other nematodes that is redundant or unnecessary in *C. elegans*.

## Figures

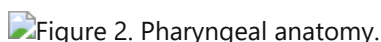


### Figure 2

Pharyngeal anatomy. This figure, based on reconstruction from electron micrographs by [Albertson and Thomson \(1976\)](#), shows the anatomy of the [pharynx](#). (a) Schematic of a transverse view. Three [pharyngeal muscle](#) cells situated with triradiate symmetry surround the pharyngeal lumen. Their contractile fibers are radial so that when they contract, the pharyngeal lumen opens. Their apical surface is lined by cuticle, whereas their basal surface is lined by a basal lamina. Between the [pharyngeal muscle](#) cells at the apices of the lumen are three marginal cells. Together, the marginal cells and muscle cells constitute a single-cell-thick epithelium that separates the environment (connected to the pharyngeal lumen) from the fluid-filled interior of the worm, the [pseudocoelom](#). Pharyngeal neurons are embedded in grooves of the [pharyngeal muscle](#) basal membranes in each of the three sectors. (b) Lateral view, anterior to the left. The [pharynx](#) is divided into three functional parts: the corpus, isthmus, and terminal bulb. The corpus is further subdivided into the procorpus and the [metacorpus](#). There are five types of large muscles in the [pharynx](#), arranged from anterior to posterior: pm3 in the procorpus, pm4 in the [metacorpus](#), pm5 in the isthmus, and pm6 and pm7 in the terminal bulb. Three types of small muscles, pm1 and pm2 at the anterior end and pm8 at the posterior end, are not shown here. (Note that these muscles are called [m1–m8](#) by [Albertson and Thomson \[1976\]](#). The names pm1–pm8 are used here to avoid confusion with the motor neurons M1–M5.) (Adapted, with permission, from [Avery and Horvitz 1989](#) [copyright 1989 by Cell Press] and from [Raizen and Avery 1994](#) [copyright 1994 by Cell Press].)



### Figure 3

Pumping and isthmus peristalsis. (a) Pumping. A pump consists of a nearly simultaneous contraction of the corpus, anterior isthmus, and terminal bulb, followed by relaxation. Corpus and isthmus muscles are radially oriented (see [Fig. 2a](#)) ([Albertson and Thomson 1976](#)), so the lumen opens when they contract, sucking in liquid and suspended bacteria. Terminal bulb muscle contraction inverts the grinder, breaking bacteria that are in front of the grinder and passing the debris back to the [intestine](#) ([Doncaster 1962](#)). Relaxation returns the grinder to its relaxed position and allows the lumen of the corpus to close, expelling liquid. Bacteria trapped by a mechanism that is not fully understood accumulate in the back of the corpus and anterior half of the isthmus. (b) Isthmus peristalsis. The feeding cycle is closed by a peristaltic contraction of the posterior isthmus muscles, which carries bacteria from the middle of the isthmus to the grinder. (Reprinted, with permission, from [Avery and Horvitz 1989](#) [copyright 1989 by Cell Press].)



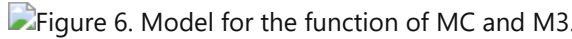
### Figure 4

Pressure differences during feeding. At rest, the pharyngeal lumen is closed except for a small region around the grinder, which is at high pressure (*a*). During a pump (*b*), the lumen of the corpus and anterior isthmus are at ambient pressure, open to the outside fluid. The lumen around the grinder is at high pressure, connected to the intestinal lumen by the open pharyngeal-intestinal valve. These two regions are separated by the closed posterior isthmus. After a pump, the muscles have relaxed (*c*) and the lumen is closed. About one out of four pumps is followed by isthmus peristalsis, a wave of contraction that begins in the middle of the isthmus and moves posteriorly, carrying the bacteria to the terminal bulb. Toward the end of the peristalsis (*d*), the isthmus lumen is connected to the terminal bulb lumen and is at high pressure. The sizes of the pharyngeal and intestinal lumens are exaggerated for clarity.

Figure 5. Electrical recordings from pharyngeal muscle.

## Figure 5

Electrical recordings from [pharyngeal muscle](#). (*a*) Intracellular recording from a terminal bulb muscle cell. (E) Excitation, the sharp rise in membrane potential that begins the action potential; (R) repolarization, the sharp drop in membrane potential that ends the action potential. (*b*) Electropharyngeomgram from a wild-type worm. E and R label E-phase and R-phase spikes, which correspond to the E and R phases of action potentials. *a* and *b* were recorded separately from different pharynges. Time scale is the same for *a* and *b*. Current scale bar applies only to *b*. (Adapted from [Davis et al. 1995](#).)

Figure 6. Model for the function of MC and M3.

## Figure 6

Model for the function of MC and M3. The figure shows four schematic traces. The top three represent hypothesized intracellular recordings from an MC neuron, an [M3](#) neuron, and a corpus muscle cell. The bottom trace is a schematic EPG. According to this model, MC is the pacemaker for rapid regular pharyngeal pumping. It fires regularly at a frequency of up to four times a second. Each time it fires, it produces an excitatory postsynaptic potential (*thick line*) in the [pharyngeal muscle](#) cell, usually raising the potential above the threshold necessary to trigger a muscle action potential. The muscle action potential causes contraction. [M3](#) senses this contraction and fires in response, producing inhibitory postsynaptic potentials in the muscle, which hasten the drop in membrane potential. Eventually, the threshold for repolarization is reached and the action potential ends. The end of the action potential is rapidly followed by relaxation. Occasionally, MC fails to trigger an action potential. In this case, the excitatory postsynaptic potential is seen as a solitary positive spike in the EPG. The EPG is the time derivative of muscle membrane potential summed over all pharyngeal muscles. Sharp changes in muscle membrane potential such as postsynaptic potentials and the beginning and end of the action potential appear as spikes. The small spike that occurs between corpus muscle action potentials is caused by repolarization of terminal bulb muscles. (Adapted from [Raizen and Avery 1994](#).)

Generated from local HTML

# Chapter 24. Feeding and Defecation — III Defecation Motor Program

---

Defecation is achieved by periodically activating a stereotyped sequence of muscle contractions ([Croll and Smith 1978](#)). The period does not change with temperature. When assayed at temperatures from 19°C to 30°C in the presence of plentiful food, defecation occurs every 45 seconds, with a standard deviation of less than 3 seconds at 20°C ([Liu and Thomas 1994](#); Iwasaki *et al.* 1995). In the hermaphrodite, each defecation begins with the contraction of the posterior body-wall muscles in all four muscle quadrants ([Fig. 7](#)). This locally increases internal pressure, causing the fluid contents of the intestinal lumen to be squeezed anteriorly. About 1 second later, these muscles relax, causing the intestinal contents to flow posteriorly, where they tend to collect in a bolus in the preanal region. About 1 second after this relaxation is complete, the body muscles near the head contract in all four muscle quadrants. This head contraction drives the rigid [pharynx](#) like a piston back into the anterior [intestine](#) ([Fig. 7](#)), perhaps to aid in concentrating gut contents near the [anus](#). Just as the anterior body contraction reaches its zenith, three types of muscles near the [anus](#) contract nearly simultaneously (Figs. [7](#) and [8](#)): the two intestinal muscles, the [anal](#) depressor, and the [anal](#) sphincter. The intestinal muscles wrap around the posterior gut and appear to further pressurize the intestinal contents. The [anal](#)-depressor muscle runs from the dorsal wall of the [anus](#) to the dorsal body wall and contracts to open the [anal](#) canal ([Thomas 1990](#)). The [sphincter muscle](#) is dilated prior to the [anal muscle](#) contractions and contracts nearly simultaneously with the other [anal](#) muscles, probably acting either to further squeeze the posterior [intestine](#) ([Reiner and Thomas 1995](#)) or to limit outflow of lumen contents ([McIntire \*et al.\* 1993b](#)). The four [anal](#) muscles are called the enteric muscles. They are interconnected by gap junctions ([White \*et al.\* 1986](#)), and their coupled contractions are called the [expulsion](#) (or enteric) muscle contraction ([E.p](#) or EMC).

In summary, defecation is carried out by three distinct motor steps: the posterior [body](#) muscle [contraction](#) (pBoc), the [anterior](#) [body](#) muscle [contraction](#) (aBoc), and the [expulsion](#) [muscle](#) [contraction](#) ([E.p](#) or EMC). Together, these steps constitute the [defecation](#) [motor](#) [program](#) (DMP). Most aspects of the defecation motor program are quite similar in the male, but the control of the [anal](#) seal is dramatically different in the adult male and will be considered in a later section.

Such a complex set of contractions might seem overdone, but observation of several other free-living nematode species reveals that the pattern of the motor steps is conserved during evolution, although the precise timing of the cycle and the motor steps varies somewhat (E. Jorgensen and J.H. Thomas, unpubl.). Elimination of any of the motor steps by mutation, including aBoc, which appears to be the least important step, causes detectable constipation. This suggests that each step contributes significantly to defecation volume. We speculate that precise control of defecation volume is achieved by a combination of all three motor steps and that this level of control has adaptive value.

## A. Neuronal Patterning

### 1. Mutants

A large number of mutations that disturb the DMP have been isolated. Most were identified by screening directly for constipated mutants ([Thomas 1990](#); E. Jorgensen, pers. comm.). This method of isolation biases toward mutations that cause a sharp reduction in the amount of feces expelled per time. Mutants with less severe defects have been isolated in smaller mutagenesis screens by direct observation of defecation cycles ([Iwasaki \*et al.\* 1995](#)). In addition, observation of behavioral mutants isolated on the basis of other mutant defects has identified several mutants with altered defecation ([Thomas 1990](#); [Reiner \*et al.\* 1995](#)). Summaries of mutants with altered motor programs, cycle period abnormalities, or muscle excitation defects have been published previously ([Thomas 1990](#); [Iwasaki \*et al.\* 1995](#); [Reiner and Thomas 1995](#)). The most severely constipated mutants probably have a degree of constipation that approximates the complete elimination of the defecation motor program. Mutants such as [gex-1](#) and [exp-2](#) never produce active enteric-muscle contractions, and they expel gut contents

about ten times less often than the wild type. Release of gut contents in these mutants often does not coincide with the remaining parts of the DMP. Following such a release (which is explosive and often clears nearly the entire gut lumen), the animal continues to feed normally and gradually becomes more constipated, as each defecation cycle fails to expel any gut contents. Eventually the animal becomes severely constipated but continues to feed well, suggesting little or no feedback regulation of feeding. It is a tribute to the power of the [pharynx](#) that eventually it fills the gut to the bursting point, the [anus](#) is forced open, and a new constipation cycle begins. The release of gut contents in such mutants can occur at any time during the defecation cycle and is not associated with any visible muscle contractions, suggesting that the release is caused by internal pressure. This pattern is phenocopied by killing the enteric muscles in the wild type, indicating that the pattern does not require enteric muscles and is not a mutant artifact. Severely constipated mutants and animals missing the enteric muscles are viable and fertile and appear behaviorally normal, although they mature slowly and are scrawny and small, characteristics of malnourishment ([Avery 1993a](#)). On the basis of these observations, it seems unlikely that overt expression of the defecation motor program is essential for viability or fertility. Despite this, large screens for constipated mutants have failed to identify mutations that eliminate the motor program ([Thomas 1990](#); E. Jorgensen et al., unpubl.), suggesting that such mutations are rare.

In addition to providing the raw material for more detailed investigations of defecation behavior, the pattern of mutant defects has some interesting properties. In theory, a series of stereotyped motor steps might be controlled in various ways. In a dependent-pathway model, each step depends on execution of the previous step. In this case, the periodicity of defecation and the timing of motor steps would be determined by simple delays after the execution of each dependent step. In an extreme alternative model, a cycle controller exists that is independent of motor steps and this controller sequentially activates motor steps at appropriate times. A hybrid model could involve a cycle controller that receives checkpoint feedback about the execution of motor steps, in a manner similar to mechanisms proposed for the cell cycle ([Hartwell and Kastan 1994](#)). The phenotypes of defecation mutants support a fairly strict controller model: Most defecation mutants affect only one part of the motor program, leaving periodicity and other parts of the motor program relatively unaffected ([Thomas 1990](#)). Similarly, most periodicity mutants leave the motor program unaffected ([Iwasaki et al. 1995](#)).

## 2. Motor Neurons

The precision of the defecation motor program demands exact spatial and temporal coordination. It is presumed that this coordination is mediated by the [nervous system](#), but there is direct evidence for only two of the motor steps, aBoc and Exp. [unc-25](#) mutants, which lack detectable amounts of the neurotransmitter GABA, are deficient in activation of the [E.p](#) step ([Thomas 1990; McIntire et al. 1993a](#)). Antibodies to GABA stain the neurons [AVL](#) and [DVB](#), and killing both [AVL](#) and [DVB](#) with a laser microbeam eliminates enteric-muscle contractions ([McIntire 1993b](#)). [DVB](#) makes a neuromuscular junction with the [anal](#) depressor ([White et al. 1986](#); E. Jorgensen, pers. comm.), and [AVL](#) forms a process with varicosities adjacent to the [anal](#) depressor muscle, although no clear neuromuscular junction is seen (E. Jorgensen, pers. comm.). No other neurons that have cell bodies or processes in the [anal](#) region are required for EMCs ([McIntire 1993b](#)). These data indicate that [AVL](#) and [DVB](#) are excitatory GABAergic motor neurons for the enteric muscles. It is also known that exogenous serotonin inhibits EMCs ([Ségalat et al. 1995](#)), although it is unclear how this functions *in vivo*.

Studies of [AVL](#) and [DVB](#) raise interesting points that may be generally significant for nematode neurons. First, [AVL](#) and [DVB](#) are partially redundant in activating EMCs. When either neuron alone is killed, EMC frequency is nearly normal, but when both are killed, EMCs are eliminated ([McIntire et al. 1993b](#)). We discuss neuronal redundancy near the end of this chapter. A second interesting point is that the EMC defect caused by killing [AVL](#) and [DVB](#) is more severe (~0% EMC) than that caused by the absence of GABA. In [unc-25](#) mutants, about 15% of cycles have an EMC ([Thomas 1990; McIntire 1993b](#)). Neuron kills in an [unc-25](#) mutant show that the residual EMCs in the absence of GABA require [DVB](#) but not [AVL](#) (E. Jorgensen, pers. comm.; J.H. Thomas, unpubl.), despite the fact that [DVB](#) is slightly less important than [AVL](#) for EMC activation in the wild type ([McIntire et al. 1993b](#)). These findings suggest that [DVB](#) employs a second EMC-activating neurotransmitter that is absent from [AVL](#). A plausible candidate transmitter is the peptide FLRFamide ([Schinkmann and Li 1992](#); see [Rand and Nonet](#), this

volume), since it is present in [DVB](#) but not [AVL](#), and it is known that peptides commonly accompany small molecular transmitters in other organisms.

A third interesting point is that GABA appears to be an excitatory transmitter for the enteric muscles. Usually in mammals, and in all other characterized cases in *C. elegans*, GABA is an inhibitory transmitter (see, e.g., [Tobin 1991](#); [McIntire et al. 1993a](#)). It is unlikely that GABA indirectly excites enteric muscles by inhibiting the action of an inhibitory neuron: Both [AVL](#) and [DVB](#) make output to the enteric muscles, and no other neuron in the region is required for normal EMCs ([White et al. 1986](#); [McIntire et al. 1993b](#)). If GABA is indeed excitatory, it might act on a novel ionotropic GABA receptor or it might act via a metabotropic receptor and a second-messenger system. A G-protein  $G_o$  is expressed in the enteric muscles, but it is not known whether this G-protein is a target of GABA ([Mendel et al. 1995](#); [Ségalat et al. 1995](#)). The [exp-1](#) gene, mutations in which are unusual in producing a defecation phenotype identical to that of [unc-25](#), is a plausible candidate for encoding this novel GABA receptor ([Thomas 1990](#); E. Jorgensen, pers. comm.; J.H. Thomas, unpubl.).

A final point is that [AVL](#) functions redundantly with [DVB](#) in activating EMCs, but killing [AVL](#) alone causes a strong aBoc-defective phenotype ([McIntire 1993b](#)). Mutants that lack GABA function have a normal aBoc step ([Thomas 1990](#)). These facts indicate that [AVL](#) has a nonredundant role in activating aBoc and that this function does not require GABA. [AVL](#) probably does not directly activate the head muscles that contract during aBoc, because no process from [AVL](#) passes anywhere near those muscles ([White et al. 1986](#)). By the conventional definition of neuron types, [AVL](#) is an interneuron using one transmitter for one muscle contraction (aBoc), and it is a motor neuron using a second transmitter (GABA) for a second muscle contraction (EMC). Functional complexity has also been described for the sensory neuron ASH, which mediates response to both nose touch and osmotic stimuli, possibly using different neurotransmitters ([Bargmann et al. 1990](#); [Kaplan and Horvitz 1993](#); [Hart et al. 1995](#); [Maricq et al. 1995](#)). We speculate that such complexity of neuron function is common in nematodes, perhaps as a result of the limited repertoire of available neurons.

Ten genes have been identified that mutate to an aBoc and [Exp](#)-defective (Aex) phenotype reminiscent of killing [AVL](#) and [DVB](#) ([Thomas 1990](#); J.H. Thomas, unpubl.; E. Jorgensen, pers. comm.). We think it likely that these genes are required for the function or activation of [AVL](#) and [DVB](#), rather than any of their specific transmitter systems, since we expect that elimination of any one transmitter would not produce an Aex phenotype. The strongest *aex* mutations cause a phenotype nearly identical to killing [AVL](#) and [DVB](#), but some other *aex* mutations result in a weaker phenotype, in which aBoc and [E.p](#) are more frequently present. It is unknown whether or not these *aex* mutations are null. In addition to the tight connection between the aBoc and [E.p](#) steps, there is also some indication that pBoc and [E.p](#) are connected in some manner not yet understood. Although many mutants that are deficient in pBoc have normal Exps, [egl-8](#) mutants ([Trent et al. 1983](#)) have a very weak pBoc and a variably reduced EMC frequency, as do some other less-characterized mutants (K. Iwasaki and J.H. Thomas, unpubl.; E. Jorgensen, pers. comm.).

### 3. pBoc Activation

The body-wall muscles used for pBoc and aBoc are the same as those used for locomotion. During locomotion, the dorsal and ventral body muscles are reciprocally contracted and relaxed to generate bends in the body, and the motor neurons that control these movements have been identified ([Stretton et al. 1985](#); [White et al. 1986](#); [McIntire et al. 1993b](#)). In contrast, during pBoc and aBoc, dorsal and ventral body muscles are contracted simultaneously, causing the body to shorten locally ([Fig. 7](#)). A large number of mutants have been identified that profoundly affect locomotion, including many that severely perturb the locomotory motor neurons (see [Hedgecock and Garriga](#), this volume). None of these mutants is defective in pBoc ([Thomas 1990](#); J.H. Thomas, unpubl.; E. Jorgensen, pers. comm.), indicating that activation of pBoc occurs by a distinct pathway. (This may be true for aBoc as well, but the aBoc contraction is less robust and has not been analyzed in as much detail.) The source of pBoc activation is mysterious, since laser kills suggest that no neuron in the region of these muscles is required for their contraction (E. Jorgensen, pers. comm.). It is possible that some neuron acts at a distance to activate pBoc, perhaps through the pseudocoelomic space, or pBoc may be activated by a nonneuronal pathway, for example, by the hypodermal syncytium.

## 4. Excitation of the Enteric and Egg-laying Muscles

Many of the mutations that affect enteric muscle contraction share two properties: They are semi-dominant and they also affect egg-laying muscle contraction ([Greenwald and Horvitz 1980, 1986; Trent et al. 1983; Park and Horvitz 1986a; Levin and Horvitz 1993; Reiner et al. 1995; Weinshenker et al. 1995](#)). Many of these mutations also affect additional muscle groups and were originally identified by these other muscle defects ([Brenner 1974; Greenwald and Horvitz 1980, 1986; Trent et al. 1983; Park and Horvitz 1986a; Avery 1993b; Levin and Horvitz 1993](#); R. Waterston, pers. comm.). The muscle specificity of these mutations is summarized in [Table 1](#). For each of these mutants, the muscle myofilaments appear to be relatively unaffected. Polarized-light microscopy showed that their muscle organization is normal, and each mutant can contract its [anal](#)-depressor muscle when it is shot with a laser ([Reiner et al. 1995](#)). The mutants do not lay eggs in response to excitatory transmitters that are thought to act directly on egg-laying muscle ([Trent et al. 1983](#)). These results suggest that these genes affect muscle excitation but not contractile function.

An extraordinary feature of the *egl/exp* mutations is that every one of them is dominant, despite the fact that nearly all were isolated in standard  $F_2$  screens designed to detect recessive mutants. Most mutations causing abnormal myofilament structure are recessive ([Waterston 1988; Fire and Moerman](#), this volume) as is characteristic of mutations affecting most processes. Deficiencies eliminating 8 of the 12 genes exist, and none of these cause dominant muscle defects, indicating that the dominance of the *egl/exp* mutation is due to a gain of function. Putative loss-of-function mutations have been identified for eight of the *egl/exp* genes and seven of these produce no obvious phenotype. It will be interesting to learn why so many muscle excitation genes are identified by dominant mutations. We speculate that excitation of these muscles involves a number of negative regulatory pathways, which can mutate to the easily detected *Egl* or *E.p* phenotypes only by gain of function. Loss-of-function mutations in such genes would cause the relatively subtle phenotype of stronger muscle contraction. An example of such a negative regulator of neuronal and muscle excitation is  $K^+$  channels, which function to shape and terminate action potentials.

## B. The Defecation Cycle Clock

The defecation cycle period of 45 seconds is regular in single animals over time and among animals, with a standard deviation of only a few seconds ([Fig. 9](#)). The cycle period has several properties that are characteristic of biological clocks: The period is constant over a range of temperatures (temperature compensation), the oscillation phase is maintained in the absence of entraining cues, and the oscillation can be reset by certain perturbations ([Liu and Thomas 1994](#)). Defecation periodicity is nearly constant in animals assayed at temperatures ranging from 19°C to 30°C ([Liu and Thomas 1994](#)). In contrast to the defecation cycle, other processes such as growth rate, pharyngeal pumping, and the duration of the defecation motor program (time from pBoc to *E.p*) are strongly affected by temperature changes ([Iwasaki et al. 1995](#); L. Avery, unpubl.). When an animal spontaneously leaves the bacterial lawn, the defecation motor program is not expressed. When the animal returns to the lawn, the phase of the defecation cycle tends to be maintained, indicating that the cycle phase can be maintained in the absence of overt expression of the motor program ([Liu and Thomas 1994](#)). Finally, light-touch mechanosensation can reset the defecation phase. When an animal is gently touched at various times during a defecation cycle, the next DMP occurs 45 seconds after the touch ([Thomas 1990; Liu and Thomas 1994](#)), suggesting that the clock has been reset to zero. Mutants that lack touch response ([Chalfie and Sulston 1981](#)) fail to reset, showing that a sensory stimulus is responsible for the reset. These findings strongly suggest that a temperature-compensated clock controls the defecation cycle period.

Dilution of food causes graded lengthening of the defecation cycle. Animals feeding on a very thin lawn of bacteria have regular cycles with periods as long as 80 seconds ([Liu and Thomas 1994](#)). Surprisingly, there are only modest effects of feeding rate and constipation on the defecation cycle. Several different mutants severely defective in pharyngeal pumping have defecation cycles that are typically 50 to 60 seconds long, suggesting that slow feeding can lengthen the cycle slightly ([Thomas 1990](#); D.W.C. Liu and J.H. Thomas, unpubl.). The fact that dilute food can lengthen the cycle period more dramatically than feeding defects suggests that part of this

regulation is sensory-mediated. However, pleiotropic chemosensory-defective mutants such as [osm-3](#) and [osm-5](#) have nearly normal response to food dilution ([Thomas 1990](#); D.W.C. Liu and J.H. Thomas, unpubl.), suggesting that at least part of this sensory regulation is mechanosensory. Severely constipated mutants have a characteristic oscillation in cycle period: Just after an explosive release of gut contents, the defecation cycle is about 50 seconds long, but as the animals become constipated over the next ten cycles or so, this gradually drops to about 35 seconds (D.J. Reiner et al., unpubl.). Since this pattern is observed in various mutants and in wild-type animals lacking the enteric muscles or [AVL](#) and [DVB](#), we think that the oscillating cycle period is due to the cyclical constipation that the animals experience.

## 1. Mutants

Circadian rhythms, with a period of about 1 day (*circa dia*), are being analyzed genetically and molecularly in several organisms, including cyanobacterium, plants, *Drosophila*, *Neurospora*, and mouse (see, e.g., [Konopka and Benzer 1971](#); [Hall 1990](#); [Kondo et al. 1994](#); [McClung et al. 1989](#); [Vitaterna et al. 1994](#)). Ultradian rhythms, with a period of less than 24 hours, are also widespread but have been the subject of relatively little genetic analysis (see, e.g., [Edmunds 1988](#)). Its high frequency, tight periodicity, and ease of observation make defecation periodicity amenable to genetic analysis.

A number of defecation cycle period (Dec) mutants have been identified, genetically mapped, and characterized phenotypically ([Thomas 1990](#); [Iwasaki et al. 1995](#)). Most such mutations do not cause substantial constipation and are identified and analyzed by direct observation of defecation cycles. A total of 12 genes have been identified that can mutate to affect the defecation cycle period specifically (Figs. [9](#) and [10](#)). For each mutation, feeding and defecation motor steps appear to be grossly normal. Mutations in these genes fall into two major groups: short cycle (Dec-s) and long cycle (Dec-L; we use the capital L to distinguish it from the numeral "1"). Mutations in seven genes cause a short cycle period. These mutants can be divided into three subclasses based on detailed phenotype. Mutations in [flr-1](#), [flr-3](#), and [flr-4](#) are recessive and cause a very short mean cycle period, especially at 25°C where cycles are often less than 20 seconds. Mutations in these three genes were first identified and named for their fluoride resistance (Flr) phenotype ([Katsura et al. 1994](#)), but it is unclear how the Dec-s and Flr phenotypes are related. Mutations in two other genes, [dec-7](#) and [unc-16](#), are recessive and cause moderately short cycle periods. Finally, Dec-s mutations in two genes, [dec-9](#) and [dec-10](#), are semidominant, and genetic deficiency tests suggest that both mutations are gain-of-function. None of these last four Dec-s genes and none of the Dec-L genes confer fluoride resistance. All five identified Dec-L mutations are recessive and each Dec-L gene is defined by a single mutation. [dec-2](#) and [dec-4](#) alone among all of the Dec mutations cause an altered motor program: The interval between the pBoc and [E.p](#) steps is slightly longer than normal ([Iwasaki et al. 1995](#)). The recently described [clk-1](#) mutant also has a Dec-L phenotype and, unlike other Dec mutants, [clk-1](#) affects the timing of many other behaviors and developmental events ([Wong et al. 1995](#)).

The phenotypes of the clock mutants and the motor program mutants are parsimoniously explained by the model in Figure 11. In this model, a clock runs separately from the motor program and periodically initiates a motor program. Each step in the motor program can be individually affected by mutation without perturbing the clock, so the motor steps are depicted as branching from each other after the program initiation step. The *aex* genes are depicted as affecting a step common to aBoc and [E.p](#), probably the activation or function of [AVL](#) and [DVB](#). One of the chief challenges of future research will be to move beyond this formal model by deciphering the cellular and molecular pathways that underlie the genetic pathway.

## 2. Temperature Compensation

In general, biochemical reactions occur faster at higher temperatures. The fact that the defecation cycle period remains nearly constant over a range of temperatures implies that a specific mechanism compensates the cycle period at different temperatures. In contrast to the wild type, most *dec* mutants have temperature-dependent cycle periods ([Fig. 10](#)). Temperature-dependent phenotypes can be caused by heat- or cold-sensitive gene products, but only a small subset of mutations produce such thermolability. The high frequency of temperature-dependent *dec* mutants implies that they do not result from thermolabile gene products. Supporting this

interpretation, some *dec* mutations confer pleiotropic phenotypes that are not temperature-dependent ([Iwasaki et al. 1995](#)). The simple interpretation is that temperature compensation is an intrinsic feature of the clock mechanism, rather than a separate circuit that regulates cycle periodicity. In *Drosophila* and *Neurospora*, mutations in *per* and *frq* cause temperature-compensation defects in addition to abnormal circadian rhythms ([Loros and Feldman 1986; Konopka et al. 1989](#)), suggesting that this clock is also integrated with temperature compensation.

All of this begs the question of why the defecation cycle should be temperature-compensated. Presumably, the rate of defecation is the major determinant of the residence time of food in the gut, and this residence time must influence the thoroughness of digestion and absorption of nutrients. Assuming that the rate of digestive processes increases with temperature, the temperature compensation of the defecation cycle means that nutrient extraction is less complete at lower temperatures. We have no idea why this is adaptive.

## C. Developmental Changes in the Male

During larval stages, the male [anus](#) appears to be identical to the hermaphrodite [anus](#): Hydrostatic pressure maintains the [anal](#) seal and enteric muscles break this seal transiently during defecation. However, during the generation of the mature [male tail](#) at the L4 molt, the [anal](#) canal is modified to form a cloacal/[anal](#) canal, and this canal is open directly to the exterior (see [Fig. 8](#)). The [anal](#) depressor, the most important larval enteric muscle, repositions its ventral attachment site to become a spicule protractor that functions in male mating ([Sulston et al. 1980](#)). On the basis of its structure and the lack of a defecation defect when killed, the [anal](#) depressor no longer plays a significant part in adult male defecation ([Reiner and Thomas 1995](#)). Despite the fact that there is no plausible hydrostatic pressure seal, gut contents do not discharge in the adult male except during a defecation motor program. This seal is established by hypertrophy of the [anal-sphincter muscle](#) during the late L4 ([Sulston et al. 1980](#)) and a reversal in the excitation of the muscle ([Reiner and Thomas 1995](#)). Tonic contraction of the [anal](#) sphincter seals the adult male intestinal lumen between defecations. During ejaculation, the sphincter hypercontracts, causing the [intestine](#) to shift dorsally ([Fig. 8](#)), which probably aids in opening the [vas deferens](#) for sperm passage ([Sulston et al. 1980](#)). During the expulsion step of defecation, the sphincter relaxes to allow intestinal contents to pass ([Reiner and Thomas 1995](#)).

The structural changes in the male [anal](#) sphincter must be associated with changes in excitability, since it converts from contraction during expulsion in the larva ([McIntire et al. 1993b; Reiner and Thomas 1995](#)) to tonic contraction punctuated by relaxation during expulsion in the adult. Strangely, GABA appears to mediate both the larval contraction and the adult relaxation, since [unc-25](#) mutants are deficient in both events ([Reiner and Thomas 1995](#)). Failure of the sphincter to relax in [unc-25](#) adult males results in a severe Con phenotype that is fully relieved by killing the [sphincter muscle](#) ([Reiner and Thomas 1995](#)). Similarly, mutations in other genes ([unc-46](#), [unc-47](#) and [unc-49](#)) implicated in general GABA function cause a Con phenotype in the adult male that is relieved by killing the sphincter. [unc-49](#) encodes a GABA-A receptor (B. Bamber and E. Jorgensen, pers. comm.), consistent with a role specifically in relaxation of the [sphincter muscle](#) in the adult male. Killing [AVL](#) and [DVB](#), other *exp* mutations, and *aex* mutations causes constipation in larvae of both sexes but not in the adult male. These results suggest that these *exp* and *aex* genes are required either for the function of [AVL](#) and [DVB](#) or specifically for muscle excitation (since only sphincter relaxation seems to be essential to prevent constipation in the adult male). The fact that [AVL](#) and [DVB](#) are not required for adult male defecation indicates that additional [GABAergic neurons](#) must be recruited to regulate the sphincter. The [male tail](#) contains several unidentified GABA-containing [neurons](#) that might play this part (S. McIntire and E. Jorgensen, pers. comm.).

Another developmental twist in male defecation is that the enteric muscles probably change their electrical coupling at this time. In the hermaphrodite (and presumably in the larval male), the three classes of enteric muscles are coupled by gap junctions ([White et al. 1986](#)) and all the muscles contract nearly simultaneously. However, in the adult male, the intestinal muscles contract during the expulsion step while the sphincter relaxes, and the [anal](#) depressor functions independently ([Reiner and Thomas 1995](#)). Although they have not been reconstructed by electron microscopy, it seems likely the gap junctions joining the enteric-muscle arms are lost in the adult male.

## Figures

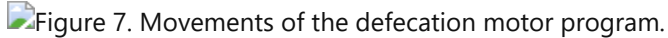


### Figure 7

Movements of the defecation motor program. (Intercycle) An animal is between defecation motor programs. (pBoc) An animal at the peak of the posterior [body muscle](#) contraction (pBoc), with the tail compressed and the fluid gut contents pressed anteriorly. (Relaxation) An animal just after pBoc has relaxed and before anterior [body muscle](#) contraction (aBoc) starts, with the gut contents concentrated in the preanal region. (aBoc) An animal at the peak of the aBoc contraction, with the head compressed and the [pharynx](#) driven back into the [intestine](#). (E.p) While the anterior body is still contracted, the enteric muscles contract (expulsion muscle contraction, EMC), opening the [anus](#) and allowing the animal's internal pressure to expel gut contents.



### Figure 8

Adult hermaphrodite and adult male [anal](#) regions. The [sphincter muscle](#) enlarges and forms an attachment to the dorsal body wall that is absent in the hermaphrodite. The intestinal muscles are similar in the two sexes and appear to have the same function of squeezing the posterior [intestine](#) during expulsion. The [anal](#) depressor does not function in male defecation and is not shown. The larval male is structurally and functionally similar to the hermaphrodite. (Adapted from [Reiner and Thomas 1995](#).)

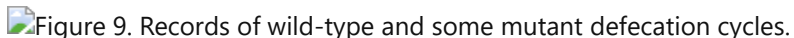


### Figure 9

Records of wild-type and some mutant defecation cycles. Each dot or letter is one second. "p" is pBoc and "x" is Exp. aBoc is not shown. Scale at the top of each panel is in seconds. *flr-1* appears to miss occasional cycles, for example, on line three of the record shown. The periodicity of the *flr-1* animal was established both by eye alignment and by the MESA program ([Dowse and Ringo 1989](#)), which were in good agreement. Assays were with wild type, *flr-1(sa96)*, *dec-7(sa296)*, and *dec-2(sa89)*, all at 20°C.

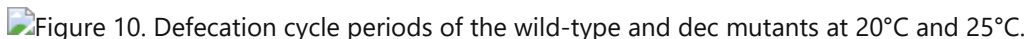


### Figure 10

Defecation cycle periods of the wild-type and *dec* mutants at 20°C and 25°C. (Solid bars) 20°C; (hatched bars) 25°C. Genes are shown below each bar. The y-axis shows mean cycle period (seconds/cycle). The standard error of the mean is indicated at the top of each bar. The asterisk indicates significant difference between the means at 20°C and 25°C for a given mutant ( $p < 0.01$  using the two-tailed t-test and the Mann-Whitney test). The pound sign indicates a marginal significance ( $p < 0.05$  using the Mann-Whitney test for data sets deviating from the normal distribution). The horizontal dashed line in each panel is the wild-type mean at 20°C. At least ten animals were observed for ten cycles each for each bar. The left panel shows the Dec-s mutants and the right panel shows the Dec-L mutants. Strains were *flr-1(sa96)*, *flr-3(ut9)*, *flr-4(sa201)*; *dec-7(sa296)*, *unc-16(e109)*, *dec-9(sa293)*, *dec-10(sa294)*, *dec-2(sa89)*, *dec-1(sa48)*, *dec-12(sa295)*, *dec-11(sa292)*, and *dec-4(sa73)*. The arrowhead on the *dec-4* mutant at 25°C indicates rare activation of the motor program. (Adapted from [Iwasaki et al. 1995](#).)



### Figure 11

A genetic model of defecation. A cycle generator controls the timing of defecation. A branching pathway controls the individual motor steps. Genes affect various steps as indicated by lines crossing the pathways. The model is based largely on the phenotypes of mutants and when [AVL](#) and [DVB](#) are killed.

## Tables

**Table 1 Summary of *egl/exp* genes and affected muscle groups**

Gene	Pharyngeal muscle	Body-wall muscle	Egg-laying muscle	Enteric muscle
<i>egl-2(sd)</i>	+	+	d	d
<i>egl-23(sd)</i>	+	+	d	d
<i>egl-36(sd)</i>	+	+	d	d
<i>exp-3(sd)</i>	+	+	d	d
<i>exp-4(sd)</i>	+	+	d	d
<i>exp-2(sd)</i> <sup>a</sup>	d	+	d	d
<i>unc-93(sd)</i>	+	d	d	d
<i>sup-9(sd)</i>	d	d	d	d
<i>sup-10(sd)</i>	+	d	d	d
<i>egl-30(sd)</i>	+	d	d	d
<i>unc-103(sd)</i>	+	d	d	d
<i>unc-58(sd)</i>	+	h	h	n.d.
<i>unc-90(sd)</i>	+	h	h	n.d.
<i>unc-105(sd)</i>	+	h	h	n.d.
<i>eat-12(sd)</i>	h	h	h	n.d.
<i>unc-43(sd)</i>	+	h	d	d
<i>unc-43(r)</i>	+	d	h	n.d.
<i>unc-110(sd)</i> <sup>a</sup>	+	d	h	n.d.

(+)

Similar to wild type; (d) defective contraction; (h) hypercontracted; (n.d.) not determined (it is suspected that these mutants have a hyperactivated enteric-muscle contraction but this is difficult to observe).

a

These two mutations cause recessive lethality and data are for the heterozygote.

Generated from local HTML

# Chapter 24. Feeding and Defecation — IV Conclusions

---

The [nervous system](#) of *C. elegans*, consisting in the adult hermaphrodite of 302 [neurons](#) of 118 anatomical types ([Albertson and Thomson 1976](#); [White et al. 1986](#)), is simple enough that one can hope to understand how it functions as a whole. It is unique among neurobiological model systems in this regard. It was partly with this idea in mind that Brenner began work on *C. elegans* in 1965 ([Brenner 1973](#); [Wood 1988](#)). It is only now after 30 years that we are beginning to understand enough about *C. elegans* behavior and its implementation by the [nervous system](#) to fulfill his vision. Brenner and White's program of anatomical reconstruction had to be completed. It also took technical advances such as White's development of laser microsurgery as a broadly applicable technique. In the last several years, most of the obvious *C. elegans* behaviors have been studied in one or more laboratories, and functions have been assigned to many [neuron](#) types.

The pharyngeal [nervous system](#) is to the *C. elegans* [nervous system](#) what the *C. elegans* [nervous system](#) is to the more complex nervous systems of other animals: a smaller, simpler system that can be studied as a unit. We believe we now have an overview of the main functions of the pharyngeal [nervous system](#). We are beginning to attain such an overview for the extrapharyngeal [nervous system](#). Have we learned any general lessons? Which lessons are specific to *C. elegans*, and which can be applied to more complicated nervous systems?

## A. Multifunctional Neurons

[neurons](#) are conventionally classified as [sensory neurons](#), [interneurons](#), or motor neurons. Sensory neurons have sensory endings that detect changes in their environment and are presynaptic to other [neurons](#). [Interneurons](#) receive input from and send output to other [neurons](#). Motor neurons send their output to muscle cells or other effectors. This classification works very well in vertebrates and applies to most [neurons](#) in classical arthropod, annelid, and mollusc systems. It breaks down badly in *C. elegans*. [Albertson and Thomson \(1976\)](#), [Ward et al. \(1975\)](#), and [White et al. \(1986\)](#) found that many [neurons](#) appeared anatomically to be multifunctional. For instance, the pharyngeal neuron [M3](#) has apparent sensory endings, yet sends its output to muscle. Functional studies have confirmed the multifunctionality of several [neuron](#) types. There is evidence that [pharyngeal neurons](#) [MC](#) and [M3](#) are indeed sensorimotor. We have discussed the evidence that [AVL](#) has output both to enteric muscles and to [head neurons](#), and it therefore appears to be both a motor neuron and an [interneuron](#). We think that the high frequency of multifunctional [neurons](#) in *C. elegans* was selected to allow complex behavior to be programmed with a smaller number of [neurons](#) than would otherwise be necessary.

## B. Redundancy

Redundancy is a pervasive theme in *C. elegans* [nervous system](#) function. Examples can be drawn from defecation and feeding. Either [AVL](#) or [DVB](#) is sufficient for nearly normal EMC frequency, but when both are killed, EMCs nearly cease ([McIntire et al. 1993b](#)). Neither of the [pharyngeal neurons](#) [M3](#) or [I5](#) is necessary for nearly normal transport of bacteria within the [pharynx](#), but when both are killed, bacterial transport within the isthmus becomes inefficient. For many more examples of redundancy for these and for other behaviors, see [Bargmann and Horvitz \(1991a\)](#) and [Riddle](#) (this volume).

Nervous system redundancy is nearly universal through the animal kingdom. For instance, the [dopaminergic neurons](#) of the human substantia nigra are necessary for normal movement, but Parkinson's disease does not develop until about 80% of them have died ([Bernheimer et al. 1973](#); [Calne and Zigmond 1991](#)). Similarly, no single [neuron](#) in the 30-neuron lobster stomatogastric ganglion is necessary for pacemaker activity ([Selverston and Miller 1980](#); [Eisen and Marder 1982](#); [Miller and Selverston 1982a,1982b](#)). Nevertheless, the repeated discovery of redundancy in the *C. elegans* [nervous system](#) was a surprise. The naive prediction is that in a small [nervous system](#), every cell must count, and there should not be multiple cells doing the same thing. Redundancy requires explanation. The existence of redundancy even in the stripped-down *C. elegans* [nervous system](#) suggests that the explanation must be basic to the nature of [nervous system](#) function.

[Thomas \(1993a\)](#) suggested four ways in which genetic redundancy could be maintained: selection for cumulative function, fidelity of function, divergent functions of molecules whose functions overlap, and emergent functions. His scheme can also be applied to neuronal redundancy. For the two examples given above, EMC control and bacterial transport, selection for divergent function may be part of the explanation. [AVL](#) and [DVB](#) functions overlap in the excitation of expulsion muscles, but [AVL](#) is uniquely necessary for aBoc, and there is evidence that [DVB](#) provides a chemical stimulus to the enteric muscles that [AVL](#) does not (see above). [I5](#) and [M3](#) also have divergent functions. In fact, they promote effective transport by entirely different mechanisms: [M3](#) triggers pharyngeal relaxation, whereas [I5](#) inhibits [M3](#) and has in addition an [M3](#)-independent effect on the isthmus. [Liu and Sternberg \(1995\)](#) have shown that there is a similar type of functional but not mechanistic redundancy in male mating, where two [sensilla](#), the hook and the postcloacal sensillum, are involved in the location of the [vulva](#) by unrelated mechanisms.

Redundant [neurons](#) are probably maintained by selection for fidelity as well. Although either [AVL](#) or [DVB](#) is sufficient for the production of EMCs, the EMCs are not as reliable when only one of these [neurons](#) is present as when both are. Similarly, bacterial transport in the isthmus is often slightly abnormal when just [I5](#) is killed. Selection for fidelity may be an important general mechanism that promotes [nervous system](#) redundancy. It is believed that much synaptic transmission is quantal, with only one or a few vesicles of transmitter released per impulse and frequent failure ([Kandel 1991](#)). This would be especially true at small synapses, such as those of *C. elegans*. Extra [neurons](#) are one way of increasing the reliability of transmission.

Implicit in this discussion is the idea that redundancy is never complete: Killing a [neuron](#) should always have an effect if one looks closely enough. This is true for both of the cases discussed here. EMCs occasionally fail when either [DVB](#) or [AVL](#) is killed, and [AVL](#) is also necessary for aBoc. Killing either [M3](#) or [I5](#) delays growth to adulthood by a few hours, and the effect of killing both is not synergistic, but additive ([Avery 1993b](#)).

Generated from local HTML

## **Chapter 24. Feeding and Defecation — Acknowledgments**

---

We thank E. Jorgensen, members of the Avery lab, members of the Thomas lab, and the reviewers for their comments on the manuscript. L.A. is supported by a fellowship from the Klingenstein Foundation, J.H.T. is supported by the Searle Scholar's Program/Chicago Community Trust, and both authors are recipients of research grants from the U.S. Public Health Service.

Generated from local HTML

# **Chapter 25. Chemotaxis and Thermotaxis**

---

## **Contents**

- [I Introduction](#)
- [II \*C. elegans\* Responds to a Variety of Chemicals](#)
- [III The Behavioral Mechanism of Chemotaxis and Thermotaxis](#)
- [IV Cellular Analysis of Chemosensory and Thermosensory Neurons](#)
- [V Genetic and Molecular Analysis of Chemosensation and Thermosensation](#)
- [VI Regulation of Chemotaxis and Thermotaxis by Experience](#)
- [VII Conclusions and Prospects](#)
- [Acknowledgments](#)

Generated from local HTML

## Chapter 25. Chemotaxis and Thermotaxis — I Introduction

---

Chemosensation and thermosensation are two important sensory mechanisms that *Caenorhabditis elegans* uses to interact with its environment. Behavioral and genetic similarities between chemotaxis and thermotaxis indicate that these two types of tracking behaviors share molecular and cellular components.

*C. elegans* modifies many aspects of its behavior on the basis of chemical cues. Bacteria (its food) or bacterial metabolites stimulate feeding, defecation, and egg laying ([Horvitz et al. 1982](#); [Avery and Horvitz 1990](#); [Thomas 1990](#); [Avery and Thomas](#), this volume). The chemosensory system also detects a pheromone that regulates entry into the alternative dauer larva stage (see [Riddle](#), this volume). Other pheromones contribute to mating between males and hermaphrodites (see [Emmons and Sternberg](#), this volume). This chapter focuses on chemotaxis, the migration of animals toward bacteria (their food) or defined chemicals ([Ward 1973](#); [Dusenberry 1974](#)).

Temperature is a major determinant of the animal's metabolism. As a cold-blooded animal, *C. elegans* has a limited temperature range (~12– 26°C) at which it is viable and fertile. Thermotaxis behaviors allow animals to track to a preferred temperature (see [Hedgecock and Russell 1975](#)).

Generated from local HTML

## Chapter 25. Chemotaxis and Thermotaxis — II *C. elegans* Responds to a Variety of Chemicals

In the soil, *C. elegans* lives at an air-water interface and is exposed to both liquid and airborne chemicals. It detects most water-soluble attractants in the micromolar concentration range ([Ward 1973; Dusenberry 1980a](#)) and volatile molecules in the picomolar concentration range (B. Terrill and D. Dusenberry, pers. comm.). Volatile molecules travel quickly through diffusion and turbulence in the air, whereas water-soluble molecules in the soil tend to diffuse more slowly. Taken together, these results suggest that water-soluble chemicals are used mainly for short-range chemotaxis to bacteria, and volatile chemicals can be used for longer-range chemotaxis to distant food sources.

Chemical attractants and repellents for *C. elegans* have been identified by screening large numbers of volatile and nonvolatile chemicals ([Table 1](#)). Salts, some amino acids, some nucleotides, and some vitamins act as water-soluble attractants ([Ward 1973; Dusenberry 1974; Bargmann and Horvitz 1991a](#)), as do many different volatile organic molecules ([Bargmann et al. 1993](#)). Many of the attractants are byproducts of bacterial metabolism, so they could be chemical cues in the animal's natural environment.

The ability of *C. elegans* to discriminate between related chemicals has been demonstrated in saturation experiments, in which high concentrations of one attractant block or do not block responses to a second attractant ([Ward 1973; Bargmann et al. 1993](#)). These experiments indicate that *C. elegans* can distinguish among many different chemicals, including chemicals that vary only slightly in their structures. At least five classes of water-soluble attractants and seven classes of volatile attractants have been defined by these studies. It is likely that these different classes of molecules are recognized by different receptor proteins (see below).

Repulsive substances include some specific water-soluble chemicals, acids, many compounds at high osmotic strength, and a few volatile molecules ([Ward 1973; Dusenberry 1974, 1975; Bargmann et al. 1993](#); J. Culotti and J.H. Thomas, pers. comm.). All of these compounds are toxic or hazardous to the organism, causing paralysis and death. Other equally toxic compounds are not avoided by the animal, so avoidance responses are mediated by specific neuronal mechanisms and not by tissue damage.

### Tables

**Table 1** Attractive and repulsive substances

Attractants	
Water-soluble	Volatile
Na <sup>+</sup> , K <sup>+</sup> , Li <sup>+</sup> Ca <sup>++</sup> , Mg <sup>++</sup>	alcohols
Cl <sup>-</sup> , SO <sub>4</sub> <sup>-</sup> , NO <sub>3</sub> <sup>-</sup> , Br <sup>-</sup> , I <sup>-</sup>	ketones
cAMP, cGMP	diketones
Biotin	esters
Lysine, histidine, cysteine, serotonin	pyrazines
Basic pH	thiazoles aldehydes aromatics ethers
Repellents	
Water-soluble	Volatile

High osmotic strength	heptanol, octanol, nonanol
Acid pH	nonanone
Copper ions	benzaldehyde
Sodium dodecyl sulfate	2,4,5-trimethylthiazole
Δ-tryptophan	ethyl heptanoate

Generated from local HTML

## Chapter 25. Chemotaxis and Thermotaxis — III The Behavioral Mechanism of Chemotaxis and Thermotaxis

---

The standard chemotaxis assay measures the ability of *C. elegans* to track to the point source of a chemical gradient on an agar assay plate ([Fig. 1a](#)) ([Ward 1973](#)). Chemotaxis of individual animals is measured by watching the tracks that they leave on the agar; chemotaxis of populations of animals is measured by counting animals at the attractant source over time. To generate the chemotaxis behavior, an animal must recognize a chemical, orient itself in the gradient, and move in a coordinated fashion to the peak concentration of attractant. The mechanism by which chemotaxis is accomplished is only partly understood. Since all of the essential chemosensory structures are in the head (see below), *C. elegans* does not respond to a gradient by comparing concentrations of attractant at its head and tail ([Ward 1973](#)). Nor does the nematode compare attractant concentrations on its left and right, since killing the [neurons](#) in either the left or the right chemosensory organ does not prevent chemotaxis ([Bargmann and Horvitz 1991a](#)).

Experiments with tethered animals indicate that *C. elegans* can directly sense temporal changes in chemical concentration ([Dusenberry 1980b](#)). Individual animals were tethered and exposed to different concentrations of chemicals, and their responses were monitored by videotaping. Tethered animals display movement patterns that can be recognized as forward-directed or backward-directed, although the animals do not actually change their position. An abrupt decrease in the concentration of attractant (salt) leads the animal to display backward-directed movement, whereas an increase in the concentration of attractant suppresses the spontaneous frequency of backward movement. This behavior pattern is analogous to the mechanism of bacterial chemotaxis, in which bacteria move in long smooth lines (running) in the presence of increasing concentrations of attractant, but change direction frequently (tumbling) in the presence of decreasing concentrations of attractant ([Berg and Brown 1972](#); [Berg 1993](#)).

Observation of freely moving animals in attractant gradients indicates that spatial integration of chemosensory information also contributes to chemotaxis. On agar plates, *C. elegans* swims on its side, making sinusoidal movements in the dorsal-ventral plane. Animals that have bent necks as a consequence of a [vab-10](#) mutation migrate to the peak of the gradient in a spiral pattern, apparently because they keep their heads precisely directed toward the attractant source ([Ward 1973](#)). This observation suggests that the nematode can detect the steepest gradient of attractant and direct its movement in that direction. It is likely that both temporal and spatial cues are integrated during chemotaxis in the normal environment.

Thermotaxis behaviors can be observed by watching tracking patterns of individual animals in radial thermal gradients ([Fig. 1b](#)) or by observing the distribution of animals in linear thermal gradients ([Hedgecock and Russell 1975](#)). After cultivation at temperatures from 15°C to 26°C, *C. elegans* first moves along the temperature gradient and then chooses an optimal temperature, which normally corresponds to its cultivation temperature. Animals then display "isoclines" of movement in the radial gradient, in which they circle the plate at precisely the preferred temperature. This smooth movement at the preferred temperature requires that the animal detect thermal gradients of less than 0.1°C. Like chemotaxis, normal thermotaxis probably includes both spatial and temporal integration of thermal cues. Some mutants or laser-operated animals are only abnormal in migration to a preferred temperature and can make crude isotherms at a temperature other than the preferred temperature ([Mori and Ohshima 1995](#)). This observation implies that migration to a preferred temperature and isothermal tracking require distinct cellular or molecular mechanisms ([Hedgecock and Russell 1975](#); I. Mori and Y. Ohshima, unpubl.).

Avoidance of noxious chemicals can occur by at least two different behavior patterns. A high concentration of repellent, such as high osmotic strength, acid, or octanol, can induce a rapid reversal response, which is followed by a change of direction ([Culotti and Russell 1978](#); [Troemel et al. 1995](#)). This fast response does not require the spatial and temporal resolution characteristic of chemotaxis or thermotaxis. In addition, animals in the presence of a gradient of volatile repellents display a form of negative chemotaxis, in which they travel down the gradient to the lowest concentration of odorant (B. Kimmel and C. Bargmann, unpubl.).

## Figures

Figure 1. Chemotaxis and thermotaxis behaviors.

### Figure 1

Chemotaxis and thermotaxis behaviors. Shown in both cases are tracks of a single worm on an agar plate. (a) Animal in the presence of a gradient of biotin, with the biotin source marked at B. The animal was allowed to move freely on the agar plate for 1 hour. (b) Animal in a radial thermal gradient. The animal first moved to the acclimation temperature and then circled in isotherms at that temperature.

Generated from local HTML

## Chapter 25. Chemotaxis and Thermotaxis — IV Cellular Analysis of Chemosensory and Thermosensory Neurons

---

Three types of sensory organs in *C. elegans* hermaphrodites appear to be chemosensory, based on the fact that they are associated with openings in the cuticle that allow the enclosed [neurons](#) to contact the outside world ([Fig. 2, top](#)) ([Ward et al. 1975](#); [Ware et al. 1975](#)). Two bilaterally symmetric amphids in the animal's head each contains the endings of 12 types of [sensory neurons](#), two bilaterally symmetric phasmids in the tail each contains the endings of two types of [sensory neurons](#), and six inner labial sensory organs in the head each contains the endings of two types of [sensory neurons](#). Amphid [neurons](#) responsible for chemosensory and thermosensory behaviors have been identified through behavioral analysis of animals in which defined [neurons](#) were killed using a laser microbeam. At this point, cell ablations have not revealed functions for the phasmid and inner labial sensory organs.

The 12 [neurons](#) in each amphid can be distinguished from one another by their morphology and by their connections to other [neurons](#) ([Fig. 2, bottom](#)). Each [neuron](#) is bipolar, with one sensory process (dendrite) and one presynaptic process (axon) emanating from the cell body. The dendrites extend to the nose and terminate in sensory cilia about 5  $\mu\text{m}$  long. All of the axons extend to the [nerve ring](#), where they make synaptic connections with other [neurons](#) and each other ([White et al. 1986](#)).

The [sensory neurons](#) of the amphid can be divided into three classes based on their dendritic morphology and function ([Ward et al. 1975](#); [Ware et al. 1975](#)). Eight types of [neurons](#) (ADF, ADL, ASE, ASG, ASH, ASI, ASJ, ASK) have one or two long slender cilia that are directly exposed to the environment through the amphid pore ("exposed" cells). These [neurons](#) detect mostly water-soluble chemicals ([Table 2](#)) ([Bargmann et al. 1990](#); [Bargmann and Horvitz 1991a,b](#); [Kaplan and Horvitz 1993](#); [Troemel et al. 1995](#)). Three types of [neurons](#) (AWA, AWB, AWC) have flattened, branched cilia that are near the amphid pore, but enclosed by a support cell called the amphid sheath cell ("wing" cells). These [neurons](#) detect volatile odorants ([Bargmann et al. 1993](#); B. Kimmel and C. Bargmann, unpubl.). One type of [neuron](#) (AFD) has a complex, brush-like dendritic membrane structure at the sensory ending which is embedded in the amphid sheath cell ("finger" cell). This [neuron](#) detects thermal cues ([Mori and Ohshima 1995](#)).

The functions of the chemosensory and thermosensory [neurons](#) inferred from cell-killing experiments are listed in [Table 2](#). These [sensory neurons](#) are not required for postembryonic viability, but some of the [amphid neurons](#) have an essential function in regulating the dauer/non-dauer developmental decision ([Bargmann and Horvitz 1991b](#)). ADF, ASG, and ASI regulate dauer larva initiation, and ASJ mediates dauer recovery. If all of these [neurons](#) are killed, or if all [amphid neurons](#) are killed, the animals arrest permanently in the dauer stage and therefore never become fertile adults (see [Riddle](#), this volume).

One limitation of the laser data is that some [neurons](#) might alter their chemical responsiveness when other [neurons](#) are killed. However, analyses of cell function and the expression of cell-specific markers after cell killing have not revealed extensive respecification of the chemosensory neurons after postembryonic cell ablation ([Bargmann and Horvitz 1991a](#)). A second caution is that the [neurons](#) probably have other functions in chemosensation that have not been studied. Nevertheless, some generalities about sensory [neuron](#) function can be made from the existing data.

First, no two types of [neurons](#) have identical functions, except for the bilateral left/right pairs that define one cell type ([Table 2](#)). Second, each type of [neuron](#) has a particular sensory specificity. As mentioned above, cilium morphologies correlate with sensory function, so that water-soluble, volatile, and thermal cues are each recognized mainly by specialized types of sensory endings. Most [neurons](#) recognize several different chemical cues. The chemical specificities of different [neurons](#) can overlap; for example, two types of [neurons](#) sense thiazole and four types of [neurons](#) sense salts. The ASH neurons are particularly broad in their apparent sensory function; they detect water-soluble repellents (high osmotic strength) ([Bargmann et al. 1990](#)), volatile repellents (octanol) ([Troemel et al. 1995](#)), and a mechanical repellent (light touch to the nose) ([Kaplan and Horvitz 1993](#)). These polymodal neurons may be analogous to pain-sensing neurons in vertebrates.

Third, each [neuron](#) directs a particular set of behavioral responses. Individual [sensory neurons](#) detect either attractive or repulsive cues, but not both. However, some [neurons](#) that sense attractants also have functions in egg laying (E. Sawin, pers. comm.) or the regulation of dauer formation. Behavioral specificity is probably encoded by the synaptic connections between the [sensory neurons](#) and their partners in the [nerve ring](#). For example, the ASH and ADL neurons, which mediate avoidance responses, synapse extensively onto the AVA and AVD [interneurons](#), which in turn synapse directly onto the motor [neurons](#) that initiate backward movement ([White et al. 1986](#)). The ASE, AWC, AFD, and AWA neurons, which are important in chemotaxis and thermotaxis, all synapse extensively onto the [AIY](#) and AIZ interneurons.

The functions of both [sensory neurons](#) and [interneurons](#) in thermotaxis have been analyzed in cell-killing experiments ([Mori and Ohshima 1995](#)). Killing the AFD [sensory neurons](#) leads to a severe athermotactic (non-temperature-responsive) phenotype in some animals, and a cryophilic (cold-seeking) phenotype in others. Killing either the [AIY](#) or the AIZ interneurons leads to less severe, mistactic phenotypes that are interesting because they are opposite to each other: Killing [AIY](#) causes a cryophilic phenotype, whereas killing AIZ causes a thermophilic (heat-seeking) phenotype. Thus, it is likely that thermotaxis to a preferred temperature requires two reciprocal behavioral components directed by the [AIY](#) and AIZ [neurons](#). The regulation of these two behavioral components could be achieved in two ways. First, [AIY](#) could regulate AIZ directly by its chemical synapses, since AIZ is the most prominent postsynaptic partner of [AIY](#) ([White et al. 1986](#)). Second, both [AIY](#) and AIZ [neurons](#) could regulate one or more downstream [neurons](#) in opposite directions. For example, the RIA [interneurons](#) could directly receive chemical signals from both [AIY](#) and AIZ ([White et al. 1986](#)). Killing the RIA [neurons](#) leads to partially defective thermotaxis, indicating that RIA is one of the downstream targets of [AIY](#) and AIZ. Killing either the AFD [sensory neurons](#) or [AIY interneurons](#) abolishes isothermal tracking, whereas killing the AIZ [interneurons](#) spares isothermal tracking movements in about half the operated animals ([Mori and Ohshima 1995](#)). The molecular components required for isothermal movement may reside in the [neural](#) circuit including AFD and [AIY](#) but not AIZ.

The functions of the [interneurons](#) in chemotaxis have not been analyzed in detail. Killing any single class of [interneuron](#) (AIA, AIB, [AIY](#), AIZ, or RIA) does not prevent chemotaxis, suggesting some redundancy in this response (C. Bargmann, unpubl.).

The *C. elegans* male possesses all of the chemosensory [neurons](#) found in the hermaphrodite. It also has 79 additional [neurons](#), of which many have exposed sensory endings that might have chemosensory functions ([Sulston et al. 1980; Hodgkin 1983](#)). Four male-specific CEM neurons have cilia that are exposed through the cephalic sensory organs in the head. These [neurons](#) are similar in structure to the [amphid sensory neurons](#), but no function has been demonstrated for them. At least 20 [neurons](#) in the [male tail](#) are also associated with sensory pores that suggest a chemosensory function. The functions of these [tail neurons](#) in male mating have been analyzed by killing [neurons](#) and observing mating behaviors ([Liu and Sternberg 1995](#)). Potential chemosensory [neurons](#) in the [male tail](#) include the sensory [ray neurons](#) that help the male identify the hermaphrodite [vulva](#) during mating, and the spicule [neurons](#) that regulate sperm release after the [vulva](#) has been located (see [Emmons and Sternberg](#), this volume).

## Figures

Figure 2. Anatomy of chemosensory and thermosensory neurons.

### Figure 2

Anatomy of chemosensory and thermosensory [neurons](#). (*Top*) Location of the major chemosensory and thermosensory organs. Dendrites extend from the sensory openings to the cell bodies of the [neurons](#); axons extend from the cell bodies to enter the [nerve ring](#) (in the head) or the [ventral nerve cord](#) (in the tail). Anterior is at left and dorsal is up. Only [neurons](#) on the left side of the animal are shown; all of these [neurons](#) have symmetric homologs on the right side. (*Bottom*) Amphid structure and cilium morphology of [amphid neurons](#). (*Left*) Structure of the amphid opening. A pore in the cuticle is produced by the amphid socket cell (so). Eleven

[amphid neurons](#) are associated with the pore, eight of which are exposed to the external environment and three of which are embedded in the amphid sheath (sh). The AFD [neuron](#) is embedded in the sheath but not associated with the pore. Bar, 1  $\mu\text{m}$ . (Reprinted, with permission, from [Bargmann et al. \[1993\]](#), adapted from [Perkins et al. \[1986\]](#).) (Right) Structure of the sensory endings of the [amphid neurons](#). Bar, 1  $\mu\text{m}$ . (Adapted from [Ward 1973](#).)

## Tables

**Table 2**Neuronal functions defined by laser ablation

	<b>Neuron</b>	<b>Function</b>
Sensory neurons	AWA	volatile chemotaxis; diacetyl, pyrazine, thiazole
	AWB	volatile avoidance
	AWC	volatile chemotaxis; benzaldehyde, butanone, isoamyl alcohol, thiazole
	AFD	thermotaxis
	ASE	$\text{Na}^+$ , $\text{Cl}^-$ , cAMP, biotin, lysine chemotaxis, egg laying
	ADF	dauer pheromone; $\text{Na}^+$ , $\text{Cl}^-$ , cAMP, biotin chemotaxis (minor)
	ASG	dauer pheromone (minor); $\text{Na}^+$ , $\text{Cl}^-$ , cAMP, biotin, lysine chemotaxis (minor)
	ASH	osmotic avoidance, nose touch avoidance, volatile avoidance
	ASI	dauer pheromone; $\text{Na}^+$ , $\text{Cl}^-$ , cAMP, biotin, lysine chemotaxis (minor)
	ASJ	dauer pheromone (recovery)
Interneurons	ASK	lysine chemotaxis, egg laying
	ADL	octanol avoidance, water-soluble avoidance
	AIY	thermophilic movement (thermotaxis)
	AIZ	cryophilic movement (thermotaxis)
	RIA	thermotaxis

Generated from local HTML

# Chapter 25. Chemotaxis and Thermotaxis — V Genetic and Molecular Analysis of Chemosensation and Thermosensation

---

A variety of behavioral screens have been used to identify mutant animals with defects in chemosensory or thermosensory behaviors (Table 3) (Ward 1973; Dusenberry et al. 1975; Hedgecock and Russell 1975; Lewis and Hodgkin 1977), including direct screens for chemotaxis-defective (*che* and *tax*) and thermotaxis-defective (*ttx*) mutants. Animals with defective responses to volatile odorants, but not water-soluble attractants (*odr* mutants), and animals with defects in osmotic avoidance (*osm* mutants) have also been identified (Culotti and Russell 1978; Bargmann et al. 1993; J.H. Thomas, pers. comm.). Chemotaxis-defective mutants have also been identified in morphological screens for animals with deformed sensory cilia. Exposed [sensory neurons](#) of the amphid and phasmid take up fluorescent dyes including FITC and DiO; animals that do not take up these dyes (*dyf* mutants) have defects in the [sensory neurons](#) or the support cells associated with the amphids (Perkins et al. 1986; Starich et al. 1995). Since a subset of chemosensory [neurons](#) regulate the dauer/non-dauer developmental decision, some mutants that were first detected based on defects in dauer formation (*daf*) also have chemosensory defects and vice versa (Lewis and Hodgkin 1977; Albert et al. 1981; Riddle et al. 1981). The class of mutants that fails to take up FITC includes genes named *che*, *osm*, *dyf*, and *daf*.

## A. Genes Required for Cilium Structure and Function

Approximately 25 genes are required for normal formation of the [amphid sensilla](#) and normal dye filling of the [sensory neurons](#) (Perkins et al. 1986; Starich et al. 1995). The chemosensory and [mechanosensory neurons](#) are the only ciliated cells in *C. elegans*, and thus many genes required specifically for cilium function should be detected in these screens. Most of the dye-filling mutants examined by electron microscopy have been shown to have stunted or malformed sensory cilia (Lewis and Hodgkin 1977; Albert et al. 1981; Perkins et al. 1986). One group of cilium structure genes affects all sensory cilia, including the [amphid neurons](#), [phasmid neurons](#), [inner labial neurons](#), and the [mechanosensory neurons](#) associated with the inner and outer labial sensory organs and the cephalic sensory organs. Many of these mutants affect particular ciliary structures, such as the distal or medial cilium elements (Perkins et al. 1986). Although the products of these genes have not been identified, it is likely that they encode components of the cilia and molecules required for cilium assembly.

A few of the cilium structure mutants are more selective in the [neurons](#) that they affect. Several genes affect the amphid and [phasmid neurons](#), but not other [sensory neurons](#), suggesting a functional similarity between the amphids in the head and the phasmids in the tail (Perkins et al. 1986). In *osm-3* mutants, only the exposed [amphid neurons](#) and the [phasmid neurons](#) are abnormal. Even within the amphid, the wing [neurons](#) (which sense volatile odorants) and the AFD [neurons](#) (which sense temperature) are normal in *osm-3* mutants. *osm-3* encodes a novel kinesin-related protein (Shakir et al. 1993b). Its similarity to microtubule-directed motors suggests a function in assembly or action of the microtubule-rich cilia of the [sensory neurons](#). *osm-3* appears to be expressed in the exposed [sensory neurons](#) of the amphid and phasmid, as well as the exposed [IL2 neurons](#) of the inner labial sensory organs (Tabish et al. 1995). The [IL2 neurons](#), however, are structurally normal in *osm-3* mutants.

Assembly of each sensory organ involves interactions between the [sensory neurons](#) and two nonneuronal cell types, the socket and the sheath cells (Ward et al. 1975; Ware et al. 1975). The socket cell attaches the sensory organ to the cuticle and, in the case of chemosensory organs, makes the pore in the cuticle. The sheath cell surrounds the dendrites of the [sensory neurons](#) and secretes a matrix around the chemosensory cilia. Some cilium structure genes affect the support cells of the sensory organs, rather than the [sensory neurons](#) themselves. Mutations in the *daf-6* gene lead to degenerations of the amphid and phasmid sheath cells (Albert et al. 1981). Genetic mosaic analysis indicates that *daf-6* acts within the sheath cells (Herman 1984). Other genes, including *che-14*, have been suggested to act within the sheath or socket cells on the basis of the morphological defects observed in these mutants by electron microscopy (Perkins et al. 1986). This subset of cilium structure genes may

be involved in support cell function or sensory organ assembly (for a discussion of organogenesis in the [male tail](#), see [Emmons and Sternberg](#), this volume).

Most of the cilium structure mutants are pleiotropically defective in chemotaxis to volatile and nonvolatile odorants, avoidance of repellents, and mechanosensation in the nose, behaviors that are mediated by ciliated [sensory neurons](#). These mutants display normal thermotaxis behaviors and normal morphology of the AFD [sensory neurons](#) ([Perkins et al. 1986](#)). Interestingly, different cilium structure mutants have different effects on dauer larva formation. The most severe cilium-defective mutant, [daf-19](#), is dauer-constitutive; it forms dauer larvae regardless of food or population density. All cilium structure mutants except [daf-19](#) show some rudimentary or malformed cilia, but [daf-19](#) mutants have no recognizable cilium structures ([Perkins et al. 1986](#)). Since killing the [sensory neurons](#) leads to a dauer-constitutive phenotype ([Bargmann and Horvitz 1991b](#)), these results suggest that the [sensory neurons](#) in [daf-19](#) mutants are functionally silent. In contrast, all of the other cilium structure mutants are dauer-defective; they never or rarely form dauer larvae. When the [sensory neurons](#) were killed in two mutants of this class [che-2](#) and [daf-10](#), the mutants did form dauer larvae ([Bargmann and Horvitz 1991b](#)). Therefore, the [sensory neurons](#) in these cilium structure mutants can prevent dauer formation, but they are no longer regulated correctly by external stimuli.

## B. *unc-86* and *lin-32* Affect Chemotaxis and Thermotaxis and Interneuron Cell Lineages

Some mutants are characterized by the loss of many sensory responses without obvious structural defects in the [sensory neurons](#). Animals mutant for the [unc-86](#) gene lack responses mediated by the AWC, ASE, and AFD [sensory neurons](#) (chemotaxis and thermotaxis), but they retain at least some function of the AWA [sensory neurons](#) (chemotaxis) and the ASH [sensory neurons](#) (avoidance) ([Bargmann et al. 1993](#); [Mori and Ohshima 1995](#); C. Bargmann, unpubl.). *UNC-86* protein is not expressed in [amphid sensory neurons](#), but it is expressed in the AIZ [interneurons](#), which are directly implicated in thermotaxis and probably important for chemotaxis as well ([Finney and Ruvkun 1990](#); [Mori and Ohshima 1995](#)). Lineage changes in [unc-86](#) mutants prevent the generation of the AIZ neurons ([Chalfie et al. 1981](#)). *unc-86* encodes a POU-class homeodomain-containing transcription factor that controls cell lineage and cell fate during development ([Finney et al. 1988](#); see [Ruvkun](#), this volume).

A second transcription factor required in the lineages that give rise to the AIZ [interneurons](#) is encoded by the [lin-32](#) gene, which is a *C. elegans* homolog of the *achaete-scute* family of neurogenic genes ([Zhao and Emmons 1995](#)). *lin-32* mutants have multiple lineage defects and defects in survival and differentiation of [neurons](#), but their amphid chemosensory [neurons](#) are present and morphologically normal ([Zhao and Emmons 1995](#); C. Kenyon and E. Hedgecock, pers. comm.; C. Bargmann, unpubl.). *lin-32* mutants display broad chemotaxis defects; they are probably defective in processing of chemosensory information by the AIZ [neurons](#) and other [neurons](#) ([Bargmann et al. 1993](#)).

## C. *tax-2*, *tax-4*, *daf-11*, and *daf-21* Affect Multiple Sensory Behaviors and Chemosensory Axon Outgrowth

[tax-2](#), [tax-4](#), [daf-11](#), and [daf-21](#) mutants have behavioral defects that are similar to those of [unc-86](#) mutants. All of these mutants have defects in AWC-mediated and ASE-mediated chemotaxis, but not AWA-mediated chemotaxis ([Dusenberry et al. 1975](#); [Bargmann et al. 1993](#); [Vowels and Thomas 1994](#); C. Coburn et al., in prep.). In addition, all except [daf-11](#) exhibit essentially athermotactic (non-temperature-responsive) phenotypes in thermotaxis ([Dusenberry et al. 1975](#); [Hedgecock and Russell 1975](#); I. Mori et al., unpubl.).

Animals mutant for these four genes also have characteristic axon outgrowth defects (C. Coburn et al., in prep.), in which some chemosensory axons are elongated or inappropriately branched compared to those of wild-type animals. By inference, the normal function of these genes limits or inhibits axon outgrowth of those [neurons](#). Only a few chemosensory [neurons](#) show these defects, typically one or two per animal. The axons of many other [neurons](#) are normal in these mutants, suggesting that their defects are relatively specific to the sensory systems.

All four of these genes also affect sensory control of dauer larva formation. [\*daf-11\*](#) and [\*daf-21\*](#) have a strong dauer-constitutive phenotype and form nearly all dauer larvae at high temperatures (Riddle et al. 1981; Thomas et al. 1993). [\*daf-11\*](#) and [\*daf-21\*](#) have been proposed to act in the [\*sensory neurons\*](#) early in dauer formation (Vowels and Thomas 1994); the appearance of a sensory axon phenotype in these mutants supports this model. [\*tax-2\*](#) and [\*tax-4\*](#) have a slight dauer-constitutive phenotype (C. Coburn et al., in prep.). In addition, [\*tax-2\*](#) and [\*tax-4\*](#) strongly suppress the dauer-constitutive phenotype of [\*daf-11\*](#) and [\*daf-21\*](#), indicating that they can play an important part in dauer larva formation (C. Coburn et al., in prep.).

Temperature-sensitive alleles of [\*tax-2\*](#) and [\*daf-11\*](#) have been used to define the times at which these genes act to influence axon guidance and chemosensory behavior (C. Coburn et al., in prep.). The chemosensory [\*neurons\*](#) are born in the embryo and function by the first larval stage. However, the [\*tax-2\*](#) and [\*daf-11\*](#) gene products are required until the adult stage to maintain normal axon morphology in the adult. Conversely, providing these gene products as late as the fourth larval stage can rescue the axon guidance defects in the mutants. These results indicate that axon morphology is plastic long after the initial neuronal connections are made.

[\*daf-11\*](#) encodes a predicted transmembrane guanylyl cyclase, and [\*tax-2\*](#) and [\*tax-4\*](#) encode two potential subunits of a cyclic-nucleotide-gated channel (D. Birnby and J.H. Thomas, pers. comm.; C. Coburn and C. Bargmann; H. Komatsu et al.; both unpubl.). These sequence similarities suggest that cGMP is an important second messenger in chemosensory and thermosensory transduction and in chemosensory axon morphology. Cyclic-nucleotide-gated channels are implicated in olfactory and photosensory transduction in vertebrates ([Fesenko et al. 1985](#); [Nakamura and Gold 1987](#)), and thus this function may be conserved across diverse sensory systems.

## D. Genes Required for the Function of Specific Sensory Neurons

Some chemosensory mutants display defects in only a few cell types. For example, the behavioral defects in [\*che-1\*](#), [\*che-6\*](#), [\*che-15\*](#), and [\*che-16\*](#) mutants are mostly limited to functions of the ASE [\*sensory neurons\*](#) (Ward 1973; E. Troemel and C. Bargmann, unpubl.), and the genes [\*osm-7\*](#), [\*osm-8\*](#), [\*osm-11\*](#), and [\*osm-12\*](#) appear to affect the functions of the ASH [\*sensory neurons\*](#) (J.H. Thomas, unpubl.). In these cases, one cell type is functionally silent but morphologically intact, although subtle morphological defects have been observed in [\*che-1\* amphid neurons](#) ([Lewis and Hodgkin 1977](#)). These genes might affect the specification of particular cell types in development, or they might be required for cell-type-specific neuronal functions.

One gene required for the function of a specific olfactory [\*neuron\*](#) type is [\*odr-7\*](#) ([Sengupta et al. 1994](#)). [\*odr-7\*](#) null mutants lack all function of the AWA olfactory [\*neurons\*](#), but the AWA [\*neurons\*](#) are present and morphologically normal in the mutants. [\*odr-7\*](#) encodes a protein with a zinc finger DNA-binding domain related to those of the steroid receptor superfamily. Unlike other members of this family, it lacks a typical steroid- or ligand-binding domain. Expression of [\*odr-7\*](#) is limited to the AWA [\*neurons\*](#), apparently within their nuclei, supporting the idea that it encodes a transcription factor involved in AWA function.

What is the role of [\*odr-7\*](#) in the AWA [\*neurons\*](#)? A missense mutation in the [\*odr-7\*](#) gene shows an interesting partial loss of AWA function ([Sengupta et al. 1994](#)). AWA [\*neurons\*](#) detect both diacetyl and pyrazine, and the missense mutants are defective only in the response to diacetyl. The clean separation of diacetyl and pyrazine responses argues that [\*odr-7\*](#) does not simply specify a cell as AWA or non-AWA. Instead, this result suggests that the [\*odr-7\*](#) gene product helps determine the sensory specificity of the AWA olfactory [\*neurons\*](#), perhaps by regulating olfactory receptors or other olfactory signaling molecules within the AWA [\*neurons\*](#). This model is supported by the observation that expression of [\*odr-10\*](#), the potential diacetyl receptor, is controlled by [\*odr-7\*](#) (see Section H below; [Sengupta et al. 1996](#)).

## E. A Glutamate Receptor Participates in Integration of Sensory Information

An interesting class of mutants lacks some, but not all, of the responses mediated by one type of sensory [\*neuron\*](#). The olfactory mutants exemplified by [\*odr-2\*](#) and [\*odr-4\*](#) have defects in a subset of olfactory responses mediated by one [\*neuron\*](#) type ([Bargmann et al. 1993](#)). For example, strong [\*odr-4\*](#) mutants do not respond to diacetyl

(sensed by AWA), but they do respond to pyrazine (also sensed by AWA). These selective defects would be expected of genes that are involved in olfactory recognition and signal transduction within the olfactory [neurons](#).

Alternatively, genes in this group might be involved in downstream integration of sensory information, as has been observed for a *C. elegans* glutamate receptor gene (see [Driscoll and Kaplan](#), this volume). Null mutations in *glr-1*, a putative AMPA-type glutamate receptor, lead to a specific defect in avoidance of nose touch ([Hart et al. 1995; Maricq et al. 1995](#)). Nose touch is detected by the ASH [sensory neurons](#) ([Kaplan and Horvitz 1993](#)), which also detect high osmotic strength, but avoidance of high osmotic strength is normal in *glr-1* null mutants. *glr-1* is expressed in the interneurons that are postsynaptic to the ASH [sensory neurons](#) ([Hart et al. 1995; Maricq et al. 1995](#)), and mosaic analysis indicates that the gene acts in the interneurons ([Hart et al. 1995](#)).

Taken together, these results suggest that nose touch and high osmotic strength generate distinct signals to the [interneurons](#). One model is that activation of the ASH [neurons](#) by nose touch leads to glutamate release, which transmits a signal to the [interneurons](#) via the *glr-1* receptor. Activation of the ASH [neurons](#) by high osmotic strength can transmit a signal to the [interneurons](#) without using the *glr-1* receptor. This might occur if the ASH [neuron](#) contains two different neurotransmitters, or if the downstream [neurons](#) express multiple classes of transmitter receptors, or if complex signals from multiple [sensory neurons](#) contribute to the response.

## F. Candidate Receptors for Chemosensation

A family of G-protein-coupled seven-transmembrane domain receptors are thought to be the olfactory receptors in vertebrates ([Buck and Axel 1991](#)), although their ligands are unknown. Similarly, a group of more than 40 seven-transmembrane domain receptors include strong candidates for chemosensory receptors in *C. elegans* ([Troemel et al. 1995](#)). These genes, which are called *sra*, *srb*, *srg*, *srd*, *sre*, and *sro* genes, are unrelated in sequence to other known seven-transmembrane receptors, with the exception of *sro-1*, which is distantly related to opsin genes. At least 11 of these genes are expressed in subsets of chemosensory [neurons](#), but 3 are expressed outside the chemosensory system. Therefore, although some of these genes might encode chemosensory receptors, others probably have different functions.

As yet, there is no functional evidence that these genes interact with chemoattractants in the [sensory neurons](#). However, their sequences and their expression patterns are consistent with such a role. In addition, their expression patterns fit predictions about chemosensory receptors made by previous analyses of chemosensation in *C. elegans*. For example, saturation and cross-adaptation patterns in chemosensation indicate that multiple receptors might be expressed in one sensory [neuron](#) ([Bargmann et al. 1993; Colbert and Bargmann 1995](#)). Consistent with this model, one [neuron](#) (ASK) can express at least four different receptors of the *sra* and *srg* classes. In addition, laser ablation experiments indicate that a single attractant can be detected by two or more classes of [sensory neurons](#) and some *sra*, *srb*, and *sre* genes are expressed in several different chemosensory [neurons](#). Three different genes, *sra-1*, *sra-6*, and *srd-1*, are expressed in male-specific chemosensory [neurons](#) ([Troemel et al. 1995](#)). Therefore, these genes are candidate receptors for pheromones during male/hermaphrodite mating in *C. elegans*. The cells that have been shown to express *sr* genes detect water-soluble attractants, repellents, or pheromones; no expression of these genes has been observed in the AWA, AWB, or AWC [neurons](#) that detect volatile molecules.

## G. *odr-10* Defines a Potential Olfactory Receptor-Odorant Interaction

*odr-10* mutants were isolated in behavioral screens for animals that fail to chemotax to the odorant diacetyl ([Sengupta et al. 1996](#)). Interestingly, their chemotaxis to all other tested odorants was found to be normal. *odr-10* encodes a potential seven-transmembrane domain receptor that is distinct from the candidate *sr* receptors, although it has a distant similarity to the *srd* genes as well as a distant similarity to some vertebrate candidate olfactory receptors. At least ten additional genes that are similar to *odr-10* have been identified by the *C. elegans* genome sequencing consortium (R. Waterston et al., pers. comm.). Reporter gene fusions with *odr-10* are expressed only in the AWA [neurons](#), which detect diacetyl, and expression of *odr-10* is regulated by *odr-7*, the

putative AWA transcriptional regulator ([Sengupta et al. 1996](#)). A tagged ODR-10 protein appears to be localized to the AWA sensory cilia. These results are consistent with a sensory function for [\*odr-10\*](#).

Its sequence, expression pattern, and mutant phenotype suggest that [\*odr-10\*](#) might encode an olfactory receptor for diacetyl. These observations provide a first view of a defined odorant-receptor interaction in vivo. On the basis of genetic analysis, [\*odr-10\*](#) function is highly odorant-specific: Even odorants that are very similar in structure to diacetyl appear to be recognized normally in [\*odr-10\*](#) mutants. It is possible that other members of the [\*odr-10\*](#) gene family encode receptors for other odorants.

## H. *ttx-1* Affects Thermotaxis and AFD Sensory Ending Morphology

Screens for thermotaxis-defective mutants have yielded some genes with specific functions in the thermosensory pathways. [\*ttx-1\*](#) mutants are cryophilic and severely defective in isothermal tracking on a thermal gradient ([Hedgecock and Russell 1975](#); I. Mori and Y. Ohshima, unpubl.), but they show normal or nearly normal responses to a variety of chemical stimuli ([Dusenberry and Barr 1980](#)).

The AFD thermosensory [neurons](#) have a rudimentary cilium accompanied by a complex microvillar or brush-like structure at their sensory endings. This sensory structure is absent in [\*ttx-1\*](#) mutants, suggesting that it is important for thermosensation ([Perkins et al. 1986](#)). At this point, the molecular mechanism of thermosensation is unknown. However, the brush-like structure might contribute to thermosensation by increasing membrane surface area if membrane fluidity helps detect temperature or it might change its shape at different temperatures and act as a thermometer. Alternatively, thermosensation could be initiated by thermoreceptor proteins in the AFD projections. A precedent for a receptor-type thermosensor exists in bacterial thermosensation: In *Escherichia coli*, the four transmembrane chemoreceptors can also function as thermoreceptors via a temperature-dependent conformational change ([Nara et al. 1991](#)). [\*ttx-1\*](#) mutants are also hypersensitive to dauer pheromone ([Golden and Riddle 1984a](#)). Since the dauer pheromone sensitivity of wild-type animals increases at high temperature, the pheromone hypersensitivity of [\*ttx-1\*](#) mutants may imply that at least part of the thermosensory system responsible for thermotaxis is also used in dauer formation ([Golden and Riddle 1984b](#)).

Mutations in [\*ttx-2\*](#) and [\*ttx-3\*](#) genes result in a cryophilic phenotype that is similar to that of [\*ttx-1\*](#) mutants (I. Mori et al., unpubl.). The molecular characterization of these *ttx* genes might reveal components of the thermosensory signal transduction pathway.

## Tables

**Table 3** Chemotaxis- and thermotaxis-defective mutants

Cilium structure mutants	
All or most ciliated neurons	<a href="#">che-2</a> , <a href="#">che-3</a> , <a href="#">che-10</a> , <a href="#">che-11</a> , <a href="#">che-13</a> , <a href="#">daf-10</a> , <a href="#">daf-13</a> , <a href="#">osm-1</a> , <a href="#">osm-5</a> , <a href="#">osm-6</a>
Amphid and phasmid neurons	<a href="#">osm-3</a>
Socket and sheath cell defects	<a href="#">che-12</a> , <a href="#">che-14</a> , <a href="#">daf-6</a>
Not reconstructed	<a href="#">dyf-1</a> – <a href="#">dyf-13</a>
Normal chemosensory cilia, multiple sensory defects	
Interneuron lineage defects	<a href="#">unc-86</a> , <a href="#">lin-32</a>
Axon guidance defects	<a href="#">tax-2</a> , <a href="#">tax-4</a> , <a href="#">daf-11</a> , <a href="#">daf-21</a>
Other	<a href="#">che-7</a> , <a href="#">tax-6</a> , <a href="#">mec-2</a>
Genes that affect one or a few cell types	
ASE function (water-soluble chemotaxis)	<a href="#">che-1</a> , <a href="#">che-6</a> , <a href="#">che-15</a> , <a href="#">che-16</a>

AWA function (volatile chemotaxis)	<a href="#"><u>odr-7</u></a>
AWC function (volatile chemotaxis)	<a href="#"><u>odr-1</u></a> , <a href="#"><u>odr-5</u></a>
ASH function (osmotic avoidance)	<a href="#"><u>osm-7</u></a> , <a href="#"><u>osm-8</u></a> , <a href="#"><u>osm-11</u></a> , <a href="#"><u>osm-12</u></a>
AFD function (thermotaxis)	<a href="#"><u>ttx-1</u></a> , <a href="#"><u>ttx-2</u></a> , <a href="#"><u>ttx-3</u></a>
AWC, AWA, ASH functions	<a href="#"><u>odr-3</u></a> , <a href="#"><u>osm-9</u></a>
Genes that affect some, but not all, of the functions of a sensory cell	
ASH (nose-touch-, osmotic avoidance+)	<a href="#"><u>glr-1</u></a>
AWC (benzaldehyde-, butanone+)	<a href="#"><u>odr-2</u></a> , <a href="#"><u>odr-4</u></a>
AWA (diacetyl-, pyrazine+)	<a href="#"><u>odr-4</u></a> , <a href="#"><u>odr-10</u></a>

For details and references, see text.

Generated from local HTML

## Chapter 25. Chemotaxis and Thermotaxis — VI Regulation of Chemotaxis and Thermotaxis by Experience

---

*C. elegans* displays flexibility in many of its behavioral responses, and both chemotaxis and thermotaxis behaviors can be modified by the experience of the animal (see [Jorgensen and Rankin](#), this volume). Thermotaxis intrinsically contains an experience-dependent component, since the preferred temperature to which *C. elegans* will thermotax depends on the temperature at which it was raised ([Hedgecock and Russell 1975](#)). Animals shifted from one temperature to another shift their preference to the new temperature over approximately 4 hours ([Hedgecock and Russell 1975](#); I. Mori and Y. Ohshima, unpubl.).

Starvation is an important modulator of thermotaxis ([Hedgecock and Russell 1975](#)). Animals that have been starved for 2–4 hours avoid their cultivation temperature instead of approaching it (I. Mori and Y. Ohshima, unpubl.). These animals might have learned to avoid that adverse temperature, or they might have a general suppression of thermotaxis. To examine this response more closely, animals were cultivated at one temperature, starved for 2 hours either at the old temperature or at a new temperature, and then cultivated with food at the new temperature (I. Mori and Y. Ohshima, unpubl.). Regardless of starvation, animals that had sensed the new temperature 2 hours longer acquired a preference for the new temperature more rapidly. This result implies that acclimation to the exposed temperature occurs under all conditions, whereas starvation inhibits thermotaxis, which is the behavioral expression of the acclimation. The mechanism by which sensation of food is transmitted to the behavioral expression of temperature acclimation is unknown. Starvation also regulates chemotaxis responses. Starved animals appear to be suppressed in their responses to water-soluble attractants and some repellents but are enhanced in their attraction to some volatile attractants (H. Colbert et al., unpubl.). This regulation may allow starved animals to seek out distant food sources that release airborne chemicals.

A specific behavioral modification can occur after prolonged exposure to odorants. Animals exposed to high concentrations of an attractive odorant in the absence of food slowly lose their sensitivity to that attractant over a few hours ([Colbert and Bargmann 1995](#)). These adapted animals still respond normally to other chemical attractants, including those that are detected by the same chemosensory [neurons](#) as the adapting attractant. If the adapting odorant is removed, animals recover their sensitivity to the odorant over the course of a few hours. The mechanisms of adaptation and recovery are not well understood, but their odorant selectivity indicates that they are not due to silencing of the [sensory neurons](#). Rather, some specific change must block the ability of the sensory [neuron](#) to direct chemotaxis to a subset of its normal ligands.

Mutations in two genes, [adp-1](#) and [osm-9](#), lead to defects in adaptation to specific volatile odorants ([Colbert and Bargmann 1995](#)). Like some of the olfactory mutants described above, these genes have odorant-specific functions. Both benzaldehyde and isoamyl alcohol are sensed by the AWC olfactory [neurons](#), but [adp-1](#) affects only adaptation to benzaldehyde, and [osm-9](#) affects only adaptation to isoamyl alcohol. Like olfaction itself, olfactory adaptation appears to be a complex process that is regulated separately for different olfactory molecules.

Generated from local HTML

## Chapter 25. Chemotaxis and Thermotaxis — VII Conclusions and Prospects

---

*C. elegans* provides an opportunity to examine behaviors at a number of levels. Because the [nervous system](#) is so compact and well-described, the contributions of individual [neurons](#) to complex behaviors such as chemosensation and thermosensation can be defined in detail. This circuit information has been useful for the isolation and analysis of chemosensory and thermosensory genes. The increased understanding of the sensory systems provided by cellular and genetic analyses should allow a series of questions about these behaviors to be addressed.

First, what are the molecules directly involved in sensory recognition and signaling? These results should follow from analysis of the chemotaxis- and thermotaxis-defective mutants and from further genetic analysis of the candidate receptor genes. There is a special opportunity to gain new insights into thermosensation, which is not well understood in any animal.

Second, how do the chemosensory and thermosensory [neurons](#) develop their chemical specificity and behavioral specificity? Do molecules such as [odr-7](#) act in other sensory cell types to determine sensory specificity? The first synapses of the sensory [neuron](#) onto [interneurons](#) differ for [neurons](#) that mediate attraction and repulsion, suggesting an early sorting of chemosensory information. What genetic mechanisms allow different [amphid neurons](#) to recognize different targets in the [nerve ring](#), thereby generating distinct responses? The development of the sensory organs can also be addressed by further study of the cilium structure genes.

Third, how is chemosensory information integrated by the [nervous system](#)? The neuronal circuit for thermotaxis reveals functions for the AFD [sensory neurons](#) and at least three types of [interneurons](#). How does the sensory [neuron](#) transmit information about temperature to the circuit, and how do the [interneurons](#) generate a precise isothermal tracking behavior? How do [interneurons](#) integrate information from groups of [sensory neurons](#)? Will the complexity of function exemplified by the role of the [glr-1](#) glutamate receptor in sensory signaling be general or will most [sensory neurons](#) have more simple coding properties? These questions will be particularly interesting to ask for [neurons](#) that regulate both chemotaxis and egg laying or both chemotaxis and dauer larva formation. How can one sensory [neuron](#) generate two different responses to two different chemicals?

Finally, how are chemotaxis and thermotaxis behaviors regulated to generate more flexible behaviors? How does the animal change its thermal preferences over time? Are more complex forms of learning and behavioral modification present in *C. elegans*? The availability of mutants that are specifically defective in olfactory adaptation suggests that these problems will be tractable at a molecular level.

Generated from local HTML

## **Chapter 25. Chemotaxis and Thermotaxis — Acknowledgments**

---

We thank Noelle Dwyer, Emily Troemel, Ikuro Kawagishi, and several reviewers for their comments and discussion.

Generated from local HTML

# **Chapter 26. Genetic and Environmental Regulation of Dauer Larva Development**

---

## **Contents**

- [I Introduction](#)
- [II The Dauer State](#)
- [III Developmental Transitions](#)
- [IV A Network of Gene Functions](#)
- [V Summary and Conclusions](#)
- [Acknowledgments](#)

Generated from local HTML

# Chapter 26. Genetic and Environmental Regulation of Dauer Larva Development — I Introduction

---

Dauer larvae were first identified as a special larval stage of insect-parasitic nematodes. These larvae, which differed structurally from all other stages of the same species, were termed "dauerlarven" by [Fuchs \(1915\)](#). The dauer (enduring) stage of *Caenorhabditis elegans* is formed when environmental conditions are inadequate for successful reproduction. In abundant food, the animal develops continuously through the four larval stages (L1–L4) to the adult. Coincident with increased population density and limited food supply, development is arrested at the second molt, and the third-stage larva that is formed is structurally and behaviorally specialized for dispersal and long-term survival ([Cassada and Russell 1975](#)). Dauer larvae do not feed, but they can survive at least four to eight times the normal 2-week life span of *C. elegans* ([Klass and Hirsh 1976](#)). When favorable conditions are encountered, the dauer larva begins to feed and resumes development to the adult. Both entry into and exit from the dauer stage are developmental responses to specific chemosensory cues. These cues inform the larva whether there will be sufficient food available to support its reproduction.

The environmental cues are first assessed and integrated throughout the L1 stage ([Golden and Riddle 1984b](#)). The primary cue is a *Caenorhabditis*-specific pheromone constitutively released by the nematodes ([Golden and Riddle 1984c](#)). The pheromone is very stable and hydrophobic and has chromatographic properties similar to those of hydroxylated fatty acids and bile acids. The concentration of pheromone reflects nematode population density. Temperature and food modulate the response to pheromone at intermediate pheromone concentrations. The food signal is released by bacterial cells and reflects the bacterial food supply. This signal is unstable and hydrophilic, with chromatographic properties similar to those of nucleosides or carbohydrates. A high ratio of pheromone to food favors dauer larva formation and maintenance of the dauer state ([Golden and Riddle 1984b](#)), whereas the opposite condition favors continuous growth and stimulates dauer larvae to recover ([Golden and Riddle 1982](#)). Temperature modulates the response to the food/pheromone balance, with higher growth temperatures favoring the dauer state; a similar temperature-dependent response to the same pheromone activity is observed with *Caenorhabditis briggsae* ([Golden and Riddle 1984a](#)).

If the present and anticipated future environments are suitable for reproduction, the larva becomes developmentally committed to continued growth by the L1 molt. However, the timing of commitment is not precise. In an experiment using very stringent environmental conditions (high pheromone and low food concentrations more than sufficient for the induction of 100% dauer larvae if the animals were exposed from the time of hatching), about 10% of the L2 larvae were induced to form dauer larvae if they were shifted to dauer-inducing conditions within 2 hours after the first molt ([Golden and Riddle 1984b](#)).

Once committed to nondauer development, increased tricarboxylic acid (TCA) cycle activity ensues ([Wadsworth and Riddle 1989](#)) as energy metabolism shifts to a phase in which ingested nutrients are rapidly deployed to the construction of a reproductive system and to increasing the body mass. (There are only 31 hours from the first molt to the beginning of egg laying at 25°C.) However, if the food supply is insufficient, the second-stage larva prepares for food deprivation by slowing development (a 13-hour predauer, or L2d stage, instead of a 7-hour L2 stage) and by accumulating fat in its intestinal and hypodermal cells ([Popham and Webster 1979](#); [Albert and Riddle 1988](#)). The L2d retains the potential for continuous development; it can molt to the L3 stage if environmental conditions improve ([Golden and Riddle 1984b](#)).

Developmental arrest and dispersal are traits found in a variety of free-living and parasitic nematodes, from the closely related, free-living *C. briggsae* ([Yarwood and Hansen 1969](#); [Fodor et al. 1983](#)) to distantly related parasites ([Hotez et al. 1993](#)). In parasitic species, the dauer or infective form, which is frequently an obligate stage in the life cycle, moves from one host to another. The dispersal stage is usually the third stage, as it is in *C. elegans*. Examples of species with third-stage dauer dispersal are *Steinernema* and *Heterorhabditis* (parasites of insects) and *Strongyloides stercoralis* (a parasite of humans). *Steinernema* dauer larvae are used commercially for biological control of insects ([Poinar 1990](#)).

Occasionally, species disperse as an arrested fourth stage. For example, the pine wilt nematode *Bursaphelenchus xylophilus* ([Mamiya 1984](#)) molts once in the egg to hatch as an L2 larva. It proliferates for generations in the resin canals of a host pine tree. As the tree becomes infected with bark beetles, specialized third-stage (predauer) larvae develop, migrate to the insect pupal cases, and then molt to the dauer stage. As the adult beetle emerges, these larvae enter its trachea for transport to another pine tree ([Dropkin 1989](#)). It is possible that nematode population density in the resin canals may also regulate the decision between propagative and dispersal life cycles, but the existence of a *Bursaphelenchus* dauer-inducing pheromone has not been investigated.

A quite different example of arrested fourth-stage development is provided by *Ostertagia ostertagi*, the adults of which are digestive tract parasites of cattle ([Evans and Perry 1976](#)). Eggs are passed in the feces, and the larvae feed on dung to reach the infective third stage. If ingested by a new host, they either resume development, mate, and reproduce or, as winter approaches, arrest development again at the third molt and overwinter in the gastric glands. This seasonal effect, which seems to be mediated through the endocrine system of the host, prevents the release of eggs in cold weather. Hence, the life cycle of *Ostertagia* includes an obligate infective stage for host finding, followed by a facultative diapause that is regulated by environmental conditions. The above species, which occupy diverse habitats, have presumably evolved diverse sensory receptors appropriate for their environments. However, the internal signal transduction and transcriptional controls used to achieve developmental arrest may conceivably be quite similar to those of *C. elegans*.

Research on the *C. elegans* dauer larva has been reviewed elsewhere ([Riddle 1988; Thomas 1993b](#)). This chapter describes what is currently known about the dauer larva and the mechanisms by which its formation and recovery are regulated by environmental signals. Branched genetic pathways for dauer formation, which represent a network of overlapping functions, have been constructed. Molecular studies have revealed numerous components in these signal transduction/transcriptional regulation pathways, including a ligand, putative receptor molecules, putative second messengers, and downstream transcription factors ([Fig. 1](#)). It appears that certain chemosensory [neurons](#) use a member of the transforming growth factor  $\beta$  (TGF- $\beta$ ) superfamily as a neuromodulator, perhaps to control the synthesis or secretion of a systemic hormone that, in turn, controls transcriptional events in [all cells](#) in the body in accordance with a threshold of chemosensory signaling. Other [sensory neurons](#) may use guanylyl-cyclase-mediated signaling in parallel with TGF- $\beta$  signaling, apparently to influence the same transcriptional controls. A putative pheromone receptor present on these chemosensory [neurons](#) may act through G proteins to control synthesis of the TGF- $\beta$ -like ligand. A third pathway, which involves 3-phosphoinositide signaling, specifies both larval diapause and adult longevity.

Both the genetics and cell-killing experiments have revealed redundant or overlapping [neural](#) functions that may reflect roles for different [neurons](#) in transducing different environmental signals or may simply reflect a system of fine tuning or optimization of the developmental controls ([Bargmann and Horvitz 1991b; Schackwitz et al. 1996](#)). Selection for enhanced fidelity is one explanation for the evolution of redundant gene functions ([Thomas 1993a](#)). The dauer/nondauer developmental switch is the major decision *C. elegans* makes during its life. Given its boom and bust lifestyle in the soil ([Riddle et al.](#), this volume), an appropriate decision whether to grow and reproduce or to disperse to a new location is critical for survival, and optimization of the sensory/developmental response should be highly adaptive. An erroneous decision to grow would result in less than optimal progeny production or survival. Similarly, an erroneous decision to disperse would, at best, slow the generation time and would sacrifice rapid reproduction to an uncertain future.

## Figures

Figure 1. Model encompassing three levels of dauer/nondauer signaling as discussed in this chapter: environmental cues, signal transduction pathway components including a neurotransmitter/neuromodulator to integrate the cues over time, and a hormonal signal that controls transcription in target tissues.

## Figure 1

Model encompassing three levels of dauer/nondauer signaling as discussed in this chapter: environmental cues, signal transduction pathway components including a neurotransmitter/neuromodulator to integrate the cues over time, and a hormonal signal that controls transcription in target tissues. Amphid ASI chemosensory [neurons](#) secrete the DAF-7 ligand (putative neuromodulator) unless inhibited by dauer pheromone. Putative pheromone receptors on the amphid sensory dendrites mediate a signal transduction pathway in ASI and other [neurons](#) that prevents transcription of the [\*daf-7\*](#) gene. [\*daf-7\*](#) function is required for nondauer development at 25°C, but it is redundant with other functions at lower temperatures. Failure to activate the DAF-1/DAF-4 receptor (expressed in chemosensory and [interneurons](#)) allows activation of the DAF-12 nuclear hormone receptor, perhaps by allowing biosynthesis or secretion of a ligand (a dauer-inducing hormone). The cellular specificity of [\*daf-12\*](#) expression is not known, but this model places it in [all cells](#) to activate dauer morphogenesis and/or repress continuous development. In parallel with [\*daf-7\*](#) signaling, [\*daf-11\*](#) and [\*daf-21\*](#) act to inhibit dauer-promoting activity of amphid ASJ [neurons](#), likewise resulting in the inactivation of DAF-12. Heterotrimeric G proteins expressed in the chemosensory cells have been implicated in both [\*daf-11\*](#) and in [\*daf-7\*](#) signaling by their role in mediating the response to pheromone. Another control on the transcriptional switch involves the AGE-1 (a.k.a. DAF-23) PI3-kinase. The regulation of this branch of the pathway is not understood, but its activity affects adult life span as well as the dauer/nondauer switch. The T-bar symbols represent indirect inhibitory effects, not direct molecular interactions.

Generated from local HTML

# Chapter 26. Genetic and Environmental Regulation of Dauer Larva Development — II The Dauer State

---

## A. Morphology

Dauer larvae are easily distinguished from other developmental stages. They are thin and dense due to shrinkage of the hypodermis at the dauer-specific molt ([Cassada and Russell 1975](#); [Albert and Riddle 1988](#)). They acquire resistance to detergent treatment about 1 hour after radial shrinkage of the body ([Swanson and Riddle 1981](#)), presumably as a result of cuticle modification and the occlusion of the [buccal cavity](#) ([Fig. 2](#)) ([Cassada and Russell 1975](#); [Popham and Webster 1979](#); [Albert and Riddle 1983, 1988](#)).

Transverse-section electron micrographs of the cuticle show a thickened outer cortex and a dauer-specific, striated inner layer ([Cassada and Russell 1975](#); [Popham and Webster 1978](#); [Cox et al. 1981b](#)). The dauer cuticle has lateral ridges (alae) not present on L2, L3, or L4 larvae that are visible with Nomarski optics. A detergent-soluble 37-kD hydrophobic protein exposed on the surface of the dauer larva is not found on other stages ([Blaxter 1993a](#)). Many tissues and organs exhibit dauer-specific morphology: Pharyngeal pumping is suppressed ([Cassada and Russell 1975](#)) and the isthmus and terminal bulb of the [pharynx](#) are constricted ([Vowels and Thomas 1992](#)); the lumen of the intestine is shrunken and the microvilli are condensed ([Popham and Webster 1979](#)); the [excretory gland](#) lacks secretory granules ([Nelson et al. 1983](#)); and several [sensory neurons](#) exhibit altered position or dendrite orientation ([Albert and Riddle 1983](#)).

The anterior sensory ultrastructure of the dauer larva was examined in several specimens and compared with that of the L2 larva ([Albert and Riddle 1983](#)). In some instances, comparisons were made with L3, postdauer L4, and adult stages. Whereas sensory morphology in different nondauer stages remains constant, it differs in the dauer larva, providing an example of developmental plasticity in the [nervous system](#) ([Jorgensen and Rankin](#), this volume). Dauer-specific sensory modifications in the amphids, [inner labial neurons](#), and the deirids may play a part in dauer-specific behavior.

The amphids are a pair of prominent chemosensory organs located on either side of the head. Each amphid consists of two support cells and 12 [neurons](#), eight of which are exposed to the environment through a pore in the cuticle near the tip of the head ([Ward et al. 1975](#); [Ware et al. 1975](#); [Bargmann and Mori](#), this volume).

Dendritic processes extend anteriorly from cell bodies located near the [circumpharyngeal nerve ring](#), and axons extend into the ring. A sheath cell forms the channel for the dendritic processes and presumably secretes the matrix of material observed in the channel. A socket cell joins the anterior end of the channel to the cuticle. Amphidial [neurons](#) AWC, AFD, ASG, and ASI and the amphidial sheath cell are altered in shape or position in the dauer stage ([Albert and Riddle 1983](#)). [neurons](#) ASG and ASI are displaced posteriorly within the dauer amphidial channel. [Neuron](#) AFD has significantly more microvillar projections in the dauer stage than in L2, L3, or postdauer L4 larvae. Wing-like processes of the two dauer AWC [neurons](#) form a much wider arc in transverse section, including extensive overlap of these cells. Such overlap does not occur in an L2. Whereas L2 larvae possess two separate bilateral amphidial sheath cells, the left and right sheath cells can be continuous in the dauer larva. The AWC [neurons](#) are involved in chemotaxis to volatile attractants, the AFD [neurons](#) are involved in thermotaxis, and ASG and ASI inhibit dauer formation ([Bargmann and Mori](#), this volume).

Whereas the amphidial pores remain open in the dauer larva, the inner labial channels are virtually occluded ([Albert and Riddle 1983](#)). The relative positions of the dendritic tips of the two types of [inner labial neurons](#) are reversed in the dauer stage compared to the L2 and postdauer L4 stages. The inner labial neuron 1 (IL1) rather than IL2 is more anterior in each of the six [sensilla](#), and the IL2 cilia are only one-third as long as those in the L2. Since the IL2 [neuron](#) is thought to be chemosensory, and IL1 is thought to be mechanosensory, it is possible that IL2 chemosensory input may be reduced or absent in dauer larvae. Finally, the deirid ([ADE](#)) mechanosensory dendrites exhibit a dauer-specific structure and orientation. The dendritic tip of each [neuron](#) in the dauer stage is attached to the body wall cuticle by a substructure not observed in L2 or postdauer L4 stages, and it is oriented

parallel to the longitudinal axis of the body. These sensory terminals are oriented perpendicular to the cuticle in other stages.

## B. Behavior

On an agar surface, dauer larvae tend to lie motionless unless disturbed, perhaps to conserve energy reserves. They do, however, move rapidly in response to touch. The slender body and specialized cuticle may allow them to break the surface tension of the medium more easily than other stages. On starved plates stored for long periods, dauer larvae will accumulate in the droplets of condensation on the lids of the plates, presumably by crawling over the inside wall of the dish. Nictation is a dauer-specific behavior in which the larva mounts a projection and stands on its tail, waving its head in the air ([Croll and Matthews 1977](#)). This behavior could possibly allow the dauer larva to attach to passing soil insects in a phoretic relationship for transport to a fresh environment.

Dauer larvae respond to thermal gradients differently from other stages ([Hedgecock and Russell 1975](#)). Adults track along isothermal lines, preferring the temperature at which they were raised, but dauer larvae seek novel temperatures. They are more thermotolerant than adults, living about three times longer when exposed to 37°C ([Anderson 1978](#)). Dauer larvae respond to reduced pheromone levels and increased food by initiating recovery. Once they begin pharyngeal pumping, they become more responsive to a chemical attractant in an orientation assay ([Albert and Riddle 1983](#)).

## C. Metabolism

The dauer larva exhibits a metabolism that is consistent with long-term survival in the absence of food. Dauer larvae have reduced TCA cycle activity but high phosphofructokinase activity relative to adults, indicating that dauer larvae have a greater capacity to metabolize glycogen ([O'Riordan and Burnell 1989](#)). The decreased TCA cycle activity relative to the glyoxylate cycle in dauer larvae indicates the importance of lipid storage as an energy reserve in the dauer stage ([Wadsworth and Riddle 1989; O'Riordan and Burnell 1990](#)).

After the L1 molt, *C. elegans* energy metabolism undergoes a major transition that is dependent on the commitment to continuous development ([Wadsworth and Riddle 1989](#)). The relative concentrations of ATP, ADP, AMP, sugar phosphates, and other metabolites result in stage-specific phosphorus nuclear magnetic resonance (NMR) spectra. These spectra are consistent with assays of isocitrate dehydrogenase and isocitrate lyase, indicating high activity of the glyoxylate pathway only during the L1 stage, whereas respiration during the L2, L3, and L4 stages occurs preferentially through the TCA cycle. Relative to the L1, L2 larvae exhibit increased isocitrate dehydrogenase activity, as well as increased concentrations of ATP and other high-energy phosphates, whereas predauer (L2d) larvae exhibit declining enzyme activities and declining levels of high-energy phosphates. Although the predominant phosphorus NMR signal in dauer larva extracts corresponds to inorganic phosphate, the higher energy state observed in growing larvae can be restored within 4 hours after wild-type dauer larvae resume feeding in bacteria. NMR analysis of living animals revealed that dauer larvae have an elevated intracellular pH relative to other stages, reflecting their unique metabolic state ([Wadsworth and Riddle 1988](#)).

On the basis of results from in vitro translation, [Snutch and Baillie \(1983\)](#) suggested that dauer larvae have reduced transcriptional activity relative to growing larvae. Using run-on transcription assays with isolated nuclei, [Dalley and Golomb \(1992\)](#) observed a depression of general RNA polymerase II transcription in dauer larvae to 11–17% of that in other stages. However, the dauer larvae could be induced for heat shock mRNAs, showing that they are competent to initiate and elongate transcripts. Interestingly, dauer larvae were found to be 15-fold enriched for Hsp90 (heat shock protein) mRNA relative to other stages. In unstressed cells, Hsp90 interacts with steroid hormone receptors, facilitating receptor activation and preventing receptors from activating transcription in the absence of hormone ([Cadepond et al. 1991](#)). Hsp90 acts as a chaperon for various protein kinases, and also complexes with other proteins ([Gething and Sambrook 1992](#)). Conceivably, Hsp90 could interact with steroid hormone receptors or other proteins to promote dauer formation. In addition, it might complex with transcriptional activators to down-regulate transcription during dauer maintenance.

Dauer larvae possess elevated activities of superoxide dismutase ([Anderson 1982](#); [Larsen 1993](#)) and catalase ([Vanfleteren and De Vreese 1995](#)), enzymes that are involved in protection against oxidative damage. They also exhibit greater tolerance to oxygen deprivation ([Anderson 1978](#)). These traits might contribute to dauer longevity ([Klass and Hirsh 1976](#); [Kenyon](#), this volume).

## Figures

Figure 2. External morphological differences between an L2 larva (A) and a dauer larva (B) are shown by scanning electron micrographs of the head.

### Figure 2

External morphological differences between an L2 larva (A) and a dauer larva (B) are shown by scanning electron micrographs of the head. The field width in each micrograph is 7.2  $\mu\text{m}$ . An internal cuticular block, which closes the [mouth](#) of the dauer completely (B), is revealed in transmission electron micrographs of transverse sections (not shown). (Reprinted, with permission, from [Riddle 1988](#).)

Generated from local HTML

# Chapter 26. Genetic and Environmental Regulation of Dauer Larva Development — III Developmental Transitions

---

## A. Heterochronic Genes

One of the genes that controls the timing of dauer larva formation is [\*lin-14\*](#), which also regulates other temporal transitions during development. In particular, the stage at which an animal may arrest as a dauer larva is affected by the level of [\*lin-14\*](#) activity ([Ambros](#), this volume). Therefore, the targets regulated by [\*lin-14\*](#) might include genes that are required to initiate dauer development in response to environmental stimuli or to trigger differentiation into the dauer larva ([Ambros and Moss 1994](#)). Animals that have reduced [\*lin-14\*](#) activity may form dauer larvae precociously (at the L1 molt), and those with increased [\*lin-14\*](#) activity may form dauer larvae late (at the L3 molt). However, both types of mutants can form dauer larvae at the L2 molt, as wild-type animals might do.

If animals do not pass through the dauer stage, [\*lin-14\*](#) controls the timing of all stages of development; in contrast, developmental timing after the dauer stage is independent of [\*lin-14\*](#) ([Liu and Ambros 1991](#)). Those [\*lin-14\*](#) mutant animals that have recovered from dauer larva arrest at the second molt undergo wild-type postdauer development. At the wild-type fourth molt of both continuous and postdauer development, hypodermal cells switch from a proliferating state to the terminally differentiated state (the larva-to-adult or L/A switch). In continuously developing [\*lin-14\*](#) mutants, the L/A switch occurs at abnormally early or late molts, but during postdauer development of the same mutants, the L/A switch occurs normally. Similar differences between dauer and nondauer development are seen with other heterochronic mutants, including [\*lin-4\*](#) and [\*lin-28\*](#) ([Liu and Ambros 1991](#)). Thus, there appears to be a regulatory signal associated with dauer larva arrest that reprograms the temporal state of cells and allows the animal to execute cell lineages appropriate to the L3 and L4 stages ([Ambros and Moss 1994](#)). Differences in expression of the *Sqt-2* phenotype may similarly reflect a reprogramming of hypodermal cells associated with dauer arrest. [\*sqt-2\*](#) L3 larvae exhibit a roller phenotype, but L4 larvae and adults do not roll. In contrast, dauer and postdauer L4 and adult stages do roll ([Cox et al. 1980](#)).

## B. Exit from the Dauer Stage

Exit from the dauer stage is affected by the same environmental factors that influence entry: pheromone, food, and temperature ([Golden and Riddle 1984b](#)). In the presence of exogenous pheromone, temperature downshifts from 25°C to 15°C induce dauer larvae to resume development, whereas temperature upshifts have no such effect. In the absence of food, removal from a pheromone-rich environment is sufficient to induce recovery in older dauer larvae but not in younger ones; dauer larvae become progressively more predisposed to recovery during the 1–2 week period after they are formed. This may result from a decrease in the dauer larva's sensitivity to pheromone.

When wild-type dauer larvae from starved cultures are put in fresh food, they become developmentally committed to recovery from the dauer state in 50–60 minutes ([Golden and Riddle 1984b](#)). One of the earliest biological markers of exit from the dauer stage is a change in surface lipophilicity; 30 minutes after exposure to food, the dauer surface starts to accept lipid probes ([Proudfoot et al. 1993b](#)). Dauer larvae begin pharyngeal pumping within 3 hours (postdauer, PD1 stage) and then molt to the L4 (PD2) stage after approximately 10 hours at 25°C. The PD1 stage retains the dauer cuticle but expands radially and grows in length prior to the PD1-PD2 molt.

Recovery from the dauer state is associated with an increase in the specific activity of enzymes of intermediary metabolism. This increase is inhibited by cycloheximide ([Reape and Burnell 1991b](#)) but not by actinomycin D ([Reape and Burnell 1992](#)). Actinomycin D treatment does prevent molting to the PD2 stage, leading [Reape and Burnell \(1991a\)](#) to conclude that RNA synthesis is not required for the transition from dauer to PD1, but it is required for the first postdauer molt. However, exit from the dauer stage is normally accompanied by a temporally regulated sequence of gene expression ([Dalley and Golomb 1992](#)). Steady-state levels of Hsp70 and

polyubiquitin mRNA rise sharply within 75 minutes and then decline within 4 hours after exposure to food. Actin and histone mRNAs increase steadily but more slowly. In contrast, Hsp90 mRNA declines sharply within 75 minutes of exposure to fresh food. Metabolic activation is accompanied by a large decrease in intracellular pH from about 7.3 to about 6.3 within 3 hours after dauer larvae encounter food ([Wadsworth and Riddle 1988](#)). This shift occurs before feeding begins, and it coincides with, or soon follows, the commitment to resume development.

Generated from local HTML

# Chapter 26. Genetic and Environmental Regulation of Dauer Larva Development — IV A Network of Gene Functions

---

## A. Mutants

More than 30 genes controlling dauer larva formation have been identified. Mutations in *daf* (*dauer* formation) genes result either in the inability to form dauer larvae in response to crowding and starvation (dauer-defective, or Daf-d) or in the formation of dauer larvae at low population density in the presence of abundant food (dauer-constitutive, or Daf-c). Nonconditional dauer-constitutive mutants form dauer larvae independently of environmental cues. Temperature-sensitive dauer-constitutive mutants form dauer larvae at high frequency only at restrictive temperatures, and if such larvae are shifted to permissive temperatures, they exit from the dauer stage and resume growth ([Swanson and Riddle 1981](#)). The latter mutants are easily selected as detergent-resistant larvae formed in abundant food ([Cassada 1975; Riddle 1977](#)).

Identifying constitutively formed dauer larvae in visual screens ([Riddle 1977; Malone and Thomas 1994](#); I. Caldicott and D. Riddle, in prep.) allows isolation of mutants that nonconditionally arrest development since heterozygous siblings can be used to propagate the mutant. In this way, nonconditional alleles of *daf-23* (now called *age-1*) and *daf-2* have been collected; these mutants arrest development at all temperatures. Mutants that form dauer-like (partial dauer) larvae nonconditionally have been identified, at least two of which, *daf-9* and *daf-15*, have been placed downstream from the *daf-c* and *daf-d* genes in the genetic pathway ([Albert and Riddle 1988](#)). Only temperature-sensitive alleles of *daf-1*, -4, -7, -8, -11, -14, and -21 have been identified, suggesting that the null phenotype of these genes is temperature-sensitive. This model has been confirmed by molecular analysis of *daf-1*, -4, and -7, since nonsense mutations, deletions, and transposon insertions all result in temperature-sensitive phenotypes ([Georgi et al. 1990; Estevez et al. 1993; Ren et al. 1996](#)). The relationship between dauer formation and thermotaxis behavior is intriguing. Some thermotaxis-defective mutants do not differ in their sensitivity to dauer-inducing pheromone, but others are either more sensitive or less sensitive ([Golden and Riddle 1984a](#)). *tax-2* and *tax-4* mutants have a slight Daf-c phenotype ([Bargmann and Mori](#), this volume).

Virtually all Daf-c mutants obtained thus far are recessive. Exceptions are the single allele of *daf-28*, which is weakly dominant and may be a gain-of-function allele ([Malone and Thomas 1994](#)), and dominant activating mutations in *gpa-2* and *gpa-3*, two genes that encode G-protein  $\alpha$  subunits ([Zwaal et al. 1997](#)). Some Daf-c mutants are maternally rescued (all progeny of a *daf*/+ heterozygote grow to the adult at 25°C, but the Daf-c homozygotes produce all Daf-c progeny at the same temperature). The maternal-effect is complete for *age-1* ([Gottlieb and Ruvkun 1994](#)), for some alleles of *daf-1* ([Riddle 1977](#)), and the single allele of *daf-21*, and it is partial for some alleles of *daf-1* ([Malone and Thomas 1994](#)) and for *daf-4*. Daf-d mutants are likewise recessive, as judged from their recessive suppression of Daf-c mutants. An exception is the weakly semidominant suppression of *daf-2* and *age-1* by *daf-16* mutations (Gottlieb and Ruvkun 1994).

About half of the mutants selected by their dauer-defective phenotype also exhibit sensory defects involving chemotaxis, male mating, or osmotic avoidance ([Riddle 1977; Culotti and Russell 1978; Albert et al. 1981](#)). Chemotaxis, osmotic avoidance, thermotaxis, and dauer formation are all mediated by the amphids (for review, see [Bargmann 1993; Bargmann and Mori](#), this volume). The sensory terminals of the exposed *neurons* consist of nonmotile cilia. A large number of mutations disrupt cilium morphogenesis, resulting not only in behavioral defects, but also in failure to absorb fluorescent dyes from the environment ([Perkins et al. 1986](#)). Of mutants in 13 genes identified as amphid dye-filling-defective (Dyf), 10 are also dauer-defective ([Starich et al. 1995](#)). The remaining three genes in the set have only one mutant allele each, so it is possible that stronger alleles might be dauer-defective as well. The Daf-c mutants *daf-11* and *daf-21* are also defective in chemotaxis ([Vowels and Thomas 1994](#)). Their gene products are thought to function in the amphid sensory cilia because the Dyf mutants are epistatic to mutations in these genes ([Vowels and Thomas 1992; Thomas et al. 1993](#)).

Mutants defective in both dauer larva formation and chemotaxis have been examined ultrastructurally, and a variety of morphological abnormalities in the dendritic endings of anterior and posterior [sensory neurons](#) were observed ([Lewis and Hodgkin 1977](#); [Albert et al. 1981](#); [Perkins et al. 1986](#)). Of all the anterior [sense organs](#) examined in mutants that are defective in both dauer larva formation and chemotaxis, only the amphids consistently displayed abnormal morphology. Mutations in one Daf-d gene, [daf-6](#), affect the amphid sheath cell so that it closes the amphid channel and creates a barrier between the [amphid neurons](#) and the environment ([Albert et al. 1981](#)). Genetic mosaic analysis also indicated that the [daf-6](#) defect is localized to the sheath cells ([Herman 1987](#)). Killing these cells in wild-type L1 larvae with a laser prevents response to dauer-inducing pheromone, whereas killing the analogous phasmid sheath cells in the tail has no effect ([Vowels and Thomas 1994](#)).

Although a high level of pheromone is the primary dauer-inducing stimulus, under nondauer-inducing conditions, the source and quantity of food become more important and can affect mutant phenotypes, as well as wild-type development. *E. coli* strain OP50, a uracil auxotroph, was chosen by [Brenner \(1974\)](#) as a convenient laboratory food source for *C. elegans* because it promoted optimal development of the organism, and its reduced growth on uracil-limiting agar medium facilitated visual identification of even small larvae. By limiting the available bacterial food supply even further, [Cassada and Russell \(1975\)](#) were able to induce dauer larva formation in wild type at a population density that did not induce dauer larva formation in the presence of more food.

Recent results indicate that not all bacterial strains have the same sensory or nutritive value, which apparently can explain discrepancies in the penetrance (percent dauer formation) reported for some Daf-c mutant strains at 15°C ([Swanson and Riddle 1981](#); [Thomas et al. 1993](#)). The apparent phenotypic differences do not reflect genetic divergence between laboratory sublines but are due to subtle differences in culture conditions. Given the importance of the ratio of pheromone to food in the formation of dauer larvae, the strain of bacteria used as a food source must be taken into account when experimental results are interpreted, or when comparing the results obtained in different laboratories. Indeed, raising animals at 27°C rather than 25°C induces constitutive dauer formation in some mutants that cannot otherwise be scored as Daf-c ([Malone et al. 1996](#)). Such observations underscore the importance of environmental conditions in dauer larva formation and raise the possibility that other cues also affect the process.

## B. Genetic Pathways

Studies of the phenotypes resulting from combinations of temperature-sensitive *daf-c* and nonconditional *daf-d* mutations have allowed the *daf* genes to be ordered into complex branched pathways ([Riddle et al. 1981](#); [Vowels and Thomas 1992](#); [Thomas et al. 1993](#); [Gottlieb and Ruvkun 1994](#); [Larsen et al. 1995](#); [Grenache et al. 1996](#)). A unified version of the pathways is shown in Figure 3. Tests for genetic epistasis ask whether a given *daf-c*; *daf-d* double mutant forms dauer larvae or grows to the adult at 25°C ([Riddle et al. 1981](#)).

The first gene in the pathway, [daf-22](#), is involved in production of the dauer-inducing pheromone ([Golden and Riddle 1985](#)). [daf-22](#) is unique among *daf-d* mutants because its phenotype can be cured by addition of exogenous pheromone to the culture medium. [daf-6](#) also acts at an early phase of the response ([Vowels and Thomas 1992](#)). As previously mentioned, the amphidial pores in [daf-6](#) mutants are blocked, preventing sensation of pheromone.

Downstream from [daf-6](#), two parallel genetic pathways corresponding to two partially distinct neuronal signaling pathways have been identified ([Thomas et al. 1993](#); [Schackwitz et al. 1996](#)). One branch includes [daf-11](#) and [daf-21](#) mutations. *Dyf* mutations that affect development of the sensory cilia suppress the temperature-sensitive *daf-c* mutations in [daf-11](#) and [daf-21](#), indicating that mutations in these two genes require normal cilium structure to induce dauer larva formation in the presence of food ([Vowels and Thomas 1992](#); [Thomas et al. 1993](#)). The second branch of *daf-c* genes includes [daf-1](#), -4, -7, -8, and -14, which are not suppressed by *dyf* mutations. These genes encode components of the TGF-β signaling pathway that are expressed in some [sensory](#)

[neurons](#) (see below). These *daf-c* mutations are fully suppressed by mutations in [\*daf-3\*](#) and [\*daf-5\*](#), which only partially suppress the *daf-c* mutations in [\*daf-11\*](#) and [\*daf-21\*](#).

The parallel nature of these two branches of the pathway was proposed on the basis of the phenotypes of animals doubly mutant for [\*daf-11\*](#) or [\*daf-21\*](#) and any of the second group of mutations ([\*daf-1\*](#), -4, -7, -8, and -14). These animals form 100% dauer larvae at all temperatures, a Daf-c phenotype more severe than observed for the single mutants at 15°C ([Thomas et al. 1993](#)). Thus, the two groups of genes have partially redundant activities that can compensate for one another under some conditions, a model that conforms to their apparent parallel activities in different [neurons](#) ([Schackwitz et al. 1996](#)).

The two branches of the dauer formation pathway converge again on [\*daf-12\*](#), which fully suppresses the Daf-c phenotype of both groups of upstream mutations. The [\*daf-12\*](#) gene encodes a nuclear hormone receptor that is required for wild-type or *daf-c* animals to form dauer larvae ([Yeh 1991](#)). *daf-c* mutations in [\*daf-2\*](#) and [\*age-1\*](#) have antagonistic activity with [\*daf-12\*](#) ([Gottlieb and Ruvkun 1994; Larsen et al. 1995](#)). The [\*age-1\*](#) gene encodes a phosphatidylinositol-3-OH (PI3) kinase catalytic subunit ([Morris et al. 1996](#)) of the class that is activated in tyrosine kinase signaling pathways ([Kapellar and Cantley 1994](#)). At this point, it is unclear whether the link between [\*age-1\*](#) phosphatidylinositol signaling and TGF-β signaling ([\*daf-1\*](#), -4, and -7) is direct or indirect.

A simple model relating the genetics to the physiology is that the two parallel groups of *daf-c* genes detect and relay environmental signals to the animal. At low temperatures, either parallel pathway can operate independently, but at high temperatures, both are required to prevent dauer larva formation. The ultimate result of these pathways is to control the relative activities of the [\*daf-12\*](#) and [\*daf-2\*](#) genes. When pheromone levels are high, DAF-12 is active, DAF-2 is inactive, and dauer larvae form. When pheromone levels are low, DAF-12 is inactive, DAF-2 is active, and nondauer development ensues. Interestingly, [\*daf-2\*; \*daf-12\*](#) double mutants often arrest as young larvae, as though the activity of one of these two genes is necessary to get the animal through larval development, either on the dauer pathway or on the nondauer pathway ([Vowels and Thomas 1992; Larsen et al. 1995](#)).

*daf-c* mutations in [\*age-1\*](#) and [\*daf-2\*](#), but not other *daf-c* genes, double adult longevity and decrease sensitivity to UV irradiation. All three phenotypes are suppressed by a mutation in [\*daf-16\*](#) ([Kenyon et al. 1993; Larsen et al. 1995; Murakami and Johnson 1996](#)). Different combinations of [\*daf-12\*](#) and [\*daf-2\*](#) alleles either enhance or suppress the extended life span, leading [Larsen et al. \(1995\)](#) to propose a direct interaction between [\*daf-2\*](#) and [\*daf-12\*](#) gene products. The [\*age-1\*](#) gene has long been studied by means of one mutant allele (*hx546*) that extends longevity by 50% ([Friedman and Johnson 1988a; Johnson et al. 1991](#)), but this mutant lacks a Daf-c phenotype unless exposed to temperatures above the normal growth range ([Malone et al. 1996](#)). Only recently has [\*age-1\*](#) been found to be allelic with [\*daf-23\*](#) ([Malone et al. 1996; Morris et al. 1996](#)).

The genetic pathways diverge after [\*daf-3\*](#) and [\*daf-5\*](#), with [\*daf-12\*](#) activity required for dauer formation, but only [\*daf-3\*](#) and [\*daf-5\*](#) are required for expression of other aspects of the [\*daf-1\*](#) group Daf-c mutant phenotype, including display of an L1 surface antigen on later larval stages ([Grenache et al. 1996](#)) and defects in behavior and appearance ([Trent et al. 1983; Thomas et al. 1993](#)).

Why is the dauer formation pathway so complex, and why were discrepancies observed between different laboratory groups? Many of the *daf* gene products probably affect response to a subset of environmental cues. The exquisite sensitivity of dauer formation to environmental conditions and the partial redundancy of the [neurons](#) that sense these conditions mean that different genes may shift in importance under different culture conditions. Furthermore, gene interactions are not always easily interpreted. First, many of the mutations used for epistasis tests were probably not null, which could weaken the interpretation for those genes. Second, some *daf-c*; *daf-d* double-mutant combinations clearly show intermediate phenotypes (coexpression), whose interpretation will necessarily be ambiguous ([Vowels and Thomas 1992; Larsen et al. 1995](#)). The relationship between these dauer-like forms and normal dauer larvae is not obvious. For example, if the dauer-like forms do not undergo dauer sensory remodeling, they might respond differently to sensory cues than do true dauer larvae. Certain *daf-c*; *daf-d* double mutants form dauer or dauer-like larvae transiently and then resume

development ([Vowels and Thomas 1992](#); [Larsen et al. 1995](#)). The appearance of transient dauer larvae makes the timing of scoring important.

An additional problem is that in many cases, the double-mutant phenotype is neither fully *daf-c* nor fully *daf-d* (partially penetrant suppression), which raises the question of the amount of suppression necessary to define an epistatic relationship. Several conventions have been used to define an epistatic relationship. For example, [Riddle et al. \(1981\)](#) considered 20% suppression of a Daf-c phenotype (scored in asynchronous populations after 3 days of growth) sufficient to place a Daf-d mutant downstream in the pathway in the absence of any information about which alleles might be null. [Larsen et al. \(1995\)](#) used 66% suppression of entry into the dauer stage 50 hours from the time eggs were laid (scoring synchronously developing populations over a 5-day period) as the minimum to define an epistatic Daf-d mutant. A useful strategy for epistasis tests has been to construct *daf-c*; *daf-d* strains that do not carry other genetic markers, and score synchronous populations for growth or dauer larva formation at a time when transient dauer formation can be observed ([Vowels and Thomas 1992](#); [Larsen et al. 1995](#)).

## C. Sensory Neurons with Overlapping Functions

Laser microsurgery has been used to identify specifically which [amphid neurons](#) participate in dauer signaling. In these studies, corresponding [neurons](#) in both amphids were killed. When [neurons](#) ADF, ASG, and ASI were killed early in the L1 stage, wild-type animals developed into dauer larvae at 20°C in abundant food, mimicking the Daf-c phenotype ([Bargmann and Horvitz 1991b](#)). However, these dauer larvae recovered within 1 day unless the ASJ [neurons](#) were also killed. Hence, under conditions favoring nondauer development, [amphid neurons](#) ADF, ASI, and ASG signal to inhibit dauer formation, and ASJ signals exit from the dauer stage. Mutants that fail to develop normal dendritic cilia are Daf-d because they fail to respond to pheromone ([Golden and Riddle 1984a](#)). It is argued that pheromone inhibits the promotion of nondauer development by ADF, ASI, and ASG. Killing the ADF, ASG, ASI, and ASJ [neurons](#) in Daf-d mutants resulted in a Daf-c phenocopy in the case of [daf-22](#) and [daf-10](#), but not in the case of [daf-3](#), [daf-5](#), [daf-12](#), or [daf-16](#) ([Bargmann and Horvitz 1991b](#)). This suggests that the latter genes act downstream from these cells, and they are required for dauer formation in the absence of the dauer-inhibiting neuronal signal ([Fig. 3](#)).

[Bargmann and Horvitz \(1991b\)](#) observed that the function of either ASI or ADF alone was sufficient to prevent dauer formation at 20°C (i.e., in two sets of L1 larvae, ADF, ASG, and ASJ were killed and ASI, ASG, and ASJ were killed, respectively). The ASG [neuron](#), on the other hand, only prevented 40% of ADF + ASI + ASJ killed L1 larvae from developing into dauer larvae. Hence, under standard laboratory conditions at 20°C, either ADF or ASI cell function is sufficient for continuous development, and ASG has an overlapping function, perhaps as an evolutionary fine-tuning mechanism for adapting pheromone response to different environments. Indeed, wild-type *Caenorhabditis* strains from different environments have been observed to differ quantitatively in their response to pheromone ([Fodor et al. 1983](#)).

Further evidence for a role of ADF in dauer formation was provided by a phenotypic analysis of [osm-3](#) osmotic avoidance mutants ([Shakir et al. 1993a](#)). [osm-3](#) encodes a kinesin-like protein that is expressed in chemosensory [neurons](#) during neurogenesis ([Tabish et al. 1995](#)). Severe [osm-3](#) mutants are deficient in amphid dye filling and they are dauer-defective (always signaling nondauer development). Weaker alleles retain some ability to concentrate fluorescein isothiocyanate (FITC) in ADF [neurons](#). The ability of ADF to absorb dye correlated with the ability to form dauer larvae in starved, crowded cultures. These results indicate that ADF is likely to be important under dauer-inducing conditions at 20°C, but why was pheromone-induced inhibition of ADF alone sufficient to permit dauer larva formation by the [osm-3](#) mutant? One might have predicted that ASI (and ASG), which did not absorb dye, would have constitutively signaled nondauer development because they remained pheromone-insensitive.

The difference in assay conditions may account for the apparent difference in the function of ASI. [Bargmann and Horvitz \(1991b\)](#) assayed constitutive dauer formation of laser-operated animals in abundant food, whereas [Shakir et al. \(1993a\)](#) assayed dauer formation in starved cultures. ASI may be less important under these

conditions than under unstarved conditions, or dye filling might not be a reliable test of pheromone-sensing ability of ASI. It is intriguing to consider that the relative roles of ADF, ASI, and ASG in signaling might change with food abundance. In abundant food, response to high pheromone levels might require inhibition of both ADF and ASI, but when food is depleted, inhibition of ADF might be sufficient to permit dauer formation because the competitive food signal is reduced.

Another possibility that could account for the difference between laser microsurgery results and mutant analysis concerns the late time of cell death after laser killing (early to mid L1). If ADF not only regulated dauer formation, but also signaled ASI in the embryo or L1 to make ASI competent to signal nondauer development, a weak *osm-3* mutation could eliminate both functions, whereas laser killing might eliminate only the later function.

The experiments of [Bargmann and Horvitz \(1991b\)](#) were designed to detect dauer-inhibiting [neurons](#), not dauer-promoting [neurons](#). [Thomas et al. \(1993\)](#) proposed parallel pathways for dauer formation based on genetic analysis. Genes like *daf-1*, which encode components of TGF- $\beta$  signaling, were proposed to define one pathway, whereas the *daf-d* genes affecting chemotaxis and the *daf-c* genes *daf-11* and *daf-21*, which also affect chemotaxis ([Vowels and Thomas 1994](#)), were proposed to define a parallel pathway. [Schackwitz et al. \(1996\)](#) hypothesized that the Daf-c phenotype of *daf-11* mutants results from the activity of dauer-promoting [neurons](#) and that loss of *daf-11* function activates these [neurons](#), resulting in constitutive dauer formation. Indeed, killing ASJ, but not other [amphid neurons](#), resulted in suppression of the *daf-11* and *daf-21* Daf-c phenotypes. This suppression was enhanced by killing [neurons](#) ASK and ADL. In contrast, killing ADF and ASI enhanced the Daf-c phenotype of *daf-11* and *daf-21* mutants. Finally, killing ASJ in wild-type larvae impaired their response to the dauer-inducing pheromone.

The results of the [neuron](#) ablation studies suggest that parallel pathways for control of dauer larva formation function in different sets of [amphid neurons](#). The model proposed by [Schackwitz et al. \(1996\)](#) is that mutations in the *daf-1* group (see [Fig. 3](#)) disrupt the inhibition of dauer formation by ADF, ASI, and ASG. Laser-operated *daf-1* and *daf-7* mutants, in which ADF, ASI, and ASG were left intact, still expressed the Daf-c phenotype. In contrast, the dauer-promoting [neuron](#), ASJ, is required for the Daf-c phenotype of *daf-11* and *daf-21* mutants to be expressed. In low levels of pheromone, the dauer-inhibiting [neurons](#) ADF, ASI, and ASG are active, and the dauer-promoting [neuron](#) ASJ is inactive. Conversely, in high levels of pheromone, ADF, ASI, and ASG are inactive and ASJ is active. Such parallel pathways have been found in the vertebrate visual system, where they are thought to enhance contrast sensitivity and improve rapid response to light changes ([Schiller et al. 1986](#)). Similarly, the fidelity of the dauer/nondauer switch may be enhanced by the parallel [neural](#) pathways.

A dauer-promoting role for ASJ in the L1 stage is surprising because these [neurons](#) function to promote dauer recovery ([Bargmann and Horvitz 1991b](#)). One possibility is that ASJ changes its function between the L1 and dauer stages. In this case, *daf-11* and *daf-21* would inactivate ASJ to help prevent dauer formation in low pheromone, but in the dauer larva, these genes would activate ASJ in low pheromone to promote recovery ([Schackwitz et al. 1996](#)). The temperature-sensitive *daf-11* mutants, in fact, recover very poorly from the dauer stage when shifted to lower temperature ([Vowels and Thomas 1994](#)). An answer to the puzzle of ASJ functions may emerge from an understanding of cross-talk with [neurons](#) of opposite function, such as ASI.

## D. Gene Products and Expression Patterns

### 1. TGF- $\beta$ Signaling

The first *daf* gene cloned, *daf-1*, had the hallmarks of a cell surface receptor with a signal peptide, a single transmembrane segment, and a cytoplasmic region with a protein serine/threonine kinase domain ([Georgi et al. 1990](#)). These and other sequence features have subsequently proved to identify it as a member of the TGF- $\beta$  receptor family ([Kingsley 1994; Massagué et al. 1994](#)). The *daf-4* gene encodes another receptor serine/threonine kinase corresponding to a type II TGF- $\beta$  receptor ([Estevez et al. 1993](#)). The type II TGF- $\beta$  receptor binds its ligand, recruits the type I receptor into a heterodimer, and activates the type I receptor by phosphorylation ([Wrana et al. 1994](#)). The type I receptor then phosphorylates downstream components in the signal transduction pathway. The

[daf-4](#) receptor was found to bind human bone morphogenetic proteins BMP-2 and BMP-4 when expressed in monkey COS cells (Estevez et al. 1993). [daf-4](#) did not bind TGF- $\beta$  or activin, and the [daf-1](#) receptor did not bind any ligand tested. The DAF-1 protein is the putative type I receptor because it possesses a "GS domain" similar to the site of phosphorylation on the TGF- $\beta$  type I receptor, and it has a smaller extracellular domain than does the DAF-4 receptor, as would be expected for a type I subunit. Type I TGF- $\beta$  receptors do not bind ligand in the absence of the type II receptor. Biochemical tests for direct interaction of DAF-1 and DAF-4 proteins have yet to be done, so the proposed relationship is based on the genetic results and by analogy with other receptors in the family.

The DAF-4 receptor participates directly in dauer/nondauer signaling, rather than playing an indirect part in [neural](#) development. Heat shock treatment of transgenic [daf-4](#) mutant animals carrying a heat-shock-inducible [daf-4](#) (+) cDNA construct demonstrated that expression of [daf-4](#) in the L1 stage was sufficient to rescue the Daf-c phenotype, and expression in the dauer stage induced exit ([Estevez et al. 1993](#)).

The putative natural ligand for DAF-4 in its role in nondauer development is the DAF-7 protein, which is a novel member of the TGF- $\beta$  superfamily ([Ren et al. 1996](#)). The [daf-7](#) gene encodes a secreted 350-amino-acid precursor that is processed at a dibasic proteolytic cleavage site to produce a 116-amino-acid mature hormone subunit. Such processing has been confirmed by amino-terminal sequencing of recombinant DAF-7 protein expressed in insect cells (P. Ren and D. Riddle, unpubl.). In this protein family, the biologically active protein is a homodimer or heterodimer joined by a disulfide bridge ([Roberts and Sporn 1990](#)). DAF-7 has sequence similarity to the BMP group of ligands, which includes the *Drosophila decapentaplegic* (*dpp*) gene product ([Padgett et al. 1993](#)), but it lacks several amino acids invariant in this group. It also has sequence similarity to TGF- $\beta$ , including two conserved cysteines found in TGF- $\beta$  and activin, but not in other superfamily members ([Kingsley 1994](#)). It is conceivable that a protein similar to DAF-7 was the evolutionary precursor to both TGF- $\beta$  and BMPs, which now represent structurally divergent subfamilies ([Fig. 4](#)).

Northern blot analysis has shown that [daf-1](#) and [daf-4](#) mRNAs are present in all developmental stages (M. Estevez and D.L. Riddle, unpubl.), but [daf-7](#) mRNA is regulated. The [daf-7](#) mRNA is rare but most abundant in the L1 stage under conditions favoring nondauer development ([Ren et al. 1996](#)). Its steady-state level decreases in the L2, but the RNA is nearly absent in the egg, L2d, and later stages. Control of [daf-7](#) transcription by food and/or pheromone is one mechanism by which the dauer/nondauer decision is made. Mutations in [daf-1](#), [daf-4](#), and [daf-7](#) all result in a Daf-c phenotype, and they define one step in the genetic pathway ([Fig. 3](#)), as would be expected for a ligand and its receptor. A low-pheromone environment activates continuous development by promoting secretion of the [daf-7](#) ligand. Ligand binding would, in turn, activate the DAF-1/DAF-4 receptor.

The repression of [daf-7](#) transcription as a result of exposure to dauer-inducing pheromone was inferred from observation of transgenic animals carrying green fluorescent protein (GFP) reporter constructs ([Ren et al. 1996](#); [Schackwitz et al. 1996](#)). The reporter gene was expressed in ASI [neurons](#) and preferentially under conditions favoring growth. [Ren et al. \(1996\)](#) observed GFP expression in hermaphrodite larvae from 4 to 5 hours after hatching, through the four larval stages and in adults, whereas [Schackwitz et al. \(1996\)](#) observed only low levels of adult expression. Neither [daf-7](#) mRNA nor GFP expression was observed in embryos, suggesting that [daf-7](#) does not have a role in sensory [neuron](#) development. During pheromone-induced dauer formation at 25°C, GFP expression was strongly suppressed in L1 larvae, both in the percentage of animals expressing GFP and in the intensity of fluorescence. As animals entered the dauer stage, weak GFP expression was no longer detected. The GFP expression results suggest that during the L1 stage, the amphid ASI [neurons](#) use DAF-7 to signal nondauer development in low pheromone and then again use DAF-7 to signal recovery from the dauer state in response to fresh food at higher growth temperatures (see [Ren et al. 1996](#)).

As described above, laser microsurgery performed at 20°C indicated that [neurons](#) ASI, ADF, and ASG were apparently redundant. The temperature itself may account for the difference between [neuron](#) ablation and GFP expression results or the surgery may not have killed ASI cells soon enough to prevent [daf-7](#) expression, so that additional [neurons](#) (perhaps DAF-7 target cells) had to be disrupted to cause dauer formation. Alternatively,

unknown transcriptional or translational regulatory elements for expression of GFP in other [neurons](#) may be absent from the reporter constructs.

In contrast with [\*daf-7\*](#), a *daf-1::gfp* fusion is expressed in more than 50 cells in the body. Many of these cells are [interneurons](#), but [amphid neurons](#) also fluoresce in the transgenic animals ([Fig. 5](#)). The amphid cells that express GFP include ASI (C. Gunther and D. Riddle, unpubl.). Expression in ASI raises the possibility of an autocrine loop in which [\*daf-7\*](#) progressively stimulates its own expression, although [Ren et al. \(1996\)](#) found that [\*daf-7\*](#) (+) activity was not required for continuous reporter gene expression in transgenic animals.

The secretion of a TGF- $\beta$ -like ligand by a sensory [neuron](#), presumably to activate a receptor on [interneurons](#) (some of which are synaptically connected via the [circumpharyngeal nerve ring](#)), might seem surprising. As precedent for this type of [neural](#) function, activin has been implicated as a neurotransmitter/neuromodulator in central [neural](#) pathways in rats for the release of oxytocin in response to suckling ([Sawchenko et al. 1988](#)). DAF-7 might act as a neuromodulator to change the activity of [neural](#) circuits over time. Sufficient DAF-7 signaling through the L1 stage could raise the system to a threshold committing the animal to nondauer development by the L1 molt. A second use of DAF-7 could be to directly modulate the activity of other chemosensory [neurons](#) that may have either synergistic or competitive activities. If, for example, DAF-7 secretion by ASI beyond a certain threshold inactivated ASJ, it would ensure a coherent signal by silencing the competitive [neurons](#).

## 2. Cyclic Nucleotide Signaling

Recently, cyclic nucleotide signaling has been implicated in the dauer/ nondauer switch by the cloning of additional genes for which mutant alleles convey a partial or complete Daf-c phenotype as well as other sensory defects. The [\*daf-11\*](#) gene encodes a transmembrane guanylyl cyclase (D. Birnby and J. Thomas, pers. comm.); activating alleles of [\*gpa-2\*](#) and [\*gpa-3\*](#), which encode  $\alpha$  subunits of heterotrimeric G proteins, convey a dominant Daf-c phenotype ([Zwaal et al. 1997](#)); and the sensory mutant genes [\*tax-2\*](#) and [\*tax-4\*](#), which have a weak Daf-c phenotype, encode subunits of a cyclic-nucleotide-gated channel ([Coburn and Bargmann 1996](#); [Komatsu et al. 1996](#)).

Heterotrimeric G proteins are components of seven transmembrane hormone and sensory receptor pathways. GTP-bound G- $\alpha$  proteins can regulate cGMP phosphodiesterase or they can activate adenylyl cyclase, and the resulting rise in cAMP can result in activation of protein kinase A. GTP-bound G- $\alpha$  can also activate phospholipase C, a key component in 3-phosphoinositide signaling pathways. The *C. elegans* [\*gpa-2\*](#) and [\*gpa-3\*](#) genes were cloned on the basis of their sequence similarity with mammalian G- $\alpha$  subunits ([Zwaal et al. 1997](#)). Expression of presumptive dominant mutations in transgenic animals resulted in a Daf-c phenotype, and this phenotype was suppressed by *daf-d* cilium structure mutations (just as *daf-c* mutations in [\*daf-11\*](#) and [\*daf-21\*](#) are suppressed), suggesting that GPA-3 functions in the amphid cilia. This location would be expected for a G protein coupled to the pheromone receptor. [\*gpa-3\*](#) reporter gene fusions were, indeed, expressed in [amphid neurons](#). Activated [\*gpa-3\*](#) mutant strains were also Daf, indicating that constitutive GPA-3 activity is deleterious to [neuron](#) function.

Loss of [\*gpa-2\*](#) function results in dauer recovery in the presence of pheromone, but [\*gpa-3\*](#) loss-of-function mutants retained pheromone responsiveness and were not able to recover under the same conditions. Hence, the [neurons](#) expressing [\*gpa-2\*](#) are involved in both dauer formation and recovery, whereas [amphid neurons](#) expressing [\*gpa-3\*](#) are involved only in dauer formation. Loss of [\*gpa-2\*](#) or [\*gpa-3\*](#) function results in reduced sensitivity to pheromone in the L1 stage and, under certain conditions, an altered food response. Mutations in [\*daf-11\*](#) and [\*daf-21\*](#) are partially suppressed by these loss-of-function mutations, but mutations in [\*daf-1\*](#) or [\*daf-8\*](#) are not, indicating that [\*gpa-2\*](#) and [\*gpa-3\*](#) may act downstream or in parallel to [\*daf-11\*](#) and [\*daf-21\*](#) and either upstream or in parallel to [\*daf-1\*](#) and [\*daf-8\*](#) ([Zwaal et al. 1997](#)). The [\*daf-11\*](#) and [\*daf-21\*](#) gene products might act through G proteins, or this suppression could be indirect, involving other [neurons](#). [\*gpa-2\*](#) and [\*gpa-3\*](#) seem to be involved primarily in the sensory response to dauer-inducing pheromone, since inactivation of these genes interferes with the pheromone response, and constitutively active GPA-2 and GPA-3 lead to a Daf-c phenotype.

The [tax-2](#) and [tax-4](#) genes encode subunits of a cyclic-nucleotide-gated channel ([Komatsu et al. 1996; Coburn and Bargmann 1996](#)) that are required for expression of the [daf-11](#) (guanylyl cyclase) mutant phenotype. Cyclic-nucleotide-gated channels are involved in olfactory and photosensory transduction in vertebrates ([Nakamura and Gold 1987](#)). The ASJ [sensory neurons](#) exhibit defects in axon outgrowth in [tax-2](#) ([Coburn and Bargmann 1996](#)) and in [daf-11](#) mutants ([Bargmann and Mori](#), this volume). These results show that cyclic nucleotides are an important intracellular messenger in *C. elegans* sensory transduction and in chemosensory axon morphology.

## E. Pleiotropy

### 1. Multiple Functions for *daf* Genes

Most of the dauer formation genes also have effects on other aspects of *C. elegans* biology. [daf-11](#) and [daf-21](#) exhibit chemotaxis and thermotaxis defects, consistent with their proposed role in sensory function ([Vowels and Thomas 1994; Bargmann and Mori](#), this volume). The Dyf mutants, which have developmental defects in the sensory cilia, also have correspondingly broad defects in chemosensory function; [dyf](#) mutations suppress [daf-11](#) and [daf-21](#) mutations. In addition to the G-protein mutants discussed above, mutations in [tax-2](#) and [tax-4](#) also suppress [daf-11](#) and [daf-12](#) mutations, suggesting a role for these *tax* genes in thermotaxis, chemotaxis, and dauer formation ([Bargmann and Mori](#), this volume).

Multiple roles in developmental or behavioral processes may not always be so obvious. For example, most Daf-c mutants are defective in egg laying (Egl), but a large number of additional Egl mutants, including [egl-4](#), lack a Daf-c phenotype ([Trent et al. 1983](#)). However, an [egl-4](#) mutant is hypersensitive to dauer-inducing pheromone, indicating that this gene may play some part in promoting nondauer development that is not detectable under normal laboratory conditions ([Golden and Riddle 1984a](#)). It is now known that mutations in more than 50 genes, including [egl-4](#), convey a Daf-c phenotype, but only when combined in specific double mutants (synthetic Daf-c mutants) (I. Katsura, pers. comm.). Such genes include those required for chemotaxis, locomotion, and defecation. For example, an [unc-31](#); [aex-3](#) double mutant is strongly Daf-c ([Avery 1993a](#)), whereas the single mutants are not.

Recently, [mig-7](#) mutants have been shown to be novel alleles of [daf-12](#). [daf-12](#) function is required not only for dauer formation, but also for proper guidance of gonadal development by the [distal tip cells](#) and for proper development of the [hypodermis](#) ([Antebi et al.](#), this volume). Different [daf-12](#) alleles have different effects on these processes. It is possible that [daf-12](#) coordinates different developmental processes in time, like the heterochronic genes. The gonadal [distal tip cells](#) stop migrating at the dauer-specific molt in response to the signal for dauer morphogenesis, and hypodermal cell divisions that would normally occur after the molt do not occur. DAF-12 may also synchronize gonadal and hypodermal development at other larval stages. It is interesting that certain [daf-12](#) mutations also double the longevity of certain [daf-2](#) mutants ([Larsen et al. 1995](#)). Mutations in [age-1](#) and [daf-2](#), but not other *daf-c* genes, increase adult longevity, increase thermotolerance, and decrease sensitivity to UV irradiation ([Kenyon et al. 1993; Larsen et al. 1995; Lithgow et al. 1995; Murakami and Johnson 1996; Kenyon](#), this volume). One hypothesis is that [daf-2](#) mutants express genes for efficient life maintenance in the adult that are normally only expressed in the dauer stage, and certain [daf-12](#) alleles enhance this expression when combined with [daf-2](#) mutations.

### 2. Multiple Functions for TGF- $\beta$ Signaling

Mutants in the [daf-1](#) group have an adult egg-laying defect ([Trent et al. 1983](#)) and dark intestinal cells, and individuals tend to accumulate ("clump") in groups near the edge of the bacterial lawn ([Thomas et al. 1993](#)). The mutants also express an L1 surface antigen on later larval stages ([Grenache et al. 1996](#)). These phenotypes are suppressed by [daf-3](#) and [daf-5](#) mutations, indicating that these two genes function in every aspect of the function of the [daf-1](#) group. However, these phenotypes are not suppressed by [daf-12](#), which may be more selective for the dauer pathway (see [Fig. 3](#)).

Mutants in [\*daf-4\*](#), the type II TGF- $\beta$  receptor, are not only Daf-c and Egl, but also small (Sma) with abnormal [\*male tail\*](#) phenotypes ([Savage et al. 1996](#)). The [\*daf-1\*](#) (putative type I receptor) mutants possess the Daf-c and adult Egl phenotypes, but they are not Sma or defective in male mating. The presence of mRNAs for both these receptors in all developmental stages, including the adult, is consistent with their use in both larval and adult behaviors. The similarity of the Daf-4 adult phenotypes to [\*sma-2\*](#), [\*sma-3\*](#), and [\*sma-4\*](#) mutants (which are not Daf-c) led [Savage et al. \(1996\)](#) to examine these genes as potentially encoding constituents of TGF- $\beta$  signaling unrelated to dauer formation. These three genes encode members of the Smad family of proteins, the founding member of which is the product of the *Mothers against decapentaplegic* (*Mad*) gene from *Drosophila* ([Sekelsky et al. 1995](#)). In *Drosophila*, the *Mad* and decapentaplegic (*dpp*) phenotypes are similar, and loss-of-function mutations in *Mad* enhance the embryonic dorsal-ventral patterning defects and adult appendage defects resulting from *dpp* mutations. Vertebrate homologs of MAD include the human DPC4 (Smad4) tumor suppressor, which associates with either the Smad1 or Smad2 proteins in response to BMP and TGF- $\beta$ , respectively ([Lagna et al. 1996](#)). Smad proteins contain a conserved carboxy-terminal transcriptional activation domain and are transported to the nucleus upon phosphorylation. Smad proteins may also form complexes with other transcription factors to activate activin-dependent transcription ([Chen et al. 1996](#)).

### 3. Dauer Signaling Downstream from DAF-4

Smad proteins act downstream from TGF- $\beta$  family receptors to activate transcription in both vertebrate and invertebrate systems. Which genes might encode the DAF counterparts to the three SMA proteins? The most likely candidates are the *daf-c* genes associated with [\*daf-1\*](#) and [\*daf-4\*](#) in the genetic pathway (see [Fig. 3](#)). In fact, three *daf* genes have recently been found to encode Smad family members: [\*daf-3\*](#) (A. Koweeck et al., pers. comm.), [\*daf-8\*](#) (A. Estevez and D. Riddle, unpubl.), and [\*daf-14\*](#) (T. Inoue and J. Thomas, pers. comm.). Mutations in [\*daf-8\*](#) and [\*daf-14\*](#) are Daf-c, but [\*daf-3\*](#) mutants are Daf-d. Given the known interactions between DPC4 and Smad1 or Smad2 ([Lagna et al. 1996](#)), it is attractive to speculate that DAF-8 and DAF-14 would inactivate DAF-3 (which is required for dauer formation) to signal nondauer development when activated by DAF-7 signaling through the DAF-1/DAF-4 receptor. This would be consistent with the observed epistasis of [\*daf-3\*](#) mutations to [\*daf-8\*](#) and [\*daf-14\*](#). Alternatively, the *daf-c* Smad genes might be in a pathway to activate nondauer development, and the [\*daf-3\*](#) Smad might be in a parallel pathway to activate dauer development. Blockage of either pathway would lead to constitutive activation of the other, but the double mutant would activate nondauer development by a mechanism not requiring [\*daf-8\*](#) or [\*daf-14\*](#).

At least three Smad family proteins are involved in transducing [\*daf-4\*](#) signals in the *daf* pathway and three others are in the *sma* pathway. The DAF-4 receptor apparently does not use the DAF-7 ligand or the DAF-1 receptor as its type I partner for specifying adult body size and [\*male tail\*](#) development. Such a type I receptor may be found among other *sma* genes. Activation of the distinct type I receptor would then result in activation of SMA-2, SMA-3, and SMA-4 proteins. The DAF-1 protein and the downstream Smad proteins in the dauer pathway are activated by the DAF-7 ligand to signal nondauer development, but these proteins apparently have no significant role in the *sma* and [\*male tail\*](#) pathways.

## Figures

Figure 3. Genetic pathway for dauer larva formation, assembled from Malone et al.

### Figure 3

Genetic pathway for dauer larva formation, assembled from [Malone et al. \(1996\)](#), [Gottlieb and Ruvkun \(1994\)](#), [Larsen et al. \(1995\)](#), and [Grenache et al. \(1996\)](#). The pathway is drawn to show wild-type gene functions that stimulate (arrow) or inhibit (T bar) subsequent steps in the pathway. They do not necessarily indicate direct regulatory interactions. Some genes affect the development of cells needed for processing environmental cues, whereas other genes encode proteins thought to be used directly in pheromone/food mediated signal transduction or control of transcription. The *daf-c* genes are [\*daf-1\*](#), [\*daf-2\*](#), [\*daf-4\*](#), [\*daf-7\*](#), [\*daf-8\*](#), [\*daf-11\*](#), [\*daf-14\*](#), [\*daf-21\*](#), and [\*age-1\*](#) (a.k.a. [\*daf-23\*](#)), mutations in which result in constitutive dauer larva formation. The *daf-d*

genes are [\*daf-3\*](#), [\*daf-5\*](#), [\*daf-6\*](#), [\*daf-10\*](#), [\*daf-12\*](#), [\*daf-16\*](#) and [\*daf-22\*](#), mutations in which result in failure to form dauer larvae. Dyf refers to [\*daf-10\*](#) and eight other *daf-d* genes, [\*che-2\*](#), [\*che-3\*](#), [\*che-11\*](#), [\*che-13\*](#), [\*osm-1\*](#), [\*osm-3\*](#), [\*osm-5\*](#), and [\*osm-6\*](#) (Vowels and Thomas 1992). In Dyf mutants, the [\*amphid neurons\*](#) fail to take up fluorescent dyes, and they are defective in amphid sensory cilium structure (Perkins et al. 1986). The pathway has three main branches. The [\*daf-1\*](#) branch involves a dauer-inhibiting signal from ASI [\*neurons\*](#), the [\*daf-11\*](#) branch involves a dauer-promoting signal from ASJ [\*neurons\*](#), and the [\*daf-2\*](#) branch involves phosphatidylinositol signaling in unknown cells that inhibits dauer formation and limits adult longevity. The Daf-c mutants in the [\*daf-1\*](#) branch of the pathway also express an L1-specific surface antigen in all larval stages, and exhibit defects in adult behavior and appearance. Expression of these phenotypes requires the function of [\*daf-3\*](#) and [\*daf-5\*](#), but not [\*daf-12\*](#), indicating a divergence of the dauer pathway from the other traits (Thomas et al. 1993; Grenache et al. 1996). The [\*daf-18\*](#) (Larsen et al. 1995), [\*daf-19\*](#), and [\*daf-28\*](#) (Malone et al. 1996) genes are not included because results of epistasis tests with existing alleles are ambiguous.

Figure 4. Sequence relationships between ten members of the TGF-β superfamily shown by phylogenetic analysis.

## Figure 4

Sequence relationships between ten members of the TGF-β superfamily shown by phylogenetic analysis. The ligand region alone (amino acids 250–350 of DAF-7) was used, starting with the first invariant cysteine. All sequences are human except DPP and 60A (*Drosophila*), nodal (mouse) and Vg1 (*Xenopus*). (BMP-4) Bone morphogenetic protein-4; (GDF-1) growth differentiation factor-1; (Act A) activin A; (MIS) Müllerian inhibiting substance.

Figure 5. GFP expression under control of the *daf-1* promoter.

## Figure 5

GFP expression under control of the [\*daf-1\*](#) promoter. The head of the L1 larva is to the left; dorsal side is up. Genomic DNA upstream of the [\*daf-1\*](#) initiator methionine codon was placed in the pPD95.75 vector (provided by A. Fire). N2 hermaphrodites coinjected with this reporter construct and plasmid pRF4, carrying *rol-6(su1006)*, yielded roller transformants with strong fluorescence in multiple [\*neurons\*](#) in the head, including [\*amphid neurons\*](#). The micrograph is overexposed to see the fluorescence in the [\*amphid processes\*](#) extending to the tip of the head and processes of [\*interneurons\*](#) in the [\*ventral nerve cord\*](#). Plasmids and other [\*neurons\*](#) in the tail (not shown) also fluoresce brightly. Autofluorescence of the small granules in the intestine is independent of injected plasmid. Magnification ×450; field width 243 µm.

Generated from local HTML

## Chapter 26. Genetic and Environmental Regulation of Dauer Larva Development — V Summary and Conclusions

---

The [neural](#) controls on facultative diapause in *C. elegans* appear to be complex. The evolution of such complex behavioral controls may have been driven by the importance of the dauer/nondauer switch in *C. elegans* life history. An ability to make the appropriate decision every time in a variety of environments should offer a strong selective advantage, so fine-tuning mechanisms may have been added since the basic switch first evolved. The major environmental cues of pheromone, food, and temperature may not be the only indicators used by the [nervous system](#). *C. elegans* presumably feeds on a variety of bacteria in the soil that have characteristics different from those of *E. coli*. The pheromone itself is a family of structurally related compounds. Although pheromone from two other hermaphroditic, dauer-forming soil nematode species had no detectable biological activity on *C. elegans* or *C. briggsae* ([Golden and Riddle 1982](#)), this does not mean that such cross-species activity cannot exist.

Numerous environmental cues in the soil may not be present in the laboratory, yet the pathways they influence may be detectable genetically and/or by cell-killing experiments. Candidate genes for processing primary sensory stimuli ([daf-11](#) and [daf-21](#)) have been identified ([Vowels and Thomas 1994](#)), but the identity of the primary receptors for the environmental stimuli has not been determined. A role for a G-protein-coupled receptor in the pheromone response is implied by the Daf-c phenotype resulting from activation of G- $\alpha$  subunits expressed in [amphid neurons](#) ([Zwaal et al. 1997](#)). It is possible that the receptor for the dauer pheromone is a member of the seven transmembrane family, a number of which have been identified in the *C. elegans* genomic sequence, and some of which are expressed in individual [amphid neurons](#) ([Troemel et al. 1995](#)).

One result of pheromone receptor signaling in ASI [neurons](#) is inhibition of [daf-7](#) transcription. Failure to activate DAF-4 receptors on the surface of other [neurons](#) promotes dauer formation or inhibits recovery via physiological mechanisms that are not understood. One clue comes from the identity of the DAF-12 protein, implicating steroid or retinoid signaling. This is the type of global signal that could direct transcriptional events in [all cells](#) in the body, and its synthesis could be controlled in specific [neurons](#) expressing both the DAF-1 and DAF-4 receptor subunits. At present, the details of neuroendocrine control of dauer morphogenesis are only speculative, but comparison with better characterized regulatory strategies used in other organisms may be informative. Molecular analysis of mutations that result in constitutive formation of dauer-like larvae also may be useful, since these animals have some dauer-like tissues and other nondauer-like tissues ([Albert and Riddle 1988](#)). The genes may encode tissue-specific transcription factors that are needed to execute nondauer development in some cells but not in others.

Even nematode species in which dauer formation is obligatory utilize sensory cues from food or their host for facultative resumption of development. For example, the dormant larvae of *Ostertagia* resume development when they detect the coming of spring from their location within a cow's stomach. Considering that *C. elegans* has recruited several types of basic signal transduction machinery used in development for signaling growth versus diapause, and wired it to specific sensory cues appropriate for its survival strategy, it seems likely that diverse parasites will have used similar internal pathways linked to different cues.

## **Chapter 26. Genetic and Environmental Regulation of Dauer Larva Development — Acknowledgments**

---

We thank C. Turner for help with Figures 1 and 3; Dr. P. Ren for the gift of Figure 4; Drs. C.V. Gunther and T. Phillips for Figure 5; Drs. C. Bargmann, J. Thomas, and J. Priess for thoughtful comments and advice; and Ms. L. Hatley for processing the manuscript.

Generated from local HTML

# **Chapter 27. Neural Plasticity**

---

## **Contents**

[I Introduction: Connectivity and Plasticity](#)

[II Synaptic Plasticity During Development](#)

[III Behavioral Plasticity in the Adult](#)

[IV Conclusions](#)

[Acknowledgments](#)

Generated from local HTML

## Chapter 27. Neural Plasticity — I Introduction: Connectivity and Plasticity

---

Neural plasticity refers to functional changes in the [nervous system](#) and therefore encompasses a range of phenomena from changes at synapses observed on a microscopic scale to changes in behavior observed in the whole animal. These diverse phenomena are related since changes in synapses are believed to underlie changes in an animal's behavior ([Greenough and Bailey 1988](#)). Ideally, both the physical changes to the [nervous system](#) and the resultant behavioral changes could be identified and studied together to yield an integrated understanding of [nervous system](#) structure and behavior.

Nervous systems were once thought to be "hardwired" during development. In most vertebrate central nervous systems, cell proliferation occurs during embryogenesis and new [neurons](#) are not added to the mature [nervous system](#) ([Jacobson 1991](#)). An unusual exception to this rule is found in some species of birds in which [neurons](#) are added to the brains of juveniles to accommodate song learning ([Paton and Nottebohm 1984](#)). Sensory systems such as the visual cortex form their functional connectivity during a limited "critical period" during development, and new connections in most systems are not made after this period ([Hubel and Wiesel 1970](#)). This stability was thought to be an essential requirement for reliable processing of sensory information. However, this general stability has been shown to have its exceptions. The [nervous system](#) of even the dimmest among us can learn new tasks and thereby reveals a degree of plasticity in our brains. Even the inability of the brain to produce new [neurons](#) has been recently challenged when it was demonstrated that mature brain cells can be induced to divide and proliferate *in vitro* ([Reynolds and Weiss 1992; Morshead et al. 1994](#)). Additionally, the functional connectivity of the visual cortex reorganizes after sensory lesions ([Das and Gilbert 1995](#)), illustrating a flexibility in a circuit once thought to be rigidly fixed.

Even a [nervous system](#) with a stable anatomical connectivity can exhibit profoundly variable output. Anatomical connectivity refers to the physical arrangement of synapses among cells of a circuit. Functional connectivity defines the effects of cells in a circuit upon one another ([Getting 1989](#)). A cell may form synapses to another cell, but these synapses have no effect on the postsynaptic cell. Thus, the synapses form part of the anatomical connectivity but not the functional connectivity. In some cases, these latent synapses can be activated to alter the output of the circuit after high-frequency electrophysiological stimulation ([Charpier et al. 1995; Liao et al. 1995](#)). In other cases, the functional connectivity may be quite dynamic; synaptic relationships between cells can change instantaneously when inputs into the circuit change ([Dickinson 1989](#)). For example, the mollusk *Tritonia* first responds to threat by reflexive withdrawal. Withdrawal is followed by rapid escape swimming, which is driven by alternating contractions of the dorsal and ventral muscles. The same group of [interneurons](#) mediate both behaviors; these cells inhibit one another when they participate in reflexive withdrawal, and they excite one another when they participate in escape swimming ([Getting 1989](#)).

Because the output of a [nervous system](#) is a function of the input into the circuit and the anatomical and functional connectivities, changes in the output can be caused by alterations to any one of these three properties. First, altering the input of a circuit can radically change the functional connectivity. These inputs can be either synaptic or humoral. Second, the functional connectivity can be changed by altering the individual strengths of the existing synapses. Third, synapses can be added or eliminated to change the anatomical connectivity. Observations of these first two mechanisms require electrophysiological recordings from the relevant circuit, and although such techniques are being developed in *Caenorhabditis elegans* ([Raizen and Avery 1994; Davis et al. 1995; Lockery and Hall 1995](#)), they have not yet been applied to the analysis of dynamic [neural](#) circuits. For this reason, we are confined to observing changes in the physical connectivity of the nematode. Nevertheless, there are several examples of such synaptic remodeling during *C. elegans* development.

The *C. elegans* [nervous system](#) is thought to be even more rigid than other nervous systems. Unlike vertebrate nervous systems, the number of cells is invariant, and anatomical reconstructions have shown that neuronal connectivity is similar between individuals ([White et al. 1986; Hall and Russell 1991](#)). For these reasons, *C. elegans* once appeared to be a poor organism in which to study [neural](#) plasticity. However, recent data indicate that the

*C. elegans* [nervous system](#) is also flexible. In this chapter, we review examples of [neural](#) plasticity during development and behavioral plasticity in adult animals, including examples of learning such as habituation and classical conditioning.

Generated from local HTML

# Chapter 27. Neural Plasticity — II Synaptic Plasticity During Development

---

During development in vertebrates, there is a dynamic interaction between a [neuron](#) and its target. In a process called activity-dependent development, the activity of the target can affect its innervation from the input [neuron](#). Thus, the connectivity cannot be hardwired; i.e., it cannot be predetermined by the genome. Studies of the vertebrate visual system indicate that many of the initial synaptic contacts appear to be temporary or inappropriate. Use of the visual system strengthens appropriate synapses and eliminates inappropriate synapses ([Constantine-Paton et al. 1990](#); [Shatz 1990](#); [Hockfield and Kalb 1993](#)). Similarly, it has been hypothesized that in the adult animal, the strengths of synapses may be altered in an activity-dependent manner during learning ([Bliss and Collingridge 1993](#); [Hawkins et al. 1993](#)). Thus, in both a developing and a mature [nervous system](#), there must be signal transduction systems that link activity of the presynaptic and postsynaptic cells and cause changes in the strength of the connection. Moreover, the mechanisms used to alter an existing circuit in a mature animal may be the same mechanisms used early in development to establish the original connectivity in the embryo ([Kandel and O'Dell 1992](#) and references therein).

## A. Neuromuscular Junction Formation

Dynamic interactions between [neuron](#) and target were first observed during the formation of vertebrate neuromuscular junctions. In early development, a muscle fiber is innervated by several motor [neurons](#). There is then a competitive interaction among the motor [neurons](#) that eliminates all but one input and serves to sharpen the compartment boundaries between adjacent motor units ([Lichtman 1995](#)). The sorting-out process is activity-dependent; it seems that the more effective motor [neuron](#) is favored and the weaker motor [neuron](#) is disfavored by a retrograde signal from the muscle.

Observations of *C. elegans* neuromuscular junctions indicate that synaptic plasticity may occur in nematode development as well. First, rudimentary plasticity is a prerequisite to normal development and growth of the animal. The length of a *C. elegans* individual increases fivefold during development, and neuromuscular junctions are added to maintain synaptic density ([Fig. 1](#)). At the end of the L1 stage, additional muscles and motor [neurons](#) are added to the embryonic [nervous system](#) and must be incorporated into the existing nerve cords ([White et al. 1978](#)). During the L4 stage, sex-specific muscles and motor [neurons](#) are added to both hermaphrodites and males. It is likely that the addition of these components requires accommodations in the existing [nervous system](#) so that a well-ordered motor system is maintained. These observations indicate that the motor [neurons](#) and target muscles interact dynamically during the formation of neuromuscular junctions, but it is not yet clear whether this is an activity-dependent interaction.

Nematodes differ from most other animals in that a motor [neuron](#) does not leave the nerve fascicle to innervate its target; instead, the muscle extends a process, the muscle arm, to the nerve cord to form a neuromuscular junction at the edge of the nerve bundle. Analyses of [unc-6](#) and [unc-104](#) mutants indicate that the migrating muscle arm may respond to chemotropic cues to locate its synaptic partner. In the absence of function from the *C. elegans* netrin homolog UNC-6, axons that normally run in the [dorsal nerve cord](#) are displaced ventrally ([Fig. 2](#)) ([Hedgecock et al. 1990](#)). In this mutant, the dorsal muscles send their arms ventrally across the lateral epidermis to locate the misplaced axons. [unc-104](#) mutants lack the neuron-specific kinesin-like protein. Although these mutants possess a relatively normal axon morphology, the motor [neurons](#) accumulate vesicles in the ventrally located cell bodies instead of transporting them dorsally into the axons ([Hall and Hedgecock 1991](#)). Muscle arms in [unc-104](#) mutants project to the vesicle-rich cell bodies instead of the axons. Both phenotypes suggest that a chemotropic molecule, perhaps stored in vesicles, is released by axons and guides the muscle arms to the motor [neurons](#). Alternatively, what we see in the adult mutant may be the result of promiscuous muscle arm projection to many targets during development and only the correct projection may persist, stabilized by adhesive interactions during neuromuscular formation. In either case, these mutants reveal that the muscle can respond flexibly to perturbations of the motor [neurons](#).

Axonal outgrowth in *C. elegans* does not depend on the target muscle. During embryogenesis, when the [ventral cord motor neurons](#) are extending axons, the muscles have already differentiated; i.e., the muscle cells are in place, the contractile apparatus is assembled, and the muscles are spontaneously contracting ([Durbin 1987](#); [Hresko et al. 1994](#)). However, in animals in which the muscle precursors have been killed, the DD motor neurons still extend processes into the dorsal cord ([Plunkett et al. 1996](#)).

The motor [neuron](#) may not be completely passive in the search for a synaptic partner. Reconstructions of adult worms demonstrate that motor [neuron](#) axons shift to the edge of the nerve cord to form neuromuscular junctions with the muscle arms ([White et al. 1976](#)). Although this displacement seems to be a very subtle migration on the part of the [neuron](#), it may reflect a latent ability of the motor [neuron](#) to actively seek a synaptic partner. When a motor neuron's normal target has been killed, the motor [neuron](#) can extend a process to an ectopic muscle ([Plunkett et al. 1996](#)). Thus, both the muscle and the motor [neuron](#) can respond to perturbations in a plastic manner to form a neuromuscular junction.

Moreover, the regionalization of junctions in *C. elegans* suggests that motor [neurons](#) may compete for synaptic targets. The regions of [body muscle](#) innervated by adjacent motor [neurons](#) of the same class do not overlap ([White et al. 1976](#)). The extent of the junctional domain is not limited by the length of the axon since the axon of any particular motor [neuron](#) extends across two adjacent domains of innervation. Such a distribution may be formed by competition between members of a class for targets.

The experiments described above indicate that bidirectional communication between muscle and [neuron](#) is important for neuromuscular junction formation in *C. elegans*. As stated above, the formation of synapses between the motor [neuron](#) and the muscle is activity-dependent in vertebrates. For example, when the acetylcholine agonist carbachol is added to vertebrate neuromuscular junctions, acetylcholine receptors are inappropriately activated, and synaptic sites are eliminated to compensate for the increase in muscle depolarization ([Bloch 1986](#)). Conversely, blocking neurotransmission with curare leads to an increase in synaptic sites ([Dahm and Landmesser 1991](#)). These experiments indicate that the muscle regulates its synaptic input in an activity-dependent manner. In contrast, synaptic density is not altered in *C. elegans* mutants that have altered muscle activation. For example, the lack of acetylcholine in [cha-1](#) mutants (J. Rand, pers. comm.) or GABA in [unc-25](#) mutants (E. Jorgensen et al., unpubl.) does not lead to an increase in the frequency of neuromuscular junctions. These mutants may up-regulate the activity of the motor [neurons](#) or the responsiveness of the muscles in other ways, but by ultrastructural criteria, there seems to be no increase in synaptic density. The number and position of synaptic sites must be controlled by other signals that may include cell surface receptors, components of the extracellular matrix, secreted growth factors or peptides, or signals that pass through gap junctions ([Cash and Poo 1995](#)).

## B. DD Rewiring

The most concrete example of synaptic plasticity occurs in the DD motor [neurons](#) of the [ventral nerve cord](#) during larval development. At the end of the L1 stage, additional body muscles and five additional classes of motor [neurons](#) are born. These [neurons](#) and muscles are incorporated into the existing motor circuit. During this time, the embryonic DD motor [neurons](#) change their synaptic partners ([Fig. 3](#)). During embryonic development, the GABAergic DD motor [neurons](#) innervate the ventral muscles and receive input from the DA and DB motor [neurons](#) on the dorsal side. At the end of the L1 stage, the DD motor [neurons](#) rewire their synaptic contacts so that they form neuromuscular junctions on the dorsal side ([White et al. 1978](#)). Synaptic input from the dorsal motor [neurons](#) is lost and new inputs from the VA and VB motor [neurons](#) are developed. During this period, a new class of GABAergic motor [neurons](#), the [VD neurons](#), form neuromuscular junctions to the ventral muscles and receive input from the dorsal motor [neurons](#). One possible mechanism for this rewiring is that the generation of the VD contacts causes the DD motor [neurons](#) to rewire. However, in [unc-55](#) mutants, the VDs inappropriately form synaptic outputs onto the dorsal muscles, and the DD motor [neurons](#) rewire even in the absence of VD contacts to the ventral muscles ([Walthall and Plunkett 1995](#)). The cholinergic VA and [VB neurons](#) form new synapses to the DDs during this period. It is possible that these new inputs induce the changes in the DDs. However, in [lin-6](#) mutants, none of the postembryonic motor [neurons](#) are born, including the VA and [VB](#).

[neurons](#), and again the DD motor [neurons](#) redirect their neuromuscular junctions to the dorsal muscles ([White et al. 1978](#)). As a consequence, the [DD neurons](#) in [lin-6](#) mutants form normal outputs but have no inputs. Because the remodeling of the [DD neurons](#) does not require the presence of these other [neurons](#), it is likely that the [DD neurons](#) are executing an intrinsic program initiated during the L1 to L2 transition.

## C. Remodeling of Dauer Larva Sensory Endings

A second developmental period during which synaptic remodeling occurs is during the formation of the dauer larvae. Dauer larvae behave in a manner obviously different from nondauer larvae (see [Riddle](#), this volume). One way in which they differ is in their chemotactic behavior. Although capable of movement, dauer larvae do not chemotax to food ([Albert and Riddle 1983](#)). Instead, sensation of food initiates recovery from the dauer stage. After resuming pharyngeal pumping, the dauer larva will then chemotax to food, which eventually results in the resumption of normal development. In addition, chemosensory responses change with the age of the dauer larvae. Dauer pheromone inhibits food-induced dauer recovery, but after 1 week spent in the dauer state, animals are much less sensitive to this inhibitory effect of dauer pheromone ([Golden and Riddle 1984b](#)). These changes in chemosensory responses may be caused by the remodeling of the sensory endings that occurs during dauer formation ([Albert and Riddle 1983](#)). In the amphid, the AWC and AFD cells elaborate larger sensory processes, whereas the ASG and ASI sensory endings are retracted somewhat in the amphidial pore. In addition, the inner labial sensory endings no longer protrude at the anterior tip of the nose. The amphidial [sensory neurons](#) are important for entry (ADF, ASG, ASI) and exit (ASJ) from the dauer stage ([Bargmann and Horvitz 1991b](#)). Why are the sensory endings remodeled in the dauer larvae? These modifications might be required for the altered chemotactic behavior of the dauer larva, or they may be specializations that allow recovery from the dauer stage. Finally, the modifications may simply protect the sensory endings from the harsh environmental conditions experienced for the duration of the dauer stage.

In addition to altered chemotaxis, dauer larvae exhibit other unique behaviors ([Cassada and Russell 1975](#)). They are sluggish and do not actively forage, but they will rapidly move away if prodded. They also will climb to the top of a vertical object such as a strand of fungus and wave their bodies in the air. In the soil, this behavior may be an attempt to become lodged on the body of a passing insect and thereby propagate dispersal. It is unlikely that the remodeling of the [sensory neurons](#) can be responsible for these changes in behavior. It is more likely that alterations of the connectivity in the central [nervous system](#) or changes in the humoral environment of the worm are responsible for these new locomotory responses. A reconstruction of dauer connectivity may yield insight into the circuits mediating these behavioral changes. Molecular genetic analysis of dauer behavioral mutants could be used to identify signaling molecules contributing to the behavioral change.

## D. Synaptic Plasticity in the Male

*C. elegans* males change their behavior when they mature from larvae into adults. L4 stage male larvae behave in a manner similar to hermaphrodites. For example, L4 males exhibit slow locomotion on food and avoid media preconditioned with hermaphrodites (E. Jorgensen, unpubl.). Adult males are more active than L4 males on food, particularly in the absence of hermaphrodites, and will chemotax to hermaphrodite-conditioned media. In the presence of hermaphrodites or media preconditioned with hermaphrodites, males spontaneously back and coil, presumably in search of a mate. Once contact with an adult hermaphrodite has been made, the male proceeds through a series of steps to locate the [vulva](#), insert the spicules, and transfer sperm ([Liu and Sternberg 1995; Emmons and Sternberg](#), this volume). These behaviors in male adults but not in hermaphrodites or male larvae are probably caused by the extensive modifications to the [nervous system](#) that take place during the L4 molt. There are 87 [neurons](#) found in the adult male that are not found in the hermaphrodite ([Sulston et al. 1980, 1988](#)). It is also possible that the connectivity of the [neurons](#) common to both sexes is remodeled in the male. Although a complete reconstruction of the [nervous system](#) in an adult male has not been yet been attempted, such a reconstruction would directly address this question. Mutational analyses of male mating behavior may identify molecules that are involved in remodeling the [male nervous system](#) between the L4 and adult stages.

The behavioral changes seen in the adult male also require remodeling of existing muscles. Specifically, one of the enteric muscles that controls expulsion in the larval stages is reshaped to play a part in copulation. In the L4 male, GABA release from [AVL](#) and [DVB](#) causes contraction of the enteric muscles, including the [anal](#) depressor and sphincter muscles (for a review of the defecation cycle, see [Avery and Thomas](#), this volume). The [anal](#) depressor in the L4 male is attached on one side to the dorsal hypoderm and on the other side to the roof of the [rectum](#). During the L4 molt, the [anal](#) depressor contractile apparatus detaches from the dorsal hypoderm and attaches to the dorsal spicule protractor (Sulston et al. 1980). As a consequence, [AVL](#) and [DVB](#) are required for eversion of the spicules in the adult (E. Jorgensen, unpubl.). [AVL](#) and [DVB](#) function is also involved in enteric muscle function in the adult. In the L4 male, GABA release from [AVL](#) and [DVB](#) contracts the [sphincter muscle](#), but in the adult male, GABA relaxes the [sphincter muscle](#) ([Reiner and Thomas 1995](#)). Thus, not only do the enteric muscles become reconfigured in the adult male, but there also must be alterations at the neuromuscular junctions that change the activity of the neurotransmitter.

## Figures

Figure 1. Neuromuscular junctions are added to axons during development.

### Figure 1

Neuromuscular junctions are added to axons during development. Green fluorescent protein (GFP; [Chalfie et al. 1994](#)) was fused to the *C. elegans* homolog of the synaptic vesicle protein synaptobrevin and expressed in the D-type motor [neurons](#) (a gift from M. Nonet and Y. Jin). This fluorescent construct appears to label clusters of synaptic vesicles at neuromuscular junctions. Note the increase in synaptic sites between the motor [neurons](#) [VD8](#) and [VD9](#) in the adult (B) compared to the L2 larvae (A). (Confocal photomicrograph by K. Knobel and E. Jorgensen.)

Figure 2. Muscle arms can locate misplaced motor neurons.

### Figure 2

Muscle arms can locate misplaced motor [neurons](#). (A) In wild-type animals, processes from the muscles, called muscle arms, extend to the motor neuron axons in the dorsal and ventral cords. Only the dorsal muscles are shown. (B) In [unc-6](#) mutants, the motor neuron axons do not extend to the dorsal cord, and the muscle arms extend to the misplaced axons on the ventral side ([Hedgecock et al. 1990](#)). (C) In [unc-104](#) mutants, axonal outgrowth is normal but vesicles are not transported along the axonal processes ([Hall and Hedgecock 1991](#)). Muscle arms extend ventrally and form synapses to the vesicle-rich motor neuron cell bodies.

Figure 3. Rewiring of the DD motor neurons during larval development.

### Figure 3

Rewiring of the DD motor [neurons](#) during larval development. In the L1 larva, the [DD neurons](#) receive input from the DA and DB motor [neurons](#) and innervate the ventral muscles. These neuromuscular junctions are eliminated, and the [DD neurons](#) innervate the dorsal muscles in the L2 larva ([White et al. 1978](#)). Several classes of motor [neurons](#) are added during this period (VA, VB, VC, VD, and [AS neurons](#)). The connectivity of a new class of GABAergic motor neurons, the VDs, resembles the DD connectivity in the L1 larva.

# Chapter 27. Neural Plasticity — III Behavioral Plasticity in the Adult

---

Instead of studying the morphology of the [nervous system](#), one can observe changes in the behavior of an animal. In fact, there are a number of ways that an organism can express behavioral plasticity without a morphological change. Neuromodulators can toggle between stereotyped behavioral states. For example, the egg-laying hormone of *Aplysia* elicits a complex behavioral program by exciting and inhibiting specific [neurons](#) throughout the [nervous system](#) ([Scheller et al. 1982](#)). Alternatively, the strengths of existing synapses can be altered as a result of experience. We present evidence of such complex behavioral changes in worms ranging from examples of neuromodulators to paradigms for learning and memory.

Neuromodulators can instantaneously alter the range of synapses that are active in any particular group of [neurons](#). The modulator can thereby bias a pattern generator toward one of several output patterns.

Neuromodulators can act globally as a circulating hormone or they can act on a specific cell via synaptic connections ([Dickinson 1989](#)). In invertebrates, aminergic neurotransmitters have been demonstrated to act humorally to control behavioral states. In the lobster, a high ratio of serotonin to octopamine initiates dominant and aggressive behavior, whereas a low ratio initiates submissive behavior ([Kravitz 1990](#)). Alternatively, the neurotransmitters can act locally via synaptic contacts to strengthen or weaken a second connection in a circuit. For example, serotonergic or FMRF-amidergic synapses from [sensory neurons](#) can, respectively, strengthen or weaken response of the sea slug *Aplysia* to mechanosensory stimuli ([Byrne 1987; Montarolo et al. 1988](#)). In the mollusk *Tritonia*, a central pattern generator produces rhythmic output to the motor [neurons](#) that control swimming during escape; serotonergic input dynamically modulates synaptic strengths in this circuit during ongoing behavior ([Katz et al. 1994](#)).

## A. Aminergic Neuromodulators

The best evidence for neuromodulators in *C. elegans* comes from studies of aminergic neurotransmission. The most common aminergic neurotransmitters in invertebrates are dopamine, serotonin, histamine, and octopamine. Although a number of behaviors are affected by raising or lowering levels of aminergic neurotransmitters in worms, it is not known whether these neuromodulators are acting humorally as neurohormones or as classical neurotransmitters at discrete synapses. However, in some cases, the actions appear so global that a humoral role seems likely.

Dopamine release might signal the presence of food to a well-fed nematode. Worms alter a number of behaviors upon exiting a lawn of bacteria. They become hyperactive, stop pharyngeal pumping, and do not activate the motor movements of the defecation cycle. Upon entering a bacterial lawn, wild-type worms slow, resume pumping, and resume motor movements of the defecation cycle. Some of these changes in behavior are probably mediated by dopamine transmission. Exogenous application of dopamine causes animals to become inactive, mimicking food abundance ([Schafer and Kenyon 1995](#)). Dopamine antagonists such as haloperidol cause animals to become hyperactive, mimicking food depletion. *cat-2(e1112)* mutants have low levels of dopamine ([Sulston et al. 1975](#)), and these animals are hyperactive in the presence of food in comparison to wild-type animals (B. Sawin, pers. comm.). However, they do not lack defecation cycles nor do they exhibit slow pharyngeal pumping, which are the other two behavioral changes that take place when a worm exits food. Laser killing of the dopamine [neurons](#) phenocopies the [cat-2](#) defect and thus confirms the role of the dopaminergic [nervous system](#) in the suppression of the hyperactive behavior (B. Sawin, pers. comm.). It is not clear whether this behavior is mediated indirectly by a humoral effect or by the direct release of dopamine from [sensory neurons](#) onto postsynaptic elements of [interneurons](#). However, the dopamine [neurons](#) lack neurosecretory ultrastructure, so the effects of dopamine may be mediated at synapses ([White et al. 1986](#)).

Serotonin may signal the presence of food to a hungry worm. Worms that have been removed from food for 30 minutes are very sensitive to the presence of food; upon entering a bacterial lawn, they stop swimming, initiate rapid pharyngeal pumping, begin laying eggs, and suppress the contraction of the enteric muscles when they reinitiate the defecation cycle (B. Sawin, pers. comm.; E. Jorgensen, unpubl.). Application of exogenous serotonin

can also induce these behaviors even in a well-fed worm. Bath application of serotonin stimulates pharyngeal pumping ([Croll 1975b](#); [Avery and Horvitz 1990](#)), induces egg laying ([Trent et al. 1983](#)), causes sluggish locomotion, and inhibits enteric muscle contractions ([Ségalat et al. 1995](#)). In addition, hungry worms have altered chemotactic behaviors, and these alterations are abolished by the application of serotonin (C. Bargmann, pers. comm.). [cat-4](#) mutants lack serotonin and dopamine ([Sulston et al. 1975](#); [Desai et al. 1988](#); [Weinshenker et al. 1995](#)) and are defective for several of the behaviors that can be induced by serotonin application. These mutants pump slowly ([Avery and Horvitz 1990](#)) and are hyperactive (J. Kaplan; B. Sawin; both pers. comm.). Although these mutants are not egg-laying-defective, mutations in [cat-4](#) can enhance egg-laying defects in other mutants ([Avery et al. 1993](#)). Finally, [cat-2](#) mutants that express serotonin but not dopamine still have enhanced sensitivity to food after starvation, suggesting that dopamine is not required for this behavior (B. Sawin, pers. comm.).

Serotonin probably acts humorally as well as synaptically to mediate behavior. It is most intensely expressed in two [pharyngeal motor neurons](#), the NSMs, which appear secretory by morphology ([Albertson and Thomson 1976](#); [Horvitz et al. 1982](#)). Killing the NSMs along with other serotonergic cells phenocopies at least some of the [cat-4](#) behavioral defects (B. Sawin, pers. comm.). Since NSM synapses are directed toward the [nerve ring](#) and do not directly synapse onto the cells that are likely to mediate these behaviors, the NSMs are probably acting at a distance. In other organisms, it is known that serotonin binds seven-pass transmembrane receptors that activate trimeric G-proteins. In *C. elegans*, serotonin acts via the  $G_o$  GTPase. The  $\alpha$ -subunit of  $G_o$  is encoded by the gene [goa-1](#) ([Lochrie et al. 1991](#)), and mutations in [goa-1](#) disrupt serotonin signaling in several behaviors, including locomotion and defecation ([Mendel et al. 1995](#); [Ségalat et al. 1995](#)). Together, these results suggest a model in which a starved worm has very low levels of circulating serotonin; as a consequence, the animal is hyperactive. When it enters the bacterial lawn, serotonin is released humorally, and this induces a number of appropriate behaviors, including active pumping, restricted movement, and egg laying.

Octopamine antagonizes the effects of serotonin in lobsters ([Kravitz 1990](#)), but its functions in *C. elegans* are relatively unexplored. Octopamine is found in *C. elegans*, but the cells expressing octopamine have not been identified ([Horvitz et al. 1982](#)). In contrast to serotonin application, octopamine causes loopy or kinked locomotion and depresses egg laying and pharyngeal pumping. Phenolamine, an octopamine antagonist in invertebrates, stimulates egg laying. Thus, serotonin and octopamine appear to act antagonistically in *C. elegans* as they appear to do in other invertebrates, but the basic cell biology of octopamine neurotransmission has not yet been investigated.

## B. Peptidergic Neuromodulators

Neuropeptides can act as hormones, neuromodulators, or neurotransmitters ([Krieger 1983](#)). Although there is circumstantial evidence that neuropeptides can act independently and at a distance to modify the activity of many [neurons](#), it is believed that most neuropeptides act in concert with a classical neurotransmitter to simply modify the output of the primary neurotransmitter on the postsynaptic cell ([Cooper et al. 1991](#)). This may make the study of neuropeptides by genetic methods rather difficult because mutants lacking a specific neuropeptide may have only subtle changes in behavior unrecognizable in the rather crude behavioral screens that are presently practical.

The actions of modulatory peptides are only beginning to be explored in nematodes. Studies so far have concentrated on a single family of peptides, the FMRFamide-like peptides (FLPs). When *C. elegans* is stained with an antibody that recognizes all members of this family, about 10% of the [neurons](#) express FMRFamide immunoreactivity, including motor [neurons](#) and [interneurons](#) ([Schinkmann and Li 1992](#)). Some of these peptides are likely to originate from the gene, [flp-1](#), that encodes multiple peptides ending with the amino acid sequence FLRF ([Rosoff et al. 1992](#); see [Rand and Nonet](#), this volume). One [neuron](#) class that expresses a FMRFamide-like peptide is the VC class of motor [neurons](#). The VCs synapse to the ventral body muscles and the vulval muscles. Because egg laying requires the contraction of the vulval muscles, the effect of FLRFamide on egg laying was tested. Application of FLRFamide alone caused no change in egg laying, but it was capable of potentiating the induction of egg laying by serotonin. A genetic analysis of these peptides has been complicated by the discovery of at least four genes that could encode FMRFamide-like peptides (C. Li, pers. comm.).

An analysis of the role of peptides in nematodes has been more extensively carried out in the parasitic nematode *Ascaris*. Because of its large size, *Ascaris* is more amenable to electrophysiological analyses, and despite the disparity in size, the *Ascaris* and *C. elegans* nervous systems are remarkably similar ([Stretton et al. 1985](#)). In *Ascaris*, a large number of neuropeptides have been characterized by immunoreactivity ([Stretton et al. 1991](#)), and 12 peptides related to FMRFamide have been purified (AF1–12). Bioactivity of some of these peptides has been tested. AF1 abolishes the spontaneous oscillations of the ventral cord inhibitory motor [neurons](#) by reducing the input resistance of the membrane ([Cowden et al. 1989](#)). AF2 causes rhythmic contractions of the [body muscle](#) ([Cowden and Stretton 1993](#)), and AF4 induces continuous contraction of the [body muscle](#) ([Cowden and Stretton 1995](#)). Despite the extreme differences in lifestyle, the parasitic *Ascaris* and the free-living *C. elegans* nervous systems are remarkably similar in cell number, morphology, and neurotransmitter type. However, in *C. elegans*, less than 10% of the [neurons](#) are immunoreactive for FMRFamide-like peptides; in *Ascaris*, more than 60% of the [neurons](#) express FMRFamide-like immunoreactivity ([Cowden et al. 1993](#)). The differences in peptide distribution between these two species might be mechanisms to generate very different behaviors in nematode species that share an evolutionarily rigid [nervous system](#) ([Stretton et al. 1991](#)).

## C. Sensory Adaptation

A simple form of behavioral plasticity as a result of experience is sensory adaptation. Sensory adaptation is the decrease or fatigue of sensory [neuron](#) response following prolonged exposure to sensory input. In most cases, the sensory response recovers after the stimulus has been removed. In *C. elegans*, responses to soluble compounds (taste) and responses to volatile compounds (olfaction) show a decrease following prolonged exposure ([Ward 1973](#); [Dusenbery 1980b](#); [Colbert and Bargmann 1995](#)). Similarly, worms raised at a specific temperature will avoid other temperatures, but after 2 hours, they no longer avoid these novel temperatures ([Hedgecock and Russell 1975](#)). Olfactory adaptation is selective, i.e., an animal will not move toward an adapted odorant, but it will still move toward a novel odorant, even when the two odorants are sensed by the same olfactory [neuron](#) (see [Bargmann and Mori](#), this volume). Mutational analysis has shown that the molecular mechanisms for adaptation differ for different odorants. [Colbert and Bargmann \(1995\)](#) characterized two mutants that show normal chemotactic responses to volatile compounds but fail to adapt to different subsets of odors mediated by the AWC [neurons](#): [adp-1](#) mutants fail to adapt to benzaldehyde and butanone but adapt to isoamyl alcohol, and [osm-9](#) mutants do not fully adapt to isoamyl alcohol or butanone but adapt normally to benzaldehyde.

## D. Learning and Memory

Another way that behavior can change as a result of experience is through learning. Traditionally, theorists have divided learning into two categories: nonassociative and associative. Nonassociative learning occurs when an individual is exposed to a single type of stimulus and behavior is changed as a result of that exposure. Examples of nonassociative learning include habituation and sensitization. Like sensory adaptation, habituation is a simple decrement in response to a repeated stimulus, but it can be distinguished from sensory adaptation by a number of features (see below). Sensitization is an increase in response to a wide variety of stimuli following a noxious stimulus. Associative learning occurs when animals learn to link a stimulus or behavior with a second temporally associated stimulus. Associative learning includes classical conditioning and operant conditioning. The most prominent example of classical conditioning is Pavlov's experiments with dogs in which the animal learns to associate the ringing of a bell with food. In operant conditioning, an animal learns to associate one of its own behaviors with a stimulus. For example, in B.F. Skinner's classic operant conditioning experiments, a rat learns to press a lever for a reward of food.

Whereas learning is a change in behavior as a result of experience, memory is the ability to store and recall those changes to behavior. Research on both vertebrates and invertebrates has suggested that there may be a number of phases of memory (ranging from two in *Aplysia* to three in rats and birds to four in flies; for review, see [DeZazzo and Tully 1995](#)). Memory can last in these various phases from as short as seconds as is found in short-term memory or as long as hours to a lifetime as is found in long-term memory. The cellular and molecular

mechanisms behind these phases of memory seem to be distinct. For example, long-term but not short-term memory can be disrupted by treatments such as electroconvulsive shock or inhibitors of protein synthesis ([Davis and Squire 1984](#)).

## 1. Habituation

Perhaps the simplest and most ubiquitous form of learning is habituation, which is a decrease in a response to a given stimulus after repeated trials. Observations of worms that bumped into glass beads ([Croll 1975a](#)) or that had been touched with a fine hair ([Chalfie et al. 1985](#)) demonstrated that the backing response declined with repeated mechanosensory stimulation. However, to distinguish this decrement in response from sensory adaptation or fatigue, a number of features of habituation must be observed ([Groves and Thompson 1970](#)). For example, habituation occurs more slowly with more intense stimuli or with longer interstimulus intervals. Habituation can be built up with repeated training sessions. Habituation, sensory adaptation, and fatigue all diminish gradually with time, but the rate of recovery from habituation depends on the interstimulus intervals of training. Finally, only habituation can be rapidly abolished with the application of a novel or noxious stimulus in a phenomenon known as dishabituation.

One simple stimulus that can be used to study habituation in *C. elegans* is a controlled tap to the side of the petri dish ([Rankin et al. 1990](#)). Such a tap causes an animal that is motionless or moving forward to move backward. As taps are repeated, the average distance a worm moves backward decreases. Following habituation training, an electrical stimulus delivered to the agar on either side of the worm causes dishabituation, i.e., the shock restores the normal response to tap.

In other organisms such as *Aplysia* ([Rankin and Carew 1987](#)) and rat ([Davis 1970](#)), the speed and degree of response decrement are dependent on the interstimulus interval. Similarly, worms rapidly habituate to stimuli delivered at 10-second intervals but slowly and less completely to stimuli delivered at 60-second intervals ([Fig. 4](#)) ([Rankin and Broster 1992](#)). Spontaneous recovery from habituation is also dependent on the interstimulus interval. Worms recover more rapidly from habituation induced by short interstimulus intervals than they do from long interstimulus intervals ([Rankin and Broster 1992](#)). These data indicate that the different intervals are recorded in the [nervous system](#) at least 1 hour after the delivery of the last stimulus and can continue to influence behavior differentially. They also suggest that habituation to short and long stimulus intervals may recruit different cellular mechanisms.

Work with other organisms (e.g., *Aplysia*; [Carew and Kandel 1973](#)) has shown that with repeated habituation training sessions, two things happen: (1) a build up of habituation over blocks of trials and (2) the possibility of the formation of long-term memory. A paradigm used to study long-term habituation in *Aplysia* was modified and applied to *C. elegans* ([Beck and Rankin 1995](#)). In this paradigm, worms were given three blocks of 20 stimuli each and stimuli within blocks were delivered every 60 seconds, with an hour rest between blocks. To determine whether the training produced long-term habituation, these same worms were given a block of 20 stimuli at 60-second intervals on the second day. The results showed that there was a build up of habituation over the course of the three training blocks on the first day. In addition, the worms were capable of long-term memory as demonstrated by retaining memory of habituation training for at least 24 hours. This long-term memory was disrupted by heat shock during the rest intervals ([Beck and Rankin 1995](#)). The current hypothesis is that heat shock disrupts cellular processes such as protein synthesis that are necessary for memory formation ([Davis and Squire 1984](#)).

Although habituation is a form of learning found in many organisms, surprisingly, little is known about the cellular processes underlying this form of learning. Studies in *Aplysia* ([Bailey and Chen 1983](#)) have suggested that there may be a decrease in the amount of neurotransmitter available for release in terminals that have undergone habituation training. Although studies in *C. elegans* have not yet progressed to the molecular level, *C. elegans* with its simple [nervous system](#) may offer new insights into the cellular mechanisms underlying habituation. Two interacting [neural](#) circuits are activated during response to head and tail touch ([Chalfie et al. 1985](#); see [Driscoll and Kaplan](#), this volume). Stimulation of the tail [touch receptors](#) activates the [interneurons](#) that direct the worm to move forward, and stimulation of the head [touch receptors](#) activate the [interneurons](#) that

direct the animal to move backward. In response to tap, these [neural](#) circuits are activated simultaneously and the behavior results from an integration of two competing outputs ([Wicks and Rankin 1995](#)).

Given that the observed response to tap in intact animals is actually an integration of two competing responses, what is the response of each of the competing circuits alone to habituation training? The two circuits do not produce the same pattern of behavioral outputs in response to habituation training ([Wicks and Rankin 1996](#)). When the posterior touch [neurons](#) (PLM) are killed, the circuit that moves the animal backward can be viewed in isolation. In the operated animals, the reversals habituate more slowly and less completely than they do in the wild-type worms. Ablation of the anterior touch [neurons ALM](#) and [AVM](#) produce animals that respond to tap by accelerating forward. When such ablated animals are given habituation training, a different pattern of response was observed. With short interstimulus intervals (10 seconds), accelerations first increase in magnitude (sensitization) before habituating. With long interstimulus intervals (60 seconds), there is no evidence of sensitization. Again, the data suggest that habituation in unoperated animals is the result of a balance of two competing behaviors: reversals and accelerations. For example, with short interstimulus intervals, animals rapidly habituate within the first few stimuli. This rapid habituation may reflect the increased input of the sensitized accelerations that decrease the magnitude of the reversals. As habituation continues, reversals become infrequent and the animals often accelerate forward in response to tap. Presumably, the rapid habituation of reversals and the slower habituation of accelerations are integrated as a net movement forward. These results suggest that there might not be a single mechanism underlying habituation, nor might [all cells](#) involved in a behavior respond in the same way to repeated stimulation. Instead, each cell type may have a unique response to repeated stimulation, and the behavior that is observed is the integrated output of all of the cell types.

In the future, genetic analyses of the mechanisms involved in the long- and short-term memory phases of habituation should lead to additional insights into the similarities and differences between memory processes in this simple [nervous system](#) and in more complex organisms such as *Drosophila*, *Aplysia*, and mammals.

## 2. Sensitization

A second form of nonassociative learning is sensitization ([Groves and Thompson 1970](#)), which refers to the increase in reflexive responses due to the application of a noxious stimulus. Sensitization is not a form of associative learning because the stimulus is not specifically paired with another stimulus. The stimulus merely raises the arousal level of the animal so that all reflex pathways are facilitated. Sensitization in *C. elegans* has been demonstrated in several ways, but it has not been investigated to the same extent as habituation. Sensitization was first shown by presenting worms with a single tap, then a stronger stimulus, in the form of trains of taps, and then looking at the response to a single tap again ([Rankin et al. 1990](#)). Worms showed larger responses to the single tap following the train of taps than they did to the initial single tap.

## 3. Associative Learning

In the simple nonassociative forms of learning, an animal alters its behavior to a single stimulus; in contrast, in associative learning, an animal learns to use a previously neutral stimulus to predict the presence or absence of a second more significant stimulus. *C. elegans* is capable of this more advanced form of learning as demonstrated by several different paradigms. Examples of associative learning by *C. elegans* come from classical conditioning paradigms in response to chemosensory stimuli (J.Y.M. Wen et al., in prep.). In this discriminative classical conditioning assay, one ion is associated with food and a second ion is associated with the absence of food; the conditioned animals will then selectively migrate to the ion paired with food. First, adult hermaphrodites are deprived of food for 5 hours, and then an ion, either sodium or chloride, is presented to the animals with bacteria for the first hour and the other ion is presented without bacteria for a second hour. In the test phase, the animals are then given a choice between diffusive gradients of sodium and chloride for 1.5 hours. The results show that conditioned animals display significant preference for the ion paired with food and that the preference lasts up to 7 hours after training ([Fig. 5](#)). Switching the order of the conditioning stimuli did not affect the results. Presentation of the ion paired with no food before presentation of the ion paired with food resulted in identical degrees of learning.

Learning can be assayed in individual animals as well. In this paradigm, worms are conditioned in liquid medium in test tubes containing solutions of the ions and *Escherichia coli*. To test for learning, individuals are placed on test plates with a gradient of each of the ions, and the initial heading of the worm is assayed. Conditioned animals show initial headings similar to their final accumulation; thus, learning can be assayed within 30 seconds, rather than waiting the 1.5 hours required in the chemotaxis assay.

*C. elegans* can also learn aversive associations. In this type of experiment, an ion, such as sodium or chloride, is paired with a noxious stimulus, and thereafter the worms avoid the conditioned ion. For example, adult hermaphrodites can first be conditioned with an ion associated with an aversive stimulus such as garlic. Subsequently, when tested in a chemotaxis assay, these animals avoided the ion that had been paired with garlic ([Fig. 5C](#)). Aversive learning can also be tested in individuals as well as in populations. In this kind of experiment, worms are exposed to an attractive ion and the aversive stimulus, for example, copper ion. To test for learned aversion, conditioned worms are placed on a spot containing the paired or unpaired ion in the absence of copper, and the time required for the animal to leave the spot is measured.

The eventual goal is to employ genetic techniques in *C. elegans* to identify molecules essential for learning and memory. Having established that *C. elegans* shows discriminative classical conditioning in a variety of paradigms, van der Kooy and colleagues screened for mutants defective in associative learning (J.Y.M. Wen et al., in prep.). They isolated two lines of ethylmethanesulfonate (EMS)-induced learning-deficient mutants that show normal chemosensory responses but no evidence for classical conditioning in any of the discriminative classical conditioning paradigms. These mutations define two loci, [\*lrn-1\*](#) and [\*lrn-2\*](#) ([learn](#)).

Another possible case of associative learning is a phenomenon first described by [Hedgecock and Russell \(1975\)](#), who demonstrated not only that *C. elegans* could detect thermal gradients and selectively migrate along an isothermic contour, but also that such thermotaxis could be modified by experience. The temperature at which the animals were raised and fed determines the temperature to which they migrate. A brief starvation of 2 hours induces strong dispersion from the starvation temperature; a 4-hour period of starvation decreases these responses ([Hedgecock and Russell 1975](#); [Mori and Ohshima 1995](#)). Although it is possible that dispersion from the starvation temperature involves a learned association between a specific temperature and a lack of food, new data indicate that starvation may simply suppress thermotaxis (see [Bargmann and Mori](#), this volume).

## Figures



## Figure 4

Habituation in *C. elegans*. (A) Habituation of backing to trains of taps for 30 stimuli delivered at a 10-sec interstimulus interval (ISI). (B) Habituation of backing to trains of taps for 30 stimuli delivered at a 60-sec interstimulus interval. The shorter interstimulus interval (10 sec) produces greater and more rapid decrement than the longer interstimulus interval (60 sec). Habituation is expressed as the mean percent of the initial backing response (INIT). Bars indicate the standard error of the mean. (Modified, with permission, from [Rankin and Broster 1992](#); copyright by the American Psychological Association.)



## Figure 5

Classical conditioning in the *C. elegans* wild type and in [\*lrn-1\*](#) and [\*lrn-2\*](#) mutants. (A) Both wild-type and mutant lines show the same response levels in an unconditioned (without training) discrimination test. (B) In appetitive conditioning, one ion is paired with *E. coli* (CS+) and the other ion without *E. coli* (CS-). Wild-type animals show conditioning by preferring the CS+; neither mutant strain shows a preference for the CS+. (C) In aversive conditioning, the CS+ ion is paired with garlic extract. Wild-type worms show conditioning by preferring the CS- ion; neither mutant strain avoids the CS+ ion. Bars indicate the standard error of the mean. (Modified from J.Y.M. Wen et al., in prep.)

Generated from local HTML

## Chapter 27. Neural Plasticity — IV Conclusions

---

For such a simple organism, *C. elegans* shows a great deal of behavioral plasticity. The conclusion that one must draw is that behavioral plasticity is an important component in the everyday life of a worm. Once well-defined learning paradigms become established in *C. elegans*, genetic analysis in this organism may resolve several long-standing issues in our studies of learning and memory. First, what are the molecules that mediate [neural](#) plasticity? Genetic analysis of associative learning, combined with studies of the proteins involved in neurotransmission (see [Rand and Nonet](#), this volume), will identify the molecular substrates of synaptic strengthening and weakening. Second, does long-term potentiation (LTP) equal learning? A long-standing debate in the field of learning and memory has been whether the mechanisms that underlie cellular models of learning such as LTP reflect the mechanisms used in the formation of memory as measured in behavioral assays. Genetic analysis can circumvent this dispute because the initial criteria for selecting a mutant will be a demonstrable defect in a learning task. Third, is plasticity in the adult related to plasticity in the embryo? Genetic studies may reveal that the mechanisms that establish connectivity in the embryo are the same as those that modify behavior in the adult.

Studies in *C. elegans* may eventually link the different levels at which plasticity is measured, so that we will have a mechanistic understanding of changes in behavior. Such experiments will demonstrate how changes in the behavior of an animal are caused by physiological or morphological changes in a [neural](#) circuit. In turn, the changes in the [neural](#) circuit can then be correlated with the activity of molecules in individual cells.

Generated from local HTML

## **Chapter 27. Neural Plasticity — Acknowledgments**

---

The authors are grateful to the numerous *C. elegans* workers who provided unpublished data. We thank Mike Nonet and Yishi Jin for the VAMP-GFP construct, Karla Knobel for the photographs in Figure 1, and Karen Yook for carefully reading the manuscript.

Generated from local HTML

# **Chapter 28. Environmental Factors and Gene Activities That Influence Life Span**

---

## **Contents**

[I The Study of Life Span](#)

[II Theories of Aging](#)

[III Aging in \*C. elegans\*](#)

[IV The Search for Genes that Control the Rate of Aging](#)

[V Prospects](#)

[Acknowledgments](#)

Generated from local HTML

## Chapter 28. Environmental Factors and Gene Activities That Influence Life Span — I The Study of Life Span

---

How the rate of aging is determined is unknown. It is often assumed that aging is the result of an inevitable process of decay and degeneration. However, there are reasons to believe that the aging process is actively regulated. For example, [germ cells](#) and transformed cells do not age, which indicates that aging is not a necessary feature of eukaryotic cells. In addition, the rate of aging is strikingly different in different species; e.g., the life spans of mice, canaries, and bats (all small warm-blooded animals) are 2, 13, and 30 years or more, respectively (for an extensive review of the phylogenetic variation of aging rates, see [Finch 1990](#)). In addition, control of the rate of aging by the endocrine system has been implicated in many different types of organisms; e.g., marsupial mice and certain species of salmon and insects undergo a rapid process of senescence following reproduction, and the endocrine system has been shown to delay senescence in the queen bee. Life span can also be extended in many species that enter a state of diapause or dormancy under unfavorable environmental conditions, an extreme example of which is the *Caenorhabditis elegans* dauer larva. The rate of aging in vertebrates and many other animals can also be altered in response to food availability.

Together, these observations suggest that the rate of aging is actively regulated. As with other biological processes, it may be possible to dissect the aging process using genetics, and in fact, a number of intriguing aging mutants have been isolated in several species (for review, see [Jazwinski 1996](#)). The most striking of these mutants have been isolated in *C. elegans* and are discussed in this chapter.

Like other organisms, *C. elegans* goes through a visible aging process. This is not widely appreciated because in exponentially growing cultures, old individuals comprise a vanishingly small proportion of the population. Young adults move, pump, and defecate actively, whereas older adults move, pump, and defecate more slowly ([Bolanowski et al. 1981](#); [Kenyon et al. 1993](#); [Duhon and Johnson 1995](#)). As in other organisms, the levels of lysosomal hydrolases and lipofuscin-like granules increase as *C. elegans* ages ([Klass 1977](#); [Bolanowski et al. 1983](#)). Old worms actually look “old,” even to the untrained observer. During the final stages of life, they become pale, lose turgor pressure, and appear flaccid and decrepit (see [Johnson et al. 1984](#)). A day or two before they die, they stop moving altogether. Initially, they move if prodded, but at the final stages, only the nose wiggles feebly. When examined using Nomarski optics, the individual cells and nuclei of old worms appear indistinct and mottled and often contain vacuole-like holes and inclusion bodies. The entire process of development and senescence is completed in a very short time: just over 2 weeks.

Major breakthroughs in this important field will likely be made with *C. elegans* for two reasons. First, it has a very short life span, so is experimentally tractable for genetic studies of aging. Second, since conserved molecular mechanisms govern other aspects of its cell and developmental biology, the findings stand a good chance of being universally applicable.

This chapter is divided into three sections. In the first section, popular theories of aging are discussed. Although it is possible (perhaps even likely) that none of these theories are correct, they are presented here because they have influenced the study of *C. elegans* aging and have prompted many of the experiments carried out on the life-span mutants. In the next sections, the life-span mutants of *C. elegans* are described, along with attempts to determine whether the properties of these mutants support or contradict the different aging theories.

# Chapter 28. Environmental Factors and Gene Activities That Influence Life Span — II Theories of Aging

---

How does one study the aging process? (For a comprehensive review, see [Finch 1990](#).) Unlike most biological processes, the endpoint of the aging process is degenerative in nature, which has suggested that the rate of aging is set by something that damages cells rather than something more elegant, such as the cell cycle machinery. Therefore, researchers have long been tabulating physiological and structural differences between old and young cells and postulating that one or more of these differences is actually the cause of aging. The problem with this approach is that any of the correlates of aging could be a downstream process by which a central regulatory mechanism, perhaps a more elegant mechanism, brings about cell senescence. Specific hypotheses are collectively termed the "theories of aging" (for specific references, see [Finch 1990](#)). Leading theories are discussed below.

## A. Oxidative Damage

One theory posits that aging is caused by oxidative damage. Since different species have different life spans, this model implies that long-lived organisms are relatively more resistant to oxidative damage; e.g., they may have more effective ways of scavenging reactive oxygen species. Although this model is popular, there is no direct evidence that aging is caused by oxidative damage. One experiment that appeared to support this theory ([Orr and Sohal 1994](#); a report that overexpression of superoxide dismutase and catalase in *Drosophila* extends life span) is now in doubt (see [Tower 1996](#)).

## B. Telomere Shortening

The telomeres of cultured mammalian cells undergoing senescence become shorter with consecutive cell divisions. This has suggested the possibility that telomere shortening causes aging, for example, by perturbing the expression states of genes located near the ends of chromosomes ([Harley et al. 1990](#); [Allsopp et al. 1992](#)). Although telomere shortening may play a part in limiting the life span of cells that continue to divide, it seems unlikely to contribute to the aging process that occurs in cells that are postmitotic. The aging process is not limited to dividing cells. For example, in humans, neither muscle cells nor central [nervous system neurons](#) divide during adulthood, yet both exhibit progressive morphological signs of age during senescence. Likewise, in *C. elegans*, senescence occurs without cell division, since the [somatic cells](#) of adults are postmitotic. Only when it is possible to inhibit telomere shortening in dividing cells will it be possible to learn whether telomere shortening is responsible for cell senescence or whether it is simply another correlate of aging.

## C. Progeny Production

Evolutionary theory posits that the rate of aging is set indirectly as a consequence of selection for reproductive success. Under conditions in which resources are limited, these resources are invested in producing progeny, rather than in maintaining the survival of older, reproductively less fit, individuals. (If resources were not limiting, it might be possible for a species to evolve high levels of fecundity as well as a long life span.) This model is supported by the observation that some species, such as certain salmon, are programmed to undergo rapid senescence following reproduction. Some theorists also make a related but distinct assumption that there is likely to be a trade-off between fecundity and life span within a single individual; i.e., if its energy is expended on production of progeny, it will not be available for longevity. If the trade-off theory is true, one might expect a decrease in progeny production to cause increased longevity. Implicit in this hypothesis is the idea that an individual has a fixed amount of energy to use during its life span. In this way, it is like a battery-powered alarm clock, which runs longer if the alarm is turned off. However, living organisms are more like electric than battery-run alarm clocks if food is not limiting. Thus, the necessity for a trade-off within a single individual is not clear.

## D. Metabolic Rate

Another theory of aging states that the length of life span is controlled by the rate of metabolism. The faster a species burns calories, the more rapidly it ages. In fact, there is a correlation between metabolic rate and life span in certain groups of animals, such as birds and mammals (excluding primates). However, the many striking exceptions to this rule argue strongly that metabolic rate cannot be the sole determinant of the rate of senescence. Likewise, long-lived mutants exist in *C. elegans* that do not have lowered metabolic rates ([Vanfleteren and DeVreese 1995, 1996](#)), as described below.

## E. Regulation by an Aging Program

Unlike the theories described above, which are stochastic in nature, an alternative theory is that the aging process is programmed in some way. This theory suggests that life span is determined by a timing mechanism that controls and coordinates the rates of aging between different tissues in an organism. In principle, such a mechanism could also link the process of aging to other age-related events, such as puberty and menopause. This rate-setting mechanism would be influenced by environmental conditions and by gene activities that influence specific age-related processes (e.g., balding in humans). This model is attractive because it can explain the remarkably similar qualities shared by young, middle-aged, and old animals of many species with very different life spans. It can also account for the rapid, hormonally controlled onset of aging that occurs after reproduction in certain species of salmon and in marsupial mice (for review, see [Russell 1987](#)) and for the coordinated acceleration of many age-dependent phenotypes associated with aging in humans afflicted with the accelerated-aging progeria syndromes. Finally, it can explain how mutations in single genes, described below, can profoundly affect the rate of aging of an entire organism.

If there is an aging program, then there must be a regulatory mechanism that can control the rate at which the timing mechanism runs the aging process (see [Kenyon 1996](#)). It is necessary to postulate this in order to explain the striking differences in life spans of different species and in aging mutants. Note that there may be a fine line between this theory and some of the other aging theories; e.g., the master regulator could be an enzyme that repairs oxidative damage at a fixed, species-specific rate. Alternatively, there could be a distinct molecular timer that is molecularly unlike anything known to be degenerative in nature, which, in turn, would bring about senescence. An example of such a timer is the *lin-14* antisense RNA timer that patterns stage-specific lineage patterns in *C. elegans* ([Lee et al. 1993](#); [Wightman et al. 1993](#)). The notion that there is a mechanism that regulates aging can be reconciled with the views of evolutionary theorists (who argue that there can be no direct selection and thus no “molecular program” for longevity) if it is assumed that, directly or indirectly, selective forces (or even unselected chance mutations) can influence the rate of action of a universal mechanism that brings about senescence.

## F. Caloric Intake

Environment can influence life span in many ways, for example, by improving the health of an individual or, conversely, by causing illness. However, one environmental influence, food, has a well-documented and very interesting effect on the rate of aging. Vertebrates such as rats can live up to 60% longer than normal if they are fed a diet low in calories. This is remarkable, since these “calorically restricted” individuals are robust and healthy and have normal rates of metabolism. Calorically restricted animals do not produce progeny. However, once food is restored, they become fertile, even if they have reached an age at which well-fed rats would be postreproductive. In principle, caloric restriction could act to reset a normal control mechanism that governs the rate of aging. If an aging timer runs at different rates in different species, perhaps it can be reset within a single individual. Alternatively, caloric restriction could induce a type of aging process (or anti-aging process) that is fundamentally different from normal aging.

# Chapter 28. Environmental Factors and Gene Activities That Influence Life Span — III Aging in *C. elegans*

---

## A. Life Spans of Well-fed Adults

What is the life span of *C. elegans*? Even in highly inbred, presumably homozygous strains of *C. elegans*, not all individuals die at the same time; therefore, mean life span is determined by examining populations of animals. In a survey of wild strains of *C. elegans*, [Johnson and Hutchinson \(1993\)](#) found that hermaphrodites of the strains they examined had similar life spans. However, in some strains, males had shorter life spans than hermaphrodites, whereas in other strains, males had longer life spans. More recently, D. Gems and D.L. Riddle (pers. comm.) have shown that different isolates of the N2 strain of *C. elegans* have significantly different life spans, ranging from 12 to 18 days at 20°C. It is not clear whether strain-specific differences in life spans are due to changes in a single gene or in multiple genes. Whatever the case, because the life span of *C. elegans* is somewhat strain-specific, it is important to compare the life spans of candidate mutants with those of their direct parents. In addition, in cases where mutations isolated a relatively long time ago are found to have life spans that differ from that of N2, it is safest to isolate new alleles and compare their life spans with those of the direct parental line, or at least to show that the life-span phenotype is linked genetically to the allele in question.

Unfortunately, even when a single strain is analyzed and all known variables are held constant, some degree of variability can still exist between the life-span curves observed in different experiments. This means that in all life span studies, controls must be carried out in parallel, and apparent differences between strains must be tested for reproducibility.

## B. Environmental Influences

### 1. Temperature

The life span of *C. elegans* is influenced by temperature. For example, [Klass \(1977\)](#) found that the mean life span of *C. elegans* cultured in liquid media was 23 days at 16°C, but 9 days at 25°C. One might assume that the different rates of growth at different temperatures are a direct consequence of the intrinsic thermodynamic properties of chemical reaction rates. However, [Wong et al. \(1995\)](#) found that mutants defective in *clk* (*clock*) genes are unable to adjust their rate of growth to changes in temperature. Wild-type animals actively decrease or increase their rate of development in response to temperature changes. In contrast, *clk* mutants cultured to the two-cell stage at 15°C or 25°C and then shifted to 20°C were unable to either increase or decrease their rate of development effectively. Thus, the *clk* genes are required to reset the rate of development in response to changes in temperature. This is a provocative finding, and it will be interesting to learn its molecular basis. These mutants also have altered life spans, as discussed below.

### 2. Food

#### a. Larval Arrest

If L1 larvae hatch in the absence of food, their growth is arrested. When they resume feeding, they grow normally to adulthood, and their subsequent adult life span is the same as that of a worm that hatches in the presence of food ([Johnson et al. 1984](#)).

#### b. Dauer Formation

*C. elegans* has a discrete response to food limitation early in life: It enters an alternative developmental stage, the dauer. Unlike the normal feeding state, the dauer can live for many months. Dauers are an alternative L3 state and are discussed in detail by [Riddle](#) (this volume). Dauer formation is potentiated by food limitation and high temperature. The dauer state is induced by a constitutively produced dauer pheromone, whose concentration

increases as the animals crowd together around the remaining food. The dauer state can be induced only in L1 and early L2 larvae. The dauer differs from the adult in many ways. Its growth is arrested, and it contains intestinal granules that are thought to store food (dauers appear dark for this reason). It is encased by a dauer-specific cuticle that is relatively resistant to dehydration. Dauers have reduced metabolic rates ([O'Riordan and Burnell 1989, 1990](#)), elevated levels of superoxide dismutase, and are relatively resistant to oxidative stress ([Anderson 1982; Larsen 1993; Vanfleteren 1993](#)). They also have elevated levels of several heat shock proteins ([Dalley and Golomb 1992; R. Shmookler Reis, pers. comm.](#)). Animals that exit from the dauer state resume growth and have subsequent life spans that are similar to those of animals that have not arrested at the dauer stage ([Klass and Hirsh 1976](#)).

It is not known what metabolic or physiological changes contribute to the longevity of the dauer. The finding that several dauer-constitutive mutations can increase the life spans of fertile adults (see below) raises the possibility that dauers do not live longer simply because their growth is arrested, but rather because they express an active longevity program of some sort.

### c. Caloric Restriction

As discussed above, the life spans of healthy vertebrates can be extended dramatically by caloric restriction. Likewise, [Klass \(1977\)](#) reported that the life span of *C. elegans* can be extended by about 50% by growth in liquid cultures with a relatively low concentrations of bacteria.

## 3. Reproduction

The most straightforward way of determining whether progeny production influences life span is to sterilize animals and measure their life spans. This has been done in several ways. First, the life spans of worms unable to make sperm have been examined and found to be similar to those of wild type. These include [fer-15](#) mutants, which produce defective sperm ([Klass 1983; Friedman and Johnson 1988a](#)), and [fem](#) mutants, which produce oocytes instead of sperm ([Kenyon et al. 1993](#)). In addition, life span is not affected by ablation of the gonad and [germ cells](#) ([Kenyon et al. 1993](#)). Therefore, in *C. elegans*, the production of progeny per se does not affect life span.

One sterile mutant, [spe-26](#), has been reported to have an extended life span ([Van Voorhies 1992](#)); however, in this case, the effect on life span is probably unrelated to the sperm defect, since the magnitude of the life-span extension in these mutants is not correlated with the degree of sterility in different [spe-26](#) alleles (S. Ward, pers. comm.).

Does the act of mating itself affect life span? It appears that it does but it is not clear how. [Van Voorhies \(1992\)](#) found that mating decreased the life span of males. In fact, male life span appears to be shortened by mating, or attempted mating, with either males or hermaphrodites. When males are grown singly, their life spans are increased, an effect not seen with hermaphrodites (D. Gems and D.L. Riddle, pers. comm.). In the case of hermaphrodites, [Van Voorhies \(1992\)](#) found that mating did not affect the life span. However, in a subsequent, more extensive study, mating with males was found to reduce hermaphrodite life span by up to one half ([Gems and Riddle 1996](#)). The act of copulation itself seems to decrease life span, because sterile males that attempt to copulate also accelerate the death of hermaphrodites.

## 4. Oxygen Levels

Changes in oxygen concentration perturb the life span of *C. elegans* ([Honda et al. 1993](#)). When animals are cultured in a high concentration of oxygen, their life spans are shortened, and when they are cultured in a low concentration of oxygen, their life spans are lengthened. Furthermore, a strain with reduced levels of superoxide dismutase was more sensitive to the effects of oxygen. These findings suggest that oxidative damage can accelerate the aging process in *C. elegans* and argue that in nature, oxygen levels have a role in setting the normal life span.

## 5. DNA Damage

[Hartman et al. \(1988\)](#) questioned whether the effectiveness of DNA repair systems might determine the life expectancy of *C. elegans*. To address this issue, they asked whether there was a correlation between life span and sensitivity to three different DNA-damaging agents in recombinant inbred strains (described below) whose mean life spans range from 13 to 30 days. They found that there was no such correlation. This finding argues that the efficacy of DNA repair is not a limiting factor in determining the life span of wild-type *C. elegans*.

## 6. Relationship between Programmed Cell Death and Senescence

Mutations in *ced* genes, which alter programmed cell death, do not affect life span (R. Horvitz, pers. comm.). It thus seems likely that the regulation of programmed cell death (apoptosis) is fundamentally different from the process of organismal senescence and aging.

Generated from local HTML

# **Chapter 28. Environmental Factors and Gene Activities That Influence Life Span — IV The Search for Genes that Control the Rate of Aging**

---

Aging in *C. elegans* does not have to be studied only by testing specific theories. Instead, one can look for mutants and follow where they lead. The remainder of this review describes the search for genes that affect the rate of aging.

## **A. Identification of Genetic Polymorphisms Affecting Aging**

One way to identify genes affecting life span is to look for preexisting mutations affecting life span that are present in natural populations. These can be identified by crossing different wild strains and then inbreeding their progeny in hopes of establishing lines homozygous for new combinations of alleles. [Johnson and Wood \(1982\)](#) crossed the *C. elegans* strains *Bristol* and *Bergerac* and established presumably homozygous recombinant-inbred (RI) lines, each of which descended from a different F<sub>2</sub> animal following 18 rounds of self-fertilization. Whereas their starting strains both had life spans of approximately 18 days, the inbred lines had life spans ranging from 10 to 30 days. These findings indicate that there are genes affecting life expectancy that are polymorphic in natural populations. An important consideration is whether the RI lines still undergo normal senescence. One way to address this concern is to ask whether the probability of death increases exponentially with age, which is the case in normal wild populations of many different species ([Johnson 1987](#)). These RI lines do show an exponential increase in mortality rate with age with the slopes varying between strains with different mean life spans. In addition, their degree of motor activity is also correlated with their relative stage in the life cycle. These findings are consistent with the idea that the RI lines are aging in a normal way. The alleles segregating in these populations did not coordinately affect the rate of growth to adulthood, indicating that the processes of development and senescence can vary independently of one another ([Johnson 1987](#)). Fertility and life span segregated independently as well, arguing against an evolutionary trade-off between these two features ([Shook et al. 1996](#)). The life-span polymorphisms segregating within these lines ([Shook et al. 1996](#)) and similar independently isolated RI lines ([Ebert et al. 1993](#)) have been mapped to a total of five broadly defined genetic regions. It will be interesting to learn what gene products are responsible for these effects on life span.

A major limitation of the approach of looking for life-span genes by crossing wild populations is that one can only identify genes that are already polymorphic in natural populations. It is possible that important regulatory genes will be missed because they do not happen to differ between these strains. For this reason, it seems wise to isolate mutants.

## **B. Early History of *C. elegans* Life-span Mutants**

The early history of life-span genetics in *C. elegans* illustrates how theories of aging can influence the interpretation of life-span mutants (for another example, see [Partridge and Harvey 1993](#)). The first collection of life-span mutants was assembled in a screen of 8000 F<sub>2</sub> clones from a single pool of descendants of 200 mutagenized L3 animals ([Klass 1983](#)). A temperature-sensitive sperm-defective *fer-15* mutation was included to control progeny production. Individual lines were established from the F<sub>2</sub> progeny of mutagenized hermaphrodites at the permissive temperature, and pools of animals from each clone were shifted to the nonpermissive temperature and allowed to age. In this screen, Klass found eight clones whose life span had been extended. The mutants were not outcrossed, and like many newly isolated mutants, they appeared to be unhealthy. Klass found that the mutants had lower rates of food ingestion than wild type. He had observed that caloric restriction increases *C. elegans* life span and concluded that "the results of our screening procedure argue that [specific aging genes] are rare...It is most probable that none of the mutants with increased life spans bear mutations in specific aging genes. Rather, life span may simply be increased because of the reduction in food uptake... ."

Several years later, Johnson (1986; [Friedman and Johnson 1988a,b](#)) found that the unhealthy appearance of one mutant, which he called *age-1*, disappeared when the strain was outcrossed. The outcrossed mutant did not have reduced levels of food uptake, but still lived longer. However, Johnson noted that the mutant, which still carried the closely linked *fer-15* mutation, had decreased fertility relative to control animals ([Friedman and Johnson 1988a](#)). Johnson concluded that the mutant animals lived longer because they failed to produce progeny, stating that "It is likely that the action of *age-1* in lengthening life results not from eliminating a programmed aging function but rather from reduced hermaphrodite self-fertility or from some unknown metabolic or physiologic alteration. The *age-1* gene should not be interpreted as an example of a genetic locus whose primary function is to keep time so as to cause programmed aging or senescence. Indeed, such genes are unlikely to exist in iteroparous organisms because of a lack of selective pressure for the evolution of such loci." The *fer-15* fertility mutation was later crossed away, and the resulting healthy and fully fertile *age-1* mutants still had their extended life spans. The *age-1* gene is now known to regulate dauer formation as well as life span ([Malone et al. 1996](#); [Morris et al. 1996](#)). Time will tell to what extent our new interpretations of *age-1* (described below) are still biased by the powerful theories of aging.

Although it is not clear how many genomes were represented in Klass' screen, the number is probably small, since the 200 mutagenized animals were reproductively immature. Furthermore, three *age-1* mutants all contained an additional *unc-31* allele ([Friedman and Johnson 1988b](#)), suggesting that they were siblings. Thus, this relatively unbiased screen for life-span mutants was clearly far from saturation. Thus far, *age-1* is the only *C. elegans* gene identified by its life-span Age phenotype ([Klass 1983](#); also see [Duhon et al. 1996](#)).

## C. Life-span Mutations and Dauer Formation

### 1. Overview

As described by [Riddle](#) (this volume), dauer larvae are developmentally arrested, sexually immature, resistant to starvation and desiccation, and long-lived. Dauer formation is normally induced when the animals reach high population density during periods of food limitation. When food is restored, dauers resume growth and become adults that have normal 2–3-week life spans ([Klass and Hirsh 1976](#)). Mutations in two genes that regulate dauer formation ([Riddle et al. 1981](#)) can also increase the life spans of active, fertile adults. These genes are *daf-2* ([Kenyon et al. 1993](#)) and *daf-23* ([Larsen et al. 1995](#)). The most severe mutations at either locus produce nonconditional dauer larvae constitutively ([Gottlieb and Ruvkun 1994](#); [Riddle 1988](#)). In addition, reduction of function of *daf-2* or *daf-23* gene activities can produce a dramatic extension of life span. The *daf-2* (e1370) mutation is a temperature-sensitive dauer-constitutive mutation. However, when these animals are cultured at the permissive temperature or shifted to the nonpermissive temperature following the larval decision point for dauer formation, they become adults that live more than twice as long as wild type. The *daf-23* alleles identified by their dauer phenotype are all nonconditional mutations. However, the mutants are maternally rescued for dauer formation ([Gottlieb and Ruvkun 1994](#)), and these maternally rescued animals are also long-lived nondauer adults ([Larsen et al. 1995](#)). The *daf-23* and *age-1* mutations have now been shown to be allelic, and the gene is now referred to as *age-1* ([Malone et al. 1996](#); [Morris et al. 1996](#)). Because these *daf-2* and *age-1* mutations are thought to reduce gene activity, one can infer that in wild-type animals, these genes act to accelerate the aging process. The *age-1* gene has now been cloned and found to encode a phosphatidylinositol-3-OH kinase family member ([Morris et al. 1996](#)). This implies that a phosphatidylinositol signaling pathway involving the *age-1* kinase regulates dauer formation and life span. Morris et al. suggest that the gene may be involved in neuroendocrine signaling. So far, this is the only *C. elegans* life-span gene that has been cloned. Its site of action is unknown.

The ability of *daf-2* and *age-1* mutations to extend life span is dependent on the activities of two additional genes, *daf-16* and *daf-18* ([Kenyon et al. 1993](#); [Dorman et al. 1995](#); [Larsen et al. 1995](#)). Both of these genes are thought to act downstream from *daf-2* and *age-1* in the dauer pathway because they are required for dauer formation in *daf-2* or *age-1* mutants. On their own, *daf-16* mutations do not have a marked effect on life span (see [Kenyon et al. 1993](#)); however, they may cause a small but consistent decrease in life span ([Larsen et al. 1995](#)).

The [\*daf-18\*](#) gene is defined by a single allele ([Riddle et al. 1981](#)) that also causes some animals to have grossly misshapen midbody regions and to die prematurely from internal hatching ([Dorman et al. 1995; Larsen et al. 1995](#)), and thus no firm conclusions can be drawn at this time about the wild-type role of [\*daf-18\*](#) in either dauer formation or life span.

In summary, four genes that act in the dauer pathway, [\*age-1\*](#), [\*daf-2\*](#), [\*daf-16\*](#), and probably [\*daf-18\*](#), also act in a single pathway for life-span control: In the wild type, [\*daf-2\*](#) and [\*age-1\*](#) activities shorten life span, possibly by down-regulating [\*daf-16\*](#) and [\*daf-18\*](#). In contrast, [\*daf-16\*](#) and possibly [\*daf-18\*](#) function in a process that extends life span. In the regulation of the dauer state, [\*daf-16\*](#) activity is required for maintenance of the dauer; it will be interesting to learn whether its activity is required continuously to maintain adult youthfulness in [\*daf-2\*](#) and [\*age-1\*](#) mutants.

Do all genes in the dauer pathway affect adult life span? Surprisingly, the answer is no. As described by [Riddle](#) (this volume), the regulation of dauer formation is complex. It comprises at least two parallel regulatory pathways: The group-1 pathway appears to involve the [\*neuron\*](#) ASJ and a signaling pathway similar to the photoreception signaling pathway ([Thomas et al. 1993](#); J. Thomas; C. Bargmann; both pers. comm.). The group-2 pathway involves a transforming growth factor- $\beta$  (TGF- $\beta$ )-like signaling cascade that may affect the ADF, ASI, and ASG [\*neurons\*](#) ([Georgi et al. 1990; Bargmann and Horvitz 1991b; Estevez et al. 1993; Thomas et al. 1993; Ren et al. 1996; Schackwitz et al. 1996](#)). It seems likely that the [\*daf-2\*](#) and [\*age-1\*](#) genes act downstream from these two pathways, because mutations that reduce or eliminate the functions of either [\*daf-2\*](#) or [\*age-1\*](#) trigger dauer formation in animals in which the group-1 or group-2 pathways have been put in the dauer-repressing states by mutation or by ablation of [\*sensory neurons\*](#) that act in these pathways ([Thomas et al. 1993](#); J. Thomas, pers. comm.).

Surprisingly, [\*daf-2\*](#) and [\*age-1\*](#) mutations are the only dauer-constitutive mutations that appear to extend life span. Mutations in neither the group-1 pathway ([Kenyon et al. 1993](#)) nor the group-2 signaling pathway ([Kenyon et al. 1993; Larsen et al. 1995](#)) affect life span. The discrepancy between these upstream mutants and the life-span mutants ([\*daf-2\*](#) and [\*age-1\*](#)) is particularly striking when one considers the fact that [\*daf-2\*](#) (*ts*) mutants have extended life spans even at temperatures too low to induce dauer formation. At these low temperatures, mutations in the group-1 and -2 genes do not extend life span. Moreover, group-1 and -2 mutants have normal life spans even when they are cultured at high temperature, which is capable of inducing dauer formation very efficiently. (In these experiments, the animals are shifted to the high, dauer-inducing temperature after they have passed the critical period for dauer formation.)

We know that reduction of [\*daf-2\*](#) or [\*age-1\*](#) function induces life-span extension, and thus these findings suggest that mutations in these two upstream branches of the pathway do not cause [\*daf-2\*](#) or [\*age-1\*](#) levels to fall when animals are shifted to 25°C late in development. One way to explain this is to postulate that group-1 and group-2 pathways only function in young larvae, where they specifically regulate entry into the dauer stage (see [Kenyon et al. 1993](#)).

Dauer formation by dauer-constitutive mutations in the group-1 and group-2 pathways requires activity of the [\*daf-12\*](#) gene ([Riddle et al. 1981; Vowels and Thomas 1992](#)). When [\*daf-12\*](#) is missing, these mutants are unable to enter the dauer state. Is [\*daf-12\*](#) activity required for the life-span extension of [\*daf-2\*](#) mutants? When certain [\*daf-2\*](#); [\*daf-12\*](#) double mutants are placed under dauer-inducing conditions, they go through the first stage of dauer formation, entering an alternative L2 state called L2d; however, instead of progressing to the dauer state, they arrest development as young larvae ([Vowels and Thomas 1992](#)). A plausible explanation for this is that in the absence of [\*daf-12\*](#), animals cannot become dauers, but in the absence of [\*daf-2\*](#) activity, they cannot progress to adulthood either ([Vowels and Thomas 1992; Larsen et al. 1995](#)). It is possible to ask whether [\*daf-12\*](#) activity is required for the longevity of [\*daf-2\*](#) mutants by shifting [\*daf-2\*](#); [\*daf-12\*](#) double mutants to the nonpermissive temperature when they have passed the dauer decision point or by growing animals at 20°C. Under these conditions, one can observe different, allele-specific effects on life span ([Dorman et al. 1995; Larsen et al. 1995](#)). In one allelic combination, dauer formation is completely suppressed, but life span extension is unaffected. Thus, the activity of [\*daf-12\*](#) required for dauer formation is not required for life-span extension. Nevertheless, in certain

allelic combinations, [\*daf-12\*](#) activity does influence life span. Depending on the allele, maximum life span can be shortened, or lengthened up to fourfold over wild type. It will be interesting to determine the molecular basis for these interactions.

Why do [\*daf-2\*](#) and [\*age-1\*](#) mutations control both life span and dauer formation? Do mutations in these genes simply induce dauer formation in adults? This seems unlikely for several reasons. First, Johnson has carefully characterized the life cycle of *age-1(hx546)* mutants. The mutation does not markedly affect the timing of larval molts, length of embryogenesis, food uptake, movement, or behavior ([Friedman and Johnson 1988a](#)). In addition, the results of population studies suggest that these animals are undergoing a typical type of senescence but at a rate that is slower than normal for *C. elegans* ([Johnson 1990](#)). Movement rates decrease more slowly in [\*age-1\*](#) mutants than in wild type ([Duhon and Johnson 1995](#)).

[Kenyon et al. \(1993\)](#) characterized several behaviors of [\*daf-2\*](#) (*e1370*) mutants. Like [\*age-1\*](#) animals, long-lived [\*daf-2\*](#) adults resemble wild type in body size and general appearance ([\*daf-2\*](#) mutants contain intestinal granules that make them appear dark; however, this is also true of [\*daf-7\*](#) mutants [[Vowels and Thomas 1992](#)], which do not have extended life spans). The increase in [\*daf-2\*](#) (*e1370*) longevity at 20°C occurs with only a slight decrease in hermaphrodite self-fertility ([Kenyon et al. 1993](#)), and some alleles have wild-type fertility ([Larsen et al. 1995](#)). In addition, [\*daf-2\*](#) adults move normally. Like wild type, [\*daf-2\*](#) adults move more slowly as they age (some [\*daf-2\*](#) alleles also adopt a dauer-like resting posture), but the ability to move decreases at a slower rate than normal ([Kenyon et al. 1993](#)). Young [\*daf-2\*](#) adults also pump normally ([Kenyon et al. 1993](#)). Surprisingly, the rate of pumping falls off at the same rate as in the wild type. However, this decrease in the rate of pumping probably reflects a decreased requirement for food when egg laying is completed, rather than a wild-type rate of senescence. It makes sense that animals not rapidly producing progeny would need less food, and in fact, wild-type animals that do not produce progeny because their gonad has been ablated pump more slowly than normal (C. Kenyon, unpubl.).

Since longevity can be uncoupled from the vast majority of dauer characteristics, why do the same mutations affect both dauer formation and adult life span? Perhaps it is simply a coincidence. Alternatively, perhaps these weak dauer-constitutive mutations uncouple expression of a life-span extension mechanism normally activated in dauers from the morphological features of the dauer. Possibly different dauer-specific features have different thresholds for expression; i.e., partial loss of gene function allows the expression of a life-span extension program but not expression of the other morphological and behavioral features of the dauer program ([Kenyon et al. 1993; Larsen et al. 1995](#)).

How is the life-span extension seen in [\*daf-2\*](#) and [\*age-1\*](#) mutants related to normal life span? This is a key question. There are two possibilities. First, it is possible that [\*daf-2\*](#) and [\*age-1\*](#) mutations somehow elicit a bypass pathway that overrides the normal aging process to extend life. Alternatively, it is possible that the [\*daf-2\*](#) and [\*age-1\*](#) mutations somehow reset a natural life-span-determining mechanism to a longer life-span setting (see [Kenyon 1996](#)). The rate of aging can be different between species; perhaps these mutations cause *C. elegans* to age in exactly the same way that normally occurs in a slightly longer-lived species. If the [\*daf-2\*](#) and [\*age-1\*](#) gene functions are conserved, it will be interesting to learn whether there is a general correlation between their activity levels and the rate of aging in other species.

A number of processes associated with the different theories of aging have been examined in [\*age-1\*](#) and/or [\*daf-2\*](#) mutants in hopes of inferring the cause of their longevity. In the next sections, the results of these studies are discussed.

## 2. Rate of Oxidative Damage

[\*age-1\*](#) or [\*daf-2\*](#) mutants might live longer because they have lower levels of oxidative damage or a greater capacity to repair oxidative damage. In fact, catalase and superoxide dismutase levels were elevated in older [\*age-1\*](#) and [\*daf-2\*](#) worms ([Larsen 1993; Vanfleteren 1993; Vanfleteren and DeVreese 1995](#)). [\*age-1\*](#) worms also showed increased resistance to hydrogen peroxide ([Larsen 1993](#)) and paraquat ([Vanfleteren 1993](#)). (However, it should be noted that paraquat is an anion generator which, unlike four other anion generators, does not exert an oxygen-

dependent toxic effect as it should if it increased anion production [Blum and Fridovich 1983]. It therefore cannot be assumed that paraquat toxicity is due to increased anions.) These findings are consistent with the hypothesis that changes in the life spans of *age-1* mutants are due to increased resistance to oxidative damage. However, it is important to emphasize that increased ability to repair oxidative damage could be a correlate, rather than a cause, of longevity.

Melov et al. (1994, 1995) have asked whether *age-1* mutants have a reduced frequency of deletion formation in mitochondrial DNA. These authors found a statistically significant decrease in the rate at which deletions form in *age-1* mutants, consistent with the hypothesis that these mutants are better able to repair DNA damage than is the wild type.

### 3. Increased Thermotolerance and UV Resistance

Interestingly, *age-1* and *daf-2* mutants are more resistant to heat shock and UV damage than wild type. Moreover, this resistance is suppressed by *daf-16* mutations (Lithgow et al. 1995; Murakami and Johnson 1996). Are these forms of stress resistance likely to be the cause of the longevity of these animals? UV resistance is correlated with longevity (Murakami and Johnson 1996), but heat shock resistance is not, because dauer-constitutive *daf-7* and *daf-4* mutants, which do not have extended adult life spans, are also heat-resistant (Lithgow et al. 1995). However, the physiological change that leads to heat resistance could be necessary but simply not sufficient for life-span extension. Lithgow et al. (1994) have found that exposing wild-type worms to heat pulses causes a small but statistically significant increase in life span (Lithgow et al. 1995). Whether repeated heat pulses might have a substantial effect on life span remains to be tested. For a recent review of oxidative damage, environmental stress, and life span, see Martin et al. (1996).

### 4. Telomere Shortening

The model that telomere shortening causes senescence has not been tested in the *C. elegans* life-span mutants; however, this model seems unlikely to explain the extended life spans of *daf-2* and *age-1* mutants because the increase in life span is postmitotic.

### 5. Rate of Metabolism

The fact that long-lived *age-1* and *daf-2* mutants can be fully fertile, move normally, and exhibit a normal pumping rate suggests that their metabolism has not been grossly slowed. To test this directly, Vanfleteren and DeVreese (1995) measured the rate of oxygen consumption in wild-type and *age-1* animals. These authors found that the metabolic rate of *age-1* animals is similar to that of wild type up to day seven of adulthood. After this time, the rate of oxygen consumption in *age-1* animals is actually higher than in wild type, which is consistent with the fact that *age-1* animals at this age are much more active than wild type. This is an extremely important observation, because it indicates that these mutants are not simply living at a slower rate. Vanfleteren and DeVreese (1995) have also asked whether the "metabolic potential" of *age-1* and *daf-2* mutants is greater than the wild type. To do this, they asked how effectively a luminescent substrate, lucigenin, could be oxidized by a given amount of nematode extract in the presence of the reducing agent NADPH. Their test measures the level of superoxide anions, which are produced as a byproduct of cellular metabolic activity. This "metabolic potential" is similar in wild type, *daf-2*, and *age-1* worms up to about day five of adulthood. After this age, it becomes higher in *age-1* mutants than in the wild type. In addition, the levels of the metabolic enzymes isocitrate dehydrogenase, isocitrate lyase, and malate synthase are all down-regulated in wild-type worms but to a lesser extent (or not at all) in *age-1* and *daf-2* mutant adults. These findings indicate that *age-1* and *daf-2* mutants do not live longer because their metabolic rate has been slowed. In contrast, relative to wild type, the metabolic rate actually increases with age.

The metabolism of *age-1* and *daf-2* adults is similar to that of dauers in some ways, but different in others: The levels of catalase, superoxide dismutase, isocitrate lyase, and malate synthase are elevated in both dauers and *age-1* and *daf-2* adults. Conversely, alkaline and acid phosphatase activities are lower in both dauers and *age-1* and *daf-2* adults. The activity of isocitrate dehydrogenase, in contrast, is decreased in the dauer stage but

elevated in both [age-1](#) and [daf-2](#) adults. Likewise, the metabolic rate of dauers is decreased relative to L3 larvae, and about the same as mid-stage adults, whereas that of [age-1](#) and [daf-2](#) adults is increased relative to adults of comparable age.

## 6. Trade-off between Longevity and Fertility

At 20°C, [daf-2](#) mutants have fairly normal or completely normal brood sizes, depending on the allele. However, at 25°C, they appear to have fewer progeny, and in some [daf-2](#) mutants, such as *e1370*, these progeny can be produced by very old hermaphrodites ([Larsen et al. 1995](#); C. Kenyon, unpubl.). This indicates that [daf-2](#) gene activity can influence reproduction but that the effect on reproduction can be uncoupled from the effect on life span. The reproductive potential of [daf-2](#) animals is not clear, because the number of self-progeny is limited by the number of sperm and mating with males can affect hermaphrodite life span ([Gems and Riddle 1996](#)). To ask directly whether the longevity of [daf-2](#) mutants could be caused by any type of change in the reproductive system, [Kenyon et al. \(1993\)](#) ablated (*Z1-Z4*), the gonad and germ cell precursors, in wild-type and in [daf-2](#) mutants. Under these conditions, the life span of wild type was normal and that of [daf-2](#) animals was still extended. Thus, the longevity of [daf-2](#) mutants cannot be attributed to a change in the reproductive system.

## 7. Caloric Restriction and Endocrine Control of Life Span

The fact that dauer formation is induced by food limitation, which also induces longevity in vertebrates, makes one wonder whether [age-1](#) and [daf-2](#) mutations might be altering a conserved caloric restriction pathway. In both cases, food limitation increases life span. As discussed above, the major effect of caloric restriction in *C. elegans* appears to be to promote entry into the long-lived dauer state, although it has been reported to extend the life span of nondauer adults as well ([Klass 1977](#)).

Is it possible that [age-1](#) and [daf-2](#) mutants have extended life spans because they do not feed or metabolize nutrients properly? This possibility has not been ruled out, but it seems unlikely. [daf-2](#) and [age-1](#) mutants do not have a starved appearance or altered feeding behavior, and they can produce progeny as rapidly as the wild type, suggesting that they are healthy (see [Kenyon et al. 1993](#); [Larsen et al. 1995](#)). In addition, under axenic conditions, the life span of *C. elegans* is extended; however, under these conditions, [age-1](#) and [daf-2](#) mutants still live much longer than the wild type ([Vanfleteren and DeVreese 1995](#)).

An alternative possibility is that [daf-2](#) and [age-1](#) mutations are part of a regulatory switch that is activated by caloric restriction. Specifically, in wild-type worms, food restriction would down-regulate [daf-2](#) and [age-1](#) activity, presumably through the endocrine pathway that regulates dauer formation. (These two genes could act within a neurosecretory system or in the response of target tissues to such a system.) This, in turn, would result in downstream events, including dauer formation and life-span extension. In this model, lowering [daf-2](#) or [age-1](#) activities by mutation would not prevent worms from ingesting or metabolizing food, but it would trigger life-span extension. Thus, these mutants may be reaping all of the benefits of caloric restriction without going hungry.

How likely is it that [age-1](#) and [daf-2](#) functions have been conserved in evolution? It seems possible that a mechanism arose early in evolution that allowed life span to be increased under the dangerous condition of food limitation. During the subsequent evolution of *C. elegans*, other dauer features could have been added to the original life-span extension program, so that now their expression is tightly coexpressed. In this model, homologs of [daf-2](#) or [age-1](#) in vertebrates might also be down-regulated by caloric restriction. This would result in life-span extension, but of course not dauer morphology. This is a hypothesis that should be possible to test once more genes and molecules in the pathway are identified.

In addition to the parallels that can be drawn between caloric restriction and dauer formation, both of which involve food intake, one can draw a separate parallel that does not involve food. This parallel involves the neuroendocrine system, which has been shown to influence life span in certain postreproductive insects, marsupial mice, and certain salmon (see [Finch 1990](#); [Morris et al. 1996](#)), and it regulates dauer formation in *C. elegans*. Perhaps the [age-1](#) and [daf-2](#) genes influence life span through a conserved endocrine pathway.

Finally, the dauer state itself is an example of a state of diapause, or dormancy, which is a period of slowed growth and metabolism observed in many types of organisms. Like dauer formation, diapause or dormancy in other organisms can be induced by unfavorable living conditions. In a number of species, including species of insects, amphibians, and fish, diapause or dormancy is associated with life-span extension (for review, see [Finch 1990](#)). It would be interesting to learn whether these states involve the activities of genes similar to [age-1](#) and [daf-2](#), and if so, whether it would be possible to uncouple the life-span extensions normally associated with diapause from the other features of dormancy, as appears to have occurred in the reduction of function [daf-2](#) and [age-1](#) mutants of *C. elegans*.

It is important to emphasize that even if the [age-1](#) and [daf-2](#) genes act to induce a special longevity pathway, this does not mean that these long-lived animals do not age "normally." It is possible that these mutations influence the function of a regulatory mechanism that establishes the rate of aging. It may be that there is a highly conserved "senescer" present in all animals that brings about senescence (see [Kenyon 1996](#)). The rate at which this senescer "runs" the aging process may be subject to regulation: Perhaps the rate-setting mechanism of the senescer can be changed easily by mutation during natural selection or by the influence of environmental signals. Thus, [age-1](#) and [daf-2](#) mutations may have the effect of causing *C. elegans* to age in exactly the same way that a longer-lived member of a different species ages. In fact, it is worth pondering the possibility that humans, with their long life spans, harbor reduction of function mutations in genes in a conserved [age-1](#) / [daf-2](#) life-span pathway.

## D. Genes That Decrease the Rate of Development and Extend Life Span

A second set of mutations, called the *clk* (*clock*) mutations, also affect life span ([Wong et al. 1995; Lakowski and Hekimi 1996](#)). Unlike [daf-2](#) and [age-1](#) mutations, [clk-1](#), [clk-2](#), and [clk-3](#) mutations disrupt the timing of many events including the length of embryonic and larval development; the length of the cell cycle; the duration of the pumping, defecation, and swimming cycles; and the rate of egg laying. In general, each of these events proceeds much more slowly than normal in the *clk* mutants, which suggests that unlike [age-1](#) and [daf-2](#) mutants, these animals may have a lower rate of metabolism. In addition, unlike the wild type, where the variation in these rates between individuals is low, the variation in *clk* mutants is quite high. For example, although the mean period of embryogenesis is longer in *clk* mutants, some embryos develop more quickly than normal. The *clk* genes therefore appear to coordinate the timing of developmental processes and also make them occur in a highly reproducible fashion.

As described above, one of the most interesting features of the *clk* mutants is that they are unable to adjust their rates of development and behavior to either increases or decreases in temperature. This is a finding that changes the way one thinks about the effect of temperature on biological processes: It indicates that temperature adaptation is subject to regulation by specific gene products, rather than simply being an intrinsic response of chemical and biochemical processes themselves to heat.

All three *clk* genes have life spans that are slightly longer than normal at all temperatures. Whereas the mean life span of N2 was 15 days at 18°C, the life span of [clk-1](#) mutants was about 18–19 days ([Lakowski and Hekimi 1996](#)). The life spans of *clk* mutants can increase even more in certain double-mutant combinations. For example, the mean life span of [clk-1 clk-2](#) double mutants is about 28 days at 18°C. Unlike [age-1](#) mutants, which have nearly normal rates of growth to adulthood, a substantial fraction of the increase in life span of the *clk* mutants is due to extended development to adulthood (e.g., [clk-1 clk-2](#) double mutants take 6 days rather than 2.5 days to reach adulthood at 18°C).

The [gro-1](#) mutant, which resembles *clk* mutants in many respects, suppresses rather than enhances the extended life spans of the *clk* mutants. The mutation does not suppress the long life span of [age-1](#) mutants, so its effect seems to be specific for the *clk* mutants. Curiously, on its own, this mutation extends life span slightly.

Do the *clk* mutants act in the same pathway as the genes affecting dauer formation? The phenotypes of these two mutants seem to be quite different: *clk* mutants affect the rate of growth to adulthood (decreasing the rate of cell division), and they slow down many periodic behavioral processes. In contrast, [age-1](#) mutants grow to

adulthood at a rate that is similar to that of normal worms. Like dauer-constitutive mutations in many genes, [\*daf-2\*](#) mutants take an additional day to develop, but this is not because cell division is retarded; instead, these mutants enter and pause in the L2d stage ([Swanson and Riddle 1981](#); J.H. Thomas, pers. comm.; C. Kenyon, unpubl.). Likewise, *clk* mutants have not been reported to affect dauer formation, although this has not been tested rigorously. If *clk* mutations act in the same pathway as [\*age-1\*](#) and [\*daf-2\*](#) mutations, then [\*daf-16\*](#) activity should be required for life-span extension. The life spans of putative [\*clk-1\*](#) ; [\*daf-16\*](#) double mutants have been examined by two groups who, unfortunately, report opposite results. [Lakowski and Hekimi \(1996\)](#) report that, unlike [\*daf-2\*](#) and [\*age-1\*](#) mutants, the life-span increase of *clk* mutants is not suppressed by a [\*daf-16\*](#) mutation. In contrast, [Murakami and Johnson \(1996\)](#) report that the adult life span of [\*clk-1\*](#) ; [\*daf-16\*](#) double mutants is similar to that of wild type. It is not clear why this discrepancy exists; it is unfortunate, since it is important to determine whether these mutations affect the same or different pathways.

The life spans of *clk*; [\*daf-2\*](#) mutants are reported to be much longer than either single mutant, with a mean life span up to five times as long as wild type ([Lakowski and Hekimi 1996](#)). This is the longest life span reported for *C. elegans*; in contrast, the life spans of [\*daf-2\*](#) ;(e1370) [\*age-1\*](#) double mutants are similar to that of either single mutant at 25°C and only slightly longer at 15°C ([Dorman et al. 1995](#)). A cautionary note: Unlike [\*daf-2\*](#) ;(e1370) [\*age-1\*](#) double mutants, *clk*; [\*daf-2\*](#) double mutants are very sluggish. [\*daf-2 unc-32\*](#) double mutants also have extremely long life spans (P. Larsen, pers. comm.), which raises the possibility that the *clk*; [\*daf-2\*](#) double mutants have long life spans because they are sluggish. To test this, it is necessary to determine the life spans of many different [\*daf-2\*](#) ;*unc* double mutants; particularly with *unc* mutations that do not affect the [\*nervous system\*](#) (since many neuronal *unc* mutations have been found to influence dauer formation; see [Riddle](#), this volume).

Why do *clk* mutations lengthen life span? It seems possible that mutations in *clk* genes effectively slow the rate at which "time passes" for these worms. For example, the primary role of the *clk* genes may be to set the rate of metabolism which, in turn, sets the rate of many developmental and behavioral processes, as well as the rate of aging. This interpretation is consistent with one of the theories of aging, which states that metabolic rate sets the rate of aging. In fact, although this model cannot explain many notable exceptions, including the [\*age-1\*](#) and [\*daf-2\*](#) mutants ([Vanfleteren and DeVreese 1995](#) and in prep.), long-lived calorically restricted vertebrates, and many of the examples mentioned earlier, there is an intriguing correlation between metabolic rate and life span within certain phyla in nature (see [Finch 1990](#)). Alternatively, it is also possible that *clk* genes set the rates of metabolism and the rates of other timed processes in parallel.

Generated from local HTML

## **Chapter 28. Environmental Factors and Gene Activities That Influence Life Span — V Prospects**

---

Compared to our understanding of other biological processes, such as pattern formation, the cell cycle, and gene expression, we know very little about aging. Possibly because of this, it is surprising how many people have strong, fixed opinions about how it works. In closing, I would like to argue on behalf of additional screens for life-span mutants (see [Duhon et al. 1996](#)). Of all of the mutants described in this review, only one, [\*age-1\*](#), was identified in an unbiased screen for life-span mutants, and that screen was far from saturation. All of the others were first identified because of other phenotypes. It is possible that we have already identified all of the *C. elegans* life-span genes, but this seems unlikely to me. [\*age-1\*](#) and [\*daf-2\*](#) mutants still age, and we do not know how this takes place. We do not know whether there are genes that function downstream from [\*daf-16\*](#) specifically to affect life span without affecting dauer formation. The *clk* mutants may affect a second life-span pathway, and we do not know whether additional life-span pathways exist. There have been no screens for mutants with accelerated rates of aging. It is exciting to have an unexplored frontier like this to investigate. Pure genetic and subsequent molecular analysis, done in a way that is unbiased by the expectations of theorists, seems like the best way to make progress.

Generated from local HTML

## **Chapter 28. Environmental Factors and Gene Activities That Influence Life Span — Acknowledgments**

---

I thank Pam Larsen, Tom Johnson, Gary Ruvkun, and Don Riddle, as well as members of the Kenyon lab, for comments on the manuscript and Don Riddle for his infinite patience.

Generated from local HTML

# Chapter 29. Evolution

---

## Contents

[I Introduction](#)

[II Phylogenetic Context for \*C. elegans\*](#)

[III Character Evolution](#)

[IV Other Directions](#)

[V Conclusions](#)

[Acknowledgments](#)

Generated from local HTML

## Chapter 29. Evolution — I Introduction

---

Nematodes, and *Caenorhabditis elegans* in particular, provide excellent material for the study of evolution for two main reasons. First, because of the wealth of information from *C. elegans* on the genetic hierarchies underlying the development of the organism's features (characters), candidate loci can be targeted for studying their possible roles in character evolution. Although these studies (reviewed in the second half of this chapter) are just beginning, many evolutionary changes are similar to mutant phenotypes, suggesting that much of evolution may proceed by changes at the kinds of regulatory loci defined by genetic studies.

Second, because nematodes diverged early in metazoan evolution (possibly before the divergence of deuterostomes from protostomes), the primitive features that they share with other metazoan groups must have resembled those features in the ancient ancestor common to all these groups. Because *C. elegans* uses the same mechanisms and molecules as other Metazoa for pattern formation, cell signaling, cell fate determination, etc., the common ancestor also had these features. Besides maintaining this important position within the Metazoa, there is enormous diversity within the phylum Nematoda, and even within the family Rhabditidae, to which *C. elegans* belongs. This diversity (the greater portion of which must yet be explored; [Sudhaus 1991](#)) can be exploited to address fundamental questions about patterns and processes of evolution if the relationships of taxa within these groups can be established. The phylogenetic context of *C. elegans* is therefore reviewed in the first half of this chapter.

Placing the *C. elegans* model in a phylogenetic and evolutionary context can help identify which biological questions are relevant over a phylogenetically broad range of taxa. Because different pairs of organisms shared ancestors at different times, similarities between organisms that are due to shared ancestry (homologies) may be shared at distinct hierarchical levels of organization. But similarities may also arise from convergence. A phylogenetic framework is thus essential for drawing the historical inference about whether the form of a feature (character state) is primitive or derived and is ultimately required for assessing the explanatory power of the model system ([Kellogg and Shaffer 1993](#); [Sidow and Thomas 1994](#)).

Generated from local HTML

# Chapter 29. Evolution — II Phylogenetic Context for *C. elegans*

---

The methodologies of phylogenetic reconstruction have evolved rapidly since [Hennig \(1950\)](#) established an explicit methodological foundation on the basis of Darwin's (see p. 111 in Darwin 1859) principle of Divergence of Character, whereby historical relationships are inferred from suites of characters in extant taxa (see pp. 102–126 in [Sudhaus and Rehfeld 1992](#)). Numerical methods for phylogeny reconstruction are currently available that are based on different assumptions and algorithms (for review, see [Felsenstein 1988; Swofford and Olsen 1990](#)), the most common of which are parsimony ([Fitch 1971; Swofford 1993](#)), maximum likelihood ([Felsenstein 1993](#)), and "distance methods" such as neighbor-joining ([Saitou and Nei 1987](#)) and minimum evolution ([Rzhetsky and Nei 1992](#)). Statistical methods are also employed to evaluate the confidence associated with particular groupings ([Felsenstein 1985; Kishino and Hasegawa 1989; Rzhetsky and Nei 1992](#)).

## A. Relationship of *C. elegans* to Other Animals

Because nematodes diverged at some very early time during metazoan evolution, they are simultaneously problematic and valuable as representatives of the Metazoa: problematic because the long period of time since they shared a last common ancestor with other Metazoa suggests that many features will be specific to nematodes, but valuable because of their position in the "outgroup" to most metazoan forms. (The outgroup is the set of taxa outside the monophyletic group, or clade, under study; representative outgroup taxa are generally added to a comparison of monophyletically related taxa for the purpose of resolving the root of the phylogenetic tree or to infer ancestral states.) Since understanding the relationships of animals is critical to understanding their biology, it is particularly important that we develop a sound phylogenetic framework for the well-characterized genetic models such as *Caenorhabditis*, *Drosophila*, and *Mus*, representing nematodes, arthropods, and vertebrates, respectively. The possible phylogenetic relationships among these animals can be expressed as three distinct hypotheses ([Fig. 1](#)). In these scenarios, arthropods and vertebrates are more closely related to each other than either is to nematodes ([Fig. 1a](#)), nematodes are more closely related to arthropods than to vertebrates ([Fig. 1b](#)), or nematodes are more closely related to vertebrates than to arthropods ([Fig. 1c](#)). These alternative relationships present critical differences for interpreting information from model organisms. For example, if *C. elegans* were more closely related to *Drosophila* than to vertebrates ([Fig. 1b](#)), the observation of any biological feature in both *C. elegans* and *Drosophila* would have little predictive value for that feature in humans. However, as a representative outgroup taxon to a wide range of other Metazoa (i.e., the rest of the Bilateria; [Fig. 1a](#)), any feature found during investigations of *C. elegans* and identified in any one "ingroup" taxon such as *Drosophila* could be predicted in other ingroup taxa (e.g., vertebrates), unless the feature was lost in subsequent lineages ([Sidow and Thomas 1994](#)).

How then are nematodes likely to be related to other Metazoa? During the past 100 years, Nematoda (usually categorized as a class) has been generally included along with other "pseudocoelomates" such as Rotifera, Kinorhyncha, Gastrotricha, Nematomorpha, Chaetognatha, Acanthocephala, Priapula, and Loricifera in catchall groups (generally categorized as phyla) like Nemathelminthes (=Pseudocoelomata) or Aschelminthes ([Grobben 1908; Cobb 1919; Chitwood and Chitwood 1950; Hyman 1951; Barnes 1987; Brusca and Brusca 1990; Willmer 1990](#)). These groupings depend on the assumption that an often poorly defined character (e.g., the "pseudocoel") is shared because of a derived change in a common ancestor. Thus, it is uncertain if Nemathelminthes is monophyletic, and if so, the relationship of the sister group of Nematoda (usually assumed to be Nematomorpha) is unclear.

Fossil evidence has been helpful in reconstructing the evolution of several animal taxa; but there are *no* fossils relevant to the origin of Nematoda or deep nematode relationships. Of greater importance for reconstructing relationships are suites of independently evolving, derived and clearly homologous characters shared by extant phyla that could be related to nematodes, but there are few such morphological characters (see pp. 9–12 and 305–306 in [Maggenti 1981](#)). With this paucity of clear data, many different scenarios have been proposed for the origin of nematodes (see pp. 27–28 in [Andrássy 1976](#); see p. 9 in [Maggenti 1981](#)). A recent review of metazoan

relationships placed nematodes as an early branch of the Protostoma, but with the qualification that this placement was "contentious" ([Conway Morris 1993](#)).

Despite some misgivings about the present selection of molecular data ([Conway Morris 1994](#); [Philippe et al. 1994](#)), the continued accumulation of such data is likely to provide a much better resolution of metazoan relationships, primarily because the potential database for independent characters is so great. However, *C. elegans* was excluded from the early molecular studies of metazoan evolution using 18S rRNA sequences ([Field et al. 1988](#); [Lake 1990](#); but see [Cedergren et al. 1988](#); [Hendricks et al. 1988](#); [Brandl et al. 1992](#)) because the sequence and secondary structure of *C. elegans* 18S rRNA are more different from those of other animals than are fungal or plant rRNAs ([Ellis et al. 1986](#); [Hendricks et al. 1988](#)).

Currently, an "outgroup" position for *C. elegans* ([Fig. 1a](#)) is favored by the molecular data, including sequences of the two large single-copy nuclear genes for RNA polymerase II and III ([Sidow and Thomas 1994](#)), mitochondrial rDNA ([Okimoto et al. 1994](#)), cytochrome c ([Vanfleteren et al. 1994](#)), and 18S rRNA ([Winnepenningckx et al. 1995](#); for the phylogenetic use of other *C. elegans* genes, see also [Friedlander et al. 1994](#)). Most of these sequences appear to have evolved more rapidly in *C. elegans* than in other animals. A dramatic difference in evolutionary rate between *C. elegans* and other animals could result in an artifactual placement of *C. elegans* as an outgroup to more slowly evolving taxa (although it is important to note that no increased rate was observed for the two RNA polymerase genes compared; [Sidow and Thomas 1994](#)). However, as sequence data accumulate to provide a better representation of the genome and of phylogenetic diversity (see [Waterston et al.](#); [Blaxter and Bird](#); both this volume), we can expect that hypotheses about the systematic placement of nematodes (and *C. elegans* in particular) within the Metazoa will be tested with greater and greater rigor.

## B. Relationship of *C. elegans* to Other Nematodes

Nematode systematics is currently based primarily on morphology, although molecular studies have been initiated. To the extent that the variation in these morphological characters reflects the hierarchy of their evolutionary relationships, the classification can be considered a phylogenetic hypothesis and a way to view the relationship of *C. elegans* to other nematodes. Nematode classifications can differ substantially from author to author, or suggest largely unresolved phylogenies, so we will not attempt to thoroughly compare current classifications. We refer readers to the works of [Andrássy \(1976, 1983, 1984\)](#), [Sudhaus \(1976\)](#), [Maggenti \(1981\)](#), [Lorenzen \(1981, 1994\)](#), [Poinar \(1983\)](#), and [Malakhov \(1994\)](#) for discussions of various classification systems.

Figure 2 presents a general view of possible relationships among the major orders of nematodes based primarily on Malakhov (see p. 188 in [Malakhov 1994](#)). A taxonomic principle shared by some nematologists is a fundamental division of nematodes into two groups, the Adenophorea and Secernentea (which includes *C. elegans*). This dichotomous classification does not, however, reflect the probable origin of the Secernentea within Adenophorea (i.e., Adenophorea is probably paraphyletic), as is represented in the three subclasses (Enoplia, Chromodoria, and Rhabditia) recognized by some investigators (see [Fig. 2](#)) ([Andrássy 1976, 1984](#); [Lorenzen 1981, 1994](#); [Malakhov 1994](#)). Adenophorea dominate marine and (to a lesser extent) freshwater sediments, occupying a wide range of ecological habitats. However, a small number of parasitic groups have arisen within this class, such as the marine invertebrate parasites in the order Marimermithida, the invertebrate parasites in Mermithida, the largely vertebrate parasites of Dioctophymida and Trichocephalida, and the plant parasites in the order Dorylaimida ([Fig. 2](#)). In contrast, the Secernentea are nearly unknown in marine environments (except as parasites of marine vertebrates), and although most are free-living terrestrial species, a large number of important parasitic forms have evolved in this class (see [Blaxter and Bird](#), this volume).

The order Rhabditida is depicted as one of several lineages in the Secernentea and bears features considered primitive for the class ([Fig. 2](#)). For example, many Rhabditida and most Adenophorea are free-living microbotrophs, suggesting that the ancestral Secernentea were also free-living microbotrophs (see pp. 175–201 in [Malakhov 1994](#)). Although some members of the Rhabditida may have conserved features ancestral to Secernentea, this order has radiated into one of the most diverse and abundant groups of nematodes known, including a wide array of specialized associations with animals, e.g., the true parasitic families Rhabdiasidae and

Strongyloididae. Other families are Steinernematidae and Heterorhabditidae, which include entomopathogenic species currently used in biological control ([Poinar 1983](#)). Cephalobidae (e.g., *Cephalobus* and *Acrobeloides*), Panagrolaimidae (e.g., *Panagrellus redivivus*), and Diplogastridae (e.g., *Pristionchus*) include many terrestrial free-living and invertebrate-associated species generally used in comparisons with Rhabditidae (which includes *C. elegans*). (Note that [Andrássy \[1984\]](#) considers similar subdivisions as suborders and [Maggenti \[1981\]](#) elevates Diplogastridae to a separate order, Diplogastrida.) Other secernentean orders depicted ([Fig. 2](#)) are the stylet-bearing plant parasitic order Tylenchida and the true zooparasitic orders Ascaridida and Strongylida. The placement of parasitic taxa within such a classification is made difficult by their extreme morphological divergence from the other groups (which could be phylogenetically closely related), probable convergence between different nematode groups, and lack of data about larval characters and diversity. In addition, most systematic treatments are specialized for particular ecological groups (e.g., either free-living or parasitic, but not both), frustrating a comprehensive evolutionary approach to nematode systematics (see pp. 175–201 in [Malakhov 1994](#)).

The family Rhabditidae has been described in several different contexts; Figure 3 depicts one possible scenario for this group based on [Sudhaus \(1976\)](#), amended. In this evolutionary hypothesis, lineages lead to four genera. The lineage leading to genus *Rhabditis* is further divided into several evolutionary lineages giving rise to several subgenera, although similar taxa have been accorded generic status by many authors (see, e.g., [Dougherty 1955](#); [Andrássy 1983](#)).

Our understanding of nematode relationships is based on very few clearly homologous characters for such a diverse animal group. Consequently, classifications differ depending on the characters emphasized. Without more characters upon which to base our understanding of relationships, we will continue to lack a firm evolutionary framework for nematodes. Thus, the future of nematode systematics is likely to be based largely on the wealth of independent molecular characters.

[Fitch et al. \(1995\)](#) recently demonstrated the utility of 18S rRNA sequences as a source of molecular characters for developing a phylogenetic framework for ten nematode species in the family Rhabditidae. In addition, these authors found that the level of molecular divergence between morphologically similar nematodes in the same family is fivefold greater than the divergence found (in the same molecule) between different classes of tetrapod vertebrates as morphologically different, for example, as crocodiles and mice (cf. [Turbeville et al. 1991](#); [Rzhetsky and Nei 1992](#)). Although there is no metric for the amount of divergence (molecular or morphological) that defines a particular taxonomic level, either these are very ancient lineages or this molecule (or the nematode genome) evolves very rapidly, or both. [Vanfleteren et al. \(1994\)](#) used a vertebrate molecular clock to estimate times of divergence between Ascaridida and Rhabditida/Strongylida (~500 Myr ago) and between Strongylida and Rhabditida (~400 Myr ago), possibly corresponding to the diversification of potential hosts for the parasitic forms from the late Cambrian period to the early Devonian period. However, because different phylogenetic branches vary greatly in rates of accumulation of molecular substitutions (see previous section) and the calibration for taxon-specific molecular clocks requires a fossil record (no informative record exists for nematodes), such estimates are likely to have a very large variance.

Several additional 18S rDNA sequences have recently been determined for nematodes representing major taxonomic groups within the order Rhabditida. A phylogenetic hypothesis based on the analysis of these sequences is shown in Figure 4. In addition, the sequence of an Adenophorean nematode (*Plectus acuminatus*) can be included as an outgroup to root the tree. Several aspects of this molecular phylogeny are noteworthy. First, the fact that the root occurs on the *Zeldia* lineage supports a more recent common ancestor of (suborders) Diplogastrina and Rhabditina than for either of these groups and Cephalobina, an observation supported by additional sequences from genes for the largest subunit of RNA polymerase II and the large (28S) subunit of ribosomal RNA (J.G. Baldwin et al., in prep.). Second, as has been noted earlier ([Fitch et al. 1995](#)), the branching order among the Rhabditidae is very similar to that proposed by [Sudhaus \(1976\)](#), amended ([Fig. 3](#)) based on morphological characters. Finally, this analysis suggests that the vertebrate parasites *Nematodirus* and *Haemonchus* (traditionally included in order Strongylida) arose within family Rhabditidae. Thus, the phylogenetic

framework will direct the comparison of these parasitic species with the apparently closely related rhabditids, comparisons that may not have otherwise been made or appreciated.

The hypothesis represented in Figure 4 can be useful for the interpretation of comparative studies. However, significant resolution of several of the relationships will require additional sequences from appropriate loci. Also, the individual species included represents a poor sampling of diverse groups. The monophyly of each taxonomic group remains to be evaluated by the inclusion of additional informative taxa.

## C. Relationships within *Caenorhabditis*

Approximately 17 *Caenorhabditis* species have been described ([Sudhaus 1976](#) and pers. comm.; K. Kiontke, pers. comm.). The majority of these are known only from fixed material and only four are currently available as live cultures at the *Caenorhabditis* Genetics Center: *C. elegans*, *C. briggsae*, *C. remanei*, and *C. sp.* The latter strain, CB5161, was previously referred to as *C. remanei* but is now considered to be an undescribed species (W. Sudhaus, pers. comm.). In addition, the strains (EM464 and VT733) described by [Baird et al. \(1994\)](#) as *C. vulgaris* are synonymous with *C. remanei*. These four species (which represent sister species in the *Elegans* species group) are remarkably similar morphologically ([Sudhaus 1976](#)) and, as shown by the 18S rDNA data, form a distinct monophyletic group within the Rhabditidae ([Fitch et al. 1995](#)). The single prominent difference among these four species is that *C. elegans* and *C. briggsae* are hermaphroditic, whereas *C. remanei* (strains EM464 and VT733) and *C. sp.* (strain CB5161) are gonochoristic (dioecious).

One of the first molecular comparisons between *Caenorhabditis* species demonstrated that despite the extreme morphological conservation, the genomes of *C. elegans* and *C. briggsae* differ extensively ([Emmons et al. 1979](#)). This large genetic divergence is also supported by the 18S rDNA data, which suggest divergences between *Caenorhabditis* species as large as those between orders in tetrapod classes ([Fitch et al. 1995](#)). During the last several years, comparisons among *Caenorhabditis* species have been extended to include many genes (see, e.g., [Thomas and Wilson 1991](#); [Lee et al. 1992](#); [Xue et al. 1992](#); [Lee et al. 1993](#); [Krause et al. 1994](#); [Fitch et al. 1995](#)). In all cases, these comparisons have shown extensive differences between the species, indicating that this extreme molecular divergence is not limited to a particular type of gene. Indeed, this difference between *Caenorhabditis* species has been used to map gene structures and regulatory elements by "phylogenetic footprinting" (see, e.g., [Zucker-Aprison and Blumenthal 1989](#); term coined by [Tagle et al. 1988](#)). Although direct and homologous comparisons are not always possible, the pairwise differences between *Caenorhabditis* species for several genes appears to be comparable to the level of difference between homologous genes of mammalian orders (cf. [Rzhetsky and Nei 1992](#)). That the same level of genetic divergence can result in morphologically almost indistinguishable species such as those in the *Elegans* species group or in species as morphologically distinct as elephants and mice convincingly demonstrates several principles: (1) genome evolution is uncoupled from morphological evolution ([King and Wilson 1975](#)), (2) much of the genome can change during evolutionary periods of morphological stasis, and because of this, (3) selection is probably a stronger force than drift in shaping novel morphologies or maintaining static morphologies in most cases.

Whether or not the extreme molecular divergence reflects a long period of absolute time or simply a rapid accumulation of change, it is clear that a great deal more evolution has taken place within the *Elegans* species group than is suggested by morphology alone. A clear understanding of the relationship among the species of the *Elegans* group is necessary to understand the evolutionary history of that change. Unfortunately, it is not possible to resolve the relationships among these four species based on more than 7 kb of sequence information from several genes ([Fitch et al. 1995](#); J.T. Vida et al., in prep). These four species seem to have diverged at a similar time, although additional data may ultimately resolve their history.

An additional problem with the evolutionary framework for the *Elegans* group is that molecular data from a closely related outgroup taxon are presently not available. There exists a very large "evolutionary gap" between the *Elegans* group and other representative genera from the Rhabditidae ([Fitch et al. 1995](#); W.K. Thomas et al., in prep.). Recently, however, molecular data from an as yet undescribed species (strain PS1010) supported a closer

relationship to *Caenorhabditis* than to any other tested taxa (W.K. Thomas et al., in prep). Additional such species (K. Kiontke, pers. comm.) should help our understanding of the evolution of *Caenorhabditis*.

## D. Intraspecific Variation in *C. elegans*

*C. elegans* (Maupas 1899) is considered to be a cosmopolitan species. Our knowledge of *C. elegans* diversity is based on comparisons of the independent isolates collected during the last 20 years. At this time, more than 20 different *C. elegans* strains have been isolated from the soil of different continents, namely, North America, Europe, and Australia. This variety of strains allows the genetic diversity within this species to be investigated.

One of the first demonstrations of genetic variability between *C. elegans* strains was a comparison of nuclear restriction fragment length differences (RFLDs) by [Emmons et al. \(1979\)](#). In this study, significant differences were found between the Bristol (N2) and Bergerac (BO) strains. This was due in part to the fact that the BO strain has many more copies of the transposable element Tc1 than does the N2 strain. Among the strains currently available, there are 12 distinct Tc1 patterns for the strains with low numbers of that element and 6 distinct high-copy-number patterns (J. Hodgkin, pers. comm., see [Plasterk and van Luenen](#), this volume). In contrast to the high degree of RFLD variation, a survey of 24 enzyme loci ([Butler et al. 1981](#)) found no detectable protein differences between the Bristol and Bergerac strains; a survey of arbitrarily primed polymerase chain reaction (PCR) products ([van der Knaap et al. 1993](#)) also resulted in no significant intraspecific differences. In addition, a comparison of the gene sequences for the calmodulin-like nuclear gene ([cal-1](#)) from 11 isolates including the N2 and BO strains found no differences in either the protein-coding sequence or the single intron of that gene ([Thomas and Wilson 1991](#)). Taken together, these results suggest that significant genetic differences between strains exist, but that these may be predominantly due to transposable-element-mediated changes or other types of rearrangements, and that the level of other types of genetic variations in the nuclear genome of *C. elegans* is low. Although this observation underscores the potential importance of transposable elements, a more thorough survey for point mutations between strains is needed to clarify the relative contributions of each mutational class to variation in this nematode species.

To further evaluate the relationships among strains, [Thomas and Wilson \(1991\)](#) compared mitochondrial DNA sequences from 11 different isolates of widespread geographic origin and found that the level of nucleotide difference was low (<2%) between strains. These sequences identified four different mitochondrial haplotypes, and phylogenetic analysis supported the existence of at least two distinct groups. One group comprising three haplotypes embraced strains of widespread geographic origin including both the N2 and BO isolates. A second distinct group included strains from Australia, California, and British Columbia in a single mitochondrial haplotype. Although direct comparisons are difficult, the level of difference found in the mitochondrial genomes of *C. elegans* strains is comparable to that found among the mitochondrial genomes of humans. This low level of mitochondrial divergence is also consistent with the low level of nucleotide substitution in the nuclear genome of *C. elegans* strains.

It is possible to construct a phylogeny representing the mitochondrial genome history of these strains because this genome is assumed not to recombine and each mitochondrial genome will therefore have a single evolutionary history. In contrast, for the nuclear genome of *C. elegans*, different loci can be separated by recombination and each locus may have an evolutionary history independent of other loci. In this light, it is interesting to consider the possibility that *C. elegans* strains evolve with no effective outcrossing. If this is true, we would expect that all regions of the nuclear genome would have a single shared history (and this history should be congruent with the mitochondrial history).

A critical and widespread analysis of nuclear loci is as yet not possible. However, in a study of five low-copy-number strains, [Egilmez et al. \(1995\)](#) mapped 20 variable Tc1 loci and found that the inferred relationship among strains is consistent with the character patterns at 19 of the 20 loci. This observation suggests that interbreeding between the lineages defined by these strains has been limited. Nevertheless, one Tc1 polymorphism is not consistent with this relationship. For this site, we must assume either the parallel insertion (or loss) of a Tc1 at that locus or that locus has been separated from the others by crossing and recombination. Although these

preliminary results support a model of *C. elegans* evolution where strains are isolated and mixis is rare, more data are required. There are many more Tc1 polymorphisms that when mapped (as in [Egilmez et al. 1995](#)) can be evaluated for congruence among sites. Additional mapped polymorphisms such as copulatory plug formation ([Barker 1994](#)) and mitochondrial sequences will provide a more thorough evaluation of *C. elegans* strain evolution.

An additional, interesting question about the closely related (and thus recently diverged) strains of *C. elegans* concerns the origin of the *C. elegans* strains with high copy numbers of Tc1 elements (HCN strains). Recently, by mapping 35 Tc1 sites occupied in the Bergerac strain of *C. elegans* and comparing the occupancy of those sites in other HCN strains of *C. elegans*, [Egilmez et al. \(1995\)](#) proposed that all high-copy-number strains arose from a single common ancestor, suggesting that mutator strains appear rarely (or transiently) in the history of *C. elegans*. This proposal assumes that the ancestral condition in *C. elegans* is a low number of Tc1 elements, an assumption based on the observation that the vast majority of isolates are low copy number. Furthermore, the Tc1 patterns suggest that the BO strain represents this early event and that the other HCN strains (DH424 and TR403) are derived from subsequent "backcrossing" to low-copy-number strains. This backcrossing is consistent with the fact that the different HCN strains have different mitochondrial haplotypes. However, it will be necessary to test these hypotheses in a phylogenetic context.

Although our understanding of genetic diversity within *C. elegans* is just beginning, this species represents a rare opportunity to evaluate the details of genome evolution only possible for organisms with such detailed genetic information.

## Figures



### Figure 1

Three possibilities of relationships of *C. elegans* ("the" nematode) to *Drosophila melanogaster* ("the" arthropod) and *Mus musculus* ("the" vertebrate): (a) nematodes as an outgroup taxon to vertebrates and arthropods; (b) nematodes more closely related to arthropods than to vertebrates; (c) nematodes more closely related to vertebrates than to arthropods. Obviously, these hypotheses (like the model systems themselves) are overly simplistic representations for enormously diverse phylogenetic groups. Although present data favor *a* or *b*, robustly distinguishing which hypothesis is most likely depends on the accumulation of much more data.

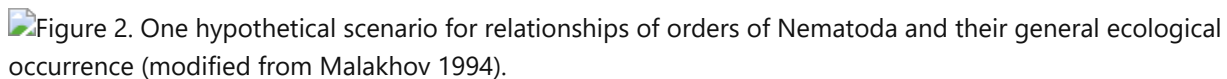


### Figure 2

One hypothetical scenario for relationships of orders of Nematoda and their general ecological occurrence (modified from [Malakhov 1994](#)). Note that multifurcations represent *uncertainties* in branching arrangements rather than simultaneous speciation events. The classification derived from this evolutionary scenario proposes three subclasses ([Malakhov 1994](#)). According to other classification systems, Adenophorea encompasses the subclasses Enoplia and Chromodoria, whereas Secernentea corresponds to Rhabditia. Branching relationships within the Rhabditia do not reflect possible paraphyly, i.e., the Rhabditida may be an artificial group that includes a common ancestor but not all of its descendants. Note also that the scheme does not show the occurrence of several animal parasitic groups in "marine" environments (e.g., there are ascarid parasites in marine vertebrates).

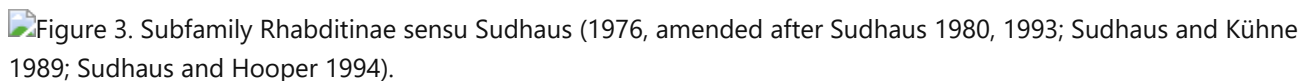


### Figure 3

Subfamily Rhabditinae *sensu* [Sudhaus \(1976\)](#), amended after [Sudhaus 1980, 1993](#); [Sudhaus and Kühne 1989](#); [Sudhaus and Hooper 1994](#)). Note that multifurcations represent *uncertainties* in branching arrangements rather than simultaneous speciation events. Other authors often refer to similar taxa, but with the depicted subgenera raised to genera within a family called Rhabditidae. Note that *Rhabditis* is paraphyletic according to Sudhaus (1993) since genus *Heterorhabditis* is included here within *Rhabditis*. Also shown is a hypothesis for relationships among some of these taxa as inferred from 18S rDNA ([Fitch et al. 1995](#)). (Dashed line) Alternative possibility for the relationship of *Caenorhabditis* to the other taxa.

Generated from local HTML

## Chapter 29. Evolution — III Character Evolution

---

Model systems like *C. elegans* are an important resource for the study of character evolution because they provide a detailed picture of how characters are constructed at morphological, developmental, genetic, and molecular levels. If evolutionary changes can be reconstructed at these elementary levels, several important, largely unanswered, evolutionary questions will be realistically approachable. Among these guiding questions are the following: (1) What kinds of, and how many, genetic changes are principally involved in adaptive (or nonadaptive) character transformations? The architects of the neo-Darwinian synthesis argued that most (if not all) adaptations involve alleles at many loci, each of which has a small effect ([Provine 1971](#)). However, the theoretical foundation for this view is surprisingly weak, and the empirical evidence is mixed ([Barton and Turelli 1989](#); [Orr and Coyne 1992](#)). (2) How significantly do “developmental constraints” bias or limit phenotypic variability and thus the range of possible responses of an organism to selection ([Maynard Smith et al. 1985](#); see p. 75 in [Hall 1992](#))? Developmental constraints are predicted to arise from the interdependent and hierarchical nature of the developmental process, yet the same integrated nature of development makes the evolution of complex systems possible (see pp. 439–440 in [Futuyma 1986](#)).

Most of the data reviewed in this section have been taken from comparative studies, which seek general principles by studying similar features or processes in different species. For example, the largely invariant cell lineages of nematodes related to *C. elegans* have allowed detailed interspecific comparisons of cell lineages ([von Ehrenstein and Schierenberg 1980](#); [Sternberg and Horvitz 1981, 1982](#); [Ambros and Fixsen 1987](#); [Skiba and Schierenberg 1992](#)). Phylogenetically based reconstructions of character changes should be even more informative than interspecific comparisons because the polarity of changes may be inferred in addition to suggesting candidate loci involved (see, e.g., [Fitch and Emmons 1995](#)). Given a phylogenetic hypothesis, the first step in any analysis of character evolution is to reconstruct hypothetical ancestral states at the nodes of the phylogenetic tree. Methods of character reconstruction have been discussed in detail elsewhere ([Wiley 1981](#); [Maddison et al. 1984](#); [Ax 1987](#); [Swofford and Maddison 1987](#); [Funk and Brooks 1990](#); [Harvey and Pagel 1991](#); [Maddison and Maddison 1992](#)).

### A. Deep Homologies

The molecular developmental and pattern-forming mechanisms found in flies and vertebrates are also found in *C. elegans*, suggesting that a “tool kit” of basic regulatory mechanisms was already present in the common ancestor of the Metazoa (for review, see [Manak and Scott 1994](#)). Despite the largely invariant cell lineages so uncharacteristic of most animals, *C. elegans* uses the same mechanisms as other metazoans to specify cell fates. For example, not only do *C. elegans* [\*lin-12\*](#) and *Drosophila Notch* share homology at the sequence level, but they are also functionally homologous; the intracellular domains of these transmembrane proteins are regulated by the extracellular domains and intrinsically cause cell-fate transformations ([Struhl et al. 1993](#)). Applying phylogeny (see [Fig. 1a](#)), the prediction can be made that vertebrate homologs of the [\*lin-12\*](#) /Notch signaling mechanism should not only be found, but be functionally equivalent as well ([Struhl et al. 1993](#)), although the tissues or organs in which they operate may not necessarily be homologous. Indeed, such vertebrate homologs of components in the [\*lin-12\*](#) /Notch signaling pathway are found, and the signaling function is similar as well ([Jariault et al. 1995](#); [Levitin and Greenwald 1995](#)).

So many other such molecular-functional homologies have been observed between *C. elegans* and other metazoan species, like flies and vertebrates, that “the relevance of functional studies in tractable model systems is established beyond dispute” ([Akam et al. 1994](#)). For example, the molecules and mechanisms of neurogenesis are phylogenetically conserved among worms, flies, and vertebrates: [\*lin-32\*](#) /*achaete-scute* determines neuroblast cell fate in the peripheral [\*nervous system\*](#) ([Zhao and Emmons 1995](#)), [\*unc-6\*](#) netrin is associated with axonal guidance ([Goodman 1994](#)), and synaptotagmin is a component of the synapse in these animals ([Nonet et al. 1993](#)).

The most striking evidence for the conservation of function is the ability of a molecule from one species to function in a different species in the same manner as its endogenous homolog. For example, human *bcl-2* can regulate cell death in *C. elegans* as a replacement for endogenous *ced-9* (Vaux et al. 1992; Hengartner and Horvitz 1994b). Elegant interspecific substitutions in *Drosophila* have demonstrated similar conservation of molecular function for *Hox* genes (McGinnis et al. 1990; Malicki et al. 1990) and even their regulatory elements (Malicki et al. 1992). The *Drosophila* *Hox* proteins Scr and Antp can in turn substitute in a specific manner for their homologs (*lin-39* and *mab-5*, respectively) in *C. elegans* in controlling three different cell fate decisions: regulation of Q neuroblast migrations, specification of ventral serotonergic neurons, and specification of male ray sensilla (Hunter and Kenyon 1995).

Perhaps the most dramatic example of a conserved metazoan character is the HOM-C cluster of *Antp*-type *Hox* genes (see Ruvkun, this volume). Not only are there molecular sequence homologies and, in most cases, conservation of gene order, but a basic anterior-posterior (A-P) axial patterning function is also conserved (for review, see Manak and Scott 1994). In *C. elegans* and other Metazoa, this axial patterning function interprets A-P asymmetry and regulates diversification of several different kinds of cellular fields (Wang et al. 1993). Slack et al. (1993) have suggested that the phylum-specific body plan (assuming there is such a thing) of each metazoan is prefigured by a characteristic A-P expression pattern of the *Hox* genes at a particular developmental stage (the "phylotypic stage"). The proposed archetypal pattern for the Metazoa is called the "zootype." Of course, types are not ancestors. But with the other comparisons discussed above, this typological viewpoint does emphasize the striking conservation of molecular mechanisms used in development. Despite this conservation, an even more remarkable diversity of forms has evolved. But how?

As is evident from studies that include *C. elegans*, diversity in the patterns controlled by the HOM-C genes could arise by (a) changes in the cluster itself, (b) changes in how these genes are regulated, or (c) changes in the target molecules they affect (Kenyon 1994; Ruvkun, this volume).

### a. Changes in the cluster itself

Because the four *Hox* genes in the *C. elegans* HOM-C cluster are homologous to four subfamilies of *Hox* genes in other species, the ancestor of the Bilateria may have had a HOM-C arrangement similar to that in *C. elegans* (Salser and Kenyon 1994), with gene duplications proliferating these basic types in other lineages (Ruddle et al. 1994). That both *ceh-23* and its mammalian homologs *Dlx1* and *Dlx2* are found near their respective HOM-C cluster suggests that the ancestral cluster might also have contained such a fifth gene (Manak and Scott 1994). A phylogenetic analysis of vertebrate and *Drosophila* HOM-C genes suggests a three-gene cluster in the metazoan ancestor, corresponding to the classes represented by *ceh-13*, *lin-39* + *mab-5*, and *egl-5* (Schubert et al. 1993), further suggesting to us that the inverted arrangement of *ceh-13* and *lin-39* relative to their homologs in *Drosophila* and vertebrates (Salser and Kenyon 1994) arose in a nematode-specific lineage. Representing even more primitively diverging lineages than *C. elegans*, at least two HOM-C genes exist in *Hydra*, corresponding to *ceh-13* and *lin-39* (Shenk et al. 1993), and at least one exists in sponges (Degnan et al. 1995). Although one might worry about possible effects of intergenic "conversions" interfering with homology assignments, the possibility of intergenic recombination has apparently not been tested as it has in other multigene clusters (cf. Fitch and Goodman 1991). Changes in the *Hox* genes could well have been associated with morphological changes; for example, more paralogs may have allowed increased body plan complexity in arthropods and especially vertebrates (Holland et al. 1994), although increased *Hox* cluster complexity does not always correlate simply with morphological diversity (W.J. Bailey et al., in prep.).

### b. Changes in how these genes are regulated

Changes in the regulation of the HOM-C genes must also have occurred, since they can be regulated by different systems in different species and can be regulated differently in different cell types or at different times during development of the same species (see Ruvkun, this volume). For example, the regulation of *Hox*-dependent patterning in *C. elegans* can occur both by extrinsic, position-dependent signaling, as in the regulation of *mab-5* expression in P<sub>9</sub> and P<sub>10</sub> (Salser et al. 1993), and by cell-autonomous, lineage-dependent mechanisms, as in the

autonomous action of [\*lin-39\*](#) to sustain [\*QR\*](#) neuroblast migration ([Clark et al. 1993](#)). In fact, cell-fate determination by cellular environment or lineage may involve similar underlying mechanisms that cause and maintain cell division asymmetry ([Jan and Jan 1995](#)). Because of this underlying similarity in mechanism, the requirement for an environmental signal in *Hox* regulation—or for any other developmental step—could conceivably be replaced during evolution by relatively simple changes affecting the regulation of an intrinsic factor ([Wolpert 1994](#); adumbrated by [Sulston et al. 1983](#)). Selection for such a transformation could involve a tradeoff between faster, possibly more reliable specification of cell identities *versus* ability to regulate and respond to environmental contingencies ([Wolpert 1994](#)). The release from a requirement for an environmental signal might also allow evolutionary changes in pattern or morphology as, for example, has perhaps occurred as one factor in the evolution of a posterior [\*vulva\*](#) in some Rhabditidae ([Sommer and Sternberg 1994](#)).

### c. Changes in the target molecules they effect

Although few loci are actually known to be targets of *Hox* regulation, candidates do exist (see [Sternberg and Emmons](#), this volume). The diversity of cellular responses to the same *Hox* genes suggests that evolutionary changes could also arise from changes in the responses of target genes or the kinds of developmental processes regulated by the *Hox* genes (see [Ruvkun](#), this volume).

Homology is arguably the most important concept in all of systematics; yet 153 years after its explicit definition by Owen (see pp. 374 and 379 in Owen 1843), the definition of and criteria for recognizing homology are still highly polemical topics ([Hall 1994](#)). Developmental and genetic studies in *C. elegans* and related species should help define how homologous characters (e.g., organs) can be formed by changes in developmental or genetic regulatory mechanisms or, conversely, how the same mechanisms may be used to form analogous (or even entirely different) characters. (The long-standing, albeit dubious, position of shared developmental process as “requisite evidence” for homology has been recently reviewed by [Hall \[1995\]](#).) For example, although there is deep homology between *C. elegans* and other Metazoa at the level of a shared A-P patterning mechanism, it is unclear how homology at the level of A-P patterning could relate to homologies between specific organs, because this mechanism is used in patterning different features in different ways. Conversely, homologous structures in even closely related species can use different developmental mechanisms. For example, [\*vulva\*](#) development requires gonad induction in some species (e.g., *C. elegans*) or is gonad-independent in other species (e.g., *Teratorhabditis palmarum*; [Sommer and Sternberg 1994](#); described later).

The recent discovery of a *Pax-6* homolog in *C. elegans* ([\*vab-3\* / \*mab-18\*](#); [Chisholm and Horvitz 1995](#); [Zhang and Emmons 1995](#)) may help us understand the role of this gene in the evolution of photosensation. Although the molecular homologies among the *Drosophila* paired/homeobox-containing gene *eyeless*, mouse and rat *Small eye*, and human *Pax-6* (all involved in eye development) have led some to suggest that arthropod and vertebrate eye organs are homologous ([Quiring et al. 1994](#); [Zuker 1994](#)), the body of data strongly suggests that eye organs of vertebrates and arthropods are convergent and analogous ([Salvini-Plawen and Mayr 1977](#)). On the other hand, an ancestral role for *Pax-6* seems likely in early photoreceptor evolution. The *C. elegans* homolog, [\*vab-3\* / \*mab-18\*](#), is involved in specifying the identity of a peripheral sense organ ([Zhang and Emmons 1995](#)) as well as head and other structures ([Chisholm and Horvitz 1995](#)). A propensity (“constraint”) for [\*mab-18\* / \*pax-6\*](#) to be involved in head development and/or the development of sensory elements might increase its probability for involvement in the convergent evolution of photosensory structures; i.e., the developmental pathway in which *Pax-6* is a component may have provided a “preadaptation” for the repeated evolution of sight. In this light, it is intriguing that *C. elegans* also may have a photoresponse ([Burr 1985](#)).

## B. Evolution of Early Embryogenesis in Nematoda

One of the more variable features in nematode development is also one of the earliest: How do nematodes initially establish A-P asymmetry? Sperm entry point specifies the A-P axis in *C. elegans* ([Kemphues and Strome](#), this volume) and predicts the posterior end of the developing embryo in all Rhabditidae observed (B. Goldstein, pers. comm.). But in at least some species of the related family Cephalobidae, A-P axis specification is not coupled to sperm entry and must therefore be specified by another asymmetric cue. Indeed, parthenogens are

quite common in this family (P. De Ley, pers. comm.) and develop with no sperm at all (B. Goldstein, pers. comm.).

Although other secernentean nematodes observed so far also show asymmetric cleavage of the [zygote](#), species in the adenophorean order Enoplida demonstrate equal and apparently symmetric cleavages to the eight-cell stage (see pp. 142–147 in [Malakhov 1994](#); E. Schierenberg, pers. comm.). Malakhov (see pp. 143–144 and 165–167 in [Malakhov 1994](#)) noted the striking variability of geometric arrangement in the blastomeres and suggested that enoplid development is primitive for Nematoda. Like other nematodes, cleavage is not spiralian (see p. 284 in [Nielsen 1995](#)) and cannot be used to support a monophyletic relationship of nematodes with spiralian groups such as Mollusca and Articulata. Although endodermal determinants in enoplid blastomeres have segregated by the eight-cell stage (see p. 166 in [Malakhov 1994](#)), early blastomere regulation is supported by fate-mapping and blastomere isolation experiments (D. Voronov and E. Schierenberg, pers. comm.). In addition, early segregation of the germ line cannot be detected (see p. 166 in [Malakhov 1994](#); E. Schierenberg, pers. comm.).

Although the “primitive” enoplids do not demonstrate cell constancy and cell fates appear to be shuffled when the cell lineage “trees” of representatives from different orders of the Chromodoria are compared (see pp. 165–169 and 187 in [Malakhov 1994](#)), the cell lineage tree of early embryogenesis is remarkably conserved in Rhabditia, at least across orders Ascaridida and Rhabditida ([Skiba and Schierenberg 1992](#)). The main differences between representative species within Rhabditida are in the timing of the somatic cell divisions relative to those of the germ line. The time between early somatic cell divisions can vary 13-fold between species of the same order; the markedly shorter time for *C. elegans* embryogenesis may result from the availability of maternally stored material ([Skiba and Schierenberg 1992](#)). That germ-line divisions are relatively constant, on the other hand, could reflect a requirement for early separation of germ line from soma to “preserve germ-line quality” in these species ([Skiba and Schierenberg 1992](#)), although this begs the question as to how such “quality” is preserved in enoplid embryos. Another difference involves the polarity of the P<sub>2</sub> cleavage, which is reversed in a *Cephalobus* species (family Cephalobidae) relative to that in *C. elegans* ([Schierenberg 1987](#)) and other Rhabditidae ([Skiba and Schierenberg 1992](#)). That the same polarity reversal is seen in *Bradyrhema rigidum* may suggest that the *Cephalobus*-type polarity is ancestral to Rhabditida ([Skiba and Schierenberg 1992](#)).

## C. Evolution of Postembryonic Cell Lineages in Rhabditida

An understanding of the genetic and developmental pathways specifying cell lineages in *C. elegans* provides the means for developing hypotheses about candidate loci involved in the evolution of cell lineages in related taxa. Comparisons between Rhabditida species have demonstrated how the patterns of postembryonic cell lineages can differ ([Sternberg and Horvitz 1981, 1982](#); [Ambros and Fixsen 1987](#); [Sommer and Sternberg 1995](#)). [Ambros and Fixsen \(1987\)](#) interpreted the cell lineage differences that they observed between rhabditid species as particular cell-fate transformations (cell fate referring to either a differentiated state or a pattern of descendant cell lineages). On the basis of phenotypes of known mutations, they then suggested candidate loci at which evolutionary changes could be postulated to underlie the cell lineage differences observed between species:

*Temporal* (heterochronic) transformations were postulated to explain differences in cell lineage patterns that were “retarded” or “precocious” relative to the corresponding *C. elegans* cell lineage. For example, a [seam](#)-cell duplication that is specific to the L2 in *C. elegans* was reiterated in another rhabditid species in the L3 or L4 stage ([Ambros and Fixsen 1987](#)). Because this difference was similar to “retarded” mutants in genes of the *C. elegans* heterochronic regulatory pathway ([Ambros and Moss 1994](#); see [Ambros](#), this volume), some of these genes are good candidate loci for such evolutionary transformations.

*Spatial* transformations were used to describe homeotic changes in the fate of one cell to the fate of a cell in a different location, relative to its fate in *C. elegans*. For example, the lineages of [P5.p](#) and [P7.p](#) in one rhabditid species were identical to the 3<sup>o</sup>-type lineages of P(3,4,8).p and furthermore did not appear to participate in vulval morphogenesis ([Ambros and Fixsen 1987](#)), in contrast to the behavior of P(5,7).p in *C. elegans* and in most other rhabditid species ([Sommer and Sternberg 1995](#)). [Ambros and Fixsen \(1987\)](#) observed the similarity to [lin-12](#)

mutants that can reduce the number of cell fates to 1° and 3° (also suggesting that “homeotic transformations” may not necessarily involve genes that are generally thought of as “homeotic”).

*Sexual* transformations referred to changes in sex-specific cell fate to that of the opposite sex, relative to its fate in *C. elegans*. Changes in sex determination genes or in genes involved in the response to the sex determination pathway could have been responsible.

[Ambros and Fixsen \(1987\)](#) raised several important caveats in proposing candidate loci for evolutionary changes. First, a species difference could be interpreted as one of several kinds of transformations (certain heterochronic differences could also be interpreted as homeotic differences, for example). Second, none of the mutants suggested as pointers to candidate loci caused *precisely* the same changes as the observed interspecific differences, suggesting that modulatory mutations in interacting genes would be important. Third, there are allele-specific differences in developmental effects, suggesting that different changes at single loci could produce a diversity of pattern changes.

[Sommer et al. \(1994\)](#) classified cell lineage differences into five types ([Fig. 5](#)), primarily based on comparisons between species of different families in order Rhabditida ([Sternberg and Horvitz 1981, 1982; Skiba and Schierenberg 1992](#)): (1) switch in the fate of a cell to a fate associated with another cell, (2) reversal in the polarity of a sublineage, (3) change in the number of rounds of cell division, (4) change in the relative timing of cell division, and (5) change in the segregation of lineage potential. Defining cell lineage differences in terms of such patterns can help to avoid the ambiguities in interpreting lineage differences in terms of temporal, spatial, or sexual transformations. [Sommer et al. \(1994\)](#) also suggested many candidate loci as plausible players in effecting particular kinds of cell lineage differences (for specific examples, see the legend to [Fig. 5](#)).

Two suggestions resulting from their survey are especially intriguing. First, there are many instances of interspecific differences in cell fate involving programmed cell death ([Sternberg and Horvitz 1981, 1982; Sommer et al. 1994](#)). Such differences can result in significant morphological differences (e.g., death of a distal tip cell in *Panagrellus* is cellularly sufficient to explain the difference between its one-armed gonad in the female and the two-armed [hermaphrodite gonad](#) of *Caenorhabditis*; [Sternberg and Horvitz 1981](#)). Cell death could be switched on or off fairly easily by blocking response to a survival factor, since such factors can be cell-type-specific ([Ellis and Horvitz 1991](#)). Second, additional rounds of cell divisions might allow the formation of new equivalence groups and allow cell diversification in the analogous manner in which gene duplications may allow functional diversity ([Chalfie et al. 1981](#); but see [Hughes \[1994\]](#) for rethinking the diversification of duplicates dogma). As a corollary to these suggestions, cell death may be “used” to dispose of redundant cells (e.g., if redundant functions interfere or are simply not required). For example, [Avery and Horvitz \(1987\)](#) showed that if it is allowed to survive its normally programmed death, the sister of [M4](#) can become a functioning [M4-like neuron](#).

In summary, because the kinds of cell lineage differences that have been observed after cell or genetic ablation in *C. elegans* are in many cases similar to observed interspecific differences, such interspecific differences could have a relatively simple cellular or genetic basis. For example, significant—yet coherent—evolution of a suite of features could result from simple, single changes at major regulatory loci in the genetic hierarchy that coordinately govern the cell lineages for ontogenetically related characters. Obviously, this hypothesis has yet to be tested with empirical data for any particular case. But the fact that single changes at specifiable loci can be postulated at all strongly suggests that there could be many exceptions to the neo-Darwinian dogma that evolution proceeds necessarily as gradual change at multiple loci that each have small effect.

## D. Evolution of Vulva Development in Rhabditida

Vulval position along the A-P axis varies greatly in nematodes, as does gonad morphology (see pp. 136–147 in [Chitwood and Chitwood 1950](#)). Because of their anatomical and functional associations, gonad morphology and vulval position are likely to influence each other, as in the case for *C. elegans* ([Greenwald](#), this volume). A strict correlation between gonad morphology and [vulva](#) position cannot be made, however, showing that these two features are somewhat independently variable ([Sudhaus and Hooper 1994](#)). Nevertheless, some covariation is recognizable. In Rhabditidae, female gonads are most often didelphic (with two uteri) and amphidelphic (the

uteri are opposed at the vagina). In this case, the [vulva](#) is always located midbody (40–65% of the body length from the head). In nematodes outside of Rhabditidae, didelphic gonads may be parallel, with the [vulva](#) positioned either anteriorly or posteriorly (see p. 137 in [Chitwood and Chitwood 1950](#)). Monodelphic forms also appear in a distribution that suggests a great deal of convergence, and in Rhabditida, they are associated with both central and posterior vulvae (see pp. 141–143 in [Chitwood and Chitwood 1950; Sudhaus and Hooper 1994](#)). Vulval position per se is thus not generally informative for phylogenetic relationships, but it is a very promising system for studying character evolution, especially since the *C. elegans* [vulva](#) is such a well-understood character (see [Greenwald](#), this volume).

Recent comparative studies ([Sommer and Sternberg 1994, 1995, 1996a; Sommer et al. 1994](#)) have defined interspecific differences in vulval features in terms of differences in underlying developmental mechanisms. Aspects that have changed during vulval evolution in Rhabditida are (a) lineages generated by vulval precursor cells (VPCs), (b) specific VPCs that contribute vulval tissue (i.e., 1<sup>o</sup> and 2<sup>o</sup> fates), (c) number of cells in the [VPC](#) equivalence group, and (d) changes in the relative contributions of position-dependent prebias, induction, and lateral signaling.

### a. Lineages generated by vulval precursor cells

Although the 1<sup>o</sup> lineages are conserved, a number of species differences occur in the 2<sup>o</sup> and especially 3<sup>o</sup> lineages. This suggests that alterations in the 2<sup>o</sup> and 3<sup>o</sup> lineages are likely to be tolerated as long as enough cells are present to provide a “scaffold” for the vulval structure ([Sommer et al. 1994; Sommer and Sternberg 1995](#); see also [Sternberg and Horvitz 1982](#)). In *Pelodera* and *Rhabditoides*, the polarity of asymmetry in the 3<sup>o</sup> lineages is reversed between cells anterior and posterior of the 1<sup>o</sup> cells (3<sup>o</sup> asymmetry is not observed in *C. elegans*). That the anterior-type asymmetry is the ground state for the posterior cell (demonstrated by gonadal cell ablation) suggests a role for the gonad induction signal in reversing the polarity of asymmetry in the posterior 3<sup>o</sup> lineages. Cell lineages also show variability *within* some species ([Sommer et al. 1994; Sommer and Sternberg 1995](#)). Not only may 3<sup>o</sup> lineage patterns be variable, but there may be different numbers of cells expressing 3<sup>o</sup> lineages. Both *Pelodera* and *Caenorhabditis* show variability in expression of a 3<sup>o</sup> lineage by [P3.p](#) and by [P9.p](#) in *Pelodera*. Variation is obviously important in evolutionary change, although the contribution of a genetic component to this intraspecific cell lineage variation has not yet been shown.

### b. Specific VPCs that contribute vulval tissue

In most Rhabditidae, vulval tissue is derived from three VPCs, P(5-7).p; only one case has been reported where one [VPC](#) cell was involved ([Ambros and Fixsen 1987](#)). A species in Diplogastridae, *Pristionchus pacificus*, also uses P(5-7).p ([Sommer and Sternberg 1996a, b](#)). Although all the Rhabditidae observed so far express 1<sup>o</sup> lineages from only one [VPC](#) (usually [P6.p](#)), species analyzed from family Panagrolaimidae express 1<sup>o</sup> lineages from two VPCs, [P6.p](#) and [P7.p](#) ([Sternberg and Horvitz 1982; Sommer and Sternberg 1995, 1996b](#)). In the latter case, the anchor cell (AC) comes to rest above cells from both lineages, instead of just [P6.p](#) as in *C. elegans*. Interestingly, the AC frequently adopts a position between [P5.p](#) and [P6.p](#) in an undescribed species closely related to *C. elegans* (strain PS1010), correlating with a subsequent anterior shift in the patterning of vulval fates to P(4-6).p. [Sommer and Sternberg \(1995\)](#) suggest that such variation in AC position and inductive effect was one important step of several in the evolutionary differences between rhabditid and panagrolaimid vulval patterning. The panagrolaimid-type patterning could be considered apomorphic (i.e., a derived feature) instead of primitive if either Panagrolaimidae (suborder Cephalobina) and Diplogastridae (suborder Diplogastrina) or Panagrolaimidae and Rhabditidae are most closely related pairs ([Fig. 6a,b](#)); but if Diplogastridae and Rhabditidae are most closely related ([Fig. 6c](#)), nothing can yet be concluded about the primitive state of this aspect of vulval patterning.

### c. Number of cells in the VPC equivalence group

In many species, the vulval “equivalence group” probably changes during development as axial prepatterns become defined, e.g., from at least eight cells in *Panagrellus* before the (randomly interdigitating) Pn migrations into the ventral cord to six cells afterward ([Sternberg and Horvitz 1982](#)). Although interspecific differences in the regulation of axial prepattern (e.g., the prepattern set up by the *Hox* system) theoretically could produce differences in the number of Pn.p cells in the equivalence group, the size of the vulval equivalence group does not seem to have changed much by such a mechanism. (Perhaps there is a slight posterior shift in *Panagrellus*, where the equivalence group encompasses P(4-9).p and the [vulva](#) is produced by P(5-8).p.) However, programmed cell death limits the size of the equivalence group to only four cells—P(4-7).p—in the diplogastrid, *Pristionchus*; convergently, cell death also limits equivalence group size in a rhabditid species ([Sommer and Sternberg 1996a](#)). It would be interesting to see if the same genes are responsible for these possibly convergent changes.

#### d. Changes in the relative contributions of position-dependent prebias, induction, and lateral signaling

That the vulval equivalence group itself is quite conserved is intriguing, considering the amount of vulval heterotopy (change in relative position) that occurs in these species (see above). P(3-8).p in *Cruznema* and P(4-8).p in *Teratorhabditis* and *Mesorhabditis* migrate posteriorly; P(5-7).p then produce the vulval lineages ([Sommer and Sternberg 1994](#)). In *Cruznema*, where the [vulva](#) forms at a position 80% of body length, the posterior positioning of the VPCs results in a delay of gonad induction to the L3 (somehow the AC manages to find the previously migrated VPCs). P(3-8).p cells are presumably equivalent in their potentials prior to induction. However, in *Mesorhabditis* and *Teratorhabditis*, the P(4-8).p cells are only partially equivalent; for example, [P5.p](#) and [P6.p](#) have a strong potential to adopt a 1° fate, but [P4.p](#) cannot ([Sommer and Sternberg 1994](#)). In addition, AC induction is not required, providing another example of an evolutionary change between autonomous and nonautonomous specification of cell fates. The partial equivalence resulting from the position-dependent prebias in these cells must be further refined by some mechanism, probably by lateral signaling (e.g., [P4.p](#) cannot adopt a 2° fate alone but requires the presence of a 1° [P5.p](#)), suggesting that the role for lateral signaling in patterning vulval fates has become critical in these species. Induction from some other source cannot be ruled out, however ([Sommer and Sternberg 1994](#)).

Changes in the contributions of cell migration, competence, induction, and lateral signaling to vulval patterning have thus occurred in the evolution of a posterior [vulva](#). Current studies of the developmental genetic basis for these processes in *C. elegans* are likely to suggest candidate loci for evolutionary changes. For example, to identify the genetic changes underlying the evolution of a posterior [vulva](#) in two of three species (very likely to be a derived feature), we might look for changes in the expression of LIN-3 or LET-23 homologs in or near the VPCs to explain loss of response to induction. Alternatively, we might look for changes in cell-autonomous expression of the MAB-5 homolog in the VPCs as one possible explanation for their posterior migration. Another approach is to genetically dissect these mechanisms in other species. For example, mutants in *Pristionchus* allow survival of Pn.p cells that would normally die to limit vulval equivalence group size; these cells also respond to inductive signal, further suggesting that apoptotic constraint on the equivalence group is a derived trait ([Sommer and Sternberg 1996a](#)). These mutants should also reveal processes and genes likely to underlie evolutionary changes.

Integrated with phylogenetic analysis, studies of developmental mechanisms in the model system are also likely to provide unique insights into possible sources of constraint on variation. Axial pre patterning of the vulval equivalence group in *C. elegans* involves the HOM-C gene [lin-39](#) ([Clark et al. 1993](#)). Because it is used for axial patterning in many different cell types during development, most changes in [lin-39](#) regulation would probably be pleiotropic. Such pleiotropy could hypothetically pose a constraint on the possible pathways for vulval heterotopic changes ([Sommer and Sternberg 1994](#)). But first, we must determine whether or not a constraint is even suggested in the distribution of evolutionary changes. If all rhabditid species with a posterior [vulva](#) shared a common ancestor with a posterior [vulva](#), the commonality of [VPC](#) migration might have less to do with “constraint” than with simply sharing a single ancestral change ([Sommer et al. 1994](#)). Using a correlated changes

statistic ([Maddison 1990](#)), we can test the null hypothesis that evolutionary changes to migrating VPCs are randomly associated with evolutionary changes to posterior vulvae. In fact, the correlation may not be significant if there have been only two such changes on a variety of possible cladograms ( $p = 0.03–0.09$ ; D. Fitch, unpubl.). However, if there have been three such changes (i.e., if all three taxa had different ancestors with central vulvae), the correlation becomes decidedly more significant ( $p = 0.002–0.02$ ). Therefore, a robust phylogenetic framework in combination with such comparative data will allow a more rigorous evaluation of possible biases in the evolution of such developmental mechanisms.

## E. Evolution of Male Tail Development in Rhabditida

One of the most important morphological characters classically and currently used for phylogenetic inferences is the male copulatory apparatus ([Chitwood and Chitwood 1950](#); [Andrássy 1976, 1983, 1984](#); [Sudhaus 1974, 1976, 1980](#)). The size, location, and conformation of caudal alae (bursa or “fan” of secernenteans), the arrangements of the caudal papillae (“ray” [sensilla](#)), the shapes of the spicules and [gubernaculum](#), and the form of the tail tip are all features that are variable and have been considered phylogenetically informative at some level. Because the developmental and genetic mechanisms underlying ray patterning have been a subject of study in *C. elegans* ([Emmons 1992](#); [Emmons and Sternberg](#), this volume), evolutionary changes in morphology may be understood in terms of changes affecting elementary mechanisms.

Because evolutionary reconstruction depends on defining the units (homologs) that change, comprehensive attempts to reconstruct ray pattern evolution in the Rhabditidae (see, e.g., [Sudhaus 1976](#)) have been hampered by lack of a firm understanding of homologous relationships among rays. This problem is solved at least for the Rhabditidae by tracing ray development from the time ray cells are born in the [lateral hypodermis](#) ([Fitch and Emmons 1995](#); see below). In *C. elegans*, the relationship between the adult rays and the nine bilateral pairs of ray cell groups generated by the R(1–9) lineages during the L4 stage was traced by individual neuronal cell ablations ([Sulston et al. 1980](#); corrected in [Sulston et al. 1988](#)) and by correlating the final positions of the ray cells in the L4 epidermis (observed by immunofluorescence staining) with the attachment sites of particular ray tips ([Fig. 7](#)) ([Baird et al. 1991](#); [Fitch and Emmons 1995](#); see [Emmons and Sternberg](#), this volume). The latter method was applied in a comparison of ten different Rhabditidae ([Fitch and Emmons 1995](#)). An unambiguous correspondence between ray cell groups can be made on the basis of the striking similarities in cell arrangements at the earliest stage the cell lineages are complete. Homology assignments for individual rays can be made accordingly (Figs. [7](#) and [8](#)).

That the genital papilla precursor cell lineages in *Panagrellus redivivus* (family Panagrolaimidae) are nearly identical to the ray precursor cell lineages of *C. elegans* ([Sternberg and Horvitz 1982](#)) suggests that these lineages may be highly conserved within the Rhabditidae as well. Although correspondences have not yet been traced to the rays in the adult (despite the assignment of numbers to rays by Sternberg and Horvitz [1982]), the positions of ray cell nuclei born in the *P. redivivus* L4 hypodermis also suggest a spatial pattern of cells predicted from the rhabditid comparisons. Both this pattern and the lineage suggest that the difference in ray number between *C. elegans* and *P. redivivus* is due to absence of ray homologs 1 and 2 in *P. redivivus*.

Other differences in ray number can also be explained using this ray homology system. Individual rays can be lost or in rare variants gained (e.g., *Rhabditis blumi*; [Fitch and Emmons 1995](#)). That several rhabditid species appear to have ten rays instead of nine is due to the placement of the phasmid anterior of the three posterior rays (consistent with a predicted polarity reversal of the first division of T, suggesting [lin-44](#) involvement). The phasmid in these species can still be distinguished from the rays by retaining the ability to stain with FITC ([Fitch and Emmons 1995](#)). The ability to propose homologies for individual rays suggests that the position-specific axial patterning system underlying diversification of these rays may be as highly conserved as it seems to be for vulval precursor cells.

Whereas relative arrangements of the ray cells after their birth are the same in different rhabditid species, differences in adult ray arrangements are preceded by species-specific shifts of cell contacts between ray cells and hypodermal or other ray cells ([Fitch and Emmons 1995](#)). From these observations of species differences in

ray-cell associations, and given the demonstrations of ray nonequivalence in *C. elegans* ([Baird et al. 1991](#); [Chow and Emmons 1994](#); see [Sternberg and Emmons](#), this volume), evolutionary changes could result from changes in specificities of cell recognition or adhesion proteins or changes in the regulation of such proteins by the pattern formation mechanisms responsible for determining ray identities ([Fitch and Emmons 1995](#)). Because genes for ray pattern formation are known in *C. elegans*, candidate loci can be proposed that might be foci for evolutionary changes (D.H.A. Fitch, in prep.).

Additionally, when these species differences in [male tail](#) characters are analyzed in the context of a phylogeny (or alternative phylogenies), robustly supported polarities for many of the evolutionary changes in morphology and development can be identified ([Fitch 1997](#)). Of these character state changes, at least four resemble the phenotypic changes caused by known mutations in *C. elegans* ([Fig. 8](#)). Knowing the evolutionary polarity of changes that were likely (or at least possible) in this historical context allows testable hypotheses to be formulated about underlying changes in specific genetic and developmental mechanisms. For example, if an evolutionary hypomorphic change to [lin-32](#) resulted in the loss of the ray 8 homolog sublineage in *Rhabditis blumi* ([Fig. 8](#)), transformation with a restored-function [lin-32](#) transgene (representing the ancestral state) should atavistically restore the lost ray 8.

## F. Other Characters

Stoma ([buccal cavity](#)) characters are also an important phylogenetically informative character (see pp. 66–69 in [Chitwood and Chitwood 1950](#)). Since [Steiner \(1933\)](#), a pentapartite scheme based primarily on cuticular differentiation has been used to characterize variation in this structure in several nematode groups, including Rhabditida. Again, characterization of variation depends on a viable hypothesis of homologous relationships. In combination with ultrastructure information from *C. elegans* ([Albertson and Thomson 1976](#); [Wright and Thomson 1981](#), [De Ley et al. \(1995\)](#)) have proposed homologies among stomatal features of Rhabditida, emphasizing cellular processes surrounding the stoma rather than the stoma lining itself. It will be interesting to see how these new characters will be used in phylogenetic reconstruction and conversely how they may have evolved.

Body size has classically been of interest in the study of macroevolutionary patterns (evolutionary size increases deemed phyletic trends have been canonized as "Cope's Rule"; see p. 368 in [Futuyma 1986](#)); but body size is interesting in its own right as an evolving character. Changes in body size have occurred frequently during the evolution of the Rhabditidae and appear to correlate sometimes with cell proliferation and at other times with increases in cell size associated with genomic endoreduplication (A. Leroi and S. Emmons, pers. comm.).

Molecular characters are important not only for reconstructing phylogenies, but in their own right as evolving biological features. That Tc1-like transposable elements are features of nematode genomes, and that some share sequence similarity to vertebrate elements ([Radice et al. 1994](#); [Plasterk and van Luenen](#), this volume), suggests they may be ancient features of the metazoan genome. The trend that synonymous codon usage in *C. elegans* is extremely biased in highly expressed genes and relatively unbiased in lowly expressed genes ([Stenico et al. 1994](#)) suggests that codon usage has been shaped by selection favoring a limited number of translationally optimal codons ([Stenico et al. 1994](#)), although perhaps there are caveats to such generalizations (see, e.g., [Fitch and Strausbaugh 1993](#)).

Because genes are organized as operons in both eubacteria and archaebacteria, operons may have been primitive in ancestral eukaryotes. To determine if the operons found in *C. elegans* have been primitively conserved or recently derived, it is necessary to know if such operons are conserved throughout the nematode phylum. Recently, *Oscheius* sp. homologs to the ribosomal protein gene rp21 and the gene for ribosomal protein L27 were found to have features associated with operons (e.g., there is only 87 bp of intercistronic sequence between the genes, and the rp21 homolog is *trans*-spliced to a SL2 homolog, a leader sequence utilized for downstream genes in *C. elegans* operons; D. Zorio, et al., pers. comm.).

## Figures

Figure 5. Possible kinds of changes in cell lineage pattern (redrawn from Sommer et al.).

## Figure 5

Possible kinds of changes in cell lineage pattern (redrawn from [Sommer et al. 1994](#)). (P) Precursor cell; (A–D) different cell types. Because these changes are similar to known mutations, possible loci contributing to such changes have been suggested ([Sommer et al. 1994](#)), corresponding to the numbered boxes as follows. (1) Mutations in *ces-1* and *ces-2* cause programmed death of specific cells (if D represents a cell death, for example); (2) mutations in *lin-18* and *lin-44* cause altered polarity of cell lineages; (3) mutations in *unc-86* result in reiterations of some lineages; (5) *mex-1* mutations cause defective localization of the SKN-1 determinant. [Sommer et al. \(1994\)](#) also cite specific examples of interspecific lineage differences; for example, (4) *Z1* division is delayed in *P. redivivus* relative to *C. elegans*.

## Figure 6

Most parsimonious reconstructions for the evolution of anchor cell-vulval precursor cell interactions. Depending on the relationships of the taxa, the association of the anchor cell specifically with *P6.p* could have been apomorphic (derived, one possibility in tree c) or ancestral (as in trees a and b). Because the relationships are not yet well known (although [Fig. 4](#) suggests tree c), any of these scenarios is possible.

## Figure 4

A phylogenetic hypothesis for 16 nematodes based on preliminary analyses of 18S rDNA sequences ([Putland et al. 1993](#); [Zarlenga et al. 1994a,b](#); [Fitch et al. 1995](#); J.G. Baldwin et al., in prep.). The branching order shown is the most parsimonious, based on 911 alignment positions (aligned as by J.G. Baldwin et al., in prep.). Rooting was performed using *Plectus acuminatus* as an outgroup. Only branches found in 70% or more of bootstrap analyses are shown; other branches are collapsed to form multifurcations (which represent uncertainties in branching order). The same branching order is observed for either maximum parsimony as implemented in PAUP ([Swofford 1993](#)) or neighbor-joining as implemented in MEGA ([Kumar et al. 1993](#)). The classification is based largely on that of [Malakhov \(1994\)](#).

## Figure 7

Schematics of the boundaries of ray and hypodermal cells in the left lateral tail hypodermis of an archetypal early (a) and late (b) L4 male rhabditid after the ray lineages are completed (adapted from [Fitch and Emmons 1995](#)). The morphology of a hypothetical adult *male tail* is also shown (c). Anterior is to the left, posterior to the right. In a and b, gray lines represent the body outline; black lines represent cell boundaries. In c, the outlines of the rays, phasmid, and fan are depicted, but not the underlying hypodermal cells. The relative positions in which ray cells and their associated Rn.p hypodermal cells are born in the *lateral hypodermis* (schematized in a) are highly conserved in the Rhabditidae so far investigated ([Fitch and Emmons 1995](#)) and probably represent the ancestral condition. This rhabditid developmental ground state (a) thus allows ray homologies to be defined, as denoted by the numerals near clusters of ray cells at early L4 (a), ray structural cells at late L4 (b), or adult rays (c). If the ray structural cells (numbered circles in b) remained at the same positions in which the ray cells were born (a), a hypothetical, default pattern of rays in the adult (c) would arise from *male tail* morphogenesis. Ray patterns in the rhabditid groups represented in Figs. 3 and 8 therefore result from shifts in the positions of the ray cells after they are born in the *lateral hypodermis* ([Fitch and Emmons 1995](#)).

## Figure 8

A portion of the reconstruction of morphological and morphogenetic changes (numbers in boxes on lineages) likely to have occurred during [male tail](#) evolution in the Rhabditidae (adapted from D.H.A. Fitch, in prep.). Hypothetical forms of male tails are constructed for ancestors inferred at the nodes (an L4 stage showing cell boundaries and an adult stage are shown for each taxon). Reconstructed changes: (1) ray 3 adopts a ray-4-like identity and often fuses with ray 4; (2) acquisition of a novel ray 6 morphology (e.g., tapered instead of cylindrical); (3) loss of the ray 8 sublineage (failure of R8 to divide); (4) change in tail tip morphology from blunt (peloderan) to pointy (leptoderan). Respective candidate genetic changes that could have produced these morphological changes are *mab-5(gf)*, a variety of changes such as changes in [\*mab-18\*](#), [\*lin-32\(lf\)\*](#), and [\*lep-1\(lf\)\*](#), where the polarity of the postulated type of genetic change is designated according to conventional genetic notation (i.e., *lf* = loss of function, *gf* = gain of function).

Generated from local HTML

## Chapter 29. Evolution — IV Other Directions

---

[Baird et al. \(1992\)](#) have extended the early investigations by [Osche \(1952\)](#) into the mechanisms of species isolation among the most closely related *Caenorhabditis* species. Using *Caenorhabditis* for such studies obviously takes advantage of *C. elegans* genetics to understand the genetic basis of reproductive isolation. One result has been the reaffirmation of "Haldane's Rule" (hybrid inviability affects the heterogametic sex); further genetic tests can address predictions made from other systems (see, e.g., [Orr 1993](#)).

Hermaphroditism has evolved several times in the history of the Rhabditidae ([Maupas 1900](#); [Potts 1910](#); [Sudhaus 1976](#)), but the evolutionary mechanism for why this reproductive strategy has arisen poses interesting problems at both the genetic level and the population level. Sperm-limited fecundity, as seen in these hermaphrodites, is unusual in Metazoa. Using *C. elegans* mutants in which the timing of the spermatogenesis-to-oogenesis switch varied, [Hodgkin and Barnes \(1991\)](#) showed that the timing of this switch is critical in maximizing population growth rate on a limited resource. The population dynamics have also been modeled ([Barker 1992](#)). One model has been proposed that derives an optimum self-fertile hermaphrodite/male sex ratio and predicts that the *C. elegans* mating system will select for males with promiscuous copulatory behavior and largely "disinterested" hermaphrodites ([Hedgecock 1976](#)). The evolution of sex determination itself poses an enormously interesting problem as well. Although sex determination in flies, worms, mice, and humans involves a clear binary fate decision that is genetically determined, the overall mechanisms are not conserved ([Parkhurst and Meneely 1994](#)), and it is presently unclear how this diversity has evolved.

Ecological and coevolutionary studies of interactions between nematodes and other species have provided classic examples of ecological succession (see, e.g., [Sudhaus 1981](#)), host-parasite specificity (see, e.g., [Mitter and Brooks 1983](#); [Blaxter and Bird](#), this volume), the origins of parasitism (see, e.g., [Sudhaus and Schulte 1988](#)), and so on; but current studies have also focused on interactions involving *Caenorhabditis* species (see, e.g., [Sudhaus 1974](#); [Sudhaus and Kühne 1989](#); [Baird et al. 1994](#)). For example, K. Kiontke (pers. comm.) has shown a highly specific phoretic relationship between a *Caenorhabditis* species and a drosophilid fruit fly. Although identification of the loci involved in determining this interaction is a long way off, it is intriguing to speculate that two genetic model systems could be used to study the evolution of an ecological relationship at the genetic level.

Obviously, many other fundamental parameters of nematode evolution have yet to be explored (with or without *C. elegans* as a model), such as dispersal and gene flow between natural populations, ecological niches and species interactions, and life history strategies.

Generated from local HTML

## Chapter 29. Evolution — V Conclusions

---

Incorporation of *C. elegans* into a phylogenetic picture of the Metazoa reveals deep homologies in a set of building blocks for developmental modules that can be assembled in a variety of ways to construct “endless forms most beautiful and most wonderful.” Convergences are thus possible, and perhaps even likely if a mechanism is highly constrained. Conversely, diverged or analogous developmental mechanisms may underlie homologous features. Taking account of these issues in the context of questions such as “How have living things become what they are, and what are the laws which govern their forms?” (see p. 1 in Bateson 1894) requires *both* an understanding of how structure is determined by developmental genetic mechanisms *and* an understanding of the ways that these structures and elementary mechanisms can and have changed.

Incorporation of a model system into a phylogenetic framework informs both pursuits. We no longer need to be reproached because “those who are in contact with the facts and material necessary for this study care little for the problem, or at least rarely make it the first of their aims, and on the other hand those who care most for the problem have hoped to solve it in another way” (see p. 574 in Bateson 1894). Reconstructing the requisite phylogenetic framework for lineages nearly as deep as Metazoa itself is a daunting task. Yet, in combination with other kinds of phylogenetically informative characters and the biological variation within this enormously diverse phylum, molecular sequences promise to add a fundamentally important information base for approaching such problems.

Although the analysis of worm character evolution in the context of such a phylogeny is not likely to divulge the precise developmental genetic changes that transformed our hominoid ancestors into humans only a few millions of years ago, it will provide models for how evolution works with development to make living forms. From models arise predictions. Only then can we evaluate and incorporate notions about general mechanisms into the body of explanatory principles being built by integrative approaches in biology. Perhaps in this context, Ralph Waldo Emerson's words provide a special perception:

*And, striving to be man, the worm  
Mounts through all the spires of form.  
May-Day (1867)*

Generated from local HTML

## **Chapter 29. Evolution — Acknowledgments**

---

For communication of results before publication and comments on the manuscript, the authors are greatly indebted to Tom Blumenthal, Paul De Ley, Scott Emmons, Jim Garey, Bob Goldstein, Richard Gordon, Tom Johnson, Karin Kiontke, Armand Leroi, Patrick Phillips, Einhard Schierenberg, David Shook, Ralf Sommer, Walter Sudhaus, and an anonymous reviewer.

Generated from local HTML

# **Chapter 30. Parasitic Nematodes**

---

## **Contents**

[I The Nematode World](#)

[II An Introduction to Some Nematode Parasites](#)

[III Antinematode Compounds and Their Targets](#)

[IV The Nematode Surface](#)

[V Parasite Genes and Genomes](#)

[VI Future Prospects](#)

[Acknowledgments](#)

Generated from local HTML

## Chapter 30. Parasitic Nematodes — I The Nematode World

---

Of every five animals on the planet, four are nematodes ([Platt 1994](#)). The vast majority are free-living microbivores, but many species have adopted a parasitic lifestyle. Most plants and animals have at least one parasitic nematode species uniquely adapted to exploit the concentration of food and resources that the host species represents. The reasons for the success of the Nematoda as parasites probably include the presence of an environmentally protective cuticle, facultative diapause (like the dauer stage of *Caenorhabditis elegans*), biochemical adaptations to existence in extreme conditions, and the use of a variety of reproductive strategies. Some parasitic nematodes are the subject of extensive research efforts, often aimed at understanding their lifestyle and ecology so as to control or manage them better.

The choice of the free-living rhabditid *C. elegans* as a model for metazoan development has been fortunate for the study of other nematodes, particularly parasites. Although only distantly related to most parasitic species, *C. elegans* displays the morphological conservatism of the phylum and shares structures found to be important to parasitic species. It also has a characteristic nematode biochemistry and has proved to be sensitive to all the major nematicidal drugs. In this chapter, we first provide an overview of the diversity and importance of parasitic nematodes and subsequently describe three systems where research on *C. elegans* is having a significant impact on parasitology.

Historically, the study of nematodes has fragmented into three major branches (plant nematology, animal parasitology, and free-living nematology) that have had little impact on one another. Plant nematology emphasizes the study of plant pathology and crop protection. Veterinary and human nematode parasitology have been closely linked through the use of model parasite-host combinations in the elucidation of pathogenesis and immunity. Research on free-living nematodes has emphasized taxonomic, ecological, and nutritional studies. Because research on *C. elegans* impinges on all these areas, the three fields are growing closer together while the horizons of traditional nematology are expanding.

Nematodes infect plants and invertebrate and vertebrate animals. The relationships between nematodes and their hosts vary from necromenic association (where the nematode uses the host both to transport it to new food sources and as a source of food upon its death) to complex life cycles involving multiple intermediate hosts. In this spectrum, it is often difficult to distinguish a “true” parasitic lifestyle from that of a predator which invades its food source and devours it from the inside out. *Xiphinema index*, a dorylaimid plant “parasite” that grazes upon plant roots by piercing them with a pharyngeal stylet, remains outside its hosts and moves from root to root. Other plant-eating species, such as *Criconemella xenoplax*, are sedentary ectoparasites. True parasites are mainly internal, in the gut (e.g., *Haemonchus contortus*), in roots (e.g., *Meloidogyne incognita*), or within tissues (e.g., *Brugia malayi*), or even intracellular (e.g., the human-infective muscle-cell parasite *Trichinella spiralis*). Host ranges vary widely. Some animal parasites such as the rhabditid *Heterorhabditis bacteriophora* (which invades insect larvae) are promiscuous and will enter and reproduce in several species, whereas others are exquisitely specific to a single host or host-vector combination. Some nematodes will enter and developmentally arrest in many species (known as paratenic hosts) but will only complete their reproductive cycle in a limited range of hosts (e.g., the ascarid *Toxocara canis* reproduces only in dogs and cats but can infect and cause pathology in many vertebrates including humans).

The phylogenetic relationship of parasitic nematode groups to free-living species such as *C. elegans* remains problematic. Although it is clear that there are relatively easily defined groups of parasites and nonparasites ([Anderson 1992](#)), the morphological conservation within the phylum coupled with remarkable instances of convergence makes deep-level phylogenetics difficult ([Andrássy 1976](#); [Lorenzen 1994](#); [Malakhov 1994](#)). Some species such as *Steinerinema* (insect hosts) and *Strongyloides* (mammalian hosts) are clearly closely related to *C. elegans*, but the relationships of others such as the ascarids and filarids are obscure ([Fig. 1](#)) (see [Fitch and Thomas](#), this volume). Molecular phylogenies have been constructed for local groups, including the rhabditids ([Fitch et al. 1995](#)), ascarids ([Nadler 1992](#)), and filarids ([Xie et al. 1994](#)), but a robust phylum-wide analysis is yet to be performed.

## Figures

Figure 1. Relationships of the nematodes mentioned in this chapter.

### Figure 1

Relationships of the nematodes mentioned in this chapter. Taxonomy taken from [Anderson \(1992\)](#) and [Malakhov \(1994\)](#).

Generated from local HTML

## Chapter 30. Parasitic Nematodes — II An Introduction to Some Nematode Parasites

---

### A. A Rhabditid Pathogen of Insects: *Heterorhabditis bacteriophora*

*H. bacteriophora* is a microbivore that uses an insect host ([Fig. 2](#)) as a nutrient-rich breeding place in which to cultivate symbiotic bacteria ([Gaugler and Kaya 1990](#); [Nealson 1991](#)). Infective L3 larvae (which are functionally analogous to *C. elegans* dauer larvae) invade the insect via the body wall, alimentary canal, or respiratory tree and migrate to the hemocoel, where by defecation or regurgitation they release spores of the bacterium *Xenorhabdus* spp. These bacteria multiply, killing the host and providing a food source for the nematode larvae. *Xenorhabdus* spp. secrete antibiotics that prevent multiplication of other microflora, resulting in a nearly pure bacterial culture. In the presence of sufficient food, L1 larvae develop through four molts (~50 hr at 25°C) into reproductive adults, hermaphrodites, and males. Approximately 300 eggs are produced per hermaphrodite ([Zioni \[Cohen-Nissan\] et al. 1992a](#)). *H. bacteriophora* can be grown monoxenically in fermenters through many generations on *Xenorhabdus* spp. and other bacterial food sources. However, if the food supply is scarce (the usual case after the second generation has matured in the insect carcass), eggs hatch and develop into infective L3 larvae which migrate away from the corpse to actively seek new hosts. The host-seeking behavior includes nictation (raising the head and body in the air and weaving from side to side), a behavior also seen in *C. elegans* dauer larvae and in the infective L3 larvae of many parasitic species. The infective L3 larvae are nonfeeding but carry *Xenorhabdus* spp. with which to infect a new host in specialized structures in the intestine.

*H. bacteriophora*, and species with similar life cycle habits such as *Steinernema carpocapsae*, are being cultivated as biocontrol agents for insect pests of many crops ([Gaugler and Kaya 1990](#); [Glazer et al. 1991](#)) and are commercially available to even the casual gardener. In attempts to improve the infectivity and survivorship of the nematodes, genetic analyses have been initiated ([Glazer et al. 1991](#)), which include isolation of visible mutants ([Zioni \[Cohen-Nissan\] et al. 1992b](#)) and genetic transformation with *C. elegans* markers ([Hashmi et al. 1995](#)).

Other rhabditid parasites also have a facultative switch between multiplicative forms and direct development to infective larvae. In *Strongyloides ratti*, larvae that develop from eggs laid by free-living sexual adults enter the dauer-like infective L3 stage, invade the rat host, and develop into parthenogenetic females ([Viney 1994](#)). L1s of *S. ratti* emerging from the host in feces can either develop directly to infective L3 or produce adults, the progeny of which are committed to develop to the infective L3. This property is under genetic control ([Viney et al. 1992](#)) and is strikingly similar to the dauer developmental pathway in *C. elegans* (see [Riddle](#), this volume).

### B. A Strongylid Gut Parasite of Sheep: *Haemonchus contortus*

*H. contortus*, the sheep barber pole worm ([Fig. 3](#), bottom), is a serious temperate agricultural pathogen ([Smyth 1994](#)). Adult *H. contortus* reside in the host gut where they use a buccal capsule equipped with cuticular teeth to feed on mucosal blood. This can result in anemia and weight loss and can be fatal. Its life cycle is direct, i.e., it does not involve an intermediate vector host ([Fig. 3](#), top).

The host gut is a harsh environment: low oxygen tension, acid pH, digestive enzyme and detergent secretions, and niche competition from both commensal bacteria and other gut parasites. Adaptations to gut life include the development of microaerobic metabolism and the probable use of host blood as both a protein and an oxygen source ([Rogers 1962](#)). Like many gut nematodes, *H. contortus* expresses globins found in its cuticle and muscle. Nematode muscle ([Blaxter et al. 1994b](#)) and cuticle ([Blaxter et al. 1994a](#)) globins have oxygen affinities about 100-fold higher than host hemoglobins, and they act as oxygen transport chains to feed aerobic muscle activity. In addition to myoglobin, the larger ascarids also have pseudocoelomic globins. Their function is more enigmatic, as they have affinities 10,000-fold above that of the host and are thus rarely if ever deoxygenated ([De Baere et al. 1992](#); [Blaxter 1993b](#); [Kloeck et al. 1993b](#)). *C. elegans* expresses a muscle globin isoform very like those found in gut parasites ([Kloeck et al. 1993a](#)).

The infected host can clear *H. contortus* infections naturally through a combination of specific and nonspecific immune responses. Infections can also be cleared by drug treatment, but serious outbreaks of resistance to many drugs, including benzimidazoles and avermectins, have been found in the field ([Prichard 1994](#)). One potentially novel management approach is the development of a vaccine based on nematode gut antigens, which, because they are exposed to host antibody during feeding, are promising targets ([Jasmer et al. 1993; Smith et al. 1993](#)).

Early L4 larvae can arrest development in the host ([Armour and Duncan 1987](#)). This diapause is induced by the onset of winter. The larvae re-enter the growth cycle after overwintering in their host and thus reinfect pasture and new lambs in the first flush of spring. The arrest and escape appear to result from sensing of (host) environmental cues by the larva. Similar sensing of periodic changes in the host environment is also found in other parasites, including the ascarid *Toxocara canis*, where arrested larvae in the tissues of the bitch become activated around day 42 of pregnancy and infect puppies transplacentally ([Lewis and Maizels 1993](#)). In field isolates of the soybean cyst nematode *Heterodera glycines*, the onset of winter (presumably involving growth status of the host plant) also induces diapause in unhatched L2 larvae within the cysts (T. Niblack and G. Tylka, pers. comm.). Exit from arrest and hatching of diapaused cysts requires, in addition to host signals exuded from roots of the subsequent year's crop, a vernalization period.

## C. A Spirurid Parasite of Humans That Causes Lymphatic Filariasis: *Brugia malayi*

The World Health Organization has identified lymphatic filariasis and elephantiasis, caused by the related nematodes *Brugia malayi* and *Wuchereria bancrofti*, as among the most important human tropical diseases, affecting 120 million people ([WHO 1992; Ottesen and Ramachandran 1995](#)). The diseases caused by *B. malayi* and related species are spectral, ranging from acute febrile attacks associated with invasion and establishment of infection to chronic disfiguring disease. Elephantiasis, the gross enlargement of lower and upper limbs and genitals ([Fig. 4, right](#)), is thought to result from a structural failure of the lymphatic system which causes edema, lymph stasis, and permanent limb enlargement. Opportunistic fungal and bacterial infection can take hold, leading to deposition of scar tissue.

The *Brugia* life cycle involves an intermediate vector host, one of several species of mosquitoes ([Fig. 4, left](#)). Microfilariae (or L1) in the blood meal invade the mosquito hemocoel, move to the flight muscles, and mature through two molts to the infective L3 that migrates to the proboscis in preparation for reintroduction to the primary (human) host. The L3 migrate through the skin to the lymphatics, molting twice to become dioecious adults. The adults can survive attack by both nonspecific and specific host immune effectors for many years. One mechanism appears to be epicuticular expression of enzymes (including glutathione peroxidase and superoxide dismutase) that effectively disarm the oxygen radical attack of activated immune effector cells ([Cookson et al. 1993; Tang et al. 1994, 1995; Ou et al. 1995b](#)). One of the characteristics of filarial infected populations is the large proportion of people who harbor active infection (in that they have circulating microfilariae) but have no obvious pathology ([Maizels et al. 1993](#)). Immune responses to the parasite are suppressed in these individuals and progression to disease may be associated with breakage of this tolerance. Understanding the molecular mechanisms underlying immune tolerance may permit effective termination of infection ([Maizels and Lawrence 1991](#)). Current drug treatment for *Brugia* infection is with the microfilaricidal diethylcarbamazine (DEC), which has no effect in vitro, implying that it acts through potentiation of host responses ([Maizels and Denham 1992](#)).

## D. Tylenchid Root-knot Parasites of Plants: *Meloidogyne* spp

Plant-parasitic nematodes reduce the yield of the world's 40 major food staples and cash crops by an average of 12.3% ([Sasser and Freckman 1987](#)), with the root-knot nematodes (*Meloidogyne* spp.) being the main contributors to these losses. Collectively, the members of this genus have a host range of more than 2000 plant species. Their control is essential to maintain intensive crop production, but deregistration of chemical nematicides for environmental or human health reasons threatens to result in unchecked damage in many countries.

Root-knot nematodes are obligate root endoparasites ([Fig. 5](#), left). Larvae hatch in the soil as L2s, invade the root near the tip, and migrate between cells to take up a sedentary position in or near the developing vascular cylinder, where a permanent feeding site is established ([Jones 1981; Wyss et al. 1992](#)). The nematode feeds from up to ten cells using a hollow, extendible stomatostyle ([Fig. 5](#), right), which is used to penetrate the cell wall and withdraw nutrients. In response to as yet unidentified nematode signal(s), those cells are induced to undergo mitosis without cytokinesis and become multinucleate “giant cells” with morphology and ultrastructure indicating a role in nutrient transfer. Analysis of giant cell transcripts suggests that giant cells are a chimeric cell type, with features of developing xylem, transfer cells, and meristematic tissues ([Bird and Wilson 1994a,b; Wilson et al. 1994](#); D. Bird, unpubl.). Genes expressed specifically in giant cells are prime targets for generation of transgenic resistant plants ([Williamson et al. 1992; Opperman et al. 1994b](#); C. Opperman et al., in prep.).

Resistance to animal parasites is often characterized by an immune response, the vigor of which is genetically determined. In plant-nematode interactions, there is clear demonstration of similar interactions between the genotypes of host and parasite, and this is exploited in the breeding of resistant plants. The plant resistance reaction typically is an induced necrosis of the feeding site with the elaboration of reactive oxygen species and other enzymatic defenses. Several resistance genes from plants active in rejection of bacterial and fungal pathogens have been isolated ([Staskawicz et al. 1995](#)). Loci determining resistance to nematode infection have been mapped in plant genomes ([J.Y. Ho et al. 1992](#)), and their characterization is expected in the near future.

*Meloidogyne* species are dioecious, although males of most agriculturally important species are uncommon in the wild. Reproduction is typically parthenogenetic; only a small number of obligatorily amphimictic species have been described ([Triantaphyllou 1985](#)). Parthenogenesis can involve a meiotic event (e.g., *M. hapla* and *M. chitwoodi*), in which the egg absorbs the second polar body to restore diploidy, or through apomixis, where there is no meiotic reduction. In the latter case (e.g., *M. arenaria*, *M. javanica*, and *M. incognita*), mitotic divisions generate a binucleate oocyte from which embryogenesis proceeds directly. In some species (e.g., *M. hapla*), parthenogenesis is clearly facultative, but it remains a subject of debate as to whether fecund matings ever occur for the apomictic species. The parthenogenetic mode is perhaps a reason why it has been possible to develop cell lines from *Meloidogyne* ([Manoussis and Ellar 1990](#)).

## Figures



### Figure 2

Life cycle of *H. bacteriophora*. Each side of the hexagon represents a life cycle stage, with the corners the molts/hatching. The parallel lines indicate a period of developmental arrest (comparable to the *C. elegans* dauer larva). The internal circular arrow shows the time taken to complete development at 25°C ([Zioni \[Cohen-Nissan\] et al. 1992a](#)).



### Figure 3

(Top) Life cycle of *H. contortus*. Conventions are the same as those in [Fig. 2](#): the shaded part indicates the free-living portion of the cycle. (Bottom) An adult female *H. contortus* isolated from sheep intestine (photograph courtesy of E. Munn). The twisted gut and gonad that give this species its name is visible.



### Figure 4

(Left) Life cycle of *B. malayi*. Conventions are the same as those in [Fig. 2](#): the shaded part indicates the portion of the cycle in the mosquito vector. (Right) The effects of filarial infection: elephantiasis of the lower leg

(photograph courtesy of S. Williams). (*Inset*) Microfilariae (L1s) that circulate in the blood. Bar, 100  $\mu\text{m}$ .  
(Photograph courtesy of B. Gregory.)

Figure 5. (Left) Life cycle of *Meloidogyne* spp.

## Figure 5

(Left) Life cycle of *Meloidogyne* spp. Conventions are the same as those in [Fig. 2](#); the shaded part indicates the portion of the cycle spent in the soil. (Right) Longitudinal section through the head of a *Meloidogyne incognita* L2 migrating in roots of red clover. Part of the lumen of the 16- $\mu\text{m}$  long, fully retracted stomatostyle (stylet) is visible. Two of the three stylet protractor muscle groups, each attached at one end to one of the three knobs at the base of the stylet, are apparent. (Reprinted, with permission, from [Endo and Wergin 1973](#).)

Generated from local HTML

## Chapter 30. Parasitic Nematodes — III Antinematode Compounds and Their Targets

---

The negative impact of nematodes on human and animal health and nutrition has resulted in an active search for effective nematicides. These drugs are often active against all nematodes rather than just the indicator species, and thus the search for improved compounds can use free-living species such as *C. elegans*. Although space does not permit consideration of all drugs and targets, two systems are described here where *C. elegans* research has had an impact on the understanding of drug action.

### A. Benzimidazoles

The benzimidazoles (BZ; e.g., thiabendazole, benomyl, and mebendazole) disrupt microtubule assembly by binding to the nucleotide-binding site of specific isotypes of  $\beta$ -tubulin. They are potent nematicides in use worldwide for treatment of gut nematode infections of humans and domestic animals. Tissue-dwelling filarial parasites are unaffected. *C. elegans* is BZ-sensitive, and BZ-resistant lines have been obtained by mutagenesis ([Driscoll et al. 1989](#)). All of the BZ-resistant lines tested were mutant at a single locus ([\*ben-1\* III](#)) which encodes a  $\beta$ -tubulin. Although [\*ben-1\*](#) mutants are wild type in the absence of drug, a number have gene deletions, suggesting that [\*ben-1\*](#) is a dispensable gene. These observations have important implications for the generation of resistance in economically important species. If the BZ target is dispensable, the generation of resistance might be a relatively frequent event in natural populations.

Genetic resistance to BZ and derivatives is increasingly common in the field ([Prichard 1994](#); [Roos et al. 1995](#)). In *H. contortus*, field resistance is associated with a rise in the population frequency of restriction fragment length polymorphisms (RFLPs) linked to particular  $\beta$ -tubulin isotype I alleles and a loss of heterozygosity ([Roos et al. 1990](#)). This correlates with a biochemical loss of high-affinity BZ-binding sites, and an increase in low-affinity sites, in tubulins prepared from parasites ([Lacey and Gill 1994](#)). Similar changes occur under in vitro selection regimes ([Kwa et al. 1993](#); [Roos et al. 1995](#)). Comparison of an *H. contortus*  $\beta$ -tubulin isotype I gene (*Hc tub-1*) from European BZ-sensitive and BZ-resistant isolates revealed a substitution of phenylalanine (sensitive) for tyrosine (resistant) at residue 200, near a segment of the nucleotide-binding site ([Kwa et al. 1994](#)). An equivalent mutation has also been seen in BZ-resistant fungi. Thiabendazole-resistant [\*ben-1\*](#) *C. elegans* can be rescued (to sensitivity) by transformation with the drug-sensitive allele of *Hc tub-1*, although the rescued animals remain resistant to benomyl ([Kwa et al. 1994, 1995](#); [Roos et al. 1995](#)).

*C. elegans* may be an effective test-bed for next-generation BZ derivative testing ([Roos et al. 1995](#)), but this assertion must be tempered by the realization that the level of susceptibility of *C. elegans* to BZ is on the order of that of resistant strongylid nematodes. The strongylids have additional high-affinity sites that bind BZ stably at 37°C, whereas *C. elegans* tubulin fractions bind BZ only at lower temperatures ([Russell and Lacey 1991](#)). Intestinal parasites (ascarids and strongylids) are also much more sensitive to BZ than are the tissue-dwelling filarids, and this may be related to the different routes of nutrition in these two groups. The gut of the intestinal parasites is well developed, and gut cell microtubule arrays may be the significant site of action of BZ in these species ([Kohler and Bachmann 1981](#)). The filarids have atrophied guts and obtain a significant portion of their nutrition transcuticularly (see below) ([Chen and Howells 1981](#); [Howells and Chen 1981](#)).

### B. The Avermectins

The avermectins (AVMs) are semisynthetic derivatives of fungally derived macrocyclic lactones ([Putter et al. 1981](#)) which are effective against many invertebrates including nematodes ([Rohrer and Schaeffer 1995](#)). They are widely used for veterinary treatment of gut parasites and treatment of human river blindness caused by the filarial *Onchocerca volvulus* ([Bennett et al. 1988](#)) and are also effective against plant-parasitic species ([Sasser et al. 1982](#)). AVMs appear to act through the inhibition of a glutamate-gated chloride channel present on muscle cells ([Cully et al. 1994](#)). These compounds inhibit pharyngeal pumping at  $\geq 10^{-10}$  M and affect general motility at  $\geq 10^{-8}$  M

([Avery and Horvitz 1990](#); [Holden-Dye and Walker 1990](#); [Geary et al. 1993](#)). Chloride channels of  $10^{-11}$  to  $10^{-10}$  M sensitivity have been described from isolated somatic muscle cells of *Ascaris suum* ([Martin and Pennington 1989](#)). At higher concentrations, inhibitory GABA responses are also blocked ([Holden-Dye and Walker 1990](#)). The effect of AVMs on gut parasites may be through a specific blockage of the pharyngeal pump rather than general paralysis.

*C. elegans* can readily be mutated to give an [AVM](#)-resistant phenotype, Avr ([Novak 1992](#); C. Johnson, pers. comm.). The most common phenotype observed is that of low-level resistance. Such mutations are recessive and map to more than 20 loci. Detailed genetic mapping showed that [avr-1](#) is allelic to a previously known locus, [che-3](#), and that [avr-5](#) is allelic to [osm-3](#). The [che-3](#) and [osm-3](#) animals are defective in dye filling of amphid and plasmid [neurons](#) and chemotaxis and fail to avoid high osmolarity due to defects in their ciliated [neurons](#) ([Perkins et al. 1986](#); [Stravich et al. 1995](#)). Examination of nematode strains carrying mutations at other [avr](#) loci showed that many of these also displayed amphid defects, such as the Df (dye-filling negative) phenotype (C. Johnson, pers. comm.). The [avr-1](#) gene has been cloned and shown to encode a cytoplasmic dynein (W. Grant, pers. comm.), presumed to be active in amphidial neuronal transport processes. [AVM](#)-resistant parasitic nematodes, which can be readily generated by laboratory selection ([Echevarria 1993](#)), are becoming a serious threat in the real world ([Prichard 1994](#)). Like *C. elegans* Avr lines, [AVM](#)-resistant *H. contortus* have [AVM](#)-binding sites identical to those of wild type ([Rohrer 1994](#)). The anatomical correlation between the observed site of highest sensitivity to [AVM](#) in parasitic species (the pharyngeal musculature) and the site of action of [avr](#) mutants ([amphid neurons](#)) is interesting. Two models can be envisaged, one in which the amphid defects prevent access of the drug to a periamphidial essential site (C. Johnson, pers. comm.) and another in which the [amphid neurons](#) affected by the mutations inhibit the [pharynx](#) in wild-type animals in the presence of [AVM](#), and genetic ablation of these [neurons](#) results in insensitivity to the drug (T. Geary, pers. comm.). It is reassuring to note that mutations conferring high-level or dominant resistance in *C. elegans* are rare (C. Johnson and P. Hunt, pers. comm.); hopefully, the same is true of parasitic species.

In gut parasites such as *H. contortus*, AVMs are adultcidal. However, adult filariae are relatively resistant, and the main effect is against microfilariae (L1s). Both adults and microfilaria have atrophied guts, and most nutritional exchange is across the cuticle ([Chen and Howells 1981](#); [Howells and Chen 1981](#)). Gut-dwelling species also use this route ([Ho et al. 1990](#), 1992; [Geary et al. 1993](#)), but the significance of transcuticular exchange in *C. elegans* and other free-living species is an open question. As AVMs have no lethal effect in vitro on microfilariae, their action may be through potentiation of a host attack or down-regulation of a parasite defense (as is also noted for another antifilarial drug, DEC [[Maizels and Denham 1992](#)]). The lack of activity against the macrofilariae (adults) of important human (e.g., *Onchocerca*, *Brugia*) and veterinary (e.g., *Dirofilaria immitis*, the dog heartworm) parasites is puzzling and is inspiring a search for both the mechanism of relative resistance in these stages and the development of active analogs.

Generated from local HTML

# Chapter 30. Parasitic Nematodes — IV The Nematode Surface

---

Nematode surfaces are targets for passive and active environmental assault, including attacks by the immune system of a host, the attachment of bacterial spores and fungal traps, and extremes of desiccation or salinity. The cuticle must therefore play a part in defense, and the biosynthesis and maintenance of the cuticle surface are of central importance ([Bird and Bird 1991](#)). For many drugs, it would appear that the hypodermal membrane is the diffusion-limiting structure ([Ho et al. 1990; Geary et al. 1995](#)). For attacking pathogens, cells, antibodies, or protein effectors, the perceived surface can be the surface coat, the epicuticle, or outer structural layers. We review here the nonstructural components of the cuticle; the structural components are described elsewhere ([Kramer 1994b](#); see [Kramer](#), this volume).

The cuticle is an acellular, dynamic, biochemical compartment, rather than a simple inert exoskeleton. The external plasma membrane of a nematode is that of the hypodermis (epidermis), but the cuticle is enveloped by the membrane-like epicuticle ([Wright 1987](#)). The cuticle is reconstructed at each molt, but pulse-chase labeling demonstrates continuous production and export of surface components, and transcripts for both collagen and noncollagenous proteins are found in intermolt and molting animals ([Selkirk et al. 1989, 1990; Johnstone 1992; Johnstone et al. 1994; Gems et al. 1995](#)).

## A. The Surface Coat

The surface coat or glycocalyx lies external to the epicuticle ([Blaxter et al. 1992; Spiegel and McClure 1995](#)). It can vary widely in apparent thickness both between species and between life cycle stages in a species. Surface coats can be seen with the transmission electron microscope, either in negative stains or after staining with cationic ferritin or ruthenium red, and they have been demonstrated in most species examined ([Bird and Bird 1991](#)). The coat in *C. elegans* is~ approximately 5 nm thick and is seen in all stages ([Zuckerman et al. 1979; Jansson et al. 1986](#)). The surface coat is dynamic in that components appear to be synthesized continuously ([Page and Maizels 1992](#)), and coat material is readily shed on environmental or antibody insult. The surface coat of *T. canis* larvae is synthesized in pharyngeal and [excretory](#) glands and thus voided through the [mouth](#) and [excretory pore](#). Transcuticular secretion of surface coat components also occurs in *T. canis* and *Heterodera schachtii* ([Aumann et al. 1991; Endo and Wyss 1992](#)).

The surface coats of nematodes are polyanionic (probably due to sulfate or phosphate groups) and contain carbohydrate and mucin-like proteins ([Zuckerman et al. 1979; Himmelhoch and Zuckerman 1983; Jansson et al. 1986; Page et al. 1992](#)). The composition of the *C. elegans* coat is not known in detail, but it probably includes the O-glycosylated target of the antibody M38 ([Table 1](#)) ([Hemmer et al. 1991; Politz and Philipp 1992](#)). Other candidates for components of the *C. elegans* coat are the products of the Exc mutants. These mutants have degenerate or pathological changes in the [excretory](#) cell ranging from swelling of the lumen into cysts (e.g., [exc-1](#) and [let-653](#)) to the formation of multiple lumens (e.g., [exc-3](#)). The lumen of the [excretory](#) cell has a well-developed surface coat, and the [let-653](#) gene product is a serine/threonine-rich protein with similarities to mammalian cell surface mucins ([Jones and Baillie 1995](#)). In infective larvae of the ascarid *T. canis*, the coat is made up of a small number of proteoglycans and mucin-like glycoproteins that share carbohydrate determinants ([Maizels and Page 1990](#)). The structure of this O-glycan has been solved and contains novel sugar linkages ([Khoo et al. 1991](#)). The major coat component ( $M_r$  120,000) is a mucin-like protein containing 12 seven-amino-acid repeats rich in serine ([Gems et al. 1995](#)). An *M. incognita* adult-specific cDNA from the [excretory gland](#), encoding a mucin-like protein, may be part of the surface coat (D. Bird and T.-J. Chen, unpubl.).

*C. elegans* wild-type cuticles bind few if any lectins (the [male tail](#) binds WGA and SBA at low levels, as does the vulval slit in hermaphrodites [[McClure and Zuckerman 1982; Zuckerman and Kahane 1983; Link et al. 1988, 1992](#)]). Attachment of the spores of some nematophagous fungi is confined to sensory openings and the [vulva](#) ([Barron 1977; Jansson 1994](#)). This absence of reactivity may reflect the relative success of a survival strategy whereby the information content of the surface is reduced, rendering it biochemically invisible to sensory or adhesive products of predators and parasites. Active shedding of the coat by animal parasites is thought to be

an adaptive defense against immune attack ([Blaxter et al. 1992](#)). The same may be true for free-living species avoiding the adhesive traps and spores of fungi and bacteria. A dispensable coat may slough off attached molecules (and thus cells, spores, or traps) and act as a dispensable sink for enzymatic effector mechanisms. Shed material may then act as a decoy to divert attention from the corpus of the organism.

In contrast, the surfaces of plant-parasitic nematodes bind a range of lectins, often (depending on the species) in specific temporal and spatial patterns ([Spiegel and McClure 1995](#)). Carbohydrate-binding, lectin-like activity is expressed on the surface of *M. javanica* L2s ([Spiegel et al. 1995](#)). Many plant-parasitic nematodes avoid eliciting host defense or wound responses even during the invasion and migratory phases, or when resident in the host (see [Fig. 5](#), left). It is possible that the surface coat mimics host self-identity, as antibodies raised to the *M. incognita* surface specifically cross-react with host phloem cells ([Bird and Wilson 1994b](#)) and the major surface coat glycan of *T. canis* resembles the host LewisX determinant ([Khoo et al. 1991](#)).

## B. The Epicuticle

The epicuticle is an electron-dense layer at the exterior boundary of the cuticle visible in negatively stained sections of nematodes. It has the appearance of a trilaminar plasma membrane but is usually significantly wider (6–40 µm). In freeze-fracture studies of many secernentean species, the outer leaflet appears smooth, whereas the inner leaflet has sparse “intramembranous” particles ([de Souza et al. 1993; Lee et al. 1993; Peixoto and de Souza 1994](#)). The *C. elegans* dauer epicuticle differs by having particles in the outer leaflet ([Peixoto and de Souza 1994](#)). Transcuticular uptake of nutrients and drugs by *Brugia* and *Ascaris* suggests that the epicuticle may not be a homogeneous or complete lipid barrier ([Howells 1983; Ho et al. 1990](#), 1992). In many enoplidian (adenophorean) nematode species, especially marine free-living ones, the cuticle and epicuticle contain microscopic pores ([Bird and Bird 1991](#)).

The epicuticle is the first new layer to be laid down during molting ([Lee 1970; Wright and Hong 1989](#)). Whether or how it is replenished during the intermolt periods is unknown. The epicuticle contains lipid. Surface labeling studies using IODOGEN reagent (which attaches radioiodine to unsaturated lipids) reveal that the epicuticular lipid is a distinct subset of the total lipid of the nematode and also that it varies with life cycle stage ([Scott et al. 1988; Blaxter 1993a](#); M. Blaxter, unpubl.). Unlike mammalian cells, there appears to be no glycolipid on the surface of *C. elegans* ([Blaxter 1993a](#)), but glycolipids have been described from whole lipid extracts of *C. elegans* ([Chitwood et al. 1995](#)), *Ascaris suum*, *Nippostrongylus brasiliensis* ([Dennis et al. 1995](#)), and *O. volvulus* ([Maloney and Semprevivo 1991](#)).

Like more conventional membranes, the epicuticle will take up tagged lipid analogs from the surrounding medium in vitro ([Kennedy et al. 1987](#)), and a model of the organization of the epicuticle has been produced (Proudfoot et al. 1990, 1991). Adults of *C. elegans* and many parasitic species selectively take up 18-carbon aliphatic lipids but not analogs with shorter chain lengths. The headgroup of the C18 lipid must be anionic ([Kennedy et al. 1987; Proudfoot et al. 1991](#)). The mobility of these inserted lipids, measured by fluorescence recovery after photobleaching, is low in parasites compared to that seen in mammalian plasma membranes ([Kennedy et al. 1987](#)). In contrast, the nonpolar lipid probe NBD-cholesterol readily inserts into the adult parasite epicuticle and is laterally mobile ([Proudfoot et al. 1991](#)). Adult *C. elegans* show nearly unrestricted lateral mobility ([Proudfoot et al. 1991](#)), but dauer larvae (and infective larvae of many vertebrate parasites) are refractory to lipid probe insertion ([Proudfoot et al. 1991](#)). This may have a role in resistance to desiccation. One of the earliest biological markers of exit from the dauer stage in *C. elegans* is a change in surface lipophilicity. By 30 minutes after exposure to food, long before the molt to L4, the dauer surface starts to accept lipid probes ([Proudfoot et al. 1991, 1993b](#)). In parasites, a similar change is observed when arrested infective larvae encounter their definitive host (Proudfoot et al. 1991b). For filarial nematodes, the change is more rapid than that seen in *C. elegans* and can be triggered by exposure to host-like pH, carbon dioxide concentrations, or temperature ([Proudfoot et al. 1991](#)). There is evidence for the involvement of second-messenger-mediated signaling in the control of this event ([Proudfoot et al. 1993a](#)).

## C. Noncollagenous Proteins at the Nematode Surface

Antisera from experimental and natural hosts and surface-directed labeling techniques have been used to identify noncollagenous "surface antigens" in many parasitic species. These proteins may have roles in nutrition, defense, or cuticle maintenance. The diversity of surface proteins of nematode parasites is low compared to that seen on mammalian cells and may reflect a necessity to avoid the immune response. In the best known system, *Brugia malayi*, several of these surface proteins have been cloned and shown to encode products with recognizable functions.

The major surface glycoprotein of *B. malayi* adults is an *N*-glycosylated glutathione peroxidase (GPX) homolog ([Maizels et al. 1989](#); [Cookson et al. 1992](#)) which is made in the hypodermis and secreted through the cuticle ([Selkirk et al. 1990](#)). The filarial GPX is inactive against hydrogen peroxide but is active against lipid peroxides ([Tang et al. 1995](#)) and is thus well placed to protect the epicuticle from peroxidative disruption. Tissue-dwelling parasites are exposed to a chemical arsenal that can do severe damage to membrane lipids ([Selkirk et al. 1993](#)). A second protein on the filarial surface is a secreted superoxide dismutase that is presumed to eliminate superoxide generated by the lipoperoxidase ([Tang et al. 1994](#); [Ou et al. 1995a](#)). The homolog of a third *B. malayi* surface protein was first cloned from the related cutaneous filarid *O. volvulus* ([Lustigman et al. 1992](#)) and is similar to cystatin proteinase inhibitors. It may be involved in cuticle maintenance or in abrogating the effects of proteases released by immune effector cells. An abundant complex of proteins from *B. malayi*, called the nematode polyprotein antigen (NPA) ([McReynolds et al. 1993](#)), has homologs in *Ascaris suum*, where it is the most abundant protein of the pseudocoelomic fluid and is not surface located ([McGibbon et al. 1990](#); [Spence et al. 1993](#)), and in *C. elegans*, where the location is unknown (J. Moore and M. Blaxter, unpubl.). The NPAs are lipid carrier proteins ([Kennedy et al. 1995](#)) and are highly allergenic in *Ascaris* infections ([McGibbon et al. 1990](#)). They are made as large (>350 kD) polyproteins and then cleaved at tetrabasic protease sites to give 15-kD monomers ([Poole et al. 1992](#); [Paxton et al. 1993](#)). In *B. malayi*, the processing is incomplete, resulting in a ladder of monomer, dimer, etc. ([Tweedie et al. 1993](#)). Homologs of all these filarial surface proteins have been isolated from *C. elegans* or identified in the genome or cDNA sequence (M. Blaxter, unpubl.).

In vertebrate parasitic species, the antigenicity and pattern of proteins present at the surface change during development. Surface properties can change at each molt or within one intermolt on timescales ranging from days to minutes ([Maizels et al. 1983a,b](#); [Philipp and Rumjanek 1984](#); [Proudfoot et al. 1993a,b](#)). These changes correspond to developmental events in the nematode and the generation of immune responses in the host and have been suggested to be part of an immune evasion mechanism ([Philipp et al. 1980](#)).

In *C. elegans*, the cuticles of different stages are morphologically distinct and contain distinct sets of collagens ([Cox et al. 1981c](#), [1989](#); [Politz and Edgar 1984](#)) and cuticlin ([Sebastiano et al. 1991](#)). Surface labeling of *C. elegans* N2 adults with the nonpenetrating IODOGEN reagent reveals a simple pattern of surface proteins ([Politz et al. 1990](#); [Blaxter 1993a](#)). Each stage has a distinct set of surface molecules ([Table 1](#)) revealed by antibody binding ([Politz et al. 1987](#); [Hemmer et al. 1991](#)) and surface radioiodination profiles ([Politz et al. 1987](#); [Blaxter, 1993a](#); M. Blaxter, unpubl.). In particular, the dauer larva and the post-dauer L4 cuticle express the same surface proteins, but the post-dauer adult reverts to the normal pattern ([Table 1](#)) (M. Blaxter, unpubl.). The dauer-like surface phenotype of post-dauer L4s adds to data suggesting that this stage is not identical to directly developed L4 ([Liu and Ambros 1989](#); [Kramer 1994a](#)). The finding that the free-living *C. elegans* also changes its complement of surface proteins (and antigenicity) suggests that modulation of the surface is a basic part of the nematode developmental program, albeit one that may have been exploited by successful parasites to evade the host. The *C. elegans* cuticle is an excellent model for understanding parasitic species ([Politz and Philipp 1992](#)). As most parasites are dioecious (and probably highly heterozygous) and brood sizes can be large, it is likely that significant antigenic polymorphism could be selected under immune pressure, but neither the existence of such polymorphism nor its importance has been assessed. The *C. elegans* locus *srf-1* determines adult cuticular surface reactivity to an antibody raised against cuticle material; polymorphism at this locus has been detected in wild populations ([Politz et al. 1987](#)). Such variation may reflect selection by predators.

## D. Genes Controlling Surface Identity in *C. elegans*

The Srf phenotype is defined by changed reactivity at the surface to antibody or lectin reagents in the absence of morphological disruption of the cuticle ([Table 2](#)). The *srf* loci can be divided into three groups. The first group, composed of [\*srf-1\*](#), [\*srf-2\*](#), [\*srf-3\*](#), and [\*srf-5\*](#) mutants ([Politz et al. 1987, 1990](#); [Link et al. 1988, 1992](#)), has only cuticle phenotypes that arise from the novel exposure of antibody epitopes or lectin-binding sites at the cuticle surface. The structure of the cuticle is otherwise intact, except in the [\*srf-3\*](#) dauer larva which is abnormally SDS-sensitive. Surface coat or epicuticle lipid composition is changed ([Blaxter 1993a](#)), but there is no change in detergent- or 2-mercaptoethanol-soluble WGA-binding glycoproteins (M. Silverman et al., unpubl.). The [\*srf-2\*](#), [\*srf-3\*](#), and [\*srf-5\*](#) L1 larvae do not bind the M38 antibody (S. Politz, pers. comm.). These *srf* mutations also abrogate expression of the radioactively labeled 6.5/12.5-kD species. The phenotype can be modeled as the loss of a masking or overlying layer which reveals moieties present but unavailable to extrinsic reagents in the wild-type cuticle.

The second group is composed of the pleiotropic *srf* loci, [\*srf-4\*](#), [\*srf-8\*](#), and [\*srf-9\*](#), that share an additional suite of defects in both internal and external structures. These include protruding vulvae and a low-penetrance multivulval phenotype (see [Greenwald](#), this volume), male infertility, probably due to distorted copulatory bursae and abnormal spicules (see [Emmons and Sternberg](#), this volume), defects in gonadal morphology, distortion of body shape, and uncoordinated movement (muscle cells are normal, but defects in [neural](#) cell projections were noted) ([Link et al. 1992](#)). These loci may be involved in secretion or specification of external matrix, both apically (cuticle) and basally (basement membranes). The internal defects would then arise from misrouting or misspecification of position, and the cuticle defects from misexpression of integral cuticle proteins ([Link et al. 1992](#); see [Kramer](#), this volume).

The third group of *srf* mutations affects the timing of surface antigen expression. Mutations in [\*srf-6\*](#) result in the inappropriate expression at later larval stages of an antigen that is normally present only on L1 larvae. No other Srf-6 phenotype has been detected. Certain temperature sensitive dauer-constitutive (Daf-c) mutants are also in this class, revealing a link between dauer larva development and surface antigen switching. Heterochronic expression of the L1 antigen by these mutants is independent of dauer larva formation. Some genes affect both surface antigen switching and dauer larva formation (e.g., [\*daf-1\*](#) and [\*daf-4\*](#)), whereas other gene activities (e.g., [\*srf-6\*](#) and [\*daf-12\*](#)) are process-specific (see [Riddle](#), this volume). Continued expression of the O-glycoprotein is probably due to failure of the switch from the L1 to the L2 cuticle type and similar controls may underlie both dauer- and cuticle-type switching ([Hemmer et al. 1991](#); S. Politz, pers. comm.).

## Tables

**Table 1** Surface markers of *C. elegans*

Stage	Surface proteins identified with IODOGEN			Anti-surface reagents	
	6.5 kD/12 kD	80 kD	37 kD	M38	WGA/SBA
Normal development					
L1	+	-	-	+	-
L2	+	+	-	-	-
L3	+	+	-	-	-
L4	+	+	-	-	-
adult hermaphrodite	+	-	-	-	+ vulva
adult male	+	-	-	-	+ bursa
Dauer development					
L2d	+	+	-	-	-
dauer	-	-	+	-	-
post-dauer L4	-	-	+	-	-

**Table 2**The phenotypes of *srf* mutants of *C. elegans*

		Antibody/lectin phenotypes					Surface radiolabeling	Other	
Locus		WGA	SBA	Ab117 <sup>a</sup>	M38 <sup>b</sup>	Other	phenotypes <sup>c</sup>	phenotypes	Reference
Wild type	-	vulva, bursa	vulva, bursa	vulva, bursa	L1s only	-	heterodimer +ve	-	
<i>srf-1</i>	II	-	-	n.d.	n.d.	adults do not label with anti-wild- type adult serum	heterodimer -ve changed surface lipid,	none	<a href="#">Politz et al. (1987)</a>
<i>srf-2</i>	I	+	+	whole cuticle	no binding	express masked epitopes as larvae and adult	heterodimer -ve changed surface lipid	none	<a href="#">Politz et al. (1990)</a>
<i>srf-3</i>	IV	+	+	whole cuticle	no binding	express masked epitopes as larvae and adults	heterodimer -ve changed surface lipid	dauer SDS-s <sup>d</sup>	<a href="#">Politz et al. (1990); Link et al. (1992)</a>
<i>srf-4</i>	V	+	+	whole cuticle	L1s only		heterodimer -ve changed surface lipid	Vul, Muv <sup>e</sup> , Mab, Egl, <sup>f</sup> Unc, <sup>g</sup> , dauer SDS-s	Link et al. (1992)
<i>srf-5</i>	X	+	+	whole cuticle	no binding		heterodimer -ve changed surface lipid	none	Link et al. (1992)
<i>srf-6</i>	II	n.d.	n.d.	n.d.	all stages		n.d.	ts Daf <sup>h</sup>	<a href="#">Hemmer et al. (1991)</a>
<i>srf-8</i>	V	+	+	whole cuticle	L1s only		heterodimer -ve changed surface lipid	Vul, Muv, Mab, Egl, Unc, dauer SDS-s	Link et al. (1992)
<i>srf-9</i>	V	+	+	whole cuticle	L1s only		heterodimer -ve changed surface lipid	Vul, Muv, Mab, Egl, Unc, dauer SDS-s	Link et al. (1992)

n.d

indicates not determined.

a

[Link et al. \(1988\)](#); <sup>b</sup>[Hemmer et al. \(1991\)](#); S. Politz (pers. comm.); <sup>c</sup>[Politz et al. \(1990\)](#); [Blaxter \(1993a\)](#).

d

Dauer larvae do not survive 1 hour treatment with SDS.

e

Protruding vulvae, low penetrance multivulval.

f

Male infertility due to misformed bursa, gonadal abnormalities.

g

Uncoordinated movement, defective [neural](#) projections.

h

Temperature-sensitive dauer formation at 25°C.

Generated from local HTML

# Chapter 30. Parasitic Nematodes — V Parasite Genes and Genomes

---

One of the major contributions to parasitology made by *C. elegans* research has been the ready availability of homologs and paralogs of genes of interest in a tractable genetic model. Gene cloning from most parasites is in its infancy and is frequently led by the availability of probes from *C. elegans*. Often the closest or only homolog of a parasite gene, chosen for serodiagnostic or vaccine potential, is an otherwise anonymous open reading frame or cDNA from the genome project. For example, the closest homologs of *O. volvulus* Ov20, a component of a candidate multisubunit river blindness vaccine, are the *C. elegans* genes [F02A9.2/3](#), which are expressed in [body wall muscle](#) ([Tree et al. 1995](#)). Other *C. elegans* homologs are helping to elucidate the functions of filarial surface antigen genes ([Cookson et al. 1993](#); [Paxton et al. 1993](#)) and vaccine candidates ([Limberger and McReynolds 1990](#)).

## A. Parasite Genomes

Parasitic nematodes have genome sizes broadly similar to that of *C. elegans*. Some, such as *Meloidogyne* spp. genomes, appear to be a little smaller ([Pableo et al. 1988](#)), whereas others, such as the *B. malayi* genome, are a little larger. The *B. malayi* genome has a greater content of repetitive DNA than does *C. elegans*, 27% versus 17% ([Maina et al. 1987](#)), including 10,000 copies of a 322-bp tandem repeat, comprising 12% of the genome and arranged at~ approximately four loci ([McReynolds et al. 1986](#); [Williams et al. 1987](#)). Many filarids have a markedly skewed DNA base composition with as little as 27% GC (compared to 36% in *C. elegans*). Several animal parasites (ascarids) undergo programmed chromatin diminution, which involves the fragmentation of chromosomes in [all somatic cells](#) and the amplification of specific subchromosomal fragments ([Tobler et al. 1992](#); [Goday and Pimpinelli 1993](#); [Müller 1995](#)). These nematodes discard much of their highly repetitive DNA in the soma, but some single-copy genes are also eliminated ([Aeby et al. 1986](#); [Etter et al. 1991](#)).

Other aspects of parasitic nematode gene number, organization, and expression are well modeled by *C. elegans*. Introns tend to be short, although a preponderance of very short introns (37–80 bases) is not observed. As in *C. elegans* ([Krause and Hirsh 1987](#)), most parasitic nematode genes appear to use the universal spliced leader mini-exon (SL1) ([Joshua et al. 1991](#); [Tackacs et al. 1988](#); [Nilsen et al. 1989](#); [Blaxter et al. 1994b](#); [Blumenthal and Steward](#), this volume), and this feature has been used to construct full-length cDNA libraries using reverse transcriptase–polymerase chain reaction (RT-PCR) with SL1 and oligo(dT) primers from minimal quantities of parasite mRNAs ([Martin et al. 1995](#); [Scott et al. 1995](#); [Yenbutr and Scott 1995](#)). Neither operons ([Spieth et al. 1993](#); [Blumenthal and Speith 1995](#)) nor alternate spliced leaders such as SL2 ([Huang and Hirsh 1989](#); [Ross et al. 1995](#)) have yet been demonstrated in parasitic nematodes.

## B. Parasite Genome Projects

The *C. elegans* expressed sequence tag (EST) projects ([McCombie et al. 1992](#); [Waterston et al. 1992](#); see [Waterston et al.](#), this volume) have proven to be very effective sources of genetic information. A similar approach is being applied to the filarial parasite *B. malayi* to overcome a bottleneck in the discovery of new genes. cDNA libraries derived from the infective L3, the adult, and the microfilaria (L1) have been sampled and more than 1000 partial cDNA sequences have been obtained (M. Blaxter et al., unpubl.; S. Williams and B. Slatko, pers. comm.). Approximately 50% of the *C. elegans* cDNA sequences have no clear homologs in the databases. It might be expected that a significant proportion of these will be nematode-specific genes involved in the machinery of being a nematode, and the *B. malayi* dataset may contain homologs of otherwise anonymous *C. elegans* genes. As expected, a significant number of the *B. malayi* cDNAs are most similar to otherwise anonymous *C. elegans* genes, and a significant dataset of homologs is being assembled. Small EST cDNA-sequencing projects have also been initiated for root-knot and soybean cyst nematodes (C.H. Opperman, pers. comm.). In vertebrate species, synteny, or the similarity in gene linkage relationships, has been a powerful tool for genome initiatives. The degree of synteny between different nematode genera and families is unknown, but molecular evidence suggests deep divergence ([Vanfleteren et al. 1994](#); see [Fitch and Thomas](#), this volume). The EST data from parasitic species will allow comparison with *C. elegans* at this genomic level.

Gene identification in plant-parasitic nematodes has emphasized functions pertinent to agricultural concerns. Of particular interest are parasite genes able to confer a host-resistance breaking phenotype (virulence). Such loci not only are important in the field (where they specify nematode "pathotype"), but might also define functions intimately associated with parasitism. Most studies have focused on the cyst (*Heterodera* and *Globodera* spp.) and burrowing (*Radopholus* spp.) nematodes, as these are amphimictic and thus amenable to genetic analysis (Jeroen et al. 1994; Opperman et al. 1994a). In one approach (C.H. Opperman and K. Dong, pers. comm.), three essentially homozygous strains of *H. glycines* were generated by sib matings in single cyst selections. Controlled crosses have been performed between these strains, and F<sub>1</sub>, F<sub>2</sub>, and F<sub>3</sub> progeny have been scored for virulence on different soy bean cultivars, identifying a number of unlinked dominant and recessive loci associated with virulence on particular hosts. This is not unexpected, as soybean breeders have identified at least four recessive genes and one or more dominant major genes, each probably with multiple allelic states, that confer resistance to *H. glycines*; different cultivars contain different permutations of these genes. To map the virulence (and other) loci, approximately 1600 recombinant inbred lines have been established from progeny of the crosses, and random 10-mers have been tested on parental DNA to identify RAPD markers (C.H. Opperman and K. Dong, pers. comm.). To expand the utility of this and other maps, a uniform genetic nomenclature for parasitic nematodes, modeled after the *C. elegans* conventions but with several important differences, has been developed (Bird and Riddle 1994).

Generated from local HTML

## Chapter 30. Parasitic Nematodes — VI Future Prospects

---

We have presented several areas where *C. elegans* serves as a model nematode for parasitic nematode research and where parasitological research provides insights into *C. elegans* biology. However, there are aspects of parasitic nematode biology, such as the evolution of parasitism and resistance to host defenses, that studies on *C. elegans* have yet to illuminate. In both plant and animal parasite systems, major questions remain to be answered concerning the ability of the nematodes to persist in the presence of an otherwise intact immune/defense system. Parasites have coevolved with their hosts and have a number of adaptations that are evolutionary novelties. For example, the lymphatic filarial nematodes specifically and actively immunosuppress their hosts such that microfilarial levels in the bloodstream can reach greater than  $10^3$  per milliliter in the absence of clinical symptoms ([Nutman et al. 1987](#); [Lawrence et al. 1994](#); [Nutman 1995](#)). The breaking of this immune tolerance not only heralds clearance of the circulating parasites, but can also lead to gross pathology (elephantiasis) ([Maizels and Lawrence 1991](#)). *Trichinella spiralis* lives within muscle cells where it induces a dedifferentiation into a “nurse cell” and the production of a nexus of capillaries to provide it with nutrition ([Jasmer 1995](#)). Root-knot nematodes induce their hosts to provide a feeding site that has biochemical and anatomical adaptations to support the nematode ([Sijmons et al. 1994](#)).

Although parasitic species have evolved a wide range of specializations for survival as parasites, these adaptations have been built on a frame of basic nematode anatomy and thus may have *C. elegans* counterparts. For example, the highly developed pharyngeal glands of root-knot nematodes, believed to be the source of the feeding-site inductive signal ([Hussey 1989](#)), are presumably homologous to the *C. elegans* pharyngeal glands. Nematode gut antigens will vaccinate against animal intestinal parasites ([Jasmer et al. 1993](#); [Smith et al. 1993](#)); the *C. elegans* homologs may also offer insights into possible chemotherapeutic targets. The gut cysteine proteases of *C. elegans* have their closest homologs in parasitic nematodes, and antiprotease drug development using *C. elegans* models may expedite real-world trials ([Ray and McKerrow 1992](#)). Acetylcholinesterases (AChEs) are targets of effective antinematode drugs, but due to environmental concerns, the drugs are subject to increasing regulation ([Prichard 1994](#)). Luckily, the AChEs are under extensive study in *C. elegans* (see [Rand and Nonet, this volume](#)). This work can only gain from and feed into the study of AChE in other species ([Arpagaus et al. 1992a,b](#); [Blackburn and Selkirk 1992](#); [Opperman and Chang 1992](#)). In addition, *C. elegans* can be used as a transgenic test bed to study the function of parasite genes in the absence of their host genome, as has been achieved for BZ-resistant *H. contortus* tubulins ([Kwa et al. 1995](#)).

Significantly, *C. elegans* may itself be a parasite. The congeneric *C. remanei (vulgaris)* was isolated in a phoretic association with snails and millipedes ([Baird et al. 1994](#)), and other rhabditids use mollusks, annelids, and arthropods as transport hosts and food sources ([Chitwood and Chitwood 1974](#); [Nicholas 1984](#)). The rhabditid *Steinernema* are parasites of insect larvae, and members of the genus *Strongyloides* are parasites of vertebrates ([Smyth 1994](#)). The *C. elegans* dauer larva is in this view an adaptation not only to poor environmental conditions, but also to association with a transport host (see [Riddle, this volume](#)). A short reproductive cycle and hermaphroditic sexual mode make sense for a small invertebrate living off locally rich but globally sparse food sources.

The significance of studies on *C. elegans* to the understanding of parasitism cannot be understated, and the interest of parasitologists in *C. elegans* research and vice versa will continue to benefit from the fruitful trade in concepts, systems, reagents, and ideas.

## **Chapter 30. Parasitic Nematodes — Acknowledgments**

---

We thank J. Allen, T. Geary, W. Grant, C. Johnson, C. Opperman, and S. Politz for constructive comments on the manuscript and for kind sharing of unpublished data, and B. Endo, S. Williams, B. Gregory, and E. Munn for photographs. M.B. is funded by the Wellcome Trust, the World Health Organization, and the Leverhulme Trust. D.B. is supported by the USDA National Research Initiative.

Generated from local HTML

# **Appendix 1 Genetics**

---

## **Contents**

[Part A Genetic Nomenclature](#)

[Part B List of Laboratory Strain and Allele Designations](#)

[Part C Skeleton Genetic Map](#)

[Part D List of Characterized Genes](#)

[Acknowledgments](#)

[Gene List](#)

Generated from local HTML

# Appendix 1 Genetics — Part A Genetic Nomenclature

---

The genetic nomenclature summarized here is based on the original proposals for *Caenorhabditis elegans* nomenclature ([Horvitz et al. 1979](#)), plus additional recommendations that have been distributed in *The Worm Breeder's Gazette*.

## Genetic Loci

Genes are given names consisting of three italicized letters, a hyphen, and an arabic number, e.g., [dpy-5](#) or [let-37](#) or [mlc-3](#). The gene name may be followed by an italicized Roman numeral, to indicate the linkage group on which the gene maps, e.g. *dpy-5 I* or *let-37 X* or *mlc-3 III*.

For genes defined by mutation, the gene names refer to the mutant phenotype originally detected and/or most easily scored: *umpy* (DumPY) in the case of [dpy-5](#), and *lethal* (LEThal) in the case of [let-37](#).

For genes defined by cloning, on the basis of sequence similarity, the gene name refers to the predicted protein product or RNA product: Myosin Light Chain in the case of [mlc-3](#), SuperOxide Dismutase in the case of [sod-1](#), Ribosomal RNA in the case of [rrn-1](#).

Genes with related properties are usually given the same three-letter name and different numbers. For example, the 3 known myosin light chain genes are indicated [mlc-1](#), [mlc-2](#), [mlc-3](#), and the more than 20 different *umpy* genes are indicated [dpy-1](#), [dpy-2](#), [dpy-3](#), and so on.

There are no specific recommendations for designating cloned sequences that are not homologous to known genes. Most genomic clones have been provided by the *C. elegans* mapping/sequencing consortium (based at the Sanger Centre, Cambridge, UK, and the Genome Sequencing Center, St. Louis, USA; see Waterston et al., this volume). Cosmid clones generated by the consortium are named on the basis of the vector, either pJB8 (initial letters B, C, D, E, R, M, ZC) or a Lorist vector (initial letters K, T, W, F, ZK). Phage clones (in Lambda 2001) are identified by the initial letters A, ZL, YSL. YACs (yeast artificial chromosome clones) are identified by the initial letter Y, e.g., Y3D5.

Sequences that are predicted to be genes are named on the basis of the sequenced cosmid, plus a number. For example, the genes predicted for the cosmid T05G3 are called T05G3.1, T05G3.2, etc. DNA clones that have not been generated by the consortium are usually designated by the laboratory strain designation (see below), a # symbol and an isolation number, e.g., MT#JAL6.

## Homologous Genes

If a homolog of a known *C. elegans* gene is identified in a related species such as *Caenorhabditis briggsae*, it can be given the same gene name, preceded by two italic letters referring to the species, and a hyphen. For example, [Cb-tra-1](#) is the name for the *C. briggsae* homolog of the *C. elegans* gene [tra-1](#).

The *C. elegans* homolog of a gene identified and named in another organism can be distinguished by the same convention, using "Ce-" as an optional prefix. For example, [Ce-snt-1](#) defines the *C. elegans* synaptotagmin gene.

## Alleles and Mutations

Every mutation has a unique designation. Mutations are given names consisting of one or two italicized letters followed by an italicized Arabic number, e.g., *e61* or *mn138* or *st5*. The letter prefix refers to the laboratory of isolation, as registered with the Caenorhabditis Genetics Center (CGC). There are currently more than 150 registered laboratories (see Part B). For example, *e* refers to the MRC Laboratory of Molecular Biology (Cambridge, U.K.), and *st* refers to the laboratory of R.H. Waterston (Washington University, St. Louis, Missouri).

When gene and mutation names are used together, the mutation name is included in parentheses after the gene name, e.g., *dpy-5(e61)*, *let-37(mn138)*. When unambiguous, e.g., if only one mutation is known for a given gene, gene names are used in preference to mutation names ([let-37](#) rather than *mn138*).

Suffixes indicating characteristics of a mutation can follow a mutation name. These are usually two-letter nonitalicized letters, e.g., *hc17ts*, where *ts* stands for temperature sensitive.

The wild-type allele of a gene is defined as that present in the Bristol N2 strain, stored frozen at the CGC and other locations. Wild-type alleles can be designated by a plus sign immediately after the gene name, *dpy-5+*, or by including the plus sign in parentheses, *dpy-5(+)*. The widely understood convention of a superscript plus sign, *dpy-5<sup>+</sup>*, has also been used.

There is no special nomenclature for suppressor mutations. Most extragenic suppressor loci are called *sup* (40 loci defined so far, with a wide variety of properties and mechanisms). Some more specific classes have been established, such as *smu* (Suppressor of Mec and Unc), and *smg* (Suppressor with Morphogenetic effect on Genitalia). Intragenic suppressors or modifiers are indicated by adding a second mutation name within parentheses; for example, *unc-17(e245e2608)* is an intragenic partial revertant of *unc-17(e245)*.

Mutations known to be chromosomal rearrangements, rather than intragenic lesions, are named somewhat differently, as described below.

## RFLPs

Polymorphic sites, which are usually RFLPs (restriction fragment length polymorphisms), are designated by an italic letter *P* and an italic number, preceded by the allele prefix for the laboratory responsible for identifying the site. For example, *eP2* and *eP98* are RFLPs identified at the MRC Laboratory of Molecular Biology, and *stP17* and *stP196* are RFLPs identified in the laboratory of R. H. Waterston.

## Transgenes

Transformation of *C. elegans* with exogenous DNA usually leads to the formation of a transmissible extrachromosomal array containing many copies of the injected DNA, but sometimes chromosomal integration of the injected DNA can occur. Extrachromosomal arrays are given italicized names consisting of the laboratory allele prefix, the two letters *Ex*, and a number. Integrated transgenes are designated by italicized names consisting of the laboratory allele prefix, the two letters *Is*, and a number. Both *Ex* and *Is* can optionally be followed by genotypic or molecular information describing the transgene, in brackets, e.g., *eEx3* or *els2* or *stEx5 [sup-7(st5) unc-22(+)]*.

## Genotypes

Mutants carrying more than one mutation are designated by sequentially listing mutant genes or mutations according to the left-right (= up-down) order on the genetic map. A skeleton genetic map is provided in Part C. Different linkage groups are separated by a semicolon and given in the order *I, II, III, IV, V, X, f*. *I–V* are the five autosomes, *X* is the *X* chromosome, and *f* refers to free duplications or chromosomal fragments. For example: *dpy-5(e61) I; bli-2(e768) II; unc-32(e189) III*.

Heterozygotes, with allelic differences between chromosomes, are designated by separating mutations on the two homologous chromosomes with a slash. Where unambiguous, wild-type alleles can be designated by a plus sign alone, or even omitted, e.g., *dpy-5(e61) unc-13(+) / dpy-5(+) unc-13(e51) I* can also be written *dpy-5 +/+ unc-13* or *dpy-5/unc-13*.

## Transposons

*C. elegans* transposons are called *Tc1*, *Tc2*, etc., where each number represents a different family. Transposon names are not italicized except when included in a genotype. Transposon insertions in genes are indicated by adding *::Tc* to the relevant mutation name, as an optional descriptor. Thus, a mutation of the gene *unc-54*, called *r293*, is a *Tc1* insertion and can therefore be written *unc-54(r293::Tc1)*.

## Chromosomal Aberrations

Duplications (*Dp*) deficiencies (*Df*), inversions (*In*), and translocations (*T*) are known in *C. elegans* cytogenetics; these are given italicized names consisting of the laboratory mutation prefix, the relevant abbreviation, and a number, optionally followed by the affected linkage groups in parentheses, for example, *eT1(III;V)*, *mnDp5(X;f)*, where *f* indicates a free duplication. Chromosomal balancers of unknown structure can be designated using the abbreviation C, for example, *mnC1 (II)*.

## Phenotypes

Phenotypic characteristics can be described in words, e.g., dumpy animals or uncoordinated animals. If more convenient, a nonitalicized three-letter abbreviation, which usually corresponds to a gene name, may be used. The first letter of a phenotypic abbreviation is capitalized, e.g., Unc for uncoordinated, Dpy for dumpy. If necessary to distinguish among related but distinguishable phenotypes, the relevant gene number can be added, e.g., Unc-4 and Unc-13, to differentiate the distinct phenotypes produced by mutations in the two genes [\*unc-4\*](#) and [\*unc-13\*](#). Abbreviations that do not correspond to gene names can also be used, e.g., Muv for multiple vulval development.

A common convention, when comparing a mutant with the wild type, is to use the prefix non- to refer to the wild-type phenotypes, for example, non-Lin (= wild-type cell lineage) or Dpy non-Unc (= wild type with respect to movement, but dumpy with respect to body shape).

## Proteins

The protein product of a gene can be referred to by the relevant gene name, written in nonitalic capitals, for example, the protein encoded by [\*unc-13\*](#) can be called UNC-13. Where more than one protein product is predicted for a gene (usually as a result of alternative message processing), the different proteins are distinguished by additional capital letters, for example, TRA-1A, TRA-1B.

## Strains

A strain is a set of individuals of a particular genotype with the capacity to produce more individuals of the same genotype. Strains are given nonitalicized names consisting of two uppercase letters followed by a number. The letter prefixes refer to the laboratory of origin and are different from mutation letter prefixes (see Part B). For example, CB1833 is a strain of genotype *dpy-5(e61) unc-13(e51)*, constructed at the MRC Laboratory of Molecular Biology (strain prefix CB, allele prefix *e*), and MT688 is a strain of genotype *unc-32(e189) +/+ lin-12(n137) III; him-5(e1467) V*, constructed in the laboratory of H.R. Horvitz at M.I.T. (strain prefix MT, allele prefix *n*).

Some 3-letter laboratory designations are also in use (see Part B), to refer to strains of nematode species other than *C. elegans*.

Generated from local HTML

## Appendix 1 Genetics — Part B List of Laboratory Strain and Allele Designations

3-LETTER LABORATORY DESIGNATIONS (NO ALLELE DESIGNATION)

### Footnotes

\*

As registered with the Caenorhabditis Genetics Center, 1995.

### Tables

<u>AB</u>	aa	Bird, Alan	CSIRO Adelaide, Australia
AE	at	Sluder, Ann	University of Georgia, Athens GA
AF	sz	Fodor, Andras	Hungarian Academy of Sciences, Szeged, Hungary
AG	av	Golden, Andy	National Cancer Institute, Frederick MD
AL	ic	Alfonso, Aixa	University of Iowa, Iowa City IA
AQ	lj	Schafer, Bill	University of California, San Diego CA
AS	id	Spence, Andrew	University of Toronto, Canada
AT	yj	Politz, Sam	Worcester Polytechnic Institute, Worcester MA
AV	me	Villeneuve, Anne	Stanford University, Stanford CA
AZ	ru	Austin, Judith	University of Chicago, Midway IL
BA	hc	Ward, Sam	University of Arizona, Tucson AZ
BC	s	Baillie, Dave	Simon Fraser University, Vancouver, Canada
BE	sc	Edgar, Bob	University of California, Santa Cruz CA
BG	nw	Goodwin, Betsy	Northwestern University, Chicago IL
BH	hb	Honda, Barry	Simon Fraser University, Vancouver, Canada
BL	in	Blumenthal, Tom	Indiana University, Bloomington IN
BM	bb	Mitchell, David	Boston Biomedical Research Institute, Boston MA
BP	hy	Podbilewicz, Benjamin	Technion Institute, Haifa, Israel
BR	by	Baumeister, Ralf	LMB/Genzentrum, Munich, Germany
BS	oz	Schedl, Tim	Washington University, St. Louis MO
BW	ct	Wood, Bill	University of Colorado, Boulder CO
CB	e	Hodgkin, Jonathan	MRC-LMB, Cambridge, England
CD	dc	Johnson, Carl	NemaPharm Inc., Boston MA
CF	mu	Kenyon, Cynthia	University of California, San Francisco CA
CH	cg	Kramer, Jim	Northwestern University, Chicago IL
CL	dv	Link, Chris	University of Denver, Denver CO
CR	-	Rubin, Charles	Albert Einstein College of Medicine, Bronx NY
CW	fc	Morgan, Phil	Case Western Reserve University, Cleveland OH
CX	ky	Bargmann, Cori	University of California, San Francisco CA

CZ	ju	Chisholm, Andrew & Jin, Yishi	University of California, Santa Cruz CA	
DA	ad	Avery, Leon	University of Texas Southwestern Medical Center, Dallas TX	
DB	rv	Bird, David	University of California, Riverside CA	
DD	d	Otsuka, Tony	Illinois State University, Normal IL	
DF	ny	Fitch, David	New York University, New York NY	
DG	tn	Greenstein, David	Vanderbilt University, Nashville TN	
DH	b	Hirsh, David	Columbia University, New York NY	
DM	ra	Moerman, Don	University of British Columbia, Vancouver, Canada	
DP	ed	Pilgrim, Dave	University of Alberta, Edmonton, Canada	
DR	m	Riddle, Don	University of Missouri, Columbia	MO
DS	tx	Shakes, Diane	University of Houston, Houston TX	
DT	jb	Stinchcomb, Dan	Synergen, Boulder CO	
DU	un	Titus, Margaret	Duke University, Durham NC	
DZ	ez	Zarkower, Dave	University of Minnesota, Minneapolis MN	
EA	ls	Aamodt, Eric	LSUMC, Shreveport LA	
EE	up	Bucher, Beth	University of Pennsylvania, Philadelphia PA	
EF	ab	Ferguson, Chip	University of Chicago, Chicago IL	
EG	ox	Jorgensen, Erik	University of Utah, Salt Lake City UT	
EH	lw	Shaw, Jocelyn	University of Minnesota, St. Paul	MN
EJ	dx	Lambie, Eric	Dartmouth College, Hanover NH	
EL	om	Maine, Eleanor	Syracuse University, Syracuse NY	
EM	bx	Emmons, Scott	Albert Einstein College of Medicine, Bronx NY	
ER	jd	Walhall, Bill	Georgia State University, Atlanta GA	
ES	kg	Schierenberg, Einhard	University of Cologne, Germany	
ET	ek	Kipreos, Edward	University of Georgia, Athens GA	
EU	or	Bowerman, Bruce	University of Oregon, Eugene OR	
FF	f	Thierry-Mieg, Danielle	CNRS, Montpellier, France	
FH	ec	Meneely, Phil	Haverford College, Haverford PA	
FK	ks	Ohshima, Yasumi	Kyushu University, Fukuoka, Japan	
FR	sw	Muller, Fritz	University of Fribourg, Fribourg, Switzerland	
FS	tf	Roberts, Tom	Florida State University, Tallahassee FL	
FX	tm	Mitani, Shohei	Tokyo Women's College, Tokyo, Japan	
GB	sf	Benian, Guy	Emory University, Atlanta GA	
GE	t	Schnabel, Ralf	MPI, Martinsried, Germany	
GG	g	*(von Ehrenstein, G)	MPI, Gottingen, Germany	
GR	mg	Ruvkun, Gary	Massachusetts General Hospital, Boston MA	
GS	ar	Greenwald, Iva	Columbia University, New York NY	
GT	a	Dusenbery, David	Georgia Institute of Technology, Atlanta GA	

HE	su	Epstein, Henry	Baylor College of Medicine, Houston TX
HG	yw	Wilson, David	University of Miami, Coral Gables FL
HH	hs	Hecht, Ralph	University of Houston, Houston TX
HK	kh	Kagawa, Hiro	Okayama University, Okayama, Japan
HR	sb	Mains, Paul	University of Calgary, Calgary, Canada
HU	jv	Varkey, Jacob	Humboldt State University, Arcata CA
IA	ij	Johnstone, Iain	University of Glasgow, Glasgow, Scotland
IM	ur	Wadsworth, Bill	UMDNJ, Piscataway NJ
JA	we	Ahringer, Julie	University of Cambridge, Cambridge, England
JC	ut	Katsura, Isao	National Institute of Genetics, Mishima, Japan
JF	mt	Freedman, Jonathan	Duke University, Durham NC
JH	ax	Seydoux, Geraldine	Johns Hopkins University, Baltimore MD
JJ	zu	Priess, Jim	FHCRC, Seattle WA
JK	q	Kimble, Judith	University of Wisconsin, Madison WI
JL	fm	Lissemore, Jim	John Carroll University, University Heights OH
JM	ca	McGhee, Jim	University of Calgary, Calgary, Canada
JP	gn	Nelson, Greg	Jet Propulsion Laboratory, Pasadena CA
JR	w	Rothman, Joel	University of Wisconsin, Madison WI
JT	sa	Thomas, Jim	University of Washington, Seattle WA
JW	je	Way, Jeff	Rutgers University, Piscataway NJ
KB	um	Bennett, Karen	University of Missouri, Columbia MO
KC	wx	Chow, King	HKUST, Hong Kong
KE	ha	Edwards, Kaye	Haverford College, Haverford PA
KK	it	Kemphues, Ken	Cornell University, Ithaca NY
KM	gv	Krause, Mike	National Institutes of Health, Bethesda MD
KP	nu	Kaplan, Josh	Massachusetts General Hospital, Boston MA
KR	h	Rose, Ann	University of British Columbia, Vancouver, Canada
LC	pa	Loer, Curtis	Lafayette College, Easton PA
LK	gs	Manser, Jim	Harvey Mudd College, Claremont CA
LM	sd	Satelle, David	University of Cambridge, Cambridge, England
LR	rk	Rokeach, Luis	Universite de Montreal, Montreal, Canada
LS	cx	Segalat, Laurent	CNRS-IMPC, Valbonne, France
LT	wk	Padgett, Rick	Waksman Institute, Piscataway NJ
LU	lr	DeStasio, Beth	Lawrence University, Appleton WI
LV	wc	Venolia, Lee	Williams College, Williamstown MA
MB	ib	Burnell, Ann	St. Patrick's College, Maynooth, Ireland
MC	gc	Crowder, Mike	Washington University, St Louis MO
MF	hm	Treinin, Millet	Hebrew University, Jerusalem, Israel

MH	ku	Han, Min	University of Colorado, Boulder CO
MJ	k	Miwa, Johji	NEC Fundamental Research Labs, Tsukuba, Japan
MK	hx	Klass, Michael	Abbott Labs, Abbott Park IL
ML	mc	Labouesse, Michel	IGBMC, Strasbourg, France
MM	an	Hamelin, Michel	Merck Research Labs, Rahway NJ
MP	lb	Wolinsky, Eve	NYU Medical School, New York NY
MQ	qm	Hekimi, Siegfried	McGill University, Montreal, Canada
<u>MS</u>	lc	Sutherlin, Marie	University of Nebraska, Lincoln NE
MT	n	Horvitz, Bob	MIT, Cambridge MA
MW	wm	Wickens, Marv	University of Wisconsin, Madison WI
NA	gb	Bazzicalupo, Paolo	IIGB, Napoli, Italy
NC	wd	Miller, David	Vanderbilt University, Nashville TN
NE	rp	Pertel, Ruth	FDA, Cold Spring Harbor Laboratory Washington, D.C.
NF	tk	Nishiwaki, Kyoji	NEC Fundamental Research Labs, Tsukuba, Japan
NG	gm	Garriga, Gian	University of California, Berkeley CA
NH	ay	Stern, Michael	Yale University, New Haven CT
NJ	rh	Hedgecock, Ed	Johns Hopkins University, Baltimore MD
NL	pk	Plasterk, Ronald	NKI, Amsterdam, The Netherlands
NM	js	Nonet, Mike	Washington University, St Louis MO
NS	nr	Server, Fred	Cambridge NeuroScience Research, Cambridge MA
NT	uc	Perry, Marc	University of Toronto, Toronto, Canada
NW	ev	Culotti, Joe	Mt. Sinai Hospital Research Institute, Toronto, Canada
NY	yn	Li, Chris	Boston University, Boston MA
OK	cu	Okkema, Pete	University of Illinois, Chicago IL
PA	hv	Trent, Carol	Western Washington University, Bellingham WA
PB	bd	Baird, Scott	Wright State University, Dayton OH
PC	ub	Candido, Peter	University of British Columbia, Vancouver, Canada
PD	cc	Fire, Andy	Carnegie Institution, Baltimore MD
PH	hf	Hartman, Phil	Texas Christian University, Fort Worth TX
PJ	j	Jacobson, Lew	University of Pittsburgh, Pittsburgh PA
PK	cr	Kuwabara, Patty	MRC-LMB, Cambridge, England
PR	p	*(Russell, Dick)	University of Pittsburgh, Pittsburgh PA
PS	sy	Sternberg, Paul	Caltech, Pasadena CA
PY	oy	Sengupta, Piali	Brandeis University, Waltham MA
PX	fx	Phillips, Patrick	University of Texas, Arlington TX
RB	ok	Barstead, Bob	Oklahoma Med. Res. Found., Oklahoma City OK
RC	g	Cassada, Randy	University of Freiburg, Freiburg, Germany
RE	v	Ellis, Ron	University of Michigan, Ann Arbor MI

RG	ve	Rougvie, Ann	University of Minnesota, St. Paul MN
RL	da	Rose, Lesilee	University of California, Davis CA
RM	md	Rand, Jim	Oklahoma Med. Res. Found., Oklahoma City OK
RS	tu	Sommer, Ralf	MPI, Tubingen, Germany
RW	st	Waterston, Bob	Washington University, St. Louis MO
SB	be	Sudhaus, Walter	Free University of Berlin, Berlin, Germany
SC	lm	Miller, Leilani	Santa Clara University, Santa Clara CA
SD	ga	Kim, Stuart	Stanford University, Stanford CA
SF	pc	Coffino, Philip	University of California, San Francisco CA
SG	ds	Scheel, Jochen	MPI, Tubingen, Germany
SL	eb	L'Hernault, Steve	Emory University, Atlanta GA
SM	px	Mango, Susan	University of Utah, Salt Lake City UT
SP	mn	Herman, Bob	University of Minnesota, St. Paul MN
SQ	zk	Siddiqui, Shahid	Toyohashi University, Toyohashi, Japan
SR	rs	Shmookler Reis, Robert	University of Arkansas, Little Rock AR
SS	bn	Strome, Susan	Indiana University, Bloomington IN
SW	se	Waring, David	FHCRC, Seattle WA
TB	ch	Burglin, Thomas	Biocenter, Basel, Switzerland
TD	tc	Lew, Ken	Forsyth Dental Center, Boston MA
TJ	z	Johnson, Tom	University of Colorado, Boulder CO
TK	kn	Ishii, Naoaki	Tokai University Med. School, Kanagawa, Japan
TM	sj	Honda, Shuji	Jet Propulsion Laboratory, Pasadena CA
TN	cn	Hosono, Ryuji	Kanazawa University, Ishikawa, Japan
TP	ka	Page, Tony	University of Glasgow, Glasgow, Scotland
TR	r	Anderson, Phil	University of Wisconsin, Madison WI
TT	tb	Babu, P	Tata Institute, Bombay, India
TU	u	Chalfie, Marty	Columbia University, New York NY
TW	cj	Collins, John	University of New Hampshire, Durham NH
TY	y	Meyer, Barbara	University of California, Berkeley CA
UC	la	Mancillas, Jorge	University of California, Los Angeles CA
UG	bg	Bogaert, Thierry	University of Gent, Gent, Belgium
UK	In	Nawrocki, Leon	University College, London, England
UL	le	Hope, Ian	University of Leeds, Leeds, England
UT	mm	van der Kooy, Derek	University of Toronto, Toronto, Canada
UW	wb	Woods, Robin	University of Winnipeg, Winnipeg, Canada
VB	sv	Tuck, Simon	University of Umea, Sweden
VD	sn	*(Van Doren, Kevin)	Syracuse University, Syracuse NY
VT	ma	Ambros, Victor	Dartmouth College, Hanover NH

WG	au	Grant, Warwick	CSIRO, Armidale, Australia
WH	oj	White, John	University of Wisconsin, Madison WI
WJ	sh	Sharrock, Bill	University of Minnesota, St. Paul MN
WK	lx	Katz, Wendy	University of Kentucky, Lexington KY
WM	ne	Mello, Craig	University of Massachusetts, Worcester MA
WR	oh	Morgan, Bill	The College of Wooster, Wooster OH
WS	op	Hengartner, Michael	CSHL, Cold Spring Harbor NY
WW	xx	Samoiloff, Martin	University of Manitoba, Winnipeg, Canada
XA	qa	multiple users	CGC, MRC-LMB, Cambridge, England
YK	ms	Kohara, Yuji	National Institute of Genetics, Mishima, Japan
ZB	bz	Driscoll, Monica	Rutgers University, Piscataway NJ
ZZ	x	Lewis, Jim	University of Texas, San Antonio TX

\*

Deceased.

CEW	Winter, Carlos	University of Sao Paulo, Sao Paulo, Brazil
DWF	Freckman, Diane	Colorado State University, Fort Collins CO
LSJ	Lu, Nancy	San Jose State University, San Jose CA
PDL	De Ley, Paul	University of Gent, Gent, Belgium

Generated from local HTML

## Appendix 1 Genetics — Part C Skeleton Genetic Map

---

The current genetic map of *Caenorhabditis elegans* includes more than 1600 mapped genes and more than 500 genetic deficiencies and duplications. Detailed inspection of the map, as well as all the underlying genetic data, is possible via the public access database ACeDB, which is updated at frequent intervals. A printed version of the genetic map is also distributed every two years by the Caenorhabditis Genetics Center. The most recent printed version, compiled in 1995, took up about 45 pages. The figure shown here provides only a skeleton version of the map, illustrating the overall organization of each chromosome and indicating the location of a limited number of well-mapped genes. All rearrangements have been omitted.

Each of the six chromosomes is shown in vertical orientation, with the left end at the top and right end at the bottom. Numerical map coordinates, based on recombinational distances in centimorgans, are shown; these are defined relative to a zero position on each chromosome. All positions to the left (upward) of this have negative coordinates, and all positions to the right (downward) have positive coordinates. There are no defined centromeres on *C. elegans* chromosomes, so these zero positions were originally chosen arbitrarily, each corresponding to a standard marker (shown in bold type) located at the approximate middle of each linkage group. Each of the six chromosomes is 45–50 cM in recombinational length. Each of the five autosomes, but not the X chromosome, has a centrally located cluster of higher gene density. The approximate extent of these clusters (as determined most recently by [Barnes et al. 1995](#)) is shown by a thicker line.

Generated from local HTML

## Appendix 1 Genetics — Part D List of Characterized Genes

---

Genes are listed in alphabetical order of gene names. Most genes in this list have been defined by the isolation of one or more mutant alleles, but an increasing number have been defined only by the cloning and characterization of the wild-type gene.

Each *gene name category* (e.g., *dpy*) is preceded by an explanation of the gene name (**d** um **p**y : shorter than wild type) and by the strain designation of the laboratory assigning gene names within that category (CB). A full listing of these strain designations is provided in Part B. In some cases, assignment of gene names within a category is made by the *Caenorhabditis Genetics Center* (CGC).

Each gene entry begins with the *gene name* and its *chromosomal location* (all in bold type): the name and relevant linkage group (**I**, **II**, **III**, **IV**, **V**, or **X**) are followed by the map coordinate of the gene on that linkage group, as determined for the 1995 Genetic Map of *C. elegans*. A skeleton genetic map is provided (Part C). Genes that have been mapped precisely are usually given positions to two decimal places. Less precisely mapped genes are usually given positions to one or zero decimal places. Genes with very approximate positions are indicated by L, LC, C, RC, R (left, left-center, center, right-center, right). Some genes have not been mapped beyond linkage assignment (position given as N). Finally, some genes have been defined molecularly but have not yet been assigned to any location on the physical map of the genome; the position of these is given as ?.

Genes for which no mutations have yet been identified are indicated NMK (no mutations known). For all other genes, the *reference allele* is given in bold type. This is usually the mutation that has been studied in most detail, and a brief description of the relevant mutant phenotype follows. Penetrance of mutant phenotypes is 100% unless otherwise noted. Most mutations have been induced with ethylmethanesulfonate (EMS); alleles induced with other mutagens are usually indicated by an appended descriptor (see abbreviations below). Additional descriptive abbreviations for the allele (e.g., ts, ird) may also be used and are explained below. Other abbreviations used are:

### ES (Ease of Scoring)

This indicates (very approximately) how easy it is to recognize a particular mutant phenotype. ES3 = easy to score; ES2 = hard to score (may become easier with practice); ES1 = very hard to score except by special means (such as enzyme assay or cell lineage analysis); ES0 = impossible to score, which may be the case for particular stages, sexes, or genetic background. In general, the ES score refers to ease of scoring at the stage when the mutation is maximally expressed. ES scores have only been included where relevant and known, and omitted for genes such as *let* genes.

### ME (Male mating Efficiency)

This is recorded, where known, by an ME score, where ME0 = no successful mating, ME1 = rare successful mating, ME2 = poor mating, ME3 = fair-to-excellent mating. Hermaphrodite mating efficiency is recorded where relevant and known by a corresponding HME score.

### OA (Other Alleles)

The number of additional alleles is listed by an OA score, followed by a list of some or all of these alleles, together with brief phenotypic descriptions for alleles with properties significantly different from that of the reference allele. Most mutations result in partial or complete loss of function and are recessive. Unusual alleles may exhibit gain-of-function properties, or dominant negative effects, and therefore lead to phenotypes very different from that of the reference allele. If only one allele is known, this is often indicated by NA1 (Number of Alleles 1). Total number of alleles for each gene is based on data reported to the CGC and is therefore likely to be an underestimate in many cases.

## Synonyms

Previously used gene names are included in the list, with cross reference to the current gene name. These previously used names are also included in each gene entry and prefixed by "pka" (previously known as).

## References

A few key references are listed at the end of each entry, in brackets, e.g., [Herman and Hedgecock 1995]. The most recent key reference has been included wherever possible, because this can be used to trace earlier publications. A list of comprehensive references for each gene is not feasible, for reasons of space. Such listings can be obtained by means of databases such as ACeDB. A large amount of additional information in this list is based on unpublished observations communicated to the CGC or reported in the Worm Breeder's Gazette. The sources of this and further information are indicated in the reference list by the strain codes for the relevant laboratories (Part B), given in alphabetical order. It is not feasible, again for reasons of space, to acknowledge separately all of the hundreds of individual workers who have communicated information used in the compilation of this list.

## Phenotypic abbreviations

aci

acetaldehyde-induced

amb

amber nonsense (UAG)

cs

cold-sensitive (phenotype stronger at low temperatures)

des

diethylsulfate-induced

dm

dominant

fdi

formaldehyde-induced

gf

gain-of-function

gri

gamma-ray-induced

icr

induced by ICR compounds

ird

intragenic revertant of dominant

lf

loss-of-function

mat

maternal-effect	
mm	maternal expression of wild-type allele required for viability
mn	either maternal or embryonic expression of wild-type allele required for viability
mnp	paternal expression of wild-type allele required for viability
mnz	paternal expression of wild-type allele insufficient for viability
mut	mutator induced (usually transposon-associated)
nm	both maternal and embryonic expression of wild-type allele required for viability
oc	ochre nonsense (UAA)
op	opal nonsense (UGA)
pat	paternal effect
pdi	induced by $^{32}\text{P}$ decay
sd	semidominant (incompletely dominant)
spo	spontaneous
tci	transposon ( $\text{Tc}$ ) insertion
te	allele derived by transposon excision
ts	temperature-sensitive (phenotype stronger at higher temperature)
uvi	ultraviolet irradiation-induced
uvp	ultraviolet plus psoralen-induced
xri	

X irradiation-induced

## Other abbreviations

In many places, standard phenotypic abbreviations are used, such as Unc for uncoordinated and Ric for resistance to inhibitors of cholinesterase. These are defined in the relevant gene category. Identified cells and [neurons](#) are given standard names (see [Wood et al. 1988](#)).

aa

amino acids

°C

degrees centigrade (15°C = 15 degrees Centigrade, etc.)

Con

constipated

Daf-c

constitutive formation of dauer larvae

Daf-d

defective in dauer larva formation

ES

ease of scoring (see above)

FITC

fluoroscein isothiocyanate

GABA

gamma amino butyric acid

HME

hermaphrodite mating efficiency (see above)

kb

kilobases

kD

kilodaltons

ME

mating efficiency (see above)

MMS

methylmethanesulfonate

Muv

multivulva

NA1

number of alleles one

NMK

no mutations known

OA

other alleles (see above)

TSP

temperature-sensitive period

UTR

untranslated region

Vul

vulvaless

wt

wild-type

Generated from local HTML

## **Appendix 1 Genetics — Acknowledgments**

---

The compilation of this list was made possible only by the use of the database ACeDB, developed by Richard Durbin and Jean Thierry-Mieg, and by the continuing operation of the Caenorhabditis Genetics Center (CGC) and the work of its present and past personnel (Bob Herman, Theresa Stiernagle, Sylvia Martinelli, Don Riddle, Peg MacMorris, Mark Edgley, Mary O'Callaghan). The CGC is supported by a contract from the NIH National Center for Research Resources.

Additional material and corrections for the list were also provided by many individuals, notably Leon Avery, David Baillie, Tom Barnes, Thomas Burglin, Estella Chen, Mark Edgley, Jaime Garcia-Anoveros, Iva Greenwald, Bob Herman, Kouichi Iwasaki, Lisa Kadyk, Michael Krause, Steve L'Hernault, Eric Lambie, Chris Larminie, Michel Leroux, Jim McCarter, Antony Page, Ronald Plasterk, David Reiner, Don Riddle, Ann Rose, Raja Rosenbluth, Tim Schedl, Geraldine Seydoux, Ann Sluder, Michael Stern, Paul Sternberg, Helen Stewart, Jim Thomas, and Sam Ward. Finally, it is essential to acknowledge the role of the entire *C. elegans* research community in providing published and unpublished information, and to apologize for all errors, omissions, and misapprehensions.

Generated from local HTML

## Appendix 1 Genetics — Gene List

---

### A to C

#### *abl*

**abl** (vertebrate oncogene)-related [CGC].

#### ***abl-1 X 2.06***

NMK. Major transcript 4.4 kb; sequence (~400 aa) has 62% identity with oncogene *v-abl* in predicted kinase domain. [[Goddard et al. 1986](#)]

#### *ace*

**a cetyl c holin e sterase abnormality [PR, RM].**

#### ***ace-1 X 24.11 p1000***:

class-A acetylcholinesterase reduced 100%; no behavioral phenotype alone (ES1 ME3), but *ace-2;ace-1* is uncoordinated (hypercontracted) and *ace-2;ace-3;ace-1* is L1-lethal; mosaic focus in muscle. OA6: e1572, etc. CLONED: sequence predicts 609 aa; 37% identity with *Torpedo* acetylcholinesterase; *p1000* is W99op. [[Herman and Kari 1985](#); [Arpagaus et al. 1994](#)] [FF]

#### ***ace-2 I – 4.93 g72***:

class-B acetylcholinesterase reduced 98%; no behavioral phenotype alone (see [\*ace-1\*](#)). ES1 ME3. OA11: g73, etc. [[Culotti et al. 1981](#)]

#### ***ace-3 II 22.65 dc2***:

class-C acetylcholinesterase reduced >95%; no behavioral phenotype alone (see [\*ace-1\*](#)). ES1. OA1: *dc3*. [[Johnson et al. 1988](#)]

#### *ach*

**a denylyl c yclase h omolog family [CGC].**

#### ***ach-1 ?***

NMK. Encodes protein with N-terminal similarity to yeast adenylyl cyclase; Ras binding; C-terminal similarity to gelsolin/villin; immunofluorescence indicates ACH-1 centrosome associated at mitosis, not during interphase. [CGC]

#### *acr*

**a cetyl c holine r eceptor-related [CGC].**

#### ***acr-1***

= *lev-1*

#### ***acr-2 X – 2.73***

NMK. Structural and functional similarity to non- $\alpha$ -subunit of nicotinic acetylcholine receptor. [LM, CGC]

#### *act*

**act** in [RW].

#### ***act-1***

See [\*act-123\*](#).

#### ***act-2***

See [act-123](#).

### ***act-3***

See [act-123](#).

### ***act-4 X -6.27***

NMK.

### ***act-5 III 20.3***

NMK. Sequence predicts protein with closer similarity to vertebrate cytoplasmic actin than *act-123*, *act-4*; *act-5:lacZ* expressed only in microvillous intestinal cells and [excretory](#) cell. [RW]

### ***act-123 V 2.92 st15***

(pka *unc-92*) sd; both *st15* and *st15/+* small, slow-growing, uncoordinated, almost paralyzed; abnormal thin-filament ultra-structure in muscle. ES3 ME0. OA4 (sd): *st22ts* (25°C phenotypes similar to *st15*), *st119* (dominant paralyzed, recessive larval-lethal, etc.). All are dominant neomorphic mutations of one of the three clustered actin genes; double-mutant intragenic revertants wt in phenotype even if [act-1](#) or [act-3](#) disrupted (e.g., *st22st283* internal deficiency in [act-3](#)). See also [emb-22](#). CLONED: encodes three actin genes, [act-1](#), [act-2](#), [act-3](#); mutant alterations in either *act-1* (*st118* is K18T, D11N), [act-3](#) (*st15* is Y143N, *st22* and *ad767* are both Q334K), or both *act-2* and [act-3](#) (*ad468*, recessive, lethal with dominant [pharynx](#) muscle defect). [[Files et al. 1983](#); [Krause et al. 1989](#)] [DA]

### ***adm***

**AD A M** family proteins [BP]. Disintegrin plus metalloprotease domains.

### ***adm-1 III R***

NMK. Sequence predicts protein with extensive similarity to ADAM (disintegrin plus metalloprotease domains) family. [BP]

### ***adn***

**ad** *hesio n* defect [NJ].

### ***adn-1 I 3.62 rh110***

: uncoordinated; detected by extra [neurons](#) stained by monoclonal antibody M44 (normally stains only [neuron](#) PVP); additional pair of [neurons](#) stain (? AVH or AVJ); no obvious axon outgrowth defects, very minor Mig defects. OA>5: *rh38sd* (Unc and slightly Dpy, many axon trajectories abnormal, [excretory](#) canals short, [distal tip cells](#) detach from [germ cells](#), and first polar bodies rest in abnormally posterior positions). *rh38/+* is not Unc, but has axonal, canal, distal tip cell, and polar body abnormalities; *rh38/Df* approximately wt; intragenic revertants (*rh38rh408*, *rh38rh410*) are impenetrant Uncs, *rh240*. [NJ]

### ***adn-2 V 0.46 rh162***

: [excretory](#) canals short; alae abnormal; [distal tip cells](#) detach from [germ cells](#); first polar body ends up in posterior positions. [NJ]

### ***adp***

sensory **ad** a **p** tation abnormal [CX].

### ***adp-1 II 2.5 ky20***

: fails to adapt to a subset of odorants detected by [neuron](#) AWC (benzaldehyde, butanone); normal adaptation to diacetyl, isoamyl alcohol. See also [osm-9](#). [[Colbert and Bargmann 1995](#)]

### ***aex***

**a** Boc, **ex** pulsion defects in defecation [JT].

**aex-1 I 2.24 sa9**

: defecation-defective, severely constipated; anterior body contraction (aBoc) and expulsion muscle contraction ([E.p](#)) steps of defecation nearly always missing; adult males not constipated and mate well. OA3: *sa10*, *sa27* (weaker), *sa49* (weaker). [[Thomas 1990](#); [Reiner and Thomas 1995](#)] [JT]

**aex-2 X 1.1 sa3**

: defecation-defective, severely constipated; expulsion muscle contraction ([E.p](#)) nearly always absent, anterior body contraction (aBoc) either absent or mistimed; adult male unaffected and mates well. OA1: *sa21* (similar). [[Thomas 1990](#); [Reiner and Thomas 1995](#)] [JT]

**aex-3 X – 19.00 ad418**

: defecation-defective, slightly constipated; anterior body contraction (aBoc) and expulsion muscle contraction ([E.p](#)) missing in five of six defecation cycles; adult males unaffected and mate well; interactions (Daf-c and Eat) with [unc-31](#). OA3: *sa5*, *ad696*, *n2166*. CLONED: cosmid C02H7. [[Thomas 1990](#); [Reiner and Thomas 1995](#)] [JT, DA]

**aex-4 X – 10.11 sa22**

: defecation-defective, moderately constipated; anterior body contraction (aBoc) and expulsion muscle contraction ([E.p](#)) missing in about six of seven defecation cycles; adult males unaffected and mate well. [[Thomas 1990](#); [Reiner and Thomas 1995](#)] [JT]

**aex-5 I 27.19 sa23**

: defecation-defective, moderate to severe constipation; expulsion muscle contraction ([E.p](#)) missing in about nine of ten defecation cycles; anterior body contraction (aBoc) usually missing as well; adult males unaffected and mate well. OA3: *sa41*, *sa42*, *sa43* (all similar). [[Thomas 1990](#); [Reiner and Thomas 1995](#)] [JT]

**aex-6 I 21.82 sa24**

: defecation-defective, moderately to severely constipated; expulsion muscle contraction ([E.p](#)) missing in about nine of ten defecation cycles; anterior body contraction (aBoc) usually also missing; slightly sluggish and slight egg-laying defect (Egl). [[Thomas 1990](#); [Reiner and Thomas 1995](#)] [JT]

**age**

**age** ing abnormal [TJ].

**age-1 II RC hx546**

: increased life span; increased thermotolerance; increased resistance to UV, paraquat; increased life span dependent on *daf-16*, *daf-18*; dauer-constitutive alleles (*m333*, *mg44*, *mg55*, *mg109*) are nonconditional, maternal-effect mutants that form dauer and dauer-like larvae; maternally rescued adults are Egl. NA6. CLONED: encodes largest subunit of RNA polymerase II. [[Friedman and Johnson 1988](#); [Bird and Riddle 1989](#); [Morris et al. 1996](#); [Malone et al. 1996](#); [Larson et al. 1995](#); [Lithgow et al. 1995](#)] [GR, TJ, JT]

**ali**

**al** ae **i** nconspicuous [CB].

**ali-1 V 3.31 e1934**

: faint or invisible alae in L1. ES1 ME3 NA1. [CF]

**ama**

**ama** nitin resistance abnormal [DR].

**ama-1 IV 0.05 m118**

: sd; heterozygote *m118*/+ resistant to 400 µg/ml α-amanitin; no other phenotype. ES1. OA>30 (intragenic revertants); *m118m221* (L1-lethal, probable null), *m118m235* (including late larval-lethal), *m118m252* (embryonic-lethal), *m118m238ts* (sterile adult), etc. Also hyperresistant allele: *m118m526* (sterile 25°C, 80% embryonic-lethal at 20°C). CLONED: encodes a phosphatidyl inositol-3-OH kinase catalytic subunit. [Rogalski et al. 1988, 1990]

### ***ama-2* V 4.84 m323**

: dm; heterozygote *m323*/+ resistant to 100 µg/ml α-amanitin; recessive-lethal. ES1 NA1. CLONED: encodes a phosphatidylinositol-3-OH kinase catalytic subunit. [Rogalski et al. 1988]

### ***anc***

***anc*** horage of nuclei abnormal [CB].

### ***anc-1* I – 1.43 e1753**

: amb; nuclei of hypodermal cells not elastically anchored; other cytoskeletal abnormalities; no gross phenotype; enhances *Mul* phenotype of *lin-15* mutants, without change in lineage; *e1753*/Df very unhealthy. ES1. OA4: *e1802*, *e1873*, *e1874*, *e1885* (all resemble *e1753*; all alleles tend to revert spontaneously by intragenic reversion). [Hedgecock and Thomson 1982] [CZ]

### ***aph***

***a*** nterior ***p*** harynx-defective [JJ].

### ***aph-1* I 3.63 zu123**

: maternal-effect-lethal, no *anterior pharynx*; resembles Glp-1 embryonic phenotype but no *Lag* or germ-line phenotypes; maternal rescue complete. OA1: *zu147* (weaker allele). [JJ]

### ***aph-2* I 5.06**

Mutation maternal-effect-lethal, no *anterior pharynx*; resembles Aph-1; Egl. CLONED: novel protein, 722 aa with signal sequence; antibody staining indicates APH-2 present on membranes of all late oocytes and early blastomeres. [JJ]

### ***apl***

***a*** myloid ***p*** recusror- ***I*** ike [NY].

### ***apl-1* X – 5.91 pk53**

: Tc1 insertion; no known phenotype. CLONED: encodes several alternatively processed transcripts; longest ORF 608 aa with extensive similarity to human amyloid precursor protein, but no β-amyloid peptide. [Daigle and Li 1993] [NY]

### ***apx***

***a*** nterior ***p*** harynx in e ***x*** cess [JJ].

### ***apx-1* V – 10.21 or3**

: maternal-effect-lethal; extra anterior *pharyngeal cells*; ABp fails to produce intestinal valve cells. OA1: *zu183*. CLONED: predicted protein with similarity to Delta, Serrate, LAG-2; can substitute for *lag-2* if fused to *lag-2* promoter. [Mello et al. 1994; Gao and Kimble 1995; Fitzgerald and Greenwald 1995] [JJ, BB, JK, GS]

### ***arf***

**A** DP ***r*** ibosylation ***f*** actor family [CGC]. See also *arl*.

### ***arf-1* III – 1.36**

NMK. Encodes 181-aa predicted class I ARF. [CGC, MQ]

***arf-2***

= *arl-5*

***arf-3 IV 3.53***

NMK. Encodes predicted class II ARF. [MQ]

***arg***

**a** pex- **r** elated **g** enes [JJ].

***arg-1 X – 15.47***

NMK. Encodes predicted protein related to APX-1; transgene overexpression can rescue [\*lag-2\*](#) mutants. [JJ]

***arl***

**ar** f- **l** ike **p** roteins [CGC]. See also *arf*.

***arl-1 III 0.15***

NMK. Encodes predicted ARL. C38D4.8 [MQ]

***arl-2 III 0.70***

NMK. Encodes predicted ARF-like protein. ZK632.8. [MQ]

***arl-3 II 0.80***

NMK. Encodes predicted ARL (ARL1-like). F54C9. [MQ]

***arl-4 II 1.60***

NMK. Encodes predicted ARF-like protein. ZK1320. [MQ]

***arl-5 II 0.79***

NMK. pka *arf-2*. Encodes predicted 184-aa ARL2-like protein. [MQ]

***arp***

**a** ctin- **r** elated **p** roteins [RW].

***arp-1 II 23.5***

NMK. Sequence predicts protein having 50% homology with actin, 67% with vertebrate actin-related protein; antibody staining suggests located at cell division remnant. [RW]

***art***

steroid **a** lpha **r** educ **t** ase-related [PK].

***art-1 II – 0.19***

NMK. Significant similarity to rat SC2 gene; downstream gene in operon with [\*sod-1\*](#) . [[Kuwabara and Shah 1994](#)] [PK]

***atn***

**a** c **t** ini **n** [RW].

***atn-1 V 4.22***

NMK. 3.6-kb RNA; encodes  $\alpha$ -actinin homolog; almost complete cDNA encodes predicted 926-aa polypeptide; 63% identical to chick smooth muscle  $\alpha$ -actinin. [[Barstead and Waterston 1991b](#)]

***avr***

**a** v ermectin **r** esistance abnormal [CD].

**avr-1**

= *che-3*

**avr-5**

= *osm-3*

**avr-15 ? ad1051**

: Eat phenotype, lacks [M3](#)-derived IPSP; isolated [pharynx](#) insensitive to iontophoretically applied glutamate. [CD, AD]

**bas**

**b** iogenic **a** mine **s** ynthesis-related [LC].

**bas-1 III – 0.81 ad446**

: serotonin-deficient (no detectable serotonin immunoreactivity); serotonin immunoreactivity restored by exposure to serotonin, but not to 5-hydroxytryptophan; poor male turning behavior. [[Loer and Kenyon 1993](#)] [LC, DA]

**bas-2 II 0.83**

NMK. Encodes predicted biogenic amine synthesis enzyme. [LC]

**ben**

**ben** omyl resistance abnormal [TU].

**ben-1 III – 6.43 e1880**

: ts, sd; resistant to 14 µM benomyl; no other phenotype. ES1. OA>20: *e1910, u102, u134*, etc. (all somewhat ts and sd). CLONED: encodes β-tubulin. [[Driscoll et al. 1989](#)]

**bli**

**bli** stered cuticle [CB].

**bli-1 II 3.03 e769**

: adult symmetrically blistered, especially head; enhanced 25°C. ES3 (old adult) ME2. OA6: *e770, e935* (weaker allele), *e993spo, e1610*, etc. Spontaneous mutations frequent. [[Brenner 1974](#)] [CB]

**bli-2 II – 1.26 e768**

: adult blistered, especially head; slightly small; enhanced 25°C. ES3 (old adult) ME2. OA3: *e107, e527, e772*. [[Brenner 1974](#)] [CB]

**bli-3 I – 18.72 e767**

: small irregular shape; variable slight blistering in adult. ES2 (adult late larvae) ME1. OA1: *n529*. [[Brenner 1974](#)] [CB]

**bli-4 I 0.90 e937**

: adult blistered, especially head; penetrance 90%; unique class I allele. ES3 (old adult) ME1. OA13: all other alleles result in late embryonic lethality; most are class II, fail to complement *e937*, e.g., *h42, h199, h254, h1403*. Also *s90* (pka [let-77](#), class III allele, late larval-lethal, complements *e937* but not other alleles). CLONED: multiple alternatively spliced transcripts, encoding predicted endoproteases (KEX2/subtilisin class) with different C-termini. [[Peters et al. 1991; Thacker et al. 1995](#)] [KR]

**bli-5 III – 18.72 e518**

: small dumpyish adult; blistered, especially around [pharynx](#); abnormal bursa in adult male. ES3 (adult late larvae) ME0. OA1: s277 (induced on *eT1*). [[Brenner 1974](#)] [CB, BC]

***bli-6 IV 3.15 sc16***

: adult blistered, both head and body; often small blisters. ES3 (old adult). OA>4: *n776sd*, *mn4dm* (*mn4*/+ always blistered), revertants of *mn4*. Null phenotype uncertain. [[Park and Horvitz 1986a](#)] [BE, SP]

***bop***

**b** last **o** mere **p** olarity-defective [JJ].

***bop-1***

= *mom-1*

***bor***

**bor** dering behavior abnormal [RC].

***bor-1 X 17.37 g320***

: spo, sd; homozygous mutant worms stay near the border of a bacterial lawn, congregate in groups of 10–50+ individuals; usually leads to extensive burrowing; bordering dependent on volatile component(s) of live bacteria; allele *g320* isolated from Freiburg wild isolate RC301, which may contain autosomal Bor enhancers. ES1 ME3. OA2: *ad609*, *n1353* (both EMS-induced in N2, recessive, stronger Bor phenotype than *g320*). [RC, DR, DA]

***cad***

**ca** thepsin **D** -deficient [PJ].

***cad-1 II 23.05 j1***

: 90% reduced cathepsin D; gut cells appear more vacuolated and bubbly; gross phenotype wt. OA2: *j12*, *j14* (similar). Probable structural gene for cathepsin D. [[Jacobson et al. 1988](#)]

***caf***

**caf** feine resistance abnormal [PH]. See also *dyf*.

**caf-1**

= *osm-3*

***caf-2***

= *che-3*

***cah***

**c** cyclase- **a** ssociated protein **h** omolog [CGC].

***cah-1 X 24.08 pk56***

: Tc1 insertion, no known phenotype; sequenced cDNA just 5' to [\*mec-4\*](#) has similarity to yeast CAP (cyclase-associated protein) gene. [TU].

***cal***

**cal** modulin family [CGC].

***cal-1 V 4.31***

NMK. Sequence related to calmodulin and troponin C. [[Salvato et al. 1986](#)]

***can***

**CAN** cell abnormality [NJ]. CAN cell processes run along [excretory](#) canal; ablation of CAN cells lethal.

**can-1 III 6.85 rh67**

: CAN migrates normally, but retains a [neuronal](#) phenotype and usually dies; animals pale and have withered tails. [NJ]

**cap**

actin **cap** ping protein [RW].

**cap-1 IV 3.33**

NMK. Encodes homolog of actin capping protein,  $\alpha$ -subunit; functional in yeast. [[Waddle et al. 1993](#)]

**cap-2 II 3.05**

NMK. Encodes homolog of actin capping protein,  $\beta$ -subunit; functional in yeast. [[Waddle et al. 1993](#)]

**cat**

**cat** echolamine abnormality [CB].

**cat-1 X – 4.18 e1111**

: amb; dopamine and serotonin absent from [neuron](#) processes, present in cell bodies; poor male turning behavior; enhanced foraging behavior, suppressed by serotonin agonists; serotonin immunoreactivity restored by exogenous serotonin or 5-hydroxytryptophan; ES1 ME1. OA1: n733. [[Sulston et al. 1975](#); [Loer and Kenyon 1993](#)] [KP, LC]

**cat-2 II – 18.15 e1112**

: dopamine reduced >95%, serotonin normal; no defect in male turning behavior. ES1 ME3 NA1. [[Sulston et al. 1975](#); [Loer and Kenyon 1993](#)] [LC]

**cat-3 III N e1333**

: (lost); dopamine reduced in [neuron](#) processes. [[Sulston et al. 1975](#)]

**cat-4 V 2.76 e1141**

: dopamine reduced >90%, serotonin reduced or absent; poor male turning behavior; enhanced foraging behavior, suppressed by serotonin agonists; serotonin immunoreactivity restored by exogenous serotonin or 5-hydroxytryptophan; cuticle-defective; hypersensitive to SDS, levamisole, hypochlorite. ES1 ME2 NA1. [[Sulston et al. 1975](#); [Loer and Kenyon 1993](#)] [DA, KP, LC]

**cat-5 V N e1334**

: (lost); variable displacement of CEPD cell bodies and other cells. [[Sulston et al. 1975](#)]

**cat-6 V 4.96 e1861**

: [sensory neurons](#) CEP, [ADE](#), [PDE](#) take up FITC; tubular body of CEP cilia disrupted; abnormal cilia in CEP, OLL; slightly defective dauer formation. ES1 ME3 NA1. [[Hedgecock et al. 1987](#); [Perkins et al. 1986](#)]

**cct**

**c** haperonin **c** ontaining **I** CP-1 [PC].

**cct-1 II 0.78 pk58**

: Tc1 insertion, no known phenotype; pka [tcp-1](#); encodes one of 7–9 related subunits of eukaryotic cytosolic chaperonin; ortholog of mouse Ccta (66% aa sequence identity). [[Leroux and Candido 1995](#)] [PC]

**cct-2 II 0.9**

NMK. Encodes one of 7–9 related subunits of eukaryotic cytosolic chaperonin CCT; ortholog of mouse Cctb (66% aa sequence identity) [PC]

**cct-4 II 0.78**

NMK. Encodes one of 7–9 related subunits of eukaryotic cytosolic chaperonin CCT; ortholog of mouse Cctd (63% aa sequence identity) [PC]

**cct-5 III – 3.70**

NMK. Encodes one of 7–9 related subunits of eukaryotic cytosolic chaperonin CCT; ortholog of mouse Ccte (68% aa sequence identity) [PC]

**cct-6 III – 1.2**

NMK. Encodes one of 7–9 related subunits of eukaryotic cytosolic chaperonin CCT; ortholog of mouse Cctz (67% aa sequence identity) [PC]

**cdc**

**c**ell **d**ivision **c**ycle-related [CGC].

**cdc-42 II – 0.5 pk57**

: Tc1 insertion; no known phenotype; encodes homolog of CDC42 (188 aa, 85% identity to human sequence, complements yeast mutant). [[Chen et al. 1993b](#)]

**cdh**

**c**a **dh** erin family [BW].

**cdh-1 III – 11.31**

NMK. Encodes cadherin-related protein; 11-kb embryonic transcript. [BW, NL]

**cdh-2 V 18.09**

NMK. Encodes cadherin-related protein; 11-kb embryonic transcript. [BW, NL]

**cdh-3 III – 0.58 pk87**

: te; viable, grossly wt; allele is deletion derived from *pk77tci*; encodes a cadherin-related protein; 10-kb transcript detected on Northern blots, in late-stage embryo and L1 larval RNA; *cdh:lac-Z* expressed in [seam cells](#), comma-stage through to 3-fold embryos; a few other as yet unidentified hypodermal cells also stain in the anterior; overexpression of truncated transgene leads to Pun ([pharynx](#) detachment) phenotype. [BW, NL]

**ced**

**ce** II **d**eath abnormality [CB].

**ced-1 I 10.77 e1735**

: programmed cell deaths abnormal; dying cells arrest at highly refractile stage; killer cells fail to engulf target cells; engulfment group A (*ced-1,6,7*); no gross phenotype. ES1. OA>10: *n1506spo*, *e1754*, *e1797*, *e1798*, *e1799*, *e1800*, *e1801*, *e1814*, *n691*, *n2000*, *n2092* (all alleles similar) [[Hedgecock et al. 1983](#); [Ellis et al. 1991a](#)] [MT]

**ced-2 IV – 17.79 e1752**

: programmed cell deaths abnormal; dying cells arrest at highly refractile stage; killer cells fail to engulf target cells; engulfment group B (*ced-2,5,10*: suppress Vul phenotype of [lin-24](#), [lin-33](#)); extensive maternal rescue; no gross phenotype. ES1. OA1: *n1994*. [[Hedgecock et al. 1983](#); [Ellis et al. 1991a](#)] [MT]

**ced-3 IV 8.17 n717**

: programmed cell deaths fail to occur; epistatic to [\*ced-1\*](#), [\*ced-2\*](#), and [\*nuc-1\*](#); recessive suppressor of [\*egl-1\*](#) and of egg-laying defect of [\*egl-41\*](#) homozygotes; semidominant suppressor of *egl-1(n487)/+* and *egl-41(n1069)/+* heterozygotes; no gross phenotype. ES1 (ES2 in [\*egl-1\*](#) background) ME3. OA>10: *n718*, *n1129*, *n1163*, *n1164*, *n1165*, *n1286*, *pk59tci*. CLONED: 2.9-kb RNA; predicted protein 503 aa, 56 kD; similarity (29% identity) to mammalian ICE (interleukin-1 $\beta$  converting enzyme); antibodies detect 34-kD and 12-kD species. [[Yuan et al. 1993](#)] [MT]

#### ***ced-4 III – 2.44 n1162***

: programmed cell deaths fail to occur; recessive suppressor of [\*egl-1\*](#) and [\*egl-41\*](#) homozygotes; no gross phenotype. ES1 (ES2 in [\*egl-1\*](#) background) ME3. OA>10: *n1894*, *n1920*, *n1461* (Tc4 insertion, also revertants *n1561n1712*, *n1416n1713*), *n2273* (anomalous allele, enhances cell death by synergy with [\*ced-9\*](#) [*lf*], but reduces cell death alone), etc. CLONED: major transcript 2.2 kb; encodes 549-aa novel protein, 65 kD (confirmed by antibody); minor 2.3-kb transcript (alternatively spliced, may inhibit cell death). [[Yuan and Horvitz 1992](#)] [MT]

#### ***ced-5 IV 4.65 n1812***

: programmed cell deaths abnormal; dying cells arrest at highly refractile stage; killer cells fail to engulf target cells; engulfment group B (*ced-2,5,10* : suppress Vul phenotype of [\*lin-24\*](#), [\*lin-33\*](#)); Mig, hermaphrodite [\*distal tip cells\*](#) execute extra turns; extensive maternal rescue; no gross phenotype. OA1: *n2002*. CLONED: 5.6-kb transcript; predicted protein 180 kD, novel. [[Ellis et al. 1991a](#)] [MT, NF, ZB]

#### ***ced-6 III – 1.52 n2095***

: programmed cell deaths abnormal; dying cells arrest at highly refractile stage; killer cells fail to engulf target cells; engulfment group A (*ced-1,6,7*); extensive maternal rescue; no gross phenotype. OA1: *n1813*. [[Ellis et al. 1991a](#)] [MT]

#### ***ced-7 III 0.49 n1892***

: programmed cell deaths abnormal; dying cells arrest at highly refractile stage; killer cells fail to engulf target cells; engulfment group A (*ced-1,6,7*); extensive maternal rescue; no gross phenotype. OA6: *n1893*, *n1896*, *n1996*, *n1997*, *n1998*, *n2001*, *n2094*. CLONED: encodes predicted 191-kD protein, with similarity to ABC transporter proteins. [[Ellis et al. 1991a](#)] [MT; ZB]

#### ***ced-8 X – 0.03 n1891***

: programmed cell deaths abnormal and protracted; dying cells arrest at highly refractile stage; killer cells fail to engulf target cells; superficially resembles engulfment group A (*ced-1,6,7*), but synergizes with weak [\*ced-3\*](#) alleles in preventing cell death; no gross phenotype. OA3: *n1999*, *n2090*, *n2093*. CLONED: encodes predicted novel protein. [[Ellis et al. 1991a](#)] [MT]

#### ***ced-9 III 2.40 n1950***

: sd; gf allele, reduced cell deaths; intragenic *lf* revertants increase cell death: *n1950n2077* (partial sterility, Mel, very sick embryo), *n1950n2161* (weaker *lf*, Mel, ectopic cell deaths in embryo), *n1653ts* (weak *lf*, viable). CLONED: 2.1-kb ([\*cyt-1\*](#) + [\*ced-9\*](#)) and 1.3-kb transcripts; latter encodes 280-aa protein related to mammalian *bcl-2* (23% identity); 3' of [\*cyt-1\*](#), immediately adjacent, shares regulation. [[Hengartner et al. 1992](#); [Hengartner and Horvitz 1994b](#)] [MT]

#### ***ced-10 IV – 1.80 n1993***

: dying cells arrest at highly refractile stage; killer cells fail to engulf target cells; engulfment group B (*ced-2,5,10*: suppress Vul phenotype of [\*lin-24\*](#), [\*lin-33\*](#)); extensive maternal rescue; no gross phenotype. [Ellis et al. 1991] [MT]

#### ***ced-11 III 0.15 n2744***

: abnormal programmed cell death corpses. OA4: *n2745*, *n2832*, *n2833*, *n2834*. CLONED: encodes predicted novel protein. [MT]

### ***ceh***

**C . e** *legans* **h** omeobox [TB].

### ***ceh-1 X – 7.00***

NMK. Encodes homeoprotein with similarities to *Apis* H40, *Drosophila* NK-1. [[Hawkins and McGhee 1990](#)]

### ***ceh-2 I 0.70***

NMK. Encodes homeoprotein; antibodies stain some [pharyngeal cells](#) just before pharyngeal morphogenesis. [[Bürglin et al. 1989](#)]

### ***ceh-3***

= *pal-1*

### ***ceh-4***

= *unc-4*

### ***ceh-5 IV 4.65***

NMK. Encodes diverged homeoprotein (novel class). [[Bürglin et al. 1989](#)]

### ***ceh-6 I 2.85 mg60***

: embryonic- or L1-lethal; malformed [rectum](#), rectal rupture at or after 2-fold stage; *mg60* is 1.6-kb deletion derived from Tc1 insertion *pk33*; antibody stains strong or transiently in a variety of [neuronal](#) tissues, [excretory](#) cells, rectal cells [Y](#), [K](#), [F](#), [B](#), [U](#); encodes homeoprotein, POU III subclass. [[Bürglin et al. 1989](#)] [TB]

### ***ceh-7 II 0.81***

NMK. Encodes diverged homeoprotein (novel class). [[Bürglin et al. 1989](#)]

### ***ceh-8 I 2.48***

NMK. Encodes homeoprotein. [[Bürglin et al. 1989](#)]

### ***ceh-9 I – 19.89***

NMK. Similar to sea urchin TgHbox5. [[Hawkins and McGhee 1990](#)]

### ***ceh-10 III – 1.25***

NMK. 1.2-kb transcript; encodes 344-aa Paired-like class homeoprotein; extensive similarity to mouse Chx10, goldfish Vsx-1; *ceh-10:lacZ* expressed maximally in embryo, from 250–300-cell stage, lower in larvae, in certain [neuronal](#) nuclei ([interneurons](#) AIY, AIN, [sensory neurons](#) CEPD, motor neurons [RID](#), RMED; CAN cells, etc.); transgene can induce defects in CAN cell migration and withered tail phenotype. [[Hawkins and McGhee 1990](#); [Svendsen and McGhee 1995](#)] [JM]

### ***ceh-11***

= *egl-5*

### ***ceh-12 I 0.34***

NMK. Encodes homeoprotein. [[Schaller et al. 1990](#)]

### ***ceh-13 III – 0.67 pk20, pk36***

: Tc1 insertions; no known phenotype; encodes labial-like homeoprotein (68% identity in homeodomain). [[Schaller et al. 1990](#)]

### ***ceh-14 X – 1.83***

NMK. Encodes LIM class homeoprotein. [[Bürglin et al. 1989](#)]

***ceh-15***

= *lin-39*

***ceh-16 III – 0.17***

NMK. Encodes predicted homeoprotein; Engrailed-related. [[Kamb et al. 1989](#)]

***ceh-18 X – 9.46 mg57***

: variable defects in oogenesis, many oocytes fail to arrest in meiosis I (Emo), 11% sterile; some abnormal round eggs; impenetrant gonad arm defects (27%), larval lethality (15%), disorganized [hypodermis](#); [male gonad](#) and spermatogenesis normal; probable null allele (deletion derivative of *pk37tci*). OA2: *mg58te*, *mg61te* (weaker phenotypes); also Tc1 insertions *ms1*, *ms2*. Encodes 542-aa POU class homeoprotein; CEH-18 antibody staining absent until late embryo; at hatching, most abundant in hypodermal and muscle nuclei, later in DTC nuclei, gonad sheath nuclei; overexpression by HS construct leads to defects; antisense expression in late embryo leads to lethality; [hypodermis](#) abnormal. [[Greenstein et al. 1994](#)] [DG, GR, YK]

***ceh-19 IV 3.53***

NMK. Encodes predicted homeoprotein. [[Naito et al. 1992](#)] [YK]

***ceh-20 III – 0.81 ay9***

: Vul, Egl, SM migration defects; stronger alleles are larval-lethal, Unc, defective in Q daughter migrations, [M lineage](#); males do not mate, have defective tails. OA3: *ay412* (severe Unc, Vul), *ay37*, *ay38* (both larval-lethal). Encodes PBC class homeoprotein; antibody stains posterior of embryo, RVG and VNC of larva; weak staining in [body muscle](#) and [hypodermis](#). [[Bürglin and Ruvkun 1992](#)] [NH, TB]

***ceh-21 X – 15.42***

NMK. Encodes cut class homeoprotein (T26C11.6). [[Bürglin and Ruvkun 1992](#)] [TB]

***ceh-22 V 2.80 cc8266***

: te; pharyngeal defects, poor feeding, some larval arrest. OA1: *pk40tci*. Encodes protein related (83%) to NK-2 of *Drosophila*; candidate binding protein for [myo-2](#) enhancer; *ceh-22:lacZ* expressed in [pharyngeal muscle](#). [[Okkema and Fire 1994](#)]

***ceh-23 III – 0.54***

NMK. Encodes homeoprotein most similar to *Drosophila* Empty spiracles and Distalless; *ceh-23:lacZ* expressed primarily in [amphid sensilla](#), CAN cells. [[Wang et al. 1993](#)] [TB]

***ceh-24 V 5.57 pk92***

: Tc1 insertion, no known phenotype; encodes NK class homeoprotein; *ceh-24:lacZ* expressed in [pharynx](#) muscle , vulval muscles, some [head neurons](#). [PD]

***ceh-25 ?***

NMK. Encodes novel atypical homeoprotein. [TB]

***ceh-26 III – 0.40***

NMK. Encodes predicted protein (K12H4.1), with atypical homeodomain, similar to *Drosophila* Prospero in homeodomain and C-terminal 100 aa. [[Bürglin 1994](#)] [TB]

***ces***

***ce*** II death ***s*** election abnormal [MT].

***ces-1 I 2.91 n703***

: sisters of NSM, I2 fail to undergo programmed cell death (gf allele). OA2 (gf): *n1895*, *n1896* (similar). If alleles (probable null) wt but suppress *ces-2* mutations. CLONED: encodes zinc finger protein, most related to Snail of *Drosophila*. [[Ellis and Horvitz 1991](#)] [MT]

#### ***ces-2* I 29.06 *n732***

: sisters of NSM (but not I2) fail to undergo programmed cell death. CLONED: encodes protein related to bZIP transcription factors. [[Ellis and Horvitz 1991](#)] [MT]

#### ***cey***

**C . e** *legans* **Y** box-containing genes [PD]. See also [\*lin-28\*](#).

#### ***cey-1* II 3.07 *pk81***

: Tc1 insertion, no known phenotype; CEY-1 protein binds to internal enhancer of *unc-54* in vitro; maternal RNA maintained in germ line, lost in soma; later transcripts ubiquitous. [[Seydoux and Fire 1994](#)] [PD]

#### ***cey-2* I 0.03**

NMK. Encodes predicted Y box protein; maternal RNA maintained in germ line, lost in soma. [[Seydoux and Fire 1994](#)] [PD]

#### ***cey-3* I 0.00**

NMK. Encodes predicted Y box protein. [PD]

#### ***cha***

**ch** oline **a** cetyltransferase [PR, RM].

#### ***cha-1* IV – 3.31 *p1152***

: 99% reduced choline acetyltransferase, slow-growing, uncoordinated (coiler), Ric (resistant to aldicarb, trichlorfon); slow pumping. ES3. OA>10: *m324* (lethal, probable null), *b401ts* (ME2), *p1154*, *p1156* (anomalous allele, fails to complement [\*unc-17\*](#)), *cn101*, *n2411*, etc. Defecation cycle variable in length, often extremely long in all alleles tested; [\*unc-17\*](#) alleles *e113*, *e876* fail to complement *cha-1*. CLONED: encodes choline acetyltransferase; 37% identical to pig enzyme, 28% to *Drosophila* enzyme; antibody staining cytosolic, in motor [\*neurons\*](#); shares 5'UTR exon with [\*unc-17\*](#). [[Rand 1989](#); [Alfonso et al. 1994a,b](#)] [RM, JT, DR, DA]

#### ***che***

**che** motaxis-defective [CB]. See also *daf*, *avr*, *tax*, *dyf*.

#### ***che-1* I 1.45 *e1034***

: nonchemotactic to sodium ion; abnormal sensory neuro-anatomy especially AFD, IL2 cells. ES1 ME2. OA>5: *e1035*, *p674* (pka [\*tax-1\*](#), normal thermotaxis, poor osmotic avoidance), *p679*, *p680*, *p692*, *p696*. [[Dusenberry 1976](#); [Lewis and Hodgkin 1977](#)]

#### ***che-2* X – 19.54 *e1033***

: nonchemotactic to sodium ion; slightly small; defective in osmotic avoidance and dauer formation; males impotent; Dyf (no FITC uptake); ciliated [\*neurons\*](#) have abnormal stunted ultrastructure. ES2 ME0. OA5: *m127*, *mn330mut*, *mn395*, etc. [[Lewis and Hodgkin 1977](#); [Starich et al. 1995](#)] [DR, SP, NJ]

#### ***che-3* I 2.28 *e1124***

: nonchemotactic to sodium ion; slightly small; defective in osmotic avoidance and dauer formation; males impotent; ciliated [\*neurons\*](#) have abnormal stunted ultrastructure; Dyf (no FITC uptake); octopamine-deficient. ES2 ME0. OA>30: *e1379*, *e1253* (pka [\*che-8\*](#)), *p801* (pka [\*osm-2\*](#)), *m443mut*, *mn333mut*, *sa129*, etc.

Also *hf5* (pka *caf-2*, resistant to 30 mM caffeine; no gross phenotype; Df). High forward mutation frequency. [[Lewis and Hodgkin 1977](#); [Starich et al. 1995](#)] [NJ, SP, DR]

***che-4***

= *mec-1*

***che-5 IV N e1073***

: poor chemotaxis to sodium ion; erratic movement. ES1 ME3 NA1. [[Lewis and Hodgkin 1977](#)] [KP]

***che-6 IV N e1126***

: nonchemotactic to chloride ion; abnormal IL2 basal bodies. ES1 ME3 NA1. [[Lewis and Hodgkin 1977](#)]

***che-7 V N e1128***

: nonchemotactic to chloride ion; small. ES1 ME3 NA1. [[Lewis and Hodgkin 1977](#)]

***che-8***

= *che-3*

***che-9***

= *che-13*

***che-10 II – 2.79 e1809***

: Df (no FITC uptake by amphids or phasmids); striated ciliary rootlets missing from OLQ, IL1, BAG [sensory neurons](#); defective osmotic avoidance; males impotent. ES1. OA>5: *m525mut, mn403, n1514*. [[Perkins et al. 1986](#); [Starich et al. 1995](#)] [DR, SP, MT]

***che-11 V 3.87 e1810***

: Df (no FITC uptake by amphids or phasmids); defective in osmotic avoidance and dauer formation; irregular amphid cilia, abnormal staining, abnormal CEP cilia, etc. ES1 ME0. OA>6: *e1815, m162, mn387, mn393*. [[Perkins et al. 1986](#); [Starich et al. 1995](#)] [SP, DR]

***che-12 V 2.21 e1812***

: Df (weak FITC uptake by amphids and phasmids); amphid sheath cells fail to secrete matrix material; defective osmotic avoidance. ES1 ME3. OA3: *e1813, mn389, mn399*. [[Perkins et al. 1986](#); [Starich et al. 1995](#)]

***che-13 I 5.27 e1805***

: Df (no FITC uptake by amphids or phasmids); severely shortened axonemes and ectopic assembly of ciliary structures and microtubules in many [sensory neurons](#); defective in osmotic avoidance and dauer formation. ES1 ME0. OA2: *m523mut, n1520*. [[Perkins et al. 1986](#); [Starich et al. 1995](#)] [DR, SP]

***che-14 I N e1960***

: some FITC uptake by amphids but not by phasmids; abnormal uptake by CEP [ADE PDE](#); abnormal amphid channel due to misjoining of sheath and socket cell. ES1 NA1. [[Perkins et al. 1986](#)]

***che-15 II N n1931***

: defective chemotaxis. OA1: *n1932*. [MT, CX]

***che-16 I 2.1 n1929***

: sd; defective chemotaxis to cAMP, chloride; normal taxis to volatile odorants. OA1: *n1851*. [MT, CX]

***cib***

***c*** hanged ***i*** dentity of ***b*** lastomeres [GE].

***cib-1 I – 0.24 e2300***

: ts; maternal-effect embryonic-lethal at 25°C, wt at 15°C; TSP in oocyte, early embryo; mutant embryos exhibit abnormal delayed cleavage of [P1](#), [P2](#), [P3](#); other pleiotropic defects. OA6: e2303 (nonconditional strict Mel), e2301, e2302, e2304, e2305, e2306 (all ts, weaker than e2300). [[Schnabel and Schnabel 1990](#)]

### **cib-3 I – 7.49 t1008**

: Mel? [GE]

#### **clb**

**c** o **l** lagen, **b** asement membrane-associated [CH]. Collagen type IV.

#### **clb-1**

= *let-2*

#### **clb-2**

= *emb-9*

#### **clk**

**cl** oc **k** (biological timing) abnormal [MQ].

### **clk-1 III – 1.99 e2519**

: mat; growth and behavior slowed by up to 2-fold; profound zygotic and maternal rescue; slow postembryonic development, slow cell cycle, long life span; swimming, pumping, egg-laying, defecation all slow and irregular. OA4: *qm30* (worms viable at 20°C but become sterile at 25°C), *qm11*, *qm47*, *qm51*. CLONED: cosmid rescue (W03B11) [[Wong et al. 1995](#); [Lakowski and Hekimi 1996](#)] [MQ]

### **clk-2 III – 0.71 qm37**

: slow growth and rhythms, phenotypes similar to Clk-1; profound maternal and zygotic rescue; embryonic-lethal at 25°C, some lethality at all temperatures. NA1. [[Lakowski and Hekimi 1996](#)] [MQ]

#### **clk-3 II 21.5 qm38**

: slow growth and rhythms, phenotypes similar to Clk-1; profound maternal and zygotic rescue; no lethality. OA1: *qm53*. [[Lakowski and Hekimi 1996](#)] [MQ]

#### **clr**

**cl** ea **r** [CB].

### **clr-1 II – 1.95 e1745**

: ts; starved translucent appearance at 20°C, facilitating Nomarski visualization of [neuron](#) processes; phenocopied by growth on 1 mM orthovanadate; inviable at 25°C; suppresses *egl-15(n1477ts)* and SM Mig defect of *egl-17(1313)*. ES3 (25°C) ES2 (20°C). OA>30: e2530 (slightly stronger phenotype, putative null), *ut41* (non-ts-lethal); most alleles isolated as [egl-15](#) suppressors, some of these viable, non-Clr. See also *soc*. CLONED: encodes protein with similarity to protein tyrosine phosphatases. [[Clark et al. 1992](#); [DeVore et al. 1995](#)] [NJ, MT, NH, JC]

#### **cod**

**co** pulation- **d** efective [PS].

### **cod-1 V 1.59 sy193**

: males unable to insert spicules during mating. [PS]

### **cod-2 I 10.00 sy43**

: males unable to insert spicules during mating, spicule muscle defect. [PS]

***cod-3 IV 2.7 sy166***

: copulation-defective males. [PS]

***cod-4 III – 1.99 sy180***

: males have difficulty inserting spicules during mating. [PS]

***cod-5 II 0.12 sy181***

: males fail to execute proper turning behavior during mating. [PS]

***cod-6 III – 0.93 sy186***

: males fail to insert spicules during mating. [PS]

***cod-7 I 0.10 sy190***

: males unable to insert spicules during mating. [PS]

***cod-8 III N sy176***

: synthetic spicule insertion-defective with *cod-9(sy226)*. [PS]

***cod-9 IV N sy226***

: synthetic spicule insertion-defective with *cod-8(sy1760)*. [PS]

***cod-10 I 9.04 sy38***

: males fail to initiate mating behavior and have a variable tail abnormality that can include abnormal rays, breaks in the alae, and occasional pseudovulvae-like structures. NA1. [PS]

***cod-11 I N sy35***

: males fail to execute proper turning behavior during mating; sex-specific muscle defects. [PS]

***cod-12 II N sy419***

: males defective in vulval location during mating. [PS]

***cod-13 III N sy420***

: males defective in vulval location during mating. [PS]

***cod-14 IV N sy421***

: males defective in vulval location during mating. [PS]

***cod-15 I N sy423***

: males defective in vulval location during mating. [PS]

***col***

**col** lagen genes [CH]. Families defined by *dpy-13*, *dpy-10*, *col-6*, *sqt-1*, *col-8*, *dpy-7*.

**col-1**

= *sqt-3*

***col-2 IV 4.58***

NMK. Transcript abundant only in dauer larvae; encodes 300-aa collagen, [\*dpy-13\*](#) family (59% identical to SQT-3). [[Kramer et al. 1982](#); [Cox and Hirsh 1985](#)]

***col-3 IV 3.95***

NMK. Transcript present in all stages, abundant in L4, decreases in adult. [[Cox and Hirsh 1985](#)]

***col-4 IV* 3.49**

NMK. Misnamed, not a true collagen; contains 23 repeats of 15-aa sequence GAPPSSGGPGPF(D/N)PS; no transcript detected. [[Cox et al. 1985](#)] [CH]

***col-5 IV* 5.50**

NMK. Hybridizes to collagen probe. [[Cox et al. 1985](#)]

***col-6 II* 0.44**

NMK. Transcript abundant only in dauer larvae; encodes collagen; *col-6* family includes *col-12,13,14,36,40*. [[Cox and Hirsh 1985](#)]

***col-7 I* 2.0**

NMK. Transcript present in dauer, adult; not detected in egg or L4. [[Cox and Hirsh 1985](#); [Liu et al. 1995](#)] [VT]

***col-8 III – 0.80***

NMK. Transcript present in dauer larvae, adults; not detected in egg or L4; encodes collagen; *col-8* family includes *col-19,35,39*. [[Cox and Hirsh 1985](#)]

***col-9 X* 13.12**

NMK. Hybridizes to collagen probe. [[Cox et al. 1985](#)]

***col-10 ?***

NMK. Transcript present at all stages, most abundant in L4. [[Cox and Hirsh 1985](#)]

***col-11 ?***

NMK. Transcripts present at all stages, 7-fold increase in adult. [[Cox and Hirsh 1985](#)]

***col-12 V* 2.57**

NMK. Transcripts detected late in each larval stage, at lethargus; encodes collagen, *col-6* family; linked to *col-13*. [[Cox and Hirsh 1985](#)] [IA]

***col-13 V* 2.57**

NMK. Transcript present at all stages; encodes collagen, *col-6* family; linked to *col-12*. [[Cox and Hirsh 1985](#)]

***col-14 ?***

NMK. Transcript present at all stages; encodes collagen, *col-6* family. [[Cox and Hirsh 1985](#)]

***col-15 ?***

NMK. Transcript present in dauer, L4, adult; not detected in egg. [[Cox and Hirsh 1985](#)]

***col-16 ?***

NMK. Transcript present in dauer, L4, adult; not detected in egg. [[Cox and Hirsh 1985](#)]

***col-17 ?***

NMK. Transcript present in dauer, L4, probably absent from adult; not detected in egg. [[Cox and Hirsh 1985](#); [Liu et al. 1995](#)] [VT]

***col-18 ?***

NMK. Transcript present in dauer, adult; not detected in egg or L4. [[Cox and Hirsh 1985](#)]

***col-19 ?***

NMK. Transcript present in dauer, adult; not detected in egg or L4; encodes collagen, *col-8* family. [[Cox and Hirsh 1985](#); [Liu et al. 1995](#)] [VT]

**col-20 ?**

NMK. Linked to [col-17](#) . [[Cox and Hirsh 1985](#)]

**col-33 IV 0.08**

NMK. Encodes collagen. [[von Mende et al. 1988](#)]

**col-34 IV 0.01**

NMK. Encodes collagen; adjacent and closely related to collagen gene [dpy-13](#) . [[von Mende et al. 1988; Bird 1992](#)] [CH]

**col-35 ?**

NMK. Encodes collagen, [col-8](#) family. [[Kramer 1994a](#)] [CH]

**col-36 II 0.3**

NMK. Encodes 307-aa collagen, [col-6](#) family; transcript present L1, L1-L2, L2-dauer, not eggs, late larvae, adults. C15G2. [[Levy and Kramer 1993](#)]

**col-37 V 3.61**

NMK [KE].

**col-39 II 2.88**

NMK. Encodes collagen, [col-8](#) family. [[Kramer 1994a](#)] [CH]

**col-40 II – 16.62**

NMK. Encodes 292-aa collagen, [col-6](#) family; transcript present L1, L2-dauer, not L2. [[Levy and Kramer 1993](#)]

**cpr**

**c**ysteine **p**rotease family [CGC].

**cpr-1 V 8.24**

NMK. Encodes 329-aa protein (pka [gcp-1](#)) with 40–50% identity to cysteine proteases; 1.1-kb transcript [intestine](#)-specific, present in larvae and adults, not embryos. [[Ray and McKerrow 1992](#)]

**cpr-2 V 3.48**

NMK. Encodes protein with similarity to cysteine protease. [[Ray and McKerrow 1992](#)]

**cpr-3 V 8.3**

NMK. Encodes protein with significant similarity to proteases of cathepsin B family (EST *cm12b6*); 50% identity to CPR-1. [[Larminie and Johnstone 1996](#)] [IA]

**cpr-4 V 0.16**

NMK. Encodes protein with significant similarity to proteases of cathepsin B family (EST *cm14e3*). [[Larminie and Johnstone 1996](#)] [IA]

**cpr-5 V – 19.9**

NMK. Encodes protein with significant similarity to proteases of cathepsin B family (EST *cm04d10*). [[Larminie and Johnstone 1996](#)] [IA]

**cpr-6 X – 2.75 pk91**

: Tc1 insertion, no known phenotype; encodes protein with significant similarity to proteases of cathepsin B family (EST *cm01a5*). [[Larminie and Johnstone 1996](#)] [IA]

***crf***

See *nhr*.

***crf-1***

= *nhr-1*

***crf-2***

= *nhr-2*

***crt***

**C**al **R**e **T**iculin family [CGC].

***crt-1 V – 1.13***

NMK. Encodes predicted 395-aa calreticulin (61% identity to mouse calreticulin). [[Smith 1992](#)]

***cut***

**CUT** iclin [NA].

***cut-1 II 3.16***

NMK. Cross-hybridization to *Drosophila* vitelline membrane protein gene (pka [vmp-1](#)); encodes collagenase-resistant cuticle component; predicted 423 aa, *trans*-spliced to SL1; transcript highest in dauer; CUT-1 present in cortical layer (all stages) and under alae (dauers). [[Sebastian et al. 1991](#)] [NA]

***cut-2 V 5.16***

NMK. Cross-hybridizes to *Drosophila* vitelline membrane protein gene (pka [vmp-2](#)); encodes collagenase-resistant cuticle component; predicted 231-aa secreted protein, repetitious, some similarity to CUT-1; CUT-2 present in cortical layer (all stages) and under alae (dauers). [[Lassandro et al. 1994](#)] [NA]

***cwn***

**C***aenorhabditis WN* T family [CF].

***cwn-1 II – 18.97 mu109***

: embryonic-lethal; early arrest as disorganized embryo at 2–3-fold stage; allele obtained by psoralen screen for lethals rescued by [cwn-1](#) transgene. OA1: *mu110*. CLONED: 1.4-kb transcript, *trans*-spliced; most abundant in embryo; encodes 372-aa Wnt homolog. [[Shackleford et al. 1993](#)] [CF]

***cwn-2 IV 4.58***

NMK. 1.5-kb transcript; most abundant in embryo; encodes predicted 362-aa Wnt homolog. [[Shackleford et al. 1993](#)] [CF]

***cya***

**CY** clin **A** [CGC].

***cya-1 III 0.13***

NMK. Encodes predicted cyclin A. [[Kreutzer et al. 1995](#)] [KB].

***cya-2 II – 14.80***

NMK. 1.4-kb transcript; encodes predicted cyclin A. [[Kreutzer et al. 1995](#)] [KB]

***cyb***

**CY** clin **B** [CGC].

***cyb-1 IV 4.73***

NMK. 72% identity to sea urchin cyclin B. [[Kreutzer et al. 1995](#)] [KB]

### **cyb-2 V 8.50**

NMK. Encodes predicted cyclin B. [[Kreutzer et al. 1995](#)] [KB]

### **cyp**

**cy** clo **p** hilin-related [TP].

### **cyp-1 V 5.84**

NMK. Cyclophilin family, *trans*-spliced to SL1; partial sequence identity 83% to human CYP gene, 74% to yeast CSBY; possible signal peptide. YAC Y14B8. [[Page et al. 1996](#)] [WS, TP]

### **cyp-2 III 21.51**

NMK. Cyclophilin family; partial sequence identity 64% to human CYP gene, 66% to yeast CSBY. Cosmid ZK526. [[Page et al. 1996](#)] [WS]

### **cyp-3 V 7**

NMK. Cyclophilin family, *trans*-spliced to SL1. YAC Y15F7. [[Page et al. 1996](#)] [TP]

### **cyp-4 II 3.04**

NMK. Cyclophilin family (diverged CsA-binding domain). Cosmid M106. [[Page et al. 1996](#)] [WS]

### **cyp-5 I 29.9**

NMK. Cyclophilin family, *trans*-spliced to SL1. Cosmid B0467. [[Page et al. 1996](#)] [TP]

### **cyp-6 III – 26.3**

NMK. Cyclophilin family; signal peptide. Cosmid C51B6. [[Page et al. 1996](#)] [TP]

### **cyp-7 V N**

NMK. Cyclophilin family; signal peptide. [[Page et al. 1996](#)] [TP]

### **cyp-8 X 0.65**

NMK. Cyclophilin family (diverged CsA-binding domain). Cosmid D1009. [[Page et al. 1996](#)] [TP]

### **cyp-9 III – 5.70**

NMK. Cyclophilin family (diverged CsA-binding domain), *trans*-spliced to SL2. Cosmid C14B1. [[Page et al. 1996](#)] [TP]

### **cyp-10 II 0.15**

NMK. Cyclophilin family (diverged CsA-binding domain). Cosmid B0252. [[Page et al. 1996](#)] [TP]

### **cyp-11 II 0.81**

NMK. Cyclophilin family (diverged CsA-binding domain). Cosmid T01B7. [[Page et al. 1996](#)] [TP]

### **cyt**

**cyt** ochrome [CGC].

### **cyt-1 III 2.40**

NMK. Transcripts 2.1-kb (cyt-1 + ced-9) and 0.75 kb; encodes 182-aa presumptive cytochrome  $b_{560}$ ; 3'end overlaps [ced-9](#), shared regulation. [[Hengartner and Horvitz 1994b](#)] [MT, WS]

## **D to F**

### ***dad***

***d***efender against ***a*** poptotic ***d***eath (homologs of mammalian DAD) [JR].

### ***dad-1* ?**

Tc1 insertions obtained; no phenotype known. CLONED: 0.55-kb transcript, encodes 113-aa predicted protein, >60% identity to vertebrate DAD-1; transgene overexpression inhibits cell death; *Ce-dad-1* functional in hamster cells. [[Sugimoto et al. 1995](#)] [JR]

### ***daf***

***da***uer larva ***f***ormation abnormal [DR].

### ***daf-1 IV – 28.04 m40***

: ts, mat; constitutive dauer formation at 25°C, reversible by shift to 15°C; dark [intestine](#); clumpy; exhibits Srf-6 phenotype even at 16°C; no effect on life span. ES3 (L3). NA17: *n690* (Egl type C), *sa184 e1287, e1146, m402::Tc1*, etc. CLONED: 2.5-kb transcript, encodes predicted 669-aa receptor Ser/Thr kinase, member of TGF-β receptor family. [[Georgi et al. 1990](#); [Malone and Thomas 1994](#); [Larsen et al. 1995](#)] [DR, AT]

### ***daf-2 III – 7.98 e1370***

: ts; constitutive dauer formation at 25°C, reversible by shift to 15°C; increased adult life span, increased thermotolerance, UV resistance; non-Srf; ES3 (L3). OA>40: *e979, m577, m41* (wt at 15°C), *sa223* (sterile), *m65* (nonconditional), etc. Most alleles (not *e1370*) hypersensitive to dauer pheromone. [[Larsen et al. 1995](#); [Malone and Thomas 1994](#); [Dorman et al. 1995](#); [Murakami and Johnson 1996](#)] [DR, CF, JT, AT]

### ***daf-3 X – 19.35 e1376***

: defective dauer formation. ES1 ME3 OA7. CLONED: encodes dwarfin/MAD/DPC-4 family protein. [[Riddle et al. 1981](#); [Thomas et al. 1993](#)] [GR]

### ***daf-4 III – 1.52 m63***

: ts; constitutive dauer formation at 25°C; reversible by shift to 15°C; at all temperatures, small and defective in intestinal endocytosis, similar to Sma-2; Srf-6 at 16°C; type-E Egl; weak maternal rescue. ME0: males have crumpled spicules, fused and displaced rays. ES3 (L3) ES2 (other stages); all alleles ts Daf. OA7: *e1364, m72amb, m592* (also ts for Sma), etc. Most alleles resemble *m63*. CLONED: encodes predicted 744-aa receptor Ser/Thr kinase, related to TGF-β type II receptor kinases, binds human BMP-4. [[Estevez et al. 1993](#)] [DR, JT, PB, PJ, AT]

### ***daf-5 II 23.33 e1386***

: defective dauer formation. ES1 ME3. OA11: *e1385*, etc. [[Riddle et al. 1981](#); [Thomas et al. 1993](#)] [DR]

### ***daf-6 X 19.07 e1377***

: defective dauer formation; abnormal chemotaxis; defective osmotic avoidance; poor male mating; abnormal sensory anatomy, especially amphidial sheath cells (resembles Che-14); Dyf. ES1 ME2 OA6. [[Albert et al. 1981](#); [Perkins et al. 1986](#); [Starich et al. 1995](#)] [DR, SP]

### ***daf-7 III – 26.16 e1372***

: ts; constitutive dauer formation at 25°C, reversible at 15°C; type-C Egl at all temperatures; dark [intestine](#); clumpy; Srf-6 at 16°C; no effect on life span. ES3 (L3). OA11: *m62amb, m83op, m696* (internal deletion), *m434::Tc1*, etc. All alleles Egl and ts Daf. CLONED: encodes novel member of TGF-β superfamily, possible ligand for DAF-1/DAF-4 receptor, expressed in ASI [neurons](#). [[Golden and Riddle 1984a](#); [Larsen et al. 1995](#)] [DR, JT, AT]

### ***daf-8 I 2.87 m85***

: ts; constitutive dauer formation at 25°C, reversible by shift to 15°C; type-C Egl at all temperatures; dark [intestine](#); clumpy; Srf-6 at 16°C. ES3 (L3). OA7: *e1393ts* (weak allele), etc. CLONED: encodes dwarfin/MAD/DPC-4 family protein. [[Golden and Riddle 1984a](#); [Malone and Thomas 1994](#)] [DR, JT]

#### ***daf-9 X L e1406***

: constitutive formation of abnormal dauer-like larvae irreversible (genetically lethal); does not form true dauers in pheromone. ES3 (L3). OA6: *m677*. [[Albert and Riddle 1988](#)] [DR]

#### ***daf-10 IV 4.13 e1387***

: defective dauer formation; abnormal chemotaxis and osmotic avoidance; males impotent; abnormal sensory anatomy, especially amphidial [neurons](#) and sheath cells, cephalic [neurons](#); Df; octopamine-deficient. ES1 ME0. OA10: *m79*, *p821* (pka [osm-4](#)), *m534mut*, etc. [[Albert et al. 1981](#); [Starich et al. 1995](#)] [DR, SP]

#### ***daf-11 V 3.19 m47***

: ts; constitutive dauer formation at 25°C, reversible by shift to 15°C; defective chemotaxis, normal osmotic avoidance; Odr (defective in response to benzaldehyde, not to diacetyl); impenetrant Srf-6; no effect on life span. ES3 (L3). OA9: *m84* (Daf non-Odr), *m597::Tc1*, *sa203* (high penetrance at 15°C), etc. CLONED: encodes predicted transmembrane guanyl cyclase. [[Golden and Riddle 1984a](#); [Vowels and Thomas 1994](#)] [DR, JT, AT]

#### ***daf-12 X 2.12 m20***

: defective dauer formation; cell migration and lineage defects. ES1 ME3 (ME0 at 25°C). OA>20: *m25* (pka *daf-20*), *rh84* (pka [mig-7](#), [distal tip cells](#) fail to reflex, fail to express *unc-5:lacZ*), etc. At least six phenotypic classes; some alleles lead to heterochronic defects; some alleles enhance Age phenotype of [daf-2](#). CLONED: encodes protein similar to nuclear hormone receptors. [[Larsen et al. 1995](#); [Hedgecock et al. 1987](#)] [DR, NJ]

#### ***daf-13 X – 6.14 m66***

: formation of SDS-sensitive dauer larvae. ES1 ME3 NA1. [[Riddle et al. 1981](#)] [DR]

#### ***daf-14 IV 4.52 m77***

: ts; constitutive dauer formation at 25°C, incomplete penetrance, reversible by shift to 15°C; type-C Egl; dark [intestine](#); clumpy; Srf-6 at 16°C; no effect on adult life span. ES3 (L3). OA1: *sa340* (21% dauers at 25°C, derived from [egl-21](#) strain). CLONED: cosmid rescue; encodes dwarfin/MAD/DPC-4 family protein. [[Golden and Riddle 1984a](#); [Larsen et al. 1995](#); [Thomas et al. 1993](#)] [DR, GR, JT]

#### ***daf-15 IV 4.24 m81***

: constitutive formation of abnormal dauer-like larvae irreversible (genetically lethal); does not form true dauers in pheromone. ES3 (L3) OA7. [[Albert and Riddle 1988](#)] [DR, JK]

#### ***daf-16 I 3.76 m26***

: defective dauer formation; suppresses Age phenotype of *age-1*, *daf-2*. ES1 ME3 NA15 (*m27*, pka *daf-17*; *mg11*, possible defect in maintenance of dauer state). [[Riddle et al. 1981](#); [Gottlieb and Ruvkun 1994](#); [Murakami and Johnson 1996](#)] [DR, GR]

#### ***daf-17***

= *daf-16*

#### ***daf-18 IV – 29.15 e1375***

: defective dauer formation; forms some dauer-like larvae when starved; partly suppresses Age phenotype of *daf-2*, *age-1*. ES1 ME3 NA1. [[Larsen et al. 1995](#)] [DR]

#### ***daf-19 II 1.84 m86***

: ts; constitutive dauer formation at 25°C, reversible by shift to 15°C; defective chemotaxis and osmotic avoidance; Df; fails to take up FITC at 15°C or 25°C; cilia but not ciliary rootlets missing from [sensory neurons](#). ES3 (L3) ME0. OA5: *m334* (nonconditional), *sa190*, *sa232*. CLONED: cosmid rescue. [[Perkins et al. 1986](#); [Malone and Thomas 1994](#)] [DR, JT]

***daf-20***

= *daf-12*

***daf-21 V 6.42 p673***

: ts, mat; constitutive dauer formation; poor recovery even at low temperature; defective chemotaxis, defective response to some volatile odorants (benzaldehyde, isoamyl alcohol, like Daf-11); normal osmotic avoidance; slightly lethargic, semi-sterile at 25°C; strong maternal rescue; *p673/Df* is not Daf-c. NA1. [[Vowels and Thomas 1994](#)] [DR, JT]

***daf-22 II 12.07 m130***

: defective dauer formation (suppressible by exogenous dauer pheromone); defective dauer pheromone production. ES1 NA1. [[Golden and Riddle 1985](#)] [DR, JT]

***daf-23 II 3.53***

= *age-1*

***daf-24***

= *daf-19*.

***daf-25 I L m362***

: ts, mat; constitutive formation of dauer larvae at 25°C, poor dauer recovery at 15°C; adults Egl. ES3 (L3) OA3. [DR]

***daf-26 IV L m442***

: defective dauer formation; not Df. ES1 NA1. [DR]

***daf-27 III N***

(lost)

***daf-28 V 23.76 sa191***

: ts; constitutive dauer formation; dauer larvae resume development within 2 hours, even at 25°C; semidominant, 10% of *sa191*/+ animals form dauers; probable gf mutation. NA1. [[Malone and Thomas 1994](#); [Malone et al. 1996](#)]

***daf-29 II L m683***

: nonconditional constitutive formation of abnormal dauer-like larvae; two molts; does not form true dauers in pheromone. ES2 OA1. [DR]

***daf-30 IV C m654***

: nonconditional constitutive formation of abnormal dauer-like larvae; two molts; does not form true dauers in pheromone. ES2 OA1. [DR]

***daf-31 IV C m655***

: nonconditional constitutive formation of abnormal dauer-like larvae; three molts; dauer-like [pharynx](#); does not form true dauers in pheromone. ES2 NA1. [DR]

***daf-32 V N m688***

: nonconditional constitutive formation of abnormal dauer-like larvae; two molts; does not form true dauers in pheromone. ES2 NA1. [DR]

***daf-33 III L m687***

: nonconditional constitutive formation of abnormal dauer-like larvae; three molts; does not form true dauers in pheromone. ES2 NA1. [DR]

***daf-34 III L m651***

: nonconditional constitutive formation of abnormal dauer-like larvae; two molts; does not form true dauers in pheromone. ES2 OA4. [DR]

***daf-35 III R m678***

: nonconditional constitutive formation of abnormal dauer-like larvae; two molts; does not form true dauers in pheromone. ES2 NA1. [DR]

***deb***

**de** nse **b** ody component [RW].

***deb-1 IV 3.33 st385***

: amb; Pat (paralyzed embryonic arrest at 2-fold); disorganized muscle; some pharyngeal pumping. OA1: *st555* (similar). CLONED: encodes dense body component, vinculin. [[Barstead and Waterston 1991a](#); [Williams and Waterston 1994](#)]

***dec***

**de** fecation **c** ycle period abnormal [JT]. See also *flr-1,3,4*.

***dec-1 X 17.73 sa48***

: long defecation cycle period, shorter at 25°C. [[Iwasaki et al. 1995](#)] [JT]

***dec-2 III 22.42 sa89***

: long defecation cycle period; slightly slow growing and scrawny; appears to feed normally. [[Iwasaki et al. 1995](#)] [JT]

***dec-4 IV 3.25 sa73***

: long defecation cycle period; slightly slow growing and scrawny, reduced brood especially at 25°C; appears to feed normally. [[Iwasaki et al. 1995](#)] [JT]

***dec-7 III 1.04 sa92***

: ts, short defecation cycle period at 20°C, longer at 25°C; appears to feed normally. OA1: *sa296*. [[Iwasaki et al. 1995](#)] [JT]

**dec-8**

= *unc-43*

***dec-9 IV 4.65 sa293***

: short defecation cycle period; semidominant; appears to feed normally. [[Iwasaki et al. 1995](#)] [JT]

***dec-10 X 2.15 sa294***

: short defecation cycle period; dominant; appears to feed normally. [[Iwasaki et al. 1995](#)] [JT]

***dec-11 IV 15.00 sa292***

: long defecation cycle period; slightly slow growing and scrawny; appears to feed normally. [[Iwasaki et al. 1995](#)] [JT]

## **dec-12 I – 11.13 sa295**

: long defecation cycle period; slightly slow growing and scrawny; appears to feed normally. [[Iwasaki et al. 1995](#)] [JT]

## **deg**

**deg** eneration of certain [neurons](#) [TU].

### **deg-1 X – 1.32 u38**

: ts, dm; touch-insensitive and prod-insensitive only in tail; PVC [interneurons](#) degenerate at L1/L2, certain other [neurons](#) die at hatching (some IL1, also probably [AVG](#)) or L4 molt (probably AVD). ES2. OA1 (dominant): *u529* (identical). Intragenic revertants (e.g., *u38u175*) are wt (probable null phenotype). Also recessive gf allele: *u506* (cs embryonic-lethal, arrest at 2-fold with cell degenerations at 15°C; see also *des-1,4*) CLONED: encodes predicted membrane protein; two transmembrane domains surrounding Cys-rich domain; Deg alleles are A707V (*u38*, second transmembrane domain) and A393T (*u506*, predicted extracellular). [[Chalfie and Wolinsky 1990](#); [Hong and Driscoll 1994](#); [Garcia-Anoveros et al. 1995](#)] [MP, TU]

### **deg-2 X – 0.61**

NMK. Encodes predicted 730-aa protein; resembles DEG-1, MEC-4 (54% identity over 469 aa); missense transgene leads to progressive Tab as L3, probably due to death of [neuron](#) PVC; suppressed by *mec-6(e1342)*. [TU]

### **deg-3 V 3.43 u662**

: dominant uncoordinated, Tab in tail; subset of [neurons](#) undergo progressive degeneration; see also *des-2,3*. OA>8 pseudo-wt intragenic revertants, e.g., *u662u692*, *u662u693* : wt phenotype. CLONED: encodes α-subunit of nicotinic acetylcholine receptor; *u662* is missense change in second transmembrane domain. [[Treinin and Chalfie 1995](#)]

## **des**

**de** generation **s** uppressor [TU].

### **des-1 X – 15.3 u586**

: maternal-effect suppressor of cs embryonic lethality caused by *deg-1(u506)*; does not suppress larval degenerations, Tab phenotype; no obvious phenotype alone. NA1. [TU]

### **des-2 II N**

Mutation acts as a suppressor of *deg-3(u662)*. [[Treinin and Chalfie 1995](#)] [TU]

### **des-3 III N**

Mutation acts as a suppressor of *deg-3(u662)*. [[Treinin and Chalfie 1995](#)] [TU]

### **des-4 X N u552**

: maternal-effect suppressor of cs embryonic lethality caused by *deg-1(u506)*; does not suppress larval degenerations, Tab phenotype. NA1. [TU]

## **dhc**

**d** ynein **h** eavy **c** hain [RW].

### **dhc-1 I – 1.6**

NMK. 14.5-kb transcript, *trans*-spliced to SL1; encodes predicted 4568-aa protein that has significant homology with cytoplasmic and axonemal dyneins. [[Lye et al. 1995](#)] [RW]

## **dif**

**dif** ferentiation abnormal [CB].

**dif-1 IV 3.40 e2562**

: maternal-effect embryonic-lethal (mn); embryos arrest at the completion of gastrulation with little or no tissue differentiation; probable null. OA4: e2577 (similar), e2591cs (100% dead eggs at 15°C, variably viable and sometimes dumpy at 25°C; TSP 5–8 hours embryo), etc. CLONED: 1.2-kb transcript, present at all stages; encodes predicted 312-aa protein with similarity to mitochondrial carrier proteins. [[Ahringer 1995](#)]

**dif-2 IV 4.85 e2576**

: cs; maternal-effect embryonic-lethal (mn); embryos arrest at the completion of gastrulation, with little or no tissue differentiation; e2576 is cs, with more differentiation at 25°C than at 15°C, but is inviable at both temperatures. NA1. [JA]

**dig**

**di** spliced **g** onad [MT].

**dig-1 III – 0.94 n1321**

: gonad displaced, usually to anterior; 13% have dorsal gonad; phenotype enhanced in *n1321/Df*, additional failures of adherence in various tissues, twisted [pharynx](#), defects in ciliated sensory endings; defective head withdrawal (Not phenotype), normal osmotic avoidance; similarities to Mig-4. OA6: *n1480*, *n2467* (Not, defects in CEP, OLQ, AWC, AFD sensory endings; IL1 and IL2 processes abnormal), *nu52*, *nu336* (severe sensory defects, somewhat Unc, very small brood), *nu319ts* (weak; TSP embryonic). [[Thomas et al. 1990](#)] [KP, NJ]

**dom**

**do** wnstream of **m** es [SS]. Genes sharing operons with *mes* genes.

**dom-3 I – 0.38**

NMK. Novel predicted 393-aa protein; downstream gene in operon with [mes-3](#). [[Zorio et al. 1994](#); [Paulsen et al. 1995](#)] [SS]

**dom-6 IV 3.92**

NMK. Encodes protein with similarity to CSK1; regulatory subunit of cyclin-dependent kinase; downstream gene in operon with [mes-6](#). [SS]

**dpy**

**d** um **py** [CB].

**dpy-1 III – 19.41 e1**

: strong dumpy; mosaic analysis indicates focus in *hyp7*, also required in other hypodermal syncytia; suppresses some alleles of [glp-1](#). ES3 ME1. OA>20: e6, e830xri, e874pdi, e1177icr, f14, s513, etc. High forward mutation frequency. [[Brenner 1974](#); [Hedgecock and Herman 1995](#)] [EL]

**dpy-2 II – 0.00 e8**

: dumpy left roller; early larvae non-dumpy; suppresses some alleles of *glp-1*, *emb-5*. ES3 ME1. OA>10: e115, sc38ts, sc78sd, e489 (pka [rol-2](#)), e961, q292, etc. CLONED: encodes collagen; 41% identical to adjacent gene [dpy-10](#). [[Brenner 1974](#); [Levy et al. 1993](#)] [CH]

**dpy-3 X – 15.78 e27**

: medium dumpy (nonroller); L1 non-dumpy; suppresses some alleles of *glp-1*, *emb-5*. ES3 (all stages) ME1. OA>10 : e2079, sc26 (left roller dumpy), e182 (pka [dpy-12](#), medium dumpy, ES3 [adult], ME1), m39ts [[Brenner 1974](#)] [EL]

***dpy-4 IV 12.41 e1166***

: sd, icr; large dumpy; *e1166*/+ slightly dumpy. ES3 (adult) ES1 (larva) ME3. OA1: *e1158sd,icr*. [[Cox et al. 1980](#)] [DR]

***dpy-5 I 0.00 e61***

: strong dumpy; early larvae non-dumpy; *e61*/+ very slightly dumpy; homozygote suppressed by Smg, hemizygote enhanced by Smg. ES3 ME1. OA7: *e565, e907pdi, s102, s111fdi, s1300::Tc1, s1706spo*. CLONED: encodes novel protein, 257 aa; has signal sequence. [[Brenner 1974; Hodgkin et al. 1989](#)] [KR]

***dpy-6 X 0.00 e14***

: small dumpy, nonroller. ES3 ME0. OA6: *e1502aci, f10, f11, n754*, etc. [[Brenner 1974](#)]

***dpy-7 X – 1.81 e88***

: dumpy (nonroller); suppresses some alleles of *glp-1, emb-5*. ES3 ME1. OA>8: *e1324ts, sc27ts* (left roller dumpy), *m38, e2076, q288*, etc. CLONED: *trans*-spliced to SL1; encodes typical cuticular collagen, 318 aa, no close relatives; four missense alleles sequenced; expressed at each larval stage 5.5 hours prelethargus. [[Johnstone et al. 1992](#)] [IA]

***dpy-8 X – 5.80 e130***

: medium dumpy (nonroller); suppresses some alleles of *glp-1, emb-5*. ES3 ME1. OA>10: *e1281ts, sc24ts* (left roller dumpy), *sc44, e2279, q287* (weak?), etc. [Brenner 1971; [Maine and Kimble 1989](#)]

***dpy-9 IV – 28.03 e12***

: large dumpy. ES3 (adult) ES1 (larvae) ME2. OA3: *e424, e858, e1164icr*. [[Brenner 1974](#)]

***dpy-10 II 0.00 e128***

: small dumpy (nonroller); sometimes poor survival from freezing; non-null; suppresses some alleles of *glp-1, emb-5*. ES3 (all stages) ME1. OA>10: *e223, sc48* (left roller dumpy), *sc30ts* (pka *rol-7*, left roller dumpy at 25°C), *cn64* (dominant left roller), *q291, s364fdi*, etc. CLONED: encodes collagen 41% identical to DPY-2; *e128* is splicing defect, *cg36* (left roller dumpy, ochre, probable null). [[Brenner 1974; Levy et al. 1993](#)] [CH]

***dpy-11 V 0.00 e224***

: medium dumpy. ES3 (adult) ES2 (larvae) ME2. Males Ram (lumpy rays) at 25°C. OA>10: *e33, e1180icr* (these and most other alleles have much stronger dumpy “piggy” phenotype, etc.), *e455, e733, e752, s287* (induced on *eT1*), *s10, s261, s360fdi*, etc. [[Brenner 1974; Baird and Emmons 1990](#)] [CB]

***dpy-12***

= *dpy-3*

***dpy-13 IV 0.00 e184***

: sd; strong dumpy; *e184*/+ medium dumpy. ES3 (all stages) ME2. NA13: *e458, e1165icr, e225* (pka [\*dpy-16\*](#)): recessive medium dumpy, *e458, m399::Tc1, e1165*, etc. CLONED: encodes 302-aa collagen; [\*dpy-13\*](#) family includes *col-2, col-34, sqt-3*; *e184* is in-frame deletion, *e458* is 673-bp deletion, null, strong dumpy; expressed at each larval stage, 4–2.5 hours prelethargus. [[Brenner 1974; von Mende et al. 1988](#)] [CH, IA]

***dpy-14 I 1.40 e188***

: ts; medium dumpy adult, strong dumpy L1 (20°C); ts-lethal (25°C); lethality enhanced by Smg. ES3 (all stages 20°C). Synthetic lethal with some mutations at 20°C. ME2. OA2: *n497, s70*. CLONED: cosmid rescue. [[Brenner 1974; McKim et al. 1992](#)] [KR, TR]

***dpy-15***

= *sqt-3*

### ***dpy-16***

= *dpy-13*

### ***dpy-17 III – 2.16 e164***

: medium dumpy, spindle-shaped adult; old adults sometimes less dumpy; strong dumpy L1; low penetrance defects in outgrowth of posterior canal cell processes. ES3 (all stages) ME2. OA6: *e1345ts*, *e905pdi*, *e1295icr*, *e1345*, *e2145*, etc. [[Brenner 1974](#)] [NJ]

### ***dpy-18 III 8.50 e364***

: amb; medium dumpy. ES3 (adult) ES2 (larvae) ME2. Males have abnormal lumpy rays (Ram) at 25°C. OA>10: *e499*, *e1270*, *e1862*, *s361fdi*, *s1304* (induced on [\*eT1\*](#)), *bx26* (Ram at 25°C), *h662*. [[Brenner 1974](#); [Baird and Emmons 1990](#)] [PB]

### ***dpy-19 III – 0.16 e1259***

: ts, des, mat; dumpy (20°C, 25°C); wt (15°C); abnormal Q and Q daughter migrations. ES3 (adult 25°C). Weaker phenotype if mother *dpy-19*/+. ME0 (25°C) ME3 (15°C). OA3: *e1314ts*, *n1347*, *pk102*. [DR, MT, CF]

### ***dpy-20 IV 5.18 e1282***

: ts; medium dumpy (20°C), weak dumpy (15°C), strong dumpy, round-nosed (25°C); TSP during L1 and L2 stages. ES3 (25°C all stages) ME2 (20°C). OA>10: other alleles mostly severe round-headed dumpy (20°C), inviable, or almost inviable (15°C), *e1362*, *e1415*, *cn142* (strongest allele), *e2017amb* (slightly weaker), *cn322*, etc. *m474::Tc1*: strong dumpy, reverts to Dpy (*m474s2033*) or wt (*m474m495*). CLONED: rare 1.9-kb RNA, most abundant in L2; encodes predicted 359-aa novel protein. [[Hosono et al. 1982](#); [Clark et al. 1995](#)] [BC]

### ***dpy-21 V 12.97 e428***

: weak dumpy (XX); non-dumpy (XO); lethal to 2A;3X. ES3 (adult) ES1 (larvae). Some X chromosome transcript levels elevated in XX and XO. ME3. OA2: *e459* (resembles *e428*), *ct16* (very weak phenotype). [[Hodgkin 1983](#); [Meyer and Casson 1986](#)] [TY]

### ***dpy-22 X 1.94 e652***

: variable, scrawny, dumpy, slow growing (XX); very abnormal small or inviable male (XO); reduced X chromosome expression. ES2 (all stages XX) ES3 (all stages XO) ME0 NA1. [[Meneely and Wood 1987](#); [Plenefisch et al. 1989](#)]

### ***dpy-23 X – 7.34 e840***

: variable dumpy, head swollen around [pharynx](#), inviable at 15°C (XX); HSN migration defect; variable [QL](#) and DTC Mig defects also; inviable on low-phosphate media; very abnormal or inviable males (XO). ES2 (XX) ES3 (XO) ME0. OA1: *gm17* (similar). [[Meneely and Wood 1987](#)] [CB, BG]

### ***dpy-24 I 5.27 s71***

: weak dumpy; abnormal DTC migration. ES3 (adult) ES1 (larvae) NA1. [[Hedgecock et al. 1987](#)] [BC, BS]

### ***dpy-25 II – 4.49 e817***

: sd; strong dumpy, inviable at 15°C; *e817*/+ medium dumpy. ES3 (all stages). Intragenic revertants may be wt, probable null phenotype. ME1 NA1. [[Hodgkin 1983](#); [Chen et al. 1992](#)] [PD]

### ***dpy-26 IV 5.91 n199***

: mat; XX daughters of *n199*/+ mothers are maternally rescued weak dumpy phenotype with protruding [vulva](#) (ES2) 4% Him; XX daughters of *n199/n199* mothers are severely dumpy and Him (2% of brood) or die as embryos or young larvae (98% of XX brood); XO *n199* animals are non-dumpy almost wt males (ME3); similar or slightly stronger phenotypes in *n199/Df*. OA3: *n198* (resembles *n199*), *y6* (weaker phenotypes),

*y65*. CLONED: encodes predicted 1263-aa novel protein; antibody staining indicates DPY-26 associated with X chromosomes in XX, diffuse nuclear in XO. [[Plenefisch et al. 1989](#)] [TY]

#### ***dpy-27 III – 5.04 rh18***

: mat; XX phenotype is zygotic weak dumpy maternal-effect dumpy/near lethal-like Dpy-26 but non-Him. ES2. XO phenotype nearly wt male (ME3). OA5: *y57* (weaker allele), *y44*, *y42*, *y56am*, *y49* (strongest allele) CLONED: encodes 1469-aa protein with similarities to chromosome structural proteins, specifically localized to X chromosomes in XX but not XO animals. [[Plenefisch et al. 1989](#); [Chuang et al. 1994](#)]

#### ***dpy-28 III 5.15 y1***

: ts, mat; at 24°C, XX phenotype is zygotic weak dumpy, 3% Him, maternal-effect dumpy/near lethal; XO phenotype wt male (ME3); XX viable at 15°C, 0.4% Him. OA1: *s939* (non-ts, Him, >99% maternal XX lethality at 15°C, >90% at 20°C). [[Plenefisch et al. 1989](#)]

#### ***dpy-29***

= *sdc-3*

#### ***dpy-30 V 3.70 y130***

: maternal ts-lethal to XX animals, as a result of X chromosome overexpression; fully penetrant at restrictive temperature (25°C); XO animals viable abnormal males, scrawny, slow-growing, mating-defective. OA1: *y228am*. CLONED: 0.6-kb transcript, encodes 123-aa novel protein; antibody staining indicates DPY-30 ubiquitous nuclear protein, present in both sexes; upstream gene in operon with [\*rnp-1\*](#). [[Hsu and Meyer 1994](#); [Hsu et al. 1995](#)]

#### ***dyf***

**dy** e **f** illing of [neurons](#) defective [SP]. In wt, 16 amphid and [phasmid neurons](#) will take up fluorescent dyes (FITC, DiO). See also *daf*, *che*, *osm*, *tax*, *avr*.

#### ***dyf-1 I – 0.45 mn335***

: mut; defective in dye filling (FITC or DiO) of amphid and [phasmid neurons](#); chemotaxis-defective. ME2. [[Starich et al. 1995](#)]

#### ***dyf-2 III 21.71 m543***

: mut; defective in dye (FITC or DiO) filling of amphid and [phasmid neurons](#); chemotaxis-defective. ME4 (both alleles). OA1: *m160*. [[Starich et al. 1995](#)]

#### ***dyf-3 IV – 5.25 m185***

: defective in dye (FITC or DiO) filling of amphid and [phasmid neurons](#); chemotaxis-defective. ME4 (*m185*) ME2 (*mn331*) ME1 (*sa122*). OA2: *mn331mut*, *sa122*. [[Starich et al. 1995](#)]

#### ***dyf-4 V 4.23 m158***

: defective in dye (FITC or DiO) filling of amphid and [phasmid neurons](#); chemotaxis-defective. ME4 (*m158*) ME4 (*m177*) ME3 (*mn332*). OA2: *m177*, *mn332mut*. [[Starich et al. 1995](#)]

#### ***dyf-5 I 3.70 mn400***

: defective in dye (FITC or DiO) filling of amphid and [phasmid neurons](#); animals slightly short; chemotaxis-defective. ME2. [[Starich et al. 1995](#)]

#### ***dyf-6 X 2.46 m175***

: defective in dye (FITC or DiO) filling of amphid and [phasmid neurons](#); chemotaxis-defective. ME3 (*m175*) ME4 (*mn346*). OA1: *mn347mut*. [[Starich et al. 1995](#)]

#### ***dyf-7 X 1.95 m537* :**

*mut*; defective in dye (FITC or DiO) filling of amphid and [phasmid neurons](#); chemotaxis-defective. ME1. [Starich et al. 1995]

***dyf-8 X 12.79 m539***

: mut; defective in dye (FITC or DiO) filling of amphid and [phasmid neurons](#); animals slightly short; chemotaxis-defective. ME1. [Starich et al. 1995]

***dyf-9 V 23.47 n1513***

: defective in dye (FITC or DiO) filling of amphid and [phasmid neurons](#); chemotaxis-defective. ME1 (*n1513*) ME3 (*sa121*). OA1: *sa121*. [Starich et al. 1995]

***dyf-10 I 1.55 e1383***

: defective in dye (FITC or DiO) filling of amphid and [phasmid neurons](#); chemotaxis-defective. ME4 NA1. [Starich et al. 1995]

***dyf-11 X – 17.86 mn392***

: defective in dye (FITC or DiO) filling of amphid and [phasmid neurons](#); animals slightly short; chemotaxis-defective. ME3 NA1. [Starich et al. 1995]

***dyf-12 X 1.93 sa127***

: defective in dye (FITC or DiO) filling of amphid and [phasmid neurons](#); chemotaxis-defective. ME3. OA3: *nr272*, *nr2477*, *nr2344* (dominant Avr allele, heterozygotes 98% non-Dyf, but many have less uptake than wt). [Starich et al. 1995]

***dyf-13 II 0.22 mn396***

: defective in dye (FITC or DiO) filling of amphid and [phasmid neurons](#); usually 1–2 [amphid neurons](#) dye fill (FITC or DiO); reduced growth rate and reduced and variable brood sizes; mildly chemotaxis-defective. ME2 NA1. [Starich et al. 1995]

***dyn***

***dyn*** amin-related [CX].

***dyn-1 ? ky51***

: ts reversible uncoordinated phenotype; encodes protein with similarity to vertebrate dynamin; antibody staining indicates high in axons. OA1: *pk76tci*. [CX]

***eat***

***eat*** ing abnormal (pharyngeal defects) [DA].

***eat-1 IV 4.85 e2343***

: slow, irregular pumping, body slightly long and thin, movement slightly sluggish. OA1: *ad427* (stronger phenotype). [Avery 1993a] [DA]

***eat-2 II 22.46 ad465***

: medium-strong Eat: slow, often regular pumping; somewhat hypersensitive to arecoline (cholinergic agonist), most L1s arrested by 5 mM; lose synaptic transmission from MC motor [neuron](#). OA>10: *ad451*, *ad453*, *ad459*, *ad570*, *ad692*. Complex complementation, five classes. [Avery 1993a; Raizen et al. 1995] [DA]

***eat-3 II 1.31 ad426***

: generally disgusting worm; very slow, irregular pumping; sluggish; Egl; dies on recovery from dauer; strong maternal rescue effect; [\*eat-3\*](#) progeny of an *eat-3/+* mother move normally and have only a weak Eat phenotype. NA1. [Avery 1993a] [DA]

***eat-4* III 0.14 *ad572***

: xri; weak Eat; normal pumps interspersed with abnormal pumps in which corpus contractions feeble but long-lasting, and terminal bulb contractions long-lasting but of normal strength; phenotype resembles that caused by killing pharyngeal [M3 neurons](#), but is stronger; lacks [M3](#)-derived IPSPs; other behavioral defects include Not, Fab, Che, Ttx; possibly general defect in glutamatergic [neurons](#). OA6: *ad537*, *ad613*, *ad801*, *ad818*, *ad819*, *ky5*. CLONED: encodes possible transporter protein, "NERD" family (45% identity to rat brain phosphate transporter); *eat-4: lacZ* expressed in multiple [neurons](#). [[Avery 1993a](#)] [CX, DA, KP]

***eat-5* I 1.87 *ad464***

: corpus and terminal bulb contractions not synchronized; usually the terminal bulb pumps more slowly than the corpus; phenotype less penetrant in adults; defective dye-coupling between terminal bulb and corpus. NA1. CLONED: encodes predicted protein related to UNC-7, *Drosophila* Passover (four transmembrane domains). [[Avery 1993a](#)] [DA]

***eat-6* V 4.83 *ad467***

: strong relaxation-defective; [pharynx](#) often fails to relax or relaxes slowly; long yawns occur, where the corpus stays open for seconds, punctuated with erratic partial relaxations; terminal bulb usually more strongly affected than the corpus, but the motions of the two precisely synchronized; relaxation transient reduced in size in electropharyngeograms; hypersensitive to inhibitors of Na/K ATPase; synthetic lethal with [eat-11](#) (*ad541*). OA2: *ad601xri*, *ad792*. CLONED: encodes  $\alpha$ -subunit of Na/K ATPase (pka [spa-1](#)). [[Avery 1993a](#); [Davis et al. 1995](#)] [DA]

***eat-7* IV – 17.60 *ad450***

: narcoleptic; [eat-7](#) worms when undisturbed fall "asleep"; tend to become starved; sleeping worms do not move or pump, and probably do not defecate; disturbing them wakes them up, and while awake act fairly normal. OA1: *ad540*. [[Avery 1993a](#)] [DA]

***eat-8* III – 25.63 *ad697***

: brief, rare pumps; pumping otherwise normal in Nomarski, except pumps sometimes so brief as to be only coordinated twitches; penetrant, strong Eat. OA1: *ad599*. [[Avery 1993a](#)] [DA]

***eat-9* I 23.58 *e2337***

: slightly starved; irregular pumping. NA1. [[Avery 1993a](#)] [DA]

***eat-10* IV – 27.99 *ad606***

: strong Eat; slippery isthmus and corpus. NA1. [[Avery 1993a](#)] [DA]

***eat-11* I 2.24 *ad541***

: weak Eat: slippery corpus; slightly long; movement slightly loopy (i.e., bends deeper than normal); hypersensitive to arecoline (cholinergic agonist), will not grow at concentrations  $\geq 1$  mM; synthetic-lethal with [eat-6](#); suppressed by [egl-30](#) (gf), [exp-2](#) (gf). NA1. [[Avery 1993a](#)] [DA, JT]

***eat-12***

= *egl-19*

***eat-13* X 1.16 *ad522***

: strong Eat; slippery [pharynx](#); possible terminal bulb relaxation defect. NA1. [[Avery 1993a](#)] [DA]

***eat-14* X 5.40 *ad573***

: medium or weak Eat; grinder sometimes fails to relax fully between pumps; resembles [phm-2](#) in motion defect, but weaker, and no obvious anatomical abnormalities exist. NA1. [[Avery 1993a](#)] [DA]

***eat-15* I 1.80 *ad602***

: medium to weak Eat: slippery isthmus, corpus, and grinder. NA1. [[Avery 1993a](#)] [DA]

***eat-16* I 3.88 *ad702***

: strong Eat: slippery isthmus and corpus. [[Avery 1993a](#)] [DA]

***eat-17* X 23.83 *ad707***

: strong Eat: stuffs corpus and isthmus; abnormality in pharyngeal muscles pm6 and pm7 contraction timing. [[Avery 1993a](#)] [DA]

***eat-18* I 23.60 *ad820***

: sd; Eat; starved; homozygote has slow pharyngeal pumping, defective MC neurotransmission, and lacks I-phase transients in the EPG (ES3); *ad820*/+ pumps slower than wt but faster than *ad820/ad820* and not very starved (ES1). OA1: *ad1110* (putative If allele). [[Raizen et al. 1995](#)] [DA]

***eft***

**e** longation **f** ac **t** or [CGC].

***eft-1* III – 1.1**

NMK. Encodes 849-aa protein; C-terminal has 47–58% similarity to elongation factors; N-terminal has homology with GTP-binding proteins; lacks diphtheria toxin target His (Tyr instead). [[Ofulue and Candido 1992](#)]

***eft-2* I 3.62**

NMK. Encodes protein with >80% similarity to elongation factor EF2 from yeast, *Drosophila*, humans. [[Ofulue and Candido 1992](#)]

***eft-3* III – 0.82**

NMK. Encodes 463-aa protein with 83% identity to EF1 $\alpha$ ; *eft-3:lacZ* fusion expressed widely, but not in [intestine](#) or [body wall muscle](#). [FK]

***eft-4* X – 1.09**

NMK. Encodes EF1 $\alpha$  protein; amino acid sequence identical to [\*eft-3\*](#). [FK]

***egl***

**eg** g **I** laying-defective [MT]. Egl-c : egg-laying-constitutive; drug response categories define response to serotonin and to imipramine (serotonin re-uptake inhibitor).

Type A: egg laying not stimulated by either serotonin or imipramine (probable defects in [vulva](#) or sex muscles)

Type B: stimulated by serotonin, not imipramine

Type C: stimulated by imipramine and by serotonin

Type D: stimulated by imipramine, not by serotonin

Type E: variable response

***egl-1* V 6.18 *n487***

: sd, ts; transient bloating Egl; stimulated by serotonin, not imipramine; HSN cells undergo programmed cell death, hence [\*ced-3\*](#) suppressible; no phenotype in male; *n487*/+ is ts Egl (penetrance 85% at 25°C, 60% at 20°C). ES2 (adult) ME3. OA3: *n986*, *n987* (both stronger non-ts alleles, *n987*/+ penetrance >95%), *n1084* (weaker than *n487*). [[Ellis and Horvitz 1986](#); [Desai and Horvitz 1989](#)] [MT]

***egl-2* V – 20.40 *n693***

: dm; severe bloating Egl; stimulated by imipramine, not serotonin; weak uncoordinated kinker phenotype; muscle activation-defective (flaccid, long); defecation-defective, severely constipated; [E.p](#) (expulsion muscle contraction) nearly always missing, corrected by imipramine; egg-laying and defecation muscles appear normal by polarized light. ES3 (adult) ME1 (abnormal bursal morphology, cloacal structures protrude, poor vulval location; weak similar phenotype in *n693/+*). Probable gf allele. OA>4: intragenic revertants, e.g., *n693n905*, *n693sa326* (phenotypically wt). Also second sd allele: *n2656*. [[Trent et al. 1983](#); [Reiner and Thomas 1995](#)] [JT]

#### ***egl-3 V 2.33 n150***

: ts; moderate bloating Egl; stimulated by serotonin and by imipramine; coiler phenotype. ES3 (adult 25°C) ES2 (larvae, males) ME2. OA3: *n588* (weakly semidominant), *n729*. [[Trent et al. 1983](#)] [MT]

#### ***egl-4 IV – 15.30 n478***

: transient bloating Egl; variable drug response; overresponds to dauer pheromone. ES2 (adult) ME1 (no obvious morphological defect). OA4: *n477*, *n479ts*, *n579*, *n612*. [[Trent et al. 1983](#); [Golden and Riddle 1984a](#)]

#### ***egl-5 III – 0.54 n486***

: moderate bloating Egl; stimulated by serotonin, not imipramine; uncoordinated coiler phenotype; Mec in posterior; HSN cell bodies absent or displaced and serotonin-negative; not suppressed by [ced-3](#). ES3 (adult) ME0. OA>10: *e2495*, *u202*, *e2399*, *e2502*, *e2506*, *e2508*, *n1066*, *n1067*, *n1439* (weakest allele, males can mate), *n945amb* (strongest allele), *n988*, *n989*. CLONED: encodes Abd-B class homeoprotein (pka [ceh-11](#)) [[Chisholm 1991](#); [Wang et al. 1993](#)] [CF, MT]

#### ***egl-6 X – 12.73 n592***

: sd; transient bloating Egl; variable drug response; uncoordinated weak kinker phenotype. ES2 ME2 NA1. [[Trent et al. 1983](#)] [MT]

#### ***egl-7 III – 3.18 n575***

: sd, ts; moderate bloating at 25°C, unhealthy; some bloating at 15°C; stimulated by serotonin and by imipramine. ES2 (adult 25°C) ME2 NA1. [[Trent et al. 1983](#)] [MT]

#### ***egl-8 V – 20.25 n488***

: transient variable bloating; variable drug response; Unc; Pbo, pBoc defecation contractions weak or very weak. ES2 (adult) ME0 (variable Mab: fan-defective, missing rays). OA5: *sa28* (pka [pbo-2](#)), *sa32ts*, *sa46* (weaker), *sa47*. [[Trent et al. 1983](#); [Thomas 1990](#)]

#### ***egl-9 V 2.64 n586***

: ts; transient bloating at 25°C; variable drug response; resistant to paralysis by toxin from *Pseudomonas aeruginosa*. ES2 (adult 25°C) ME3. OA3: *n571* (non-ts), *sa307*, *sa330*. [[Trent et al. 1983](#)] [MT, JT]

#### ***egl-10 V 4.18 n692***

: sd, ts; transient bloating, sluggish weak kinker; type B/C; HSN appears normal; weakly semidominant, partially ts. ES3 (adult) ES2 (other stages) ME2. OA9: *n480ts* (slight bloating; stimulated by serotonin and by imipramine), *n1068*, *n1083*, *n1185*, etc. CLONED: predicted protein has distant similarity to yeast signal transduction component, Sst2p. [[Trent et al. 1983](#); [Koelle and Horvitz 1996](#)] [MT]

#### ***egl-11 V 3.19 n587***

: ts; transient bloating at 25°C; variable drug response. ES2 (adult 25°C) ME2. [[Trent et al. 1983](#)] [MT]

#### ***egl-12 V 16.12 n602***

: sd; transient bloating; variable drug response; weakly semidominant. ES2 (adult) ME2. OA1: *n599* (recessive). [[Trent et al. 1983](#)] [MT]

***egl-13* X – 3.84 n483**

: penetrance 70%; severe bloating or bag-of-worms phenotype (insensitive to serotonin and imipramine); minority wt. ES3/0 (adult) ME3. OA1: *e1447*. [[Trent et al. 1983](#)] [MT]

***egl-14* X – 3.66 n549**

: transient bloating; variable drug response. ES2 (adult) ME0 (no obvious morpho-Mab, poor vulva location) NA1. [[Trent et al. 1983](#)] [MT]

***egl-15* X 2.49 n484**

: moderate to severe bloating; 60% form bag-of-worms (insensitive to serotonin, imipramine); vulval and uterine muscles defective because of defects in sex myoblast migrations; Soc suppresses and is suppressed by clr-1 mutations. ES3 (adult) ME3. OA>10: *n1458*, *n1459*, *ay1* (all three resemble *n484*, class 1). Also stronger alleles (class II, putative null): *n1454*, *n1456*, *n1478* (all larval-lethal, L1 arrest). Also class III alleles: *n1477ts*, *n1460*, *n1780*, *n1784* (all scrawny, Egl, Soc). Also class IV alleles: *n1783*, *n1775* (Soc, no other phenotype). CLONED: 4.2-kb transcript, encodes predicted 1040-aa FGFR-type receptor tyrosine kinase; transgene overexpression leads to Clr phenotype. [[Stern and Horvitz 1991](#); [DeVore et al. 1995](#)] [MT, NH]

***egl-16***

= *sdc-1*

***egl-17* X – 19.55 e1313**

: moderate to severe bloating; 30% form bag-of-worms; insensitive to serotonin and imipramine; severe posterior displacement of hermaphrodite sex muscles (due to gonadal repulsion); enhancer of weak Tra mutation; suppressed by clr-1 mutations. ES3 (adult) ME3. OA9: *ay6*, *n1377*, *ay10* (putative null); all similar. CLONED: cosmid rescue; *ay6*, *n1377* are deletions. [[Stern and Horvitz 1991](#); [Clark et al. 1993](#)] [MT, NH]

***egl-18* IV – 15.67 n162**

: variable bloating; a few form bag-of-worms; variable drug response; vulval abnormalities; low penetrance Vab. ES3/1 (adult) ME0 (variable Mab, rays blobby or missing, fan abnormal). OA2: *n474*, *n475*. [[Trent et al. 1983](#)] [MT]

***egl-19* IV 3.38 n582**

: sd; moderate bloating; stimulated by imipramine, not by serotonin; slow and floppy; long; *n582/Df* more severe phenotypes. ES3 (adult) ES2 (other stages) ME1. NA(If)>10: *st556* (pka pat-5), *st576*, *st577* (all embryonic-lethal, severe Pat, probable null phenotype). Also apparent gf alleles: *ad695sd* (pka eat-12, weak Eat: terminal bulb stays contracted for longer than normal, sometimes >1 sec; corpus action normal; muscle hyperactivated, sticky pumping, short, *ad695/+* similar but weaker phenotypes), *n2368* (Eat: delayed relaxation and repolarization of terminal bulb; Egl: eggs of <10 nuclei are laid, vulval muscles show spontaneous contraction; Dpy: may be due to body muscles hypercontraction; Mab: protruding spicules. *n2368/+* has a phenotype similar to but weaker than *n2368*. ES3 ME0. *n2368* but not *n2368/+* has a cs Pat phenotype, penetrant at 12°C. ME0. Intragenic revertants, e.g., *n2368ad979* are recessive Pat) CLONED: may encode calcium channel subunit. [[Avery 1993a](#); [Williams and Waterston 1994](#)] [DA, MT]

***egl-20* IV 4.43 n585**

: ts; moderate bloating at 25°C; variable drug response; pleiotropic Mig, some but not all migrations defective, QL daughters migrate anteriorly. ES3 (adult) ME0 (variable Mab: blobby rays, small fan, displaced sex muscles, etc.) NA1. [[Trent et al. 1983](#); [Garriga and Stern 1994](#)] [CF, MT]

***egl-21* IV 4.63 n611**

: ts; transient bloating at 25°C; variable drug response; partially temperature-sensitive; uncoordinated weak coiler; abnormal 5-HT signaling. ES2 (adult) ME2. OA2: *n476*, *n576*. [[Trent et al. 1983](#)] [KP, MT]

***egl-22***

= *unc-31*

***egl-23 IV 10.68 n601***

: dm; severe bloating (insensitive to serotonin and imipramine); some animals form bag-of-worms; uncoordinated sluggish phenotype (recessive); vulval muscles contract under laser stimulation; muscle activation defective (flaccid, long); defecation-defective; moderate constipation but almost never have expulsion (*E.p*) contraction. ES3 (adult) ES1 (larvae) ME3. OA>4: intragenic revertants *n601sa179*, etc.; all phenotypically wt (probable null). Also second *sd* allele. [[Trent et al. 1983](#); [Reiner and Thomas 1995](#)] [JT, MT]

***egl-24 III – 1.06 n572***

: variable bloating (insensitive to serotonin and imipramine); some animals wt; variable Unc and Lon phenotypes. ES2 (adult) ME2 NA1. [[Trent et al. 1983](#)] [MT]

***egl-25 III – 1.51 n573***

: variable bloating (insensitive to serotonin and imipramine); variable abnormal tail morphology. ES2 (adult) ME0 (no obvious morphological defect) NA1. [[Trent et al. 1983](#)] [MT]

***egl-26 II – 18.21 n481***

: variable bloating; insensitive to serotonin and imipramine; 60% adults form bag-of-worms; abnormal *vulva*; suppressor of Tra-3. ES2 (adult) ME3. OA1: *e1952* (pka *egl-48*, HME1/2, stronger suppressor of Tra-3). [[Trent et al. 1983](#); [Hodgkin 1986](#)] [CB, MT]

***egl-27 II 0.12 n170***

: variable bloating, moderate to severe; variable drug response; possibly abnormal *vulva*; Mig. Males Lin, very abnormal: reduced rays, short spicules, swollen bursa, hermaphroditic *tail spike*. ES2 (adult) ES3 (adult male) ME0. OA1: *e2394*. [[Trent et al. 1983](#); [Desai et al. 1988](#)] [CZ, MT]

***egl-28 II 1.58 n570***

: ts; transient bloating at 25°C; variable drug response; partially temperature-sensitive; Dpy; ES2 (adult) ME0 (occasional Mab, also variable Spe defect in germ line) NA1. [[Trent et al. 1983](#)] [MT]

***egl-29 II 5.32 n482***

: variable, some animals wt, some form bag-of-worms (80%); insensitive to serotonin and imipramine; variably abnormal *vulva* (protrusive; abnormal VU pi fate). ES2 (adult) ME3 NA1. [[Trent et al. 1983](#)] [MT, PS]

***egl-30 I – 13.53 n686***

: sd; moderate bloating, variable drug response; Unc slow, very sluggish phenotype, Sma, Gro; muscle activation defective (flaccid, long). ES3 (adult) ES2 (other stages) ME0 (slight morpho-Mab). OA>10 (dominant): *n715sd* (uncoordinated paralyzed phenotype, *n715/+* has type-C bloating), *ad805*, *ad803*, *ad806*, *ad809*, *ad810* (recessive-lethal, flaccid arrest at hatching), *ad813*, *ad814*. The strongest gf alleles are homozygous-lethal; homozygotes hatch, but paralyzed, with no or feeble contractions of body wall, pharyngeal, and defecation muscles; homozygotes, however, move normally during embryonic elongation; many dominant suppressors of *eat-11*. Also intragenic revertants: *n715n1190*, *n715n1189* (candidate lf: weak Egl, possibly hyperactive), *pk45tci*. Null phenotype uncertain. CLONED: corresponds to *gqa-1*, α-subunit of G protein q (80% identity to mammalian Gqα). [[Trent et al. 1983](#); [Park and Horvitz 1986a](#); [Brundage et al. 1996](#)] [DA, MT, PS]

***egl-31 I 3.07 n472***

: moderate to severe bloating; insensitive to serotonin and imipramine; some animals form bag-of-worms (20%) or rupture at *vulva*; sex muscles variably defective because of abnormalities in early *M lineage*; Unc

poor backing phenotype; Lon? ES2 (adult) ES2 (other stages) ME0 (males have [M lineage](#) defect also) NA1. [[Trent et al. 1983](#)] [CZ, MT]

***egl-32 I 3.96 n155***

: ts; moderate bloating; variable drug response; partially temperature-sensitive; suppressible by [daf-3](#). ES2 (adult) ME3 (some males have abnormal somatic gonads, some have abnormal or feminized germ lines) NA1. [[Trent et al. 1983](#)] [MT]

***egl-33 I 3.96 n151***

: ts; moderate to severe bloating at 25°C; insensitive to serotonin and imipramine; some animals form bag-of-worms (40%) or rupture at [vulva](#); Gro; Unc kinker phenotype at 25°C. ES3 (adult 25°C) ES2 (larvae 25°C) ME2 NA1. [[Trent et al. 1983](#)] [MT]

***egl-34 I – 2.41 n171***

: variable bloating; variable drug response; some animals wt, some form bag-of-worms (10%). ES2 (adult) ME0 (variable Mab: blobby rays, misshapen bursa, sex muscle defects). OA1: e1452. [[Trent et al. 1983](#)] [CZ, MT]

***egl-35 III 17.53 n694***

: ts; transient bloating at 25°C; sensitive to serotonin and to imipramine; Unc, unhealthy; precocious HSN differentiation. ES2 (adult 25°C) ME3/ME0 (variable Mab: some tail deformity at 25°C, less at 20°C) NA1. [[Trent et al. 1983](#)] [CZ, MT]

***egl-36 X 1.95 n728***

: dm; severe bloating; insensitive to serotonin and imipramine; 50% adults form bag-of-worms; abnormal defecation ([E.p](#)), weakly constipated; Sma? ES2 (adult). Muscle activation defective (flaccid, long). ME3. n728/+ has similar phenotype. NA1. [[Trent et al. 1983](#); [Park and Horvitz 1986a](#); [Reiner and Thomas 1995](#)] [JT, MT]

***egl-37 II 1.41 n742***

: ts; transient bloating at 25°C; variable drug response. ES2 (adult 25°C) ME3 NA1. [[Trent et al. 1983](#)] [MT]

***egl-38 IV 4.46 n578***

: severe bloating; insensitive to serotonin and imipramine; almost no egg laying; >90% adults form bag-of-worms (>90%); defect in vulval-[uterine](#) attachment, persistent survival of AC; uncoordinated very sluggish phenotype; abnormal [vulva](#). ES3 (all stages). OA2: sy294 (pka [lin-50](#), males have abnormal tails with [U](#) and [B lineage](#) defects; hermaphrodites also have abnormal tails, frequently sterile), s1775. [[Trent et al. 1983](#)] [MT, PS]

***egl-39***

= *unc-16*

***egl-40 IV 4.19 n606***

: ts, sd; transient bloating; sensitive to serotonin and imipramine; partially temperature-sensitive; Dpy; overresponds to dauer pheromone. ES2 (adult 25°C) ME3 NA1. [[Trent et al. 1983](#); [Golden and Riddle 1984a](#)] [MT]

***egl-41 V 5.67 n1077***

: cs, sd; moderate bloating; sensitive to serotonin, not to imipramine; HSN cells absent in adult ( [ced-3](#) suppressible); other indications of weak masculinization of XX animals (CEM cells survive; weak suppressor of *tra-2[gf]*); also XO animals sometimes weakly feminized, especially at 25°C. Penetrance of *n1077/+* XX: 60% Egl at 20°C. ES2 (adult) ES1 (other stages). OA3: *n1069*, *n1074*, *e2055* (all similar). [[Desai and Horvitz 1989](#); [Hodgkin et al. 1985](#)] [CB, MT]

***egl-42* II 0.31 n995**

: sd; moderate bloating; stimulated by serotonin, not imipramine; HSN appear normal; slight bloating in n995/+ . ES2 (adult) ME2 OA1 (n996sd). [[Desai and Horvitz 1989](#)] [MT]

***egl-43* II 1.81 n997**

: moderate bloating; stimulated by serotonin, not imipramine; HSN cell bodies serotonin-positive but misplaced posteriorly along path of HSN migration; aberrant variable HSN processes; abnormal IL2 wiring. ES2 (adult) ES1 (other stages) ME2. OA1: n1079. CLONED: 2.5- and 1.8-kb transcripts, encode 517-aa or 360-aa zinc finger proteins, related to mouse Evi-1. [[Desai and Horvitz 1989](#); [Garriga and Stern 1994](#)] [KP, MT, NG]

***egl-44* II – 1.69 n998**

: moderate bloating; stimulated by serotonin, not imipramine; HSN cell bodies do not contain serotonin; axon defects; slow growth; serotonin levels increased if synapse formation blocked; ectopic expression of *mec-7* . ES2 (adult) ME2. OA2: n1080, n1087 (strongest allele). [[Desai and Horvitz 1989](#)] [MT, TU]

***egl-45* III – 0.54 n999**

: moderate bloating; stimulated by serotonin, not imipramine; HSN cell bodies sometimes degenerate in L4, absent in adult and never contain serotonin; Unc; axon defects; some sterility; n999/Df often very unhealthy, slow, sterile; HSN degeneration suppressed by *unc-76* and *unc-42* mutations. ES2 (adult) ES1 (other stages) ME1 (variable morpho-Mab: posterior bulges in fan, some spicule and muscle defects). NA1. CLONED: encodes novel predicted protein. [[Desai and Horvitz 1989](#)] [MT]

***egl-46* V 0.13 n1127**

: moderate bloating; stimulated by serotonin, not imipramine; HSN cell bodies do not contain serotonin; torpid Unc and Lin (abnormal Q lineage) phenotypes; axon defects; serotonin levels increased if HSN synapse formation blocked; ectopic expression of *mec-7*; n1127/Df similar. ES2 (adult) ES1 (other stages) ME2. OA3: n1075, n1076. [[Desai and Horvitz 1989](#)] [MT, TU]

***egl-47* V 2.57 n1081**

: dm; moderate bloating; stimulated by serotonin, not imipramine; HSN appear normal; slightly Unc, kinking tendency; probable gf allele. ES2 (adult) ME2. OA1: n1082dm. [[Desai and Horvitz 1989](#)] [MT]

***egl-48***

= *egl-26*

***egl-49* X N n1107**

: ts, sd; Egl; stimulated by serotonin, not imipramine; HSN appear normal. ME2 NA1. [[Desai and Horvitz 1989](#)] [MT]

***egl-50* II 23.50 n1086**

: cs; Egl; stimulated by serotonin, not imipramine; HSN appear normal; slight Dpy; weak Tra (some intersexes at 15°C), weak Him. ME2. [[Desai and Horvitz 1989](#)] [MT]

***ego***

**e** nhancer of **g**. **l**p- **o** ne ( [glp-1](#) ) [EL].

***ego-1* I 2.04 om18**

: recessive enhancer of *glp-1(bn18)* at 20°C; reduced germ cell number, 50% of wt in young adult, delayed spermatogenesis, abnormal unfertilized oocytes. NA1. [[Qiao et al. 1995](#)] [EL]

***ego-2* I 6.88 om33**

: recessive enhancer of *glp-1(bn18)* at 20°C; also interacts with *glp-4(om14)*. NA1. [[Qiao et al. 1995](#)] [EL]

#### ***ego-3* V 6.31 *om40***

: recessive enhancer of *glp-1(bn18)* at 20°C; reduced germ cell number, 50% of wt in young adult, delayed spermatogenesis; some proximal germ-line proliferation; abnormal unfertilized oocytes, some somatic gonad abnormalities; severe Unc as larva, not as adult. NA1. [[Qiao et al. 1995](#)] [EL]

#### ***ego-4* III 0.82 *om30***

: recessive enhancer of *glp-1(bn18)* at 20°C; reduced germ cell number, 30% of wt in young adult, defective oocytes (MeI, usually mid-embryonic arrest). OA1: *om60*. [[Qiao et al. 1995](#)] [EL]

#### ***ego-5* III 0.70 *om31***

: recessive enhancer of *glp-1(bn18)* at 20°C; reduced germ cell number, 30% of wt in young adult, defective oocytes (MeI, late embryonic arrest). OA1: *om62*. [[Qiao et al. 1995](#)] [EL]

#### ***eha***

**e** gg-laying **h** ormone of *Aplysia*, related [CGC].

#### ***eha-1* I 3.72**

NMK. Hybridizes to *Aplysia* probe. [CGC]

#### ***eln***

See *eft*.

#### ***elt***

**e** rythroid- **I** like **t** ranscription factor family [BL].

#### ***elt-1* IV 4.45 *zu180***

: zygotic recessive-lethal; makes no hypodermis; extra cell divisions in all hypodermal lineages, extra neuron-like cells. OA1: *pk60* (Tc1 insertion, no known phenotype). CLONED: 1.7-kb transcript, *trans-spliced* to SL1; encodes GATA family protein, functional in yeast; transcripts most abundant in germ line, especially male; *elt-1:lacZ* expressed in embryo from 50-cell stage. [[Spieth et al. 1991b](#)] [BL, JJ, JM]

#### ***elt-2* X 1.95 *pk46***

: Tc1 insertion, no known phenotype; encodes GATA family protein; transcripts maximal in embryo, absent from oocytes; *elt-2:lacZ* expressed specifically in intestinal cells, from 2 **E** cell stage onward. [[Hawkins and McGhee 1995](#)] [JM]

#### ***elt-3* X 15.5**

NMK. Encodes GATA family protein. [BL, CGC]

#### ***emb***

**emb** ryogenesis abnormal [RC].

#### ***emb-1* III – 4.46 *hc57***

: ts, mm; at 25°C, 1–24-cell arrest; no pseudocleavage-defective cytoplasmic streaming; normal and defective execution before one-cell stage; viable at 16°C. OA1: *hc62ts* (similar phenotype). [[Miwa et al. 1980](#)] [MJ]

#### ***emb-2* III – 5.09 *hc58***

: ts, mnz; at 25°C, lima bean arrest; abnormal blastocoel; division rates slowed ~20%; normal execution in oogenesis or early cleavage; defective execution later; viable at 16°C, slightly slow divisions. NA1. [[Miwa et al. 1980](#)] [MJ]

***emb-3* IV 3.84 *hc59***

: ts, mm; at 25°C, lima bean arrest; early nuclear and cytoplasmic abnormalities; abnormal blastocoel; division rates slightly faster; normal and defective execution before fertilization. NA1. [[Miwa et al. 1980](#)] [MJ]

***emb-4* V 21.06 *hc60***

: ts, mm; at 25°C, lima bean arrest; slow division rates especially [E lineage](#); shift to 25°C in L1 results in defective gonadogenesis. Subviable at 16°C: 60% of eggs fail to hatch, many larvae die or have gross morphological abnormalities. NA1. [[Miwa et al. 1980](#)] [MJ]

***emb-5* III – 3.36 *hc61***

: ts, mm; at 25°C, lima bean arrest; misplaced gut granule birefringence; abnormal gastrulation division rates slowed (except [E lineage](#), precocious), Ea divides a/p; normal and defective execution at 24-cell stage; shift to 25°C in L1 results in defective gonadogenesis; viable at 16°C; suppressible by mutations in *dpy-2,3,7,8,10*. OA3: *g16ts*, *g65ts* (similar to *hc61*), *hc67ts* (division rates faster than wt, otherwise like *hc61*). CLONED: 5.4-kb transcript, encodes predicted 1521-aa protein; some similarity to yeast nuclear protein SPT6. [[Miwa et al. 1980](#); [Nishiwaki et al. 1993](#); [Hubbard et al. 1996](#)] [MJ]

***emb-6* I – 0.47 *hc65***

: ts, mm; at 25°C, 14-cell arrest; no gut granule birefringence; division rates very slow; normal and defective execution before first cleavage; viable at 16°C. OA1: *g36ts* (similar). [[Miwa et al. 1980](#); Denich et al. 1984] [MJ]

***emb-7* III – 3.12 *hc66***

: ts, mm; at 25°C, lima bean arrest; division rates slightly slowed; normal and defective execution before first division; viable at 16°C but slightly abnormal division rates. OA2: *b84ts* (pka [zyg-4](#), 25°C embryonic arrest <100 nuclei; L1 temperature shift-up affects gonadogenesis), *b64*. [[Miwa et al. 1980](#)] [MJ]

***emb-8* III – 4.44 *hc69***

: ts, mm; at 25°C, eggs osmotically sensitive; variable arrest (early to mid-cleavage); division rates slowed; viable at 16°C, but eggs are fragile. NA1. CLONED: cosmid rescue (ZC235). [[Miwa et al. 1980](#)] [MJ]

***emb-9* III 0.47 *hc70***

: sd, ts, nn; at 25°C, early pretzel arrest; a few animals hatch and die in L1; ts for larval growth (arrest shortly after any shift to 25°C); normal and defective execution in late embryogenesis. OA>10: *g23ts*, *g34ts*, *b117ts*, *b189ts* (pka [zyg-6](#)) (all similar to *hc70*), *mj70ts* (Mig, abnormal Q daughter migration). Also Pat alleles: *st540*, *st545* (paralyzed arrest at 2-fold, late paralysis, no elongation). Putative nulls recessive, arrest at 3-fold stage; strong missense alleles arrest at 2-fold. CLONED: pka [clb-2](#); encodes 1758-aa basement membrane collagen (type IV),  $\alpha 1$  chain. [Denich et al. 1984; [Sibley et al. 1993](#)] [CH, MJ, RW]

***emb-10* I 1.75 *hc63***

: ts; embryonic arrest. OA1: *k12ts* (sterile; viable at 16°C). [MJ]

***emb-11* IV 4.73 *g4***

: ts, mm; osmotically sensitive eggs at 25.6°C (leaky at 25°C); 94% arrest during early proliferation; escapers mostly arrest in L1; temperature shift-up in L1 or L4 results in abnormal gonadogenesis; adults dumpy at 25°C, uncoordinated at 16°C. OA1: *g7ts* (similar phenotypes but lower penetrance). [[Cassada et al. 1981](#)] [RC]

***emb-12* I 2.06 *g5***

: ts, mm; osmotically sensitive eggs at 25.6°C (leaky at 25°C); 72% arrest during early proliferation; escapers have abnormal gonads; temperature shift-up in L1 results in incompletely penetrant gonad defects; viable

at 16°C. NA1. [[Cassada et al. 1981](#)] [RC]

**emb-13 III – 11.73 g6**

: ts, nm; at 25°C, 99% eggs arrest at lima bean; no gut granule birefringence; reduced cytoplasmic streaming before first cleavage slow divisions; E, D, and P lineages early; escapers arrest as larvae, abnormal gonadogenesis; L1 temperature shift-up results in larval arrest, abnormal gonad; viable at 16°C, variably long. NA1. [[Cassada et al. 1981](#); Denich et al. 1984] [RC]

**emb-14 I 1.67 g43**

: ts, nm; osmotically sensitive eggs at 25°C; 100% eggs arrest during proliferation; escapers arrest as larvae; L1 temperature shift-up results in some gonad abnormality; viable at 16°C; poor male mating. OA1: g14ts,mm? (similar phenotypes, lower penetrance). [[Cassada et al. 1981](#)] [RC]

**emb-15 X 7.61 g15**

: ts, mnz; at 25°C, 97% eggs arrest at pretzel; prolonged mitoses during cleavage; escapers arrest L1–L4; viable at 16°C. NA1. [[Cassada et al. 1981](#); Denich et al. 1984] [RC]

**emb-16 III – 0.80 g19**

: ts, mm; at 25°C, 91% eggs arrest at lima bean; misplaced gut granule birefringence; E lineage early, MS delayed; escapers arrest in L1 abnormal gonadogenesis; L1 temperature shift-up affects gonadogenesis; viable at 16°C, somewhat uncoordinated. NA1. [[Cassada et al. 1981](#); Denich et al. 1984] [RC]

**emb-17 I N g20**

: ts, mnz; at 25°C, 100% eggs arrest at lima bean; normal gut granule birefringence; eggs variably irregular in shape; some lineages early, some delayed; L1 or L4 temperature shift-up affects gonadogenesis; at 16°C, uncoordinated; synthetic lethal with many *dpy* mutations. NA1. [[Cassada et al. 1981](#); Denich et al. 1984] [RC]

**emb-18 V 2.21 g21**

: ts, mm; at 25°C, 100% eggs arrest at lima bean; normal gut granule birefringence; eggs variably round in shape; C and E lineages late, P4 early; escapers arrest L2–L4; L1 temperature shift-up affects gonadogenesis; slightly long at 16°C. NA1. [[Cassada et al. 1981](#); Denich et al. 1984] [RC]

**emb-19 I 2.06 g22**

: ts, mm; osmotically sensitive eggs at 25°C; 100% arrest during early proliferation; escapers arrest L1–L4; L1 temperature shift-up affects gonadogenesis; viable at 16°C. NA1. [[Cassada et al. 1981](#)] [RC]

**emb-20 I 13.31 g27**

: ts, mm; osmotically sensitive eggs at 25.6°C (leaky at 25°C); 96% eggs arrest during early proliferation; escapers viable F<sub>1</sub> Emb; viable at 16°C. OA1: g26. [[Cassada et al. 1981](#)] [RC]

**emb-21 II 0.58 g31**

: ts, mm; at 25°C, 90% eggs arrest 26–30 cell stage; no gut granule birefringence; variable round eggs; large ooplasmic granules, prolonged mitoses especially AB; escapers arrest L2–L3, abnormal gonadogenesis; L1 temperature shift-up affects gonadogenesis. NA1. [[Cassada et al. 1981](#); Denich et al. 1984] [RC]

**emb-22 V 1.39 g32**

: ts, nm; at 25°C, 100% eggs arrest at lima bean; misplaced gut granule birefringence; strong ooplasmic streaming, erratic pronuclear migration, no polar body formation, all mitoses prolonged; temperature shift-up at all stages after lima bean results in immediate arrest; viable at 16°C. NA1. Tightly linked to and possibly identical with act-123. [[Cassada et al. 1981](#); Denich et al. 1984] [RC]

***emb-23* II 2.94 g39**

: ts, mm; at 25°C, 100% eggs arrest at lima bean; misplaced gut granule birefringence; very large ooplasmic granules; [MS](#), C, and P<sub>2</sub> divisions late; escapers arrest L1–L2 abnormal gonads; L1 temperature shift-up results in L1–L2 arrest abnormal gonads; viable at 16°C. NA1. [[Cassada et al. 1981](#); Denich et al. 1984] [RC]

***emb-24* III 0.02 g40**

: ts, mnz; at 25°C, 100% eggs arrest at pretzel; normal gut granule birefringence; [E lineage](#) late; L1 temperature shift-up results in L1–L3 arrest; viable at 16°C, but many defective embryos. NA1. [[Cassada et al. 1981](#); Denich et al. 1984] [RC]

***emb-25* III – 0.37 g45**

: ts, mm; at 25°C, 100% eggs arrest at 100–250 cells; normal gut granule birefringence; eggs variably long in shape; later divisions slow or incomplete; escapers arrest L1–L2; L1 temperature shift-up results in L1–L2 arrest; viable at 16°C. NA1. [[Cassada et al. 1981](#); Denich et al. 1984] [RC]

***emb-26* IV 2.45 g47**

: ts, mm; at 25.6°C (leaky at 25°C), 80% eggs arrest at lima bean; abnormal gut granule birefringence; slow ooplasmic streaming, cleavage timing alterations; escapers arrest L1–L4 abnormal gonads; L1 temperature shift-up affects gonadogenesis; viable at 16°C, slightly long, poor male mating; meiotic phenotype at 20°C (pka [him-12](#)), self-progeny 8% XO male, low brood size (65% unhatched eggs), males sire many inviable zygotes. ES3 (progeny) ME2 NA1. [[Cassada et al. 1981](#); Denich et al. 1984] [RC]

***emb-27* II 0.78 g48**

: ts, mm, pat : at 25°C, 100% eggs arrest at one-cell stage; no polar body formation, no pseudocleavage, 30% fail to reform pronucleus; pronuclear migration and fusion are slow or absent, pronuclei disintegrate; escapers viable adults, F<sub>1</sub> Emb; males crossed with wt hermaphrodites sire progeny that arrest at 100-cell stage; mutant hermaphrodites crossed with wt males also produce embryos arrested at 100-cell stage; pleiotropic defect in gametogenesis (cf. [emb-30](#)); L1 temperature shift-up results in viable adult F<sub>1</sub> Emb; viable at 16°C. NA1. [[Cassada et al. 1981](#); Denich et al. 1984] [DS, RC]

***emb-28* V 13.87 g49**

: ts, mm; at 25.6°C (leaky at 25°C), 91% arrest at lima bean; misplaced gut granule birefringence; very large ooplasmic granules; slow and abnormal first cleavage, later divisions slow; escapers viable with abnormal gonad; L1 temperature shift-up results in viable adult F<sub>1</sub> Emb; viable at 16°C. NA1. [[Cassada et al. 1981](#); Denich et al. 1984] [RC]

***emb-29* V – 18.40 g52**

: ts, nn; at 25°C, 100% eggs arrest before mitosis during 150–200-cell stage; misplaced gut granule birefringence; some divisions delayed; escapers arrest L2–L4; L1 or L4 temperature shift-up affects gonadogenesis; probably general G<sub>2</sub>/M cell cycle arrest; viable at 16°C. OA4: *b262* (similar phenotypes), *s819*, *s1613*, *s1666fdi*. CLONED: cosmid rescue? [Denich et al. 1984; [Hecht et al. 1987](#)] [BC, HH]

***emb-30* III 1.29 g53**

: ts, mm, pat; round osmotically sensitive eggs at 25°C; 96% eggs arrest at one-cell stage; ooplasmic streaming somewhat abnormal, only one polar body; no pseudocleavage; no pronuclear migration or fusion; some endomitosis; escapers are viable adults, F<sub>1</sub> Emb; males crossed with wt hermaphrodites sire progeny that arrest at 100-cell stage; pleiotropic defect in gametogenesis? (cf. [emb-27](#)); L1 temperature shift-up results in viable adult F<sub>1</sub> Emb; viable at 16°C, slightly uncoordinated. NA1. CLONED: cosmid rescue; operon includes [tbg-1](#), so [emb-30](#) may correspond to [tbg-1](#). [[Cassada et al. 1981](#); Denich et al. 1984] [RC, SQ]

***emb-31 IV 2.92 g55***

: ts, mm; at 25°C, 100% eggs arrest at lima bean; normal gut granule birefringence; abnormal blastocoel and gastrulation; escapers sometimes arrest in L1–L2; abnormal gonads; L1 temperature shift-up affects gonadogenesis; viable at 16°C. NA1. [[Cassada et al. 1981](#)] [RC]

***emb-32 III – 6.65 g58***

: ts, mnz; at 25.6°C (leaky at 25°C), 97% eggs arrest at lima bean; normal gut granule birefringence; ooplasmic streaming slow, cleavage timing altered, late divisions slow; escapers arrest in L2; L1 temperature shift-up results in L2 arrest, abnormal gonadogenesis; viable at 16°C, dumpy. NA1. [[Cassada et al. 1981](#); Denich et al. 1984] [RC]

***emb-33***

= *glp-1*

***emb-34 III 0.26 g62***

: ts, nm; at 25°C, 100% eggs arrest at lima bean; abnormal gut granule birefringence; egg shape variable; some pseudocleavage failure, erratic pronuclear migration; first mitosis prolonged, later divisions prolonged and skewed; L1 temperature shift-up results in L1 arrest; viable at 16°C. NA1. [[Cassada et al. 1981](#); Denich et al. 1984] [RC]

***emb-35 IV 0.23 g64***

: ts, mnz; at 25.6°C (leaky at 25°C), 97% eggs arrest at lima bean; normal gut granule birefringence; later divisions delayed and prolonged, P<sub>4</sub> early; escapers small, arrest L1–L4; L1 temperature shift-up results in some larval arrest, dumpy adults F<sub>1</sub> Emb; viable at 16°C. NA1. [[Cassada et al. 1981](#); Denich et al. 1984] [RC]

***emo***

**e** ndo **m** itotic **o** ocytes [BS]. Formerly *oar*.

***emo-1 V 2.83 oz1***

: oocyte diakinesis arrest-defective; hermaphrodite sterile; in hermaphrodite, unfertilized oocytes in diakinesis undergo DNA endoreduplication and become polyploid. OA1: *oz151* (embryonic-lethal). CLONED: cosmid F32D8. [[Iwasaki et al. 1996](#)] [BS]

***emo-2 III – 1 oz136***

: recessive-sterile, endomitotic oocytes. [BS]

***emo-3 IV 5.8 oz138***

: recessive-sterile, endomitotic oocytes. [BS]

***emo-4 V N oz145***

: recessive-sterile, endomitotic oocytes. [BS]

***emo-5 II N oz148***

: recessive-sterile, endomitotic oocytes. [BS]

***emo-6 III – 1 oz154***

: recessive-sterile, endomitotic oocytes. [BS]

***emo-5 II N oz148***

: recessive-sterile, endomitotic oocytes. [BS]

***emo-6 III – 1 oz154***

: recessive-sterile, endomitotic oocytes. [BS]

#### ***enu***

**en** hancer of **u** ncoordinated behavior [CB].

#### ***enu-1 II N ev419***

: sd; no phenotype alone but enhances uncoordinated phenotype of *vab-8(ev411)*; ES3 (in *ev411* background) ES0 (without *ev411*). NA1. [NW]

#### ***epi***

**epi** thelialization abnormal [NJ].

#### ***epi-1 IV 4.72 rh165***

: basal lamina missing or defective in epidermis, gonad, [intestine](#); [pharynx](#) normal; some migrations defective; body wall myofilaments disorganized; [uterus](#) and spermatheca fail to epithelialize, release proliferating [germ cells](#); sterile. OA3: *rh152* (weaker allele, mostly sterile), *gm1*, *gm80* (more severe?). CLONED: encodes predicted protein with similarity to laminin A (pka [lgx-3](#) ). [NJ, GS, NG]

#### ***evl***

abnormal **e** version of **v u l** va [GS].

#### ***evl-1 V 2.4 ar115***

: everted [vulva](#), sterile; normal L4 vulval invagination, abnormal [uterus](#), abnormal oocytes. NA1. [[Seydoux et al. 1993](#)]

#### ***evl-2 II – 2.4 ar119***

: everted [vulva](#), sterile; normal L4 vulval invagination, abnormal [uterus](#), abnormal oocytes. NA1. [[Seydoux et al. 1993](#)]

#### ***evl-3 II 1.8 ar99***

: everted [vulva](#), sterile; normal L4 vulval invagination, no [uterine](#) cavity, abnormal distal germ line, no sperm or oocytes. OA2: *ar100*, *ar118* (both similar). [[Seydoux et al. 1993](#)]

#### ***evl-4 II RC ar101***

: everted [vulva](#), sterile; abnormal L4 vulval invagination, abnormal [uterus](#), abnormal oocytes. OA1: *ar116* (similar). [[Seydoux et al. 1993](#)]

#### ***evl-5 V – 0.5 ar105***

: everted [vulva](#), sterile; abnormal L4 vulval invagination, abnormal [uterus](#), abnormal oocytes. NA1. [[Seydoux et al. 1993](#)]

#### ***evl-6 IV 5 ar120***

: everted [vulva](#), sterile; abnormal L4 vulval invagination, abnormal [uterus](#), abnormal oocytes. NA1. [[Seydoux et al. 1993](#)]

#### ***evl-7 IV 1.8 ar108***

: everted [vulva](#), sterile; abnormal L4 vulval invagination, abnormal [uterus](#), no oocytes. NA1. [[Seydoux et al. 1993](#)]

#### ***evl-8 III RC ar102***

: everted [vulva](#) (or sometimes no vulval induction), sterile; abnormal L4 vulval invagination, abnormal [uterus](#), abnormal oocytes. NA1. [[Seydoux et al. 1993](#)]

***evl-9 I RC ar121***

: everted [vulva](#), sterile; abnormal L4 vulval invagination, abnormal [uterus](#), distal germ line abnormal, abnormal oocytes, no sperm. NA1. [[Seydoux et al. 1993](#)]

***evl-10 I 0.5 ar95***

: everted [vulva](#), sterile; abnormal L4 vulval invagination, abnormal [uterus](#), distal germ line abnormal, no sperm or oocytes. NA1. [[Seydoux et al. 1993](#)]

***evl-11 V – 1.6 ar114***

: everted [vulva](#), sterile; abnormal L4 vulval invagination, no [uterine](#) cavity, abnormal oocytes. OA1: *ar113* (similar). [[Seydoux et al. 1993](#)]

***evl-12 V 3.2 ar109***

: everted [vulva](#) (or sometimes no vulval induction), sterile; abnormal L4 vulval invagination, no [uterine](#) cavity, abnormal oocytes. NA1. [[Seydoux et al. 1993](#)]

***evl-13 IV 3.3 ar107***

: everted [vulva](#), sterile; abnormal L4 vulval invagination, no [uterine](#) cavity, no oocytes. NA1. [[Seydoux et al. 1993](#)]

***evl-14 III – 3.3 ar96***

: everted [vulva](#), sterile; no L4 vulval invagination, abnormal [uterus](#) and oocytes. OA2: *ar97, ar112* (both similar) [[Seydoux et al. 1993](#)]

***evl-15 IV L ar126***

: everted [vulva](#), sterile; no L4 vulval invagination, abnormal [uterus](#), no oocytes. NA1. [[Seydoux et al. 1993](#)]

***evl-16 I RC ar93***

: everted [vulva](#), sterile; no L4 vulval invagination, abnormal [uterus](#) and oocytes, distal germ line abnormal. NA1. [[Seydoux et al. 1993](#)]

***evl-17 I RC ar94***

: everted [vulva](#), sterile; no L4 vulval invagination, abnormal [uterus](#) and oocytes, distal germ line abnormal. NA1. [[Seydoux et al. 1993](#)]

***evl-18 III L ar117***

: everted [vulva](#), sterile; no L4 vulval invagination, abnormal [uterus](#), distal germ line abnormal, no sperm or oocytes. NA1. [[Seydoux et al. 1993](#)]

***evl-19 III RC ar98***

: everted [vulva](#), sterile; no L4 vulval invagination, abnormal [uterus](#), distal germ line abnormal, no sperm or oocytes. NA1. [[Seydoux et al. 1993](#)]

***evl-20 II 0.9 ar103***

: everted [vulva](#), sterile; no L4 vulval invagination, abnormal [uterus](#), distal germ line abnormal, no sperm or oocytes. NA1. [[Seydoux et al. 1993](#)]

***evl-21 III L ar122***

: everted [vulva](#) (or sometimes no [vulva](#)), sterile; no L4 vulval invagination, abnormal [uterus](#), distal germ line abnormal, no sperm. NA1. [[Seydoux et al. 1993](#)]

***evl-22 II LC ar104***

: everted [vulva](#), sterile; no L4 vulval invagination, no [uterine](#) cavity, no sperm or oocytes. NA1. [[Seydoux et al. 1993](#)]

#### **evl-23 IV 3.4 ar106**

: everted [vulva](#) (or sometimes no [vulva](#)), sterile; no L4 vulval invagination, no [uterine](#) cavity, abnormal oocytes. NA1. [[Seydoux et al. 1993](#)]

#### **evl-24 IV 4 ar124**

: everted [vulva](#), sterile; no L4 vulval invagination, no [uterine](#) cavity or oocytes, distal germ line abnormal. NA1. [[Seydoux et al. 1993](#)]

#### **exc**

[exc](#) retoxy canal abnormal [NJ].

#### **exc-1 X 21.24 rh26**

: [excretory](#) canal defect; large vacuoles appear randomly along the [excretory](#) canal, especially at the tips; 100% penetrant; often visible by low-power microscopy. NA1. [NJ]

#### **exc-2 X – 5.24 rh90**

: [excretory](#) canal defect; canals very short and consist of a series of vacuoles; luminal coat partly detached, floats in canal; 100% penetrant; usually visible by low-power microscopy. OA1: *rh105*. [NJ]

#### **exc-3 X 1.12 rh186**

: [excretory](#) canal defect; canals shortened and animal somewhat pale; defect visible only by Nomarski microscopy. OA1: *rh207*. [NJ]

#### **exc-4 I 25.31 rh133**

: [excretory](#) canal defect; vacuoles appear in canal during embryogenesis and drastically shorten canal by hatch; animals pale, slightly Unc, and often killed by growth of large vacuoles at the [excretory](#) cell body; defect visible by low-power microscopy. OA1: *n2400* [NJ]

#### **exc-5 IV 4.30 rh232**

: [excretory](#) canal defect; large vacuoles appear randomly along the [excretory](#) canal; 100% penetrant; often visible by low-power microscopy. OA2: *n2669* (weaker allele, smaller vacuoles), *n2672*. [NJ]

#### **exc-6 X 21.00 rh103**

: [excretory](#) canal defect; canal varies in length from no outgrowth to almost complete outgrowth; frequent small vacuoles and extra branchings in the canal lumen visible only by Nomarski microscopy; animal somewhat pale. NA1. [NJ]

#### **exc-7 II 1.59 rh252**

: [excretory](#) canal defect; canal invariably short with multiple cysts of varying size clustered along length, especially at the tips; visible only by Nomarski microscopy; animal somewhat pale. NA1. [NJ]

#### **exc-8 X N rh210**

: [excretory](#) canal defect; resembles Exc-6. NA1. [NJ]

#### **exp**

[exp](#)ulsion step of defecation abnormal [JT].

#### **exp-1 II – 0.87 sa6**

: severe to moderate constipation; [E.p](#) contraction present about every sixth cycle, slight Egl; defecation phenotype resembles Unc-25, Unc-47; GABA staining normal; *sa6/Df* similar. NA1. [[Thomas 1990](#); [Reiner](#)

[and Thomas 1995](#)] [JT]

**exp-2 V – 0.32 sa26**

: sd; recessive-lethal; *sa26*/+ strongly dominant, severely constipated, jerky Unc; expulsion muscle contraction always absent from defecation cycle ([E.p](#)), severe egg-laying defect (type-A Egl); serotonin nonresponsive; egg laying and [anal muscle](#) normal as observed by polarized light, pumping very shallow but rapid; muscle activation defective (flaccid, long). NA1 (gf). Intragenic revertants, e.g., *sa26sa66* *sa26sa68*, recessive-lethal, no dominant [E.p](#) phenotype. [[Thomas 1990](#); [Reiner and Thomas 1995](#)] [DA, JT]

**exp-3 V 21.73 n2372**

: sd; severely bloated egg-laying-defective (type A); frequently forms bag-of-worms; also semidominantly defective for expulsion step of defecation; rarely has expulsion ([E.p](#)); severely constipated; egg-laying and enteric muscles grossly normal by polarized light microscopy; muscle activation defective (flaccid, long). ES3 (adult) ES2 (larvae) ME3 NA1. [[Reiner et al. 1995](#)] [JT]

**exp-4 IV – 4.96 n2373**

: sd; moderately bloated egg-laying-defective (type A); infrequently forms bag-of-worms; also semidominantly defective for expulsion step of defecation; infrequently has expulsion defect ([E.p](#)); moderately constipated; egg-laying and enteric muscles grossly normal by polarized light microscopy; muscle activation defective (flaccid, long). ES3 (adult) ES2 (larvae) ME3 NA1. [[Reiner et al. 1995](#)] [JT]

***fab***

**f**oraging behavior **ab** normal [KP].

***fab-1 I N ky2***

: hyperactive foraging; suppressed by serotonin agonists and uptake inhibitors. [KP]

***fab-2 I N n2460***

: hyperactive foraging; suppressed by serotonin agonists but not by imipramine. [KP]

***fab-3 III N n2462***

: hyperactive foraging; suppressed by serotonin agonists but not by imipramine. [KP].

***fab-4 V R n2466***

: hyperactive foraging; suppressed by serotonin agonists and uptake inhibitors. [KP]

***fat***

**fat** ty acid desaturase [CGC].

***fat-1 IV 8.3***

NMK. Encodes fatty acid desaturase (EST *cm10e11*); complements *Arabidopsis* mutant *fad2* (deficient in 18:3 fatty acid synthesis). [CGC]

***fem***

**fem** inization. Formerly *isx* (**i**nter **s**e **x**) [CB].

***fem-1 IV 1.99 e1965***

: mat; XO animals transformed into fertile females if mother homozygous, into intersexes if mother heterozygous; XX animals females if mother homozygous, females or hermaphrodites if mother heterozygous; null allele. ES3 (XO adult) ES2 (XX adult) ME0. OA>20: *e1991amb* (resembles *e1965*), *e1949*, etc. Also many ts alleles: *hc17ts* (pka [isx-1](#), causes only partial XO feminization at 25°C; XX self-fertile at 20°C), *e1918ts*, *e1988ts*, *e1973ts*. CLONED: 2.4-kb transcript, encodes 656-aa protein with six ANK repeats;

antibody staining indicates present in both sexes, both germ line and soma. [[Doniach and Hodgkin 1984](#); [Spence et al. 1990](#); [Gaudet et al. 1996](#)] [AS]

#### **fem-2 III – 26.79 e2105**

: ts, mat; XO animals transformed into fertile females (25°C) or intersexes (20°C) if mother homozygous, into abnormal males if mother heterozygous; XX animals fertile females if mother homozygous, hermaphrodite if mother heterozygous; XX phenotype non-ts; *e2105/Df* similar phenotypes. ES3 (XO adult) ES2 (XX progeny) ME0. OA>5: *e2102* (Q182oc, similar to *e2105*), *b245ts* (pka [\*isx-2\*](#), weaker missense allele, causes only partial XO feminization at 25°C, XX self-fertile at 20°C), *q117ts* (missense). CLONED: encodes predicted 449-aa protein, with similarity to protein phosphatase class 2C; allele *e2105* (probable null) is double mutant, *b245tse2005op*. [[Kimble et al. 1984](#); [Hodgkin 1986](#); [Pilgrim et al. 1995](#)] [DP]

#### **fem-3 IV 4.13 e1996**

: sd, mat, oc; XO animals transformed into fertile females if mother homozygous, into intersexes if mother heterozygous; XX animals fertile females; some *e1996/+* XX animals female, some *e1996/+* sons of *e1996* mothers are feminized. ES3 (XO adult) ES2 (XX adult) ME0. OA>20 *e1950*, *e2068amb*, *e2006ts* (XX self-fertile at 20°C). Also gf, ts alleles: *q20sd,ts* (at 25°C, XX germ line makes only sperm; at 15°C, XX germ line makes oocytes and excess sperm). ES3 (progeny) ME3. OA8(gf): *q22ts* (weaker), *q95ts* (strongest allele, 80% Mog even at 15°C). CLONED: 1.7-kb and 1.55-kb (minor) transcripts; former encodes predicted 388-aa novel protein; gf alleles are alterations in 3'UTR; transgene overexpression of [\*fem-3\*](#) leads to extensive masculinization of XX soma. [[Hodgkin 1986](#); [Ahringer et al. 1992](#)] [CB, JK, AS]

#### **fer**

**fer** tilization-defective [BA]. See also *spe*.

#### **fer-1 I 2.91 hc1**

: ts; hermaphrodites and males grown at 25°C produce nonfunctional nonmotile sperm with short pseudopods; membranous organelles fail to fuse with sperm plasma membrane; TSP in L4; similar phenotype in *hcl/Df*. ES2 (adult). Self-fertility <1% (25°C), 100% (16°C); sperm normal if grown at <25°C. OA7: *hc80* (nonconditional), *hc24* (leaky ts), *b232*, etc. CLONED: cosmid rescue (C02D7); 7-kb transcript, encodes probable novel protein. [[Ward et al. 1981](#)] [BA]

#### **fer-2 III 7.28 hc2**

: ts; hermaphrodites and males grown at 25°C produce nonfunctional nonmotile sperm with aberrant pseudopods, perinuclear tubules; TSP L2–L4; self-fertility 2% (25°C), 70% (16°C). ES2 (adult) NA1. [[Ward et al. 1981](#)] [BA]

#### **fer-3 II N hc3**

: ts; hermaphrodites and males grown at 25°C produce nonfunctional nonmotile sperm with some aberrant pseudopods, perinuclear tubules; TSP L3–L4; self-fertility 1% (25°C), 60% (16°C). ES2 (adult) NA1. [[Ward et al. 1981](#)] [BA]

#### **fer-4 V 2.75 hc4**

: ts; hermaphrodites and males grown at 25°C produce nonfunctional nonmotile sperm with aberrant pseudopods, perinuclear tubules; skewed transmission ratio from *hc4/+* males, implying haplo-expression; self-fertility 3% (25°C), 50% (16°C). ES2 (adult) NA1. *hc4/Df* hermaphrodites have abnormal gonads with no oocyte production, no rescue by wt sperm. [[Ward et al. 1981](#)] [BA]

#### **fer-5**

= *fer-6*

#### **fer-6 I 2.89 hc6**

: ts; hermaphrodites and males grown at 25°C produce few sperm with defective pseudopods and retention of fibrous bodies; self-fertility 1% (25°C), 50% (16°C); TSP L4. ES2 (adult) NA1. (*hc23ts* [pka [fer-5](#)] is probably reisolate of *hc6*.) [\[Ward et al. 1981\]](#) [BA]

#### ***fer-7 I – 1.92 hc34***

: ts; hermaphrodites and males grown at 25°C produce nonfunctional nonmotile sperm; self-fertility 6% (25°C), 40% (16°C); TSP L4. ES2 (adult) NA1. [\[Argon and Ward 1980\]](#) [BA]

#### ***fer-14 I 25.45 hc14***

: ts; hermaphrodites and males grown at 25°C produce nonfunctional motile spermatozoa; sperm from Fer-14 males can outcompete wt hermaphrodite sperm; self-fertility <0.5% (25°C), 8% (16°C). ES2 (adult) NA1. [BA, DS, SL]

#### ***fer-15 II 0.77 hc15***

: ts; hermaphrodites and males grown at 25°C produce [spermatids](#) that fail to activate into spermatozoa; self-fertility <1% (25°C), 100% (16°C). ES2 (adult); similar phenotype in *hc15/Df. OA2: hc89, b26*. See also *age-1*. [\[Roberts and Ward 1982a\]](#) [BA, TJ, SL]

#### ***fib***

**fib** rillarin

#### ***fib-1* ?**

NMK. Similarity to fibrillarin; upstream gene in operon with [rps-16](#). [\[Zorio et al. 1994\]](#) [BL]

#### ***fkh***

**f** or **k h** ead family of transcription factors [JM].

#### ***fkh-1 V 25 pk48***

: Tc1 insertion; no known phenotype. CLONED: three transcripts, present in all stages, highest in embryo; *fkh-1:lacZ* expressed primarily in gut; >75% identity to *Drosophila fork head* in DNA-binding domain. [JM]

#### ***flp***

**F** MRFamide-**I** like **P** peptide [NY].

#### ***flp-1 IV N pk41***

: Tc1 insertion; no known phenotype. CLONED: encodes FMRF-containing neuropeptides; six exons, four encode FMRFamide-like peptides; alternatively spliced transcripts. [\[Rosoff et al. 1992\]](#) [NY]

#### ***flr***

**fl** uo **r** ide resistance abnormal [JC]. See also *dec*.

#### ***flr-1 X 12.39 ut1***

: resistant to 400 µg/ml NaF; slow growth; small. OA5: *ut2, ut4, ut6, ut11, sa96* (very short defecation cycle period, often with weak or missing motor program steps, Con, scrawny, and slow growing; fluoride-resistant; appears to feed normally). CLONED: encodes protein with some similarity to DEG-1/MEC-4 family. [\[Katsura et al. 1994; Iwasaki et al. 1995\]](#) [JC, JT]

#### ***flr-2 V 3.49 ut5***

: partially resistant to 400 µg/ml NaF; normal defecation. OA1: *ut71*. [\[Katsura et al. 1994\]](#) [JC, JT]

#### ***flr-3 IV – 29.14 ut9***

: resistant to 400 µg/ml NaF; slow growth; small; very short defecation cycle period. OA2: *ut8, ut10*. CLONED: encodes protein with some similarity to kinases, but lacks ATP-binding consensus. [\[Katsura et al.](#)

[1994; Iwasaki et al. 1995](#)] [JC, JT]

**flr-4 X 19.96 ut3**

: resistant to 400 µg/ml NaF; slow growth; small. OA2: *ut7, sa201* (ts, at 25°C, very short defecation cycle period, often with weak or missing motor program steps, Con, scrawny, and slow growing; fluoride-resistant; appears to feed normally). CLONED: cosmid rescue (F09B12). [[Katsura et al. 1994](#); [Iwasaki et al. 1995](#)] [JC, JT]

**flr-5 V 1.89 ut73**

: partially resistant to 400 µg/ml NaF; normal defecation. [[Katsura et al. 1994](#)] [JC, JT]

**flu**

**flu** orecence of gut abnormal [CB].

**flu-1 V N e1002**

: sd; increased gut fluorescence, bluish purple; low orthoamino-phenol content, low kynurenone hydroxylase. ES1 ME2 OA5. [[Babu 1974](#); [Siddiqui and Babu 1980](#)]

**flu-2 X – 3.61 e1003**

: reduced gut fluorescence, dull green; high orthoamino-phenol content, low kynureninase levels, enhanced mutagen sensitivity. ES1 ME3 OA4. [[Babu 1974](#); [Bhat and Babu 1980](#)]

**flu-3 II N e1001**

: increased gut fluorescence, purple. ES1 ME2 OA2. [[Babu 1974](#)]

**flu-4 X N e1004**

: increased gut fluorescence, blue. ES1 ME3 NA1. [[Babu 1974](#)]

**fog**

**f** eminization **o** f **g** erm line [CB].

**fog-1 I – 4.45 e1959**

: sd; homozygous XX animals transformed into fertile females; homozygous XO animals somatically male, make oocytes in germ line; heterozygous XO animals somatically male with both sperm and oocytes in germ line. ES2 (adults). OA>10: *e2121, e1959, e2122, q155, q253ts* (fertile at 15°C). [[Barton and Kimble 1990](#); [Ellis and Kimble 1995](#)] [JK, RE]

**fog-2 V 24.94 q71**

: XX animals transformed into females; XO animals wt males. ES3 (adult XX) ME3 OA5. [[Schedl and Kimble 1988](#)] [BS]

**fog-3 I 4.56 q469**

: XX animals transformed into females; XO animals somatically male, make oocytes in germ line; *q469/Df* similar; no dominant phenotypes. ES3 (adult XX) ME0. OA>10: *q441, q443, q470, q520fdi, q502uvp, oz137, oz147*. [[Ellis and Kimble 1995](#)] [RE]

**fox**

**f** eminizing site **o** n **X** chromosome [CB].

**fox-1 X – 14.00**

Extra copies of locus lead to dominant XO lethality and feminization. CLONED: 1.8-kb transcript, encodes predicted 415-aa protein with RNP motif. [[Hodgkin et al. 1994](#)] [CB, TY]

**ftt**

**f**ourteen-**t**hree-**t**hree (14-3-3) family [DS].

#### **ftt-1 IV 5.31**

NMK. Encodes predicted protein 78% identical to *Drosophila* and bovine 14-3-3 proteins. [[Wang and Shakes 1994](#)] [DS]

#### **ftt-2 X N**

NMK. Encodes predicted protein with similarity to 14-3-3 proteins. [DS]

## **G to K**

### **gbr**

**G A B A r** eceptor family [CGC].

#### **gbr-1 III 13.91**

NMK. Cross-hybridization to GABA receptor probe. [CGC]

### **gcp**

See *cpr*.

### **ges**

**g**ut **es** terase [JM].

#### **ges-1 V – 18.93 ca1**

: electrophoretic variant of major gut esterase, no other phenotype. ES1 ME3. OA>10: *ca4*, *ca6*, etc. (all electrophoretic variants), *ca6ca7*, *ca6ca9*, *ca10*, *ca11*, etc. (null mutations, major gut esterase activity absent, no other phenotype), *pk47*, *pk49* (Tc1 insertions; deletion derivatives also obtained). CLONED: encodes gut-specific esterase, expressed from 200-cell stage onward; extensive promoter analysis. [[McGhee et al. 1990](#); [Aamodt et al. 1991](#)] [JM]

### **gld**

**g**erm **l**ine **d**ifferentiation abnormal [BS].

#### **gld-1 I 2.24 q485**

: hermaphrodite [germ cells](#) enter meiosis, fail in pachytene, reenter mitosis, and form large proximal germ-line tumor; males unaffected; probable null phenotype. ES3 (adult) ME3. OA>15: multiple phenotypic classes and subclasses:

class A: *q268*, *q365* (probable nulls, resemble *q485*)

class B: *q93oz12* (sperm, then [germ cells](#) arrested in pachytene)

class C: *q93* (gf, Mog)

class D: *q126* (gf, Fog)

class E: *q266* (gf, Fog, abnormal oocytes)

class F: *q343* (sperm, then abnormal oocytes)

Complex complementation. CLONED: encodes predicted 463- or 466-aa proteins, with similarity to shrimp GRP33, mouse Src-associated protein Sam68; includes KH (possible RNA-binding) domain. [[Francis et al. 1995a,b](#); [Jones and Schedl 1995](#)] [BS]

#### **gld-2 I N q497**

: [germ cells](#) enter meiosis, fail in pachytene, make enlarged oocyte-like cells; spermatogenesis also defective in males; in presence of extragenic modifier (*q525*), proximal germ line becomes mitotic. NA1. [JK]

## **glh**

**g**erm **l**ine **h**elicase [KB].

### **glh-1 I 1.34**

NMK (but may correspond to [let-545](#)). Encodes predicted 70-kD protein with RNA helicase similarity, DEAD box, four zinc finger motifs; expression correlated with germ line; antibody staining suggests associated with P granules. [[Roussell and Bennett 1993](#)] [KB]

### **glh-2 I 1.14**

NMK. Encodes predicted protein, 80% identity with [glh-1](#). [KB]

## **glp**

**g**erm **l**ine **p**roliferation abnormal [JK].

### **glp-1 III 0.14 q46**

: [germ cells](#) divide only a few times in both XX and XO, forming 10–20 sperm; [somatic gonad](#) superficially wt; mosaic analysis indicates germ-line focus. ES3 (adult). OA>10: *q35*, *q50* (both have weaker phenotype than *q46*, some oocyte production; fertilized eggs arrest during embryogenesis), *e2072* (Mel, late embryonic arrest, no [AB](#)-derived [pharyngeal cells](#), variable hypodermal defects), *e2141ts*, *e2144ts* (both Mel at 25°C), *g60ts,mm* (*pka* [emb-33](#); at 25°C, 100% eggs arrest at lima bean or earlier, misplaced gut granule birefringence; escapers have abnormal gonadogenesis; L1 temperature shift-up results in viable adult F<sub>1</sub> Emb; viable at 16°C). Also gf alleles: *q35sd* (causes Muv, extra vulval differentiation, mimics *lin-12[glf]*), *oz112gf* (dominant germ-line tumorous in both sexes, some Muv, extra vulval differentiation). See also *sog*, *ego*, *lag*, *lin-12*, etc; *lag* functions redundant with [lin-12](#). CLONED: 4.4-kb transcripts, encodes 1295-aa transmembrane receptor, closely related to LIN-12, *Drosophila* Notch, etc.; extracellular ten EGF-like repeats, other repeats; intracellular six ANK repeats, etc.; antibody staining indicates GLP-1 membrane-associated in early embryo, [AB](#) descendants, mitotic [germ cells](#), not detected in gametes; very extensive developmental and molecular analysis. [[Austin and Kimble 1987, 1989; Priess et al. 1987; Yochem and Greenwald 1989; Crittenden et al. 1994](#)] [JK, BS, GE, JR, GS]

### **glp-3 III – 0.81 q145**

: sterile, no germ-line proliferation in hermaphrodites or males; about three undifferentiated [germ cells](#) per gonad arm; no somatic defects. OA4: *q156*, *q171*, *q363*, *q456* (all similar). [JK]

### **glp-4 I 20.84 bn2**

: ts; hermaphrodites raised at 25°C sterile, ~12 germ-line nuclei, nonreflexed gonad arms; males at 25°C ~16 germ-line nuclei, normal soma; [germ cells](#) arrested at meiotic prophase; fertile at 16°C; TSP throughout larval development. OA3: *om14* (proliferation normal; oocytes small, irregular; other germ-line abnormalities), *om23* (weaker phenotypes), *om24*. Also probable intragenic revertants of *bn2*: *bn2bn39*, *bn2bn40* (some fertility at 25°C). [[Beanan and Strome 1992; Qiao et al. 1995](#)] [EL, SS]

## **glr**

**g**lutamate **r**eceptor family [CX].

### **glr-1 III – 0.18 n2461**

: fails to respond to light nose touch (Not) or to harsh body touch (Tab); other sensory responses normal; *n2461/Df* similar. ME3. Missense mutation. OA1: *ky176te, sd* (non-null deletion, Not, Mec; slightly sluggish; other sensory responses normal; *ky176/+* Not, Mec). CLONED: encodes predicted 962-aa protein with similarity to AMPA-class glutamate receptors (40% identity to rat GluRB); *glr-1:GFP* expressed in 17 [neuron](#) classes. [[Maricq et al. 1995; Hart et al. 1995](#)] [CX, KP]

## **goa**

**G** protein **Q**, **A** lpha subunit [PS].

**goa-1 I 2.04 sy192**

: hyperactive, Egl-c; defective male mating. OA3: *pk39* (Tc1 insertion, similar phenotypes), *n363*, *n1134* (some axon guidance defects?). CLONED: encodes homolog of mammalian G-protein  $\alpha$ -subunit (>80% identity); *goa-1:lacZ* expressed in most [neurons](#), some muscle cells, [pharynx](#), [distal tip cells](#); transgene overexpression leads to lethargy, slow pumping, egg-laying defects, irregular defecation. [[Mendel et al. 1995](#); [Segalat et al. 1995](#)] [KP, PS]

**gon**

**gon** ad development abnormal [CB].

**gon-1 IV 4.31 e1254**

: defective formation of [somatic gonad](#) primordium; much germ-line proliferation, almost no gamete maturation, variable vulval induction, no [uterus](#); *e1254/Df* similar. ES3 ME0 (male [somatic gonad](#) also abnormal). OA4: *e2547*, *e2551*, *q517*, *q518* (similar). [[Hodgkin et al. 1989](#)] [CB, JK]

**gon-2 I 2.88 q362**

: partial maternal-effect gonadless ([Z1](#) and [Z4](#) often fail to divide). OA3: *q388ts* (zygotic sterile at 25°C, fertile 15°C, upshift gives Gon progeny), *dx12*, *dx13*. CLONED: cosmid rescue (T01H8) [EJ]

**gon-3 IV N e2548**

: abnormal [somatic gonad](#), late defect, sterile. NA1. [CB]

**gon-4 IV 4.53 e2575**

: abnormal gonad development, sterile; [vulva](#) development mostly abnormal, some spermatogenesis, little oogenesis; often failure of division of [Z1](#), [Z4](#). OA2: *q519*, *q521*. [CB, JK]

**gon-5 I N e2550**

: abnormal [somatic gonad](#), late defect, sterile. NA1. [CB]

**gon-6 II N e2586**

: abnormal [somatic gonad](#), late defect, sterile. NA1. [CB]

**gon-7 V N e2589**

: abnormal [somatic gonad](#), late defect, sterile. NA1. [CB]

**gon-9 I N e2611**

: abnormal gonad development, sterile. [CB]

**gon-10 V 6.36 e1795**

: hermaphrodites have very abnormal swollen proximal gonad with apparent giant oocytes, additional nongonadal somatic abnormalities, sterile, variable tail malformation. NA1. [CB]

**gon-11 I 3.8 dx5**

: ts; partial maternal-effect gonadless ([Z1](#) and [Z4](#) undergo few or no divisions); zygotic germ-line phenotype, proximal proliferation. NA1. [EJ]

**gpa**

**G** protein, **A** lpha subunit [PS].

**gpa-1 V 3.18 pk15**

: te; deletion of most of coding region, derived from Tc1 insertion *pk1*; no detectable phenotype. Also *pk14te* (smaller deletion). CLONED: 48% identity to GPA-3; *gpa-1:lacZ* expressed in some amphid and phasmid neurons, spicular neurons, some anterior pharyngeal cells. [[Lochrie et al. 1991](#); [Zwaal et al. 1993](#)] [PS, NL]

#### ***gpa-2 V 1.54 pk16***

: te; deletion of most of coding sequence, derived from Tc1 insertion *pk19*; no obvious phenotype, some reduction in dauer formation, stronger with *gpa-3(0)*. OA>50: numerous Tc1 insertions analyzed. CLONED: *gpa-2:lacZ* expressed in phasmid neurons, some nerve ring neurons, PVT, sphincter. [[Lochrie et al. 1991](#); [Zwaal et al. 1993](#)] [PS, NL]

#### ***gpa-3 V 1.97 pk35***

: te, deletion of most of coding sequence, derived from Tc1 insertion *pk12*; no obvious phenotype, some reduction in dauer formation, stronger with *gpa-2(0)*. CLONED: 48% identity to GPA-1; *gpa-3:lacZ* expressed in amphid and phasmid neurons. [[Lochrie et al. 1991](#); [Zwaal et al. 1993](#)] [PS, NL]

#### ***gpb***

**G** p rotein, **B** eta subunit [PS].

#### ***gpb-1 II 3.99 pk13***

: Tc1 insertion, also excision derivative *pk44*; recessive- lethal, arrests at L1 stage with very little body wall or pharyngeal muscle activity; in absence of maternal rescue, arrests as early embryonic-lethal. [[Zwaal et al. 1996](#)] [JA, NL]

#### ***gpd***

**g** lyceraldehyde 3- **p** hosphate **d** ehydrogenase [HH].

#### ***gpd-1 II 2.38***

NMK. Encodes glyceraldehyde-3-phosphate-dehydrogenase, minor isozyme (GAPDHase-1), ubiquitous, predominant expression in embryo; sequence closest to *gpd-4*. [[Barrios et al. 1989](#)] [HH]

#### ***gpd-2 X – 13.05***

NMK. Encodes glyceraldehyde-3-phosphate-dehydrogenase, major muscle-specific isozyme (GAPDHase-2); expression increases postembryonically; middle gene in operon between *mai-1* and *gpd-3*. [[Barrios et al. 1989](#); [Spieth et al. 1993](#)] [HH, BL]

#### ***gpd-3 X – 13.05***

Deleted in Bergerac strains; no apparent phenotype; encodes glyceraldehyde-3-phosphate-dehydrogenase, major muscle-specific isozyme (GAPDHase-2); expression increases postembryonically; final gene in operon with *mai-1*, *gpd-2*. [[Barrios et al. 1989](#); [Spieth et al. 1993](#)] [HH, BL]

#### ***gpd-4 II 1.95***

NMK. Encodes glyceraldehyde-3-phosphate-dehydrogenase, minor isozyme (GAPDHase-1); ubiquitous, predominant expression in embryo; sequence closest to *gpd-1*. [[Barrios et al. 1989](#)] [HH]

#### ***gqa***

**G** protein, class **Q** , **A** lpha subunit [PS].

#### ***gqa-1***

= *egl-30*

#### ***gro***

**gro** wth rate abnormal [CB].

***gro-1* III – 1.99 e2400**

: spo, mat; postembryonic growth rate greatly reduced; increased resistance to heat shock; some increase in life span; tends to avoid bacterial lawn; complete maternal rescue. ES0 (zygotic) ES2 ME2. Polymorphic in wild isolate (Palm Canyon, California). NA1. [CB, DR]

***gro-2* IV 9.46 e2442**

: spo, mat; postembryonic growth rate greatly reduced, tends to avoid bacterial lawn; spontaneous mutation from cross with Bergerac strain; complete maternal rescue. ES0 (zygotic) ES2 ME2 NA1. [CB, MQ]

***gro-3* I 18.67 e2556**

: spo, mat; no obvious zygotic phenotype; in absence of maternal rescue, homozygotes are very slow growing, slow moving, Egl, tend to avoid bacterial lawn. ES0 (zygotic) ES2 ME1. e2556 spontaneous in N2 background. NA1. [CB]

***gsa***

**G** protein, **S**, **A** lpha subunit [FK].

***gsa-1* I – 13.37 pk75**

: excision derivative of *pk27tci*, 1.8-kb deletion; recessive-lethal, L1/L2 arrest. CLONED: encodes 375-aa predicted protein; 66% identity with rat Gsa; *gsa-1:lacZ* expressed in many cells from late embryo onward. [Zwaal et al. 1993] [NL]

***gst***

**g**lutathione **S**-transferase [GS].

***gst-1* III 0.12**

NMK. Encodes predicted glutathione-S-transferase P subunit; *trans*-spliced to SL2. [[Weston et al. 1989](#)]

***gum***

**gu** t **m** orphology abnormal [EJ].

***gum-1* I 1.1 q373**

: accumulates large, possibly aqueous vesicles in gut, leading to marbled appearance under Nomarski. OA2: *dx2ts*, *oz162*. [EJ]

***gum-2* IV N e1747**

: gut cells have spongy appearance under Nomarski; in L4, [intestine](#) less patchy than wt under dissecting scope. OA2: *e1739* (weaker?). [CB, EJ]

***gum-3* X N e1823**

: gut cells have spongy appearance under Nomarski. OA1: *q433*. [CB, EJ]

***gum-4* X N q412**

: gut cells accumulate vesicles, possibly lipidaceous, leading to tapioca-like appearance under Nomarski. NA1. [EJ]

***gum-5* V – 2.5 dx4**

: causes large vesicles to accumulate in adult gut. NA1. [EJ]

***gum-6* X L oz124**

: causes large vesicles to accumulate in adult gut of hermaphrodites but not of males. NA1. [EJ]

***gus***

abnormal **g**. **l** **u** curonida **s** e [NA].

#### ***gus-1* I 25.85 *b405***

:  $\beta$ -glucuronidase activity reduced >99%; no gross phenotype. ES1. NA11: *b410* (slight activity), *gb25*, etc. Also intragenic revertants, e.g., *gb94b410*. Probable structural gene. [[Sebastian et al. 1986](#)] [NA]

#### ***gut***

***gut*** differentiation abnormal [EH].

#### ***gut-2* V 5.24 *lw6***

: **E** cells fail to gastrulate, division rate does not slow; mutant [EMS](#) not responsive to wt P<sub>2</sub> induction; *lw6/Df* similar. OA>10: *it92*, *lw63* (Gro, sterile). CLONED: cosmid rescue (T10G8). [EH, CB]

#### ***gut-4* IV 3.0 *lw4***

: Mel, no gastrulation; arrests as ball of cells without gut or [pharyngeal muscle](#) differentiation. [EH]

#### ***ham***

**H** SN **a** bnormal **m** igration [MT].

#### ***ham-1* IV 6.05 *n1438***

: multiple HSN defects, Egl, Dif; HSN and sister phasmid [neuron](#) PHB both abnormal; also disrupted asymmetry in other sister cells [RID](#), [ADE/ADA](#), ADL, ALN/[PLM](#). OA1: *n1810*. CLONED: 1.8-kb RNA, encodes 414-aa novel protein. [[Desai et al. 1988](#); [Garriga and Stern 1994](#)] [NG, NH, MT]

#### ***ham-2* X N *n1332***

: multiple HSN defects, abnormal HSN migration, reduced serotonin; Egl. [[Desai et al. 1988](#); [Garriga and Stern 1994](#)] [NG, NH, MT]

#### ***ham-3* III N *n1654***

: multiple HSN defects, abnormal HSN migration, reduced serotonin; Egl; other impenetrant Mig defects. [[Desai et al. 1988](#); [Garriga and Stern 1994](#)] [NG, NH, MT]

#### ***hcd***

**h** ermaphrodite **c** opulation **d** efective [PS].

#### ***hcd-1* II N *sy417***

: hermaphrodites fail to stimulate sperm transfer from males. [PS]

#### ***hcd-2* III N *sy418***

: hermaphrodites fail to stimulate sperm transfer from males. [PS]

#### ***hch***

**h** at **ch** ing abnormality [CB].

#### ***hch-1* X N *e1734***

: delayed hatching from eggshell rescued by protease or wt hatching fluid; [QL](#) and descendant cells migrate forward instead of backward. ES1. OA1: *e1907* (same phenotypes). [[Hedgecock et al. 1987](#); [Hishida et al. 1996](#)] [NJ]

#### ***her***

**her** maphroditization [CB].

#### ***her-1* V 2.11 *e1518***

: XX animals wt, XO animals transformed into fertile hermaphrodites. ES3 (XO). Similar phenotype in *e1518/Df*. OA>20: *e1520*, *e1561ts* (XO fertile male 15°C, fertile hermaphrodite 25°C), *q428ts* (very weak Her), etc. Also gf alleles: *n695sd,ts* (XO animals wt, XX animals partly masculinized Egl hermaphrodites; *n695/+* XX animals slightly masculinized), *y101* (stronger masculinization, still incomplete). Intragenic revertants are recessive Her-1 alleles: *n695n826*, *y1hv101* (viable deletion), etc. ES2 (XX) NA1. Intragenic revertants have class-1 phenotype. CLONED: 0.8- and 1.2-kb transcripts, XO-specific; 1.2-kb transcript necessary and sufficient; encodes 175-aa predicted cysteine-rich novel protein with signal sequence.

[[Hodgkin 1980](#); [Perry et al. 1993, 1994](#)] [NT, PA]

## ***her-2***

= *tra-1*

## ***him***

***h***igh ***i***ncidence of ***m***ales [CB].

### ***him-1 I – 0.24 e879***

: sd; self-progeny 21% XO male, 5% 3X hermaphrodite; 8% nullo-X ova as a result of reductional meiotic nondisjunction; X chromosome recombination specifically reduced 40% or more, except at left end (recombination increased); Rad; *e879/+* self-progeny 1% XO. ES3 (progeny) ME2 NA1. [[Hodgkin et al. 1979](#); [Broverman and Meneely 1994](#)]

### ***him-2 I 6.98 e1065***

: self-progeny 2% XO male; 1.5% nullo-X ova; some associated sterility. ES2 (progeny) ME3 NA1. [[Hodgkin et al. 1979](#)]

### ***him-3 IV 1.97 e1147***

: self-progeny 3.5% XO male, 2% nullo-X ova. ES2 (progeny) ME3. OA1: *e1256* (stronger allele, 11% Him, many unhatched eggs [71%]; males sire inviable zygotes; probably generalized meiotic nondisjunction; some reduction in autosomal recombination, effects on segregation of free duplications). [[Hodgkin et al. 1979](#)] [KR]

### ***him-4 X 1.57 e1267***

: icr; self-progeny 6% XO male, very low brood size; frequent gonad eversion with rupture at [vulva](#); 2% nullo-X ova; [male gonad](#) abnormal, [testis](#) fails to connect with [proctodeum](#), may be twice reflexed; Mua (muscle attachment) phenotype, general defects in transhypodermal anchorage. ES2 (adult) ME0. OA2: *e1266icr* (same phenotypes), *rh166*. [[Hodgkin et al. 1979](#)] [NJ]

### ***him-5 V 5.83 e1467***

: ts; at 20°C, self-progeny 16% XO male, 3% 3X hermaphrodite, 11% nullo-X ova as a result of reductional meiotic nondisjunction; X chromosome recombination specifically reduced 50% or more, except at left end (increased); additional sterility not due to autosomal nondisjunction (brood reduced 64% at 25°C); some embryonic lethality. ES3 (progeny) ME3. OA4: *e1490* (stronger allele: 33% Him at 20°C). CLONED: cosmid rescue K02A12. [[Hodgkin et al. 1979](#); [Broverman and Meneely 1994](#)] [FH]

### ***him-6 IV 6.25 e1423***

: self-progeny 15% XO male, 6% 3X hermaphrodite, low brood size (78% unhatched eggs), 8% nullo-X ova as a result of reductional meiotic nondisjunction; autosomal nondisjunction; males sire inviable zygotes. ES3 (progeny) ME3. OA1: *e1104* (weaker allele: 5% Him). [[Hodgkin et al. 1979](#); [Haack and Hodgkin 1991](#)] [KR]

### ***him-7 V – 5.02 e1480***

: self-progeny 3% XO male, 0.6% nullo-X ova; males make slight excess of nullo-X sperm, sire some inviable zygotes. ES2 (progeny) ME3 NA1. [[Hodgkin et al. 1979](#)]

#### ***him-8 IV 4.69 e1489***

: self-progeny 37% XO male, 6% 3X hermaphrodite, 38% nullo-X ova as a result of reductional meiotic nondisjunction; X chromosome recombination specifically reduced 90% except at left end (increased). ES3 (progeny) ME2. OA6: *mn253*, *ec51*, etc. (all >30% Him). CLONED: cosmid rescue T19G9 [[Hodgkin et al. 1979](#); [Broverman and Meneely 1994](#)] [SP, FH]

#### ***him-9 II 4.84 e1487***

: aci; self-progeny 5% males, 2% nullo-X ova. ES3 (progeny) ME3 NA1. [[Hodgkin et al. 1979](#)]

#### ***him-10 III – 1.69 e1511***

: ts; self-progeny 2% XO male (15°C), 12% male (20°C), 27% male (25°C), low brood size, many unhatched eggs at 25°C; probably some chromosome loss in premeiotic germ line: abnormal mitotic cytology, jackpots in male production. ES3 (progeny 25°C) ME3 (20°C) NA1. [[Hartman and Herman 1982](#)] [AV]

#### ***him-11 III N n318***

: self-progeny 5% XO male. ES3 (progeny) NA1. [CB]

#### ***him-12***

= *emb-26*

#### ***him-13 I N e1742***

: self-progeny 5% XO male. ES3 (progeny) NA1. [CB]

#### ***him-14 II 0.54 it44***

: ts; viable self-progeny 2–40% male, 95% dead eggs, probable generalized nondisjunction, meiotic defect. OA4: *it13*, *it21*, *it23*, *it52* (strongest allele, <3% eggs hatch). [[Kemphues et al. 1988a](#)]

#### ***him-15 III 0.32***

No point mutations; several small deletions of [\*unc-86\*](#) (such as *eDf25*, pka *e1416*) exhibit additional weak Him phenotype (2% XO males) due to deletion of adjacent *him-15*. [[Hodgkin et al. 1979](#); [Finney et al. 1988](#)] [MT]

#### ***his***

***his*** tone structural genes [EM]. Core histone genes are organized in ~11 genomic clusters, each containing at least one of H2A, H2B, H3, H4 genes.

#### ***his-1 V 9.19***

NMK. Histone-type H4, HIS1 cluster. [[Roberts et al. 1989](#)] [EM]

#### ***his-2 V 9.19***

NMK. Histone-type H3, HIS1 cluster. [[Roberts et al. 1989](#)] [EM]

#### ***his-3 V 9.19***

NMK. Histone-type H2A, HIS1 cluster. [[Roberts et al. 1989](#)] [EM]

#### ***his-4 V 9.19***

NMK. Histone-type H2B, HIS1 cluster. [[Roberts et al. 1989](#)] [EM]

#### ***his-5 V 1.60***

NMK. Histone-type H4, HIS2 cluster. [EM]

***his-6* V 1.60**

NMK. Histone-type H3, HIS2 cluster. [EM]

***his-7* V 1.60**

NMK. Histone-type H2A, HIS2 cluster. [EM]

***his-8* V 1.60**

NMK. Histone-type H2B, HIS2 cluster. [EM]

***his-9* II 16.04**

NMK. Histone-type H3, HIS3 cluster. [[Roberts et al. 1989](#)] [EM]

***his-10* II 16.04**

NMK. Histone-type H4, HIS3 cluster. [[Roberts et al. 1989](#)] [EM]

***his-11* II 16.04**

NMK. Histone-type H2B, HIS3 cluster. [[Roberts et al. 1989](#)] [EM]

***his-12* II 16.04**

NMK. Histone-type H2A, HIS3 cluster. [[Roberts et al. 1989](#)] [EM]

***his-13* II 16.04**

NMK. Histone-type H3, HIS3 cluster. [[Roberts et al. 1989](#)] [EM]

***his-14* II 16.04**

NMK. Histone-type H4, HIS3 cluster. [[Roberts et al. 1989](#)] [EM]

***his-15* II 16.04**

NMK. Histone-type H2B, HIS3 cluster. [[Roberts et al. 1989](#)] [EM]

***his-16* II 16.04**

NMK. Histone-type H2A, HIS3 cluster. [[Roberts et al. 1989](#)] [EM]

***his-17* V 1.71**

NMK. Histone-type H3, HIS4 cluster. [EM]

***his-18* V 1.71**

NMK. Histone-type H4, HIS4 cluster. [EM]

***his-19* V 1.71**

NMK. Histone-type H2A, HIS4 cluster. [EM]

***his-20* V 1.71**

NMK. Histone-type H2B, HIS4 cluster. [EM]

***his-21* V 1.71**

NMK. Histone-type H2A, HIS4 cluster. [EM]

***his-22* V 1.71**

NMK. Histone-type H2B, HIS4 cluster. [EM]

***his-23* V 1.60**

NMK. Histone-type H2B. [EM]

### **his-24 X 17.00**

NMK. Histone-type H1; contains intron, encodes polyadenylated RNA. [[Sanicola et al. 1990](#)]

### **hlh**

**h** elix- **I** oop- **h** elix transcription factor family [PD].

### **hlh-1 II – 4.52 cc450**

: amb; recessive-lethal, arrest at varying stages as lumpy dumpy with some muscle differentiation, disorganized myofilaments; encodes member of MyoD family; transcripts present transiently in **MS** descendants, stably in **D** daughters and **C** and **MS** lineages leading to **body wall muscle**; antibody staining similar (nuclear staining, persists through development of **body wall muscle** cells). [[Krause et al. 1990, 1994](#), [Chen et al. 1992](#)] [KM, PD]

### **hlh-2 I 1.83**

NMK. Encodes homolog of vertebrate E12, *Drosophila* Daughterless; *lacZ* fusion indicates transcription in some [neuronal precursors](#); antibody staining indicates all blastomere nuclei stain up to 200-cell stage, later expression complex, strong in head, ventral cord, and tail at comma stage; fewer than 20 cells stain at hatching. Cosmid K07G5. [KM]

### **hmp**

**h** u **mp** back (dorsal lumps) [JJ].

### **hmp-1 V 3.44**

Mutations zygotic-lethal, arrest at 1.25–1.5-fold stage with lumps in dorsal hypoderm. CLONED: encodes probable  $\alpha$ -catenin homolog. [JJ]

### **hsp**

**h** eat **s** hock **p** rotein family [BC].

### **hsp-1 IV 18.36**

NMK. Encodes protein related to generic *hsp70*; quite strong expression normally, only weak heat shock induction. [[Heschl and Baillie 1990](#)] [BC]

### **hsp-2 X – 12.84**

NMK. Pseudogene derived from [hsp-1](#). [[Heschl and Baillie 1990](#)] [BC]

### **hsp-3 X – 3.40**

NMK. Encodes protein related to mammalian *grp78/BiP*; not heat-shock-induced. [[Heschl and Baillie 1990](#)] [BC]

### **hsp-4 ?**

NMK. Encodes protein related to mammalian *grp78/BiP*; strongly induced by heat shock. [[Heschl and Baillie 1990](#)] [BC]

### **hsp-5 ?**

NMK. Probable pseudogene. [BC]

### **hsp-6 ?**

NMK. Encodes protein related to generic *hsp70*, mitochondrial import sequence, bacterial dnaK similarity; strongly induced by heat shock. [[Heschl and Baillie 1990](#)] [BC]

### **hsp-16A V 1.85**

NMK. Two divergently transcribed genes *hsp16-1*, *hsp16-48*, encoding 16-kD heat shock proteins (<70% identity); HSP16-1 145 aa, 92% identity to HSP16-2 and HSP16-48 143 aa, 94% identity to HSP16-41; expression depends on heat shock; transgene *lacZ* fusions expressed in many tissues (not germ line) after heat shock, strongest in muscle and [hypodermis](#). [[Russnak et al. 1985](#); [Stringham et al. 1992b](#)] [PC]

### ***hsp-16B* ?**

NMK. Two divergently transcribed genes *hsp16-2*, *hsp16-41*, encoding 16-kD heat shock proteins (<70% identity); HSP16-2 145 aa, 92% identity to HSP16-1 and HSP16-41 143 aa, 94% identity to HSP16-48; expression depends on heat shock; transgene *lacZ* fusions expressed in many tissues (not germ line) after heat shock, strongest in [intestine](#) and pharyngeal tissue; not located on physical map. [[Russnak et al. 1985](#); [Stringham et al. 1992](#)] [PC]

### ***hum***

***h*** eavy chain, ***u*** nconventional ***m*** yosin [DU].

### ***hum-1 I 3.15***

NMK. Encodes predicted unconventional myosin heavy chain, class I. [DU]

### ***hum-2 V 1.98***

NMK. Encodes predicted unconventional myosin heavy chain, class V. [DU]

### ***hum-3* ?**

NMK. Encodes predicted unconventional myosin heavy chain, class VI. [DU]

### ***hum-4 X 3.33***

NMK. Encodes predicted unconventional myosin, novel, probably class XII. [DU]

### ***hum-5 III – 4.38***

NMK. Encodes predicted 1017-aa unconventional myosin heavy chain, class I. (T02C12.1) [CB, CGC]

### ***inf***

***in*** itiation ***f*** actor for protein synthesis [CGC].

### ***inf-1 III – 0.82***

NMK. 1.7-kb RNA, encodes DEAD box RNA helicase, probable homolog of eukaryotic initiation factor 4A (71% identity to mouse eIF-4A). [[Roussell and Bennett 1992](#); [Seydoux and Fire 1994](#)] [KB]

### ***isx***

See *fem*.

### ***itr***

***i*** nositol ***t*** riphosphate ***r*** eceptor-related [CGC].

### ***itr-1 IV 3.5***

NMK. Sequence (yk33g8) has similarity to receptor for inositol 1,4,5-trisphosphate from vertebrates and *Drosophila*. [LM, CGC]

### ***kin***

protein ***kin*** ase [CGC]. See also *ksr*, *pkc*.

### ***kin-1 I 28.97***

NMK. 2.5-kb transcripts (alternatively spliced); encodes 358-aa catalytic (C $\alpha$ ) subunit of cAMP-dependent protein kinase (82% identity to murine C $\alpha$  subunit) and variant (C $\alpha'$ ) 374-aa subunit, different 56-aa at C-

terminal; SL1 *trans*-spliced. [[Gross et al. 1990](#)] [CR]

***kin-2 X – 3.72***

NMK. Encodes regulatory subunit of cAMP-dependent protein kinase (clone CR#LRI1). [CR]

***kin-3 ?***

NMK. Encodes casein kinase II $\alpha$ ; not located on physical map (clone CR#G1, Y42G4, Y52D1). [CR]

***kin-4 IV 5.07***

NMK. Encodes two protein kinase L isoforms: PKL1 (1528 aa, ST kinase, low in embryos, increases 5-fold on hatching) and PKL2 (1377 aa, different C-terminal, maximal in embryos, absent in L1). [CR]

***kin-5 IV 4.58***

NMK. Encodes predicted tyrosine kinase; transcript not detected. [FK]

***kin-6 II 3.78***

NMK. Encodes predicted tyrosine kinase; transcript not detected. [FK]

***kin-7***

= *let-23*

***kin-8 II 1.16***

NMK. Encodes transmembrane kinase of *trk*/NGFR class; contains Kringle domain. [FK]

***kin-9 X – 0.58***

NMK. Encodes predicted tyrosine kinase. [FK]

***kin-10 I 2.55***

NMK. Encodes predicted protein with similarity to casein kinase II  $\beta$ . CR#CKB1. In operon with [\*kup-2\*](#). [[Hu and Rubin 1991](#)] [CR]

***kin-11 X 0.76***

NMK. Encodes two isoforms of protein kinase C2 (PKC2A and PKC2B). Clone CR#PKC2A, cosmid E01H11. [CR]

***kin-13 VN***

NMK. Encodes kinases related to protein kinase C (PKC1A and PKC1B); transcript from proximal promoter encodes 707-aa PKC1B; antibody stains cell bodies and processes of ~75 [sensory neurons](#); transcription from distal promoter yields [\*kup-1\*](#), PKC1A (SL2 *trans*-spliced, 763 aa, additional 56 aa at N-terminal of PKC1B); B:A ratio ~40 in early development, unity in adults. [[Land et al. 1994a,b](#)] [CR]

***kin-14 I 1.75***

NMK. Encodes predicted tyrosine kinase, similarity to *v-ros*. [FK]

***kin-15 II 1.34***

Tc1 insertion: retarded development? Encodes predicted tyrosine kinase with transmembrane domain, no large extracellular domain; related to *kin-16*. [[Morgan and Greenwald 1993](#)] [WR]

***kin-16 II 1.34***

Tc1 insertion: retarded development? Encodes predicted tyrosine kinase with transmembrane domain, no large extracellular domain; related to *kin-15*. [[Morgan and Greenwald 1993](#)] [WR]

***kin-17 X – 1.86***

NMK. Encodes predicted protein kinase. [FK]

### ***kin-18* III – 1.13**

NMK. Encodes 982-aa predicted protein; residues 1–300 have similarity to Ser/Thr kinases. [CB, CGC]

### ***kra***

***k***etamine ***r***esponse ***a***nnormal [HK].

### ***kra-1* V 0.51 *kh30***

: semidominant convulsive behavior in 30 mM ketamine or other NMDA antagonists; recessive cs Unc; variable motility; weakly resistant to cholinergic agonists, ouabain; normal muscle morphology. [HK]

### ***ksr***

***k***inase ***s*** uppressor of activated ***r***as [MH].

### ***ksr-1* X – 0.61 *n2526***

: pka [\*sar-2\*](#); suppresses activated *ras*, *let-60(n1046gf)*; low penetrance larval lethality (rod-like L1 arrest, 10%); 4% abnormal vulval development; synergistic effects with *lin-45*, *mpk-1* mutations, etc.; nonsense mutation, probable null allele. OA>10: *ku68*, *ku83* (pka [\*sur-3\*](#)), *n1860*, *n2682* (similar phenotypes, impenetrant Let, Egl, Mig), *ku113*, *n2519*, *n2509*, etc. (weaker, <1% larval lethality). CLONED: 2.3-kb and rarer 2.65-kb transcripts; encodes 771-aa predicted protein with similarity to both Tyr and Ser/Thr kinases. [[Sundaram and Han 1995](#); [Kornfeld et al. 1995b](#)] [MT, MH]

### ***kup***

***k***inase ***up*** stream genes [BL]. Genes in operons with kinase genes.

### ***kup-1* V N**

NMK. Upstream in operon with [\*kin-13\*](#); encodes predicted 385-aa novel protein; antibody stains nuclei of most cells. [[Zorio et al. 1994](#)] [CR]

### ***kup-2* I 2.55**

NMK. Upstream gene in operon with [\*kin-10\*](#). [[Zorio et al. 1994](#)]

## L

### ***lag***

***l***in-12 ***a***nd ***g***lp-1 phenotype [JK].

### ***lag-1* IV 2.90 *q385***

: larval arrest at L1, characteristic Lag (Lin-12 and Glp-1) phenotype: [\*rectum/anus\*](#) and [\*excretory\*](#) cell absent (98%), sometimes twisted nose (12%). OA>10 (other alleles mostly weaker): *q416* (sometimes viable and fertile at 20°C), *q426* (low larval lethality), *om13* (viable, impenetrant embryonic and larval lethality; strong Ego, enhances *glp-1[bn18ts]*), *om27* (viable, Ego), *om108* (viable, Ego), etc. CLONED: 2.6-kb transcript, encodes protein with high similarity to *Drosophila* Suppressor of hairless. [[Lambie and Kimble 1991](#); [Christensen et al. 1996](#)] [JK]

### ***lag-2* V – 10.37 *q387***

: larval arrest at L1, characteristic Lag (Lin-12 and Glp-1) phenotype: [\*rectum/anus\*](#) absent, [\*excretory\*](#) cell absent, often twisted nose (76%); similar phenotype in *q387/Df. NA>6*: *q420* (weaker allele), *s1486* (pka [\*let-461\*](#)), *ut103*, *ut105* (both Clr). Also gf alleles: *n1255*, *sa37* (pka [\*sel-3\*](#), partly suppresses *lin-12[gf]* mutations). CLONED: encodes 400-aa membrane protein with similarity to *Drosophila* Delta and Serrate; transcript present in DTC. [[Johnsen and Baillie 1991](#); [Tax et al. 1994](#); [Henderson et al. 1994](#)] [MT, JC]

### ***lag-3* V N**

Mutation leads to larval arrest, Lag phenotype. NA1. [JK]

### **lam**

**lam** inin-related [NJ].

### **lam-1 IV 1.40 rh219**

: resembles Epi-1, basal lamina missing or defective in epidermis, gonad, [intestine](#); abnormal [excretory](#) canals, muscle cell positions, sheath cells, proximal gonad, basement membranes, ray morphology; *rh219/Df* is larval-lethal. CLONED: rescued by cosmid C24D10; encodes laminin β-chain. [NJ]

### **lan**

See *ric*.

### [\*\*lan-2\*\*](#)

= *unc-18*

### [\*\*lan-5\*\*](#)

= *ric-1*

### **lep**

**lep** toderan [male tail](#) [DF].

### **lep-1 I 3.77 bx37**

: sd; [male tail](#) tip is pointy and protrudes beyond the posterior edge of the fan, 100% penetrant; no hermaphrodite phenotype. OA1: *bx42sd* (92% penetrant). [DF]

### **lep-2 ? bx73**

: male tail tip protrudes beyond posterior edge of fan, failure of tail tip syncytium retraction. NA1. [DF]

### **let**

**let** hal [SP, KR]. See also *gon*, *lin*, *mel*, *stu*, etc.

### **let-1 X 19.78 mn119**

: early larval-lethal. OA5: *mn124*, *mn102* (late larval-lethal), *mn115* (hermaphrodite sterile, lays fertilized eggs, male sterile), etc. [[Meneely and Herman 1981](#)] [SP]

### **let-2 X 23.78 mn153**

: amb; embryonic-lethal. OA>15: (many ts; complex interallelic complementation pattern), *mn114ts* (*pka let-8*), *b246ts*, *e1470ts*, *g30ts* (inviable at 20°C), *b246ts* (viable at 20°C), *q37ts* (Mig, Q daughters affected), *st550* (embryonic-lethal, late paralysis, elongation arrest at 2-fold), etc. High forward mutation frequency. See also [sup-20](#). CLONED: encodes 1795-aa type IV (basement membrane) collagen, α2 chain (*pka clb-1*); alternative splicing [Kramer] either exon 9 (higher in embryo) or 10 (higher in larva, adult). [[Meneely and Herman 1981](#); [Sibley et al. 1993](#)] [CF, CH, MT, RW, SP]

### **let-3 X 22.44 mn104**

: amb; early larval-lethal, incompletely suppressible by [sup-5](#). NA1. [[Meneely and Herman 1981](#)] [SP]

### **let-4 X 17.42 mn105**

: amb; early larval-lethal; cystic [excretory](#) canals. NA1. [[Meneely and Herman 1981](#)] [NJ, SP]

### **let-5 X 17.54 mn106**

: amb, mat, mnz; progeny grow slowly, fail to reach adulthood. OA1: *mn132* (similar). [[Meneely and Herman 1981](#)] [SP]

***let-6 X 24.13 mn130***

: early larval-lethal. OA3: *mn108*, etc. [[Meneely and Herman 1981](#)] [SP]

***let-7 X 18.63 mn112***

: late larval-lethal, XX animals die at early L3, XO die at late L4. OA1: *mn107* (sterile). [[Meneely and Herman 1981](#)] [SP]

**let-8**

= *let-2*

***let-9 X 17.64 mn107***

: sterile; defective sperm. NA1. [[Meneely and Herman 1981](#)] [SP]

***let-10 X 22.44 mn113***

: early larval-lethal. OA1: *mn118*. [[Meneely and Herman 1981](#)] [SP]

***let-11 X 22.41 mn116***

: early larval-lethal. NA1. [[Meneely and Herman 1981](#)] [SP]

***let-12 X 20.65 mn121***

: amb; early larval-lethal. OA1: *mn125* (pka *let-17*, similar). [[Meneely and Herman 1981](#)] [SP]

***let-13 I 19.00 e1188***

: lethal. NA1. [DR]

***let-14 X 22.46 mn120***

: early larval-lethal. NA1. [[Meneely and Herman 1981](#)] [SP]

***let-15 X 21.82 mn127***

: amb; early larval-lethal. OA2: *mn123, e1471*. [[Meneely and Herman 1981](#)] [SP]

***let-16 X 23.49 mn117***

: early larval-lethal. NA1. [[Meneely and Herman 1981](#)] [SP]

**let-17**

= *let-12*

***let-18 X 21.82 mn122***

: amb; embryonic-lethal, incompletely suppressible by *sup-5*. OA2: *mn142, mn136* (late larval-lethal). [[Meneely and Herman 1981](#)] [SP]

***let-19 II 0.81 mn19***

: larval-lethal. NA1. [[Sigurdson et al. 1984](#)] [SP]

**let-20**

= *mnDf71*

***let-21 II 3.68 e1778***

: sterile uncoordinated polynucleate oocytes; abnormal positioning of germ-line nuclei. NA1. [NJ]

***let-22 II - 0.24 mn22***

: embryonic-lethal. NA1. [[Sigurdson et al. 1984](#)] [SP]

***let-23* II 1.03 *mn23***

: early larval-lethal. OA>15: *sy15* (rod-like early larval-lethal, probable null), *sy5* (similar to *sy15*, W1078op), *mn224* (early larval-lethal, non-null), *n1045* (homozygous viable, Vul at 15°C, weak Muv [hyperinduced] at 25°C; [P12](#) transformed to [P11](#) fate), *sy1* (viable, Vul, Q1318och), *sy97* (viable, Vul, ME0, abnormal spicules), *sy10* (impenetrant larval-lethal, survivors sterile, Emo, abnormal oocytes), etc. Alleles affect subset or all of five phenotypes (L1 viability, vulval induction, male spicules, oogenesis, [P12](#)). Also gf allele *sa62sd* (scrawny Muv, *sa62/+* variable Muv, 5–50%). CLONED: 4.9-kb transcript, encodes 1323-aa EGF-receptor-class tyrosine kinase (*pka kin-7*); *let-23:lacZ* expressed in many but not [all cells](#); extensive molecular and developmental analysis. See also *lfe*, *sli*, etc. [[Sigurdson et al. 1984](#); [Aroian et al. 1990](#); [Aroian and Sternberg 1991](#); [Aroian et al. 1994](#); [Koga and Ohshima 1995](#)] [FK, SP]

***let-24* II 0.69 *mn24***

: early larval-lethal. NA1. [[Sigurdson et al. 1984](#)] [SP]

***let-25* II 2.69 *mn25***

: early larval-lethal. NA1. [[Sigurdson et al. 1984](#)] [SP]

***let-26* II 4.14 *mn26***

: early larval-lethal. NA1. [[Sigurdson et al. 1984](#)] [SP]

***let-27* II N *mn27***

: early larval-lethal. NA1. [[Sigurdson et al. 1984](#)] [SP]

***let-28* II N *mn28***

: embryonic-lethal. OA1: *mn212*. [[Sigurdson et al. 1984](#)] [SP]

***let-29* II 2.99 *mn29***

: late larval-lethal. OA2: *b285* (Mel), *mn182*. [[Sigurdson et al. 1984](#); [Kemphues et al. 1988a](#)]

***let-30* II – 1.10 *mn30***

: embryonic-lethal. OA1: *mn239*. [[Sigurdson et al. 1984](#)] [SP]

***let-31* II 1.45 *mn31***

: embryonic-lethal. OA1: *mn223*. [[Meneely and Herman 1981](#)] [SP]

***let-32* II N *mn32***

: embryonic-lethal. NA1. [[Meneely and Herman 1981](#)] [SP]

***let-33* X 22.97 *mn128***

: mat, mm; Mel, homozygotes lay fertilized eggs that do not hatch; no male rescue but males fertile; *mn128/Df* sterile. NA1. [[Meneely and Herman 1981](#)] [SP]

***let-34* X 20.50 *mn134***

: early larval-lethal. NA1. [[Meneely and Herman 1981](#)] [SP]

***let-35* X 22.43 *mn135***

: early larval-lethal. NA1. [[Meneely and Herman 1981](#)] [SP]

***let-36* X 21.23 *mn140***

: slow growth, late larval-lethal or adult producing inviable progeny; rescued by mating; *mn140/Df* early larval-lethal. NA1. [[Meneely and Herman 1981](#)] [SP]

***let-37* X 22.97 *mn138***

: early larval-lethal. NA1. [[Meneely and Herman 1981](#)] [SP]

**let-38 X 21.82 mn141**

: mat, mnz; Mel, homozygotes lay fertilized eggs that do not hatch, males fertile; *mn141/Df* sterile. NA1. [[Meneely and Herman 1981](#)] [SP]

**let-39 X 21.23 mn144**

: amb; early larval-lethal, incompletely suppressible by *sup-5*. NA1. [[Meneely and Herman 1981](#)] [SP]

**let-40 X 21.82 mn150**

: ts; early larval-lethal at 25°C, dumpyish sterile with abnormal gonads at 20°C; males fertile; *mn150/Df* early larval-lethal at 20°C. NA1. [[Meneely and Herman 1981](#)] [SP]

**let-41 X 22.97 mn146**

: amb; early larval-lethal, incompletely suppressible by *sup-5*. NA1. [[Meneely and Herman 1981](#)] [SP]

**let-42 III 1.48 g38**

: leaky maternal-effect-lethal phenotype at 25°C; animals developing to adulthood sterile, frequently Evl. OA1: *oz36* (similar phenotype at 25°C; also impenetrant late-onset tumorous germ-line phenotype, strongest at 15°C; *oz36* males exhibit some tumorous germ lines, some oogenesis, and yolk synthesis). [RC, BS]

**let-43 X – 8.46 mg49**

: larval-lethal [GR, DG]

**let-44 X – 7.93 mg41**

: embryonic-lethal [GR, DG]

**let-45 I 13.60 h1292**

: lethal. NA1. [KR]

**let-46 I 13.60 h1297**

: lethal. OA3: *h1330*, *h1337*, *h1359*. [KR]

**let-47 I 13.59 h1319**

: lethal. NA1. [KR]

**let-48 I 13.60 h1320**

: lethal. NA1. [KR]

**let-49 I 27.17 st44**

: mid larval-lethal. NA1. [[Anderson and Brenner 1984](#)] [RW]

**let-50 I 27.46 st33**

: early larval-lethal. NA1. [[Anderson and Brenner 1984](#)] [RW]

**let-51 IV 4.63 s41**

: embryonic-lethal, cystic [excretory](#) canals. NA1. [[Rogalski et al. 1982](#)] [BC, NJ]

**let-52 IV 5.52 s42**

: early larval-lethal. OA2: *s2346* (homozygote and hemizygote arrest at L2), *s2381* (L3 arrest, *s2381/Df* L2 arrest). CLONED: cosmid rescue (T12G3). [[Clark et al. 1988](#)] [BC]

**let-53 IV 4.55 s43**

: late larval-lethal. NA1. [[Rogalski et al. 1982](#)] [BC]

***let-54 IV 4.06 s44***

: early larval-lethal (L1–L2 molt). OA1: s53 (similar). [[Rogalski et al. 1982](#)] [BC]

***let-55 IV 4.61 s45***

: early larval-lethal. NA1. [[Rogalski et al. 1982](#)] [BC]

***let-56 IV 5.42 s173***

: slow development, eventually reaches sterile adult stage after 7 days; s173/Df slower development initially, still reaches sterile adult stage. OA>10: s46 (late larval-lethal, hemizygote mid larval-lethal), s50, s168 (late larval-lethals), s1210, s1223, s1262 (homozygotes and hemizygotes mid larval-lethal), s173 (homozygote and hemizygote arrest as sterile adults), s2217, s2230, s2321 (resemble s173). CLONED: cosmid rescue, C11F2. [[Clark et al. 1988](#); [Clark and Baillie 1992](#)] [BC]

***let-57 IV R s47***

: sterile adult, not rescued by mating. [[Rogalski et al. 1982](#)] [BC]

***let-58 IV N s48***

: (lost) embryonic- or early larval-lethal. [[Rogalski et al. 1982](#)] [BC]

***let-59 IV 4.89 s49***

: early larval-lethal; hemizygote embryonic/early larval-lethal. OA5: s175 (pka [let-62](#), embryonic-lethal), s681, s1087, s1174, s1197. [[Rogalski and Baillie 1985](#); [Clark et al. 1988](#)] [BC]

***let-60 IV 5.17 s59***

: mid larval-lethal (leaky, escapers non-Vul). OA>10 (recessive): s1124 (strongest allele, both homozygote and hemizygote arrest as rod-like early larva; rare escapers die as Vul adult), s2336 (homozygote L3 arrest, hemizygote L2 arrest), s1155, n2021 (viable, 14% Vul), etc. Weak If mutations have mating defects. Also dominant negative alleles, OA8: sy93dm (dominant Vul, viable), sy99 (dominant Vul, recessive-lethal), sy92 (weaker dominant, recessive-lethal), etc. Also gf alleles, OA>5: n1046sd,amb (pka [lin-34](#), non-null; adult hermaphrodite Muv [penetrance 57%], normal [vulva](#) with one to three large additional protrusions; n1046/+ 17% Muv. ES2. Male gross morphology wt, ME1), n1700, sy130 (all identical to n1046), ga89ts (at 25°C, 57% Muv, near-sterile, ME0). CLONED: encodes 143-aa Ras protein; *let-60:lacZ* fusion indicates complex developmental expression, multiple functions; extensive molecular and developmental analysis. [[Rogalski et al. 1982](#); [Han and Sternberg 1990, 1991](#); [Beitel et al. 1990](#)] [BC, MH, MT, PS, SD]

***let-61 IV 4.63 s65***

: late larval-lethal; s65/Df similar. NA1. [[Clark et al. 1988](#)] [BC]

***let-62***

= *let-59*

***let-63 IV 4.69 s170***

: mid larval-lethal; s170/Df similar. OA2: s679 (late larval-lethal), s1766. [[Clark et al. 1988](#)] [BC]

***let-64 IV 4.85 s216***

: thin sterile adult progeny; not rescued by wt sperm. OA3: s171 (leaky sterile adult), s697 (pka [let-74](#), late larval-lethal, s697/Df similar), s1746. [[Clark et al. 1988](#)] [BC]

***let-65 IV 5.12 s254***

: nonconditional constitutive formation of abnormal dauer-like larvae; forms true dauers in pheromone, dauers recover to arrested state. NA11: s174, s694, s1084, s1154, s1222, s1730, s1777, m644, m650 (all

resemble *s254*), *s694* (sterile adult), *s1083* (homozygote is mid larval-lethal, hemizygote is sterile adult). [Clark et al. 1988] [BC, DR]

***let-66 IV 5.71 s176***

: early larval-lethal; *s176/Df* mid larval-lethal. OA1: *s1739* (homozygote and hemizygote both early larval-lethal). [Clark et al. 1988] [BC]

***let-67 IV 5.71 s214***

: sterile adult, rescued by wt sperm; *s214/Df* mid larval-lethal. NA1. [Clark et al. 1988] [BC]

***let-68 IV 5.77 s1258***

: early larval-lethal; *s1258/Df* similar. OA4: *s1081* (early larval-lethal), *s693*, *s696*, *s698* (some alleles arrest at sterile adult stage). [Clark et al. 1988] [BC]

***let-69 IV 4.63 s684***

: late larval-lethal. OA3: *s1111*, *s172* (both early larval-lethal, *s1111/Df* embryonic- or early larval-lethal). [Clark et al. 1988] [BC]

***let-70 IV 4.85 s689***

: mid larval-lethal. OA1: *s1132* (early larval-lethal, *s1132/Df* mid larval-lethal). [Clark et al. 1988] [BC]

***let-71 IV 4.69 s692***

: leaky sterile adult; *s692/Df* is similar. NA1. [Clark et al. 1988] [BC]

***let-72 IV 4.69 s52***

: late larval-lethal. OA1: *s695* (mid larval-lethal, *s695/Df* similar). [Clark et al. 1988] [BC]

***let-73 IV 4.85 s685***

: sterile adult; *s685/Df* similar. OA1: *s1747* (sterile adult, hemizygote similar). [Clark et al. 1988; Clark and Baillie 1992] [BC]

***let-74***

= *let-64*

***let-75 I 1.85 s101***

: early larval-lethal (L1); no pumping, pharyngeal birefringence abnormal; possibly = *myo-1*. OA3: *s107*, *s108*, *s143*. [McKim et al. 1992; Avery 1993a] [DA, KR, RW]

***let-76***

= *unc-37*

***let-77***

= *bli-4*

***let-78 I 1 s82***

: late larval-lethal. NA1. [Rose and Baillie 1980] [KR]

***let-79 I 3 s81***

: L1-lethal. NA1. [Rose and Baillie 1980] [KR]

***let-80 I 2.60 s96***

: L1-lethal. NA1. [Rose and Baillie 1980] [KR]

***let-81 I 2.24 s88***

: L1-lethal. NA1. [[Rose and Baillie 1980](#)] [KR]

***let-82* I 2.23 s85**

: L1-lethal (larva abnormal?). NA1. [[Rose and Baillie 1980](#)] [KR]

***let-83* I 2 s97**

: L1-lethal. NA1. [[Rose and Baillie 1980](#)] [KR]

***let-84* I 2.68 s91**

: late larval-lethal. NA1. [[Rose and Baillie 1980](#)] [KR]

***let-85* I 2.24 s142**

: L1-lethal. NA1. [[McKim et al. 1992](#)] [KR]

***let-86* I 1.56 s141**

: L1-lethal. NA1. [[McKim et al. 1992](#)] [KR]

***let-87* I 2.16 s106**

: semiviable; L1-lethal with *dpy-14(e188)*. OA2: *s87* (L1-lethal), *s139*. [[McKim et al. 1992](#)] [KR]

***let-88* I 2.24 s132**

: L1-lethal. NA1. [[McKim et al. 1992](#)] [KR]

***let-89* I 2.60 s133**

: L1-lethal. NA1. [[McKim et al. 1992](#)] [KR]

***let-90* I 2.24 s140**

: L1-lethal (larva abnormal?). NA1. [[McKim et al. 1992](#)] [KR]

***let-91* IV 5.00 s678**

: mid larval-lethal; *s678/Df* similar. OA2: *s753* (fails to complement *let-651* [*s1185*]), *s1720*. Anomalous complementation: *let-91(s753)/let-651(s1185)* lethal; other combinations viable. [[Clark et al. 1988](#); [Clark and Baillie 1992](#)] [BC]

***let-92* IV 5.32 s504**

: early larval-lethal; *s504/Df* similar. OA3: *s677, s2021* (homozygote and hemizygote arrest as L2), *s2209* (similar). CLONED: partial cosmid rescue B0033. [[Clark et al. 1988](#)] [BC]

***let-93* IV 5.71 s734**

: mid larval-lethal. OA2: *s2254* (homozygote arrests at L2, hemizygote at L1), *s2357* (similar). [[Clark et al. 1988](#)] [BC]

***let-94***

= *lin-3*

***let-95***

= *let-91*

***let-96* IV 4.63 s1112**

: mid larval-lethal; *s1112/Df* similar. OA1: *s1732* (late larval-lethal). [[Clark et al. 1988](#); [Clark and Baillie 1992](#)] [BC]

***let-97* IV 6.11 s1121**

: early larval-lethal; *s1121*/*Df* similar. NA1. [[Clark et al. 1988](#); [Charest et al. 1990](#)] [BC]

***let-98 IV 4.85 s1117***

: late larval-lethal; *s1117*/*Df* similar. NA1. [[Clark et al. 1988](#)] [BC]

***let-99 IV 5.81 s1201***

: Mel; *s1201*/*Df* similar; incorrect spindle orientation in AB and P<sub>1</sub>. OA1. CLONED. [[Clark et al. 1988](#); [Charest et al. 1990](#)] [BC, KK]

***let-100 IV 4.85 s1160***

: early larval-lethal; *s1160*/*Df* embryonic-lethal or early larval-lethal. NA1. [[Clark et al. 1988](#)] [BC]

***let-201 I 23.57 e1716***

: lethal. NA1. [[Anderson and Brenner 1984](#)]

***let-202 I 22.93 e1720***

: lethal. NA1. [[Anderson and Brenner 1984](#)]

***let-203 I 23.57 e1717***

: lethal. NA1. [[Anderson and Brenner 1984](#)]

***let-204 I 23.60 e1719***

: lethal. NA1. [[Anderson and Brenner 1984](#)]

***let-205 I 25.38 e1722***

: lethal. NA1. [[Anderson and Brenner 1984](#)]

***let-206 I 25.45 e1721***

: lethal. NA1. [[Anderson and Brenner 1984](#)]

***let-207 I 25.64 e1723***

: lethal. NA1. [[Anderson and Brenner 1984](#)]

***let-208 I 29.03 e1718***

: lethal. NA1. [[Anderson and Brenner 1984](#)]

***let-209***

= *rnr-1*

***let-236 II 0.23 mn88***

: larval-lethal. NA1. Possible U1 snRNP 70-kD protein? [[Sigurdson et al. 1984](#)] [SP]

***let-237 II 0.78 mn208***

: larval-lethal. OA1: *b283* (Mel, leaky). [[Sigurdson et al. 1984](#); [Kemphues et al. 1988a](#)]

***let-238 II 0.80 mn229***

: larval-lethal. NA1. [[Sigurdson et al. 1984](#)] [SP]

***let-239 II 0.83 mn217***

: embryonic-lethal. OA1: *mn93* (similar). [[Sigurdson et al. 1984](#)] [SP]

***let-240 II 1.24 mn209***

: larval-lethal. NA1. [[Sigurdson et al. 1984](#)] [SP]

***let-241* II 1.59 *mn228***

: larval-lethal. NA1. [[Sigurdson et al. 1984](#)] [SP]

***let-242* II 1.81 *mn90***

: larval-lethal. NA1. [[Sigurdson et al. 1984](#)] [SP]

***let-243* II 2.11 *mn226***

: larval-lethal. NA1. [[Sigurdson et al. 1984](#)] [SP]

***let-244* II 2.11 *mn97***

: embryonic-lethal. NA1. [[Sigurdson et al. 1984](#)] [SP]

***let-245* II 2.39 *mn185***

: embryonic-lethal. OA1: *mn221*. [[Sigurdson et al. 1984](#)] [SP]

***let-246* II 2.98 *mn99***

: embryonic-lethal. NA1. [[Sigurdson et al. 1984](#)] [SP]

***let-247* II 3.19 *mn211***

: larval-lethal. NA1. [[Sigurdson et al. 1984](#)] [SP]

***let-248* II 3.07 *mn237***

: larval-lethal. NA1. [[Sigurdson et al. 1984](#)] [SP]

***let-249* II 3.69 *mn238***

: larval-lethal. NA1. [[Sigurdson et al. 1984](#)] [SP]

***let-250* II 3.69 *mn207***

: larval-lethal. NA1. [[Sigurdson et al. 1984](#)] [SP]

***let-251* II 5.92 *mn95***

: embryonic-lethal. NA1. [[Sigurdson et al. 1984](#)] [SP]

***let-252* II 0.79 *mn100***

: embryonic-lethal. NA1. [[Sigurdson et al. 1984](#)] [SP]

***let-253* II 0.25 *mn181***

: larval-lethal; some embryonic and larval death or very slow growth to Egl adult; severe constipation; most intestinal nuclei fail to divide in L1. OA2: *mn184*, *n2142*. CLONED: cosmid rescue (F31B8). [[Sigurdson et al. 1984](#)] [SP, ML]

***let-254* II N *mn214***

: larval-lethal. NA1. [[Sigurdson et al. 1984](#)] [SP]

***let-255* II N *mn186***

: larval-lethal. OA1: *mn236*. [[Sigurdson et al. 1984](#)] [SP]

***let-256* II N *mn231***

: larval-lethal. NA1. [[Sigurdson et al. 1984](#)] [SP]

***let-257* II 24.00 *mn235***

: larval-lethal. NA1. [[Sigurdson et al. 1984](#)] [SP]

***let-258* II N *mn206***

: larval-lethal. NA1. [[Sigurdson et al. 1984](#)] [SP]

***let-259* II 22.94 *mn210***

: larval-lethal. NA1. [[Sigurdson et al. 1984](#)] [SP]

***let-260* II N *mn232***

: larval-lethal. NA1. [[Sigurdson et al. 1984](#)] [SP]

***let-261* II N *mn233***

: larval-lethal. NA1. [[Sigurdson et al. 1984](#)] [SP]

***let-262* II N *mn87***

: embryonic-lethal. NA1. [[Sigurdson et al. 1984](#)] [SP]

***let-263* II 0.20 *mn240***

: larval-lethal. NA1. [[Sigurdson et al. 1984](#)] [SP]

***let-264* II – 0.13 *mn227***

: larval-lethal. NA1. [[Sigurdson et al. 1984](#)] [SP]

***let-265* II – 0.24 *mn188***

: larval-lethal. NA1. [[Sigurdson et al. 1984](#)] [SP]

***let-266* II 5.92 *mn194***

: larval-lethal. NA1. [[Sigurdson et al. 1984](#)] [SP]

***let-267* II N *mn213***

: larval-lethal. NA1. [[Sigurdson et al. 1984](#)] [SP]

***let-268* II 1.83 *mn189***

: larval-lethal. OA1: *mn198*. [[Sigurdson et al. 1984](#)] [SP]

***let-269* II N *mn201***

: larval-lethal. NA1. [[Sigurdson et al. 1984](#)] [SP]

***let-270* II N *mn191***

: larval-lethal. NA1. [[Sigurdson et al. 1984](#)] [SP]

***let-271* II N *mn193***

: larval-lethal. NA1. [[Sigurdson et al. 1984](#)] [SP]

***let-272* IV – 3.44 *m243***

: mid larval-lethal. OA1: *m266*. [DR]

***let-273* IV – 2.87 *m263***

: early larval-lethal. NA1. [[Rogalski and Riddle 1988](#)] [DR]

***let-274* IV – 1.61 *m256***

: early larval-lethal. NA1. [[Rogalski and Riddle 1988](#)] [DR]

***let-275* IV – 0.56 *m245***

: mid larval-lethal. OA1: *m257*. [[Rogalski and Riddle 1988](#)] [DR]

***let-276 IV 0.62 m240***

: early larval-lethal. OA5: *m239* (embryonic-lethal), etc. [[Rogalski and Riddle 1988](#)] [DR]

***let-277 IV 1.43 m262***

: nonconditional constitutive formation of abnormal dauer-like larvae, forms true dauers in pheromone; dauers recover to arrested dauer-like state. OA1: *m657*. [[Rogalski and Riddle 1988](#)] [DR]

***let-278 IV - 0.06 m265***

: sterile adult. NA1. [[Rogalski and Riddle 1988](#)] [DR]

***let-279 IV 0.67 m261***

: sterile adult. NA1. [[Rogalski and Riddle 1988](#)] [DR]

***let-280 IV 1.40 m259***

: sterile adult. NA1. [[Rogalski and Riddle 1988](#)] [DR]

***let-281 IV 1.31 m247***

: sterile adult. NA1. [[Rogalski and Riddle 1988](#)] [DR]

***let-282 IV 1.31 m258***

: early larval-lethal. OA1: *m270* (sterile adult). [[Rogalski and Riddle 1988](#)] [DR]

***let-283***

= *let-282*

***let-284 IV 1.31 m267***

: early larval-lethal. NA1 [[Rogalski and Riddle 1988](#)] [DR]

***let-285 IV N m248***

: sterile adult. NA1. [[Rogalski and Riddle 1988](#)] [DR]

***let-286 IV N m269***

: sterile adult (Mel, progeny embryonic-lethal). NA1. [[Rogalski and Riddle 1988](#)] [DR]

***let-287 IV N m244***

: sterile adult. NA1. [[Rogalski and Riddle 1988](#)] [DR]

***let-288 IV 0.63 m306***

: sterile adult. NA1. [[Rogalski and Riddle 1988](#)] [DR]

***let-289 IV 3.17 s1133***

: embryonic- or early larval-lethal. OA2: *s1253*, *s2006*. [BC, DR]

***let-290 IV 3.10 s1140***

: embryonic- or early larval-lethal. OA1: *s1109?* [BC, DR]

***let-291 IV 3.27 s1139***

: embryonic- or early larval-lethal. NA1. [BC, DR]

***let-292 IV 3.37 s1146***

: embryonic- or early larval-lethal. NA1. [BC, DR]

***let-293 IV 3.01 s1166***

: embryonic- or early larval-lethal. NA1. [BC, DR]

**let-294 IV 3.39 s1103**

: embryonic- or early larval-lethal. NA1. [BC, DR]

**let-295 IV 3.13 s1175**

: embryonic- or early larval-lethal. NA1. [BC, DR]

**let-296 IV 3.37 s1250**

: embryonic- or early larval-lethal. NA1. [BC, DR]

**let-297 IV 3.39 s1989**

: embryonic- or early larval-lethal. NA1. [BC, DR]

**let-298 IV N m656**

: forms dauer-like larva; grows to sterile adult. NA1. [DR]

**let-301 IV 7.75 s1134**

: early larval-lethal. OA1: s1735. [[Charest et al. 1990](#)] [BC]

**let-302 IV 6.86 s1159**

: (lost) embryonic- or early larval-lethal. [[Charest et al. 1990](#)] [BC]

**let-303 IV 2.5 s761**

: lethal; s1160/Df embryonic- or early larval-lethal. [BC]

**let-304 IV – 0.5 s747**

: early larval-lethal. NA1. [BC]

**let-305 IV – 4.5 s762**

: sterile adult. NA1. [BC]

**let-306 IV – 7.5 s759**

: larval-lethal. NA1. [BC]

**let-307 IV 4.63 s1171**

: mid larval-lethal; s1171/Df similar. NA1. [[Clark et al. 1988](#)] [BC]

**let-308 IV 4.63 s1705**

: mid larval-lethal; s1705/Df similar. NA1. [[Clark et al. 1988](#)] [BC]

**let-309 IV 5.79 s1115**

: late larval-lethal; s1115/Df similar. OA1: s1770 (simi-lar). [[Clark et al. 1988](#); [Clark and Baillie 1992](#)] [BC]

**let-311 IV 4.89 s1195**

: late larval-lethal; s1195/Df similar. NA1. [[Clark et al. 1988](#)] [BC]

**let-312 IV 4.69 s1234**

: late larval-lethal; s1234/Df similar. NA1. [[Clark et al. 1988](#)] [BC]

**let-313 IV 9.39 s1135**

: hemizygote is sterile adult. NA1. [[Charest et al. 1990](#)] [BC]

**let-314 IV 7.78 s1206**

: hemizygote is embryonic- or early larval-lethal. NA1. [[Charest et al. 1990](#)] [BC]

***let-315 IV 7.96 s1101***

: hemizygote is mid larval-lethal. NA1. [[Charest et al. 1990](#)] [BC]

***let-316 IV 7.81 s1227***

: hemizygote is early larval-lethal. NA1. [[Charest et al. 1990](#)] [BC]

***let-317 IV 7.79 s1153***

: hemizygote is embryonic- or early larval-lethal. OA1: *s1182* (similar). [[Charest et al. 1990](#)] [BC]

***let-318 IV 9.39 s1218***

: hemizygote is sterile adult. NA1. [[Charest et al. 1990](#)] [BC]

***let-319 IV 9.39 s1754***

: late larval-lethal; *s1754/Df* similar. OA1: *s1233*. [[Charest et al. 1990](#)] [BC]

***let-320 IV 8.80 s1248***

: hemizygote is sterile adult. OA1: *s1757* (similar). [[Charest et al. 1990](#)] [BC]

***let-321 IV 9.39 s1228***

: hemizygote is sterile adult. NA1. [[Charest et al. 1990](#)] [BC]

***let-322 IV 9.07 s1238***

: hemizygote is early to mid larval-lethal. NA1. [[Charest et al. 1990](#)] [BC]

***let-323 IV 9.67 s1719***

: sterile adult; *s1719/Df* similar. NA1. [[Charest et al. 1990](#)] [BC]

***let-324 IV 9.53 s1727***

: early larval-lethal; *s1727/Df* similar. NA1. [[Charest et al. 1990](#)] [BC]

***let-325 IV 7.79 s1738***

: mid larval-lethal; *s1738/Df* sterile adult. NA1. [[Charest et al. 1990](#)] [BC]

***let-326 V – 19.36 s1404***

: early larval-lethal. OA1: *s238* (mid larval-lethal). [[Johnsen and Baillie 1991](#)] [BC]

***let-327 V – 16.00 s247***

: cs larval-lethal; slow developer, translucent adult. OA3: *s1485, s1496* (morphological abnormalities, lethal 25°C), *s1799*. [[Johnsen and Baillie 1991](#)] [BC]

***let-328***

= *unc-62*

***let-329 V – 0.51 s575***

: early larval-lethal. NA1. [[Johnsen and Baillie 1991](#)] [BC]

***let-330 V – 11.37 s573***

: mid larval-lethal; highly mutable. NA18: *s1425* (early larval-lethal), *s1429, s1463, s1468, s1497, s1515, s1517, s1518, s1583, s1638, s1702spo, s955*, etc. Also *s1433, s1497, s1518* (anomalous complementation, possible weaker alleles). [[Johnsen and Baillie 1991](#)] [BC]

***let-331 V – 2.80 s427***

: cs mid larval-lethal or sterile adult. OA1: *s1608* (slow development, sterile). [[Johnsen and Baillie 1991](#)] [BC]

***let-332 V 0.56 s234***

: embryonic-lethal. OA6: *s369*, *s1021* (some escapers), *s1441*, *s1464* (late embryonic-lethal), *s1498*, *s1567*. [[Johnsen and Baillie 1991](#)] [BC]

***let-333***

= *rol-3*

***let-334 V 1.70 s908***

: early larval-lethal. OA1: *s383* (mid larval-lethal). [[Johnsen and Baillie 1991](#)] [BC]

***let-335 V 0.89 s1439***

: early larval-lethal. OA5: *s232*, *s1412*, *s1476* (tends to coil), *s1520* (escapers to sterile Evl adult), *s1523*. [[Johnsen and Baillie 1991](#)] [BC]

***let-336 V – 22.20 s1413***

: early larval-lethal. OA2: *s1420*, *s1495*. [[Johnsen and Baillie 1991](#)] [BC]

***let-337 V 0.46 s825***

: mid larval-lethal. OA4: *s1426* (early larval-lethal), *s382*, *s1018*, *s1024*. Some alleles early larval-lethal, some Mel. [[Johnsen and Baillie 1991](#)] [BC]

***let-338 V – 5.83 s1020***

: mid larval-lethal. OA1: *s503gri* (similar) [[Johnsen and Baillie 1991](#)] [BC]

***let-339 V 0.56 s1444***

: early larval-lethal. OA2: *s1019* (cs Mel), *s1469* (variable, embryonic- to mid larval-lethal). [[Johnsen and Baillie 1991](#)] [BC]

***let-340 V 1.70 s1508***

: early larval-lethal. OA1: *s1022* (mid larval-lethal). [[Johnsen and Baillie 1991](#)] [BC]

***let-341 V – 5.39 s1031***

: embryonic-lethal. OA>8: *s1415*, *s1421*, *s1454*, *s1516*, *s1534*, *s1571*, *s2118fdi*, *ut58* (early larval-lethal, Clr phenotype), *n1613ts* (variable Vul phenotype at 25°C, some suppression by *let-60[gf]*) [[Johnsen and Baillie 1991](#)] [BC, JC, MT]

***let-342 V – 4.88 s1029***

: early larval-lethal; *s1029/sDf27* similar, *s1029/sDf50* is sterile adult. OA4: *s1487*, *s1549*, *s1616*, *s1442* (weaker allele, *s1442/sDf50* is viable). Some alleles mid larval-lethal. [[Johnsen and Baillie 1991](#)] [BC]

***let-343 V 0.56 s1025***

: embryonic-lethal. OA5: *s816*, *s1410*, *s1428*, *s1579*, *s1465* (cs, slow development). [[Johnsen and Baillie 1991](#)] [BC]

***let-344 V – 5.78 s376***

: embryonic-lethal. OA1: *s1555* (mid larval-lethal). [[Johnsen and Baillie 1991](#)] [BC]

***let-345 V – 4.55 s578***

: mid larval-lethal. OA4: *s1452*, *s1509*, *s1510*, *s1690fdi*. Some alleles late larval-lethal. [[Johnsen and Baillie 1991](#)] [BC]

***let-346 V 0.56 s1619***

: mid larval-lethal. OA6: *s373*, *s1026*, *s1575*, *s1580* (mid/late larval-lethal, Evl), *s1630* (sterile adult, rescued by mating), *s2166fdi*. [[Johnsen and Baillie 1991](#)] [BC]

***let-347 V – 11.40 s1035***

: late larval-lethal. NA1. [[Johnsen and Baillie 1991](#)] [BC]

***let-348 V – 5.67 s1436***

: early larval-lethal. OA3: *s1622* (resembles *s1436*), *s998gri*, *s1448* (slow development to Mel adult, embryonic-lethal), *s1622*. [[Johnsen and Baillie 1991](#)] [BC]

***let-349 V N s217***

: early larval-lethal. OA3: *s502gri*, *s572* (cs, late larval-lethal), *s1965uvi*. [[Johnsen and Baillie 1991](#)] [BC]

***let-350 V – 2.70 s250***

: sterile adult. OA1: *s2126fdi*. [[Johnsen and Baillie 1991](#)] [BC]

***let-351 I – 1.28 h43***

: mid larval-lethal. NA1. [[Howell et al. 1987; McKim et al. 1992](#)] [KR]

***let-352 I – 0.15 h45***

: late larval-lethal/sterile adult. NA1. [[Howell et al. 1987](#)] [KR]

***let-353 I – 1.46 h46***

: mid larval-lethal. NA1. [[Howell and Rose 1990](#)] [KR]

***let-354 I – 1.30 h79***

: mid larval-lethal, no dominant effect. OA>20 (recessive-lethal). Also three dominant alleles: *ct42*, *ct76*, *ct77* (all three alleles lead to recessive zygotic larval lethality, dominant embryonic Mel). [[Howell and Rose 1990; Mains et al. 1990a](#)] [HR, KR]

***let-355 I 0.00 h81***

: sterile adult. NA1. [[Howell et al. 1987](#)] [KR]

***let-356 I – 2.21 h83***

: mid larval-lethal. OA3: *h501*, *h679*, *h871*. [[Howell and Rose 1990](#)] [KR]

***let-357 I – 3.11 h89***

: sterile adult. OA1: *h132*. [[Howell et al. 1987](#)] [KR]

***let-358***

= *lin-6*

***let-359 I – 0.37 h94***

: sterile adult. NA1. [[Howell et al. 1987](#)] [KR]

***let-360 I – 5.12 h96***

: late larval-lethal. NA1. [[Howell et al. 1987](#)] [KR]

***let-361 I – 0.24 h97***

: late larval/early adult lethal. OA3: *h113*, *h116*, *h323gri*. [[Howell et al. 1987](#)] [KR]

***let-362 I – 13.45 h86***

: embryonic-lethal. OA1: *h93*. [[Howell et al. 1987](#)] [KR]

***let-363* I – 0.24 *h98***

: late larval-lethal. OA4: *h111* (early adult arrest), *h60*, *h114*, *h131* (lethal). [[Howell et al. 1987](#)] [KR]

***let-364* I – 0.24 *h104***

: sterile adult. NA1. [[Howell et al. 1987](#)] [KR]

***let-365* I – 5.35 *h108***

: sterile adult. OA2: *h129*, *h295* (sterile adult). [[Howell et al. 1987](#)] [KR]

***let-366* I – 1.77 *h112***

: mid larval-lethal. OA6: *h265* (lethal), etc. [[Howell and Rose 1990](#)] [KR]

***let-367* I 0.02 *h119***

: sterile adult. NA1. CLONED: cosmid rescue (C12H4). [[Howell et al. 1987](#)] [KR]

***let-368* I – 2.28 *h121***

: early larval-lethal. OA1: *h826* (sterile adult, no rescue by mating). [[Howell et al. 1987](#)] [KR]

***let-369* I – 2.22 *h125***

: early larval-lethal. OA1: *h864* (mid larval-lethal). [[Howell et al. 1987](#)] [KR]

***let-370* I – 0.01 *h128***

: sterile adult or Mel with larval lethality. OA1: *h270*. [[Howell et al. 1987](#)] [KR]

***let-371* I – 0.20 *h123***

: sterile adult. NA1. [[Howell et al. 1987](#)] [KR]

***let-372* I – 2.23 *h126***

: sterile adult. NA1. [[Howell et al. 1987](#)] [KR]

***let-373* I – 1.86 *h234***

: early larval-lethal. OA2: *h570*, *h573* (early larval-lethal). [[Howell and Rose 1990](#)] [KR]

***let-374* I – 1.45 *h251***

: mid larval-lethal. NA1. [[Howell and Rose 1990](#)] [KR]

***let-375* I – 0.61 *h259***

: leaky sterile adult. OA1: *h391* (similar). [[Howell and Rose 1990](#)] [KR]

***let-376* I 0.03 *h130***

: early larval-lethal. OA6: *h416* (lethal), etc. CLONED: cosmid rescue (M01A12) [[Howell et al. 1987](#)] [KR]

***let-377* I 0.22 *h110***

: early larval-lethal. OA2: *h443*, *h766*. [[Howell et al. 1987](#)] [KR]

***let-378* I 0.21 *h124***

: sterile adult. OA3: *h181*, *h401*, *h563*. CLONED: cosmid rescue (C07F10) [[Howell et al. 1987](#)] [KR]

***let-379* I 0.41 *h127***

: embryonic- or early larval-lethal. OA2: *h186*, *h712*. [[Howell et al. 1987](#)] [KR]

***let-380* I 0.94 *h80***

: late larval-lethal. OA2: *h675*, *h831*. [[Howell et al. 1987](#)] [KR]

***let-381* I 0.90 *h107***

: embryonic- or early larval-lethal. OA2: *h495*, *h747*. CLONED: cosmid F26B1. [[Howell et al. 1987](#)] [KR]

***let-382* I 1.23 *h82***

: mid larval-lethal. OA1: *h476*. [[Howell et al. 1987](#)] [KR]

***let-383* I 1.24 *h115***

: early to mid larval-lethal. OA3: *h389*, *h527*, *h727*. [[Howell et al. 1987](#); [McKim et al. 1992](#)] [KR]

***let-384* I 0.74 *h84***

: late larval-lethal or sterile adult. OA3: *h388*, *h454*, *h865*. [[Howell et al. 1987](#)] [KR]

***let-385* I 1.36 *h85***

: early larval-lethal; highly mutable. OA>15: *h578* (late larval-lethal), *h940*, etc. [[Howell et al. 1987](#); [McKim et al. 1992](#)] [KR]

***let-386* I 1.20 *h117***

: mid larval-lethal. OA4: *h678*, etc. [[Howell et al. 1987](#)] [KR]

***let-387* I 0.90 *h87***

: mid to late larval-lethal. OA1: *h183*. [[Howell et al. 1987](#)] [KR]

***let-388* I 0.42 *h88***

: early larval-lethal. OA2: *h729*, *h843*. [[Howell et al. 1987](#)] [KR]

***let-389* I 1.56 *h680***

: early larval-lethal. OA10: *h428*, *h106* (both early larval-lethal), *h698* (late larval-lethal). Complex complementation; *h698/h428* is fertile. [[Howell et al. 1987](#); [McKim et al. 1992](#)] [KR]

***let-390* I 1.23 *h44***

: late larval-lethal or sterile adult. NA1. [[Howell et al. 1987](#)] [KR]

***let-391* I 0.87 *h91***

: late larval-lethal or sterile adult. OA3: *h823* (early/mid larval-lethal), *h736*, *h475*. [[Howell et al. 1987](#)] [KR]

***let-392* I 1.24 *h120***

: early larval-lethal. OA8: *h122*, etc. [[Howell et al. 1987](#); [McKim et al. 1992](#)] [KR]

***let-393* I 0.01 *h225***

: early larval-lethal. OA1: *h375* (similar). CLONED: cosmid rescue (F40D12).

***let-394* I 1.40 *h262***

: early to mid larval-lethal. OA6: *h361* (sterile adult), etc. CLONED: cosmid rescue (T14D10). [[McKim et al. 1992](#)] [KR]

***let-395* I 0.01 *h271***

: sterile adult, undeveloped gonad. NA1. CLONED: partial cosmid rescue (M01A12), to Mel with arrest at cleavage stage. [KR]

***let-396* I 0.88 *h217***

: early larval-lethal. OA4: *h354*, etc. [KR]

***let-397* I 1.24 *h228***

: early larval-lethal. OA2: *h221*, *h445*. [[McKim et al. 1992](#)] [KR]

***let-398 I 1.31 h257***

: arrests L2. NA1. CLONED: partial cosmid rescue (K01B11). [[McKim et al. 1992](#)] [KR]

***let-399 I 1.34 h273***

: L4-lethal. NA1. [[McKim et al. 1992](#)] [KR]

***let-400 I 1.58 h269***

: early to mid larval-lethal. OA5: *h878*, *h590gri*, etc. [[McKim et al. 1992](#)] [KR]

***let-401 V - 0.75 s193***

: mid larval-lethal. NA1. [[Johnsen and Baillie 1991](#)] [BC]

***let-402 V - 0.33 s1526***

: early larval-lethal. OA2: *s127* (mid larval-lethal), *s500gri*. [[Johnsen and Baillie 1991](#)] [BC]

***let-403 V - 0.09 s1482***

: early larval-lethal. OA3: *s120* (mid/late larval-lethal), *s246*, *s498gri*. [[Johnsen and Baillie 1991](#)] [BC]

***let-404 V 0.50 s119***

: mid larval-lethal. NA1. [[Johnsen and Baillie 1991](#)] [BC]

***let-405 V 0.89 s116***

: early larval-lethal. OA2: *s388*, *s829*. Some alleles mid larval-lethal. [[Johnsen and Baillie 1991](#)] [BC]

***let-406 V 0.62 s514***

: mid larval-lethal (gri). NA1. CLONED: cosmid rescue (F58G4). [[Johnsen and Baillie 1991](#)] [BC]

***let-407 V 1.88 s830***

: early larval-lethal. OA3: *s118*, *s1631* (early larval-lethal), *s2122fdi*. [[Johnsen and Baillie 1991](#)] [BC]

***let-408 V 0.89 s827***

: embryonic-lethal. OA1: *s195* (late larval-lethal). CLONED: cosmid rescue (F18B11). [[Johnsen and Baillie 1991](#)] [BC]

***let-409 V 1.61 s823***

: early larval-lethal. OA6: *s206* (early larval-lethal), *s1480* (early larval-lethal, curls), *s1507*, *s1528*, *s1546*, *s1547*. [[Johnsen and Baillie 1991](#)] [BC]

***let-410 V 0.48 s815***

: mid larval-lethal. OA1: *s1565* (similar). [[Johnsen and Baillie 1991](#)] [BC]

***let-411 V 0.76 s1595***

: mid larval-lethal. OA3: *s223* (late larval-lethal), *s1453*, *s1553*. YAC rescue of *s1553* (Y69E9). [[Johnsen and Baillie 1991](#)] [BC]

***let-412 V 1.60 s1598***

: sterile adult roller. OA1: *s579* (Mel, embryonic lethality). [[Johnsen and Baillie 1991](#)] [BC]

***let-413 V 1.43 s128***

: embryonic-lethal. OA3: *s1431*, *s1451*, *s1455*. YAC rescue of *s1451* (Y69E9). [[Johnsen and Baillie 1991](#)] [BC]

***let-414 V 0.89 s114***

: mid larval-lethal. OA1: *s207*. CLONED: cosmid rescue (F18B11). [[Johnsen and Baillie 1991](#)] [BC]

***let-415 V – 1.65 s1525***

: early larval-lethal. OA2: *s1505* (late larval-lethal), *s129* (mid/late larval-lethal). [[Johnsen and Baillie 1991](#)] [BC]

***let-416 V 1.61 s113***

: late larval-lethal. NA1. [[Johnsen and Baillie 1991](#)] [BC]

***let-417 V – 0.99 s204***

: early larval-lethal. OA3: *s1313*, *s1424*, *s1679fdi*. [[Johnsen and Baillie 1991](#)] [BC]

***let-418 V N s1617***

: sterile adult, Evl, partial rescue at 15°C. OA1: *s1045* (sterile Evl adult at 24°C, Mel [early larval-lethal] at 20°C). [[Johnsen and Baillie 1991](#)] [BC]

***let-419 V – 2.54 s1483***

: early/mid larval-lethal. OA2: *s219* (mid larval-lethal), *s1539*. [[Johnsen and Baillie 1991](#)] [BC]

***let-420 V – 2.70 s1046***

: sterile adult, Evl. OA6: *s723gri*, *s1058*, *s1478*, *s1573*, *s1584*, *s1603* (abnormal tail). [[Johnsen and Baillie 1991](#)] [BC]

***let-421 V C s1477***

: embryonic-lethal. OA3: *s288* (leaky), *s1460* (dumpy, mid larval-lethal), *s1632* (dumpy, curls, escapers late larval-lethal, Evl). [[Johnsen and Baillie 1991](#)] [BC]

***let-422 V C s194***

: early larval-lethal. OA6: *s738gri*, *s739gri*, *s1312*, *s1563*, *s1578* (ts, rescued at 15°C), *s1548*. [[Johnsen and Baillie 1991](#)] [BC]

***let-423 V 0.82 s818***

: early larval-lethal. OA1: *s1550* (early/mid larval-lethal). YAC rescue of *s1550* (Y69E9). [[Johnsen and Baillie 1991](#)] [BC]

***let-424 V 1.44 s384***

: sterile adult. OA2: *s248*, *s1587* (similar). Mixed cosmid rescue. [[Johnsen and Baillie 1991](#)] [BC]

***let-425 V 0.56 s385***

: sterile adult. NA1. [[Johnsen and Baillie 1991](#)] [BC]

***let-426 V – 17.76 s1527***

: early larval-lethal. OA1: *s826* (mid larval-lethal). [[Johnsen and Baillie 1991](#)] [BC]

***let-427 V 2.10 s1057***

: sterile adult. NA1. [[Johnsen and Baillie 1991](#)] [BC]

***let-428 V – 2.70 s1490***

: dumpy, late larval-lethal (ruptures). OA1: *s1070* (sterile adult). [[Johnsen and Baillie 1991](#)] [BC]

***let-429 V – 0.62 s584***

: sterile adult. OA1: *s1597* (slow development, morphological abnormalities). [[Johnsen and Baillie 1991](#)] [BC]

***let-430 V – 5.67 s1042***

: sterile adult. NA1. [[Johnsen and Baillie 1991](#)] [BC]

***let-431 V – 20.44 s1049***

: sterile adult. OA1: *s1044* (similar). [[Johnsen and Baillie 1991](#)] [BC]

**let-432**

= *lin-40*

***let-433 V 1.61 s950***

: sterile adult. NA1. CLONED: cosmid rescue (T24H5). [[Johnsen and Baillie 1991](#)] [BC]

***let-434 V 1.59 s1904***

: sterile adult, gri. NA1. CLONED: cosmid rescue (ZK307). [[Johnsen and Baillie 1991](#)] [BC]

***let-436 V 1.25 s1403***

: early larval-lethal. NA1. [[Johnsen and Baillie 1991](#)] [BC]

***let-437 V – 20.98 s1405***

: mid larval-lethal, abnormal tail. NA1. [[Johnsen and Baillie 1991](#)] [BC]

***let-438 V 0.56 s2114***

: fdi, lethal. NA1. [[Johnsen and Baillie 1991](#)] [BC]

***let-439 V – 0.04 s1407***

: early larval-lethal. OA3: *s1503*, *s1522*, *s1524* (all similar) [[Johnsen and Baillie 1991](#)] [BC]

***let-440 V – 2.70 s1411***

: very early larval-lethal. OA4: *s1440*, *s1552*, *s1560*, *s1589* (similar). [[Johnsen and Baillie 1991](#)] [BC]

***let-441 V 2.04 s1414***

: early larval-lethal (ts, leaky at 20°C, rescued at 15°C). NA1. [[Johnsen and Baillie 1991](#)] [BC]

***let-442 V 0.56 s1416***

: early/mid larval-lethal. OA2: *s1430ts* (partial rescue to sterile adult at 15°C), *s1535*. [[Johnsen and Baillie 1991](#)] [BC]

***let-443 V – 0.87 s1417***

: early larval-lethal. NA1. [[Johnsen and Baillie 1991](#)] [BC]

***let-444 V – 0.41 s1418***

: early larval-lethal. OA2: *s1459*, *s1569* (Mel). [[Johnsen and Baillie 1991](#)] [BC]

***let-445 V 1.15 s1419***

: Mel (larval-lethal, tight coiler). [[Johnsen and Baillie 1991](#)] [BC]

***let-447 V – 21.52 s1457***

: Mel (embryonic-lethal, arrest pre-lima bean); *s1457/Df* lays more eggs than homozygote. OA1: *s1654fdi* (resembles *s1457*) [[Johnsen and Baillie 1991](#)] [BC]

***let-448 V – 20.98 s1363***

: mut; mid/late larval-lethal. NA1. [[Johnsen and Baillie 1991](#)] [BC]

***let-449 V 1.43 s1343***

: mut; early larval-lethal. NA1. YAC rescue (Y69E9) [[Johnsen and Baillie 1991](#)] [BC]

***let-450 V – 22.60 s2160***

: fdi (lost). [[Johnsen and Baillie 1991](#)] [BC]

***let-452 V – 2.70 s1434***

: early larval-lethal. NA1. [[Johnsen and Baillie 1991](#)] [BC]

***let-453 V – 20.98 s2167***

: lethal. NA1. [[Johnsen and Baillie 1991](#)] [BC]

***let-454 V 2.04 s1423***

: mid larval-lethal; double cuticle, no pumping. NA1. [[Johnsen and Baillie 1991](#)] [BC]

***let-455 V – 7.07 s1447***

: early larval-lethal. OA1: *s1511* (similar). [[Johnsen and Baillie 1991](#)] [BC]

***let-456 V 1.43 s1479***

: early larval-lethal. NA1. YAC rescue (Y69E9). [[Johnsen and Baillie 1991](#)] [BC]

***let-458 V – 20.98 s1443***

: early larval-lethal. NA1. [[Johnsen and Baillie 1991](#)] [BC]

***let-459 V – 6.46 s1432***

: mid larval-lethal. OA1: *s1615* (Mel [embryonic-lethal], not rescued by mating). [[Johnsen and Baillie 1991](#)] [BC]

***let-460 V 1.79 s1664***

: early larval-lethal, fdi. NA1. [[Johnsen and Baillie 1991](#)] [BC]

***let-461***

= *lag-2*

***let-462 V – 0.04 s1594***

: embryonic/early larval-lethal. OA3: *s1481* (larval-lethal, molting problem), *s1590*, *s1956uvi*. [[Johnsen and Baillie 1991](#)] [BC]

***let-463 V – 0.47 s2168***

: lethal. NA1. [[Johnsen and Baillie 1991](#)] [BC]

***let-464 V 1.59 s1504***

: embryonic/early larval-lethal. OA1: *s1530* (early larval-lethal). [[Johnsen and Baillie 1991](#)] [BC]

***let-466 V – 7.42 s1063***

: Mel (early larval-lethal). OA1: *s990* (Mes, maternal-effect sterile). [[Johnsen and Baillie 1991](#)] [BC]

***let-467 V 1.74 s1521***

: early larval-lethal. NA1. [[Johnsen and Baillie 1991](#)] [BC]

***let-468 V 0.56 s1533***

: early larval-lethal. NA1. [[Johnsen and Baillie 1991](#)] [BC]

***let-469 V 0.48 s1582***

: sterile adult, rescued by mating. NA1. [[Johnsen and Baillie 1991](#)] [BC]

**let-470 V 1.99 s1581**

: mid larval-lethal. OA1: *s1629ts* (slow development at 20°C, normal at 15°C). [[Johnsen and Baillie 1991](#)] [BC]

**let-471 V 0.48 s1570**

: Mel (early larval-lethal, rescued by mating). NA1. [[Johnsen and Baillie 1991](#)] [BC]

**let-472 V 0.48 s1605**

: mid larval-lethal, morphological abnormalities. NA1. [[Johnsen and Baillie 1991](#)] [BC]

**let-473 V 0.23 s1602**

: early larval-lethal, trapped in old cuticle. NA1. [[Johnsen and Baillie 1991](#)] [BC]

**let-474 V 1.43 s1577**

: early larval-lethal. NA1. YAC rescue (Y69E9). [[Johnsen and Baillie 1991](#)] [BC]

**let-475 V 1.99 s1606**

: sterile adult. NA1. [[Johnsen and Baillie 1991](#)] [BC]

**let-476 V 0.18 s1621**

: ts; sterile adult at 20°C, rescued by mating; fertile at 15°C. NA1. [[Johnsen and Baillie 1991](#)] [BC]

**let-478 V – 9.04 s1620**

: early larval-lethal; *s1620/sDf50* is Mel (embryonic-lethal). NA1. [[Johnsen and Baillie 1991](#)] [BC]

**let-479 V – 0.03 s1576**

: sterile Evl adult, lays unfertilized eggs; rescued by mating; partial rescue at 15°C. NA1. [[Johnsen and Baillie 1991](#)] [BC]

**let-480 V C s1607**

: sterile adult, not rescued by mating. NA1. [[Johnsen and Baillie 1991](#)] [BC]

**let-481 V L s1636**

: early larval-lethal. NA1. [[Johnsen and Baillie 1991](#)] [BC]

**let-500 III/V N s2165**

: embryonic-lethal (induced on *eT1*). NA1. [[Johnsen and Baillie 1991](#)] [BC]

**let-501 I – 1.91 h714**

: early larval-lethal. OA1: *h498* (mid larval-lethal). [[Howell and Rose 1990](#)] [KR]

**let-502 I – 1.37 h392**

: mid larval-lethal. OA5: *h783* (late larval-lethal), *h509* (sterile adult), *ca201sd* (embryonic arrest, early morphogenesis; *ca201/+* sometimes abnormal), *h732*, *h835* (both mid larval-lethal). All alleles probable dominant negatives. CLONED: encodes protein with similarity to human myotonic dystrophy kinase. [[Howell and Rose 1990](#)] [HR, JM, KR]

**let-503 I – 1.46 h313**

: sterile adult. OA1: *h418* (similar). [[Howell and Rose 1990](#)] [KR]

**let-504 I – 1.53 h844**

: late larval-lethal. OA3: *h448* (sterile adult), *h327*, *h888* (late larval-lethals). [[Howell and Rose 1990](#)] [KR]

***let-505 I – 1.53 h426***

: late larval-lethal. NA1. [[Howell and Rose 1990](#)] [KR]

***let-506 I – 1.46 h300***

: late larval-lethal. NA1. [[Howell and Rose 1990](#)] [KR]

***let-507 I – 1.46 h439***

: leaky sterile adult. NA1. [[Howell and Rose 1990](#)] [KR]

***let-508 I – 0.92 h452***

: late larval-lethal. OA1: *h995*. [[Howell and Rose 1990](#)] [KR]

***let-509 I – 1.91 h867***

: leaky late larval-lethal/sterile adult. OA2: *h521* (leaky sterile adult), *h522*. [[Howell and Rose 1990](#)] [KR]

***let-510 I – 1.91 h740***

: lethal. NA1. [[Howell and Rose 1990](#)] [KR]

***let-511 I – 1.91 h755***

: early larval-lethal. NA1. [[Howell and Rose 1990](#)] [KR]

***let-512 I 0.69 h797***

: mid larval-lethal. OA5: *h351*, etc. [KR]

***let-513 I 0.57 h752***

: sterile adult. NA1. [KR]

***let-514 I 0.65 h753***

: early/mid larval-lethal. NA1. CLONED: partial cosmid rescue (C32E7), to sterile adult, no oocytes. [KR]

***let-515 I – 2.50 h730***

: early larval-lethal. OA3: *h223* (late larval-lethal), *h139*, *h149* (both Mel). [KR]

***let-516 I – 1.91 h144***

: sterile adult. OA1: *h456*. [KR]

***let-517 I – 2.50 h264***

: lethal. OA1: *h757*, *h1398*. [KR]

***let-518 I – 2.50 h316***

: embryonic/early larval-lethal. NA1. [KR]

***let-519 I – 2.50 h405***

: lethal. NA1. [KR]

***let-520 I 1.64 h690***

: L4-lethal. OA1: *h1003* (similar). [[McKim et al. 1992](#)] [KR]

***let-521 I 1.35 h704***

: L4-lethal. NA1. [[McKim et al. 1992](#)] [KR]

***let-522 I 1.73 h735***

: early larval-lethal. OA2: *h240*, *h519*. [[McKim et al. 1992](#)] [KR]

***let-523* I 1.73 *h751***

: early larval-lethal. OA1: *h479*. [[McKim et al. 1992](#)] [KR]

***let-524* I 1.80 *h442***

: early larval-lethal. OA4: *h53gri*, etc. [[McKim et al. 1992](#)] [KR]

***let-525* I 1.73 *h874***

: mid larval-lethal. OA1: *h410*. [[McKim et al. 1992](#)] [KR]

***let-526* I – 0.12 *h185***

: lethal. NA1. CLONED: cosmid rescue (C01G8). [KR]

***let-527* I 1.80 *h207***

: early larval-lethal. OA3: *h209* (mid larval-lethal), *h357* (some maternal rescue to Spe adult), *h932* (early larval-lethal). [[McKim et al. 1992](#)] [KR]

***let-528* I 1.40 *h1012***

: late larval-lethal. OA1: *h58spo* (similar). [[McKim et al. 1992](#)] [KR]

***let-529* I 1.36 *h238***

: early larval-lethal. OA3: *h249*, *h342*, *h516* (similar). [[McKim et al. 1992](#)] [KR]

***let-530* I 0.02 *h798***

: early larval-lethal. OA5: *h359*, etc. CLONED: partial cosmid rescue (M01A12) of *h798*, to Mel (cleavage arrest). [KR]

***let-531* I 0.36 *h733***

: late larval-lethal. OA1: *h767*. [KR]

***let-532* I 0.39 *h715***

: embryonic-lethal. NA1. CLONED: cosmid rescue (anomalous?). [KR]

***let-533* I N *h845***

: lethal. NA1. [KR]

***let-534* I 1.31 *h260***

: mid larval-lethal, coiler Unc. OA1: *h196* (mid larval-lethal). CLONED: cosmid rescue (T14D10). [[McKim et al. 1992](#)] [KR]

***let-535* I 2.42 *h993***

: mid larval-lethal. OA1: *h999* (similar). [[McKim et al. 1992](#)] [KR]

***let-536* I 3.11 *h882***

: late larval-lethal. NA1. [[McKim et al. 1992](#)] [KR]

***let-537***

= *mek-2*

***let-538* I 2.42 *h990***

: sterile adult. NA1. [[McKim et al. 1992](#)] [KR]

***let-539* I 1.82 *h938***

: mid larval-lethal. NA1. [[McKim et al. 1992](#)] [KR]

***let-540 I 2.03 h884***

: late larval-lethal. NA1. [[McKim et al. 1992](#)] [KR]

***let-541 I 3.11 h886***

: early larval-lethal. NA1. [[McKim et al. 1992](#)] [KR]

***let-542 I 1.94 h986***

: early larval-lethal. NA1. [[McKim et al. 1992](#)] [KR]

***let-543 I 1.37 h792***

: L4-lethal. NA1. [[McKim et al. 1992](#)] [KR]

***let-544 I 1.27 h692***

: sterile adult. NA1. [[McKim et al. 1992](#)] [KR]

***let-545 I 1.45 h842***

: sterile adult, very few germ-line nuclei; no oocytes or sperm. NA1. CLONED: cosmid rescue (T21G5).

Possibly = *glh-1*. [[McKim et al. 1992](#)] [KR]

***let-546 I – 15.00 h227***

: lethal. NA1. [KR]

***let-547 I – 15.00 h277***

: lethal. NA1. [KR]

***let-548 I – 11.55 h356***

: lethal. NA1. [KR]

***let-549 I – 7.68 h193***

: lethal. NA1. [KR]

***let-550 I N h291***

: sterile adult. NA1. [KR]

***let-551 V 17.28 e2517***

: early/mid larval-lethal at 20°C; sterile adult at 15°C; mutator-induced. [CB]

***let-552 II – 5.25 e2542***

: most animals arrest as L1 hatchlings; small dumpy warped appearance; occasional escapers reach fertile adulthood, with extreme dumpy phenotype; rare progeny have same phenotype; spontaneous mutation. NA1. [CB]

***let-553 II R e2617***

: mut; Evl, often ruptures at L4 molt; normal spermatogenesis; Mel; variable embryonic arrest up to many cells; no morphogenesis; many distorted eggs, never laid. [CB]

***let-571 I – 7.88 h347***

: lethal. NA1. [KR]

***let-572 I – 15.00 h220***

: lethal. NA1. [KR]

***let-573 I – 8.17 h247***

: lethal. NA1. [KR]

***let-574 I N h317***

: sterile adult. NA1. [KR]

***let-575 I N h345***

: lethal. OA1: *h728*. [KR]

***let-576 I N h816***

: early larval-lethal. OA1: *h494*. [KR]

***let-577 I N h503***

: early larval-lethal. NA1. [KR]

***let-578 I N h512***

: lethal. NA1. [KR]

***let-579 I N h705***

: mid larval-lethal. NA1. [KR]

***let-580 I N h709***

: lethal. NA1. [KR]

***let-581 I N h725***

: mid larval-lethal. OA1: *h876* (similar). [KR]

***let-582 I N h726***

: lethal. NA1. [KR]

***let-583 I N h738***

: early/mid larval-lethal. NA1. [KR]

***let-584 I N h743***

: sterile adult. OA1: *h746* (similar). [KR]

***let-585 I N h784***

: early larval-lethal. NA1. [KR]

***let-586 I N h846***

: mid larval-lethal. NA1. [KR]

***let-587 I N h849***

: mid larval-lethal. NA1. [KR]

***let-588 I – 1.45 h318***

: sterile adult, occasionally lays a few eggs. NA1. [KR]

***let-589 I – 1.91 h319***

: Mel, embryonic arrest. NA1. [KR]

***let-590 I – 1.45 h320***

: sterile adult. NA1. [KR]

***let-595 I C h353***

: lethal. OA1: *h372*. [KR]

***let-598 I C h213***

: lethal. OA1: *h813*. [KR]

***let-599 I – 0.12 h290***

: sterile adult. NA1. [KR]

***let-601 I 1.00 h281***

: embryonic-lethal. NA1. CLONED: cosmid rescue (ZC338). [KR]

***let-602 I 0.88 h283***

: early larval-lethal. OA2: *h374*, *h497*. CLONED: mixed cosmid rescue (including C46H8); partial rescue to sterile adult, no oocytes. [JS, KR]

***let-603 I 0.43 h289***

: sterile adult (gonad tumorous mass). OA3: *h408*, *h437*, *h812* (sterile adults). CLONED: partial cosmid rescue (C32E7); rescued to Mel. [KR]

***let-604 I 1.23 h293***

: sterile adult. OA1: *h490* (similar). [KR]

***let-605 I 1.30 h312***

: sterile Unc adult; *h312/Df* sterile, Evl, strong coiler Unc. OA4 (all alleles Unc). [\[McKim et al. 1992\]](#) [KR]

***let-606 I 1.05 h292***

: sterile adult. NA1 [KR]

***let-607 I 1.24 h402***

: embryonic-lethal. NA1. [KR]

***let-608 I 1.13 h706***

: early larval arrest, lives 1–2 weeks. OA2. [KR]

***let-610 I 1.13 h695***

: sterile adult. NA1. [KR]

***let-611 I 0.89 h850***

: early/mid larval-lethal. OA2. CLONED: mixed cosmid rescue (including C48E7); rescue to sterile adult, no oocytes. [KR]

***let-613 I C h198***

: lethal. NA1. [KR]

***let-651 IV 4.66 s1165***

: mid larval-lethal. OA1: *s1185* (mid larval-lethal, fails to complement *let-91[s753]*). [\[Clark and Baillie 1992\]](#) [BC]

***let-652 IV 4.66 s1086***

: mid larval-lethal; *s1086/Df* similar. NA1. [\[Clark and Baillie 1992\]](#) [BC]

***let-653 IV 5.41 s1733***

: early larval-lethal; arrest stage is late L1 to early L2; cystic [excretory](#) canals. OA2: *s2270* (homozygote arrests L2 with vacuole anterior to posterior pharyngeal bulb, hemizygote arrests L1), *s2377* (homozygote sterile adult, hemizygote arrests L2). CLONED: encodes predicted 694-aa secreted protein, with features characteristic of mucin glycoproteins. [[Jones and Baillie 1995](#)] [BC, NJ]

***let-654***

= *sem-3*

***let-655 IV 4.95 s1748***

: sterile adult, *s1748/Df* similar. NA1. [[Clark and Baillie 1992](#)] [BC]

***let-656 IV 5.78 s1753***

: sterile adult, *s1753/Df* similar. OA1: *s1767* (similar). [[Clark and Baillie 1992](#)] [BC]

***let-657 IV 4.59 s1254***

: hemizygotes arrest as embryo/early larva. OA3: *s1143, s1164, s1236*. [BC]

***let-658 IV 4.49 s1149***

: hemizygote arrests as late larva. OA2: *s1107, s1194*. [BC]

***let-659 IV 4.49 s1152***

: hemizygote arrests as early larva. NA1. [BC]

***let-660 IV 5.38 s1996***

: sterile adult (leaky). NA1. [BC]

***let-661 IV 5.61 s2203***

: homozygote and hemizygote arrest as L2 larva. NA1. CLONED: partial cosmid rescue (K04H1). [BC]

***let-662 IV 5.71 s2219***

: homozygote and hemizygote arrest as leaky sterile adult. NA1. [BC]

***let-664 IV 5.35 s2374***

: homozygote and hemizygote arrest as sterile adult. NA1. [BC]

***let-702 III – 1.1 s2483***

: early larval-lethal. NA1. [BC]

***let-705 III – 1.45 s2451***

: early larval-lethal. NA1. [BC]

***let-706 III – 5.46 s2480***

: early larval-lethal. NA1. [BC]

***let-707 III – 2.28 s2462***

: early larval-lethal. NA1. [BC]

***let-708***

= *let-764*

***let-713 III C s2449***

: early/mid larval-lethal. OA1: *s2470* (early larval-lethal). [BC]

***let-714 III – 1 s2582***

: early larval-lethal. OA2: *s2481* (mid/late larval-lethal), *s2465* (sterile). [BC]

***let-715 III – 3.05 s2618***

: variable sterile adult. NA1. [BC]

***let-716 III – 1.43 s2457***

: early larval-lethal. OA1: *s2626* (similar). [BC]

***let-720 III – 20.5 s2610***

: sterile adult. NA1. [BC]

***let-721 III C s2447***

: sterile adult. NA1. [BC]

***let-722 III – 1.0 s2448***

: early larval-lethal. OA2: *s2588* (pka [\*let-744\*](#), mid larval-lethal), *s2450* (pka [\*let-772\*](#), sterile adult). [BC]

***let-723 III C s2434***

: sterile adult. NA1. [BC]

***let-725 III C s2454***

: sterile adult. NA1. [BC]

***let-728 III C s2573***

: early/mid larval-lethal. NA1. [BC]

***let-733 III – 2.34 s2621***

: variable sterile adult. NA1. [BC]

***let-734 III – 2.3 s2479***

: early larval-lethal. NA1. [BC]

***let-737 III – 2.82 s2477***

: mid larval-lethal. NA1. [BC]

***let-744***

= *let-722*

***let-745***

= *let-765*

***let-747 III C s2456***

: early/mid larval-lethal. NA1. [BC]

***let-749 III – 2.36 s2467***

: sterile adult. NA1. [BC]

***let-754 III C s2622***

: mid larval-lethal. NA1. [BC]

***let-755 III C s2600***

: early/mid larval-lethal. NA1. [BC]

***let-758 III – 5.46 s2607***

: sterile adult. NA1. [BC]

***let-759 III – 4.52 s2595***

: sterile adult. NA1. [BC]

***let-761 III – 1.68 s2461***

: early larval-lethal. NA1. [BC]

***let-764 III – 1.5 s2616***

: early larval-lethal. OA1: *s2443* (pka [\*let-708\*](#), early larval arrest). [BC]

***let-765 III – 1.04 s2575***

: early larval-lethal; L2 arrests with lineage abnormalities; in males, *B.a* and *B.p* equal in size; *s2575/Df* arrests at L1. OA1: *s2630* (pka [\*let-745\*](#), mid larval-lethal). [BC]

***let-766 III C s2463***

: early larval-lethal. NA1. [BC]

***let-767 III C s2464***

: early larval-lethal. NA1. [BC]

***let-768 III C s2592***

: mid/late larval-lethal. OA2: *s2482* (sterile), *s2628* (later larval arrest). [BC]

***let-771 III – 1.5 s2442***

: sterile adult. NA1. [BC]

***let-772***

= *let-722*

***let-774 III C s2615***

: early larval-lethal. NA1. [BC]

***let-778 III – 2.2 s2584***

: early larval-lethal. NA1. [BC]

***let-782 III – 1.68 s2591***

: variable sterile adult. NA1. [BC]

***let-783 III C s2601***

: embryonic or early larval-lethal. NA1. [BC]

***let-786 III – 1.43 s2631***

: early larval-lethal. NA1. [BC]

***let-789 III – 2.2 s2606***

: sterile adult. NA1. [BC]

***let-852 II 3 cc502***

: early larval-lethal. OA3: *cc50* (mid larval-lethal), *cc504* (late larval-lethal). [PD]

***let-853 II 3 cc505***

: embryonic-lethal. OA2. [PD]

***let-854 II 3 cc507***

: embryonic-lethal. OA1. [PD]

***let-855 II 3 cc509***

: early larval-lethal. OA8. [PD]

***let-856 II 3 cc514***

: mid larval-lethal. OA6. [PD]

***let-857 II 3 cc516***

: embryonic-lethal. OA5. [PD]

***let-858 II 3 cc500***

: embryonic-lethal. OA2. Two strongest alleles arrest at 1.5/2.5-fold elongation stage, often with head vacuoles; transgenically rescued animals survive to sterile adult; abnormal germ line. CLONED: partial cosmid rescued (F33A8), to viable sterile adult phenotype; 2.8-kb transcript, predicted 90-kD novel protein. [PD]

***let-974 III - 0.3 s230***

: late larval-lethal. NA1. [BC, KR]

***let-975 III - 0.3 s255***

: sterile adult. NA1. [BC]

***let-976 III - 0.3 s267***

: lethal. NA1. [BC, KR]

***let-977 III - 0.3 s966***

: sterile adult. NA1. [BC, KR]

***let-978 III - 0.3 s1050***

: sterile adult. OA1: s377 (similar). [BC, KR]

***let-979 III - 0.1 s231***

: lethal. NA1. [BC, KR]

***let-980 III - 0.1 s424***

: mid larval-lethal. NA1. [BC, KR]

***let-981 III - 0.1 s453***

: lethal. OA3: s222, s529 (larval-lethal), s1072 (sterile adult). CLONED: cosmid rescue (ZK643). [BC, KR]

***let-982 III 0 s386***

: lethal. NA1. [BC, KR]

***let-983 III 0 s442***

: lethal. OA1: s1080 (sterile adult). CLONED: partial cosmid rescue (F44E2). [BC, KR]

***let-984 III 0 s428***

: lethal. OA1: s294 (larval-lethal). [BC, KR]

***let-985 III 0 s980***

: larval-lethal. NA1. [BC, KR]

***let-986 III 0 s1065***

: sterile adult. NA1. [BC, KR]

***let-987 III 0 s1078***

: sterile adult. NA1. [BC, KR]

***lev***

**lev** amisole resistance abnormal [ZZ]. See also *tmr*.

***lev-1 IV 8.05 e211***

: (pka [tmr-1](#)) almost normal movement in absence of drugs; uncoordinated but not hypercontracted in 1 mM levamisole. ES2 ME3. OA>10: x22, e289, x577, etc. Also two rare semidominant alleles with uncoordinated phenotype: x21 (uncoordinated Egl-c, ME3), x63. CLONED: corresponds to [acr-1](#), encoding subunit of nicotinic acetylcholine receptor. [[Lewis et al. 1980a,b](#), [1987b](#)] [ZZ, MQ]

***lev-7***

= *unc-63*

***lev-8 X 5.09 x15***

: almost normal movement in absence of drugs; weakly resistant to 1 mM levamisole; body contracts but head does not; more resistant at 25°C. ES2 NA1. [[Lewis et al. 1980a](#), [1987a](#)] [ZZ]

***lev-9 X - 2.52 x16***

: almost normal movement in absence of drugs; weakly resistant to 1 mM levamisole. ES2 OA2. [[Lewis et al. 1980a](#), [1987a](#)] [ZZ]

***lev-10 I 23.83 x17***

: almost normal movement in absence of drugs; weakly resistant to 1 mM levamisole. ES2 NA1. [[Lewis et al. 1980a](#), [1987a](#)] [ZZ]

***lev-11 I 25.44 x12***

: slightly long, uncoordinated, mild twitcher phenotype; grows well in 1 mM levamisole; strong semidominant suppressor of *unc-90(e1463)*. ES3 ME2. OA6: x1 (twitcher), e1724 (lethal). Also Pat (paralyzed arrest at 2-fold) alleles: *st536* (severe paralysis), *st577*, *st566* (some pharyngeal pumping). Greatly reduced staining for tropomyosin, probably corresponds to structural gene *tmy-1*. [[Lewis et al. 1980a](#); [Williams and Waterston 1994](#)] [HK, ZZ]

***lfe***

**L**et-23 **f**e rtility effector/regulator [PS].

***lfe-1 IV N sy290***

: suppresses sterility of [let-23](#) mutations. [PS]

***lfe-2 I N sy326***

: suppresses sterility of [let-23](#) mutations. [PS]

***lgx***

**L**in-12 and **g**lp-1 **X**-hybridizing [GS].

***lgx-1 X - 4.80***

NMK. Encodes predicted protein with EGF-like repeats. [GS]

***lgx-2 IV 3.15***

NMK. Encodes predicted protein with EGF-like repeats. [GS]

### ***Igx-3***

= *epi-1*

### ***lin***

**lin** eage abnormal [CB].

### ***lin-1 IV – 8.36 e1777***

: amb; adult hermaphrodite has multiple (one to four) vulval protrusions, often bursts at abnormal [vulva](#) during L4 molt. ES3 (adult)/ES1 (larvae) HME2; adult male has rudimentary ectopic hooks. ES1 ME0. OA>20: *e1026*, *n431amb* (phenotype resembles *e1777*), *e1275* (weaker, slightly ts phenotype; ME1), *n746*, *n1141*, etc. CLONED: encodes predicted protein with strong similarity to ETS family transcription factors. [[Ferguson and Horvitz 1985](#); [Beitel et al. 1995](#); [Katz et al. 1995](#)] [GS, MT]

### ***lin-2 X 7.49 e1309***

: adult hermaphrodite Vul (penetrance 93%). ES2 (adult)/ES1 (larvae) HME2 ME3 (adult male wt). NA13: *e1453amb* (non-null, lower penetrance than *e1309*, 50% Vul), *n105ts* (penetrance 24% at 15°C, 90% at 25°C), *n768* (weak allele, multiple vulval protrusions, penetrance at 21%), *n397* (deletes most of gene), etc. CLONED: encodes predicted protein with PDZ domain, similarity to guanylate kinase, *Drosophila* Discs large; mutants delocalize LET-23. [[Ferguson et al. 1985](#); [Simske et al. 1996](#)] [MT, SD]

### ***lin-3 IV 4.81 e1417***

: adult hermaphrodite Vul (penetrance 89%); HME2 ME2 (adult male wt). OA>10: *n378* (resembles *e1417*), *n1059* (early larval-lethal), *n1058* (early larval-lethal/sterile adult), *s751* (pka [let-94](#), late larval-lethal, *s751/Df* early larval-lethal), *s1750* (homozygote and hemizygote mid larval-lethal), etc. CLONED: encodes proteins with similarity to EGF family; transgene overexpression leads to Muv (extra vulval differentiation). [[Hill and Sternberg 1992](#); [Katz et al. 1995](#)] [BC, MT, PS]

### ***lin-4 II – 0.88 e912***

: pdi; heterochronic, retarded; adult hermaphrodites have long, abnormal movement, Vul, lack adult cuticle. ES3 (adult) ES1 (larvae) HME0 (20°C)/HME1 (15°C). Adult males lack copulatory structures. ME0. OA1: *ma161* (resembles *e912*). CLONED: encodes two small RNAs with no coding potential. [[Lee et al. 1993](#); [Wightman et al. 1993](#)] [GR, VT]

### ***lin-5 II 0.56 e1348***

: thin, sterile, and uncoordinated after L1; all postembryonic divisions fail from defective cytokinesis, although DNA replication continues; no sexual maturation in either sex. ES3 ME0. OA1: *e1457* (similar phenotypes). CLONED: cosmid rescue (C03G3) [[Sulston and Horvitz 1981](#); [Albertson et al. 1978](#)] [MT]

### ***lin-6 I – 9.44 e1466***

: thin, sterile, and uncoordinated after L1; most postembryonic divisions absent or defective from absence of DNA synthesis; Q and I divisions normal; no sexual maturation in either sex. ES3 ME0. OA1 (pka [let-358](#)). [[Sulston and Horvitz 1981](#)] [MT]

### ***lin-7 II 22.94 e1413***

: amb; adult hermaphrodite Vul (penetrance 98%); HME2 ME3 (adult male wt). OA>10: *e974amb*, *n308* (both resemble *e1413*), *n308cs* (penetrance 95% at 15°C, 28% at 25°C), *n385*, *n764*, etc. CLONED: encodes predicted 33-kD protein with PDZ domain, similarity to junction-associated proteins; mutants delocalize LET-23. [[Sulston and Horvitz 1981](#); [Hoskins et al. 1996](#); [Simske et al. 1996](#)] [MT, SD]

### ***lin-8 II – 8.39 n111***

: adult hermaphrodite wt, Muv in homozygotes with *lin-9*, *lin-35*, *lin-36*, or [\*lin-37\*](#). ME3 (male wt). Mosaic analysis indicates action is cell nonautonomous. OA1: *n762*. [[Ferguson and Horvitz 1989](#); [Hedgecock and Herman 1995](#)] [MT]

***lin-9* III – 0.00 *n112***

: adult hermaphrodite wt, Muv in homozygotes with [\*lin-8\*](#) or [\*lin-38\*](#). OA2: *n942*, *n943* (both sterile non-Muv alone; sterile Muv with [\*lin-8\*](#), etc.). CLONED: encodes predicted 642-aa novel protein, hydrophobic, possible C-terminal transmembrane domains. [[Ferguson and Horvitz 1989](#)] [MT]

***lin-10* I 2.49 *e1439***

: adult hermaphrodite Vul (penetrance 95%); HME2 ME3 (adult male wt). Similar phenotype in *e1439/Df*. OA>5: *e1438*, *n299*, *n1299*, *n1329*, *n1638amb*, etc. CLONED: encodes predicted 407-aa novel protein; antibody staining indicates ubiquitous, cytoplasmic. [[Kim and Horvitz 1990](#)] [MT, SD]

***lin-11* I 4.88 *n389***

: adult hermaphrodite Vul (penetrance 100%); 2° lineages become symmetrical; HME0; slightly uncoordinated; adult male slightly uncoordinated; wt morphology. ME1. OA3: *n382* (resembles *n389*), *n672sd* (*n672/+* is 5% Vul), *n566* (weaker allele HME2). CLONED: encodes LIM class homeoprotein; *lin-11:lacZ* expressed in some [\*VPC\*](#) 2° descendants, some gonadal cells, [\*VC neurons\*](#), some [\*head neurons\*](#). [[Freyd et al. 1990](#)] [MT]

***lin-12* III 0.12 *n941***

: abnormal [\*vulva\*](#), sterile, small; many lineage transformations. ES3 ME0. Also gf alleles: *n137sd* : adult hermaphrodite Muv, many lineage transformations. ES3 ME1 (*n137/+* ME3). OA>15(gf): *n177* (resembles *n137*), *n676*, *n302*, *n379* (these alleles have semidominant Vul phenotype, probably less hypermorphic). Also intragenic revertants of dominant alleles OA>50 (ird): most have lf phenotype, e.g., *n137n720*, *n676n909amb* (resemble *n941*), *n137n460ts* (wt at 25°C, Muv at 15°C). Many other non-null alleles with tissue-specific effects, also TcI-insertion null alleles. See also *sel*, *lag*, *glp-1*; Lag functions redundant with *glp-1*. CLONED: encodes 1429-aa protein, transmembrane receptor related to GLP-1, *Drosophila* Notch; 13 EGF-like repeats and other repeats in extracellular domain, 6 ANK repeats in intracellular domain; very extensive developmental and molecular analyses, many mutations sequenced. [[Greenwald et al. 1983](#); [Wilkinson et al. 1994](#); [Wilkinson and Greenwald 1995](#)] [GS]

***lin-13* III – 0.60 *n387***

: ts, mat; adult hermaphrodite Muv and sterile at 25°C, maternally rescued at 15°C (*n387* progeny of *n387/+* are wt but produce sterile F<sub>2</sub> only); males have occasional ventral protrusions. ME0. *n387/Df* at 25°C is early larval-lethal. OA1: *n388* (similar). CLONED: cosmid rescue (K04F4) [[Ferguson and Horvitz 1985](#), 1989] [GS, MT]

***lin-14* X 3.33 *n526n540***

: ird; lf allele (class II, a<sup>-</sup>b<sup>-</sup>), precocious heterochronic lineage alterations in ectoderm; abnormal development of [\*vulva\*](#), endoderm, and mesoderm; abnormal cuticle formation; precocious dauer entry at L1 molt. ES2. Male more severely affected, only three molts, gonadal development abnormal; similar phenotype in *n536n540/Df*. OA>10: *n179ts*, etc.; also *n355n679ird,ts* (class V, a<sup>-</sup>b<sup>+</sup>, only early events precocious), *n360ts* (class III, a<sup>+</sup>b<sup>-</sup>, only late events precocious). Also gf alleles: *n536sd* (class I, retarded heterochronic alterations in many lineages; abnormal vulval development, cuticle formation, supernumerary molts, extra divisions in sex mesoblasts, [\*intestine\*](#), etc.; gonadal lineages normal. ES3), *n355sd* (similar). Numerous intragenic revertants; for both lf and gf mutations, late lineages less affected if animal develops via dauer stage. CLONED: two 3.5-kb transcripts, differing 5', encoding 70-kD novel proteins; antibodies stain nuclei; protein levels high in L1, reduced or absent later; gf mutations affect 3'UTR. [[Ruvkun and Giusto 1989](#); [Wightman et al. 1993](#)] [GR, VT]

***lin-15* X 22.32 n309**

: adult hermaphrodite Muv, [vulva](#) either normal or nonfunctional, two to six ventral protrusions; some animals rupture during L4 molt; adult males have one to three ventral protrusions, rudimentary ectopic hook. ME0. Possibly enhanced phenotype in *n309/Df*. OA>10: *e1763*, *n765ts* (wt at 15°C, Muv at 25°C, maternal-effect Muv at 20°C), *n767* (class-A allele, wt alone, Muv in homozygotes with *lin-9,35,36,37*), *n744* (class-B allele, wt alone, Muv with *lin-8,38*), etc. CLONED: locus encodes two collinear transcripts, B (5') and A (3', SL2 *trans-spliced*); encode predicted 1440-aa and 719-aa novel proteins. [[Ferguson and Horvitz 1989](#); [Clark et al. 1994](#); [Huang et al. 1994](#)] [MT, PS]

***lin-16* III – 0.81 e1743**

: thin, sterile, uncoordinated after L1; extensive failure of postembryonic divisions; no polyplloid cells; most Vn.p cells join syncytium. [TU]

***lin-17* I – 7.63 n671**

: adult hermaphrodite slightly uncoordinated, long, irregularly shaped tail, [vulva](#) may be nonfunctional; many hermaphrodites (50%) have single small protrusion posterior to vulvas; some gonadal abnormality and sterility; abnormally long [excretory](#) canals; diverse asymmetric cell divisions are symmetric or reversed. ES2. Male tail grossly abnormal, may rupture during L2 molt. ME0. OA4: *n677* (resembles *n671*), *n669* (less penetrant for Muv phenotype), *e2257*, etc. CLONED: encodes predicted membrane protein (seven transmembrane domains), 28% identity to *Drosophila* Frizzled. [[Sternberg and Horvitz 1988](#); [Herman et al. 1995](#); [Sawa et al. 1996](#)] [MT]

***lin-18* X – 8.15 e620**

: some (<50%) hermaphrodites have single small protrusion posterior to [vulva](#), occasional vulval rupture; polarity of 2° lineages variably disrupted; slight maternal-effect; slightly ts; *e620/Df* stronger phenotype. ES2 ME3 (males phenotypically wt). OA1: *n1051amb,ts* (resembles *e620*). [[Ferguson et al. 1985](#)] [MT, PS]

***lin-19* III 2.51 e1756**

: normal L1, extra cell divisions in most postembryonic lineages (about 4-fold increase; extra cells smaller, but differentiate); sterile. ES3 (adult) ME0 NA1. CLONED: encodes predicted 697-aa protein, 28% identity to yeast Cdc53p. [[Kipreos et al. 1996](#)] [NJ]

***lin-20***

= *vab-3*

***lin-21* III – 0.46 e1751**

: sd; uncoordinated, abnormal migration of Q [neuroblasts](#), both [QL](#) and [QR](#) migrate posteriorly; ectopic V ray papillae; reverts spontaneously to wt. NA1. Molecular data indicate *e1751* is a tandem duplication of ~100 kb that includes [mab-5](#). [[Hedgecock et al. 1987](#)] [NJ, CF]

***lin-22* IV – 6.87 n372**

: V1–V4 divide like V5, resulting in multiple ectopic [postdeirids](#) in hermaphrodites and males, and multiple ectopic rays in males; males also have hermaphroditic Pn.ps and are mostly missing lateral alae. ES1 (hermaphrodite) ES2 (male) ME2. OA1: *n1113*. CLONED: predicted protein has similarity to bHLH proteins, *Drosophila* Hairy. [[Horvitz et al. 1983](#); [Waring et al. 1992](#)] [CF, MT]

***lin-23* II – 0.38 e1883**

: extra cell divisions in all postembryonic lineages, apparently stochastic; sterile, eggs undergo many cell divisions, no morphogenesis. ES3 (adult) ME0. OA3: *e1924*, *e1925*, *e1521* (pka [stu-1](#), thin, sterile, loopy, uncoordinated). CLONED: predicted protein has similarity to yeast Cdc4p. [[Miller et al. 1993](#)] [NJ]

***lin-24* IV 5.71 n432**

: sd; adult hermaphrodite Vul (*n432* 95% Egl, *n432/+* 55% Egl); Pn.p cells degenerate, dependent on *ced-2,5,10*. ES2 ME3 (male wt). Probably neomorphic, *n432/nDf27* is 54% Egl, *+/nDf27* is wt. OA1: *n1057amb* (non-null, *n1057* and *n1057/Df* are wt, *n1057/+* is 33% Egl). Null phenotype probably wt. [[Ferguson et al. 1987](#); [Ellis et al. 1991a](#)] [MT]

#### ***lin-25 V 4.51 e1446***

: adult hermaphrodite Vul, 11% sterile; [VPC](#) all 3° except [P6.p](#); suppresses *lin-1, let-60(gf)*, not *lin-12(gf)*. ES2 HME1 ME0 (males morphologically wt). OA9: *n545ts* (resembles *e1446* at 25°C; 8% Vul at 15°C), *n1063, ku78, ar90* (probable null, resembles *e1446*), etc. CLONED: encodes predicted 1139-aa novel protein. [[Tuck and Greenwald 1995](#)] [GS]

#### ***lin-26 II 0.48 n156***

: adult hermaphrodites Vul (>99%), slightly small and fat; HME1; general hypodermal and support cell defects, hypodermal cells die or neuralize; 2% sterile. ES2. Males very small scrawny, rounded tail; ME0. *n156/Df* is larval-lethal. OA4: *mc1, mc2* (both embryonic-lethal), *pk38tci, mc15* (deletion derivative). CLONED: encodes predicted zinc finger transcription factor; antibody stains [hypodermis](#), support cells, [uterine](#) cells. [[Labouesse et al. 1994](#)] [MT, ML]

#### ***lin-27 I N b151***

: ts, mat, mn; at 25°C, hermaphrodite sterile with ball-shaped gonad; other lineage abnormalities (e.g., M descendants); male sterile with normal gonad morphology. NA1. [DH, JK]

#### ***lin-28 I 2.71 n719***

: precocious heterochronic alterations in many ectodermal lineages, more severe than *lin-14(null)*; precocious abnormal [vulva](#) development; Egl; abnormal cuticle formation; only three molts; hermaphrodite and male V5.pa make ray cells in L2; gonadal development normal; late lineages less affected if animal develops via dauer stage. ES3 ME0. OA3: *n947, n1119, n1120* (all resemble *n719*). CLONED: 1.5- and 1.6-kb transcripts, encode predicted Y-box protein. [[Liu and Ambros 1991](#); [Arasu et al. 1991](#)] [GR, VT]

#### ***lin-29 II 4.28 n333***

: retarded heterochronic alterations in L4 [seam cells](#); no adult alae formed; supernumerary divisions; also Egl, Evl; phenotype not affected by development via dauer stage. ES3 ME0 (males have short spicules). OA3: *n546* (*smg*-suppressible), *n1440, n836, ga94* (adult cuticle but abnormal [vulva](#)). CLONED: 1.8- and 2.4-kb transcripts (different 5'), present throughout larval development, maximal L4; 2.4 kb encodes 50-kD protein with five zinc fingers; antibody shows LIN-29 stage-specific expression in nuclei of [seam cells](#), [hyp-7](#) of L4, some vulval nuclei also. [[Rougvie and Ambros 1995](#)] [VT, GR]

#### ***lin-30 III N e1908***

: many late embryonic and postembryonic lineage failures due to abnormal cytokinesis; variable; homozygous-viable. NA1. [[Mitani et al. 1993](#)] [NJ]

#### ***lin-31 II – 5.25 n301***

: adult hermaphrodite Muv, [vulva](#) either functional or nonfunctional protrusion; 0–4 small ventral protrusions; [VPC](#) cells adopt 1°/2°/3° fate at random. ES3 (adult). Male gross morphology wt, ME0; similar phenotype in *n301/Df* mosaic analysis indicates cell-autonomous action. OA>10: *e1750, e2181, n376, n428, n1301*. CLONED: 1.5-transcript, expressed throughout development, encodes predicted 237-aa protein with similarity to Fork head/HNF-3 transcription factors; *lin-31*:GFP expressed in [P3.p–P8.p](#). [[Miller et al. 1993, 1996](#)] [SD]

#### ***lin-32 X – 14.12 e1926***

: many [neuroblasts](#) adopt hypodermal fates (Q, postdeirid, ray [neuroblasts](#) make only [seam](#) or syncytial nuclei); Q/V5 embryonic division delayed; various embryonic [sensory neurons](#) absent or displaced; loopy

foraging; anterior rays most affected; mutant phenotypes more severe in *e1926/Df*. ES1 (hermaphrodite) ES3 (adult male). OA2: *u282* (stronger, 90% of males lack rays; also lack [PLM](#), [AVM](#), [PVM neurons](#), hence touch-insensitive in tail), *bx46* (intermediate phenotype). CLONED: encodes predicted bHLH transcription factor, 66% identity to *Drosophila* Atonal; transgene overexpression leads to ectopic ray papillae. [[Zhao and Emmons 1995](#)] [EM, KP]

***lin-33 IV 2.54 n1043***

: sd; adult hermaphrodite Vul (*n1043* 95% Egl, *n1043/+* 77% Egl); Pn.p cells undergo cell death (*ced-2,5,10*-dependent). ES2 ME3 (male gross morphology wt). OA1: *n1044* (similar). Null phenotype uncertain. [[Ferguson et al. 1987](#); [Ellis et al. 1991a](#)] [MT]

***lin-34***

= *let-60*

***lin-35 I 0.74 n745***

: almost wt alone (reduced fertility); Muv (extra vulval differentiation) in homozygotes with *lin-8*, *lin-38*, or *lin-15(n767)*. ES2. OA1: *n373* (similar). [[Ferguson and Horvitz 1989](#)] [MT, PS]

***lin-36 III – 0.42 n766***

: wt alone; Muv in homozygotes with *lin-8*, *lin-38*, or *lin-15(n767)*; mosaic analysis indicates autonomous action in [VPC](#). ES2 ME3. OA3: *n772* (similar), *n750*, etc. CLONED: encodes predicted 926-aa novel protein. [[Ferguson and Horvitz 1989](#)] [MT, PS]

***lin-37 III – 0.77 n758***

: wt alone; Muv in homozygotes with *lin-8*, *lin-38*, or *lin-15(n767)*. ES2 NA1. [[Ferguson and Horvitz 1989](#)] [MT, PS]

***lin-38 II 12.81 n751***

: almost wt alone (reduced fertility); Muv in homozygotes with *lin-9*, *lin-35*, *lin-36*, *lin-37*, or *lin-15(n744)*. ES2. OA1: *n761* (similar). [[Ferguson and Horvitz 1989](#)] [MT, PS]

***lin-39 III – 0.65 n709***

: ts; some or all P3.aap–[P8.aap](#) (presumptive [VC neurons](#)) die in hermaphrodites (ES1); variably Egl (ES2); variably abnormal vulval divisions; multiple defects in specification of fates in midbody. ME3. OA1: *n1490*, *mu26*. CLONED: encodes homeoprotein (pka [ceh-15](#)) related to *Drosophila* Dfd/Scr; *lin-39:lacZ* expressed in central body region of egg, larva, adult. [[Clark et al. 1993](#); [Wang et al. 1993](#)] [CF, MT]

***lin-40 V – 8.35 e2173***

: sterile Evl adult, multiple defects; males very abnormal. ES3 ME0. OA>15: *s1053* (pka [let-432](#)), *s1345mut*, *s1351mut*, *s1669fdi*, *s1675fdi*, *s1704*, *s1916uvi*, etc. Homozygous developmental arrest stages range from early/mid larval-lethal to Mel (early larval-lethal); sterile and Mel adults are Evl; complex complementation, at least five classes; high mutation frequency; also dominant effects on sperm number (dominant increase in *Df/+*, decrease in some alleles). [[Johnsen and Baillie 1991](#)] [BC]

***lin-41 I 4.89 ma104***

: heterochronic defect in L4/A switch. [VT]

***lin-42 II – 12.78 n1089***

: precocious HSN differentiation; heterochronic defect in L4/A switch. [MT, VT]

***lin-43 I – 1 ma103***

: thin sterile Evl adult, patches of adult alae missing; general failure of L3 and L4 [seam](#) cell divisions, and other cell divisions; probable cell cycle defect. NA1. [VT]

***lin-44 I – 1.60 n1792***

: polarities of B, F, U, T divisions reversed; *n1792/Df* similar; mosaic analysis indicates nonautonomous action. OA1: *n2111* (similar). CLONED: encodes member of Wnt family; *lin-44:lacZ* and *lin-44:GFP* expressed in tail tip [hypodermis](#). [Herman et al. 1995] [EH, MT, SP]

***lin-45 IV 3.27 sy96***

: subviable, >90% die as rod-like L1, escapers mostly Egl, Vul; suppresses [\*lin-15\*](#) Muv; impenetrant [\*P12\*](#) to [\*P11\*](#) transformation; partial maternal rescue of larval lethality; effects on male development resemble F and U ablation. OA1: *n2018cs* (most animals Vul or inviable at 15°C, 25% non-Vul at 25°C). CLONED: pka [\*raf-1\*](#); encodes 813-aa predicted protein with extensive similarity to raf kinases; dominant-negative transgene frequently Vul. [Han et al. 1993] [MH, MT, PS]

***lin-46 V 6***

Mutation suppresses Lin-28; some lateral hypodermal cells divide at fourth molt rather than form alae; enhanced by starvation. [VT]

***lin-47 X 1.83 sy32***

: males have abnormal spicules; B-cell lineage defect, possibly additional defects. [PS]

***lin-48 III – 7.54 sy234***

: males have abnormal spicules; defects in [\*B\*](#), [\*E\*](#), and [\*U\*](#) lineages. [PS]

***lin-49 IV 3.97 sy238***

: males have short crumpled spicules; defects in [\*E\*](#) and [\*U\*](#) lineages; both males and hermaphrodites sickly and have some “scarring” at the [rectum](#); *sy238/Df* animals arrest at mid-larval stage, heavy scarring at int/rect junction; males have B-lineage defect. OA1: *s1198* (stronger, mid larval-lethal). [PS, BC]

***[lin-50](#)***

= *egl-38*

***lir***

[\*\*l\*\*](#) *n-26-* [\*\*r\*\*](#) elated [ML].

***lir-1 II 0.48 pk96***

: Tc1 insertion, no known phenotype; encodes predicted protein related and 5'to *lin-26*. [ML]

***lir-2 II 0.48***

NMK. Encodes predicted protein related and 5'to *lin-26*. [ML]

***lmr***

[\*\*l\*\*](#) [\*\*a\*\*](#) [\*\*m\*\*](#) inin [\*\*r\*\*](#) eceptor-related [CGC].

***lmr-1 III – 2.69***

NMK. Cross-hybridization to laminin receptor probe. [GS]

***lon***

[\*\*l\*\*](#) [\*\*o\*\*](#) [\*\*n\*\*](#) g [CB].

***lon-1 III – 1.68 e185***

: ~50% longer than wt at all stages, markedly tapering tail and head; low penetrance tendency to form constriction behind head, may result in auto-decapitation; eggs elongated. ES3. Male bursa elongated.

ME0. OA5: *e43*, *e1820*, *n1130*, etc. (some have stronger Lon phenotype than *e185*, all show some decapitation). [[Brenner 1974](#)] [MT]

#### ***lon-2* X – 6.17 e678**

: ~50% longer than wt at all stages; some embryonic lethality. ES3. Male bursa slightly elongated, ME3 (ME0 at 25°C?). OA4: *e405*, *e434*, *n1346*, *n1630*, etc. (all similar to *e678*). [[Brenner 1974](#)]

#### ***lon-3* V 4.16 e2175**

: mut; adult about 50% longer than wt. ES3 (adult) ME1. NA1. [CB, KE]

#### ***lrp***

**L** DL- **r** ece **p** tor-related [GS]. LDL, low-density lipoprotein.

#### ***lrp-1* I 2.18**

NMK. Encodes predicted protein of 4753 aa, extensive homology with mammalian LRP (4525 aa). [[Yochim and Greenwald 1993](#)] [GS]

#### ***lrx***

**I** p **X** -hybridizing [GS].

#### ***lrx-1* V 3.73**

NMK. Cross-hybridization to [\*lrp-1\*](#) probe. [GS]

## **M to N**

#### ***mab***

**m** ale **ab** normal [CB].

#### ***mab-1***

= *smg-1*

#### ***mab-2* I 0.35 e1241**

: adult male missing 6–18 copulatory rays as a result of variable failures of V and T lineages; bursa often grossly distorted. ME0/ME1. Hermaphrodite gross phenotype normal; late hypodermal V and T divisions variably defective. ES1 (hermaphrodite) ES3 (adult male). NA1. [[Hodgkin 1983](#); [Link et al. 1988](#)] [CB]

#### ***mab-3* II 1.67 e1240**

: adult [\*male tail\*](#) morphology grossly abnormal, often with hermaphrodite [\*tail spike\*](#); adult male synthesizes yolk proteins; V lineages abnormal, other defects. ES3 (adult male) ME0. Hermaphrodite wt. OA4: *e1921ts*, *e2093* (similar but slightly weaker phenotypes than *e1240*), *e2093*, *e2212*. [[Shen and Hodgkin 1988](#)] [CB]

#### ***mab-4* III 8.20 e1252**

: adult male has swollen bursa. ES3 ME1. Adult hermaphrodite has protruding [\*vulva\*](#). ES2 NA1. [[Hodgkin 1983](#); [Link et al. 1988](#)] [CB]

#### ***mab-5* III – 0.55 e1239**

: postembryonic lineages and migrations in preanal region generally abnormal; adult [\*male tail\*](#) morphology thin, grossly abnormal; V rays missing, T rays present; sex mesoblast lineages, etc., abnormal. ES3 (male) ME0. Hermaphrodite gross phenotype wt, but V divisions, Q migrations, [\*coelomocytes\*](#) all abnormal. ES1 (hermaphrodite). Mosaic analysis indicates cell-autonomous; similar mutant phenotypes in *e1239/Df*. OA>8: *e1936*, *e2011* (Q24och), *e2088* (all resemble *e1239*), etc. Also *bx54sd* (dominant missense, ray fusion phenotype). See also *lin-21*. CLONED: HOM-C member, encodes homeoprotein related to Antennapedia; extensive molecular analysis. [[Kenyon 1986](#); [Cowing and Kenyon 1992](#); [Salser and Kenyon 1996](#)] [CF]

***mab-6* II – 0.95 *e1249***

: adult male has very swollen bursa. ES2 ME1. Hermaphrodite wt. NA1. [[Hodgkin 1983; Link et al. 1988](#)] [CB]

***mab-7* X – 19.15 *e1599***

: adult male slightly small, all bursal rays swollen; bursal fan reduced. ES2 ME1. Hermaphrodite slightly dumpy. ES2. OA1: *e2150*. [[Hodgkin 1983; Link et al. 1988](#)] [CB]

***mab-8* II – 1.21 *e1250***

: adult male has swollen bursa, adult hermaphrodite has protruding [vulva](#). ES2 ME1 NA1. [[Hodgkin 1983; Link et al. 1988](#)] [CB]

***mab-9* II – 14.49 *e1245***

: amb; [male tail](#) morphology and development grossly abnormal, [B lineage](#) defective, resembles [Y lineage](#); also probable [F](#) to [U](#) lineage transformation; many males die or rupture during L4 molt; *e1245/Df* similar. ES3 (male) ME0. Hermaphrodite grossly wt, sometimes constipated as a result of rectal abnormalities. OA2: *e2410, e2376* (weaker allele). [[Chisholm and Hodgkin 1989](#)]

***mab-10* II 3.04 *e1248***

: adult male has slightly swollen bursa, reduced fan, thin rays; some adult males have supernumerary molt, second adult cuticle; *e1248/Df* more severe. ES2 ME0. Hermaphrodite has slightly protruding [vulva](#). ES2 NA1. [[Hodgkin 1983; Link et al. 1988](#)] [CB, CL]

***mab-11***

= *smg-2*

***mab-12* IV – 15.43 *e2166***

: adult male has swollen bursa; adult hermaphrodite has protruding [vulva](#). ES2 ME1. [[Hodgkin et al. 1989](#)]

***mab-13***

= *smg-3*

***mab-14***

= *smg-4*

***mab-15***

= *smg-5*

***mab-16***

= *smg-6*

***mab-17* I N *e2167***

: adult male has bulged tail tip, loss of T rays; unstabilized *hyp7* retraction, defective fan. NA1. [CB, EM]

***mab-18* X 1.95 *bx23***

: ray 6 to ray 4 transformation, resulting in fused double ray 4. OA1: *bx79*. See also *vab-3*. CLONED: [\*mab-18\*](#) activity provided by shorter transcripts from [\*vab-3\*](#), encoding only homeodomain; *mab-18*:GFP expressed in ray 6 sublineage from L4 onward. [[Zhang and Emmons 1995](#)] [CZ, EM]

***mab-19* X – 2.83 *bx38***

: variable loss of T rays (lineage defect), some retention of [tail spike](#), gonad morphology defects; hermaphrodite brood size reduced to 100; partly suppressed by many *dpy* mutations, or stress; synthetic-lethal with many [\*unc-17\*](#) alleles; *bx38/Df* is lethal. OA1: *bx83* (similar). [[Sutherlin and Emmons 1994](#)] [EM]

***mab-20 I – 10.41 bx24***

: displacements and fusions in rays 1, 2, 3, 4, 8, 9; R1,2,4 probably transformed to R3; variable bulges in posterior body region. OA1: *bx61ts* (weaker). [[Baird et al. 1991](#); [Chow and Emmons 1994](#)] [EM]

***mab-21 III – 3.61 bx53***

: transformation of thick ray 6 to a thin ray, which is anteriorly displaced and fuses with ray 4 (>95%); tenth ray derived from T.apapa, between rays 5 and 7, found in ~50% of sides scored; both males and hermaphrodites have slightly shorter body length (~85% of wt); reduced brood size; males backward Unc, reduced mating efficiency; mosaic focus cell autonomous for R6, nonautonomous for T.apapa; probable hypomorph, *bx53/Df* is embryonic-lethal. OA2: *bx41, sy155* (similar). CLONED: encodes predicted 386-aa novel protein. [[Baird et al. 1991](#); [Chow et al. 1995](#)] [KC, EM, PS]

***mab-22 III N bx59***

: ts; extensive loss of rays at 25°C, not 15°C; divisions appear normal, possible ray assembly defect. NA1. [EM]

***mab-23 V 2.47 e2518***

: spo; no phenotype in hermaphrodite, [male tail](#) very swollen, rays indistinct. ME0. Vancouver wild isolate KR314 is naturally homozygous for *e2518*. [CB]

***mab-24 I N e2169***

: variable V5 and V6 ray loss or misplacement; uncoordinated, poor backing, forward coiler. [EM]

***mab-25 I N bx27***

: ts; [male tail](#) swollen, fan reduced, missing ray; wrinkled; ts-lethal. [EM]

***mab-26 IV – 29.20 bx80***

: sd; fusions among all rays; also head, body, and (especially) tail deformities; *bx80/+* shows impenetrant R4 to R3 transformation. [[Chow and Emmons 1994](#)] [EM]

***mab-27 X 17.01 sy202***

: males have abnormal spicules; both males and hermaphrodites exhibit a slight "loopy" Unc; possibly also very weakly penetrant lineage defect. NA1. [PS]

***mad***

[ma](#) ternal effect [d](#) umpy [MQ].

***mad-1 I 25 qm39***

: hatchlings short and deformed, resemble Dpy-17; at later stages variable, anterior body short, posterior half thin; high larval lethality; full zygotic rescue, almost complete maternal rescue. NA1. [[Hekimi et al. 1995](#)] [MQ]

***mad-2 I 6 qm62***

: adults short, lethargic but hyperactive for foraging movement, very rapid pumping after touch; tails abnormal in both sexes; very slow development; high larval lethality; full zygotic and maternal rescue. OA1: *qm58*. [[Hekimi et al. 1995](#)] [MQ]

***mad-3 V 5.8 qm64***

: hatchlings of variable length, shortest die; adults short, unhealthy; high embryonic and larval lethality; full zygotic and maternal rescue. NA1. [[Hekimi et al. 1995](#)] [MQ]

***mah***

**mah** i (uncoordinated in Japanese) [TN].

***mah-2 X – 1.32 cn110***

: ts, sd; rigid paralysis on shift to 30°C, reversible on shift-down. NA1. [[Hosono et al. 1985](#)]

***mai***

**m** itochondrial **A** TPase **i** nhibitor [BL].

***mai-1 X – 13.05***

NMK. Upstream transcript in operon with *gpd-2,3*; encodes predicted homolog of mitochondrial ATPase inhibitor, but lacks import signal. [[Spieth et al. 1993](#)]

***mal***

**m** aternal effect m **al** formed (morphologically abnormal) [MQ].

***mal-1 IV 9.5 qm27***

: variable, dorsal protrusions on head and tail, head frequently twisted; high embryonic and larval lethality; full zygotic and maternal rescue. NA1. [[Hekimi et al. 1995](#)] [MQ]

***mal-2 V 24 qm31***

: variably deformed; frequently hypertrophic ventral side of head; high embryonic and larval lethality; no zygotic rescue, full maternal rescue. OA2: *qm16, qm35*. [[Hekimi et al. 1995](#)] [MQ]

***mal-3 I 0.8 qm34***

: head frequently deformed because buccal opening displaced ventrally, dorsally, or laterally; some embryonic lethality, very high larval lethality; full zygotic and maternal rescue. NA1. [[Hekimi et al. 1995](#)] [MQ]

***mal-4 II 0.7 qm36***

: hypertrophic left side of the head, usually anterior to terminal bulb of **pharynx**; high larval lethality; full zygotic and maternal rescue. NA1. [[Hekimi et al. 1995](#)] [MQ]

***mau***

**ma** ternal effect **u** ncoordinated [MQ].

***mau-1 V – 19.5 e2507***

: variable Unc (kinking, coiling, or paralysis); Egl; neuroanatomical defects; some lethality; full zygotic and maternal rescue. OA1: *qm6*. [[Hekimi et al. 1995](#)] [MQ]

***mau-2 I 2.42 qm4***

: kinky Unc, Egl; neuroanatomical defects; short **excretory** canals; Egl; some lethality; full zygotic rescue, almost complete maternal rescue, no maternal rescue of Egl. OA2: *qm5, qm40*. [[Hekimi et al. 1995](#)] [MQ]

***mau-3 IV 3.5 qm10***

: Unc, progressive paralysis, abnormal muscle anatomy; full zygotic and maternal rescue. NA1. [[Hekimi et al. 1995](#)] [MQ]

***mau-4 X 24 qm45***

: Unc, stiff posterior body, withered tail; some lethargy; full zygotic rescue, almost complete maternal rescue. OA2: *qm18, qm19* (both ts alleles, wt at 15°C, mutant 20°C, lethal 25°C). [[Hekimi et al. 1995](#)] [MQ]

***mau-5 III – 15 qm17***

: progressive sluggishness and jerky forward movement; Egl; abnormal muscle anatomy; full maternal and zygotic rescue. NA1. [[Hekimi et al. 1995](#)] [MQ]

#### ***mau-6 V 3 qm50***

: progressive paralysis, full paralysis, and rapid death after fourth molt; some larval lethality; complete zygotic rescue, almost complete maternal rescue. NA1. [[Hekimi et al. 1995](#)] [MQ]

#### ***mau-7 IV – 28 qm56***

: Unc, lethargic, kinky jerky ratchet-like movements in reverse; constipated ([E.p](#)); some lethality; full zygotic and maternal rescue. NA1. [[Hekimi et al. 1995](#)] [MQ]

#### ***mau-8 IV 3.45 qm57***

: Unc, lethargic, kinky jerky ratchet-like movements in reverse; constipated ([E.p](#)); some lethality; full zygotic and maternal rescue. NA1. [[Hekimi et al. 1995](#)] [MQ]

### ***mec***

**mec** hanosensory abnormality [TU]. Defects in avoidance response to light touch.

#### ***mec-1 V 0.62 e1066***

: (pka [che-4](#)) touch-insensitive; lethargic; microtubule cells lack extracellular mantle, often displaced; some amphidial neurons also displaced, defective fasciculation. ES2 ME2. OA>50: *e1292, e1336, u39amb*, etc. Most alleles resemble *e1066* but may lack amphidial [neuron](#) displacement. [[Perkins et al. 1986](#)]

#### ***mec-2 X – 4.61 u8***

: amb; touch-insensitive; lethargic. ES2. OA>50: *e75* (pka [che-9](#); recessive, ME3), *u7cs, e1084* (probable null), *e1514, e1608dm, u284sd*, etc. Alleles vary in phenotype from weak recessive to strong dominant Mec; complex complementation. CLONED: encodes predicted 440-aa protein with central similarity to human stomatin (65% identity over 247 aa); *mec-2:lacZ* expressed in cell bodies and processes of [touch cells](#), some other neurons. [[Chalfie and Au 1989; Huang et al. 1995](#)] [TU]

#### ***mec-3 IV 4.63 e1338***

: touch-insensitive; lethargic; microtubule cells small and lacking processes, [ALM](#) and [PLM](#) cells displaced. ES2 ME2. OA>10: *e1498, e1612, u467amb*, etc. Also revertant allele *e1498u124* ([ALM](#) and [PLM](#) processes abnormally long). CLONED: encodes LIM class homeoprotein, expressed in [touch receptors](#), FLP, [PVD](#); extensive molecular analysis. [[Way and Chalfie 1989; Xue et al. 1993; Wang and Way 1996](#)] [JW, TU]

#### ***mec-4 X 24.08 u52***

: amb; touch-insensitive; lethargic. ES2 ME2. OA>50: *e1339* (weak allele, sometimes touch sensitive in tail), *e1497, u45ts*, etc. Also dominant Deg alleles: *e1611dm* (pka [mec-13](#), touch-insensitive, microtubule cells become vacuolated and die in *e1611* and *e1611/+*; neomorphic. ES2 ME3. Intragenic revertants (e.g., *e1611 e1879*) resemble *u52*. OA2 (dominant). CLONED: encodes protein related to mammalian ENaC sodium channel subunit; *deg* alleles are bulky missense changes at A442; see also *deg-1, mec-10*. [[Driscoll and Chalfie 1991; Hong and Driscoll 1994; Lai et al. 1996](#)] [TU, ZB]

#### ***mec-5 X 22.41 e1340***

: touch-insensitive; lethargic; mantle of microtubule cells not stained by peanut lectin. ES2 ME3. OA>30: *e1503ts, e1504, e1790*, etc. (many are ts). CLONED: encodes 329-aa collagen. [[Chalfie and Au 1989; Huang and Chalfie 1994; Du et al. 1996](#)] [TU]

#### ***mec-6 I 1.46 e1342***

: touch-insensitive; lethargic; suppresses Deg phenotype of [mec-4](#) (dm), [deg-1](#) (dm), [deg-2](#) (dm). ES2 ME3. OA>10: *e1609spo, u247ts* (may be Mec only in head), *e1472, u450gri* (deletion null), etc. CLONED: encodes

degenerin homolog, related to MEC-4, MEC-10. [[Chalfie and Au 1989](#); [Huang and Chalfie 1994](#)] [MP, TU, ZB]

#### ***mec-7 X – 1.31 e1343***

: sd, ts; touch-insensitive; lethargic at 25°C; microtubule cells lack 15-protofilament microtubules; *e1343*/+ variably touch-insensitive at 25°C, wt at 15°C. ES2 ME3. OA>30: *n434dm* (dominant at all temperatures), *e1506* (recessive at all temperatures), *e1527*, *u278* (missense, causes ectopic touch cell branching), *u443* (deletion null), etc. Most alleles incompletely dominant and ts. CLONED: encodes β-tubulin; antibody stains strongly in [touch cells](#), weakly in some others (FLP, [PWD](#)); 45 alleles sequenced. [[Savage et al. 1989](#); [Hamelin et al. 1992](#); [Gu et al. 1996](#)] [NW, TU]

#### ***mec-8 I 3.70 e398***

: amb; touch-insensitive; lethargic; disrupted fasciculation of amphid and phasmid channel cilia; Dyr, synthetic-lethal with some [unc-52](#) alleles (*e444*); Pat. ES2 ME2. NA16: *mn364* (recessive-lethal, Pat), *mn412* (Mel, Gro), *u74*, *u456*, *rh170*, *mn472*, *u391*. See also *smu*. CLONED: encodes protein with two copies of RNP-predicted RNA-binding domain. [[Perkins et al. 1986](#); [Lundquist et al. 1996](#)] [SP, NJ, EH, TU]

#### ***mec-9 V 2.11 u27***

: amb; touch-insensitive; lethargic. ES2 ME2. OA>30: *e1494*, *e1852*, *u164amb*, etc. CLONED: 2-kb and 3-kb transcripts, trans-spliced to SL1 and SL2, encode protein with Kunitz-type serine protease inhibitor domains, EGF-like repeats; *mec-9*:GFP expressed in [touch cells](#) and [PWD](#) (3-kb promoter) or more extensively (2-kb promoter). [[Chalfie and Au 1989](#); [Huang and Chalfie 1994](#); [Du et al. 1996](#)] [TU]

#### ***mec-10 X – 0.57 e1515***

: touch-insensitive; lethargic. ES2 ME3. OA5: *e1715*, etc. CLONED: encodes 724-aa degenerin protein, related to MEC-4, DEG-1, vertebrate ENaC sodium channel components. [[Huang and Chalfie 1994](#)] [MP, TU, ZB]

#### ***mec-11***

= *mec-7*

#### ***mec-12 III – 10.34 e1605***

: touch-insensitive; lethargic. ES2 ME3. NA15: *e1607* (weaker allele), *u94sd* (*u94*/+ touch-insensitive in head only), *u247sd*, etc. Weak alleles often lack synaptic branch of [AVM](#); strong alleles have few microtubules in microtubule cell processes, no 15-protofilament microtubules. CLONED: encodes α-tubulin (pka [tba-3](#)); *mec-12:lacZ* expressed in [touch cells](#), some other [neurons](#) also. [[Chalfie and Au 1989](#); [Gu et al. 1996](#)] [NW, SQ, TU]

#### ***mec-13***

= *mec-4*

#### ***mec-14 III – 0.76 u55***

: touch-insensitive; lethargic. ES2. OA8: *u82*, *u296*, etc. [[Chalfie and Au 1989](#); [Huang and Chalfie 1994](#); [Gu et al. 1996](#)] [TU]

#### ***mec-15 II 1.83 u215***

: ts; touch-insensitive; lethargic. ES2 (25°C). OA4: *u75*, etc. (all alleles partially ts). [[Chalfie and Au 1989](#); [Huang and Chalfie 1994](#); [Gu et al. 1996](#)] [TU]

#### ***mec-16***

= *tab-1*

#### ***mec-17 IV 3.55 u265***

: larvae touch-sensitive, older animals touch-insensitive; *mec-3:lacZ* expression not maintained in [touch cells](#). NA1. [[Chalfie and Au 1989](#); [Way and Chalfie 1989](#)] [TU]

#### ***mec-18 X N u228***

: touch-insensitive; lethargic. OA5: *u69*, *u138*, *u182*, etc. [[Chalfie and Au 1989](#); [Huang and Chalfie 1994](#); [Gu et al. 1996](#)] [TU]

#### ***mef***

related to vertebrate **MEF** 2 transcription factors [KM].

#### ***mef-2 I 3.4***

NMK. Encodes homolog of vertebrate MEF2; *lacZ* fusions indicate transcription after 1.5-fold stage in a few head cells, more extensive in most tissues except gut from 3-fold stage on, to adulthood; cosmid F27D1. [KM]

#### ***mei***

**mei** otic abnormality [KK].

#### ***mei-1 I 2.61 b284***

: Mel, embryonic lethality, abnormal oocyte meiosis leading to lethal aneuploidy; normal male meiosis. OA>20: *ct46dm,ts* (gf allele, normal meiosis followed by abnormal mitoses), intragenic revertants of *ct46*, e.g., *ct44 ct99* (putative null, abnormal meiosis), *ct46 ct82* (antimorphic), *ct46 ct103* (viable, weak Him), additional phenotypic classes. See also *mei-2*, *mel-26*, *zyg-9*. CLONED: two transcripts encoding 472- and 475-aa predicted proteins with similarity to ATPases; antibody stains meiotic spindles I and II. [[Mains et al. 1990b](#); [Clark-Maguire and Mains 1994a,b](#)] [HR]

#### ***mei-2 I 1.24 ct102***

: Mel, embryonic arrest as mass of cells without morphogenesis; abnormal oocyte meiosis; dominant suppressor of [\*mei-1\*](#) (dm), [\*mel-26\*](#) (dm). OA1: *ct98* (dominant suppressor of [\*mei-1\*](#) [dm], slight recessive Mel, weak Him, viable). [[Mains et al. 1990b](#)] [HR]

#### ***mek***

**M** AP kinase kinase or **e** rk **k** inase [MH].

#### ***mek-1 ?***

NMK. Encodes predicted protein related to mammalian MEK. [MH, MT, FK]

#### ***mek-2 I – 5.55 n2678***

: sterile, Vul; suppresses Muv phenotype of [\*let-60\* \(gf\)](#). OA: *h294* (pka [\*let-537\*](#)), *n2156* (both similar to *n2678*), *n1859*, *n1989*, *n2537* (weaker allele, some fertility), *n1859*, *n1989* (weak alleles, homozygous viable but much early larval lethality, rod-like morphology), *q425* (pka *glv-1*, sterile Vul adult hermaphrodite, makes sperm but no oocytes, all [\*VPC\*](#) tertiary), *ku114* (viable, suppresses [\*let-60\* \(gf\)](#)), etc. CLONED: 55% identity to human MEK1. [[Church et al. 1995](#); [Kornfeld et al. 1995a](#); [Wu et al. 1995](#)] [EJ, KR, MH, MT]

#### ***mel***

**m** aternal- **e** ffect- **I** ethal [KK].

#### ***mel-1 II – 0.33 it19***

: strict maternal-effect embryonic-lethal. OA1: *b315*. [[Kemphues et al. 1988a](#)]

#### ***mel-2 II LC it20***

: strict maternal-effect embryonic-lethal. OA1: *it22*. [[Kemphues et al. 1988a](#)]

***mel-3* II – 0.33 *b281***

: strict maternal-effect embryonic-lethal. OA1: *it8*. [Kemphues et al. 1988a]

***mel-4* II LC *it43***

: strict maternal-effect embryonic-lethal. OA1: *it12ts* (6% viable). [[Kemphues et al. 1988a](#)]

***mel-5* II LC *b314***

: maternal-effect embryonic-lethal, some zygotic rescue. NA1. [[Kemphues et al. 1988a](#)]

***mel-6***

= *mel-8*

***mel-7* II LC *it36***

: strict maternal-effect embryonic-lethal. NA1. [[Kemphues et al. 1988a](#)]

***mel-8* II 1.12 *it39***

: maternal-effect embryonic-lethal, 71% zygotic rescue by mating with males. OA>15: *b312* (stronger allele, only 19% rescue), *it3*, *it27* (pka *mel-6*), *t1120*, *t1152*, etc. Highly mutable gene. [[Kemphues et al. 1988a](#)] [GE]

***mel-9* II 1.12 *b293***

: ts; maternal-effect embryonic-lethal, some escapers; reasonable zygotic rescue. NA1. [[Kemphues et al. 1988a](#)]

***mel-10* II 0.57 *it10***

: maternal-effect embryonic-lethal (0.5% hatch), no zygotic rescue. NA1. [[Kemphues et al. 1988a](#)]

***mel-11* II 1.12 *it26***

: maternal-effect embryonic-lethal, extensive zygotic rescue. NA1. [[Kemphues et al. 1988a](#)]

***mel-12* II 0.57 *it42***

: maternal-effect embryonic-lethal, leaky, some zygotic rescue. NA1. [[Kemphues et al. 1988a](#)]

***mel-13* II 3.36 *b306***

: strict maternal-effect embryonic-lethal. NA1. [[Kemphues et al. 1988a](#)]

***mel-14* II RC *it24***

: maternal-effect embryonic-lethal (0.2% egg hatch), slight zygotic rescue. OA2: *b291*, *b292*. [[Kemphues et al. 1988a](#)]

***mel-15* II 5.62 *it38***

: maternal-effect embryonic-lethal, leaky. OA1: *it7ts* (0.9% egg hatch at 25°C, extensive zygotic rescue). [[Kemphues et al. 1988a](#)]

***mel-16* II RC *b298***

: maternal-effect embryonic-lethal. NA1. [[Kemphues et al. 1988a](#)]

***mel-17* II RC *b299***

: maternal-effect embryonic-lethal, leaky, some zygotic rescue. NA1. [[Kemphues et al. 1988a](#)]

***mel-18* II 3.37 *b300***

: maternal-effect embryonic-lethal, slight zygotic rescue. NA1. [[Kemphues et al. 1988a](#)]

***mel-19* II 3.37 *b310***

: maternal-effect embryonic-lethal, leaky, no zygotic rescue. NA1. [[Kemphues et al. 1988a](#)]

***mel-20* II RC *b317***

: maternal-effect embryonic-lethal, complete zygotic rescue. NA1. [[Kemphues et al. 1988a](#)]

***mel-21***

= *mex-1*

***mel-22* II 5.62 *it30***

: maternal-effect embryonic-lethal, no zygotic rescue. NA1. [[Kemphues et al. 1988a](#)]

***mel-23* III 3.83 *ct45***

: dm, ts; dominant maternal-effect-lethal at 25°C, recessive nonconditional lethal; at 25°C, all embryos from *ct45*/+ mothers have early defects, arrest at 28-cell stage; also dominant zygotic defects in [male tail](#). NA1. [[Mains et al. 1990a](#)] [HR]

***mel-24* IV 4.05 *ct59***

: sd, ts; dominant maternal-effect-lethal, variable; at 25°C, many progeny from *ct59*/+ mothers arrest during embryogenesis; homozygotes nonconditional Mel. NA1. [[Mains et al. 1990a](#)] [HR]

***mel-25* V 2.87 *ct60***

: dm, ts; dominant maternal-effect-lethal at 25°C, recessive nonconditional sterile; at 25°C, progeny from *ct60*/+ mothers have early defects, arrest at early morphogenesis; also dominant zygotic defects in [male tail](#). [[Mains et al. 1990a](#)] [HR]

***mel-26* I 3.56 *ct61***

: dm, ts; dominant maternal-effect-lethal; at 25°C, most embryos from *ct61*/+ mothers have early cleavage defects, arrest prior to morphogenesis; at 15°C, impenetrant maternal-effect Vab; more severe defects in progeny from homozygous mothers. OA1: revertant *ct61sb4* is a recessive maternal-effect-lethal. [[Mains et al. 1990a](#)] [HR]

***mel-27* III – 1.07 *e2561***

: mm; embryos arrest with about 100 cells that do not adhere to each other and resemble a bag of marbles; no tissue differentiation; homozygous mutant mothers slightly clear and sick, with [hypodermis](#) variably pulled away from cuticle along the body. NA1. [JA]

***mel-28* III – 2.38 *e2567***

: mm; polar bodies sometimes large, mitotic spindles look weak; DNA does not separate properly at mitotic divisions when viewed in tubulin/DNA-stained embryos; globs of DNA can be seen at midbodies, and sometimes most of the DNA goes to one cell. NA1. [JA]

***mel-29* V 2.22 *e2596***

: mm; embryos arrest as balls of cells with gut granules, twitching, [hypodermis](#), and [neurons](#), but they appear to lack pharyngeal tissue. NA1. [JA]

***mel-30* II 1.98 *e2595***

: mm; embryos arrest as balls of cells with gut granules, twitching, [hypodermis](#), and [neurons](#), but apparently lacking pharyngeal tissue; founder cell divisions slow relative to P-cell divisions. NA1. [JA]

***mel-31* III – 2.2 *s2438***

: variable sterile or Mel (embryonic-lethal). NA1. [BC]

## **mes**

**m** aternal- **e** ffect **s** terile [SS].

### **mes-1 X 6.31 bn7**

: ts; grandchildless; at 25°C, 70% of progeny develop into sterile adults; P<sub>2</sub> and P<sub>3</sub> divisions variably defective, P<sub>4</sub> transformed into D-like muscle precursor, generating additional muscle cells, no [germ cells](#). OA9: [bn74](#) (deletion null, ts impenetrant Mes resembling *bn7*), *bn24*, *q222*, etc. (all ts, impenetrant). CLONED: cosmid rescue (C38D5). [[Strome et al. 1995](#)]

### **mes-2 II 23.01 bn11**

: grandchildless; progeny undergo normal embryogenesis but develop into agametic adults; few [germ cells](#) made; XO germ line less affected; normal P granule staining. OA2: *bn27*, *bn48*. CLONED: 2.5-kb transcript, encodes SET domain protein, closest similarity to *Drosophila* Enhancer of zeste. [[Capowski et al. 1991](#)] [SS]

### **mes-3 I – 0.38 bn35**

: grandchildless; progeny undergo normal embryogenesis but develop into agametic adults; few [germ cells](#) made; normal P granule staining; XO germ line less affected. OA4: *bn53* (stronger allele), *bn21ts* (100% sterile 25°C, 2% 16°C; T-shift suggests action in early embryo). CLONED: 3.1-kb transcript, encodes predicted 754-aa novel protein; transcripts not restricted to germ line; in operon with *dom-3*. [[Capowski et al. 1991](#); [Paulsen et al. 1995](#)] [SS]

### **mes-4 V 5.29 bn50**

: grandchildless; progeny undergo normal embryogenesis but develop into agametic adults (only ten [germ cells](#) made); normal P granule staining; XO germ line much less affected. OA3: *bn23*, *bn58*, *bn67* (all similar). [[Capowski et al. 1991](#)] [SS]

### **mes-5 III – 1.69 bn37**

: ts; grandchildless; progeny undergo normal embryogenesis but develop into agametic adults. [[Capowski et al. 1991](#)] [SS]

### **mes-6 IV 3.92 bn66**

: grandchildless; progeny undergo normal embryogenesis but develop into agametic adults. OA3: *bn38*, *bn64*, *bn69*. CLONED: encodes predicted protein with WD40 repeats.; in operon with *dom-6*. [[Capowski et al. 1991](#)] [SS]

## **mev**

**me** thyl **v** iologen (paraquat) resistance abnormal [TK].

### **mev-1 III 2.33 kn1**

: 4-fold increase in paraquat sensitivity; hypersensitive to high oxygen concentration; reduced brood size, reduced life span, increased age-associated fluorescence; rare supernumerary divisions in gut cells. [[Honda et al. 1993](#)] [TK, TM]

### **mev-2 X – 18.74 kn2**

: increased paraquat sensitivity. [TK, TM]

### **mev-3 I 0.51 kn3**

: increased paraquat sensitivity, hypersensitive to oxygen. [TK, TM]

## **mex**

**m** uscle in **ex** cess [JJ].

***mex-1* II 5.38 zu121**

: maternal-effect-lethal mutation, resulting in four [AB](#) granddaughters of the eight-cell-stage embryo following a pattern of development nearly identical to the posterior blastomere [MS](#); this results in embryos that produce excess muscle and [pharynx](#). OA9: zu120, zu122, zu140, zu173, zu221, it9 (pka [mel-21](#)). [Mello et al. 1992b] [JJ, KK]

***mex-2* II N**

: Mutation maternal-effect-lethal, leading to production of excess muscle cells, like Mex-1. [JJ]

***mex-3* I – 17.42 zu142**

: maternal-effect-lethal mutations, resulting in the production of excess muscle; excess muscle derived from the anterior blastomere [AB](#) of the two-cell-stage embryo. OA8: zu155, zu203, zu205, zu208, zu211, etc. CLONED: encodes novel predicted protein with two KH domains; mRNA accumulates at anterior pole of [zygote](#) after fertilization. [JJ]

***mig***

cell [mig](#) ration abnormal [CB].

***mig-1* I – 16.68 e1787**

: abnormal migration of Q [neuroblasts](#) (both [QL](#) and [QR](#) migrate anteriorly); HSN migration also abnormal; Egl. ES1. OA3: n1354, n1654. [Hedgecock et al. 1987; Desai et al. 1988] [NJ]

***mig-2* X N rh17**

: variable abnormal migration of Q [neuroblasts](#), HSN cells, CAN cells, etc.; Egl; uncoordinated; axon defects. OA1. [Hedgecock et al. 1987; Desai et al. 1988] [NJ]

***mig-3***

= *unc-39*

***mig-4* III 5.2 rh51**

: phenotype resembles Dig-1; gonad primordium detached from body wall in embryo, variable attachment in mid-L1; abnormal [Z1](#) and [Z4](#) migrations; [pharynx](#) twisted. OA1. [Hedgecock et al. 1987] [NJ]

***mig-5* II 0.79 rh147:**

ts, mat; complex phenotype, abnormal cell migrations; cell lineage and cell fate defects; often two linker cells in male; *rh147/Df* similar; both maternal and zygotic rescue. OA1: *rh94* (weaker). CLONED: encodes predicted 666-aa intracellular protein; three domains with high similarity to *Drosophila* Dishevelled, Discs large. [Hedgecock et al. 1987] [NJ]

***mig-6* V 1.02 e1931**

: [distal tip cells](#) fail to migrate, sterile. OA2: *oz90*, *oz113*. [Hedgecock et al. 1987] [NJ, BS]

***mig-7***

= *daf-12*

***mig-8* X – 2.07 rh50**

: [distal tip cells](#) fail to reflex, fail to express *unc-5:lacZ*; see also *daf-12*. [Hedgecock et al. 1987] [NJ]

***mig-10* III – 0.31 ct41**

: incomplete CAN, HSN, [ALM](#) migrations; shortened [excretory](#) canals; additional defects; mosaic analysis indicates nonautonomy, possible hypodermal focus. OA1: *e2527*. CLONED: encodes predicted 650-aa

protein with similarity to human Grb7, Grb10, including pleckstrin homology domain. [[Desai et al. 1988](#)] [LK]

***mig-11* III – 1.42 *ct78***

: defective CAN migrations; other migrations defective at low penetrance. [LK, CX]

***mig-12* II N *n1706***

: defective HSN migration, Egl, insensitive to serotonin. OA1 (*mu71*). [[Desai et al. 1988](#)] [CF]

***mig-13* X – 5.78 *mu31***

: defects in migration of cells descended from [QR](#); positions of a few other cells (BDU, [ALM](#), left [coelomocytes](#)) sometimes abnormal; HSN wt. [CF]

***mig-14* II 20.84 *mu71***

: [QL](#) descendants migrate to anterior, [QR](#) descendants and HSNs have shortened migrations, BDU posteriorly displaced; mild Egl. [CF]

***mig-15* X 1.63 *rh148***

: [QL](#) migration resembles [QR](#); pleiotropic defects in [hypodermis](#). [CF]

***mlc***

***m*** yosin ***I*** ight ***c*** hain [TR].

***mlc-1* X 24.11**

: Deletion mutants (e.g., *sup-10* [*n184*]) viable, normal muscle; increased lethality of [mlc-2](#) (0); resembles mammalian nonmuscle MLC; expressed in both [pharynx](#) and body wall; not *trans*-spliced. [[Cummins and Anderson 1988](#)] [TR]

***mlc-2* X 24.11**

: Deletion mutant exhibits pharyngeal pumping defect, 10% reach fertile adulthood (most males reach adulthood); deletion of both [mlc-1](#) and [mlc-2](#) leads to lethal arrest as short lumpy paralyzed L1/L2; resembles mammalian nonmuscle MLC; expressed in both [pharynx](#) and body wall; SL1 *trans*-spliced. [[Cummins and Anderson 1988](#); [Rushforth et al. 1993](#)] [TR]

***mlc-3* III – 0.61**

NMK. Encodes alkali (essential) MLC; >40% identity to vertebrate and invertebrate MLC; transcripts of 1.05 and 0.75 kb. [TR]

***mog***

***m*** asculinization ***o*** f ***g*** erm line [JK].

***mog-1* III 0.99 *q223***

: hermaphrodite germ line makes 300–500 sperm, no oocytes; no somatic defects; males wt; *q223/Df* similar. OA5: *q151*, *q161*, *q370*, *q471* (all similar), *q473* (viable, some oogenesis, more at 15°C). *mog-1;fem-1* or *mog-1;fem-3* double-mutant hermaphrodites make oocytes, but are Mel (variable embryonic arrest). [[Graham and Kimble 1993](#)]

***mog-2* II – 4.66 *q75***

: ts Mog; at 25°C, hermaphrodite germ line makes mostly sperm, rare abnormal oocytes; mostly fertile at 15°C, but no viable progeny (Mel); also Mel if feminized by [fem-3](#). NA1. [[Graham et al. 1993](#)]

***mog-3* III – 3.02 *q74***

: ts Mog; at 25°C, most hermaphrodites make only sperm, 13% make "oooids"; at 15°C, fertile but Mel; also Mel if feminized by *fem-3*. NA1. [[Graham et al. 1993](#)]

#### ***mog-4 II 24.00 q233***

: ts Mog; at 25°C, incompletely penetrant Mog; hermaphrodite germ line makes mostly sperm, some abnormal oocytes; at 15°C, sterile, non-Mog; Mel if feminized by *fem-3*. NA1. [[Graham et al. 1993](#)]

#### ***mog-5 II – 0.87 q449***

: ts Mog; at 25°C, fully penetrant Mog; hermaphrodite germ line makes only sperm; at 15°C, sterile non-Mog; Mel if feminized by *fem-3*. NA1. [[Graham et al. 1993](#)]

#### ***mog-6 II 2.86 q465***

: ts Mog; at 25°C, fully penetrant Mog; hermaphrodite germ line makes only sperm; at 15°C, sterile non-Mog; Mel if feminized by *fem-3*. NA1. [[Graham et al. 1993](#)]

#### ***mom***

**m ore o f M S** (additional [MS](#)-like pharyngeal tissue) [JJ].

#### ***mom-1 X – 3.2 zu188***

: pka *bop-1*, maternal-effect embryonic-lethal; E blastomere makes pharyngeal and muscle tissue (similar to [MS](#) blastomere); cleavage plane of ABar also altered. OA7: *or10, or46, or65, or70, se2, zu204, zu237*. [JJ]

#### ***mor***

**mor** phological abnormality (round nose) [CB].

#### ***mor-1 III 1.29 e1071***

: head less pointed than wt, slightly rounded nose, especially at 25°C. ES2 (adult) ME3 NA1. [[Lewis and Hodgkin 1977](#); [Hodgkin 1983](#)]

#### ***mor-2 IV 2.04 e1125***

: head less pointed than wt, rounded nose. ES2 (adult) ME3. OA1: *e2015* (similar). [[Hodgkin 1983](#)]

#### ***mpk***

**m a p k** inase [SD].

#### ***mpk-1 III – 3.80 ku1***

: (pka [sur-1](#)) suppresses activated *ras* ([let-60 \[gfl\]](#)), variable Vul, cs Egl, rod-like early larval lethality phenotypes; impenetrant defects in [P6.p](#) lineage. OA>10: *ku30* (lineage defects), *ku33, ku34, ku38* (all Egl), *n2521* (activated *ras* suppressor, normal lineage alone; mosaic analysis indicates cell autonomy), *oz140, pk79tci*, etc. CLONED: encodes 375-aa predicted protein, 75–80% identical to mammalian MPK, closest to ERK2 subfamily. [[Lackner et al. 1994](#); [Wu and Han 1994](#)] [MH, MT, SD]

#### ***mpk-2 II – 2.84***

NMK. Encodes predicted MAP kinase. [[Lackner et al. 1994](#)] [SD]

#### ***mrp***

**m ultidrug r esistance associated p rotein family** [NL].

#### ***mrp-1 X N***

: Deletion allele viable, increased sensitivity to cadmium and arsenite; encodes predicted protein similar to human MRP. [NL]

#### ***mrp-2 X N***

NMK. Encodes predicted protein similar to human MRP. [NL]

***mrp-3* ?**

NMK. Encodes predicted protein similar to human MRP. [NL]

***mrp-4* ?**

NMK. Encodes predicted protein similar to human MRP. [NL]

***msp***

**m ajor s perm p rotein** [BA].

***msp-3 II – 3.57***

NMK. Encodes major sperm protein MSP (16 kD); in cluster of three genes including *msp-3*. [[Ward et al. 1988](#)] [BA]

***msp-10 IV 4.58***

NMK. Encodes MSP (16 kD); *msp-56* cluster. [[Ward et al. 1988](#)] [BA]

***msp-19 IV 1.61***

NMK. Encodes MSP (16 kD); *msp-113* cluster. [[Ward et al. 1988](#)] [BA]

***msp-24 IV 4.58***

NMK. Transcribed pseudogene for MSP; *msp-77* cluster. [[Ward et al. 1988](#)] [BA]

***msp-29 II – 3.0***

NMK. Encodes MSP (16 kD); *msp-152* cluster. [[Ward et al. 1988](#)] [BA]

***msp-31 II – 3.0***

NMK. Encodes MSP (16 kD); *msp-152* cluster. [[Ward et al. 1988](#)] [BA]

***msp-32 II – 3.0***

NMK. Encodes MSP (16 kD); *msp-152* cluster. [[Ward et al. 1988](#)] [BA]

***msp-33 II – 3.0***

NMK. Encodes MSP (16 kD); *msp-152* cluster. [[Ward et al. 1988](#)] [BA]

***msp-36 IV 4.58***

NMK. Encodes MSP (16 kD); *msp-77* cluster. [[Ward et al. 1988](#)] [BA]

***msp-37 IV 4.58***

NMK. Pseudogene for MSP; *msp-77* cluster. [[Ward et al. 1988](#)] [BA]

***msp-38 IV 4.58***

NMK. Encodes MSP (16 kD); *msp-77* cluster. [[Ward et al. 1988](#)] [BA]

***msp-40 II – 3.7***

NMK. Encodes MSP (16 kD); *msp-3* cluster. [[Ward et al. 1988](#)] [BA]

***msp-41 II – 3.7***

NMK. Encodes MSP (16 kD); *msp-3* cluster. [[Ward et al. 1988](#)] [BA]

***msp-45 II – 2.69***

NMK. Encodes MSP (16 kD); defines *msp-45* cluster (five genes, one pseudogene). [[Ward et al. 1988](#)] [BA]

***msp-46* II – 3.0**

NMK. Encodes MSP (16 kD); [\*msp-45\*](#) cluster. [[Ward et al. 1988](#)] [BA]

***msp-47* II – 3.0**

NMK. Encodes MSP (16 kD); [\*msp-45\*](#) cluster. [[Ward et al. 1988](#)] [BA]

***msp-48* II – 3.0**

NMK. Pseudogene for MSP; [\*msp-45\*](#) cluster. [[Ward et al. 1988](#)] [BA]

***msp-49* II – 3.0**

NMK. Encodes MSP (16 kD); [\*msp-45\*](#) cluster. [[Ward et al. 1988](#)] [BA]

***msp-50* II – 3.0**

NMK. Encodes MSP (16 kD); [\*msp-45\*](#) cluster. [[Ward et al. 1988](#)] [BA]

***msp-51* IV 1.61**

NMK. Encodes MSP (16 kD); [\*msp-113\*](#) cluster. [[Ward et al. 1988](#)] [BA]

***msp-52* IV 1.61**

NMK. Encodes MSP (16 kD); [\*msp-113\*](#) cluster. [[Ward et al. 1988](#)] [BA]

***msp-53* IV 1.61**

NMK. Encodes MSP (16 kD); [\*msp-113\*](#) cluster. [[Ward et al. 1988](#)] [BA]

***msp-54* IV 1.61**

NMK. Encodes MSP (16 kD); [\*msp-113\*](#) cluster. [[Ward et al. 1988](#)] [BA]

***msp-56* IV 4.58**

NMK. Encodes MSP (16 kD); sequenced; defines [\*msp-56\*](#) cluster (three genes). [[Ward et al. 1988](#)] [BA]

***msp-60* II – 1.0**

NMK. Encodes MSP (16 kD); [\*msp-142\*](#) cluster. [[Ward et al. 1988](#)] [BA]

***msp-61* II – 1.0**

NMK. Pseudogene for MSP; [\*msp-142\*](#) cluster. [[Ward et al. 1988](#)] [BA]

***msp-62* II – 1.0**

NMK. Pseudogene for MSP; [\*msp-142\*](#) cluster. [[Ward et al. 1988](#)] [BA]

***msp-63* II – 1.0**

NMK. Pseudogene for MSP; [\*msp-142\*](#) cluster. [[Ward et al. 1988](#)] [BA]

***msp-64* II – 1.0**

NMK. Pseudogene for MSP; [\*msp-142\*](#) cluster. [[Ward et al. 1988](#)] [BA]

***msp-70* IV 4.6**

NMK. Pseudogene for MSP; [\*msp-77\*](#) cluster. [[Ward et al. 1988](#)] [BA]

***msp-71* II – 3.07**

NMK. Encodes MSP (16 kD); near [\*msp-152\*](#). [[Ward et al. 1988](#)] [BA]

***msp-72* V 2.39**

NMK. Pseudogene for MSP. [[Ward et al. 1988](#)] [BA]

***msp-74* II – 3.0**

NMK. Encodes MSP (16 kD); near [\*msp-45\*](#) . [Ward et al. 1988] [BA]

***msp-76* IV 4.58**

NMK. Encodes MSP (16 kD); near [\*msp-56\*](#) . [Ward et al. 1988] [BA]

***msp-77* IV 4.58**

NMK. Encodes MSP (16 kD); defines cluster of three genes, three pseudogenes. [Ward et al. 1988] [BA]

***msp-78* IV 4.58**

NMK. Encodes MSP (16 kD); near [\*msp-56\*](#) . [Ward et al. 1988] [BA]

***msp-81* IV 4.58**

NMK. Encodes MSP (16 kD); [\*msp-56\*](#) cluster. [Ward et al. 1988] [BA]

***msp-113* IV 1.61**

NMK. Encodes MSP (16 kD); defines cluster of at least six genes including [\*msp-19\*](#) and [\*msp-113\*](#) (both transcribed). [Ward et al. 1988] [BA]

***msp-142* II – 1.03**

NMK. Encodes MSP (16 kD); defines cluster of two genes, four pseudogenes including [\*msp-142\*](#) (transcribed). [Ward et al. 1988] [BA]

***msp-152* II – 3.21**

NMK. Encodes MSP (16 kD); defines cluster of five genes including [\*msp-152\*](#) (transcribed). [Ward et al. 1988] [BA]

***mtl***

**m** e **t** a **l**lothionein [CR].

***mtl-1* V 0.24**

NMK. Encodes 75-aa metallothionein; accumulates after exposure to CdCl<sub>2</sub>; *mtl-1:lacZ* expressed constitutively in [\*pharynx\*](#) and in [\*intestine\*](#) after cadmium treatment or heat shock; response lower in adult. [Freedman et al. 1993]

***mtl-2* V 5.79**

NMK. Encodes 63-aa metallothionein; accumulates after exposure to CdCl<sub>2</sub>; *mtl-1:lacZ* expressed in [\*intestine\*](#) after cadmium treatment or heat shock. [Freedman et al. 1993]

***mua***

**mu** scle **a** ttachment abnormal [NJ].

***mua-1* II – 0.04 *rh160***

: progressive paralysis, with loss of muscle-to-cuticle attachments; both muscle-muscle and muscle-[\*hypodermis\*](#) links lost from L2 onward; may lead to secondary Gon, Egl defects, etc.; detachment suppressed by muscle mutants such as [\*unc-54\*](#) ; *rh160/Df* similar. NA1. CLONED: encodes predicted 246-aa protein with three zinc fingers, Sp1 family. [NJ]

***mua-2* III 10.21 *rh119***

: progressive detachment of muscles during larval development. [NJ]

***mua-3* III 1.78 *rh169***

: progressive detachment of muscles during larval development, possibly defective in reformation of muscle-cuticle links at each molt. CLONED: encodes predicted 3617-aa protein with transmembrane domain, large extracellular domain containing 52 EGF repeats, 5 LDL repeats, etc. [NJ]

***mua-4* III – 1.79 *rh177* :**

progressive detachment of muscles during larval development. [NJ]

***mua-5* IV C *rh179***

: progressive detachment of muscles during larval development. OA1: *rh180*. [NJ]

***mua-6* X 23.52 *rh85***

: progressive paralysis, defective muscle attachments like Mua-1; poor growth; most homozygotes arrest as larvae; adults Egl; Smg-suppressible. NA1. [NJ]

***mua-7* III R**

Mutation leads to defective muscle attachment. [NJ]

***mud***

**m** aternal-effect **u** ncoordinated and **d** umpy [MQ].

***mud-1* III – 3.2 *qm21***

: hatchlings of variable length, very poor movement; adults short, kinky Unc; very high embryonic and larval lethality; full zygotic and maternal rescue, except for incomplete maternal rescue of Dpy phenotype. OA1: *qm22*. [[Hekimi et al. 1995](#)] [MQ]

***mum***

**m** aternal-effect **u** ncoordinated and **m** alformed (morphologically abnormal) [MQ].

***mum-1* IV 4.6 *qm32***

: variably deformed body, [pharynx](#); severe Unc, strong kinker or paralyzed; defects in neuroanatomy, [excretory](#) system, gonads; high embryonic and larval lethality; extensive (>95%) maternal and zygotic rescue; *qm32/Df* lethal. NA1. [[Hekimi et al. 1995](#)] [MQ]

***mum-2* IV 4.4 *qm33***

: variably deformed body, [pharynx](#); severe Unc, strong kinker or paralyzed; defects in neuroanatomy, [excretory](#) system, gonads; high larval lethality; extensive (>95%) maternal and zygotic rescue; *qm33/Df* sterile. NA1. [[Hekimi et al. 1995](#)] [MQ]

***mum-3* III 3 *qm46***

: variably deformed body, [pharynx](#); severe Unc, strong kinker or paralyzed; defects in neuroanatomy, [excretory](#) system, gonads; some larval lethality; complete maternal and zygotic rescue. NA1. [[Hekimi et al. 1995](#)] [MQ]

***mup***

**m** scle **p** ositioning abnormal [NJ].

***mup-1* II – 7.76 *e2430***

: ts; viable, inappropriately attached or detached muscles; dumpy; phenotype least severe at 20°C; suppressed by *dpy-2,10,11*; some maternal rescue; weakest allele. OA9: *e2485ts*, *e2436*, *e2347*, *e2434*, *e2439* (strong allele, mostly embryonic arrest at 3-fold stage or kinked L1, extensive misattachment of muscles), etc. [[Goh and Bogaert 1991](#)]

***mup-2* X – 2.89 *e2346***

: ts; embryonic temperature shift leads to lethal mispositioning and deformity of body-wall muscle; larval temperature shift leads to sterility, defects in oviduct muscle. OA1: *up7* (nonconditional, lethal with arrest as kinked larva; probable null, nonsense mutation). CLONED: encodes troponin T homolog. [[Myers et al. 1996](#)] [EE, UG]

### ***mup-4 III – 0.73 mg36***

: lethal, embryonic arrest at 3-fold, defective muscle attachment, abnormal [hypodermis](#); muscle cells collapse from ventral side, retract from head and tail; some embryos arrested earlier; mosaic analysis indicates focus in AB. OA>5: *ar60*, *mg23*, *mg36*, *s2433*, etc. [BC, EE, GR]

### ***mut***

**mut** ator [CB].

### ***mut-1 ? e1396***

: possible mutator locus. [DR]

### ***mut-2 I 2 r459***

: mutator, increased transposition of Tc1 and Tc3, Tc4, etc.; 1.7% Him. [[Collins et al. 1987](#)] [TW]

### ***mut-3 ? r456***

: mutator, increased transposition of Tc1; 1.5% Him. [[Collins et al. 1987](#)]

### ***mut-4 I 1.5 st700***

: mutator, increased transposition of Tc1. [[Mori et al. 1988a](#)]

### ***mut-5 II 1 st701***

: mutator, increased transposition of Tc1; *mut-4* -derived. [[Mori et al. 1988a](#)]

### ***mut-6 IV 3 st702***

: mutator, increased transposition of Tc1; *mut-4* -derived. [[Mori et al. 1988a](#)]

### ***myb***

**myb** (vertebrate oncogene)-related [CGC].

### ***myb-2 X 21.83***

NMK. Possible *myb* homolog? [CGC]

### ***myo***

**myo** sin (heavy chain, class II) [CB].

### ***myo-1 I 1.86***

NMK (but may correspond to [let-75](#)). Encodes pharyngeal myosin. [[Dibb et al. 1989](#); [Avery 1993a](#); [Okkema et al. 1993](#)]

### ***myo-2 X 7.74***

NMK. Encodes pharyngeal myosin. [[Dibb et al. 1989](#); [Okkema and Fire 1994](#)]

### ***myo-3 V 3.79 st386***

: severe Pat (paralyzed embryonic arrest at 2-fold stage); very abnormal muscle ultrastructure, no MYO-3 staining. OA2 (Pat): *st563*, *st565*. Also duplication alleles: *e1407sd* (pka [sup-3](#)), partial suppressor of certain mutations of muscle genes *unc-15*, *unc-54*, *unc-87*, *e1390*, etc. Also supersuppressor alleles (unstable). All probably tandem duplications or further amplifications of [myo-3](#). See also [sus-1](#). [[Dibb et al. 1989](#); [Maruyama et al. 1989](#); [Williams and Waterston 1994](#)]

**myo-4**

= *unc-54*

**ncc**

**n**ematode **c**ell **c**ycle-associated [CB]. See also *cdc*.

***ncc-1 III 0.69***

NMK. Encodes 38-kD protein, homolog of fission yeast p34 cdc2 kinase, 65% identity to human cdc2 but has sequence PSTAVR rather than PSTAIR; can complement some alleles of budding yeast Cdc28p. [[Mori et al. 1994](#)] [PS]

**ncl**

**n**u **c**l eoli abnormal [CB].

***ncl-1 III – 0.60 e1865***

: abnormal large nucleoli in most cells; intestinal and germ-line nucleoli not markedly larger. ES1. Cell autonomous, widely used cell marker for mosaic analysis. OA1: *e1942* (similar phenotype). [[Herman 1989](#); [Hedgecock and Herman 1995](#)] [NJ]

***ncl-2 IV 4.14 e1896***

: abnormal refractile nucleoli especially in [germ cells](#); few ribosomes, abnormal nucleoli seen in EM sections; progressive deterioration; sterile. ES2 NA1. [NJ]

**nex**

an **nex** in family [CGC].

***nex-1 III – 2.1***

NMK. Encodes protein with 42% identity to bovine annexin IV; antibody stains pharyngeal grinder, gland cells, spermathecal folds. [[Creutz et al. 1996](#)] [CGC]

***nex-2 III 2.4***

NMK. Encodes predicted protein with annexin similarity. [[Creutz et al. 1996](#)] [CGC]

***nex-3 III – 3.7***

NMK. Encodes predicted protein with annexin similarity. [[Creutz et al. 1996](#)] [CGC]

**nhr**

**n**uclear **h**ormone **r**eceptor superfamily [AE].

***nhr-1 X 24.12 pk43***

: Tc1 insertion, no known phenotype; encodes member of nuclear hormone receptor superfamily (pka [crf-1](#)); predicted 439 aa; deletion (associated with [sup-10](#) [*n184*]) probably homozygous viable. [BH, AE]

***nhr-2 I 0.30***

NMK. Encodes member of nuclear hormone receptor superfamily (pka [crf-2](#)); 50% identity to mouse thyroid hormone receptor in zinc finger region; NHR-2 present in embryonic nuclei at two-cell stage, ubiquitous until gastrulation, later diminishes; transcript in maternal germ line; antisense expression leads to posterior necrosis in L4, adult. [[Seydoux and Fire 1994](#); [Seydoux et al. 1996](#)] [AE, GR]

***nhr-3 IV 4.58***

NMK. Nuclear hormone receptor superfamily. Cosmid ZZH8. [AE]

***nhr-4 X 17.00***

NMK. Nuclear hormone receptor superfamily. YAC Y52F5, etc. [AE]

***nhr-5 IV 13.02***

NMK. Nuclear hormone receptor superfamily. YAC Y73F8. [AE]

***nhr-6 III – 6.31***

NMK. Similarity to steroid hormone receptor. Sequenced: C48D5.1. Also named *ceb-1*, *cnr-8*. [[Kostrouch et al. 1995](#)] [AE]

***nhr-7 IV 4.98***

NMK. Nuclear hormone receptor superfamily. YAC Y72H7, etc. [AE]

***nhr-8 IV 3.41***

NMK. Nuclear hormone receptor superfamily. YAC Y50A3, etc. [AE]

***nhr-9 III – 0.78***

NMK. Nuclear hormone receptor superfamily. Sequenced: ZK418.1. [GR]

***nhr-10 III – 0.77***

NMK. Nuclear hormone receptor superfamily. Sequenced: B0280.8. [GR]

***nhr-11 IV 4.05***

NMK. Nuclear hormone receptor superfamily. YAC Y54B5. [AE]

***nhr-13 V – 14.96***

NMK. Nuclear hormone receptor superfamily. YAC Y50H8, etc. [AE]

***nhr-17 X 7.49***

NMK. Nuclear hormone receptor superfamily. Sequenced: C02B4.2 [AE]

***nhr-18 V – 14.54***

NMK. Nuclear hormone receptor superfamily. Cosmid W02G2. [AE]

***nhr-19 II 1.59***

NMK. Nuclear hormone receptor superfamily. Sequenced: E02H1.7 [AE]

***nhr-20 III – 3.81***

NMK. Nuclear hormone receptor superfamily. Sequenced: F43C1.4 [AE]

***nhr-21 II 0.35***

NMK. Nuclear hormone receptor superfamily. Sequenced: F21D12.1? [AE]

***nhr-22 II – 0.25***

NMK. Nuclear hormone receptor superfamily. Sequenced: K06A1.4 [AE]

***nmy***

n onmuscle my osin [CGC].

***nmy-1 X – 13.33***

NMK. Encodes predicted nonmuscle myosin heavy chain. [DU]

***nob***

k nob -like tail ( no b ackside) [BW].

***nob-1* III 13.89 *ct223***

: early L1-lethal with normal head, spherical gut, round posterior; defect in E cell arrangement at 100-cell stage; affects *pal-1:lacZ* expression; *ct223/Df* similar. OA2: *ct351* (similar), *ct230* (weaker, viable; abnormal tail, 65% fertile; males have missing rays, crumpled spicules). [BW]

***nob-2***

= *pal-1*

***nob-3* I 3.70 *ct315***

: homozygotes L1-lethal or embryonic-lethal, malformed posterior. CLONED: cosmid rescue. [BW]

***nob-5***

= *unc-62*

***nop***

no p pseudocleavage [KK].

***nop-1* III – 1.5 *it142***

: mat; embryos from homozygous *nop-1* mothers have no pseudocleavage contractions or furrow during the first cell cycle; abnormal actin distribution; normal cytoplasmic streaming and partition; 79% of embryos hatch and grow into fertile adults. [[Rose et al. 1995](#)]

***not***

no se t ouch response abnormal [KP].

***not-1***

= *eat-4*

***not-3***

= *glr-1*.

***nuc***

nuc lease [CB].

***nuc-1* X 7.05 *e1392***

: amb; major endodeoxyribonuclease reduced >95%; condensed chromatin persists after programmed cell death; DNA in intestinal lumen not degraded. ES1 ME3. OA2: *n887* (resembles *e1392*), *n334* (weaker allele). [[Hedgecock et al. 1983](#); [Ellis et al. 1991a](#)] [MT]

## O to R

***odc***

o rnithine d e c arboxylase [SF].

***odc-1* V 0.61 *pc13***

: null allele (partial excision of Tc1 insert *pk32*), no detectable ODC activity; no obvious phenotype; hermaphrodite brood size reduced 35%; encodes 423-aa protein, homologous to other eukaryotic ODCs. [[Macrae et al. 1995](#)] [SF]

***odr***

od o r ant response abnormal [CX].

***odr-1* X 12.52 *n1930***

: defective chemotaxis to some volatile odorants. OA2: *n1933*, *n1936* (similar). [[Bargmann et al. 1993](#)]

***odr-2 V 0.63 n1939***

: defective chemotaxis to some volatile odorants; *n1939/Df* similar. OA2: *n2148*, *n2145*. CLONED: encodes predicted ~200-aa protein, GPI-linked. [[Bargmann et al. 1993](#)] [CX]

***odr-3 V 4.40 n2150***

: reduced response to all volatile odorants; defective osmotic avoidance; some chemotactic defects; cilia of sensory [neuron](#) AWC stunted. OA1: *n2046* (weaker phenotypes). [[Bargmann et al. 1993](#)]

***odr-4 III – 0.90 n2144***

: defective chemotaxis to some volatile odorants; *n2144/Df* similar. NA1. [[Bargmann et al. 1993](#)]

***odr-5 X 1.64 ky9* :**

defective chemotaxis to some volatile odorants, same subset as Odr-1. NA1. [[Bargmann et al. 1993](#)]

***odr-7 X 7.90 ky4***

: defective chemotaxis to some volatile odorants; nonsense mutant. OA1: *ky55* (defective chemotaxis to diacetyl, other responses normal; missense). CLONED: encodes predicted protein with similarity to NHR DNA-binding domain; *odr-7*:GFP expressed only in AWA [sensory neurons](#). [[Sengupta et al. 1994](#)] [CX]

***odr-8 IV***

: Mutant phenotype resembles Odr-4. OA4. [CX]

***odr-9 ? ky27***

: diacetyl response defective. [CX]

***odr-10 X – 2.19 ky32***

: diacetyl response defective. [[Sengupta et al. 1996](#)] [CX]

***ogr***

**o**ocyte- and **g**erm-line- **r**elated [KK].

***ogr-1 V 5.79***

Tc1 insert, no phenotype; 3.3-kb transcript, oogenesis-associated; 2.8-kb ORF encoding novel predicted protein. [[Guo and Kemphues 1995](#)] [DT, KK]

***ooc***

**ooc**yte formation abnormal [SP].

***ooc-1 II 3.04 mn250***

: mat, mm; hermaphrodites lay fertilized eggs that do not hatch. ES3 (progeny) NA1. [[Sigurdson et al. 1984](#)]

***ooc-2 II 0.59 mn249***

: mat, mm; hermaphrodites lay fertilized eggs that do not hatch. ES3 (progeny) NA1. [[Sigurdson et al. 1984](#)]

***ooc-3 II 3.45 mn241***

: mat, mm; hermaphrodites lay fertilized eggs that do not hatch. ES3 (progeny) NA1. [[Sigurdson et al. 1984](#)]

***ooc-4 III 2.26 e2078***

: sterile, abnormal, or missing oocytes; some spermatogenesis; males fertile. [CB]

***ops***

**ops** in-related [CGC].

***ops-1 I 1.37***

NMK. Cross-hybridization to opsin probe. [BC]

***ops-2 V 1.06***

NMK. Cross-hybridization to opsin probe. [BC]

***ops-3 III 0.63***

NMK. Cross-hybridization to opsin probe. [BC]

***ops-4 III – 6.40***

NMK. Cross-hybridization to opsin probe. [BC]

***ops-5 X 2.45***

NMK. Cross-hybridization to opsin probe. [BC]

***ora***

**Onchocerciasis- related antigen family [MQ].**

***ora-1 IV 3.54 eDf28 :***

(pka e927) deletes [unc-24](#) and [ora-1](#), no apparent phenotype other than Unc-24; encodes predicted protein related to 22-kD antigenic protein from *Onchocerca volvulus*. [MQ]

***ora-2 X 18.0***

NMK. Encodes predicted protein related to [ora-1](#) and 22-kD antigenic protein from *Onchocerca*. Cosmid F40E10. [MQ]

***osm***

**osm** otic avoidance defective [PR].

***osm-1 X 23.99 p808***

: fails to avoid 4 M fructose or 4 M NaCl; poor chemotaxis to NaCl; normal thermotaxis; fails to take up FITC; Daf-d; severely shortened axonemes, ectopic assembly of ciliary structures and microtubules in many [sensory neurons](#). ES1 ME2. OA>10: *p816* (similar phenotype, lower fertility), *e1803*, *e1804*, *p808*, *p816*, *m530mut*, etc. CLONED: encodes predicted 1738-aa protein, very acidic; related to human brain protein of unknown function. [[Perkins et al. 1986](#); [Starich et al. 1995](#)]

**osm-2**

= *che-3*

***osm-3 IV – 2.26 p802***

: fails to avoid 4 M fructose or 4 M NaCl; nonchemotactic; defective dauer formation; normal thermotaxis; fails to take up FITC; eliminates distal segment of amphid channel; cilia in other ciliated [neurons](#) normal; octopamine-deficient. ES1 ME3. OA>7: *e1806*, *e1811*, *hf3* (pka [caf-1](#), resistant to 30 mM caffeine, Daf), etc. CLONED: encodes 672-aa kinesin-like protein; *osm-3:lacZ* expressed in all 26 [sensory neurons](#) with external openings. [[Tabish et al. 1995](#); [Starich et al. 1995](#)]

**osm-4**

= *daf-10*

***osm-5 X – 12.20 p813***

: fails to avoid 4 M fructose or 4 M NaCl; poor chemotaxis to NaCl; normal thermotaxis; fails to take up FITC; Daf-d; severely shortened axonemes, ectopic assembly of ciliary structures and microtubules in many [sensory neurons](#); also males suicidal, poor mating. ES1 ME1. OA>6: *m184, mn397*. [[Perkins et al. 1986](#); [Starich et al. 1995](#)] [SP, DR]

#### ***osm-6 V 3.44 p811***

: fails to avoid 4 M fructose or 4 M NaCl; poor chemotaxis to NaCl; normal thermotaxis; fails to take up FITC; Daf-d; severely shortened axonemes, ectopic assembly of ciliary structures and microtubules in many [sensory neurons](#). ES1 ME1. OA>6: *m511, m533mut*. CLONED: cosmid R07A10. [[Perkins et al. 1986](#); [Starich et al. 1995](#)] [SP, DR]

#### ***osm-7 III 21.48 n1515***

: defective osmotic avoidance; defective chemotaxis; slow pharyngeal pumping; FITC uptake normal. NA1. [CX, MT, JT]

#### ***osm-8 II 0.68 n1518***

: defective osmotic avoidance. NA1. [MT, JT]

#### ***osm-9 IV – 3.26 n1601***

: defective in osmotic avoidance, also in nose touch avoidance (Not); Adp (partly defective adaptation to isoamyl alcohol and butanone); normal chemotaxis. OA5: *n1516, n1603, n2473, ky10* (similar). [[Colbert and Bargmann 1995](#)] [JT, KP, MT]

#### ***osm-10 III – 0.65 n1602***

: specifically defective in osmotic avoidance; normal chemotaxis; normal garlic avoidance; normal nose touch response. NA1. CLONED: cosmid rescue. [[Bargmann et al. 1990](#)] [CX, KP]

#### ***osm-11 X 23.49 n1604***

: defective osmotic avoidance. NA1. [MT, JT]

#### ***osm-12 III 13.33 n1601***

: defective osmotic avoidance. NA1. [MT, JT]

#### ***ost***

**ost** eonectin [CGC].

#### ***ost-1 IV – 29.28***

NMK. Encodes predicted protein with 38% identity to mammalian extracellular matrix protein SPARC/Osteonectin; *ost-1:lacZ* expressed in [body wall muscle, vulval muscle](#); transgene overexpression leads to deformity, variable locomotion defects. [[Schwarzauer and Spencer 1993](#)]

#### ***pag***

**pa** ttern of reporter **g** ene expression abnormal [CGC].

#### ***pag-1 III – 1.88 ls2***

: homozygotes exhibit overexpression of [\*mec-7\*-\*lacZ\*](#) fusion transgene; recessive; some additional axonal defects. ES1 OA4. [EA]

#### ***pag-3 X 19.49 ls20***

: homozygotes exhibit misexpression of the [\*mec-7\*](#) gene, *mec-7 lacZ* and *mec-4 lacZ* fusion genes in the BDU [neurons](#); also causes a reverse kinked uncoordinated phenotype and occasional axonal guidance errors in the [PLM](#) and BDU [neurons](#). NA1. [[Jia et al. 1996](#)] [EA]

## ***pal***

**p**osterior **a**lae [CF].

### ***pal-1* III – 2.63 e2091**

: adult males lack V6-derived rays, alae extend into tail region; V6 lineage transformed into V1–V4; cell autonomous action; variable additional defects, some embryonic lethality. OA3: *mu13* (similar to e2091), *ct224* (pka [nob-2](#), lethal with arrest at hatching, severely deformed posterior, deletion null), *ct281*. CLONED: 1.25- and 1.45-kb transcripts, encode homeoprotein (pka [ceh-3](#)) with similarity to *Drosophila* Caudal, mouse Cdx-1. [[Waring and Kenyon 1991](#); [Waring et al. 1992](#)] [CF, BW]

### ***pal-2* IV 4.05 e2260**

: adult males have ectopic alae extending into tail region; slight ray abnormalities and mispositioning; tail [seam](#) probably transformed to body [seam](#); e2260/Df similar; hermaphrodite wt. ME2 NA1. [[Hodgkin et al. 1989](#)] [CB]

## ***par***

embryonic **par** titioning abnormal [KK].

### ***par-1* V 5.92 b274**

: mat; homozygous hermaphrodites produce embryos that arrest with many differentiated cells, no detectable gut granules; first cleavage symmetrical, defective P granule localization. ES3 (progeny). OA>10: *it51*, *it90* (both missense changes in kinase domain), *e2012*, *it32*, *it102*, *lw7* (leaky, Mes), *lw39gri* (deletion), etc. CLONED: 4.4-kb transcript, germ-line-enriched, encodes predicted 1192-aa Ser/Thr kinase; antibody staining indicates 126-kD protein with specific asymmetric membrane localizations in early blastomeres. [[Kemphues et al. 1988b](#); [Guo and Kemphues 1995](#)] [JJ, KK]

### ***par-2* III – 24.71 it46**

: ts, mat; homozygous hermaphrodites produce 90% (16°C) to 99% (25°C) arrested embryos, escapers sterile; abnormal early cleavages, both spindles transverse at second cleavage (failure of P<sub>1</sub> rotation), defective P granule localization. ES3 (progeny). OA7: *it5ts* (weaker phenotype), *e2030* (Mes, grandchildless), *it87* (weak), *jb2*, etc. All ts; temperature shift indicates not needed after second cleavage. CLONED: encodes predicted novel protein; antibody staining indicates specific asymmetric cortical localizations in early blastomeres. [[Cheng et al. 1995](#)] [KK]

### ***par-3* III – 1.44 e2074**

: amb; maternal-effect-lethal mutation, affects first two embryonic cell cycles; abnormal pseudocleavage, streaming, P granule localization; second cleavage spindle orientation variable, often both longitudinal (ectopic rotation in [AB](#)). OA5: *it54* (leaky, Mes), *it71amb* (null), *it62*, *it91*. CLONED: encodes predicted 138-kD novel protein; antibody staining indicates specific asymmetric peripheral localizations in early blastomeres. [[Cheng et al. 1995](#)] [KK]

### ***par-4* V 13.74 it47**

: ts; maternal-effect-lethal at 25°C; arrest as multicellular mass, no morphogenesis, no gut granules; abnormally small and round eggs; abnormal early cleavages, etc.; 4% hatch at 15°C, develop to sterile adult. OA9: *it33* (nonconditional, fully penetrant Mel; putative null); *it57ts* (viable at 15°C, Mel at 25°C), *it74*, *it75*, *it120*, etc. [[Morton et al. 1992](#)] [KK]

### ***par-5* IV 5.31 it55**

: maternal-effect-lethal; second cleavage spindles transverse, asters spherical (resembles Par-2); most embryos lack gut granules. OA1. [[Morton et al. 1992](#)] [KK]

### ***par-6* I 13.9 zu170**

: spo; maternal-effect-lethal, resembles Par-3 but terminal arrest with more gut differentiation; improper P granule localization; dominant suppressor of weak [par-2](#) mutations. OA2: zu174, zu222. [JJ, KK]

### ***pat***

**p**aralyzed **a**rrest at embryonic **t**wo-fold stage [RW].

#### ***pat-2 III – 0.02 st543***

: severe Pat phenotype; disrupted assembly of myofilament lattice. OA6: *st422, st538, st567* (weaker, some pharyngeal pumping), etc. CLONED: encodes  $\alpha$  integrin. [[Williams and Waterston 1994](#)] [RW]

#### ***pat-3 III – 4.52 st423***

: severe Pat phenotype; disrupted myofilament lattice. OA>8: *st564* (weaker allele), *st423, st552, st564, rh54* (embryonic-lethal, mosaic analysis indicates autonomous defects in cell attachment, morphogenesis, etc.), *rh151* (sterile), *rh96* (mild; short [excretory](#) canals, variable Mig defects). CLONED: 3-kb transcript, encodes  $\beta$  integrin. [[Williams and Waterston 1994](#); [Gettner et al. 1995](#)] [CF, NJ, RW]

#### ***pat-4 III – 27.19 st552***

: severe Pat phenotype. OA3: *st551, st579, st580* (all similar). [[Williams and Waterston 1994](#)] [RW]

### ***pat-5***

= *egl-19*

#### ***pat-6 IV – 28.00 st561***

: severe Pat phenotype. OA1: *st570* (weaker, some pharyngeal pumping). [[Williams and Waterston 1994](#)] [RW]

#### ***pat-8 IV 2.98 st554***

: severe Pat phenotype; some pharyngeal pumping. [[Williams and Waterston 1994](#)] [RW]

#### ***pat-9 X 23.00 st558***

: severe Pat phenotype; some pharyngeal pumping. [[Williams and Waterston 1994](#)] [RW]

#### ***pat-10 I – 0.47 st568***

: severe Pat phenotype; some pharyngeal pumping. OA1: *st575*. Probably corresponds to [tnc-1](#), encoding troponin C. [[Williams and Waterston 1994](#)] [HK, RW]

#### ***pat-11 I 0.44 st541***

: mild Pat phenotype; paralyzed pharyngeal muscles. [[Williams and Waterston 1994](#)] [RW]

#### ***pat-12 III – 26.59 st430 :***

mild Pat phenotype; some pharyngeal pumping. [[Williams and Waterston 1994](#)] [RW]

### ***pbo***

**pBo** c contraction step (posterior body) of defecation defective [JT].

#### ***pbo-1 III – 3.58 sa7***

: posterior body contraction during defecation very weak or absent; aBoc and [E.p](#) steps, and cycle period, normal; constipated; very slow growing. NA1. [[Thomas 1990](#)] [JT]

#### ***pbo-2***

= *egl-8*

#### ***pbo-3 II N sa304***

: extra pBoc in about 20% of cycles, other aspects of motor program normal; weak phenotype. OA1: *sa290*. [JT]

***pbo-4 X 2.2 sa300***

: pBoc weak but often present, slightly constipated, non-Egl; apparently normal feeding. NA1. [JT]

***pbo-5 V 2.3 sa242***

: pBoc step of defecation motor program completely absent; other aspects of motor program and timing normal; apparently normal feeding. NA1. [JT]

***pbo-6 IV 3.5 sa243***

: pBoc step of defecation motor program completely absent; other aspects of motor program and timing normal; apparently normal feeding. NA1. [JT]

***pbo-7 V 3.1 sa297***

: pBoc step of defecation motor program completely absent; other aspects of motor program and timing normal; apparently normal feeding. NA1. [JT]

***pcm***

***p***rotein ***c***arboxyl ***m***ethyltransferase [CGC].

***pcm-1 V – 1.3 qa201***

: Tc1 insertion, enzyme null, viable, reduced dauer survival; encodes 225-aa protein, 53% identical with human L-isoaspartyl methyltransferase; methylates L-isoaspartyl peptides in vitro. [[Kagan and Clarke 1995](#)]

***pdi***

***p***rotein ***d***isulfide ***i***somerase [TP].

***pdi-1 III – 5.70***

NMK. Encodes protein disulfide isomerase. Cosmid C14B1. [TP]

***pel***

***p***harynx and ***e***longation-defective [JR].

***pel-1* ?**

Most severe mutations lead to absence of discernible [pharynx](#), reduced number of cells expressing pharyngeal antigens. OA2. [JR]

***pel-2 IV N***

Mutant blocked in late stages of pharyngeal differentiation and morphogenesis. [JR]

***pel-3 I N***

Mutant exhibits nearly complete elongation, variably blocked in pharyngeal morphogenesis. [JR]

***pel-4 III N***

Mutant blocked in late stages of pharyngeal differentiation and morphogenesis. [JR]

***pes***

***p***atterned ***e***xpression ***s***ite [UL]. Loci conferring patterned expression on inserted reporter transgenes.

***pes-1 IV 1.2 pk72***

: Tc1 insertion, no known phenotype; resident gene encodes two predicted proteins with 45–50% identity to *Drosophila* Fork head transcription factor, diverged class; *pes-1:lacZ* expressed in some embryonic nuclei,

transiently in subset of early [AB](#) descendants, all early [D](#) descendants, and in [Z1](#), [Z4](#) from end of migration to early L1. Clone UL#24C7, cosmid F57F11. [[Hope 1991](#), 1994] [UL]

#### ***pes-2 I 9.0***

NMK. Resident gene encodes novel protein; *pes-2:lacZ* expressed in many nuclei from 14-cell stage (not C, D, or P4), after 200 min only in ABn, especially [hypodermis](#). Clone UL#100G5, cosmid F56G4. [[Young and Hope 1993](#)] [UL]

#### ***pes-3 III 0.13***

NMK. *pes-3:lacZ* expressed in nuclei of body wall muscles, vulval muscles. Clone UL#4F5, cosmid ZK506. [[Hope 1991](#)] [UL]

#### ***pes-4 ?***

NMK. *pes-4:lacZ* expressed in nuclei of three rectal epithelial cells, from L1 to adult; also dispersed expression in [pharynx](#). Clone UL#26D10, not located on physical map. [[Young and Hope 1993](#)] [UL]

#### ***pes-5 II 4.25***

NMK. *pes-5:lacZ* expressed strongly in most embryonic nuclei from 28-cell stage; not detected beyond comma stage or postembryonically. Clone UL#38E5, cosmid T27D12. [[Young and Hope 1993](#)] [UL]

#### ***pes-6 IV 3.15***

NMK. *pes-6:lacZ* expressed throughout H-shaped [excretory](#) cell, also in nuclei of [lateral hypodermis](#). Clone UL#64A1, YAC 55E1. [[Young and Hope 1993](#)] [UL]

#### ***pes-7 I 27.1***

NMK. *pes-7:lacZ* expressed in all [ganglia](#), [ventral nerve cord](#); predominantly nuclear, some in neurites, [vulva](#), spermatheca; staining from embryonic elongation onward. Clone UL#25C4, cosmid K04H8. [[Young and Hope 1993](#)] [UL]

#### ***pes-8 X 0.70***

NMK. *pes-8:lacZ* expression in three rectal epithelial cells from L1 onward, spermatheca from L4, [uterus](#) in adult (Ut-1, Ut-2, Use); adult male [proctodeum](#). Clone UL#38E12, cosmid F18G5. [[Young and Hope 1993](#)] [UL]

#### ***pes-9 V 5.9 pk22***

: Tc1 insertion, no known phenotype; *pes-1:lacZ* expressed in nuclei of 2–8 cells in early embryo (28–80-cell stage). Clone UL#80G8, YAC Y40H4. [[Young and Hope 1993](#)] [UL]

#### ***pes-10 ? pk74***

: Tc1 insertion, no known phenotype; no maternal transcripts, zygotic transcripts present transiently in each somatic lineage from four-cell stage; *pes-10:lacZ* expression similar. [[Seydoux and Fire 1994](#)] [PD]

#### ***pes-22 X – 6.3***

NMK. *pes-22:lacZ* expressed behind pharyngeal terminal bulb, probably lobes of [excretory gland](#) cell; L1 larvae have apparent gut nuclear staining. Clone UL#161G10, cosmid K05B2. [UL]

#### ***pes-23 X – 2.18***

NMK. *pes-23:lacZ* expressed in cells of [uterus](#) wall, staining luminal near spermatheca, basolateral or cytoplasmic nearer [vulva](#). Clone UL#9F7, cosmid F14B8. [[Hope 1991](#)] [UL]

#### ***pex***

**p** achytene **ex** it [EJ].

#### ***pex-1 I 14.5 dx8***

: sterile; pachytene exit blocked in hermaphrodite oogenesis; germ-line phenotype resembles [mpk-1](#) and [mek-2](#) mutants. NA1. [EJ]

### **pgl**

[P\\_g](#) ranu | e abnormality [SS].

### **pgl-1 IV 3.3 ct131**

: germ-line P granules unstained by some (not all) monoclonal antibodies; 5% sterile, Mes if grown at 26°C.  
CLONED: cosmid rescue (B0318). [SS]

### **pgp**

[P\\_g](#) lyco p rotein family [NL].

### **pgp-1 IV 6.10 pk17**

: deletion derived from *pk28tci*, no apparent drug sensitivity or other phenotype. CLONED: encodes 1321-aa P glycoprotein, 61–65% identical to mammalian P glycoproteins; transcripts relatively low, peak early; *pgp-1:lacZ* expressed in [intestine](#), throughout development; tagged PGP-1 detected in gut apical membrane. [[Broeks et al. 1995](#)] [NL]

### **pgp-2 I 0.42**

NMK. Encodes P glycoprotein, 61–65% identical to mammalian P glycoproteins; transcripts low in egg, higher subsequently. [[Lincke et al. 1993](#)] [NL]

### **pgp-3 X 3.18 pk18**

: deletion derived from *pk30tci*, increased sensitivity to colchicine and to chloroquine; gross phenotype wt. CLONED: encodes 1254-aa P glycoprotein, 61–65% identical to mammalian P glycoproteins; transcripts present throughout development; *pgp-1:lacZ* expressed in [intestine](#), throughout development; tagged PGP-3 detected in apical membranes of gut and of [excretory](#) cell. [[Broeks et al. 1995](#)] [NL]

### **pgp-4 X 3.17 pk34, pk82**

: Tc1 insertions, no known phenotype; encodes predicted 1265-aa P glycoprotein similar to PGP-3 (75% identity); *pgp-4:lacZ* expressed only in [excretory](#) cell. [[Lincke et al. 1993](#)] [NL]

### **pha**

[pha](#) rynx development abnormal [GE].

### **pha-1 III 5.93 e2123**

: ts; at 25°C, zygotic embryonic-lethal, [pharynx](#) fails to undergo late differentiation and morphogenesis; early [pharynx](#) development normal. OA>5: *e2468* (unconditional), *t1001ts*, *e2286* (weak, 38% hatch and arrest), *t1002* (weak, some survival to late larval arrest), etc. See also extragenic suppressors: *sup-35,36,37*. CLONED: 2.2-kb embryonic transcript, encodes 491-aa predicted protein with some similarity to bZIP transcription factors; *pha-1:lacZ* expressed transiently in all pharyngeal precursor cells. [[Granato et al. 1994](#)] [GE]

### **pha-2 X – 19.41 ad572**

: misshapen [pharynx](#) worms hatch with [pharynx](#) of correct gross shape, but disorganized, with nuclei misplaced; most homozygotes arrest in L1, escapers grow up to become very starved adults with deformed pharynges with abnormally small terminal bulb, thick nucleated isthmus; weakly cs (more survival beyond L1 at 25°C than at 15°C). ES2 ME3 NA1. [[Avery 1993a](#)] [DA]

### **pha-3 IV 5.68 ad607**

: misshapen [pharynx](#), isthmus tapered, thinner at the front, rather than uniform; corpus also deformed; [metacorpus](#) often open when relaxed; no larval arrest, very slow growth; *ad607/Df* grow more slowly, usually or always sterile. ES2 NA1. [[Avery 1993a](#)] [DA]

#### ***pha-4* V 25.18 *q490***

: zygotic-lethal; embryonic arrest with no [pharynx](#), absence of pharyngeal antigens; [intestine](#) not connected to [rectum](#), some rectal cells often missing; most embryos fail to elongate; *q490/Df* similar. OA6: *q400*, *n2498*, *q506* (similar), *q500* (weaker), etc. [[Mango et al. 1994a](#)] [JK]

#### ***phm***

**ph** aryngal **m** uscle abnormal [DA].

#### ***phm-1***

= *unc-89*

#### ***phm-2* I 9.41 *ad538***

: pharyngeal grinder cannot assume full forward position, terminal bulb muscles appear short (too strong?); space behind the grinder usually distorted into a continuously open cavity; male spicules protrude. ES2 ME0. OA1: *ad597*. [[Avery 1993a](#)] [DA]

#### ***phm-3* III – 12.28 *ad493***

: [pharyngeal muscle](#) birefringence reduced, pharyngeal contractions feeble. ES1 ME3 NA1. [[Avery 1993a](#)] [DA]

#### ***pho***

acid **pho** sphatase, intestinal [JM].

#### ***pho-1* II – 1.20 *ca101***

: electrophoretic variant in major acid phosphatase, no other phenotype. NA1. Purified protein is homodimeric glycoprotein, 55-kD subunit; activity detected at luminal edge of most gut cells, but not of six most anterior. [[Beh et al. 1991](#)] [JM]

#### ***pie***

**p** harynx, **i** ntestine in **e** xcess [JJ].

#### ***pie-1* III 17.25 *zu154***

: maternal-effect-lethal, often with two distinct pharynges; additional [pharynx](#) and intestinal tissue from P<sub>2</sub> (transformed to [EMS](#) fate). OA1. CLONED: encodes zinc finger protein, localized to nuclei of germ-line blastomeres. [[Mello et al. 1992b, 1996; Mango et al. 1994b](#)] [EU, JJ]

#### ***plg***

copulatory **pl** u **g** formation [CB].

#### ***plg-1* III 0.63 *e2001***

: dm, spo; males lay down gelatinous blob over [vulva](#) of mated hermaphrodites; allele isolated from natural *C. elegans* strain from Stanford, California. ES1 ME3 NA1. [[Barker 1994](#)] [CB]

#### ***pop***

**po** sterio **p** harynx-defective [JJ].

#### ***pop-1* I – 5.40 *zu189***

: mut; maternal-effect embryonic-lethal, no [MS](#)-derived [pharyngeal cells](#); [MS](#) blastomere adopts the fate of sister blastomere E; resulting embryos have twice the wt amount of gut. NA1. CLONED: encodes predicted

487-aa protein with HMG box; antibody stains nuclei of oocytes, early blastomeres. [[Lin et al. 1995](#)] [JJ]

### **ppp**

**p**yro **p**hos **p**horylase family [PK].

### **ppp-1 II - 0.19**

NMK. Upstream gene in operon with [tra-2](#). [[Kuwabara and Shah 1994](#)] [PK]

### **prk**

**p**im (mammalian oncogene)-**r**elated **k**inase [NL].

### **prk-1 III - 0.80 pk25**

: Tc1 insertion, no known phenotype; encodes predicted protein with 40% identity to murine Pim1, but longer C-terminus. [NL]

### **prk-2 III - 8.5 pk26**

: Tc1 insertion, no known phenotype; encodes predicted protein with 40% identity to murine Pim1, but longer C-terminus. [NL]

### **pry**

**p**oly **r**a **y** [CF].

### **pry-1 I 22.17 mu38**

: adult males make no alae but instead have ectopic rays; hermaphrodites sometimes Muv; descendants of [QR](#) stay in the posterior; postderid often missing; causes late ectopic expression of *lin-39*, *mab-5*, and [egl-5](#). See also *spy*. [CF]

### **ptl**

**p**rotein with **t**au-**I** like repeats [CGC].

### **ptl-1 III - 26.3**

NMK. Two transcripts, differing 3'ends, encoding proteins of 413- and 453-aa, containing, respectively, four and five tandem repeats; 50% identical to vertebrate tau/MAP repeats. [CGC]

### **pun**

**p**harynx **un** attached [BW].

### **pun-1 I N ct359 :**

lethal; L1 larval arrest; buccal capsule not attached to buccal [hypodermis](#); variable dumpy to severely disrupted [hypodermis](#). [BW]

### **pvp**

**PVP interneurons** abnormal [NJ]

### **pvp-1 X 3.55 rh114**

: PVP axons fail to stain with MAb 44; no other phenotype detected. [NJ]

### **rab**

**rab** family [NM].

### **rab-3 II - 1.21 y250**

: mild Unc, Che, Egl defects; Ric. OA1: *y251* (similar; both *y250* and *y251* are missense alleles). Encodes homolog of mammalian *rab3* (73% identity to human Rab3a); dominant-negative transgene leads to Ric, some Unc, or L1 lethality like [cha-1](#) (0). [NM]

***rac***

**rac** related [CGC].

***rac-1 IV – 3***

NMK. 1.7- and 0.9-kb transcripts, encode 191-aa predicted protein with 82% identity to human Rac1 (Ras superfamily). [[Chen et al. 1993a](#)]

***rad***

**rad** iation sensitivity abnormal [SP].

***rad-1 I 6.21 mn155***

: extremely hypersensitive to UV, X, and  $\gamma$  irradiation, not to UV psoralen. ES1 ME3 NA1. [[Hartman and Herman 1982](#); [Hartman and Marshall 1992](#)] [PH]

***rad-2 V 1.10 mn156* :**

extremely hypersensitive to UV, X, and  $\gamma$  irradiation; some sensitivity to chronic MMS treatment; not hypersensitive to UV psoralen. ES1 ME3 NA1. [[Hartman and Herman 1982](#); [Hartman and Marshall 1992](#)] [PH]

***rad-3 I 1.47 mn157***

: extremely hypersensitive to UV, not to X irradiation; hypersensitive to chronic MMS treatment (L1 arrest in 0.1 mM); reduced brood size (58% of wt); reduced photoproduct excision; not hypersensitive to UV psoralen. ES1 ME3. [[Hartman et al. 1988](#); [Hartman and Marshall 1992](#)] [PH]

***rad-4 V – 9.46 mn158***

: cs; hypersensitive to UV and to acute MMS treatment, not to X irradiation; reduced X chromosome nondisjunction (partly suppresses some *him* mutations); reduced brood size (34% of wt at 20°C); <25% eggs hatch at 15°C. ES1 ME2 NA1. [[Hartman and Herman 1982](#)] [PH]

***rad-5 III – 2 mn159***

: ts; hypersensitive to UV and X irradiation, not to MMS; reduced brood size at 20°C (7% of wt); sterile at 25°C; increased spontaneous mutability. ES2 ME2 NA1. [[Hartman and Herman 1982](#)] [PH]

***rad-6 III 3.46 mn160***

: hypersensitive to UV and X irradiation, not to MMS; hermaphrodites less viable (<50%) than males at 25°C, equal viability at 15°C. ES1 ME3 NA1. [[Hartman and Herman 1982](#)] [PH]

***rad-7 IV 6.05 mn161***

: hypersensitive to UV, not to X irradiation or MMS; reduced brood size (25% of wt); not hypersensitive to UV psoralen. ES1 ME3 NA1. [[Hartman and Herman 1982](#); [Hartman and Marshall 1992](#)] [PH]

***rad-8 I 0.47 mn163***

: hypersensitive to UV, not to X irradiation or MMS; reduced brood size (7% of wt); young hermaphrodites lay many inviable eggs; hypersensitive to paraquat, high oxygen concentration (lethal at 60%) (see also *mev*); increased life span at 16°C. ES1 ME0 NA1. [[Hartman and Herman 1982](#); [Ishii et al. 1994](#)] [TJ, TK, PH]

***rad-9 III – 2 mn162***

: hypersensitive to UV, not to X irradiation or MMS; reduced brood size (9% of wt). ES1 ME1 NA1. [[Hartman and Herman 1982](#)] [PH]

***raf***

**raf** (oncogene)-related [CGC].

**raf-1**

= *lin-45*

***ram***

**ra** y **m** orphology abnormal [PB].

***ram-1 I 9.92 bx34***

: adult males have lumpy, amorphous ray morphology; *bx34*/+ has variably swollen ray tips; fails to complement unlinked *ram* Mutations; hermaphrodite wt. ME3 NA1. [[Baird and Emmons 1990](#)] [PB]

***ram-2 II 1.74 bx39***

: ts; adult males have lumpy, amorphous ray morphology; *bx39*/+ has variably swollen ray tips; fails to complement unlinked *ram* mutations; hermaphrodite wt. ME3 NA1. [[Baird and Emmons 1990](#)] [PB]

***ram-3 II 19.74 bx32***

: adult males have lumpy, amorphous ray morphology; *bx32*/+ has variably swollen ray tips; fails to complement unlinked *ram* mutations; hermaphrodite wt. ME3 NA1. [[Baird and Emmons 1990](#)] [PB]

***ram-4 IV – 0.21 bx25***

: ts; adult males have lumpy, amorphous ray morphology; *bx25*/+ has variably swollen ray tips; fails to complement unlinked *ram* mutations; hermaphrodite wt; *bx25/Df* similar. ME3. OA?: *bx48*, *bx56ts* (possible alleles). [[Baird and Emmons 1990](#)] [PB]

***ram-5 X 17.71 bx30***

: adult males have lumpy, amorphous ray morphology; *bx30*/+ has variably swollen ray tips; fails to complement unlinked *ram* mutations; hermaphrodite wt. ME3 NA1. [[Baird and Emmons 1990](#)] [PB]

***rbp***

**R** NA- **b** inding **p** rotein family. See also *rnp*.

***rbp-1 ?***

NMK. Encodes hnRNP-like protein. Acc # [D10877](#). [[Stenico et al. 1994](#)]

***rec***

**rec** ombination abnormal [KR].

***rec-1 I 25 s180***

: increases meiotic recombination in gene clusters, reduces recombination on chromosome arms; distribution of crossovers in Rec-1 approximates physical map. ES1 ME3 NA1. [[Rose and Baillie 1979b](#); [Zetka and Rose 1995b](#)] [KR]

***rho***

**rho** -related [CGC]

***rho-1 ?***

NMK. 2-kb RNA, encodes 192-aa protein with 88% identity to human RhoA; immunofluorescence indicates 24 kD, ubiquitous, enriched in [nerve ring](#) and tip of head; not located on physical map; see also *cdc-42*, *rac-1*. [[Chen and Lim 1994](#)]

***ric***

**r** esistant to **i** nhibitors of **c** holinesterase [RM]. Inhibitors are drugs such as lannate, aldicarb, trichlorfon. See also *lan* (lannate-resistant), *lar* (lannate-resistant), *tcf* (trichlorfon-resistant).

***ric-1* III – 0.68 e239**

: (pka *lar-5*), resistant to cholinesterase inhibitors. OA2: *n1337* (pka *ric-5*). [[Bargmann et al. 1990](#); [Nguyen et al. 1995](#)] [CX, RM]

***ric-2***

= *snt-1*

***ric-3* IV 3.5 *md158* :**

Unc; small, slow growing, resistant to cholinesterase inhibitors. [[Nguyen et al. 1995](#)] [RM]

***ric-4* V 2.11 *md1088***

: Unc; slow movement, great difficulty backing; small, slow growing, resistant to cholinesterase inhibitors. OA2: *md1136*, *md1192*. CLONED: encodes predicted protein with similarity to SNAP-25 (57% identity to *Drosophila* SNAP-25). [[Nguyen et al. 1995](#)] [RM, TY]

***ric-5***

= *ric-1*

***rnp***

***rnp*** (RNA binding) domain containing [TY].

***rnp-1* V 3.70 *pk73***

: Tc1 insertion, no known phenotype. CLONED: encodes predicted 305-aa protein with two RNP domains, one NBP zinc finger; downstream gene in operon with *dpy-30*. [[Hsu et al. 1995](#)] [TY]

***rok***

***rok*** regulator ***o*** f ***k*** inase [PS].

***rok-1* IV 6.3 *sy187***

: negatively regulates vulval differentiation; at 20°C, no phenotype alone; at 25°C, some excess vulval differentiation; more in *sli-1* (*sy243*) background. [PS]

***rol***

***rol*** ler [CB].

***rol-1* II 7.55 *e91***

: adults left-handed rollers. ES3 (adult) ME1. OA1: *sc22ts* (left roller, slightly dumpy adult at 25°C). [[Cox et al. 1980](#)]

***rol-2***

= *dpy-2*

***rol-3* V 1.45 *e754***

: adults left-handed rollers. ES3 (adult) ME1. OA1 (viable): *e202*. Also lethal alleles (high forward mutation rate), OA>10: *s126*, *s422* (pka *let-333*), *s742gri*, *s833*, *s1040ts* (lethality suppressed by *srl-1* or *srl-2*), *s1408*, *s1519*, etc. Lethal arrest for most alleles early/mid larval. CLONED: cosmid rescue (B0340). [[Cox et al. 1980](#); [Barbazuk et al. 1994](#)] [BC]

***rol-4* V 4.38 *sc8***

: adults and L4 larvae left-handed rollers. ES3 (adult) ME2. OA2: *b238ts* (at 25°C, rolls only in adult, wt at 16°C). [[Cox et al. 1980](#)]

***rol-5***

= *sqt-1*

#### ***rol-6* II 0.81 *e187***

: adults, L3, and L4 larvae right-handed rollers. ES3 (adults, late larvae) ME0. Similar phenotype in *e187/Df*. OA6 (recessive): *sc90*, *n1177* (both have no phenotype alone but fail to complement *e187*). Also intragenic revertants *e187 n1270* (wt), etc.; null phenotype probably wt. Also neomorphic allele: *su1006dm* (both *su1006* and *su1006/+* severe right-handed rollers in L3, L4, adult; phenotype more extreme than *e187*). *su1006* widely used as dominant transformation marker (ES3 ME1). CLONED: encodes collagen, *sqt-1* family. [[Cox et al. 1980](#); [Kramer et al. 1990](#); [Mello et al. 1992a](#); [Park and Kramer 1994](#)] [CH]

#### ***rol-7***

= *dpy-10*

#### ***rol-8* II 0.88 *sc15***

: adults left-handed rollers. OA1: *sc102*. [[Kusch and Edgar 1986](#)] [BE]

#### ***rol-9* V 25.18 *sc148***

: adults strong right-handed roller, late larvae weak roller; *sc148/+* sometimes very weak roller. ES3 (adult). OA1: *sc149*. [BE]

#### ***rop***

**Ro** (Ro) ribonucleo **p** rotein family [LR].

#### ***rop-1* V 2.4**

NMK. Encodes predicted 643-aa protein, 36% identity to human and *Xenopus* Ro proteins; antibody detects 69-kD protein, which coprecipitates with and binds to small Y RNA encoded by *yrn-1*. [[Van Horn et al. 1995](#); [Labbe et al. 1995](#)] [LR]

#### ***rpc***

**R** NA **p** olymerase, type III (**C**).

#### ***rpc-1* IV 3.31**

NMK. 4.8-kb transcript, strong hybridization to largest subunit of yeast RNA polymerase III. [[Riddle and Bird 1989](#)] [DR]

#### ***rpl***

**R** ibosomal **p** rotein of **L** arge subunit [CGC]. Numbering follows standard scheme for eukaryotic ribosomes.

#### ***rpl-29* ?**

NMK. 0.6-kb transcript, *trans*-spliced to SL1; encodes predicted ribosomal protein (87% identical to yeast). [[Bektesh et al. 1988](#)] [DH]

#### ***rpl-37* III – 6.99**

NMK. *Trans*-spliced to SL1; encodes predicted ribosomal protein L37 (54% identical to rat). [[Bektesh et al. 1988](#)] [DH]

#### ***rps***

**R** ibosomal **p** rotein of **S** mall subunit [CGC]. Numbering follows standard scheme for eukaryotic ribosomes.

#### ***rps-16* ? N**

NMK. Encodes predicted ribosomal protein S16; downstream gene in operon with *fib-1*. [[Zorio et al. 1994](#)] [BL]

**rrn**

ribosomal **RN**A [CGC].

**rrn-1 I 29.99**

Structural locus for rRNA (pka NOR); ~55 tandem copies of 18S, 5.8S, and 28S rRNAs; mutation *let* (e2000) (pka *let-209*) associated with partial deletion; also *eDp20* (I;II) duplicates this locus; mutation *e2345* is transgene induced break in *rrn-1*. [[Ellis et al. 1986](#)] [PD]

**rrp**

ras-related **p**rotein [MH].

**rrp-1 IV 3.99**

NMK. Encodes Ras-related protein. [MH]

**rrp-2 IV 4.93**

NMK. Encodes Ras-related protein. [MH]

**rrs**

ribosomal **R**NA, **s**mall [CGC].

**rrs-1 V 10.81**

Structural locus for 5S RNA and SL1; ~110 tandem copies of 1-kb sequence coding for 5S RNA, alternating with sequence encoding SL1; *e2482* (pka [zen-1](#)) and *w1* are deletions of this locus leading to embryonic lethality (arrest at 200–300 cells, no compaction) or to L1 lethality if SL1 supplied transgenically. [[Nelson and Honda 1986](#); [Krause and Hirsh 1987](#); [Ferguson et al. 1996](#)] [JR]

**rsn**

**R**NA, **s**mall **n**uclear [BL]. snRNAs specified by small disperse gene families (6–12 members).

**rsn-1 I 12.34**

NMK. Cluster of three genes for U2 RNA. [[Thomas et al. 1990](#)] [BL]

**rsn-2 II 15.96**

NMK. Cluster of two genes for U2 RNA. [[Thomas et al. 1990](#)] [BL]

**rsn-3 II 17.59**

NMK. Cluster of two genes for U2 RNA. [[Thomas et al. 1990](#)] [BL]

**rsn-4 V 9.97**

NMK. Encodes U2 RNA. [[Thomas et al. 1990](#)] [BL]

**rsn-5 I 9.66**

NMK. Encodes U2 RNA. [[Thomas et al. 1990](#)] [BL]

**rsn-6 ?**

NMK. Encodes U2 RNA. [[Thomas et al. 1990](#)] [BL]

**rsn-7 V – 21.23**

NMK. Cluster of two genes for U6 RNA. [[Thomas et al. 1990](#)] [BL]

**rsn-8 V 3.43**

NMK. Cluster of two genes for U4 RNA. [[Thomas et al. 1990](#)] [BL]

***rsn-9* V 3.48**

NMK. Encodes U4 RNA. [[Thomas et al. 1990](#)] [BL]

***rsn-10* IV 3.37**

NMK. Encodes U5 RNA. [[Thomas et al. 1990](#)] [BL]

***rsn-11* I 1.40**

NMK. Encodes U1 RNA; see also [\*hsp-16\*](#). [[Thomas et al. 1990](#)] [BL]

***rsn-12* ?**

NMK. Pseudogene for U5 RNA. [[Thomas et al. 1990](#)] [BL]

***rsn-13* IV 6.27**

NMK. Two genes for U5 RNA, located in intron and 3' of [\*unc-31\*](#). [CB, CGC]

***rtm***

**R** NA, **t** transfer, **m** = methionine [CGC].

***rtm-1* I 11.36**

NMK. Encodes tRNA<sup>Met</sup>. [[Khosla and Honda 1989](#)]

***rtm-2* II 7.41**

NMK. Encodes tRNA<sup>Met</sup>. [[Khosla and Honda 1989](#)]

***rtm-3 X* – 0.63**

NMK. Encodes tRNA<sup>Met</sup>. [[Khosla and Honda 1989](#)]

***rtm-4* ?**

NMK. Encodes tRNA<sup>Met</sup>. [[Khosla and Honda 1989](#)]

***rtr***

**R** NA, **t** transfer, **r** = arginine [CGC].

***rtr-1* I 0.33**

NMK. Encodes tRNAArgACG. [[Schaller et al. 1991](#)]

***rtw***

**R** NA, **t** transfer, **w** = tryptophan [CGC].

***rtw-1***

= *sup-5*

***rtw-2***

= *sup-7*

***rtw-3* II 8.30**

NMK. Probable tRNA<sup>Trp</sup> pseudogene, variant base at A19. [[Kondo et al. 1990](#)]

***rtw-4***

= *sup-24*

***rtw-5* IV 5.14**

NMK. Probable tRNA<sup>Trp</sup> pseudogene, variant base at A46. [[Kondo et al. 1990](#)]

***rtw-6 IV 3.38***

NMK. Encodes tRNA<sup>Trp</sup>. [[Kondo et al. 1990](#)]

***rtw-7 IV 1.63***

NMK. Encodes tRNA<sup>Trp</sup>. [[Kondo et al. 1990](#)]

***rtw-8***

= *sup-28*

***rtw-9***

= *sup-29*

***rtw-10***

= *sup-21*

***rtw-11***

= *sup-33*

***rtw-12***

= *sup-34*

***rtx***

**R** NA, **t** ransfer, **x** = selenocysteine [CGC].

***rtx-1 IV – 28.78***

NMK. Encodes predicted tRNA for selenocysteine. [CGC]

***ryr-1***

= *unc-68*

**S to T**

***sch***

**s**odium **ch**annel [CGC].

***sch-1 V 4.59***

NMK. Cross-hybridizes to sodium channel probe. [KR]

***sdc***

**s**ex and **d**osage **c**ompensation [TY].

***sdc-1 X 23.48 n485***

: (pka [egl-16](#)) mat; very variable bloating; some animals form bag-of-worms (type A) or explode at [vulva](#); abnormal vulval morphology; some masculinization of XX animals (especially at 15°C); weaker phenotype if mother *n485*/+. ES2/3 (adult) ME2. XX progeny of *n485/Df* mothers have incompletely penetrant partially male (Tra) phenotype. OA>5: *e2426*, *n485*, *y4*, *y67ts* (30% masculinized at 20°C), etc. Most alleles have apparent dosage compensation defects, variable masculinizing effects. CLONED: encodes 1203-aa protein with seven N-terminal zinc fingers. [[Villeneuve and Meyer 1990a](#); [Nonet and Meyer 1991](#)] [TY]

***sdc-2 X 4.67 y15***

: XX animals inviable and masculinized, XO animals wt; no maternal rescue. ES3 (XX) ME3. OA>20: *y46*, *y74*, *y55* (weaker, *Egl* or *Tra* phenotypes). CLONED: 9.2-kb transcript, encodes predicted 2962 novel protein (344 kD), highly charged. [[Nusbaum and Meyer 1989](#)] [TY]

### ***sdc-3* V 6.91 *y126***

: mat; deletion null, XX animals inviable if mother homozygous; rare escapers dumpy hermaphrodite; cryptic masculinization; XO phenotype wt. OA>10: *y122*, *y127*, *y143* (similar). Also *sdc-3* (*Tra*) alleles: *y52* (XX viable, masculinized), *y137* (weaker). Also *sdc-3* (*Dpy*) alleles: *y100* (XX inviable or dumpy, no masculinization), *y128*, etc. CLONED: 7-kb transcript present in embryo, L1, L2; encodes 2150-aa protein, with possible ATP-binding site (affected in *Tra* mutations), two C-terminal zinc fingers (affected in *Dpy* mutations). [[DeLong et al. 1993](#); [Klein and Meyer 1993](#)] [TY]

### ***sel***

***s*** suppressor/ ***e*** nhancer of ***I*** ineage defect [GS].

### ***sel-1* V 4.46 *e1948***

: pka [\*sup-25\*](#); recessive suppressor of [\*lin-12\*](#) hypomorph (*n676 n930ts*), partial suppressor of [\*glp-1\*](#) hypomorph; no effect on [\*lin-12\*](#) amorph; no phenotype alone; no suppression of *lin-3*, *egl-15*, etc. OA4: *ar23*, *ar29*, *ar73*, *ar77*. CLONED: encodes predicted 650-aa protein with signal sequence. [[Sundaram and Greenwald 1993b](#); [Grant and Greenwald 1996](#)] [GS]

### ***sel-2* III – 2.92 *n655***

: interacts with [\*lin-12\*](#) (*n302sd*). [GS]

### ***sel-3***

= *lag-2*

### ***sel-4* II – 16.37 *n1259***

: suppressor of [\*lin-12\*](#) hypermorph (*n302sd*). [JT, MT]

### ***sel-5* III – 2.97 *n1524***

: suppressor of [\*lin-12\*](#) hypermorphs (*n302sd*, etc.); mosaic analysis indicates focus in VU not AC. [JT, MT]

### ***sel-6* V 20.39 *n1256***

: suppressor of [\*lin-12\*](#) hypermorph (*n302sd*). [JT, MT]

### ***sel-7* X 17.31 *n1253***

: suppressor of [\*lin-12\*](#) hypermorph (*n302sd*) [JT, MT]

### ***sel-9* V 1.60 *ar22***

: suppressor of hypomorphic [\*lin-12\*](#) allele, partial suppressor of [\*glp-1\*](#) hypomorph; no effect on [\*lin-12\*](#) amorph; no phenotype alone; probable gf mutation. OA1: *ar26*. [[Sundaram and Greenwald 1993b](#)] [GS]

### ***sel-10* V 5.46 *ar41***

: recessive suppressor of [\*lin-12\*](#) hypomorph allele, partial suppressor of [\*glp-1\*](#) hypomorph; some effect on [\*lin-12\*](#) amorph; properties affected by extragenic modifier; no phenotype alone. OA1: *ar28*. [[Sundaram and Greenwald 1993](#)] [GS]

### ***sel-11* V 3.19 *ar39***

: recessive suppressor of [\*lin-12\*](#) hypomorph, partial suppressor of [\*glp-1\*](#) hypomorph; no effect on [\*lin-12\*](#) amorph; no phenotype alone; probable gf mutation. OA1: *ar84*. [[Sundaram and Greenwald 1993](#)] [GS]

### ***sel-12* X – 18.86 *ar131***

: (pka [sum-1](#)) recessive suppressor of Muv phenotype of [lin-12](#) hypermorph *n950*; impenetrant Egl in [lin-12](#) (+) background. OA3: *ar133*, *ar171* (100% Egl, *ar171/Df* similar, *W225op*). CLONED: encodes predicted 467-aa protein, nine transmembrane domains; related to human presenilin genes (S182) and to SPE-4. [Levit and Greenwald 1995] [GS]

### ***sem***

**se x m uscle abnormality [MT].**

#### ***sem-1 X 14.34 n1382***

: Egl, hermaphrodite sex muscles fail to divide. ME3. [MT, NH]

#### ***sem-2 I – 0.27 n1343***

: mut; Egl, hermaphrodite sex muscles adopt [body wall muscle](#) fate. ME3. OA5: some alleles have additional phenotypes, four are embryonic-lethal, arrest 1.5-fold with bloated head. [MT, NH, RW]

#### ***sem-3 IV 4.92 n1655***

: Egl (5-HT-resistant); hermaphrodite sex muscles show subtle positioning defects. ME3. OA>3: *n1905*, *s1734* (pka [let-654](#), hemizygote mid larval-lethal). [Clark and Baillie 1992] [BC, NH]

#### ***sem-4 I 1.66 n1378***

: Egl, hermaphrodite sex muscles fail to differentiate; additional axon and lineage defects. ME0 (severe Mab) HME3. OA3: *h769*, *n2087*, *n1971* (stronger allele, two mesodermal and six [neuronal](#) cell types pleiotropically affected; two additional [touch cells](#) formed in tail), etc. CLONED: encodes predicted protein with six C2H2 zinc finger motifs. [Desai et al. 1988; Mitani et al. 1993; Basson and Horvitz 1996] [MT, NH, TU]

#### ***sem-5 X – 0.66 n2030***

: Vul, hermaphrodite sex muscles show subtle positioning defect, Soc (suppressor of [clr-1](#)), impenetrant Mel (rod-like larval-lethal); pleiotropic effects on migration, vulval induction, etc. ME0. OA5: strong alleles *n1619*, *n2019*; weaker alleles *n1781*, *n2195* (Soc, weak Egl, ME3), *n1619*, *n1779* (synergizes with alleles of *unc-71*, *unc-73*, *egl-15*, *egl-17*, to give stronger Sem defect). CLONED: encodes predicted SH3-SH2-SH3 protein with 60% identity to human Grb2, functional equivalence. [Clark et al. 1992; Stern et al. 1993; DeVore et al. 1995] [MT, NH]

### ***shv***

**sh i v a (4-armed) gonad [BS].**

#### ***shv-1 II 1.63 oz128***

: sd; homozygous hermaphrodite sometimes sterile and often contains a multiple-armed [somatic gonad](#) with three or four [distal tip cells](#); male appears normal; probable gf allele. NA1 (gf). Also recessive intragenic revertants: *oz128 oz157* (hermaphrodite-sterile with defect in germ-line proliferation; partial lf), etc. [BS]

### ***sip***

**s tress i nduced p rotein [CGC].**

#### ***sip-1 III 2.53***

NMK. Expression in gonad and early embryo, increased after treatment with >0.2 mM cadmium; encodes novel protein related to heat shock proteins. [CR]

### ***skn***

**sk i n ([hypodermis](#)) in excess [JJ].**

***skn-1* IV 2.16 zu67**

: mat; maternal-effect embryonic-lethal, extra internal hypodermal cells, fails to produce [pharynx](#) and [intestine](#); [EMS](#) adopts P2-like fate ([MS](#) more affected than E). OA>5: *or12*, *or13*, etc. CLONED: encodes predicted transcription factor; antibody stains early nuclei, differential localization to [EMS](#), not detectable beyond 12-cell stage. [[Bowerman et al. 1992a, 1993](#)] [EU, JJ]

***skn-4* III 2 *or16***

: mat; maternal-effect embryonic-lethal, extra hypodermal cells; [EMS](#) lineage defective (E more affected than [MS](#)). [EU]

***sli***

***sli-1 X – 19.09 sy143***

: suppressor of Vul phenotype of [let-23](#) hypomorph; other [let-23](#) defects suppressed, but not sterility; Muv phenotype in combination with [unc-101](#); low penetrance head morphology defect in [let-23](#) (+) background; *sy143/Df* similar. OA>10: *sy263* (weaker), *sy129*, etc. CLONED: encodes homolog of mammalian oncogene *c-cbl* (55% identity over 390 aa, containing RING finger motif; *sy129* missense). [[Jongeward et al. 1995; Yoon et al. 1995](#)] [PS]

***sls***

***sls-1 I – 1.64***

NMK. Encodes *trans*-spliced leader, SL2 $\alpha$ . [[Huang and Hirsh 1989; Ross et al. 1995](#)] [CR]

***sls-2 III C***

NMK. Encodes *trans*-spliced leaders, three SL2 variants (SL3 $\alpha$ , SL4, SL5). [[Ross et al. 1995](#)] [CR]

***sls-3 I 3.39***

NMK. Encodes *trans*-spliced leader, SL2 variant (SL3 $\beta$ ). [[Ross et al. 1995](#)] [CR]

***sls-4 I 3.39***

NMK. Encodes *trans*-spliced leader, SL2 variant (SL3 $\gamma$ ). [[Ross et al. 1995](#)] [CR]

***sma***

***sma-1 V 3.44 e30***

: short round-headed, especially in early larvae; adults have slight rolling tendency. ES3. OA>10: *e656*, *e2075* (pka [sma-7](#), ME2), *e1160*, *e2090*, *n504*, etc. CLONED: encodes predicted cytoskeletal protein. [[Brenner 1974](#)] [AZ]

***sma-2 III – 0.06 e502* :**

short, somewhat dumpy; males have crumpled spicules, abnormal rays; synthetic-lethal with some morphological mutants; mosaic analysis indicates cell autonomous action; similar to Sma-3, Sma-4, Daf-4. ES3 (adult) ME0. OA>5: *e172*, *e297*, *e1491* (weaker), *s262* (induced on [eT1](#)), etc. CLONED: encodes Dwarfin family protein. [[Baird et al. 1991; Savage et al. 1996](#)] [LT, PB]

***sma-3 III – 0.91 e491***

: short, somewhat dumpy; males have crumpled spicules, abnormal rays; similar to Sma-2, Sma-4, Daf-4. ES3 (adult) ME0. OA2: *e637*, *e958*. CLONED: encodes Dwarfin family protein. [[Baird et al. 1991; Savage et al.](#)

[1996](#)] [LT, PB]

**sma-4 III – 1.26 e729**

: short nondumpy; males have crumpled spicules, abnormal rays. ES3 (adult) ME0. OA1: *e805*. [[Brenner 1974](#); [Savage et al. 1996](#)] [LT, PB]

**sma-5 X 6.74 n678**

: very small adult, slow-growing; small in L1 and L2. ES3 NA1. [MT]

**sma-6 II 0.08 e1482**

: short adult and late larvae; *e1482/Df* similar. ES2 ME3. NA1. [CB]

**sma-7**

= *sma-1*

**sma-8 V 3.19 e2111**

: dm; short blunt head; *e2111/+* similar phenotype. ES3. OA1: *n716sd* (recessive-lethal). [[Park and Horvitz 1986a](#); [Chen et al. 1992](#)] [PD]

***smg***

**s** uppressor with **m** orphogenetic effect on **g** enitalia (**s** uppressor affecting **m** essa **g** e stability) [CB]. All *smg* mutations act as allele-specific suppressors of mutations in many different genes; also enhance certain mutations; affect mRNA stability.

**smg-1 I 1.50 e1228**

: adult male has swollen bursa. ES3 (adult male) ME1. Adult hermaphrodite has protruding [vulva](#). ES2. Recessive suppressor of *unc-54(r293)*, *tra-2(e1209)*, etc.; [unc-54](#) nonsense RNAs accumulate. OA>10: *e1233*, *e2134spo* (similar phenotypes), *ma127*, *ma131*, *r861*, *r913spo*, etc. CLONED: 7.8-kb transcript, encodes predicted protein with some kinase similarity in C-terminal. [[Hodgkin et al. 1989](#); [Pulak and Anderson 1993](#)] [TR]

**smg-2 I – 17.91 e2008**

: adult male has swollen bursa. ES3 ME1. Adult hermaphrodite has protruding [vulva](#) ES2. Recessive suppressor of *unc-54(r293)*, *tra-2(e1209)*, etc.; [unc-54](#) nonsense RNAs accumulate. OA>10: *e2423*, *ma114*, *ma122*, *r863*, *r920::Tc4*, *r908* (deletion), etc. CLONED: encodes predicted protein with 36–69% similarity to yeast Upf1p. [[Hodgkin et al. 1989](#); [Pulak and Anderson 1993](#)] [TR]

**smg-3 IV 3.16 ma117**

: adult male has swollen bursa, adult hermaphrodite has protruding [vulva](#). ME1. Recessive suppressor of *unc-54(r293)*, *tra-2(e1209)*, etc.; suppression reduced by maternal rescue; [unc-54](#) nonsense RNAs accumulate. OA>3: *ma115*, *r867*, etc. [[Hodgkin et al. 1989](#); [Pulak and Anderson 1993](#)] [TR]

**smg-4 V 2.25 ma116**

: adult male has swollen bursa, adult hermaphrodite has protruding [vulva](#). ME1. Recessive suppressor of *unc-54(r293)*, *tra-2(e1209)*, etc.; suppression reduced by maternal rescue; [unc-54](#) nonsense RNAs accumulate. OA3: *r1181*, *e2615psu*, *e2616psu*. CLONED: YAC and phage rescue. [[Hodgkin et al. 1989](#); [Pulak and Anderson 1993](#)] [CB, TR]

**smg-5 I 1.29 r860**

: adult male has swollen bursa, adult hermaphrodite has protruding [vulva](#). ME1. Recessive suppressor of *unc-54(r293)*, *tra-2(e1209)*, etc.; [unc-54](#) nonsense RNAs accumulate. OA1: *r919::Tc1*. CLONED: encodes 549-aa novel protein; 56-kD protein detected by Western; SMG-5 interacts with SMG-7 in vitro and in vivo. [[Hodgkin et al. 1989](#); [Pulak and Anderson 1993](#)] [TR]

### ***smg-6* III – 16.27 r896**

: adult male has swollen bursa, adult hermaphrodite has protruding [vulva](#). ME1. Recessive suppressor of *unc-54(r293)*, *tra-2(e1209)*, etc.; suppression reduced by maternal rescue; [unc-54](#) nonsense RNAs accumulate. OA9: *r886* (similar), *r1059* (embryonic-lethal), *r1062* (early larval-lethal), *r1014* (late larval-lethal). [[Hodgkin et al. 1989](#); [Pulak and Anderson 1993](#)] [TR]

### ***smg-7* IV 3.27 r1131**

: Tc1 insertion; suppresses *unc-54(r293)*, *tra-2(e1209)*, *dpy-5(e61)*; [unc-54](#) nonsense mRNAs accumulate; hermaphrodites are Pvul, males are Mab. CLONED: encodes predicted 53-kD protein with three tetratricopeptide repeats; 54-kD protein detected by Western; SMG-7 interacts with SMG-5 in vitro and in vivo. [TR]

### ***smu***

**s** uppressor of **m** ec and **u** nc [SP]. Specific action on certain alleles of [mec-8](#) and *unc-52*.

### ***smu-1* I 18.06 mn415**

: suppresses Mec (touch-insensitive) and Dyf (dye-filling defective) phenes of *mec-8(u218ts)*, Mec phene of *mec-8(mn472ts)*, Dyf phene of most [mec-8](#) alleles, variable cs arrest of *mec-8(u74)* and *mec-8(mn463)*, Unc phene of [unc-52](#) (*e669su250ts*), and synthetic lethality of [mec-8](#) (*u218ts*); [unc-52](#) (*e669su250ts*). Essentially wt phenotype alone. OA2: *mn417*, *mn433*. [[Lundquist and Herman 1994](#)] [SP]

### ***smu-2* II – 7.12 mn416**

: suppresses Mec (touch-insensitive) and Dyf (dye-filling defective) phenes of [mec-8](#) (*u218ts*), Mec phene of [mec-8](#) (*mn472ts*), Dyf phene of most [mec-8](#) alleles, variable cs arrest of [mec-8](#) (*u74*) and *mec-8(mn463)*, Unc phene of [unc-52](#) (*e669su250ts*), and synthetic lethality of [mec-8](#) (*u218ts*); [unc-52](#) (*e669su250ts*). Essentially wt phenotype alone. [[Lundquist and Herman 1994](#)] [SP]

### ***snb***

**s** y **n** apto **b** revin-related [CGC].

### ***snb-1* V 0.17 md247**

: lethargic, jerky, Ric, accumulates acetylcholine. CLONED: encodes synaptobrevin homolog (67% identity to human VAMP-1) [NM, RM]

### ***snt***

**s** y **n** apto **t** agmin-related.

### ***snt-1* II 0.10 md125**

: (pka [ric-2](#)) uncoordinated, slight shrinker, small, slow-growing, resistant to cholinesterase inhibitors; some pumping and defecation defects. OA2: *ad596* (pka [unc-121](#), Unc, worse when starved; ME2), *n2665*. CLONED: encodes synaptotagmin (54% identity to mammalian synaptotagmin) [[Nonet et al. 1993](#); [Nguyen et al. 1995](#); [Schafer et al. 1996](#)] [NM, RM]

### ***soc***

**s** uppressor **o** f **c** lr [NH].

### ***soc-1* VL n1789**

: gri; suppressor of [clr-1](#); scrawny alone. OA9: *n1778*, *n1788* (similar), etc. [[DeVore et al. 1995](#)] [NH]

### ***soc-2* IV C n1774**

: suppressor of [clr-1](#). OA1. [[DeVore et al. 1995](#)] [NH]

### ***sod***

**s** uper **o**xide **d**ismutase [CGC].

**sod-1 II 0.20 pk67**

: Tc1 insertion, no known phenotype; encodes 158-aa Cu/Zn superoxide dismutase gene; upstream gene in operon with [art-1](#). [[Larsen 1993](#); [Kuwabara and Shah 1994](#)] [MT]

**sod-2 I 2.72**

NMK : Encodes manganese superoxide dismutase. [TK]

**sod-3 ?**

NMK : Encodes 227-aa manganese superoxide dismutase. CLONED: encodes manganese superoxide dismutase. [[Giglio et al. 1994](#)]

**sog**

**s** uppressor **o**f **g** *lp-1* [EL].

**sog-1 I 1.91 q305**

: recessive suppressor of ts [glp-1](#) alleles *q224*, *q231*, suppresses both germ-line and embryonic defects; does not suppress stronger [glp-1](#) alleles; no phenotype alone; other alleles exhibit complex non-allelic noncomplementation with mutations of other *sog* genes. OA1: *q298*. [[Maine and Kimble 1993](#)] [EL]

**sog-2 II 2.42 q299**

: recessive suppressor of ts [glp-1](#) alleles *q224* and *q231*, suppresses both germ-line and embryonic defects; does not suppress stronger [glp-1](#) alleles; no phenotype alone. [[Maine and Kimble 1993](#)] [EL]

**sog-3 IV 3.04 q294**

: recessive suppressor of ts [glp-1](#) alleles *q224* and *q231*, suppresses both germ-line and embryonic defects; does not suppress stronger [glp-1](#) alleles; no phenotype alone. [[Maine and Kimble 1993](#)] [EL]

**sog-4 V 1.47 q301**

: recessive suppressor of ts [glp-1](#) alleles *q224* and *q231*, suppresses both germ-line and embryonic defects; does not suppress stronger [glp-1](#) alleles; no phenotype alone. OA1: *q304*. [[Maine and Kimble 1993](#)] [EL]

**sog-5 X – 5.33 q297**

: recessive suppressor of ts [glp-1](#) alleles *q224* and *q231*, suppresses both germ-line and embryonic defects; does not suppress stronger [glp-1](#) alleles; no phenotype alone. [[Maine and Kimble 1993](#)] [EL]

**sog-6 IV 4.23 q300**

: recessive suppressor of ts [glp-1](#) alleles *q224* and *q231*, suppresses both germ-line and embryonic defects; does not suppress stronger [glp-1](#) alleles; no phenotype alone. OA1: *q306*. [[Maine and Kimble 1993](#)] [EL]

**sog-10 III – 2.59 q162**

: suppressor of germ-line defect of some weak [glp-1](#) alleles; cs Fog phenotype alone, *q162/Df* stronger Fog. [[Maine and Kimble 1993](#)] [EL]

**spa**

**s** odium/ **p** otassium **A** TPase family [CGC].

**spa-1**

= *eat-6*

**spe**

**spe** rmatogenesis abnormal [BA].

***spe-1* II 0.40 *mn47***

: hermaphrodites and males produce aberrant [spermatids](#) that fail to activate into spermatozoa; [spermatids](#) exhibit unusual and rapid cytoplasmic movement. ES2 (adult) NA1. [[Sigurdson et al. 1984](#)]

***spe-2* II 1.59 *mn63***

: pat; hermaphrodites lay self-fertilized eggs that do not hatch, but eggs are viable if cross-fertilized by *mn63* sperm from *mn63/+* males; also Sqv (squashed [vulva](#)) phenotype, morphology of L4 [vulva](#) abnormal (invagination considerably reduced). OA>5: *n2843*, *n2847*, *n2850*, *n2851*, *n3036*, *n2822*, *n2825* (somewhat fertile). CLONED: encodes predicted novel protein; possible transmembrane domain. [[Sigurdson et al. 1984](#)] [MT]

***spe-3* II – 0.89 *mn230***

: pat; hermaphrodites lay self-fertilized eggs that do not hatch, but eggs are viable if cross-fertilized by *mn230* sperm from *mn230/+* males. (Same Spe phenotype as [spe-2](#), but non-Sqv.) ES3 (progeny) NA1. [[Sigurdson et al. 1984](#)]

***spe-4* I 2.04 *hc78***

: hermaphrodites and males produce primary [spermatocytes](#) that contain four haploid nuclei; males retain these [spermatocytes](#) while hermaphrodites resorb them when oogenesis begins; self-fertility 0%; similar phenotype in *hc78/Df*; fibrous body membranous organelle formation disrupted. ES2 (adult). OA2: *hc81*, *q347* (deletion null). CLONED: 1.3-kb transcript, spermatogenesis-specific; encodes predicted 465-aa protein, probable seven transmembrane domains; similarity to human S182 (Alzheimer's associated) and SEL-12; SPE-4 segregates to [spermatids](#). [[L'Hernault and Arduengo 1992](#)] [SL]

***spe-5* I – 0.25 *hc93***

: hermaphrodites and males produce primary [spermatocytes](#) that occasionally begin first meiotic division but do not differentiate further; abnormal fibrous body–membranous organelle complex; self-fertility <1%. ES2 (adult). OA3: *hc110*, etc. (all slightly leaky, cs). CLONED: encodes predicted 25-kD protein, four transmembrane domains, large hydrophilic domain. [[L'Hernault et al. 1988](#)] [SL]

***spe-6* III 9.78 *hc49***

: hermaphrodites and males produce primary [spermatocytes](#) that do not differentiate further; no division, eventual degeneration; SP fails to assemble into fibrous body–membranous organelle. ES2 (adult). OA3: *hc92*, *hc143*, also nonallelic failure to complement *eDf19*. [[Varkey et al. 1993](#)] [BA, HU]

***spe-7* II N *mn252***

: hermaphrodites and males produce primary [spermatocytes](#) that do not differentiate further. ES2 (adult) NA1. [[Varkey et al. 1993](#)] [BA, SP]

***spe-8* I – 17.38 *hc40***

: hermaphrodites produce nonfunctional nonmotile sperm with uniformly aberrant pseudopods; male sperm normal; self-fertility <1% (16°C or 25°C). ES2 (adult). OA5: *hc50*, *hc53*, etc. [[L'Hernault et al. 1988](#); [Shakes and Ward 1989a](#)] [BA]

***spe-9* I 9.54 *hc52***

: ts; hermaphrodites and males grown at 25°C produce motile sperm that are fertilization-defective; self-fertility <1% (25°C), 100% (16°C). ES2 (adult). OA3: *hc88ts*, also nonconditional alleles. [[L'Hernault et al. 1988](#)] [SL]

***spe-10* V 2.67 *hc104***

: ts; hermaphrodites and males produce nonfunctional but motile sperm with short pseudopods; severe defects in fibrous body–membranous organelle. ES2 (adult) NA1. [[Shakes and Ward 1989b](#)] [BA, DS]

***spe-11 I – 0.10 hc77***

: ts; hermaphrodites and males grown at 25°C produce motile sperm that fertilize oocytes leading to abnormal early development; self-fertility 3% (25°C), 100% (16°C); similar phenotype in *hc77/Df*. ES2 (adult). OA3: *hc90* (nonconditional sterile). CLONED: encodes 299-aa novel protein, highly charged and hydrophilic; transcript present only in sperm, but forced transgene expression in oocyte can rescue Spe phenotype; SPE-11 in perinuclear halo of mature sperm. [[Hill et al. 1989](#); [Browning and Strome 1996](#)] [SS]

***spe-12 I 2.60 hc76***

: hermaphrodites produce nonfunctional sperm, fertilization defective; males are fertile; similar phenotype in *hc76/Df*, [\*spermatids\*](#) activated by ionophores, arrest as spiky intermediates after protease activation; self-fertility <1% (16°C or 25°C). ES2 (adult) NA1. CLONED: transcript only in spermatogenic germ line, predicted protein novel? [[L'Hernault et al. 1988](#); [Shakes and Ward 1989a](#)] [BA]

***spe-13 I – 20.00 hc137***

: ts; at 25°C, [\*spermatids\*](#) can activate to form crawling sperm, unable to fertilize; low hermaphrodite self-fertility at 15°C. NA1. [[L'Hernault et al. 1988](#)] [SL]

***spe-15 I – 15.97 hc75***

: ts; at 25°C, [\*spermatids\*](#) can activate to form crawling sperm, unable to fertilize; low hermaphrodite self-fertility at 15°C. NA1. [[L'Hernault et al. 1988](#)] [SL]

***spe-16 III 7.27 hc54***

: ts; at 25°C, hermaphrodites make nonfunctional sperm with wt cytology. [SL]

***spe-17 IV 5.5 hcDf1***

: mutation defined by *hcDf1*, *hDf13*; hermaphrodite brood size 3; abnormal spermatogenesis with ribosomes attaching to fibrous body–membranous organelle. CLONED: 0.56-kb transcript, encodes 142-aa novel predicted protein, highly charged, Ser- and Thr-rich. [[L'Hernault et al. 1993](#)] [SL]

***spe-26 IV 4.6 hc138***

: accumulates defective [\*spermatocytes\*](#); pleiotropic effects in increasing life span (Age phenotype), thermotolerance, UV resistance. OA5: *hc139*, *hc140*, *it112*, *it118*, *hc107ts* (Spe, non-Age); 5/6 alleles ts. CLONED: encodes 570-aa protein containing five tandem 50-aa scruin/kelch repeats, possible actin-binding domains. [[Van Voorhies 1992](#); [Varkey et al. 1995](#); [Murakami and Johnson 1996](#)] [BA, HU, KK]

***spe-27 IV 2.57 it132***

: ts; hermaphrodites produce nonfunctional sperm, males are fertile; hypomorphic allele. OA>3: some alleles probably null. CLONED: transcript only in spermatogenic germ line, encodes novel predicted protein. [[Minniti et al. 1996](#)] [BA]

***spe-29 IV 4.40 it127***

: leaky hermaphrodites produce nonfunctional sperm, almost self-sterile (brood 4–10 at 20°C, 1–2 at 16°C or 25°C); males fertile, no sperm defect; *spe-29/Df* similar. NA1. [BA, SL]

***spy***

**s** uppressor of **p** olyra **y**. [CF].

***spy-1 X – 2.15 mu63***

: spo; suppresses *pry-1(mu38)*; *mu63* alone leads to ts defect in the migration of the [\*QL\*](#) descendants. NA1. [CF]

***sqt***

**sq** ua **t** [BE, CB].

**sqt-1 II 3.19 scl**

: sd; homozygotes short, dumpyish in adult and L4; roll in L3; *scl*/+ non-dumpy right-handed rollers in adult, L4, L3. ES3 ME1. OA>10 (dominant): *su1005*, *e1584* (resemble *scl*), *e1350* (recessive dumpy), etc. Also recessive alleles, e.g., *sc13* (pka *rol-5*, adults, L3, L4 larvae left-handed rollers. ES3 [adult, late larvae]), *sc101* (long), *sc33ts* (at 25°C, rolls only in adult, at 16°C wt), etc. Complex complementation patterns; null phenotype probably wt. CLONED: encodes 32-kD collagen, *sqt-1* family includes *rol-6*; expressed each larval stage, 4–2.5 hours prelethargus. [[Kramer et al. 1988](#); [Park and Kramer 1994](#)] [CH, IA]

**sqt-2 II – 18.22 sc3**

: sd; homozygotes slightly dumpyish in adult, late larvae; roll in L3; *sc3*/+ non-dumpy right-handed roller in adult, L4, L3. ES3 (adult). OA6: *sc14* (stronger phenotype than *sc3*), *e1486*, *sc108*, etc. [[Kusch and Edgar 1986](#)]

**sqt-3 V 3.96 sc63**

: ts, sd; homozygotes at 25°C are non-roller dumpy, heterozygotes (*sc63*/+) are non-dumpy left-handed rollers in adult; high penetrance deformed tail at 25°C. ES3 ME0 (25°C). At 15°C, slightly dumpy. OA3: *sc80ts* (resembles *sc63*), *e24sd,ts* (pka *dpy-15*, dumpy inviable at 25°C, *e24*/+ dumpy at 25°C, sometimes Lon at 15°C), *sc42* (recessive left roller), *e2117ts* (extreme dumpy, early larval-lethal at 25°C). CLONED: encodes 295-aa collagen (pka *col-1*, *dpy-13* family; mutations all missense; expressed at each larval stage, 4–2.5 hours prelethargus. [[Kramer et al. 1982](#); [van der Keyl et al. 1994](#)] [IA]

**sqv**

**sq** uashed **v** ulva [MT].

**sqv-1 IV 3.83 n2820**

: morphology of L4 [vulva](#) abnormal (invagination considerably reduced); hermaphrodites almost self-sterile. OA5: *n2819*, *n2828*, *n2848*, *n2849*, *n2824* (all self-sterile?). [MT]

**sqv-2 II – 6.00 n2826**

: morphology of L4 [vulva](#) abnormal (invagination considerably reduced); hermaphrodites self-sterile. OA4: *n2821* (somewhat fertile), *n3037*, *n3038*, *n2826*, *n2821*. [MT]

**sqv-3 III 0.70 n2823 :**

morphology of L4 [vulva](#) abnormal (invagination considerably reduced); hermaphrodites self-sterile. OA2: *n2841*, *n2842*. CLONED: encodes predicted protein with similarity to β-1,4-galactosyltransferase. [MT]

**sqv-4 V 2.76 n2840**

: morphology of L4 [vulva](#) abnormal (invagination considerably reduced); hermaphrodites self-sterile. OA1: *n2827*. [MT]

**sqv-5 I 7.15 n3039**

: morphology of L4 [vulva](#) abnormal (invagination considerably reduced); hermaphrodites self-sterile. [MT]

**sqv-6 V 0.99 n2845**

: morphology of L4 [vulva](#) abnormal (invagination considerably reduced); hermaphrodites self-sterile. [MT]

**sqv-7 II 0.20 n2844**

: morphology of L4 [vulva](#) abnormal (invagination considerably reduced); hermaphrodites self-sterile. OA1: *n2839* (somewhat fertile). [MT]

**sra**

**s**erpentine **r**eceptor family, class **A** ( $\alpha$ ) [CX]. *sra-1* to *sra-9* clustered, 35% identity overall; *sra-10,11,12* clustered, 20–25% identity to *sra-1*, etc.

#### ***sra-1* II 1.4**

NMK. Encodes predicted serpentine receptor; *sra-1*:GFP expressed in male spicule [neurons](#) SPD/SPV; *sra-1* to *sra-9* clustered. [[Troemel et al. 1995](#)] [CX]

#### ***sra-2* II 1.4**

NMK. Encodes predicted serpentine receptor; *sra-1* to *sra-9* clustered. [[Troemel et al. 1995](#)] [CX]

#### ***sra-3* II 1.4**

NMK. Encodes predicted serpentine receptor; *sra-1* to *sra-9* clustered. [[Troemel et al. 1995](#)] [CX]

#### ***sra-4* II 1.4**

NMK. Encodes predicted serpentine receptor; *sra-1* to *sra-9* clustered. [[Troemel et al. 1995](#)] [CX]

#### ***sra-5* II 1.4**

NMK. Probable pseudogene; may encode predicted serpentine receptor; *sra-1* to *sra-9* clustered. [[Troemel et al. 1995](#)] [CX]

#### ***sra-6* II 1.4**

NMK. Encodes predicted serpentine receptor; *sra-6*:GFP expressed in [sensory neurons](#) ASK, ASI (faint), [interneuron](#) PVQ; also in male spicule [neurons](#) SPD/SPV; *sra-1* to *sra-9* clustered. [[Troemel et al. 1995](#)] [CX]

#### ***sra-7* II 1.4**

NMK. Encodes predicted serpentine receptor; *sra-7*:GFP expressed in sensory [neuron](#) ASK; *sra-1* to *sra-9* clustered. [[Troemel et al. 1995](#)] [CX]

#### ***sra-8* II 1.4**

NMK. Encodes predicted serpentine receptor; *sra-1* to *sra-9* clustered. [[Troemel et al. 1995](#)] [CX]

#### ***sra-9* II 1.4**

NMK. Encodes predicted serpentine receptor; *sra-9*:GFP expressed in sensory [neuron](#) ASK; *sra-1* to *sra-9* clustered. [[Troemel et al. 1995](#)] [CX]

#### ***sra-10* II 3.05**

NMK. Encodes predicted serpentine receptor; *sra-10*:GFP expressed in sensory [neuron](#) URX, [interneuron](#) ALA, additional [interneurons](#), [pharyngeal neurons](#), muscle; *sra-10,11,12* clustered. [[Troemel et al. 1995](#)] [CX]

#### ***sra-11* II 3.05**

NMK. Encodes predicted serpentine receptor; *sra-11*:GFP expressed in [interneurons AIY](#), AVB, one pharyngeal [neuron](#); *sra-10,11,12* clustered. [[Troemel et al. 1995](#)] [CX]

#### ***sra-12* II 3.05**

NMK. Encodes predicted serpentine receptor; *sra-10,11,12* clustered. [[Troemel et al. 1995](#)] [CX]

#### ***sr*b**

**s**erpentine **r**eceptor family, class **B** (Beta) [CX]; 30% identity overall, distant similarity to *sra* class.

#### ***sr*b-1 II – 2.6**

NMK. Encodes predicted serpentine receptor; *sr*b-1 to *sr*b-5 possible operon. [[Troemel et al. 1995](#)] [CX]

#### ***sr*b-2 II – 2.6**

NMK. Encodes predicted serpentine receptor; [\*srb-1\*](#) to [\*srb-5\*](#) possible operon. [Troemel et al. 1995] [CX]

#### ***srb-3 II – 2.6***

NMK. Encodes predicted serpentine receptor; [\*srb-1\*](#) to [\*srb-5\*](#) possible operon. [Troemel et al. 1995] [CX]

#### ***srb-4 II – 2.6***

NMK. Probable pseudogene; may encode predicted serpentine receptor; [\*srb-1\*](#) to [\*srb-5\*](#) possible operon. [Troemel et al. 1995] [CX]

#### ***srb-5 II – 2.6***

NMK. Encodes predicted serpentine receptor; [\*srb-1\*](#) to [\*srb-5\*](#) possible operon. [Troemel et al. 1995] [CX]

#### ***srb-6 II 1.95***

NMK. Encodes predicted serpentine receptor; *srb-6*:GFP expressed in [sensory neurons](#) ADL, ASH, ADF (faint), PHA, PHB; also in vulval region; clustered with *srd-1,2*. [Troemel et al. 1995] [CX]

#### ***srb-7 III – 0.8***

NMK. Probable pseudogene; may encode predicted serpentine receptor; *srb-7,8,9* clustered. [Troemel et al. 1995] [CX]

#### ***srb-8 III – 0.8***

NMK. Encodes predicted serpentine receptor; *srb-7,8,9* clustered. [Troemel et al. 1995] [CX]

#### ***srb-9 III – 0.8***

NMK. Encodes predicted serpentine receptor; *srb-7,8,9* clustered. [Troemel et al. 1995] [CX]

#### ***srb-10 III – 0.9***

NMK. Probable pseudogene; may encode predicted serpentine receptor; *srb-10,11* clustered. [Troemel et al. 1995] [CX]

#### ***srb-11 III – 0.9***

NMK. Encodes predicted serpentine receptor; *srb-10,11* clustered. [Troemel et al. 1995] [CX]

#### ***src***

***src*** oncogene similarity.

#### ***src-1 ?***

NMK Tc5 insertion obtained; encodes protein with similarity to *src* oncogene; not yet located on physical map. [KR]

#### ***srd***

***s*erpentine *r*eceptor family, class **D** (Delta)** [CX].

#### ***srd-1 II 1.95***

NMK. Encodes predicted serpentine receptor; 48% identity to linked gene [\*srd-2\*](#); *srd-1*:GFP expressed in sensory [neuron](#) ASI; also only in male, sensory [neuron](#) ADF, [male tail neurons](#) (R8/R9?). [Troemel et al. 1995] [CX]

#### ***srd-2 II 1.95***

NMK. Encodes predicted serpentine receptor; 48% identity to linked gene *srd-1*. [Troemel et al. 1995] [CX]

#### ***sre***

***s*erpentine *r*eceptor family, class **E** (Epsilon)** [CX].

### ***sre-1* II 0.5**

NMK. Encodes predicted serpentine receptor; 28% identity to *sre-2*; *sre-1*:GFP expressed in [sensory neurons](#) ADL, ASJ (faint). [[Troemel et al. 1995](#)] [CX]

### ***sre-2* II 0.75**

NMK. Encodes predicted serpentine receptor; 28% identity to *sre-1*. [[Troemel et al. 1995](#)] [CX]

### ***srf***

***s u rf*** ace antigenicity abnormal [AT]. Also ectopic surface binding of lectin or antibody.

### ***srf-1* II 4.35 *yj1***

: adult cuticle fails to bind adult-specific antiserum; gross morphology wt. [[Politz et al. 1990](#)] [AT]

### ***srf-2* I 5.35 *yj262***

: increased binding of anticuticle serum, ectopic lectin WGA binding, no labeling with L1-specific MAb M38; gross morphology wt. OA>20: *yj133*, *yj422*, *ct104*, *ct117*, *dv1*, *dv2*, *dv37*, etc. All alleles recessive. [[Hemmer et al. 1991](#); [Link et al. 1992](#)] [AT, CL]

### ***srf-3* IV 6.36 *yj10***

: increased binding of anticuticle serum, ectopic WGA lectin binding, no labeling with L1-specific MAb M38; gross morphology wt; fragile cuticle, increased drug permeability, reduced SDS resistance of dauers. OA1: *ct107*. [[Hemmer et al. 1991](#); [Link et al. 1992](#)] [AT, CL]

### ***srf-4* V 23.95 *ct109***

: altered cuticle labeling, ectopic WGA lectin binding, pleiotropic defects: Unc, Egl, Mab, Mig (DTC); variable [neuronal](#) abnormalities, SDS-sensitive dauers; enhances [\*lin-12\* \(gf\)](#). OA7: *ct113*, *dv11*, *dv39*, etc. [[Link et al. 1992](#)] [CL]

### ***srf-5* X 12.62 *ct115***

: ectopic surface binding of lectins SBA, WGA. OA5: *ct114*, *dv18*, *dv32*, *dv40*, etc. [[Link et al. 1992](#)] [CL]

### ***srf-6* II 0.08 *yj13***

: all larval stages (but not adult) label with L1-specific MAbs M37, M38; gross phenotype wt; see also *daf-1,4,7,8,11,14* (related phenotype). OA4: *yj41*, *yj43*, *yj5*, *yj15*. [AT, DR]

### ***srf-8* V 3.07 *dv38***

: altered cuticle labeling, ectopic WGA lectin binding, pleiotropic defects: Unc, Egl, Mab, Mig (DTC); variable [neuronal](#) abnormalities, SDS-sensitive dauers; enhances [\*lin-12\* \(gf\)](#). [[Link et al. 1992](#)] [CL]

### ***srf-9* V 1.46 *dv4***

: altered cuticle labeling, ectopic WGA lectin binding, pleiotropic defects: Unc, Egl, Mab, Mig (DTC); variable [neuronal](#) abnormalities, SDS-sensitive dauers; enhances [\*lin-12\* \(gf\)](#). OA1: *dv16*. [[Link et al. 1992](#)] [CL]

### ***srg***

***s*erpentine *r*eceptor family, class **G** (Gamma) [CX]; 10–30% overall identity.**

### ***srg-1* III – 1.0**

NMK. Encodes predicted serpentine receptor; in possible operon, *srg-1* to *srg-9*. [[Troemel et al. 1995](#)] [CX]

### ***srg-2* III – 1.0**

NMK. Encodes predicted serpentine receptor; *srg-2*:GFP expressed in sensory [neuron](#) ASK; in possible operon, *srg-1* to *srg-9*. [[Troemel et al. 1995](#)] [CX]

***srg-3 III – 1.0***

NMK. Encodes predicted serpentine receptor; in possible operon, [\*srg-1\*](#) to *srg-9*. [[Troemel et al. 1995](#)] [CX]

***srg-4 III – 1.0***

NMK. Encodes predicted serpentine receptor; in possible operon, [\*srg-1\*](#) to *srg-9*. [[Troemel et al. 1995](#)] [CX]

***srg-5 III – 1.0***

NMK. Encodes predicted serpentine receptor; in possible operon, [\*srg-1\*](#) to *srg-9*. [[Troemel et al. 1995](#)] [CX]

***srg-6 III – 1.0***

NMK. Encodes predicted serpentine receptor; in possible operon, [\*srg-1\*](#) to *srg-9*. [[Troemel et al. 1995](#)] [CX]

***srg-7 III – 1.0***

NMK. Encodes predicted serpentine receptor; in possible operon, [\*srg-1\*](#) to *srg-9*. [[Troemel et al. 1995](#)] [CX]

***srg-8 III – 1.1***

NMK. Encodes predicted serpentine receptor; *srg-8*:GFP expressed in sensory [neuron](#) ASK; stronger in larvae; in possible operon, [\*srg-1\*](#) to *srg-9*. [[Troemel et al. 1995](#)] [CX]

***srg-9 III – 1.1***

NMK. Encodes predicted serpentine receptor; in possible operon, [\*srg-1\*](#) to *srg-9*. [[Troemel et al. 1995](#)] [CX]

***srg-10 III – 3.4***

NMK. Encodes predicted serpentine receptor; in possible operon, *srg-10,11,13*. [[Troemel et al. 1995](#)] [CX]

***srg-11 III – 3.4***

NMK. Possible pseudogene; may encode predicted serpentine receptor; in possible operon, *srg-10,11,13*. [[Troemel et al. 1995](#)] [CX]

***srg-12 III – 0.1***

NMK. Encodes predicted serpentine receptor; sequence most diverged among *srg* genes; *srg-12*:GFP expressed in gut, [excretory](#) cell. [[Troemel et al. 1995](#)] [CX]

***srg-13 III – 3.5***

NMK. Encodes predicted serpentine receptor; *srg-13*:GFP expressed in sensory [neuron](#) PHA; in possible operon, *srg-10,11,13*. [[Troemel et al. 1995](#)] [CX]

***srl***

**s** uppressor of **r** *ol-3* **I** lethality [BC].

***srl-1 II N s2501***

: recessive suppressor of lethal phenotype of *rol-3(s1040)*; Rol phenotype of [\*rol-3\*](#) generally not suppressed; homozygous [\*srl-1\*](#) males display aberrant tail morphologies. OA3: *s2503*, *s2500*, *s2502*. Some nonallelic noncomplementation with *srl-2*. [[Barbazuk et al. 1994](#)] [BC]

***srl-2 III LC s2504***

: recessive suppressor of lethal phenotype of *rol-3(s1040)* as well as several other (but not all) [\*rol-3\*](#) alleles; Rol phenotype of [\*rol-3\*](#) generally not suppressed; homozygous [\*srl-2\*](#) males display aberrant tail morphologies. OA3: *s2506*, *s2507*, *s2508*. Some nonallelic noncomplementation with [\*srl-1\*](#). [[Barbazuk et al. 1994](#)] [BC]

***sro***

**s**erpentine **r**eceptor, class **O** (opsin similarity) [CX].

***sro-1* II 0.4**

NMK. Encodes predicted receptor, distant similarity to opsin; *sro-1*:GFP expressed in sensory [neuron](#) ADL, [neuron](#) SIA. [Troemel et al. 1995] [CX]

***ssb***

**s** ingle **s** tranded DNA-**b** inding protein family [FH].

***ssb-1* III N *pk61***

: Tc1 insertion, no known phenotype; encodes 178-aa, 23-kD nuclear protein with N-terminal similarity to bacterial SSB; binds single-strand TTTCAATA (candidate feminizing element). [FH]

***ssp***

**s** perm- **sp** ecific genes [BA]. Transcripts only in spermatogenic tissue; often small Transcripts in msp clusters.

***ssp-1* IV 4.58**

NMK. Sperm-specific transcript, 1.0 kb. [BA]

***ssp-2* IV 4.58**

NMK. Sperm-specific transcript, 0.8 kb. [BA]

***ssp-3* IV 4.58**

NMK. Sperm-specific transcript, 0.9 kb; member of multigene family. [BA]

***ssp-4* IV 4.58**

NMK. Sperm-specific transcript, 0.9 kb; related to *ssp-3*. [BA]

***ssp-7* IV 1.61**

NMK. Sperm-specific transcript, 1.4 kb. [BA]

***ssp-9* IV 1.19**

NMK. Sperm-specific transcript, 0.5 kb; related to *ssp-10*. [BA]

***ssp-10* IV 4.58**

NMK. Sperm-specific transcript, 0.5 kb; member of multigene family. [BA]

***ssp-12* IV 4.58**

NMK. Sperm-specific transcript, 1.2 kb. [BA]

***ssp-13* IV 4.58**

NMK. Sperm-specific transcript, 1.7 kb. [BA]

***ssp-14* IV 4.58**

NMK. Sperm-specific transcript, 1.2 kb. [BA]

***ssp-17* IV 4.58**

NMK. Sperm-specific transcript, 0.8 kb. [BA]

***ssp-18* IV 4.58**

NMK. Sperm-specific transcript, 1.2 kb. [BA]

***stp***

**S** H2-containing **t** yrosine **p** phosphatase family [CGC].

***stp-1* II – 0.87**

NMK. Encodes predicted protein related to SH2-containing tyrosine phosphatase family. [CGC]

***stu***

**st** erile **u** ncoordinated [CB].

**stu-1**

= *lin-23*

***stu-2* II 2.01 e2297**

: spo; thin, sterile, uncoordinated; males similar; [testis](#) thin but well formed, contains sperm; no rays or fan, spicules rudimentary. ES3 NA1. [CB]

***stu-3* V 25.09 q265**

: uncoordinated, sterile, Vul. [BS]

***stu-4* I – 4.44 e2406**

: ts; sterile Unc; extensive failures of postembryonic cell division at 25°C, many polyploid nuclei, probable defect in karyokinesis; hermaphrodites and males viable and fertile at 15°C. [CB]

***stu-6* X 5.43 e2408**

: sterile and uncoordinated but not defective in cell division: small, variably dumpy, often second vulval protrusion posteriorly. Abnormal gonad arms, abnormal oocytes; ventral cord has abnormal positioning of nuclei and commissures, cord sometimes detached from [hypodermal ridge](#). [CB]

***sud***

**su** pernumerary cell **d** ivisions.

***sud-1* II 0.92**

: Mutation leads to embryonic lethality, high cell number; possible failure to repress cell cycle at end of proliferation phase. [GE]

***sum***

**su** ppressor of **m** ultivulva phenotype [GS].

**sum-1**

= *sel-12*

***sup***

**sup** pressor [CB]. See also *sel*, *sli*, *smg*, *smu*.

***sup-1* III 11.65 e995**

: dm; dominant allele-specific suppressor of *unc-17(e245)*; does not suppress *unc-17(e876)*; no phenotype alone. ES3 (in presence of *e245*) ME3. OA>5: *e996xri*, *e1827*, *e1955*, etc. (all similar). See also *unc-123*. [CB, RM]

***sup-2* X 1.44 e997**

: dm; dominant allele-specific suppressor of *unc-17(e245)*; does not suppress *unc-17(e876)*; no phenotype alone. ES3 (in presence of *e245*) ME3. Weaker suppressor than [\*sup-1\*](#). NA1. [CB, RM]

**sup-3**

= *myo-3*

### **sup-4**

= *sup-5*

### ***sup-5 III – 0.11 e1464***

: sd; amber suppressor, partially or completely suppresses amber alleles of >40 different genes; slow-growing cs (sterile at 15°C), otherwise no phenotype alone; alteration in tRNA<sup>Trp</sup> anticodon. ES3 (in presence of *unc-13[e450]*, etc.) ME1. OA>20: all identical to *e1464*, e.g., *e1877dm* (pka *sup-4*, dominant suppressor of *unc-51* [e369amb]). Corresponds to *rtw-1*, tRNA<sup>Trp</sup> structural gene. [[Waterston and Brenner 1978](#); [Wills et al. 1983](#)]

### ***sup-6 II 12.21 st19***

: dm; dominant suppressor of *unc-13(e309)*; recessive lethal; also suppresses certain *daf* mutations; does not suppress amber or ochre alleles of *unc-54*. ES3. [PD, RW]

### ***sup-7 X – 2.89 st5***

: sd; strong amber suppressor, partially or completely suppresses amber alleles of >40 different genes; slow growing or sterile below 22°C, grows best at 23°C; suppression strongest at low temperature; otherwise no gross phenotype alone; alteration in tRNA<sup>Trp</sup> anticodon. ES3 (in presence of *unc-13[e450]*, etc.) ME2. OA5 all identical to *st5*. Corresponds to *rtw-2*, tRNA<sup>Trp</sup> structural gene. [[Waterston 1981](#); [Wills et al. 1983](#)]

### ***sup-8 V – 0.01 e1563***

: dm, uvi; dominant suppressor of *unc-17(e245)*; no phenotype alone. ES3 in presence of *e245*. NA1. [CB]

### ***sup-9 II – 11.92 n180***

: recessive suppressor of *unc-93(e1500)*, no phenotype alone; probably null allele. ES3 (in presence of *e1500*) ME3. OA>20(lf): *n180spo*, *n192uvi*, *n186*, *n350* (all resemble *n180*). Also neomorphic dominant allele: *n1550sd* (severe rubberband, almost sterile, inviable; *n1550/+* strong “rubberband” Unc-93 phenotype; muscle activation defective [flaccid, long]). Also dominant-negative suppressor alleles: *n1435*, *n242* (semidominant suppressors of *sup-10[n983]*). [[Greenwald and Horvitz 1980](#); [Levin and Horvitz 1993](#)] [JT, MT]

### ***sup-10 X 24.12 n183***

: recessive suppressor of *unc-93(e1500)*, no phenotype alone; probably null allele. ES3 (in presence of *e1500*) ME3. OA>20(lf): *n181spo*, *n245gri*, *n184* (large viable deletion, also removes *mlc-1*, *nhr-1*), *n185*, *n221*, *n1034*, etc. Also neomorphic dominant allele: *n983dm* (uncoordinated “rubberband” Unc-93 paralysis, muscle activation defective [flaccid, long]); suppressed by intragenic revertants, *unc-93* null alleles, etc.) CLONED: sequence predicts 332-aa protein, possible signal sequence, transmembrane domain. [[Greenwald and Horvitz 1980](#); [Levin and Horvitz 1993](#)] [JT, MT]

### ***sup-11 I – 5.89 n403***

: dm; dominant suppressor of *unc-93(e1500)*, recessive small scrawny slow growing phenotype. ES3. OA9 (dominant): *n401*, *n402*, *n404*, *n406*, etc. (all resemble *n403*). Also alleles derived from *n403*, e.g., *n403n406* (recessive suppressor of *unc-93[e1500]*, no phenotype alone). OA7 (recessive). Also putative null alleles derived from *n403*, e.g., *n403n682* (no suppressive effect, recessive-lethal, late embryo arrest). OA3: *n403n681amb* (partly suppressed by *sup-5*, L1-lethal). [[Greenwald and Horvitz 1982](#)] [MT]

### ***sup-12 X – 8.31 st89***

: recessive suppressor of *unc-60(e677)* and other *unc-60* alleles (*e723*, *e890*); alone, abnormal gonad and minor changes in *body wall muscle* ultrastructure. ES3 (in presence of *e677*). OA>10: *st86* (suppresses lethal allele *unc-60[s1586]* to viable ts sterile phenotype), etc. [[Francis and Waterston 1985](#)] [BC]

### ***sup-13 III 0.00 st210***

: strong recessive suppressor of *unc-78*(*e1217*) and at least two other *unc-78* alleles (*e1221*, *st43*); no phenotype alone. ES3 (in presence of *e1217*). [RW]

***sup-16 IV N st500***

: sd; semidominant suppressor of *unc-52*(*e669*) and at least one other *unc-52* allele (*e1421*); does not suppress *unc-13*(*e1091*); no phenotype alone. ES3 (in presence of *e669*). [RW]

***sup-17 I 3.04 n316***

: allele and lineage nonspecific suppressor of *lin-12* dominant mutations, weakly dominant; phenotype alone is recessive Dpy, recessive Egl; abnormal vulval cell lineages; *male tail* abnormal; Egl and Dpy phenotypes stronger at 25°C. ES2 ME0. Similar degree of suppression of *lin-12(dom)* in *nDf24/+* and *n316/+*; also *n316/nDf24* is maternal-effect-lethal. OA>5: *n1260* (weakly sd, ts; at 15°C, phenotype non-Dpy non-Egl very weak suppressor ME3; at 25°C, phenotype similar to *n316*, *n1258*, *n1306*, etc. [[Trent et al. 1983](#)] [JT, MT]

***sup-18 III – 0.71 n463***

: spo; strong recessive suppressor of *sup-10*(*n983*), weak suppressor of *unc-93*(*e1500*); no phenotype alone. OA>10: *n527*, *n528*, *n1010*, *n1033*, *n1038*, etc. [[Greenwald and Horvitz 1986](#)] [MT]

***sup-19 V 19.24 m210***

: weak recessive suppressor of *unc-15*(*e73*). [[Brown and Riddle 1985](#)] [DR]

***sup-20 X 16.97 n821***

: recessive suppressor of *unc-105*(*n490*); mosaic analysis indicates focus in muscle cells. OA2 (viable suppressor alleles): *n1168*, *n1169*. Also many recessive-lethal alleles (embryonic arrest), probable nulls; suppressor alleles fail to complement *let-2*, probably allelic. [[Park and Horvitz 1986b](#); [Liu et al. 1996](#)] [MT, RW]

***sup-21 X 0.63 e1957***

: sd; amber suppressor, partially or completely suppresses amber mutations in many genes but not in *unc-13*; no phenotype alone. ES3 (in presence of *tra-3[e1107]*, etc.) ME3. OA1: *e2064* (identical). Anticodon mutation in tRNA<sup>Trp</sup> (*rtw-10*). [[Kondo et al. 1990](#)]

***sup-22 IV – 2.53 e2057***

: weak amber suppressor, suppresses amber mutations in a few genes (*tra-3*, *dpy-20*); no phenotype alone. ES3 (in presence of *tra-3[e1107]*) ME3 NA1. [[Hodgkin 1985](#); [Kondo et al. 1990](#)]

***sup-23 IV 1.82 e2059***

: weak amber suppressor, suppresses amber mutations in a few genes (*tra-3*, *dpy-20*, *lin-1*); no phenotype alone. ES3 (in presence of *tra-3[e1107]*) ME3 NA1. [[Hodgkin 1985](#); [Kondo et al. 1990](#)]

***sup-24 IV 13.01 st354***

: weak amber suppressor, suppresses *unc-52*(*e669*), weakly suppresses *unc-13*(*e450*); no gross phenotype alone. ES3 (in presence of *unc-52[e669]*) OA7 (identical). Anticodon mutation in tRNA<sup>Trp</sup> (*rtw-4*). [[Kondo et al. 1990](#)]

***sup-25***

= *sel-1*

***sup-26 III – 3.37 n1091***

: sd; suppressor of *her-1* (*n695sd*); no phenotype alone. OA1: *ct49sd* (similar). [BW, LK]

***sup-27 V 6.86 n1092***

: sd; suppressor of [her-1](#) (n695sd); no phenotype alone. OA1: *n1102sd* (similar). [BW, LK]

***sup-28 X 0.64 e1958***

: (pka [sup-21](#)), amber suppressor, suppresses *tra-3(e1107)*, *dpy-20(e2017)*, but not *unc-13(e450)*; no gross phenotype alone. ES3 (in presence of *tra-3[e1107]*) ME3 OA2 (identical). Anticodon mutation in tRNA<sup>Trp</sup> (*rtw-8*). [[Kondo et al. 1990](#)]

***sup-29 IV – 2.82 e1986***

: (pka [sup-22](#)) very weak amber suppressor, suppresses *tra-3(e1107)*; no phenotype alone. ES3 (in presence of *tra-3[e1107]*) ME3 OA2 (identical). Anticodon mutation in tRNA<sup>Trp</sup> (*rtw-9*). [[Kondo et al. 1990](#)]

***sup-30 IV R e1992***

: weak recessive suppressor of *tra-3(e1767)*. NA1. [[Hodgkin 1986](#)]

***sup-31 IV 6 e2042***

: xri; weak recessive suppressor of *tra-3(e1767)*. NA1. [[Hodgkin 1986](#)]

***sup-32 X 0 e2058***

: (pka *sup-21*), amber suppressor, suppresses *tra-3(e1107)*, *dpy-20(e2017)*; probably not a tRNA<sup>Trp</sup> mutation. OA1: *e2061* (weaker). [[Hodgkin 1985](#); [Kondo et al. 1990](#)]

***sup-33 X 0 st389***

: amber suppressor, suppresses *unc-52(e669)*, *dpy-20(e2017)*, not *unc-13(e450)*. NA1. Anticodon mutation in tRNA<sup>Trp</sup> (*rtw-11*). [[Kondo et al. 1990](#)]

***sup-34 I – 17.71 e2227***

: weak amber suppressor, suppresses *tra-3(e1107)*, weakly suppresses *unc-52(e669)*; anticodon mutation in tRNA<sup>Trp</sup> (*rtw-12*). NA1. [[Kondo et al. 1990](#)]

***sup-35 III 5.81 e2220***

: recessive suppressor of ts alleles of [pha-1](#) (e2123 and *t1001*); no other phenotype. OA>100: *e2221*, *e2223*, etc. [[Schnabel et al. 1991](#)]

***sup-36 IV N e2217***

: recessive suppressor of ts alleles of [pha-1](#) (e2123 and *t1001*); no other phenotype. OA26: *e2218*, *e2219*, etc. [[Schnabel et al. 1991](#)]

***sup-37 V N e2214***

: recessive suppressor of ts alleles of [pha-1](#) (e2123 and *t1001*); no other phenotype. OA7: *e2215*, *e2216*, etc. [[Schnabel et al. 1991](#)]

***sup-38 IV 10.91 ra5***

: sd; semidominant suppressor of class-1 (paralyzed) [unc-52](#) alleles; does not suppress Unc-52 gonad defects, nor lethal (class 2 and 3) [unc-52](#) alleles; in wt background, *ra5* homozygotes exhibit some muscle fragility, low brood size (<30); probable gf allele. OA4(sd): *ra14* (brood <10), *ra18*, *ra21* (weaker). Also intragenic revertants: *ra5ra60* (MeI, progeny die as larvae; rescued zygotically; probable null), *ra5ra55* (leaky, viable). Also If allele: *n2667* (abnormal axon growth, processes missing in left [ventral nerve cord](#)). [[Gilchrist and Moerman 1992](#)] [DM, EG, MT]

***sup-39 II 0.22 je5***

: dominant suppressor of *unc-73(e936)*; impenetrant embryonic-lethal, escapers almost wt, abnormal double row of oocyte nuclei. OA1: *je6*. [[Run et al. 1996](#)] [JW]

***sup-40 I 0.57 lb130***

: dominant suppressor of *unc-8(e15)*, *unc-8(n491)*; also recessive phenotypes, independent of [unc-8](#) genotype: slow growth, sterility (abnormal oocytes), swollen hypodermal nuclei in adult, resistant to NDG (nordihydroguaiaretic acid). [[Shreffler et al. 1995](#)] [MP]

***sup-41 IV 1.86 lb125***

: dominant suppressor of *unc-8(e15)*, *unc-8(n491)*; also partial suppressor of *deg-1(u38)*. [[Shreffler et al. 1995](#)] [MP]

***sup-42 X N lb88***

: recessive suppressor of *unc-8(n491)*; very mild sluggish Unc phenotype alone; 25% eggs fail to hatch. [[Shreffler et al. 1995](#)] [MP]

***sur***

**su** ppressor of activated [let-60](#) **r** as [MH].

**sur-1**

= *mpk-1*

***sur-2 I 26.28 ku9***

: suppressor of [let-60](#) (*gf*); pleiotropic effects; some gonadal abnormality, vulval defects, larval lethality, Egl, [male tail](#) defects; *ku9/Df* stronger Vul phenotype. OA7: *ku9*, *ku31*, *ku42*, *ku115amb* (all similar to *ku9*; all nonsense mutations), *ku60* (Egl non-Vul), etc. CLONED: 5-kb transcript, enriched in embryo and early larva; encodes predicted 1586-aa novel protein; *sur-2:lacZ* expressed in [VPC](#) during vulval differentiation. [[Singh and Han 1995](#)] [MH]

**sur-3**

= *ksr-1*

***sur-4 III 5.33 ku23***

: sd; suppressor of *let-60(gf)*; no obvious phenotype alone. [MH]

***sus***

**su** ppressor of **s** uppressor [DR].

***sus-1 III – 12.57 m156***

: reduces suppression by [sup-3](#) alleles; enhances paralyzed phenotype of *unc-15(e73)*, *unc-54(e190)*; no phenotype alone. ES1. OA1: *m155*. [[Brown and Riddle 1985](#)]

***suv***

**su** ppressor of **V** ul phenotype [MT].

***suv-1 X – 15.81 n1329***

: suppresses Vul phenotype of *lin-10(n1390)*; complex suppressive or enhancing interactions with other [vulva](#) determination genes; no phenotype alone. OA11. [MT]

***suv-2 X 5.60 n1694***

: suppresses Vul phenotype of *lin-10(n1390)*. OA6. [MT]

***suv-3 ?***

Mutations suppress Vul phenotype of *lin-10(n1390)*. OA3. [MT]

***suv-4 ?***

Mutations suppress Vul phenotype of *lin-10(n1390)*. OA1. [MT]

***suv-5* ?**

Mutations suppress Vul phenotype of *lin-10(n1390)*. OA1. [MT]

***syr***

***sy*** nthetic ***r*** oller [JW].

***syr-1 II – 18 je11***

: no phenotype alone, recessive roller in the presence of *sup-39(je5)*; possibly allelic with [\*sqt-2\*](#) (similar map position). [JW]

***tab***

***t*** ouch response ***ab*** normal [TU]. Defective in response to strong touch, as opposed to light touch (Mec).

***tab-1 II 0.16 u271***

: fails to respond to prod (strong touch). NA1. [TU]

***tax***

chemo ***tax*** is abnormal [GT]. See also *che*.

***tax-1***

= *che-1*

***tax-2 II N p671***

: defects in chemotaxis (all attractants), athermotactic; Odr; dye-filling reveals some amphid and phasmid axon defects. OA5: *p691*, *p694*, *ks10*, etc. [[Dusenberry 1976](#)] [CX, FK]

***tax-3 A ? p673***

: defects in chemotaxis (most attractants), athermotactic. NA1. [[Dusenberry 1976](#)] [FK]

***tax-4 III – 0.26 p678***

: defective chemotaxis to Na, cAMP; repelled by Cl; athermotactic; reduced brood size. OA3: *p674*, *ks28*, *ks11* (athermotactic; defects in sensory axon outgrowth). CLONED: encodes predicted 772-aa transmembrane protein with 36% identity to human cGMP-gated ion channel. [[Dusenberry 1976](#)] [FK]

***tax-5 V N p672***

: defective chemotaxis to Na; repelled by cAMP. NA1. [[Dusenberry 1976](#)]

***tax-6 ? p675***

: defective chemotaxis to Na, Cl, cAMP; thermophilic; small. NA1. [FK]

***tba***

***t*** u ***b*** ulin, ***A*** lpha [CGC].

***tba-1 I 3.92***

NMK. Encodes α-tubulin; *tba-1:lacZ* expressed in [touch cells](#), motor [neurons](#), and certain other [neurons](#). [[Fukushige et al. 1995](#)] [SQ]

***tba-2 I 16.20***

NMK. Encodes α-tubulin; *tba-2:lacZ* expressed in [touch cells](#), motor [neurons](#), and certain other [neurons](#). [SQ]

***tba-3***

= *mec-12*

***tba-4* ?**

NMK. Encodes  $\alpha$ -tubulin. [SQ]

***tba***

**t u b ulin, B eta** [CGC].

***tbb-1 III 4.40***

NMK. Encodes  $\beta$ -tubulin. [NW]

***tbb-2 III – 4.39***

NMK. Encodes  $\beta$ -tubulin. [NW]

***tbg***

**t u b ulin, G amma** [CGC].

***tbg-1 III 0.61***

NMK. Possibly corresponds to [\*emb-30\*](#); encodes predicted  $\gamma$ -tubulin; final gene in operon with genes for ubiquitin conjugating enzyme, RNA polymerase subunit; antisense expression of [\*tbg-1\*](#) leads to embryonic arrest at one-cell stage, Emb-30 phenocopy. [SQ]

***tbp***

**T ATA b ox-binding p rotein family** [CGC].

***tbp-1* ?**

NMK. Encodes 340-aa protein, 85% identity to human TATA box-binding protein (TBP) in C-terminal half; recombinant TBP-1 binds [\*hsp-16\*](#) TATA box. [[Lichtsteiner and Tjian 1993](#)]

***tbx***

**T b o x family** [CGC]. Similarity to mouse T locus product, putative transcriptional regulator.

***tbx-2 III – 2.4***

NMK. Similarity to mouse T-box genes, closest to mouse Tbx2 (70% identity in T box domain). (F21H11.3) [[Aguilnik et al. 1995](#)]

***tbx-7 III – 1.1***

NMK. Similarity to mouse T-box genes. (ZK328) [[Aguilnik et al. 1995](#)]

***tbx-8 III 2.41***

NMK. Similarity to mouse T-box genes; T07C4.2; related to [\*tbx-9\*](#), divergent Transcripts. [[Aguilnik et al. 1995](#)]

***tbx-9 III 2.41***

NMK. Similarity to mouse T-box genes; T07C4.6; related to [\*tbx-8\*](#), divergent Transcripts. [[Aguilnik et al. 1995](#)]

***tcf***

**t ri c hlor f on-resistant**. See *ric*.

***tcf-1***

= *unc-41*

***tcp***

**Tc** ha **p** eronin. See *cct*.

***tcp-1***

= *cct-1*

***tkr***

**t** achy **k**inin **r**eceptor family [CGC].

***tkr-1 III 0.48 pk69***

: Tc1 insertion, no known phenotype; encodes predicted protein with similarity to tachykinin receptors. [CGC, NL]

***tmr***

**t** etra **m** isole- **r**esistant. See *lev*.

***tmr-1***

= *lev-1*

***tmr-2***

= *unc-38*

***tmr-3***

= *unc-63*

***tmr-4***

= *unc-29*

***tmy***

**t**ropo **m**yosin [HK].

***tmy-1 I 25.44***

Probably corresponds to [\*lev-11\*](#); three transcripts encoding tropomyosin, probable body wall and nonmuscle isoforms (284 aa, different C-termini) and pharyngeal isoform (256 aa, different promoter). [[Kagawa et al. 1995](#)] [HK]

***tnc***

**t**ropo **n** in **C** [HK].

***tnc-1 I - 0.30***

NMK. Encodes predicted 161-aa protein, three calcium-binding domains; closest similarity to vertebrate cardiac troponin C; see [\*pat-10\*](#); *tnc-1:lacZ* expressed in [body wall muscle](#). [HK]

***tni***

**t**ropon **n** in **I** [HK].

***tni-1 X 0.0***

NMK. Encodes predicted 242-aa protein, similarity to troponin I; *tni-1:lacZ* expressed in [body wall muscle](#). [HK]

***tni-2 X N***

NMK. Encodes predicted protein with similarity to troponin I; *tni-2:lacZ* expressed in [body wall muscle](#). [HK]

***toh***

**to** llis **h** [LT]. Tolloid and BMP-1 family.

**toh-1 III – 5.12**

NMK. Encodes protein with similarity to tolloid and BMP-1 regulatory metalloproteases. [LT]

**toh-2 III – 0.76**

NMK. Encodes protein with BMP-1 similarity. [LT]

**tpa**

**tpa** (**t** etradecanoyl **p** horbol **a** cetaate)-resistant [MJ].

**tpa-1 IV – 27.65 k501**

: sd; resistant to 0.1  $\mu$ M TPA. OA>4. CLONED: two Transcripts, different 5'ends; encode 80-kD (A) and 65-kD (B) proteins; closest similarity to mammalian PKC  $\delta$ . [[Tabuse et al. 1989](#); [Sano et al. 1995](#)] [MJ]

**tra**

sexual **tra** nsformer (XX animals masculinized) [CB].

**tra-1 III 6.69 e1099**

: XX animals transformed into low-fertility males; gonad morphology variable, testes reduced in size, few sperm made; XO phenotype male, similar gonad defects. ES3 ME1 (XX, XO). OA>20 (recessive): *e1834*ird (deletion, probable null, resembles *e1099*), *e1781*amb (soma male, gonad contains sperm and apparent oocytes), *e1488* (gonad and [intestine](#) hermaphrodite [self-fertile], rest of body male), *e1732* (gonad more masculinized than body, Smg-suppressible), *rh132* (gonad male, tail hermaphrodite), etc. Also gf alleles: *e1575*sd (pka [her-2](#), both XX and XO animals transformed into fertile females by *e1575* or *e1575*+/). ES3 ME0. OA>20 (dominant): many weaker than *e1575*, causing incomplete or slight feminization. Also intragenic revertants of dominants, XX masculinizing. OA>30 (ird). Also additional phenotypic classes, complex properties. CLONED: 1.5- and 5-kb Transcripts, encoding 288-aa and 1110-aa proteins with two and five zinc finger motifs; similarity to GLI family. [[Hodgkin 1987a](#); [Zarkower and Hodgkin 1992](#); [Barnes and Hodgkin 1996](#)] [CB, DZ, JK]

**tra-2 II 0.16 e1095**

: sd; XX animals transformed into infertile males with abnormal tail anatomy; gonad morphology male, normal spermatogenesis; XO phenotype wt male; *e1095*+/ XX is Egl hermaphrodite; probable null phenotype. ES3 ME3 (XO) ME0 (XX). OA>20 (recessive): *e1425*amb (resembles *e1095*), *q276* (XX animals transformed into mating males, anomalous non-null), *f70* (masculinized self-fertile hermaphrodite), *e1875* (slightly Egl hermaphrodite, very weak allele), *b202*ts (self-fertile hermaphrodite at 16°C, Tra-2 at 25°C), *e1209* (XX intersexual, Smg suppressible), etc. Also hypermorphic gf alleles: *e2020*dm (XX animals completely feminized, XO animals fertile males, slightly feminized; *e2020*+/ XX also female). OA>6 (hypermorphic): *e2046*, etc. (all weaker than *e2020*). Also constitutive "eg" gf alleles: *e2531*dm (*e2531* and *e2531*+/ XO animals hermaphrodite, no effect on XX). OA9 (constitutive): all resemble *e2531*. Intragenic revertants of both gf types are If (XX masculinizing). Also "mx," mixed effect alleles: *e1941*, *e2021* (dominant feminizing effect on XX germ line, recessive weak masculinization of XX soma). CLONED: 1.8-, 1.9-, 4.7-kb Transcripts; largest encodes 1475-aa TRA-2A membrane protein, nine predicted transmembrane domains; probable HER-1 receptor; transgene overexpression of TRA-2A feminizes XO animals; complex regulation and expression; downstream gene in operon with [ppp-1](#). [[Klass et al. 1976](#); [Doniach 1986](#); [Kuwabara et al. 1992](#); [Kuwabara 1996a](#)] [BG, CB, JK, PK]

**tra-3 IV 11.75 e1107**

: amb, mat; XX progeny of homozygous parents are abnormal sterile males or intersexes, occasionally self-fertile, especially at 15°C (15°C brood 1% of wt); XO phenotype wt; either maternal or zygotic expression of *tra-3*(+) sufficient for normal XX hermaphrodite development. ES3 (progeny testing) ME0 (XX) ME3 (XO).

OA>5: *e1525amb*, *e1767* (non-amb), *y240*, etc. (resemble *e1107*, probable nulls), *bn75ts* (Mog 25°C), *e2333* (XX anatomically wt hermaphrodite with increased brood size). Amber alleles very efficiently suppressed; used for [\*sup-7\*](#) transgene selection. CLONED: encodes predicted protein with similarity to vertebrate protease calpain, but lacking calcium-binding domains. [[Hodgkin 1986](#); [Fire 1986](#); [Hodgkin and Barnes 1991](#); [Barnes and Hodgkin 1996](#)] [CB]

### ***ttx***

**t** hermo **t** a **x** is abnormal [FK].

### ***ttx-1 V N p767***

: mutant animals strongly cryophilic; hypersensitive to dauer pheromone; [neuron](#) AFD lacks "fingers" (microvilli). [[Perkins et al. 1986](#)] [FK]

### ***ttx-2 III – 1.60 ks4***

: mutant animals cryophilic, occasionally move isothermally on a thermal gradient; stronger phenotype if grown 15°C; no obvious abnormality in chemotaxis to NaCl, osmotic avoidance, male mating, or dauer formation. CLONED: cosmid rescue (F52H10) [FK]

### ***ttx-3 X 6.90 ks5***

: mutant animals cryophilic, almost completely defective in isothermal tracking; no obvious abnormalities in chemotaxis to NaCl, osmotic avoidance, male mating, or dauer formation. [FK]

## **U to Z**

### ***ubc***

**ub** iquitin **c** onjugating enzymes [PC].

### ***ubc-1 IV – 0.01***

NMK. Encodes ubiquitin conjugating enzyme, homolog of yeast Ubc2p/Rad6p (52% partial sequence identity). Cosmid C04E2. [[Leggett et al. 1995](#)] [PC]

### ***ubc-2 IV 4.87***

NMK. Encodes ubiquitin conjugating enzyme, 134 aa; 95% identical to *Drosophila* DUC1, 85% identical to yeast Ubc4p/Ubc5p (can complement yeast mutant); *ubc-2:lacZ* strong in larval [nervous system](#), weaker in adult; corresponds to Let-70. [[Zhen et al. 1993, 1996](#)] [PC]

### ***ubq***

**ub** i **q** uitin structural genes [PC].

### ***ubq-1 III – 1.14***

NMK. Encodes polyubiquitin; *ubq-1:lacZ* expressed in [all cells](#) of embryo, L1; later mainly in muscle cells. [[Graham et al. 1989](#); [Stringham et al. 1992a](#)] [PC]

### ***ubq-2 III 17.3***

NMK. Encodes ubiquitin fused to 52-aa ribosomal protein; transcript both *cis*- and *trans*-spliced (SL1), expressed at all stages; abundance not affected by heat stress. [[Jones et al. 1995](#)] [PC]

### ***unc***

**unc** oordinated [CB].

### ***unc-1 X – 18.74 e719***

: recessive kinker, putative null; suppresses anaesthetic hypersensitivity of [unc-79](#) and [unc-80](#) mutants. ES3 ME1. OA>10 (recessive): *e50*, *e68*, *e114* (anomalous allele, transdominant suppressor of *n494sd*), etc. Also

neomorph/antimorph gf alleles: *e94sd* (former reference allele, recessive kinker; *e94/+* is weak coiler. ES2 ME2), *e1598dm* (pka [unc-102](#), both homozygote and *e1598/+* are strong Ric coilers; intragenic revertants of *e1598* resemble *e719*. ES3 ME0). OA>8 (dominant and semidominant): *n496*, *n775* (strongly dominant), *n494* (weakly semidominant), etc. Complex complementation among [unc-1](#) alleles. [Park and Horvitz 1986a; Morgan and Sedensky 1994] [CW]

#### ***unc-2 X – 13.67 e55***

: weak kinker, sluggish, thin; hypersensitive to serotonin, fails to desensitize to dopamine. ES3 ME2. OA>10: *e97*, *e129*, *e2379* (Unc, only subtle defect in adaptation), *mu74* (resembles *e55*, deletion, probable null), *pk95tci*, etc. CLONED: 7.5-kb transcript, present throughout development, encodes protein homologous (41–65%) to  $\alpha 1$  subunit of mammalian [neuronal](#) voltage-sensitive calcium channel. [Schafer and Kenyon 1995] [DM]

#### ***unc-3 X 18.54 e151***

: weak coiler tends to coil, tail active, good head movement; very disorganized [ventral nerve cord](#); mosaic analysis indicates mutant focus in [ventral cord motor neurons](#); similar phenotype in *e151/Df*. ES3 ME1. OA>5: *e54* (weaker allele), *e95*, *mn419*, *p1001*, etc. CLONED: polymorphisms identified in *mn419* and derivatives (cosmid F42D1). [Brenner 1974; Herman 1987] [NG, SP]

#### ***unc-4 II 1.72 e120***

: large, healthy, active, moves forward well but cannot back; ventral cord VA motor [neurons](#) have normal anatomy but most have synaptic inputs appropriate to VB motor [neurons](#). ES3 ME1. OA>15: *e26*, *e2151*, *e2308*, *e2320* (deletion null, resembles *e120*), *e2322ts* (TSP L2-L3), *wd1*, etc. See also [unc-37](#). CLONED: rare 1.2-kb transcript, encodes homeoprotein (pka [ceh-4](#)); *unc-4:lacZ* expressed in VA but not VB motor [neurons](#). [White et al. 1992; Miller et al. 1992] [NC]

#### ***unc-5 IV 1.96 e53***

: severe coiler, grows well; L1 also severe coiler; dorsal hypodermal cells abnormal, [dorsal nerve cord](#) absent or almost absent, cord commissures fail to reach targets; muscle arms misdirected; distribution of cell bodies in ventral cord disorganized; abnormal gonad arms; Egl-c. ES3 ME0. OA>10: *e553* (resembles *e53*), *e152* (weaker phenotype behaviorally and anatomically, dorsal cord partially formed), *bx8*, *ev447*, *st1001tci*, etc. See also [unc-6](#), [unc-40](#). CLONED: 3.0- and 3.1-kb Transcripts (different 5'), encode predicted 919-aa transmembrane protein, two Ig domains and two TSP domains; mosaic analysis indicates autonomous action in [neurons](#). DTC; ectopic expression in [touch cells](#) can cause improper dorsalward migration. [Hedgecock et al. 1990; Leung-Hagesteijn et al. 1992; Hamelin et al. 1993] [NW]

#### ***unc-6 X – 2.17 e78***

: slight kinker, poor backing; large, healthy, slightly fat; dorsal extensions of DD and [VD neurons](#) grow in aberrant directions, fail to reach dorsal cord; ventral cord disorganized; abnormal gonad arms, etc. ES3 ME1. OA>20: *e7*, *e181*, *ev400* (pka [unc-106](#), uncoordinated, high frequency of phasmid axon displacement), *n593*, *n594*, etc. Some alleles (*rh202*, *rh204*, *rh402*, etc.) defective only in dorsalward migrations; null alleles defective in both dorsalward and ventralward migrations; see also [unc-5](#), [unc-40](#). CLONED: encodes extracellular matrix component (591 aa plus 21-aa signal sequence), laminin related at N-terminal, homologous to vertebrate netrins. [Ishii et al. 1992] [NJ, NW, TK]

#### ***unc-7 X 20.35 e5***

: moves backward better than forward, kinker in forward movement, active, healthy, slightly thin; suppresses anaesthetic hypersensitivity of [unc-79](#) and [unc-80](#) mutants; *e5/Df* similar, null phenotype. ES3 ME0. OA>20: *e42*, *e65* (pka [unc-12](#), weaker), *bx5:Tc1*, *st197*, *mn384* (weaker allele), etc. Also revertants *bx5mn369*, etc. CLONED: main transcript 2.9 kb, encodes predicted 522-aa membrane protein related to EAT-5, *Drosophila* Passover (26% identity), etc.; possible gap junction component. [Starich et al. 1993; Morgan and Sedensky 1994] [EH, SP]

### ***unc-8* IV 2.98 e49**

: moves well but slowly and irregularly, often kinking both forward and backward; swollen [ventral cord motor neurons](#); *e49*/+ very slightly uncoordinated. ES2 ME1 NA1 (recessive). Also dominant coiler alleles: *e15sd* (pka [unc-28](#), ES3 ME0), *n491sd* (homozygotes strong coilers, *n491*/+ coiler, slightly weaker phenotype). Intragenic revertants of *n491* (e.g., *n491n1192*) are wt, thus [unc-8](#) null phenotype may be wt. OA3 (dominant): *n492*, *n773*. See also extragenic suppressors *sup-40,41,42*. [[Park and Horvitz 1986a](#); [Shreffler et al. 1995](#)] [MP]

### ***unc-9* X 11.57 e101**

: moves backward better than forward, slight kinker in forward movement, active, healthy; larvae more severely uncoordinated; suppresses anaesthetic hypersensitivity of [unc-79](#) and [unc-80](#); male fan slightly reduced, spicules tend to protrude. ES2 ME0. OA3: *ec27*, *bx5*, *e111*. CLONED: cosmid rescue (R12H7). [[Brenner 1974](#); [Morgan and Sedensky 1994](#)] [CW, MQ]

### ***unc-10* X – 1.25 e102**

: weak coiler, tends to back, loopy movement in reverse; fairly active; slightly small and thin; Ric. ES3 ME2. OA1: *e126*. [[Brenner 1974](#); [Nguyen et al. 1995](#); [Schafer et al. 1996](#)]

### ***unc-11* I – 2.38 e47**

: kinker, jerky ratchet-like movement especially in reverse; slow pharyngeal pumping; slightly small and thin; Ric, elevated acetylcholine levels, hypersensitive to levamisole; some migration defects. ES3 ME2. OA3: *e511*, *e1024* (weaker), *h1008*. CLONED: cosmid rescue (C32E8); multiple Transcripts. [[Brenner 1974](#); [Nguyen et al. 1995](#)] [AL, NJ, RM, TN]

### ***unc-12***

= *unc-7*

### ***unc-13* I 2.03 e51**

: paralyzed, kinky, small, irregular pharyngeal pumping; able to lay eggs; Ric, high acetylcholine levels; variable neuroanatomical defects. ES3 ME0. OA>30: *e450amb*, *e312amb* (non-null), *e309* (suppressed by [sup-6](#)), *s69fdi*, *s178fdi*, etc. All alleles similar to *e51* or slightly weaker. CLONED: very large gene (>35 kb), encodes 1734-aa novel protein containing phorbol ester (diacylglycerol)-binding site; antibodies detect 190-kD UNC-13. [[Brenner 1974](#); [Ahmed et al. 1992](#); [Nguyen et al. 1995](#)]

### ***unc-14* I 1.80 e57**

: very sluggish, almost paralyzed; small and dumpyish, tends to coil; some egg retention; PVP defects. ES3 ME0. OA>5: *e157* (multiple aspects of axon outgrowth affected; nerve processes contain large abnormal varicosities), *e608*, *e866*, *e1119*, etc. CLONED: cosmid rescue (R05H7). [[Brenner 1974](#); [McIntire et al. 1992](#)] [FK, MQ, MT, NJ]

### ***unc-15* I 2.01 e73**

: limp paralyzed phenotype, larvae move slightly better; Egl; disorganized muscle structure; suppressed by [sup-3](#); *e73*/+ slightly slow. ES3 ME0. OA>10: *e1214amb* (more severe phenotype than *e73*, not suppressed by [sup-3](#)), *e1402ts* (moves well at 15°C, paralyzed at 25°C), *ut37* (lethal embryonic arrest at 4-fold stage), *r404*, *r408*, *m81*, *s40*, *su228*, etc. CLONED: encodes 886-aa paramyosin; extensive structural analysis. [[Kagawa et al. 1989](#); [Gengyo-Ando and Kagawa 1991](#); [Epstein et al. 1993](#)] [HE, HK]

### ***unc-16* III 0.54 e109**

: very sluggish small; males more active. ES3 ME2. OA1: *n730ts* (pka [egl-39](#), transient bloating at 25°C; sensitive to serotonin and imipramine; uncoordinated sluggish weak coiler phenotype. ES3 (adult 25°C) ES2 (other stages 25°C) ME2. [[Brenner 1974](#); [Trent et al. 1983](#)] [JT]

#### ***unc-17* IV – 3.31 e245**

: severe coiler at all stages, rather small and thin; slow irregular pumping; Ric, resistant to 0.1 mM lannate; suppressed by *sup-1*, *sup-2*, and *sup-8*; normal ChAT (choline acetyltransferase) levels. ES3 ME0. OA>10: *ut64* (embryonic-lethal, coiler, probable null), *e335*, *e464*, etc. (most viable alleles resemble *e245* or slightly weaker). Also anomalous alleles: *e113* (less uncoordinated phenotype, drug-sensitive, loopy movement, reduced ChAT levels, Egl-c), *e876* (similar), *p1156* (Smg-suppressible, fails to complement both *unc-17* and *cha-1*). *cha-1-unc-17* is a complex locus. CLONED: 2-kb transcript, 5'UTR exon shared with *cha-1*; encodes predicted 532-aa vesicular acetylcholine transporter; 12 transmembrane domains; antibody staining punctate, most motor synapses. [[Alfonso et al. 1993, 1994a,b](#)] [AL, RM]

#### ***unc-18* X – 1.39 e81**

: paralyzed, kinky, thin at all stages; able to lay eggs; Ric, elevated levels of acetylcholine. ES3 ME0. OA>1: *e174* (pka *unc-19*, similar), *e234* (pka *lan-2*, Ric), *e2146*, *b403*, *cn347*, *md118*, *md193*, etc. CLONED: encodes predicted 591-aa protein with similarity to yeast Sly1p, Sec1p, Slp1p secretory proteins; antibody stains along axons in nerve cords. [[Gengyo-Ando et al. 1993; Nguyen et al. 1995](#)] [RM, TN]

#### ***unc-19***

= *unc-18*

#### ***unc-20* X – 11.84 e112**

: ts; at 25°C, severe kinker, some coiling; active, healthy; some head muscle contraction; defects in longitudinal axon elongation in VNC. ES3 (25°C) ME0 (25°C); wt at 15°C. OA>5: (six Smg-enhanced or Smg-dependent alleles). [[Brenner 1974; Schafer et al. 1996](#)] [NG, TR]

#### ***unc-21***

= *unc-29*

#### ***unc-22* IV 5.45 e66**

: twitcher at all stages; moves slowly with constant trembling; thin; abnormal muscle structure; unable to hypercontract and therefore levamisole-resistant; Egl; *e66*/+ twitches in 1% nicotine; ES3 ME0. OA>200: *s32amb* (resembles *e66*), *m52dm*, *e105* (muscle structure near normal), *e2428*, *s7*, *s12* (near-normal muscle structure), *s2038*, *st792*, etc. Many Tc1 insertions, plus precise and imprecise excision revertants; most *unc-22*/+ heterozygotes twitch in nicotine. CLONED: large gene (>30 kb), transcript ~19 kb, encodes 6049-aa twitchin: single kinase domain, multiple copies of fibronectin-like and Ig-like repeats; antibody staining indicates twitchin associated with thick filaments. [[Waterston et al. 1980; Benian et al. 1989, 1993](#)] [GB]

#### ***unc-23* V 1.88 e25**

: "benthead" phenotype, progressive dystrophy of head musculature so that adult head is bent dorsally or ventrally, hence very poor forward movement, good reverse movement; defects in muscle attachment (Mua); Egl; phenotype partly suppressed by growth in liquid. ES3 (adult) ME1. OA>10: *e324* (resembles *e25*), *e611* (pka *vab-4*, impenetrant allele), *e988*, *e2154*, etc. [[Waterston et al. 1980](#)] [CB, DR, NJ]

#### ***unc-24* IV 3.53 e138**

: amb; weak kinker, tends to back, often forms omega shape; fairly active, healthy; severe kinker in L1; suppresses anaesthetic hypersensitivity of *unc-79* and *unc-80* mutants. ES3 ME1. OA>10: *e448*, *e927pdi*, *e1172icr*, *e2386*, *q327*, etc. CLONED: cosmid rescue (C56C3). [[Riddle and Brenner 1978; Morgan et al. 1991; Barnes et al. 1996](#)] [MQ]

#### ***unc-25* III 20.94 e156**

: shrinker, contracts both dorsally and ventrally when prodded; slow; loopy Fab; poor backing; slightly small; *E.p* defect in defecation; deficient in GABA; some neuroanatomical defects (D motor [neurons](#)); adult male severely constipated. ES3 ME2. OA>5: *e265*, *e591*, *sa4*, *sa25* (similar). CLONED: encodes 416-aa GAD

(glutamic acid decarboxylase), 45% identity to human GAD65,67; *unc-25:lacZ* expressed in all [GABAergic neurons](#). [Thomas 1990; McIntire et al. 1993a,b; Reiner and Thomas 1995] [CZ, JT, MT]

#### ***unc-26 IV 8.18 e205***

: amb; severe kinker, small, scrawny, flaccid, little movement; slow pharyngeal pumping; Ric. ES3 ME0. OA>10: *e176, e345* (pka [unc-48](#)), *e314* (strong [E.p.](#), weak Unc, Eat), *e2340, m2, n1307, s1710mut, ad473, ad701*, etc. Some (5/18) alleles have expulsion defect in defecation; gene is recombinationally large. [Charest et al. 1990; Avery 1993a] [DA, EG, JT, RM]

#### ***unc-27 X 0.32 e155***

: sluggish, poor backing, slightly dumpy; abnormal [body muscle](#); some neuroanatomical defects. ES3 ME2 NA1. Also sd alleles: *su142sd* (pka [unc-99](#)), very slow, almost paralyzed; can lay eggs; abnormal faint muscle birefringence and ultrastructure, collections of thick or thin filaments. ES3 ME1). OA3 (sd): *su195* (forms thin-filament paracrystals), *su215*, etc. [Brenner 1974; Zengel and Epstein 1980] [SQ]

#### **[unc-28](#)**

= *unc-8*

#### ***unc-29 I 3.20 e193***

: very sluggish L1, moves better as adult; weak kinker, head region stiff, moves better in reverse; fairly active; resistant to 1 mM levamisole; sensitive to hypo-osmotic shock. ES3 ME2. OA>50: *e1072amb, e330* (pka [unc-21](#)), *e403* (pka [unc-56](#)), *e2311, x30, x554*, etc. CLONED: encodes non- $\alpha$ -subunit of nicotinic acetylcholine receptor. [Lewis et al. 1980a,b; Fleming et al. 1993] [ZZ]

#### ***unc-30 IV 7.79 e191***

: shrinker, contracts both dorsally and ventrally when touched; slow good forward movement but poor backing, rather small; VD and DD motor [neuron](#) axons are displaced and fail to stain with anti-GABA antibodies; PVP [neurons](#) also abnormal. ES3 ME2. OA>10: *e165, e318, e646 (R44och)*, *e926pdi* (deletion), *e2505, bx8*, etc. CLONED: encodes predicted 318-aa protein with homeodomain, most similar to UNC-4; antibody stains D [neurons](#) and some other [neurons](#); ectopic transgene expression induces GABA expression; locus naturally duplicated in some strains. [McIntire et al. 1993a; Jin et al. 1994] [CZ, MT]

#### ***unc-31 IV 6.27 e169***

: ts; very slow and sluggish, moves better in absence of bacteria; insensitive to prodding; constitutive pharyngeal pumping; weak Daf-c; poor dauer recovery; Egl; more active when starved; no obvious changes in neuroanatomy. ES2 ME1. OA>10: *e69amb, e86, e375amb, n1304* (all resemble *e169*), *n422ts* (pka [egl-22](#)), variable transient bloating at 25°C, stimulated by serotonin and imipramine; uncoordinated limp paralyzed phenotype. ES3 [adult, larvae], *e928* (strongest allele, deletion null; resembles *e169*), *n577ts, st198, u378, z1*, etc. CLONED: encodes predicted 138-kD novel protein; antibody stains axons of most [neurons](#); see also [rsn-13](#). [Avery et al. 1993] [CB, DA, MT]

#### ***unc-32 III 0.00 e189***

: severe coiler, little movement in adult; moves well in L1 but coils in response to touch in L2 and later stages; rather small and thin; weakly Egl-c; Ric. ES3 ME0. OA>5: *f123* (lethal, *f123/e189* coiler), *f121* (lethal, *f121/e189* almost wt), *ut61, ut111* (embryonic-lethals, irregular shape). Most alleles lethal. CLONED: probably encodes protein that has homology with glutathione reductase (ZK637.10); downstream gene in operon. [Brenner 1974; Nguyen et al. 1995] [FF, JC]

#### ***unc-33 IV – 3.54 e204***

: very slow, almost paralyzed; tends to curl; dumpyish; weak FITC uptake; amphid, phasmid, [PDE](#), PVP axons abnormal; multiple defects in axonogenesis; abnormally abundant [neuronal](#) microtubules. ES3 ME0. OA>10: *e572, e1358, m7, mn260::Tc4, rh1030::Tc4*, etc. CLONED: 2.8-, 3.3-, 3.8-kb Transcripts (different

5'ends) encoding predicted 523-aa, 679-aa, 854-aa proteins; antibody stains all [neuron](#) processes in larvae and adults. [[Hedgecock et al. 1987](#); [Li et al. 1992](#)] [EH, SP]

#### ***unc-34 V – 20.39 e315***

: ts; at 20°C, fairly severe coiler, somewhat active, grows well; male has crumpled [copulatory spicules](#); variable defects in VD and DD commissures; at 15°C, moves much better; low-penetrance withered tail phenotype (CAN cell defect) and [excretory](#) cell abnormalities. ES3 (20°C) ME0. OA>5: e566 (strongest allele, non-ts, coils at all temperatures; defects in axonal elongation and fasciculation), *e951pdi*, *s138gri*, etc. [[Brenner 1974](#); [McIntire et al. 1992](#)] [CX, NG, NW, MT]

#### ***unc-35 I – 14.40 e259***

: loopy irregular forward movement, poor backing; active, slightly thin. ES2 ME2 NA1. [[Brenner 1974](#); [Schafer et al. 1996](#)]

#### ***unc-36 IIII – 0.33 e251***

: very slow, almost paralyzed, thin; loopy at rest; normal [ventral nerve cord](#) ultrastructure; Ric; hypersensitive to serotonin, fails to adapt to dopamine (like Unc-2); hypersensitive to calcium channel modulators such as verapamil; pharyngeal pumping slow and irregular, slippery corpus and isthmus; increased sensitivity to arecoline; mosaic analysis indicates focus in [nervous system](#). ES3 ME0. OA>8: *e418* (resembles *e251*); *eT1(III;V)* (pka *unc-72[e873]*, presumed breakpoint, ME1), *e1501*, *e2341*, *ad698*, etc. CLONED: encodes predicted proteins with similarity (~45% identity) to α2-subunit of L-type calcium channel. [[Brenner 1974](#); [Rosenbluth and Baillie 1981](#); [Avery 1993a](#); [Nguyen et al. 1995](#); [Schafer et al. 1996](#)] [AQ, MT]

#### ***unc-37 I 1.30 e262***

: weak coiler, fairly active; phenotype similar to Unc-4. ES2 ME1. OA2 (recessive): *s80* (pka [let-76](#), L1-lethal), *h763* (Unc, adult sterile). Also dominant suppressors of *unc-4(e2322ts)*: *wd14*, *wd16*, *wd17*, *wd18* (no phenotype alone, allele-specific dominant suppressors of *e2322*). Intragenic revertants, e.g., *wd17wd19*, resemble *h763*. CLONED: encodes predicted 614-aa protein with similarity to groucho-related transcription factors, six WD40 repeats in C-terminal. [[Miller et al. 1993](#)] [NC]

#### ***unc-38 I – 0.55 e264***

: weak kinker, sluggish, slightly dumpyish, sometimes Egl; resistant to 1 mM levamisole in body but not in head; sensitive to hypo-osmotic shock. ES3 ME2. OA>40: *e213*, *e743*, *x20*, etc. CLONED: encodes subunit of nicotinic acetylcholine receptor. [[Lewis et al. 1980a,b](#)] [ZZ]

#### ***unc-39 V 5.85 e257***

: fairly severe kinker, can move forward and backward; fairly active, slightly dumpy; often withered tail as a result of 80% penetrant CAN migration defect; other migrations also variably defective; 15% of hermaphrodites have third gonad arm arising from additional [somatic gonad](#) founder, "Z5"; *e257/Df* more severe phenotypes. ES2 ME1. OA2: *ct73* (pka [mig-3](#), abnormal migration of CAN cells), *rh72*. [[Hedgecock et al. 1987](#); [Manser and Wood 1990](#)] [CF, NJ]

#### ***unc-40 I 0.29 e271***

: weak kinker, dumpyish, slow but fairly active; Egl; variable defects in VD and DD commissures; general failure in ventralward migrations. ES2 ME0. OA>5: *e1430* (pka [unc-91](#)), *e1478*, *n324*, *n473*, *ev457* (probable null), etc. CLONED: encodes predicted large protein with transmembrane domain, extracellular fibronectin and Ig domains; related to chicken neogenin, human tumor suppressor DCC; *unc-40*:GFP expressed in cells undergoing circumferential migrations or extensions. [[Hedgecock et al. 1990](#)] [NW]

#### ***unc-41 V 2.29 e268***

: weak kinker, irregular jerky movement, slightly small; VD1, VD2, DD1 cell bodies mispositioned, usually anteriorly; RVG organization disrupted; Ric; elevated acetylcholine levels; *e268/Df* similar. ES3 ME0. OA8: *e252, e399, e1175, e1294, cn252::Tc1*, etc. (similar). Also anomalous alleles: *e554, e1162* (normal acetylcholine levels, larger size, sd Unc phenotype). CLONED: partial sequence indicates novel predicted protein. [[Nguyen et al. 1995](#)] [RM, TN]

#### ***unc-42 V 2.21 e270***

: medium kinker, sometimes backs in response to tail touch, slightly small, fairly active, grows well; Egl-c; HSN fasciculation abnormal. ES3 ME1. Similar phenotypes in *e270/Df*. OA>5: *e419, e623, e2325, s260, m435*, etc. [[Brenner 1974](#)] [NG]

#### ***unc-43 IV 4.55 e408***

: slow, lazy, slightly rippling movement; poor backing; thin; almost paralyzed, tends to shrink and relax when prodded; larvae move better; Egl-c. ES3 (adult) ME1. OA>5: *e266* (similar Unc, Egl-c, echo in defecation cycle; exhibits muscle activation defects in some tissues, muscle hyperactivation in others), *e300* (shorter than *e408*, shrinking more marked), *e755, sa200* (pka [\*dec-8\*](#), weaker allele, Dec non-Unc; *sa200/Df* is Unc). Also gf allele: *n498sd* small, almost paralyzed, Egl; Daf-c at 27°C; *n498/+* less severe. Intragenic revertants, e.g., *n498n1179*, have recessive uncoordinated phenotype. [[Park and Horvitz 1986a](#)] [JT]

#### ***unc-44 IV 2.75 e362***

: paralyzed coiler, dumpy, tends to curl; weak FITC uptake; amphid, phasmid, PVP, [\*PDE\*](#), and other axons abnormal. ES3 ME0. NA11: *e427, e638, e1197* (multiple defects in axonal elongation, fasciculation, etc.), *e1260, q331::Tc1, rh1013::Tc1, st200::Tc5*, etc. CLONED: multiple Transcripts up to 14 kb in length, encoding proteins related to mammalian ankyrin, up to 23 repeats of 33-aa ANK repeat. [[McIntire et al. 1992](#); [Otsuka et al. 1995](#)] [DD]

#### ***unc-45 III – 27.13 e286***

: ts; at 25°C, limp paralyzed Egl; muscle ultrastructure defective, few thick filaments; males move better; slow at 20°C, wt at 15°C. ES3 (adult 25°C) ME0. OA>5: *m94ts, r450ts, su2002* (some ts alleles have stronger 20°C phenotype than *e286*). Also lethal Pat alleles: *st601, st603* (limited embryonic development beyond 2-fold, no pharyngeal pumping, failure to assemble thick filaments), *st604* (weaker allele, some maternal rescue), *wc2, wc4, wc5*. [[Venolia and Waterston 1990](#)] [LV]

#### ***unc-46 V – 2.27 e177***

: shrinker contracts both dorsally and ventrally when prodded; slow, good forward movement, poor backing; slightly small; adult male moderately constipated. ES3 ME2. OA2: *e300, e642*. [[Brenner 1974](#); [McIntire et al. 1993a](#); [Reiner and Thomas 1995](#)] [MT]

#### ***unc-47 III 1.85 e307***

: very poor backing, good slow forward movement; slight shrinker (contracts both dorsally and ventrally when prodded); small; abnormal staining with anti-GABA antibodies (accumulates GABA); adult male severely constipated. ES3 ME2. OA2: *e542, e707*. [[Brenner 1974](#); [McIntire et al. 1993a](#); [Reiner and Thomas 1995](#)] [EG, JT, MT]

#### ***unc-48***

= *unc-26*

#### ***unc-49 III 3.33 e382***

: shrinker, contracts both dorsally and ventrally when prodded; slow; poor backing, slightly small; probable defect in inhibitory GABA receptor function; adult male weakly constipated. ES3 ME2. OA>5: *e407, e468, e929, n1324*, etc. CLONED: encodes predicted GABA-A receptor; in probable operon with two other GABA receptor subunits. [[Brenner 1974](#); [McIntire et al. 1993a](#); [Reiner and Thomas 1995](#)] [EG, MT]

***unc-50* III 2.39 e306**

: weak kinker, slow but fairly active; resistant to 1 mM levamisole, sensitive to hypo-osmotic shock; extracts lack levamisole binding. ES3 ME1. OA6: e425, etc. (all similar). CLONED: encodes predicted 301-aa novel protein, possible transmembrane domain. [[Lewis et al. 1980a](#)] [MT, WS, ZZ]

***unc-51* V 24.42 e369**

: amb; paralyzed dumpy tends to curl; Egl; dorsal extensions of DD and [VD neurons](#) grow in aberrant directions, fail to reach [dorsal nerve cord](#); amphid, phasmid, [PDE](#), and other axons abnormal; multiple defects in axon elongation, fasciculation, etc. Abnormal axon ultrastructure: varicosities, cisternae, abnormal vesicles. ES3 ME0. OA>10: e389, e432, e584, e1212, etc. CLONED: 3.1-kb transcript, encodes predicted 856-aa protein with similarity to Ser/Thr kinases; *unc-51:lacZ* expressed in [neurons](#). [[Hedgecock et al. 1985](#); [McIntire et al. 1992](#); [Ogura et al. 1994](#)] [FK, FR]

***unc-52* II 23.33 e444**

: adults limp, paralyzed except for head region; thin; Egl; larvae move well; progressive dystrophy, body muscles fail to accumulate myofilaments; class-1 allele. ES3 (adult) ME0. OA>10 (class 1): e669amb (well suppressed), e998 (stronger phenotype), su200, r290, etc. Also class-2 mutations: st549 (lethal, severe Pat, no organized myofilament lattice; probable null), st546, st560, etc. (all similar to st549). Also class-3 mutation: ut111 (lethal, arrest at 2-fold; not paralyzed; complements class-1 alleles). See also *sup-38*, *smu*. CLONED: multiple Transcripts (4.0, 6.5, 8.0 kb) generated by alternative RNA processing; encode proteins related to perlecan (matrix heparan sulfate proteoglycan). [[Rogalski et al. 1993, 1995](#)] [DM]

***unc-53* II 3.07 e404**

: sluggish, poor backing, dumpyish; somewhat Egl; multiple defects in neuronal outgrowth, branching; also defects in [excretory](#) canal extension, gonad arm growth; males have abnormal bursal anatomy. ES2 ME0. OA>5: n152, n166, n569 (synergizes with *sem-5[n177]* to give strong Sem migration defect), e2432, e2499, etc. Null phenotype uncertain; some lethality in strong alleles. CLONED: multiple Transcripts (different 5'ends); one encodes 1528-aa protein, predicted to bind actin, ATP/GTP; may interact with SEM-5; transgene overexpression leads to extension of growth cones along A-P axis. [[Hedgecock et al. 1987](#); [Hekimi and Kershaw 1993](#)] [UG]

***unc-54* I 27.21 e190**

: limp paralyzed phenotype at all stages; larvae can move slightly more than adults; Egl; muscle ultrastructure very disorganized, few thick filaments. ES3 ME0. OA>50 (recessive): e1108amb, e1301ts, e675sd, and s291 (in-frame internal deletion mutants, almost paralyzed, slight twitchers), etc. Also unusual suppressor alleles, OA>15: s74 (dominant suppressor of *unc-22[s12]*, recessive slow, stiff; normal muscle ultrastructure). Also dominant antimorphic alleles, OA>10: e1152sd (severe rigid paralysis, small; e1152/+ paralyzed weaker phenotype. ES3 ME0), r344 (recessive lethal, r344/+ severely paralyzed), etc. Intragenic revertants have recessive paralyzed phenotype; some recessive alleles (r274, e1420, etc.) are dominant antimorphs in *smg* background. CLONED: encodes MHC B (MYO-4), major [body wall muscle](#) myosin heavy chain; 6-kb message, 1117-aa protein; extensive molecular analysis. [[Epstein et al. 1974](#); [McLachlan and Karn 1982](#); [Dibb et al. 1989](#); [Bejsovec and Anderson 1990](#)] [TR, RW]

***unc-55* I 2.36 e402**

: slow, very poor backing, tends to coil ventrally; healthy; abnormal [VD neurons](#) (adopt DD synaptic pattern); mosaic analysis indicates focus in [VD neurons](#). ES3 ME0. OA>11: e523, etc. [[Walhall and Plunkett 1995](#)] [ER]

***unc-56***

= *unc-29*

***unc-57* I – 0.99 e406**

: strong kinker, active; small and thin; slow pharyngeal pumping; tends to hypercontract. ES3 ME2. OA>5: e590, e957, e1190, st199, ad592, etc. [[Brenner 1974](#); [Avery 1993a](#)] [DA]

#### ***unc-58 X 1.51 e665***

: dm; "shaker" animals short, rigidly paralyzed with constant shaking of body; e665/+ phenotype similar but weaker, animals slightly longer and less rigid; muscle hyperactivated, sticky pumping, short. ES3 ME0. OA4 (dominant): e415, n495 (similar), e778 (weaker phenotype), etc. Dominant alleles revert intragenetically, e.g., e665e2112, recessive weak Unc (probable null phenotype). [[Brenner 1974](#); [Park and Horvitz 1986a](#)] [JT]

#### ***unc-59 I 22.49 e261***

: poor backward movement, forward better; thin; [vulva](#) variably abnormal, often protrusive, sometimes ruptured; many postembryonic lineage abnormalities resulting from variable failures in cytokinesis; gonad lineages sometimes defective; variable defects in neuroanatomy; males have very abnormal tail anatomy. ES2 ME0. OA3: e1005 (pka [unc-88](#)), e1465, n391. [[Brenner 1974](#); [White et al. 1982](#)] [MT]

#### ***unc-60 V – 18.92 e723***

: limp paralyzed or very slow; thin; Egl; abnormal muscle ultrastructure with large aggregates of thin filaments; recessively suppressed by [sup-12](#). ES3 ME0. OA>10: e677 (pka [unc-66](#)), e890 (both resemble e723), e890, s1310 (induced on eT1), s1586 (500-bp deletion, larval-lethal). Also r398, s1307 (both antidystrophic alleles). CLONED: 1.3- and 0.7-kb alternative Transcripts encoding 165-aa and 152-aa predicted proteins with 38% identity, sharing only first exon and first methionine; both have similarity to actin depolymerizing proteins (cofilin, destin). [[Waterston et al. 1980](#); [McKim et al. 1994](#)] [BC]

#### ***unc-61 V 6.49 e228***

: poor backing, irregular waveform in forward movement; thin; protrusive [vulva](#); variable defects in neuroanatomy; [male tail](#) very abnormal (rays absent, spicules reduced, etc.). ES3 ME0 NA1. [[Brenner 1974](#); [Siddiqui and Culotti 1991](#)] [SQ]

#### ***unc-62 V – 5.49 e644***

: slightly slow, irregular, sometimes rippling movement, especially in reverse; slightly dumpy; variable abnormalities in VD and DD commissures; [male tail](#) abnormal, bursa small, fan reduced, rays variably absent; 19% of embryos Nob. ES2 ME0. OA2: s472spo (pka [let-328](#), lethal, probable null), ct344 (pka [nob-5](#), partial maternal-effect Nob, disorganized posterior). [[Brenner 1974](#); [Johnsen and Baillie 1991](#)] [BC, BW]

#### ***unc-63 I – 0.24 e214***

: weak kinker, slow, inactive; resistant to 1 mM levamisole, sensitive to hypo-osmotic shock; elevated acetylcholine levels. ES3 ME2. OA>50: x13 (pka [lev-7](#), Lev, Ric, poor backing; ES3 ME3), x18, x37, etc. (most alleles resemble e214). Also rare exceptional alleles: x26 (almost normal movement, slight levamisole resistance), b404 (Ric, trichlorfon-resistant, slight Lev, slight Unc), x33 (more resistant in body than in head). Previous reference allele "e384" is double mutant with [unc-11](#). [[Lewis et al. 1980a](#); [Nguyen et al. 1995](#)] [AL, RM, TN, ZZ]

#### ***unc-64 III 21.46 e246***

: sluggish, will move either forward or backward if prodded but almost immediately jams up; Ric; healthy; elevated acetylcholine levels. ES2 ME0. OA>1 (some alleles lead to severe paralysis). CLONED: encodes predicted syntaxin homolog. [[Brenner 1974](#); [Nguyen et al. 1995](#)] [NM, RM, TN]

#### ***unc-65 V 6.57 e351***

: slow, moves well, slightly poor backing; partially lannate-resistant (Ric); healthy; sometimes Egl. ES2 ME2. OA1: e355. [[Brenner 1974](#)]

#### ***unc-66***

= unc-60

#### **unc-67 I – 2.39 e713**

: sluggish, can move well both forward and backward but frequently pauses or jams up. ES2 ME2 NA1. [Brenner 1974] [MQ]

#### **unc-68 V 0.62 e540**

: weak kinker, slow, thin; slight shrinker; head region but not body resistant to 1 mM levamisole, ouabain. ES3 ME2. OA>15: *x14, x24, e932, e2313, s92spo, r1162* (presumed null, deletes all transmembrane domains), etc. (all resemble e540). CLONED: 30-kb gene, 43 exons; encodes 4902-aa ryanodine receptor (43% identity to mammalian cardiac RYR). [Brenner 1974; Lewis et al. 1980a] [HK, TR]

#### **unc-69 III 2.32 e587**

: medium coiler, inactive, small; abnormalities in VD and DD commissures, longitudinal axon elongation. ES3 ME0. OA1: *e602*. CLONED: cosmid rescue (C46D2). [Brenner 1974] [NG, SQ, WS]

#### **unc-70 V 0.50 e524**

: ts, sd; irregular loopy movement, sometimes coiling, active; grows well; *e524/+* weak coiler at 25°C. ES2 ME2. OA1 (sd): *n493sd* (curly, uncoordinated, non-ts). revertants, e.g., *n493n1170ird*, have recessive-lethal phenotype, early L1 arrest (probable null phenotype). OA7 (ird) 8. Also lethal alleles, OA>5: *s115, s1406, s1639*, etc. (all early/mid larval-lethals, dominant weak Unc). Dominance of many alleles strongly enhanced by *smg* background. [Park and Horvitz 1986a; Johnsen and Baillie 1991] [TR]

#### **unc-71 III 20.30 e541**

: strong kinker, especially in reverse; fairly active; commissures sometimes on wrong side; variable defects in axonal elongation and fasciculation; synergizes with *sem-5(n1779)* to give Sem migration defect. ES3 ME2. OA1: *ay7*. YAC rescue (Y37D8). [McIntire et al. 1992; Garriga and Stern 1994] [NG, NH]

#### **unc-72**

= unc-36

#### **unc-73 I – 1.85 e936**

: coiler, small and dumpyish, inactive; commissures often on wrong side; variable defects in axon growth and fasciculation; occasional lineage defects; reduced Z migration; male copulatory spicules short and crumpled; synergizes with *sem-5(n1779)* to give Sem migration defect. ES3 ME0. OA>3: *rh40, ev454::Tc1, e936je3* (intragenic change, recessive-lethal and dominant suppressor of e936). See also *sup-39*. CLONED: 7.7- and 7.3-kb Transcripts, encode >200-kD protein related to Rho-type guanine nucleotide exchange factors, yeast Cdc24p. [McIntire et al. 1992; Garriga and Stern 1994; Run et al. 1996] [NJ, JW, NW]

#### **unc-74 I – 1.45 e883**

: weak kinker, slow, slightly small; resistant to 1 mM levamisole, sensitive to hypo-osmotic shock; L1 movement very poor, no backing. ES3 ME2. OA>25: *x19* (resembles e883), etc. [Lewis et al. 1980a] [ZZ]

#### **unc-75 I 9.55 e950**

: weak coiler especially in reverse; moves forward well; sluggish, short; Ric. ES3 ME2. OA2: *h1041, h1042* (both lethal). [Brenner 1974; Nguyen et al. 1995] [KR, RM]

#### **unc-76 V 7.01 e911**

: pdi, inactive, tends to curl, dumpyish; Egl-c; amphid, phasmid, PDE, PVP, other axons abnormal; dorsal extensions of DD and VD neurons frequently grow in abnormal directions, often fail to connect to dorsal nerve cord; defects in axonal elongation and fasciculation along nerve cords. ES3 ME0 NA1. CLONED: 1.8-

kb Transcripts, encode predicted 385-aa or 376-aa novel proteins; epitope-tagged UNC-76 detected in axons. [[Hedgecock et al. 1987](#); [McIntire et al. 1992](#)] [MT]

***unc-77 IV 1.92 e625***

: irregular loopy movement both forward and reverse; active, thin; sometimes protrusive [vulva](#); slight movement abnormality in *e625*+. ES2 ME2 NA1. [[Brenner 1974](#); [Schafer et al. 1996](#)]

***unc-78 X – 9.15 e1217***

: slow, abnormal [body muscle](#) birefringence; abnormal muscle ultrastructure with large aggregates of thin filaments; suppressed to wt by [sup-13](#). ES2 ME0. OA>5: *e1221*, *st43*, etc. [[Waterston et al. 1980](#)]

***unc-79 III – 4.03 e1068***

: irregular movement, somewhat sluggish ("fainter"); hypersensitive to volatile anaesthetics. ES2 ME3. OA>5: *e1031*, *e1291*, *e1510*, *ec1*, etc. [[Sedensky and Meneely 1987](#); [Morgan et al. 1991](#)] [CW]

***unc-80 V 18.70 e1272***

: slightly sluggish, tends to pause ("fainter"), good movement; hypersensitive to volatile anaesthetics. ES1 ME3. OA2: *e1069*, *m513*. [[Sedensky and Meneely 1987](#); [Morgan et al. 1991](#)] [CW]

***unc-81 III 17.56 e1122***

: slightly irregular movement. ES1 ME3 NA1. [CB, ZZ]

***unc-82 IV 2.59 e1220***

: slow, good movement; abnormal reduced muscle birefringence, abnormal [body muscle](#) ultrastructure with enlarged thick filaments; weaker [pharyngeal muscle](#) abnormalities. ES2 ME2. OA>5: *e1323*, *r194*, *st1323*, etc. (all resemble *e1220*). [[Waterston et al. 1980](#)] [RW]

***unc-83 V – 0.09 e1408***

: ts, reverse kinker as adult, variably Egl; L1 moves well; variable failures in postembryonic migration of Pn nuclei into ventral cord and (some alleles) embryonic migrations of *hyp-7* hypodermal nuclei; all alleles are ts for Pn defect, non-ts for *hyp-7* defect; unmigrated Pn nuclei mostly fail to divide; adult male phenotype variable, some mate at 25°C, all mate at 15°C. ES3 ME3 (15°C). NA11: *337amb*,*ts*, *e1409amb*,*ts* (suppressible only for *hyp-7* defect), *n159*, *n1218*, etc. [[Sulston and Horvitz 1981](#)] [MH, MT]

***unc-84 X 13.48 e1410***

: ts, reverse kinker as adult; L1 moves well; variable failures in nuclear migrations; same phenotypes as *unc-83(e1408)*. ES3 ME3 (15°C). OA>10: *e1174*, *e1748*, *n296*, *n1325*, etc. (all alleles ts, resemble *e1410*). Complex complementation pattern; null phenotype probably incompletely penetrant. CLONED: 2.5-kb and 3.5-kb Transcripts (different 3'ends); latter encodes predicted 1100-aa protein with transmembrane domain, similarity to fission yeast SPB-associated protein Sad. [[Sulston and Horvitz 1981](#)] [MH, MT]

***unc-85 II – 3.32 e1414***

: amber, kinker in adult, cannot back; L1 moves well; many postembryonic lineages abnormal as a result of defective cytokinesis in cell division; all phenotypes similar to or slightly weaker than those of *unc-59(e261)*. ES3 ME0. OA2: *n319*, *n471*. [[Horvitz and Sulston 1980](#); [White et al. 1982](#)] [MT]

***unc-86 III – 0.32 eDf25***

: pka *e1416*, lethargic; Mec ([touch cells](#) absent); Egl (HSN cells fail to differentiate); nonchemotactic to NaCl; lineage abnormalities involving reiterative divisions of [neuroblasts](#), hence supernumerary [neurons](#) and missing [neurons](#); 2% Him. ES3 ME2. OA>30: *e1507* (Mec, Egl, non-Him, ME3), *n848ts* (superficially wt at 20°C, Mec and Egl at 25°C), *n306*, *n1132*, *n846* (amorph), *u371::Tc3*, *rh1029::Tc3*, *n1351::Tc4*, etc. Alleles form graded series; *e1416/Df* is ME0; Him alleles (*e1416*, *n303*, etc.) are viable deletions of >15 kb, affecting both *unc-86* and *him-15*. CLONED: rare 1.9-kb transcript, encodes 467-aa POU-class

homeoprotein; antibody staining indicates UNC-86 nuclear, specific to daughter nuclei affected by [unc-86](#) mutations; extensive promoter analysis. [Chalfie et al. 1981; Finney et al. 1988; Baumeister et al. 1996] [GR]  
**unc-87 I 1.31 e1216**

: limp paralyzed or very sluggish; somewhat Egl; larvae more paralyzed; abnormal [body muscle](#) birefringence and ultrastructure; thin filaments in small bundles. ES3 ME0. OA>10: *e1459amb* (phenotype more severe than *e1216*), *st39*, *r320*, etc. CLONED: encodes predicted 40-kD protein with similarities to vertebrate smooth muscle proteins calponin, *Drosophila mp20*; localized to I bands; alternative splicing. [Waterston et al. 1980; Goetinck and Waterston 1994a,b] [RW]

### **[unc-88](#)**

= *unc-59*

### **[unc-89 I – 1.60 e1460](#)**

: good movement, slightly small, thin, and transparent; abnormal reduced birefringence in body wall and [pharyngeal muscle](#); thick filaments disarranged, no M-line. ES1 ME3. OA>10: *st85amb*, *r291*, *ad539* (*pk1 phm-1*, worms small and starved, feeble pharyngeal contractions), *e2338amb*, *st515::Tc1*, etc. CLONED: encodes 750-kD protein related to UNC-22 (twitchin); antibodies stain middle of A bands. [Waterston et al. 1980; Benian et al. 1996] [GB]

### **[unc-90 X 0.27 e1463](#)**

: sd, homozygotes small, rigidly paralyzed (hypercontracted); mostly sterile (not viable); abnormal pharyngeal pumping, abnormal muscle birefringence and ultrastructure; muscle hyperactivated, sticky pumping, short; heterozygote *e1463/+* slowish, somewhat dumpy; muscle disorganization resembles homozygote but less severe; suppressed semidominantly by *lev-11(x12)*; [unc-54](#) null alleles also epistatic to *e1463*. ES3 (homozygote) NA1 (sd). Intragenic revertants of *e1463* are wt (probable null phenotype). [Waterston et al. 1980] [JT, RW]

### **[unc-91](#)**

= *unc-40*

### **[unc-92](#)**

= *act-123*

### **[unc-93 III – 5.86 e1500](#)**

: sd, adults paralyzed, Egl; slightly long; abnormal muscle; contract and relax when prodded ("rubberband" phenotype); muscle activation defective (flaccid, long). ES3 ME0. Poor mating in *e1500/+* males; neomorphic allele, gf. OA1 (gf): *n200* (resembles *e1500* but less severe phenotype). Both gf alleles suppressed by *sup-9,10,11,18*. Also lf alleles: *n392* (no phenotype alone but fails to complement *e1500*), *n393*, etc. Intragenic revertants of *e1500* all have similar wt lf phenotype: *e1500n234amb,des*, *e1500n200spo*, *e1500n243gri*, *e1500n1415::Tc1*, etc. OA>30 (ird). CLONED: 2.2-kb Transcripts (slightly different 5'), encoding 700- and 705-aa predicted novel proteins with multiple (5–10) possible transmembrane domains. [Greenwald and Horvitz 1980; Levin and Horvitz 1992] [MT]

### **[unc-94 I 0.79 su177](#)**

: slow, especially in adult; abnormal patchy muscle birefringence and ultrastructure; collections of thin and "intermediate" filaments (no staining with anti-intermediate filament antibodies). ES2 ME2 NA1. [Zengel and Epstein 1980] [HE]

### **[unc-95 I 23.80 su106](#)**

: sd, very slow or paralyzed, Egl; abnormal variable muscle birefringence; disorganized sarcomeres with collections of thin filaments. ES3. OA3: *su33amb* (similar phenotypes, ME0), etc. [Zengel and Epstein 1980] [HE]

***unc-96 X – 18.21 su151***

: very slightly slow, slightly Egl, moves well; abnormal muscle birefringence and ultrastructure, collections of thin filaments near ends of cells. ES1 ME3 NA1. [[Zengel and Epstein 1980](#)] [HE]

***unc-97 X – 4.55 su110***

: limp paralyzed adults, Egl; larvae paralyzed, slightly curled; variable abnormal muscle birefringence; small, easily disrupted sarcomeres. ES3 ME0 NA1. [[Zengel and Epstein 1980](#)] [HE]

***unc-98 X – 1.67 su130***

: slow somewhat Egl; abnormal muscle birefringence and ultrastructure, collections of thin filaments; poorly organized A and I bands; variable defects in neuroanatomy. ES2 ME1 NA1. [[Zengel and Epstein 1980](#); [Siddiqui and Culotti 1991](#)] [HE, SQ]

***unc-99***

= *unc-27*

***unc-100 I 22.48 su149***

: sd, slow, small, dumpyish; male bursa swollen; *su149*/+ slightly slow and small. ES3 ME0. OA2: *su115*, etc. [[Zengel and Epstein 1980](#)] [HE]

***unc-101 I 13.51 m1***

: des, coiler; very sluggish, moves poorly; slightly Egl; slightly short; defecation defects, abnormal FITC staining; subviable; adult males have abnormal tails and spicules. OA>8: *rh6*, *sy108*, *sy161*, *sy241*. Mutations suppress weak Vul mutants such as *let-23(sy1)*; Muv phenotype in combination with *sli-1*. CLONED: encodes clathrin adaptor protein, ortholog of mouse AP47 (>75% identity; AP47 can substitute for [\*unc-101\*](#)). [[Lee et al. 1994](#)] [DR, PS]

***unc-102***

= *unc-1*

***unc-103 III – 3.77 e1597***

: sd, homozygote severe kinker, little movement; slight Egl; *e1597*/+ somewhat less severe kinker; muscle activation defective (flaccid, long); neomorphic (gf) allele. ES3 ME0. OA1 (gf): *n500*. Also intragenic revertants: *e1597n1212spo* (wt, probable null), *e1597n1213*, *n500n1211*, etc. OA5 (ird). [[Park and Horvitz 1986a](#)] [JT, MT]

***unc-104 II 0.22 e1265***

: severe coiler; Ric; defects in neuroanatomy; poor response to dauer pheromone; abnormal transport of synaptic vesicles; *e1265/Df* probably lethal. ES3 ME0. OA>5: *rh43* (viable, severe), *rh142* (sublethal), *ut60* (lethal, arrests as coiler), *ut104*, *e2184::Tc1*, *rh1016*, *rh1017*. CLONED: >30-kb gene, 6-kb transcript, encodes 1584-aa kinesin family protein. [[Otsuka et al. 1991](#); [Hall and Hedgecock 1991](#); [Nguyen et al. 1995](#)] [DD, NJ]

***unc-105 II 0.67 n490***

: sd; small, hypercontracted, rigid paralytic; very poor growth; abnormal muscle structure; muscle hyperactivated, sticky pumping, short; *n490*/+ similar but less severe phenotype; probable neomorphic gf allele; suppressed by mutations in [\*unc-15\*](#), [\*unc-22\*](#), [\*unc-45\*](#), [\*unc-54\*](#), etc.; see also [\*sup-20\*](#). ES3. OA2 (gf): *n506* (less severe; ME0), *n1274*. Also intragenic revertants: *n490n804* (wt, no behavioral or muscular abnormality; probable null phenotype), *n490n820*, etc. OA>10 (ird). CLONED: encodes degenerin family member, related to amiloride-sensitive Na channels. [[Park and Horvitz 1986a,b](#); [Liu et al. 1996](#)] [MT, RW]

***unc-106***

= *unc-6*

***unc-107***

= *vab-8*

***unc-108 I – 1.92 n501***

: dm; sluggish, poor backing; similar phenotype in *n501*+/-. ES3. OA1: *n777*. Possibly haplo-insufficient locus. [[Park and Horvitz 1986a](#)]

***unc-109 I 2.56 n499***

: dm; recessive-lethal, embryonic arrest; *n499*+/ uncoordinated, paralyzed, muscle defective. ES3 NA1. [[Park and Horvitz 1986a](#)]

***unc-110 X 0.41 e1913***

: dm; recessive-lethal; *e1913*+/ uncoordinated, thin, very sluggish, tends to shrink and relax when prodded, Egl; exhibits muscle activation defects in some tissues, muscle hyperactivation in other tissues. ES3 NA1 (dm). Also intragenic revertant: *e1913e2383* (wt, ME3). [CB, JT]

***unc-111 V 0.3 r346***

: moves well; disorganized [body wall muscle](#); partial suppressor of *unc-105(n490)*. ES1 NA1. [TR]

***unc-112 V 6.20 r367***

: adults paralyzed and thin except for head region; Egl; disorganized [body wall muscle](#), frayed myofilament lattice; partial suppressor of *unc-105(n490)*; young larvae nearly wt (phenotypes very similar to *unc-52*). ES3 (adult) ME0. OA2: *st562* (severe Pat [paralyzed arrest at 2-fold], some pharyngeal pumping), *st581* (Pat). Probable dense body component. [[Williams and Waterston 1994](#)] [DM, TR, RW]

***unc-113 V 0.3 r449***

: slightly slow; disorganized [body wall muscle](#); partial suppressor of *unc-105(n490)*. ES3 NA1. [TR]

***unc-114 V N r476***

: paralyzed; Egl; disorganized [body wall muscle](#); partial suppressor of *unc-105(n490)*. ES3 ME0 NA1. [TR]

***unc-115 X 1.69 e2225***

: mut; uncoordinated movement, severe kinker; muscle structure appears normal. OA1: *mn481*. CLONED: predicted protein has N-terminal LIM domain, C-terminal villin headpiece similarity. [FF, SP]

***unc-116 III – 0.29 e2281***

: Tc5 insertion; L1 coiler; poor backing; variable misplacement of axons, [excretory](#) canals. OA>3: *e2282*, *e2310*, *pk211*, *rh24* (severe phenotype, high embryonic lethality at first cleavages; abnormal membrane inventories, defective endocytosis, axon guidance defects). CLONED: encodes predicted 815-aa protein, extensive similarity to kinesin heavy chain. [[Patel et al. 1993](#)] [FF, NJ, UC]

***unc-117 X – 11.8 e2330***

: mut; larval kinker, adults less affected; slow and loopy. NA1. [FF]

***unc-118 X 1 e2331***

: mut; kinker, especially in larva; variable; null possibly sterile. NA1. [FF]

***unc-119 III 5.33 e2498***

: Tc1 insertion; severe Unc, almost paralyzed adults, dumpyish, tends to curl; Daf-d, partial Egl, partial Dyr; normal muscle ultrastructure. ES3 ME0. OA3: *ed3op*, *ed4oc*, *ed9* (all similar). CLONED: encodes predicted 219-aa novel protein; *unc-119*:GFP expressed extensively in axons. [[Maduro and Pilgrim 1995](#)]

***unc-120 I 2.74 st364***

: ts; progressive paralysis at 20°C; mature adults very sluggish at 15°C; number of thick and thin filaments variably reduced; sterile at 25°C. [RW]

***unc-121***

= *snt-1*

***unc-122 I 26.29 e2520***

: medium coiler at all stages; moves forward well when stimulated, tends to coil up when moving backward or at rest; coiling usually ventral, occasionally dorsal. ES2 ME1/ME2 NA1. [CB]

***unc-123 III 13.32 jd5***

: sd; temperature-sensitive, semidominant, uncoordinated; coils dorsally when moving backward, or moves in circles, dorsal aspect oriented centrally; almost wt at 15°C; possibly allelic with *sup-1*. NA1. Also revertant *jd5jd10* (subtle movement defect, dominant suppressor of *unc-17[e245]*). [ER]

***unc-124 X – 2 hs10***

: cs; uncoordinated at 11°C, kinker; wt at 23°C; phenotype reversible within hours of temperature shift, throughout development; dominant interaction with some *unc-7* alleles. NA1. [[Hecht et al. 1996](#)] [HH]

***unc-125 X – 15 hs11***

: cs, dm; uncoordinated (coiled, kinked, slow) at 11°C, wt at 23°C; phenotype reversible within minutes of temperature shift, throughout development; *hs11/+* similar. NA1. [[Hecht et al. 1996](#)] [HH]

***unc-126 III – 0.4 hs12***

: cs; severely paralyzed at 11°C, wt at 23°C; tsP early. NA1. [[Hecht et al. 1996](#)] [HH]

***unc-127 V 0.1 hs13***

: cs; uncoordinated coiler at 11C, wt at 23°C; TSP early. NA1. [[Hecht et al. 1996](#)] [HH]

***unc-128 X 8.24 rh110***

: uncoordinated; detected by extra *neurons* stained by monoclonal antibody M44 (normally stains only PVP), additional pair of *neurons* stain (? AVH or AVJ); no obvious axon outgrowth defects, very minor Mig defects. NA1. [NJ]

***unc-129 IV 4.10 ev554***

: uncoordinated, variable kinker, healthy; DD and *VD neurons* grow in aberrant directions; suppresses guidance defects caused by ectopic UNC-5. OA2: *ev557*, *ev566*. CLONED: cosmid rescue (C53D6). [NW]

***uts***

***uts*** unidentified *trans*-spliced ***s*** equence [CGC].

***uts-1 V 4.57***

NMK. Abundant 0.6-kb transcript (SL13), *trans*-spliced to SL1; encodes predicted novel protein. [[Bektesh et al. 1988](#)] [DH]

***uts-2 I 3.39***

NMK. 0.5-kb transcript (SL17), *trans*-spliced to SL1; encodes predicted novel protein. [[Bektesh et al. 1988](#)] [DH]

***uts-3 IV 6.03***

NMK. 0.35-kb transcript (SL52), *trans*-spliced to SL1; encodes predicted novel protein. [[Bektesh et al. 1988](#)] [DH]

***uts-4* IV 5.90**

NMK. 0.6- and 0.9-kb Transcripts (SL109), *trans*-spliced to SL1; encode predicted novel protein. [[Bektesh et al. 1988](#)] [DH]

***uvt***

unidentified **v**itellogenin-linked **t**ranscript [BL]. Genes near *vit* genes.

***uvt-1* X – 1.4**

NMK. Abundant 0.5-kb transcript present in larvae, adults. [[Heine and Blumenthal 1986](#)]

***uvt-2* X – 5.9**

NMK. Rare 1.3-kb transcript present in larvae, adult hermaphrodites. [[Heine and Blumenthal 1986](#)]

***uvt-3* X – 5.9**

NMK. 2.7-kb transcript present in embryos, larvae. [[Heine and Blumenthal 1986](#)]

***uvt-4* X – 5.9**

NMK. Abundant 2.6-kb transcript present at all stages, less abundant in adults; dosage-compensated. [[Heine and Blumenthal 1986](#); [Meyer and Casson 1986](#)]

***uvt-5* X – 12.5**

NMK. Rare 1.2-kb transcript present in larvae, adults. [[Heine and Blumenthal 1986](#)]

***uvt-6* X – 12.5**

NMK. Rare transcript present only in adult hermaphrodites. [[Heine and Blumenthal 1986](#)]

***uvt-7* X – 12.7**

NMK. 2.3-kb transcript present in embryos, adult hermaphrodites. [[Heine and Blumenthal 1986](#)]

***uxt***

unidentified **x**-linked **t**ranscripts [TY].

***uxt-1* X – 2.9**

NMK. 1.25-kb transcript, dosage-compensated. [[Meyer and Casson 1986](#)]

***uxt-2* X C**

NMK. 1.45-kb transcript, not dosage-compensated. [[Meyer and Casson 1986](#)]

***vab***

**v**ariable **ab**normal morphology [CB].

***vab-1* II – 3.46 e2**

: notched head, variable dystrophy of ventral cephalic region, especially in L1; <70% penetrance. ES3/0 ME3. OA>10: *e1063* (35% penetrance), *e2027spo* (>90% penetrance), *e699*, etc. [[Brenner 1974](#); [Lewis and Hodgkin 1977](#)] [CB, CZ]

***vab-2* IV – 2.36 e96**

: notched head, especially in L1; resembles [\*vab-1\*](#) alleles; 65% penetrance. ES3/0 ME3. OA3: *e141*, *e1208* (50% penetrance), *sy167*. [[Brenner 1974](#); [Lewis and Hodgkin 1977](#)] [CB, CZ]

***vab-3* X 1.97 e648**

: notched head, especially in L1; 100% penetrance, dystrophy of ventral head regions, disorganized hypodermal and anterior sensory anatomy; nonchemotactic to NaCl; Emo; adult [\*male tail\*](#) variably

deformed. ES3 ME0. OA8: *e41*, *e1062* (resemble *e648*), *e1178* (severe allele, 60% larval-lethal), *e2429*, *sy66*, *sy281* (weak alleles), *e1796* (pka [lin-20](#), abnormal lineages for HO, H1, G1, and G2; Mig defects in DTC). CLONED: encodes 455-aa predicted protein with paired domain, Pax6 homolog; *vab-3*:GFP expressed in head precursors at 100-cell stage; see also *mab-18*. [[Lewis and Hodgkin 1977](#); [Chisholm and Horvitz 1995](#)] [CZ, EM]

#### ***vab-4***

= *unc-23*

#### ***vab-5 ? e108***

: low-penetrance notched head. [CB]

#### ***vab-6 III – 27.17 e697***

: dumpyish, lumpy appearance, especially in L1; sometimes twisted body. ES3 (L1) ME2. OA1: *e1023* (resembles *e697*). [[Hodgkin 1983](#)] [CB]

#### ***vab-7 III 5.34 e1562* :**

hermaphrodite tail abnormal, sometimes twisted, tail whip never normal, often bobbed; variably uncoordinated with bent tail; adult [male tail](#) deformed; abnormal positioning of Cpap descendants, etc.; probable null, nonsense mutation; *e1562/Df* similar phenotypes. ES3 ME0. OA>4 (mostly weaker). CLONED: encodes homolog of *Drosophila* homeoprotein Eve (Even-skipped); Transcripts present in four posterior cells during gastrulation. [[Hodgkin 1983](#); [Ahringer 1996](#)] [JA, NJ]

#### ***vab-8 V 3.63 e1017***

: posterior half thin, pale, uncoordinated; anterior half normal; adult [male tail](#) anatomy vestigial; failure of posterior migration of CAN cells; rare animals have normal posterior morphology and one correctly placed CAN cell; most posteriorly directed migrations of cells and growth cones abnormal; similar phenotypes in *e1017/Df*. ES3 ME0. OA>5: *ct33* (resembles *e1017*, abnormal HSN migration), *ev411* (pka [unc-107](#), slightly uncoordinated, partially shortened phasmid axons; Unc phenotype enhanced by one or two doses of *enu-1*[*ev419*], *ev411*; *ev419* severely uncoordinated, cannot back, very short phasmid axons). Multiple phenotypic classes; some mutations affect only certain migrations. CLONED: multiple Transcripts. [[Hedgecock et al. 1987](#); [Wightman et al. 1996](#)] [JW, LK, NG, NJ, NW]

#### ***vab-9 II 0.79 e1744***

: slightly dumpy; tail whip knobbed at all stages except adult male (adult [male tail](#) tip slightly swollen); variably Egl. ES3 (larvae) ME2. OA2: *e1775*, *e2016* (resemble *e1744*, slightly dumpier). [Hodgkin 1974]

#### ***vab-10 I 7.46 e698***

: degenerate head, bent dorsally or ventrally; penetrance 50%; generally poor growth; adult [male tail](#) invariably thin, fan and rays reduced in size; Mua (defective muscle attachment). ES3/1 ME0 NA1. [[Hodgkin 1983](#)] [NJ]

#### ***vab-11 IV – 10.2 e1255***

: tail irregular, variably blebbled or shortened in adult hermaphrodite; some animals have enlarged [excretory](#) canals; adult males have swollen bursa, sometimes fused rays, normal spicules. ES2 (adult) ME1 NA1. [CB]

#### ***vet***

***v*** ery ***e*** arly ***t*** ranscripts [BW].

#### ***vet-1 I 0.89***

NMK. Abundant pregastrulation transcript; encodes coiled-coil protein. [[Schauer and Wood 1990](#); [Seydoux et al. 1996](#)] [BW]

***vet-2* ?**

NMK. Abundant pregastrulation transcript. [[Schauer and Wood 1990; Seydoux et al. 1996](#)] [BW]

***vet-3* ?**

NMK. Abundant pregastrulation transcript. [[Schauer and Wood 1990](#)] [BW]

***vet-4* ?**

NMK. Abundant pregastrulation transcript. [[Schauer and Wood 1990; Seydoux et al. 1996](#)] [BW]

***vet-5* ?**

NMK. Abundant pregastrulation transcript. [[Schauer and Wood 1990; Seydoux et al. 1996](#)] [BW]

***vet-6 I 18.05***

NMK. Abundant pregastrulation transcript; encodes novel protein; *vet-6:lacZ* expressed in many cells from 28-cell stage to end of gastrulation. [[Schauer and Wood 1990](#)] [BW]

***vet-7 II – 11.98***

NMK. Abundant pregastrulation transcript. [[Schauer and Wood 1990; Seydoux et al. 1996](#)] [BW]

***vet-8 II – 13.09***

NMK. Abundant pregastrulation transcript. [[Schauer and Wood 1990](#)] [BW]

***vet-9 IV – 28.99***

NMK. Abundant pregastrulation transcript. [[Schauer and Wood 1990](#)] [BW]

***vet-10 X 24.09***

NMK. Abundant pregastrulation transcript. [[Schauer and Wood 1990](#)] [BW]

***vet-11 I 14.18***

NMK. Abundant pregastrulation transcript. [[Schauer and Wood 1990](#)] [BW]

***vex***

**v** ulval **ex** ecution-defective [SY].

***vex-1 II C sy207***

: abnormal mitosis in division of vulval precursor [P6.p](#); *sy207/Df* similar. [PS]

***vhp***

**VH** 1 dual specificity **p** phosphatase-related.

***vhp-1 II – 2.32***

NMK. Encodes predicted protein with similarity to VH1 dual specificity phosphatase family; previously F08B1.1. [CGC]

***vit***

**vit** ellogenin family [BL].

***vit-1 X – 1.38***

NMK. Pseudogene with 95% similarity to [\*vit-2\*](#); Transcripts not detected. [[Spieth et al. 1985b](#)]

***vit-2 X 5.93***

NMK. 4.9-kb transcript, specific to adult hermaphrodite [intestine](#); encodes vitellogenin yp170B (67% identity to VIT-5); extensive promoter analysis. [[Spieth et al. 1985b; MacMorris et al. 1994](#)] [BL]

***vit-3* X – 12.53**

NMK. Encodes vitellogenin yp170A; gene adjacent and nearly identical to [\*vit-4\*](#) . [[Spieth et al. 1985b](#)] [BL]

***vit-4* X – 12.53**

NMK. Encodes vitellogenin yp170A (95% identical to VIT-5); gene adjacent and nearly identical to [\*vit-3\*](#) . [[Spieth et al. 1985b](#)] [BL]

***vit-5* X – 12.73**

NMK. 4.9-kb transcript, specific to adult hermaphrodite [\*intestine\*](#); encodes 1603-aa vitellogenin yp170A. [[Spieth et al. 1985a](#)] [BL]

***vit-6* IV 3.76**

NMK. 5.1-kb transcript, specific to adult hermaphrodite [\*intestine\*](#); encodes VIT-180, 180-kD protein distantly related to VIT-5 (30% identity); cleaved to yp115 and yp88. [[Spieth and Blumenthal 1985](#)] [BL]

***vmp***

**v** itelline **m** embrane **p** rotein-related [NA].

***vmp-1***

= *cut-1*

***vmp-2***

= *cut-2*

***xol***

**XO** I ethal [TY].

***xol-1* X – 0.59 y9**

: XO animals die as embryos or small crumpled feminized L1 larvae with disorganized cellular structures; XX animals viable, apparently wt hermaphrodites; also enhances XX pseudomale phenotype of *tra-2*, *tra-3*, *her-1(gf)*, to fertile mating male phenotype; 35–50-kb deletion null. OA>10: *y70*, *y95*, *y138* (nonsense), *mn467* (XO lethal but no XX Tra enhancement), *e2533*, *e2583*, etc. CLONED: multiple Transcripts (1.5, 2.2, 2.5 kb) present 10-fold higher in XO than XX embryo; encode novel predicted proteins with three different C-termini; 2.2-kb transcript necessary and sufficient for [\*xol-1\*](#) activity; transgene overexpression leads to XX lethality. [[Miller et al. 1988](#); [Rhind et al. 1995](#)] [TY]

***yp***

t **y** rosine **p** hos **p** hatase family [CGC].

***yp*-1 II 3.06**

NMK. Encodes predicted tyrosine phosphatase. [CR]

***yrn***

**Y RN** A [CGC].

***yrn-1* IV 3.40**

NMK. Encodes 105-nucleotide RNA with structural similarity to vertebrate Y RNAs; associated with and bound by ROP-1; also bound by human Ro protein. [[van Horn et al. 1995](#)]

***zen***

**z**ygotic hypodermal **en** closure-defective [JR].

***zen-1***

= *rrs-1*

### ***zen-2* II N**

: Mutation leads to embryonic lethality; may be specifically defective in ventralward hypodermal migrations. [JR]

### ***zen-3* V N**

Mutation leads to embryonic lethality; failure to express [seam](#) cell antigens, may make too few hypodermal cells. [JR]

### ***zyg***

***zyg*** ote (embryo)-defective [DH].

### ***zyg-1* II – 1.96 b1**

: ts, mm; L4 shift-up results in embryonic arrest at 2–20 nuclei; first cleavage plane distorted, endomitosis; L1 shift-up results in abnormal gonadogenesis, Evl, Unc, weak Egl, Mab; spindle formation defects; viable at 16°C. OA>5, complex phenotypes, most alleles only Mel: *it4* (Mel, Evl), *it25ts*, *it29*, *it37*. CLONED: cosmid rescue (C08D10). [[Wood et al. 1980](#); [Kemphues et al. 1988a](#)] [KK]

### ***zyg-2* I 1.87 b10**

: ts, mm; L4 shift-up results in embryonic arrest at <25–50 nuclei, early cleavage slow; TSP before fertilization; L1 shift-up results in abnormal gonadogenesis, male sterility; viable at 16°C, male fertility low at 16°C. OA1: *g57*. [[Wood et al. 1980](#); Denich et al. 1984]

### ***zyg-3* II – 2.06 b18**

: ts, sd, mn; L4 shift-up results in embryonic arrest at >200 nuclei; eggs lyse in vitro; TSP short, during early cleavage; L1 shift-up results in abnormal gonadogenesis, male sterility; viable at 16°C. NA1. [[Wood et al. 1980](#)]

### ***zyg-4***

= *emb-7*

### ***zyg-5* II N b89**

: ts, nm; L4 shift-up results in embryonic arrest at <25 nuclei, few early cleavages; eggs lyse in vitro; TSP during cleavage; L1 shift-up results in larval arrest (L1 to L3); slight dominant reduction in fertility; viable at 16°C. NA1. [[Wood et al. 1980](#)]

### ***zyg-6***

= *emb-9*

### ***zyg-7* III 0.32 b187**

: ts, mn; L4 shift-up results in embryonic arrest; L1 shift-up results in some L4 arrest, males fertile; viable at 16°C. NA1. [[Wood et al. 1980](#)]

### ***zyg-8* III 13.89 b235**

: ts, mnp; L4 shift-up results in embryonic arrest at >200 nuclei; first cleavage abnormal giving three or four blastomeres; phenotype paternally rescued by *b235/+* sperm cytoplasm; L1 shift-up results in viable adult, F<sub>1</sub> embryonic arrest; male sterility; viable at 16°C. NA1. [[Wood et al. 1980](#)]

### ***zyg-9* II 0.78 b244**

: ts; maternal-effect embryonic-lethal after larval shift-up; meiotic and mitotic spindle abnormalities, defects in first mitotic divisions, like [\*mei-1\* \(gf\)](#), [\*mel-26\* \(gf\)](#). OA>5: *it3* (Mel, no zygotic rescue), *b288ts,mm*,

*b*279, *b*301, *b*307. [[Kemphues et al. 1988a](#); [Mains et al. 1990b](#)] [HR, KK]

***zyg-10 III C b261***

: ts, mn?; L4 shift-up results in embryonic arrest, abnormal skewed first cleavage, small P<sub>1</sub> blastomere; TSP during oogenesis; L1 shift-up results in viable adult hermaphrodite, fertile male; viable at 16°C. NA1. [[Wood et al. 1980](#)]

***zyg-11 II 0.62 mn40***

: amb; maternal-effect-lethal, abnormal metaphase at meiosis II, symmetrical first cleavage, extensive early defects. OA>5: *b2ts* (TSP before fertilization; L1 shift-up Mel), *it11ts*, *it1*, *it2* (weak), *it28*, *it34* (mostly strict Mel), *b290* (Mel, leaky, zygotic rescue). CLONED: Transcripts not confined to germ line; encodes novel protein. [[Kemphues et al. 1988a](#); [Carter et al. 1990](#)] [KK]

***zyg-12 II – 1.89***

Putative single mutation in wild strain Bergerac, ts, mm; L4 shift-up results in embryonic arrest at >200 nuclei, normal early cleavages; TSP before fertilization; L1 shift-up results in abnormal gonadogenesis, male sterility; viable at 20°C, 16°C. NA1. [[Wood et al. 1980](#)]

***zyg-13 IV – 28.03 b126***

: sd, ts, mm; maternal-effect-lethal after L4 shift-up, abnormal gonadogenesis after L1 shift-up; *b126*/+ reduced fertility. [[Wood et al. 1980](#)] [BW]

***zyg-14***

= *par-1*

Generated from local HTML

## Appendix 2 Neurotransmitter Assignments for Specific Neurons

The putative neurotransmitter for many neurons is indicated in the table on the following pages; most assignments are likely but not absolutely certain. Some assignments have not been verified for all developmental stages, and the listing of male-specific neurons or male-specific staining is not complete. Some neurons may contain and/or use more than one transmitter. Not listed are approximately 20 not yet identified putative cholinergic neurons (J. Duerr, pers. comm.). In addition, neuropeptide-like immunoreactivities have been observed in a wide variety of neurons both in *Ascaris* ([Sithigorngul et al. 1990, 1996](#); [Cowden et al. 1993](#)) and in *C. elegans* ([Schinkmann and Li 1992](#)).

<b>Transmitter<sup>a</sup></b>	<b>Cell<sup>b</sup></b>	<b>Criteria<sup>c</sup></b>	<b>Comments</b>	<b>References</b>
ACh	ALN(2)	2		J. Duerr (pers. comm.)
	AS(11)	2,3,4		<a href="#">Stretton et al. (1978); Johnson and Stretton (1985)</a> ; J. Duerr (pers. comm.)
	CA(4)	4	male	C. Johnson (pers. comm.)
	DA(9)	2,3,4		<a href="#">Stretton et al. (1978); Johnson and Stretton (1985)</a> ; J. Duerr (pers. comm.)
	DB(7)	2,3,4		<a href="#">Stretton et al. (1978); Johnson and Stretton (1985)</a> ; J. Duerr (pers. comm.)
	HSN(2)	2,5	staining weak and variable; reduction of ACh synthesis does not function	<a href="#">Weinshenker et al. (1995)</a> ; J. Duerr (pers. comm.)
	M1	2		J. Duerr (pers. comm.)
	M2(2)	2		J. Duerr (pers. comm.)
	<a href="#">M4</a>	2	staining variable; reduction of ACh synthesis does not function	J. Duerr; L. Avery (both pers. comm.)
	M5	2		J. Duerr (pers. comm.)
	MC	3,5	staining weak or nonexistent	<a href="#">Raizen et al. (1995)</a> ; J. Duerr (pers. comm.)
	<a href="#">PLN(2)</a>	2		J. Duerr (pers. comm.)
	SAA(4)	2		J. Duerr (pers. comm.)
	SAB(3)	2		J. Duerr (pers. comm.)
	SDQ(2)	2		J. Duerr (pers. comm.)
	SIA(4)	2		J. Duerr (pers. comm.)
	SIB(4)	2		J. Duerr (pers. comm.)
	SMB(4)	2		J. Duerr (pers. comm.)
	SMD(4)	2		J. Duerr (pers. comm.)
	VA(12)	2,3		J. Duerr (pers. comm.)
	VB(11)	2,3		J. Duerr (pers. comm.)
	VC(6)	2		J. Duerr (pers. comm.)
GABA	<a href="#">AVL</a>	1A,2,3		<a href="#">McIntire et al. (1993b)</a> ; Y. Jin (pers. comm.)
	DD(6)	1A,1B, 2,3,4		<a href="#">Stretton et al. (1978); Johnson and Stretton (1987); McIntire et al. (1993b)</a> ; Y. Jin (pers. comm.)

<b>Transmitter<sup>a</sup></b>	<b>Cell<sup>b</sup></b>	<b>Criteria<sup>c</sup></b>	<b>Comments</b>	<b>References</b>
	<a href="#">DVB</a>	1A,1B, 2,3,4		<a href="#">Guastella et al. (1991); McIntire et al. (1993b)</a> ; Y. Jin (pers. comm.)
	RIS	1A,2		<a href="#">McIntire et al. (1993b)</a> ; Y. Jin (pers. comm.)
	RME(4)	1A,1B, 2,3,4		<a href="#">Guastella et al. (1991); McIntire et al. (1993b)</a> ; Y. Jin (pers. comm.)
	VD(13)	1A,1B, 2,3,4		<a href="#">Stretton et al. (1978); Johnson and Stretton (1987); McIntire et al. (1993b)</a> ; Y. Jin (pers. comm.)
DA	<a href="#">ADE(2)</a>	1A,3		<a href="#">Sulston et al. (1975)</a> ; B. Sawin (pers. comm.)
	CEP(4)	1A,3		<a href="#">Sulston et al. (1975)</a> ; B. Sawin (pers. comm.)
	<a href="#">PDE(2)</a>	1A,3		<a href="#">Sulston et al. (1975)</a> ; B. Sawin (pers. comm.)
	R5A(2)	1A	male tail	<a href="#">Sulston and Horvitz (1977)</a> .
	R7A(2)	1A	male tail	<a href="#">Sulston and Horvitz (1977)</a> .
	<a href="#">R9A(2)</a>	1A	male tail	<a href="#">Sulston and Horvitz (1977)</a> .
5-HT	ADF(2)	1A		G. Garriga and C. Bargmann (pers. comm.)
	CA(4)	1A	male; CA1-CA4 only; staining weak in <i>C. elegans</i> ; no staining in <i>Ascaris</i>	<a href="#">Loer and Kenyon (1993); Johnson et al. (1996)</a> .
	CP(6)	1A,1B, 3	male; CP1-CP6 only; very strong staining	<a href="#">Loer and Kenyon (1993); Johnson et al. (1996)</a> .
	HSN(2)	1A,5	strong staining; loss of 5-HT in <i>cat-4</i> or <i>bas-1</i> does not prevent function	<a href="#">Desai et al. (1988); Weinshenker et al. (1995)</a> .
	NSM(2)	1A,1B	very strong staining	<a href="#">Horvitz et al. (1982); Johnson et al. (1996)</a> .
	RIG(2)	1A	might be AIM or <a href="#">AIY</a> instead of RIG	J. Kaplan; B. Sawin (both pers. comm.)
	<a href="#">RIH</a>	1A		G. Garriga and J. Thomas (pers. comm.)
	R1A/B(2)	1A	male tail	<a href="#">Loer and Kenyon (1993)</a> .
	R3A/B(2)	1A	male tail	<a href="#">Loer and Kenyon (1993)</a> .
	<a href="#">R9A/B(2)</a>	1A	male tail	<a href="#">Loer and Kenyon (1993)</a> .
	VC(2)	1A	VC4 and <a href="#">VC5</a> only	G. Garriga (pers. comm.)
GLU	ASH(2)	3		<a href="#">Hart et al. (1995); Maricq et al. (1995)</a>
	<a href="#">M3</a>	3,5		<a href="#">Avery and Thomas (this volume)</a>

a

Neurotransmitter abbreviations: (ACh) Acetylcholine, (GABA)  $\gamma$ -aminobutyric acid; (DA) dopamine; (5-HT) serotonin; (GLU) glutamate.

b

If a cell type includes more than one cell, the number of cells in the class is indicated in parentheses.

c

Criteria:

(1A)

The transmitter is present in the *C. elegans* cell, identified by immunostaining (for GABA and 5-HT) and/or by formaldehyde-induced fluorescence (for DA and 5-HT).

(1B)

The transmitter is present in the comparable cell in *Ascaris*, identified by immunostaining for GABA or 5-HT.

(2)

The biosynthetic enzyme is present in the cell, determined by antibodies to choline acetyltransferase or by reporter gene expression of *unc-25*.

(3)

Supported by mutant data, i.e., loss of transmitter (in *cha-1*, *unc-25*, or *cat*) or loss of receptor (in postsynaptic partner) is associated with loss of cell function.

(4)

Supported by physiological, pharmacological, and/or biochemical studies of the homologous cell(s) from *Ascaris*.

(5)

Supported by other data, such as *C. elegans* electrophysiology or pharmacology studies.

Generated from local HTML

## Appendix 3 Codon Usage in *C. elegans*

---

Synonymous codon usage in *C. elegans* was investigated by Stenico et al. (1994). The major conclusion of this analysis was that synonymous codon usage patterns vary among genes in a manner correlated with their expression level. Some genes have extremely biased codon usage: these genes appear to be expressed at higher levels, and it was inferred that natural selection has favored a limited number of translationally optimal codons. Other genes (apparently those expressed at low levels) have relatively unbiased codon usage, although there was some nonrandomness consistent with context-dependent mutational biases. These results echo those found in a number of unicellular eukaryotes and in *Drosophila melanogaster* (see Sharp et al. 1995). Here the analyses of codon usage in *C. elegans* have been updated using similar techniques, but with a much larger dataset.

All nuclear protein-coding sequences annotated as deriving from *C. elegans* were extracted from the GenBank/EMBL/DDBJ DNA sequence data library (GenBank release 92), using the ACNUC retrieval system (Gouy et al. 1985). Duplicate sequences, partial sequences, and sequences containing ambiguous codons or multiple stop codons were excluded, yielding a total dataset of 4027 open reading frames (ORFs). Although some of these sequences were determined by the "traditional" approach—i.e., the genes were identified and sequenced because of some known function or phenotype—many others were found within cosmids sequenced as part of the genome project and many of the genes thus identified remain putative. Therefore, gene sequences were first designated as (1) "genes" if the sequence was determined by the traditional approach, (2) "probable genes" if the cosmid-contained sequence exhibited significant similarity to a sequence from another species, or (3) "unidentified reading frames (URFs)" if identified only as an open reading frame within a cosmid sequence.

Overall codon usage in 312 genes (not shown) was found to be very similar to that in 168 genes previously examined (Stenico et al. 1994). Codon usage in 2238 URFs was not very different from that in 90 URFs previously examined (Stenico et al. 1994). As before, URF codon usage differed somewhat from that in genes, in being generally much less biased. Codon usage in 1477 probable genes showed a pattern of bias intermediate between that in genes and URFs. These observations suggest that the dataset of genes examined by the traditional approach contains a disproportionate number of relatively highly expressed genes, whereas the majority of the URFs are lowly expressed (and perhaps some are not in fact genes). Further analyses were restricted to the dataset of genes and probable genes (totaling 1789 sequences).

Codon usage in these genes was subjected to correspondence analysis, a statistical technique for characterizing major trends in multivariate data (see Stenico et al. 1994). As previously found, a single major trend among genes ("axis 1") was identified. The nature of the trend in codon usage along axis 1 is shown in Table 1, which contains codon usage values for three subsets of this dataset: the 10% of genes from each extreme of the axis (one extreme exhibiting high bias and the other low bias) and the 10% of genes lying at the center of the axis. Each subset shows codon usage summed over 178 genes: The total numbers of codons in each case are 73164 (High), 109120 (Middle), and 80249 (Low). The data are presented as raw codon usage values ( $N$ ) and relative synonymous codon usage values (RSCU). RSCU is calculated as the observed value ( $N$ ) divided by that expected if all synonyms for an amino acid were used equally.

Comparison of the RSCU values for the High (bias) and Low (bias) datasets illustrates the considerable variation in codon usage among *C. elegans* genes. For example, for Phe, UUC seems to be heavily favored over UUU in some genes (the High subset), whereas the opposite is true in others (the Low subset). The Middle subset of genes exhibit codon usage patterns intermediate between the High and Low subsets. These patterns are consistent with codon usage in any particular gene reflecting a balance between the population genetic processes of mutation, selection, and random genetic drift, with the point of balance depending on the strength of selection on that gene. Thus, for Phe, UUC seems to be the translationally optimal codon in a wide range of species, and its high frequency in the High subset is inferred to be due to strong natural selection. In contrast, in the Low subset, U-ending codons occur at high frequency (and C-ending codons at low frequency) for all four amino acids with U at the second codon position, consistent with neighboring nucleotide-dependent mutation biases. Codon usage in the Middle subset of genes is similar to the total codon usage of the 1789 taken as a

whole. Thus, it is a guide to the “typical” codon usage of *C. elegans*, but the heterogeneity among genes reflected in the contrast between the High and Low subsets should always be borne in mind.

Twenty two codons that occur at significantly ( $p < 0.01$ ) higher frequencies in the High subset than in the Low subset (indicated by an asterisk) are inferred to be those that are translationally optimal. These include 21 codons identified by Stenico et al. (1994), plus UCU (for Ser), which was only marginally significant ( $0.01 < p < 0.05$ ) in the earlier analysis. Another Ser codon, AGC, has not been included in this set of optimal codons because its frequency in the High subset, while significantly higher than in the Low subset, is still lower than for four other Ser codons. The degree of codon usage bias in any gene can then be quantified by  $F_{op}$ , the frequency of these optimal codons as a fraction of the total usage of codons for the 18 amino acids with more than one codon. These  $F_{op}$  values range between 0.17 and 0.89 and represent a succinct summary of the major trend in codon usage bias revealed by the correspondence analysis:  $F_{op}$  and position on axis 1 are extremely highly correlated (correlation coefficient 0.97).

Strong bias in favor of translationally optimal codons has generally been interpreted as reflecting selection for efficiency of translation. Thus, the genes with the highest bias are those with the highest expression levels. This appears to be the case in *C. elegans*. The genes with the highest  $F_{op}$  values (lying at the high bias extreme of axis 1) include those encoding ribosomal proteins, translation elongation factors, actins, and histones, all of which are expressed at very high levels. The genes with the lowest  $F_{op}$  values (lying at the low bias extreme of axis 1) include those encoding regulatory proteins, generally expected to be expressed at very low levels. Furthermore, within gene families whose members are expressed at different levels, those expressed at higher levels have higher  $F_{op}$  values (Stenico et al. 1994). An alternative hypothesis, recently proposed for *Drosophila* genes, is that optimal codons are selected primarily for accuracy of translation (Akashi 1994). Since many abundant proteins (such as those listed above) are also highly conserved proteins, it can be difficult to disentangle the potential effects of selection for efficiency and/or accuracy; we are currently investigating this problem.

## Tables

**Table 1**Codon usage in *C. elegans*

		High		Middle		Low	
		N	RSCU	N	RSCU	N	RSCU
Phe	UUU	315	0.26	2103	0.93	2440	1.25
	UUC*	2139	1.74	2405	1.07	1472	0.75
Leu	UUA	49	0.05	930	0.63	1449	1.28
	UUG	946	1.04	2049	1.38	1599	1.41
Leu	CUU*	2052	2.26	2465	1.66	1517	1.34
	CUC*	2066	2.28	1541	1.04	666	0.59
	CUA	66	0.07	732	0.49	769	0.68
	CUG	268	0.30	1173	0.79	784	0.69
Ile	AUU	1179	0.96	3310	1.67	2971	1.71
	AUC*	2483	2.01	1884	0.95	984	0.57
	AUA	40	0.03	752	0.38	1257	0.72
	Met	AUG	1473	—	3000	—	2142
Val	GUU	1722	1.51	2678	1.62	2057	1.68
	GUC*	2057	1.81	1360	0.83	624	0.51

		High		Middle		Low	
		N	RSCU	N	RSCU	N	RSCU
	GUA	215	0.19	1041	0.63	1194	0.97
	GUG	564	0.49	1514	0.92	1028	0.84
Ser	UCU*	1104	1.64	2020	1.35	1381	1.25
	UCC*	1400	2.08	1087	0.73	580	0.53
	UCA	517	0.77	2345	1.57	2120	1.92
	UCG	466	0.69	1182	0.79	757	0.69
Pro	CCU	166	0.15	1074	0.78	929	1.00
	CCC	91	0.08	496	0.36	299	0.32
	CCA*	3994	3.60	2958	2.14	1862	2.00
	CCG	192	0.17	999	0.72	634	0.68
Thr	ACU	1167	1.25	2271	1.39	1478	1.30
	ACC*	1990	2.14	1005	0.61	417	0.37
	ACA	410	0.44	2309	1.41	1977	1.74
	ACG	158	0.17	972	0.59	660	0.58
Ala	GCU*	2777	1.82	2525	1.47	1559	1.40
	GCC*	2631	1.72	1159	0.68	466	0.42
	GCA	537	0.35	2342	1.36	1887	1.69
	GCG	171	0.11	840	0.49	546	0.49
Tyr	UAU	432	0.44	1783	1.13	1695	1.35
	UAC*	1523	1.56	1382	0.87	815	0.65
ter	UAA	137	2.31	85	1.42	73	1.23
	UAG	27	0.46	36	0.60	33	0.56
His	CAU	479	0.68	1621	1.25	1330	1.40
	CAC*	935	1.32	973	0.75	564	0.60
Gln	CAA	2363	1.35	3365	1.32	2302	1.44
	CAG*	1147	0.65	1720	0.68	896	0.56
Asn	AAU	726	0.49	3360	1.23	2936	1.47
	AAC*	2237	1.51	2115	0.77	1049	0.53
Lys	AAA	781	0.30	4255	1.22	3863	1.42
	AAG*	4373	1.70	2720	0.78	1585	0.58
Asp	GAU	2046	1.01	4061	1.39	3246	1.52
	GAC*	1991	0.99	1771	0.61	1028	0.48
Glu	GAA	2110	0.79	5038	1.32	3991	1.45
	GAG*	3255	1.21	2621	0.68	1524	0.55
Cys	UGU	321	0.53	1210	1.13	1066	1.36
	UGC*	895	1.47	925	0.87	504	0.64

		High		Middle		Low	
		N	RSCU	N	RSCU	N	RSCU
ter	UGA	14	0.24	58	0.97	72	1.21
Trp	UGG	591	—	1039	—	921	—
Arg	CGU*	1665	2.66	1442	1.43	595	0.82
	CGC*	935	1.49	548	0.54	185	0.26
	CGA	168	0.27	1391	1.38	1252	1.73
	CGG	39	0.06	481	0.48	404	0.56
Ser	AGU	148	0.22	1454	0.98	1286	1.17
	AGC	409	0.61	859	0.58	485	0.44
Arg	AGA	906	1.45	1773	1.76	1486	2.06
	AGG	43	0.07	408	0.41	409	0.57
Gly	GGU	797	0.45	1393	0.91	953	0.92
	GGC	351	0.20	703	0.46	363	0.35
	GGA*	5807	3.29	3560	2.33	2446	2.36
	GGG	108	0.06	449	0.29	387	0.37

\*

Optimal codons (see text).

Generated from local HTML

## **Appendix 4 On-line *C. elegans* Resources**

---

The wide use of the Internet and World Wide Web (WWW) in the scientific community and the corresponding rapid development of hypertext browser programs have made a bewildering array of on-line resources available for biological researchers. The tables and text on the following pages give brief descriptions and electronic addresses of several major Web sites providing access to information on *C. elegans*, categorized by general type of data.

The sites listed here constitute a basic set of the major electronic *C. elegans* resources on the Web. Each site, customized by its keepers, may contain links to many other more specific resources such as specialized programs written by *C. elegans* researchers, data search engines, electronic versions of standard print materials (e.g., the *Worm Breeder's Gazette*), photographic images of worms, the Bionet *C. elegans* discussion group, and many others. Discovering the wealth of information that is now literally at one's fingertips requires only standard computer hardware, a graphical link to the Internet, and a bit of time.

### **Contents**

[Part A ACeDB Resources](#)

[Part B \*C. elegans\* Genome Project and Related Sources](#)

[Part C Other Information Sources](#)

Generated from local HTML

## Appendix 4 On-line *C. elegans* Resources — Part A ACeDB Resources

ACeDB (a *C. elegans* database) has become the standard electronic mechanism for collection, linking, and display of data on *C. elegans*, as well as other organisms. The programmers make available by anonymous ftp the program source code; executable binaries for several common Unix, Macintosh, and Windows platforms; and raw data files. Updates to the data and program are published at these sites several times a year. The source code can be used to compile an executable system on computers for which precompiled binaries are not usually available.

The Web has made obtaining ACeDB documentation an easy task as well. Two major sites provide FAQs (Frequently Asked Questions), detailed descriptions of program function and features, and E-mail addresses of people who can be contacted for help.

Finally, for the researcher who does not want to bother with setting up ACeDB on a local computer system, the data are available through ACeDB installations executable over the Web. Data access can be slow, depending on network traffic, but the data are available through these sites using only a limited-function network terminal.

### Tables

Program source code, compiled binaries, data
<a href="ftp://ncbi.nlm.nih.gov/repository/acedb">ftp://ncbi.nlm.nih.gov/repository/acedb</a>
<a href="ftp://ftp.sanger.ac.uk/pub/acedb">ftp://ftp.sanger.ac.uk/pub/acedb</a>
<a href="ftp://lirmm.lirmm.fr/genome/acedb">ftp://lirmm.lirmm.fr/genome/acedb</a>
Documentation
<a href="http://probe.nalusda.gov:8000/acedocs/index.html">http://probe.nalusda.gov:8000/acedocs/index.html</a>
<a href="http://genome.wustl.edu/gsc/ace/acedocs/ace.html">http://genome.wustl.edu/gsc/ace/acedocs/ace.html</a>
WWW-executable program
<a href="http://probe.nalusda.gov:8300/other/index.html">http://probe.nalusda.gov:8300/other/index.html</a>
<a href="gopher://weeds.mgh.harvard.edu/77/.index/">gopher://weeds.mgh.harvard.edu/77/.index/</a>
Caenorhabditis_elegans_Genome

Generated from local HTML

## **Appendix 4 On-line *C. elegans* Resources — Part B *C. elegans* Genome Project and Related Sources**

The *C. elegans* Genome Project had generated 50 million nucleotides of DNA sequence by the end of July, 1996, and this number is expected to grow to 100 million by the end of 1998. The data are currently available in finished and "in-process" form from the Web sites of both sequencing centers. The sequence is posted on these sites prior to appearance in GenBank or ACeDB and is retrieved most commonly by cosmid name. A project funded by the Canadian Genome and Technology program (CGAT) in the D.L. Baillie and A.M. Rose laboratories operates as a complement to the Genome Project. These labs are systematically creating *C. elegans* strains transformed with sequenced cosmids and making them available to the research community on request. The Web site lists cosmids for which strains are currently available and cosmids for which strains are to be constructed.

### **Tables**

Sanger Centre, Cambridge, England	<a href="http://www.sanger.ac.uk/~sjj/C.elegans_Home.html">http://www.sanger.ac.uk/~sjj/C.elegans_Home.html</a>
Washington University, St. Louis, Missouri, USA	<a href="http://genome.wustl.edu/gsc/gschmpg.html">http://genome.wustl.edu/gsc/gschmpg.html</a>
Transgenic <i>C. elegans</i> strains	<a href="http://darwin.mbb.sfu.ca/imbb/dbaillie/cosmid.html">http://darwin.mbb.sfu.ca/imbb/dbaillie/cosmid.html</a>

Generated from local HTML

## **Appendix 4 On-line *C. elegans* Resources — Part C Other Information Sources**

---

Leon Avery's *C. elegans* Server at University of Texas Southwestern Medical Center is one of the most comprehensive *C. elegans* sites on the Web. It is often the first stop for anyone looking for anything to do with *C. elegans*, as it contains a variety of useful information and a number of links to other sites. Of particular interest are details about upcoming *C. elegans* meetings, complete with electronic versions of abstracts, and a complete set of links to Web sites maintained by individual *C. elegans* labs. This site is maintained very actively.

The Caenorhabditis Genetics Center at the University of Minnesota operates a gopher site to provide access to its accumulated data on *C. elegans* strains, assigned gene names and laboratory and allele prefixes, a bibliography of *Caenorhabditis* publications, tables of contents from the international and regional *C. elegans* meetings, articles appearing in the *Worm Breeder's Gazette*, and the WBG subscriber list. The site is searchable, and full data lists are available for downloading.

Finally, the Nematode Educational Resource Server, maintained by the laboratory of Sam Ward at the University of Arizona, primarily targets scientists using or planning to use nematodes in teaching. It provides sample course syllabi and lab exercises and a set of links to sites offering general teaching resources, and it maintains a list of open teaching positions and a mailing list of scientists interested in teaching.

### **Tables**

<i>C. elegans</i> Server at UTSW	<a href="http://eatworms.swmed.edu">http://eatworms.swmed.edu</a>
<i>C. elegans</i> laboratory Web site list	<a href="http://eatworms.swmed.edu/Worm_labs">http://eatworms.swmed.edu/Worm_labs</a>
Caenorhabditis Genetics Center Gopher	<a href="gopher://elegans.cbs.umn.edu:70/1">gopher://elegans.cbs.umn.edu:70/1</a>
Nematode Educational Resource Server	<a href="http://worm.biosci.arizona.edu/NERS/NERShome.html">http://worm.biosci.arizona.edu/NERS/NERShome.html</a>

Generated from local HTML

# Bibliography

---

[A](#) · [B](#) · [C](#) · [D](#) · [E](#) · [F](#) · [G](#) · [H](#) · [I](#) · [J](#) · [K](#) · [L](#) · [M](#) · [N](#) · [O](#) · [P](#) · [Q](#) · [R](#) · [S](#) · [T](#) · [U](#) · [V](#) · [W](#) · [X](#) · [Y](#) · [Z](#)

## A

1. Aamodt E J, Chung M A, McGhee J D. Spatial control of gut-specific gene expression during *Caenorhabditis elegans* development. *Science*. 1991;252:579–582. [[PubMed: 2020855](#)]
2. Abad P, Quiles C, Tares S, Piotte C, Castagnone-Sereno P, Abdon M, Dalmaso A. Sequences homologous to Tc(s) transposable elements of *Caenorhabditis elegans* are widely distributed in the phylum nematoda. *J. Mol. Evol.* 1991;33:251–258. [[PubMed: 1661782](#)]
3. Abdul Kader N, Brun J. Induction detection and isolation of temperature-sensitive lethal and/or sterile mutants in nematodes. I. The free-living nematode *C. elegans*. *Rev. Nematol.* 1978;1:27–37.
4. Abe H, Ohsima S, Obinata T. A cofilin-like protein is involved in the regulation of actin assembly in developing skeletal muscle. *J. Biochem. (Tokyo)*. 1989;106:696–702. [[PubMed: 2691511](#)]
5. Abe H, Endo T, Yamamoto K, Obinata T. Sequence of cDNA's encoding actin depolymerizing factor and cofilin embryonic chicken skeletal muscle: Two functionally distinct actin-regulatory proteins exhibit high structural homology. *Biochemistry*. 1990;29:7420–7425. [[PubMed: 1699599](#)]
6. Abe M, Takahashi K, Hiwada K. Effect of calponin on actin-activated myosin ATPase activity. *J. Biochem.* 1990;108:835–838. [[PubMed: 2150518](#)]
7. Adams J C, Watt F M. Regulation of development and differentiation by the extracellular matrix. *Development*. 1993;117:1183–1198. [[PubMed: 8404525](#)]
8. Adams M D, Kerlavage A R, Fleischmann R D, Fuldner R A, Bult C J, Lee N H, Kirkness E F, Weinstock K G, Gocayne J D, White O, Sutton G, Blake J A, Brandon R C, Chiu M -W, Clayton R A, Cline R T, Cotton M D, Earle-Hughes J, Fine L D, FitzGerald L M, FitzHugh W M, Fritchman J L, Geoghegan N S M, Glodek A, Gnehm et al C L. Initial assessment of human gene diversity and expression patterns based upon 83 million nucleotides of cDNA sequence.(suppl.). *Nature*. 1995;377:3–174. [[PubMed: 7566098](#)]
9. Adams T H, Boyland M T, Timberlake W E. *brlA* is necessary and sufficient to direct conidiophore development in *Aspergillus nidulans*. *Cell*. 1988;54:353–362. [[PubMed: 3293800](#)]
10. Aeby P, Spicher A, De Chastonay Y, Muller F, Tobler H. Structure and genomic organisation of proretrovirus-like elements partially eliminated from the somatic genome of *Ascaris lumbricoides*. *EMBO J.* 1986;5:3353–3360. [[PMC free article: PMC1167333](#)] [[PubMed: 3816762](#)]
11. Agabian N. Trans splicing of nuclear pre-mRNAs. *Cell*. 1990;61:1157–1160. [[PubMed: 2142018](#)]
12. Agulnik S I, Bollag R J, Silver L M. Conservation of the T-box family from *Mus musculus* to *Caenorhabditis elegans*. *Genomics*. 1995;25:214–219. [[PubMed: 7774921](#)]
13. Ahmed S, Maruyama I N, Kozma R, Lee J, Brenner S, Lim L. The *Caenorhabditis elegans unc-13* gene product is a phospholipid-dependent high-affinity phorbol ester receptor. *Biochem. J.* 1992;287:995–999. [[PMC free article: PMC1133105](#)] [[PubMed: 1445255](#)]
14. Ahnn J, Fire A. A screen for genetic loci required for body-wall muscle development during embryogenesis in *Caenorhabditis elegans*. *Genetics*. 1994;137:483–498. [[PMC free article: PMC1205971](#)] [[PubMed: 8070659](#)]
15. Ahringer J. "Post-transcriptional regulation of *fem-3* a sex-determining gene of *C. elegans*." [Ph.D. thesis] University of Wisconsin-Madison. 1991. [[PubMed: 1702880](#)]
16. Ahringer J. Embryonic tissue differentiation in *Caenorhabditis elegans* requires *dif-1* a gene homologous to mitochondrial solute carriers. *EMBO J.* 1995;14:2307–2316. [[PMC free article: PMC398338](#)] [[PubMed: 7774589](#)]
17. Ahringer J. Posterior patterning by the *Caenorhabditis elegans* even-skipped homolog *vab-7*. *Genes Dev.* 1996;10:1120–1130. [[PubMed: 8654927](#)]
18. Ahringer J, Kimble J. Control of the sperm-oocyte switch in *Caenorhabditis elegans* hermaphrodites by the *fem-3*'untranslated region. *Nature*. 1991;349:346–348. [[PubMed: 1702880](#)]

19. Ahringer J, Rosenquist T A, Lawson D N, Kimble J. The *C. elegans* gene *fem-3* is regulated post-transcriptionally. *EMBO J.* 1992;11:2303–2310. [[PMC free article: PMC556697](#)] [[PubMed: 1376249](#)]
20. Akam M, Holland P, Wray G. Preface. *Suppl. Development.* 1994;
21. Akashi H. Synonymous codon usage in *Drosophila melanogaster*: Natural selection and translational accuracy. *Genetics.* 1994;136:927–935. [[PMC free article: PMC1205897](#)] [[PubMed: 8005445](#)]
22. Akerib C C, Meyer B J. Identification of Xchromosome regions in *C. elegans* that contain sex-determination signal elements. *Genetics.* 1994;138:1105–1125. [[PMC free article: PMC1206251](#)] [[PubMed: 7896094](#)]
23. Aksoy S. Spliced leader RNA and 5S rRNA genes in *Herpetomonas* spp. are genetically linked. *Nucleic Acids Res.* 1992;20:913. [[PMC free article: PMC312040](#)] [[PubMed: 1542583](#)]
24. Albert P S, Riddle D L. Developmental alterations in sensory neuroanatomy of the *Caenorhabditis elegans* dauer larva. *J. Comp. Neurol.* 1983;219:461–481. [[PubMed: 6643716](#)]
25. Albert P S, Riddle D L. Mutants of *Caenorhabditis elegans* that form dauer-like larvae. *Dev. Biol.* 1988;126:270–293. [[PubMed: 3350212](#)]
26. Albert P S, Brown S J, Riddle D L. Sensory control of dauer larva formation in *Caenorhabditis elegans*. *J. Comp. Neurol.* 1981;198:435–451. [[PubMed: 7240452](#)]
27. Albertson D G. Localization of the ribosomal genes in *Caenorhabditis elegans* chromosomes by *in situ* hybridization using biotin-labeled probes. *EMBO J.* 1984a;3:1227–1234. [[PMC free article: PMC557503](#)] [[PubMed: 6378619](#)]
28. Albertson D G. Formation of the first cleavage spindle in nematode embryos. *Dev. Biol.* 1984b;101:61–72. [[PubMed: 6692980](#)]
29. Albertson D G. Mapping muscle protein genes by *in situ* hybridization using biotin-labeled probes. *EMBO J.* 1985;4:2493–2498. [[PMC free article: PMC554534](#)] [[PubMed: 4054096](#)]
30. Albertson D G. Mapping chromosome rearrangement breakpoints to the physical map of *Caenorhabditis elegans* by fluorescent *in situ* hybridization. *Genetics.* 1993;134:211–219. [[PMC free article: PMC1205424](#)] [[PubMed: 8514130](#)]
31. Albertson D G, Thomson J N. The *pharynx* of *Caenorhabditis elegans*. *Philos. Trans. R. Soc. Lond. B Biol. Sci.* 1976;275:299–325. [[PubMed: 8805](#)]
32. Albertson D G, Thomson J N. The kinetochores of *Caenorhabditis elegans*. *Chromosoma.* 1982;86:409–428. [[PubMed: 7172865](#)]
33. Albertson D G, Thomson J N. Segregation of holocentric chromosomes at meiosis in the nematode *Caenorhabditis elegans*. *Chromosome Res.* 1993;1:15–26. [[PubMed: 8143084](#)]
34. Albertson D G, Fishpool R M, Birchall P S. Fluorescent *in situ* hybridization for the detection of DNA and RNA. *Methods Cell Biol.* 1995;48:339–364. [[PubMed: 8531734](#)]
35. Albertson D G, Sulston J E, White J G. Cell cycling and DNA replication in a mutant blocked in cell division in the nematode *Caenorhabditis elegans*. *Dev. Biol.* 1978;63:165–178. [[PubMed: 631425](#)]
36. Alexandre C, Jacinto A, Inghan P W. Transcriptional activation of *hedgehog* target genes in *Drosophila* is mediated by the Cubitus interruptus protein, a member of the GLI family of zinc finger DNA-binding proteins. *Genes Dev.* 1996;10:2003–2013. [[PubMed: 8769644](#)]
37. Alfonso A, Grundahl K, McManus J R, Rand J B. Cloning and characterization of the choline acetyltransferase structural gene (*cha-1*) from *C. elegans*. *J. Neurosci.* 1994a;14:2290–2300. [[PMC free article: PMC6577154](#)] [[PubMed: 8158270](#)]
38. Alfonso A, Grundahl K, Duerr J S, Han H P, Rand J B. The *Caenorhabditis elegans unc-17* gene: A putative vesicular acetylcholine transporter. *Science.* 1993;261:617–619. [[PubMed: 8342028](#)]
39. Alfonso A, Grundahl K, McManus J R, Asbury J M, Rand J B. Alternative splicing leads to two cholinergic proteins in *Caenorhabditis elegans*. *J. Mol. Biol.* 1994b;241:627–630. [[PubMed: 8057385](#)]
40. Allsopp R C, Vaziri H, Paterson C, Goldstein S, Younglai E V, Furcht A B, Greider C W, Harley C B. Telomere length predicts replicative capacity of human fibroblasts. *Proc. Natl. Acad. Sci.* 1992;89:10114–10118. [[PMC free article: PMC50288](#)] [[PubMed: 1438199](#)]
41. Allsopp T E, Wyatt S, Paterson H F, Davies A M. The proto-oncogene *bcl-2* can selectively rescue neurotrophic factor-dependent neurons from apoptosis. *Cell.* 1993;73:295–307. [[PubMed: 8477446](#)]

42. Alnemri E S, Robertson N M, Fernandez T F, Croce C M, Litwack G. Overexpressed full-length human BCL2 extends the survival of baculovirus-infected Sf9 insect cells. Proc. Natl. Acad. Sci. 1992;89:7295–7299. [[PMC free article: PMC49696](#)] [[PubMed: 1502141](#)]
43. Amaar Y G, Baillie D L. Cloning and characterization of the *C. elegans* histidyl-tRNA synthetase gene. Nucleic Acids Res. 1993;21:4344–4347. [[PMC free article: PMC310070](#)] [[PubMed: 8414990](#)]
44. Ambros V. A hierarchy of regulatory genes controls a larva-to-adult developmental switch in *C. elegans*. Cell. 1989;57:49–57. [[PubMed: 2702689](#)]
45. Ambros V, Fixsen W, Raff R A, Raff E C, editors. Development as an evolutionary process. New York: Alan Liss; 1987. Cell lineage variation among nematodes. pp. 139–159.
46. Ambros V, Horvitz H R. Heterochronic mutants of the nematode *Caenorhabditis elegans*. Science. 1984;266:409–416. [[PubMed: 6494891](#)]
47. Ambros V, Horvitz H R. The *lin-14* locus of *Caenorhabditis elegans* controls the time of expression of specific postembryonic developmental events. Genes Dev. 1987;1:398–414. [[PubMed: 3678829](#)]
48. Ambros V, Moss E G. Heterochronic genes and the temporal control of *C. elegans* development. Trends Genet. 1994;10:123–127. [[PubMed: 8029828](#)]
49. Ameisen J C, Idziorek T, Billaut-Mulot O, Loyens M, Tissier J -P, Potentier A, Ouassis A. Apoptosis in an unicellular eukaryote (*Trypanosoma cruzi*): Implications for the evolutionary origin and role of programmed cell death in the control of cell proliferation, differentiation and survival. Cell Death Differ. 1995;2:285–300. [[PubMed: 17180034](#)]
50. Anderson G L. Responses of dauer larvae of *Caenorhabditis elegans* (Nematoda: Rhabditidae) to thermal stress and oxygen deprivation. Can. J. Zool. 1978;56:1786–1791.
51. Anderson G L. Superoxide dismutase activity in the dauerlarvae of *Caenorhabditis elegans*. Can. J. Zool. 1982;60:288–291.
52. Anderson P. Molecular genetics of nematode muscle. Annu. Rev. Genet. 1989;23:507–525. [[PubMed: 2694942](#)]
53. Anderson P. Mutagenesis. Methods Cell Biol. 1995;48:31–58. [[PubMed: 8531732](#)]
54. Anderson P, Brenner S. A selection for myosin heavy chain mutants in the nematode *Caenorhabditis elegans*. Proc. Natl. Acad. Sci. 1984;81:4470–4474. [[PMC free article: PMC345612](#)] [[PubMed: 6589606](#)]
55. Anderson P, Emmons S W, Moerman D G. Discovery of Tc1 in the nematode *Caenorhabditis elegans*. In: Fedoroff N, Botstein D, editors. The dynamic genome. Cold Spring Harbor, New York: Cold Spring Harbor Laboratory Press; 1992. pp. 319–333.
56. Anderson R C. Nematode parasites of vertebrates. Their development and transmission. England: C.A.B. International; 1992.
57. Andrassy I. Evolution as a basis for the systematization of nematodes. London: Budapest: Pitman Publishing; Akademiai Kiado; 1976.
58. Andrassy I. A taxonomic review of the suborder Rhabditina (Nematoda: Secernentia). Paris: ORSTOM (L'Office de la Recherche Scientifique et Technique Outre-Mer); 1983.
59. Andrassy I. Klasse Nematoda (Ordnungen Monhysterida Desmoscolecida Araeolaimida, Chromadorida, Rhabditida). Stuttgart: Gustav Fischer Verlag; 1984.
60. Angstadt J D, Stretton A O. Slow active potentials in ventral inhibitory motor neurons in the nematode *Ascaris*. J. Comp. Physiol. 1989;166:165–177. [[PubMed: 2607486](#)]
61. Anya A O. Physiological aspects of reproduction in nematodes. Adv. Parasitol. 1976;14:267–351. [[PubMed: 769504](#)]
62. Arasu P, Wightman B, Ruvkun G. Temporal regulation of *lin-14* by the antagonistic action of two other heterochronic genes, *lin-4* and *lin-28*. Genes Dev. 1991;5:1825–1833. [[PubMed: 1916265](#)]
63. Ardizzi J P, Epstein H F. Immunohistochemical localization of myosin heavy chain isoforms and paramyosin in developmentally and structurally diverse muscle cell types of the nematode *Caenorhabditis elegans*. J. Cell Biol. 1987;105:2763–2770. [[PMC free article: PMC2114684](#)] [[PubMed: 3320053](#)]
64. Arduengo P M, Appleberry O K, L'Hernault S W. Immunocytochemical localization of *spe-4*, a protein required for spermatogenesis in *C. elegans*. (abstr.). Mol. Biol. Cell. 1994;5:219a. [[PubMed: 7865889](#)]

65. Arena J P, Liu K K, Paress P S, Cully D F. Avermectin-sensitive chloride currents induced by *Caenorhabditis elegans* RNA in *Xenopus* oocytes. Mol. Pharmacol. 1991;40:368–374. [[PubMed: 1716730](#)]
66. Arena J P, Liu K K, Paress P S, Schaeffer J M, Cully D F. Expression of a glutamate-activated chloride current in *Xenopus* oocytes injected with *Caenorhabditis elegans* RNA—Evidence for modulation by avermectin. Mol. Brain. Res. 1992;15:339–348. [[PubMed: 1279355](#)]
67. Argon Y. "Genetic and biochemical analysis of sperm-defective mutants of *C. elegans*." [Ph.D. thesis]. Harvard University; Massachusetts: 1980.
68. Argon Y, Ward S. *Caenorhabditis elegans* fertilization-defective mutants with abnormal sperm. Genetics. 1980;96:413–433. [[PMC free article: PMC1214308](#)] [[PubMed: 7196361](#)]
69. Armour J, Duncan M. Arrested larval development in cattle nematodes. Parasitol. Today. 1987;3:171–176. [[PubMed: 15462948](#)]
70. Aroian R V, Sternberg P. Multiple functions of *let-23* a *Caenorhabditiselegans* receptor tyrosine kinase gene required for vulval induction. Genetics. 1991;128:251–267. [[PMC free article: PMC1204464](#)] [[PubMed: 2071015](#)]
71. Aroian R V, Lesa G M, Sternberg P W. Mutations in the *Caenorhabditis elegans* *let-23* EGFR-like gene define elements important for cell-type specification and function. EMBO J. 1994;13:360–366. [[PMC free article: PMC394816](#)] [[PubMed: 8313880](#)]
72. Aroian R V, Koga M, Mendel J E, Ohshima Y, Sternberg P W. The *let-23* gene necessary for *Caenorhabditis elegans* vulval induction encodes a tyrosine kinase of the EGF receptor subfamily. Nature. 1990;348:693–699. [[PubMed: 1979659](#)]
73. Aroian R V, Ley A D, Koga M, Ohshima Y, Kramer J M, Sternberg P W. Splicing in *Caenorhabditis elegans* does not require an AG at the 3'splice site. Mol. Cell. Biol. 1993;13:626–637. [[PMC free article: PMC358941](#)] [[PubMed: 8417357](#)]
74. Arpagaus M, Richier P, Bergé J -B, Toutant J -P. Acetylcholinesterases of the nematode *Steinernema carpocapsae*. Characterisation of two types of amphiphilic forms differing in their mode of membrane association. Eur. J. Biochem. 1992a;207:1101–1108. [[PubMed: 1323459](#)]
75. Arpagaus M, Fedon Y, Cousin X, Chatonnet A, Bergé J -B, Fournier D, Toutant J P. cDNA sequence, gene structure, and in vitro expression of *ace-1*, the gene encoding acetylcholinesterase of class A in the nematode *Caenorhabditis elegans*. J. Biol. Chem. 1994;269:9957–9965. [[PubMed: 8144590](#)]
76. Arpagus M, Richier P, L'Hermite Y, Le Roy F, Bergé J -B, Thierry-Mieg D, Toutant J -P. Nematode acetylcholinesterases: Several genes and molecular forms of their products. In: Shafferman A, Velan B, editors. Multidisciplinary approaches to cholinesterase functions. New York: Plenum Press; 1992b. pp. 65–74.
77. Artavanis-Tsakonas S, Matsuno K, Fortini M E. Notch signaling. Science. 1995;286:225–232. [[PubMed: 7716513](#)]
78. Assad J A, Shephard G M, Corey D P. Tip-link integrity and mechanical transduction in vertebrate hair cells. Neuron. 1991;7:985–994. [[PubMed: 1764247](#)]
79. Atkin A L, Altamura N, Leeds P, Culbertson M R. The majority of yeast UPF1 co-localizes with polyribosomes in the cytoplasm. Mol. Biol. Cell. 1995;6:611–625. [[PMC free article: PMC301219](#)] [[PubMed: 7545033](#)]
80. Auge-Gouillou C, Bigot Y, Pollet N, Hamelin M, Meunier-Rotival M, Periquet G. Human and other mammalian genomes contain transposons of the *mariner* family. FEBS Lett. 1995;368:541–546. [[PubMed: 7635217](#)]
81. Aumann J, Robertson W M, Wyss U. Lectin binding to cuticle exudates of sedentary *Heterodera schachtii* (*Nematoda:Heteroderidae*) second stage juveniles. Rev. Nematol. 1991;14:113–118.
82. Ausiello D A, Stow J L, Cantiello H F, Bruno de Almeida J, Benos D. Purified epithelial Na<sup>+</sup> channel complex contains the pertussis toxin-sensitive Gα<sub>i-3</sub> protein. J. Biol. Chem. 1992;267:4759–4765. [[PubMed: 1311319](#)]

83. Austin C R. Observations on the penetration of the sperm into mammalian eggs. *Aust. J. Sci. Res.* 1951;4:581–596. [[PubMed: 14895481](#)]
84. Austin J, Kenyon C. Cell contact regulates neuroblast formation in the *Caenorhabditis elegans* lateral epidermis. *Development*. 1994a;120:313–324. [[PubMed: 8149911](#)]
85. Austin J, Kenyon C. Developmental timekeeping. Marking time with antisense. *Curr. Biol.* 1994b;4:366–369. [[PubMed: 7857401](#)]
86. Austin J, Kimble J. *glp-1* is required in the germ line for regulation of the decision between mitosis and meiosis in *Caenorhabditis elegans*. *Cell*. 1987;51:589–599. [[PubMed: 3677168](#)]
87. Austin J, Kimble J. Transcript analysis of *glp-1* and *lin-12* homologous genes required for cell interactions during development of *Caenorhabditis elegans*. *Cell*. 1989;58:565–571. [[PubMed: 2758467](#)]
88. Avery L. The genetics of feeding in *Caenorhabditis elegans*. *Genetics*. 1993a;133:897–917. [[PMC free article: PMC1205408](#)] [[PubMed: 8462849](#)]
89. Avery L. Motor neuron M3 controls [pharyngeal muscle](#) relaxation timing in *Caenorhabditis elegans*. *J. Exp. Biol.* 1993b;175:283–297. [[PubMed: 8440973](#)]
90. Avery L, Horvitz H R. A cell that dies during wild-type *C. elegans* development can function as a neuron in a *ced-3* mutant. *Cell*. 1987;51:1071–1078. [[PMC free article: PMC3773210](#)] [[PubMed: 3690660](#)]
91. Avery L, Horvitz H R. Pharyngeal pumping continues after laser killing of the pharyngeal [nervous system](#) of *C. elegans*. *Neuron*. 1989;3:473–485. [[PubMed: 2642006](#)]
92. Avery L, Horvitz H R. Effects of starvation and neuroactive drugs on feeding in *Caenorhabditis elegans*. *J. Exp. Zool.* 1990;253:263–270. [[PubMed: 2181052](#)]
93. Avery L, Wasserman S. Ordering gene function: The interpretation of epistasis in regulatory hierarchies. *Trends Genet.* 1992;8:312–316. [[PMC free article: PMC3955268](#)] [[PubMed: 1365397](#)]
94. Avery L, Bargmann C I, Horvitz H R. The *Caenorhabditis elegans unc-31* gene affects multiple [nervous system](#)-controlled function. *Genetics*. 1993;134:455–464. [[PMC free article: PMC1205489](#)] [[PubMed: 8325482](#)]
95. Avery L, Lockery S, Raizen D M. Electrophysiological methods in *C. elegans*. In: Epstein H F, Shakes D C, editors. *Caenorhabditis elegans: Modern biological analysis of an organism*. New York: Academic Press; 1995a. pp. 251–269.
96. Avery L, Raizen D, Lockery S. Electrophysiological methods. In: Epstein H F, Shakes D C, editors. *Caenorhabditis elegans: Modern biological analysis of an organism*. San Diego: Academic Press; 1995b. pp. 251–269.
97. Ayme-Southgate A, Vigoreaux J, Benian G M, Pardue M L. *Drosophila* has a twitchin/titin gene that appears to encode projectin. *Proc. Natl. Acad. Sci.* 1991;88:7973–7977. [[PMC free article: PMC52427](#)] [[PubMed: 1910171](#)]
98. Ayme-Southgate A, Southgate R, Saide J, Benian G, Pardue M. Both synchronous and asynchronous muscle isoforms of projectin (the *Drosophila* Bent locus product) contain functional kinase domains. *J. Cell Biol.* 1995;128:393–403. [[PMC free article: PMC2120353](#)] [[PubMed: 7844153](#)]
99. Ax P. The phylogenetic system: The systematization of organisms on the basis of their phylogenesis. England: Wiley, Chichester; 1987.
100. Azzaria M, Goszczynski B, Chung M A, Kalb J M, McGhee J D. A *fork head/HNF-3* homolog expressed in the pharynx and intestine of the *Caenorhabditis elegans* embryo.. *Dev. Biol.* 1996;178:289–303. [[PubMed: 8812130](#)]

## B

101. Babity J M, Starr T V B, Rose A M. Tc1 transposition and mutator activity in a Bristol strain of *Caenorhabditis elegans*. *Mol. Gen. Genet.* 1990;222:65–70. [[PubMed: 1978238](#)]
102. Babu P. Biochemical genetics of *Caenorhabditis elegans*. *Mol. Gen. Genet.* 1974;135:39–44.

103. Bailey C H, Chen M. Morphological basis of long-term habituation and sensitization in *Aplysia*. Science. 1983;220:91–93. [[PubMed: 6828885](#)]
104. Baird S E, Emmons S W. Properties of a class of genes required for ray morphogenesis in *Caenorhabditis elegans*. Genetics. 1990;126:335–344. [[PMC free article: PMC1204188](#)] [[PubMed: 2245913](#)]
105. Baird S E, Fitch D H A, Emmons S W. *Caenorhabditis vulgaris* sp.n. (Nematoda: Rhabditidae): A necromenic associate of pill bugs and snails. Nematologica. 1994;40:1–11.
106. Baird S E, Sutherlin M E, Emmons S W. Reproductive isolation in Rhabditidae (Nematoda: Secernentea);--> mechanisms that isolate six species of three genera. Evolution. 1992;46:585–594. [[PubMed: 28568672](#)]
107. Baird S E, Fitch D H, Kassem I A, Emmons S W. Pattern formation in the nematode epidermis: Determination of the arrangement of peripheral [sense organs](#) in the *C. elegans* [male tail](#). Development. 1991;113:515–526. [[PubMed: 1782863](#)]
108. Baker T A, Luo L. Identification of residues in the Mu transposase essential for catalysis. Proc. Natl. Acad. Sci. 1994;91:6654–6658. [[PMC free article: PMC44261](#)] [[PubMed: 7912831](#)]
109. Ballinger D G, Benzer S. Targeted gene mutations in *Drosophila*. Proc. Natl. Acad. Sci. 1989;86:9402–9406. [[PMC free article: PMC298504](#)] [[PubMed: 2556711](#)]
110. Barbazuk W B, Johnsen R C, Baillie D L. The generation and genetic analysis of suppressors of lethal mutations in the *Caenorhabditis elegans rol-3(V)* gene. Genetics. 1994;136:129–143. [[PMC free article: PMC1205765](#)] [[PubMed: 8138151](#)]
111. Bargmann C I. Genetic and cellular analysis of behavior in *C. elegans*. Annu. Rev. Neurosci. 1993;16:47–71. [[PubMed: 8460900](#)]
112. Bargmann C I, Horvitz H R. Chemosensory neurons with overlapping functions direct chemotaxis to multiple chemicals in *C. elegans*. Neuron. 1991a;7:729–742. [[PubMed: 1660283](#)]
113. Bargmann C I, Horvitz H R. Control of larval development by chemosensory neurons in *Caenorhabditis elegans*. Science. 1991b;251:1243–1246. [[PubMed: 2006412](#)]
114. Bargmann C I, Hartwig E, Horvitz H R. Odorant-selective genes and neurons mediate olfaction in *C. elegans*. Cell. 1993;74:515–527. [[PubMed: 8348618](#)]
115. Bargmann C I, Thomas J H, Horvitz H R. Chemosensory cell function in the behavior and development of *Caenorhabditis elegans*. Cold Spring Harbor Symp. Quant. Biol. 1990;55:529–538. [[PubMed: 2132836](#)]
116. Barker D M. Evolution of sperm shortage in a selfing hermaphrodite. Evolution. 1992;46:1951–1955. [[PubMed: 28567744](#)]
117. Barker D M. Copulatory plugs and paternity assurance in the nematode *Caenorhabditis elegans*. Anim. Behav. 1994;48:147–156.
118. Barnes E D. Invertebrate zoology 5th ed. Philadelphia: Saunders College Publishing; 1987.
119. Barnes T M. "Molecular analysis of the tra-3 region of the *Caenorhabditis elegans* genome." [Ph.D. thesis]. Cambridge University; England: 1991.
120. Barnes T M. OPUS: A growing family of gap junction proteins? Trends Genet. 1994;10:303–305. [[PubMed: 7974741](#)]
121. Barnes T M, Hodgkin J. The *tra-3* sex-determination gene of *Caenorhabditis elegans* encodes a member of the calpain regulatory protease family. EMBO J. 1996;15:4477–4484. [[PMC free article: PMC452177](#)] [[PubMed: 8887539](#)]
122. Barnes T M, Kohara Y, Coulson A, Hekimi S. Meiotic recombination, noncoding DNA and genomic organization in *Caenorhabditis elegans*. Genetics. 1995;141:159–179. [[PMC free article: PMC1206715](#)] [[PubMed: 8536965](#)]
123. Barnes T M, Jin Y, Horvitz H R, Ruvkun G, Hekimi S. The *Caenorhabditis elegans* behavioral gene *unc-24* specifies a novel bipartite protein similar to both erythrocyte band 7.2 (stomatin) and nonspecific lipid transfer protein. J. Neurochem. 1996;67:46–57. [[PubMed: 8667025](#)]
124. Barrios L, Vonkhorpon P, Honda S, Albertson D G, Hecht R M, Huang X -Y. Genomic organization of the glyceraldehyde-3-phosphate dehydrogenase gene family of *Caenorhabditis elegans*. J. Mol. Biol.

- 1989;206:411–424. [[PubMed: 2716055](#)]
125. Barron G L. The nematode-destroying fungi. Guelph: Canadian Biological Publications; 1977.
126. Barstead R J, Waterston R H. The basal component of the nematode dense-body is vinculin. *J. Biol. Chem.* 1989;264:10177–10185. [[PubMed: 2498337](#)]
127. Barstead R J, Waterston R H. Vinculin is essential for muscle function in the nematode. *J. Cell Biol.* 1991a;114:715–724. [[PMC free article: PMC2289884](#)] [[PubMed: 1907975](#)]
128. Barstead R J, Waterston R H. Cloning sequencing and mapping of an alpha-actinin gene from the nematode *Caenorhabditis elegans*. *Cell Motil. Cytoskel.* 1991b;20:69–78. [[PubMed: 1756579](#)]
129. Bartnik E, Osborn M, Weber K. Intermediate filaments in muscle and epithelial cells of nematodes. *J. Cell Biol.* 1986;102:2033–2041. [[PMC free article: PMC2114260](#)] [[PubMed: 3519620](#)]
130. Barton M K, Kimble J. *fog-1* a regulatory gene required for specification of spermatogenesis in the germ line of *Caenorhabditis elegans*. *Genetics*. 1990;125:29–39. [[PMC free article: PMC1204007](#)] [[PubMed: 2341035](#)]
131. Barton M K, Schedl T, Kimble J. Gain-of-function mutations of *fem-3*, a sex-determination gene in *Caenorhabditis elegans*. *Genetics*. 1987;115:107–119. [[PMC free article: PMC1203045](#)] [[PubMed: 3557107](#)]
132. Barton N, Turelli M A. Evolutionary quantitative genetics: How little do we know? *Annu. Rev. Genet.* 1989;23:337–370. [[PubMed: 2694935](#)]
133. Basler K, Struhl G. Compartment boundaries and the control of *Drosophila* limb pattern by hedgehog protein. *Nature*. 1994;368:208–214. [[PubMed: 8145818](#)]
134. Basson M, Horvitz H R. The *Caenorhabditis elegans* gene *sem-4* controls neuronal and mesodermal cell development and encodes a zinc-finger protein. *Genes Dev.* 1996;10:1953–1965. [[PubMed: 8756352](#)]
135. Bate C M, Grunewald E B. Embryogenesis of an insect [nervous system](#) II: A second class of neuron precursor cells and the origin of the intersegmental connectives. *J. Embryol. Exp. Morphol.* 1981;61:317–330. [[PubMed: 7264548](#)]
136. Bates S, Vousden K H. p53 in signaling checkpoint arrest or apoptosis. *Curr. Opin. Genet. Dev.* 1996;6:12–18. [[PubMed: 8791489](#)]
137. Bateson W. Materials for the study of variation treated with especial regard to discontinuity in the origin of species. London: Macmillan; 1894.
138. Baumeister R, Liu Y, Ruvkun G. Lineage-specific regulators couple cell lineage asymmetry to the transcription of the *Caenorhabditis elegans* POU gene *unc-86* during neurogenesis. *Genes Dev.* 1996;10:1395–1410. [[PubMed: 8647436](#)]
139. Beall C J, Sepanski M A, Fyrberg E A. Genetic dissection of *Drosophila* myofibril formation: Effects of actin and myosin heavy chain null mutations. *Genes Dev.* 1989;3:131–140. [[PubMed: 2714648](#)]
140. Beanan M, Strome S. Characterization of a germ-line proliferation mutation in *Caenorhabditis elegans*. *Development*. 1992;116:755–766. [[PubMed: 1289064](#)]
141. Beck C D O, Rankin C H. Heat-shock disrupts long-term memory consolidation in *Caenorhabditis elegans*. *Learn. Memory*. 1995;2:161–167. [[PubMed: 10467573](#)]
142. Beck K, Hunter I, Engel J. Structure and function of laminin: Anatomy of a multidomain glycoprotein. *FASEB J.* 1990;4:148–160. [[PubMed: 2404817](#)]
143. Beh C T, Ferrari D C, Chung M A, McGhee J D. An acid phosphatase as a biochemical marker for intestinal development in the nematode *Caenorhabditis elegans*. *Dev. Biol.* 1991;147:133–143. [[PubMed: 1652526](#)]
144. Beitel G J, Clark S G, Horvitz H R. *Caenorhabditis elegans* gene *let-60* acts as a switch in the pathway of vulval induction. *Nature*. 1990;348:503–509. [[PubMed: 2123303](#)]
145. Beitel G J, Tuck S, Greenwald I, Horvitz H R. The *Caenorhabditis elegans* gene *lin-1* encodes an ETS-domain protein and defines a branch in the vulval induction pathway. *Genes Dev.* 1995;9:3149–3162. [[PubMed: 8543158](#)]
146. Bejanin S, Cervini R, Mallet J, Berrard S. A unique gene organization for two cholinergic markers, choline acetyltransferase and a putative vesicular transporter of acetylcholine. *J. Biol. Chem.*

- 1994;269:21944–21947. [PubMed: 8071313]
147. Bejsovec A, Anderson P. Myosin heavy-chain mutations that disrupt *Caenorhabditis elegans* thick filament assembly. *Genes Dev.* 1988;2:1307–1317. [PubMed: 3203908]
148. Bejsovec A, Anderson P. Functions of the myosin ATP and actin binding sites are required for *C. elegans* thick filament assembly. *Cell.* 1990;60:133–140. [PubMed: 2136805]
149. Bektesh S, Hirsh D. *C. elegans* mRNAs acquire a spliced leader through a *trans*-splicing mechanism. *Nucleic Acids Res.* 1988;16:5692. [PMC free article: PMC336799] [PubMed: 3387244]
150. Bektesh S, Doren K V, Hirsh D. Presence of the *Caenorhabditis elegans* spliced leader on different mRNAs and in different genera of nematodes. *Genes Dev.* 1988;2:1277–1283. [PubMed: 3203906]
151. Belardetti F, Campbell W B, Falck J R, Demontis G, Roslowsky M. Products of heme-catalyzed transformation of the arachidonate derivative 12-HPETE open S-type K<sup>+</sup> channels in *Aplysia*. *Neuron.* 1989;3:497–505. [PubMed: 2642008]
152. Belgrader P, Cheng J, Maquat L E. Evidence to implicate translation by ribosomes in the mechanism by which nonsense codons reduce the nuclear level of human triosephosphate isomerase mRNA. *Proc. Natl. Acad. Sci.* 1993;90:482–486. [PMC free article: PMC45687] [PubMed: 8421679]
153. Bellen H J, O'Kane C J, Wilson C, Grossniklaus U, Pearson R K, Gehring W J. P-element-mediated enhancer detection: A versatile method to study development in *Drosophila*. *Genes Dev.* 1989;34:1288–1300. [PubMed: 2558050]
154. Belote J M, Lucchesi J C. Control of X chromosome transcription by the maleless gene in *Drosophila*. *Nature.* 1980a;285:573–575. [PubMed: 7402300]
155. Belote J M, Lucchesi J C. Male-specific lethal mutations of *Drosophila melanogaster*. *Genetics.* 1980b;96:165–186. [PMC free article: PMC1214287] [PubMed: 6781985]
156. Benian G M, L'Hernault S W, Morris M E. Additional sequence complexity in the muscle gene, *unc-22*, and its encoded protein, twitchin, of *Caenorhabditis elegans*. *Genetics.* 1993;134:1097–1104. [PMC free article: PMC1205578] [PubMed: 8397135]
157. Benian G M, Tilney T L, Tang X, Borodovsky M. The *Caenorhabditis elegans* gene *unc-89*, required for muscle M-line assembly, encodes a giant modular protein composed of Ig and signal transduction domains. *J. Cell Biol.* 1996;132:835–848. [PMC free article: PMC2120741] [PubMed: 8603916]
158. Benian G M, Kiff J E, Neckelmann N, Moerman D G, Waterston R H. Sequence of an unusually large protein implicated in regulation of myosin activity in *C. elegans*. *Nature.* 1989;342:45–50. [PubMed: 2812002]
159. Bennett J L, Williams J F, Dave V. Pharmacology of ivermectin. *Parasitol. Today.* 1988;4:226–228. [PubMed: 15463103]
160. Bennett K L, Ward S. Neither germline-specific nor several somatically expressed genes are lost or rearranged during embryonic chromatin diminution in the nematode *Ascaris lumbricoides* var. *suum*. *Dev. Biol.* 1986;118:141–147. [PubMed: 3770294]
161. Bennett M K, Scheller R H. A molecular description of synaptic vesicle membrane trafficking. *Annu. Rev. Biochem.* 1994;63:63–100. [PubMed: 7979250]
162. Benos D J, Saccomani G, Sariban-Sohraby S. The epithelial sodium channel: Subunit number and location of the amiloride binding site. *J. Biol. Chem.* 1987;262:10613–10618. [PubMed: 2440868]
163. Berg H. Random walks in biology. Princeton, New Jersey: Princeton University Press; 1993.
164. Berg H C, Brown D A. Chemotaxis in *E. coli* analysed by three-dimensional tracking. *Nature.* 1972;239:500–504. [PubMed: 4563019]
165. Bernheimer H, Birkmayer W, Hornykiewicz O, Jellinger K, Seitelberg F. Brain dopamine and the syndromes of Parkinson and Huntington: Clinical, morphological, and neurochemical correlations. *J. Neurol. Sci.* 1973;20:415–455. [PubMed: 4272516]
166. Besson J -M, Chaouch A. Peripheral and spinal mechanisms of nociception. *Physiol. Rev.* 1987;67:67–186. [PubMed: 3543978]
167. Betschart B, Wyss K. Analysis of the cuticular collagens of *Ascaris suum*. *Acta Trop.* 1990;47:297–305. [PubMed: 1978530]

168. Bhanot P, Brink M, Samos C H, Hsieh J C, Wang Y, Macke J P, Andrew D, Nathans J, Nusse R. A new member of the *frizzled* family of *Drosophila* functions as a Wingless receptor. *Nature*. 1996;382:225–230. [[PubMed: 8717036](#)]
169. Bhat K, Poole S, Schedl P. The mitimere and pdm1 genes collaborate during specification of the RP2/sib lineage in *Drosophila* neurogenesis. *Mol. Cell. Biol.* 1995;15:4052–4063. [[PMC free article: PMC230644](#)] [[PubMed: 7623801](#)]
170. Bhat S G, Babu P. Mutagen sensitivity of kynureninase mutants of the nematode *Caenorhabditis elegans*. *Mol. Gen. Genet.* 1980;180:635–638. [[PubMed: 6936603](#)]
171. Bier E, Vaessin H, Shepherd S, Lee K, McCall K, Barbel S, Ackerman L, Carretto R, Uemura T, Grell E, Jan L Y, Jan Y N. Searching for pattern and mutation in the *Drosophila* genome with a P-lacZ vector. *Genes Dev.* 1989;3:1273–1287. [[PubMed: 2558049](#)]
172. Biessmann H, Mason J M. Genetics and molecular biology of telomeres. *Adv. Genet.* 1992;30:185–249. [[PubMed: 1456111](#)]
173. Bigot Y, Hamelin M, Capy P, Periquet G. Mariner-like elements in hymenopteran species: Insertion site and distribution. *Proc. Natl. Acad. Sci.* 1994;91:3408–3412. [[PMC free article: PMC43586](#)] [[PubMed: 8159761](#)]
174. Bird A F, Bird J. The structure of nematodes 2nd edition. San Diego: Academic Press; 1991.
175. Bird D M. Sequence comparison of the *Caenorhabditis elegans* *dpy-13* and *col-34* genes, and their deduced collagen products. *Gene*. 1992;120:261–266. [[PubMed: 1398138](#)]
176. Bird D M, Riddle D L. Molecular cloning and sequencing of *ama-1* the gene encoding the largest subunit of *Caenorhabditis elegans* RNA polymerase II. *Mol. Cell. Biol.* 1989;9:4119–4130. [[PMC free article: PMC362490](#)] [[PubMed: 2586513](#)]
177. Bird D M, Riddle D L. A genetic nomenclature for parasitic nematodes. *J. Nematol.* 1994;26:138–143. [[PMC free article: PMC2619496](#)] [[PubMed: 19279876](#)]
178. Bird D M, Wilson M A. DNA sequence and expression analysis of root-knot nematode elicited giant cell transcripts. *Mol. Plant-Microbe Interact.* 1994a;7:419–424. [[PubMed: 8012051](#)]
179. Bird D M, Wilson M A. Plant molecular and cellular responses to nematode infection. In: Lamberti F, et al., editors. NATO ARW:Advances in molecular plant nematology. New York: Plenum Press; 1994b. pp. 181–195.
180. Blackburn C C, Selkirk M E. Characterisation of the secretory acetylcholinesterases from adult *Nippostrongylus brasiliensis*. *Mol. Biochem. Parasitol.* 1992;53:79–88. [[PubMed: 1501647](#)]
181. Blackwell T K, Bowerman B, Priess J R, Weintraub H. Formation of a monomeric DNA binding domain by Skn-1 bZIP and homeodomain elements. *Science*. 1994;266:621–628. [[PubMed: 7939715](#)]
182. Blair S S, Brower D L, Thomas J B, Zavortink M. The role of apterous in the control of dorsoventral compartmentalization and PS integrin gene expression in the developing wing of *Drosophila*. *Development*. 1994;120:1805–1815. [[PubMed: 7924988](#)]
183. Blaxter M L. The cuticle surface proteins of wild type and mutant *Caenorhabditis elegans*. *J. Biol. Chem.* 1993a;268:6600–6609. [[PubMed: 8503957](#)]
184. Blaxter M L. Nemoglobins: Divergent nematode globins. *Parasitol. Today*. 1993b;9:353–360. [[PubMed: 15463668](#)]
185. Blaxter M L, Ingram L, Tweedie S. Sequence, expression and evolution of the globins of the nematode *Nippostrongylus brasiliensis*. *Mol. Biochem. Parasitol.* 1994a;68:1–14. [[PubMed: 7891734](#)]
186. Blaxter M L, Page A P, Rudin W, Maizels R M. Nematode surface coat: Actively evading immunity. *Parasitol. Today*. 1992;8:243–247. [[PubMed: 15463630](#)]
187. Blaxter M L, Vanfleteren J, Xia J, Moens L. Structural characterisation of an *Ascaris* myoglobin. *J. Biol. Chem.* 1994b;269:30181–30186. [[PubMed: 7982924](#)]
188. Bliss T V, Collingridge G L. A synaptic model of memory: Long-term potentiation in the hippocampus. *Nature*. 1993;361:31–39. [[PubMed: 8421494](#)]
189. Bloch R J. Loss of acetylcholine receptor clusters induced by treatment of cultured rat myotubes with carbachol. *J. Neurosci.* 1986;6:691–700. [[PMC free article: PMC6568452](#)] [[PubMed: 3958790](#)]

190. Bloom K. The centromere frontier: Kinetochore components microtubule-based motility, and the CEN-value paradox. *Cell*. 1993;73:621–624. [[PubMed: 8500159](#)]
191. Blum J, Fridovich I. Superoxide hydrogen peroxide and oxygen toxicity in two free-living nematode species. *Arch. Biochem. Biophys.* 1983;222:35–43. [[PubMed: 6687666](#)]
192. Blumenthal T. Trans-splicing and polycistronic transcription in *Caenorhabditis elegans*. *Trends Genet.* 1995;11:132–136. [[PubMed: 7732590](#)]
193. Blumenthal T, Speith J, Boothroyd J C, Komuniecki R, editors. Molecular approaches to parasitology. New York: Wiley-Liss; 1995. *Trans-splicing specificity and polycistronic units in Caenorhabditis elegans*. pp. 281–298.
194. Blumenthal T, Thomas J. *Cis* and *trans* mRNA splicing in *C. elegans*. *Trends Genet.* 1988;4:305–308. [[PubMed: 3070853](#)]
195. Blumenthal T, Squire M, Kirtland S, Cane J, Donegan M, Spieth J, Sharrock W. Cloning of a yolk protein gene family from *Caenorhabditis elegans*. *J. Mol. Biol.* 1984;174:1–18. [[PubMed: 6546952](#)]
196. Bokhari C J, Godward M B E. The ultrastructure of the diffuse kinetochore in *Luzula nivea*. *Chromosoma*. 1980;79:125–136.
197. Bolanowski M A, Jacobson L A, Russell R L. Quantitative measures of aging in the nematode *Caenorhabditis elegans*. II. Lysosomal hydrolases as markers of senescence. *Mech. Ageing Dev.* 1983;21:295–319. [[PubMed: 6412000](#)]
198. Bolanowski M A, Russell R L, Jacobson L A. Quantitative measures of aging in the nematode *Caenorhabditis elegans*. I. Population and longitudinal studies of two behavioral parameters. *Mech. Ageing Dev.* 1981;15:279–295. [[PubMed: 7253717](#)]
199. Bolten S, Powell-Abel P, Fischhoff D, Waterston R. The *sup-7(st5)* X gene of *C. elegans* encodes a transfer RNA<sup>Trp</sup><sub>UAG</sub> amber suppressor. *Proc. Natl. Acad. Sci.* 1984;81:6784–6788. [[PMC free article: PMC392016](#)] [[PubMed: 6093119](#)]
200. Bon S, Lamouroux A, Vigny A, Massoulié J, Mallet J, Henry J P. Amphiphilic and nonamphiphilic forms of bovine and human dopamine β-hydroxylase. *J. Neurochem.* 1991;57:1100–1111. [[PubMed: 1654385](#)]
201. Bonen L. Trans-splicing of pre-mRNA in plants animals, and protists. *FASEB J.* 1993;7:40–46. [[PubMed: 8422973](#)]
202. Bork P, Bairoch A. Extracellular protein modules. A proposed nomenclature. poster C02. *Trends Biol. Sci.* 1995;20
203. Boulianne G L, Trimble W S. Identification of a second homolog of *N*-ethylmaleimide-sensitive fusion protein that is expressed in the [nervous system](#) and secretory tissues of *Drosophila*. *Proc. Natl. Acad. Sci.* 1995;92:7095–7099. [[PMC free article: PMC41478](#)] [[PubMed: 7624376](#)]
204. Bour B A, O'Brien M A, Lockwood W L, Goldstein E S, Bodmer R, Taghert P H, Abmayr S M, Nguyen H T. *Drosophila MEF2*, a transcription factor that is essential for myogenesis. *Genes Dev.* 1995;9:730–741. [[PubMed: 7729689](#)]
205. Bourchuladze R, Frenguelli B, Blendy J, Cioffi D, Schutz G, Silva A J. Deficient long-term memory in mice with a targeted mutation of the cAMP-responsive element-binding protein. *Cell*. 1994;79:59–68. [[PubMed: 7923378](#)]
206. Boveri T. Zellen Studien. *J. na. Z. Naturwiss.* 1888;22:685.
207. Boveri T. Ueber die teilung centrifugierte eier von *Ascaris megalocephala*. *Wilhelm Roux Arch. Entwicklungsmech. Org.* 1910;30:101–125.
208. Bowerman B, Eaton B A, Priess J R. *skn-1*, a maternally expressed gene required to specify the fate of ventral blastomeres in the early *C. elegans* embryo. *Cell*. 1992a;68:1061–1075. [[PubMed: 1547503](#)]
209. Bowerman B, Draper B W, Mello C C, Priess J R. The maternal gene *skn-1* encodes a protein that is distributed unequally in early *C. elegans* embryos. *Cell*. 1993;74:443–452. [[PubMed: 8348611](#)]
210. Bowerman B, Tax F E, Thomas J H, Priess J R. Cell interactions involved in development of the bilaterally symmetrical intestinal valve cells during embryogenesis in *Caenorhabditis elegans*. *Development*. 1992b;116:1113–1122. [[PubMed: 1295733](#)]

211. Brandl R, Mann W, Sprinzl M. Mitochondrial tRNA and the phylogenetic position of Nematoda. *Biochem. Syst. Ecol.* 1992;20:325–330.
212. Braselton J P. The ultrastructure of the non-localized kinetochores of *Luzula* and *Cyperus*. *Chromosoma.* 1971;36:89–99.
213. Braselton J P. The ultrastructure of the meiotic kinetochores of *Luzula*. *Chromosoma.* 1981;82:143–151.
214. Bray D. Cell movements. New York: Garland Publishers; 1992.
215. Brenner S. The genetics of behavior. *Br. Med. Bull.* 1973;29:269–271. [[PubMed: 4807330](#)]
216. Brenner S. The genetics of *Caenorhabditis elegans*. *Genetics.* 1974;77:71–94. [[PMC free article: PMC1213120](#)] [[PubMed: 4366476](#)]
217. Brenner S. Wood W B, editor. The nematode *Caenorhabditis elegans*. Cold Spring Harbor, New York: Cold Spring Harbor Laboratory; 1988. Foreword.
218. Brezinsky L, Wang G V L, Humphreys T, Hunt J. The transposable element Uhu from Hawaiian *Drosophila*—Member of the widely dispersed class of Tc1-like transposons. *Nucleic Acids Res.* 1990;18:2053–2059. [[PMC free article: PMC330682](#)] [[PubMed: 2159635](#)]
219. Brierly H L, Potter S S. Distinct characteristics of loop sequences of two *Drosophila* foldback transposable elements. *Nucleic Acids Res.* 1985;13:485–500. [[PMC free article: PMC341010](#)] [[PubMed: 2987798](#)]
220. Britten R J. Active gypsy/Ty3 retrotransposons or retroviruses in *Caenorhabditis elegans*. *Proc. Natl. Acad. Sci.* 1995;92:599–601. [[PMC free article: PMC42789](#)] [[PubMed: 7530364](#)]
221. Broeks A, Janssen H W R M, Calafat J, Plasterk R H A. A P-glycoprotein protects *Caenorhabditis elegans* against natural toxins. *EMBO J.* 1995;14:1858–1866. [[PMC free article: PMC398285](#)] [[PubMed: 7743993](#)]
222. Brose N, Hofmann K, Hata Y, Südhof T C. Mammalian homologues of *Caenorhabditis elegansunc-13* gene define novel family of C<sub>2</sub>-domain proteins. *J. Biol. Chem.* 1995;270:25273–25280. [[PubMed: 7559667](#)]
223. Brose N, Petrenko A G, Südhof T C, Jahn R. Synaptotagmin: A calcium sensor on the synaptic vesicle surface. *Science.* 1992;256:1021–1025. [[PubMed: 1589771](#)]
224. Broverman S A, Meneely P M. Meiotic mutants that cause a polar decrease in recombination on the X chromosome of *Caenorhabditis elegans*. *Genetics.* 1994;136:119–127. [[PMC free article: PMC1205764](#)] [[PubMed: 8138150](#)]
225. Brown S J, Riddle D L. Gene interactions affecting muscle organization in *C. elegans*. *Genetics.* 1985;110:421–440. [[PMC free article: PMC1202572](#)] [[PubMed: 4018568](#)]
226. Brown W, Tyler-Smith C. Centromere activation. *Trends Genet.* 1995;11:337–339. [[PubMed: 7482782](#)]
227. Browning H, Strome S. A sperm-supplied factor required for embryogenesis in *C. elegans*. *Development.* 1996;122:391–404. [[PubMed: 8565851](#)]
228. Brundage L, Avery L, Katz A, Kim U -J, Mendel J E, Sternberg P W, Simon M I. Mutations in a *C. elegans* Gqa gene disrupt movement, egg-laying and viability. *Neuron.* 1996;16:999–1009. [[PMC free article: PMC4444781](#)] [[PubMed: 8630258](#)]
229. Brunk C F, Sadler L A. Characterization of the promoter region of *Tetrahymena* genes. *Nucleic Acids Res.* 1990;18:323–329. [[PMC free article: PMC330270](#)] [[PubMed: 2129549](#)]
230. Brusca R C, Brusca G J. Invertebrates. Sunderland, Massachusetts: Sinauer Associates; 1990.
231. Bruzik J P, Doren K V, Hirsh D, Steitz J A. *Trans* splicing involves a novel form of small nuclear ribonucleoprotein particles. *Nature.* 1988;335:559–562. [[PubMed: 2971142](#)]
232. Bryan G J, Jacobson J W, Hartl D L. Heritable somatic excision of a *Drosophila* transposon. *Science.* 1987;235:1636–1638. [[PubMed: 3029874](#)]
233. Bucher E A, Greenwald I. A genetic mosaic screen of essential zygotic genes in *Caenorhabditis elegans*. *Genetics.* 1991;128:281–292. [[PMC free article: PMC1204466](#)] [[PubMed: 2071016](#)]
234. Buck L, Axel R. A novel multigene family may encode odorant receptors: A molecular basis for odor recognition. *Cell.* 1991;65:175–187. [[PubMed: 1840504](#)]

235. Bump N J, Hackett M, Huginin M, Seshagiri S, Brady K, Chen P, Ferenz C, Franklin S, Ghayur T, Li P, Licari P, Mankovich J, Shi L, Greenberg A H, Miller L K, Wong W W. Inhibition of ICE family proteases by baculovirus antiapoptotic protein p35. *Science*. 1995;269:1885–1888. [PubMed: 7569933]
236. Burden-Gulley S M, Payne H R, Lemmon V. Growth cones are actively influenced by substrate-bound adhesion molecules. *J. Neurosci.* 1995;15:4370–4381. [PMC free article: PMC657725] [PubMed: 7790914]
237. Burghardt R C, Foor W E. Membrane fusion during spermiogenesis in *Ascaris*. *J. Ultrastruct. Res.* 1978;62:190–202. [PubMed: 650734]
238. Bürglin T R. A *C. elegans* prospero homologue defines a novel domain. *Trends Biochem. Sci.* 1994;19:70–71. [PubMed: 7909177]
239. Bürglin T R, Arai R, et al., editors. *Biodiversity and evolution*. Tokyo: The National Science Museum Foundation; 1995. *The evolution of homeobox genes*. pp. 291–336.
240. Bürglin T R, Ruvkun G. New motif in PBX genes (letter). *Nat. Genet.* 1992;1:319–320. [PubMed: 1363814]
241. Bürglin T R, Ruvkun G. The *Caenorhabditis elegans* homeobox gene cluster. *Curr. Opin. Genet. Dev.* 1993;3:615–620. [PubMed: 7902148]
242. Bürglin T R, Finney M, Coulson A, Ruvkun G. *Caenorhabditis elegans* has scores of homeobox-containing genes. *Nature*. 1989;341:239–243. [PubMed: 2571091]
243. Bürglin T R, Ruvkun G, Coulson A, Hawkins N C, McGhee J D, Schaller D, Wittmann C, Muller F, Waterston R H. Nematode homeobox cluster. *Nature*. 1991;351:703. [PubMed: 1676487]
244. Burke D J, Ward S. Identification of a large multigene family encoding the major sperm protein of *Caenorhabditis elegans*. *J. Mol. Biol.* 1983;171:1–29. [PubMed: 6315956]
245. Burns M E, Augustine G J. Synaptic structure and function: Dynamic organization yields architectural precision. *Cell*. 1995;83:187–194. [PubMed: 7585936]
246. Burr A H. The photomovement of *Caenorhabditis elegans* a nematode which lacks ocelli: Proof that the response is to light, not radiant heating. *Photochem. Photobiol.* 1985;41:577–582. [PubMed: 4011710]
247. Burri M, Tromvoukis Y, Bopp D, Frigerio G, Noll M. Conservation of the paired domain in metazoans and its structure in three isolated human genes. *EMBO J.* 1989;8:1183–1190. [PMC free article: PMC400932] [PubMed: 2501086]
248. Burridge K, Fath K, Kelly T, Nuckolls G, Turner C. Focal adhesions: Transmembrane junctions between extracellular matrix and the cytoskeleton. *Annu. Rev. Cell Biol.* 1988;4:487–525. [PubMed: 3058164]
249. Bushman F D. Dodging the genes. *Curr. Biol.* 1993;3:533–535. [PubMed: 15335696]
250. Bussey H, Kaback D B, Zhong W W, Vo D T, Clark M W, Fortin N, Hall J, Ouellette B F F, Keng T, Barton A B, Su Y, Davies C J, Storms R K. The nucleotide sequence of chromosome I from *Saccharomyces cerevisiae*. *Proc. Natl. Acad. Sci.* 1995;92:3809–3813. [PMC free article: PMC42051] [PubMed: 7731988]
251. Butler M H, Wall S M, Luehrsen K R, Fox G E, Hecht R M. Molecular relationships between closely related strains and species of nematodes. *J. Mol. Evol.* 1981;18:18–23. [PubMed: 7334524]
252. Byerly L, Masuda M O. Voltage-clamp analysis of the potassium current that produces a negative-going action potential in *Ascaris* muscle. *J. Physiol.* 1979;288:263–284. [PMC free article: PMC1281425] [PubMed: 469718]
253. Byerly L, Cassada R C, Russell R L. The life cycle of the nematode *Caenorhabditis elegans*. I. Wild type growth and reproduction. *Dev. Biol.* 1976;51:23–33. [PubMed: 988845]
254. Byrne J H. Cellular analysis of associative learning. *Physiol. Rev.* 1987;67:329–439. [PubMed: 3550838]

## C

255. Cabrera C V. The generation of cell diversity during early neurogenesis in *Drosophila*. *Development*. 1992;115:893–901. [PubMed: 1451665]
256. Cabrera C V, Alonso M C. Transcriptional activation by heterodimers of the *achaete-scute* and *daughterless* gene products of *Drosophila*. *EMBO J.* 1991;10:2965–2973. [PMC free article: ]

[PMC453011](#)] [[PubMed: 1915272](#)]

257. Cadepond F, Schweizer-Groyer G, Segard-Maurel I, Jibard N, Hollenberg S M, Giguere V, Evans R M, Baulieu E E. Heat shock protein 90 as a critical factor in maintaining glucocorticosteroid receptor in a nonfunctional state. *J. Biol. Chem.* 1991;266:5834–5841. [[PubMed: 2005120](#)]
258. Caizzi R, Caggese C, Pimpinelli S. Bari-1, a new transposon-like family in *Drosophila melanogaster* with a unique heterochromatic organization. *Genetics*. 1993;133:335–345. [[PMC free article: PMC1205323](#)] [[PubMed: 8382176](#)]
259. Calne D B, Zigmond M J. Compensatory mechanisms in degenerative neurologic diseases. Insights from Parkinsonism. *Arch. Neurol.* 1991;48:361–363. [[PubMed: 2012508](#)]
260. Campuzano S, Modolell J. Patterning of the *Drosophila nervous system*: The *achaete/scute* gene complex. *Trends Genet.* 1992;8:202–208. [[PubMed: 1496555](#)]
261. Canessa C M, Horsberger J D, Rossier B C. Functional cloning of the epithelial sodium channel: Relation with genes involved in neurodegeneration. *Nature*. 1993;361:467–470. [[PubMed: 8381523](#)]
262. Canessa C M, Merillat A M, Rossier B C. Membrane topology of the epithelial sodium channel in intact cells. *Am. J. Physiol.* 1994a;267:C1682–1690. [[PubMed: 7810611](#)]
263. Canessa C M, Schild L, Buell G, Thorens B, Gautschi I, Horisberger J -D, Rossier B C. Amiloride-sensitive epithelial Na<sup>+</sup> channel is made of three homologous subunits. *Nature*. 1994b;367:463–467. [[PubMed: 8107805](#)]
264. Cangiano G, La Volpe A. Repetitive DNA sequences located in the terminal portion of the *Caenorhabditis elegans* chromosomes. *Nucleic Acids Res.* 1993;21:1133–1139. [[PMC free article: PMC309273](#)] [[PubMed: 8096635](#)]
265. Capowski E E, Martin P, Garvin C, Strome S. Identification of grandchildless loci whose products are required for normal germ-line development in the nematode *Caenorhabditis elegans*. *Genetics*. 1991;129:1061–1072. [[PMC free article: PMC1204771](#)] [[PubMed: 1783292](#)]
266. Capy P, Anxolabehere D, Langin T. The strange phylogenies of transposable elements: are horizontal transfers the only explanation? *Trends Genet.* 1994;10:7–12. [[PubMed: 8146915](#)]
267. Capy P, Koga A, David J R, Hartl D L. Sequence analysis of active *mariner* elements in natural populations of *Drosophila simulans*. *Genetics*. 1992;130:499–506. [[PMC free article: PMC1204867](#)] [[PubMed: 1312979](#)]
268. Carew T J, Kandel E R. Acquisition and retention of long-term habituation in *Aplysia*: Correlation of behavioral and cellular processes. *Science*. 1973;182:1158–1160. [[PubMed: 4750613](#)]
269. Carroll P T. Membrane-bound choline-O-acetyltransferase in rat hippocampal tissue is associated with synaptic vesicles. *Brain Res.* 1994;633:112–118. [[PubMed: 8137149](#)]
270. Carroll S B, Scott M P. Zygotically active genes that affect the spatial expression of the *fushi tarazu* segmentation gene during early *Drosophila* embryogenesis. *Cell*. 1986;45:113–126. [[PubMed: 3082519](#)]
271. Carter P W, Roos J M, Kemphues K J. Molecular analysis of *zyg-11*, a maternal-effect gene required for early embryogenesis of *Caenorhabditis elegans*. *Mol. Gen. Genet.* 1990;221:72–80. [[PubMed: 2325632](#)]
272. Cash S, Poo M. Presynaptic differentiation and retrograde signalling during the early phase of synaptogenesis. *Sem. Dev. Biol.* 1995;66:185–193.
273. Cassada R C, McMahon D M, Fox C F, editors. *Developmental biology: Pattern formation and gene regulation*. New York: W.A. Benjamin; 1975. The dauer larva of *C. elegans*: A specific developmental arrest inducible environmentally and genetically. pp. 539–547.
274. Cassada R C, Russell R L. The dauer larva, a post-embryonic developmental variant of the nematode *Caenorhabditis elegans*. *Dev. Biol.* 1975;46:326–342. [[PubMed: 1183723](#)]
275. Cassada R, Isnenghi E, Culotti M, von Ehrenstein G. Genetic analysis of temperature-sensitive embryogenesis mutants in *Caenorhabditis elegans*. *Dev. Biol.* 1981;84:193–205. [[PubMed: 7250492](#)]
276. Caudy M, Vässin H, Brand M, Tuma R, Jan L Y, Jan Y N. *daughterless*, a *Drosophila* gene essential for both neurogenesis and sex determination, has sequence similarities to *myc* and the *achaete-scute*

- complex. *Cell*. 1988;55:1061–1067. [PubMed: 3203380]
277. Caulagi V R, Rajan T V. The structural organization of an alpha 2 (type IV) basement membrane collagen gene from the filarial nematode *Brugia malayi*. *Mol. Biochem. Parasitol.* 1995;70:227–229. [PubMed: 7637709]
278. Cedergren R, Gray M W, Abel Y, Sankoff D. The evolutionary relationships among known life forms. *J. Mol. Evol.* 1988;28:98–122. [PubMed: 3148747]
279. Chacravarti S, Horchar T, Jefferson B, Laurie G W, Hassell J R. Recombinant domain III of perlecan promotes cell attachment through its RGD's sequence. *J. Biol. Chem.* 1995;270:404–409. [PubMed: 7814401]
280. Chalfie M, Au M. Genetic control of differentiation of the *Caenorhabditis elegans* touch receptor neurons. *Science*. 1989;243:1027–1033. [PubMed: 2646709]
281. Chalfie M, Sulston J. Developmental genetics of the mechanosensory neurons of *Caenorhabditis elegans*. *Dev. Biol.* 1981;82:358–370. [PubMed: 7227647]
282. Chalfie M, Thomson J N. Organization of neuronal microtubules in the nematode *C. elegans*. *J. Cell. Biol.* 1979;82:278–289. [PMC free article: PMC2110421] [PubMed: 479300]
283. Chalfie M, Thomson J N. Structural and functional diversity in the neuronal microtubules of *C. elegans*. *J. Cell. Biol.* 1982;93:15–23. [PMC free article: PMC2112106] [PubMed: 7068753]
284. Chalfie M, White J, Wood W B, editor. The nematode *Caenorhabditis elegans*. Cold Spring Harbor, New York: Cold Spring Harbor Laboratory; 1988. The nervous system. pp. 337–391.
285. Chalfie M, Wolinsky E. The identification and suppression of neurodegeneration in *Caenorhabditis elegans*. *Nature*. 1990;345:410–416. [PubMed: 2342572]
286. Chalfie M, Driscoll M, Huang M X. Degenerin similarities. *Nature*. 1993;361:504. [PubMed: 8429902]
287. Chalfie M, Horvitz H R, Sulston J E. Mutations that lead to reiterations in the cell lineages of *C. elegans*. *Cell*. 1981;24:59–69. [PubMed: 7237544]
288. Chalfie M, Thomson J N, Sulston J E. Induction of neuronal branching in *C. elegans*. *Science*. 1983;221:61–63. [PubMed: 6857263]
289. Chalfie M, Tu Y, Euskirchen G, Ward W W, Prasher D C. Green fluorescent protein as a marker for gene expression. *Science*. 1994;263:802–805. [PubMed: 8303295]
290. Chalfie M, Sulston J E, White J G, Southgate E, Thomson J N, Brenner S. The neural circuit for touch sensitivity in *C. elegans*. *J. Neurosci.* 1985;5:956–964. [PMC free article: PMC6565008] [PubMed: 3981252]
291. Chamberlin H M. "Cell fate specification during *Caenorhabditis elegans* male tail development." [Ph.D. thesis]. California Institute of Technology; Pasadena: 1994. [PMC free article: PMC43666]
292. Chamberlin H M, Sternberg P W. Multiple cell interactions are required for fate specification during male spicule development in *Caenorhabditis elegans*. *Development*. 1993;118:297–323. [PubMed: 8223264]
293. Chamberlin H M, Sternberg P W. The *lin-3/let-23* pathway mediates inductive signalling during male spicule development in *Caenorhabditis elegans*. *Development*. 1994;120:2713–2721. [PubMed: 7607066]
294. Chamberlin H M, Sternberg P W. Mutations in the *Caenorhabditis elegans* gene *vab-3* reveal distinct roles in fate specification and unequal cytokinesis in an asymmetric cell division. *Dev. Biol.* 1995;170:679–689. [PubMed: 7649393]
295. Chan S K, Jaffe L, Capovilla M, Botas J, Mann R S. The DNA binding specificity of Ultrabithorax is modulated by cooperative interactions with extradenticle, another homeoprotein. *Cell*. 1994;78:603–615. [PubMed: 7915199]
296. Chan S S -Y, Zheng H, Su M -W, Wilk R, Killeen M T, Hedgecock E M, Culotti J G. UNC-40, a *C. elegans* homolog of DCC (Deleted in Colorectal Cancer), is required in motile cells responding to UNC-6 netrin cues. *Cell*. 1996;87:187–195. [PubMed: 8861903]
297. Chan W, Kordeli E, Bennett V. 440-kD ankyrinB: Structure of the major developmentally regulated domain and selective localization in unmyelinated axons. *J. Cell Biol.* 1993;123:1463–1473. [PMC free article: PMC2290908] [PubMed: 8253844]

298. Chang M C. Fertilizing capacity of spermatozoa deposited in fallopian tubes. *Nature*. 1951;168:997–998. [PubMed: 14882325]
299. Chant J, Pringle J R. Patterns of bud-site selection in the yeast *Saccharomyces cerevisiae*. *J. Cell Biol.* 1995;129:751–765. [PMC free article: PMC2120437] [PubMed: 7730409]
300. Chao M V. Neurotrophin receptors: A window into neuronal differentiation. *Neuron*. 1992;9:583–593. [PubMed: 1327010]
301. Charest D L, Clark D V, Green M E, Baillie D L. Genetic and fine-structure analysis of *unc-26* (IV) and adjacent regions in *Caenorhabditis elegans*. *Mol. Gen. Genet.* 1990;221:459–465. [PubMed: 2381425]
302. Sharpier S, Behrends J C, Triller A, Faber D S, Korn H. “Latent” inhibitory connections become functional during activity-dependent plasticity. *Proc. Natl. Acad. Sci.* 1995;92:117–120. [PMC free article: PMC42828] [PubMed: 7816799]
303. Chen L, Krause M, Sepanski M, Fire A. The *Caenorhabditis elegans* MYOD homologue HLH-1 is essential for proper muscle function and complete morphogenesis. *Development*. 1994;120:1631–1641. [PubMed: 8050369]
304. Chen L, Krause M, Draper B, Weintraub H, Fire A. Body-wall muscle formation in *Caenorhabditis elegans* embryos that lack the MyoD homolog *hlh-1*. *Science*. 1992;256:240–243. [PubMed: 1314423]
305. Chen M, Obar R A, Schroeder C C, Austin T W, Poodry C A, Wadsworth S C, Vallee R B. Multiple forms of dynamin are encoded by *shibire*, a *Drosophila* gene involved in endocytosis. *Nature*. 1991;351:583–586. [PubMed: 1828536]
306. Chen R, Ingraham H A, Treacy M N, Albert V R, Wilson L, Rosenfeld M G. Autoregulation of *pit-1* gene expression mediated by two *cis*-active promoter elements. *Nature*. 1990;346:583–586. [PubMed: 2142999]
307. Chen S N, Howells R E. *Brugia pahangi*: Uptake and incorporation of nucleic acid precursors by microfilariae and macrofilariae *in vitro*. *Exp. Parasitol.* 1981;51:296–306. [PubMed: 6970680]
308. Chen W, Lim L. The *Caenorhabditis elegans* small GTP-binding protein RhoA is enriched in the *nerve ring* and *sensory neurons* during larval development. *J. Biol. Chem.* 1994;269:32394–32404. [PubMed: 7798239]
309. Chen W, Lim H H, Lim L. A new member of the *rassuperfamily*, the *rac1* homologue from *Caenorhabditis elegans*. *J. Biol. Chem.* 1993a;268:320–324. [PubMed: 7677998]
310. Chen W, Lim H H, Lim L. The *CDC42* homologue from *Caenorhabditis elegans*. *J. Biol. Chem.* 1993b;268:13280–13285. [PubMed: 8514766]
311. Chen X, Rubock M J, Whitman M. A transcriptional partner for MAD proteins in TGF- $\beta$  signalling. *Nature*. 1996;383:691–696. [PubMed: 8878477]
312. Cheng J, Belgrader P, Zhou X, Maquat L E. Introns are *cis*-effectors of the nonsense-codon-mediated reduction in nuclear mRNA abundance. *Mol. Cell. Biol.* 1994;14:6317–6325. [PMC free article: PMC359158] [PubMed: 8065363]
313. Cheng N N. “Genetic and developmental analysis of *par-2* a gene required for cytoplasmic localization and cleavage patterning in *Caenorhabditis elegans*.” [Ph.D. thesis]. Cornell University; Ithaca, New York: 1991.
314. Cheng N N, Kirby C M, Kemphues K J. Control of cleavage spindle orientation in *Caenorhabditis elegans*: The role of the genes *par-2* and *par-3*. *Genetics*. 1995;139:549–559. [PMC free article: PMC1206366] [PubMed: 7713417]
315. Chia C P, Shariff A, Savage S A, Luna E J. The integral membrane protein, ponticulin, acts as a monomer in nucleating actin assembly. *J. Cell Biol.* 1993;120:909–922. [PMC free article: PMC2200087] [PubMed: 8432731]
316. Chiba C M, Rankin C H. A developmental analysis of spontaneous and reflexive reversals in the nematode *C. elegans*. *J. Neurobiol.* 1990;21:543–554. [PubMed: 2376729]
317. Chin-Sang I D, Spence A M. *C. elegans* sex-determining protein FEM-2 is a protein phosphatase that promotes male development and interacts directly with FEM-3. *Genes Dev.* 1996;10:2314–2325. [PubMed: 8824590]

318. Chisholm A. Control of cell fate in the tail region of *C. elegans* by the gene *egl-5*. *Development.* 1991;111:921–932. [PubMed: 1879361]
319. Chisholm A D, Hodgkin J. The *mab-9* gene controls the fate of B the major male-specific blast cell in the tail region of *Caenorhabditis elegans*. *Genes Dev.* 1989;33:1413–1423. [PubMed: 2606353]
320. Chisholm A D, Horvitz H R. Patterning of the *Caenorhabditis elegans* head region by the *Pax-6*-family member *vab-3*. *Nature.* 1995;377:52–55. [PubMed: 7659159]
321. Chitwood B G, Chitwood M B. Introduction to nematology. Baltimore: University Park Press; 1950.
322. Chitwood B G, Chitwood M B. Introduction to nematology (reprinted). Baltimore, Maryland: University Park Press; 1974.
323. Chitwood D J, Feldlaufer M F. Ecdysteroids in axenically propagated *Caenorhabditis elegans* and culture medium. *J. Nematol.* 1990;22:598–607. [PMC free article: PMC2619082] [PubMed: 19287765]
324. Chitwood D J, Lusby W R, Thompson M J, Kochansky J P, Howarth O W. The glycosylceramides of the nematode *Caenorhabditis elegans* contain an unusual, branched-chain sphingoid base. *Lipids.* 1995;30:567–573. [PubMed: 7651085]
325. Chow K L, Emmons S W. HOM-C/Hox genes and four interacting loci determine the morphogenetic properties of single cells in the nematode *male tail*. *Development.* 1994;120:2579–2593. [PubMed: 7956833]
326. Chow K L, Hall D, Emmons S W. The *mab-21* gene of *C. elegans* encodes a novel protein required for choice of alternate cell fates. *Development.* 1995;121:3615–3626. [PubMed: 8582275]
327. Christensen S, Kodoyanni V, Bosenberg M, Friedman L, Kimble J. *lag-1*, a gene required for *lin-12* and *glp-1* signaling in *Caenorhabditis elegans* is homologous to human CBF1 and *Drosophila Su(H)*. *Development.* 1996;122:1373–1383. [PubMed: 8625826]
328. Chuang P -T, Albertson D G, Meyer B J. DPY-27: A chromosome condensation protein homolog that regulates *C. elegans* dosage compensation through association with the X chromosome. *Cell.* 1994;79:459–474. [PubMed: 7954812]
329. Chuang P -T, Lieb J D, Meyer B J. Sex-specific assembly of a dosage compensation complex on the nematode X chromosome. *Science.* 1996;274:1736–1739. [PubMed: 8939870]
330. Chuong C M, Jiang T X, Yin E, Widelitz R B. cDCC (chicken homologue to a gene deleted in colorectal carcinoma) is an epithelial adhesion molecule expressed in the basal cells and involved in epithelial-mesenchymal interaction. *Dev. Biol.* 1994;164:383–397. [PubMed: 8045341]
331. Church D, Guan K -L, Lambie E J. Three genes of the MAP kinase cascade, *mek-2*, *mpk-1/sur-1* and *let-60 ras*, are required for meiotic cell cycle progression in *Caenorhabditis elegans*. *Development.* 1995;121:2525–2535. [PubMed: 7671816]
332. Ciaramella M, Bazzicalupo P, La Volpe A. Structure, evolution and properties of a novel repetitive DNA family in *Caenorhabditis elegans*. *Nucleic Acids Res.* 1988;16:8213–8231. [PMC free article: PMC338554] [PubMed: 3419918]
333. Cigan A M, Donahue T F. Sequence and structural features associated with translational initiator regions in yeast—A review. *Gene.* 1987;59:1–18. [PubMed: 3325335]
334. Citi S, Kendrick-Jones J. Regulation of non-muscle myosin structure and function. *BioEssays.* 1987;7:155–159. [PubMed: 3318821]
335. Clandinin T R, Mains P E. Genetic studies of *mei-1*gene activity during the transition from meiosis to mitosis in *Caenorhabditis elegans*. *Genetics.* 1993;134:199–210. [PMC free article: PMC1205422] [PubMed: 8514128]
336. Clark D V, Baillie D L. Genetic analysis and complementation by germ-line transformation of lethal mutations in the *unc-22 IV* region of *Caenorhabditis elegans*. *Mol. Gen. Genet.* 1992;232:97–105. [PubMed: 1552909]
337. Clark D V, Johnsen R C, McKim K S, Baillie D L. Analysis of lethal mutations induced in a mutator strain that activates transposable elements in *Caenorhabditis elegans*. *Genome.* 1990;33-1:109–114. [PubMed: 2158925]
338. Clark D V, Rogalski T M, Donati L M, Baillie D L. The *unc-22(IV)* region of *Caenorhabditis elegans*:Genetic analysis of lethal mutations. *Genetics.* 1988;129:345–353. [PMC free article:

[PMC1203417](#)] [[PubMed: 3396868](#)]

339. Clark D V, Suleman D S, Beckenbach K A, Gilchrist E J, Baillie D L. Molecular cloning and characterization of the *dpy-20* gene of *Caenorhabditis elegans*. *Mol. Gen. Genet.* 1995;247:367–378. [[PubMed: 7770042](#)]
340. Clark K L, Halay E D, Lai E, Burley S K. Co-crystal structure of the HNF-3/*fork head* DNA-recognition motif resembles histone H5. *Nature*. 1993;364:412–415. [[PubMed: 8332212](#)]
341. Clark S G, Chisholm A D, Horvitz H R. Control of cell fates in the central body region of *C. elegans* by the homeobox gene *lin-39*. *Cell*. 1993;74:43–55. [[PubMed: 8101475](#)]
342. Clark S G, Lu X, Horvitz H R. The *Caenorhabditis elegans* locus *lin-15*, a negative regulator of a tyrosine kinase signaling pathway, encodes two different proteins. *Genetics*. 1994;137:987–997. [[PMC free article: PMC1206075](#)] [[PubMed: 7982579](#)]
343. Clark S G, Stern M J, Horvitz H R. *C. elegans* cell-signalling gene *sem-5* encodes a protein with SH2 and SH3 domains. *Nature*. 1992;356:340–344. [[PubMed: 1372395](#)]
344. Clark-Maguire S, Mains P E. *mei-1* a gene required for meiotic spindle formation in *Caenorhabditis elegans*, is a member of a family of ATPases. *Genetics*. 1994a;136:533–546. [[PMC free article: PMC1205806](#)] [[PubMed: 8150281](#)]
345. Clark-Maguire S, Mains P E. Localization of the *mei-1* gene product of *Caenorhabditis elegans*, a meiotic-specific spindle component. *J. Cell Biol.* 1994b;126:199–209. [[PMC free article: PMC2120096](#)] [[PubMed: 8027178](#)]
346. Cleary M L, Smith S D, Sklar J. Cloning and structural analysis of cDNAs for *bcl-2* and a hybrid *bcl-2*/immunoglobulin transcript resulting from the t(14;-->18) translocation. *Cell*. 1986;47:19–28. [[PubMed: 2875799](#)]
347. Cleavinger P J, McDowell J W, Bennett K L. Transcription in nematodes: Early *Ascaris* embryos are transcriptionally active. *Dev. Biol.* 1989;133:600–604. [[PubMed: 2471658](#)]
348. Clem R J, Fechheimer M, Miller L K. Prevention of apoptosis by a baculovirus gene during infection of insect cells. *Science*. 1991;254:1388–1390. [[PubMed: 1962198](#)]
349. Cline T W. A sex-specific temperature-sensitive maternal effect of the *daughterless* mutation of *Drosophila melanogaster*. *Genetics*. 1976;84:723–742. [[PMC free article: PMC1213604](#)] [[PubMed: 827461](#)]
350. Cline T W. Two closely linked mutations in *Drosophila melanogaster* that are lethal to opposite sexes and interact with *daughterless*. *Genetics*. 1978;90:683–698. [[PMC free article: PMC1213913](#)] [[PubMed: 105964](#)]
351. Cline T W. Evidence that *sisterless-a* and *sisterless-b* are two of several discrete “numerators”: Of the X/A sex determination signal in *Drosophila* that switch *Sxl* between two alternative stable expression states. *Genetics*. 1988;119:829–862. [[PMC free article: PMC1203469](#)] [[PubMed: 3137120](#)]
352. Cline T W. The *Drosophila* sex determination signal: How do flies count to two? *Trends Genet.* 1993;9:385–390. [[PubMed: 8310535](#)]
353. Cline T W, Meyer B J. Vive la différence: Males vs. females in flies vs. worms. *Annu. Rev. Genet.* 1996;30:637–701. [[PubMed: 8982468](#)]
354. Cobb N A. The orders and classes of nemas. *Contrib. Sci. Nematol.* 1919;8:213–216.
355. Coburn C M, Bargmann C I. A putative cyclic nucleotide-gated channel is required for sensory development and function in *C. elegans*. *Neuron*. 1996;17:695–706. [[PubMed: 8893026](#)]
356. Cohen C, Lanar D E, Parry D A. Amino acid sequence and structural repeats in schistosome paramyosin match those of myosin. *Biosci. Rep.* 1987;7:11–16. [[PubMed: 3620600](#)]
357. Cohen C, Szent-Gyorgyi A G, Kendrick-Jones J. Paramyosin and the filaments of molluscan “catch” muscles. I. Paramyosin: Structure and assembly. *J. Mol. Biol.* 1971;56:223–237. [[PubMed: 5551393](#)]
358. Cohen C, Lowey S, Harrison R G, Kendrick-Jones J, Szent-Gyorgyi A G. Segments from myosin rods. *J. Mol. Biol.* 1970;47:605–609. [[PubMed: 5461464](#)]
359. Cohen-Dayag A, Eisenbach M. Potential assays for sperm capacitation in mammals. *Am. J. Physiol.* 1994;267:C1167–C1176. [[PubMed: 7977680](#)]

360. Colamarino S A, Tessier-Lavigne M. The axonal chemoattractant netrin-1 is also a chemorepellent for trochlear motor axons. *Cell*. 1995;81:621–629. [[PubMed: 7758116](#)]
361. Colbert H A, Bargmann C I. Odorant-specific adaptation pathways generate olfactory plasticity in *C. elegans*. *Neuron*. 1995;14:803–812. [[PubMed: 7718242](#)]
362. Cole K D, Kandala J C, Kister W S. Isolation of the gene for testes-specific H1 histone variant H1t. *J. Biol. Chem.* 1986;216:7178–7183. [[PubMed: 2423516](#)]
363. Collinge M, Matrisian P E, Zimmer W E, Shattuck R L, Lukas T J, Van Eldik L J, Watterson D M. Structure and expression of a calcium-binding protein gene contained within a calmodulin-regulated protein kinase gene. *Mol. Cell. Biol.* 1992;12:2359–2371. [[PMC free article: PMC364408](#)] [[PubMed: 1373815](#)]
364. Collins J, Anderson P. The Tc5 family of transposable elements in *Caenorhabditis elegans*. *Genetics*. 1994;137:771–781. [[PMC free article: PMC1206037](#)] [[PubMed: 8088523](#)]
365. Collins J, Forbes E, Anderson P. The Tc3 family of transposable elements in *Caenorhabditis elegans*. *Genetics*. 1989;121:47–55. [[PMC free article: PMC1203604](#)] [[PubMed: 2537252](#)]
366. Collins J, Saari B, Anderson P. Activation of a transposable element in the germ line but not the soma of *Caenorhabditis elegans*. *Nature*. 1987;328:726–728. [[PubMed: 3039378](#)]
367. Colloms S D, van Luenen H G A M, Plasterk R H A. DNA binding activities of the *Caenorhabditis elegans* Tc3 transposase. *Nucleic Acids Res.* 1994;22:5548–5554. [[PMC free article: PMC310115](#)] [[PubMed: 7838706](#)]
368. Condeelis J. Life at the leading edge: The formation of cell protrusions. *Annu. Rev. Cell Biol.* 1993;9:411–444. [[PubMed: 8280467](#)]
369. Conrad R, Lea K, Blumenthal T. SL1 *trans*-splicing specified by AU-rich synthetic RNA inserted at the 5'end of *Caenorhabditis elegans* pre-mRNA. *RNA*. 1995;1:164–170. [[PMC free article: PMC1369070](#)] [[PubMed: 7585246](#)]
370. Conrad R, Liou R F, Blumenthal T. Functional analysis of a *C. elegans* trans-splice site acceptor. *Nucleic Acids Res.* 1993a;21:913–919. [[PMC free article: PMC309224](#)] [[PubMed: 8451190](#)]
371. Conrad R, Liou R F, Blumenthal T. Conversion of a *trans*-spliced *C. elegans* gene into a conventional gene by introduction of a splice donor site. *EMBO J.* 1993b;12:1249–1255. [[PMC free article: PMC413329](#)] [[PubMed: 8458337](#)]
372. Conrad R, Thomas J, Spieth J, Blumenthal T. Insertion of part of an intron into the 5'untranslated region of a *Caenorhabditis elegans* gene converts it into a *trans*-spliced gene. *Mol. Cell. Biol.* 1991;11:1921–1926. [[PMC free article: PMC359875](#)] [[PubMed: 1848665](#)]
373. Constantine-Paton M, Cline H T, Debski E. Patterned activity, synaptic convergence, and the NMDA receptor in developing visual pathways. *Annu. Rev. Neurosci.* 1990;13:129–154. [[PubMed: 2183671](#)]
374. Conway Morris S. The fossil record and the early evolution of the Metazoa. *Nature*. 1993;361:219–225.
375. Conway Morris S. Why molecular biology needs palaeontology. *Suppl. pp. Development*. 1994;1–13. [[PubMed: 8119118](#)]
376. Cooke R. The actomyosin engine. *FASEB J.* 1995;9:636–642. [[PubMed: 7768355](#)]
377. Cookson E, Blaxter M L, Selkirk M E. Identification of the major soluble cuticular glycoprotein of lymphatic filarial nematode parasites as a secretory homologue of glutathione peroxidase. *Proc. Natl. Acad. Sci.* 1992;89:5837–5841. [[PMC free article: PMC49392](#)] [[PubMed: 1631065](#)]
378. Cookson E, Tang L, Selkirk M E. Conservation of primary structure of gp29, the major soluble cuticular glycoprotein, in three species of lymphatic filariae. *Mol. Biochem. Parasitol.* 1993;58:155–160. [[PubMed: 8459826](#)]
379. Cooper J R, Bloom F E, Roth R H. The biochemical basis of neuropharmacology. New York: Oxford University Press; 1991.
380. Cornillon S, Foa C, Davoust J, Buonavista N, Gross J D, Golstein P. Programmed cell death in *Dictyostelium*. *J. Cell Sci.* 1994;107:2691–2704. [[PubMed: 7876338](#)]
381. Costa M, Weir M, Coulson A, Sulston J, Kenyon C. Posterior pattern formation in *C. elegans* involves position-specific expression of a gene containing a homeobox. *Cell*. 1988;55:747–756. [[PubMed:](#)

[2903796](#)

382. Coulson A R. "The physical map of the genome of *Caenorhabditis elegans*." [Ph.D. thesis]. The Open University; Milton Keynes, England: 1994.
383. Coulson A R, Sulston J, Brenner S, Karn J. Toward a physical map of the genome of the nematode *C. elegans*. Proc. Natl. Acad. Sci. 1986;83:7821–7825. [[PMC free article: PMC386814](#)] [[PubMed: 16593771](#)]
384. Coulson A R, Waterston R H, Kiff J E, Sulston J E, Kohara Y. Genome linking with yeast artificial chromosomes. Nature. 1988;335:184–186. [[PubMed: 3045566](#)]
385. Coulson A R, Kozono Y, Lutterbach B, Shownkeen R, Sulston J, Waterston R. YACs and the *C. elegans* genome. BioEssays. 1991;13:413–417. [[PubMed: 1953703](#)]
386. Cowan A E, McIntosh J R. Mapping the distribution of differentiation potential for intestine muscle, and hypodermis during early development in *Caenorhabditis elegans*. Cell. 1985;41:923–932. [[PubMed: 3891098](#)]
387. Cowden C, Stretton A O W. AF2, an *Ascaris*neuropeptide: Isolation, sequence, and bioactivity. Peptides. 1993;14:423–430. [[PubMed: 8332542](#)]
388. Cowden C, Stretton A O W. Eight novel FMRFamide-like neuropeptides isolated from the nematode *Ascaris suum*. Peptides. 1995;16:491–500. [[PubMed: 7651904](#)]
389. Cowden C, Stretton A O W, Davis R E. AF1, a sequenced bioactive neuropeptide isolated from the nematode *Ascaris suum*. Neuron. 1989;2:1465–1473. [[PubMed: 2627377](#)]
390. Cowden C, Sithigorngul P, Brackley P, Guastella J, Stretton A O. Localization and differential expression of FMRFamide-like immunoreactivity in the nematode *Ascaris suum*. J. Comp. Neurol. 1993;333:455–468. [[PubMed: 8349852](#)]
391. Cowing D W, Kenyon C. Expression of the homeotic gene *mab-5* during *Caenorhabditis elegans* embryogenesis. Development. 1992;116:481–490. [[PubMed: 1363090](#)]
392. Cox G N. Molecular biology of the cuticle collagen gene families of *Caenorhabditis elegans* and *Haemonchus contortus*. Acta Trop. 1990;47:269–281. [[PubMed: 1978527](#)]
393. Cox G N. Molecular and biochemical aspects of nematode collagens. J. Parasitol. 1992;78:1–15. [[PubMed: 1738051](#)]
394. Cox G N, Hirsh D. Stage-specific patterns of collagen gene expression during development of *Caenorhabditis elegans*. Mol. Cell. Biol. 1985;5:363–372. [[PMC free article: PMC366719](#)] [[PubMed: 2983191](#)]
395. Cox G N, Kramer J M, Hirsh D. Number and organization of collagen genes in *Caenorhabditis elegans*. Mol. Cell. Biol. 1984;4:2389–2395. [[PMC free article: PMC369069](#)] [[PubMed: 6513921](#)]
396. Cox G N, Kusch M, Edgar R S. Cuticle of *Caenorhabditis elegans*: Its isolation and partial characterization. J. Cell Biol. 1981a;90:7–17. [[PMC free article: PMC2111847](#)] [[PubMed: 7251677](#)]
397. Cox G N, Shamansky L M, Boisvenue R J. *Haemonchus contortus*: The 3A3 collagen gene is a member of an evolutionarily conserved family of nematode cuticle collagens. Exp. Parasitol. 1990;70:175–185. [[PubMed: 2404780](#)]
398. Cox G N, Staprans S, Edgar R S. The cuticle of *Caenorhabditis elegans*. II. Stage-specific changes in ultrastructure and protein composition during postembryonic development. Dev. Biol. 1981b;86:456–470. [[PubMed: 6269931](#)]
399. Cox G N, Carr S, Kramer J M, Hirsh D. Genetic mapping of *Caenorhabditis elegans* collagen genes using DNA polymorphisms as phenotypic markers. Genetics. 1985;109:513–528. [[PMC free article: PMC1216285](#)] [[PubMed: 3979813](#)]
400. Cox G N, Kusch M, DeNevi K, Edgar R S. Temporal regulation of cuticle synthesis during development of *Caenorhabditis elegans*. Dev. Biol. 1981c;84:277–285. [[PubMed: 20737865](#)]
401. Cox G N, Laufer J S, Kusch M, Edgar R S. Genetic and phenotypic characterization of roller mutants of *Caenorhabditis elegans*. Genetics. 1980;95:317–339. [[PMC free article: PMC1214229](#)] [[PubMed: 17249038](#)]
402. Cox G N, Fields C, Kramer J M, Rosenzweig B, Hirsh D. Sequence comparisons of developmentally regulated collagen genes of *Caenorhabditis elegans*. Gene. 1989;76:331–344. [[PubMed: 2753356](#)]

403. Craig R. Structure of A segments from frog and rabbit skeletal muscle. *J. Mol. Biol.* 1977;109:69–81. [PubMed: 300111]
404. Craig S P, Muralidhar M G, McKerrow J H, Wang C C. Evidence for a class of very small introns in the gene for hypoxanthine-guanine phosphoribosyl-transferase in *Schistosoma mansoni*. *Nucleic Acids Res.* 1989;17:1635–1647. [PMC free article: PMC331826] [PubMed: 2701934]
405. Craigie R. Hotspots and warm spots: Integration specificity of retroelements. *Trends Genet.* 1992;8:187–190. [PubMed: 1323152]
406. Craigie R, Mizuuchi M, Mizuuchi K. Site-specific recognition of the bacteriophage Mu ends by MuA protein. *Cell.* 1984;39:387–394. [PubMed: 6094016]
407. Creutz C E, Snyder S L, Daigle S N, Redick J. Identification, localization and functional implications of an abundant nematode annexin. *J. Cell Biol.* 1996;132:1079–1082. [PMC free article: PMC2120750] [PubMed: 8601586]
408. Crittenden S L, Troemel E R, Evans T C, Kimble J. GLP-1 is localized to the mitotic region of the *C. elegans* germ line. *Development.* 1994;120:2901–2911. [PubMed: 7607080]
409. Crofton H D. *Nematodes*. London: Hutchinson University Library; 1966.
410. Croll N A. Indolealkylamines in the coordination of nematode behavioral activities. *Can. J. Zool.* 1975a;53:894–903. [PubMed: 1079747]
411. Croll N A. Components and patterns in the behavior of the nematode *Caenorhabditis elegans*. *J. Zool.* 1975b;176:159–176.
412. Croll N A. When *C. elegans*(Nematoda: Rhabditidae) bumps into a bead. *Can. J. Zool.* 1976;54:566–570.
413. Croll N A, Matthews B E. *Biology of nematodes* 66–67. New York: John Wiley; 1977.
414. Croll N A, Smith J M. Integrated behavior in the feeding phase of *Caenorhabditis elegans* (Nematoda). *J. Zool.* 1978;184:507–517.
415. Csank C, Taylor F M, Martindale D W. Nuclear pre-mRNA introns: Analysis and comparison of intron sequences from *Tetrahymena thermophila* and other eukaryotes. *Nucleic Acids Res.* 1990;18:5133–5141. [PMC free article: PMC332134] [PubMed: 2402440]
416. Cui Y, Hagan K W, Zhang S, Peltz S W. Identification and characterization of genes that are required for accelerated degradation of mRNAs containing a premature translation termination codon. *Genes Dev.* 1995;9:423–436. [PubMed: 7883167]
417. Cully D F, Vassilatis D K, Liu K K, Paress P S, Van Der Ploeg L H T, Schaeffer J M, Arena J P. Cloning of an avermectin-sensitive glutamate-gated chloride channel from *Caenorhabditis elegans*. *Nature.* 1994;371:707–711. [PubMed: 7935817]
418. Culotti J G. Axon guidance mechanisms in *Caenorhabditis elegans*. *Curr. Opin. Genet. Dev.* 1994;4:587–595. [PubMed: 7950328]
419. Culotti J G, Klein W L. Occurrence of muscarinic acetylcholine receptors in wild type and cholinergic mutants of *Caenorhabditis elegans*. *J. Neurosci.* 1983;3:359–368. [PMC free article: PMC6564492] [PubMed: 6822867]
420. Culotti J G, Russell R L. Osmotic avoidance defective mutants of the nematode *Caenorhabditis elegans*. *Genetics.* 1978;90:243–256. [PMC free article: PMC1213887] [PubMed: 730048]
421. Culotti J G, Von Ehrenstein G, Culotti M R, Russell R L. A second class of acetylcholinesterase-deficient mutants of the nematode *Caenorhabditis elegans*. *Genetics.* 1981;97:281–305. [PMC free article: PMC1214394] [PubMed: 7274655]
422. Cummins C, Anderson P. Regulatory myosin light-chain genes of *Caenorhabditis elegans*. *Mol. Cell. Biol.* 1988;8:5339–5349. [PMC free article: PMC365636] [PubMed: 3244358]

## D

423. Daboussi M, Langin T, Brygoo Y. Fot1, a new family of fungal transposable elements. *Mol. Gen. Genet.* 1992;232:12–16. [PubMed: 1313143]

424. Dahm L M, Landmesser L T. The regulation of synaptogenesis during normal development and following activity blockade. *J. Neurosci.* 1991;11:238–255. [[PMC free article: PMC6575191](#)] [[PubMed: 1898747](#)]
425. Daigle I, Li C. *apl-1* a *Caenorhabditis elegans* gene encoding a protein related to the human  $\beta$ -amyloid protein precursor. *Proc. Natl. Acad. Sci.* 1993;90:12045–12049. [[PMC free article: PMC48122](#)] [[PubMed: 8265668](#)]
426. Dalley B K, Golomb M. Gene expression in the *Caenorhabditis elegans* dauer larva: Developmental regulation of Hsp90 and other genes. *Dev. Biol.* 1992;151:80–90. [[PubMed: 1577199](#)]
427. Darwin C. The origin of species by means of natural selection or the preservation of favoured races in the struggle for life. London: John Murray; 1859. [[PMC free article: PMC5184128](#)] [[PubMed: 30164232](#)]
428. Darzynkiewicz E, Stepinski J, Jin Y, Haber D, Sijuwade T, Tahara S M.  $\beta$ -globin mRNAs capped with  $m_1^7G$ ,  $m_2^{2,7}G$ , or  $m_3^{2,2,7}G$  differ in intrinsic translation efficiency. *Nucleic Acids Res.* 1988;16:8953–8962. [[PMC free article: PMC3386451](#)] [[PubMed: 3174438](#)]
429. Das A, Gilbert C D. Long-range horizontal connections and their role in cortical reorganization revealed by optical recording of cat primary visual cortex. *Nature*. 1995;375:780–784. [[PubMed: 7596409](#)]
430. Dascher C, Ossig R, Gallwitz D, Schmitt H D. Identification and structure of four yeast genes (SLY) that are able to suppress the functional loss of YPT1, a member of the RAS superfamily. *Mol. Cell. Biol.* 1991;11:872–885. [[PMC free article: PMC359739](#)] [[PubMed: 1990290](#)]
431. Davis H P, Squire L R. Protein synthesis and memory: A review. *Psychol. Rev.* 1984;96:518–559. [[PubMed: 6096908](#)]
432. Davis J S. Assembly processes in vertebrate skeletal thick filament formation. *Annu. Rev. Biophys. Chem.* 1988;17:217–239. [[PubMed: 3293585](#)]
433. Davis J Q, McLaughlin T, Bennett V. Ankyrin-binding proteins related to [nervous system](#) cell adhesion molecules: Candidates to provide transmembrane and intercellular connections in adult brain. *J. Cell Biol.* 1993;121:121–133. [[PMC free article: PMC2119766](#)] [[PubMed: 8458865](#)]
434. Davis M. Effects of interstimulus interval length and variability on startle-response habituation in the rat. *J. Comp. Physiol. Psychol.* 1970;72:177–192. [[PubMed: 5489452](#)]
435. Davis M C, Ward J G, Herrick G, Allis C D. Programmed nuclear death: Apoptotic-like nuclear degradation of specific nuclei in conjugating *Tetrahymena*. *Dev. Biol.* 1992;154:419–432. [[PubMed: 1426647](#)]
436. Davis M W, Somerville D, Lee R Y N, Lockery S, Avery L, Fambrough D M. Mutations in the *Caenorhabditis elegans* Na,K-ATPase  $\alpha$ -subunit gene, *eat-6*, disrupt excitable cell function. *J. Neurosci.* 1995;15:8408–8418. [[PMC free article: PMC4445131](#)] [[PubMed: 8613772](#)]
437. Davis R E. Spliced leader RNA trans-splicing in metazoa. *Parasitol. Today*. 1996;12:33–40. [[PubMed: 15275306](#)]
438. Davis R E, Stretton A O. Signaling properties of *Ascaris* motorneurons: Graded active responses graded synaptic transmission, and tonic transmitter release. *J. Neurosci.* 1989;9:403–414. [[PMC free article: PMC6569786](#)] [[PubMed: 2563763](#)]
439. Davis R E, Singh H, Botka C, Hardwick C, Meanawy M A E, Villanueva J. RNA trans-splicing in *Fasciola hepatica*: Identification of a spliced leader (SL) RNA and SL sequences on mRNAs. *J. Biol. Chem.* 1994;269:20026–20030. [[PubMed: 8051087](#)]
440. Dawid I B, Toyama R, Taira M. LIM domain proteins. *C.R. Acad. Sci. Paris*. 1995;318:295–306. [[PubMed: 7788499](#)]
441. De Baere I, Liu L, Moens L, Van Beeumen J, Gielens C, Richelle J, Trottmann C, Finch J, Gerstein M, Perutz M. Polar zipper sequence in the high-affinity hemoglobin of *Ascaris suum*: Amino acid sequence and structural interpretation. *Proc. Natl. Acad. Sci.* 1992;89:4638–4642. [[PMC free article: PMC49138](#)] [[PubMed: 1584800](#)]

442. de Bono M, Hodgkin J. Evolution of sex determination in *Caenorhabditis*: Unusually high divergence of *tra-1* and its functional consequences. *Genetics*. 1996;144:587–595. [[PMC free article: PMC1207552](#)] [[PubMed: 8889522](#)]
443. de Bono M, Zarkower D, Hodgkin J. Dominant feminizing mutations implicate protein-protein interactions as the main mode of regulation of the nematode sex-determining gene *tra-1*. *Genes Dev.* 1995;9:155–167. [[PubMed: 7851791](#)]
444. De Camilli P, Benfenati F, Valtorta F, Greengard P. The synapsins. *Annu. Rev. Cell Biol.* 1990;6:433–460. [[PubMed: 1980418](#)]
445. Degnan B M, Degnan S M, Giusti A, Morse D E. A Hox/Hom homeobox gene in sponges. *Gene*. 1995;155:175–177. [[PubMed: 7721087](#)]
446. Deitiker P R, Epstein H F. Thick filament substructures in *Caenorhabditis elegans*: Evidence for two populations of paramyosin. *J. Cell Biol.* 1993;123:303–311. [[PMC free article: PMC2119837](#)] [[PubMed: 8408214](#)]
447. Deits T, Farrance M, Kay E S, Medill L, Turner E E, Weidman P J, Shapiro B M. Purification and properties of ovoperoxidase, the enzyme responsible for hardening the fertilization membrane of the sea urchin egg. *J. Biol. Chem.* 1984;259:13525–13533. [[PubMed: 6490663](#)]
448. del Castillo J, Morales T. The electrical and mechanical activity of the esophageal cell of *Ascaris lumbricoides*. *J. Physiol.* 1967;50:603–629. [[PMC free article: PMC2225679](#)] [[PubMed: 11526849](#)]
449. del Castillo J, de Mello W C, Morales T. Inhibitory action of GABA on *Ascaris* muscle. *Experientia*. 1964;20:141–143. [[PubMed: 5853680](#)]
450. De Ley P, Van de Velde M C, Mounport D, Baujard P, Coomans A. Ultrastructure of the stoma in Cephalobidae, Panagrolaimidae and Rhabditidae, with a proposal for a revised stoma terminology in Rhabditida (Nematoda). *Nematologica*. 1995;41:153–182.
451. DeLong L, Casson L P, Meyer B J. Assessment of X chromosome dosage compensation in *Caenorhabditis elegans* by phenotypic analysis of *lin-14*. *Genetics*. 1987;117:657–670. [[PMC free article: PMC1203239](#)] [[PubMed: 3428573](#)]
452. DeLong L, Plenefisch J D, Klein R D, Meyer B J. Feedback control of sex determination by dosage compensation revealed through *Caenorhabditis elegans sdc-3* mutations. *Genetics*. 1993;133:875–896. [[PMC free article: PMC1205407](#)] [[PubMed: 8462848](#)]
453. Denk W, Holt J R, Shepherd G M G, Corey D P. Calcium imaging of single stereocilia in hair cells: Localization of transduction channels at both ends of the tip links. *Neuron*. 1996;15:1311–1321. [[PubMed: 8845155](#)]
454. Dennis R D, Baumeister S, Smuda C, Lochnit C, Waider T, Geyer E. Initiation of chemical studies on the immunoreactive glycolipids of adult *Ascaris suum*. *Parasitology*. 1995;110:611–624. [[PubMed: 7596644](#)]
455. Deppe U, Schierenberg E, Cole T, Krieg C, Schmitt D, Yoder B, von Ehrenstein G. Cell lineages of the embryo of the nematode *Caenorhabditis elegans*. *Proc. Natl. Acad. Sci.* 1978;75:376–380. [[PMC free article: PMC411251](#)] [[PubMed: 272653](#)]
456. Desai C, Horvitz H R. *Caenorhabditis elegans* mutants defective in the functioning of the motor neurons responsible for egg laying. *Genetics*. 1989;121:703–721. [[PMC free article: PMC1203655](#)] [[PubMed: 2721931](#)]
457. Desai C, Garriga G, McIntire S L, Horvitz H R. A genetic pathway for the development of the *Caenorhabditis elegans* HSN motor neurons. *Nature*. 1988;336:638–646. [[PubMed: 3200316](#)]
458. de Souza W, Souto-Padron T, Dreyer G, Dias de Andrade L. *Wuchereria bancrofti*: Freeze-fracture study of the epicuticle of microfilariae. *Exp. Parasitol.* 1993;76:287–292. [[PubMed: 8500588](#)]
459. DeVore D L, Horvitz H R, Stern M J. An FGF receptor signaling pathway is required for the normal cell migrations of the sex myoblasts in *C. elegans* hermaphrodites. *Cell*. 1995;83:611–620. [[PubMed: 7585964](#)]
460. Dey C S, Deitiker P R, Epstein H F. Assembly-dependent phosphorylation of myosin and paramyosin of native thick filaments in *Caenorhabditis elegans*. *Biochem. Biophys. Res. Commun.* 1992;186:1528–1532. [[PubMed: 1324668](#)]

461. DeZazzo J, Tully T. Dissection of memory formation: From behavioral pharmacology to molecular genetics. *Trends Neurosci.* 1995;18:212–218. [PubMed: 7610491]
462. DiAntonio A, Schwarz T L. The effect on synaptic physiology of synaptotagmin mutations in *Drosophila*. *Neuron*. 1994;12:909–920. [PubMed: 7909234]
463. Dibb N J, Maruyama I N, Krause M, Karn J. Sequence analysis of the complete *Caenorhabditis elegans* myosin heavy chain gene family. *J. Mol. Biol.* 1989;205:603–613. [PubMed: 2926820]
464. Dibb N J, Brown D M, Karn J, Moerman D G, Bolten S L, Waterston R H. Sequence analysis of mutations that affect the synthesis, assembly and enzymatic activity of *unc-54* myosin heavy chain of *C. elegans*. *J. Mol. Biol.* 1985;183:543–551. [PubMed: 4020869]
465. Dickinson P. Modulation of simple motor patterns. *Semin. Neurosci.* 1989;1:15–24.
466. Dion M, Brun J L. Cartographie génique du Nematode libre *Caenorhabditis elegans* Maupas 1900, variété Bergerac. I. Etude de deux mutants nains. *Mol. Gen. Genet.* 1971;112:133–151. [PubMed: 5115378]
467. Dixon D K, Jones D, Candido E P M. The differentially expressed 16-kD heat shock genes of *Caenorhabditis elegans* exhibit differential changes in chromatin structure during heat shock. *DNA Cell Biol.* 1990;9:177–191. [PubMed: 2160246]
468. Dlugosz A A, Antin P B, Nachmias V T, Holtzer H. The relationship between stress fiber-like structures and nascent myofibrils in cultured cardiac myocytes. *J. Cell Biol.* 1984;99:2268–2278. [PMC free article: PMC2113583] [PubMed: 6438115]
469. Doak T G, Doerder F P, Jahn C L, Herrick G. A proposed superfamily of transposase genes: Transposon-like elements in ciliated protozoa and a common “D35E” motif. *Proc. Natl. Acad. Sci.* 1994;91:942–946. [PMC free article: PMC521429] [PubMed: 8302872]
470. Dodemont H, Riemer D, Ledger N, Weber K. Eight genes and alternative RNA processing pathways generate an unexpectedly large diversity of cytoplasmic intermediate filament proteins in the nematode *Caenorhabditis elegans*. *EMBO J.* 1994;13:2625–2638. [PMC free article: PMC395137] [PubMed: 8013462]
471. Doe C Q, Chu-LaGraff Q, Wright D M, Scott M P. The *prospero* gene specifies cell fates in the *Drosophila* central nervous system. *Cell*. 1991;65:451–464. [PubMed: 1673362]
472. Doncaster C C. Nematode feeding mechanisms. I. Observations on *Rhabditis* and *Pelodera*. *Nematologica*. 1962;8:313–320.
473. Donelson J E, Zeng W. A comparison of trans-splicing in trypanosomes and nematodes. *Parasitol. Today*. 1990;6:327–334. [PubMed: 15463258]
474. Doniach T. Activity of the sex-determining gene *tra-2* is modulated to allow spermatogenesis in the *C. elegans* hermaphrodite. *Genetics*. 1986;114:53–76. [PMC free article: PMC1202941] [PubMed: 3770471]
475. Doniach T, Hodgkin J. A sex-determining gene *fem-1*, required for both male and hermaphrodite development in *Caenorhabditis elegans*. *Dev. Biol.* 1984;106:223–235. [PubMed: 6541600]
476. Dorman J B, Albinder B, Shroyer T, Kenyon C. The *age-1* and *daf-2* genes function in a common pathway to control the lifespan of *Caenorhabditis elegans*. *Genetics*. 1995;141:1399–1406. [PMC free article: PMC1206875] [PubMed: 8601482]
477. Dougherty E C. The genera and species of subfamily Rhabditinae Micoletzky 1922 (Nematoda): A nomenclatorial analysis-including an addendum on the composition of the family Rhabditidae Örley, 18. *J. Helminthol.* 1955;29:105–152. [PubMed: 13306933]
478. Dougherty E C, Calhoun H G. Possible significance of free-living nematodes in genetic research. *Nature*. 1948;161:29. [PubMed: 18900748]
479. Dougherty E C, Nigon V. A new species of the free-living nematode genus *Rhabditis* of interest in comparative physiology and genetics. *J. Parasitol.* 1949;35:11.
480. Dougherty E C, Hansen E L, Nicholas W L, Mollett J A, Yarwood E A. Axenic cultivation of *Caenorhabditis briggsae*(Nematoda: Rhabditidae) with unsupplemented and supplemented chemically defined media. *Ann. N.Y. Acad. Sci.* 1959;77:176–217.

481. Dowse H B, Ringo J M. The search for hidden periodicities in biological time series revisited. *J. Theor. Biol.* 1989;139:487–515.
482. Draper B W, Mello C C, Bowerman B, Hardin J, Priess J R. MEX-3 is a KH domain protein that regulates blastomere identity in early *C. elegans* embryos. *Cell*. 1992;87:205–216. [[PubMed: 8861905](#)]
483. Drelich M, Wilhelm R, Mous J. Identification of amino acid residues critical for endonuclease and integrase activities of HIV-1 IN protein *in vitro*. *Virology*. 1992;188:459–468. [[PubMed: 1585629](#)]
484. Dreyfus D H, Emmons S W. A transposon-related palindromic repetitive sequence from *C. elegans*. *Nucleic Acids Res.* 1991;19:1871–1877. [[PMC free article: PMC328117](#)] [[PubMed: 1674369](#)]
485. Driscoll M. Molecular genetics of cell death in the nematode *Caenorhabditis elegans*. *J. Neurobiol.* 1992;23:1327–1351. [[PubMed: 1469391](#)]
486. Driscoll M, Chalfie M. The *mec-4* gene is a member of a family of *Caenorhabditis elegans* genes that can mutate to induce neuronal degeneration. *Nature*. 1991;349:588–593. [[PubMed: 1672038](#)]
487. Driscoll M, Chalfie M. Developmental and abnormal cell death in *C. elegans*. *Trends Neurosci.* 1992;15:15–19. [[PubMed: 1374952](#)]
488. Driscoll M, Dean E, Reilly E, Bergholz E, Chalfie M. Genetic and molecular analysis of a *Caenorhabditis elegans*  $\beta$ -tubulin that conveys benzimidazole sensitivity. *J. Cell Biol.* 1989;109:2993–3003. [[PMC free article: PMC2115974](#)] [[PubMed: 2592410](#)]
489. Dropkin V H. Introduction to plant nematology. New York: John Wiley; 1989. pp. 190–198.
490. Du H, Gu G, William C, Chalfie M. Extracellular proteins needed for *C. elegans* mechanosensation. *Neuron*. 1996;16:183–194. [[PubMed: 8562083](#)]
491. Dübendorfer A, Hilfiker-Kleiner D, Nöthiger R. Sex determination mechanisms in dipteran insects: The case of *Musca domestica*. *Semin. Dev. Biol.* 1992;3:349–356.
492. Duggal C L. Sex attraction in the free-living nematode *Panagrellus redivivus*. *Nematologica*. 1978;24:213–221.
493. Duhon S A, Johnson T E. Movement as an index of vitality: Comparing wild type and the *age-1* mutant of *Caenorhabditis elegans*. *J. Gerontol.* 1995;50:B254–261. [[PubMed: 7671016](#)]
494. Duhon S A, Murakami S, Johnson T E. Direct isolation of longevity mutants in the nematode *Caenorhabditis elegans*. *Dev. Genet.* 1996;18:114–153. [[PubMed: 8934876](#)]
495. Durbin R. "Studies on the development and organisation of the [nervous system](#) of *Caenorhabditis elegans*." [Ph.D. thesis]. University of Cambridge; England: 1987.
496. Dusenberry D B. Countercurrent separation: A new method for studying behavior of small aquatic organisms. *Proc. Natl. Acad. Sci.* 1973;70:1349–1352. [[PMC free article: PMC433494](#)] [[PubMed: 4514305](#)]
497. Dusenberry D B. Analysis of chemotaxis in the nematode *Caenorhabditis elegans* by countercurrent separation. *J. Exp. Zool.* 1974;188:41–47. [[PubMed: 4822548](#)]
498. Dusenberry D B. The avoidance of D-tryptophan by the nematode *Caenorhabditis elegans*. *J. Exp. Zool.* 1975;193:413–418. [[PubMed: 1176914](#)]
499. Dusenberry D B. Chemotactic behavior of mutants of the nematode *Caenorhabditis elegans* that are defective in their attraction to NaCl. *J. Exp. Zool.* 1976;198:343–352.
500. Dusenberry D B. Behavior of free-living nematodes. In: Zuckerman B M, editor. *Nematodes as biological models* vol. 1. New York: Academic Press; 1980a. pp. 127–158.
501. Dusenberry D B. Responses of the nematode *C. elegans* to controlled chemical stimulation. *J. Comp. Physiol.* 1980b;136:327–331.
502. Dusenberry D B, Barr J. Thermal limits and chemotaxis in mutants of the nematode *Caenorhabditis elegans* defective in thermotaxis. *J. Comp. Physiol.* 1980;137:353–356.
503. Dusenberry D B, Sheridan R E, Russell R L. Chemotaxis-defective mutants of the nematode *Caenorhabditis elegans*. *Genetics*. 1975;80:297–309. [[PMC free article: PMC1213328](#)] [[PubMed: 1132687](#)]
504. Dush M K, Martin G R. Analysis of mouse Evx genes: Evx-1 displays graded expression in the primitive streak. *Dev. Biol.* 1992;151:273–287. [[PubMed: 1349539](#)]

## E

505. Ebens A J, Garren H, Cheyette B N, Zipursky S L. The *Drosophila anachronism* locus, A glycoprotein secreted by glia inhibits neuroblast proliferation. *Cell.* 1993;74:15–27. [[PubMed: 7916657](#)]
506. Ebert R H II, Cherkasova V A, Dennis R A, Wu J H, Ruggles S, Perrin T E, Shmookler Reis R J. Longevity-determining genes in *Caenorhabditis elegans*: Chromosomal mapping of multiple noninteractive loci. *Genetics.* 1993;135:1003–1010. [[PMC free article: PMC1205733](#)] [[PubMed: 8307318](#)]
507. Echevarria F A M. Laboratory selection for ivermectin resistance in *Haemonchus contortus*. *Vet. Parasitol.* 1993;49:265–270. [[PubMed: 8249250](#)]
508. Eddy E M. Germ plasm and the differentiation of the germ line. *Int. Rev. Cytol.* 1975;43:229–280. [[PubMed: 770367](#)]
509. Edgar L G. "Control of spermatogenesis in the nematode *Caenorhabditis elegans*." [Ph. D. thesis]. University of Colorado; Boulder: 1982.
510. Edgar L G, McGhee J D. Embryonic expression of a gut-specific esterase in *Caenorhabditis elegans*. *Dev. Biol.* 1986;114:109–118. [[PubMed: 3956859](#)]
511. Edgar L G, McGhee J D. DNA synthesis and the control of embryonic gene expression in *C. elegans*. *Cell.* 1988;53:589–599. [[PubMed: 3131016](#)]
512. Edgar L G, Wolf N, Wood W B. Early transcription in *Caenorhabditis elegans* embryos. *Development.* 1994;120:443–451. [[PubMed: 7512022](#)]
513. Edgar R S, Wood W B. The nematode *C. elegans*: A new organism for intensive biological study. *Science.* 1977;198:1285–1286. [[PubMed: 9292051](#)]
514. Edgar R S, Cox G N, Kusch M, Politz J C. The cuticle of *Caenorhabditis elegans*. *J. Nematol.* 1982;14:248–258. [[PMC free article: PMC2618170](#)] [[PubMed: 19295706](#)]
515. Edgley M L, Riddle D L. The nematode *Caenorhabditis elegans*. In: O'Brien S J, editor. *Genetic maps:Locus maps of complex genomes* 6th edition. Cold Spring Harbor, New York: Cold Spring Harbor Laboratory Press; 1993. pp. 3281–3.
516. Edgley M L, Baillie D L, Riddle D L, Rose A M. Genetic balancers. *Methods Cell Biol.* 1995;48:147–184. [[PubMed: 8531724](#)]
517. Edmunds L N. Cellular and molecular bases of biological clocks. New York: Springer Verlag; 1988.
518. Edwards M K, Wood W B. Location of specific messenger RNAs in *Caenorhabditis elegans* by cytological hybridization. *Dev. Biol.* 1983;97:375–390. [[PubMed: 6343161](#)]
519. Eckman F H, Durbin R. ACeDB and Macace. *Methods Cell Biol.* 1995;48:583–605. [[PubMed: 8531744](#)]
520. Egan C R, Chung M A, Allen F L, Heschl M F P, Van Buskirk C L, McGhee J D. A gut-to- *pharynx/tail* switch in embryonic expression of the *Caenorhabditis elegans ges-1* gene centers on two GATA sequences. *Dev. Biol.* 1995;170:397–419. [[PubMed: 7649372](#)]
521. Egilmez N K, Shmookler Reis R J. Age-dependent somatic excision of transposable element Tc1 in *Caenorhabditis elegans*. *Mutat. Res.* 1994;316:17–24. [[PubMed: 7507565](#)]
522. Egilmez N K, Ebert II R H, Shmookler Reis R J. Strain evolution in *Caenorhabditis elegans*: Transposable elements as markers of interstrain evolutionary history. *J. Mol. Evol.* 1995;40:372–381. [[PubMed: 7769614](#)]
523. Eide D, Anderson P. The gene structures of spontaneous mutations affecting a *Caenorhabditis elegans* myosin heavy chain gene. *Genetics.* 1985a;109:67–79. [[PMC free article: PMC1202484](#)] [[PubMed: 2981757](#)]
524. Eide D, Anderson P. Transposition of Tc1 in the nematode *Caenorhabditis elegans*. *Proc. Natl. Acad. Sci.* 1985b;82:1756–1760. [[PMC free article: PMC397351](#)] [[PubMed: 2984668](#)]
525. Eide D, Anderson P. Novel insertion mutations in *Caenorhabditis elegans*. *Mol. Cell. Biol.* 1985c;5:1–6. [[PMC free article: PMC366670](#)] [[PubMed: 3982411](#)]
526. Eide D, Anderson P. Insertion and excision of *Caenorhabditis elegans* transposable element Tc1. *Mol. Cell. Biol.* 1988;8:737–746. [[PMC free article: PMC363199](#)] [[PubMed: 2832734](#)]
527. Einheber S, Fischman D A. Isolation and characterization of a cDNA encoding avian skeletal muscle C protein: An intracellular member of the immunoglobulin superfamily. *Proc. Natl. Acad. Sci.*

- 1990;87:2157–2161. [[PMC free article: PMC53645](#)] [[PubMed: 2315308](#)]
528. Eisen J S, Marder E. Mechanisms underlying pattern generation in lobster stomatogastric ganglion as determined by selective inactivation of identified neurons. III. Synaptic connections of electrically coupled pyloric neurons. *J. Neurophysiol.* 1982;48:1392–1415. [[PubMed: 6296329](#)]
529. Ellemberger T E, Brandl C J, Struhl K, Harrison S C. The GCN4 basic region leucine zipper binds DNA as a dimer of uninterrupted  $\alpha$  helices: Crystal structure of the protein-DNA complex. *Cell.* 1992;71:1223–1237. [[PubMed: 1473154](#)]
530. Ellis H M. "Genetic control of programmed cell death in the nematode *Caenorhabditis elegans*." [Ph.D. thesis]. Massachusetts Institute of Technology; Cambridge: 1985.
531. Ellis H M, Horvitz H R. Genetic control of programmed cell death in the nematode *C. elegans*. *Cell.* 1986;44:817–829. [[PubMed: 3955651](#)]
532. Ellis R E, Horvitz H R. Two *C. elegans* genes control the programmed deaths of specific cells in the pharynx. *Development.* 1991;112:591–603. [[PubMed: 1794327](#)]
533. Ellis R E, Kimble J. The *fog-3* gene and regulation of cell fate in the germ line of *Caenorhabditis elegans*. *Genetics.* 1995;139:561–577. [[PMC free article: PMC1206367](#)] [[PubMed: 7713418](#)]
534. Ellis R E, Jacobson D M, Horvitz H R. Genes required for the engulfment of cell corpses during programmed cell death in *Caenorhabditis elegans*. *Genetics.* 1991a;129:79–94. [[PMC free article: PMC1204584](#)] [[PubMed: 1936965](#)]
535. Ellis R E, Sulston J E, Coulson A R. The rDNA of *C. elegans*: Sequence and structure. *Nucleic Acids Res.* 1986;14:2345–2364. [[PMC free article: PMC339662](#)] [[PubMed: 3960722](#)]
536. Ellis R E, Yuan J, Horvitz H R. Mechanisms and functions of cell death. *Annu. Rev. Cell Biol.* 1991b;7:663–698. [[PubMed: 1809356](#)]
537. Emmons S W, Wood W B, editor. The nematode *Caenorhabditis elegans*. Cold Spring Harbor, New York: Cold Spring Harbor Laboratory; 1988. The genome. pp. 47–79.
538. Emmons S W. From cell fates to morphology: Developmental genetics of the *Caenorhabditis elegans* male tail. *BioEssays.* 1992;14:309–316. [[PubMed: 1637362](#)]
539. Emmons S W, Yesner L. High-frequency excision of transposable element Tc1 in the nematode *Caenorhabditis elegans* limited to somatic cells. *Cell.* 1984;36:599–605. [[PubMed: 6321037](#)]
540. Emmons S W, Klass M R, Hirsh D. Analysis of the constancy of DNA sequences during development and evolution of the nematode *Caenorhabditis elegans*. *Proc. Natl. Acad. Sci.* 1979;76:1333–1337. [[PMC free article: PMC383245](#)] [[PubMed: 286315](#)]
541. Emmons S W, Roberts S, Ruan K. Evidence in a nematode for regulation of transposon excision by tissue-specific factors. *Mol. Gen. Genet.* 1986;202:410–415. [[PubMed: 3012268](#)]
542. Emmons S W, Yesner L, Ruan K, Katzenberg D. Evidence for a transposon in *Caenorhabditis elegans*. *Cell.* 1983;32:55–65. [[PubMed: 6297788](#)]
543. Endo B Y, Wergin W P. Ultrastructural investigation of clover roots during early stages of infection by the root-knot nematode *Meloidogyne incognita*. *Protoplasma.* 1973;78:365–379.
544. Endo B Y, Wyss U. Ultrastructure of cuticular exudations in parasitic juvenile *Heterodera schachtii* as related to cuticle structure. *Protoplasma.* 1992;166:67–77.
545. Engel W K, Bishop D W, Cunningham G G. Tubular aggregates in type II muscle fibers: Ultrastructural and histochemical correlation. *J. Ultrastruct. Res.* 1970;31:507–525. [[PubMed: 4912968](#)]
546. Engelman A, Craigie R. Identification of conserved amino acid residues critical for human immunodeficiency virus type 1 integrase function *in vitro*. *J. Virol.* 1992;66:6361–6369. [[PMC free article: PMC240128](#)] [[PubMed: 1404595](#)]
547. Engels W R, Johnson-Schlitz D M, Eggleston W B, Sved J. High frequency P element loss in *Drosophila* is homolog dependent. *Cell.* 1990;62:515–525. [[PubMed: 2165865](#)]
548. Epstein H, Bernstein S. Genetic approaches to understanding muscle development. *Dev. Biol.* 1992;154:231–244. [[PubMed: 1426637](#)]
549. Epstein H, Fischman D. Molecular analysis of protein assembly in muscle development. *Science.* 1991;251:1039–1044. [[PubMed: 1998120](#)]

550. Epstein H F, Shakes D C. Methods in cell biology, vol. 48, *Caenorhabditis elegans*: Modern biological analysis of an organism. New York: Academic Press; 1995.
551. Epstein H F, Thomson J N. Temperature-sensitive mutation affecting myofilament assembly in *Caenorhabditis elegans*. *Nature*. 1974;250:579–580. [[PubMed: 4845659](#)]
552. Epstein H F, Casey D L, Ortiz I. Myosin and paramyosin of *Caenorhabditis elegans* embryos assemble into nascent structures distinct from thick filaments and multi-filament assemblages. *J. Cell Biol.* 1993;122:845–858. [[PMC free article: PMC2119588](#)] [[PubMed: 8349734](#)]
553. Epstein H F, Ortiz I, MacKinnon L A T. The alteration of myosin isoform compartmentation in specific mutants of *Caenorhabditis elegans*. *J. Cell Biol.* 1986;103:985–993. [[PMC free article: PMC2114276](#)] [[PubMed: 3745277](#)]
554. Epstein H F, Waterston R H, Brenner S. A mutant affecting the heavy chain of myosin in *Caenorhabditis elegans*. *J. Mol. Biol.* 1974;90:291–300. [[PubMed: 4453018](#)]
555. Epstein H F, Berliner G C, Casey D L, Ortiz I. Purified thick filaments from the nematode *Caenorhabditis elegans*: Evidence for multiple proteins associated with core structures. *J. Cell Biol.* 1988;106:1985–1995. [[PMC free article: PMC2115133](#)] [[PubMed: 3384852](#)]
556. Epstein H F, Miller 3rd D M, Ortiz I, Berliner G C. Myosin and paramyosin are organized about a newly identified core structure. *J. Cell Biol.* 1985;100:905–915. [[PMC free article: PMC2113503](#)] [[PubMed: 3972901](#)]
557. Epstein H F, Lu G Y, Deitiker P R, Ortiz I, Schmid M F. Preliminary three-dimensional model for nematode thick filament core. *J. Struct. Biol.* 1995;115:163–174. [[PubMed: 7577237](#)]
558. Erickson J, Eiden L, Hoffman B. Expression cloning of a reserpine-sensitive vesicular monoamine transporter. *Proc. Natl. Acad. Sci.* 1992;89:10993–10997. [[PMC free article: PMC50469](#)] [[PubMed: 1438304](#)]
559. Erickson J, Varoqui H, Schafer M, Modi W, Diebler M, Weihe E, Rand J, Eiden L, Bonner T, Usdin T. Functional identification of a vesicular acetylcholine transporter and its expression from a “cholinergic” gene locus. *J. Biol. Chem.* 1994;269:21929–21932. [[PubMed: 8071310](#)]
560. Escoubas J M, Prère M F, Fayet O, Salvignol I, Galas D, Zerbib D, Chandler M. Translational control of transposition activity of the bacterial insertion sequence IS1. *EMBO J.* 1991;10:705–712. [[PMC free article: PMC452705](#)] [[PubMed: 1848178](#)]
561. Estevez M, Attisano L, Wrana J L, Albert P S, Massagué J, Riddle D L. The *daf-4* gene encodes a bone morphogenetic protein receptor controlling *C. elegans* dauer larva development. *Nature*. 1993;365:644–649. [[PubMed: 8413626](#)]
562. Etemad-Moghadam B, Guo S, Kemphues K J. Asymmetrically distributed PAR-3 protein contributes to cell polarity and spindle alignment in early *C. elegans* embryos. *Cell*. 1995;83:743–752. [[PubMed: 8521491](#)]
563. Etter A, Aboutanos M, Tobler H, Müller F. Eliminated chromatin of *Ascaris* contains a gene that encodes a putative ribosomal protein. *Proc. Natl. Acad. Sci.* 1991;88:1593–1596. [[PMC free article: PMC51070](#)] [[PubMed: 2000367](#)]
564. Euling S, Ambros V. Heterochronic genes control cell cycle progress and developmental competence of *C. elegans* *vulva* precursor cells. *Cell*. 1996a;84:667–676. [[PubMed: 8625405](#)]
565. Euling S, Ambros V. Reversal of cell fate determination in *Caenorhabditis elegans* vulval development. *Development*. 1996b;122:2507–2515. [[PubMed: 8756295](#)]
566. Evans A A F, Perry R M. Survival strategies in nematodes. In: Croll N A, editor. The organization of nematodes. New York: Academic Press; 1976. pp. 383–424.
567. Evans R M. The steroid and thyroid hormone receptor superfamily. *Science*. 1988;240:889–895. [[PMC free article: PMC6159881](#)] [[PubMed: 3283939](#)]
568. Evans T C, Crittenden S L, Kodoyianni V, Kimble J. Translational control of maternal glp-1 mRNA establishes an asymmetry in the *C. elegans* embryo. *Cell*. 1994;77:183–194. [[PubMed: 8168128](#)]

## F

569. Fatt H V, Dougherty E C. Genetic control of differential heat tolerance in two strains of the nematode *Caenorhabditis elegans*. *Science*. 1963;141:266–267. [[PubMed: 17841565](#)]
570. Favre R, Hermann R, Cermola M, Hohenberg H, Muller M, Bazzicalupo P. Immunogold labelling of CUT-1, CUT-2 and cuticlin epitopes in *Caenorhabditis elegans* and *Heterorhabditis* sp. processed by high pressure freezing and freeze-substitution. *J. Submicrosc. Cytol. Pathol.* 1995;27:341–347. [[PubMed: 7545536](#)]
571. Fawcett D W. Bloom and Fawcett's textbook of histology 12th ed. Philadelphia: W.B. Saunders; 1994.
572. Fayet O, Ramond P, Polard P, Prére M F, Chandler M. Functional similarities between retroviruses and the IS3 family of bacterial insertion sequences? *Mol. Microbiol.* 1990;4:1771–1777. [[PubMed: 1963920](#)]
573. Fedoroff N V, Berg D E, Howe M M, editors. Mobile DNA. Washington, D.C.: American Society for Microbiology; 1989. Maize transposable elements. pp. 375–411.
574. Felsenstein J. Confidence limits on phylogenies: An approach utilizing the bootstrap. *Evolution*. 1985;39:783–791. [[PubMed: 28561359](#)]
575. Felsenstein J. Phylogenies from molecular sequences: Inference and reliability. *Annu. Rev. Genet.* 1988;22:521–565. [[PubMed: 3071258](#)]
576. Felsenstein J. PHYLIP: Phylogenetic inference package, version 3.5c. Seattle: University of Washington; 1993.
577. Felsenstein K M, Emmons S W. Structure and evolution of a family of interspersed repetitive DNA sequences in *C. elegans*. *J. Mol. Evol.* 1987;25:230–240. [[PubMed: 3118041](#)]
578. Ferguson E L, Horvitz H R. Identification and characterization of 22 genes that affect the vulval cell lineages of the nematode *Caenorhabditis elegans*. *Genetics*. 1985;110:17–72. [[PMC free article: PMC1202554](#)] [[PubMed: 3996896](#)]
579. Ferguson E L, Horvitz H R. The multivulva phenotype of certain *Caenorhabditis elegans* mutants results from defects in two functionally redundant pathways. *Genetics*. 1989;123:109–121. [[PMC free article: PMC1203774](#)] [[PubMed: 2806880](#)]
580. Ferguson E L, Sternberg P W, Horvitz H R. A genetic pathway for the specification of the vulval cell lineages of *Caenorhabditis elegans*. *Nature*. 1987;326:259–267. [[PubMed: 2881214](#)]
581. Ferguson K C, Heid P J, Rothman J H. The SL1 trans-spliced leader performs an essential embryonic function in *Caenorhabditis elegans* that can also be supplied by SL2 RNA. *Genes. Dev.* 1996;10:1543–1556. [[PubMed: 8666237](#)]
582. Ferreiro B, Kintner C, Zimmerman K, Anderson D, Harris W A. XASH genes promote neurogenesis in *Xenopusembryos*. *Development*. 1994;120:3649–3655. [[PubMed: 7821228](#)]
583. Ferro-Novick S, Novick P. The role of GTP-binding proteins in transport along the exocytic pathway. *Annu. Rev. Cell. Biol.* 1993;9:575–599. [[PubMed: 8280472](#)]
584. Fesenko E E, Kolesnikov S S, Lyubarsky A L. Induction by cGMP of cationic conductance in plasma membrane of retinal rod outer segment. *Nature*. 1985;313:310–313. [[PubMed: 2578616](#)]
585. Fetterer R H, Rhoads M L, Urban J F. Synthesis of tyrosine-derived cross-links in *Ascaris suum* cuticular proteins. *J. Parasitol.* 1993;79:160–166. [[PubMed: 8459325](#)]
586. Fichant G A, Burks C. Identifying potential tRNA genes in genomic DNA sequences. *J. Mol. Biol.* 1991;220:659–671. [[PubMed: 1870126](#)]
587. Field K G, Olsen G J, Land D J, Giovannoni S J, Ghiselin M T, Raff E C, Pace N C, Raff R A. Molecular phylogeny of the animal kingdom. *Science*. 1988;239:748–753. [[PubMed: 3277277](#)]
588. Fields C. Information content of *Caenorhabditis elegans* splice site sequences varies with intron length. *Nucleic Acids Res.* 1990;18:1509–1512. [[PMC free article: PMC330518](#)] [[PubMed: 2326191](#)]
589. Files J, Hirsh D. Ribosomal DNA of *C. elegans*. *J. Mol. Biol.* 1981;149:223–240. [[PubMed: 7310881](#)]
590. Files J, Carr S, Hirsh D. Actin gene family of *Caenorhabditis elegans*. *J. Mol. Biol.* 1983;164:355–375. [[PubMed: 6302275](#)]
591. Finer J T. Single myosin molecule mechanics: Piconewton forces and nanometre steps. *Nature*. 1994;368:113–119. [[PubMed: 8139653](#)]

592. Finney M. "The genetics and molecular biology of unc-86 a *C. elegans* cell lineage gene." [Ph.D. thesis]. Massachusetts Institute of Technology; Cambridge: 1987.
593. Finney M, Ruvkun G. The *unc-86* gene product couples cell lineage and cell identity in *C. elegans*. *Cell*. 1990;63:895–905. [[PubMed: 2257628](#)]
594. Finney M, Ruvkun G, Horvitz H R. The *C. elegans* cell lineage and differentiation gene *unc-86* encodes a protein with a homeodomain and extended similarity to transcription factors. *Cell*. 1988;55:757–769. [[PubMed: 2903797](#)]
595. Fire A. Integrative transformation of *Caenorhabditis elegans*. *EMBO J*. 1986;5:2673–2680. [[PMC free article: PMC1167168](#)] [[PubMed: 16453714](#)]
596. Fire A, Waterston R H. Proper expression of myosin genes in transgenic nematodes. *EMBO J*. 1989;8:3419–3428. [[PMC free article: PMC401492](#)] [[PubMed: 2583105](#)]
597. Fire A, Harrison S, Dixon D. A modular set of lacZ fusion vectors for studying gene expression in *Caenorhabditis elegans*. *Gene*. 1990;93:189–198. [[PubMed: 2121610](#)]
598. Fischer von Mollard G, Stahl B, Li C, Südhof T C, Jahn R. Rab proteins in regulated exocytosis. *Trends Biochem. Sci.* 1994;19:164–168. [[PubMed: 8016866](#)]
599. Fischman D A, Vaughan K, Weber F, Einheber S, Ozawa E, et al., editors. *Frontiers of muscle research; -> Muscle contraction and muscle dystrophy*. Amsterdam: Elsevier; 1991. Myosin binding proteins: Intracellular members of the immunoglobulin superfamily. pp. 211–222.
600. Fisk G, Thummel C. Isolation, regulation, and DNA-binding properties of three *Drosophila* nuclear hormone receptor superfamily members. *Proc. Natl. Acad. Sci.* 1995;92:10604–10608. [[PMC free article: PMC40660](#)] [[PubMed: 7479849](#)]
601. Finch C E. Longevity, senescence, and the genome. Illinois: University of Chicago Press; 1990.
602. Fitch D H A. Evolution of male tail development in rhabditid nematodes related to *Caenorhabditis elegans*. *Syst. Biol.* 1997;46:145–179. [[PubMed: 11975351](#)]
603. Fitch D H A, Emmons S W. Variable cell positions and cell contacts underlie morphological evolution of the rays in the male tails of nematodes related to *Caenorhabditis elegans*. *Dev. Biol.* 1995;170:564–582. [[PubMed: 7649384](#)]
604. Fitch D H A, Goodman M. Phylogenetic scanning: A computer-assisted algorithm for mapping gene conversions and other recombinational events. *Comp. Appl. Biosci.* 1991;7:207–215. [[PubMed: 2059846](#)]
605. Fitch D H A, Strausbaugh L D. Low codon bias and high rates of synonymous substitution in *Drosophila hydei* and *D. melanogaster* histone genes. *Mol. Biol. Evol.* 1993;10:397–413. [[PubMed: 8487638](#)]
606. Fitch D H A, Bugaj-Gaweda B, Emmons S W. 18S ribosomal RNA gene phylogeny for some Rhabditidae related to *Caenorhabditis*. *Mol. Biol. Evol.* 1995;12:346–358. [[PubMed: 7700158](#)]
607. Fitch W M. Toward defining the course of evolution: Minimal change for a specific tree topology. *Syst. Zool.* 1971;20:406–416.
608. Fitzgerald K, Greenwald I. Interchangeability of *Caenorhabditis elegans* DSL proteins and intrinsic signalling activity of their extracellular domains in vivo. *Development*. 1995;121:4275–4282. [[PubMed: 8575327](#)]
609. Fitzgerald K, Wilkinson H, Greenwald I. *glp-1* can substitute for *lin-12* in specifying cell fate decisions in *C. elegans*. *Development*. 1993;119:1019–1027. [[PubMed: 8306872](#)]
610. Fixsen W D. "The genetic control of hypodermal cell lineages during nematode development." [Ph.D. thesis]. Massachusetts Institute of Technology; Cambridge: 1985.
611. Fixsen W, Sternberg P, Ellis H, Horvitz R. Genes that affect cell fates during the development of *Caenorhabditis elegans*. *Cold Spring Harbor Symp. Quant. Biol.* 1985;50:99–104. [[PubMed: 3868513](#)]
612. Fleming J T, Tornoe C, Riina H A, Coadwell J, Lewis J A, Sattelle D B, Pichon Y, editor. *Comparative molecular neurobiology*. Basel: Birkhäuser Verlag; 1993. Acetylcholine receptor molecules of the nematode *Caenorhabditis elegans*. pp. 65–80. [[PubMed: 8422541](#)]
613. Fodor A, Deak P. The isolation and genetic analysis of a *Caenorhabditis elegans* translocation (*szT1*) strain bearing an X chromosome balancer. *J. Genet.* 1985;64:143–167.

614. Fodor A, Riddle D L, Nelson F K, Golden J W. Comparison of a new wild-type *Caenorhabditis briggsae* with laboratory strains of *C. briggsae* and *C. elegans*. *Nematologica*. 1983;29:203–217.
615. Foe V E, Alberts B M. Studies of nuclear and cytoplasmic behavior during the five mitotic cycles that precede gastrulation in *Drosophila* embryogenesis. *J. Cell Sci.* 1983;61:31–70. [[PubMed: 6411748](#)]
616. Foor W E. Spermatozoan morphology and [zygote](#) formation in nematodes.(suppl.) . *Biol. Reprod.* 1970;2:177–202. [[PubMed: 4939239](#)]
617. Foor W E, Adiyodi K G, Adiyodi R G, editors. *Reproductive biology of invertebrates II:Spermatogenesis and sperm function*. New York: John Wiley; 1983. Nematoda. pp. 221–256.
618. Fortini M, Artavanis-Tsakonas S. The *suppressor of hairless* protein participates in Notch receptor signaling. *Cell*. 1994;79:273–282. [[PubMed: 7954795](#)]
619. Francis G R, Waterston R H. Muscle organization in *Caenorhabditis elegans*: Localization of proteins implicated in thin filament attachment and I-band organization. *J. Cell Biol.* 1985;101:1532–1549. [[PMC free article: PMC2113919](#)] [[PubMed: 2413045](#)]
620. Francis R, Waterston R H. Muscle cell attachment in *Caenorhabditis elegans*. *J. Cell Biol.* 1991;114:465–479. [[PMC free article: PMC2289102](#)] [[PubMed: 1860880](#)]
621. Francis R, Maine E, Schedl T. Analysis of multiple roles of *gld-1* in germline development: Interactions with the sex determination cascade and the *glp-1* signaling pathway. *Genetics*. 1995a;139:607–630. [[PMC free article: PMC1206369](#)] [[PubMed: 7713420](#)]
622. Francis R, Barton M K, Kimble J, Schedl T. *gld-1*, a tumor suppressor gene required for oocyte development in *Caenorhabditis elegans*. *Genetics*. 1995b;139:579–606. [[PMC free article: PMC1206368](#)] [[PubMed: 7713419](#)]
623. Franz G, Savakis C. *Minos* a new transposable element from *Drosophila hydei*, is a member of the Tc1-like family of transposons. *Nucleic Acids Res.* 1991;19:6646. [[PMC free article: PMC329244](#)] [[PubMed: 1661410](#)]
624. Franz G, Loukeris T G, Dialetaki G, Thompson C R L, Savakis C. Mobile *Minos* elements from *Drosophila hydei* encode a two-exon transposase with similarity to the paired DNA-binding domain. *Proc. Natl. Acad. Sci.* 1994;91:4746–4750. [[PMC free article: PMC43865](#)] [[PubMed: 8197129](#)]
625. Freedman J H, Slice L W, Dixon D, Fire A, Rubin C S. The novel metallothionein genes of *Caenorhabditis elegans*. *J. Biol. Chem.* 1993;268:2554–2564. [[PubMed: 8428932](#)]
626. French A S. Mechanotransduction. *Annu. Rev. Physiol.* 1992;54:135–152. [[PubMed: 1373277](#)]
627. Freyd G. "Molecular analysis of the *Caenorhabditis elegans* cell lineage gene lin-11." [Ph.D. thesis]. Massachusetts Institute of Technology; Cambridge: 1991. [[PMC free article: PMC52683](#)] [[PubMed: 1924383](#)]
628. Freyd G, Kim S K, Horvitz H R. Novel cysteine-rich motif and homeodomain in the product of the *Caenorhabditis elegans* cell lineage gene *lin-11*. *Nature*. 1990;344:876–879. [[PubMed: 1970421](#)]
629. Freytag J W, Noelken M E, Hudson B G. Physical properties of collagen-sodium dodecyl sulfate complexes. *Biochemistry*. 1979;18:4761–4768. [[PubMed: 497168](#)]
630. Friedlander T P, Regier J C, Mitter C. Phylogenetic information content of five nuclear gene sequences in animals: Initial assessment of character sets from concordance and divergence studies. *Syst. Biol.* 1994;43:511–525.
631. Friedman D B, Johnson T E. A mutation in the *age-1* gene in *Caenorhabditis elegans* lengthens life and reduces hermaphrodite fertility. *Genetics*. 1988a;118:75–86. [[PMC free article: PMC1203268](#)] [[PubMed: 8608934](#)]
632. Friedman D B, Johnson T E. Three mutants that extend both mean and maximum life span of the nematode *Caenorhabditis elegans* define the *age-1* gene. *J. Gerontol.* 1988b;43:B102–109. [[PubMed: 3385139](#)]
633. Friedman P A, Platzer E G, Eby J E. Species differentiation in *C. briggsae* and *C. elegans*. *J. Nematol.* 1977;9:197–203. [[PMC free article: PMC2620237](#)] [[PubMed: 19305593](#)]
634. Fuchs G. Die naturgeschichte der nematoden und einiger anderer parasiten.. *Zool. Jahrb. Abt. System.* 1915;38

635. Fukushige T, Yasuda H, Siddiqui S S. Selective expression of the *tba-1* $\alpha$  tubulin gene in a set of mechanosensory and motor neurons during the development of *Caenorhabditis elegans*. *Biochim. Biophys. Acta.* 1995;1261:401–416. [[PubMed: 7742369](#)]
636. Fukushige T, Schroeder D F, Allen F L, Gosczynski B, McGhee J D. Modulation of gene expression in the embryonic digestive tract of *C. elegans*. *Dev. Biol.* 1996;178:276–288. [[PubMed: 8812129](#)]
637. Fujimoto D. Occurrence of dityrosine in cuticlin a structural protein from *Ascaris* cuticle. *Comp. Biochem. Physiol. B.* 1975;51:205–207.
638. Fujimoto D, Kanaya S. Cuticlin: A noncollagen structural protein from *Ascaris* cuticle. *Arch. Biochem. Biophys.* 1973;157:1–6. [[PubMed: 4352055](#)]
639. Fujimoto D, Horiuchi K, Hirama M. Isotryptyrosine, a new cross-linking amino acid isolated from *Ascaris* cuticle collagen. *Biochem. Biophys. Res. Commun.* 1981;99:637–643. [[PubMed: 7236289](#)]
640. Funk V A, Brooks D R. Phylogenetic systematics as the basis of comparative biology. Washington, D.C.: Smithsonian Institution Press; 1990.
641. Furst D O, Osborn M, Nave R, Weber K. The organization of titin filaments in the half-sarcomere revealed by monoclonal antibodies in immunoelectron microscopy: A map of ten nonrepetitive epitopes starting at the Z line extends close to the M line. *J. Cell Biol.* 1988;106:1563–1572. [[PMC free article: PMC2115059](#)] [[PubMed: 2453516](#)]
642. Furthmayr H, Timpl R. Characterization of collagen peptides by sodium dodecylsulfate-polyacrylamide electrophoresis. *Anal. Biochem.* 1971;41:510–516. [[PubMed: 4326447](#)]
643. Furukawa T, Kawaichi M, Matsunami N, Ryo H, Nishida Y, Honjo T. The *Drosophila* RBP-J $\kappa$  gene encodes the binding protein for the immunoglobulin J $\kappa$  recombination signal sequence. *J. Biol. Chem.* 1991;266:23334–23340. [[PubMed: 1744127](#)]
644. Futuyma D J. Evolutionary biology 2nd ed. Sunderland, Massachusetts: Sinauer Associates; 1986.
645. Fyrberg C, Labey S, Bullard B, Leonard K, Fyrberg E. *Drosophila* projectin: Relatedness to titin and twitchin and correlation with lethal(4) 102cda and bent-Dominant mutants. *Proc. R. Soc. Lond. B Biol. Sci.* 1992;249:33–40. [[PubMed: 1359548](#)]

## G

646. Gabius H -J, Graupner G, Cramer F. Activity patterns of aminoacyl-tRNA synthetases, tRNA methylases, arginyltransferase and tubulin: Tyrosine ligase during development and ageing of *Caenorhabditis elegans*. *Eur. J. Biochem.* 1983;131:231–234. [[PubMed: 6832143](#)]
647. Gallagher P J, Herring B P. The carboxyl terminus of the smooth muscle myosin light chain kinase is expressed as an independent protein telokin. *J. Biol. Chem.* 1991;266:23945–23952. [[PMC free article: PMC2836763](#)] [[PubMed: 1748667](#)]
648. Gamer L W, Wright C V. Murine Cdx-4 bears striking similarities to the *Drosophila* caudal gene in its homeodomain sequence and early expression pattern. *Mech. Dev.* 1993;43:71–81. [[PubMed: 7902125](#)]
649. Gao D, Kimble J. APX-1 can substitute for its homologue LAG-2 to direct cell interactions throughout *C. elegans* development. *Proc. Natl. Acad. Sci.* 1995;92:9839–9842. [[PMC free article: PMC40898](#)] [[PubMed: 7568229](#)]
650. Garcea R L, Schachat F, Epstein H F. Coordinate synthesis of two myosins in wild type and mutant nematode muscle during larval development. *Cell.* 1978;15:421–428. [[PubMed: 719748](#)]
651. Garcia E P, Gatti E, Butler M, Burton J, De Camilli P. A rat brain Sec1 homologue related to Rop and UNC18 interacts with syntaxin. *Proc. Natl. Acad. Sci.* 1994;91:2003–2007. [[PMC free article: PMC43297](#)] [[PubMed: 8134339](#)]
652. Garcia I, Martinou I, Tsujimoto Y, Martinou J -C. Prevention of programmed cell death of sympathetic neurons by the *bcl-2* proto-oncogene. *Science.* 1992;258:302–304. [[PubMed: 1411528](#)]
653. García-Añoveros J. "Genetic analysis of degenerin proteins in *Caenorhabditis elegans*." [Ph.D. thesis]. Columbia University; New York: 1995.

654. García-Añoveros J, Ma C, Chalfie M. Regulation of *Caenorhabditis elegans* degenerin proteins by a putative extracellular domain. *Curr. Biol.* 1995;5:441–448. [[PubMed: 7627559](#)]
655. Garcia-Fernández J, Baguñà J, Saló E. Planarian homeobox genes: Cloning, sequence analysis, and expression. *Proc. Natl. Acad. Sci.* 1991;88:7338–7342. [[PMC free article: PMC52290](#)] [[PubMed: 1714599](#)]
656. Garcia-Fernández J, Marfany G, Baguñà J, Saloacute;--> E. Infiltration of mariner elements. *Nature.* 1993;364:109. [[PubMed: 8391644](#)]
657. Garriga G, Stern M J. Hams and Egl: Genetic analysis of cell migration in *Caenorhabditis elegans*. *Curr. Opin. Genet. Dev.* 1994;4:575–580. [[PubMed: 7950326](#)]
658. Garriga G, Desai C, Horvitz H R. Cell interactions control the direction of outgrowth, branching and fasciculation of the HSN axons of *Caenorhabditis elegans*. *Development.* 1993a;117:1071–1087. [[PubMed: 8325236](#)]
659. Garriga G, Guenther C, Horvitz H R. Migrations of the *Caenorhabditis elegans* HSNs are regulated by *egl-43*, a gene encoding two zinc finger proteins. *Genes Dev.* 1993b;7:2097–2109. [[PubMed: 8224840](#)]
660. Garriga G, Guenther C, Horvitz H R. Migrations of the *Caenorhabditis elegans* HSNs are regulated by *egl-43* a gene encoding two zinc finger proteins. *Genes Dev.* 1993c;7:2097–2109. [[PubMed: 8224840](#)]
661. Garrity P A, Zipursky S L. Neuronal target recognition. *Cell.* 1995;83:177–185. [[PubMed: 7585935](#)]
662. Garrod D. Desmosomes and hemidesmosomes. *Curr. Opin. Cell Biol.* 1993;5:30–40. [[PubMed: 8448028](#)]
663. Gaudet J, VanderElst I, Spence A M. Post-transcriptional regulation of sex determination in *Caenorhabditis elegans*: Widespread expression of the sex-determining gene *fem-1* in both sexes. *Mol. Biol. Cell.* 1996;7:1107–1121. [[PMC free article: PMC275962](#)] [[PubMed: 8862524](#)]
664. Gaugler R, Kaya H. The entomopathogenic nematodes in biological control. Boca Raton: CRC Press; 1990.
665. Gautel M, Leonard K, Labeit S. Phosphorylation of KSP motifs in the C-terminal region of titin in differentiation myoblasts. *EMBO J.* 1993;12:3827–3834. [[PMC free article: PMC413666](#)] [[PubMed: 8404852](#)]
666. Geary T G, Blair K L, Ho N F H, Sims S M, Thompson D P, Boothroyd J C, Komuniecki R, editors. Molecular approaches to parasitology. New York: Wiley-Liss; 1995. Biological functions of nematode surfaces. pp. 191–205.
667. Geary T G, Sims S M, Thomas E M, Vanover L, Davis J P, Winterrowd C A, Klein R D, Ho N F H, Thompson D P. *Haemonchus contortus*: Ivermectin-induced paralysis of the [pharynx](#). *Exp. Parasitol.* 1993;77:88–96. [[PubMed: 8344410](#)]
668. Gems D, Riddle D L. Longevity in *Caenorhabditis elegans* reduced by mating but not gamete production. *Nature.* 1996;379:723–725. [[PubMed: 8602217](#)]
669. Gems D G, Ferguson C J, Robertson B D, Nieves R, Page A P, Blaxter M L, Maizels R M. An abundant trans-spliced mRNA from *Toxocara canis* infective larvae encodes a 26-kDa protein with homology to phosphatidylethanolamine binding proteins. *J. Biol. Chem.* 1995;270:18517–18522. [[PubMed: 7629180](#)]
670. Gendreau S B, Moskowitz I P G, Terns R M, Rothman J H. The potential to differentiate epidermis is unequally distributed in the [AB lineage](#) during early embryonic development in *Caenorhabditis elegans*. *Dev. Biol.* 1994;166:770–781. [[PubMed: 7813794](#)]
671. Gengyo-Ando K, Kagawa H. Single charge change on the helical surface of the paramyosin rod dramatically disrupts thick filament assembly in *Caenorhabditis elegans*. *J. Mol. Biol.* 1991;219:429–441. [[PubMed: 2051482](#)]
672. Gengyo-Ando K, Kamiya Y, Yamakawa A, Kodaira K, Nishiwaki K, Miwa J, Hori I, Hosono R. The *C. elegans unc-18* gene encodes a protein expressed in motor neurons. *Neuron.* 1993;11:703–711. [[PubMed: 8398155](#)]
673. Georgi L, Albert P S, Riddle D L. *daf-1*, a *C. elegans* gene controlling dauer larva development, encodes a novel receptor protein kinase. *Cell.* 1990;61:635–645. [[PubMed: 2160853](#)]

674. Geppert M, Bolshakov V Y, Siegelbaum S A, Takei K, De Camilli P, Hammer R E, Südhof T C. The role of Rab3A in neurotransmitter release. *Nature*. 1994a;369:493–497. [[PubMed: 7911226](#)]
675. Geppert M, Goda Y, Hammer R E, Li C, Rosahl T W, Stevens C F, Südhof T C. Synaptotagmin I: A major  $\text{Ca}^{2+}$  sensor for transmitter release at a central synapse. *Cell*. 1994b;79:717–727. [[PubMed: 7954835](#)]
676. Gething M J, Sambrook J. Protein folding in the cell. *J. Cell Biol.* 1992;355:33–45. [[PubMed: 1731198](#)]
677. Getting P A, Cohen A H, et al., editors. Neural control of rhythmic movements. New York: John Wiley; 1988. Comparative analysis of invertebrate central pattern generators. pp. 101–128.
678. Getting P A. Emerging principles governing the operation of [neural](#) networks. *Annu. Rev. Neurosci.* 1989;12:185–204. [[PubMed: 2648949](#)]
679. Gettner S N, Kenyon C, Reichardt L F. Characterization of *beta-pat-3* heterodimers, a family of essential integrin receptors in *C. elegans*. *J. Cell Biol.* 1995;129:1127–1141. [[PMC free article: PMC2120502](#)] [[PubMed: 7744961](#)]
680. Gilbert M, Starck J, Beguet B. Role of the gonad cytoplasmic core during oogenesis of the nematode *Caenorhabditis elegans*. *Biol. Cell*. 1984;50:77–85. [[PubMed: 6234041](#)]
681. Gierl A, Lutnicke S, Saedler H. TnpA product encoded by the transposable element En-1 of *Zea mays* is a DNA binding protein. *EMBO J.* 1988;7:4045–4053. [[PMC free article: PMC455112](#)] [[PubMed: 2854053](#)]
682. Giese K, Cox J, Grosschedl R. The HMG domain of lymphoid enhancer factor 1 bends DNA and facilitates assembly of functional nucleoprotein structures. *Cell*. 1992;69:185–195. [[PubMed: 1555239](#)]
683. Giglio M P, Hunter T, Bannister J V, Bannister W H, Hunter G J. The manganese superoxide dismutase gene of *Caenorhabditis elegans*. *Biochem. Mol. Biol. Int.* 1994;33:37–40. [[PubMed: 8081211](#)]
684. Gilbert M A, Starck J, Beguet B. Role of the gonad cytoplasmic core during oogenesis of the nematode *Caenorhabditis elegans*. *Biol. Cell*. 1984;50:77–85. [[PubMed: 6234041](#)]
685. Gilchrist E J, Moerman D G. Mutations in the *sup-38* gene of *Caenorhabditis elegans* suppress muscle-attachment defects in *unc-52* mutants. *Genetics*. 1992;132:431–442. [[PMC free article: PMC1205147](#)] [[PubMed: 1427037](#)]
686. Glazer I, Gaugler R, Segal D. Genetics of the nematode *Heterorhabditis bacteriophora* strain HP88: The diversity of beneficial traits. *J. Nematol.* 1991;23:324–333. [[PMC free article: PMC2619164](#)] [[PubMed: 19283134](#)]
687. Gochnauer M B, McCoy E. Responses of a soil nematode *Rhabditis briggsae* to antibiotics. *J. Exp. Zool.* 1954;125:377–406.
688. Goday C, Pimpinelli S. The occurrence role and evolution of chromatin diminution in nematodes. *Parasitol. Today*. 1993;9:319–322. [[PubMed: 15463793](#)]
689. Goddard J M, Weiland J J, Capecchi M R. Isolation and characterization of *Caenorhabditis elegans* DNA sequences homologous to the *v-abl* oncogene. *Proc. Natl. Acad. Sci.* 1986;83:2172–2176. [[PMC free article: PMC323253](#)] [[PubMed: 3457381](#)]
690. Goetinck S, Waterston R H. The *Caenorhabditis elegans* UNC-87 protein is essential for the maintenance but not assembly, of bodywall muscle. *J. Cell Biol.* 1994a;127:71–78. [[PMC free article: PMC2120180](#)] [[PubMed: 7929572](#)]
691. Goetinck S, Waterston R H. The *Caenorhabditis elegans* muscle-affecting gene *unc-87* encodes a novel thin filament-associated protein. *J. Cell Biol.* 1994b;127:79–93. [[PMC free article: PMC2120179](#)] [[PubMed: 7929573](#)]
692. Goff S P. Genetics of retroviral integration. *Annu. Rev. Genet.* 1992;26:527–544. [[PubMed: 1482125](#)]
693. Goh P, Bogaert T. Positioning and maintenance of embryonic [body wall muscle](#) attachments in *C. elegans* requires the *mup-1* gene. *Development*. 1991;111:667–681. [[PubMed: 1879334](#)]
694. Goldberg J. Worm mapping. *Discover*. 1991;12:22.
695. Golden J W, Riddle D L. A pheromone influences larval development in the nematode *Caenorhabditis elegans*. *Science*. 1982;218:578–580. [[PubMed: 6896933](#)]
696. Golden J W, Riddle D L. A pheromone-induced developmental switch in *Caenorhabditis elegans*: Temperature-sensitive mutants reveal a wild-type temperature-dependent process. *Proc. Natl. Acad.*

- Sci. 1984a;81:819–823. [PMC free article: PMC344929] [PubMed: 6583682]
697. Golden J W, Riddle D L. The *Caenorhabditis elegans* dauer larva: Developmental effects of pheromone, food, and temperature. Dev. Biol. 1984b;102:368–378. [PubMed: 6706004]
698. Golden J W, Riddle D L. A *Caenorhabditis elegans* dauer-inducing pheromone and an antagonistic component of the food supply. J. Chem. Ecol. 1984c;10:1265–1280. [PubMed: 24318910]
699. Golden J W, Riddle D L. A gene affecting production of the *C. elegans* dauer-inducing pheromone. Mol. Gen. Genet. 1985;198:534–536. [PubMed: 3859733]
700. Goldstein B. Induction of gut in *Caenorhabditis elegans* embryos. Nature. 1992;357:255–257. [PubMed: 1589023]
701. Goldstein B. Establishment of gut fate in the *E* lineage of *C. elegans*: The roles of lineage-dependent mechanisms and cell interactions. Development. 1993;118:1267–1277. [PubMed: 8269853]
702. Goldstein B. Cell contacts orient some division axes in the *Caenorhabditis elegans* embryo. J. Cell Biol. 1995a;129:1071–1080. [PMC free article: PMC2120481] [PubMed: 7744956]
703. Goldstein B. An analysis of the response to gut induction in the *C. elegans* embryo. Development. 1995b;121:1227–1236. [PubMed: 7743934]
704. Goldstein B, Hird S N. Specification of the anteroposterior axis in *C. elegans*. Development. 1996;122:1467–1474. [PubMed: 8625834]
705. Goldstein B, Hird S N, White J G. Cell polarity in early *C. elegans* development., pp. Dev. Suppl. 1993:279–287. [PubMed: 8049483]
706. Goldstein P. The synaptonemal complexes of *Caenorhabditis elegans*: Pachytene karyotype analysis of male and hermaphrodite wild-type and *him* mutants. Chromosoma. 1982;86:577–593. [PubMed: 7172867]
707. Goldstein P. Triplo-X hermaphrodite of *Caenorhabditis elegans*: Pachytene karyotype analysis, synaptonemal complexes, and pairing mechanisms. Can. J. Genet. Cytol. 1984;26:13–17.
708. Goldstein P. The synaptonemal complexes of *Caenorhabditis elegans*: The dominant *him* mutant *mnT6* and pachytene karyotype analysis of the X-autosome translocation. Chromosoma. 1986;93:256–260. [PubMed: 3948601]
709. Goldstein P, Slaton D E. The synaptonemal complexes of *Caenorhabditis elegans*: comparison of wild-type and mutant strains and pachytene karyotype analysis of wild-type. Chromosoma. 1982;84:585–597. [PubMed: 7075356]
710. Goodall G J, Filipowicz W. The AU-rich sequences present in the introns of plant nuclear pre-mRNAs are required for splicing. Cell. 1989;58:473–483. [PubMed: 2758463]
711. Goodier J L, Davidson W S. Tc1 transposon-like sequences are widely distributed in salmonids. J. Mol. Biol. 1994;241:26–34. [PubMed: 8051704]
712. Goodman C S. The likeness of being: Phylogenetically conserved molecular mechanisms of growth cone guidance. Cell. 1994;78:353–356. [PubMed: 8062381]
713. Goodwin E B, Okkema P G, Evans T C, Kimble J. Translational regulation of *tra-2* by its 3' untranslated region controls sexual identity in *Caenorhabditis elegans*. Cell. 1993;75:329–339. [PubMed: 8402916]
714. Goshima Y, Nakamura F, Strittmatter P, Strittmatter S M. Collapsin-induced growth cone collapse mediated by an intracellular protein related to UNC-33. Nature. 1995;376:509–514. [PubMed: 7637782]
715. Gossett L A, Hecht R, Epstein H F. Muscle differentiation in normal and cleavage-arrested mutant embryos of *Caenorhabditis elegans*. Cell. 1982;30:193–204. [PubMed: 7127470]
716. Gossett L A, Kelvin D J, Sternberg E A, Olson E N. A new myocyte-specific enhancer binding factor that recognizes a conserved element associated with multiple muscle-specific genes. Mol. Cell. Biol. 1989;9:5022–5033. [PMC free article: PMC363654] [PubMed: 2601707]
717. Gottlieb S, Ruvkun G. *daf-2* *daf-16* and *daf-23*: Genetically interacting genes controlling dauer formation in *Caenorhabditis elegans*. Genetics. 1994;137:107–120. [PMC free article: PMC1205929] [PubMed: 8056303]
718. Gould A P, White R A H. *Connectin* a target of homeotic gene control in *Drosophila*. Development. 1992;116:1163–1174. [PubMed: 1363542]

719. Gould S J. Ontogeny and phylogeny. Cambridge, Massachusetts: Belknap Press; 1977.
720. Gouy M, Gautier C, Attimonelli M, Lanave C, Di Paola G. ACNUC—A portable retrieval system for nucleic acid sequence databases: Logical and physical designs and usage. *Comput. Appl. Biosci.* 1985;1:167–172. [[PubMed: 3880341](#)]
721. Graham P, Kimble J. The *mog-1* gene is required for the switch from spermatogenesis to oogenesis in *Caenorhabditis elegans*. *Genetics*. 1993;133:919–931. [[PMC free article: PMC1205409](#)] [[PubMed: 8462850](#)]
722. Graham P L, Schedl T, Kimble J. More *mog* genes that influence the switch from spermatogenesis to oogenesis in the hermaphrodite germ line of *Caenorhabditis elegans*. *Dev. Genet.* 1993;14:471–484. [[PubMed: 8111975](#)]
723. Graham R W, Jones D, Candido E P M. UbiA, the major ubiquitin locus in *Caenorhabditis elegans*, has unusual structural features and is constitutively expressed. *Mol. Cell. Biol.* 1989;9:268–277. [[PMC free article: PMC362169](#)] [[PubMed: 2538720](#)]
724. Granato M, Schnabel H, Schnabel R. Genesis of an organ: Molecular analysis of the *pha-1* gene. *Development*. 1994;120:3005–3017. [[PubMed: 7607088](#)]
725. Grant B D, Greenwald I. The *Caenorhabditis elegans sel-1* gene a negative regulator of *lin-12* and *glp-1*, encodes a predicted extracellular protein. *Genetics*. 1996;143:237–247. [[PMC free article: PMC1207257](#)] [[PubMed: 8722778](#)]
726. Gray N F. Diseases of nematodes (ed. G.O. Poinar and H.-B. Jansson) vol. II, Boca Raton, Florida: CRC Press; 1988. pp. 3–38.
727. Green P, Lipman D, Hillier L, Waterston R H, States D, Claverie J M. Ancient conserved regions in new gene sequences and the protein databases. *Science*. 1993;259:1711–1716. [[PubMed: 8456298](#)]
728. Greenough W T, Bailey C H. The anatomy of a memory: Convergence of results across a diversity of tests. *Trends Neurosci.* 1988;11:142–147.
729. Greenstein D, Hird S, Plasterk R H A, Andachi Y, Kohara Y, Wang B, Finney M, Ruvkun G. Targeted mutations in the *Caenorhabditis elegans* POU homeo box gene *ceh-18*cause defects in oocyte cell cycle arrest, gonad migration, and epidermal differentiation. *Genes Dev.* 1994;8:1935–1948. [[PubMed: 7958868](#)]
730. Greenwald I. *lin-12* a nematode homeotic gene, is homologous to a set of mammalian proteins that include epidermal growth factor. *Cell*. 1985;43:583–590. [[PubMed: 3000611](#)]
731. Greenwald I. Structure/function studies of LIN-12/Notch proteins. *Curr. Opin. Genet. Dev.* 1994;4:556–562. [[PubMed: 7950324](#)]
732. Greenwald I S, Horvitz H R. *unc-93(e1500)*: A behavioral mutant of *Caenorhabditis elegans* that defines a gene with a wild-type null phenotype. *Genetics*. 1980;96:147–164. [[PMC free article: PMC1214286](#)] [[PubMed: 6894129](#)]
733. Greenwald I S, Horvitz H R. Dominant suppressors of a muscle mutant define an essential gene of *Caenorhabditis elegans*. *Genetics*. 1982;101:211–225. [[PMC free article: PMC1201857](#)] [[PubMed: 7173602](#)]
734. Greenwald I S, Horvitz H R. A visible allele of the muscle gene *sup-10 X* of *C. elegans*. *Genetics*. 1986;113:63–72. [[PMC free article: PMC1202801](#)] [[PubMed: 3710144](#)]
735. Greenwald I, Seydoux G. Analysis of gain-of-function mutations of the *lin-12* gene of *Caenorhabditis elegans*. *Nature*. 1990;346:197–199. [[PubMed: 2164160](#)]
736. Greenwald I S, Sternberg P W, Horvitz H R. The *lin-12* locus specifies cell fates in *Caenorhabditis elegans*. *Cell*. 1983;34:435–444. [[PubMed: 6616618](#)]
737. Greenwald I S, Coulson A R, Sulston J E, Priess J R. Correlation of the physical and genetic maps in the *lin-12*region of *C. elegans*. *Nucleic Acids Res.* 1987;15:2295–2307. [[PMC free article: PMC340635](#)] [[PubMed: 2882468](#)]
738. Grenache D G, Caldicott I, Albert P S, Riddle D L, Politz S M. Environmental induction and genetic control of surface antigen switching in the nematode *Caenorhabditis elegans*. *Proc. Natl. Acad. Sci.* 1996;93:12388–12393. [[PMC free article: PMC38001](#)] [[PubMed: 8901591](#)]

739. Grewal P S. Relative contribution of nematodes (*Caenorhabditis elegans*) and bacteria towards the disruption of flushing patterns and losses in yield and quality of mushrooms (*Agaricus bisporus*). Ann. Appl. Biol. 1991;119:483–499.
740. Grobben K. Die systematische Einteilung des Tierreiches. Verh. K. Zool. Bot. Ges. Wien. 1908;58:491–511.
741. Groenen M A M, Timmers E, van der Putte P. DNA sequences at the ends of the genome of bacteriophage MU essential for transposition. Proc. Natl. Acad. Sci. 1985;82:2087–2091. [PMC free article: PMC397497] [PubMed: 2984681]
742. Gross R E, Bagchi S, Lu X, Rubin C S. Cloning, characterization and expression of the gene for the catalytic subunit of cAMP-dependent protein kinase in *Caenorhabditis elegans*. J. Biol. Chem. 1990;265:6896–6907. [PubMed: 2324104]
743. Grosschedl R, Giese K, Pagel J. HMG domain proteins: Architectural elements in the assembly of nucleoprotein structures. Trends Genet. 1994;10:94–100. [PubMed: 8178371]
744. Groves P M, Thompson R F. Habituation: A dual process theory. Psychol. Rev. 1970;77:419–450. [PubMed: 4319167]
745. Gruss P, Walther C. Pax in development. Cell. 1992;69:719–722. [PubMed: 1591773]
746. Gu G, Caldwell G A, Chalfie M. Genetic interactions affecting touch sensitivity in *Caenorhabditis elegans*. Proc. Natl. Acad. Sci. 1996;93:6577–6582. [PMC free article: PMC39067] [PubMed: 8692859]
747. Guastella J, Stretton A O W. Distribution of H-3-GABA uptake sites in the nematode *Ascaris*. J. Comp. Neurol. 1991;307:598–608. [PubMed: 1869634]
748. Guastella J, Johnson C D, Stretton A O W. GABA-immunoreactive neurons in the nematode *Ascaris*. J. Comp. Neurol. 1991;307:584–597. [PubMed: 1869633]
749. Guillermot F, Lo L C, Johnson J E, Auerbach A, Anderson D J, Joyner A L. Mammalian *achaete-scute* homolog 1 is required for the early development of olfactory and autonomic neurons. Cell. 1993;75:463–476. [PubMed: 8221886]
750. Guo C B. "mig-5: A gene that controls cell fate determination and cell migration in *C. elegans* is a member of the dsh family." [Ph.D. thesis]. Johns Hopkins University; Baltimore, Maryland: 1995.
751. Guo S, Kemphues K J. *par-1*, a gene required for establishing polarity in *C. elegans* embryos, encodes a putative Ser/Thr kinase that is asymmetrically distributed. Cell. 1995;81:611–620. [PubMed: 7758115]
752. Guo X D, Kramer J M. The two *Caenorhabditis elegans* basement membrane (type IV) collagen genes are located on separate chromosomes. J. Biol. Chem. 1989;264:17574–17582. [PubMed: 2793871]
753. Guo X, Johnson J J, Kramer J M. Embryonic lethality caused by mutations in basement membrane collagen of *C. elegans*. Nature. 1991;349:707–709. [PubMed: 1996137]

## H

754. Haack H, Hodgkin J. Tests for parental imprinting in the nematode *Caenorhabditis elegans*. Mol. Gen. Genet. 1991;228:482–485. [PubMed: 1896016]
755. Haecker G, Vaux D L. A sticky business. Curr. Biol. 1995;5:622–624. [PubMed: 7552172]
756. Hagiwara S, Byerly L. Calcium channel. Annu. Rev. Neurosci. 1981;4:69–125. [PubMed: 6261668]
757. Halder G, Callaerts P, Gehring W J. Induction of ectopic eyes by targeted expression of the eyeless gene in *Drosophila*. Science. 1995;267:1788–1792. [PubMed: 7892602]
758. Hall B K. Evolutionary developmental biology. London: Chapman and Hall; 1992.
759. Hall B K. Introduction. In: Hall B K, editor. Homology: The hierarchical basis of comparative biology. San Diego: Academic Press; 1994. pp. 1–19.
760. Hall B K. Homology and embryonic development. In: Hecht M K, et al., editors. Evolutionary biology. New York: Plenum Press; 1995. pp. 1–37.
761. Hall D H, Hedgecock E M. Kinesin-related gene *unc-104* is required for axonal transport of synaptic vesicles in *C. elegans*. Cell. 1991;65:837–847. [PubMed: 1710172]

762. Hall D H, Russell R L. The posterior [nervous system](#) of the nematode *Caenorhabditis elegans*: Serial reconstruction of identified neurons and complete pattern of synaptic interactions. *J. Neurosci.* 1991;11:1–22. [[PMC free article: PMC6575198](#)] [[PubMed: 1986064](#)]
763. Hall D H, Gu G, Garcia-Anoveros J, Gong L, Chalfie M, Driscoll M. Neuropathology of degenerative cell death in *Caenorhabditis elegans*. *J. Neurosci.* 1997;17:1033–1045. [[PMC free article: PMC6573168](#)] [[PubMed: 8994058](#)]
764. Hall J C. Genetics of circadian rhythms. *Annu. Rev. Genet.* 1990;24:659–697. [[PubMed: 2088180](#)]
765. Hall J, Kankel D. Genetics of acetylcholinesterase in *Drosophila melanogaster*. *Genetics*. 1976;83:517–535. [[PMC free article: PMC1213530](#)] [[PubMed: 821817](#)]
766. Hamelin M, Scott I M, Way J C, Culotti J G. The *mec-7* Beta-tubulin gene of *Caenorhabditis elegans* expressed primarily in the [touch receptor neurons](#). *EMBO J.* 1992;11:2885–2893. [[PMC free article: PMC556769](#)] [[PubMed: 1639062](#)]
767. Hamelin M, Zhou Y, Su M W, Scott I M, Culotti J G. Expression of the UNC-5 guidance receptor in the touch neurons of *C. elegans* steers their axons dorsally. *Nature*. 1993;364:327–330. [[PubMed: 8332188](#)]
768. Han M, Sternberg P W. *let-60* a gene that specifies cell fates during *C. elegans* vulval induction, encodes a ras protein. *Cell*. 1990;63:921–931. [[PubMed: 2257629](#)]
769. Han M, Sternberg P W. Analysis of dominant-negative mutations of the *Caenorhabditis elegans let-60 ras* gene. *Genes Dev.* 1991;5:2188–2198. [[PubMed: 1748278](#)]
770. Han M, Aroian R V, Sternberg P W. The *let-60* locus controls the switch between vulval and nonvulval cell fates in *Caenorhabditis elegans*. *Genetics*. 1990;126:899–913. [[PMC free article: PMC1204287](#)] [[PubMed: 2076820](#)]
771. Han M, Golden A, Han Y, Sternberg P W. *C. elegans lin-45 raf* gene participates in *let-60ras*-stimulated vulval differentiation. *Nature*. 1993;363:133–140. [[PubMed: 8483497](#)]
772. Hannon G J, Maroney P A, Nilsen T W. U small nuclear ribonucleoprotein requirements for nematode *cis*- and *trans*- splicing *in vitro*. *J. Biol. Chem.* 1991;266:22792–22695. [[PubMed: 1835972](#)]
773. Hannon G J, Maroney P A, Denker J A, Nilsen T W. *Trans* splicing of nematode pre-messenger RNA *in vitro*. *Cell*. 1990a;61:1247–1255. [[PubMed: 2163760](#)]
774. Hannon G J, Maroney P A, Ayers D G, Shambaugh J D, Nilsen T W. Transcription of a nematode trans-spliced leader RNA requires internal elements for both initiation and 3'end-formation. *EMBO J.* 1990b;9:1915–1922. [[PMC free article: PMC551899](#)] [[PubMed: 2347310](#)]
775. Hannon G J, Maroney P A, Yu Y -T, Hannon G E, Nilsen T W. Interaction of U6 snRNA with a sequence required for function of the nematode SL RNA in *trans*-splicing. *Science*. 1992;258:1775–1780. [[PubMed: 1465612](#)]
776. Hansson J H, Nelson-Williams C, Suzuki H, Schild L, Shimkets R, Lu Y, Canessa C, Iwasaki T, Rossier B C, Lifton R P. Hypertension caused by a truncated epithelial sodium channel γ subunit: Genetic heterogeneity of Liddle syndrome. *Nature Genet.* 1995;11:76–82. [[PubMed: 7550319](#)]
777. Harley C B, Futcher A B, Greider C W. Telomeres shorten during aging of human fibroblasts. *Nature*. 1990;345:458–460. [[PubMed: 2342578](#)]
778. Harrington W F. Contractile proteins in muscle. In: Neurath H, editor. *The proteins* vol. 3, New York: Academic Press; 1979. pp. 246–409.
779. Harris H E, Tso M W, Epstein H F. Actin and myosin-linked calcium regulation in the nematode *Caenorhabditis elegans*. Biochemical and structural properties of native filaments and purified proteins. *Biochemistry*. 1977;16:859–865. [[PubMed: 139159](#)]
780. Harris J E, Crofton H D. Structure and function in the nematodes: Internal pressure and cuticular structure in *Ascaris*. *J. Exp. Biol.* 1957;34:116–130.
781. Harris J, Honigberg L, Robinson N, Kenyon C. Neuronal cell migration in *C. elegans*: Regulation of Hox gene expression and cell position. *Development*. 1996;122:3117–3131. [[PubMed: 8898225](#)]
782. Harris L J, Rose A M. Somatic excision of transposable element Tc1 from the Bristol genome of *Caenorhabditis elegans*. *Mol. Cell. Biol.* 1986;6:1782–1786. [[PMC free article: PMC367707](#)] [[PubMed: 3023903](#)]

783. Harris L J, Baillie D L, Rose A M. Sequence identity between an inverted repeat family of transposable elements in *Drosophila* and *Caenorhabditis*. Nucleic Acids Res. 1988;16:5991–5998. [[PMC free article: PMC336842](#)] [[PubMed: 2840637](#)]
784. Harrison S D, Broadie K, van de Goor J, Rubin G M. Mutations in the *Drosophila Rop* gene suggest a function in general secretion and synaptic transmission. Neuron. 1994;13:555–566. [[PubMed: 7917291](#)]
785. Hart A C, Sims S, Kaplan J M. Synaptic code for sensory modalities revealed by *C. elegans* [GLR-1](#) glutamate receptor. Nature. 1995;378:82–85. [[PubMed: 7477294](#)]
786. Hartenstein V, Posakony J W. A dual function of the *notch* gene in *Drosophila* sensillum development. Dev. Biol. 1990;142:13–30. [[PubMed: 2227090](#)]
787. Hartman P S, Herman R K. Radiation-sensitive mutants of *Caenorhabditis elegans*. Genetics. 1982;102:159–178. [[PMC free article: PMC1201931](#)] [[PubMed: 7152245](#)]
788. Hartman P S, Marshall A. Inactivation of wild-type and *rad* mutant *Caenorhabditis elegans* by 8-methoxypsoralen and near-ultraviolet light. Photochem. Photobiol. 1992;55:103–111. [[PubMed: 1603841](#)]
789. Hartman P S, Simpson V J, Johnson T, Mitchell D. Radiation sensitivity and DNA repair in *Caenorhabditis elegans* strains with different mean life spans. Mutat. Res. 1988;208:77–82. [[PubMed: 3380112](#)]
790. Hartwell L H, Kastan M B. Cell cycle control and cancer. Science. 1994;266:1821–1828. [[PubMed: 7997877](#)]
791. Harvey P H, Pagel M D. The comparative method in evolutionary biology. England: Oxford University Press; 1991.
792. Hashmi S, Ling P, Hashmi G, Reed M, Gaugler R, Trimmer W. Genetic transformation of nematodes using arrays of micromechanical piercing structures. BioTechniques. 1995;19:766–770. [[PubMed: 8588914](#)]
793. Hata Y, Slaughter C A, Südhof T C. Synaptic vesicle fusion complex contains unc-18 homologue bound to syntaxin. Nature. 1993;366:347–351. [[PubMed: 8247129](#)]
794. Hawkins M G, McGhee J D. *elt-2* a second GATA factor from the nematode *Caenorhabditis elegans*. J. Biol. Chem. 1995;270:14666–14671. [[PubMed: 7782329](#)]
795. Hawkins N C, McGhee J D. Homeobox containing genes in the nematode *Caenorhabditis elegans*. Nucleic Acids Res. 1990;18:6101–6106. [[PMC free article: PMC332412](#)] [[PubMed: 1978282](#)]
796. Hawkins R D, Kandel E R, Siegelbaum S A. Learning to modulate transmitter release: Themes and variations in synaptic plasticity. Annu. Rev. Neurosci. 1993;16:625–665. [[PubMed: 8096376](#)]
797. Hawley R S. Chromosomal sites necessary for normal levels of meiotic recombination in *Drosophila melanogaster*. I. Evidence for and mapping of the sites. Genetics. 1980;94:625–646. [[PMC free article: PMC1214164](#)] [[PubMed: 6772522](#)]
798. Hawley R S, Kucherlapati R, Smith G R, editors. Genetic recombination. American Society for Microbiology; 1988. Exchange and chromosomal segregation in eukaryotes. pp. 497–527.
799. Hawley R S, Irick H, Zitron A E, Haddox D A, Lohe A, New C, Whitley M D, Arbel T, Jang J, McKim K, Childs G. There are two mechanisms of achiasmate segregation in *Drosophila* females, one of which requires heterochromatic homology. Dev. Genet. 1992;13:440–467. [[PubMed: 1304424](#)]
800. Hay B A, Wolff T, Rubin G M. Expression of baculovirus P35 prevents cell death in *Drosophila*. Development. 1994;120:2121–2129. [[PubMed: 7925015](#)]
801. He F, Jacobson A. Identification of a novel component of the nonsense-mediated mRNA decay pathway by use of an interacting protein screen. Genes Dev. 1995;9:437–454. [[PubMed: 7883168](#)]
802. Heath J P. A worm's eye view of motility. Curr. Biol. 1992;2:301–303. [[PubMed: 15335941](#)]
803. Hecht R M, Norman M A, Vu T, Jones W. A novel set of uncoordinated mutants in *C. elegans* uncovered by cold-sensitive mutations. Genome. 1996;39:459–464. [[PubMed: 8984009](#)]
804. Hecht R M, Berg Z M, Rao P N, Davis F M. Conditional absence of mitosis-specific antigens in a temperature-sensitive embryonic-arrest mutant of *Caenorhabditis elegans*. J. Cell Sci. 1987;87:305–314. [[PubMed: 3308930](#)]

805. Hedgecock E M. The mating system of *Caenorhabditis elegans*: Evolutionary equilibrium between self- and cross-fertilization in a facultative hermaphrodite. Am. Nat. 1976;110:1007–1012.
806. Hedgecock E M, Herman R K. The *ncl-1* gene and genetic mosaics of *Caenorhabditis elegans*. Genetics. 1995;141:989–1006. [[PMC free article: PMC1206860](#)] [[PubMed: 8582642](#)]
807. Hedgecock E M, Russell R L. Normal and mutant thermotaxis in the nematode *Caenorhabditis elegans*. Proc. Natl. Acad. Sci. 1975;72:4061–4065. [[PMC free article: PMC433138](#)] [[PubMed: 1060088](#)]
808. Hedgecock E M, Thomson J N. A gene required for nuclear and mitochondrial attachment in the nematode *Caenorhabditis elegans*. Cell. 1982;30:321–330. [[PubMed: 6889924](#)]
809. Hedgecock E M, Culotti J G, Hall D H. The *unc-5*, *unc-6*, and *unc-40* genes guide circumferential migrations of pioneer axons and mesodermal cells on the epidermis in *C. elegans*. Neuron. 1990;2:61–85. [[PubMed: 2310575](#)]
810. Hedgecock E M, Sulston J E, Thomson J N. Mutations affecting programmed cell deaths in the nematode *Caenorhabditis elegans*. Science. 1983;220:1277–1279. [[PubMed: 6857247](#)]
811. Hedgecock E M, Culotti J G, Hall D H, Stern B D. Genetics of cell and axon migrations in *Caenorhabditis elegans*. Development. 1987;100:365–382. [[PubMed: 3308403](#)]
812. Hedgecock E M, Culotti J G, Thomson J N, Perkins L A. Axonal guidance mutants of *Caenorhabditis elegans* identified by filling [sensory neurons](#) with fluorescein dyes. Dev. Biol. 1985;111:158–170. [[PubMed: 3928418](#)]
813. Hedrick L, Cho K R, Fearon E R, Wu T C, Kinzler K W, Vogelstein B. The DCC gene product in cellular differentiation and colorectal tumorigenesis. Genes Dev. 1994;8:1174–1183. [[PubMed: 7926722](#)]
814. Heierhorst H E, Probst W C, Vilim F S, Buku A, Weiss K R. Autophosphorylation of molluscan twitchin and interaction of its kinase domain with calcium/calmodulin. J. Biol. Chem. 1994;269:21086–21093. [[PubMed: 8063728](#)]
815. Heierhorst J, Lederis K, Richter D. Presence of a member of the Tc1-like transposon family from nematodes and *Drosophila* within the vasotocin gene of a primitive vertebrate, the pacific hagfish *Eptatretus stouti*. Proc. Natl. Acad. Sci. 1992;89:6798–6802. [[PMC free article: PMC49591](#)] [[PubMed: 1379721](#)]
816. Heine U, Blumenthal T. Characterization of regions of the *Caenorhabditis elegans* X chromosome containing vitellogenin genes. J. Mol. Biol. 1986;188:301–312. [[PubMed: 3735423](#)]
817. Hekimi S, Kershaw D. Axonal guidance defects in a *Caenorhabditis elegans* mutant reveal cell-extrinsic determinants of neuronal morphology. J. Neurosci. 1993;13:4254–4571. [[PMC free article: PMC6576365](#)] [[PubMed: 8410186](#)]
818. Hekimi S, Boutis P, Lakowski B. Viable maternal-effect mutations that affect development of the nematode *Caenorhabditis elegans*. Genetics. 1995;141:1351–1364. [[PMC free article: PMC1206872](#)] [[PubMed: 8601479](#)]
819. Hemmer R M, Donkin S G, Chin K J, Grenache D G, Bhatt H, Politz S M. Altered expression of an L1-specific, O-linked cuticle surface glycoprotein in mutants of the nematode *Caenorhabditis elegans*. J. Cell Biol. 1991;115:1237–1247. [[PMC free article: PMC2289243](#)] [[PubMed: 1955471](#)]
820. Henderson S T, Gao D, Lambie E J, Kimble J. *lag-2* may encode a signaling ligand for the GLP-1 and LIN-12 receptors of *C. elegans*. Development. 1994;120:2913–2924. [[PubMed: 7607081](#)]
821. Hendricks L, van Broeckhoven C, Vandenberghe A, van de Peer Y v e s, de Wachter R. Primary and secondary structure of the 18S ribosomal RNA of the bird spider *Eurypelma californica* and evolutionary relationships among eukaryotic phyla. Eur. J. Biochem. 1988;177:15–20. [[PubMed: 3181152](#)]
822. Hengartner M O, Horvitz H R. Activation of *C. elegans* cell death protein CED-9 by an amino-acid substitution in a domain conserved in Bcl-2. Nature. 1994a;369:318–320. [[PubMed: 7910376](#)]
823. Hengartner M O, Horvitz H R. *C. elegans* cell survival gene *ced-9* encodes a functional homolog of the mammalian proto-oncogene *bcl-2*. Cell. 1994b;76:665–676. [[PubMed: 7907274](#)]
824. Hengartner M O, Horvitz H R. The ins and outs of programmed cell death in *C. elegans*. Philos. Trans. R. Soc. Lond. B Biol. Sci. 1994c;345:243–246. [[PubMed: 7846120](#)]

825. Hengartner M O, Horvitz H R. Programmed cell death in *Caenorhabditis elegans*. Curr. Opin. Genet. Dev. 1994;4:581–586. [[PubMed: 7950327](#)]
826. Hengartner M O, Ellis R E, Horvitz H R. *C. elegans* gene *ced-9* protects cells from programmed cell death. Nature. 1992;356:494–499. [[PubMed: 1560823](#)]
827. Henikoff S. Detection of *Caenorhabditis* transposon homologs in diverse organisms. New Biol. 1992;4:382–388. [[PubMed: 1320399](#)]
828. Hennig W. Grundzüge einer Theorie der phylogenetischen Systematik. Berlin: Deutscher Zentralverlag; 1950.
829. Henry R W, Sadowski C L, Kobayashi R, Hernandez N. A TBP-TAF complex required for transcription of human snRNA genes by RNA polymerases II and III. Nature. 1995;374:653–656. [[PubMed: 7715707](#)]
830. Herman M A. "Cell interactions and the polarity of cell divisions during *Caenorhabditis elegans* development." [Ph.D. thesis]. Massachusetts Institute of Technology; Cambridge: 1991.
831. Herman M A, Horvitz H R. The *Caenorhabditis elegans* gene *lin-44* controls the polarity of asymmetric cell divisions. Development. 1994;120:1035–1047. [[PubMed: 8026318](#)]
832. Herman M A, Vassilieva L L, Horvitz H R, Shaw J E, Herman R K. The *C. elegans* gene *lin-44*, which controls the polarity of certain asymmetric cell divisions, encodes a Wnt protein and acts cell nonautonomously. Cell. 1995;83:101–110. [[PubMed: 7553861](#)]
833. Herman R K. Analysis of genetic mosaics of the nematode *Caenorhabditis elegans*. Genetics. 1984;106:165–180. [[PMC free article: PMC1202392](#)] [[PubMed: 6434374](#)]
834. Herman R K. Mosaic analysis of two genes that affect nervous system structure in *Caenorhabditis elegans*. Genetics. 1987;116:377–388. [[PMC free article: PMC1203149](#)] [[PubMed: 3609726](#)]
835. Herman R K. Mosaic analysis in the nematode *Caenorhabditis elegans*. J. Neurogenet. 1989;5:1–24. [[PubMed: 2649650](#)]
836. Herman R K. Mosaic analysis. Methods Cell Biol. 1995;48:128–146. [[PubMed: 8531723](#)]
837. Herman R K, Hedgecock E M. Limitation of the size of the vulval primordium of *Caenorhabditis elegans* by *lin-15* expression in the surrounding hypodermis. Nature. 1990;348:169–171. [[PubMed: 2234080](#)]
838. Herman R K, Kari C K. Muscle-specific expression of a gene affecting acetylcholinesterase in the nematode *Caenorhabditis elegans*. Cell. 1985;40:509–514. [[PubMed: 3971421](#)]
839. Herman R K, Kari C K. Recombination between small X chromosome duplications and the X chromosome in *Caenorhabditis elegans*. Genetics. 1989;121:723–737. [[PMC free article: PMC1203656](#)] [[PubMed: 2721932](#)]
840. Herman R K, Albertson D G, Brenner S. Chromosome rearrangements in *Caenorhabditis elegans*. Genetics. 1976;83:91–105. [[PMC free article: PMC1213508](#)] [[PubMed: 1269921](#)]
841. Herman R K, Kari C K, Hartman P S. Dominant X-chromosome nondisjunction mutants of *Caenorhabditis elegans*. Genetics. 1982;102:379–400. [[PMC free article: PMC1201947](#)] [[PubMed: 6890921](#)]
842. Herman R K, Madl J E, Kari C K. Duplications in *Caenorhabditis elegans*. Genetics. 1979;92:419–435. [[PMC free article: PMC1213968](#)] [[PubMed: 573721](#)]
843. Herr W, Sturm R A, Clerc R G, Corcoran L M, Baltimore D, Sharp P A, Ingraham H A, Rosenfeld M G, Finney M, Ruvkun G, Horvitz H R. The POU domain: A large conserved region in the mammalian *pit-1*, *oct-1*, *oct-2* and *Caenorhabditis elegans unc-86* gene products. Genes Dev. 1988;2:1513–1516. [[PubMed: 3215510](#)]
844. Heschl M F P, Baillie D L. Functional elements and domains inferred from sequence comparisons of a heatshock gene in two nematodes. J. Mol. Evol. 1990;31:3–9. [[PubMed: 2116528](#)]
845. Hevelone J, Hartman P S. An endonuclease from *Caenorhabditis elegans*: partial purification and characterization. Biochem. Genet. 1988;26:447–461. [[PubMed: 3228446](#)]
846. Higgins B J, Hirsh D. Roller mutants of the nematode *Caenorhabditis elegans*. Mol. Gen. Genet. 1977;150:63–72. [[PubMed: 834177](#)]

847. Hill D P, Strome S. An analysis of the role of microfilaments in the establishment and maintenance of asymmetry in *Caenorhabditis elegans* zygotes. *Dev. Biol.* 1988;125:75–84. [[PubMed: 3275427](#)]
848. Hill D P, Strome S. Brief cytochalasin-induced disruption of microfilaments during a critical interval in 1-cell *C. elegans* embryos alters the partitioning of developmental instructions to the 2-cell embryo. *Development*. 1990;108:159–172. [[PubMed: 2190787](#)]
849. Hill D P, Shakes D C, Ward S, Strome S. A sperm-supplied product essential for initiation of normal embryogenesis in *Caenorhabditis elegans* is encoded by the paternal-effect embryonic lethal gene, *spe-11*. *Dev. Biol.* 1989;136:154–166. [[PubMed: 2806718](#)]
850. Hill R J, Sternberg P W. The gene *lin-3* encodes an inductive signal for vulval development in *C. elegans*. *Nature*. 1992;358:470–476. [[PubMed: 1641037](#)]
851. Himmelhoch S, Zuckerman B M. *Caenorhabditis elegans*: Characters of negatively charged groups on the cuticle and intestine. *Exp. Parasitol.* 1983;55:299–305. [[PubMed: 6852168](#)]
852. Hinshaw J E, Schmid S L. Dynamin self-assembles into rings suggesting a mechanism for coated vesicle budding. *Nature*. 1995;374:190–192. [[PubMed: 7877694](#)]
853. Hirano T, Mitchison T J. A heteromeric coiled-coil protein required for mitotic chromosome condensation in vitro. *Cell*. 1994;79:449–458. [[PubMed: 7954811](#)]
854. Hirata J, Nakagoshi H, Nabeshima Y, Matsuzaki F. Asymmetric segregation of the homeodomain protein prospero during *Drosophila* development. *Nature*. 1995;377:627–630. [[PubMed: 7566173](#)]
855. Hird S N, White J G. Cortical and cytoplasmic flow polarity in early embryonic cells of *Caenorhabditis elegans*. *J. Cell Biol.* 1993;121:1343–1355. [[PMC free article: PMC2119718](#)] [[PubMed: 8509454](#)]
856. Hird S N, Paulsen J E, Strome S. Segregation of germ granules in living *Caenorhabditis elegans* embryos: Cell-type-specific mechanisms for cytoplasmic localization. *Development*. 1996;122:1303–1312. [[PubMed: 8620857](#)]
857. Hirsh D. Tryptophan transfer RNA as the UGA suppressor. *J. Mol. Biol.* 1971;58:439–458. [[PubMed: 4933412](#)]
858. Hirsh D, Vanderslice R. Temperature-sensitive developmental mutants of *Caenorhabditis elegans*. *Dev. Biol.* 1976;49:220–235. [[PubMed: 943345](#)]
859. Hirsh D, Oppenheim D, Klass M. Development of the reproductive system of *Caenorhabditis elegans*. *Dev. Biol.* 1976;49:200–219. [[PubMed: 943344](#)]
860. Hishida R, Ishihara T, Knodo K, Katsura I. *hch-1*: A gene required for normal hatching and normal migration of a neuroblast in *C. elegans*, encodes a protein related to TOLLOID and BMP-1. *EMBO J.* 1996;15:4111–4112. [[PMC free article: PMC452133](#)] [[PubMed: 8861940](#)]
861. Hitt A L, Hartwig J H, Luna E J. Ponticulin is the major high affinity link between the plasma membrane and the cortical actin network in *Dictyostelium*. *J. Cell Biol.* 1994;126:1433–1444. [[PMC free article: PMC2290950](#)] [[PubMed: 8089176](#)]
862. Ho J Y, Weide R, Ma H M, Vanwordragen M F, Lambert K N, Koornneef M, Zabel P, Williamson V M. The root-knot nematode resistance gene (MI) in tomato—Construction of a molecular linkage map and identification of dominant cDNA markers in resistant genotypes. *Plant J.* 1992;2:971–982. [[PubMed: 1302643](#)]
863. Ho N F H, Geary T G, Barsuhn C L, Sims S M, Thompson D P. Mechanistic studies in the transcuticular delivery of antiparasitic drugs II: *ex vivo/in vivo* correlation of solute transport by *Ascaris suum*. *Mol. Biochem. Parasitol.* 1992;52:1–14. [[PubMed: 1625697](#)]
864. Ho N F H, Geary T G, Raub T J, Barshun C L, Thompson D P. Biophysical transport properties of the cuticle of *Ascaris suum*. *Mol. Biochem. Parasitol.* 1990;41:153–166. [[PubMed: 2398915](#)]
865. Hockenberry D, Nuñez G, Milliman C, Schreiber R D, Korsmeyer S J. Bcl-2 is an inner mitochondrial membrane protein that blocks programmed cell death. *Nature*. 1990;348:334–336. [[PubMed: 2250705](#)]
866. Hockenberry D M, Oltvai Z N, Yin X -M, Milliman C L, Korsmeyer S J. Bcl-2 functions in an antioxidant pathway to prevent apoptosis. *Cell*. 1993;75:241–251. [[PubMed: 7503812](#)]
867. Hockfield S, Kalb R G. Activity-dependent structural changes during neuronal development. *Curr. Opin. Neurobiol.* 1993;3:87–92. [[PubMed: 8453296](#)]

868. Hodgkin J. More sex-determination mutants of *Caenorhabditis elegans*. Genetics. 1980;96:649–664. [PMC free article: PMC1214367] [PubMed: 7262542]
869. Hodgkin J. Male phenotypes and mating efficiency in *Caenorhabditis elegans*. Genetics. 1983;103:43–64. [PMC free article: PMC1202023] [PubMed: 17246100]
870. Hodgkin J. Novel nematode amber suppressors. Genetics. 1985;111:287–310. [PMC free article: PMC1202644] [PubMed: 17246299]
871. Hodgkin J. Sex determination in the nematode *Caenorhabditis elegans*: Analysis of *tra-3*suppressors and characterization of the *fem* genes. Genetics. 1986;114:15–52. [PMC free article: PMC1202928] [PubMed: 3770465]
872. Hodgkin J. A genetic analysis of the sex-determining gene *tra-1* in the nematode *Caenorhabditis elegans*. Genes Dev. 1987a;1:731–745. [PubMed: 3428597]
873. Hodgkin J. Primary sex determination in the nematode *C. elegans*.(suppl.) . Development. 1987b;101:5–15. [PubMed: 3503722]
874. Hodgkin J. Wood W B, elegans C, editors. The nematode *Caenorhabditis elegans*. Cold Spring Harbor, New York: Cold Spring Harbor Laboratory; 1988. Sexual dimorphism and sex determination. pp. 243–280.
875. Hodgkin J. Sex determination in the nematode *Caenorhabditis*. Semin. Dev. Biol. 1992;3:307–317.
876. Hodgkin J. Molecular cloning and duplication of the nematode sex-determining gene *tra-1*. Genetics. 1993;133:543–560. [PMC free article: PMC1205342] [PubMed: 8384144]
877. Hodgkin J, Albertson D. Isolation of dominant XO-feminizing mutations in *Caenorhabditis elegans*: New regulatory *tra* alleles and an X chromosome duplication with implications for primary sex determination. Genetics. 1995;141:527–542. [PMC free article: PMC1206753] [PubMed: 8647390]
878. Hodgkin J, Barnes T M. More is not better: Brood size and population growth in a self-fertilizing nematode. Proc. R. Soc. Lond. B Biol. Sci. 1991;246:19–24. [PubMed: 1684664]
879. Hodgkin J, Brenner S. Mutations causing transformation of sexual phenotype in the nematode *Caenorhabditis elegans*. Genetics. 1977;86:275–287. [PMC free article: PMC1213677] [PubMed: 560330]
880. Hodgkin J, Doniach T, Shen M. The sex determination pathway in the nematode *Caenorhabditis elegans*: Variations on a theme. Cold Spring Harbor Symp. Quant. Biol. 1985;50:585–593. [PubMed: 3868496]
881. Hodgkin J A, Horvitz H R, Brenner S. Nondisjunction mutants of the nematode *Caenorhabditis elegans*. Genetics. 1979;91:67–94. [PMC free article: PMC1213932] [PubMed: 17248881]
882. Hodgkin J, Plasterk R H A, Waterston R H. The nematode *Caenorhabditis elegans* and its genome. Science. 1995;270:410–414. [PubMed: 7569995]
883. Hodgkin J, Zellan J D, Albertson D G. Identification of a candidate primary sex determination locus, *fox-1*, on the X chromosome of *Caenorhabditis elegans*. Development. 1994;120:3681–3689. [PubMed: 7821230]
884. Hodgkin J, Papp A, Pulak R, Ambros V, Anderson P. A new kind of informational suppression in the nematode *Caenorhabditis elegans*. Genetics. 1989;123:301–313. [PMC free article: PMC1203802] [PubMed: 2583479]
885. Hofmann M -C, Abramian D, Millan J L. A haploid and diploid cell cycle coexist in an *in vitro* immortalized spermatogenic cell line. Dev. Genet. 1995;16:119–127. [PubMed: 7736662]
886. Hofmann M -C, Hess R A, Goldberg E, Millan J L. Immortalized *germ cells* undergo meiosis *in vitro*. Proc. Natl. Acad. Sci. 1994;91:5533–5537. [PMC free article: PMC44030] [PubMed: 8202522]
887. Holden-Dye L, Walker R J. Avermectin and avermectin derivatives are antagonists at the 4-aminobutyric acid (GABA) receptor on the somatic muscle cells of *Ascaris*;--> is this the site of anthelmintic action? Parasitology. 1990;101:265–271. [PubMed: 2175874]
888. Holland P W W, Garcia-Fernàndez J, Williams N A, Sidow A. Gene duplications and the origins of vertebrate development. *Suppl.*, pp. Development. 1994;125–133. [PubMed: 7579513]
889. Holmes K C, Popp D, Gebhardt W, Kabsch W. Atomic model of the actin filament. Nature. 1990;347:44–49. [PubMed: 2395461]

890. Honda S, Epstein H F. Modulation of muscle gene expression in *Caenorhabditis elegans*: Differential levels of transcripts mRNAs, and polypeptides for thick filament proteins during nematode development. Proc. Natl. Acad. Sci. 1990;87:876–880. [[PMC free article: PMC53371](#)] [[PubMed: 2300580](#)]
891. Honda S, Ishii N, Suzuki K, Matsuo M. Oxygen-dependent perturbation of life span and aging rate in the nematode. J. Gerontol. 1993;48:B57–61. [[PubMed: 8473689](#)]
892. Hong K, Driscoll M. A transmembrane domain of the putative channel subunit MEC-4 influences mechanotransduction and neurodegeneration in *C. elegans*. Nature. 1994;367:470–473. [[PubMed: 8107806](#)]
893. Hope I A. “Promoter trapping” in *Caenorhabditis elegans*. Development. 1991;113:399–408. [[PubMed: 1782857](#)]
894. Hope I A. PES-1 is expressed during early embryogenesis in *Caenorhabditis elegans* and has homology to the *fork head* family of transcription factors. Development. 1994;120:505–514. [[PubMed: 8162851](#)]
895. Horowitz R, Maruyama K, Podolsky R J. Elastic behavior of connecting filaments during thick filament movement in activated skeletal muscle. J. Cell Biol. 1989;109:2169–2176. [[PMC free article: PMC2115863](#)] [[PubMed: 2808523](#)]
896. Horowitz R, Kempner E S, Bisher M E, Podolsky R J. A physiological role for titin and nebulin in skeletal muscle. Nature. 1986;323:160–164. [[PubMed: 3755803](#)]
897. Horvitz H R, Wood W B, editor. The nematode *Caenorhabditis elegans*. Cold Spring Harbor, New York: Cold Spring Harbor Laboratory; 1988. Genetics of cell lineage. pp. 157–190.
898. Horvitz H R, Sulston J E. Isolation and genetic characterization of cell-lineage mutants of the nematode *Caenorhabditis elegans*. Genetics. 1980;96:435–454. [[PMC free article: PMC1214309](#)] [[PubMed: 7262539](#)]
899. Horvitz H R, Shaham S, Hengartner M O. The genetics of programmed cell death in the nematode *Caenorhabditis elegans*. Cold Spring Harbor Symp. Quant. Biol. 1994;59:377–385. [[PubMed: 7587090](#)]
900. Horvitz H R, Brenner S, Hodgkin J, Herman R K. A uniform genetic nomenclature for the nematode *Caenorhabditis elegans*. Mol. Gen. Genet. 1979;175:129–133. [[PubMed: 292825](#)]
901. Horvitz H R, Chalfie M, Trent C, Sulston J E, Evans P D. Serotonin and octopamine in the nematode *Caenorhabditis elegans*. Science. 1982;216:1012–1014. [[PubMed: 6805073](#)]
902. Horvitz H R, Sternberg P W, Greenwald I S, Fixsen W, Ellis H M. Mutations that affect [neural](#) cell lineages and cell fates during the development of the nematode *Caenorhabditis elegans*. Cold Spring Harbor Symp. Quant. Biol. 1983;48:453–463. [[PubMed: 6586368](#)]
903. Hoskins R, Hajnal A, Harp S A, Kim S K. The *C. elegans* vulval induction gene *lin-2* encodes a member of the MAGUK family of cell junction proteins. Development. 1996;122:97–111. [[PubMed: 8565857](#)]
904. Hosono R. A study of morphology of *Caenorhabditis elegans*: A mutant of *Caenorhabditis elegans* with dumpy and temperature-sensitive roller phenotype. J. Exp. Zool. 1980;213:61–67.
905. Hosono R, Kamiya Y. Additional genes which result in an elevation of acetylcholine levels by mutations in *Caenorhabditis elegans*. Neurosci. Lett. 1991;128:243–244. [[PubMed: 1945043](#)]
906. Hosono R, Kuno S, Midsukami M. Temperature-sensitive mutations causing reversible paralysis in *Caenorhabditis elegans*. J. Exp. Zool. 1985;235:409–421. [[PubMed: 4056699](#)]
907. Hosono R, Sassa T, Kuno S. Mutations affecting acetylcholine levels in the nematode *Caenorhabditis elegans*. J. Neurochem. 1987;49:1820–1823. [[PubMed: 3681298](#)]
908. Hosono R, Sassa T, Kuno S. Spontaneous mutations of trichlorfon resistance in the nematode *Caenorhabditis elegans*. Zool. Sci. 1989;6:697–708.
909. Hosono R, Hirahara K, Kuno S, Kurihara T. Mutants of *Caenorhabditis elegans* with dumpy and rounded head phenotype. J. Exp. Zool. 1982;224:135–144.
910. Hosono R, Hekimi S, Kamiya Y, Sassa T, Murakami S, Nishiwaki K, Miwa J, Taketo A, Kodaira K I. The *unc-18* gene encodes a novel protein affecting the kinetics of acetylcholine metabolism in the nematode *Caenorhabditis elegans*. J. Neurochem. 1992;58:1517–1525. [[PubMed: 1347782](#)]
911. Hotez P, Hawdon J, Schad G A. Hookworm larval infectivity, arrest and amphiparatenesis: The *Caenorhabditis elegans*Daf-c paradigm. Parasitol. Today. 1993;9:23–26. [[PubMed: 15463660](#)]

912. Howard A D, Kostura M J, Thornberry N, Ding G J F, Limjuco G, Weidner J, Salley J P, Hogquist K A, Chaplin D D, Mumford R A, Schmidt J A, Tocci M J. IL-1-converting enzyme requires aspartic acid residues for processing of the IL-1 $\beta$  precursor at two distinct sites and does not cleave 31-kDa IL-1 $\alpha$ . *J. Immunol.* 1991;147:2964–2969. [PubMed: 1919001]
913. Howell A M, Rose A M. Essential genes in the *hDf6*region of chromosome I in *Caenorhabditis elegans*. *Genetics*. 1990;126:583–592. [PMC free article: PMC1204214] [PubMed: 2249758]
914. Howell A M, Gilmour S G, Mancebo R A, Rose A M. Genetic analysis of a large autosomal region in *Caenorhabditis elegans* by the use of a free duplication. *Genet. Res.* 1987;49:207–213.
915. Howells R E. The mechanisms of amino acid uptake by *Brugia pahangi* *in vitro*. *Z. Parasitenkd.* 1983;69:247–253. [PubMed: 6858312]
916. Howells R E, Chen S N. *Brugia pahangi*: Feeding and nutrient uptake *in vitro*. *Exp. Parasitol.* 1981;51:42–58. [PubMed: 7461090]
917. Hresko M C, Williams B D, Waterston R H. Assembly of body wall muscle and muscle cell attachment structures in *Caenorhabditis elegans*. *J. Cell Biol.* 1994;124:491–506. [PMC free article: PMC2119906] [PubMed: 8106548]
918. Hsu D R, Meyer B J. The *dpy-30* gene encodes an essential component of the *Caenorhabditis elegans* dosage compensation machinery. *Genetics*. 1994;137:999–1018. [PMC free article: PMC1206076] [PubMed: 7982580]
919. Hsu D R, Chuang P -T, Meyer B J. DPY-30, a novel nuclear protein essential early in embryogenesis for *C. elegans* dosage compensation. *Development*. 1995;121:3323–3334. [PubMed: 7588066]
920. Hu E, Rubin C S. Casein kinase II from *Caenorhabditis elegans*. Cloning characterization and developmental regulation of the gene encoding the  $\beta$  subunit. *J. Biol. Chem.* 1991;266:19796–19802. [PubMed: 1918084]
921. Hu S, Parker M, Lei J, Wilce M, Benian G, Kemp B. Insight into autophosphorylation from the crystal structure of twitchin kinase. *Nature*. 1994;369:581–584. [PubMed: 8202162]
922. Huang L S, Tzou P, Sternberg P W. The *lin-15*locus encodes two negative regulators of *Caenorhabditis elegans*vulval development. *Mol. Biol. Cell.* 1994;5:395–412. [PMC free article: PMC301050] [PubMed: 8054684]
923. Huang M. "Mechanosensory genes in *Caenorhabditis elegans*." [Ph.D. thesis]. Columbia University; New York: 1995.
924. Huang M, Chalfie M. Gene interactions affecting mechanosensory transduction in *Caenorhabditis elegans*. *Nature*. 1994;367:467–470. [PubMed: 7509039]
925. Huang M, Gu G, Ferguson E L, Chalfie M. A stomatin-like protein is needed for mechanosensation in *C. elegans*. *Nature*. 1995;378:292–295. [PubMed: 7477350]
926. Huang X -Y, Hirsh D. A second *trans*-spliced RNA leader sequence in the nematode *Caenorhabditis elegans*. *Proc. Natl. Acad. Sci.* 1989;86:8640–8644. [PMC free article: PMC298343] [PubMed: 2813415]
927. Huang X -Y, Barrios L A M, Vonkhorporn P, Honda S, Albertson D G, Hecht R M. Genomic organization of the glyceraldehyde-3-phosphate dehydrogenase gene family of *Caenorhabditis elegans*. *J. Mol. Biol.* 1989;206:411–424. [PubMed: 2716055]
928. Hubbard E J A, Dong Q, Greenwald I. Evidence for functional association between EMB-5 and LIN-12 in *Caenorhabditis elegans*. *Science*. 1996;273:112–115. [PubMed: 8658178]
929. Hubel D H, Wiesel T N. The period of susceptibility to the physiological effects of unilateral eye closure in kittens. *J. Physiol.* 1970;206:419–436. [PMC free article: PMC1348655] [PubMed: 5498493]
930. Hudson B G, Reeders S T, Tryggvason K. Type IV collagen—Structure, gene organization, and role in human diseases—Molecular basis of Goodpasture and Alport syndromes and diffuse leiomyomatosis. *J. Biol. Chem.* 1993;268:26033–26036. [PubMed: 8253711]
931. Hudspeth A J. Extracellular current flow and the site of transduction by vertebrate hair cells. *J. Neurosci.* 1982;2:1–10. [PMC free article: PMC6564293] [PubMed: 6275046]
932. Hudspeth A J. How the ear's works work. *Nature*. 1989;341:397–404. [PubMed: 2677742]
933. Hughes A L. The evolution of functionally novel proteins after gene duplication. *Proc. R. Soc. Lond. B.* 1994;256:119–124. [PubMed: 8029240]

934. Hunter C P, Kenyon C. Specification of anteroposterior cell fates in *Caenorhabditis elegans* by *Drosophila* Hox proteins. *Nature*. 1995;377:229–232. [[PubMed: 7675107](#)]
935. Hunter C P, Wood W B. The *tra-1* gene determines sexual phenotype cell-autonomously in *C. elegans*. *Cell*. 1990;63:1193–1204. [[PubMed: 2261640](#)]
936. Hunter C P, Wood W B. Evidence from mosaic analysis of the masculinizing gene *her-1* for cell interactions in *C. elegans* sex determination. *Nature*. 1992;355:551–555. [[PubMed: 1741033](#)]
937. Hussey R S. Disease-inducing secretions of plant-parasitic nematodes. *Annu. Rev. Phytopathol.* 1989;27:123–141.
938. Hutter H, Schnabel R. *glp-1* and inductions establishing embryonic axes in the *Caenorhabditis elegans*. *Development*. 1994;120:2051–2064. [[PubMed: 7925009](#)]
939. Hutter H, Schnabel R. Establishment of left-right asymmetry in the *C. elegans* embryo: A multistep process involving a series of inductive events. *Development*. 1995a;121:3417–3424. [[PubMed: 7588074](#)]
940. Hutter H, Schnabel R. Specification of anterior-posterior differences within the [AB lineage](#) in the *C. elegans* embryo: A polarising induction. *Development*. 1995b;121:1559–1568. [[PubMed: 7789283](#)]
941. Huxley H E, Hanson J. Changes in the cross-striations of muscle contraction and their structural interpretation. *Nature*. 1954;173:973–977. [[PubMed: 13165698](#)]
942. Hyman A A. Centrosome movement in the early divisions of *Caenorhabditis elegans*: A cortical site determining centrosome position. *J. Cell Biol.* 1989;109:1185–1193. [[PMC free article: PMC2115774](#)] [[PubMed: 2768338](#)]
943. Hyman A A, White J G. Determination of cell division axes in the early embryogenesis of *Caenorhabditis elegans*. *J. Cell Biol.* 1987;105:2123–2135. [[PMC free article: PMC2114830](#)] [[PubMed: 3680373](#)]
944. Hyman L H. The invertebrates: Acanthocephala Aschelminthes and Entoprocta, vol. 3. New York: McGraw-Hill; 1951.
945. Hynes R O, Lander A D. Contact and adhesive specificities in the associations, migrations, and targeting of cells and axons. *Cell*. 1992;68:303–322. [[PubMed: 1733501](#)]

## I

946. Illmensee K, Mahowald A P. Transplantation of posterior polar plasm in *Drosophila*. Induction of [germ cells](#) at the anterior pole of the egg. *Proc. Natl. Acad. Sci.* 1974;71:1016–1020. [[PMC free article: PMC388152](#)] [[PubMed: 4208545](#)]
947. Ingham P W, Pinchin S M, Howard K R, Ish-Horowicz D. Genetic analysis of the *hairy* locus in *Drosophila melanogaster*. *Genetics*. 1985;111:463–486. [[PMC free article: PMC1202654](#)] [[PubMed: 17246301](#)]
948. Isberg R R, Lazaar A L, Syvanen M. Regulation of Tn5 by the right-repeat proteins: Control at the level of the transposition reaction? *Cell*. 1982;30:883–892. [[PubMed: 6291787](#)]
949. Ishii N, Suzuki N, Hartman P S, Suzuki K. The effects of temperature on the longevity of a radiation-sensitive mutant *rad-8* of the nematode *Caenorhabditis elegans*. *J. Gerontol.* 1994;49:B117–B120. [[PubMed: 8169328](#)]
950. Ishii N, Wadsworth W G, Stern B D, Culotti J G, Hedgecock E M. UNC-6, a laminin-related protein, guides cell and pioneer axon migrations in *C. elegans*. *Neuron*. 1992;9:873–881. [[PubMed: 1329863](#)]
951. Ishijima A, Harada Y, Kojima H, Funatsu T, Higuchi H, Yanagida T. Single molecule analysis of the actomyosin motor using nanomanipulation. *Biochem. Biophys. Res. Commun.* 1994;199:1057–1063. [[PubMed: 8135779](#)]
952. Isnenghi E, Cassada K, Smith C, Denitch K, Radnia A, von Ehrenstein G. Maternal effects and temperature-sensitive period of mutations affecting embryogenesis in *Caenorhabditis elegans*. *Dev. Biol.* 1983;98:465–480. [[PubMed: 6683689](#)]
953. Israel A, Yano O, Logeat F, Kieran M, Kourilsky P. Two purified factors bind to the same sequence in the enhancer of mouse MHC class I genes: One of them is a positive regulator induced upon

- differentiation of teratocarcinoma cells. Nucleic Acids Res. 1989;17:5245–5257. [[PMC free article: PMC318108](#)] [[PubMed: 2668878](#)]
954. Italiano J E, Roberts T M, Stewart M, Fontana C A. Reconstitution *in vitro* of the motile apparatus from the amoeboid sperm of *Ascaris* shows that filament assembly and bundling move membranes. Cell. 1996;84:105–114. [[PubMed: 8548814](#)]
955. Iwasaki K, Temin H M. The efficiency of RNA 3'end formation is determined by the distance between the cap site and the poly(A) site in spleen necrosis virus. Genes Dev. 1990;4:2299–2307. [[PubMed: 1703980](#)]
956. Iwasaki K, Liu D W C, Thomas J H. Genes that control a temperature-compensated clock in *Caenorhabditis elegans*. Proc. Natl. Acad. Sci. 1995;92:10317–10321. [[PMC free article: PMC40787](#)] [[PubMed: 7479775](#)]
957. Iwasaki K, McCarter J, Francis R, Schedl T. *emo-1*, a *Caenorhabditis elegans* Sec61p gamma homologue, is required for oocyte development and ovulation. J. Cell Biol. 1996;134:699–714. [[PMC free article: PMC2120936](#)] [[PubMed: 8707849](#)]
958. Izsvák Z, Ivics Z D G, Hackett P B. Characterization of a Tc1-like transposable element in zebrafish (*Danio rerio*). Mol. Gen. Genet. 1995;247:312–322. [[PubMed: 7770036](#)]

## J

959. Jacobson J W, Medhora M M, Hartl D. Molecular structure of a somatically unstable transposable element in *Drosophila*. Proc. Natl. Acad. Sci. 1986;83:8684–8688. [[PMC free article: PMC386995](#)] [[PubMed: 3022302](#)]
960. Jacobson L A, Jen-Jacobson L, Hawdon J M, Owens G P, Bolanowski M A, Emmons S W, Shah M V, Pollock R A, Conklin D S. Identification of a putative structural gene for cathepsin D in *Caenorhabditis elegans*. Genetics. 1988;119:355–363. [[PMC free article: PMC1203418](#)] [[PubMed: 3396869](#)]
961. Jacobson M. Developmental neurobiology. New York: Plenum Press; 1991. pp. 41–93.
962. Jacobson M D, Raff M C. Programmed cell death and Bcl-2 protection in very low oxygen. Nature. 1995;374:814–816. [[PubMed: 7536895](#)]
963. Jacobson M D, Burne J F, King M P, Myiashita T, Reed J C, Raff M C. Bcl-2 blocks apoptosis in cells lacking mitochondrial DNA. Nature. 1993;361:365–369. [[PubMed: 8381212](#)]
964. Jan L Y, Jan Y N. Potassium channels and their evolving gates. Nature. 1994;371:119–122. [[PubMed: 8072541](#)]
965. Jan Y N, Jan L Y. Maggot's hair and bug's eye: Role of cell interactions and intrinsic factors in cell fate specification. Neuron. 1995;14:1–5. [[PubMed: 7826628](#)]
966. Janknecht R, Nordheim A. Gene regulation by ETS proteins. Biochim. Biophys. Acta. 1993;1155:346–356. [[PubMed: 8268191](#)]
967. Jansson H -B. Adhesion of conidia of *Drechmeria coniospora* to *Caenorhabditis elegans* wild type and mutants. J. Nematol. 1994;26:430–435. [[PMC free article: PMC2619527](#)] [[PubMed: 19279912](#)]
968. Jansson H -B, Jeyaprakash A, Coles G C, Marban-Mendoza N, Zuckerman B M. Fluorescent and ferritin labelling of cuticle surface carbohydrates of *Caenorhabditis elegans* and *Panagrellus redivivus*. J. Nematol. 1986;18:570–574. [[PMC free article: PMC2618573](#)] [[PubMed: 19294228](#)]
969. Jantsch-Plunger V. "Gene expression and regulation of the unc-54 myosin heavy chain gene of *C. elegans*: Characterization of an enhancer element and enhancer binding factors." [Ph.D. thesis]. Vienna University; Austria: 1993.
970. Jantsch-Plunger V, Fire A. Combinatorial structure of a [body muscle](#)-specific transcriptional enhancer in *Caenorhabditis elegans*. J. Biol. Chem. 1994;269:27021–27028. [[PubMed: 7929443](#)]
971. Jarman A P, Sun Y, Jan L Y, Jan Y N. Role of the proneural gene, atonal, in formation of *Drosophila* chordotonal organs and photoreceptors. Development. 1995;121:2019–2030. [[PubMed: 7635049](#)]
972. Jarriault S, Brou C, Loget F, Schroeter E H, Kopan R, Israel A. Signalling downstream of activated mammalian Notch. Nature. 1995;377:355–358. [[PubMed: 7566092](#)]

973. Jasmer D P. *Trichinella spiralis*: Subversion of differentiated mammalian skeletal muscle cells. Parasitol. Today. 1995;11:185–188.
974. Jasmer D P, Perryman L E, Conder G A, Crow S, McGuire T. Protective immunity to *Haemonchus contortus* induced by immunoaffinity isolated antigens that share a phylogenetically conserved carbohydrate gut surface epitope. J. Immunol. 1993;151:5450–5460. [PubMed: 7693812]
975. Jazwinski S M. Longevity genes and aging. Science. 1996; 273:54–58. [PubMed: 8658195]
976. Jeroen N A M, van der Voort R, Roosien J, van Zandvoort P M, Folkertsma R T, van Enckevort E L J G, Janssen R, Gommers F J, Bakker J. Linkage mapping in potato cyst nematodes. In: Lamberti F, et al., editors. NATO ARW:Advances in molecular plant nematology. New York: Plenum Press; 1994. pp. 57–63.
977. Jia Y, Xie G, Aamodt E. *pag-3*, a *Caenorhabditis elegans* gene involved in touch neuron gene expression and coordinated movement. Genetics. 1996;142:141–147. [PMC free article: PMC1206942] [PubMed: 8770591]
978. Jin Y, Hoskins R, Horvitz H R. Control of type-D GABAergic neuron differentiation by *C. elegans* UNC-30 homeodomain protein. Nature. 1994;372:780–783. [PubMed: 7997265]
979. Johnsen R C, Baillie D L. Formaldehyde mutagenesis of the eT1 balanced region in *Caenorhabditis elegans*. Mutat. Res. 1988;201:137–147. [PubMed: 3419443]
980. Johnsen R C, Baillie D L. Genetic analysis of a major segment [*LGV(left)*] of the genome of *Caenorhabditis elegans*. Genetics. 1991;129:735–752. [PMC free article: PMC1204741] [PubMed: 1752418]
981. Johnson C D, Russell R L. Multiple molecular forms of acetylcholinesterase in the nematode *Caenorhabditis elegans*. J. Neurochem. 1983;41:30–46. [PubMed: 6864228]
982. Johnson C D, Stretton A O. Neural control of locomotion in *Ascaris*: Anatomy electrophysiology, and biochemistry. In: Zukerman B, editor. Nematodes as biological models. New York: Academic Press; 1980. pp. 159–195.
983. Johnson C D, Stretton A O. Localization of choline acetyltransferase within identified motorneurons of the nematode *Ascaris*. J. Neurosci. 1985;5:1984–1992. [PMC free article: PMC6565288] [PubMed: 4020429]
984. Johnson C D, Stretton A O. GABA-immunoreactivity in inhibitory motor neurons of the nematode *Ascaris*. J. Neurosci. 1987;7:223–235. [PMC free article: PMC6568839] [PubMed: 3543249]
985. Johnson C D, Smith S P, Russell R L. Electrophorus electricus acetylcholinesterases: Separation and selective modification by collagenase. J. Neurochem. 1977;28:617–624. [PubMed: 192853]
986. Johnson C D, Reinitz C A, Sithigorngul P, Stretton A O W. Neuronal localization of serotonin in the nematode *Ascaris suum*. J. Comp. Neurol. 1996;367:352–360. [PubMed: 8698897]
987. Johnson C D, Rand J B, Herman R K, Stern B D, Russell R L. The acetylcholinesterase genes of *C. elegans*: Identification of a third gene (*ace-3*) and mosaic mapping of a synthetic lethal phenotype. Neuron. 1988;1:165–173. [PubMed: 3272166]
988. Johnson C D, Duckett J G, Culotti J G, Herman R K, Meneely P M, Russell R L. An acetylcholinesterase-deficient mutant of the nematode *Caenorhabditis elegans*. Genetics. 1981;97:261–279. [PMC free article: PMC1214393] [PubMed: 7274654]
989. Johnson R C, Yin J C P, Reznikoff W S. Control of Tn5 transposition in *Escherichia coli* is mediated by protein from the right repeat. Cell. 1982;30:873–882. [PubMed: 6291786]
990. Johnson T E. Molecular and genetic analysis of a multivariate system specifying behavior and life span. Behav. Genet. 1986;16:221–235. [PubMed: 3707485]
991. Johnson T E. Aging can be genetically dissected into component processes using long-lived lines of *Caenorhabditis elegans*. Genetics. 1987;84:3777–3781. [PMC free article: PMC304959] [PubMed: 3473482]
992. Johnson T E. Increased life-span of *age-1* mutants in *Caenorhabditis elegans* and lower Gompertz rate of aging. Science. 1990;249:908–912. [PubMed: 2392681]
993. Johnson T E, Hutchinson E W. Absence of strong heterosis for life span in the nematode *Caenorhabditis elegans*. Genetics. 1993;134:465–474. [PMC free article: PMC1205490] [PubMed: 868

[8325483\]](#)

994. Johnson T E, Wood W B. Genetic analysis of life-span in *Caenorhabditis elegans*. *Genetics*. 1982;79:6603–6607. [[PMC free article: PMC347176](#)] [[PubMed: 6959141](#)]
995. Johnson T E, Mitchell D H, Kline S, Kemal R, Foy F. Arresting development arrests aging in the nematode *Caenorhabditis elegans*. *Mech. Ageing Dev.* 1984;28:23–40. [[PubMed: 6542614](#)]
996. Johnson T E, Hutchinson E W, Tedesco P M, Fabian T J, Brooks A, Lithgow G J. New horizons in aging science:Proceedings of the Fourth Asia/Oceania Regional Congress of Gerontology. Tokyo: University of Tokyo Press; 1992. Cloning age-1, a gene that limits the life of *C. elegans*.
997. Johnstone I L. The cuticle of the nematode *Caenorhabditis elegans*—A complex collagen structure. *BioEssays*. 1994;16:171–178. [[PubMed: 8166670](#)]
998. Johnstone I L, Shafi Y, Barry J D. Molecular analysis of mutations in the *Caenorhabditis elegans* collagen gene *dpy-7*. *EMBO J.* 1992;11:3857–3863. [[PMC free article: PMC556895](#)] [[PubMed: 1396579](#)]
999. Jones A R, Schedl T. Mutations in *gld-1* a female germ cell-specific tumor suppressor gene in *Caenorhabditis elegans*, affect a conserved domain also found in Src-associated protein Sam68. *Genes Dev.* 1995;9:1491–1504. [[PubMed: 7601353](#)]
1000. Jones D, Candido E P M. Novel ubiquitin-like ribosomal protein fusion genes from the nematodes *Caenorhabditis elegans* and *Caenorhabditis briggsae*. *J. Biol. Chem.* 1993;268:19545–19551. [[PubMed: 7690036](#)]
1001. Jones D, Dixon D K, Graham R W, Candido E P. Differential regulation of closely related members of the *hsp-16* gene family in *Caenorhabditis elegans*. *DNA*. 1989;8:481–490. [[PubMed: 2475316](#)]
1002. Jones D, Stringham E G, Graham R W, Candido E P M. A portable regulatory element directs specific expression of the *Caenorhabditis elegans* ubiquitin gene *ubq-2* in the [somatic gonad](#). *Dev. Biol.* 1995;171:60–72. [[PubMed: 7556908](#)]
1003. Jones G H. Chiasmata. In: Moens P B, editor. *Meiosis*. Orlando: Academic Press; 1987. pp. 213–244.
1004. Jones M K G. The development and function of plant cells modified by endoparasitic nematodes. In: Zuckerman B M, Rohde R A, editors. *Plant parasitic nematodes*. New York: Academic Press; 1981. pp. 255–280.
1005. Jones S J M, Baillie D L. Characterisation of the *let-653* gene in *Caenorhabditis elegans*. *Mol. Gen. Genet.* 1995;248:719–726. [[PubMed: 7476875](#)]
1006. Jongeward G D, Clandinin T R, Sternberg P W. *sli-1*, a negative regulator of *let-23*-mediated signaling in *C. elegans*. *Genetics*. 1995;139:1553–1566. [[PMC free article: PMC1206484](#)] [[PubMed: 7789760](#)]
1007. Jorgensen E M, Hartwieg E, Schuske H, Nonet M L, Jin Y, Horvitz H R. Defective recycling of synaptic vesicles in synaptotagmin mutants of *C. elegans*. *Nature*. 1995;378:196–199. [[PubMed: 7477324](#)]
1008. Joshua G W P, Chuang R Y, Cheng S C, Lin S F, Tuan R S, Wang C C. The spliced leader gene of *Angiostrongylus cantonensis*. *Mol. Biochem. Parasitol.* 1991;46:209–218. [[PubMed: 1922196](#)]

## K

1009. Kabsch W, Mannherz H G, Suck D, Pai E F, Holmes K. Atomic structure of actin DNase complex. *Nature*. 1990;347:37–44. [[PubMed: 2395459](#)]
1010. Kagan R M, Clarke S. Protein L-isoaspartyl methyltransferase from the nematode *Caenorhabditis elegans*: Genomic structure and substrate specificity. *Biochemistry*. 1995;34:10794–10806. [[PubMed: 7662659](#)]
1011. Kagawa H, Gengyo K, McLachlan A D, Brenner S, Karn J. Paramyosin gene (*unc-15*) of *Caenorhabditis elegans*:Molecular cloning, nucleotide sequence and models for thick filament structure. *J. Mol. Biol.* 1989;207:311–333. [[PubMed: 2754728](#)]
1012. Kagawa H, Sugimoto K, Matsumoto H, Inoue T, Imaizumi H, Takuwa K, Sakube Y. Genome structure, mapping and expression of the tropomyosin gene *tmy-1* of *Caenorhabditis elegans*. *J. Mol. Biol.* 1995;251:603–613. [[PubMed: 7666414](#)]
1013. Kaiser K, Goodwin S F. “Site-selected” transposon mutagenesis of *Drosophila*. *Proc. Natl. Acad. Sci.* 1990;87:1686–1690. [[PMC free article: PMC53547](#)] [[PubMed: 1968635](#)]

1014. Kallioniemi A, Kallioniemi O -P, Sudar D, Rutovitz D, Gray J W, Waldman F, Pinkel D. Comparative genomic hybridization: A powerful new method for cytogenetic analysis of solid tumors. *Science*. 1992;258:818–821. [[PubMed: 1359641](#)]
1015. Kallunki P, Tryggvason K. Human basement membrane heparan sulfate proteoglycan core protein: A 467-kD protein containing multiple domains resembling elements of the low density lipoprotein receptor, laminin, [neural](#) cell adhesion molecules and epidermal growth factor. *J. Cell Biol.* 1992;116:559–571. [[PMC free article: PMC2289301](#)] [[PubMed: 1730768](#)]
1016. Kamb A, Weir M, Rudy B, Varmus H, Kenyon C. Identification of genes from pattern formation, tyrosine kinase, and potassium channel families by DNA amplification. *Proc. Natl. Acad. Sci.* 1989;86:4372–4376. [[PMC free article: PMC287271](#)] [[PubMed: 2734290](#)]
1017. Kandel E R. Transmitter release. In: Kandel E R, et al., editors. *Principles of [neural](#) science* 3rd edition. New York: Elsevier; 1991. pp. 194–212.
1018. Kandel E R, O'Dell T J. Are adult learning mechanisms also used for development? *Science*. 1992;258:243–245. [[PubMed: 1411522](#)]
1019. Kaplan J M, Horvitz H R. A dual mechanosensory and chemosensory neuron in *Caenorhabditis elegans*. *Proc. Natl. Acad. Sci.* 1993;90:2227–2231. [[PMC free article: PMC46059](#)] [[PubMed: 8460126](#)]
1020. Kapeller R, Cantley L C. Phosphatidylinositol 3-kinase. *BioEssays*. 1994;16:565. [[PubMed: 8086005](#)]
1021. Karn J, Brenner S, Barnett L. Protein structural domains in the *Caenorhabditis elegansunc-54* myosin heavy chain gene are not separated by introns. *Proc. Natl. Acad. Sci.* 1983;80:4253–4257. [[PMC free article: PMC384015](#)] [[PubMed: 6576334](#)]
1022. Katagiri H, Terasaki J, Murata T, Ishihara H, Ogihara T, Inukai K, Fukushima Y, Anai M, Kikuchi M, Miyazaki J. A novel isoform of syntaxin-binding protein homologous to yeast Sec1 expressed ubiquitously in mammalian cells. *J. Biol. Chem.* 1995;270:4963–4966. [[PubMed: 7890599](#)]
1023. Katsura I, Kondo K, Amano T, Ishihara T, Kawakami M. Isolation, characterization and epistasis of fluoride-resistant mutants of *Caenorhabditis elegans*. *Genetics*. 1994;136:145–154. [[PMC free article: PMC1205766](#)] [[PubMed: 8138152](#)]
1024. Katz P S, Getting P A, Frost W N. Dynamic neuromodulation of synaptic strength intrinsic to a central pattern generator circuit. *Nature*. 1994;367:729–731. [[PubMed: 8107867](#)]
1025. Katz W S, Hill R J, Clandinin T R, Sternberg P W. Different levels of the *C. elegans* growth factor LIN-3 promote distinct vulval precursor fates. *Cell*. 1995;82:297–307. [[PubMed: 7628018](#)]
1026. Katz W S, Lesa G M, Yannoukakos D, Clandinin T R, Schlessinger J, Sternberg P W. A point mutation in the extracellular domain activates LET-23, the *C. elegans* EGF receptor homology. *Mol. Cell. Biol.* 1996;16:529–537. [[PMC free article: PMC231031](#)] [[PubMed: 8552080](#)]
1027. Keino-Masu K, Masu M, Hinck L, Leonardo E D, Chan S S -Y, Culotti J G, Tessier-Lavigne M. Deleted in Colorectal Cancer (DCC) encodes a netrin receptor. *Cell*. 1996;87:175–185. [[PubMed: 8861902](#)]
1028. Keller M, Tessier L H, Chan R L, Weil J H, Imbault P. In *Euglena*, spliced leader RNA (SL RNA) and 5S rRNA genes are tandemly repeated. *Nucleic Acids Res.* 1992;20:1711–1715. [[PMC free article: PMC312261](#)] [[PubMed: 1579464](#)]
1029. Kellogg E A, Shaffer H B. Model organisms in evolutionary studies. *Syst. Biol.* 1993;42:409–414.
1030. Kelly R B. The cell biology of the nerve terminal. *Neuron*. 1988;1:431–438. [[PMC free article: PMC7135562](#)] [[PubMed: 2908445](#)]
1031. Kemphues K J, Malacinski G M, editor. *Developmental genetics of higher organisms*. New York: Macmillan; 1988. Genetic analysis of embryogenesis in *Caenorhabditis elegans*. pp. 193–219.
1032. Kemphues K J. *Caenorhabditis*. In: Glover D M, Hames E D, editors. *Frontiers in molecular biology: Genes and embryos*. London: 1989. pp. 95–126.
1033. Kemphues K J, Kusch M, Wolf N. Maternal-effect lethal mutations on linkage group II of *Caenorhabditis elegans*. *Genetics*. 1988a;120:977–986. [[PMC free article: PMC1203589](#)] [[PubMed: 3224814](#)]
1034. Kemphues K J, Priess J R, Morton D G, Cheng N. Identification of genes required for cytoplasmic localization in early *Caenorhabditis elegans* embryos. *Cell*. 1988b;52:311–320. [[PubMed: 3345562](#)]

1035. Kennedy B P, Aamodt E J, Allen F L, Chung M A, Heschl M F P, McGhee J D. The gut esterase gene (*ges-7*) from the nematodes *Caenorhabditis elegans* and *Caenorhabditis briggsae*. *J. Mol. Biol.* 1993;229:890–908. [[PubMed: 8445654](#)]
1036. Kennedy M W, Allen J E, Wright A S, McCruden A B, Cooper A. The gp15/400 polyprotein antigen of *Brugia malayi* binds fatty acids and retinoids. *Mol. Biochem. Parasitol.* 1995;71:41–50. [[PubMed: 7630382](#)]
1037. Kennedy M W, Foley M, Kuo Y -M, Kusel J R, Garland P B. Biophysical properties of the surface lipid of parasitic nematodes. *Mol. Biochem. Parasitol.* 1987;22:233–240. [[PubMed: 3553935](#)]
1038. Kennedy T E, Serafini T, de la Torre J R, Tessier-Lavigne M. Netrins are diffusible chemotropic factors for commissural axons in the embryonic spinal cord. *Cell.* 1994;78:425–435. [[PubMed: 8062385](#)]
1039. Kenyon C. A gene involved in the development of the posterior body region of *C. elegans*. *Cell.* 1986;46:477–487. [[PubMed: 3731276](#)]
1040. Kenyon C. If birds can fly, why can't we? Homeotic genes and evolution. *Cell.* 1994;78:175–180. [[PubMed: 7913878](#)]
1041. Kenyon C. Ponce d'*elegans*: Genetic quest for the fountain of youth. *Cell.* 1996;84:501–504. [[PubMed: 8598036](#)]
1042. Kenyon C, Wang B. A cluster of *Antennapedia*-class homeobox genes in a nonsegmented animal. *Science.* 1991;253:516–517. [[PubMed: 1677487](#)]
1043. Kenyon C, Chang J, Gensch E, Rudner A, Tabtiang R. A *C. elegans* mutant that lives twice as long as wild type. *Nature.* 1993;366:461–464. [[PubMed: 8247153](#)]
1044. Kerr J F R, Harmon B V. Definition and incidence of apoptosis: A historical perspective. In: Tomei L D, Cope F O, editors. *Apoptosis: The molecular basis of cell death*. Cold Spring Harbor, New York: Cold Spring Harbor Laboratory Press; 1991. pp. 5–29.
1045. Kerr J F R, Wyllie A H, Currie A R. Apoptosis: A basic biological phenomenon with wide-ranging implications in tissue kinetics. *Br. J. Cancer.* 1972;26:239–257. [[PMC free article: PMC2008650](#)] [[PubMed: 4561027](#)]
1046. Keynes R, Cook G M W. Axon guidance molecules. *Cell.* 1995;83:161–169. [[PubMed: 7585933](#)]
1047. Khan E, Mack J P G, Katz R A, Kulkosky J, Skalka A M. Retroviral integrase domains: DNA binding and the recognition of LTR sequences. *Nucleic Acids Res.* 1991;19:851–860. [[PMC free article: PMC333721](#)] [[PubMed: 1850126](#)]
1048. Khoo K -H, Maizels R M, Page A P, Taylor G W, Rendell N B, Dell A. Characterisation of nematode glycoproteins: The major O-glycans of *Toxocara canis* *excretory-secretory* antigens are O-methylated trisaccharides. *Glycobiology.* 1991;1:163–171. [[PubMed: 1823159](#)]
1049. Khosla M, Honda B M. Initiator tRNA<sup>Met</sup> genes from the nematode *Caenorhabditis elegans*. *Gene.* 1989;76:321–330. [[PubMed: 2526778](#)]
1050. Kiff J E, Moerman D G, Schriefer L A, Waterston R H. Transposon induced deletions in *unc-22* of *Caenorhabditis elegans* associated with almost normal gene activity. *Nature.* 1988;331:631–633. [[PubMed: 2829031](#)]
1051. Kim J S, Rose A M. The effect of gamma radiation on recombination in *Caenorhabditis elegans*. *Genome.* 1987;29:457–462. [[PubMed: 3609740](#)]
1052. Kim S. "Two *C. elegans* genes that can mutate to cause degenerative cell death." [Ph.D. thesis]. Massachusetts Institute of Technology; Cambridge: 1994.
1053. Kim S, Horvitz H R. The *Caenorhabditis elegans* gene *lin-10* is broadly expressed while required specifically for the determination of vulval cell fates. *Genes Dev.* 1990;4:357–371. [[PubMed: 2159938](#)]
1054. Kim Y, Nirenberg M. *Drosophila* NK-homeobox genes. *Proc. Natl. Acad. Sci.* 1989;86:7716–7720. [[PMC free article: PMC298141](#)] [[PubMed: 2573058](#)]
1055. Kim Y K, Valdivia H H, Maryon E B, Anderson P, Coronado R. High molecular weight proteins in the nematode *C. elegans* bind [<sup>3</sup>H]ryanodine and form a large conductance channel. *Biophys. J.* 1992;63:1379–1384. [[PMC free article: PMC1261442](#)] [[PubMed: 1335783](#)]

1056. Kimble J. Alterations in cell lineage following laser ablation of cells in the somatic gonad of *Caenorhabditis elegans*. *Dev. Biol.* 1981;87:286–300. [[PubMed: 7286433](#)]
1057. Kimble J, Hirsh D. The postembryonic cell lineages of the hermaphrodite and male gonads in *Caenorhabditis elegans*. *Dev. Biol.* 1979;70:396–417. [[PubMed: 478167](#)]
1058. Kimble J, Sharrock W J. Tissue-specific synthesis of yolk proteins in *Caenorhabditis elegans*. *Dev. Biol.* 1983;96:189–196. [[PubMed: 6825952](#)]
1059. Kimble J, Ward S. Wood W B, editor. The nematode *Caenorhabditis elegans*. Cold Spring Harbor, New York: Cold Spring Harbor Laboratory; 1988. Germ-line development and fertilization. pp. 191–213.
1060. Kimble J E, White J G. On the control of germ cell development in *Caenorhabditis elegans*. *Dev. Biol.* 1981;81:208–219. [[PubMed: 7202837](#)]
1061. Kimble J, Edgar L, Hirsh D. Specification of male development in *Caenorhabditis elegans*: The *fem* genes. *Dev. Biol.* 1984;105:234–239. [[PubMed: 6468762](#)]
1062. Kimble J, Hodgkin J, Smith T, Smith J. Suppression of an amber mutation by microinjection of suppressor tRNA in *C. elegans*. *Nature*. 1982;299:456–458. [[PubMed: 7121584](#)]
1063. King K L, Steward M, Roberts T M. Supramolecular assemblies of *Ascaris suum* major sperm protein (MSP) associated with amoeboid cell motility. *J. Cell Sci.* 1994a;107:2941–2949. [[PubMed: 7876359](#)]
1064. King K L, Essig J, Roberts T M, Moerland T S. Regulation of the *Ascaris* major sperm protein (MSP) cytoskeleton by intracellular pH. *Cell Motil. Cytoskel.* 1994b;27:193–205. [[PubMed: 8020106](#)]
1065. King K L, Stewart M, Roberts T M, Seavy M. Structure and macromolecular assembly of two isoforms of the major sperm protein (MSP) from the amoeboid sperm of the nematode, *Ascaris suum*. *J. Cell Sci.* 1992;101:847–857. [[PubMed: 1527183](#)]
1066. King M C, Wilson Evolution at two levels in humans and chimpanzees. *Science*. 1975;188:107–116. [[PubMed: 1090005](#)]
1067. Kingsley D M. The TGF-3 $\beta$  superfamily: New members new receptors, and new genetic tests of function in different organisms. *Genes Dev.* 1994;8:133–146. [[PubMed: 8299934](#)]
1068. Kingston I B, Pettitt J. Structure and expression of *Ascaris suum* collagen genes: A comparison with *Caenorhabditis elegans*. *Acta Trop.* 1990;47:283–287. [[PubMed: 1978528](#)]
1069. Kingston I B, Wainwright S M, Cooper D. Comparison of collagen gene sequences in *Ascaris suum* and *Caenorhabditis elegans*. *Mol. Biochem. Parasitol.* 1989;37:137–146. [[PubMed: 2482444](#)]
1070. Kipreos E T, Lander L E, Wing J P, He W W, Hedgecock E M. *cul-1* is required for cell cycle exit in *C. elegans* and identifies a novel gene family. *Cell*. 1996;85:829–840. [[PubMed: 8681378](#)]
1071. Kirby C, Kusch M, Kemphues K. Mutations in the *par* genes of *Caenorhabditis elegans* affect cytoplasmic reorganization during the first cell cycle. *Dev. Biol.* 1990;142:203–215. [[PubMed: 2227096](#)]
1072. Kirk K E, Blackburn E H. An unusual sequence arrangement in the telomeres of the germ-line micronucleus in *Tetrahymena thermophila*. *Genes Dev.* 1995;9:59–71. [[PubMed: 7828852](#)]
1073. Kishino H, Hasegawa M. Evaluation of the maximum likelihood estimate of the evolutionary tree topologies from DNA sequence data, and the branching order in Hominoidea. *J. Mol. Evol.* 1989;29:170–179. [[PubMed: 2509717](#)]
1074. Klammt C, Glazer L, Shilo B Z. *breathless*, a *Drosophila* FGF receptor homolog, is essential for migration of tracheal and specific midline glial cells. *Genes Dev.* 1992;6:1668–1678. [[PubMed: 1325393](#)]
1075. Klass M R. Aging in the nematode *Caenorhabditis elegans*: Major biological and environmental factors influencing life span. *Mech. Ageing Dev.* 1977;6:413–429. [[PubMed: 9268671](#)]
1076. Klass M R. A method for the isolation of longevity mutants in the nematode *Caenorhabditis elegans* and initial results. *Mech. Ageing Dev.* 1983;22:279–286. [[PubMed: 6632998](#)]
1077. Klass M R, Hirsh D. Nonaging developmental variant of *Caenorhabditis elegans*. *Nature*. 1976;260:523–525. [[PubMed: 1264206](#)]
1078. Klass M R, Hirsh D. Sperm isolation and biochemical analysis of the major sperm protein from *Caenorhabditis elegans*. *Dev. Biol.* 1981;84:299–312. [[PubMed: 20737868](#)]

1079. Klass M, Ammons D, Ward S. Conservation in the 5'flanking sequences of transcribed members of the *Caenorhabditis elegans* major sperm protein gene family. *J. Mol. Biol.* 1988;199:15–22. [[PubMed: 2451024](#)]
1080. Klass M R, Kinsley S, Lopez L. Isolation and characterization of a sperm-specific gene family in the nematode *Caenorhabditis elegans*. *Mol. Cell. Biol.* 1984;4:529–537. [[PMC free article: PMC368732](#)] [[PubMed: 6325882](#)]
1081. Klass M R, Wolf N, Hirsh D. Development of the [male reproductive system](#) and sexual transformation in the nematode *Caenorhabditis elegans*. *Dev. Biol.* 1976;52:1–18. [[PubMed: 986968](#)]
1082. Klein R D, Meyer B J. Independent domains of the Sdc-3 protein control sex determination and dosage compensation in *C. elegans*. *Cell.* 1993;72:349–364. [[PubMed: 8431944](#)]
1083. Klingensmith J, Nusse R. Signaling by *wingless* in *Drosophila*. *Dev. Biol.* 1994;166:396–414. [[PubMed: 7813765](#)]
1084. Klingensmith J, Nusse R, Perrimon N. The *Drosophila* segment polarity gene *dishevelled* encodes a novel protein required for response to the wingless signal. *Genes Dev.* 1994;8:118–130. [[PubMed: 8288125](#)]
1085. Klobutcher L A, Jahn C L. Developmentally controlled genomic rearrangements in ciliated protozoa. *Curr. Opin. Genet. Dev.* 1991;1:397–403. [[PubMed: 1668650](#)]
1086. Kloek A P, Sherman D R, Goldberg D E. Novel gene structure and evolutionary context of *Caenorhabditis elegans* globin. *Gene.* 1993a;129:215–221. [[PubMed: 8325507](#)]
1087. Kloek A P, Yiang J, Matthews F S, Goldberg D E. Expression, characterisation and crystallization of oxygen-avid *Ascaris* hemoglobin domains. *J. Biol. Chem.* 1993b;268:17669–17671. [[PubMed: 8349648](#)]
1088. Klug A, Schwabe J W R. Zinc fingers. *FASEB J.* 1995;9:597–604. [[PubMed: 7768350](#)]
1089. Knoblich J A, Jan L Y, Jan Y N. Asymmetric segregation of Numb and Prospero during cell division. *Nature.* 1995;377:624–627. [[PubMed: 7566172](#)]
1090. Kodoyianni V, Maine E, Kimble J. Molecular basis of loss-of-function mutations in the *glp-1* gene of *Caenorhabditis elegans*. *Mol. Biol. Cell.* 1992;3:1199–1213. [[PMC free article: PMC275687](#)] [[PubMed: 1457827](#)]
1091. Koelle M R, Horvitz H R. EGL-10 regulates G protein signalling in the *C. elegans* [nervous system](#) and shares a conserved domain with many mammalian proteins. *Cell.* 1996;84:115–125. [[PubMed: 8548815](#)]
1092. Koenig J H, Ikeda K. Disappearance and reformation of synaptic vesicle membrane upon transmitter release observed under reversible blockage of membrane retrieval. *J. Neurosci.* 1989;9:3844–3860. [[PMC free article: PMC6569944](#)] [[PubMed: 2573698](#)]
1093. Koga M, Ohshima Y. Mosaic analysis of the *let-23* gene function in vulval induction of *Caenorhabditis elegans*. *Development.* 1995;121:2655–2666. [[PubMed: 7671826](#)]
1094. Kohler P, Bachmann R. Intestinal tubulin as possible target for the chemotherapeutic action of mebendazole in parasitic nematodes. *Mol. Biochem. Parasitol.* 1981;4:325–336. [[PubMed: 7335116](#)]
1095. Kolodkin A L, Matthes D J, O'Connor T P, Patel N H, Admon A, Bentley D, Goodman C S. Fasciclin IV: Sequence, expression, and function during growth cone guidance in the grasshopper embryo. *Neuron.* 1992;9:831–845. [[PubMed: 1418998](#)]
1096. Kolson D L, Russell R L. A novel class of acetylcholinesterase revealed by mutations, in the nematode *Caenorhabditis elegans*. *J. Neurogenet.* 1985a;2:93–110. [[PubMed: 4020535](#)]
1097. Kolson D L, Russell R L. New acetylcholinesterase-deficient mutants of the nematode *Caenorhabditis elegans*. *J. Neurogenet.* 1985b;2:69–91. [[PubMed: 4020534](#)]
1098. Komatsu H, Mori I, Rhee J S, Akaike N, Ohshima Y. Mutations in a cyclic nucleotide-gated channel lead to abnormal thermosensation and chemosensation in *C. elegans*. *Neuron.* 1996;17:707–718. [[PubMed: 8893027](#)]
1099. Kondo K, Hodgkin J, Waterson N R. Differential expression of five tRNA<sup>Trp</sup><sub>UAG</sub> amber suppressors in *Caenorhabditis elegans*. *Mol. Cell. Biol.* 1988;8:3627–3635. [[PMC free article: PMC365418](#)] [[PubMed: 3130300](#)]

[3221861\]](#)

1100. Kondo K, Makovec B, Waterston R H, Hodgkin J. Genetic and molecular analysis of eight tRNA<sup>Trp</sup> amber suppressors in *Caenorhabditis elegans*. *J. Mol. Biol.* 1990;215:7–19. [[PubMed: 2398498](#)]
1101. Kondo T, Tsinoremas N F, Golden S S, Johnson C H, Kutsuna S, Ishiura M. Circadian clock mutants of cyanobacteria. *Science*. 1994;266:1233–1236. [[PubMed: 7973706](#)]
1102. Konopka R J, Benzer S. Clock mutants of *Drosophila melanogaster*. *Proc. Natl. Acad. Sci.* 1971;68:2112–2116. [[PMC free article: PMC389363](#)] [[PubMed: 5002428](#)]
1103. Konopka R J, Pittendrigh C, Orr D. Reciprocal behaviour associated with altered homeostasis and photosensitivity of *Drosophila* clock mutants. *J. Neurogenet.* 1989;6:1–10. [[PubMed: 2506319](#)]
1104. Kopan R, Nye J S, Weintraub H. The intracellular domain of mouse Notch: A constitutively activated repressor of myogenesis directed at the basic helix-loop-helix region of MyoD. *Development*. 1994;120:2385–2396. [[PubMed: 7956819](#)]
1105. Kornfeld K, Guan K -L, Horvitz H R. The *Caenorhabditis elegans* gene *mek-2* is required for vulval induction and encodes a protein similar to the protein kinase MEK. *Genes Dev.* 1995a;9:756–768. [[PubMed: 7729691](#)]
1106. Kornfeld K, Hom D B, Horvitz H R. The *ksr-1* gene encodes a novel protein kinase involved in *ras*-mediated signaling in *Caenorhabditis elegans*. *Cell*. 1995b;83:903–913. [[PubMed: 8521514](#)]
1107. Korsmeyer S J, Shutter J R, Veis D J, Merry D E, Oltvai Z N. Bcl-2/Bax: A rheostat that regulates an anti-oxidant pathway and cell death. *Semin. Cancer Biol.* 1993;4:327–333. [[PubMed: 8142617](#)]
1108. Kosaka T, Ikeda K. Reversible blockage of membrane retrieval and endocytosis in the garland cell of the temperature-sensitive mutant of *Drosophila melanogaster shibire(ts)*. *J. Cell Biol.* 1983;97:499–507. [[PMC free article: PMC2112522](#)] [[PubMed: 6411734](#)]
1109. Kostrouch Z, Kostrouchova M, Rall J E. Steroid/thyroid hormone receptor genes in *Caenorhabditis elegans*. *Proc. Natl. Acad. Sci.* 1995;92:156–159. [[PMC free article: PMC42836](#)] [[PubMed: 7816808](#)]
1110. Krajewski S, Tanaka S, Takayama S, Schibler M J, Fenton W, Reed J C. Investigation of the subcellular distribution of the bcl-2 oncoprotein: Residence in the nuclear envelope, endoplasmic reticulum, and outer mitochondrial membranes. *Cancer Res.* 1993;53:4701–4714. [[PubMed: 8402648](#)]
1111. Kramer J M. Structures and functions of collagens in *Caenorhabditis elegans*. *FASEB J.* 1994a;8:329–336. [[PubMed: 8143939](#)]
1112. Kramer J M. Genetic analysis of extracellular matrix in *C. elegans*. *Annu. Rev. Genet.* 1994b;28:95–116. [[PubMed: 7893143](#)]
1113. Kramer J M, Johnson J J. Analysis of mutations in the *sqt-1* and *rol-6* collagen genes of *Caenorhabditis elegans*. *Genetics*. 1993;135:1035–1045. [[PMC free article: PMC1205736](#)] [[PubMed: 8307321](#)]
1114. Kramer J M, Cox G N, Hirsh D. Comparisons of the complete sequences of two collagen genes from *Caenorhabditis elegans*. *Cell*. 1982;30:599–606. [[PubMed: 7139711](#)]
1115. Kramer J M, Cox G N, Hirsh D. Expression of the *Caenorhabditis elegans* collagen genes *col-1* and *col-2* is developmentally regulated. *J. Biol. Chem.* 1985;260:1945–1951. [[PubMed: 2578467](#)]
1116. Kramer J M, French R P, Park E -C, Johnson J J. The *Caenorhabditis elegans* *rol-6* gene, which interacts with the *sqt-1* collagen gene to determine organismal morphology, encodes a collagen. *Mol. Cell. Biol.* 1990;10:2081–2089. [[PMC free article: PMC360555](#)] [[PubMed: 1970117](#)]
1117. Kramer J M, Johnson J J, Edgar R S, Basch C, Roberts S. The *sqt-1* gene of *C. elegans* encodes a collagen critical for organismal morphogenesis. *Cell*. 1988;55:555–565. [[PubMed: 3180220](#)]
1118. Krause M, Hirsh D. A *trans*-spliced leader sequence on actin mRNA in *C. elegans*. *Cell*. 1987;49:753–761. [[PMC free article: PMC7133374](#)] [[PubMed: 3581169](#)]
1119. Krause M, Wild M, Rosenzweig B, Hirsch D. Wild-type and mutant actin genes in *Caenorhabditis elegans*. *J. Mol. Biol.* 1989;208:381–392. [[PubMed: 2795655](#)]
1120. Krause M, Fire A, Harrison S W, Priess J, Weintraub H. CeMyoD accumulation defines the [body wall muscle](#) cell fate during *C. elegans* embryogenesis. *Cell*. 1990;63:907–919. [[PubMed: 2175254](#)]

1121. Krause M, Fire A, White-Harrison S, Weintraub H, Tapscott S. Functional conservation of nematode and vertebrate myogenic regulatory factors.(suppl.) . J. Cell Sci. 1992;16:111–115. [[PubMed: 1338434](#)]
1122. Krause M, Harrison S W, Xu S -Q, Chen L, Fire A. Elements regulating cell- and stage-specific expression of the *C. elegans* MyoD family homolog *hh-1*. Dev. Biol. 1994;166:133–148. [[PubMed: 7958441](#)]
1123. Kravitz E A. Hormonal control of behavior: Amines as gain-setting elements that bias behavioral output in lobsters. Am. Zool. 1990;30:595–608.
1124. Kreutzer M A, Richards J P, De Silva-Udawatta M N, Temenak J J, Knoblich J A, Lehner C F, Bennett K L. *Caenorhabditis elegans* cyclin A- and B-type genes: A cyclin A multigene family, an ancestral cyclin B3 and differential germline expression. J. Cell Sci. 1995;108:2415–2424. [[PubMed: 7545687](#)]
1125. Krieger D T. Brain peptides: What where, and why? Science. 1983;222:975–985. [[PubMed: 6139875](#)]
1126. Krumlauf R, Marshall H, Studer M, Nonchev S, Sham M H, Lumsden A. Hox homeobox genes and regionalization of the [nervous system](#). J. Neurobiol. 1993;24:1328–1340. [[PubMed: 7901322](#)]
1127. Kuhn D M, Arthur R, Yoon H, Sankaran K. Tyrosine hydroxylase in secretory granules from bovine adrenal medulla. J. Biol. Chem. 1990;265:5780–5786. [[PubMed: 1969407](#)]
1128. Kulkosky J, Jones K S, Katz R A, Mack J P, Skalka A M. Residues critical for retroviral integrative recombination in a region that is highly conserved among retroviral/retrotransposon integrases and bacterial insertion sequence transposases. Mol. Cell. Biol. 1992;12:2331–2338. [[PMC free article: PMC364405](#)] [[PubMed: 1314954](#)]
1129. Kumar S. ICE-like proteases in apoptosis. Trends Biochem. Sci. 1995;20:198–202. [[PubMed: 7610484](#)]
1130. Kumar S, Tamura K, Nei M. MEGA: Molecular evolutionary genetic analysis, version 1.01. University Park: Pennsylvania State University; 1993.
1131. Kumar S, Kineshita M, Noda M, Copeland N G, Jenkins N A. Induction of apoptosis by the mouse *Nedd2* gene, which encodes a protein similar to the product of the *Caenorhabditis elegans* cell death gene *ced-3* and the mammalian IL-1 $\beta$  converting enzyme. Genes Dev. 1994;8:1613–1626. [[PubMed: 7958843](#)]
1132. Kumazaki T, Hori H, Osawa S, Ishii N, Suzuki K. The nucleotide sequences of 5S rRNAs from a rotifer, *Brachionus plicatilis*, and two nematodes, *Rhabditis tokai* and *C. elegans*. Nucleic Acids Res. 1982;10:7001–7004. [[PMC free article: PMC326980](#)] [[PubMed: 6891053](#)]
1133. Kunze R, Starlinger P. The putative transposase of transposable element Ac from *Zea mays* L. interacts with subterminal sequences of Ac. EMBO J. 1989;8:3177–3185. [[PMC free article: PMC401433](#)] [[PubMed: 2555157](#)]
1134. Kusch M, Edgar R S. Genetic studies of unusual loci that affect body shape of the nematode *Caenorhabditis elegans* and may code for cuticle structural proteins. Genetics. 1986;113:621–639. [[PMC free article: PMC1202859](#)] [[PubMed: 3732788](#)]
1135. Kuwabara P E. A novel regulatory mutation in the *C. elegans* sex determination gene *tra-2* defines a candidate ligand/receptor interaction site. Development. 1996a;122:2089–2098. [[PubMed: 8681790](#)]
1136. Kuwabara P E. Interspecies comparison reveals evolution of control regions in the nematode sex-determining gene *tra-2*. Genetics. 1996b;144:597–607. [[PMC free article: PMC1207553](#)] [[PubMed: 8889523](#)]
1137. Kuwabara P, Kimble J. A predicted membrane protein TRA-2A, directs hermaphrodite development in *C. elegans*. Development. 1995;121:2995–3004. [[PubMed: 7555725](#)]
1138. Kuwabara P E, Shah S. Cloning by synteny: Identifying *C. briggsae* homologues of *C. elegans* genes. Nucleic Acids Res. 1994;22:4414–4418. [[PMC free article: PMC308474](#)] [[PubMed: 7971272](#)]
1139. Kuwabara P E, Okkema P G, Kimble J. *tra-2* encodes a membrane protein and may mediate cell communication in the *Caenorhabditis elegans* sex determination pathway. Mol. Biol. Cell. 1992;3:461–473. [[PMC free article: PMC275596](#)] [[PubMed: 1498366](#)]
1140. Kwa M S G, Veenstra J G, Roos M H. Benzimidazole resistance in *Haemonchus contortus* is correlated with a conserved mutation at amino acid 200 in  $\beta$ -tubulin isotype 1. Mol. Biochem. Parasitol. 1994;63:299–303. [[PubMed: 7911975](#)]

1141. Kwa M S G, Kooyman F N J, Boersema J H, Roos M H. Effect of selection for benzimidazole resistance in *Haemonchus contortus* on beta-tubulin isotype 1 and isotype-2 genes. *Biochem. Biophys. Res. Commun.* 1993;191:413–419. [[PubMed: 8096381](#)]
1142. Kwa M S G, Veenstra J G, van Dijk M, Roos M H.  $\beta$ -tubulin genes from the parasitic nematode *Haemonchus contortus* modulate drug resistance in *Caenorhabditis elegans*. *J. Mol. Biol.* 1995;246:500–510. [[PubMed: 7877171](#)]

## L

1143. Labbe J C, Jannatipour M, Rokeach L A. The *Caenorhabditis elegans* gene *rop-1* encodes the homologue of the human 60-kDa Ro autoantigen. *Gene.* 1995;167:227–231. [[PubMed: 8566782](#)]
1144. Labeit S, Kolmerer B. Titins: Giant proteins in charge of muscle ultrastructure and elasticity. *Science.* 1995;270:293–296. [[PubMed: 7569978](#)]
1145. Labeit S, Gautel M, Lakey A, Trinick J. Towards a molecular understanding of titin. *EMBO J.* 1992;11:1711–1716. [[PMC free article: PMC556628](#)] [[PubMed: 1582406](#)]
1146. Labeit S, Barlow D P, Gautel M, Gibson T, Holt J, Hsieh C -L, Francke U, Leonard K, Wardale J, Whiting A, Trinick J. A regular pattern of two types of 100-residue motif in the sequence of titin. *Nature.* 1990;345:273–276. [[PubMed: 2129545](#)]
1147. Labouesse M, Hartwig E, Horvitz H R. The *Caenorhabditis elegans* LIN-26 protein is required to specify and/or maintain all non-neuronal ectodermal cell fates. *Development.* 1996;122:2579–2588. [[PubMed: 8787733](#)]
1148. Labouesse M, Sookhareea S, Horvitz H R. The *Caenorhabditis elegans* gene *lin-26* is required to specify the fates of hypodermal cells and encodes a presumptive zinc-finger transcription factor. *Development.* 1994;120:2359–2368. [[PubMed: 7956818](#)]
1149. Lacey E, Gill J H. Biochemistry of benzimidazole resistance. *Acta Tropica.* 1994;56:245–262. [[PubMed: 8203306](#)]
1150. Lackner M R, Kornfeld K, Miller L M, Horvitz H R, Kim S K. A MAP kinase homologue, *mpk-1*, is involved in ras mediated induction of vulval cell fates in *Caenorhabditis elegans*. *Genes Dev.* 1994;8:160–173. [[PubMed: 8299936](#)]
1151. LaFemina R L, Schneider C L, Robbins H L, Callahan P L, LeGrow K, Roth E, Schleif W A, Emini E A. Requirement of active human immunodeficiency virus type 1 integrase enzyme for productive infection of human T-lymphoid cells. *J. Virol.* 1992;66:7414–7419. [[PMC free article: PMC240448](#)] [[PubMed: 1433523](#)]
1152. Lagna G, Hata A, Hemmati-Brivanlou A, Massagué J. Partnership between DPC4 and SMAD proteins in TGF- $\beta$  signalling pathways. *Nature.* 1996;383:832–836. [[PubMed: 8893010](#)]
1153. Lai C C, Hong K, Kinnell M, Chalfie M, Driscoll M. Sequence and transmembrane topology of MEC-4, an ion channel subunit required for mechanotransduction in *C. elegans*. *J. Cell Biol.* 1996;133:1071–1081. [[PMC free article: PMC2120861](#)] [[PubMed: 8655580](#)]
1154. Lai E, Clark K L, Burley S K, Darnell J E , Jr. Hepatocyte nuclear factor 3/fork head or “winged helix” proteins: A family of transcription factors of diverse biologic function. *Proc. Natl. Acad. Sci.* 1993;90:10421–10423. [[PMC free article: PMC47788](#)] [[PubMed: 8248124](#)]
1155. Lai E, Prezioso V R, Smith E, Litvin O, Costa R H, Darnell J E , Jr. HNF-3A, a hepatocyte-enriched transcription factor of novel structure is regulated transcriptionally. *Genes Dev.* 1990;4:1427–1436. [[PubMed: 2227418](#)]
1156. Lake J A. Origin of the metazoa. *Proc. Natl. Acad. Sci.* 1990;87:763–766. [[PMC free article: PMC53346](#)] [[PubMed: 2300560](#)]
1157. Lakey A, Ferguson C, Labeit S, Reedy M, Larkins A, Butcher G, Leonard K, Bullard B. Identification and localization of high molecular weight proteins in insect flight and leg muscle. *EMBO J.* 1990;9:3459–3467. [[PMC free article: PMC552094](#)] [[PubMed: 2209553](#)]
1158. Lakowski B, Hekimi S. Determination of life-span in *Caenorhabditis elegans* by four clock genes. *Science.* 1996;272:1010–1013. [[PubMed: 8638122](#)]

1159. Lambert S, Bennett V. From anemia to cerebellar dysfunction. A review of the ankyrin gene family. *Eur. J. Biochem.* 1993;211:1–6. [[PubMed: 8425519](#)]
1160. Lambie E J, Kimble J. Two homologous regulatory genes *lin-12* and *glp-1*, have overlapping functions. *Development.* 1991;112:231–240. [[PubMed: 1769331](#)]
1161. LaMunyon C W, Ward S. Assessing the viability of mutant and manipulated sperm by artificial insemination of *Caenorhabditis elegans*. *Genetics.* 1994;138:689–692. [[PMC free article: PMC1206219](#)] [[PubMed: 7851766](#)]
1162. Land M, Islas-Trejo A, Rubin C S. Origin, properties, and regulated expression of multiple mRNAs encoded by the protein kinase C1 gene of *Caenorhabditis elegans*. *J. Biol. Chem.* 1994a;269:14820–14827. [[PubMed: 8182089](#)]
1163. Land M, Islas-Trejo A, Freedman J H, Rubin C S. Structure and expression of a novel, neuronal protein kinase C (PKC1B) from *Caenorhabditis elegans*. *J. Biol. Chem.* 1994b;269:9234–9244. [[PubMed: 8132661](#)]
1164. Landel C P, Krause M, Waterston R H, Hirsh D. DNA rearrangements of the actin gene cluster in *Caenorhabditis elegans* accompanying reversion of three muscle mutants. *J. Mol. Biol.* 1984;180:497–513. [[PubMed: 6098683](#)]
1165. Lane T F, Sage E H. The biology of SPARC a protein that modulates cell-matrix interactions. *FASEB J.* 1994;8:163–173. [[PubMed: 8119487](#)]
1166. Langin T, Capy P, Daboussi M. The transposable element *impala*, a fungal member of the Tc1/mariner superfamily. *Mol. Gen. Genet.* 1995;246:19–28. [[PubMed: 7823909](#)]
1167. Larminie C G C, Johnstone I L. Isolation and characterization of four developmentally regulated cathepsin B-like cysteine proteases from the nematode *Caenorhabditis elegans*. *DNA Cell Biol.* 1996;15:75–82. [[PubMed: 8561899](#)]
1168. Larsen P L. Aging and resistance to oxidative damage in *Caenorhabditis elegans*. *Proc. Natl. Acad. Sci.* 1993;90:8905–8909. [[PMC free article: PMC47469](#)] [[PubMed: 8415630](#)]
1169. Larsen P L, Albert P S, Riddle D L. Genes that regulate both development and longevity in *Caenorhabditis elegans*. *Genetics.* 1995;139:1567–1583. [[PMC free article: PMC1206485](#)] [[PubMed: 7789761](#)]
1170. Laski F A, Rio D C, Rubin G M. Tissue specificity of *Drosophila* P element transposition is regulated at the level of mRNA splicing. *Cell.* 1986;44:7–19. [[PubMed: 3000622](#)]
1171. Lassandro F, Sebastiani M, Zei F, Bazzicalupo P. The role of dityrosine formation in the crosslinking of CUT-2, the product of a second cuticlin gene of *Caenorhabditis elegans*. *Mol. Biochem. Parasitol.* 1994;65:147–159. [[PubMed: 7935621](#)]
1172. Laufer J S, Bazzicalupo P, Wood W B. Segregation of developmental potential in early embryos of *Caenorhabditis elegans*. *Cell.* 1980;19:569–577. [[PubMed: 7363324](#)]
1173. Laughon A, Scott M P. Sequence of a *Drosophila* segmentation gene: Protein structure homology with DNA-binding proteins. *Nature.* 1984;310:25–30. [[PubMed: 6330566](#)]
1174. La Volpe A, Ciaramella M, Bazzicalupo P. Structure, evolution and properties of a novel repetitive DNA family in *Caenorhabditis elegans*. *Nucleic Acids Res.* 1988;16:8213–8231. [[PMC free article: PMC338554](#)] [[PubMed: 3419918](#)]
1175. Lawlor K G, Narayanan R. Persistent expression of the tumor suppressor gene DCC is essential for neuronal differentiation. *Cell Growth Differ.* 1992;3:609–616. [[PubMed: 1419911](#)]
1176. Lawrence P A. The making of a fly. London: Blackwell Scientific; 1992.
1177. Lawrence R A, Allen J E, Osborne J, Maizels R M. Adult and microfilarial stages of the filarial parasite *Brugia malayi* stimulate contrasting cytokine and Ig isotype responses in BALB/c mice. *J. Immunol.* 1994;153:1216–1224. [[PubMed: 7913112](#)]
1178. Lawson E J R, Poethig R S. Shoot development in plants: Time for a change. *Trends Genet.* 1995;11:263–268. [[PubMed: 7482775](#)]
1179. Leavitt A D, Shiue L, Varmus H E. Site-directed mutagenesis of HIV-1 integrase demonstrates differential effects on integrase functions *in vitro*. *J. Biol. Chem.* 1993;268:2113–2119. [[PubMed: 8420982](#)]

1180. Lee B J, Rajagopalan M, Kim Y S, You K H, Jacobson K B, Hatfield D. Selenocysteine tRNA<sup>[Ser]Sec</sup> gene is ubiquitous within the animal kingdom. *Mol. Cell. Biol.* 1990;10:1940–1949. [[PMC free article: PMC360540](#)] [[PubMed: 2139169](#)]
1181. Lee B S, Culbertson M R. Identification of an additional gene required for eukaryotic nonsense mRNA turnover. *Proc. Natl. Acad. Sci.* 1995;92:10354–10358. [[PMC free article: PMC40795](#)] [[PubMed: 7479783](#)]
1182. Lee D L. Moulting in nematodes: The formation of the adult cuticle during the final moult of *Nippostrongylus brasiliensis*. *Tissue Cell.* 1970;2:139–153. [[PubMed: 18631505](#)]
1183. Lee D L, Wright K A, Shivers R R. A freeze-fracture study of the cuticle of adult *Nippostrongylus brasiliensis* (Nematoda). *Parasitology.* 1993;107:545–552. [[PubMed: 8295793](#)]
1184. Lee J, Jongeward G, Sternberg P W. *unc-101*, a gene required for many aspects of *C. elegans* development and behavior, encodes a clathrin-associated protein. *Genes Dev.* 1994;8:60–73. [[PubMed: 8288128](#)]
1185. Lee R C, Feinbaum R L, Ambros V. The *C. elegans* heterochronic gene *lin-4* encodes small RNAs with antisense complementarity to *lin-14*. *Cell.* 1993;75:843–854. [[PubMed: 8252621](#)]
1186. Lee Y H, Huang X -Y, Hirsh D, Fox G E, Hecht R M. Conservation of gene organization and trans-splicing in the glyceraldehyde-3-phosphate dehydrogenase-encoding genes of *Caenorhabditis briggsae*. *Gene.* 1992;121:227–235. [[PubMed: 1446820](#)]
1187. Leeds P, Wood J M, Lee B S, Culbertson M R. Gene products that promote mRNA turnover in *Saccharomyces cerevisiae*. *Mol. Cell Biol.* 1992;12:2165–2177. [[PMC free article: PMC364388](#)] [[PubMed: 1569946](#)]
1188. Leeds P, Peltz S W, Jacobson A, Culbertson M R. The product of the yeast UPF1 gene is required for rapid turnover of mRNAs containing a premature translational termination codon. *Genes Dev.* 1991;5:2303–2314. [[PubMed: 1748286](#)]
1189. Leggett D S, Jones D, Candido E P M. *Caenorhabditis elegans ubc-1*, a ubiquitin-conjugating enzyme homologous to yeast RAD6/UBC2, contains a novel carboxy-terminal extension that is conserved in nematodes. *DNA Cell Biol.* 1995;14:883–891. [[PubMed: 7546294](#)]
1190. Lehman W, Szent-Gyorgyi A G. Regulation of muscular contraction: Distribution of actin control and myosin control in the animal kingdom. *J. Gen. Physiol.* 1975;66:1–30. [[PMC free article: PMC2226187](#)] [[PubMed: 125778](#)]
1191. Lehmann R, Ephrussi A, Marsh J, Goode J, editors. Germline development. London: CIBA Foundation; 1994. Germ plasm formation and germ cell determination in *Drosophila*. pp. 282–300. [[PubMed: 7530619](#)]
1192. Lei J, Tang X, Chambers T, Pohl J, Benian G. Protein kinase domain of twitchin has protein kinase activity and autoinhibitory region. *J. Biol. Chem.* 1994;269:21078–21085. [[PubMed: 8063727](#)]
1193. Leroux M R, Candido E P M. Molecular analysis of *Caenorhabditis elegans tcp-1* a gene encoding a chaperonin protein. *Gene.* 1995;156:241–246. [[PubMed: 7758963](#)]
1194. Leung-Hagesteijn C, Spence A M, Stern B D, Zhou Y, Su M -W, Hedgecock E M, Culotti J G. UNC-5, a transmembrane protein with immunoglobulin and thrombospondin type 1 domains, guides cell and pioneer axon migrations in *C. elegans*. *Cell.* 1992;71:289–299. [[PubMed: 1384987](#)]
1195. Levin J Z, Horvitz H R. The *Caenorhabditis elegans unc-93* gene encodes a putative transmembrane protein that regulates muscle contraction. *J. Cell Biol.* 1992;117:143–155. [[PMC free article: PMC2289394](#)] [[PubMed: 1313436](#)]
1196. Levin J Z, Horvitz H R. Three new classes of mutations in the *Caenorhabditis elegans* muscle gene *sup-9*. *Genetics.* 1993;135:53–70. [[PMC free article: PMC1205627](#)] [[PubMed: 8224828](#)]
1197. Levine R J C, Elfin M, Dewey M M, Walcott B. Paramyosin in invertebrate muscles. II. Content in relation to structure and function. *J. Cell Biol.* 1976;71:273–279. [[PMC free article: PMC2109719](#)] [[PubMed: 977650](#)]
1198. Levine R J C, Kensler R W, Stewart M, Haselgrove J C. Molecular organization of Limulus thick filaments. In: Twarog B M, et al., editors. Basic biology of muscle s: A comparative approach. New

- York: Raven Press; 1982. pp. 37–52. [PubMed: 7146953]
1199. Levitan D, Greenwald I. Facilitation of *lin-12*-mediated signalling by *sel-12* a *Caenorhabditis elegans* S182 Alzheimer's disease gene. *Nature*. 1995;377:351–354. [PubMed: 7566091]
1200. Levitan D J, Boyd L, Mello C C, Kemphues K J, Stinchcomb D T. *par-2*, a gene required for blastomere asymmetry in *C. elegans*, contains zinc-finger and ATP-binding motifs. *Proc. Natl. Acad. Sci.* 1994;91:6108–6112. [PMC free article: PMC44147] [PubMed: 8016123]
1201. Levitt A, Emmons S W. The Tc2 transposon in *Caenorhabditis elegans*. *Proc. Natl. Acad. Sci.* 1989;86:3232–3236. [PMC free article: PMC287104] [PubMed: 2541437]
1202. Levy A D, Kramer J M. Identification sequence and expression patterns of the *Caenorhabditis elegans* *col-36* and *col-40* collagen-encoding genes. *Gene*. 1993;137:281–285. [PubMed: 8299960]
1203. Levy A D, Yang J, Kramer J M. Molecular and genetic analyses of the *Caenorhabditis elegans* *dpy-2* and *dpy-10* collagen genes: A variety of molecular alterations affect organismal morphology. *Mol. Biol. Cell*. 1993;4:803–817. [PMC free article: PMC300994] [PubMed: 8241567]
1204. Levy-Lahad E, Wasco W, Poorkaj P, Romano D M, Oshima J, Pettingell W H, Yu C, Jondro P D, Schmidt S D, Wang K, Crowley A C, Fu Y -H, Guenette S Y, Galas D, Nemens E, Wijsman E M, Bird T D, Schellenberg G D, Tanzi R E. Candidate gene for the chromosome 1 familial Alzheimer's disease locus. *Science*. 1995;269:973–977. [PubMed: 7638622]
1205. Lewis J A, Fleming J T. Genetic and culture methods. *Methods Cell Biol*. 1995;48:3–29. [PubMed: 8531730]
1206. Lewis J A, Hodgkin J A. Specific neuroanatomical changes in chemosensory mutants of the nematode *Caenorhabditis elegans*. *J. Comp. Neurol*. 1977;172:489–510. [PubMed: 838889]
1207. Lewis J A, Wu C H, Berg H, Levine J H. The genetics of levamisole resistance in the nematode *Caenorhabditis elegans*. *Genetics*. 1980a;95:905–928. [PMC free article: PMC1214276] [PubMed: 7203008]
1208. Lewis J A, Wu C H, Levine J H, Berg H. Levamisole-resistant mutants of the nematode *Caenorhabditis elegans* appear to lack pharmacological acetylcholine receptors. *Neuroscience*. 1980b;5:967–989. [PubMed: 7402460]
1209. Lewis J A, Fleming J T, McLafferty S, Murphy H, Wu C. The levamisole receptor, a cholinergic receptor of the nematode *Caenorhabditis elegans*. *Mol. Pharmacol*. 1987a;31:185–193. [PubMed: 3807894]
1210. Lewis J A, Elmer J S, Skimming J, McLafferty S, Fleming J, McGee T. Cholinergic receptor mutants of the nematode *Caenorhabditis elegans*. *J. Neurosci*. 1987b;7:3059–3071. [PMC free article: PMC6569184] [PubMed: 3668616]
1211. Lewis J W, Maizels R M. Toxocara and Toxocariasis. Clinical epidemiological and molecular perspectives. Institute of Biology; 1993.
1212. L'Hernault S W, Arduengo P M. Mutation of a putative sperm membrane protein in *Caenorhabditis elegans* prevents sperm differentiation but not its associated meiotic divisions. *J. Cell Biol*. 1992;119:55–68. [PMC free article: PMC2289639] [PubMed: 1527173]
1213. L'Hernault S W, Roberts T M. Cell biology of nematode sperm. *Methods Cell Biol*. 1995;48:273–301. [PubMed: 8531729]
1214. L'Hernault S W, Benian G M, Emmons R B. Genetic and molecular characterization of the *Caenorhabditis elegans* spermatogenesis defective gene *spe-17*. *Genetics*. 1993;134:769–780. [PMC free article: PMC1205514] [PubMed: 8349108]
1215. L'Hernault S W, Shakes D C, Ward S. Developmental genetics of chromosome I spermatogenesis-defective mutants in the nematode *Caenorhabditis elegans*. *Genetics*. 1988;120:435–452. [PMC free article: PMC1203522] [PubMed: 3197956]
1216. L'Hernault S W, Shakes D, Hogan E, Ward S. Genetic analysis of spermatogenesis in the nematode *Caenorhabditis elegans*. (abstr.). *Genetics*. 1987;116:s32. [PMC free article: PMC1203522] [PubMed: 3197956]
1217. Li C, Chalfie M. Organogenesis in *C. elegans*: Positioning of neurons and muscles in the egg-laying system. *Neuron*. 1990;4:681–695. [PubMed: 2344407]

1218. Li C, Ullrich B, Zhang J Z, Anderson R G W, Brose N, Südhof T C.  $\text{Ca}^{2+}$ -dependent and -independent activities of *neural* and non- *neural* synaptotagmins. *Nature*. 1995;375:594–599. [[PubMed: 7791877](#)]
1219. Li P M, Reichert J, Freyd G, Horvitz H R, Walsh C T. The LIM region of a presumptive *Caenorhabditis elegans* transcription factor is an iron-sulfur- and zinc-containing metallodomain. *Proc. Natl. Acad. Sci.* 1991;88:9210–9213. [[PMC free article: PMC52683](#)] [[PubMed: 1924383](#)]
1220. Li W, Shaw J E. A variant Tc4 transposable element in the nematode *C. elegans* could encode a novel protein. *Nucleic Acids Res.* 1993;21:59–67. [[PMC free article: PMC309065](#)] [[PubMed: 8382791](#)]
1221. Li W, Herman R K, Shaw J E. Analysis of the *Caenorhabditis elegans* axonal guidance and outgrowth gene *unc-33*. *Genetics*. 1992;132:675–689. [[PMC free article: PMC1205206](#)] [[PubMed: 1468626](#)]
1222. Liao D, Hessler N A, Malinow R. Activation of postsynaptically silent synapses during pairing-induced LTP in CA1 region of hippocampal slice. *Nature*. 1995;375:400–404. [[PubMed: 7760933](#)]
1223. Liao L W, Rosenzweig B, Hirsh D. Analysis of a transposable element in *Caenorhabditis elegans*. *Proc. Natl. Acad. Sci.* 1983;80:3585–3589. [[PMC free article: PMC394094](#)] [[PubMed: 6304721](#)]
1224. Lichtman J W. Synapse disassembly at the neuromuscular junction. *Semin. Dev. Biol.* 1995;6:195–206.
1225. Lichtsteiner S, Tjian R. Cloning and properties of the *Caenorhabditis elegans* TATA-box-binding protein. *Proc. Natl. Acad. Sci.* 1993;90:9673–9677. [[PMC free article: PMC47632](#)] [[PubMed: 8415761](#)]
1226. Lichtsteiner S, Tjian R. Synergistic activation of transcription by UNC-86 and MEC-3 in *Caenorhabditis elegans* embryo extracts. *EMBO J.* 1995;14:3937–3945. [[PMC free article: PMC394472](#)] [[PubMed: 7664734](#)]
1227. Lidholm D, Gudmundsson G H, Boman H G. A highly repetitive, mariner-like element in the genome of *Hyalophora cecropia*. *J. Biol. Chem.* 1991;266:11518–11521. [[PubMed: 1646809](#)]
1228. Lidholm D, Lohe A R, Hartl D L. The transposable element *mariner* mediates germ line transformation in *Drosophila melanogaster*. *Genetics*. 1993;134:859–868. [[PMC free article: PMC1205522](#)] [[PubMed: 8394264](#)]
1229. Lieb J D, Capowski E E, Meneely P, Meyer B J. DPY-26, a link between dosage compensation and meiotic chromosome segregation in the nematode. *Science*. 1996;274:1732–1736. [[PubMed: 8939869](#)]
1230. Liebermann D, Hoffman-Liebermann B, Weinthal J, Childs G, Maxson R, Mauron A, Cohen S N, Kedes L. An unusual transposon with long terminal inverted repeats in the sea urchin *Strongylocentrotus purpuratus*. *Nature*. 1983;306:342–347. [[PubMed: 6316151](#)]
1231. Lilly B, Zhao B, Ranganayakulu G, Paterson B M, Schulz R A, Olson E N. Requirement of MADS domain transcription factor D-MEF2 for muscle formation in *Drosophila*. *Science*. 1995;267:688–693. [[PubMed: 7839146](#)]
1232. Limberger R J, McReynolds L A. Filarial paramyosin: cDNA sequences from *Dirofilaria immitis* and *Onchocerca volvulus*. *Mol. Biochem. Parasitol.* 1990;38:271–280. [[PubMed: 2325708](#)]
1233. Lin R, Thompson S, Priess J R. *pop-1* encodes an HMG box protein required for the specification of a mesoderm precursor in early *C. elegans* embryos. *Cell*. 1995;83:599–609. [[PubMed: 7585963](#)]
1234. Lindsley D T, Tokuyasu K T. Spermatogenesis. In: Ashburner M, Wright T R F, editors. *The genetics and biology of Drosophila* vol. 2, London: Academic Press; 1980. pp. 225–294.
1235. Lincke C R, Broeks A, The I, Plasterk R H A, Borst P. The expression of two P-glycoprotein (*pgp*) genes in transgenic *Caenorhabditis elegans* is confined to intestinal cells. *EMBO J.* 1993;12:1615–1620. [[PMC free article: PMC413375](#)] [[PubMed: 8096815](#)]
1236. Link C D, Ehrenfels C W, Wood W B. Mutant expression of male copulatory bursa surface markers in *Caenorhabditis elegans*. *Development*. 1988;103:485–495. [[PubMed: 3246219](#)]
1237. Link C D, Silverman M A, Breen M, Watt K E. Characterisation of *Caenorhabditis elegans* lectin-binding mutants. *Genetics*. 1992;131:867–881. [[PMC free article: PMC1205098](#)] [[PubMed: 1516818](#)]
1238. Liou R -F, Blumenthal T. *Trans-spliced Caenorhabditis elegans* mRNAs retain trimethylguanosine caps. *Mol. Cell. Biol.* 1990;10:1764–1768. [[PMC free article: PMC362282](#)] [[PubMed: 2157142](#)]
1239. Lissemore J L, Currie P D, Turk C M, Maine E. Intragenic dominant suppressors of *glp-1*, a gene essential for cell-signaling in *Caenorhabditis elegans*, support a role for *cdc10/SWI6*/ankyrin motifs in

- GLP-1 function. *Genetics*. 1993;135:1023–1034. [[PMC free article: PMC1205735](#)] [[PubMed: 8307320](#)]
1240. Lithgow G J, White T M, Hinerfeld D A, Johnson T E. Thermotolerance of a long-lived mutant of *Caenorhabditis elegans*. *J. Gerontol.* 1994;49:B270–B276. [[PubMed: 7963273](#)]
1241. Lithgow G J, White T M, Melov S, Johnson T E. Thermotolerance and extended life-span conferred by single-gene mutations and induced by thermal stress. *Proc. Natl. Acad. Sci.* 1995;92:7540–7544. [[PMC free article: PMC41375](#)] [[PubMed: 7638227](#)]
1242. Littleton J T, Stern M, Perin M, Bellen H J. Calcium dependence of neurotransmitter release and rate of spontaneous vesicle fusions are altered in *Drosophila synaptotagmin* mutants. *Proc. Natl. Acad. Sci.* 1994;91:10888–10892. [[PMC free article: PMC45131](#)] [[PubMed: 7971978](#)]
1243. Liu A, Ambros V. Alternative temporal control systems for hypodermal cell differentiation in *Caenorhabditis elegans*. *Nature*. 1991;350:162–165. [[PubMed: 26502479](#)]
1244. Liu D W C, Thomas J H. Regulation of a periodic motor program in *C. elegans*. *J. Neurosci.* 1994;14:1953–1962. [[PMC free article: PMC6577142](#)] [[PubMed: 8158250](#)]
1245. Liu F, Thatcher J D, Barral J M, Epstein H F. Bifunctional glyoxylate cycle protein of *Caenorhabditis elegans*: A developmentally regulated protein of intestine and muscle. *Dev. Biol.* 1995;169:399–414. [[PubMed: 7781887](#)]
1246. Liu J P, Robinson P J. Dynamin and endocytosis. *Endocrine Rev.* 1995;16:590–607. [[PubMed: 8529573](#)]
1247. Liu J, Schrank B, Waterston R H. Interaction between a putative mechanosensory membrane channel and a collagen. *Science*. 1996;273:361–364. [[PubMed: 8662524](#)]
1248. Liu K S, Sternberg P W. Sensory regulation of male mating behavior in *Caenorhabditis elegans*. *Neuron*. 1995;14:79–89. [[PubMed: 7826644](#)]
1249. Liu X, Kim C N, Yang J, Jemmerson R, Wang X. Induction of apoptotic program in cell-free extracts: Requirements for dATP and cytochrome c. *Cell*. 1996;86:147–157. [[PubMed: 8689682](#)]
1250. Liu Z C, Ambros V. Heterochronic genes control the stage-specific initiation and expression of the dauer larva developmental program in *Caenorhabditis elegans*. *Genes Dev.* 1989;3:2039–2049. [[PubMed: 2628162](#)]
1251. Liu Z C, Ambros V. Alternative temporal control systems for hypodermal cell differentiation in *Caenorhabditis elegans*. *Nature*. 1991;350:162–165. [[PubMed: 26502479](#)]
1252. Liu Z, Kirch S, Ambros V. The *Caenorhabditis elegans* heterochronic gene pathway controls stage-specific transcription of collagen genes. *Development*. 1995;121:2471–2478. [[PubMed: 7671811](#)]
1253. Livingstone D. "Studies of the unc-31 gene of *Caenorhabditis elegans*." [Ph.D. thesis] Darwin College, University of Cambridge. 1991. [[PMC free article: PMC52421](#)]
1254. Lochrie M A, Mendel J E, Sternberg P W, Simon M I. Homologous and unique G protein alpha subunits in the nematode *Caenorhabditis elegans*. *Cell Regul.* 1991;2:135–154. [[PMC free article: PMC361731](#)] [[PubMed: 1907494](#)]
1255. Lockery S R, Hall D H. Signal propagation in the *nerve ring* of the nematode *C. elegans*. 569.7 p. (abstr.). *Soc. Neurosci.* 1995;21:1454.
1256. Loer C M, Kenyon C J. Serotonin-deficient mutants and male mating behavior in the nematode *Caenorhabditis elegans*. *J. Neurosci.* 1993;13:5407–5417. [[PMC free article: PMC6576401](#)] [[PubMed: 8254383](#)]
1257. Lorenzen S. Entwurf eines phylogenetischen Systems der freilebenden Nematoden.(suppl.) . Veröff. Inst. Meeresforsch. Bremerh. 1981;7:1–472.
1258. Lorenzen S. The phylogenetic systematics of free-living nematodes. London: The Ray Society; 1994.
1259. Loros J J, Feldman J F. Loss of temperature compensation of circadian period length in the *frq-9* mutant of *Neurospora crassa*. *J. Biol. Rhythms*. 1986;1:187–198. [[PubMed: 2980965](#)]
1260. Lowenstein E J, Daly R J, Blatzer A G, Li W, Margolis B, Lammers R, Ullrich A, Skolnick E Y, Bar-Sagi D, Schlessinger J. The SH2 and SH3 domain-containing protein GRB2 links receptor tyrosine kinases to ras signalling. *Cell*. 1992;70:431–442. [[PubMed: 1322798](#)]
1261. Lu M, DiLullo D, Schultheiss T, Holtzer S, Murray J M, Choi J, Fischman D A, Holtzer H. The vinculin/sarcomeric alpha-actinin/actin nexus in cultured cardiac myocytes. *J. Cell Biol.* 1992;117:1007–1022. [[PMC free article: PMC2289484](#)] [[PubMed: 1577864](#)]

1262. Lu Q, Knoepfler P S, Scheele J, Wright D D, Kamps M P. Both Pbx-1 and E2A-Pbx1 bind the DNA motif ATCAATCAA cooperatively with the products of multiple murine Hox genes, some of which are themselves oncogenes. *Mol. Cell. Biol.* 1995;15:3786–3795. [[PMC free article: PMC230617](#)] [[PubMed: 7791786](#)]
1263. Luehrsen K R, Walbot V. Intron creation and polyadenylation in maize are directed by AU-rich RNA. *Genes Dev.* 1994;8:1117–1130. [[PubMed: 7926791](#)]
1264. Lufkin T, Dierich A, LeMeur M, Mark M, Chambon P. Disruption of the *Hox-1.6* homeobox gene results in defects in a region corresponding to its rostral domain of expression. *Cell.* 1991;66:1105–1119. [[PubMed: 1680563](#)]
1265. Luisi B F, Xu W X, Otwinowski Z, Freedman L P, Yamamoto K R, Sigler P B. Crystallographic analysis of the interaction of the glucocorticoid receptor with DNA. *Nature.* 1991;352:497–505. [[PubMed: 1865905](#)]
1266. Lumpkin E A, Hudspeth A J. Detection of  $\text{Ca}^{2+}$  entry through mechanosensitive channels localizes the site of mechanoelectrical transduction in hair cells. *Proc. Natl. Acad. Sci.* 1995;92:10297–10301. [[PMC free article: PMC40783](#)] [[PubMed: 7479771](#)]
1267. Lundquist E A, Herman R K. The *mec-8* gene of *Caenorhabditis elegans* affects muscle and sensory neuron function and interacts with three other genes: *unc-52smu-1* and *smu-2*. *Genetics.* 1994;138:83–101. [[PMC free article: PMC1206141](#)] [[PubMed: 8001796](#)]
1268. Lundquist E A, Herman R K, Rogalski T M, Mullen G P, Moerman D G, Shaw J E. The *mec-8* gene of *C. elegans* encodes a protein with two RNA recognition motifs and regulates alternative splicing of *unc-52* transcripts. *Development.* 1996;122:1601–1610. [[PubMed: 8625846](#)]
1269. Lustigman S, Brotman B, Huitman T, Prince A M, McKerrow J H. Molecular cloning and characterisation of onchocystatin, a cysteine protease inhibitor of *Onchocerca volvulus*. *J. Biol. Chem.* 1992;267:17339–17346. [[PubMed: 1512269](#)]
1270. Lye R J, Wilson R K, Waterston R H. Genomic structure of a cytoplasmic dynein heavy chain gene from the nematode *Caenorhabditis elegans*. *Cell Motil. Cytoskel.* 1995;32:26–36. [[PubMed: 8674131](#)]
1271. Lynch A S, Briggs D, Hope I A. Developmental expression pattern screen for genes predicted in the *C. elegans* genome sequencing project. *Nat. Genet.* 1995;11:309–313. [[PubMed: 7581455](#)]
1272. Lyons I, Parsons L M, Hartley L, Li R, Andrews J E, Robb L, Harvey R P. Myogenic and morphogenetic defects in the heart tubes of murine embryos lacking the homeo box gene *Nkx2-5*. *Genes Dev.* 1995;9:1654–1666. [[PubMed: 7628699](#)]

## M

1273. Ma P C M, Rould M A, Weintraub H, Pabo C O. Crystal structure of MyoD bHLH domain-DNA complex: Perspectives on DNA recognition and implications for transcriptional activation. *Cell.* 1994;77:451–459. [[PubMed: 8181063](#)]
1274. Machaca K, DeFelice L J, L'Hernault S W. A novel chloride channel localizes to *Caenorhabditis elegans* spermatids and chloride channel blockers induce spermatid differentiation. *Dev. Biol.* 1996;176:1–16. [[PubMed: 8654886](#)]
1275. Maciver S K, Wachsstock D H, Schwarz W H, Pollard T D. The actin filament-severing protein actophorin promotes the formation of rigid bundles of actin filaments crosslinked with  $\alpha$ -actinin. *J. Cell Biol.* 1991;115:1621–1628. [[PMC free article: PMC2289213](#)] [[PubMed: 1757466](#)]
1276. MacKenzie J M, Epstein H F. Paramyosin is necessary for determination of nematode thick filament length in vivo. *Cell.* 1980;22:747–755. [[PubMed: 7193096](#)]
1277. MacKenzie J M, Schachat F, Epstein H F. Immunocytochemical localization of two myosins within the same muscle cells in *Caenorhabditis elegans*. *Cell.* 1978a;15:413–420. [[PubMed: 363276](#)]
1278. MacKenzie J M, Garcea R L, Zengel J M, Epstein H F. Muscle development in *Caenorhabditis elegans*: Mutants exhibiting retarded sarcomere development. *Cell.* 1978b;15:751–762. [[PubMed: 728988](#)]
1279. Mackrell A J, Blumberg B, Haynes S R, Fessler J H. The lethal myospheroid gene of *Drosophila* encodes a membrane protein homologous to vertebrate integrin beta subunits. *Proc. Natl. Acad. Sci.*

- 1988;85:2633–2637. [[PMC free article: PMC280052](#)] [[PubMed: 3128792](#)]
1280. MacLeod A R, Karn J, Brenner S. Molecular analysis of the *unc-54* myosin heavy-chain gene of *Caenorhabditis elegans*. *Nature*. 1981;291:386–390. [[PubMed: 6264304](#)]
1281. MacLeod A R, Waterston R H, Fishpool R M, Brenner S. Identification of the structural gene for a myosin heavy chain in *Caenorhabditis elegans*. *J. Mol. Biol.* 1977;114:133–140. [[PubMed: 909083](#)]
1282. MacMorris M, Blumenthal T. In situ analysis of *C. elegans* vitellogenin fusion gene expression in integrated transgenic strains: Effect of promoter mutations on RNA localization. *Gene Expr.* 1993;3:27–36. [[PMC free article: PMC6081627](#)] [[PubMed: 8508027](#)]
1283. MacMorris M, Spieth J, Madej C, Lea K, Blumenthal T. Analysis of the VPE sequences in the *Caenorhabditis elegansvit-2* promoter with extrachromosomal tandem array-containing transgenic strains. *Mol. Cell. Biol.* 1994;14:484–491. [[PMC free article: PMC358398](#)] [[PubMed: 8264616](#)]
1284. MacMorris M, Broverman S, Greenspoon S, Lea K, Madej C, Blumenthal T, Spieth J. Regulation of vitellogenin gene expression in transgenic *Caenorhabditis elegans*: Short sequences required for activation of the *vit-2* promoter. *Mol. Cell. Biol.* 1992;12:1652–1662. [[PMC free article: PMC369608](#)] [[PubMed: 1549118](#)]
1285. Macrae M, Plasterk R H A, Coffino P. The ornithine decarboxylase gene of *Caenorhabditis elegans*: Cloning, mapping and mutagenesis. *Genetics*. 1995;140:517–525. [[PMC free article: PMC1206631](#)] [[PubMed: 7498733](#)]
1286. Maddison W P. A method for testing the correlated evolution of two binary characters: Are gains or losses concentrated on certain branches of a phylogenetic tree? *Evolution*. 1990;44:539–557. [[PubMed: 28567979](#)]
1287. Maddison W P, Maddison D R. *MacClade: Analysis of phylogeny and character evolution*. Sunderland, Massachusetts: Sinauer Associates; 1992.
1288. Maddison W P, Donoghue M J, Maddison D R. Outgroup analysis and parsimony. *Syst. Zool.* 1984;33:83–103.
1289. Madhani H D, Guthrie C. Dynamic RNA-RNA interactions in the spliceosome. *Annu. Rev. Genet.* 1994;28:1–26. [[PubMed: 7534458](#)]
1290. Madl J E, Herman R K. Polyploids and sex determination in *Caenorhabditis elegans*. *Genetics*. 1979;93:393–402. [[PMC free article: PMC1214087](#)] [[PubMed: 295035](#)]
1291. Maduro M, Pilgrim D. Identification and cloning of *unc-119* a gene expressed in the *Caenorhabditis elegans* nervous system. *Genetics*. 1995;141:977–988. [[PMC free article: PMC1206859](#)] [[PubMed: 8582641](#)]
1292. Maggenti A. *General nematology*. New York: Springer-Verlag; 1981.
1293. Maguire M P. The pattern of pairing that is effective for crossing over in complex B-A chromosome rearrangements in maize. III. Possible evidence for pairing centers. *Chromosoma*. 1986;94:71–85. [[PubMed: 3743206](#)]
1294. Mahajan R K, Vaughan K T, Johns J A, Pardee J D. Actin filaments mediate *Dictyostelium* myosin assembly in vitro. *Proc. Natl. Acad. Sci.* 1989;86:6161–6165. [[PMC free article: PMC297797](#)] [[PubMed: 2762319](#)]
1295. Maina C V, Grandea III A G, Tuyen L T K, Asikin N, Williams S A, McReynolds L A, MacInnis A J, editor. *Molecular paradigms for eradicating helminthic parasites*. New York: Alan R. Liss; 1987. *Dirofilaria immitis*: Genomic complexity and characterisation of a structural gene. pp. 193–204.
1296. Maine E M, Kimble J. Identification of genes that interact with *glp-1*, a gene required for inductive cell interactions in *Caenorhabditis elegans*. *Development*. 1989;106:133–143. [[PubMed: 2627884](#)]
1297. Maine E M, Kimble J. Suppressors of *glp-1* a gene required for cell communication during development in *Caenorhabditis elegans* define a set of interacting genes. *Genetics*. 1993;135:1011–1022. [[PMC free article: PMC1205734](#)] [[PubMed: 8307319](#)]
1298. Mains P E, Sulston J A, Wood W B. Dominant maternal-effect lethal mutations causing embryonic lethality in *Caenorhabditis elegans*. *Genetics*. 1990a;125:351–369. [[PMC free article: PMC1204025](#)] [[PubMed: 2379819](#)]

1299. Mains P E, Kemphues K J, Sprunger S A, Sulston J A, Wood W B. Mutations affecting the meiotic and mitotic divisions of the early *Caenorhabditis elegans* embryo. *Genetics*. 1990;126:593–605. [PMC free article: PMC1204215] [PubMed: 2249759]
1300. Maizels R M, Denham D A. Diethylcarbamazine (DEC): Immunopharmacological interactions of an anti-filarial drug. *Parasitology*. 1992;105:S49–S60. [PubMed: 1308929]
1301. Maizels R M, Lawrence R A. Immunological tolerance: The key feature of human filariasis? *Parasitol. Today*. 1991;7:271–276. [PubMed: 15463386]
1302. Maizels R M, Page A P. Surface associated glycoproteins from *Toxocara canis* larval parasites. *Acta Tropica*. 1990;47:355–364. [PubMed: 1978535]
1303. Maizels R M, Blaxter M L, Selkirk M E. Forms and functions of nematode surfaces. *Exp. Parasitol.* 1993;77:380–384. [PubMed: 8224093]
1304. Maizels R M, Meghji M, Ogilvie B M. Restricted sets of parasite antigens from the surface of different stages and sexes of the nematode parasite *Nippostrongylus brasiliensis*. *Immunology*. 1983a;48:107–121. [PMC free article: PMC1453999] [PubMed: 6184314]
1305. Maizels R M, Gregory W F, Kwan-Lim G -E, Selkirk M E. Filarial surface antigens: The major 29 kilodalton glycoprotein and a novel 17-200 kilodalton complex from adult *Brugia malayi* parasites. *Mol. Biochem. Parasitol.* 1989;32:213–228. [PubMed: 2927446]
1306. Maizels R M, Bundy D A P, Selkirk M E, Smith D F, Anderson R M. Immunological modulation and evasion by helminth parasites in human populations. *Nature*. 1993;365:797–805. [PubMed: 8413664]
1307. Maizels R M, Partono F, Oemijati S, Denham D A, Ogilvie B M. Cross-reactive surface antigens on three stages of *Brugia malayi*, *B. pahangi* and *B. timori*. *Parasitology*. 1983b;87:249–273. [PubMed: 6196709]
1308. Malakhov V V. Nematodes: Structure development, classification, and phylogeny. Washington, D.C.: Smithsonian Institution Press; 1994.
1309. Malicki J, Schughart K, McGinnis W. Mouse *Hox*-2.2 specifies thoracic segmental identity in *Drosophila* embryos and larvae. *Cell*. 1990;63:961–967. [PubMed: 1979525]
1310. Malicki J, Cianetti L C, Peschle C, McGinnis W. A human HOX4B regulatory element provides head-specific expression in *Drosophila* embryos. *Nature*. 1992;358:345–347. [PubMed: 1353609]
1311. Malone E A, Thomas J H. A screen for nonconditional dauer-constitutive mutations in *Caenorhabditis elegans*. *Genetics*. 1994;136:879–886. [PMC free article: PMC1205893] [PubMed: 8005442]
1312. Malone E A, Inoue T, Thomas J H. Genetic analysis of the roles of *daf-28* and *age-1* in regulating *Caenorhabditis elegans* dauer formation. *Genetics*. 1996;143:1193–1205. [PMC free article: PMC1207390] [PubMed: 8807293]
1313. Maloney M D, Semprevivo L H. Thin-layer and liquid column chromatographic analyses of the lipids of adult *Onchocerca gibsoni*. *Parasitol. Res.* 1991;77:294–300. [PubMed: 1866419]
1314. Mamiya Y, Nickle W R, editor. Plant and insect nematodes. New York: Dekker; 1984. The pine wood nematode. pp. 589–626.
1315. Manak J R, Scott M P. A class act: Conservation of homeodomain protein functions. *Suppl.*, pp. Development. 1994:61–71. [PubMed: 7579525]
1316. Mango S E, Maine E, Kimble J. Carboxy-terminal truncation activates *glp-1* protein to specify vulval fates in *Caenorhabditis elegans*. *Nature*. 1991;352:811–815. [PubMed: 1881436]
1317. Mango S E, Lambie E J, Kimble J. The *pha-4* gene is required to generate the pharyngeal primordium of *Caenorhabditis elegans*. *Development*. 1994a;120:3019–3031. [PubMed: 7607089]
1318. Mango S E, Thorpe C J, Martin P R, Chamberlain S H, Bowerman B. Two maternal genes, *apx-1* and *pie-1*, are required to distinguish the fates of equivalent blastomeres in the early *Caenorhabditis elegans* embryo. *Development*. 1994b;120:2305–2315. [PubMed: 7925031]
1319. Manley J L, Yu H, Ryner L. RNA sequence containing hexanucleotide AAUAAA directs efficient mRNA polyadenylation in vitro. *Mol. Cell. Biol.* 1985;5:373–379. [PMC free article: PMC366720] [PubMed: 2579321]
1320. Mann R, Hogness D. Functional dissection of Ultrabithorax proteins in *D. melanogaster*. *Cell*. 1990;60:597–610. [PubMed: 2105847]

1321. Manoussis T, Ellar D J. Establishment of two cell lines from the nematode *Meloidogyne incognita* (Tylenchida;--> Meloidogynidae). *Vitro Cell. Dev. Biol.* 1990;26:1105–1114.
1322. Manser J, Wood W B. Mutations affecting embryonic cell migrations in *Caenorhabditis elegans*. *Dev. Genet.* 1990;11:49–64. [PubMed: 2361334]
1323. Mapes C J. Structure and function of the nematode pharynx. II. Pumping in *PanagrellusAlectana*, and *Rhabditis*. *Parasitology*. 1965;55:583–594. [PubMed: 14342121]
1324. Maquat L E. When cells stop making sense: Effects of nonsense codons on RNA metabolism in vertebrate cells. *RNA*. 1995;1:453–465. [PMC free article: PMC1482424] [PubMed: 7489507]
1325. March P A, Wurzelmann S, Walkley S U. Morphological alterations in neocortical and cerebellar GABAergic neurons in a canine model of juvenile Batten disease. *Am. J. Med. Genet.* 1995;57:204–212. [PubMed: 7668331]
1326. Maricq A V, Peckol E, Driscoll M, Bargmann C I. Mechanosensory signalling in *C. elegans* mediated by the GLR-1 glutamate receptor. *Nature*. 1995;378:78–81. [PubMed: 7477293]
1327. Maroney P A, Hannon G J, Nilsen T W. Transcription and cap trimethylation of a nematode spliced leader RNA in a cell-free system. *Proc. Natl. Acad. Sci.* 1990a;87:709–713. [PMC free article: PMC53335] [PubMed: 2300557]
1328. Maroney P A, Hannon G J, Denker J A, Nilsen T W. The nematode spliced leader RNA participates in trans-splicing as an Sm snRNP. *EMBO J.* 1990b;9:3667–3673. [PMC free article: PMC552121] [PubMed: 2145151]
1329. Maroney P A, Hannon G J, Shambaugh J D, Nilsen T W. Intramolecular base pairing between the nematode spliced leader and its 5'splice site is not essential for trans-splicing in vitro. *EMBO J.* 1991;10:3869–3875. [PMC free article: PMC453124] [PubMed: 1935906]
1330. Maroney P A, Yu Y -T, Jankowska M, Nilsen T. Direct analysis of nematode *cis*- and *trans*-spliceosomes: A functional role for U5 snRNA in spliced leader addition *trans*-splicing and the identification of novel Sm snRNPs. *RNA*. 1996;2:735–745. [PMC free article: PMC1369411] [PubMed: 8752084]
1331. Maroney P A, Denker J A, Darzynkiewicz E, Laneve R, Nilsen T W. Most mRNAs in the nematode *Ascaris lumbricoides* are trans-spliced: A role for spliced leader addition in translational efficiency. *RNA*. 1995;1:714–723. [PMC free article: PMC1369313] [PubMed: 7585256]
1332. Marra M A, Baillie D L. Recovery of duplications by drug resistance selection in *Caenorhabditiselegans*. *Genome*. 1994;37:701–705. [PubMed: 7958827]
1333. Marra M A, Prasad S S, Baillie D L. Molecular analysis of two genes between *let-653* and *let-56* in the *unc-22*(IV) region of *Caenorhabditis elegans*. *Mol. Gen. Genet.* 1993;236:289–298. [PubMed: 8382340]
1334. Martin G M, Austad S N, Johnson T E. Genetic analysis of aging: Role of oxidative damage and environmental stresses. *Nat. Genet.* 1996;13:25–34. [PubMed: 8673100]
1335. Martin R J. Neuromuscular transmission in nematode parasites and antinematodal drug action. *Pharmacol. Ther.* 1993;58:13–50. [PubMed: 8415872]
1336. Martin R J, Pennington A. A patch clamp study of effects of dihydroavermectin on *Ascaris* muscle. *Br. J. Pharmacol.* 1989;98:747–756. [PMC free article: PMC1854754] [PubMed: 2480169]
1337. Martin S A M, Thompson F J, Devaney E. The construction of spliced leader cDNA libraries from the filarial nematode *Brugia pahangi*. *Mol. Biochem. Parasitol.* 1995;70:241–245. [PubMed: 7637712]
1338. Martin T F J. The molecular machinery for fast and slow neurosecretion. *Curr. Opin. Neurobiol.* 1994;4:626–632. [PubMed: 7849517]
1339. Martinou I, Fernandez P -A, Missotten M, White E, Allet B, Sadoul R, Martinou J -C. Viral proteins E1B19K and p35 protect sympathetic neurons from cell death induced by NGF deprivation. *J. Cell Biol.* 1995;128:201–208. [PMC free article: PMC2120324] [PubMed: 7822415]
1340. Maruyama I N, Brenner S. A phorbol ester/diacylglycerol-binding protein encoded by the *unc-13* gene of *Caenorhabditis elegans*. *Proc. Natl. Acad. Sci.* 1991;88:5729–5733. [PMC free article: PMC51951] [PubMed: 2062851]
1341. Maruyama I N, Miller D M, Brenner S. Myosin heavy chain gene amplification as a suppressor mutation in *Caenorhabditis elegans*. *Mol. Gen. Genet.* 1989;219:113–118. [PubMed: 2575705]

1342. Maruyama K, Cage P E, Bell J L. The role of connectin in elastic properties of insect flight muscle. *Comp. Biochem. Physiol.* 1977;61A:623–627.
1343. Maruyama K, Natori R, Nonomura Y. A new elastic protein from muscle. *Nature*. 1976;262:58–60. [PubMed: 934326]
1344. Massagué J, Attisano L, Wrana J L. The TGF- $\beta$  family and its composite receptors. *Trends Cell Biol.* 1994;4:172–178. [PubMed: 14731645]
1345. Maupas E. La mue et l'enkystement chez les nématodes. *Arch. Zool. Exp. Gen.* 1899;7:563–628.
1346. Maupas E. Modes et formes de reproduction des nématodes. *Arch. Zool. Exp. Gen.* 1900;8:463–624.
1347. Maynard Smith J, Burian R, Kauffman S, Alberch P, Campbell J, Goodwin B, Lande R, Raup D, Wolpert L. Developmental constraints and evolution. *Q. Rev. Biol.* 1985;60:265–287.
1348. McClintock B. Chromosome organization and genetic expression. *Cold Spring Harbor Symp. Quant. Biol.* 1951;16:13–47. [PubMed: 14942727]
1349. McClung C R, Fox B A, Dunlap J C. The *Neurospora* clock gene *frequency* shares a sequence element with the *Drosophila* clock gene *period*. *Nature*. 1989;339:558–562. [PubMed: 2525233]
1350. McClure M A, Zuckerman B M. Localisation of cuticular binding sites of concanavalin A on *Caenorhabditis elegans* and *Meloidogyne incognita*. *J. Nematol.* 1982;14:39–44. [PMC free article: PMC2618142] [PubMed: 19295672]
1351. McCombie W R, Adams M D, Kelley J M, FitzGerald M G, Utterback T R, Khan M, Dubnick M, Kerlavage A R, Venter J C, Fields C. *Caenorhabditis elegans* expressed sequence tags identify gene families and potential disease gene homologues. *Nat. Genet.* 1992;1:124–131. [PubMed: 1302005]
1352. McDowall J S. "Essential genes in hDp16/hDp19(l) of *C. elegans*." [M.Sc. thesis]. University of British Columbia; Canada: 1990.
1353. McDowall J S. "Analysis of sterile mutants in the dpy-5 unc-13(l) region of *Caenorhabditiselegans*." [Ph.D. thesis]. University of British Columbia; Canada: 1996.
1354. McGhee J D. Purification and characterization of a carboxylesterase from the intestine of the nematode *C. elegans*. *Biochemistry*. 1987;26:4101–4107. [PubMed: 3651439]
1355. McGhee J D, Birchall J C, Chung M A, Cottrell D A, Edgar L G, Svendsen P C, Ferrari D C. Production of null mutants in the major intestinal esterase gene (*ges-1*) of the nematode *Caenorhabditis elegans*. *Genetics*. 1990;125:505–514. [PMC free article: PMC1204078] [PubMed: 2379823]
1356. McGibbon A M, Christie J F, Kennedy M W, Lee T D G. Identification of the major *Ascaris* allergen and its purification to homogeneity by high-performance liquid chromatography. *Mol. Biochem. Parasitol.* 1990;39:163–172. [PubMed: 1690856]
1357. McGinnis N, Kuziora M A, McGinnis W. Human *Hox-4.2* and *Drosophila Deformed* encode similar regulatory specificities in *Drosophila* embryos and larvae. *Cell*. 1990;63:969–976. [PubMed: 1979526]
1358. McGinnis W, Krumlauf R. Homeobox genes and axial patterning. *Cell*. 1992;68:283–302. [PubMed: 1346368]
1359. McGinnis W, Levine M S, Hafen E, Kuroiwa A, Gehring W J. A conserved DNA sequence in homoeotic genes of the *Drosophila Antennapedia* and bithorax complexes. *Nature*. 1984;308:428–433. [PubMed: 6323992]
1360. McIntire S L, Jorgensen E, Horvitz H R. Genes required for GABA function in *Caenorhabditis elegans*. *Nature*. 1993a;364:334–337. [PubMed: 8332190]
1361. McIntire S L, Jorgensen E, Kaplan J, Horvitz H R. The GABAergic nervous system of *Caenorhabditis elegans*. *Nature*. 1993b;364:337–341. [PubMed: 8332191]
1362. McIntire S L, Garriga G, White J, Jacobson D, Horvitz H R. Genes necessary for directed axonal elongation or fasciculation in *C. elegans*. *Neuron*. 1992;8:307–322. [PubMed: 1739461]
1363. McKay S J. "Alignment of physical and genetic maps in *C. elegans*." [M.Sc. thesis]. University of British Columbia; Canada: 1993.
1364. McKim K S. "Analysis of chromosome I rearrangements in *Caenorhabditis elegans*." [Ph.D. thesis]. University of British Columbia; Vancouver: 1990.
1365. McKim K S, Hawley R S. Chromosomal control of meiotic cell division. *Science*. 1995;270:1595–1601. [PubMed: 7502068]

1366. McKim K S, Rose A M. Chromosome I duplications in *Caenorhabditis elegans*. Genetics. 1990;124:115–132. [[PMC free article: PMC1203899](#)] [[PubMed: 2307351](#)]
1367. McKim K S, Rose A M. Spontaneous duplication loss and breakage in *Caenorhabditis elegans*. Genome. 1994;37:595–606. [[PubMed: 7958823](#)]
1368. McKim K S, Howell A M, Rose A M. The effects of translocations on recombination frequency in *Caenorhabditis elegans*. Genetics. 1988;120:987–1001. [[PMC free article: PMC1203590](#)] [[PubMed: 3224815](#)]
1369. McKim K S, Peters K, Rose A M. Two types of sites required for meiotic chromosome pairing in *Caenorhabditis elegans*. Genetics. 1993;134:749–768. [[PMC free article: PMC1205513](#)] [[PubMed: 8349107](#)]
1370. McKim K S, Starr T, Rose A M. Genetic and molecular analysis of the *dpy-14* region in *Caenorhabditis elegans*. Mol. Gen. Genet. 1992;233:241–251. [[PubMed: 1603066](#)]
1371. McKim K S, Matheson C, Marra M A, Wakarchuk M F, Baillie D L. The *Caenorhabditis elegans unc-60* gene encodes proteins homologous to a family of actin-binding proteins. Mol. Gen. Genet. 1994;242:346–357. [[PubMed: 8107682](#)]
1372. McLachlan A D, Karn J. Periodic charge distributions in the myosin rod amino acid sequence match cross-bridge spacings in muscle. Nature. 1982;299:226–231. [[PubMed: 7202124](#)]
1373. McLachlan A D, Karn J. Periodic features in the amino acid sequence of nematode myosin rod. J. Mol. Biol. 1983;164:605–626. [[PubMed: 6341606](#)]
1374. McReynolds L A, DeSimone S M, Williams S A. Cloning and comparison of repeated DNA sequences from the human filarial parasite *Brugia malayi* and the animal parasite *Brugia pahangi*. Proc. Natl. Acad. Sci. 1986;83:797–801. [[PMC free article: PMC322952](#)] [[PubMed: 3003750](#)]
1375. McReynolds L A, Kennedy M W, Selkirk M E. The polyprotein allergens of nematodes. Parasitol. Today. 1993;9:403–406. [[PubMed: 15463678](#)]
1376. Medhora M M, MacPeek A H, Hartl D L. Excision of the *Drosophila* transposable element mariner: Identification and characterization of the Mos factor. EMBO J. 1988;7:2185–2189. [[PMC free article: PMC454541](#)] [[PubMed: 2843360](#)]
1377. Medhora M M, Maruyama K, Hartl D L. Molecular and functional analysis of the mariner mutator element Mos1 in *Drosophila*. Genetics. 1991;128:311–318. [[PMC free article: PMC1204469](#)] [[PubMed: 1649068](#)]
1378. Meier T, Therianos S, Zacharias D, Reichert H. Developmental expression of TERM-1 glycoprotein on growth cones and terminal arbors of individual identified neurons in the grasshopper. J. Neurosci. 1993;13:1498–1510. [[PMC free article: PMC6576720](#)] [[PubMed: 7681872](#)]
1379. Mello C C, Fire A. DNA transformation. In: Epstein H F, editor. *Caenorhabditis elegans: Modern biological analysis of an organism*. San Diego: Academic Press; 1995. pp. 452–482.
1380. Mello C C, Draper B W, Priess J R. The maternal genes *apx-1* and *glp-1* and establishment of dorsal-ventral polarity in the early *C. elegans* embryo. Cell. 1994;77:95–106. [[PubMed: 8156602](#)]
1381. Mello C C, Kramer J M, Stinchcomb D, Ambros V. Efficient gene transfer in *C. elegans*: Extrachromosomal maintenance and integration of transforming sequences. EMBO J. 1991;10:3959–3970. [[PMC free article: PMC453137](#)] [[PubMed: 1935914](#)]
1382. Mello C C, Draper B W, Krause M, Weintraub H, Priess J R. The *pie-1* and *mex-1* genes and maternal control of blastomere identity in early *C. elegans* embryos. Cell. 1992;70:163–176. [[PubMed: 1623520](#)]
1383. Mello C, Schubert C, Draper B, Zhang W, Lobel R, Priess J R. The PIE-1 protein and germline specification in *C. elegans* embryos. Nature. 1996;382:710–712. [[PubMed: 8751440](#)]
1384. Melov S, Hertz G Z, Stormo G D, Johnson T E. Detection of deletions in the mitochondrial genome of *Caenorhabditis elegans*. Nucleic Acids Res. 1994;22:1075–1078. [[PMC free article: PMC307932](#)] [[PubMed: 8152911](#)]
1385. Melov S, Lithgow G J, Fischer D R, Tedesco P M, Johnson T E. Increased frequency of deletions in the mitochondrial genome with age of *Caenorhabditis elegans*. Nucleic Acids Res. 1995;23:1419–1425. [[PMC free article: PMC306871](#)] [[PubMed: 7753635](#)]

1386. Mendel J E, Korswagen H C, Liu K S, Hajdu-Cronin Y M, Simon M I, Plasterk R H A, Sternberg P W. Participation of the protein G<sub>o</sub> in multiple aspects of behavior in *C. elegans*. *Science*. 1995;267:1652–1655. [[PubMed: 7886455](#)]
1387. Meneely P M, Herman R K. Lethals steriles and deficiencies in a region of the X chromosome of *Caenorhabditis elegans*. *Genetics*. 1979;92:99–115. [[PMC free article: PMC1213963](#)] [[PubMed: 574105](#)]
1388. Meneely P M, Herman R K. Suppression and function of X-linked lethal and sterile mutations in *Caenorhabditis elegans*. *Genetics*. 1981;97:65–84. [[PMC free article: PMC1214388](#)] [[PubMed: 7196363](#)]
1389. Meneely P M, Wood W B. Genetic analysis of X-chromosome dosage compensation in *Caenorhabditis elegans*. *Genetics*. 1987;117:25–41. [[PMC free article: PMC1203184](#)] [[PubMed: 3666440](#)]
1390. Metzstein M M, Hengartner M O, Tsung N, Ellis R E, Horvitz H R. Transcriptional regulator of programmed cell death encoded by *Caenorhabditis elegans* gene ces-2. *Nature*. 1996;382:545–547. [[PubMed: 8700229](#)]
1391. Meyer B J, Casson L P. *Caenorhabditis elegans* compensates for the difference in X chromosome dosage between the sexes by regulating transcript levels. *Cell*. 1986;47:871–881. [[PubMed: 3779843](#)]
1392. Mezqueldi M, Fattoum A, Derancourt J, Kassab R. Mapping the functional domains in the amino-terminal region of calponin. *J. Biol. Chem.* 1992;267:15943–15951. [[PubMed: 1639822](#)]
1393. Mickey K M, Mello C C, Montgomery M K, Fire A, Priess J R. An inductive interaction in 4-cell stage *C. elegans* embryos involves APX-1 expression in the signalling cell. *Development*. 1996;122:1791–1798. [[PubMed: 8674418](#)]
1394. Miller D M, Niemeyer C J. Expression of the *unc-4* homeoprotein in *Caenorhabditis elegans* motor neurons specifies presynaptic input. *Development*. 1995;121:2877–2886. [[PubMed: 7555714](#)]
1395. Miller D M, Niemeyer C J, Chitkara P. Dominant *unc-37* mutations suppress the movement defect of a homeodomain mutation in *unc-4*, a [neural](#) specificity gene in *Caenorhabditis elegans*. *Genetics*. 1993;135:741–753. [[PMC free article: PMC1205717](#)] [[PubMed: 7904971](#)]
1396. Miller D M, Stockdale F E, Karn J. Immunological identification of the genes encoding the four myosin heavy chain isoforms of *Caenorhabditis elegans*. *Proc. Natl. Acad. Sci.* 1986;83:2305–2309. [[PMC free article: PMC323285](#)] [[PubMed: 2422655](#)]
1397. Miller D M, Ortiz I, Berliner G C, Epstein H F. Differential localization of two myosins within nematode thick filaments. *Cell*. 1983;34:477–490. [[PubMed: 6352051](#)]
1398. Miller D M, Shen M M, Shamu C E, Bürglin T R, Ruvkun G, Dubois M L, Ghee M, Wilson L. *C. elegans unc-4* gene encodes a homeodomain protein that determines the pattern of synaptic input to specific motor neurons. *Nature*. 1992;355:841–845. [[PubMed: 1347150](#)]
1399. Miller J P, Selverston A I. Mechanisms underlying pattern generation in lobster stomatogastric ganglion as determined by selective inactivation of identified neurons. II. Oscillatory properties of pyloric neurons. *J. Neurophysiol.* 1982a;48:1378–1391. [[PubMed: 7153798](#)]
1400. Miller J P, Selverston A I. Mechanisms underlying pattern generation in lobster stomatogastric ganglion as determined by selective inactivation of identified neurons. IV. Network properties of pyloric system. *J. Neurophysiol.* 1982b;48:1416–1432. [[PubMed: 7153799](#)]
1401. Miller J, McLachlan A D, Klug A. Repetitive zinc-binding domains in the protein transcription factor IIIA from *Xenopus* oocytes. *EMBO J.* 1985;4:1609–1614. [[PMC free article: PMC554390](#)] [[PubMed: 4040853](#)]
1402. Miller K G, Alfonso A, Nguyen M, Crowell J A, Johnson C D, Rand J B. A genetic selection for *Caenorhabditis elegans* synaptic transmission mutants. *Proc. Natl. Acad. Sci.* 1996;93:12593–12598. [[PMC free article: PMC38037](#)] [[PubMed: 8901627](#)]
1403. Miller L M, Waring D A, Kim S K. Mosaic analysis using a ncl-1(+) extrachromosomal array reveals that *lin-31* acts in the Pn.p cells during *Caenorhabditis elegans* vulval development. *Genetics*. 1996;143:1181–1191. [[PMC free article: PMC1207389](#)] [[PubMed: 8807292](#)]
1404. Miller L M, Gallegos M E, Morisseau B A, Kim S K. *lin-31*, a *Caenorhabditis elegans* HNF-3/fork head transcription factor homolog, specifies three alternative cell fates in vulval development. *Genes Dev.*

- 1993;7:933–947. [PubMed: 8504934]
1405. Miller L M, Plenefisch J D, Casson L P, Meyer B J. *xol-1*: A gene that controls the male modes of both sex determination and X chromosome dosage compensation in *C. elegans*. *Cell*. 1988;55:167–183. [PubMed: 3167975]
1406. Minniti A, Sadler C, Ward S. Genetic and molecular analysis of *spe-27*, a gene required for spermiogenesis in *Caenorhabditis elegans* hermaphrodites. *Genetics*. 1996;143:213–223. [PMC free article: PMC1207255] [PubMed: 8722776]
1407. Minturn J E, Fryer J L, Geschwind D H, Hockfield S. TOAD-64, a gene expressed early in neuronal differentiation in the rat, is related to *unc-33*, a *C. elegans* gene involved in axon outgrowth. *J. Neurosci.* 1995;15:6757–6766. [PMC free article: PMC6578000] [PubMed: 7472434]
1408. Misra S, Rio D C. Cytotype control of *Drosophila* P element transposition: the 66 kD protein is a repressor of transposase activity. *Cell*. 1990;62:269–284. [PubMed: 2164887]
1409. Mitani S, Du H, Hall D H, Driscoll M, Chalfie M. Combinatorial control of touch receptor neuron expression in *Caenorhabditis elegans*. *Development*. 1993;119:773–783. [PubMed: 8187641]
1410. Mitter C, Brooks D R, Futuyma D J, Slatkin M, editors. *Coevolution*. Sunderland, Massachusetts: Sinauer Associates; 1983. Phylogenetic aspects of coevolution. pp. 65–98.
1411. Miura M, Zhu H, Rotello R, Hartwig E A, Yuan J. Induction of apoptosis in fibroblasts by IL-1 $\beta$  converting enzyme, a mammalian homolog of the *C. elegans* cell death gene *ced-3*. *Cell*. 1993;75:653–660. [PubMed: 8242741]
1412. Miwa J, Schierenberg E, Miwa S, von Ehrenstein G. Genetics and mode of expression of temperature-sensitive mutations arresting embryonic development in *Caenorhabditis elegans*. *Dev. Biol.* 1980;76:160–174. [PubMed: 7380089]
1413. Mizuuchi K. Transpositional recombination: Mechanistic insight from studies of Mu and other elements. *Annu. Rev. Biochem.* 1992a;61:1011–1051. [PubMed: 1323232]
1414. Mizuuchi K. Polynucleotidyl transfer reactions in transpositional DNA recombination. *J. Biol. Chem.* 1992b;267:21273–21276. [PubMed: 1383220]
1415. Moerman D G, Baillie D L. Genetic organization in *Caenorhabditis elegans*: Fine structure analysis of the *unc-22* gene. *Genetics*. 1979;91:95–104. [PMC free article: PMC1213933] [PubMed: 1724882]
1416. Moerman D G, Baillie D L. Formaldehyde mutagenesis in the nematode *C. elegans*. *Mutat. Res.* 1981;80:273–279. [PubMed: 7207485]
1417. Moerman D G, Waterston R H. Spontaneous unstable *unc-22* IV mutations in *C. elegans* var.Bergerac. *Genetics*. 1984;108:859–877. [PMC free article: PMC1224270] [PubMed: 6096205]
1418. Moerman D G, Waterston R H, Berg D E, Howe M M, editors. *Mobile DNA*. Washington, D.C.: American Society for Microbiology; 1989. Mobile elements in *Caenorhabditis elegans* and other nematodes. pp. 537–556.
1419. Moerman D G, Benian G M, Waterston R H. Molecular cloning of the muscle gene *unc-22* in *Caenorhabditis elegans* by Tc1 transposon tagging. *Proc. Natl. Acad. Sci.* 1986;83:2579–2583. [PMC free article: PMC323342] [PubMed: 3010313]
1420. Moerman D G, Hutter H, Mullen G P, Schnabel R. Cell autonomous expression of perlecan and plasticity of cell shape in embryonic muscle of *Caenorhabditis elegans*. *Dev. Biol.* 1996;173:228–242. [PubMed: 8575624]
1421. Moerman D G, Plurad S, Waterston R H, Baillie D L. Mutations in the *unc-54* myosin heavy chain gene of *Caenorhabditis elegans* that alter contractility but not muscle structure. *Cell*. 1982;29:773–781. [PubMed: 7151169]
1422. Moerman D G, Benian G M, Barstead R J, Schreifer L, Waterston R H. Identification and intracellular localization of the *unc-22* gene product of *Caenorhabditis elegans*. *Genes Dev.* 1988;2:93–105. [PubMed: 2833427]
1423. Monaghan P, Robertson D, Amos T A S, Dyer M J S, Mason D Y, Greaves M. Ultrastructural localization of bcl-2 protein. *J. Histochem. Cytochem.* 1992;40:1819–1825. [PubMed: 1453000]
1424. Montarolo P G, Kandel E R, Schacher S. Long-term heterosynaptic inhibition in *Aplysia*. *Nature*. 1988;333:171–174. [PubMed: 3367986]

1425. Moore M J, Query C C, Sharp P A. Splicing of precursors to mRNA by the spliceosome. In: Gesteland R F, Atkins J F, editors. *The RNA world*. Cold Spring Harbor, New York: Cold Spring Harbor Laboratory Press; 1993. pp. 303–358.
1426. Morgan P G, Sedensky M M. Mutations conferring new patterns of sensitivity to volatile anesthetics in *Caenorhabditis elegans*. *Anesthesiology*. 1994;81:888–898. [PubMed: 7943840]
1427. Morgan P G, Sedensky M M, Meneely P M. The genetics of response to volatile anesthetics in *Caenorhabditis elegans*. *Ann. N.Y. Acad. Sci.* 1991;625:524–531. [PubMed: 2058904]
1428. Morgan W R, Greenwald I S. Two novel transmembrane protein tyrosine kinases expressed during *Caenorhabditis elegans* hypodermal development. *Mol. Cell. Biol.* 1993;13:7133–7143. [PMC free article: PMC364774] [PubMed: 8413302]
1429. Mori H, Palmer R E, Sternberg P E. The identification of a *Caenorhabditis elegans* homolog of a p34<sup>cdc2</sup> kinase. *Mol. Gen. Genet.* 1994;245:781–786. [PubMed: 7830726]
1430. Mori I. “Molecular cloning of Tc1 elements tightly linked to a mutator.” [Ph.D. thesis]. Washington University; St. Louis: 1989. pp. 46–95. [PubMed: 2602714]
1431. Mori I, Ohshima Y. Neural regulation of thermotaxis in *Caenorhabditis elegans*. *Nature*. 1995;376:344–348. [PubMed: 7630402]
1432. Mori I, Moerman D G, Waterston R H. Analysis of a mutator activity necessary for germline transposition and excision of Tc1 transposable elements in *Caenorhabditis elegans*. *Genetics*. 1988a;120:397–407. [PMC free article: PMC1203519] [PubMed: 2848746]
1433. Mori I, Benian G M, Moerman D G, Waterston R H. Transposable element Tc1 of *Caenorhabditis elegans* recognizes specific target sequences for integration. *Proc. Natl. Acad. Sci.* 1988b;85:861–864. [PMC free article: PMC279655] [PubMed: 2829205]
1434. Moriyama K, Matsumoto S, Nishida E, Sakai H, Yahara I. Destrin, a mammalian actin-depolymerizing protein, is closely related to cofilin. Cloning and expression of porcine brain destrin cDNA. *J. Biol. Chem.* 1990;265:5768–5773. [PubMed: 2156828]
1435. Moronet D, Bertrand R, Pantel P, Audemard E, Kassab R. Structure of the actin-myosin interface. *Nature*. 1981;292:301–306. [PubMed: 6114435]
1436. Morris J Z, Tissenbaum H A, Runkun G. A phosphatidylinositol-3-OH kinase family member regulating longevity and diapause in *Caenorhabditis elegans*. *Nature*. 1996;382:536–539. [PubMed: 8700226]
1437. Morris S, Schmid S L. The Ferrari of endocytosis? *Curr. Biol.* 1995;5:113–115. [PubMed: 7743171]
1438. Morshead C M, Reynolds B A, Craig C G, McBurney M W, Staines W A, Morassutti D, Weiss S, van der Kooy D. Neural stem cells in the adult mammalian forebrain: A relatively quiescent subpopulation of subependymal cells. *Neuron*. 1994;13:1071–1082. [PubMed: 7946346]
1439. Morton D G, Roos J M, Kemphues K J. *par-4*, a gene required for cytoplasmic localization and determination of specific cell types in *Caenorhabditis elegans* embryogenesis. *Genetics*. 1992;130:771–790. [PMC free article: PMC1204928] [PubMed: 1582558]
1440. Moskowitz I P, Gendreau S B, Rothman J H. Combinatorial specification of blastomere identity by *glp-1*-dependant cellular interactions in the nematode *Caenorhabditis elegans*. *Development*. 1994;120:3325–3338. [PubMed: 7720570]
1441. Moulder G L, Huang M M, Waterston R H, Barstead R J. Talin requires β-integrin, but not vinculin for its assembly into focal adhesion-like structures in the nematode *Caenorhabditis elegans*. *Mol. Biol. Cell*. 1996;7:1181–1193. [PMC free article: PMC275971] [PubMed: 8856663]
1442. Mount S M. A catalogue of splice junction sequences. *Nucleic Acids Res.* 1982;10:459–471. [PMC free article: PMC326150] [PubMed: 7063411]
1443. Mount S M, Burks C, Hertz G, Stormo G D, White O, Fields C. Splicing signals in *Drosophila*: Intron size, information content, and consensus sequences. *Nucleic Acids Res.* 1992;20:4255–4262. [PMC free article: PMC334133] [PubMed: 1508718]
1444. Muhlrad D, Parker R. Premature translation termination triggers mRNA decapping. *Nature*. 1994;370:578–581. [PubMed: 8052314]

1445. Müller F, Boothroyd J C, Komuniecki R, editors. Molecular approaches to parasitology. New York: Wiley-Liss; 1995. Chromatin diminution in nematode development: An alternative means of gene regulation? pp. 191–205.
1446. Müller F, Wicky C, Spicher A, Tobler H. New telomere formation after developmentally regulated chromosomal breakage during the process of chromatin diminution in *Ascaris lumbricoides*. *Cell*. 1991;67:815–822. [[PubMed: 1934070](#)]
1447. Murakami S, Johnson T E. A genetic pathway conferring life extension and resistance to UV stress in *Caenorhabditis elegans*. *Genetics*. 1996;143:1207–1218. [[PMC free article: PMC1207391](#)] [[PubMed: 8807294](#)]
1448. Murdock A D, Dodge G R, Cohen I, Tuan R S, Iozzo R V. Primary structure of the human heparan sulfate proteoglycan from basement membrane (HSPG2/perlecan). *J. Biol. Chem.* 1992;267:8544–8557. [[PubMed: 1569102](#)]
1449. Murphy T D, Karpen G H. Localization of centromere function in a *Drosophila* minichromosome. *Cell*. 1995;82:599–609. [[PMC free article: PMC3209481](#)] [[PubMed: 7664339](#)]
1450. Murphy W J, Watkins K P, Agabian N. Identification of a novel Y branch structure as an intermediate in trypanosome mRNA processing: Evidence for *trans* splicing. *Cell*. 1986;47:517–525. [[PubMed: 3779835](#)]
1451. Myers C D, Goh P -Y, Allen T S, Bucher E A, Bogaert T. Developmental genetic analysis of troponin T mutations in striated and nonstriated muscle cells of *Caenorhabditis elegans*. *J. Cell Biol.* 1996;132:1061–1077. [[PMC free article: PMC2120761](#)] [[PubMed: 8601585](#)]
1452. Naclerio G, Cangiano G, Coulson A, Levitt A, Ruvolo V, La Volpe A. Molecular and genomic organization of clusters of repetitive DNA sequences in *Caenorhabditis elegans*. *J. Mol. Biol.* 1992;226:159–168. [[PubMed: 1619649](#)]

## N

1453. Nadler S A. Phylogeny of some ascaridoid nematodes inferred from comparison of 18S and 28S rRNA sequences. *Mol. Biol. Evol.* 1992;9:932–944. [[PubMed: 1528113](#)]
1454. Naito M, Kohara Y, Kurosawa Y. Identification of a homeobox-containing gene located between *lin-45* and *unc-24* on chromosome IV in the nematode *Caenorhabditis elegans*. *Nucleic Acids Res.* 1992;20:2967–2969. [[PMC free article: PMC312424](#)] [[PubMed: 1352400](#)]
1455. Nakamura T, Gold G H. A cyclic-nucleotide gated conductance in olfactory receptor cilia. *Nature*. 1987;325:442–444. [[PubMed: 3027574](#)]
1456. Nakashima T, Sekiguchi T, Kuraoka A, Fukushima K, Shibata Y, Komiyama S, Nishimoto T. Molecular cloning of a human cDNA encoding a novel protein, DAD1, whose defect causes apoptotic cell death in hamster BHK21 cells. *Mol. Cell. Biol.* 1993;13:6367–6374. [[PMC free article: PMC364695](#)] [[PubMed: 8413235](#)]
1457. Nakayama K, Nakayama K, Negishi I, Kuida K, Shinkai Y, Louie M C, Fields L E, Lucas P J, Stewart V, Alt F W, Loh D Y. Disappearance of the lymphoid system in Bcl-2 homozygous mutant chimeric mice. *Science*. 1993;261:1584–1588. [[PubMed: 8372353](#)]
1458. Nara T, Lee L, Imae Y. Thermosensing ability of Trg and Tap chemoreceptors in *Escherichia coli*. *J. Bacteriol.* 1991;173:1120–1124. [[PMC free article: PMC207232](#)] [[PubMed: 1991711](#)]
1459. Narahashi Y. Pronase. *Methods Enzymol.* 1970;19:651–664.
1460. National Research Council Committee on Models for Biomedical Research. Models for biomedical research: A new perspective. Washington, D.C.: National Academy Press; 1985. pp. 50–52.
1461. Nave R, Weber K. A myofibrillar protein of insect muscle related to vertebrate titin connects Z band and A band: Purification and molecular characterization of invertebrate mini-titin. *J. Cell Sci.* 1990;95:535–544. [[PubMed: 2117014](#)]
1462. Nealson K H. Luminescent bacteria symbiotic with entomopathogenic nematodes. In: Margulies L, Fester R, editors. Symbiosis as a source of evolutionary innovation. Cambridge, Massachusetts: MIT Press; 1991. pp. 205–218.

1463. Neher E, Zucker R S. Multiple calcium-dependent processes related to secretion in bovine chromaffin cells. *Neuron*. 1993;10:21–30. [[PubMed: 8427700](#)]
1464. Nelson D W, Honda B M. Genes coding for 5S ribosomal RNA of the nematode *Caenorhabditis elegans*. *Gene*. 1985;38:245–251. [[PubMed: 4065574](#)]
1465. Nelson D W, Honda B M. Genetic mapping of the 5S RNA gene cluster of the nematode *Caenorhabditis elegans*. *Can. J. Genet. Cytol.* 1986;28:545–553. [[PubMed: 3019494](#)]
1466. Nelson G A, Ward S. Vesicle fusion pseudopod extension and amoeboid motility are induced in nematode *spermatids* by the ionophore monensin. *Cell*. 1980;19:457–464. [[PubMed: 7357613](#)]
1467. Nelson G A, Roberts T, Ward S. *Caenorhabditis elegans* spermatozoan locomotion: Amoeboid movement with almost no actin. *J. Cell Biol.* 1982;92:121–131. [[PMC free article: PMC2111997](#)] [[PubMed: 7199049](#)]
1468. Nelson F K, Albert P S, Riddle D L. Fine structure of the *C. elegans* secretory-[excretory](#) system. *J. Ultrastruct. Res.* 1983;82:156–171. [[PubMed: 6827646](#)]
1469. Newman A, White J G, Sternberg P W. The *C. elegans lin-12* gene mediates induction of ventral [uterine](#) specialization by the anchor cell. *Development*. 1995;121:263–271. [[PubMed: 7768171](#)]
1470. Newman S M J, Wright T R F. A histological and ultrastructural analysis of developmental defects produced by the mutation lethal(l)myospheroid, in *Drosophila melanogaster*. *Dev. Biol.* 1981;86:393–402. [[PubMed: 6793430](#)]
1471. Nguyen M, Alfonso A, Johnson C D, Rand J B. *Caenorhabditis elegans* mutants resistant to inhibitors of acetylcholinesterase. *Genetics*. 1995;140:527–535. [[PMC free article: PMC1206632](#)] [[PubMed: 7498734](#)]
1472. Nicholas W L. The biology of free-living nematodes. Oxford: Clarendon Press; 1975.
1473. Nicholas W L. The biology of free-living nematodes 2nd edition. England: Oxford University Press; 1984.
1474. Nicholas W L, Dougherty E C, Hansen E L. Axenic cultivation of *C. briggsae* (Nematoda: Rhabditidae) with chemically undefined supplements;--> comparative studies with related nematodes. *Ann. N.Y. Acad. Sci.* 1959;77:218–236.
1475. Nicholson D W, Ali A, Thornberry N A, Vaillancourt J P, Ding C K, Gallant M, Gareau Y, Griffin P R, Labelle M, Lazebnik Y A, Munday N A, Raju S M, Smulson M E, Yamin T -T, Yu V L, Miller D K. Identification and inhibition of the ICE/CED-3 protease necessary for mammalian apoptosis. *Nature*. 1995;376:37–43. [[PubMed: 7596430](#)]
1476. Nielsen C. Animal evolution: Interrelationships of the living phyla. Oxford: Oxford University Press; 1995.
1477. Nigon V. Les modalités de la reproduction et le déterminisme du sexe chez quelques nematodes libres. *Ann. Sci. Nat. Zool. Biol. Anim.* 1949;11:1–132.
1478. Nigon V. Polyploidie experimentale chez un Nematode libre, *Rhabditis elegans Maupas*. *Bull. Biol. Fr. Belg.* 1951;85:187–225.
1479. Nigon V, Brun J. L'évolution des structures nucléaires dans l'ovogenèse de *Caenorhabditis elegans* Maupas 1900. *Chromosoma*. 1955;7:129–169. [[PubMed: 13250682](#)]
1480. Nigon V, Dougherty E C. Reproductive patterns and attempts at reciprocal crossing of *Rhabditis elegans* Maupas 1900, and *Rhabditis briggsae*. *J. Exp. Zool.* 1949;112:485–503. [[PubMed: 15404785](#)]
1481. Nigon V, Dougherty E C. A dwarf mutation in a nematode. A morphological mutant of *Rhabditis briggsae* a free-living soil nematode. *J. Hered.* 1950;41:103–109. [[PubMed: 15428631](#)]
1482. Nigon V, Guerrier P, Monin H. L'architecture polaire de l'oeuf et les mouvements des constituants cellulaires au cours des premières étapes du développement chez quelques nematodes. *Bull. Biol. Fr. Belg.* 1960;94:131–202.
1483. Nilsen T W. Trans-splicing of nematode pre-messenger RNA. *Annu. Rev. Microbiol.* 1993;47:413–440. [[PubMed: 8257104](#)]
1484. Nilsen T W, Shambaugh J, Denker J, Chubb G, Faser C, Putnam L, Bennett K. Characterization and expression of a spliced leader RNA in the parasitic nematode *Ascaris lumbricoides* var. suum. *Mol. Cell. Biol.* 1989;9:3543–3547. [[PMC free article: PMC362403](#)] [[PubMed: 2796996](#)]

1485. Nishida E, Iida K, Yonezawa N, Koyasu S, Yahara I, Sakai H. Cofilin is a component of intranuclear and cytoplasmic actin rods induced in culture. Proc. Natl. Acad. Sci. 1987;84:5262–5266. [[PMC free article](#): [PMC298835](#)] [[PubMed: 3474653](#)]
1486. Nishiwaki K, Sano T, Miwa J. *emb-5*, a gene required for the correct timing of gut precursor cell division during gastrulation in *Caenorhabditis elegans*, encodes a protein similar to the yeast nuclear protein spt-6. Mol. Gen. Genet. 1993;239:313–322. [[PubMed: 8391108](#)]
1487. Nobes C D, Hall A. Rho rac, and cdc42 GTPases regulate the assembly of multimolecular focal complexes associated with actin stress fibers, lamellipodia, and filopodia. Cell. 1995;81:53–62. [[PubMed: 7536630](#)]
1488. Noguchi J, Yanagisawa M, Imamura M, Kasuya Y, Sakurai T, Tanaka T, Masaki T. Complete primary structure and tissue expression of chicken pectoralis M-protein. J. Biol. Chem. 1992;267:20302–20310. [[PubMed: 1400348](#)]
1489. Nonet M L, Meyer B J. Early aspects of *Caenorhabditis elegans* sex determination and dosage compensation are regulated by a zinc-finger protein. Nature. 1991;351:65–68. [[PubMed: 2027384](#)]
1490. Nonet M L, Grundahl K, Meyer B J, Rand J B. Synaptic function is impaired but not eliminated in *C. elegans* mutants lacking synaptotagmin. Cell. 1993;73:1291–1305. [[PubMed: 8391930](#)]
1491. Noonan D M, Fulle A, Valente P, Cai S, Horigan E, Sasaki M, Yamada Y, Hassell J R. The complete sequence of perlecan, a basement membrane heparan sulfate proteoglycan, reveals extensive similarity with laminin A chain, low density lipoprotein-receptor, and the [neural](#) cell adhesion molecule. J. Biol. Chem. 1991;266:22939–22947. [[PubMed: 1744087](#)]
1492. Nose A, Takeichi M, Goodman C S. Ectopic expression of connectin reveals a repulsive function during growth cone guidance and synapse formation. Neuron. 1994;13:525–539. [[PubMed: 7917289](#)]
1493. Novak J. Screening for a new generation of antihelminthic compounds—*In vitro* selection of the nematode *Caenorhabditis elegans* for ivermectin resistance. Folia Microbiol. 1992;37:237–238. [[PubMed: 1505886](#)]
1494. Novick P, Brennwald P. Friends and family: The role of the rab GTPases in vesicular traffic. Cell. 1993;75:597–601. [[PubMed: 8242735](#)]
1495. Nusbaum C, Meyer B J. The *Caenorhabditis elegans* gene *sdc-2* controls sex determination and dosage compensation in XX animals. Genetics. 1989;122:579–593. [[PMC free article](#): [PMC1203732](#)] [[PubMed: 2759421](#)]
1496. Nutman T B, Boothroyd J C, Komuniecki R, editors. Molecular approaches to parasitology. New York: Wiley-Liss; 1995. Immune responses in lymphatic-dwelling filarial infections. pp. 511–523.
1497. Nutman T B, Kumaraswami V, Ottesen E A. Parasite-specific anergy in human filariasis. Insights after analysis of parasite antigen-driven lymphokine production. J. Clin. Invest. 1987;79:1516–1523. [[PMC free article](#): [PMC424428](#)] [[PubMed: 3553242](#)]
1498. Nye J S, Kopan R, Axel R. An activated *Notch* suppresses neurogenesis and myogenesis but not gliogenesis in mammalian cells. Development. 1994;120:2421–2430. [[PubMed: 7956822](#)]

## O

1499. O'Brien T P, McCully M E. Plant structure and development. A pictorial and physiological approach. Toronto: Collier-Macmillan Canada; 1969.
1500. O'Brochta D A, Gomez S P, Handler A M. P element excision in *Drosophila melanogaster* and related drosophilids. Mol. Gen. Genet. 1991;225:387–394. [[PubMed: 1850084](#)]
1501. Ofulue E N, Candido E P M. Molecular cloning and characterization of the *Caenorhabditis elegans* elongation factor 2 gene (*eft-2*). DNA Cell Biol. 1991;10:603–611. [[PubMed: 1930695](#)]
1502. Ofulue E N, Candido E P M. Isolation and characterization of *eft-1* an elongation factor 2-like gene on chromosome III of *Caenorhabditis elegans*. DNA Cell Biol. 1992;11:71–82. [[PubMed: 1739435](#)]
1503. Ogg S C, Anderson P, Wickens M P. Splicing of a *C. elegans* myosin pre-mRNA in a human nuclear extract. Nucleic Acids Res. 1990;18:143–149. [[PMC free article](#): [PMC330214](#)] [[PubMed: 2308820](#)]

1504. Ogura K, Wicky C, Magnenat L, Tobler H, Mori I, Muller F, Ohshima Y. *Caenorhabditis elegans unc-51* gene required for axonal elongation encodes a novel serine/threonine kinase. *Genes Dev.* 1994;8:2389–2400. [[PubMed: 7958904](#)]
1505. Ohsako S, Hyer J, Pantaninan G, Oliver I, Caudy M. hairy function as a DNA-binding helix-loop-helix repressor of *Drosophila* sensory organ formation. *Genes Dev.* 1994;8:2743–2755. [[PubMed: 7958930](#)]
1506. Okada Y, Yamazaki H, Sekine-Aizawa Y, Hirokawa N. The neuron-specific kinesin superfamily protein KIF1A is a unique monomeric motor for anterograde axonal transport of synaptic vesicle precursors. *Cell.* 1995;81:769–780. [[PubMed: 7539720](#)]
1507. Okagaki T, Weber F E, Fischman D A, Vaughan K T, Mikawa T, Reinach F C. The major myosin-binding domain of skeletal muscle MyBP-C (C-protein) resides in the COOH-terminal immunoglobulin C2 motif. *J. Cell Biol.* 1993;123:619–626. [[PMC free article: PMC2200114](#)] [[PubMed: 8227129](#)]
1508. Okamoto H, Thomson J M. Monoclonal antibodies which distinguish certain classes of neuronal and support cells in the nervous tissue of the nematode *Caenorhabditis elegans*. *J. Neurosci.* 1985;5:643–653. [[PMC free article: PMC6565019](#)] [[PubMed: 3882896](#)]
1509. Okimoto R, Wolstenholme D R. A set of tRNAs that lack either the T $\overline{C}$ C arm or the dihydrouridine arm: Towards a minimal tRNA adaptor. *EMBO J.* 1990;9:3405–3411. [[PMC free article: PMC552080](#)] [[PubMed: 2209550](#)]
1510. Okimoto R, Macfarlane J L, Wolstenholme D R. Evidence for the frequent use of TTG as the translation initiation codon of mitochondrial protein genes in the nematodes, *Ascaris suum* and *Caenorhabditis elegans*. *Nucleic Acids Res.* 1990;18:6113–6118. [[PMC free article: PMC332414](#)] [[PubMed: 2235493](#)]
1511. Okimoto R, Macfarlane J L, Wolstenholme D R. The mitochondrial ribosomal RNA genes of the nematodes *Caenorhabditis elegans* and *Ascaris suum*: Consensus secondary-structure models and conserved nucleotide sets for phylogenetic analysis. *J. Mol. Evol.* 1994;39:598–613. [[PubMed: 7528811](#)]
1512. Okimoto R, Macfarlane J L, Clary D O, Wolstenholm D R. The mitochondrial genomes of two nematodes, *Caenorhabditis elegans* and *Ascaris suum*. *Genetics.* 1992;130:471–498. [[PMC free article: PMC1204866](#)] [[PubMed: 1551572](#)]
1513. Okkema P G, Fire A. The *Caenorhabditis elegans* NK-2 class homeoprotein CEH-22 is involved in combinatorial activation of gene expression in [pharyngeal muscle](#). *Development.* 1994;120:2175–2186. [[PubMed: 7925019](#)]
1514. Okkema P G, Kimble J. Molecular analysis of *tra-2* a sex determining gene in *Caenorhabditis elegans*. *EMBO J.* 1991;10:171–176. [[PMC free article: PMC452626](#)] [[PubMed: 1703488](#)]
1515. Okkema P G, Harrison S W, Plunger V, Aryana A, Fire A. Sequence requirements for myosin gene expression and regulation in *Caenorhabditis elegans*. *Genetics.* 1993;135:385–404. [[PMC free article: PMC1205644](#)] [[PubMed: 8244003](#)]
1516. Olson E N. MyoD family: A paradigm for development? *Genes Dev.* 1990;4:1454–1461. [[PubMed: 2253873](#)]
1517. Olson N J, Pearson R B, Needleman D S, Hurvitz M Y, Kemp B E, Means A R. Regulatory and structural motifs of chicken gizzard myosin light chain kinase. *Proc. Natl. Acad. Sci.* 1990;87:2284–2288. [[PMC free article: PMC53671](#)] [[PubMed: 2315320](#)]
1518. Omichinski J G, Clore G M, Schaad O, Felsenfeld G, Trainor C, Appella E, Stahl S J, Gronenborn A M. NMR structure of a specific DNA complex of Zn-containing DNA binding domain of GATA-1. *Science.* 1993;261:438–446. [[PubMed: 8332909](#)]
1519. Oosumi T, Belknap W R, Garlick B. *Mariner* transposons in humans. *Nature.* 1995;378:672. [[PubMed: 7501013](#)]
1520. Opperman C H, Chang S. Nematode acetylcholinesterases: Molecular forms and their potential role in nematode behaviour. *Parasitol. Today.* 1992;8:406–411. [[PubMed: 15463554](#)]
1521. Opperman C H, Dong K, Chang S. Genetic analysis of the soybean-cyst nematode interaction. In: Lamberti F, et al., editors. NATO ARW:Advances in molecular plant nematology. New York: Plenum Press; 1994a. pp. 65–75.

1522. Opperman C H, Taylor C G, Conkling M A. Root-knot nematode-directed expression of a plant root-specific gene. *Science*. 1994;263:221–223. [[PubMed: 17839183](#)]
1523. Ordway R, Pallanck L, Ganetzky B. Neurally expressed *Drosophila* genes encoding homologs of the NSF and SNAP secretory proteins. *Proc. Natl. Acad. Sci.* 1994;91:5715–5719. [[PMC free article: PMC44067](#)] [[PubMed: 8202553](#)]
1524. O'Riordan V, Burnell A M. Intermediary metabolism in the dauer larva of the nematode *C. elegans*. I. Glycolysis gluconeogenesis, oxidative phosphorylation and the tricarboxylic acid cycle. *Comp. Biochem. Physiol.* 1989;92B:233–238.
1525. O'Riordan V, Burnell A M. Intermediary metabolism in the dauer larva. II. The glyoxylate cycle and fatty acid oxidation. *Comp. Biochem. Physiol.* 1990;95B:125–130.
1526. Orr H A. Haldane's rule has multiple genetic causes. *Nature*. 1993;361:532–533. [[PubMed: 8429905](#)]
1527. Orr H A, Coyne J A. The genetics of adaptation: A reassessment. *Am. Nat.* 1992;140:725–742. [[PubMed: 19426041](#)]
1528. Orr W, Sohal R S. Extension of life-span by overexpression of superoxide dismutase and catalase in *Drosophila melanogaster*. *Science*. 1994;263:1128–1130. [[PubMed: 8108730](#)]
1529. Osche G. Systematik und Phylogenie der Gattung *Rhabditis* (Nematoda). *Zool. Jahrb. Abt. Allg. Zool. Physiol. Tiere*. 1952;81:190–280.
1530. O'Shea E K, Klemm J D, Kim P S, Alber T. X-ray stucture of the GCN4 leucine zipper, a two-stranded, parallel coiled coil. *Science*. 1991;254:539–524. [[PubMed: 1948029](#)]
1531. Otsuka A J, Jeyaprakash A, Garcia-Anoveros J, Tang L Z, Fisk G, Hartshorne T, Franco R, Born T. The *C. elegans unc-104* gene encodes a putative kinesin heavy chain-like protein. *Neuron*. 1991;6:113–122. [[PubMed: 1846075](#)]
1532. Otsuka A J, Franco R, Yang B, Shim K -H, Tang L Z, Zhang Y Y, Boontrakulpoontawee P, Jeyaprakash A, Hedgecock E, Wheaton V I, Sobery A. An ankyrin-related gene (*unc-44*) is necessary for proper axonal guidance in *Caenorhabditis elegans*. *J. Cell Biol.* 1995;129:1081–1092. [[PMC free article: PMC2120500](#)] [[PubMed: 7744957](#)]
1533. Ottesen E A, Ramachandran C D. Lymphatic filariasis. Infection and disease: Control strategies. *Parasitol. Today*. 1995;11:129–131.
1534. Ou X, Tang L, McCrossan M, Henkle-Dührsen K, Selkirk M E. *Brugia malayi*: Localisation and differential expression of extracellular and cytoplasmic CuZn superoxide dismutases in adults and microfilariae. *Exp. Parasitol.* 1995a;80:515–529. [[PubMed: 7729487](#)]
1535. Ou X, Thomas R, Chacón M R, Tang L, Selkirk M E. *Brugia malayi*: Differential susceptibility to and metabolism of hydrogen peroxide in adults and microfilariae. *Exp. Parasitol.* 1995b;80:530–540. [[PubMed: 7729488](#)]
1536. Ouazana R, Herbage D. Biochemical characterization of the cuticle collagen of the nematode *Caenorhabditis elegans*. *Biochim. Biophys. Acta*. 1981;669:236–243. [[PubMed: 7284437](#)]
1537. Ouazana R, Garrone R, Godet J. Characterization of morphological and biochemical defects in the cuticle of a dumpy mutant of *Caenorhabditis elegans*. *Comp. Biochem. Physiol.* 1985;80B:481–484.
1538. Ouazana R, Herbage D, Godet J. Some biochemical aspects of the cuticle collagen of the nematode *Caenorhabditis elegans*. *Comp. Biochem. Physiol.* 1984;77B:51–56.
1539. Owen R. Lectures on comparative anatomy and physiology of the invertebrate animals (delivered at the Royal College of Surgeons in 1843). London: Longman, Brown, Green and Longman; 1843.

## P

1540. Pableo E C, Triantaphillou A C, Kloos W E. DNA isolation and GC base composition of four root-knot nematode (*Meloidogyne* spp.) genomes. *J. Nematol.* 1988;20:1–8. [[PMC free article: PMC2618780](#)] [[PubMed: 19290179](#)]
1541. Padgett R W, Wozney J M, Gelbart W M. Human BMP sequences can confer normal dorsal-ventral patterning in the *Drosophila* embryo. *Proc. Natl. Acad. Sci.* 1993;90:2905–2909. [[PMC free article: PMC46205](#)] [[PubMed: 8464906](#)]

1542. Page A P, Maizels R M. Biosynthesis and glycosylation of serine/threonine-rich secreted proteins from *Toxocara camnis* larvae. Parasitology. 1992;105:297–308. [[PubMed: 1454427](#)]
1543. Page A P, Hamilton A J, Maizels R M. *Toxocara canis*: Monoclonal antibodies to carbohydrate epitopes of secreted (TES) antigens localize to different secretion-related structures in infective larvae. Exp. Parasitol. 1992;75:56–71. [[PubMed: 1379195](#)]
1544. Page A P, MacNiven K, Hengartner M O. Cloning and biochemical characterization of the cyclophilin homologues from the free-living nematode *Caenorhabditis elegans*. Biochem. J. 1996;317:179–185. [[PMC free article: PMC1217461](#)] [[PubMed: 8694762](#)]
1545. Pallanck L, Ordway R, Ganetzky B. A *Drosophila* NSF mutant. Nature. 1995;376:25. [[PubMed: 7596428](#)]
1546. Papp A, Rougvie A E, Ambros V. Molecular cloning of *lin-29*, a heterochronic gene required for the differentiation of hypodermal cells and the cessation of molting in *C. elegans*. Nucleic Acids Res. 1991;19:623–630. [[PMC free article: PMC333658](#)] [[PubMed: 1672752](#)]
1547. Park E -C, Horvitz H R. Mutations with dominant effects on the behavior and morphology of the nematode *Caenorhabditis elegans*. Genetics. 1986a;113:821–852. [[PMC free article: PMC1202915](#)] [[PubMed: 3744028](#)]
1548. Park E -C, Horvitz H R. *C. elegansunc-105* mutations affect muscle and are suppressed by other mutations that affect muscle. Genetics. 1986b;113:853–867. [[PMC free article: PMC1202916](#)] [[PubMed: 3744029](#)]
1549. Park W J, Liu J C, Adler P N. The frizzled gene of *Drosophila* encodes a membrane-protein with an odd number of transmembrane domains. Mech. Dev. 1994;45:127–137. [[PubMed: 8199049](#)]
1550. Park Y -S, Kramer J M. Tandemly duplicated *Caenorhabditis elegans* collagen genes differ in their modes of splicing. J. Mol. Biol. 1990;211:395–406. [[PubMed: 1689778](#)]
1551. Park Y -S, Kramer J M. The *C. elegans* *sqt-1* and *rol-6* collagen genes are coordinately expressed during development, but not at all stages that display mutant phenotypes. Dev. Biol. 1994;163:112–124. [[PubMed: 8174767](#)]
1552. Parker R, Siciliano P G, Guthrie C. Recognition of the TACTAAC box during mRNA splicing in yeast involves base-pairing to the U2-line snRNA. Cell. 1987;49:229–239. [[PubMed: 3552247](#)]
1553. Parkhurst S M, Meneely P M. Sex determination and dosage compensation: Lessons from flies and worms. Science. 1994;264:924–932. [[PubMed: 8178152](#)]
1554. Parkhurst S M, Lipshitz H D, Ish-Horowicz D. *achaete-scute* feminizing activities and *Drosophila* sex determination. Development. 1993;117:737–749. [[PubMed: 8330537](#)]
1555. Paroush Z, Finley R Jr., Kidd T, Wainwright S M, Ingham P W, Brent R, Ish-Horowicz D. Groucho is required for *Drosophila* neurogenesis, segmentation, and sex determination and interacts directly with hairy-related bHLH proteins. Cell. 1994;79:805–815. [[PubMed: 8001118](#)]
1556. Partridge L, Harvey P H. Methuselah among nematodes. Nature. 1993;366:404–405. [[PubMed: 8247143](#)]
1557. Patel N, Thierry-Mieg D, Mancillas J R. Cloning by insertional mutagenesis of a cDNA encoding *Caenorhabditis elegans* kinesin heavy chain. Proc. Natl. Acad. Sci. 1993;90:9181–9185. [[PMC free article: PMC47526](#)] [[PubMed: 8105472](#)]
1558. Paton J, Nottebohm F N. Neurons generated in the adult brain are recruited into functional circuits. Science. 1984;225:1046–1048. [[PubMed: 6474166](#)]
1559. Paulsen J E, Capowski E, Strome S. Phenotypic and molecular analysis of *mes-3*, a maternal-effect gene required for proliferation and viability of the germ line in *C. elegans*. Genetics. 1995;141:1383–1398. [[PMC free article: PMC1206874](#)] [[PubMed: 8601481](#)]
1560. Paulsson M. Basement membrane proteins. Structure assembly, and cellular interactions. Crit. Rev. Biochem. Mol. Biol. 1992;27:93–127. [[PubMed: 1309319](#)]
1561. Pavalko F, Roberts T. *Caenorhabditis elegans* spermatozoa assemble membrane proteins onto the surface at the tips of pseudopodial projections. Cell Motil. Cytoskel. 1987;7:169–177. [[PubMed: 3555849](#)]
1562. Pavalko F, Roberts T. Posttranslational insertion of a membrane protein on *Caenorhabditis elegans* sperm occurs without *de novo* protein synthesis. J. Cell. Biochem. 1989;41:57–70. [[PubMed: 2613747](#)]

1563. Paxton W A, Yazdanbakhsh M, Kurniawan A, Partono F, Maizels R M, Selkirk M. Primary structure of and immunoglobulin E response to the repeat subunit of gp15/400 from human lymphatic filarial parasites. *Infect. Immun.* 1993;61:2827–2833. [PMC free article: PMC280927] [PubMed: 8514385]
1564. Peixoto C A, de Souza W. Cytochemical characterization of the cuticle of *Caenorhabditis elegans* (Nematoda: Rhabditoidea). *J. Submicrosc. Cytol. Pathol.* 1992;24:425–435. [PubMed: 1394094]
1565. Peixoto C A, de Souza W. Freeze-fracture characterization of the cuticle of adult and dauer forms of *Caenorhabditis elegans*. *Parasitol. Res.* 1994;80:53–57. [PubMed: 8153126]
1566. Peltz S W, Brown A H, Jacobson A. mRNA destabilization triggered by premature translation termination depends on at least three cis-acting sequence elements and one trans-acting factor. *Genes Dev.* 1993;7:1737–1754. [PubMed: 8370523]
1567. Peltz S W, Feng H, Welch E, Jacobson A. Nonsense-mediated mRNA decay in yeast. *Prog. Nucleic Acids Res. Mol. Biol.* 1994;47:271–298. [PubMed: 8016322]
1568. Peltz S W, Brewer G, Bernstein P, Hart P A, Ross J. Regulation of mRNA turnover in eukaryotic cells. *Crit. Rev. Eukaryotic Gene Expr.* 1991;1:99–126. [PubMed: 1802106]
1569. Perkins A S, Fishel R, Jenkins N A, Copeland N G. *Evi-1*, a murine zinc finger proto-oncogene, encodes a sequence-specific DNA-binding protein. *Mol. Cell. Biol.* 1991;11:2665–2674. [PMC free article: PMC360036] [PubMed: 2017172]
1570. Perkins L A, Hedgecock E M, Thomson J N, Culotti J G. Mutant sensory cilia in the nematode *Caenorhabditis elegans*. *Dev. Biol.* 1986;117:456–487. [PubMed: 2428682]
1571. Perry M D, Trent C, Robertson B, Chamblin C, Wood W B. Sequenced alleles of the *Caenorhabditis elegans* sex-determining gene *her-1* include a novel class of conditional promoter mutations. *Genetics.* 1994;138:317–327. [PMC free article: PMC1206151] [PubMed: 7828816]
1572. Perry M D, Li W, Trent C, Robertson B, Fire A, Hageman J M, Wood W B. Molecular characterization of the *her-1* gene suggests a direct role in cell signaling during *Caenorhabditis elegans* sex determination. *Genes Dev.* 1993;7:216–228. [PubMed: 8436294]
1573. Peters K, McDowall J, Rose A M. Mutations in the *bli-4* (*l*) locus of *Caenorhabditis elegans* disrupt both adult cuticle and early larval development. *Genetics.* 1991;129:95–102. [PMC free article: PMC1204585] [PubMed: 1936966]
1574. Pettitt J, Kingston I B. The complete primary structure of a nematode  $\alpha$ 2(IV) collagen and the partial structural organization of its gene. *J. Biol. Chem.* 1991;266:16149–16156. [PubMed: 1714907]
1575. Pettitt J, Kingston I B. Developmentally regulated alternative splicing of a nematode type IV collagen gene. *Dev. Biol.* 1994;161:22–29. [PubMed: 8293875]
1576. Pevsner J, Hsu S C, Scheller R H. n-Sec1: A neural-specific syntaxin-binding protein. *Proc. Natl. Acad. Sci.* 1994;91:1445–1449. [PMC free article: PMC43176] [PubMed: 8108429]
1577. Philipp M, Rumjanek F D. Antigenic and dynamic properties of helminth surface structures. *Mol. Biochem. Parasitol.* 1984;10:245–268. [PubMed: 6203035]
1578. Philipp M, Parkhouse R M E, Ogilvie B M. Changing proteins on the surface of a parasitic nematode. *Nature.* 1980;287:538–540. [PubMed: 7422005]
1579. Philippe H, Chenuil A, Adoutte A. Can the Cambrian explosion be inferred through molecular phylogeny? *Suppl.*, pp. *Development.* 1994:15–25.
1580. Pickles J O, Corey D P. Mechanoelectrical transduction by hair cells. *Trends Neurosci.* 1992;15:254–259. [PubMed: 1381121]
1581. Pierceall W E, Reale M A, Candia A F, Wright C V, Cho K R, Fearon E R. Expression of a homologue of the deleted in colorectal cancer (DCC) gene in the nervous system of developing *Xenopus* embryos. *Dev. Biol.* 1994a;166:654–665. [PubMed: 7813784]
1582. Pierceall W E, Cho K R, Getzenberg R H, Reale M A, Hedrick L, Vogelstein B, Fearon E R. NIH3T3 cells expressing the deleted in colorectal cancer tumor suppressor gene product stimulate neurite outgrowth in rat PC12 pheochromocytoma cells. *J. Cell Biol.* 1994b;124:1017–1027. [PMC free article: PMC2119968] [PubMed: 8132705]
1583. Pieribone V, Shupliakov O, Brodin L, Hilfiker-Rothenfluh S, Czernik A J, Greengard P. Distinct pools of synaptic vesicles in neurotransmitter release. *Nature.* 1995;375:493–497. [PubMed: 7777058]

1584. Pilgrim D. The genetic and RFLP characterization of the left end of linkage group *III* in *Caenorhabditis elegans*. *Genome*. 1993;36:712–724. [[PubMed: 8104844](#)]
1585. Pilgrim D B, Bell J B. Expression of a *Drosophila melanogaster* amber suppressor tRNA<sup>Ser</sup> in *Caenorhabditis elegans*. *Mol. Gen. Genet.* 1993;241:26–32. [[PubMed: 8232208](#)]
1586. Pilgrim D, McGregor A, Jackle P, Johnson T, Hansen D. The *C. elegans* sex-determination gene *fem-2* encodes a putative protein phosphatase. *Mol. Biol. Cell*. 1995;6:1159–1171. [[PMC free article: PMC301274](#)] [[PubMed: 8534913](#)]
1587. Plasterk R H A. Differences between Tc1 elements from the *C. elegans* strain Bergerac. *Nucleic Acids Res.* 1987;15:10050. [[PMC free article: PMC306555](#)] [[PubMed: 2827106](#)]
1588. Plasterk R H A. The origin of footprints of the Tc1 transposon of *Caenorhabditis elegans*. *EMBO J.* 1991;10:1919–1925. [[PMC free article: PMC452867](#)] [[PubMed: 1646714](#)]
1589. Plasterk R H A. Molecular mechanisms of transposition and its control. *Cell*. 1993;74:781–786. [[PubMed: 8397072](#)]
1590. Plasterk R H A, Groenen J T M. Targeted alterations of the *Caenorhabditis elegans* genome by transgene instructed DNA double strand break repair following Tc1 excision. *EMBO J.* 1992;11:287–290. [[PMC free article: PMC556449](#)] [[PubMed: 1740110](#)]
1591. Platt H M, Lorenzen S, editor. *The phylogenetic systematics of free-living nematodes*. London: The Ray Society; 1994. Foreword.
1592. Plenefisch J D, DeLong L, Meyer B J. Genes that implement the hermaphrodite mode of dosage compensation in *Caenorhabditis elegans*. *Genetics*. 1989;121:57–76. [[PMC free article: PMC1203606](#)] [[PubMed: 2917714](#)]
1593. Plunkett J A, Simmons R B, Walther W W. Dynamic interactions between nerve and muscle in *Caenorhabditis elegans*. *Dev. Biol.* 1996;175:154–165. [[PubMed: 8608862](#)]
1594. Pluta A F, Mackay A M, Ainsztein A M, Goldberg I G, Earnshaw W C. The centromere: Hub of chromosomal activities. *Science*. 1995;270:1591–1594. [[PubMed: 7502067](#)]
1595. Podbilewicz B, White J G. Cell fusions in the developing epithelia of *C. elegans*. *Dev. Biol.* 1994;161:408–424. [[PubMed: 8313992](#)]
1596. Poethig R S. Heterochronic mutations affecting shoot development in maize. *Genetics*. 1988a;119:959–973. [[PMC free article: PMC1203479](#)] [[PubMed: 17246439](#)]
1597. Poethig S. A non-cell-autonomous mutation regulating juvenility in maize. *Nature*. 1988b;336:82–83.
1598. Poinar G O. *The natural history of nematodes*. Englewood Cliffs, New Jersey: Prentice-Hall; 1983.
1599. Poinar G O. Taxonomy and biology of Steinernematidae and Heterorhabditidae. In: Gaugler R, Kaya H K, editors. *Entomopathogenic nematodes in biological control*. Boca Raton, Florida: CRC Press; 1990. pp. 23–61.
1600. Politz J C, Edgar R S. Overlapping stage-specific sets of numerous small collagenous polypeptides are translated in vitro from *Caenorhabditis elegans* RNA. *Cell*. 1984;37:853–860. [[PubMed: 6086147](#)]
1601. Politz S M, Philipp M. *Caenorhabditis elegans* as a model for parasitic nematodes: A focus on the cuticle. *Parasitol. Today*. 1992;8:6–12. [[PubMed: 15463517](#)]
1602. Politz S M, Chin K J, Herman D L. Genetic analysis of adult-specific surface antigenic differences between varieties of the nematode *Caenorhabditis elegans*. *Genetics*. 1987;117:467–476. [[PMC free article: PMC1203222](#)] [[PubMed: 3692138](#)]
1603. Politz S M, Politz J C, Edgar R S. Small collagenous proteins present during the molt in *Caenorhabditis elegans*. *J. Nematol.* 1986;18:303–310. [[PMC free article: PMC2618558](#)] [[PubMed: 19294182](#)]
1604. Politz S M, Phillip M, Estevez M, O'Brien P, Chin K J. Genes that can be mutated to unmask hidden antigenic determinants in the cuticle of the nematode *Caenorhabditis elegans*. *Proc. Natl. Acad. Sci.* 1990;87:2901–2905. [[PMC free article: PMC53801](#)] [[PubMed: 1691498](#)]
1605. Poodry C A, Edgar L. Reversible alteration in the neuromuscular junctions of *Drosophila melanogaster* bearing a temperature-sensitive mutation shibire. *J. Cell Biol.* 1979;81:520–527. [[PMC free article: PMC2110401](#)] [[PubMed: 110817](#)]

1606. Poole C B, Grandea A G, Maina C V, Jenkins R E, Selkirk M E, McReynolds L A. Cloning of a cuticular antigen which contains multiple tandem repeats from the filarial parasite *Dirofilaria immitis*. Proc. Natl. Acad. Sci. 1992;89:5986–5990. [[PMC free article: PMC402123](#)] [[PubMed: 1631084](#)]
1607. Popham J D, Webster J M. An alternative interpretation of the fine structure of the basal zone of the cuticle of the dauerlarva of the nematode *Caenorhabditis elegans* (Nematoda). Can. J. Zool. 1978;56:1556–1563. [[PubMed: 688112](#)]
1608. Popham J D, Webster J M. Aspects of the fine structure of the dauer larva of the nematode *Caenorhabditis elegans*. Can. J. Zool. 1979;57:794–800.
1609. Popperl H, Bieren M, Studer M, Chan S K, Aparicio S, Brenner S, Mann R S, Krumlauf R. Segmental expression of Hoxb-1 is controlled by a highly conserved autoregulatory loop dependent upon exd/pbx. Cell. 1995;81:1031–1042. [[PubMed: 7600572](#)]
1610. Posakony J W. Nature versus nurture: Asymmetric cell divisions in *Drosophila* bristle development. Cell. 1994;76:415–418. [[PubMed: 8313463](#)]
1611. Potter S S. DNA sequence of a foldback transposable element in *Drosophila*. Nature. 1982;297:201–204. [[PubMed: 6176872](#)]
1612. Potts F A. Notes on the free-living nematodes. Q. J. Microscop. Sci. 1910;55:433–484.
1613. Powell K A, Robinson P J. Dephosphin/dynamin is a neuronal phosphoprotein concentrated in nerve terminals: Evidence from rat cerebellum. Neuroscience. 1995;64:821–833. [[PubMed: 7715790](#)]
1614. Prasad S S, Baillie D L. Evolutionarily conserved coding sequences in the *dpy-20-unc-22* region of *Caenorhabditis elegans*. Genomics. 1989;5:185–198. [[PubMed: 2793177](#)]
1615. Prasad S S, Harris L J, Baillie D L, Rose A M. Evolutionary conserved regions in *Caenorhabditis* transposable elements deduced by sequence comparison. Genome. 1991;34:6–12. [[PubMed: 1851119](#)]
1616. Pressman B C. Biological applications of ionophores. Annu. Rev. Biochem. 1976;45:501–530. [[PubMed: 786156](#)]
1617. Price M G, Gomer R H. Skelemin a cytoskeletal M-disc periphery protein, contains motifs of adhesion/recognition and intermediate filament proteins. J. Biol. Chem. 1993;268:21800–21810. [[PubMed: 8408035](#)]
1618. Price M, Lazzaro D, Pohl T, Mattei M -G, Rüther U, Olivo J -C, Duboule D, Di Lauro R. Regional expression of the homeobox gene Nkx-2.2 in the developing mammalian forebrain. Neuron. 1992;8:241–255. [[PubMed: 1346742](#)]
1619. Prichard R. Anthelmintic resistance. Vet. Parasitol. 1994;54:259–268. [[PubMed: 7846855](#)]
1620. Priess J R, Hirsh D I. *Caenorhabditis elegans* morphogenesis: The role of the cytoskeleton in elongation of the embryo. Dev. Biol. 1986;117:156–173. [[PubMed: 3743895](#)]
1621. Priess J R, Thomson J N. Cellular interactions in early *C. elegans* embryos. Cell. 1987;48:241–250. [[PubMed: 3802194](#)]
1622. Priess J R, Schnabel H, Schnabel R. The *glp-1* locus and cellular interactions in early *C. elegans* embryos. Cell. 1987;51:601–611. [[PubMed: 3677169](#)]
1623. Probst W C, Cropper E C, Heierhorst J, Hooper S L, Jaffe H, Vilim F, Beushausen S, Kupfermann I, Weiss K R. AMP-dependent phosphorylation of Aplysia twitchin may mediate modulation of muscle contractions by neuropeptide cotransmitters. Proc. Natl. Acad. Sci. 1994;91:8487–8491. [[PMC free article: PMC44631](#)] [[PubMed: 8078908](#)]
1624. Prockop D J, Kivirikko K I. COLLAGENS: Molecular biology diseases, and potentials for therapy. Annu. Rev. Biochem. 1995;64:403–434. [[PubMed: 7574488](#)]
1625. Proudfoot L, Kusel J R, Smith H V, Kennedy M W, Kennedy M W, editor. Parasitic nematodes—Membranes, antigens and genes. London: Taylor and Francis; 1991. Biophysical properties of the nematode surface. pp. 1–26.
1626. Proudfoot L, Kusel J R, Smith H V, Kennedy M W. External stimuli and intracellular signalling in the modification of the nematode surface during transmission to the mammalian host environment. Parasitology. 1993a;107:559–566. [[PubMed: 7507586](#)]

1627. Proudfoot L J, Kusel J R, Smith H V, Harnett W, Worms M J, Kennedy M W. The surface lipid of parasitic nematodes: Organization, and modifications during transition to the mammalian host environment. *Acta Tropica*. 1990;47:323–330. [[PubMed: 1978532](#)]
1628. Proudfoot L J, Kusel J R, Smith H V, Harnett W, Worms M J, Kennedy M W. Rapid changes in the surface of parasitic nematodes during transition from pre- to post-parasitic forms. *Parasitology*. 1993b;107:107–117. [[PubMed: 8355993](#)]
1629. Provine W. The origins of theoretical population genetics. Chicago: University of Chicago Press; 1971.
1630. Pulak R, Anderson P. Structures of spontaneous deletions in *Caenorhabditis elegans*. *Mol. Cell. Biol.* 1988;8:3748–3754. [[PMC free article: PMC365432](#)] [[PubMed: 3221864](#)]
1631. Pulak R, Anderson P. mRNA surveillance by the *Caenorhabditis elegans* smg genes. *Genes Dev.* 1993;7:1885–1897. [[PubMed: 8104846](#)]
1632. Purcell E M. Life at low Reynolds number. *Am. J. Phys.* 1977;45:3–11.
1633. Putland R A, Thomas S M, Grove D I, Johnson A M. Analysis of the 18S ribosomal RNA gene of *Strongyloides stercoralis*. *Int. J. Parasitol.* 1993;23:149–151. [[PubMed: 8468132](#)]
1634. Putter I, MacConnell J G, Preiser F A, Haidri A A, Ristich S S, Dybas R A. Avermectins—Novel insecticides, acaricides and nematicides from a soil microorganism. *Experientia*. 1981;37:963–964.

## Q

1635. Qiao L, Lissemore J L, Shu P, Smardon A, Gelber M B, Maine E M. Enhancers of *glp-1*, a gene required for cell-signaling in *C. elegans*, define a set of genes required for germline development. *Genetics*. 1995;141:551–569. [[PMC free article: PMC1206755](#)] [[PubMed: 8647392](#)]
1636. Quiring R, Walldorf U, Kloster U, Gehring W. Homology of the *eyeless* gene of *Drosophila* to the *Small eye* gene in mice and *Aniridia* in humans. *Science*. 1994;265:785–789. [[PubMed: 7914031](#)]

## R

1637. Rabizadeh S, LaCount D J, Friesen P D, Bredesen D E. Expression of the baculovirus p35 gene inhibits mammalian [neural](#) cell death. *J. Neurochem.* 1993;61:2318–2321. [[PubMed: 8245984](#)]
1638. Radice A D, Emmons S W. Extrachromosomal circular copies of the transposon Tc1. *Nucleic Acids Res.* 1993;21:2663–2667. [[PMC free article: PMC309596](#)] [[PubMed: 8392704](#)]
1639. Radice A D, Bugaj B, Fitch D H A, Emmons S W. Widespread occurrence of the Tc1 transposon family: Tc1-like transposons from teleost fish. *Mol. Gen. Genet.* 1994;244:606–612. [[PubMed: 7969029](#)]
1640. Raff J, Allan V. Mitosis in motion. *Trends Cell Biol.* 1996;6:34–36. [[PubMed: 15157530](#)]
1641. Raff M C. Social controls on cell survival and cell death. *Nature*. 1992;356:397–400. [[PubMed: 1557121](#)]
1642. Raizen D M, Avery L. Electrical activity and behavior in the [pharynx](#) of *Caenorhabditis elegans*. *Neuron*. 1994;12:483–495. [[PMC free article: PMC4460247](#)] [[PubMed: 8155316](#)]
1643. Raizen D M, Lee R Y N, Avery L. Interacting genes required for pharyngeal excitation by motor neuron MC in *Caenorhabditis elegans*. *Genetics*. 1995;141:1365–1382. [[PMC free article: PMC1206873](#)] [[PubMed: 8601480](#)]
1644. Rajkovic A, Davis R E, Simonsen J N, Rottman F M. A spliced leader is present on a subset of mRNAs from the human parasite *Schistosoma mansoni*. *Proc. Natl. Acad. Sci.* 1990;87:8879–8883. [[PMC free article: PMC55063](#)] [[PubMed: 2247461](#)]
1645. Rand J B. Genetic analysis of the *cha-1*-*unc-17* gene complex in *Caenorhabditis*. *Genetics*. 1989;122:73–80. [[PMC free article: PMC1203695](#)] [[PubMed: 2731735](#)]
1646. Rand J B, Johnson C D. Genetic pharmacology: Interactions between drugs and gene products in *Caenorhabditis elegans*. In: Epstein H F, Shakes D C, editors. *Caenorhabditis elegans: Modern biological analysis of an organism*. New York: Academic Press; 1995. pp. 187–204. [[PubMed: 8531725](#)]
1647. Rand J B, Russell R L. Choline acetyltransferase-deficient mutants of the nematode *Caenorhabditis elegans*. *Genetics*. 1984;106:227–248. [[PMC free article: PMC1202253](#)] [[PubMed: 6698395](#)]

1648. Rand J B, Russell R L. Properties and partial purification of choline acetyltransferase from the nematode *Caenorhabditis elegans*. *J. Neurochem.* 1985a;44:189–200. [[PubMed: 3964827](#)]
1649. Rand J B, Russell R L. Molecular basis of drug-resistance mutations in *C. elegans*. *Psychopharmacol. Bull.* 1985b;21:623–630. [[PubMed: 4034879](#)]
1650. Rankin C H. Interactions between two antagonistic reflexes in the nematode *C. elegans*. *J. Comp. Physiol.* 1991;169:59–67. [[PubMed: 1941719](#)]
1651. Rankin C H, Broster B S. Factors affecting habituation and recovery from habituation in the nematode *C. elegans*. *Behav. Neurosci.* 1992;106:239–249. [[PubMed: 1590951](#)]
1652. Rankin C, Carew T J. The development of learning and memory in *Aplysia*: II. Habituation and dishabituation of the siphon withdrawal reflex. *J. Neurosci.* 1987;7:133–143. [[PMC free article: PMC6568864](#)] [[PubMed: 3806190](#)]
1653. Rankin C H, Chiba C, Beck C. *Caenorhabditis elegans*: A new model system for the study of learning and memory. *Behav. Brain Res.* 1990;37:89–92. [[PubMed: 2310497](#)]
1654. Rassoulzadegan M, Paquis-Flucklinger V, Bertino B, Sage J, Jaslin M, Miyagawa K, van Heyningen V, Besmer P, Cuzin F. Transmeiotic differentiation of male [germ cells](#) in culture. *Cell.* 1993;75:997–1006. [[PubMed: 7504588](#)]
1655. Rattray B, Rose A M. Increased intragenic recombination and nondisjunction in the Rec-1 strain of *Caenorhabditis elegans*. *Genet. Res.* 1988;51:89–93.
1656. Rauskolb C, Wieschaus E. Coordinate regulation of downstream genes by extradenticle and the homeotic selector proteins. *EMBO J.* 1994;13:3561–3569. [[PMC free article: PMC395260](#)] [[PubMed: 7914871](#)]
1657. Rauskolb C, Peifer M, Wieschaus E. Extradenticle, a regulator of homeotic gene activity, is a homolog of the homeobox-containing human proto-oncogene pbx1. *Cell.* 1993;74:1101–1112. [[PubMed: 8104703](#)]
1658. Ray C, McKerrow J H. Gut-specific and developmental expression of a *Caenorhabditis elegans* cysteine protease gene. *Mol. Biochem. Parasitol.* 1992;51:239–250. [[PubMed: 1574082](#)]
1659. Ray C, Abbott A G, Hussey R S. Trans-splicing of a *Meloidogyne incognita* mRNA encoding a putative esophageal gland protein. *Mol. Biochem. Parasitol.* 1994;68:93–101. [[PubMed: 7891751](#)]
1660. Ray C A, Black R A, Kronheim S R, Greenstreet T A, Sleath P R, Salvesen G S, Pickup D J. Viral inhibition of inflammation: Cowpox virus encodes an inhibitor of the interleukin-1 $\beta$  converting enzyme. *Cell.* 1992;69:597–604. [[PubMed: 1339309](#)]
1661. Rayment I, Holden H M. The three-dimensional structure of a molecular motor. *Trends Biochem. Sci.* 1994;19:129–134. [[PubMed: 8203020](#)]
1662. Rayment I, Holden H M, Whittaker M, Yohn C B, Lorenz M, Holmes K C, Milligan R A. Structure of the actin-myosin complex and its implications for muscle contraction. *Science.* 1993a;261:58–65. [[PubMed: 8316858](#)]
1663. Rayment I, Rypiewski W R, Schmidt-Base K, Smith R, Tomchick D R, Benning M M, Winkelmann D A, Wesenberg G, Holden H M. Three-dimensional structure of myosin subfragment-1: A molecular motor. *Science.* 1993b;261:50–58. [[PubMed: 8316857](#)]
1664. Reape T J, Burnell A M. Dauer larva recovery in *Caenorhabditis elegans*. I. The effect of mRNA synthesis inhibitors on recovery growth and pharyngeal pumping. *Comp. Biochem. Physiol.* 1991a;98B:239–243.
1665. Reape T J, Burnell A M. Dauer larva recovery in the nematode *Caenorhabditis elegans*. II. The effect of inhibitors of protein synthesis on recovery, growth and pharyngeal pumping. *Comp. Biochem. Physiol.* 1991b;98B:245–252.
1666. Reape T J, Burnell A M. Dauer larva recovery in the nematode *Caenorhabditis elegans*. III. The effect of inhibitors of protein and mRNA synthesis on the activity of the enzymes of intermediary. *Comp. Biochem. Physiol.* 1992;102B:241–245.
1667. Rebay I, Rubin G M. Yan functions as a general inhibitor of differentiation and is negatively regulated by activation of the Ras1/MAPK pathway. *Cell.* 1995;81:857–866. [[PubMed: 7781063](#)]

1668. Reed J C. Bcl-2 and the regulation of programmed cell death. *J. Cell Biol.* 1994;124:1–6. [[PMC free article: PMC2119888](#)] [[PubMed: 8294493](#)]
1669. Reed J C, Cuddy M, Haldar S, Croce C, Nowell P, Makover D, Bradley K. *BCL2*-mediated tumorigenicity of a human T-lymphoid cell line: Synergy with *MYC* and inhibition by *BCL2* antisense. *Proc. Natl. Acad. Sci.* 1990;87:3660–3664. [[PMC free article: PMC53962](#)] [[PubMed: 1692620](#)]
1670. Reichman-Fried M, Dickson B, Hafen E, Shilo B Z. Elucidation of the role of breathless, a *Drosophila* FGF receptor homolog, in tracheal cell migration. *Genes Dev.* 1994;8:428–439. [[PubMed: 8125257](#)]
1671. Reiner D J, Thomas J H. Reversal of a muscle response to GABA during *C. elegans* male development. *J. Neurosci.* 1995;15:6094–6102. [[PMC free article: PMC6577681](#)] [[PubMed: 7666193](#)]
1672. Reiner D J, Weinshenker D, Thomas J H. Analysis of dominant mutations affecting muscle excitation in *C. elegans*. *Genetics.* 1995;141:961–976. [[PMC free article: PMC1206858](#)] [[PubMed: 8582640](#)]
1673. Ren P, Lim C, Johnsen R, Albert P S, Pilgrim D, Riddle D L. Control of *C. elegans* larval development by neuronal expression of a TGF- $\beta$  homolog. *Science.* 1996;274:1389–1392. [[PubMed: 8910282](#)]
1674. Renard S, Lingueglia E, Voilley N, Lazdunski M, Barbry P. Biochemical analysis of the membrane topology of the amiloride-sensitive Na<sup>+</sup> channel. *J. Biol. Chem.* 1994;269:12981–12986. [[PubMed: 8175716](#)]
1675. Rettig J, Heinemann S H, Wunder F, Lorra C, Parcej D N, Dolly J O, Pongs O. Inactivation properties of voltage-gated K<sup>+</sup> channels altered by the presence of  $\beta$ -subunit. *Nature.* 1994;369:289–294. [[PubMed: 8183366](#)]
1676. Reynolds B A, Weiss S. Generation of neurons and astrocytes from isolated cells of the adult mammalian central [nervous system](#). *Science.* 1992;255:1707–1710. [[PubMed: 1553558](#)]
1677. Rhind N R, Miller L M, Kopczynski J B, Meyer B J. *xol-1* acts as an early switch in the *C. elegans* male/hemaphrodite decision. *Cell.* 1995;80:71–82. [[PubMed: 7813020](#)]
1678. Rhyu M S, Jan L Y, Yan Y N. Asymmetric distribution of *numb* protein during division of the sensory organ precursor cell confers distinct fates to daughter cells. *Cell.* 1994;76:477–491. [[PubMed: 8313469](#)]
1679. Riddihough G, Ish-Horowicz D. Individual stripe regulatory elements in the *Drosophila* hairy promoter respond to maternal, gap, and pair-rule genes. *Genes Dev.* 1991;5:840–854. [[PubMed: 1902805](#)]
1680. Riddle D L. A genetic pathway for dauer larva formation in *Caenorhabditis elegans*. *Stadler Genet. Symp.* 1977;9:101–120.
1681. Riddle D L, Wood W B, editor. The nematode *Caenorhabditis elegans*. Cold Spring Harbor, New York: Cold Spring Harbor Laboratory; 1988. The dauer larva. pp. 393–412.
1682. Riddle D L, Bird D M. Molecular cloning and sequencing of *ama-1*, the gene encoding the largest subunit of *Caenorhabditis elegans* RNA polymerase II. *Mol. Cell. Biol.* 1989;9:4119–4130. [[PMC free article: PMC362490](#)] [[PubMed: 2586513](#)]
1683. Riddle D L, Brenner S. Indirect suppression in *C. elegans*. *Genetics.* 1978;89:299–314. [[PMC free article: PMC1213839](#)] [[PubMed: 669254](#)]
1684. Riddle D L, Swanson M M, Albert P S. Interacting genes in nematode dauer larva formation. *Nature.* 1981;290:668–671. [[PubMed: 7219552](#)]
1685. Ridley A J, Hall A. The small GTP-binding protein rho regulates the assembly of focal adhesions and actin stress fibers in response to growth factors. *Cell.* 1992;70:389–399. [[PubMed: 1643657](#)]
1686. Ridley A J, Paterson H F, Johnston C L, Diekmann D, Hall A. The small GTP-binding protein rac regulates growth factor-induced membrane ruffling. *Cell.* 1992;70:401–410. [[PubMed: 1643658](#)]
1687. Ristoratore F, Cermola M, Nola M, Bazzicalupo P, Favre R. Ultrastructural immunolocalization of CUT-1 and CUT-2 antigenic sites in the cuticles of the nematode *Caenorhabditis elegans*. *J. Submicrosc. Cytol. Pathol.* 1994;26:437–443. [[PubMed: 8087805](#)]
1688. Roberts A B, Sporn M B, Sporn M B, Roberts A B, editors. *Handbook of experimental pharmacology 95/I Peptide growth factors and their receptors I*. Berlin: Springer-Verlag; 1990. The transforming growth factor- $\beta$ s.

1689. Roberts S B, Emmons S W, Childs G. Nucleotide sequences of *Caenorhabditis elegans* core histone genes: Genes for different histone classes share common flanking sequence elements. *J. Mol. Biol.* 1989;206:567–577. [[PubMed: 2544730](#)]
1690. Roberts S B, Sanicola M, Emmons S W, Childs G. Molecular characterization of the histone gene family of *Caenorhabditis elegans*. *J. Mol. Biol.* 1987;196:27–38. [[PubMed: 3656446](#)]
1691. Roberts T M. Crawling *Caenorhabditis elegans* spermatozoa contact the substrate only by their pseudopods and contain 2-nm filaments. *Cell Motil.* 1983;3:333–347.
1692. Roberts T M, King K L. Centripetal flow and directed reassembly of the major sperm protein (MSP) cytoskeleton in the amoeboid sperm of the nematode *Ascaris suum*. *Cell Motil. Cytoskel.* 1991;20:228–241. [[PubMed: 1773449](#)]
1693. Roberts T M, Stewart M. Nematode sperm locomotion. *Curr. Opin. Cell Biol.* 1995;7:13–17. [[PubMed: 7755984](#)]
1694. Roberts T M, Streitmatter G. Membrane-substrate contact under the spermatozoon of *Caenorhabditis elegans*, a crawling cell that lacks filamentous actin. *J. Cell Sci.* 1984;69:117–126. [[PubMed: 6490743](#)]
1695. Roberts T M, Ward S. Membrane flow during nematode spermiogenesis. *J. Cell Biol.* 1982a;92:113–120. [[PMC free article: PMC2112007](#)] [[PubMed: 7056795](#)]
1696. Roberts T M, Ward S. Centripetal flow of pseudopodial surface components could propel the amoeboid movement of *Caenorhabditis elegans* spermatozoa. *J. Cell Biol.* 1982b;92:132–138. [[PMC free article: PMC2112009](#)] [[PubMed: 7056796](#)]
1697. Roberts T M, Pavalko F M, Ward S. Membrane and cytoplasmic proteins are transported in the same organelle complex during nematode spermatogenesis. *J. Cell Biol.* 1986;102:1787–1796. [[PMC free article: PMC2114225](#)] [[PubMed: 3517007](#)]
1698. Roberts T M, Sepsenwol S, Ris H. Sperm motility in nematodes: Crawling movement without actin. In: Shatten H, Schatten G, editors. *The cell biology of fertilization*. Orlando: Academic Press; 1989. pp. 41–60.
1699. Robertson A, Thomson N. Morphology of programmed cell death in the [ventral nerve cord](#) of *Caenorhabditis elegans* larvae. *J. Embryol. Exp. Morphol.* 1982;67:89–100.
1700. Robertson H M. The mariner transposable element is widespread in insects. *Nature*. 1993;362:241–245. [[PubMed: 8384700](#)]
1701. Robertson H M. The Tc1/mariner superfamily of transposons in animals. *J. Insect Physiol.* 1995;41:99–105.
1702. Robertson H M, Lampe D J, Macleod E G. A mariner transposable element from a lacewing. *Nucleic Acids Res.* 1992;20:6409. [[PMC free article: PMC334534](#)] [[PubMed: 1335572](#)]
1703. Roditi I. *Trypanosoma vivax*: Linkage of the mini-exon (spliced leader) and 5S ribosomal RNA genes. *Nucleic Acids Res.* 1992;20:1995. [[PMC free article: PMC312321](#)] [[PubMed: 1579506](#)]
1704. Rogaev E I, Sherrington R, Rogaeva E A, Levesque G, Ikeda M, Liang Y, Chi H, Lin C, Holman K, Tsuda T, Mar L, Sorbi S, Nacmias B, Piacentini S, Amaducci L, Chumakov I, Cohen D, Lannfelt L, Fraser P E, Rommens J M, St. George-Hyslop P H. Familial Alzheimer's disease in kindreds with missense mutations in a gene on chromosome 1 related to the Alzheimer's disease type 3 gene. *Nature*. 1995;376:775–778. [[PubMed: 7651536](#)]
1705. Rogalski T M, Baillie D L. Genetic organization of the *unc-22* gene and the adjacent region in *Caenorhabditis elegans*. *Mol. Gen. Genet.* 1985;201:409–414. [[PubMed: 3866907](#)]
1706. Rogalski T M, Riddle D L. A *C. elegans* RNA polymerase II gene *ama-1 IV*, and nearby essential genes. *Genetics*. 1988;118:61–74. [[PMC free article: PMC1203267](#)] [[PubMed: 8608933](#)]
1707. Rogalski T M, Bullerjahn A M, Riddle D L. Lethal and amanitin-resistance mutations in the *Caenorhabditis elegans* *ama-1* and *ama-2* genes. *Genetics*. 1988;120:409–422. [[PMC free article: PMC1203520](#)] [[PubMed: 3197954](#)]
1708. Rogalski T M, Golomb M, Riddle D L. Mutant *Caenorhabditis elegans* RNA polymerase II with a 20,000-fold reduced sensitivity to  $\alpha$ -amanitin. *Genetics*. 1990;126:889–898. [[PMC free article: PMC1204286](#)] [[PubMed: 2076819](#)]

1709. Rogalski T M, Moerman D G, Baillie D L. Essential genes and deficiencies in the *unc-22*(IV) region of *C. elegans*. *Genetics*. 1982;102:725–736. [[PMC free article: PMC1201969](#)] [[PubMed: 7187364](#)]
1710. Rogalski T M, Gilchrist E J, Mullen G P, Moerman D G. Mutations in the *unc-52* gene responsible for body wall muscle defects in adult *Caenorhabditis elegans* are located in alternatively spliced exons. *Genetics*. 1995;139:159–169. [[PMC free article: PMC1206315](#)] [[PubMed: 7535716](#)]
1711. Rogalski T M, Williams B D, Mullen G P, Moerman D G. Products of the *unc-52* gene in *Caenorhabditis elegans* are homologous to the core protein of the mammalian basement membrane heparan sulfate proteoglycan. *Genes Dev.* 1993;7:1471–1484. [[PubMed: 8393416](#)]
1712. Rogers W P. The nature of parasitism. The relationship of some metazoan parasites to their hosts. New York: Academic Press; 1962.
1713. Rohrer S P. Ivermectin binding sites in sensitive and resistant *Haemonchus contortus*. *J. Parasitol.* 1994;80:493–497. [[PubMed: 8195956](#)]
1714. Rohrer S P, Schaeffer J M, Boothroyd J C, Komuniecki R, editors. Molecular approaches to parasitology. New York: Wiley-Liss; 1995. Ivermectin. pp. 191–205.
1715. Roos M H, Kwa M S G, Grant W N. New genetic and practical implications of selection for anthelmintic resistance in parasitic nematodes. *Parasitol. Today.* 1995;11:148–150.
1716. Roos M H, Boersma J H, Borgsteede F H M, Cornelissen J, Taylor M, Ruitenberg E J. Molecular analysis of selection for benzimidazole resistance in the sheep parasite *Haemonchus contortus*. *Mol. Biochem. Parasitol.* 1990;43:77–88. [[PubMed: 1981249](#)]
1717. Rosahl T W, Spillane D, Missler M, Herz J, Selig D K, Wolff J, Hammer R E, Malenka R C, Südhof T C. Essential functions of synapsin I and II in synaptic vesicle regulation. *Nature*. 1995;375:488–493. [[PubMed: 7777057](#)]
1718. Roscigno R F, Weiner M, Garcia-Blanco M A. A mutational analysis of the polypyrimidine tract of introns: Effects of sequence differences in pyrimidine tracts on splicing. *J. Biol. Chem.* 1993;268:11222–11229. [[PubMed: 8496178](#)]
1719. Rose A M, Baillie D L. Effect of temperature and parental age on recombination and nondisjunction in *Caenorhabditis elegans*. *Genetics*. 1979a;92:409–418. [[PMC free article: PMC1213967](#)] [[PubMed: 17248928](#)]
1720. Rose A M, Baillie D L. A mutation in *Caenorhabditis elegans* that increases recombination frequency more than three-fold. *Nature*. 1979b;281:599–600. [[PubMed: 492325](#)]
1721. Rose A M, Baillie D L. Genetic organization of the region around *unc-15*(I), a gene affecting paramyosin in *C. elegans*. *Genetics*. 1980;96:639–648. [[PMC free article: PMC1214366](#)] [[PubMed: 7262541](#)]
1722. Rose A M, Snutch T P. Isolation of the closed circular form of the transposable element Tc1 in *Caenorhabditis elegans*. *Nature*. 1984;311:485–486. [[PubMed: 6090946](#)]
1723. Rose A M, Baillie D L, Curran J. Meiotic pairing behavior of two free duplications of linkage group I in *Caenorhabditis elegans*. *Mol. Gen. Genet.* 1984;195:52–56. [[PubMed: 6593563](#)]
1724. Rose A M, Edgley M E, Baillie D L. Genetic analysis in *Caenorhabditis elegans*. In: Lamberti F, et al., editors. Advances in molecular plant nematology. New York: Plenum Press; 1994. pp. 19–33.
1725. Rose A M, Harris L J, Mawji N R, Morris W J. Tc1(Hin): A form of the transposable element Tc1 in *Caenorhabditis elegans*. *Can. J. Biochem. Cell Biol.* 1985;63:752–756. [[PubMed: 2994862](#)]
1726. Rose L S, Lamb M L, Hird S N, Kemphues K J. Pseudocleavage is dispensable for polarity and development in *C. elegans* embryos. *Dev. Biol.* 1995;168:479–489. [[PubMed: 7729583](#)]
1727. Rosenbluth J. Structural organization of obliquely striated muscle fibers in *Ascaris lumbricoides*. *J. Cell Biol.* 1965;25:495–515. [[PMC free article: PMC2106669](#)] [[PubMed: 5839255](#)]
1728. Rosenbluth R E, Baillie D L. Analysis of a reciprocal translocation *eT1*(III;-->V), in *Caenorhabditis elegans*. *Genetics*. 1981;99:415–428. [[PMC free article: PMC1214511](#)] [[PubMed: 6953041](#)]
1729. Rosenbluth R E, Cuddeford C, Baillie D L. Mutagenesis in *Caenorhabditis elegans*. I. A rapid eukaryotic mutagen test system using the reciprocal translocation, *eT1*(III;-->V). *Mutat. Res.* 1983;110:39–48.
1730. Rosenbluth R E, Cuddeford C, Baillie D L. Mutagenesis in *Caenorhabditis elegans*. II. A spectrum of mutational events induced with 1500 R of gamma-radiation. *Genetics*. 1985;109:493–511. [[PMC free](#)

[article: PMC1216284](#) [PubMed: 3979812]

1731. Rosenbluth R E, Johnsen R C, Baillie D L. Pairing for recombination in LGV of *Caenorhabditis elegans*: A model based on recombination in deficiency heterozygotes. *Genetics*. 1990;124:615–625. [[PMC free article: PMC1203955](#)] [[PubMed: 2311918](#)]
1732. Rosenbluth R E, Rogalski T M, Johnsen R C, Addison L M, Baillie D L. Genomic organization in *Caenorhabditis elegans*: Deficiency mapping on Linkage Group V(left). *Genetic Res.* 1988;52:105–118.
1733. Rosenquist T A, Kimble J. Molecular cloning and transcript analysis of *fem-3* a sex-determination gene in *Caenorhabditis elegans*. *Genes Dev.* 1988;2:606–616. [[PubMed: 3384333](#)]
1734. Rosenzweig B, Liao L W, Hirsh D. Sequence of the *C. elegans* transposable element Tc1. *Nucleic Acids Res.* 1983a;11:4201–4209. [[PMC free article: PMC326035](#)] [[PubMed: 6306578](#)]
1735. Rosenzweig B, Liao L W, Hirsh D. Target sequences for the *C. elegans* transposable element Tc1. *Nucleic Acids Res.* 1983b;11:7137–7140. [[PMC free article: PMC326443](#)] [[PubMed: 6314277](#)]
1736. Rosoff M L, Burglin T R, Li C. Alternatively spliced transcripts of the *flp-1* gene encode distinct FMRFamide-like peptides in *Caenorhabditis elegans*. *J. Neurosci.* 1992;12:2356–2361. [[PMC free article: PMC6575938](#)] [[PubMed: 1607945](#)]
1737. Ross L H, Freedman J H, Rubin C S. Structure and expression of novel spliced leader RNA genes in *Caenorhabditis elegans*. *J. Biol. Chem.* 1995;270:22066–22075. [[PubMed: 7665629](#)]
1738. Roth S, Neuman-Silberberg F S, Barcelo G, Schupbach T. *cornichon* and the EGF receptor signaling process are necessary for both anterior-posterior and dorsal-ventral pattern formation in *Drosophila*. *Cell.* 1995;81:967–978. [[PubMed: 7540118](#)]
1739. Rotin D, Bar-Sagi D, O'Brodovich H, Merilainen J, Lehto V P, Canessa C M, Rossier B C, Downey G P. An SH3 binding region in the epithelial Na<sup>+</sup> channel ( $\alpha$ rENaC) mediates its localization at the apical membrane. *EMBO J.* 1994;13:4440–4450. [[PMC free article: PMC395375](#)] [[PubMed: 7925286](#)]
1740. Rotonda J, Nicholson D W, Fazil K M, Gallant M, Gareau Y, Labelle M, Peterson E P, Raspar D M, Ruel R, Vaillancourt J P, Thornberry N A, Becker J W. The three-dimensional structure of apopain/CPP32, a key mediator of apoptosis. *Nat. Struct. Biol.* 1996;3:619–625. [[PubMed: 8673606](#)]
1741. Rougvie A E, Ambros V. The heterochronic gene *lin-29* encodes a zinc finger protein that controls a terminal differentiation event in *Caenorhabditis elegans*. *Development*. 1995;121:2491–2500. [[PubMed: 7671813](#)]
1742. Roussell D L, Bennett K L. *Caenorhabditis* cDNA encodes an eIF-4A-like protein. *Nucleic Acids Res.* 1992;20:3783. [[PMC free article: PMC334035](#)] [[PubMed: 1641346](#)]
1743. Roussell D L, Bennett K L. *glh-1* a germ-line putative RNA helicase from *Caenorhabditis* has four zinc fingers. *Proc. Natl. Acad. Sci.* 1993;90:9300–9304. [[PMC free article: PMC47555](#)] [[PubMed: 8415696](#)]
1744. Royal D, Royal M, Italiano J, Roberts T, Soll D R. In *Ascaris* sperm pseudopods, MSP fibers move proximally at a constant rate regardless of the forward rate of cellular translocation. *Cell Motil. Cytoskel.* 1995;31:241–253. [[PubMed: 7585993](#)]
1745. Ruan K, Emmons S W. Extrachromosomal copies of transposon Tc1 in the nematode *Caenorhabditis elegans*. *Proc. Natl. Acad. Sci.* 1984;81:4018–4022. [[PMC free article: PMC345359](#)] [[PubMed: 6330730](#)]
1746. Ruan K, Emmons S W. Precise and imprecise somatic excision of the transposon Tc1 in the nematode *C. elegans*. *Nucleic Acids Res.* 1987;15:6875–6881. [[PMC free article: PMC306181](#)] [[PubMed: 2821484](#)]
1747. Ruddle F H, Bentley K L, Murtha M T, Risch N. Gene loss and gain in the evolution of the vertebrates. *Suppl.*, pp. *Development*. 1994;155–161. [[PubMed: 7579516](#)]
1748. Rudnicki M A, Schnegelsberg P N, Stead R H, Braun T, Arnold H H, Jaenisch R. MyoD or Myf5 is required for the formation of skeletal muscle. *Cell*. 1993;75:1351–1359. [[PubMed: 8269513](#)]
1749. Run J -Q, Steven R, Hung M -S, van Weeghel R, Culotti J G, Way J C. Suppressors of the *unc-73* gene of *Caenorhabditis elegans*. *Genetics*. 1996;143:225–236. [[PMC free article: PMC1207256](#)] [[PubMed: 8722777](#)]
1750. Ruppel K M, Spudich J A. Myosin motor function: Structural and mutagenic approaches. *Curr. Opin. Cell Biol.* 1995;7:89–93. [[PubMed: 7755994](#)]

1751. Ruppel K M, Lorenz M, Spudich J A. Myosin structure/function: A combined mutagenesis-crystallography approach. *Curr. Opin. Struct. Biol.* 1995;5:181–186. [[PubMed: 7648319](#)]
1752. Rushforth A M, Anderson P. Splicing removes the *Caenorhabditis elegans* transposon Tc1 from most mutant pre-mRNAs. *Mol. Cell Biol.* 1996;16:422–429. [[PMC free article: PMC231018](#)] [[PubMed: 8524324](#)]
1753. Rushforth A M, Saari B, Anderson P. Site-selected insertion of the transposon Tc1 into a *Caenorhabditis elegans* myosin light chain gene. *Mol. Cell. Biol.* 1993;13:902–910. [[PMC free article: PMC358973](#)] [[PubMed: 8380898](#)]
1754. Rushlow C A, Hogan A, Pinchin S M, Howe K M, Lardelli M, Ish-Horowicz D. The *Drosophila hairy* protein acts in both segmentation and bristle patterning and shows homology to N-myc. *EMBO J.* 1989;8:3095–3103. [[PMC free article: PMC401388](#)] [[PubMed: 2479541](#)]
1755. Russell C B, Fraga D, Hinrichsen R D. Extremely short 20–33 nucleotide introns are the standard length in *Paramecium tetraurelia*. *Nucleic Acids Res.* 1994;22:1221–1225. [[PMC free article: PMC523646](#)] [[PubMed: 8165136](#)]
1756. Russell G J, Lacey E. Temperature dependent binding of mebendazole to tubulin in benzimidazole-susceptible and -resistant strains of *Trichostrongylus colubriformis* and *Caenorhabditis elegans*. *Int. J. Parasitol.* 1991;21:927–934. [[PubMed: 1787034](#)]
1757. Russell R L. Evidence for and against the theory of developmentally programmed aging. In: Warner H R, et al., editors. *Modern biological theories of aging* vol. , New York: Raven Press; 1987. pp. 35–61.
1758. Russnak R L, Jones D, Candido E P M. Locus encoding a family of small heat shock genes in *Caenorhabditis elegans*: Two genes duplicated to form a 3.8-kilobase inverted repeat. *Mol. Cell. Biol.* 1985;5:1268–1278. [[PMC free article: PMC366854](#)] [[PubMed: 4033652](#)]
1759. Ruvkun G, Giusto J. The *Caenorhabditis elegans* heterochronic gene *lin-14* encodes a nuclear protein that forms a temporal developmental switch. *Nature.* 1989;338:313–319. [[PubMed: 2922060](#)]
1760. Ruvkun G, Ambros V, Coulson A, Waterston R, Sulston J, Horvitz H. Molecular genetics of the *Caenorhabditis elegans* heterochronic gene *lin-14*. *Genetics.* 1989;121:501–516. [[PMC free article: PMC1203636](#)] [[PubMed: 2565854](#)]
1761. Ruvolo V, Hill J E, Levitt A. The Tc2 transposon of *Caenorhabditis elegans* has the structure of a self-regulated element. *DNA Cell Biol.* 1992;11:111–122. [[PubMed: 1312336](#)]
1762. Rzhetsky A, Nei M. A simple method for estimating and testing minimum-evolution trees. *Mol. Biol. Evol.* 1992;9:945–967.

## S

1763. Sachs A B. Messenger RNA degradation in eucaryotes. *Cell.* 1993;74:413–421. [[PubMed: 7688664](#)]
1764. Sackin H. Mechanosensitive channels. *Annu. Rev. Physiol.* 1995;57:333–353. [[PubMed: 7539988](#)]
1765. Saitou N, Nei M. The neighbor-joining method: A new method for reconstructing phylogenetic trees. *Mol. Biol. Evol.* 1987;4:406–425. [[PubMed: 3447015](#)]
1766. Saka Y, Sutani T, Yamashita Y, Saitoh S, Takeuchi M, Nakaseko Y, Yanagida M. Fission yeast cut3 and cut14, members of the ubiquitous protein family, are required for chromosome condensation and segregation in mitosis. *EMBO J.* 1994;13:4938–4952. [[PMC free article: PMC395434](#)] [[PubMed: 7957061](#)]
1767. Sakai T, Koga M, Ohshima Y. Genomic structure and 5' regulatory regions of the *let-23* gene in the nematode *C. elegans*. *J. Mol. Biol.* 1996;256:548–555. [[PubMed: 8604137](#)]
1768. Salminen A, Novick P J. A *ras*-like protein is required for a post-Golgi event in yeast secretion. *Cell.* 1987;49:527–538. [[PubMed: 3552249](#)]
1769. Salser S J, Kenyon C. Activation of a *C. elegans* *Antennapedia* homologue in migrating cells controls their direction of migration. *Nature.* 1992;355:255–258. [[PubMed: 1346230](#)]
1770. Salser S J, Kenyon C. Patterning *C. elegans*: Homeotic cluster genes, cell fates and cell migrations. *Trends Genet.* 1994;10:159–164. [[PubMed: 7913563](#)]

1771. Salser S J, Kenyon C. A *C. elegans* Hox gene switches ON, OFF, ON, and OFF again to regulate proliferation, differentiation, and morphogenesis. *Development*. 1996;122:1651–1661. [[PubMed: 8625851](#)]
1772. Salser S J, Loer C M, Kenyon C. Multiple HOM-C gene interactions specify cell fates in the nematode central [nervous system](#). *Genes Dev.* 1993;7:1714–1724. [[PubMed: 8103754](#)]
1773. Salvato M, Sulston J, Albertson D, Brenner S. A novel calmodulin-like gene from the nematode *Caenorhabditis elegans*. *J. Mol. Biol.* 1986;190:281–290. [[PubMed: 3783700](#)]
1774. Salvini-Plawen L, Mayr E. On the evolution of photoreceptors and eyes. *Evol. Biol.* 1977;10:207–263.
1775. Sandmeyer S B, Hansen L J, Chalker D L. Integration specificity of retrotransposons and retroviruses. *Annu. Rev. Genet.* 1990;24:491–518. [[PubMed: 1965102](#)]
1776. Sanford T, Golomb M, Riddle D L. RNA polymerase II from wild type and  $\alpha$ -amanitin-resistant strains of *C. elegans*. *J. Biol. Chem.* 1983;258:12804–12809. [[PubMed: 6630208](#)]
1777. Sanford T, Prenger J P, Golomb M. Purification and immunological analysis of RNA polymerase II from *C. elegans*. *J. Biol. Chem.* 1985;260:8064–8069. [[PubMed: 3891751](#)]
1778. Sanicola M, Ward S, Childs G, Emmons S W. Identification of a *Caenorhabditis elegans* histone H1 gene family: Characterization of a family member containing an intron and encoding a poly(A)+ mRNA. *J. Mol. Biol.* 1990;212:259–268. [[PubMed: 1969492](#)]
1779. Sano T, Tabuse Y, Nishiwaki K, Miwa J. The *tpa-1* gene of *Caenorhabditis elegans* encodes two proteins similar to  $\text{Ca}^{2+}$ -independent protein kinase CS: Evidence by complete genomic and complementary DNA sequences of the *tpa-1* gene. *J. Mol. Biol.* 1995;251:477–485. [[PubMed: 7658466](#)]
1780. Sasser J N, Freckman D W, Veech J A, Dickson D W, editors. *Vistas on nematology*. Hyattsville, Maryland: Society of Nematologists; 1987. A world perspective on nematology: The role of the society. pp. 7–14.
1781. Sasser J N, Kirkpatrick T L, Dybas R A. Efficacy of avermectins for root-knot control in tobacco. *Plant Dis.* 1982;66:691–693.
1782. Savage C, Hamelin M, Culotti J G, Coulson A, Albertson D G, Chalfie M. *mec-7* is a  $\beta$ -tubulin gene required for the production of 15-protofilament microtubules in *Caenorhabditis elegans*. *Genes Dev.* 1989;3:870–881. [[PubMed: 2744465](#)]
1783. Savage C, Xue Y Z, Mitani S, Hall D, Zakhary R, Chalfie M. Mutations in the *Caenorhabditis elegans* B-tubulin gene *mec-7*: Effects on microtubule assembly and stability and on tubulin autoregulation. *J. Cell Sci.* 1994;107:2165–2175. [[PubMed: 7983175](#)]
1784. Savage C Y, Das P, Finelli A L, Townsend S R, Sun C, Baird S E, Padgett R W. *Caenorhabditis elegans* genes *sma-2*, *sma-3*, and *sma-4* define a conserved family of transforming growth factor- $\beta$  pathway components. *Proc. Natl. Acad. Sci.* 1996;93:790–794. [[PMC free article: PMC40134](#)] [[PubMed: 8570636](#)]
1785. Savill J, Fadok V, Henson P, Haslett C. Phagocyte recognition of cells undergoing apoptosis. *Immunol. Today*. 1993;14:131–136. [[PubMed: 8385467](#)]
1786. Sawa H, Lobel L, Horvitz H R. The *Caenorhabditis elegans* gene *lin-17*, which is required for certain asymmetric cell divisions, encodes a putative seven-transmembrane protein similar to the *Drosophila* Frizzled protein. *Genes Dev.* 1996;10:2189–2197. [[PubMed: 8804313](#)]
1787. Sawchenko P E, Plotsky P M, Pfeiffer S W, Cunningham E T Jr., Vaughan J, Rivier J, Vale W. Inhibin  $\beta$  in central neural pathways involved in the control of oxytocin secretion. *Nature*. 1988;344:615–617. [[PubMed: 2457171](#)]
1788. Sawin K E, Mitchison T J. Mitotic spindle assembly by two different pathways in vitro. *J. Cell Biol.* 1991;112:925–940. [[PMC free article: PMC2288871](#)] [[PubMed: 1999463](#)]
1789. Schachat F, Garcea R L, Epstein H F. Myosins exist as homodimers of heavy chains: Demonstration with specific antibody purified by nematode mutant myosin affinity chromatography. *Cell*. 1978;15:405–411. [[PubMed: 82486](#)]

1790. Schachat F, Harris H E, Epstein H F. Two homogeneous myosins in *body wall muscle* of *Caenorhabditis elegans*. *Cell*. 1977;10:721–728. [[PubMed: 862026](#)]
1791. Schackwitz W S, Inoue T, Thomas J H. Chemosensory neurons function in parallel to mediate a pheromone response in *C. elegans*. *Neuron*. 1996;17:719–728. [[PubMed: 8893028](#)]
1792. Schafer W R, Kenyon C J. A calcium-channel homologue required for adaptation to dopamine and serotonin in *Caenorhabditis elegans*. *Nature*. 1995;375:73–78. [[PubMed: 7723846](#)]
1793. Schafer W R, Sanchez B M, Kenyon C J. Genes affecting sensitivity to serotonin in *Caenorhabditis elegans*. *Genetics*. 1996;143:1219–1230. [[PMC free article: PMC1207392](#)] [[PubMed: 8807295](#)]
1794. Schaller D, Wittmann C, Spicher A, Muller F, Tobler H. Cloning and analysis of three new homeobox genes from the nematode *Caenorhabditis elegans*. *Nucleic Acids Res*. 1990;18:2033–2036. [[PMC free article: PMC330679](#)] [[PubMed: 1970877](#)]
1795. Schaller D, Wittmann C, Lanning R, Spicher A, Müller F, Tobler H. Cloning and expression in vitro of a gene encoding tRNA<sup>Arg</sup><sub>ACG</sub> from the nematode *Caenorhabditis elegans*. *Gene*. 1991;97:273–276. [[PubMed: 1999292](#)]
1796. Schauer I E, Wood W B. Early *C. elegans* embryos are transcriptionally active. *Development*. 1990;110:1303–1317. [[PubMed: 2100265](#)]
1797. Schedin P, Hunter C P, Wood W B. Autonomy and nonautonomy of sex determination in triploid intersex mosaics of *C. elegans*. *Development*. 1991;112:833–879. [[PubMed: 1935692](#)]
1798. Schedin P, Jonas P, Wood W B. Function of the *her-1* gene is required for maintenance of male differentiation in adult tissues of *Caenorhabditis elegans*. *Dev. Genet.* 1994;15:231–239. [[PubMed: 8062456](#)]
1799. Schedl T, Kimble J. *fog-2* a germ-line-specific sex determination gene required for hermaphrodite spermatogenesis in *Caenorhabditis elegans*. *Genetics*. 1988;119:43–61. [[PMC free article: PMC1203344](#)] [[PubMed: 3396865](#)]
1800. Schedl T, Graham P L, Barton M K, Kimble J. Analysis of the role of *tra-1* in germline sex determination in the nematode *Caenorhabditis elegans*. *Genetics*. 1989;123:755–769. [[PMC free article: PMC1203887](#)] [[PubMed: 2612895](#)]
1801. Schein J E, Marra M A, Benian G M, Fields C A, Baillie D L. The use of deficiencies to determine essential gene content in the *let-56-unc-22* region of *Caenorhabditis elegans*. *Genome*. 1993;36:1148–1156. [[PubMed: 8112575](#)]
1802. Scheller R H, Jackson J F, McAllister L B, Schwartz J H, Kandel E R, Axel R. A family of genes that codes for ELH, a neuropeptide eliciting a stereotyped pattern of behavior in *Aplysia*. *Cell*. 1982;28:707–719. [[PubMed: 6284369](#)]
1803. Schierenberg E. Cell determination during early embryogenesis of the nematode *C. elegans*. *Cold Spring Harbor Symp. Quant. Biol.* 1985;50:59–68. [[PubMed: 3868497](#)]
1804. Schierenberg E. Developmental strategies during early embryogenesis of *Caenorhabditis elegans*. (suppl.) . *J. Embryol. Exp. Morphol.* 1986;97:31–44. [[PubMed: 3625117](#)]
1805. Schierenberg E. Reversal of cellular polarity and early cell-cell interaction in the embryo of *Caenorhabditis elegans*. *Dev. Biol.* 1987;122:452–463. [[PubMed: 3596018](#)]
1806. Schierenberg E. Localization and segregation of lineage-specific cleavage potential in embryos of *Caenorhabditis elegans*. *Roux's Arch. Dev. Biol.* 1988;197:282–293. [[PubMed: 28305788](#)]
1807. Schierenberg E, Junkersdorf B. The role of the eggshell and underlying vitelline membrane for pattern formation in the early *C. elegans* embryo. *Roux's Arch. Dev. Biol.* 1992;202:10–16. [[PubMed: 28305999](#)]
1808. Schierenberg E, Miwa J, Von Ehrenstein G. Cell lineages and developmental defects of temperature-sensitive embryonic arrest mutants in *Caenorhabditis elegans*. *Dev. Biol.* 1980;76:141–159. [[PubMed: 7380087](#)]
1809. Schiller P H, Sandell J H, Maunsell J H R. Functions of the ON and OFF channels of the visual system. *Nature*. 1986;322:824–825. [[PubMed: 3748169](#)]

1810. Schinkmann K, Li C. Localization of FMRFamide-like peptides in *Caenorhabditis elegans*. *J. Comp. Neurol.* 1992;316:251–260. [[PubMed: 1573054](#)]
1811. Schmeichel K L, Beckerle M C. The LIM domain is a modular protein-binding interface. *Cell.* 1994;79:211–219. [[PubMed: 7954790](#)]
1812. Schmucker D, Taubert H, Jackle H. Formation of the *Drosophila* larval photoreceptor organ and its neuronal differentiation require continuous Kruppel gene activity. *Neuron.* 1992;9:1025–1039. [[PubMed: 1463605](#)]
1813. Schnabel H, Schnabel R. An organ-specific differentiation gene *pha-1*, from *Caenorhabditis elegans*. *Science.* 1990;250:686–688. [[PubMed: 17810870](#)]
1814. Schnabel H, Bauer G, Schnabel R. Suppressors of the organ-specific differentiation gene *pha-1* of *Caenorhabditis elegans*. *Genetics.* 1991;129:69–77. [[PMC free article: PMC1204582](#)] [[PubMed: 1657704](#)]
1815. Schnabel R. Cellular interactions involved in the determination of the early *C. elegans* embryo. *Mech. Dev.* 1991;33:85–100. [[PubMed: 1911397](#)]
1816. Schnabel R. Autonomy and nonautonomy in cell fate specification of muscle in the *Caenorhabditis elegans* embryo: A reciprocal induction. *Science.* 1994;263:1449–1452. [[PubMed: 8128230](#)]
1817. Schnabel R. Duels without obvious sense: Counteracting inductions involved in body wall muscle development in the *Caenorhabditis elegans* embryo. *Development.* 1995;121:2219–2232. [[PubMed: 7635065](#)]
1818. Schnabel R, Schnabel H. Early determination in the *C. elegans* embryo: A gene *cib-1*, required to specify a set of stem-cell-like blastomeres. *Development.* 1990;108:107–119. [[PubMed: 2351058](#)]
1819. Schnabel R, Weigner C, Hutter H, Feichtinger R, Schnabel H. *mex-1* and the general partitioning of cell fate in the early *C. elegans* embryo. *Mech. Dev.* 1996;54:133–147. [[PubMed: 8652407](#)]
1820. Schriever L, Waterston R H. Phosphorylation of the N-terminal region of *Caenorhabditis elegans* paramyosin. *J. Mol. Biol.* 1989;207:451–454. [[PubMed: 2754733](#)]
1821. Schubert F R, Nieselt-Struwe K, Gruss P. The Antennapedia-type homeobox genes have evolved from three precursors separated early in metazoan evolution. *Proc. Natl. Acad. Sci.* 1993;90:143–147. [[PMC free article: PMC45616](#)] [[PubMed: 8093557](#)]
1822. Schukkink R F, Plasterk R H A. TcA the putative transposase of the *C. elegans* Tc1 transposon, has an N-terminal DNA binding domain. *Nucleic Acids Res.* 1990;18:895–900. [[PMC free article: PMC330343](#)] [[PubMed: 2156234](#)]
1823. Schultheiss T, Lin Z, Lu M, Murray J, Fischman D A, Weber K, Masaki T, Imamura M, Holtzer H. Differential distribution of subsets of myofibrillar proteins in cardiac nonstriated and striated myofibrils. *J. Cell Biol.* 1990;110:1159–1172. [[PMC free article: PMC2116089](#)] [[PubMed: 2108970](#)]
1824. Schulze K L, Littleton J T, Salzberg A, Halachmi N, Stern M, Lev Z, Bellen H J. *rop*, a *Drosophila* homolog of yeast Sec1 and vertebrate nSec1/Munc-18 proteins, is a negative regulator of neurotransmitter release in vivo. *Neuron.* 1994;13:1099–1108. [[PubMed: 7946348](#)]
1825. Schwabe J W R, Chapman L, Finch J T, Rhodes D. The crystal structure of the estrogen receptor DNA-binding domain bound to DNA: How receptors discriminate between their response elements. *Cell.* 1993;75:567–578. [[PubMed: 8221895](#)]
1826. Schwartz L M, Osborne B A. Ced-3/ICE: Evolutionarily conserved regulation of cell death. *BioEssays.* 1994;16:387–389. [[PubMed: 8080427](#)]
1827. Schwartz-Sommer Z, Huijser P, Nacken W, Saedler H, Sommer H. Genetic control of flower development by homeotic genes in *Antirrhinum majus*. *Science.* 1990;250:931–936. [[PubMed: 17746916](#)]
1828. Schwarzbauer J E, Spencer C S. The *Caenorhabditis elegans* homologue of the extracellular calcium binding protein SPARC/osteonectin affects nematode body morphology and mobility. *Mol. Biol. Cell.* 1993;4:941–952. [[PMC free article: PMC275724](#)] [[PubMed: 8257796](#)]
1829. Schwarzbauer J E, Musset-Bilal F, Ryan C S. Extracellular calcium-binding protein SPARC/osteonectin in *Caenorhabditis elegans*. *Methods Enzymol.* 1994;245:257–270. [[PubMed: 7760737](#)]

1830. Schweiguth F, Posakony J W. Suppressor of *Hairless* the *Drosophila* homolog of the mouse recombination signal-binding protein gene, controls sensory organ cell fates. *Cell*. 1992;69:1199–1212. [[PubMed: 1617730](#)]
1831. Scott A L, Yenbutr P, Eisinger S W, Raghavan N. Molecular cloning of the cuticular collagen *Bmcol-2* from *Brugia malayi*. *Mol. Biochem. Parasitol.* 1995;70:221–225. [[PubMed: 7637708](#)]
1832. Scott A L, Diala C, Moraga D A, Ibrahim M S, Redding M S, Tamashiro W K. *Dirofilaria immitis*: Biochemical and immunological characterisation of the surface antigens from adult parasites. *Exp. Parasitol.* 1988;67:307–323. [[PubMed: 2461318](#)]
1833. Sebastiano M, D'Alessio M, Bazzicalupo P.  $\beta$ -glucuronidase mutants of the nematode *Caenorhabditis elegans*. *Genetics*. 1986;112:459–468. [[PMC free article: PMC1202757](#)] [[PubMed: 3007276](#)]
1834. Sebastiano M, Lassandro F, Bazzicalupo P. *cut-1* a *Caenorhabditis elegans* gene coding for a dauer-specific noncollagenous component of the cuticle. *Dev. Biol.* 1991;146:519–530. [[PubMed: 1864469](#)]
1835. Sedensky M M, Meneely P M. Genetic analysis of halothane sensitivity in *Caenorhabditis elegans*. *Science*. 1987;236:952–954. [[PubMed: 3576211](#)]
1836. Sedensky M M, Hudson S J, Everson B, Morgan P G. Identification of a mariner-like repetitive sequence in *C. elegans*. *Nucleic Acids Res.* 1994;22:1719–1723. [[PMC free article: PMC308055](#)] [[PubMed: 8202377](#)]
1837. Ségalat L, Elkes D A, Kaplan J M. Modulation of serotonin-controlled behaviors by  $G_o$  in *Caenorhabditis elegans*. *Science*. 1995;267:1648–1651. [[PubMed: 7886454](#)]
1838. Segerberg M A, Stretton A O. Actions of cholinergic drugs in the nematode *Ascaris suum*. Complex pharmacology of muscle and motorneurons. *J. Gen. Physiol.* 1993;101:271–296. [[PMC free article: PMC2216759](#)] [[PubMed: 8455017](#)]
1839. Sekelsky J J, Newfeld S J, Raftery L A, Chartoff E H, Gelbart W M. Genetic characterization and cloning of Mothers against dpp, a gene required for decapentaplegic function in *Drosophila melanogaster*. *Genetics*. 1995;139:1347–1358. [[PMC free article: PMC1206461](#)] [[PubMed: 7768443](#)]
1840. Selkirk M E, Gregory W F, Jenkins R E, Maizels R M. Localization, turnover and conservation of gp15/400 in different stages of *Brugia malayi*. *Parasitology*. 1993;107:449–457. [[PubMed: 8278224](#)]
1841. Selkirk M E, Gregory W F, Yazdanbakhsh M, Jenkins R E, Maizels R M. Cuticular localisation and turnover of the major surface glycoprotein (gp29) of adult *Brugia malayi*. *Mol. Biochem. Parasitol.* 1990;42:31–44. [[PubMed: 1700298](#)]
1842. Selkirk M E, Nielsen L, Kelly C, Partono F, Sayers G, Maizels R M. Identification, synthesis and immunogenicity of cuticular collagens from the filarial nematodes *Brugia malayi* and *Brugia pahangi*. *Mol. Biochem. Parasitol.* 1989;32:229–246. [[PubMed: 2927447](#)]
1843. Selverston A I, Miller J P. Mechanisms underlying pattern generation in lobster stomatogastric ganglion as determined by selective inactivation of identified neurons. IV. Pyloric system. *J. Neurophysiol.* 1980;44:1102–1121. [[PubMed: 6256508](#)]
1844. Sengupta P, Chou J C, Bargmann C I. *odr-10* encodes a seven transmembrane domain olfactory receptor required for responses to the odorant diacetyl. *Cell*. 1996;84:899–909. [[PubMed: 8601313](#)]
1845. Sengupta P, Colbert H A, Bargmann C I. The *C. elegans* gene *odr-7* encodes an olfactory-specific member of the nuclear receptor superfamily. *Cell*. 1994;79:971–980. [[PubMed: 8001144](#)]
1846. Sepsenwol S, Taft S J. In vitro induction of crawling in the amoeboid sperm of the nematode parasite *Ascaris suum*. *Cell Motil. Cytoskel.* 1990;15:99–110. [[PubMed: 2311127](#)]
1847. Sepsenwol S, Ris H, Roberts T M. A unique cytoskeleton associated with crawling in the amoeboid sperm of the nematode, *Ascaris suum*. *J. Cell Biol.* 1989;108:55–66. [[PMC free article: PMC2115364](#)] [[PubMed: 2910878](#)]
1848. Serafini T, Kennedy T E, Galko M J, Mirzayan C, Jessell T M, Tessier-Lavigne M. The netrins define a family of axon outgrowth-promoting proteins homologous to *C. elegans* UNC-6. *Cell*. 1994;78:409–424. [[PubMed: 8062384](#)]
1849. Seto M, Jaeger U, Hockett R D, Graninger W, Bennett S, Goldman P, Korsmeyer S J. Alternative promoters and exons, somatic mutation and deregulation of the Bcl-2-Ig fusion gene in lymphoma.

- EMBO J. 1988;7:123–131. [[PMC free article: PMC454224](#)] [[PubMed: 2834197](#)]
1850. Seydoux G, Fire A. Soma-germline asymmetry in the distributions of embryonic RNAs in *Caenorhabditis elegans*. Development. 1994;120:2823–2834. [[PubMed: 7607073](#)]
1851. Seydoux G, Greenwald I. Cell autonomy of *lin-12* function in a cell fate decision in *C. elegans*. Cell. 1989;57:1237–1245. [[PubMed: 2736627](#)]
1852. Seydoux G, Savage C, Greenwald I. Isolation and characterization of mutations causing abnormal eversion of the vulva in *Caenorhabditis elegans*. Dev. Biol. 1993;157:423–436. [[PubMed: 8500652](#)]
1853. Seydoux G, Schedl T, Greenwald I. Cell-cell interactions prevent a potential inductive interaction between soma and germline in *C. elegans*. Cell. 1990;61:939–951. [[PubMed: 2350786](#)]
1854. Seydoux G, Mello C C, Pettitt J, Wood W B, Priess J R, Fire A. Repression of gene expression in the embryonic germ lineage of *C. elegans*. Nature. 1996;382:713–716. [[PubMed: 8751441](#)]
1855. Seymour M K, Wright K A, Doncaster C C. The action of the anterior feeding apparatus of *C. elegans* (Nematoda: Rhabditida). J. Zool. Soc. Lond. 1983;201:527–539.
1856. Shackleford G M, Shivakumar S, Shiue L, Mason J, Kenyon C, Varmus H E. Two *wnt* genes in *Caenorhabditis elegans*. Oncogene. 1993;8:1857–1864. [[PubMed: 8510930](#)]
1857. Shaham S, Horvitz H R. Developing *Caenorhabditis elegans* neurons may contain both cell-death protective and killer activities. Genes Dev. 1996a;10:578–591. [[PubMed: 8598288](#)]
1858. Shaham S, Horvitz H R. An alternatively spliced *C. elegans ced-4* RNA encodes a novel cell death inhibitor. Cell. 1996b;86:201–208. [[PubMed: 8706125](#)]
1859. Shakes D C. "A genetic and pharmacological analysis of spermatogenesis in the nematode *Caenorhabditis elegans*." [Ph.D. thesis]. Johns Hopkins University; Baltimore: 1988.
1860. Shakes D C, Ward S. Initiation of spermiogenesis in *C. elegans*: A pharmacological and genetic analysis. Dev. Biol. 1989a;134:189–200. [[PubMed: 2731646](#)]
1861. Shakes D C, Ward S. Mutations that disrupt the morphogenesis and localization of a sperm-specific organelle in *Caenorhabditis elegans*. Dev. Biol. 1989b;134:307–316. [[PubMed: 2744235](#)]
1862. Shakir M A, Miwa J, Siddiqui S S. A role of ADF chemosensory neurones in dauer formation behaviour in *C. elegans*. Neuroreport. 1993a;4:1151–1154. [[PubMed: 8219008](#)]
1863. Shakir M A, Fukushige T, Yasuda H, Miwa J, Siddiqui S S. *C. elegans osm-3* gene mediating osmotic avoidance behaviour encodes a kinesin-like protein. Neuroreport. 1993b;4:891–894. [[PubMed: 7690265](#)]
1864. Shamansky L M, Pratt D, Boisvenue R J, Cox G N. Cuticle collagen genes of *Haemonchus contortus* and *Caenorhabditis elegans* are highly conserved. Mol. Biochem. Parasitol. 1989;37:73–86. [[PubMed: 2615789](#)]
1865. Shankland M. Leech segmentation: A molecular perspective. BioEssays. 1994;16:801–808. [[PubMed: 7840757](#)]
1866. Shariff A, Luna E J. *Dictyostelium discoideum* plasma membranes contain an actin nucleating activity that requires ponticulin an integral membrane protein. J. Cell Biol. 1990;110:681–692. [[PMC free article: PMC2116041](#)] [[PubMed: 2307703](#)]
1867. Sharp P M, Averof M, Lloyd A T, Matassi G, Peden J F. DNA sequence evolution: the sounds of silence. Philos. Trans. R. Soc. Lond. B. 1995;349:241–247. [[PubMed: 8577834](#)]
1868. Sharrock W J. Yolk proteins of *Caenorhabditis elegans*. Dev. Biol. 1983;96:182–188. [[PubMed: 6337890](#)]
1869. Shatz C J. Impulse activity and the patterning of connections during CNS development. Neuron. 1990;5:745–756. [[PubMed: 2148486](#)]
1870. Shen M M, Hodgkin J. *mab-3* a gene required for sex-specific yolk protein expression and a male-specific lineage in *C. elegans*. Cell. 1988;54:1019–1031. [[PubMed: 3046751](#)]
1871. Shenk M A, Bode H R, Steele R E. Expression of *Cnox-2*, a *Hom/Hox* homeobox gene in hydra, is correlated with axial pattern formation. Development. 1993;117:657–667. [[PubMed: 8101168](#)]
1872. Sherrington R, Rogaev E I, Liang Y, Rogaeva E A, Levesque G, Ikeda M, Chi H, Lin C, Li G, Holman K, Tsuda T, Mar L, Foncin J -F, Bruni A C, Montesi M P, Sorbi S, Rainero I, Pinessi L, Nee L, Chumakov I, Pollen D, Brookes A, Sanseau P, Polinsky R J, Wasco W, Da Silva H A R, Haines J L, Pericak-Vance M A,

- Tanzi R E, Roses A D, Fraser P E, Rommens J M, St. George-Hyslop P H. Cloning of a gene bearing mis-sense mutations in early-onset familial Alzheimer's disease. *Nature*. 1995;375:754–760. [[PubMed: 7596406](#)]
1873. Shimizu S, Eguchi Y, Kosaka H, Kamiike W, Matsuda H, Tsujimoto Y. Prevention of hypoxia-induced cell death by Bcl-2 and Bcl-xL. *Nature*. 1995;374:811–813. [[PubMed: 7723826](#)]
1874. Shimkets R A, Warnick D G, Bositis C M, Nelson-Williams C, Hansson J H, Schambelan M, Gill J R, Ulick S, Milora R Y, Findling J R, Canessa C M, Rossier B C, Lifton R P. Liddle's syndrome: Heritable human hypertension caused by mutations in the  $\beta$  subunit of the epithelial sodium channel. *Cell*. 1994;79:407–414. [[PubMed: 7954808](#)]
1875. Shirataki H, Kaibuchi K, Sakoda T, Kishida S, Yamaguchi T, Wada K, Miyazaki M, Takai Y. Rabphilin-3A, a putative target protein for smg p25A/rab3A p25 small GTP-binding protein related to synaptotagmin. *Mol. Cell. Biol.* 1993;13:2061–2068. [[PMC free article: PMC359527](#)] [[PubMed: 8384302](#)]
1876. Shoemaker M O, Lau W, Shattuck R L, Kwiatkowski A P, Guerra-Santos P E, Matrisian L, Wilson E, Lukas T J, Van Eldik L J, Watterson D M. Use of DNA sequence and mutant analyses and antisense oligodeoxynucleotides to examine the molecular basis of nonmuscle myosin light chain kinase autoinhibition, calmodulin recognition, and activity. *J. Cell Biol.* 1990;111:1107–1125. [[PMC free article: PMC2116294](#)] [[PubMed: 2202734](#)]
1877. Shook D R, Brooks A, Johnson T E. Mapping quantitative trait loci affecting life history traits in the nematode *Caenorhabditis elegans*. *Genetics*. 1996;142:801–817. [[PMC free article: PMC1207020](#)] [[PubMed: 8849889](#)]
1878. Shreffler W, Margardino T, Shekdar K, Wolinsky E. The *unc-8* and *sup-40* genes regulate ion channel function in *Caenorhabditis elegans* motorneurons. *Genetics*. 1995;139:1261–1272. [[PMC free article: PMC1206455](#)] [[PubMed: 7539392](#)]
1879. Shyu A B, Belasco J G, Greenberg M E. Two distinct destabilizing elements in the *c-fos* message trigger deadenylation as a first step in rapid mRNA decay. *Genes Dev.* 1991;5:221–231. [[PubMed: 1899842](#)]
1880. Sibley M H, Graham P L, von Mende N, Kramer J M. Mutations in the  $\alpha 2(IV)$  basement membrane collagen gene of *Caenorhabditis elegans* produce phenotypes of differing severities. *EMBO J.* 1994;13:3278–3285. [[PMC free article: PMC395224](#)] [[PubMed: 8045258](#)]
1881. Sibley M H, Johnson J J, Mello C C, Kramer J M. Genetic identification, sequence, and alternative splicing of the *Caenorhabditis elegans*  $\alpha 2(IV)$  collagen gene. *J. Cell Biol.* 1993;123:255–264. [[PMC free article: PMC2119826](#)] [[PubMed: 7691828](#)]
1882. Siddiqui S. Mutations affecting axonal growth and guidance of motor neurons and [mechanosensory neurons](#) in the nematode *Caenorhabditis elegans*. (supp.). *Neurosci. Res.* 1990;13:S171–S190. [[PubMed: 1701874](#)]
1883. Siddiqui S S, Babu P. Kynurenone hydroxylase mutants of the nematode *C. elegans*. *Mol. Gen. Genet.* 1980;179:21–24. [[PubMed: 6935493](#)]
1884. Siddiqui S S, Culotti J G. Examination of neurons in wild type and mutants of *Caenorhabditis elegans* using antibodies to horseradish peroxidase. *J. Neurogenet.* 1991;7:193–211. [[PubMed: 1886035](#)]
1885. Sidow A, Thomas W K. A molecular evolutionary framework for eukaryotic model organisms. *Curr. Biol.* 1994;4:596–603. [[PubMed: 7953533](#)]
1886. Sigurdson D C, Spanier G J, Herman R K. *Caenorhabditis elegans* deficiency mapping. *Genetics*. 1984;108:331–345. [[PMC free article: PMC1202409](#)] [[PubMed: 6500256](#)]
1887. Sigurdson D C, Herman R K, Horton C A, Kari C K, Pratt S E. An X-autosome fusion chromosome of *Caenorhabditis elegans*. *Mol. Gen. Genet.* 1986;202:212–218. [[PubMed: 3458021](#)]
1888. Sijmons P C, Atkinson H J, Wyss U. Parasitic strategies of root nematodes and associated host cell responses. *Annu. Rev. Phytopathol.* 1994;32:235–259.
1889. Silberstein S, Collins P G, Kelleher D J, Gilmore R. The essential *OST2* gene encodes the 16-kD subunit of the yeast oligosaccharyltransferase, a highly conserved protein expressed in diverse eukaryotic organisms. *J. Cell Biol.* 1995;131:371–383. [[PMC free article: PMC2199988](#)] [[PubMed: 7593165](#)]

1890. Simon M A, Dodson G S, Rubin G M. An SH3-SH2-SH3 protein is required for p21<sup>Ras1</sup> activation and binds to sevenless and sos proteins *in vitro*. *Cell*. 1993;73:169–177. [[PubMed: 8462097](#)]
1891. Simon M N, Pelegrini O, Veron M, Kay R R. Mutation of protein kinase A causes heterochronic development of *Dictyostelium*. *Nature*. 1992;356:171–172. [[PubMed: 1312226](#)]
1892. Simons K, Zerial M. Rab proteins and the road maps for intracellular transport. *Neuron*. 1993;11:789–799. [[PubMed: 8240804](#)]
1893. Simpson V J, Johnson T E, Hammen R F C. *C. elegans* DNA does not contain 5-methylcytosine at any time during development or aging. *Nucleic Acids Res*. 1986;14:6711–6717. [[PMC free article: PMC311675](#)] [[PubMed: 3748820](#)]
1894. Simske J S, Kim S K. Sequential signalling during *Caenorhabditis elegans* vulval induction. *Nature*. 1995;375:142–146. [[PubMed: 7753169](#)]
1895. Simske J S, Kaech S M, Harp S A, Kim S K. LET-23 receptor localization by the cell junction protein LIN-7 during *C. elegans* vulval induction. *Cell*. 1996;85:195–204. [[PubMed: 8612272](#)]
1896. Singer I I, Solomon S, Kawka D W, Hassell J R. Extracellular matrix fibers containing fibronectin and basement membrane heparan sulfate proteoglycan coalign with focal contacts and microfilament bundles in stationary fibroblasts. *Exp. Cell Res.* 1987;173:558–571. [[PubMed: 3319658](#)]
1897. Singh N, Han M. *sur-2* a novel gene, functions late in the *let-60 ras*-mediated signaling pathway during *Caenorhabditis elegans* vulval induction. *Genes Dev.* 1995;9:2251–2265. [[PubMed: 7557379](#)]
1898. Singh R N, Sulston J E. Some observations on molting in *C. elegans*. *Nematologica*. 1978;24:63–71.
1899. Singh R, Valcarcel J, Green M R. Distinct binding specificities and functions of higher eukaryotic polypyrimidine tract-binding proteins. *Science*. 1995;268:1173–1176. [[PubMed: 7761834](#)]
1900. Siomi H, Matunis M J, Michael W M, Dreyfuss G. The pre-mRNA binding K protein contains a novelevolutionarily conserved motif. *Nucleic Acids Res*. 1993;21:1193–1198. [[PMC free article: PMC309281](#)] [[PubMed: 8464704](#)]
1901. Sithigorngul P, Cowden C, Stretton A O W. Heterogeneity of cholecystokinin/gastrin-like immunoreactivity in the [nervous system](#) of the nematode *Ascaris summ*. *J. Comp. Neurol.* 1996;370:427–442. [[PubMed: 8807446](#)]
1902. Sithigorngul P, Stretton A O W, Cowden C. Neuropeptide diversity in *Ascaris*: An immunocytochemical study. *J. Comp. Neurol.* 1990;294:362–376. [[PubMed: 2341616](#)]
1903. Skalka A M. Retroviral DNA integration: Lessons from transposon shuffling. *Gene*. 1993;135:175–182. [[PubMed: 8276256](#)]
1904. Skeath J B, Panganiban G, Selegue J, Carroll S B. Gene regulation in two dimensions: The proneural *achaete* and *scute* genes are controlled by combinations of axis-patterning genes through a common intergenic control region. *Genes Dev.* 1992;6:2606–2619. [[PubMed: 1340472](#)]
1905. Skiba F, Schierenberg E. Cell lineages developmental timing, and spatial pattern formation in embryos of free-living soil nematodes. *Dev. Biol.* 1992;151:597–610. [[PubMed: 1601187](#)]
1906. Skinner M K, Norton J N, Mullaney B P, Rosselli M, Whaley P D, Anthony C T. Cell-cell interactions and the regulation of [testis](#) function. *Ann. N.Y. Acad. Sci.* 1991;637:354–363. [[PubMed: 1785780](#)]
1907. Slack J M W, Holland P W H, Graham C F. The zootype and the phylotypic stage. *Nature*. 1993;361:490–492. [[PubMed: 8094230](#)]
1908. Small S, Kraut R, Hoey T, Warrier R, Levine M. Transcriptional regulation of a pair-rule stripe in *Drosophila*. *Genes Dev.* 1991;5:827–839. [[PubMed: 2026328](#)]
1909. Smith L T, Wertelecki W, Milstone L M, Petty E M, Seashore M R, Braverman I M, Jenkins T G, Byers P H. Human dermatosparaxis: A form of Ehlers-Danlos syndrome that results from failure to remove the amino-terminal propeptide of type I procollagen. *Am. J. Hum. Genet.* 1992;51:235–244. [[PMC free article: PMC1682688](#)] [[PubMed: 1642226](#)]
1910. Smith M J. A *C. elegans* gene encodes a protein homologous to mammalian calreticulin. *DNA Seq.* 1992;2:235–240. [[PubMed: 1627827](#)]
1911. Smith T S, Munn E A, Graham M, Tavernor A S, Greenwood C A. Purification and evaluation of the integral membrane protein H11 as a protective antigen against *Haemonchus contortus*. *Int. J.*

- Parasitol. 1993;23:271–280. [[PubMed: 8496010](#)]
1912. Smyth J D. Introduction to animal parasitology. Hodder and Stoughton; 1994.
1913. Snutch T P, Baillie D L. Alterations in the pattern of gene expression following heat shock in the nematode *Caenorhabditis elegans*. Can. J. Biochem. Cell Biol. 1983;61:480–487. [[PubMed: 6883176](#)]
1914. Snutch T P, Baillie D L. A high degree of DNA strain polymorphism associated with the major heat shock gene in *Caenorhabditis elegans*. Mol. Gen. Genet. 1984;195:329–335. [[PubMed: 6208455](#)]
1915. Snyder P M, McDonald F J, Stokes J B, Welsh M J. Membrane topology of the amiloride sensitive epithelial sodium channel. J. Biol. Chem. 1994;269:24379–24383. [[PubMed: 7929098](#)]
1916. Sokol S Y, Klingensmith J, Perrimon N, Itoh E. Dorsalizing and neuralizing properties of Xdsh, a maternally expressed *Xenopus* homolog of *dishevelled*. Development. 1995;121:1637–1647. [[PubMed: 7600981](#)]
1917. Sommer R J, Sternberg P W. Changes of induction and competence during the evolution of *vulva* development in nematodes. Science. 1994;265:114–118. [[PubMed: 8016644](#)]
1918. Sommer R J, Sternberg P W. Evolution of cell lineage and pattern formation in the vulval equivalence group of rhabditid nematodes. Dev. Biol. 1995;167:61–74. [[PubMed: 7851663](#)]
1919. Sommer R J, Sternberg P W. Apoptosis and change of competence limit the size of the *vulva* equivalence group in *Pristionchus pacificus*: A genetic analysis. Curr. Biol. 1996a;6:52–59. [[PubMed: 8805221](#)]
1920. Sommer R J, Sternberg P W. Evolution of nematode vulval fate patterning. Dev. Biol. 1996b;173:396–407. [[PubMed: 8606000](#)]
1921. Sommer R J, Carta L K, Sternberg P W. The evolution of cell lineage in nematodes. *Suppl.*, pp. Development. 1994:85–95. [[PubMed: 7579527](#)]
1922. Sosnowski B K. "Developmental localization of a sperm-specific protein and isolation of its gene in the nematode *Caenorhabditis elegans*." [Ph.D. thesis]. Johns Hopkins University; Baltimore: 1987.
1923. Spence A, Coulson A, Hodgkin J. The product of *fem-1*, a nematode sex-determining gene, contains a motif found in cell cycle control proteins and receptors for cell-cell interactions. Cell. 1990;60:981–990. [[PubMed: 2317869](#)]
1924. Spence H J, Moore J, Brass A, Kennedy M W. A cDNA encoding repeating units of the ABA-1 allergen of *Ascaris*. Mol. Biochem. Parasitol. 1993;57:339–344. [[PubMed: 8433722](#)]
1925. Spiegel Y, McClure M A. The surface coat of plant parasitic nematodes: chemical composition origin and biological role—A review. J. Nematol. 1995;27:127–134. [[PMC free article: PMC2619597](#)] [[PubMed: 19277272](#)]
1926. Spiegel Y, Inbar J, Kahane I, Sharon E. Carbohydrate-recognition domains on the surface of phytophagous mematodes. Exp. Parasitol. 1995;80:220–227. [[PubMed: 7895833](#)]
1927. Spieth J, Blumenthal T. The *Caenorhabditis elegans* vitellogenin gene family includes a gene encoding a distantly related protein. Mol. Cell. Biol. 1985;5:2495–2501. [[PMC free article: PMC366982](#)] [[PubMed: 3841791](#)]
1928. Spieth J, Denison K, Zucker E, Blumenthal T. The nucleotide sequence of a nematode vitellogenin gene. Nucleic Acids Res. 1985a;13:7129–7138. [[PMC free article: PMC322028](#)] [[PubMed: 3855245](#)]
1929. Spieth J, Brooke G, Kuerston S, Lea K, Blumenthal T. Operons in *C. elegans*: Polycistronic mRNA precursors are processed by *trans*-splicing of SL2 to downstream coding regions. Cell. 1993;73:521–532. [[PubMed: 8098272](#)]
1930. Spieth J, Denison K, Kirkland S, Cane J, Blumenthal T. The *C. elegans* vitellogenin genes: Short sequence repeats in the promoter regions and homology to the vertebrate genes. Nucleic Acids Res. 1985b;13:5283–5295. [[PMC free article: PMC321865](#)] [[PubMed: 4022780](#)]
1931. Spieth J, MacMorris M, Broverman S, Greenspoon S, Blumenthal T. Regulated expression of a vitellogenin fusion gene in transgenic nematodes. Dev. Biol. 1988;130:285–293. [[PubMed: 3181632](#)]
1932. Spieth J, Nettleton M, Zucker-Aprison E, Lea K, Blumenthal T. Vitellogenin motifs conserved in nematodes and vertebrates. J. Mol. Evol. 1991a;32:429–438. [[PubMed: 1904098](#)]
1933. Spieth J, Shim Y H, Lea K, Conrad R, Blumenthal T. *elt-1*, an embryonically expressed *Caenorhabditis elegans* gene homologous to the GATA transcription factor family. Mol. Cell. Biol. 1991b;11:4651–

4659. [PMC free article: PMC361353] [PubMed: 1875944]
1934. Spikes D A, Kramer J, Bingham P M, Doren K V. SWAP pre-mRNA splicing regulators are a novel, ancient protein family sharing a highly conserved sequence motif with the *prp21* family of constitutive splicing proteins. *Nucleic Acids Res.* 1994;22:4510–1519. [PMC free article: PMC308487] [PubMed: 7971282]
1935. Squire M D, Tornoe C, Baylis H A, Fleming J T, Barnard E A, Sattelle D B. Molecular cloning and functional co-expression of a *Caenorhabditis elegans* nicotinic acetylcholine receptor subunit (*acr-2*). *Recept. Channels.* 1995;3:107–115. [PubMed: 8581398]
1936. Stanojevic D, Small S, Levine M. Regulation of a segmentation stripe by overlapping activators and repressors in the *Drosophila* embryo. *Science.* 1991;254:1385–1387. [PubMed: 1683715]
1937. Starich T A, Herman R K, Shaw J E. Molecular and genetic analysis of *unc-7*, a *Caenorhabditis elegans* gene required for coordinated locomotion. *Genetics.* 1993;133:527–541. [PMC free article: PMC1205341] [PubMed: 7681023]
1938. Starich T A, Herman R K, Kari C K, Yeh W -H, Schackwitz W S, Schuyler M W, Collet J, Thomas J H, Riddle D L. Mutations affecting the che mosensory neurons of *Caenorhabditis elegans*. *Genetics.* 1995;139:171–188. [PMC free article: PMC1206316] [PubMed: 7705621]
1939. Starr T, Howell A M, McDowall J, Peters K, Rose A M. Isolation and mapping of DNA probes within the linkage group I gene cluster of *Caenorhabditis elegans*. *Genome.* 1989;32:365–372. [PubMed: 2744447]
1940. Staskawicz B J, Ausubel F M, Baker B J, Ellis J G, Jones J D G. Molecular genetics of plant disease resistance. *Science.* 1995;268:661–667. [PubMed: 7732374]
1941. Steiner G. The nematode *Cylindrogaster longistoma* (Stefanski) Goodey, and its relationship. *J. Parasitol.* 1933;20:66–68.
1942. Steiner N C, Clarke L. A novel epigenetic effect can alter centromere function in fission yeast. *Cell.* 1994;79:865–874. [PubMed: 8001123]
1943. Stenico M, Lloyd A T, Sharp P M. Codon usage in *Caenorhabditis elegans*: Delineation of translational selection and mutational biases. *Nucleic Acids Res.* 1994;22:2437–2446. [PMC free article: PMC308193] [PubMed: 8041603]
1944. Stern M J, Horvitz H R. *lin-17* mutations of *Caenorhabditis elegans* disrupt certain asymmetric cell divisions. *Dev. Biol.* 1988;130:67–73. [PubMed: 3181641]
1945. Stern M J, Horvitz H R. A normally attractive cell interaction is repulsive in two *C. elegans* mesodermal cell migration mutants. *Development.* 1991;113:797–803. [PubMed: 1821851]
1946. Stern M J, Marengere L E M, Daly R J, Lowenstein E J, Kokel M, Batzer A G, Olivier P, Pawson T, Schlessinger J. The human GRB2 and *Drosophila* Drk genes can functionally replace the *Caenorhabditis elegans* cell signaling gene *sem-5*. *Mol. Biol. Cell.* 1993;4:1175–1188. [PMC free article: PMC275752] [PubMed: 8305738]
1947. Sternberg P W. Lateral inhibition during vulval induction in *Caenorhabditis elegans*. *Nature.* 1988;335:551–554. [PubMed: 3419532]
1948. Sternberg P W, Horvitz H R. Gonadal cell lineages of the nematode *Panagrellus redivivus* and implications for evolution by the modification of cell lineage. *Dev. Biol.* 1981;88:147–166. [PubMed: 7286441]
1949. Sternberg P W, Horvitz H R. Postembryonic nonbonadal cell lineages of the nematode *Panagrellus redivivus*: Description and comparison with those of *Caenorhabditis elegans*. *Dev. Biol.* 1982;93:181–205. [PubMed: 7128930]
1950. Sternberg P W, Horvitz H R. Pattern formation during vulval development in *C. elegans*. *Cell.* 1986;44:761–772. [PubMed: 3753901]
1951. Sternberg P W, Horvitz H R. *lin-17* mutations of *Caenorhabditis elegans* disrupt certain asymmetric cell divisions. *Dev. Biol.* 1988;130:67–73. [PubMed: 3181641]
1952. Sternberg P W, Horvitz H R. The combined action of two intercellular signaling pathways specifies three cell fates during vulval induction in *C. elegans*. *Cell.* 1989;58:679–693. [PubMed: 2548732]

1953. Stewart G W, Argent A C, Dash B C J. Stomatin: A putative cation transport regulator in the red cell membrane. *Biochim. Biophys. Acta.* 1993;1225:15–25. [[PubMed: 7694657](#)]
1954. Stewart H I, Rosenbluth R E, Baillie D L. Most ultraviolet irradiation induced mutations in the nematode *Caenorhabditis elegans* are chromosomal rearrangements. *Mutat. Res.* 1991;249:37–54. [[PubMed: 2067542](#)]
1955. Stewart M, King K L, Roberts T M. The motile major sperm protein (MSP) forms filaments constructed from two helical subfilaments. *J. Mol. Biol.* 1994;243:60–71. [[PubMed: 7932742](#)]
1956. Stone S, Shaw J E. A *Caenorhabditis elegans act-4::lacZ* fusion: Use as a transformation marker and analysis of tissue-specific expression. *Gene.* 1993;131:167–173. [[PubMed: 8406009](#)]
1957. Storfer-Glazer F A, Wood W B. Effects of chromosomal deficiencies on early cleavage patterning and terminal phenotype in *Caenorhabditis elegans* embryos. *Genetics.* 1994;137:499–508. [[PMC free article: PMC1205972](#)] [[PubMed: 8070660](#)]
1958. Stoykova A, Gruss P. Roles of Pax-genes in developing and adult brain as suggested by expression patterns. *J. Neurosci.* 1994;14:1395–1412. [[PMC free article: PMC6577564](#)] [[PubMed: 8126546](#)]
1959. Strehler E E, Carlsson E, Eppenberger H M, Thornell L E. Ultrastructural localization of M-band proteins in chicken breast muscle as revealed by combined immunocytochemistry and ultramicrotomy. *J. Mol. Biol.* 1983;166:141–158. [[PubMed: 6854641](#)]
1960. Stretton A O W, Cowden C, Sithigorngul P, Davis R E. Neuropeptides in the nematode *Ascaris suum*. (suppl.). *Parasitology.* 1991;102:S107–S116. [[PubMed: 2057216](#)]
1961. Stretton A O W, Davis R E, Angstadt J D, Donmoyer J E, Johnson C D. Neural control of behaviour in *Ascaris*. *Trends Neurosci.* 1985;8:294–300.
1962. Stretton A O W, Fishpool R M, Southgate E, Donmoyer J E, Walrond J P, Moses J E, Kass I S. Structure and physiological activity of the motorneurons of the nematode *Ascaris*. *Proc. Natl. Acad. Sci.* 1978;75:3493–3497. [[PMC free article: PMC392804](#)] [[PubMed: 277952](#)]
1963. Stringham E G, Dixon D, Candido E P M. Expression of the polyubiquitin-encoding gene (*ubq-1*) in transgenic *Caenorhabditis elegans*. *Gene.* 1992a;113:165–173. [[PubMed: 1315299](#)]
1964. Stringham E G, Dixon D K, Jones D, Candido E P M. Temporal and spatial expression patterns of the small heat shock (*hsp16*) genes in transgenic *Caenorhabditis elegans*. *Mol. Biol. Cell.* 1992b;3:221–233. [[PMC free article: PMC275521](#)] [[PubMed: 1550963](#)]
1965. Stroher V L, Kennedy B P, Millen K J, Schroeder D F, Hawkins M G, Goszczynski B, McGhee J D. DNA-protein interactions in the *Caenorhabditis elegans* embryo: Oocyte and embryonic factors that bind to the promoter of the gut-specific *ges-1* gene. *Dev. Biol.* 1994;163:367–380. [[PubMed: 8200477](#)]
1966. Strome S, Gall J G, editor. Gametogenesis and the early embryo. New York: Alan Liss; 1986a. Establishment of asymmetry in early *Caenorhabditis elegans* embryos: Visualization with antibodies to germ cell components. pp. 77–96.
1967. Strome S. Fluorescence visualization of the distribution of microfilaments in gonads and early embryos of the nematode *Caenorhabditis elegans*. *J. Cell Biol.* 1986b;103:2241–2252. [[PMC free article: PMC2114604](#)] [[PubMed: 3782297](#)]
1968. Strome S. Generation of cell diversity during early embryogenesis in the nematode *Caenorhabditis elegans*. *Int. Rev. Cytol.* 1989;114:81–123. [[PubMed: 2661459](#)]
1969. Strome S. Determination of cleavage planes. *Cell.* 1993;72:3–6. [[PubMed: 8422680](#)]
1970. Strome S, Wood W B. Immunofluorescence visualization of germ-line-specific cytoplasmic granules in embryos larvae, and adults of *Caenorhabditis elegans*. *Proc. Natl. Acad. Sci.* 1982;79:1558–1562. [[PMC free article: PMC346014](#)] [[PubMed: 7041123](#)]
1971. Strome S, Wood W B. Generation of asymmetry and segregation of germ-line granules in early *C. elegans* embryos. *Cell.* 1983;35:15–25. [[PubMed: 6684994](#)]
1972. Strome S, Martin P, Schierenberg E, Paulsen J. Transformation of the germ line into muscle in *mes-1* embryos of *C. elegans*. *Development.* 1995;121:2961–2971. [[PubMed: 7555722](#)]
1973. Strome S, Garvin C, Paulsen J, Capowski E, Martin P, Beanan M, Marsh J, Goode J, editors. Germline development. London: CIBA Foundation; 1994. Specification and development of the germline in *Caenorhabditis elegans*. pp. 45–51. [[PubMed: 7835156](#)]

1974. Struhl G, White R. Regulation of the ultrabithorax gene of *Drosophila* by other bithorax complex genes. *Cell*. 1985;43:507–519. [[PubMed: 3935322](#)]
1975. Struhl G, Fitzgerald K, Greenwald I. Intrinsic activity of the Lin-12 and Notch intracellular domains in vivo. *Cell*. 1993;74:331–345. [[PubMed: 8343960](#)]
1976. Strunnikov A V, Hogan E, Koshland D. *SMC2*, a *Saccharomyces cerevisiae* gene essential for chromosome segregation and condensation, defines a subgroup within the SMC family. *Genes Dev.* 1995;9:587–599. [[PubMed: 7698648](#)]
1977. Strunnikov A V, Larionov V L, Koshland D. *SMC1*: An essential yeast gene encoding a putative head-rod-tail protein is required for nuclear division and defines a new ubiquitous protein family. *J. Cell Biol.* 1993;123:1635–1648. [[PMC free article: PMC2290909](#)] [[PubMed: 8276886](#)]
1978. Sudhaus W. Zur Systematik, Verbreitung, Ökologie und Biologie neuer und wenig bekannter Rhabditiden (Nematoda), 2. Teil.. *Zool. Jb. Syst.* 1974;101:417–465.
1979. Sudhaus W. Vergleichende Untersuchungen zur Phylogenie, Systematik Ökologie, Biologie und Ethologie der Rhabditidae (Nematoda). *Zoologica*. 1976;43:1–229.
1980. Sudhaus W. Systematisch-phylogenetische und biologisch-ökologische Untersuchungen an *Rhabditis*- (*Poikilolaimus*-) Arten als Beitrag zu Rassenbildung und Parallelevolution bei Nematoden. *Zool. Jb. Syst.* 1980;107:287–343.
1981. Sudhaus W. Über die Sukzession von Nematoden in Kuhfladen. *Pedobiologia*. 1981;21:271–297.
1982. Sudhaus W. Check list of species of *Rhabditis* sensu lato (Nematoda:Rhabditidae) discovered between 1976 and 1986. *Nematologica*. 1991;37:229–236.
1983. Sudhaus W. Die mittels symbiotischer Bakterien entomopathogenen Nematoden-Gattungen *Heterorhabditis* und *Steinerinema* sind keine Schwestertaxa. *Verh. Deutsch. Zool. Ges.* 1993;86:146.
1984. Sudhaus W, Hooper D J. *Rhabditis (Oscheius) guentheri* sp. n., an unusual species with reduced posterior ovary, with observations on the *Dolichura* and *Insectivora* groups (Nematoda: Rhabditidae). *Nematologica*. 1994;40:508–533.
1985. Sudhaus W, Kühne R. Nematodes associated with Psychodidae: Description of *Rhabditis berolina* sp. n. and redescription of *R. dubia* Bovien, 1937 (Nematoda: Rhabditidae), with biological and ecological notes, and a phylogenetic discussion. *Nematologica*. 1989;35:305–320.
1986. Sudhaus W, Rehfeld K. Einführung in die Phylogenetik und Systematik. Stuttgart: Gustav Fischer Verlag; 1992.
1987. Sudhaus W, Schulte F. *Rhabditis (Pelodera) strongyloides* (Nematoda) als Verursacher von Dermatitis, mit systematischen und biologischen Bemerkungen über verwandte Arten. *Zool. Jb. Syst.* 1988;115:187–205.
1988. Südhof T. The synaptic vesicle cycle: A cascade of protein-protein interactions. *Nature*. 1995;375:645–653. [[PubMed: 7791897](#)]
1989. Sugimoto A, Friesen P D, Rothman J. Baculovirus p35 prevents developmentally programmed cell death and rescues a *ced-9* mutant in the nematode *Caenorhabditis elegans*. *EMBO J.* 1994;13:2023–2028. [[PMC free article: PMC395050](#)] [[PubMed: 8187756](#)]
1990. Sugimoto A, Hozak R R, Nakashima T, Nishimoto T, Rothman J H. *dad-1*, an endogenous programmed cell death suppressor in *Caenorhabditis elegans* and vertebrates. *EMBO J.* 1995;14:4434–4441. [[PMC free article: PMC394535](#)] [[PubMed: 7556086](#)]
1991. Sukharev S I, Blount P, Martinac B, Blattner F R, Kung C. A large conductance mechanosensitive channel in *E. coli* encoded by *mscl* alone. *Nature*. 1994;368:265–268. [[PubMed: 7511799](#)]
1992. Sulston J E. Post-embryonic development in the ventral cord of *Caenorhabditis elegans*. *Philos. Trans. R. Soc. Lond. B Biol. Sci.* 1976;275:287–297. [[PubMed: 8804](#)]
1993. Sulston J E, Wood W B, editor. The nematode *Caenorhabditis elegans*. Cold Spring Harbor, New York: Cold Spring Harbor Laboratory; 1988. Cell lineage. pp. 123–155.
1994. Sulston J, Hodgkin J, Wood W B, editor. The nematode *Caenorhabditis elegans*. Cold Spring Harbor, New York: Cold Spring Harbor Laboratory; 1988. Methods. pp. 587–606.
1995. Sulston J E, Brenner S. The DNA of *C. elegans*. *Genetics*. 1974;77:95–104. [[PMC free article: PMC1213121](#)] [[PubMed: 4858229](#)]

1996. Sulston J E, Horvitz H R. Post-embryonic cell lineages of the nematode *Caenorhabditis elegans*. *Dev. Biol.* 1977;56:110–156. [PubMed: 838129]
1997. Sulston J E, Horvitz H R. Abnormal cell lineages in mutants of the nematode *Caenorhabditis elegans*. *Dev. Biol.* 1981;82:41–55. [PubMed: 7014288]
1998. Sulston J E, White J G. Regulation and cell autonomy during postembryonic development of *Caenorhabditis elegans*. *Dev. Biol.* 1980;78:577–597. [PubMed: 7190941]
1999. Sulston J E, White J G. Wood W B, editor. The nematode *Caenorhabditis elegans*. Cold Spring Harbor, New York: Cold Spring Harbor Laboratory; 1988. Appendix 1. Parts list. pp. 415–431.
2000. Sulston J E, Albertson D G, Thomson J N. The *Caenorhabditis elegans* male: Postembryonic development of nongonadal structures. *Dev. Biol.* 1980;78:542–576. [PubMed: 7409314]
2001. Sulston J, Dew M, Brenner S. Dopaminergic neurons in the nematode *Caenorhabditis elegans*. *J. Comp. Neurol.* 1975;163:215–226. [PubMed: 240872]
2002. Sulston J, Horvitz H R, Kimble J. Wood W B, editor. The nematode *Caenorhabditis elegans*. Cold Spring Harbor, New York: Cold Spring Harbor Laboratory; 1988. Appendix 3. Cell lineage. pp. 457–489.
2003. Sulston J E, Schierenberg E, White J G, Thomson J N. The embryonic cell lineage of the nematode *Caenorhabditis elegans*. *Dev. Biol.* 1983;100:64–119. [PubMed: 6684600]
2004. Sulston J, Du Z, Thomas K, Wilson R, Hillier L, Staden R, Halloran N, Green P, Thierry-Mieg J, Qiu L, Dear S, Coulson A, Craxton M, Durbin R, Berks M, Metstein M, Hawkins T, Ainscough R, Waterston R. The *C. elegans* genome sequencing project: A beginning. *Nature*. 1992;356:37–41. [PubMed: 1538779]
2005. Sundaram M, Greenwald I. Genetic and phenotypic studies of hypomorphic *lin-12* mutants of *C. elegans*. *Genetics*. 1993a;135:755–763. [PMC free article: PMC1205718] [PubMed: 8293977]
2006. Sundaram M, Greenwald I. Suppressors of a *lin-12* hypomorph define genes that interact with both *lin-12* and *glp-1* in *Caenorhabditis elegans*. *Genetics*. 1993b;135:765–783. [PMC free article: PMC1205719] [PubMed: 8293978]
2007. Sundaram M, Han M. The *Caenorhabditis elegans* *ksr-1* gene encodes a novel Raf-related kinase involved in Ras-mediated signal transduction. *Cell*. 1995;83:889–901. [PubMed: 8521513]
2008. Sussman D J, Klingensmith J, Salinas P, Adams P S, Nusse R, Perrimon N. Isolation and characterization of a mouse homolog of the *Drosophila* segment polarity gene *dishevelled*. *Dev. Biol.* 1994;166:73–86. [PubMed: 7958461]
2009. Sutherlin M E, Emmons S W. Selective lineage specification by *mab-19* during *Caenorhabditis elegans* male peripheral sense organ development. *Genetics*. 1994;138:675–688. [PMC free article: PMC1206218] [PubMed: 7851765]
2010. Sutoh K. Mapping of actin-binding sites on the heavy chain of myosin subfragment 1. *Biochemistry*. 1983;22:1579–1585. [PubMed: 6849869]
2011. Sutton R E, Boothroyd J C. Evidence for *trans* splicing in trypanosomes. *Cell*. 1986;47:527–535. [PMC free article: PMC7133315] [PubMed: 3022935]
2012. Svendsen P C, McGhee J D. The *C. elegans* neuronally expressed homeobox gene *ceh-10* is closely related to genes expressed in the vertebrate eye. *Development*. 1995;121:1253–1262. [PubMed: 7789259]
2013. Swanson M M, Riddle D L. Critical periods in the development of the *C. elegans* dauer larva. *Dev. Biol.* 1981;84:27–40. [PubMed: 7250500]
2014. Swofford D L. PAUP: Phylogenetic analysis using parsimony version 3.1. Illinois: 1993.
2015. Swofford D L, Olsen G J, Hillis D M, Moritz C, editors. Molecular systematics. Sunderland, Massachusetts: Sinauer Associates; 1990. Phylogeny reconstruction. pp. 411–501.
2016. Swofford D L, Maddison W P. Reconstructing ancestral character states under Wagner parsimony. *Math. Biosci.* 1987;87:199–229.

2017. Tabish M, Siddiqui Z K, Nishikawa K, Siddiqui S S. Exclusive expression of *C. elegans* osm-3 kinesin gene in chemosensory neurons open to the external environment. *J. Mol. Biol.* 1995;247:377–389. [PubMed: 7714894]
2018. Tabuse Y, Nishiwaki K, Miwa J. Mutations in a protein kinase C homolog confer phorbol ester resistance on *Caenorhabditis elegans*. *Science*. 1989;243:1713–1716. [PubMed: 2538925]
2019. Tackacks A M, Denker J A, Perrine K G, Maroney P A, Nilsen T W. A 22-nucleotide spliced leader sequence in the human parasitic nematode *Brugia malayi* is identical to the trans-spliced leader exon in *Caenorhabditis elegans*. *Proc. Natl. Acad. Sci.* 1988;85:7932–7936. [PMC free article: PMC282327] [PubMed: 3186698]
2020. Tagle D A, Koop B F, Goodman M, Slightom J L, Hess D L, Jones R T. Embryonic  $\epsilon$  and  $\gamma$  globin genes of a prosimian primate (*Galago crassicaudatus*): Nucleotide and amino acid sequences, developmental regulation and phylogenetic footprints. *J. Mol. Biol.* 1988;203:439–455. [PubMed: 3199442]
2021. Takahashi K, Hiwada K, Kokubo T. Isolation and characterization of a 34,000 Dalton calmodulin and F-actin-binding protein from chicken gizzard smooth muscle. *Biochem. Biophys. Res. Commun.* 1986;141:20–26. [PubMed: 3606745]
2022. Takel K, McPherson P S, Schmid S L, De Camilli P. Tubular membrane invaginations coated by dynamin rings are induced by GTP-gamma S in nerve terminals. *Nature*. 1995;374:186–190. [PubMed: 7877693]
2023. Tanaka E, Sabry J. Making the connection: Cytoskeletal rearrangements during growth cone guidance. *Cell*. 1995;83:171–176. [PubMed: 7585934]
2024. Tanaka S, Saito K, Reed J C. Structure-function analysis of the Bcl-2 oncogene: Addition of a heterologous transmembrane domain to portions of the Bcl-2 $\beta$  protein restores function as a regulator of cell survival. *J. Biol. Chem.* 1993;268:10920–10926. [PubMed: 8496157]
2025. Tang L, Gounaris K, Griffiths C, Selkirk M E. Heterologous expression and enzymatic properties of a selenium-independent glutathione peroxidase from the parasitic nematode *Brugia pahangi*. *J. Biol. Chem.* 1995;270:18313–18318. [PubMed: 7629152]
2026. Tang L, Ou X, Henkle-Dhursen K J, Selkirk M E. Extracellular and cytoplasmic CuZn superoxide dismutase from the *Brugia* lymphatic filarial parasites. *Infect. Immun.* 1994;62:961–967. [PMC free article: PMC186210] [PubMed: 8112870]
2027. Tax F E, Yeargers J J, Thomas J H. Sequence of *C. elegans* lag-2 reveals a cell-signaling domain shared with *Delta* and *Serrate* of *Drosophila*. *Nature*. 1994;368:150–154. [PubMed: 8139658]
2028. Taylor P, Radic Z. The cholinesterases: From genes to proteins. *Annu. Rev. Pharmacol. Toxicol.* 1994;34:281–320. [PubMed: 8042853]
2029. Tenzen T, Matsutani S, Ohtsubo E. Site-specific transposition of insertion sequence IS630. *J. Bacteriol.* 1990;172:3830–3836. [PMC free article: PMC213363] [PubMed: 2163390]
2030. Tessier L -H, Keller M, Chan R L, Fournier R, Weil J -H, Imbault P. Short leader sequences may be transferred from small RNAs to premature mRNAs by *trans*-splicing in *Euglena*. *EMBO J.* 1991;10:2621–2625. [PMC free article: PMC452961] [PubMed: 1868836]
2031. Thacker C, Peters K, Srayko M, Rose A M. The bli-4 locus of *Caenorhabditis elegans* encodes structurally distinct kex2/subtilisin-like endoproteases essential for early development and adult morphology. *Genes Dev.* 1995;9:956–971. [PubMed: 7774813]
2032. Theisen H, Purcell J, Bennett M, Kansagara D, Syed A, Marsh J L. *dishevelled* is required during *wingless* signaling to establish both cell polarity and cell identity. *Development*. 1994;120:347–360. [PubMed: 8149913]
2033. Theriot J. Worm sperm and advances in cell locomotion. *Cell*. 1996;84:1–4. [PubMed: 8548813]
2034. Thomas J, Lea K, Zucker-Aprison E, Blumenthal T. The spliceosomal snRNAs of *Caenorhabditis elegans*. *Nucleic Acids Res.* 1990;18:2633–2642. [PMC free article: PMC330746] [PubMed: 2339054]
2035. Thomas J D, Conrad R C, Blumenthal T. The *C. elegans* trans-spliced leader RNA is bound to Sm and has a trimethylguanosine cap. *Cell*. 1988;54:533–539. [PubMed: 3401926]

2036. Thomas J H. Genetic analysis of defecation in *Caenorhabditis elegans*. *Genetics*. 1990;124:855–872. [[PMC free article: PMC1203977](#)] [[PubMed: 2323555](#)]
2037. Thomas J H. Thinking about genetic redundancy. *Trends Genet.* 1993a;9:395–399. [[PubMed: 8310537](#)]
2038. Thomas J H. Chemosensory regulation of development in *C. elegans*. *BioEssays*. 1993b;15:791–797. [[PubMed: 8141797](#)]
2039. Thomas J H, Birnby D, Vowels J. Evidence for parallel processing of sensory information controlling dauer formation in *Caenorhabditis elegans*. *Genetics*. 1993;134:1105–1117. [[PMC free article: PMC1205579](#)] [[PubMed: 8375650](#)]
2040. Thomas J H, Stern M J, Horvitz H R. Cell interactions coordinate the development of the *C. elegans* egg-laying system. *Cell*. 1990;62:1041–1052. [[PubMed: 2401010](#)]
2041. Thomas W K, Wilson A C. Mode and tempo of molecular evolution in the nematode *Caenorhabditis*: Cytochrome oxidase II and calmodulin sequences. *Genetics*. 1991;128:269–279. [[PMC free article: PMC1204465](#)] [[PubMed: 1649066](#)]
2042. Thompson C B. Apoptosis in the pathogenesis and treatment of disease. *Science*. 1995;267:1456–1462. [[PubMed: 7878464](#)]
2043. Thornberry N A, Bull H G, Calaycay J R, Chapman K T, Howard A D, Kostura M J, Miller D K, Molineaux S M, Weidner J R, Aunins J, Elliston K O, Ayala J M, Casano F J, Chin J, Ding J F, Egger L A, Gaffney E P, Limjoco G, Palyha O C, Raju S M, Rolando A M, Salley J P, Yamin T, Lee T D, Shively J E, MacCross M M, Mumford R A, Schmidt J A, Tocci M J. A novel heterodimeric cysteine protease is required for interleukin-1 $\beta$  processing in monocytes. *Nature*. 1992;356:768–774. [[PubMed: 1574116](#)]
2044. Tilstra D J, Byers P H. Molecular basis of hereditary disorders of connective tissue. *Annu. Rev. Med.* 1994;45:149–163. [[PubMed: 8198373](#)]
2045. Timpl R, Brown J C. The laminins. *Matrix Biol.* 1994;14:275–281. [[PubMed: 7827749](#)]
2046. Tobin A J. Molecular biological approaches to the synthesis and action of GABA. *Semin. Neurosci.* 1991;3:183–190.
2047. Tobler H, Etter A, Müller F. Chromatin diminution in nematode development. *Trends Genet.* 1992;8:427–432. [[PubMed: 1492368](#)]
2048. Tower J. Aging mechanisms in fruit flies. *BioEssays*. 1996;18:799–807. [[PubMed: 8885717](#)]
2049. Tranquilla T, Cortese R, Melton D, Smith J. Sequences of four tRNA genes from *C. elegans* and the expression of *C. elegans* tRNA<sup>Leu</sup> (anticodon IAG) in *Xenopus* oocytes. *Nucleic Acids Res.* 1982;10:7919–7934. [[PMC free article: PMC327059](#)] [[PubMed: 6761649](#)]
2050. Travis A, Amsterdam A, Belanger C, Grosschedl R. LEF-1, a gene encoding a lymphoid-specific protein with an HMB domain, regulates T-cell receptor  $\alpha$  enhancer function. *Genes Dev.* 1991;5:880–894. [[PubMed: 1827423](#)]
2051. Tree T I M, Gillespie A J, Shepley K J, Blaxter M L, Tuan R S, Bradley J E. Characterisation of an immunodominant glycoprotein antigen of *Onchocerca volvulus* with homologues in other filarial nematodes and *Caenorhabditis elegans*. *Mol. Biochem. Parasitol.* 1995;69:185–195. [[PubMed: 7770083](#)]
2052. Treinin M, Chalfie M. A mutated acetylcholine receptor subunit causes neuronal degeneration in *C. elegans*. *Neuron*. 1995;14:871–877. [[PubMed: 7718248](#)]
2053. Treisman J, Harris E, Desplan C. The paired box encodes a second DNA-binding domain in the paired homeodomain protein. *Genes Dev.* 1991;5:594–604. [[PubMed: 1672661](#)]
2054. Trent C, Tsuing N, Horvitz H R. Egg-laying defective mutants of the nematode *Caenorhabditis elegans*. *Genetics*. 1983;104:619–647. [[PMC free article: PMC1202130](#)] [[PubMed: 11813735](#)]
2055. Trent C, Wood W B, Horvitz H R. A novel dominant transformer allele of the sex-determining gene *her-1* of *Caenorhabditis elegans*. *Genetics*. 1988;120:145–157. [[PMC free article: PMC1203486](#)] [[PubMed: 3220248](#)]
2056. Trent C, Purnell B, Gavinski S, Hageman J, Chamblin C, Wood W B. Sex-specific transcriptional regulation of the *C. elegans* sex-determining gene *her-1*. *Mech. Dev.* 1991;34:43–55. [[PubMed: 1716965](#)]

2057. Triantaphyllou A C, Sasser J N, Carter C C, editors. An advanced treatise on Meloidgyne. Vol. I: Biology and control. Raleigh: North Carolina State University Graphics; 1985. Cytogenetics cytotsatonomy and phylogeny of root-knot nematodes. pp. 113–126.
2058. Trinick J. Titin and nebulin: Protein rulers in muscle? *Trends Biol. Sci.* 1994;19:405–409. [[PubMed: 7817397](#)]
2059. Troemel E R, Chou J H, Dwyer N D, Colbert H A, Bargmann C I. Divergent seven transmembrane receptors are candidate chemosensory receptors in *C. elegans*. *Cell.* 1995;83:207–218. [[PubMed: 7585938](#)]
2060. Truett M A, Jones R S, Potter S S. Unusual structure of the FB family of transposable elements in *Drosophila*. *Cell.* 1981;24:753–763. [[PubMed: 6265101](#)]
2061. Tryggvason K. The laminin family. *Curr. Opin. Cell Biol.* 1993;5:877–882. [[PubMed: 8240830](#)]
2062. Tsujimoto Y, Croce C M. Analysis of the structure, transcripts, and protein products of bcl-2, the gene involved in human follicular lymphoma. *Proc. Natl Acad. Sci. USA.* 1986;83:5214–5218. [[PMC free article: PMC323921](#)] [[PubMed: 3523487](#)]
2063. Tsujimoto Y, Finger L R, Yunis J, Nowell P C, Croce C M. Cloning of the chromosome breakpoint of neoplastic B cells with the t(14;-->18) chromosome translocation. *Science.* 1984;226:1097–1099. [[PubMed: 6093263](#)]
2064. Tuck S, Greenwald I. *lin-25* a gene required for vulval induction in *Caenorhabditis elegans*. *Genes Dev.* 1995;9:341–357. [[PubMed: 7867931](#)]
2065. Tudor M, Lobocka M, Goodell M, Pettitt J, O'Hare K. The pogo transposable element family of *Drosophila melanogaster*. *Mol. Gen. Genet.* 1992;232:126–134. [[PubMed: 1313144](#)]
2066. Turbeville J M, Pfeifer D M, Field K G, Raff R A. The phylogenetic status of arthropods, as inferred from 18S rRNA sequences. *Mol. Biol. Evol.* 1991;8:669–686. [[PubMed: 1766363](#)]
2067. Turner D L, Snyder E Y, Cepko C L. Lineage-independent determination of cell type in the embryonic mouse retina. *Neuron.* 1990;4:833–845. [[PubMed: 2163263](#)]
2068. Tweedie S A R, Paxton W A, Ingram L, Maizels R M, McReynolds L A, Selkirk M E. *Brugia pahangi* and *Brugia malayi*: A surface-associated glycoprotein (gp15/400) is composed of multiple tandemly-repeated units and processed from a 400 kDa precursor. *Exp. Parasitol.* 1993;76:156–164. [[PubMed: 8454024](#)]

## U

2069. Ullrich O, Stenmark H, Alexandrov K, Huber L A, Kaibuchi K, Sasaki T, Takai Y, Zerial M. Rab GDI as a general regulator for the membrane association of rab proteins. *J. Biol. Chem.* 1993;268:18143–18150. [[PubMed: 8349690](#)]
2070. Umen J G, Guthrie C. A novel role for a U5 snRNP protein in 3'splice site selection. *Genes Dev.* 1995;9:855–868. [[PubMed: 7535718](#)]

## V

2071. Vancompernolle K, Goethals M, Huet C, Louvard D, Vandekerckhove J. G- to F-actin modulation by a single amino acid substitution in the actin binding site of actobindin and thymosin  $\beta$  4. *EMBO J.* 1992;11:4739–4746. [[PMC free article: PMC556949](#)] [[PubMed: 1464307](#)]
2072. Vancompernolle K, Gimona M, Herzog M, Van D J, Vandekerckhove J, Small V. Isolation and sequence of a tropomyosin-binding fragment of turkey gizzard calponin. *FEBS Lett.* 1990;274:146–150. [[PubMed: 2253766](#)]
2073. Vandekerckhove J, Weber K. Mammalian cytoplasmic actins are the products of at least two genes and differ in primary structure in at least 25 identified positions from skeletal muscle actins. *Proc. Natl. Acad. Sci.* 1978;75:1106–1110. [[PMC free article: PMC411417](#)] [[PubMed: 274701](#)]
2074. Vandereycken W, Engler J D, Vanmontagu M, Gheysen G. Identification and analysis of a cuticular collagen-encoding gene from the plant-parasitic nematode *Meloidogyne incognita*. *Gene.*

- 1994;151:237–242. [[PubMed: 7828882](#)]
2075. van der Keyl H, Kim H, Espey R, Oke C V, Edwards M K. *Caenorhabditis elegans* *sqt-3* mutants have mutations in the *col-1* collagen gene. *Dev. Dynam.* 1994;201:86–94. [[PubMed: 7803850](#)]
2076. van der Bliek A M, Meyerowitz E M. Dynamin-like protein encoded by the *Drosophila shibire* gene associated with vesicular traffic. *Nature*. 1991;351:411–414. [[PubMed: 1674590](#)]
2077. van der Knaap E, Rodriguez R J, Freckman D W. Differentiation of bacterial-feeding nematodes in soil ecological studies by means of arbitrarily-primed PCR. *Soil Biol. Biochem.* 1993;25:1141–1151.
2078. Vanderslice R, Hirsh D. Temperature-sensitive [zygote](#) defective mutants of *Caenorhabditis elegans*. *Dev. Biol.* 1976;49:236–249. [[PubMed: 943346](#)]
2079. van de Wetering M, Oosterwegel M, Dooijes D, Clevers H. Identification and cloning of TCF-1, a T lymphocyte-specific transcription factor containing a sequence-specific HMG box. *EMBO J.* 1991;10:123–132. [[PMC free article: PMC452620](#)] [[PubMed: 1989880](#)]
2080. Van Doren K, Hirsh D. *Trans*-spliced leader RNA exists as small nuclear ribonucleoprotein particles in *Caenorhabditis elegans*. *Nature*. 1988;335:556–559. [[PubMed: 3419533](#)]
2081. Van Doren K, Hirsh D. mRNAs that mature through *trans*-splicing in *Caenorhabditis elegans* have a trimethylguanosine cap at their 5' termini. *Mol. Cell. Biol.* 1990;10:1769–1772. [[PMC free article: PMC362283](#)] [[PubMed: 1690851](#)]
2082. Van Doren M, Bailey A M, Esnayra J, Ede K, Posakony J W. Negative regulation of proneural gene activity: hairy is a direct transcriptional repressor of *achaete*. *Genes Dev.* 1994;8:2729–2742. [[PubMed: 7958929](#)]
2083. Vanfleteren J R. Nematode chromosomal proteins II. Fractionation and identification of the histones of *Caenorhabditis elegans*. *Comp. Biochem. Physiol. B*. 1983;73:709–718. [[PubMed: 7151410](#)]
2084. Vanfleteren J R. Oxidative stress and ageing in *Caenorhabditis elegans*. *Biochem. J.* 1993;292:605–608. [[PMC free article: PMC1134253](#)] [[PubMed: 8389142](#)]
2085. Vanfleteren J R, DeVreese A. The gerontogenes *age-1* and *daf-2* determine metabolic rate potential in aging *Caenorhabditis elegans*. *FASEB J.* 1995;9:1355–1361. [[PubMed: 7557026](#)]
2086. Vanfleteren J R, DeVreese A. Rate of aerobic metabolism and superoxide production rate potential in the nematode *Caenorhabditis elegans*. *J. Exp. Zool.* 1996;274:93–100. [[PubMed: 8742689](#)]
2087. Vanfleteren J R, Van Bun S M, Van Beeumen J J. The histones of *Caenorhabditis elegans*: No evidence of stage-specific isoforms. *FEBS Lett.* 1989;257:233–237. [[PubMed: 2583267](#)]
2088. Vanfleteren J R, Van de Peer Y, Blaxter M L, Tweedie S A R, Trotman C, Lu L, Van Hauwaert M -L, Moens L. Molecular genealogy of some nematode taxa as based on cytochrome c and globin amino acid sequences. *Mol. Phylogenet. Evol.* 1994;3:92–101. [[PubMed: 8075836](#)]
2089. van Gent D C, Oude Groeneger A A M, Plasterk R H A. Mutational analysis of the integrase protein of human immunodeficiency virus type 2. *Proc. Natl. Acad. Sci.* 1992;89:9598–9602. [[PMC free article: PMC50179](#)] [[PubMed: 1409671](#)]
2090. Van Horn D J, Eisenberg D, O'Brien C A, Wolin S L. *Caenorhabditis elegans* embryos contain only one major species of Ro RNP. *RNA*. 1995;1:293–303. [[PMC free article: PMC1369082](#)] [[PubMed: 7489501](#)]
2091. van Luenen H G A M, Plasterk R H A. Target site choice of the related transposable elements Tc1 and Tc3 of *Caenorhabditis elegans*. *Nucleic Acids Res.* 1994;22:262–269. [[PMC free article: PMC523575](#)] [[PubMed: 8127662](#)]
2092. van Luenen H G A M, Colloms S D, Plasterk R H A. Mobilization of quiet, endogenous Tc3 transposons of *Caenorhabditis elegans* by forced expression of Tc3 transposase. *EMBO J.* 1993;12:2513–2520. [[PMC free article: PMC413489](#)] [[PubMed: 8389698](#)]
2093. van Luenen H G A M, Colloms S D, Plasterk R H A. The mechanism of transposition of Tc3 in *Caenorhabditis elegans*. *Cell*. 1994;79:293–301. [[PubMed: 7954797](#)]
2094. Van Voorhies W A. Production of sperm reduces nematode lifespan. *Nature*. 1992;360:456–458. [[PubMed: 1448167](#)]
2095. Varkey J P, Jansma P L, Minniti A N, Ward S. The *Caenorhabditis elegans spe-6* gene is required for major sperm protein assembly and shows second site non-complementation with an unlinked deficiency. *Genetics*. 1993;133:79–86. [[PMC free article: PMC1205300](#)] [[PubMed: 8417991](#)]

2096. Varkey J P, Muhlrad P J, Minniti A N, Do B, Ward S. The *Caenorhabditis elegans spe-26* gene is necessary to form [spermatids](#) and encodes a protein similar to the actin-associated proteins kelch and scruin. *Genes Dev.* 1995;9:1074–1086. [[PubMed: 7744249](#)]
2097. Varmus H, Brown P, Berg D E, Howe M M, editors. *Mobile DNA*. American Society for Microbiology; 1989. *Retroviruses*. pp. 53–108.
2098. Varoqui H, Diebler M F, Meunier F M, Rand J B, Usdin T B, Bonner T I, Eiden L E, Erickson J D. Cloning and expression of the vesamico binding protein from the marine ray *Torpedo*. Homology with the putative vesicular acetylcholine transporter UNC-17 from *Caenorhabditis elegans*. *FEBS Lett.* 1994;342:97–102. [[PubMed: 8143858](#)]
2099. Vaudin M, Roopra A, Hillier L, Brinkman R, Sulston J, Wilson R K, Waterston R H. The construction and analysis of M13 libraries prepared from YAC DNA. *Nucleic Acids Res.* 1995;23:670–674. [[PMC free article: PMC306736](#)] [[PubMed: 7899089](#)]
2100. Vaux D L. Toward an understanding of the molecular mechanisms of physiological cell death. *Proc. Natl. Acad. Sci.* 1993;90:786–789. [[PMC free article: PMC45754](#)] [[PubMed: 8430086](#)]
2101. Vaux D L, Cory S, Adams J M. *bcl-2* gene promotes haemopoietic cell survival and cooperates with *c-myc* to immortalize pre-B cells. *Nature*. 1988;335:440–442. [[PubMed: 3262202](#)]
2102. Vaux D L, Weissman I L, Kim S K. Prevention of programmed cell death in *Caenorhabditis elegans* by human *bcl-2*. *Science*. 1992;258:1955–1957. [[PubMed: 1470921](#)]
2103. Veis D J, Sorenson C M, Shutter J R, Korsmeyer S J. *Bcl-2*-deficient mice demonstrate fulminant lymphoid apoptosis, polycystic kidneys, and hypopigmented hair. *Cell*. 1993;75:229–240. [[PubMed: 8402909](#)]
2104. Venolia L, Waterston R H. The *unc-45* gene of *Caenorhabditis elegans* is an essential muscle-affecting gene with maternal expression. *Genetics*. 1990;126:345–353. [[PMC free article: PMC1204189](#)] [[PubMed: 2245914](#)]
2105. Vibert P, Edelstein S M, Castellani L, Elliott B. Mini-titins in striated and smooth molluscan muscles: Structure, location and immunological cross-reactivity. *J. Muscle Res. Cell Motil.* 1993;14:598–607. [[PubMed: 8126220](#)]
2106. Vielmetter J, Kayyem J F, Roman J M, Dreyer W J. Neogenin, an avian cell surface protein expressed during terminal neuronal differentiation, is closely related to the human tumor suppressor molecule deleted in colorectal cancer. *J. Cell Biol.* 1994;127:2009–2020. [[PMC free article: PMC2120299](#)] [[PubMed: 7806578](#)]
2107. Vigoreaux J O, Saide J D, Pardue M L. Structurally different *Drosophila* striated muscles utilize distinct variants of Z-band-associated proteins. *J. Muscle Res. Cell Motil.* 1991;12:340–354. [[PubMed: 1719028](#)]
2108. Villeneuve A. A *cis*-acting locus that promotes crossing over between X chromosomes in *Caenorhabditis elegans*. *Genetics*. 1994;136:887–902. [[PMC free article: PMC1205894](#)] [[PubMed: 8005443](#)]
2109. Villeneuve A M, Meyer B J. *sdc-1*: A link between sex determination and dosage compensation in *C. elegans*. *Cell*. 1987;48:25–37. [[PubMed: 3791412](#)]
2110. Villeneuve A M, Meyer B J. The role of *sdc-1* in the sex determination and dosage compensation decisions in *Caenorhabditis elegans*. *Genetics*. 1990a;124:91–114. [[PMC free article: PMC1203913](#)] [[PubMed: 2307356](#)]
2111. Villeneuve A M, Meyer B J. The regulatory hierarchy controlling sex determination and dosage compensation in *Caenorhabditis elegans*. *Adv. Genet.* 1990b;27:117–188. [[PubMed: 2190446](#)]
2112. Viney M. A genetic analysis of reproduction in *Strongyloides ratti*. *Parasitology*. 1994;109:511–515. [[PubMed: 7800419](#)]
2113. Viney M E, Matthews B E, Walliker D. On the biological and biochemical nature of cloned populations of *Strongyloides ratti*. *J. Helminthol.* 1992;66:45–52. [[PubMed: 1469259](#)]
2114. Vink C, Plasterk R H A. The human immunodeficiency virus integrase protein. *Trends Genet.* 1993;9:433–437. [[PubMed: 8122311](#)]

2115. Vinkemeier U, Obermann W, Weber K, Furst D O. The globular head domain of titin extends into the center of the sarcomeric M band: cDNA cloning, epitope mapping, and immunoelectron microscopy of two titin-associated proteins. *J. Cell Sci.* 1993;106:319–330. [[PubMed: 7505783](#)]
2116. Vinson C, Adler P. Directional non-cell autonomy and the transmission of polarity information by the *frizzled* gene of *Drosophila*. *Nature*. 1987;329:549–551. [[PubMed: 3116434](#)]
2117. Vitaterna M H, King D P, Chang A M, Kornhauser J M, Lowrey P L, McDonald J D, Dove W F, Pinto L H, Turek F W, Takahashi J S. Mutagenesis and mapping of a mouse gene, *Clock*, essential for circadian behavior. *Science*. 1994;264:719–725. [[PMC free article: PMC3839659](#)] [[PubMed: 8171325](#)]
2118. Volk T, Fessler L I, Fessler J H. A role for integrin in the formation of sarcomeric cytoarchitecture. *Cell*. 1990;63:525–536. [[PubMed: 2225065](#)]
2119. von Ehrenstein G, Schierenberg E. Cell lineages and development of *Caenorhabditis elegans* and other nematodes. In: Zuckerman B M, editor. *Nematodes as biological models* vol. 2, New York: Academic Press; 1980. pp. 1–71.
2120. von Ehrenstein G, Scheierenberg E, Miwa J, LeDouarin N, editor. *Cell lineage, stem cells and cell determination*. New York: Elsevier; 1979. *Cell lineages of wild-type and temperature-sensitive embryonic arrest mutants of Caenorhabditis elegans*. pp. 49–59.
2121. von Gersdorff H, Matthews G. Inhibition of endocytosis by elevated internal calcium in a synaptic terminal. *Nature*. 1994;370:652–655. [[PubMed: 8065451](#)]
2122. von Mende N, Bird D, Albert P S, Riddle D L. *Dpy-13*: A nematode collagen gene that affects body shape. *Cell*. 1988;55:567–576. [[PubMed: 2846184](#)]
2123. Vos J C, Plasterk R H A. Tc1 transposase of *Caenorhabditis elegans* is an endonuclease with a bipartite DNA binding domain. *EMBO J*. 1994;13:6125–6132. [[PMC free article: PMC395592](#)] [[PubMed: 7813449](#)]
2124. Vos J C, De Baere I, Plasterk R H A. Transposase is the only nematode protein required for *in vitro* transposition of Tc1. *Genes Dev*. 1996;10:755–761. [[PubMed: 8598301](#)]
2125. Vos J C, van Luenen H G A M, Plasterk R H A. Characterization of the *Caenorhabditis elegans* Tc1 transposase *in vivo* and *in vitro*. *Genes Dev*. 1993;7:1244–1253. [[PubMed: 8391505](#)]
2126. Vowels J J, Thomas J H. Genetic analysis of chemosensory control of dauer formation in *Caenorhabditis elegans*. *Genetics*. 1992;130:105–123. [[PMC free article: PMC1204785](#)] [[PubMed: 1732156](#)]
2127. Vowels J J, Thomas J H. Multiple chemosensory defects in *daf-11* and *daf-21* mutants of *Caenorhabditis elegans*. *Genetics*. 1994;138:303–316. [[PMC free article: PMC1206150](#)] [[PubMed: 7828815](#)]

## W

2128. Waddle J A, Cooper J A, Waterston R H. Transient localized accumulation of actin in *Caenorhabditis elegans* blastomeres with oriented asymmetric divisions. *Development*. 1994;120:2317–2328. [[PubMed: 7925032](#)]
2129. Wadsworth W G, Hedgecock E M. Guidance of neuroblast migrations and axonal projections in *Caenorhabditis elegans*. *Curr. Opin. Neurobiol.* 1992;2:36–41. [[PubMed: 1638133](#)]
2130. Wadsworth W G, Hedgecock E M. Hierarchical guidance cues in the developing *nervous system* of *C. elegans*. *BioEssays*. 1996;18:355–362. [[PubMed: 8639159](#)]
2131. Wadsworth W G, Riddle D L. Acidic intracellular pH shift during *Caenorhabditis elegans* larval development. *Proc. Natl. Acad. Sci.* 1988;85:8435–8438. [[PMC free article: PMC282472](#)] [[PubMed: 3186732](#)]
2132. Wadsworth W G, Riddle D L. Developmental regulation of energy metabolism in *Caenorhabditis elegans*. *Dev. Biol.* 1989;132:167–173. [[PubMed: 2917691](#)]
2133. Wadsworth W G, Bhatt H, Hedgecock E. Neuroglia and pioneer neurons express UNC-6 to provide global and local netrin cues for guiding migrations in *C. elegans*. *Neuron*. 1996;16:35–46. [[PubMed: 8562088](#)]

2134. Wahle E, Keller W. The biochemistry of 3'-end cleavage and polyadenylation of messenger RNA precursors. *Annu. Rev. Biochem.* 1992;61:419–440. [[PubMed: 1353951](#)]
2135. Waldmann R, Champigny G, Lazdunski M. Functional degenerin-containing chimeras identify residues essential for amiloride-sensitive  $\text{Na}^+$  channel function. *J. Biol. Chem.* 1995;270:11735–11737. [[PubMed: 7744818](#)]
2136. Walent J, Porter B, Martin T. A novel 145 kD brain cytosolic protein reconstitutes  $\text{Ca}^{2+}$ -regulated secretion in permeable neuroendocrine cells. *Cell.* 1992;70:765–775. [[PubMed: 1516133](#)]
2137. Walker J, Saraste M, Runswick M J, Gay N J. Distantly related sequences in  $\alpha$ - and  $\beta$ -subunits of ATP synthase, myosin, kinases and other ATP-requiring enzymes and a common nucleotide binding fold. *EMBO J.* 1982;1:945–951. [[PMC free article: PMC553140](#)] [[PubMed: 6329717](#)]
2138. Walker N P, Talanian R V, Brady K D, Dang L C, Bump N J, Ferenz C R, Franklin S, Ghayur T, Hackett M C, Hammill L D, Herzog L, Hugunin M, Houy W, Mankovich J A, McGuiness L, Orlewicz E, Paskind M, Pratt C A, Reis P, Summani A, Terranova M, Welch J P, Xiong L, Moller A, Tracey D E, Kamen R, Wong W W. Crystal structure of the cysteine protease interleukin-1 $\beta$ -converting enzyme: A (p20/p10)2 homodimer. *Cell.* 1994;78:343–352. [[PubMed: 8044845](#)]
2139. Walker P R, Sikorska M. Endonuclease activities chromatin structure, and DNA degradation in apoptosis. *Biochem. Cell Biol.* 1994;72:615–623. [[PubMed: 7654335](#)]
2140. Walrond J P, Stretton A O. Reciprocal inhibition in the motor [nervous system](#) of the nematode *Ascaris*: Direct control of ventral inhibitory motoneurons by dorsal excitatory motoneurons. *J. Neurosci.* 1985b;5:9–15. [[PMC free article: PMC6565091](#)] [[PubMed: 3965648](#)]
2141. Walrond J P, Kass I S, Stretton A O, Donmeyer J E. Identification of excitatory and inhibitory motoneurons in the nematode *Ascaris* by electrophysiological techniques. *J. Neurosci.* 1985a;5:1–8. [[PMC free article: PMC6565077](#)] [[PubMed: 3965635](#)]
2142. Walthall W W, Chalfie M. Cell-cell interactions in the guidance of late-developing neurons in *C. elegans*. *Science.* 1988;239:643–645. [[PubMed: 3340848](#)]
2143. Walthall W W, Plunkett J A. Genetic transformation of the synaptic pattern of a motoneuron class in *Caenorhabditis elegans*. *J. Neurosci.* 1995;15:1035–1043. [[PMC free article: PMC6577843](#)] [[PubMed: 7869081](#)]
2144. Walther C, Gruss P. *Pax-6* a murine paired box gene, is expressed in the developing CNS. *Development.* 1991;113:1435–1449. [[PubMed: 1687460](#)]
2145. Wang B B, Müller-Immergluck M M, Austin J, Robinson N T, Chisholm A, Kenyon C. A homeotic gene cluster patterns the anteroposterior body axis of *C. elegans*. *Cell.* 1993;74:29–42. [[PubMed: 8101474](#)]
2146. Wang K, Ramirez-Michell R, Palter D. Titin is an extraordinarily long, flexible and slender myofibrillar protein. *Proc. Natl. Acad. Sci.* 1984;81:3685–3689. [[PMC free article: PMC345283](#)] [[PubMed: 6587383](#)]
2147. Wang L, Way J C. Activation of the *mec-3* promoter in two classes of stereotyped lineages in *Caenorhabditis elegans*. *Mech. Dev.* 1996;56:165–181. [[PubMed: 8798156](#)]
2148. Wang L, Miura M, Bergeron L, Zhu H, Yuan J. *Ich-1*, an *Ice/ced-3*-related gene, encodes both positive and negative regulators of programmed cell death. *Cell.* 1994;78:739–750. [[PubMed: 8087842](#)]
2149. Wang W F, Shakes D C. Isolation and sequence analysis of a *Caenorhabditis elegans* cDNA which encodes a 14-3-3 homologue. *Gene.* 1994;147:215–218. [[PubMed: 7926802](#)]
2150. Ward S. Chemotaxis by the nematode *Caenorhabditis elegans*: Identification of attractants and analysis of the response by use of mutants. *Proc. Natl. Acad. Sci.* 1973;70:817–821. [[PMC free article: PMC433366](#)] [[PubMed: 4351805](#)]
2151. Ward S, Gall J, editor. Gametogenesis and the early embryo. New York: A.R. Liss; 1986. The asymmetric localization of gene products during the development of *Caenorhabditis elegans*. pp. 55–75.
2152. Ward S, Carrel J S. Fertilization and sperm competition in the nematode *Caenorhabditis elegans*. *Dev. Biol.* 1979;73:304–321. [[PubMed: 499670](#)]
2153. Ward S, Klass M. The location of the major protein in *C. elegans* sperm and [spermatocytes](#). *Dev. Biol.* 1982;92:203–208. [[PubMed: 7049792](#)]

2154. Ward S, Miwa J. Characterization of temperature-sensitive, fertilization-defective mutants of the nematode *Caenorhabditis elegans*. *Genetics*. 1978;88:285–303. [PMC free article: PMC1213801] [PubMed: 580424]
2155. Ward S, Argon Y, Nelson G A. Sperm morphogenesis in wild-type and fertilization-defective mutants of *Caenorhabditis elegans*. *J. Cell Biol.* 1981;91:26–44. [PMC free article: PMC2111930] [PubMed: 7298721]
2156. Ward S, Hogan E, Nelson G A. The initiation of spermatogenesis in the nematode *Caenorhabditis elegans*. *Dev. Biol.* 1983;98:70–79. [PubMed: 6345236]
2157. Ward S, Roberts T M, Nelson G A, Argon Y. The development of motility of *Caenorhabditis elegans* spermatozoa. *J. Nematol.* 1982;14:259–266. [PMC free article: PMC2618167] [PubMed: 19295707]
2158. Ward S, Thomson N, White J G, Brenner S. Electron microscopical reconstruction of the anterior sensory anatomy of the nematode *Caenorhabditis elegans*. *J. Comp. Neurol.* 1975;160:313–337. [PubMed: 1112927]
2159. Ward S, Roberts T M, Strome S, Pavalko F M, Hogan E. Monoclonal antibodies that recognize a polypeptide antigenic determinant shared by multiple *Caenorhabditis elegans* sperm-specific proteins. *J. Cell Biol.* 1986;102:1778–1786. [PMC free article: PMC2114204] [PubMed: 2422180]
2160. Ward S, Burke D J, Sulston J E, Coulson A R, Albertson D G, Ammons D, Klass M, Hogan E. Genomic organization of major sperm protein genes and pseudogenes in the nematode *Caenorhabditis elegans*. *J. Mol. Biol.* 1988;199:1–13. [PubMed: 3351915]
2161. Ware R W, Clark D, Crossland K, Russell R L. The *nerve ring* of the nematode *Caenorhabditis elegans*: Sensory input and motor output. *J. Comp. Neurol.* 1975;162:71–110.
2162. Waring D A, Kenyon C. Selective silencing of cell communication influences anteroposterior pattern formation in *C. elegans*. *Cell*. 1990;60:123–131. [PubMed: 2295086]
2163. Waring D A, Kenyon C. Regulation of cellular responsiveness to inductive signals in the developing *C. elegans* *nervous system*. *Nature*. 1991;350:712–715. [PubMed: 2023634]
2164. Waring D A, Wrisschnik L, Kenyon C. Cell signals allow the expression of a pre-existent *neural* pattern in *C. elegans*. *Development*. 1992;116:457–466. [PubMed: 1363089]
2165. Warn R M, Smith L, Warn A. Three distinct distributions of F-actin occur during the divisions of polar surface caps to produce pole cells in *Drosophila* embryos. *J. Cell Biol.* 1985;100:1010–1015. [PMC free article: PMC2113770] [PubMed: 3980576]
2166. Wasserman P M. Towards molecular mechanisms for gamete adhesion and fusion during fertilization. *Curr. Opin. Cell Biol.* 1995;7:658–664. [PubMed: 8573340]
2167. Waterman M L, Fischer W H, Jones K A. A thymus-specific member of the HMG protein family regulates the human T. cell receptor alpha enhancer. *Genes Dev.* 1991;5:656–669. [PubMed: 2010090]
2168. Waterston R H. A second informational suppressor *sup-7 X*, in *C. elegans*. *Genetics*. 1981;97:307–325. [PMC free article: PMC1214395] [PubMed: 7274656]
2169. Waterston R H. Wood W B, editor. The nematode *Caenorhabditis elegans*. Cold Spring Harbor, New York: Cold Spring Harbor Laboratory; 1988. Muscle. pp. 281–335.
2170. Waterston R H. The minor myosin heavy chain, MHC A of *Caenorhabditis elegans* is necessary for the initiation of thick filament assembly. *EMBO J.* 1989;8:3429–3436. [PMC free article: PMC401495] [PubMed: 2583106]
2171. Waterston R, Brenner S. A suppressor mutation in the nematode acting on specific alleles of many genes. *Nature*. 1978;275:715–719. [PubMed: 703836]
2172. Waterston R H, Francis G R. Genetic analysis of muscle development in *Caenorhabditis elegans*. *Trends Neurosci.* 1985;84:270–276.
2173. Waterston R H, Sulston J. The genome of *Caenorhabditis elegans*. *Proc. Natl. Acad. Sci.* 1995;92:10836–10849. [PMC free article: PMC40526] [PubMed: 7479894]
2174. Waterston R H, Epstein H F, Brenner S. Paramyosin of *Caenorhabditis elegans*. *J. Mol. Biol.* 1974;90:285–290. [PubMed: 4217841]
2175. Waterston R H, Fishpool R M, Brenner S. Mutants affecting paramyosin in *Caenorhabditis elegans*. *J. Mol. Biol.* 1977;117 [PubMed: 564970]

2176. Waterston R H, Hirsh D, Lane T R. Dominant mutations affecting muscle structure in *C. elegans* that map near the actin gene cluster. *J. Mol. Biol.* 1984;180:473–496. [[PubMed: 6527380](#)]
2177. Waterston R H, Thomson J N, Brenner S. Mutants with altered muscle structure in *Caenorhabditis elegans*. *Dev. Biol.* 1980;77:271–302. [[PubMed: 7190524](#)]
2178. Waterston R H, Moerman D G, Baillie D L, Lane T R. Schotland D M, editor. Disorders of the motor unit. New York: John Wiley; 1982. Mutations affecting myosin heavy chain accumulation and function in the nematode *Caenorhabditis elegans*. pp. 747–760.
2179. Waterston R, Martin C, Craxton M, Huynh C, Coulson A, Hillier L, Durbin R, Green P, Shownkeen R, Halloran N, Metzstein M, Hawkins T, Wilson R, Berks M, Du Z, Thomas K, Thierry-Mieg J, Sulston J. A survey of expressed genes in *Caenorhabditis elegans*. *Nature Genet.* 1992;1:114–123. [[PubMed: 1302004](#)]
2180. Waterston R H, Ainscough R, Anderson K, Berks M, Blair D, Connell M, Cooper J, Coulson A, Craxton M, Dear S, Du Z, Durbin R, Favello A, Fulton L, Green P, Halloran N, Hawkins T, Hillier L, Huynh C, Johnston L, Kershaw J, Kirsten J, Kozono Y, Laister N, Latreille P, Mortimore B, Panussis D, Percy C, Rifkin L, Roopra A, Shownkeen R, Smaldon N, Smith A, Smith M, Staden R, Sulston J, Thierry-Mieg J, Vaudin M, Vaughan K, Weinstock L, Wilson R, Wohldmann R. The genome of the nematode *Caenorhabditis elegans*. *Cold Spring Harbor Symp. Quant. Biol.* 1994;58:367–376. [[PubMed: 7956049](#)]
2181. Watts J L, Etemad-Moghadam B, Guo S, Boyd L, Draper B W, Mello C C, Priess J R, Kemphues K J. *par-6*, a gene involved in the establishment of asymmetry in early *C. elegans* embryos, mediates the asymmetric localization of PAR-3.. *Development*. 1996;122:3133–3140. [[PubMed: 8898226](#)]
2182. Way J C, Chalfie M. *mec-3* a homeobox-containing gene that specifies differentiation of the [touch receptor neurons](#) in *C. elegans*. *Cell*. 1988;54:5–16. [[PubMed: 2898300](#)]
2183. Way J C, Chalfie M. The *mec-3* gene of *Caenorhabditis elegans* requires its own product for maintained expression and is expressed in three neuronal cell types. *Genes Dev.* 1989;3:1823–1833. [[PubMed: 2576011](#)]
2184. Way J C, Run J -Q, Wang A Y. Regulation of anterior cell-specific *mec-3* expression during asymmetric cell division in *C. elegans*. *Dev. Dyn.* 1992;194:289–302. [[PubMed: 1363076](#)]
2185. Way J C, Wang L, Run J -Q, Wang A. The *mec-3* gene contains *cis*-acting elements mediating positive and negative regulation in cells produced by asymmetric cell division in *Caenorhabditis elegans*. *Genes Dev.* 1991;5:2199–2211. [[PubMed: 1684166](#)]
2186. Weigel D, Jürgens G, Küttner F, Seifert E, Jäckle H. The homeotic gene *fork head* encodes a nuclear protein and is expressed in the terminal regions of the *Drosophila* embryo. *Cell*. 1989;57:645–658. [[PubMed: 2566386](#)]
2187. Weinshenker D, Garriga G, Thomas J H. Genetic and pharmacological analysis of neurotransmitters controlling egg laying in *C. elegans*. *J. Neurosci.* 1995;15:6975–6985. [[PMC free article: PMC6577982](#)] [[PubMed: 7472454](#)]
2188. Weintraub H. The MyoD family and myogenesis: Redundancy networks, and thresholds. *Cell*. 1993;75:1241–1244. [[PubMed: 8269506](#)]
2189. Weinzierl R, Axton J M, Ghysen A, Akam M. Ultrabithorax mutations in constant and variable regions of the protein coding sequence. *Genes Dev.* 1987;1:386–397.
2190. Weisblat D A, Blair S S. Developmental indeterminacy in embryos of the leech *Helobdella triserialis*. *Dev. Biol.* 1984;101:326–354. [[PubMed: 6229436](#)]
2191. Weiss M J, Orkin S H. GATA transcription factors: Key regulators of hematopoiesis. *Exp. Hematol.* 1995;23:99–107. [[PubMed: 7828675](#)]
2192. Wells J A, Yount R G. Active site trapping of nucleotides by crosslinking two sulphydryls in myosine subfragment 1. *Proc. Natl. Acad. Sci.* 1979;76:4966–4970. [[PMC free article: PMC413059](#)] [[PubMed: 159451](#)]
2193. Weston K, Yochem J, Greenwald I S. A *Caenorhabditis elegans* cDNA that encodes a product resembling the rat glutathione S-transferase P subunit. *Nucleic Acids Res.* 1989;17:2138–2138. [[PMC free article: PMC317564](#)] [[PubMed: 2928124](#)]

2194. Wharton R, Struhl G. RNA regulatory elements mediate control of *Drosophila* body pattern by the posterior morphogen *nanos*. *Cell*. 1991;67:955–967. [[PubMed: 1720354](#)]
2195. White J, Wood W B, editor. The nematode *Caenorhabditis elegans*. Cold Spring Harbor, New York: Cold Spring Harbor Laboratory; 1988. The anatomy. pp. 81–122.
2196. White J G, Albertson D G, Anness a n d M A R. Connectivity changes in a class of motoneurone during the development of a nematode. *Nature*. 1978;271:764–766. [[PubMed: 625347](#)]
2197. White J G, Horvitz H R, Sulston J E. Neurone differentiation in cell lineage mutants of *Caenorhabditis elegans*. *Nature*. 1982;297:584–589. [[PubMed: 7088142](#)]
2198. White J, Southgate E, Durbin R, Wood W B, editor. The nematode *Caenorhabditis elegans*. Cold Spring Harbor, New York: Cold Spring Harbor Laboratory; 1988. Appendix 2. Neuroanatomy. pp. 433–455.
2199. White J G, Southgate E, Thomson J N. On the nature of undead cells in the nematode *Caenorhabditis elegans*. *Philos. Trans. R. Soc. Lond. B Biol. Sci.* 1991;331:263–271.
2200. White J G, Southgate E, Thomson J N. Mutations in the *Caenorhabditis elegans unc-4* gene alter the synaptic input to [ventral cord motor neurons](#). *Nature*. 1992;355:838–841. [[PubMed: 1538764](#)]
2201. White J G, Southgate E, Thomson J N, Brenner S. The structure of the [ventral nerve cord](#) of *Caenorhabditis elegans*. *Philos. Trans. R. Soc. Lond. B Biol. Sci.* 1976;275:327–348. [[PubMed: 8806](#)]
2202. White J G, Southgate E, Thomson J N, Brenner S. The structure of the [nervous system](#) of the nematode *C. elegans*. *Philos. Trans. R. Soc. Lond. B Biol. Sci.* 1986;314:1–340. [[PubMed: 22462104](#)]
2203. White M J D. Animal cytology and evolution. England: Cambridge University Press; 1973.
2204. Whiting A, Wardale J, Trinick J. Does titin regulate the length of muscle thick filaments? *J. Mol. Biol.* 1989;205:263–268. [[PubMed: 2926807](#)]
2205. WHO. Lymphatic filariasis: The disease and its control. Geneva: World Health Organisation; 1992.
2206. Wickens M, Kimble J, Strickland S. Translational control of developmental decisions. In: Hershey J W B, et al., editors. Translational control. Cold Spring Harbor, New York: Cold Spring Harbor Laboratory Press; 1995. pp. 411–450.
2207. Wicks S R, Rankin C H. Integration of mechanosensory stimuli in *Caenorhabditis elegans*. *J. Neurosci.* 1995;15:2434–2444. [[PMC free article: PMC6578104](#)] [[PubMed: 7891178](#)]
2208. Wicks S R, Rankin C H. The integration of antagonistic reflexes revealed by laser ablation of identified neurons determines habituation kinetics of the *Caenorhabditis elegans* tap withdrawal response. *J. Comp. Physiol. A*. 1996;179:675. [[PubMed: 8888578](#)]
2209. Wicky C, Villeneuve A M, Lauper N, Codourey L, Tobler H, Müller F. Telomeric repeats (TTAGGC)<sub>n</sub> are sufficient for chromosome capping function in *Caenorhabditis elegans*. *Proc. Natl. Acad. Sci.* 1996;93:8983–8988. [[PMC free article: PMC38581](#)] [[PubMed: 8799140](#)]
2210. Wieringa B, Hofer E, Weissmann C. A minimal intron length but no specific internal sequence is required for splicing the large rabbit B-globin intron. *Cell*. 1984;37:915–925. [[PubMed: 6204770](#)]
2211. Wightman B, Ha I, Ruvkun G. Posttranscriptional regulation of the heterochronic gene *lin-14* by *lin-4* mediates temporal pattern formation in *C. elegans*. *Cell*. 1993;75:855–862. [[PubMed: 8252622](#)]
2212. Wightman B, Bürglin T R, Gatto J, Arasu P, Ruvkun G. Negative regulatory sequences in the *lin-14* 3'- untranslated region are necessary to generate a temporal switch during *Caenorhabditis elegans* development. *Genes Dev.* 1991;5:1813–1824. [[PubMed: 1916264](#)]
2213. Wightman B, Clark S G, Taskar A M, Forrester W C, Maricq A V, Bargman C I, Garriga G. The *C. elegans* gene *vab-8* guides posteriorly directed axon outgrowth and cell migration. *Development*. 1996;122:671–682. [[PubMed: 8625818](#)]
2214. Wiley E O. Phylogenetics: The theory and practice of phylogenetic systematics. New York: Wiley; 1981.
2215. Wilkinson H A, Greenwald I. Spatial and temporal patterns of *lin-12* expression during *C. elegans* hermaphrodite development. *Genetics*. 1995;141:513–526. [[PMC free article: PMC1206752](#)] [[PubMed: 8647389](#)]

2216. Wilkinson H A, Fitzgerald K, Greenwald I. Reciprocal changes in expression of *lin-12* (receptor) and *lag-2* (ligand) prior to commitment in a *C. elegans* cell fate decision. *Cell*. 1994;79:1187–1198. [[PubMed: 8001154](#)]
2217. Williams B D, Waterston R H. Genes critical for muscle development and function in *Caenorhabditis elegans* identified through lethal mutations. *J. Cell Biol.* 1994;124:475–490. [[PMC free article: PMC2119919](#)] [[PubMed: 8106547](#)]
2218. Williams B D, Schrank B, Huynh C, Shownkeen R, Waterston R H. A genetic mapping system in *Caenorhabditis elegans* based on polymorphic sequence-tagged sites. *Genetics*. 1992;131:609–624. [[PMC free article: PMC1205034](#)] [[PubMed: 1321065](#)]
2219. Williams E J, Furness J, Walsh F S, Doherty P. Activation of the FGF receptor underlies neurite outgrowth stimulated by L1, N-CAM, and N-cadherin. *Neuron*. 1994;13:583–594. [[PubMed: 7917292](#)]
2220. Williams G T, Smith C A. Molecular regulation of apoptosis: Genetic controls on cell death. *Cell*. 1993;74:777–779. [[PubMed: 8104100](#)]
2221. Williams S A, DeSimone S M, Poole C B, McReynolds L A, MacInnis A J, editor. Molecular paradigms for eliminating helminthic parasites. New York: Alan R. Liss; 1987. Development of DNA probes to identify and speciate filarial parasites. pp. 205–214.
2222. Williamson V M, Ho J -Y, Ma H M. Molecular transfer of nematode resistance genes. *J. Nematol.* 1992;24:234–241. [[PMC free article: PMC2619266](#)] [[PubMed: 19282989](#)]
2223. Willmer P. Invertebrate relationships: Patterns in animal evolution. England: Cambridge University Press; 1990.
2224. Wills N, Gesteland R, Karn J, Barnett L, Bolten S, Waterston R. The genes *sup-7* X and *sup-5* III of *C. elegans* suppress amber nonsense mutations via altered transfer RNA. *Cell*. 1983;33:575–583. [[PubMed: 6571695](#)]
2225. Wilson C, Pearson R K, Bellen H J, O'Kane C J, Grossniklaus U, Gehring W J. P-element-mediated enhancer detection: An efficient method for isolating and characterizing developmentally regulated genes in *Drosophila*. *Genes Dev.* 1989;3:1301–1313. [[PubMed: 2558051](#)]
2226. Wilson K P, Black J A, Thomson J A, Kim E E, Griffith J P, Navia M A, Murcko M A, Chambers S P, Aldape R A, Raybuck S A, Livingston D J. Structure and mechanism of interleukin-1  $\beta$  converting enzyme. *Nature*. 1994;370:270–275. [[PubMed: 8035875](#)]
2227. Wilson M A, Bird D M, van der Knaap E. A comprehensive subtractive cDNA cloning approach to identify nematode-induced transcript in tomato. *Phytopathology*. 1994;84:299–303.
2228. Wilson R, Ainscough R, Anderson K, Baynes C, Berks M, Bonfield J, Burton J, Connell M, Copsey T, Cooper J, Coulson A, Craxton M, Dear S, Du Z, Durbin R, Favello A, Fraser A, Fulton L, Gardner A, Green P, Hawkins T, Hillier L, Jier M, Johnston L, Jones M, Kershaw J, Kirsten J, Laisster N, Latreille P, Lightning J, Lloyd C, Mortimore B, O'Callaghan M, Parson J, Percy C, Rifkin L, Roopra A, Saunders D, Shownkeen R, Sims M, Smaldon N, Smith A, Smith M, Sonnhammer E, Staden R, Sulston J, Thierry-Mieg J, Thomas K, Vaudin M, Vaughan K, Waterston R, Watson A, Weinstock L, Wilkinson-Sproat J, Wohldman P. 2.2 Mb of contiguous nucleotide sequence from chromosome III of *C. elegans*. *Nature*. 1994;368:32–38. [[PubMed: 7906398](#)]
2229. Winder S J, Walsh M P. Smooth muscle calponin. Inhibition of actomyosin MgATPase and regulation by phosphorylation. *J. Biol. Chem.* 1990;265:10148–10155. [[PubMed: 2161834](#)]
2230. Winneperenninx B, Backeljau T, Mackey L Y, Brooks J M, de Wachter R, Kumar S, Garey J R. Molecular data indicate that Aschelminthes are polyphyletic in origin and consist of at least three distinct clades. *Mol. Biol. Evol.* 1995;12:1132–1137. [[PubMed: 8524046](#)]
2231. Winter C E, Penha C, Blumenthal T. Characterization of a vitellogenin gene from the free-living nematode *Oscheius brevesophaga*. *Mol. Biol. Evol.* 1996;13:674–684. [[PubMed: 8676742](#)]
2232. Wolberger C, Vershon A K, Liu B, Johnson A D, Pabo C O. Crystal structure of a MAT $\alpha$ 2 homeodomain-operator complex suggests a general model for homeodomain-DNA interactions. *Cell*. 1991;67:517–528. [[PubMed: 1682054](#)]
2233. Wolf N, Hirsh D, McIntosh J R. Spermatogenesis in males of the free living nematode *Caenorhabditis elegans*. *J. Ultrastruct. Res.* 1978;63:155–169. [[PubMed: 671581](#)]

2234. Wolf N, Priess J, Hirsh D. Segregation of germline granules in early embryos of *Caenorhabditis elegans*: An electron microscopic analysis. *J. Embryol. Exp. Morphol.* 1983;73:297–306. [[PubMed: 6683746](#)]
2235. Wolffe A P. Structural and functional properties of the evolutionarily ancient Y-box family of nucleic acid binding proteins. *BioEssays*. 1994;16:245–251. [[PubMed: 8031301](#)]
2236. Wolpert L. The evolutionary origin of development: Cycles patterning, privilege and continuity. *Suppl., pp. Development*. 1994:79–84. [[PubMed: 7579526](#)]
2237. Wolstenholme D, Macfarlane J, Okimoto R, Clary D, Wahleithner J. Bizarre tRNAs inferred from DNA sequences of mitochondrial genomes of nematode worms. *Proc. Natl. Acad. Sci.* 1987;84:1324–1328. [[PMC free article: PMC304420](#)] [[PubMed: 3469671](#)]
2238. Wong A, Boutis P, Hekimi S. Mutations in the *clk-1* gene of *Caenorhabditis elegans* affect developmental and behavioral timing. *Genetics*. 1995;139:1247–1259. [[PMC free article: PMC1206454](#)] [[PubMed: 7768437](#)]
2239. Wong L, Adler P. Tissue polarity genes regulate the subcellular location for prehair assembly in the pupal wing. *J. Cell Biol.* 1993;123:209–221. [[PMC free article: PMC2119819](#)] [[PubMed: 8408199](#)]
2240. Wood W B, Wood W B, editor. The nematode *Caenorhabditis elegans*. Cold Spring Harbor, New York: Cold Spring Harbor Laboratory; 1988. Preface.
2241. Wood W B. Evidence from reversal of handedness in *C. elegans* embryos for early cell interactions determining cell fates. *Nature*. 1991;349:536–538. [[PubMed: 1992354](#)]
2242. Wood W B. 1988.
2243. Wood W B, Kershaw D. Handed asymmetry, handedness reversal and mechanisms of cell fate determination in nematode embryos. *Ciba Found. Symp.* 1991;162:143–159. [[PubMed: 1802640](#)]
2244. Wood W B, Meneely P, Schedin P, Donahue L. Aspects of dosage compensation and sex determination in *Caenorhabditis elegans*. *Cold Spring Harbor Symp. Quant. Biol.* 1985;50:575–593. [[PubMed: 3868495](#)]
2245. Wood W B, Hecht R, Carr S, Vanderslice R, Wolf N, Hirsh D. Parental effects and phenotypic characterization of mutants that affect early development in *Caenorhabditis elegans*. *Dev. Biol.* 1980;74:446–469. [[PubMed: 7371984](#)]
2246. Wrana J L, Attisano L, Wieser R, Ventura F, Massagué J. Mechanism of activation of the TGF- $\beta$  receptor. *Nature*. 1994;370:341–347. [[PubMed: 8047140](#)]
2247. Wright K A. The nematode's cuticle—Its surface and the epidermis: Function;--> homology;--> analogy. A current consensus. *J. Parasitol.* 1987;73:1077–1083. [[PubMed: 3325620](#)]
2248. Wright K A, Hong H. *Trichinella spiralis*: The fate of the accessory layer of the cuticle of infective larvae. *Exp. Parasitol.* 1989;68:105–107. [[PubMed: 2917626](#)]
2249. Wright K A, Thomson J N. The buccal capsule of *Caenorhabditis elegans* (Nematoda:Rhabditoidea): An ultrastructural study. *Can. J. Zool.* 1981;59:1952–1961.
2250. Wright T F. The phenogenetics of the embryonic mutant lethal myospheroid, in *Drosophila melanogaster*. *J. Exp. Zool.* 1960;143:77–99. [[PubMed: 13786827](#)]
2251. Wu Y, Han M. Suppression of activated Let-60 Ras defines a role of *Caenorhabditis elegans sur-1* MAP kinase in vulval differentiation. *Genes Dev.* 1994;8:147–159. [[PubMed: 8299935](#)]
2252. Wu Y, Han M, Guan K -L. MEK-2, a *Caenorhabditis elegans* MAP kinase kinase, functions in Ras-mediated vulval induction and other developmental events. *Genes Dev.* 1995;9:742–755. [[PubMed: 7729690](#)]
2253. Wyllie A H. Glucocorticoid-induced thymocyte apoptosis is associated with endogenous endonuclease activation. *Nature*. 1980;284:555–556. [[PubMed: 6245367](#)]
2254. Wyllie A H, Kerr J F R, Currie A R. Cell death: The significance of apoptosis. *Int. Rev. Cytol.* 1980;68:251–306. [[PubMed: 7014501](#)]
2255. Wyss U, Gründler F M W, Münch A. The parasitic behaviour of second-stage juveniles of *Meloidogyne incognita* in roots of *Arabidopsis thaliana*. *Nematologica*. 1992;38:98–111.

## X

2256. Xiang M, Zhou L, Peng Y W, Eddy R L, Shows T B, Nathans J. *Brn-3b*: A POU domain gene expressed in a subset of retinal ganglion cells. *Neuron*. 1993;11:689–701. [[PubMed: 7691107](#)]
2257. Xiang M, Zhou L, Macke J P, Yoshioka T, Hendry S H, Eddy R L, Shows T B, Nathans J. The Brn-3 family of POU domain factors: Primary structure, binding specificity, and expression in subsets of retinal ganglion cells and somatosensory neurons. *J. Neurosci.* 1995;15:4762–4785. [[PMC free article: PMC6577904](#)] [[PubMed: 7623109](#)]
2258. Xie H, Bain O, Williams S A. Molecular phylogenetic studies on filarial parasites based on 5S ribosomal spacer sequences. *Parasite*. 1994;1:141–151. [[PubMed: 9140481](#)]
2259. Xu W, Rould M A, Jun S, Desplan C, Pabo C O. Crystal structure of a paired domain-DNA complex at 2.5 Å resolution reveals structural basis for Pax developmental mutations. *Cell*. 1995;80:639–650. [[PubMed: 7867071](#)]
2260. Xue D, Horvitz H R. Inhibition of the *Caenorhabditis elegans* cell-death protease CED-3 by a CED-3 cleavage site in baculovirus p35 protein. *Nature*. 1995;377:248–251. [[PubMed: 7675111](#)]
2261. Xue D, Shaham S, Horvitz H R. The *Caenorhabditis elegans* cell-death protein CED-3 is a cysteine protease with substrate specificities similar to those of the human CPP32 protease. *Genes Dev.* 1996;10:1073–1083. [[PubMed: 8654923](#)]
2262. Xue D, Tu Y, Chalfie M. Cooperative interactions between the *Caenorhabditis elegans* homeoproteins UNC-86 and MEC-3. *Science*. 1993;261:1324–1328. [[PubMed: 8103239](#)]
2263. Xue D, Finney M, Ruvkun G, Chalfie M. Regulation of the *mec-3* gene by the *C. elegans* homeoproteins UNC-86 and MEC-3. *EMBO J.* 1992;11:4969–4979. [[PMC free article: PMC556975](#)] [[PubMed: 1361171](#)]

## Y

2264. Yamada E. The fine structure of the megakaryocytes in the mouse spleen. *Acta Anat.* 1957;29:267–290. [[PubMed: 13434640](#)]
2265. Yamada Y, Sasaki M. The laminin B2 chain has a multidomain structure homologous to the B1 chain. *J. Biol. Chem.* 1987;262:17111–17117. [[PubMed: 3680290](#)]
2266. Yamaguchi Y, Murakami K, Furusawa M, Miwa J. Germline-specific antigens identified by monoclonal antibodies in the nematode *Caenorhabditis elegans*. *Dev. Growth Differ.* 1983;25:121–131.
2267. Yandell M D, Edgar L G, Wood W B. Trimethylpsoralen induces small deletion mutations in *Caenorhabditis elegans*. *Proc. Natl. Acad. Sci.* 1994;91:1381–1385. [[PMC free article: PMC43162](#)] [[PubMed: 7906415](#)]
2268. Yang J, Kramer J M. In vitro mutagenesis of *Caenorhabditis elegans* cuticle collagens identifies a potential subtilisin-like protease cleavage site and demonstrates that carboxyl domain disulfide bonding is required for normal function but not assembly. *Mol. Cell. Biol.* 1994;14:2722–2730. [[PMC free article: PMC358638](#)] [[PubMed: 8139571](#)]
2269. Yaniv M, Folk W R, Berg P, Soll L. A single mutational modification of a tryptophan-specific transfer RNA permits aminoacylation by glutamine and translation of the codon UAG. *J. Mol. Biol.* 1981;86:245–260. [[PubMed: 4606150](#)]
2270. Yarwood E A, Hansen E L. Dauer larvae of *Caenorhabditis briggsae* in axenic culture. *J. Nematol.* 1969;1:184–189. [[PMC free article: PMC2617821](#)] [[PubMed: 19325674](#)]
2271. Yeargers E. Effect of gamma-radiation on dauer larvae of *Caenorhabditis elegans*. *J. Nematol.* 1981;13:235–237. [[PMC free article: PMC2618057](#)] [[PubMed: 19300755](#)]
2272. Yeh W H. "Genes acting late in the signalling pathway for *Caenorhabditis elegans* dauer larval development." [Ph.D. thesis]. University of Missouri; Columbia: 1991.
2273. Yeo S, Lloyd A, Kozak K, Dinh A, Dick T, Yang X, Sakonju S, Chia W. On the functional overlap between two *Drosophila* POU homeodomain genes and the cell fate specifications of a CNS neural precursor. *Genes Dev.* 1995;9:1223–1236. [[PubMed: 7758947](#)]

2274. Yenbutr P, Scott A L. Molecular cloning of a serine proteinase inhibitor from *Brugia malayi*. *Infect. Immun.* 1995;63:1745–1753. [[PMC free article: PMC173219](#)] [[PubMed: 7729881](#)]
2275. Yin J C, Vecchio M D, Zhou H, Tully T. CREB as a memory modulator: Induced expression of a dCREB2 activator isoform enhances long-term memory in *Drosophila*. *Cell*. 1995;81:107–115. [[PubMed: 7720066](#)]
2276. Yin X -M, Oltvai Z N, Korsmeyer S J. Single amino acid substitution in Bcl-2 eliminates death repressor activity and heterodimerization with Bax. *Nature*. 1994;369:321–323. [[PubMed: 8183370](#)]
2277. Yochem J, Greenwald I. *glp-1* and *lin-12* genes implicated in distinct cell-cell interactions in *Caenorhabditis elegans*, encode similar transmembrane proteins. *Cell*. 1989;58:553–563. [[PubMed: 2758466](#)]
2278. Yochem J, Greenwald I. A gene for low density lipoprotein receptor-related protein in the nematode *Caenorhabditis elegans*. *Proc. Natl. Acad. Sci.* 1993;90:4572–4576. [[PMC free article: PMC46554](#)] [[PubMed: 8506301](#)]
2279. Yochem J, Weston K, Greenwald I. The *Caenorhabditis elegans lin-12* gene encodes a transmembrane protein with overall similarity to *Drosophila notch*. *Nature*. 1988;335:547–550. [[PubMed: 3419531](#)]
2280. Yonezawa N, Nishida E, Sakai H. pH control of actin polymerization by cofilin. *J. Biol. Chem.* 1985;266:10485–10489. [[PubMed: 4055781](#)]
2281. Yoon C H, Lee J, Jongeward G D, Sternberg P W. Similarity of *sli-1*, a regulator of vulval development in *C. elegans*, to the mammalian proto-oncogene *c-cbl*. *Science*. 1995;269:1102–1105. [[PubMed: 7652556](#)]
2282. Young J M, Hope I A. Molecular markers of differentiation in *Caenorhabditis elegans* obtained by promoter trapping. *Dev. Dynam.* 1993;196:124–132. [[PubMed: 8364222](#)]
2283. Youngman S, van Luenen H G A M, Plasterk R H A. Rte-1, a retrotransposon-like element in *Caenorhabditis elegans*. *FEBS Lett.* 1996;380:1–7. [[PubMed: 8603714](#)]
2284. Yu Y -T, Maroney P A, Nilsen T W. Functional reconstitution of U6 snRNA in nematode cis- and trans-splicing: U6 can serve as both a branch acceptor and a 5' exon. *Cell*. 1993;75:1049–1059. [[PubMed: 8261508](#)]
2285. Yu Y -T, Breitbart R E, Smoot L B, Lee Y, Mahdavi V, Nadal-Ginard B. Human myocyte-specific enhancer factor 2 comprises a group of tissue restricted MADS box transcription factors. *Genes Dev.* 1992;6:1783–1798. [[PubMed: 1516833](#)]
2286. Yuan J, Horvitz H R. The *Caenorhabditis elegans* genes *ced-3* and *ced-4* act cell autonomously to cause programmed cell death. *Dev. Biol.* 1990;138:33–41. [[PubMed: 2307287](#)]
2287. Yuan J, Horvitz H R. The *Caenorhabditis elegans* cell death gene *ced-4* encodes a novel protein and is expressed during the period of extensive programmed cell death. *Development*. 1992;116:309–320. [[PubMed: 1286611](#)]
2288. Yuan J, Finney M, Tsung N, Horvitz H R. Tc4, a *Caenorhabditis elegans* transposable element with an unusual fold-back structure. *Proc. Natl. Acad. Sci.* 1991;88:3334–3338. [[PMC free article: PMC51441](#)] [[PubMed: 1849651](#)]
2289. Yuan J, Shaham S, Ledoux S, Ellis H M, Horvitz H R. The *C. elegans* cell death gene *ced-3* encodes a protein similar to mammalian interleukin-1 $\beta$  converting enzyme. *Cell*. 1993;75:641–652. [[PubMed: 8242740](#)]
2290. Yunis J J, Oken M M, Kaplan M E, Ensrud K M, Howe R R, Theologides A. Distinctive chromosomal abnormalities in histologic subtypes of non-Hodgkin's lymphoma. *N. Engl. J. Med.* 1982;307:1231–1236. [[PubMed: 7133054](#)]
2291. Yurchenco P D, Cheng Y S. Self-assembly and calcium-binding sites in laminin. A three-arm interaction model. *J. Biol. Chem.* 1993;268:17286–17299. [[PubMed: 8349613](#)]
2292. Yurchenco P D, Schittny J C. Molecular architecture of basement membranes. *FASEB J.* 1990;4:1577–1590. [[PubMed: 2180767](#)]

2293. Zakian V A. Structure and function of telomeres. *Annu. Rev. Genet.* 1989;23:579–604. [[PubMed: 2694944](#)]
2294. Zalokar M. Autoradiographic study of protein and RNA formation during early development of *Drosophila* eggs. *Dev. Biol.* 1976;49:425–437. [[PubMed: 817947](#)]
2295. Zarkower D, Hodgkin J. Molecular analysis of the *C. elegans* sex-determining gene *tra-1*: A gene encoding two zinc finger proteins. *Cell.* 1992;70:237–249. [[PubMed: 1339311](#)]
2296. Zarkower D, Hodgkin J. Zinc fingers in sex determination: Only one of the two *C. elegans* *Tra-1* proteins binds DNA *in vitro*. *Nucleic Acids Res.* 1993;21:3691–3698. [[PMC free article: PMC309867](#)] [[PubMed: 8367286](#)]
2297. Zarkower D, De Bono M, Aronoff R, Hodgkin J. Regulatory rearrangements and smg-sensitive alleles of the *C. elegans* sex-determining gene *tra-1*. *Dev. Genet.* 1994;15:240–250. [[PubMed: 7520378](#)]
2298. Zarlenga D S, Lichtenfels J R, Stringfellow F. Cloning and sequence analysis of the small subunit ribosomal RNA gene from *Nematodirus battus*. *J. Parasitol.* 1994a;80:342–344. [[PubMed: 8158485](#)]
2299. Zarlenga D S, Stringfellow F, Nobary M, Lichtenfels J R. Cloning and characterization of ribosomal RNA genes from three species of *Haemonchus* (Nematoda: Trichostrongyloidea) and identification of PCR primers for rapid differentiation. *Exp. Parasitol.* 1994b;78:28–36. [[PubMed: 8299758](#)]
2300. Zeng W, Alarcon C M, Donelson J E. Many transcribed regions of the *Onchocerca volvulus* genome contain the spliced leader sequence of *Caenorhabditis elegans*. *Mol. Cell. Biol.* 1990;10:2765–2773. [[PMC free article: PMC360637](#)] [[PubMed: 1692960](#)]
2301. Zengel J M, Epstein H F. Identification of genetic elements associated with muscle structure in *Caenorhabditis elegans*. *Cell Motil.* 1980;1:73–97. [[PubMed: 7348600](#)]
2302. Zetka M C, Müller F. Telomeres in nematodes. *Semin. Cell Dev. Biol.* 1996;7:59–64.
2303. Zetka M C, Rose A M. Sex-related differences in crossing over in *Caenorhabditis elegans*. *Genetics.* 1990;126:355–363. [[PMC free article: PMC1204190](#)] [[PubMed: 2245915](#)]
2304. Zetka M C, Rose A M. The meiotic behaviour of an inversion in *Caenorhabditis elegans*. *Genetics.* 1992;131:321–332. [[PMC free article: PMC1205007](#)] [[PubMed: 1644275](#)]
2305. Zetka M C, Rose A M. The genetics of meiosis in *Caenorhabditis elegans*. *Trends Genet.* 1995a;11:27–31. [[PubMed: 7900192](#)]
2306. Zetka M C, Rose A M. Mutant *rec-1* eliminates the meiotic pattern of crossing over. *Genetics.* 1995b;141:1339–1349. [[PMC free article: PMC1206871](#)] [[PubMed: 8601478](#)]
2307. Zhang H B, Blumenthal T. Functional analysis of an intron 3'splice site in *Caenorhabditis elegans*. *RNA.* 1996;2:380–388. [[PMC free article: PMC1369380](#)] [[PubMed: 8634918](#)]
2308. Zhang J Z, Davletov B A, Südhof T C, Anderson R G W. Synaptotagmin I is a high affinity receptor for clathrin AP-2: Implications for membrane recycling. *Cell.* 1994;78:751–760. [[PubMed: 8087843](#)]
2309. Zhang M Q, Marr T G. Fission yeast gene structure and recognition. *Nucleic Acids Res.* 1994;22:1750–1759. [[PMC free article: PMC308059](#)] [[PubMed: 8202381](#)]
2310. Zhang P, Emmons S W. Specification of sense organ identity by a *C. elegans* Pax-6 homologue. *Nature.* 1995;377:55–59. [[PubMed: 7659160](#)]
2311. Zhang S, Ruiz-Echevarria M J, Quan Y, Peltz S W. Identification and characterization of a sequence motif involved in nonsense-mediated mRNA decay. *Mol. Cell. Biol.* 1995;15:2231–2244. [[PMC free article: PMC230451](#)] [[PubMed: 7891717](#)]
2312. Zhang Y, Emmons S W. Specification of sense-organ identity by a *Caenorhabditis elegans* Pax-6 homologue. *Nature.* 1995;377:55–59. [[PubMed: 7659160](#)]
2313. Zhao C, Emmons S W. A transcription factor controlling development of peripheral [sense organs](#) in *C. elegans*. *Nature.* 1995;373:74–78. [[PubMed: 7800042](#)]
2314. Zhen M, Schein J E, Baillie D L, Candido E P M. An essential ubiquitin-conjugating enzyme with tissue and developmental specificity in the nematode *Caenorhabditis elegans*. *EMBO J.* 1996;15:3229–3237. [[PMC free article: PMC451877](#)] [[PubMed: 8670823](#)]
2315. Zhen M, Heinlein R, Jones D, Jentsch S, Candido E P M. The *ubc-2* gene of *Caenorhabditis elegans* encodes a ubiquitin-conjugating enzyme involved in selective protein degradation. *Mol. Cell. Biol.* 1993;13:1371–1377. [[PMC free article: PMC359446](#)] [[PubMed: 8441382](#)]

2316. Zhivotovsky B, Wade D, Nicotera P, Orrenius S. Role of nucleases in apoptosis. *Int. Arch. Allergy Immunol.* 1994;105:333–338. [[PubMed: 7981600](#)]
2317. Ziegler C. Titin-related proteins in invertebrate muscles. *Comp. Biochem. Physiol.* 1994;109:823–833. [[PubMed: 7828026](#)]
2318. Zigmond S H. Recent quantitative studies of actin filament turnover during cell locomotion. *Cell Motil. Cytoskel.* 1993;25:309–316. [[PubMed: 8402952](#)]
2319. Zioni (Cohen-Nissan) S, Glazer I, Segal D. Life cycle and reproductive potential of the nematode *Heterorhabditis bacteriophora* strain HP88. *J. Nematol.* 1992a;24:352–358. [[PMC free article: PMC2619286](#)] [[PubMed: 19283008](#)]
2320. Zioni (Cohen-Nissan) S, Glazer I, Segal D. Phenotypic and genetic analysis of a mutant of *Heterorhabditis bacteriophora* strain HP88. *J. Nematol.* 1992b;24:359–364. [[PMC free article: PMC2619290](#)] [[PubMed: 19283009](#)]
2321. Zorio A R, Lea K, Blumenthal T. Cloning of *Caenorhabditis* U2AF65: An alternatively spliced RNA containing a novel exon. *Mol. Cell. Biol.* 1997;17:946–953. [[PMC free article: PMC231820](#)] [[PubMed: 9001248](#)]
2322. Zorio D A R, Cheng N N, Blumenthal T, Spieth J. Operons as a common form of chromosomal organization in *C. elegans*. *Nature*. 1994;372:270–272. [[PubMed: 7969472](#)]
2323. Zucker-Aprison E, Blumenthal T. Potential regulatory elements of nematode vitellogenin genes revealed by interspecies sequence comparison. *J. Mol. Evol.* 1989;28:487–496. [[PubMed: 2504925](#)]
2324. Zuckerman B M. Nematodes as biological models, vols. 1 and 2. New York: Academic Press; 1980.
2325. Zuckerman B M, Kahane I. *Caenorhabditis elegans*: Stage-specific differences in cuticle surface carbohydrates. *J. Nematol.* 1983;15:535–538. [[PMC free article: PMC2618315](#)] [[PubMed: 19295843](#)]
2326. Zuckerman B M, Kahane I, Himmelhoch S. *Caenorhabditis briggsae* and *C. elegans*: Partial characterization of cuticle surface carbohydrates. *Exp. Parasitol.* 1979;47:419–424. [[PubMed: 446589](#)]
2327. Zuker C S. On the evolution of eyes: Would you like it simple or compound? *Science*. 1994;265:742–743. [[PubMed: 8047881](#)]
2328. Zwaal R R, Broeks A, van Meurs J, Groenen J T M, Plasterk R H A. Target-selected gene inactivation in *Caenorhabditis elegans* by using a frozen transposon insertion mutant bank. *Proc. Natl. Acad. Sci.* 1993;90:7431–7435. [[PMC free article: PMC47155](#)] [[PubMed: 8395047](#)]
2329. Zwaal R R, Ahringer J, van Luenen H G A M, Rushforth A, Anderson P, Plasterk R H A. G proteins are required for spatial orientation of early cell cleavages in *C. elegans* embryos. *Cell*. 1996;86:619–629. [[PubMed: 8752216](#)]
2330. Zwaal R R, Mendel J E, Sternberg P W, Plasterk R H. Two neuronal G proteins are involved in chemosensation of the *Caenorhabditis elegans* Dauer-inducing pheromone. *Genetics*. 1997;145:15–27. [[PMC free article: PMC1207856](#)] [[PubMed: 9055081](#)]

Generated from local HTML